

DEVELOPMENT OF A PERFORMANCE-BASED SEISMIC DESIGN PHILOSOPHY FOR MID-RISE WOODFRAME CONSTRUCTION



SEISMIC TESTING OF A FULL-SCALE TWO-STORY LIGHT-FRAME WOOD BUILDING: NEESWOOD BENCHMARK TEST



By
**Ioannis P. Christovasilis, Andre Filiatrault
and Assawin Wanitkorkul**

Technical Report MCEER-09-0005 ■ July 22, 2009

This research was conducted at the University at Buffalo, State University of New York and was supported by the National Science Foundation under Grant No. CMMI-0529903 (NEES Research) and CMMI-0402490 (NEES Operations).

Sponsored by the

National Science Foundation

NSF Grant Number CMMI-0529903 and CMMI-0402490

Project Title

Development of a Performance-Based Seismic Design
Philosophy for Mid-Rise Woodframe Construction

Project Team

Colorado State University

University of Delaware

University at Buffalo, State University of New York

Rensselaer Polytechnic Institute

Texas A&M University

Web Site

www.engr.colostate.edu/NEESWood

DISCLAIMER

This report is based upon work supported by the National Science Foundation under Grant No. CMMI-0529903 (NEES Research) and CMMI-0402490 (NEES Operations). Any opinions, findings, and conclusions or recommendations expressed in this material are those of the investigators and do not necessarily reflect the views of MCEER, the National Science Foundation, or other sponsors.

NEESWood Report No. 1

**Seismic Testing of a Full-Scale Two-Story
Light-Frame Wood Building:
NEESWood Benchmark Test**

by

Ioannis P. Christovasilis,¹ Andre Filiatrault² and Assawin Wanitkorkul¹

Publication Date: July 22, 2009

Submittal Date: November 2007

Technical Report MCEER-09-0005

NSF Grant Numbers CMMI-0529903 and CMMI-0402490

- 1 Graduate Student, Department of Civil, Structural and Environmental Engineering, University at Buffalo, State University of New York
- 2 Professor, Department of Civil, Structural and Environmental Engineering, University at Buffalo, State University of New York

MCEER

University at Buffalo, State University of New York

Red Jacket Quadrangle, Buffalo, NY 14261

Phone: (716) 645-3391; Fax (716) 645-3399

E-mail: mceer@buffalo.edu; WWW Site: <http://mceer.buffalo.edu>

Project Overview

NEESWood: Development of a Performance-Based Seismic Design Philosophy for Mid-Rise Woodframe Construction

While woodframe structures have historically performed well with regard to life safety in regions of moderate to high seismicity, these types of low-rise structures have sustained significant structural and nonstructural damage in recent earthquakes. To date, the height of woodframe construction has been limited to approximately four stories, mainly due to a lack of understanding of the dynamic response of taller (mid-rise) woodframe construction, nonstructural limitations such as material fire requirements, and potential damage considerations for nonstructural finishes. Current building code requirements for engineered wood construction around the world are not based on a global seismic design philosophy. Rather, wood elements are designed independently of each other without considering the influence of their stiffness and strength on the other structural components of the structural system. Furthermore, load paths in woodframe construction arising during earthquake shaking are not well understood. These factors, rather than economic considerations, have limited the use of wood to low-rise construction and, thereby, have reduced the economical competitiveness of the wood industry in the U.S. and abroad relative to the steel and concrete industry. This project seeks to take on the challenge of developing a direct displacement based seismic design philosophy that provides the necessary mechanisms to safely increase the height of woodframe structures in active seismic zones of the U.S. as well as mitigating damage to low-rise woodframe structures. This is accomplished through the development of a new seismic design philosophy that will make mid-rise woodframe construction a reality in regions of moderate to high seismicity. Such a design philosophy falls under the umbrella of the performance-based design paradigm.

In Year 1 of the NEESWood Project, a full-scale seismic benchmark test of a two-story woodframe townhouse unit that required the simultaneous use of the two three-dimensional shake tables at the University of Buffalo's NEES node was performed. As the largest full-scale three-dimensional shake table test ever performed in the U.S., the results of this series of shake table tests on the townhouse serve as a benchmark for both woodframe performance and nonlinear models for seismic analysis of woodframe structures. These efficient analysis tools provide a platform upon which to build the direct displacement based design (DDBD) philosophy. The DDBD methodology relies on the development of key performance requirements such as limiting inter-story deformations. The method incorporates the use of economical seismic protection systems such as supplemental dampers and base isolation systems in order to further increase energy dissipation capacity and/or increase the natural period of the woodframe buildings.

The societal impacts of this new DDBD procedure, aimed at increasing the height of woodframe structures equipped with economical seismic protection systems, is also investigated within the scope of this NEESWood project. Following the development of the DDBD philosophy for mid-rise (and all) woodframe structures, it was applied to the seismic design of a mid-rise (six-story) multi-family residential woodframe condominium/apartment building. This mid-rise woodframe structure was constructed and tested at full-scale in a series of shake table tests on the E-Defense (Miki) shake table in Japan. The use of the E-Defense shake table, the largest 3-D shake table in the world, was necessary to accommodate the height and payload of the mid-rise building.

This report is the first in a series of reports resulting from the NEESWood Project. It documents the benchmark shake table test program of a full-scale two-story wood frame townhouse building. The experimental program focused on the various construction elements that could significantly influence the seismic response of these types of buildings. The testing was divided into five phases: (1) engineered wood structural (shear) walls alone; (2) wood structural walls incorporating viscous fluid dampers; (3) installation of gypsum wallboard to engineered wood structural walls; (4) installation of gypsum wallboard to interior partition walls and ceilings; and (5) installation of stucco as exterior wall finish. Two kinds of tri-axial historical ground motions were used for the tests: a Design Basis Earthquake (DBE) with a probability of exceedance of 10% in 50 years, or a return period of 475 years; and a Maximum Credible Earthquake (MCE) with a probability of exceedance of 2% in 50 years, or a return period of 2,475 years.

This report provides a detailed analysis of the experimental results of test phases 1, 3, 4 and 5. The test results show that the installation of gypsum wallboard to the interior surfaces of the structural walls substantially improved the seismic response of the test structure. The application of exterior stucco provided further improvements, particularly in the longitudinal direction, where the shear response of the wall piers dominated. The results of test phase 2 are documented in a companion report.

Project Team

John W. van de Lindt, Ph.D., Principal Investigator: Associate Professor, Department of Civil Engineering, Colorado State University, Fort Collins, CO 80523-1372; jwv@engr.colostate.edu.

Rachel A. Davidson, Ph.D., Co-Principal Investigator: Associate Professor, Department of Civil and Environmental Engineering, University of Delaware, Newark, DE 19716-3120; rdavidso@udel.edu.

Andre Filiatrault, Ph.D. Eng., Co-Principal Investigator: Professor Department of Civil, Structural, and Environmental Engineering, State University of New York at Buffalo, Buffalo, New York 14261; af36@buffalo.edu.

David V. Rosowsky, Ph.D., Co-Principal Investigator: A.P. Florence Wiley Chair Professor and Department Head, Texas A&M University, Department of Civil Engineering, College Station, TX 77843-3136; rosowsky@tamu.edu.

Michael D. Symans, Ph.D., Co-Principal Investigator: Associate Professor, Department of Civil and Environmental Engineering, Rensselaer Polytechnic Institute, 110 8th Street, Troy, NY 12180-3590; symans@rpi.edu.

ACKNOWLEDGEMENTS

The authors gratefully acknowledge the Principal Investigators of the NEESWood Project who supported the NEESWood benchmark testing: John van de Lindt, Colorado State University; Michael Symans, Rensselaer Polytechnic Institute; David Rosowsky, Texas A&M University; and Rachel Davidson, Cornell University. The authors acknowledge also the contributions of the graduate, undergraduate and REU students that participated in the NEESWood benchmark testing: Charles Ekiert, Saeed Fathali, Jamie Hong, Dave Keller and Jeremy Gworek. The assistance of Weichi Pang, a post-doctoral associate at Texas A&M University, with the parameter identification of the sheathing-to-framing connection tests is greatly appreciated.

The contributions of the students and faculty of the Department of Construction Technology at Erie Community College, who installed the gypsum drywall for Phases 3 and 4 of testing is acknowledged. The coordination conducted Mr. Gregg Gillis in this activity was much appreciated.

The following organizations are also acknowledged for providing financial and in-kind support to the NEESWood benchmark testing described in this report: APA - The Engineered Wood Association, B&L Wholesale Supply Inc., Buffalo Plastering Inc., Erie Community College, Gambale USA, Georgia Pacific, Hartland Builders, MiTek Industries Inc., National Gypsum Company, NGC Testing Services, National Overhead Door Inc., Niagara Truss & Pallet LLC, Northeast Window and Door, Ridg-U-Rak Inc, Simpson Strong-Tie Inc., Stanley Bostitch, and Taylor Devices Inc.

Finally, the contribution of the staff of the Structural Engineering Earthquake Simulation Laboratory (SEESL) at the University at Buffalo is gratefully acknowledged.

TABLE OF CONTENTS

Section	Title	Page
1	Introduction	1
1.1	Description of the NEESWood Project.....	2
1.2	Description of NEESWood Benchmark Testing Program.....	3
2	Test Structure and Testing Objectives	7
2.1	Description of Test Structure.....	8
2.2	Experimental Set-up	11
2.3	Testing Objectives	13
3	Description of Shake Table Tests	17
3.1	Testing Sequences.....	18
3.1.1	System Identification Tests.....	18
3.1.2	Seismic Tests	18
3.2	Nomenclature of Shake Table Tests	24
3.3	Description of Test Phase 1	25
3.3.1	Description of Test Structure during Phase 1	25
3.3.2	Description of Test Phase 1 Protocol.....	29
3.4	Description of Test Phase 2	30
3.4.1	Description of Test Structure during Phase 2	30
3.4.2	Description of Test Phase 2 Protocol.....	32
3.5	Description of Test Phase 3	35
3.5.1	Description of Test Structure during Phase 3	35
3.5.2	Description of Test Phase 3 Protocol.....	37
3.6	Description of Test Phase 4	37
3.6.1	Description of Test Structure during Phase 4	37
3.6.2	Description of Test Phase 4 Protocol.....	39
3.7	Description of Test Phase 5	39
3.7.1	Description of Test Structure during Phase 5	39
3.7.2	Description of Test Phase 5 Protocol.....	42
3.8	Supplemental Weight Distribution and Total Weight of Test Structure.....	43
4	Description of Instrumentation for Shake Table Tests	49
4.1	Types of Instrumentation for Shake Table Test.....	50
4.1.1	Acceleration Measurements.....	50
4.1.2	Displacement Measurements	51
4.1.3	Force Measurements	54
4.1.4	Additional Measurements	54
4.2	Sign Convention and Instrumentation Summary.....	56
5	Determination of Material Properties	59
5.1	Moisture Content of Wood Shear Walls.....	60
5.2	Hysteretic Properties of Sheathing-to-Framing Connections	62

TABLE OF CONTENTS (CONT'D)

Section	Title	Page
5.2.1	Testing Configurations.....	62
5.2.2	Loading Protocol.....	63
5.2.3	Testing Apparatus and Test Specimens	63
5.2.4	Test Machine and Instrumentation.....	66
5.2.5	Test Results and Parameter Identification	69
5.3	Compressive Strength of Exterior Stucco.....	76
6	Results of System Identification Tests	83
6.1	Data Analysis.....	84
6.1.1	Identification of Natural Frequencies.....	84
6.1.2	Calculation of Modal Damping Ratios	86
6.1.3	Determination of Mode Shapes	87
6.2	Initial Natural Periods and Damping Ratios	89
6.3	Evolution of Natural Periods and Modal Damping Ratios	91
6.4	Variation of Structural Mode Shapes.....	97
7	Results of Seismic Tests.....	101
7.1	Shake Table Fidelity	102
7.2	Visual Damage Observations.....	108
7.3	Inter-story Drift Measurements.....	111
7.4	Absolute Acceleration Measurements	118
7.5	Wall Deformation Measurements	121
7.6	Global Hysteretic Response.....	130
7.7	Wall Line Hysteresis Loops.....	134
7.8	Experimental Capacity Spectra.....	134
7.9	Energy Response.....	140
7.10	Sill Plate Slippage.....	142
7.11	Peak Holdown Forces	145
7.12	Peak Sill Plate and Holdown Stud Uplift.....	148
7.13	Identification of Displacement Components	153
7.14	Effect of Vertical Input Excitation.....	160
8	Summary and Conclusions	165
REFERENCES		173
APPENDICES (Provided on attached CD)		
A	Architectural and Structural Drawings of Test Structure	175
B	Structural Drawings of Wood Shear Walls.....	193

TABLE OF CONTENTS (CONT'D)

Section	Title	Page
C	As-Built Sheathing Cutout and Nail Schedule for Wood Shear Walls.....	211
D	Description of Shake Table Tests	229
E	Instrumentation Setup of the Test Structure	237
F	Supplemental Weight Layouts and Total Weight of Benchmark Structure	257
G	Sheathing-to-Framing Connection Test Results	263
H	System Identification Test Results.....	277
I	Fidelity of Shake Table Motion.....	287
J	Selected Visual Damage Identification Photos.....	331
K	Selected Seismic Results: Relative Interstory Drift Time Histories.....	353
L	Selected Seismic Results: Absolute Acceleration Time Histories.....	405
M	Selected Seismic Results: Wall Deformations from Diagonal String Potentiometers	457
N	Selected Seismic Results: Base Shear Force – Displacement Hysteresis Loops.....	587
O	Selected Seismic Results: Interstory Shear Force – Displacement Hysteresis Loops.....	639
P	Selected Seismic Results: Sill Plate Slippage Time Histories.....	691
Q	Selected Seismic Results: Peak Anchor Bolt Forces	743
R	Selected Seismic Results: Peak Sill Plate and Stud Uplift	795

LIST OF FIGURES

Figure	Title	Page
1.1	NEESWood benchmark test structure	4
2.1	Illustration of two-story townhouse containing three units.	8
2.2	Floor plans of test building	9
2.3	Elevations of test building	10
2.4	(a) Extension frame of shake tables connected by steel link structure, and (b) Foundation of Test Building under Construction	12
2.5	Foundation details, a) schematic, b) photograph	13
3.1	Acceleration time-histories of unscaled Canoga Park ground motions: (a) horizontal component at 106 degrees from north, (b) horizontal component at 196 degrees from north and (c) vertical component	21
3.2	Acceleration time-histories of unscaled Rinaldi ground motions: (a) horizontal component at 318 degrees from north, (b) horizontal component at 228 degrees from north and (c) vertical component	22
3.3	Acceleration response spectra of unscaled Canoga Park record for 5% damping	23
3.4	Acceleration response spectra of unscaled Rinaldi record for 5% damping	23
3.5	Installation of floor joists during construction	26
3.6	Installation of the roof trusses of the benchmark structure	27
3.7	PHD2 Strong-tie Holdown installed at the bottom corner of a shear wall	28
3.8	South-east view of the structure after installation of the roof tiles	28
3.9	Location of fluid dampers on the structure	30
3.10	Damper-wall unit installed at the south side of the garage (view from inside)	31
3.11	The benchmark structure before the installation of the damper-wall units	33
3.12	Installation of the damper-wall units on the south-west side of the structure	34
3.13	Installation of gypsum wallboard on interior surface of a shear wall	35
3.14	View of the interior wall finishes after mudding and taping	36
3.15	Installation of gypsum wallboard on an interior partition wall	38
3.16	Installation of gypsum wallboard on the ceiling of the 2nd floor	38
3.17	Installation of vapor permeable, water-resistant tar paper on the test structure ..	40
3.18	Application of the first coat of plaster on the test structure	40
3.19	Application of the second coat of plaster on the test structure	41
3.20	Application of the third coat of plaster on the test structure	41
3.21	South-east external view of the benchmark structure after the installation of the exterior stucco finish.	42
3.22	View of the dining room from the 2nd floor	44
3.23	View of the nook	44
3.24	View of the living room	45
3.25	View of the garage	45
3.26	View of the master bedroom	46
3.27	View of bedroom #1	46

LIST OF FIGURES (CONT'D)

Figure	Title	Page
3.28	View of bedroom #2	47
4.1	Two accelerometers at the top of a first floor wall measuring accelerations in the two horizontal directions	50
4.2	Accelerometer at the bottom corner of the structure measuring acceleration in the vertical direction	51
4.3	String potentiometer located on the top plate of a second floor shear wall	52
4.4	Potentiometer installed on the test structure to measure sill plate slippage	53
4.5	Two potentiometers installed on the test structure to measure uplift displacements of stud to sill plate and sill plate to foundation	53
4.6	Anchor bolt load cell measuring tensile axial force in a PHD5 Holdown	55
4.7	Load cell measuring tensile axial force in a shear transfer anchor bolt	55
4.8	Positive directions of recorded data	56
5.1	CUREe-Caltech Woodframe Project Simplified Cyclic Testing Protocol [3]	64
5.2	Test apparatus and specimen dimensions for testing parallel to grain (left) and perpendicular to grain (right).	65
5.3	MTS micro console (left) and MTS hydraulic collet grip (right)	66
5.4	10 kip load cell (left) and ± 2 in. linear potentiometer (right)	66
5.5	Parallel to grain connection test setup with 2x4 framing	67
5.6	Perpendicular to grain connection test setup with 2x4 framing	68
5.7	Variability of peak load and corresponding deformation from the connection tests	73
5.8	SAWS hysteretic response of a sheathing-to-frame connector.....	73
5.9	Hysteresis plot and fitted model for Specimen 1 of cyclic test of 2x4 parallel to grain	75
5.10	Hysteresis plot and fitted model for Specimen 1 of cyclic test of 2x4 perpendicular to grain	75
5.11	Stress-strain curve derived from the first sample of Specimen B-3	77
6.1	Accelerometers of the test structure used in the system identification	85
6.2	Transfer Functions from two white noise tests in the longitudinal and transverse directions.....	86
6.3	Application of half-power bandwidth method	88
6.4	Use of symmetry on the application of half-power bandwidth method	88
6.5	Transfer Functions of accelerometers on the north side of the roof of the test structure for Test NWP1S04.	90
6.6	Evolution of the first natural period	92
6.7	Evolution of the second natural period	92
6.8	Evolution of the third natural period	93
6.9	Variations of normalized lateral stiffness in the north-south direction	95
6.10	Evolution of the first modal damping ratio	95

LIST OF FIGURES (CONT'D)

Figure	Title	Page
6.11	Evolution of the second modal damping ratio	96
6.12	Evolution of the third modal damping ratio	96
6.13	Mode shapes from Phase 3, (a) mode 1, $T_1 = 0.30$ sec, (b) mode 2, $T_2 = 0.22$ sec, (c) mode 3, $T_3 = 0.17$ sec	98
6.14	Mode shapes from Phase 4, (a) mode 1, $T_1 = 0.30$ sec, (b) mode 2, $T_2 = 0.22$ sec, (c) mode 3, $T_3 = 0.16$ sec	99
7.1	Ballast weights located on the shake tables and the connecting bridge	103
7.2	Acceleration response spectra of shake table motion for 5 % damping in (a) longitudinal, (b) transverse, and (c) vertical direction, for test NWP1S17 ...	106
7.3	Maximum angle of rotation of the twin shake tables in the transverse direction for seismic tests of Test Phase 5.	107
7.4	Selected visual damage identification photos	110
7.5	Correction of floor displacement time-histories for shake table rotation	111
7.6	Maximum inter-story drifts for Seismic Level 2 tri-axial tests of Phases 1, 3, 4 and 5 for (a) first floor, and (b) second floor	113
7.7	Maximum inter-story drifts for Phase 5 seismic tests for (a) first floor, and (b) second floor.	115
7.8	Second floor drift normalized by first floor drift of the same wall line along the transverse direction, for Test Phase 5	117
7.9	Maximum absolute acceleration measurements for Seismic Level 2 tri-axial tests of Phases 1, 3, 4 and 5 for (a) first floor, and (b) second floor	119
7.10	Maximum absolute acceleration measurements for Phase 5 seismic tests for (a) first floor, and (b) second floor	120
7.11	Typical configuration of a string potentiometer installed across a shear wall.....	121
7.12	(a) Wall deformation, and (b) wall-diaphragm deformation ratio of first floor walls, for Seismic Level 2 tri-axial tests of Test Phase 1, 3, 4 and 5	124
7.13	(a) Wall deformation, and (b) wall-diaphragm deformation ratio of second floor walls, for Seismic Level 2 tri-axial tests of Test Phase 1, 3, 4 and 5	125
7.14	(a) Wall deformation, and (b) wall-diaphragm deformation ratio of first floor walls, for seismic tests of Test Phase 5	127
7.15	(a) Wall deformation, and (b) wall-diaphragm deformation ratio of second floor walls, for seismic tests of Test Phase 5.	128
7.16	Global force-displacement hysteresis loops for Seismic Level 2 tri-axial tests of Phases 1, 3, 4 and 5	131
7.17	Global force-displacement hysteresis loops for the tri-axial tests of Phase 5	132
7.18	Transverse wall lines force-displacement hysteresis loops for Seismic Level 2 tri-axial tests of Phases 1, 3, 4 and 5	135
7.19	Transverse wall lines force-displacement loops for the tri-axial tests of Phase 5..	136
7.20	Experimental capacity spectra from the response of the benchmark structure (a) in the transverse direction, and (b) in the longitudinal direction	139

LIST OF FIGURES (CONT'D)

Figure	Title	Page
7.21	Relative input energy time-histories, for Seismic Level 2 tri-axial tests of Phases 1, 3, 4 and 5	141
7.22	Relative input energy time-histories, for tri-axial tests of Phase 5	141
7.23	(a) Peak sill plate slippage, and (b) sill plate slippage over story displacement ratio, for Seismic Level 2 tri-axial tests of Phases 1, 3, 4 and 5	143
7.24	(a) Peak sill plate slippage, and (b) sill plate slippage over story displacement ratio, for seismic tests of Phase 5	144
7.25	(a) Peak holdown force, and (b) peak holdown force to nominal ultimate strength ratio, for Seismic Level 2 tri-axial tests of Phases 1, 3, 4 and 5	146
7.26	(a) Peak holdown force, and (b) peak holdown force to nominal ultimate strength ratio, for seismic tests of Phase 5	147
7.27	(a) Peak uplift displacement, and (b) sill plate uplift to total uplift ratio, for Seismic Level 2 tri-axial tests of Phases 1, 3, 4 and 5	150
7.28	(a) Peak uplift displacement, and (b) sill plate uplift to total uplift ratio, for seismic tests of Phase 5	151
7.29	(a) Location and (b) configuration of the walls used for the displacement decomposition	153
7.30	(a) Sill plate uplift displacements, (b) total uplift displacements, and (c) associated inter-story displacement estimates of the south segment of the garage wall, for Test NWP1S17	155
7.31	Displacement components of garage wall E16 for (a) Test NWP1S17 and (b) Test NWP4S03	157
7.32	Displacement components at the peak inter-story drifts for the Seismic Level 2 tri-axial tests of Phases 1, 3, 4 and 5 and walls (a) E16, (b) E13, (c) E11, and (d) E8. Numerical values in each histogram indicate peak inter-story displacements	158
7.33	Displacement components at the peak inter-story drifts for the tri-axial seismic tests of Phase 5 and walls (a) E16, (b) E13, (c) E11, and (d) E8. Numerical values in each histogram indicate peak inter-story displacements	159
7.34	Building central displacements for Seismic Level 1 tri-axial and bi-axial tests of Phases 1, 3, 4, and 5	161
7.35	Building central displacements for Seismic Level 2 tri-axial and bi-axial tests of Phases 1, 3, 4, and 5	161
7.36	Building central displacements for Seismic Levels 3 and 4 tri-axial and bi-axial tests of Phase 5	162

LIST OF TABLES

Table	Title	Page
2.1	Summary of test phases and building configurations	14
3.1	Ground motions for seismic tests	20
3.2	Nomenclature of shake table tests	24
3.3	Nailing schedules used in the construction of the shear walls.....	25
4.1	Summary of instrumentation devices for each test phase	57
5.1	Moisture content readings for each wall section of the benchmark structure	61
5.2	Connection test configurations	63
5.3	Peak load and deformation at peak load for 2x4 parallel to grain connection tests	69
5.4	Peak load and deformation at peak load for 2x4 perpendicular to grain connection tests	70
5.5	Peak load and deformation at peak load for 2x6 parallel to grain connection tests	71
5.6	Peak load and deformation at peak load for 2x6 perpendicular to grain connection tests	72
5.7	Fitted hysteretic parameters for SAWS model	74
5.8	Stucco mix information	78
5.9	Exterior stucco sampling locations	79
5.10	Compressive strength and modulus of elasticity of exterior stucco	81
6.1	Initial natural periods (sec)	89
6.2	Initial damping ratios (%).....	89
7.1	Damage chart based on the visual damage observations	109
7.2	Angle of inclination and scale factor for each diagonal string potentiometer, throughout the testing phases	122

Chapter 1 Introduction

While woodframe structures have historically performed well with regard to life safety in regions of moderate to high seismicity, these types of low-rise structures have sustained significant structural and non-structural damage in recent earthquakes. To date, the height of woodframe construction has been limited to approximately four stories, mainly due to the lack of understanding of the dynamic response of taller (mid-rise) woodframe construction, non-structural limitations such as material fire requirements, and potential damage considerations for non-structural finishes. Current building code requirements for engineered wood construction around the world are not based on a global seismic design philosophy. Rather, wood elements

are designed independently of each other without consideration of the influence that their stiffness and strength have on the other structural components of the structural system. Furthermore, load paths in woodframe construction arising during earthquake shaking are not well understood. These factors, rather than economic considerations, have limited the use of wood to low-rise construction and, thereby, have reduced the economical competitiveness of the wood industry in the U.S. and abroad relative to the steel and concrete industry. As a result, the NEESWood Project was developed through the George E. Brown Junior Network for Earthquake Engineering Simulation (NEES) program of the National Science Foundation to address these shortcomings of woodframe construction.

1.1 Description of the NEESWood Project

The NEESWood project seeks to take on the challenge of developing a seismic design philosophy that will provide the necessary mechanisms to safely increase the height of woodframe structures in active seismic zones of the U.S. as well as mitigating damage to low-rise woodframe structures. This will be accomplished through the development of a new seismic design philosophy that will make mid-rise woodframe construction a reality in regions of moderate to high seismicity. Such a design philosophy falls under the umbrella of the performance-based design paradigm.

In Year 1 of the NEESWood Project, a full-scale seismic benchmark tests of a two-story woodframe townhouse that requiring the simultaneous use of the two three-dimensional shake tables at the SUNY-Buffalo NEES node is to be performed. As the largest full-scale three-dimensional shake table test ever performed in the U.S., the results of this series of shake table tests on the townhouse will serve as a benchmark for both woodframe performance and nonlinear models for seismic analysis of woodframe structures. These efficient analysis tools will provide a

platform upon which to build the performance-based seismic design (PBSD) philosophy. The PBSD methodology will rely on the development of key performance requirements such as limiting inter-story deformations. The method will incorporate the use of economical seismic protection systems such as supplemental dampers and base isolation systems in order to further increase energy dissipation capacity and/or increase the natural period of the woodframe buildings.

The societal impacts of this new PBSD procedure, aimed at increasing the height of woodframe structures equipped with economical seismic protection systems, will also be investigated within the scope of this NEESWood project. Once the PBSD philosophy for mid-rise (and all) woodframe structures has been developed, it will be applied to the seismic design of a mid-rise (five or six-story) multi-family residential woodframe apartment building. This mid-rise woodframe structure will be constructed and tested at full-scale in a series of shake table tests on the E-Defense (Miki) shake table in Japan. The use of the E-Defense shake table, the largest 3-D shake table in the world, is necessary to accommodate the height and payload of the mid-rise building. There will be a general solicitation in the U.S. and in the international earthquake engineering community for payload projects to be conducted during this series of tests, thus maximizing the benefit to cost ratio for the world's earthquake engineering community.

1.2 Description of NEESWood Benchmark Testing Program

This report discusses the benchmark shake table testing program on a full-scale two-story woodframe townhouse building conducted within the NEESWood Project. The test building represents the world's largest woodframe structure tested on a shake table. The size and weight of the test structure required the simultaneous use of the two tri-axial shake tables at the University at Buffalo UB-NEES site. The testing program is focusing on the various construction

elements that may have significant influence on the seismic response of woodframe buildings and that should be considered in performance-based seismic design.

The benchmark test structure is based on one of the four index buildings designed within the recently completed CUREE-Caltech Woodframe Project [1]. It represents one unit of a two-story townhouse containing three units, having approximately 1800 ft² of living space with an attached two-car garage, as shown in Figure 1.1. The height of the townhouse from the first floor slab to the roof eaves is 18 ft and its total weight is approximately 80 kips. The exterior walls of the townhouse test building are covered on the outside with 7/8 in. thick stucco over 7/16 in. thick OSB sheathed shear walls and 1/2 in. thick gypsum wallboard on the inside.

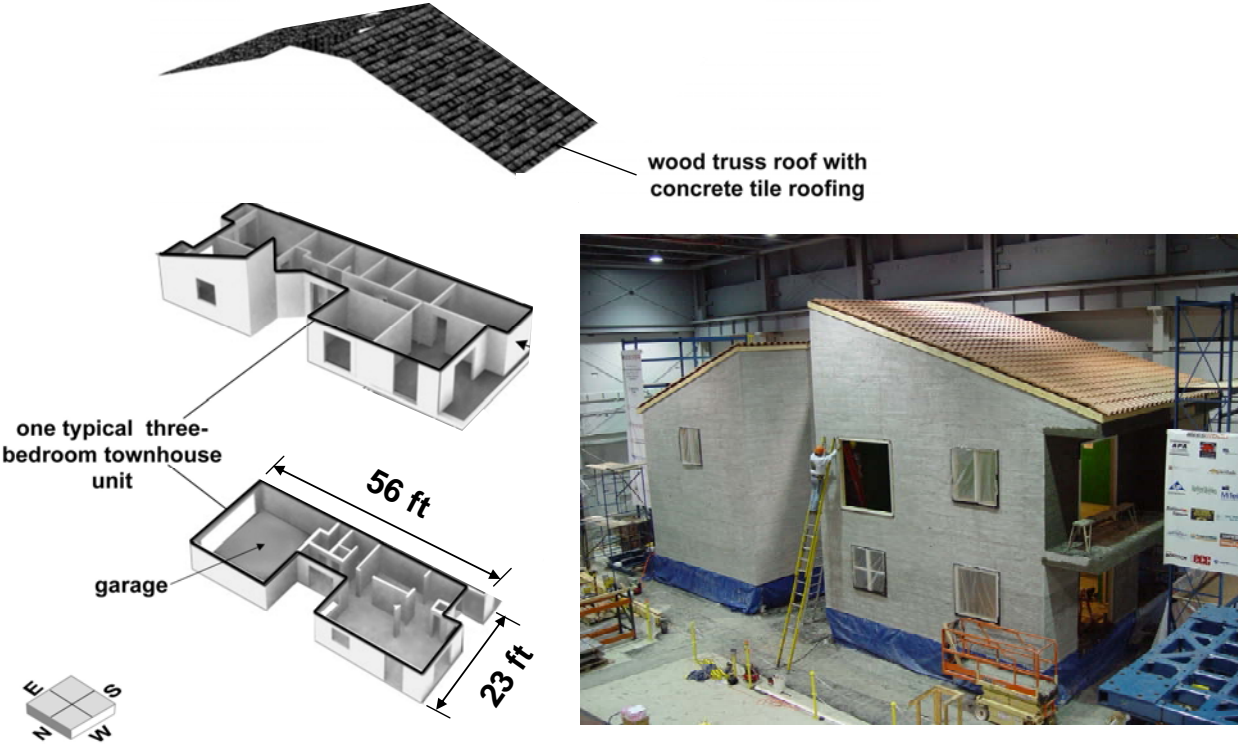


Figure 1.1: NEESWood benchmark test structure

Multiple seismic tests were conducted for various configurations of the benchmark test building. Five different seismic test phases were included in the test program. Low amplitude white noise tests were also conducted between the seismic tests of each phase to determine the variations of the dynamic characteristics of the test building as it experienced increasing levels of damage. The test structure was repaired after each test phase in an attempt to return the lateral load-resisting system to its original characteristics before the start of each subsequent test phase. Note that all test phases were performed for a constant mass of the test building by incorporating ballast weights at the floor level for the test phases in which some of the wall finish materials were omitted.

Two different types of tri-axial historical ground motions were used for the seismic tests: ordinary ground motions and near-field ground motions. The ordinary ground motions represented a Design Basis Earthquake (DBE) having a probability of exceedance of 10% in 50 years (10%/50 years), or equivalently, a return period of 475 years. The near-field ground motions represented a Maximum Credible Earthquake (MCE) having a probability of exceedance of 2% in 50 years (2%/ 50 years), or a return period of 2475 years.

The test structure was instrumented with nearly 230 displacement, acceleration, and force measuring devices to maximize the amount of information regarding the response of the structure during the various tests.

Chapter 2 Test Structure and Testing Objectives

This chapter provides a description of the benchmark structure and gives information on the experimental set-up that was used to conduct the series of shake table tests. A brief summary of the testing objectives of each test phase is included in the last section.

2.1 Description of Test Structure

The test structure considered in the NEESWood benchmark testing is one of the four index buildings designed within the recently completed CUREE-Caltech Woodframe Project [1]. It represents one unit of a two-story townhouse containing three units, having approximately 1800 ft² of living space with an attached two-car garage, as shown in Figure 2.1. This building is assumed to have been built as a “production house” in either the 1980’s or 1990’s, located in either Northern or Southern California. The design is based on engineered construction according to the seismic provisions of the 1988 edition of the Uniform Building Code [2]. The height of the townhouse from the first floor slab to the roof eaves is 18 ft and its total weight is approximately 80 kips (40 tons).

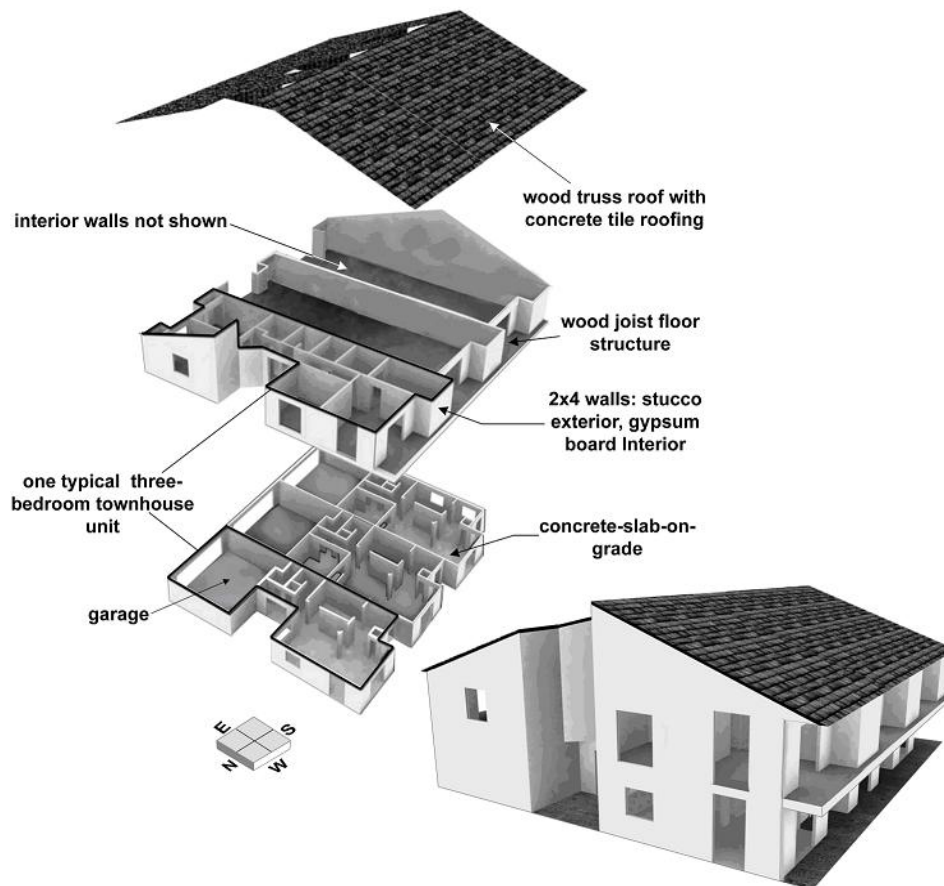


Figure 2.1: Illustration of two-story townhouse containing three units

The exterior walls of the townhouse test building were covered on the outside with 7/8 in. thick stucco over 7/16 in. thick OSB sheathed shear walls and 1/2 in. thick gypsum wallboard on the inside. Details regarding the two-story townhouse building are given by Reitherman et al. [1]. The floor plans of the test building are shown in Figure 2.2. Similarly, Figure 2.3 shows elevations of the test building. The architectural and structural plans for the final configuration (Phase 5) of the test structure are shown in Appendix A. The structural details of all shear walls in the buildings are included in Appendix B.

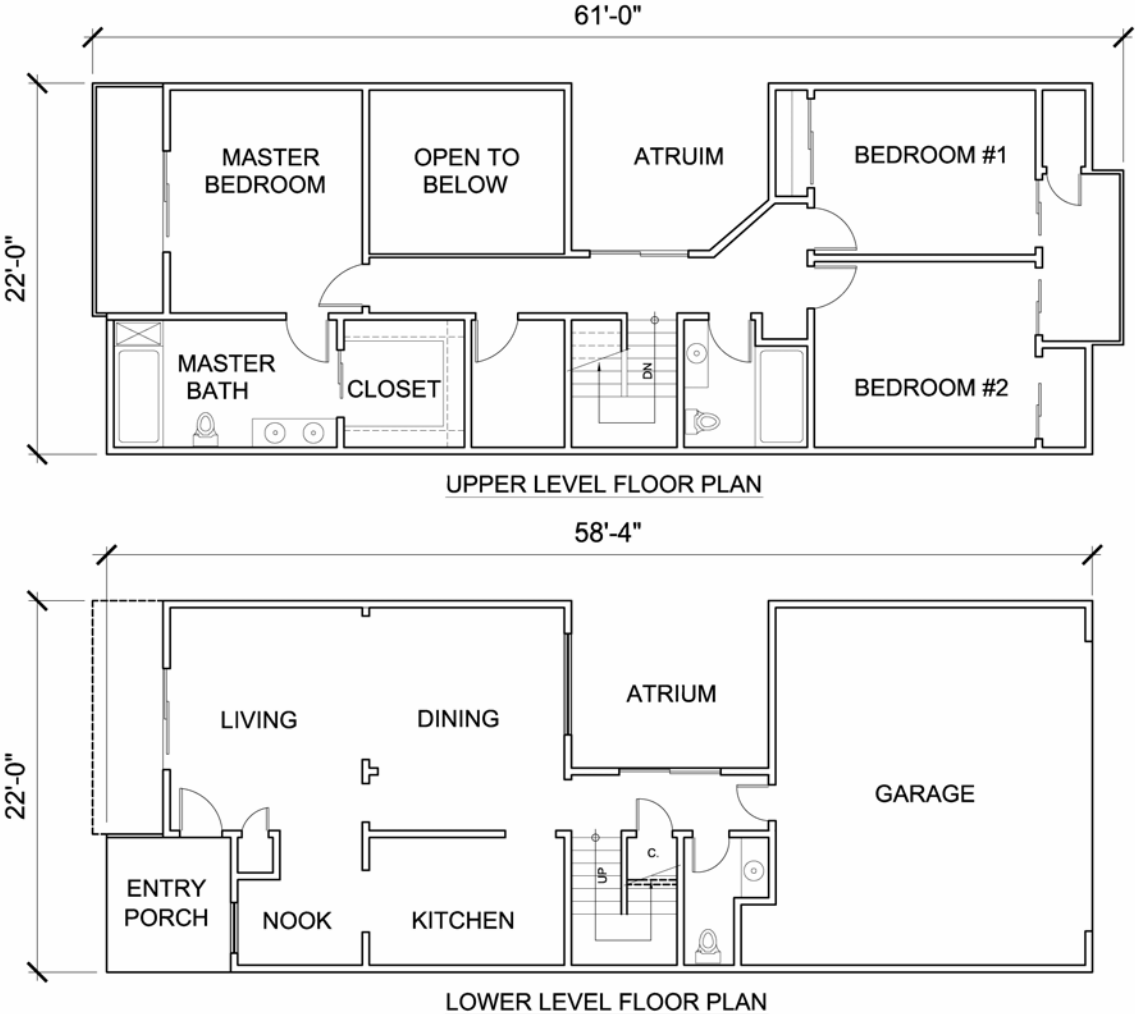


Figure 2.2: Floor plans of test building



Figure 2.3: Elevations of test building

All framing materials for the shear walls of the test building are 2x4 dimensional lumber except for the first level of the garage where 2x6 dimensional lumber is used. The top plates and end studs consist of double members, while the sole plate and the interior studs are single members. Studs are spaced at 16 in. on center. Conventional corner hold-downs are used to prevent overturning of the walls and to ensure a racking mode of deformation. The sheathing panels are 7/16 in. thick oriented strand board (OSB) installed vertically. The sheathing-to-framing connectors are pneumatically driven 8d common nails.

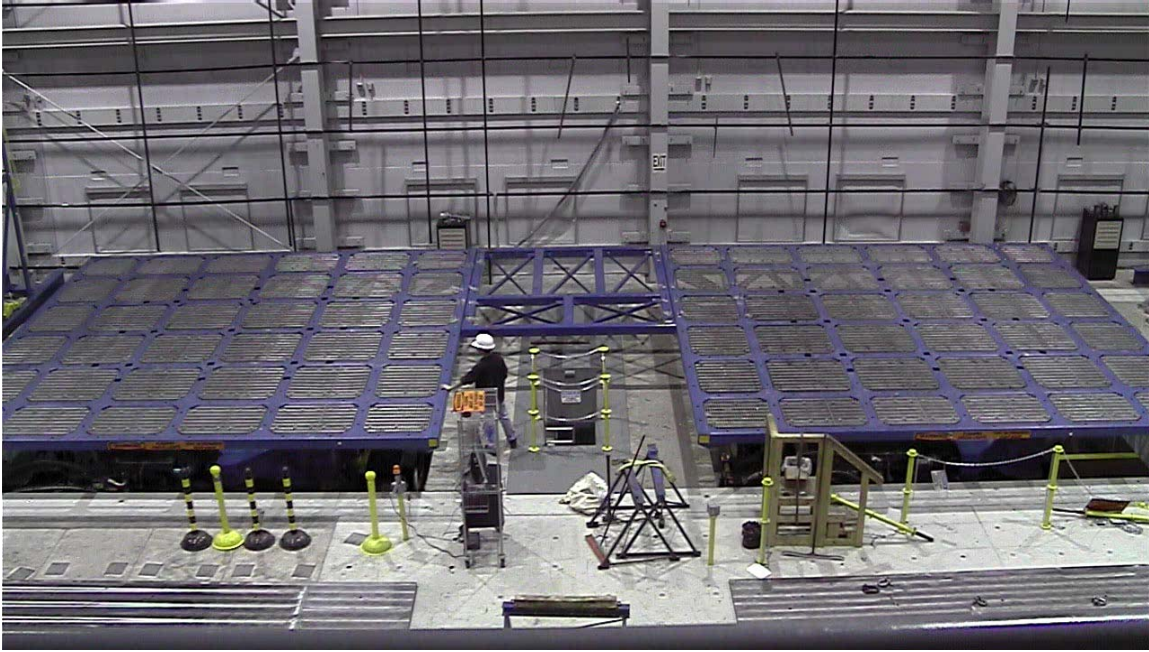
2.2 Experimental Set-up

The twin re-locatable, 50-ton, tri-axial shake tables of the Structural Engineering and Earthquake Simulation Laboratory (SEESL) at the University at Buffalo (UB) were utilized for the NEESWood benchmark experiment. Details about the earthquake-simulator characteristics can be found online at <http://nees.buffalo.edu/>.

The two tables acting in unison were required to accommodate the weight of the full-scale test building. As shown in Figure 2.4a, the 23 ft x 23 ft extension steel frames available on both of the UB-SEESL shake tables were connected together by a steel link structure to support the entire woodframe structure across the two shake tables with minimal vertical deflection. Figure 2.4b shows a photograph taken during the construction of the foundation of the test building on the two shake tables and link structure.

Threaded A-307 steel rods bolted to the existing hole pattern of the extension frame were used as anchor bolts for the sill plates, as shown in Figure 2.5a. Note that 2- $\frac{1}{4}$ in. x 2- $\frac{1}{4}$ in. x $\frac{1}{4}$ in. thick steel plate washers were installed at each anchor bolt location. At the locations of hold-down devices, $\frac{5}{8}$ in. diameter rods were used, while $\frac{1}{2}$ in. diameter rods were used at other locations. A 2- $\frac{1}{4}$ in. thick layer of grout was installed on top of the steel base beneath the pressure treated sill plates to represent a foundation, as shown in Figure 2.5b. The friction of the sill plate against the grout was similar to that of a true concrete foundation. The locations of the anchor bolts around the perimeter of the test building are given in Appendix A.

(a)

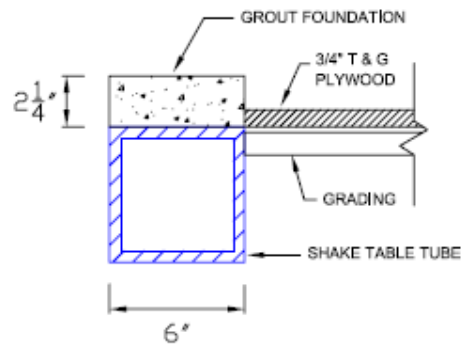


(b)



Figure 2.4: (a) Extension frame of shake tables connected by steel link structure, and (b) Foundation of Test Building under Construction

(a)



(b)



Figure 2.5: Foundation details, a) schematic, b) photograph

2.3 Testing Objectives

The objectives of the shake table testing of the NEESWood benchmark building were quite extensive and were intended to provide data for use in other tasks of the NEESWood Project (e.g., development of numerical tools, integration of results from other component tests, recommendations for code changes, determination of important parameters for performance-

based seismic design. etc.). To maximize the information that was gathered and learned, multiple tests were conducted at various stages of construction of the test building.

Conducting tests at different stages of construction allowed data to be collected on many specific building configurations. Table 2.1 presents a summary list of the test phases and the corresponding test structure configurations. Comparison of the building’s response in each of these different configurations was used to establish variations in fundamental period and damping values, determine stiffness variations for different configurations of wall finish materials and evaluate the performance of passive supplemental damping systems on the overall response of the structure. At the end of each stage of testing, damage to structural components and connections were visually inspected and recorded. Necessary repairs were made between test stages to return the structural components to their original strength and stiffness. In addition, the performance of finish materials, such as gypsum wallboard and exterior cement stucco, was visually inspected and documented. Damage observations were correlated with the force and deflection measurements of the building during those tests.

Table 2.1: Summary of test phases and building configurations

Test Phase	Test Building Configuration
1	Wood structural elements only
2	Test Phase 1 structure with passive fluid dampers incorporated into selected wood shear walls
3	Test Phase 1 structure with 1/2 in. thick gypsum wallboard installed with #6-1-1/4 in. long screws @ 16 in. O.C. on structural (load bearing) walls
4	Test Phase 3 structure with 1/2 in. thick gypsum wallboard installed with #6-1-1/4 in. mm long screws on all walls (16 in. O.C.) and ceilings (12 in. O.C.)
5	Test Phase 4 structure with 7/8 in. thick stucco installed with 16 gage steel wire mesh and 1-1/2 in. long leg staples @ 6 in. O.C. on all exterior walls

A detailed description of each of the test phases listed in Table 2.1 is provided in the next chapter. The primary objective of this shake table testing was to measure and quantify the building's overall dynamic characteristics and its component responses for various construction configurations, and to document how the distribution of forces within the structure changed between the various configurations. However, another fundamental objective was to establish relationships between ground motion severity, deflections, damage, and to provide data for defining realistic performance objectives. The data collected from the tests could then be used in the development of analytical models for complete full-scale buildings and for the prediction of damage states and failure modes. The shake table test results also provide a basis for calibration of the NEESWood Project's other individual component test results and their integration into numerical models.

Chapter 3 Description of Shake Table Tests

This chapter describes the two types of shake table tests that were performed on the test structure; that is system identification and seismic tests. The characteristics of the input motions that were used for each type of tests are reported, along with information on the recording and filtering of acquired data. In addition, a detailed description of the configuration of the structure during each of the five test phases is provided. Any repairs of the structural components that took place between or during each phase are also described.

3.1 Testing Sequences

3.1.1 System Identification Tests

The main objective of the system identification tests was to identify the dynamic characteristics of the test structure such as natural frequencies, associated mode shapes and modal damping ratios. White noise tests were considered to be adequate to effectively capture the properties mentioned above. The input excitation was an acceleration-controlled flat random noise with a frequency band between 0.5-50 Hz. The Root Mean Square (RMS) amplitude of the acceleration signal was selected to be either 0.05 g or 0.10 g and the duration of each test was 3 minutes. The sampling rate of the recorded data was 256 Hz. No additional filtering was applied to the data other than the embedded analog and anti-aliasing filters of the data acquisition system with a corner frequency of 50 Hz.

Uni-axial white noise tests were conducted in each of the three principal directions of the test structure (east-west, north-south and vertical). Typically, white noise tests in the two horizontal directions were repeated between each seismic test of each phase, in order to capture any change in the dynamic properties of the structure due to degrading inelastic response. Appendix D contains the testing sequence followed in each phase, providing the amplitude and the direction of each white noise test performed. The nominal amplitude in Test Phases 3, 4 and 5 did not exceed 0.05 g.

3.1.2 Seismic Tests

The main objective of the seismic tests was to determine the performance of the test structure under several levels of seismic shaking intensity. The input motions used for the seismic shaking were selected based on Task 1.3.2 of the CUREe-Caltech Woodframe Project [3]. Two different

sets of tri-axial historical ground motions were used for the seismic tests: ordinary ground motions and near-field ground motions. Both sets were recorded during the 1994 Northridge Earthquake in California.

The first set of ground motions was Canoga Park (CP), recorded at Topanga Canyon (USC Station 90053) at a distance of 15.8 km from the fault rupture. The acceleration time-histories of the three components of the Canoga Park record are shown in Figure 3.1. These ordinary ground motions with an amplitude-scaling factor of 1.20 were considered to represent a Design Basis Earthquake (DBE) event with a 10% probability of exceedance in 50 years or a return period of 475 years [3]. The acceleration response spectra of the three unscaled components of the Canoga Park record for 5% damping are presented in Figure 3.3.

The second set of ground motions is Rinaldi (RN), recorded at Rinaldi Receiving Station (DWP Station 77) at a distance of 7.1 km from the fault rupture. The acceleration time-histories of the three components of Rinaldi record are presented in Figure 3.2. These near-field ground motions were considered to represent a Maximum Credible Earthquake (MCE) event with a 2% probability of exceedance in 50 years or a return period of 2475 years [3]. The acceleration response spectra of the three components of the Rinaldi record for 5% damping are presented in Figure 3.4.

The order of appearance of the three components of each earthquake record in Figures 3.1 and 3.2 is based on the direction each component was applied during the seismic tests. The first components (CP 106 and RN 318) were applied in the longitudinal (east-west) direction of the test structure, while the second components (CP 196 and RN 228) were applied in the transverse (north-south) direction. The third vertical components were applied in the vertical direction of the test structure.

In addition to the 10%/50 year and 2%/50 year hazard levels, the Canoga Park ground motions were scaled to produce three additional levels of 99.9%/50 years, 50%/50 years and 20%/50 years. These lower levels of intensity were used to determine the response of the test structure under more frequently occurring ground motions. The amplitude scaling factors and the resulting peak ground accelerations for each component are listed in Table 3.1 for all levels of seismic intensity.

Summarizing, there were up to five levels of seismic tests performed. The input ground motions for the first four levels were scaled versions of the Canoga Park record while the input motions for the fifth level was the Rinaldi record, both recorded during the 1994 Northridge Earthquake. Appendix D contains the testing sequence followed during each of the test phases, providing information on the level of shaking intensity and the direction of excitation for each seismic test. Detailed description of the seismic tests for each phase is provided in the following sections. It should be noted that there were no seismic tests conducted beyond Level 2 during Test Phase 1, 3 and 4. Data from the seismic tests were recorded at a sampling rate of 256 Hz. Other than the embedded analog and anti-aliasing filters of the data acquisition system, a digital lowpass filter with a cutoff frequency of 10 Hz was applied on the acquired data.

Table 3.1: Ground motions for seismic tests

Seismic Test Level	Ground Motions (Northridge 1994)	Hazard Level	Amplitude Scaling Factor	PGA (g)		
				East-West	North-South	Vertical
1	Canoga Park	99.9% / 50 years	0.12	0.04	0.05	0.06
2	Canoga Park	50.0% / 50 years	0.53	0.19	0.22	0.26
3	Canoga Park	20.0% / 50 years	0.86	0.31	0.36	0.42
4	Canoga Park	10.0% / 50 years	1.20	0.43	0.50	0.59
5	Rinaldi	2.0% / 50 years	1.00	0.47	0.84	0.85

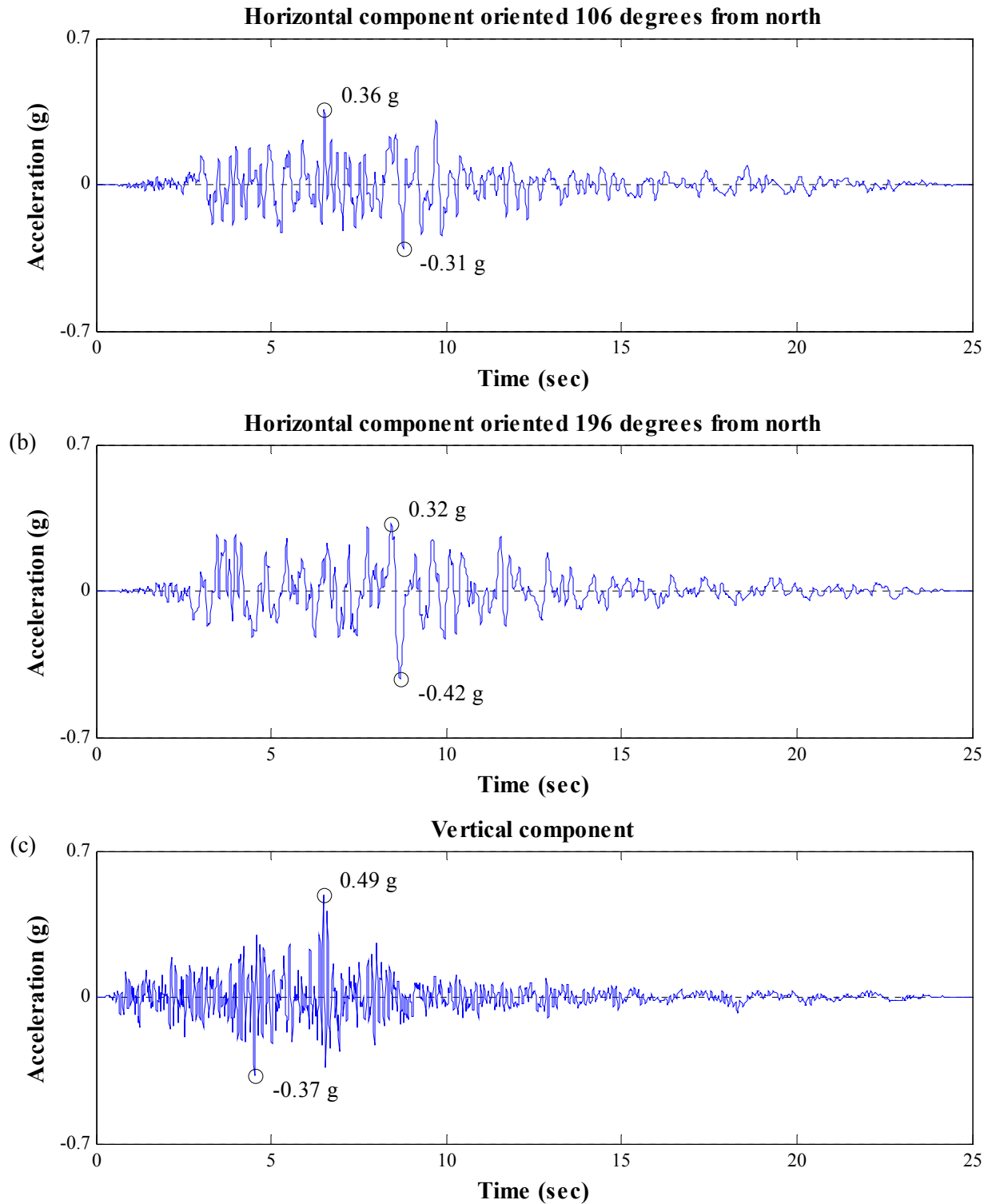


Figure 3.1: Acceleration time-histories of unscaled Canoga Park ground motions: (a) horizontal component at 106 degrees from north, (b) horizontal component at 196 degrees from north and (c) vertical component

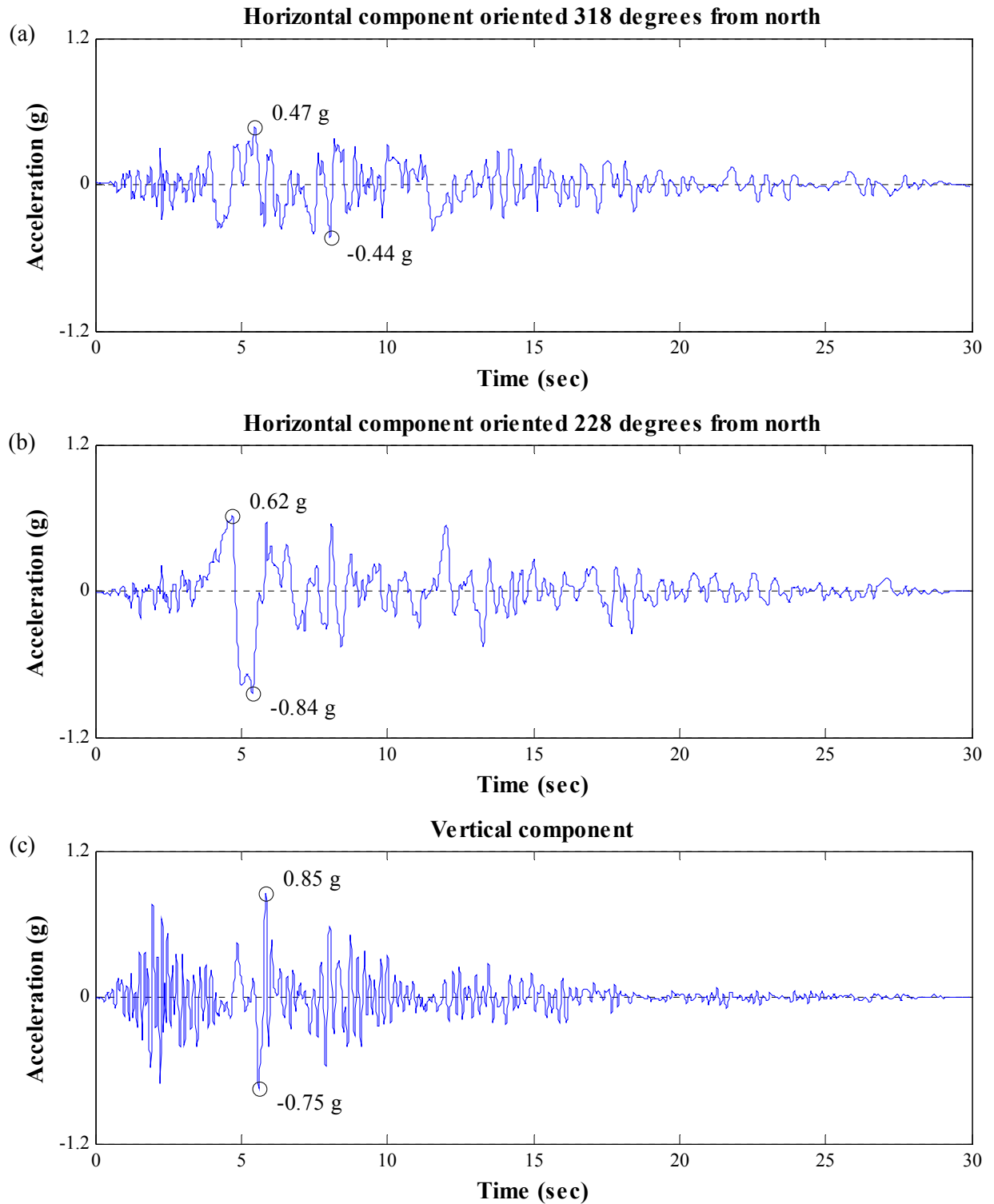


Figure 3.2: Acceleration time-histories of unscaled Rinaldi ground motions: (a) horizontal component at 318 degrees from north, (b) horizontal component at 228 degrees from north and (c) vertical component

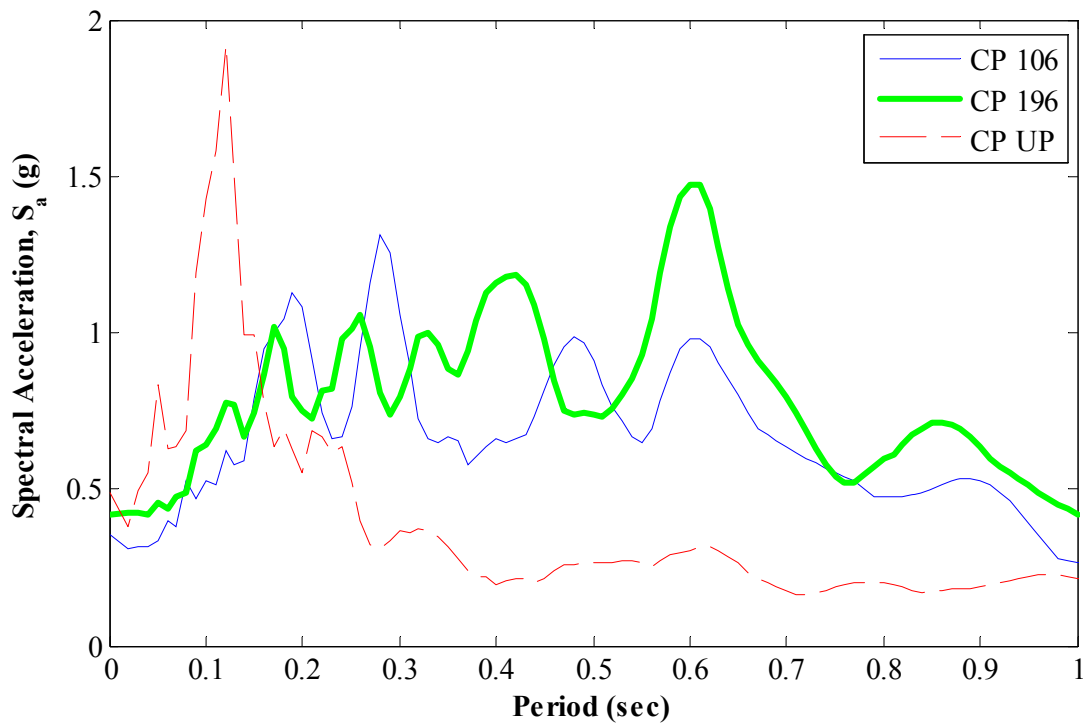


Figure 3.3: Acceleration response spectra of unscaled Canoga Park record for 5% damping

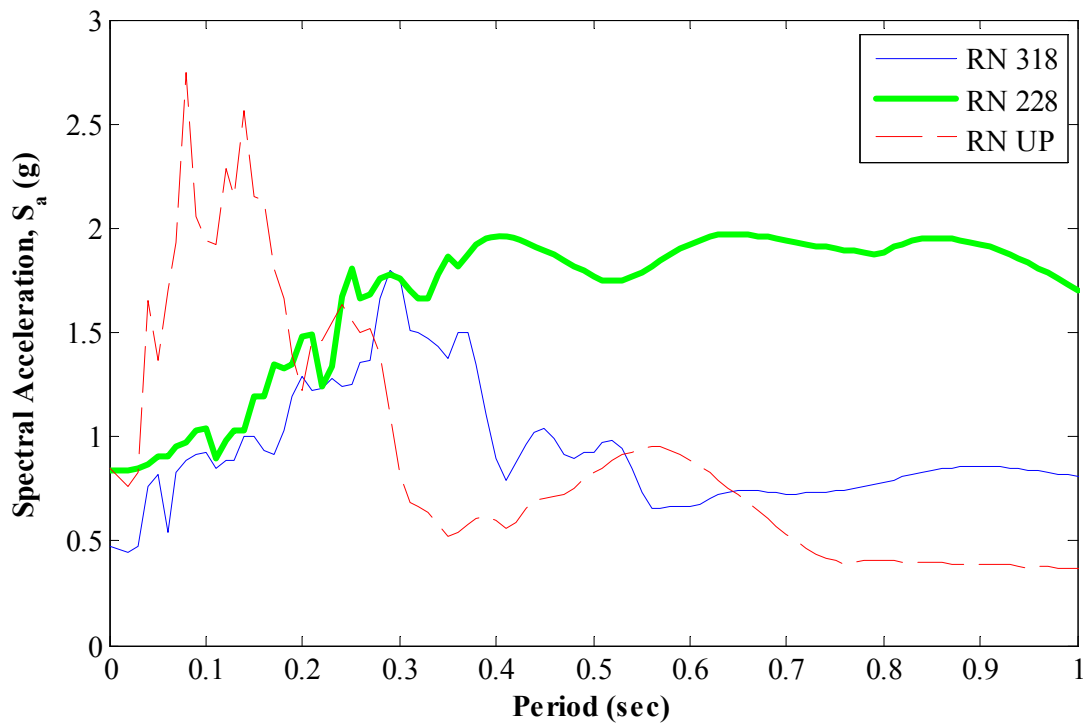


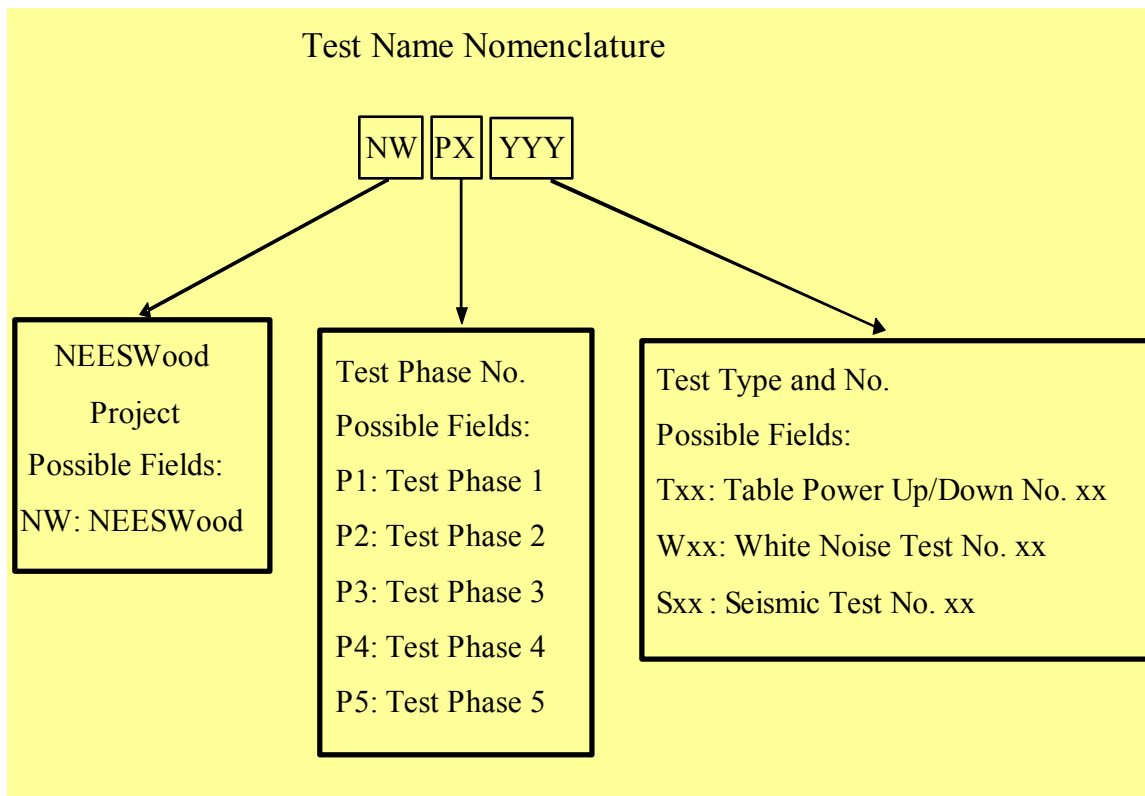
Figure 3.4: Acceleration response spectra of unscaled Rinaldi record for 5% damping

3.2 Nomenclature of Shake Table Tests

The nomenclature that was selected for the shake table tests that were conducted throughout the experimental phases is introduced and described in this section. A seven-character name was assigned to each test that was recorded by the data acquisition system. Table 3.2 lists the possible fields for each of the three parts that defined a unique name for each test.

The first two characters were the initials of the project name, which were always the same for all test names. The next two characters identified the Test Phase, part of which was the given shake table test. The last 3 characters identified the type of shake table test conducted. It should be noted that due to the size of the test structure and the complexity of the test setup, the tables' power up and down motions were recorded and were assigned test names as well.

Table 3.2: Nomenclature of shake table tests



3.3 Description of Test Phase 1

3.3.1 Description of Test Structure during Phase 1

The main objective of Test Phase 1 was to quantify the seismic behavior of the benchmark test structure when no wall finish materials were installed. The structure consisted only of the wood structural components; no additional materials such as gypsum wallboard or stucco were applied on the inner or outer surfaces of the wood shear walls. The shear walls and roof trusses were fabricated and donated by *Niagara Truss & Pallet LLC*, a local construction company, and were shipped to the University at Buffalo UB-NEES site. Appendix A contains the architectural and structural drawings of the test structure. All the drawings that are referenced in this section refer to the drawings of Appendix A unless differently stated. The shear wall framing members such as studs and top and sill plates were constructed of 2x4 Hem Fir lumber. Only the structural walls around the garage on the first floor were made of 2x6 studs and sill plates, as shown in Drawing S-13. Oriented Strand Board (OSB) sheathing panels of maximum size 4 ft x 8 ft and thickness 7/16 in. were nailed on the wood framing, made of studs spaced at 16 in. on center (O.C.), through 8d common nails. Table 3.3 presents information on the three nailing schedules that were followed in the construction of the shear walls. Sheathing edge nails were spaced at 3, 4 or 6 in. while field nails were typically spaced at 12 in.

Table 3.3: Nailing schedules used in the construction of the shear walls

Symbol	Allowable Shear (PLF)	Sheathing Material	Min. Stud at Adjoining Panel Edges	Sheathing Edge Nails	Sheathing Intermediate Nails	Anchor Bolts
{6}	260	7/16 in. OSB Sheathing	2x ↓	8d@6 in.	8d@12 in.	1/2 in. @48 in.
{4}	380			8d@4 in.	↓	1/2 in. @32 in.
{3}	490			8d@3 in.		1/2 in. @16 in.

Drawings S-7 and S-9 identify the nailing schedule for each shear wall on the first and the second floor, respectively. Appendix B contains the structural drawings of the wood shear walls and the roof trusses while Appendix C provides the actual as-built sheathing cutout and nail schedule of the shear walls, as observed on site after installation.

The floor joists were constructed of 2x12 Douglas Fir lumber spaced at 12 or 16 in. O.C., as shown in Drawing S-8 and illustrated in Figure 3.5. Roof trusses were constructed of SPF lumber and were spaced at 24 in. A photograph taken during the installation of the roof trusses on the structure is shown in Figure 3.6. The first floor shear wall sill plates were located on a 2-¼ in. thick concrete slab, which followed the perimeter of the building. The width of the concrete slab was 2 in. greater than the width of the sill plate. Drawings S-14 and S-15 present information related to the concrete slab.



Figure 3.5: Installation of floor joists during construction



Figure 3.6: Installation of the roof trusses of the benchmark structure

Holdowns ($5/8$ in. bolt diameter), as shown in Figure 3.7, and anchor bolts ($1/2$ in. bolt diameter) were used according to Drawing S-13 to anchor the sill plates to the concrete slab, while Strap-tie connectors were used to attach first and second floor walls, as identified in Drawing S-7.

The prefabricated walls were assembled on the twin shake table frames by *Hartland Builders*, a group of private contractors, who followed closely the structural notes as well as the sketches of detailed connections between structural members, which are illustrated in Drawings S-1 through S-5. All the exterior surfaces of the structure, including the inclined roof, and two interior shear walls in the north-south direction were fully sheathed with $7/16$ in. OSB panels. The roof tiles were installed by the UB-NEES staff after the construction of the structure. Figure 3.8 illustrates the structure at the end of the construction phase after the installation of the roof tiles.



Figure 3.7: PHD2 Strong-tie Holddown installed at the bottom corner of a shear wall



Figure 3.8: South-east view of the structure after installation of the roof tiles

3.3.2 Description of Test Phase 1 Protocol

Since the project consisted of five test phases, the magnitude of damage caused in early testing phases was a major concern. The intention was to repair the structural elements between each test phase, so that the structure could return to its initially identified mechanical properties. However, this might not be possible if excessive damage and large permanent deformations were observed due to inelastic response. For this reason, it was decided to specify an upper bound limit on the maximum allowed inter-story drift experienced by any structural wall, for Test Phases 1 through 4. This inter-story drift limit was set to 2%.

The test protocol that was followed during Test Phase 1 is listed in Table D.1 of Appendix D. For each of the first two seismic levels, four seismic tests were conducted. First, a tri-axial ground motion was used to simulate a real earthquake event. A bi-axial shaking followed, in the two horizontal directions, to assess the effect of the vertical component in the response of the structure. Two uni-axial seismic tests, in the longitudinal and transverse directions, completed the tetrad of tests for each level. Finally, a uni-axial Seismic Level 3 in the longitudinal direction was conducted.

No repairs took place between the seismic tests of Phase 1. However, during Test NWP1S05, there was a synchronization malfunction that led to unsynchronized motions of the twin shake tables. The test was promptly aborted, yet some of the anchor bolts located on the bridge structure failed in shear and were replaced.

3.4 Description of Test Phase 2

3.4.1 Description of Test Structure during Phase 2

Test Phase 2 was dedicated to the assessment of passive energy dissipation systems installed in light woodframe buildings. In particular, four fluid damping devices were installed in the longitudinal direction of the benchmark structure, as shown in Figure 3.9. This was the first application of fluid dampers on a full scale woodframe building. Therefore, one of the objectives of Test Phase 2 was to establish the feasibility of implementing such a seismic protection system within a full scale three-dimensional structure.

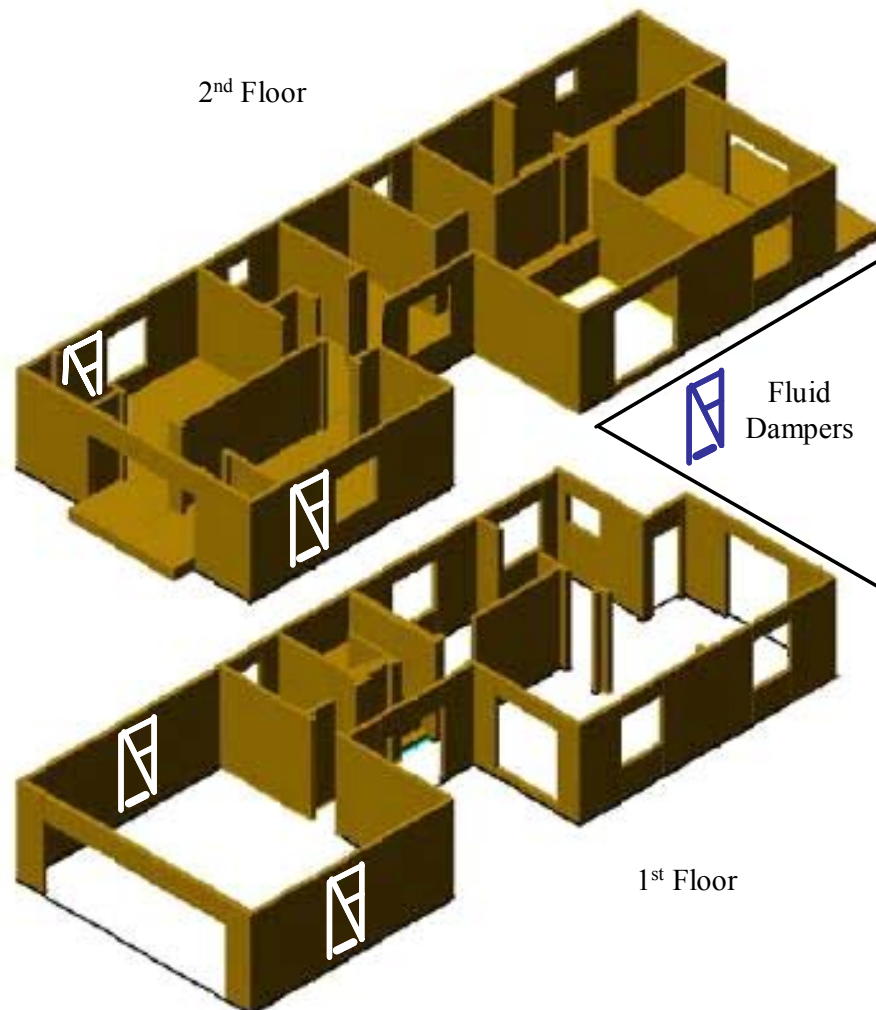


Figure 3.9: Location of fluid dampers on the structure

The viscous fluid dampers were manufactured and donated by *Taylor Devices Inc.* The dampers were nonlinear velocity-dependent devices. Therefore, the damper force \mathbf{F}_D was nonlinearly related to the velocity \mathbf{V}_D and was defined by the following equation:

$$\mathbf{F}_D = \mathbf{C} \cdot \text{sign}(\mathbf{V}_D) \cdot |\mathbf{V}_D|^\alpha \quad (3.1)$$

The dampers were designed based on the criteria of limiting the inter-story drifts to 2% for all seismic levels. The velocity exponent α and the damping coefficient \mathbf{C} were designed to be equal to 0.5 and 1.5 kips-(sec/in)^{0.5}, respectively. The maximum displacement stroke was ± 1.5 in. and the maximum force capacity was 7 kips. Each damping device was incorporated inside the wood shear wall at the desired location in the structure. Figure 3.10 shows the south damper-wall unit, installed at the garage of the benchmark structure.

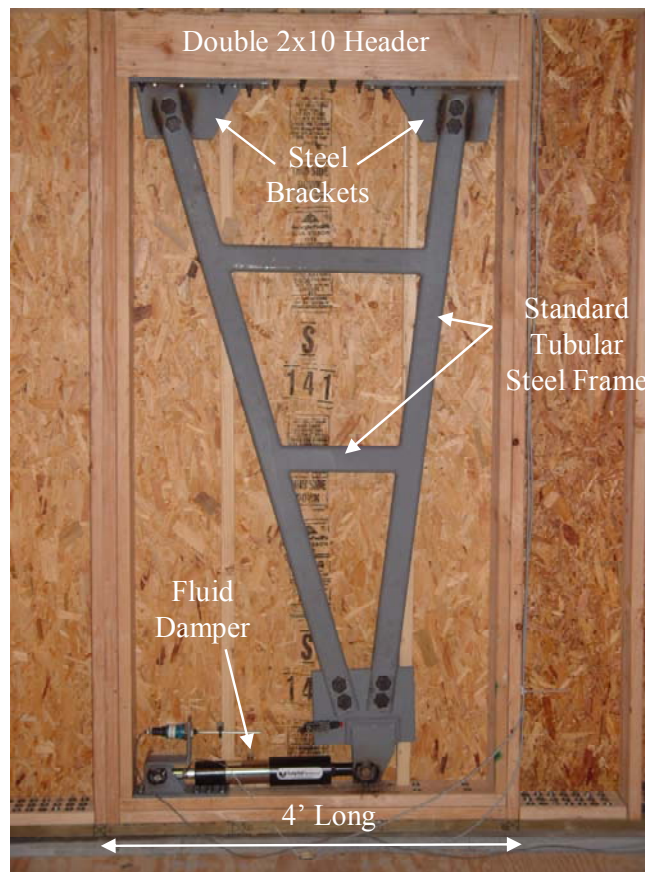


Figure 3.10: Damper-wall unit installed at the south side of the garage (view from inside)

The unit incorporated a stiff standard tubular steel frame, which transfers the relative drift from the top to the bottom of the wall. The frame was connected to a double 2x10 header at the top and to the damper at the bottom. Wood framing was provided around the perimeter. The width of each damper-wall unit was 4 ft to accommodate the standard width of wood sheathing panels.

The damper-wall units were designed and fabricated at Rensselaer Polytechnic Institute (RPI) and were shipped to the UB-NEES site for installation within the test structure. Since the structure was already built during Test Phase 1, the implementation of the damper-wall units required the unsheathing of the existing shear walls and the extraction of the studs and sill plates at the location of the dampers. Lag screws were used to connect the damper wall unit with the top and bottom plates and transfer the shear force. Additionally, epoxy was applied at the bottom sill plate for additional shear strength capacity. This can be regarded as a retrofit application.

Figure 3.11 shows the benchmark structure before the installation of the damper-wall units and after the extraction of sheathing and wood framing of the existing walls. Figure 3.12 shows the installed damper-wall units at the southwest side of the townhouse before the application of the sheathing panels. Two of the wood shear walls of the benchmark structure were repaired before the beginning of Test Phase 2. These were the interior structural walls, I-1 and I-27 as identified in Appendix B, which were located at the first floor and oriented in the north-south direction. OSB Sheathing panels were replaced for both of the walls, except for the small sheathing pieces around the interior door. One damaged stud was also replaced from Wall I-27.

3.4.2 Description of Test Phase 2 Protocol

The test protocol that was followed during Test Phase 2 is listed in Table D.2 of Appendix D. The seismic tests during this phase were conducted only in the longitudinal and vertical direction

of the structure. For each seismic test level, two seismic tests were conducted. First, a bi-axial ground motion in the two directions mentioned above was applied, followed by a uni-axial shaking in the longitudinal direction to assess the effect of the vertical component on the response of the structure. The testing sequence was repeated twice, each time applying a retrofit scheme to increase the effectiveness of the damping system by attempting to increase the rigidity of the wall-to-framing connections. This would lead to engagement of the damping devices at smaller wall displacements. Bi-axial tests were conducted up to Seismic Level 4. During the last test, the structure was subjected to a uni-axial Seismic Level 5 input motion. After the completion of that test, the dampers were disconnected, by releasing the oil pressure in the devices, and three uni-axial seismic tests (Level 3 through Level 5) were performed to directly compare the response of the “bare” structure with that of the structure containing the damper-wall units.



Figure 3.11: The benchmark structure before the installation of the damper-wall units



Figure 3.12: Installation of the damper-wall units on the south-west side of the structure

3.5 Description of Test Phase 3

3.5.1 Description of Test Structure during Phase 3

The main objective of Test Phase 3 was to assess the effect of interior wall finishes on the seismic performance of the benchmark structure. Following Test Phases 1 and 2, when the structure consisted only of the wood shear walls, gypsum wallboard was installed on the interior surface of the exterior perimeter walls, as well as on both sides of the two interior structural shear walls, located on the first level in the north-south direction. The intention was to evaluate the effect of gypsum wallboard applied only on the structural walls of the structure, which are structurally connected to adjacent roof and floor diaphragms.

Gypsum wall panels, 1/2 in. thick, were fastened on the studs of the shear walls using #6x1-1/4 in. long screws at 16 in. O.C., as shown in Figure 3.13.



Figure 3.13: Installation of gypsum wallboard on interior surface of a shear wall

Mudding and taping of the joints between the gypsum panels was appropriately applied, as shown in Figure 3.14. The wallboards were then sanded to smooth the mudded surfaces before painting. The installation of the gypsum wall finishes was performed by students from the Erie Community College (ECC) in Buffalo.

Before the application of the gypsum wall finishes, the damper-wall units that were tested in Phase 2 were removed. Studs and sheathing were installed at these locations according to the initial structural drawings. Two sheathing panels were also replaced on Wall E-10. The total width of those two panels was 48 in., so a full OSB sheathing panel was applied instead. The garage door, donated by *National Overhead Inc.*, was also installed before the execution of the Phase 3 shake table tests.



Figure 3.14: View of the interior wall finishes after mudding and taping

3.5.2 Description of Test Phase 3 Protocol

The test protocol that was followed during Test Phase 3 is listed in Table D.3 of Appendix D. Four seismic tests were conducted, two for each of the first two seismic test levels. First, a tri-axial ground motion was used to simulate a real earthquake event and, secondly, a bi-axial shaking followed, in the two horizontal directions, to assess the effect of the vertical component on the response of the structure. Note that seismic tests did not exceed Seismic Test Level 2, in order to limit the peak inter-story drift at any wall of the structure below the threshold value of 2%, as mentioned in Section 3.3.2.

3.6 Description of Test Phase 4

3.6.1 Description of Test Structure during Phase 4

Following a logical sequence in the seismic investigation of the benchmark structure, the next step was to evaluate the effect of gypsum wall finishes, applied on every wall of the townhouse as well as on the ceiling of the two floors. This would give the opportunity to compare the response of the structure between Test Phases 3 and 4 and explicitly assess the effect of interior wall finishes applied on structural and non-structural members. Gypsum wall panels, 1/2 in. thick, were fastened on the studs of interior partition walls using #6x1-1/4 in. long screws at 16 in. O.C., as shown in Figure 3.15. Gypsum wallboard of the same thickness was installed on the ceiling, as well, using the same screws, applied at 12 in. O.C., as shown in Figure 3.16. After completing the installation of the interior wall finishes, all interior surfaces were painted green to facilitate the observations of cracks in the gypsum. This concluded the preparations for Test Phase 4.



Figure 3.15: Installation of gypsum wallboard on an interior partition wall



Figure 3.16: Installation of gypsum wallboard on the ceiling of the 2nd floor

3.6.2 Description of Test Phase 4 Protocol

The test protocol that was followed during Test Phase 4 is listed in Table D.4 of Appendix D. The testing sequence was identical to the testing sequence of Test Phase 3. Four seismic tests were conducted, two for each of the first two seismic test levels. First, a tri-axial ground motion was performed, followed by a bi-axial shaking in the two horizontal directions.

3.7 Description of Test Phase 5

3.7.1 Description of Test Structure during Phase 5

The main objective of Test Phase 5 was to investigate the seismic effect of exterior wall finishes on the seismic response of the test structure. For this purpose, stucco was applied on the exterior surface of the townhouse. This concluded the additional construction phases of the test structure, which was at that point as would have been built in California in the 1980's or 1990's.

The stucco consisted of a mesh of wire lath (16 gauge steel wire mesh) and 3 coats of Portland cement-based plaster. First, vapor permeable, water-resistant tar paper was applied on the exterior surface of the structure (see Figure 3.17). The paper protected the sheathing and interior of the walls from outside moisture intrusion without trapping moisture vapor in the walls. Then, the wire mesh was attached to the exterior surface through 1-1/2 in. long leg staples, attached to the studs and spaced at 6 in. O.C. The first two coats of plaster were 3/8 in. thick each while the finish coat was 1/8 in. thick. Figures 3.18, 3.19 and 3.20 illustrate the exterior of the structure during application of the first, second and third coat, respectively, while Figure 3.21 shows the structure after the completion of this construction phase.



Figure 3.17: Installation of vapor permeable, water-resistant tar paper on the test structure



Figure 3.18: Application of the first coat of plaster on the test structure



Figure 3.19: Application of the second coat of plaster on the test structure



Figure 3.20: Application of the third coat of plaster on the test structure

Doors and windows were donated and installed by *Northeast Window and Door* in preparations for Phase 5 seismic tests.

3.7.2 Description of Test Phase 5 Protocol

The test protocol that was followed during Test Phase 5 is listed in Table D.5 of Appendix D. Two seismic tests were conducted for each of the first four seismic test levels. First, a tri-axial ground motion was used to simulate a real earthquake event and, thereafter, a bi-axial shaking followed, in the two horizontal directions, to assess the effect of the vertical component in the response of the structure. Test Phase 5 was the only phase that executed a tri-axial seismic test of Seismic Test Level 5. This was the last seismic test performed and was part of a Media Day that was held to conclude the UB-NEES benchmark testing series.



Figure 3.21: South-east external view of the benchmark structure after the installation of the exterior stucco finish

In preparations for this Media Day, the structure was fully furnished as if occupied by a 4-member family. Figures 3.22 through 3.28 illustrate the furnished rooms of the house. A car and two heaters full of water were placed in the garage, as shown in Figure 3.25. One of the heaters was anchored to the wall, while the other was not. Similarly, the library and the small table with the TV on top, which were located in bedroom #1 shown in Figure 3.27, were also anchored to the floor. Anchorage of all non-structural components was executed according to existing standards and guidelines ([4], [5], [6]).

3.8 Supplemental Weight Distribution and Total Weight of Test Structure

As a result of changes in wall finish materials throughout the test phases, supplemental weights were installed in the test structure to maintain a constant seismic weight of approximately 80 kips. The mass of the structure for Test Phase 5 was used as the reference mass because interior gypsum wallboard and exterior stucco were installed for this phase. Therefore, any supplemental weights installed in previous test phases were removed during Test Phase 5.

Appendix F contains all the information related to the supplemental weights for Test Phases 1 through 4. The weights were located on the 2nd floor level and were effectively anchored on the floor using straps. Various materials were used such as gypsum wallboards, concrete pavers, roof shingles and pavers to simulate the weight of wall finishes that were not installed at each particular phase. Figures F.1 to F.3 show the exact location and the total weight of each particular material used in each test phase.

Table F.1 presents the total tributary weight (self and supplemental) near the specific locations of the associated accelerometers, for each test phase (see Table E.1 and Figure E.1 of Appendix E or Figure 6.1 for accelerometers' nomenclature).



Figure 3.22: View of the dining room from the 2nd floor



Figure 3.23: View of the nook



Figure 3.24: View of the living room



Figure 3.25: View of the garage



Figure 3.26: View of the master bedroom



Figure 3.27: View of bedroom #1



Figure 3.28: View of bedroom #2

Chapter 4 Description of Instrumentation for Shake Table Tests

The benchmark structure was instrumented with approximately 230 instruments during the shake table tests. Various types of sensors were selected to measure accelerations, displacements and forces in the structure during identification and seismic testing. Appendix E contains information related to instrumentation. It provides a list of the type and number of sensors that were used in each test phase (Tables E.1 to E.8 of Appendix E), as well as comprehensive instrumentation plans of the locations of each specific instrument (Figures E.1 to E.8 of Appendix E). Descriptions and general locations of each type of instrument follow.

4.1 Types of Instrumentation for Shake Table Tests

4.1.1 Acceleration Measurements

More than 70 accelerometers were used to measure accelerations in the test structure during the shake table tests. Pairs of accelerometers, as shown in Figure 4.1, which measured accelerations along the two horizontal directions, were placed on each corner of each floor of the benchmark structure. This allowed monitoring the motion of all external sides and accurately extracting mode shapes from identification tests. Vertical accelerometers were also placed at the bottom of the first floor walls, at the corners of the test structure, as shown in Figure 4.2, to capture any uplifting or rocking motion of the walls. Accelerometers were placed at other locations as well, as illustrated in Figure E.1 of Appendix E.



Figure 4.1: Two accelerometers at the top of a first floor wall measuring accelerations in the two horizontal directions



Figure 4.2: Accelerometer at the bottom corner of the structure measuring acceleration in the vertical direction

4.1.2 Displacement Measurements

Twenty one linear string potentiometers were used to measure the absolute displacements of the shake tables and the benchmark structure with respect to a stationary reference system. The west and north sides of both the test structure and the shake tables were instrumented as shown in Figure E.2 of Appendix E to obtain absolute displacements in the two horizontal directions. String potentiometers were also installed on selected shear walls of the structure to determine the racking deformations of the sheathing panels (see Figure 4.3). The string potentiometers, oriented diagonally, measured the displacements between two points at the beginning and at the end of the wall, one located in the middle of the top plate and the other in the middle of the bottom plate. Some string pots that were connected also to the floor diaphragms to measure the true inter-story drift that can be compared to the racking deformation of the walls.



Figure 4.3: String potentiometer located on the top plate of a second floor shear wall

The locations of the diagonal string potentiometers during all testing phases are illustrated in Figures E.3 and E.4 of Appendix E.

Another type of displacement measuring devices used was the linear potentiometers. These instruments were calibrated for a small displacement range (of the order of 2 in.). Ten potentiometers were used to capture the sill plate slippage of shear walls around the perimeter of the structure with respect to the foundation (see Figure 4.4). Twenty six pairs of potentiometers were installed to measure the uplift displacement of the sill plate of selected walls with respect to the foundation, as well as the uplift displacement of the external stud with respect to the sill plate (see Figure 4.5). Instrumentation plans for the location of the potentiometers are provided in Figures E.5 and E.6 of Appendix E.

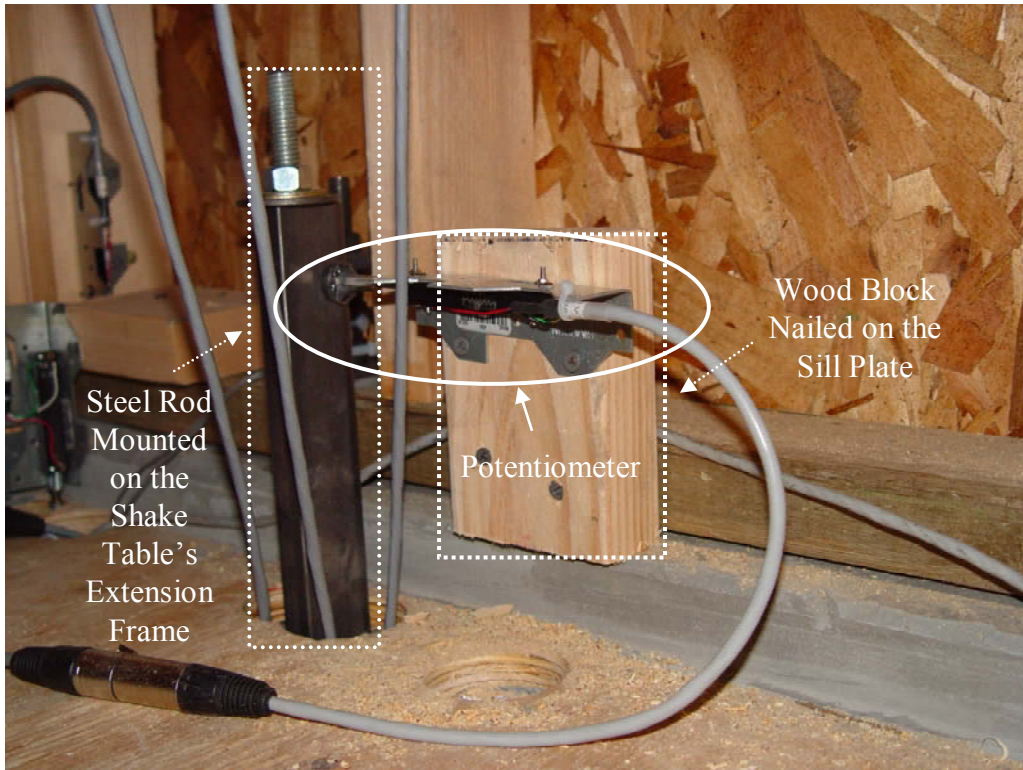


Figure 4.4: Potentiometer installed on the test structure to measure sill plate slippage

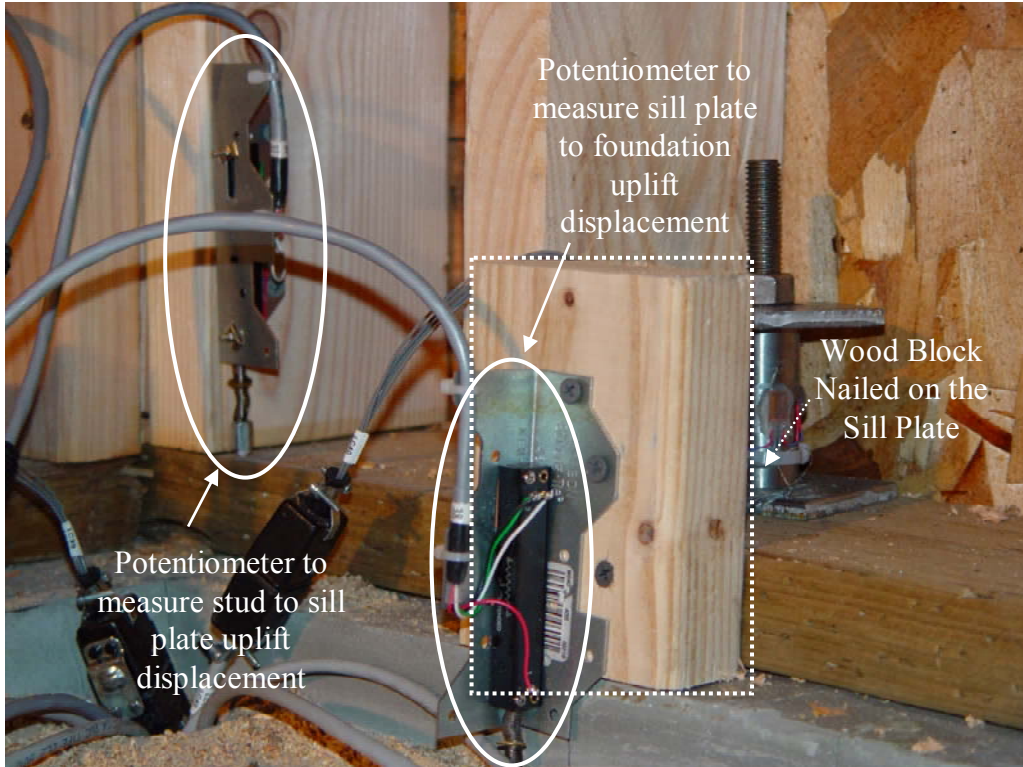


Figure 4.5: Two potentiometers installed on the test structure to measure uplift displacements of stud to sill plate and sill plate to foundation

4.1.3 Force Measurements

More than 50 load cells were used to measure tensile axial forces on the shear transfer anchor bolts and Holdown anchor bolts of the first floor shear walls. The load cells were made of a piece of a cylindrical steel pipe that had an inside diameter slightly larger than the diameter of the anchor bolt. Four strain gages (two in the direction of the axial force and two in the circumferential direction) were wired to form a full Wheatstone bridge that was sensitive to strains related to axial forces across the load cell. Figures 4.6 and 4.7 show two load cells installed in a Holdown and an anchor bolt of first floor walls, respectively. Figure E.7 of Appendix E illustrate the position of each load cell for all testing phases.

4.1.4 Additional Measurements

Apart from the devices described above and that were used throughout all testing phases, there were some additional instruments that were installed only during Test Phase 2. These were related to the 4 damper-wall units that were tested in that particular phase. As shown in Figure E.8 of Appendix E, a temposonic transducer and a load cell were utilized for each damper-wall unit to measure the displacements and the forces across the dampers.

In addition to the instrumentation devices installed on the test structure, data was also acquired through the embedded instruments that exist in the shake tables. Of particular interest were the Roll and Pitch rotations of each shake table, which are related to rotation with respect to the two horizontal axes. Thus, four additional measurements (2 rotation time-histories for each shake table) were added in the test datasheets.



Figure 4.6: Anchor bolt load cell measuring tensile axial force in a PHD5 Holddown



Figure 4.7: Load cell measuring tensile axial force in a shear transfer anchor bolt

4.2 Sign Convention and Instrumentation Summary

The sign convention was selected so that all measured data such as accelerations, displacements and forces were measured positive in the directions shown in Figure 4.8. These were towards the east and the north directions, for the horizontal components, and towards the sky, for the vertical components. The Roll and Pitch rotations of the shake tables were modified to yield positive displacements of floor diaphragms, per the sign convention defined above, for positive values of rotation of the shake tables, assuming the structure to be rigid.

Table 4.1 provides a summary of the type and total number of instruments that were recording data during each of the five test phases. A total number of approximately 230 sensors were used during the five different test phases, to effectively capture the detailed seismic response of the test structure.

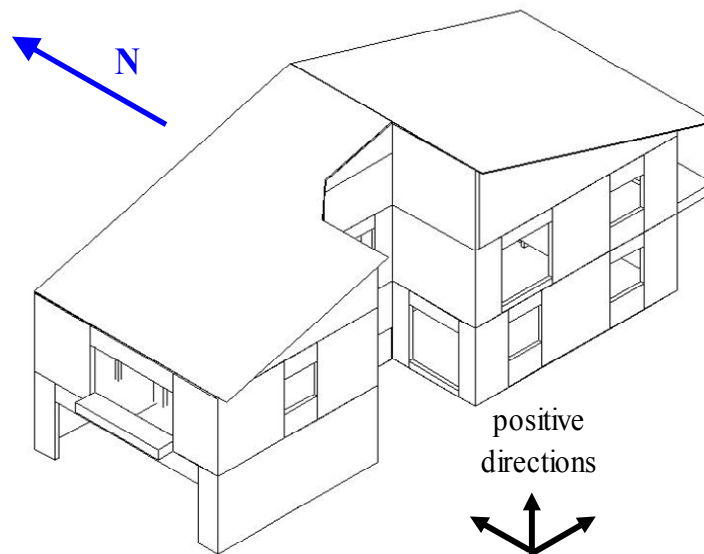


Figure 4.8: Positive directions of recorded data

Table 4.1: Summary of instrumentation devices for each test phase

Instrumentation Devices	Test Phase				
	1	2	3	4	5
Accelerometers	71	71	71	71	70
String Potentiometers - Absolute Displacements	21	21	21	21	21
String Potentiometers - Shear Deformations	23	17	19	21	21
Potentiometers - Sill Plate Slippage	10	10	10	10	10
Potentiometers - Sill Plate Uplift	52	52	52	52	52
Load Cells - Anchor Bolt Forces	53	50	54	57	57
Load Cells - Viscous Dampers	0	4	0	0	0
Temposonic Transducers - Viscous Dampers	0	4	0	0	0
Total Number of Channels	230	229	227	232	231

Chapter 5 Determination of Material Properties

This chapter focuses on the determination of the properties of the materials that were used in the construction of the NEESWood benchmark structure. More specifically, information is presented in three parts. The first part describes the moisture content readings in the wood members that took place before the execution of the experiments of Test Phase 1. The second part contains information related to the sheathing-to-framing connection tests that were conducted to determine the hysteretic properties of the specific nail connectors, sheathing type and thickness that were incorporated in the NEESWood benchmark structure. The final part describes how the compressive strength of exterior stucco wall finish was determined.

5.1 Moisture Content of Wood Shear Walls

The moisture content readings were conducted by Charles Ekiert, an REU (Research Experiences for Undergraduates) student, after the construction of the benchmark structure and before any test phase. It is noted that at that time, the test structure consisted only of the structural wood shear walls; no exterior or interior wall finishes were installed. The following text is taken from Ekiert's log book:

“On Thursday June 1, 2006 between 13:00 and 14:00 hour's moisture readings were measured using an EXTECH model 407777 heavy duty moisture meter. The moisture meter contained preset material setting, which was calibrated in the factory. The moisture meter was set to a material type two before any measurements were taken; which is the preset material number for Hem Fir.

The studs in each prefabricated wall were tested by picking any random three studs in the wall panel and measuring the moisture content in those studs. The three measurements were then averaged to determine the representative moisture content of the wall studs in each wall panel.

The top and sill plates in each prefabricated wall panel were also measured for the moisture content. The moisture content in both the sill and top plates were determined by taking moisture measurement at each end of the wall panel along with one measurement in the middle of the plate. The three measurements were then averaged to determine the representative moisture content for both the sill and top plates”.

Table 5.1 lists the averaged moisture content for each wall section of the benchmark structure. The wall sections that correspond to the wall numbers shown in Table 5.1 are identified in Appendix B.

Table 5.1: Moisture content readings for each wall section of the benchmark structure

1 st Floor	Moisture Content (%)			2 nd Floor	Moisture Content (%)		
Wall #	Sill plate	Studs	Top plate	Wall #	Sill plate	Studs	Top plate
E-1	11.7	11.9	11.7	E-17	12.4	11.5	11.6
E-2	13.0	12.1	11.5	E-18	11.2	11.5	11.5
E-4	13.9	11.6	12.3	E-19	12.1	11.5	11.3
E-5	12.5	12.4	11.3	E-20	11.5	11.4	11.3
E-6	12.8	10.9	11.7	E-21	12.7	11.5	12.9
E-7	11.4	11.6	11.0	E-22	11.2	11.6	12.4
E-8	12.0	11.7	11.6	E-23	11.1	11.4	11.2
E-9	14.3	11.8	11.7	E-24	11.1	10.5	11.3
E-10	13.3	11.9	11.3	E-25	11.2	11.0	11.1
E-11	13.7	11.4	12.3	E-26	11.5	11.5	11.2
E-12	16.9	12.7	13.0	E-27	11.9	11.5	11.3
E-13	12.5	11.4	12.5	E-28	11.3	11.4	11.4
E-16	12.6	11.8	11.4	E-29	11.3	12.1	9.7
E-35	13.7	11.6	13.5	E-30	11.9	11.2	10.9
E-36	12.1	11.5	11.6	E-31	11.5	11.3	13.2
E-37	11.9	12.0	12.4	E-32	11.2	11.7	11.2
I-1	12.7	11.7	10.8	E-33	11.7	11.3	11.4
I-2	12.9	13.1	12.4	I-9	11.7	11.2	11.6
I-5	13.1	11.4	12.3	I-10	11.3	12.2	11.9
I-6	12.9	11.3	11.3	I-11	12.1	11.8	12.8
I-27	12.7	11.8	11.6	I-12	11.9	11.4	11.5
I-28	12.8	11.6	12.0	I-13	11.9	11.3	11.9
Average	13.0	11.8	11.9	I-14	12.2	11.7	11.5
				I-15	12.5	11.0	11.3
				I-16	11.2	11.6	11.2
				I-17	12.6	12.3	11.8
				I-18	12.2	11.4	14.0
				I-19	11.6	11.7	11.5
				I-20	11.4	12.1	11.5
				I-21	11.4	11.2	11.5
				I-22	13.0	11.4	11.8
				I-23	11.8	11.2	11.5
				E-34	11.0	11.6	11.2
				Average	11.7	11.5	11.6

The average moisture content was rather constant throughout the walls of the structure, ranging between 11.5% and 13.0%. Slightly higher values were measured for the 1st floor prefabricated walls. The moisture content measured corresponded to dry conditions ($M.C. \leq 19\%$) and certified the “healthy” condition of the wood structural members.

5.2 Hysteretic Properties of Sheathing-to-Framing Connections

Connection tests of sheathing-to-framing assemblies were performed to determine the hysteretic properties of the connections for use in analytical modeling. The connection tests were conducted by two REU students, Charles Ekiert and Jamie Hong, and the results have been reported in [7].

5.2.1 Testing Configurations

The assemblies were constructed of the same materials that were used in the benchmark structure. Thus, the specimens consisted of Oriented Strand Board (OSB) sheathing panels, 7/16 in. thick, nailed on 2x4 or 2x6 Hem Fir lumber framing through 8d common nails of length and diameter of 2-1/2 in. and 0.113 in., respectively. Details on the dimensions of the specimens are presented in the next sections.

Two different test configurations were used; in the first configuration the specimens were loaded in such a way to produce nail deformation parallel to the grain of the framing lumber, while in the second configuration the nail deformations were imposed along a direction perpendicular to the grain of the framing lumber. A total number of thirteen specimens were built for each test configuration. Table 5.2 shows all the different configurations of the connections tests.

Table 5.2: Connection test configurations

Loading Direction Relative to Grain	Sheathing	Framing	Nailing	No. of Specimens
Parallel	7/16 in. OSB	2x4 Hem Fir	8d Common Nails	13
Parallel		2x6 Hem Fir		
Perpendicular		2x4 Hem Fir		
Perpendicular		2x6 Hem Fir		

5.2.2 Loading Protocol

For each test configuration, four displacement-controlled monotonic tests were conducted up to failure of the test samples. The displacement Δ , defined as 60% of the displacement occurring at 80% of the maximum recorded load after strength degradation in the test specimen, was averaged among the monotonic tests and was used to define the reference amplitude of the Simplified Cyclic Loading Protocol, which had been developed under Task 1.3.2 of the CUREE-Caltech Woodframe Project [3].

Figure 5.1 shows the displacement protocol as a fraction of Δ . The simplified loading history starts with six cycles of 0.05Δ . The initial cycles are followed by seven primary cycles of 0.075Δ and 0.1Δ . Next, the number of primary cycles is reduced to four of amplitude 0.2Δ and 0.3Δ . Finally the number of primary cycles is reduced to three cycles of amplitude 0.4Δ , 0.7Δ , 1.0Δ , and 2.0Δ . The loading rate of testing was 0.2 cycles per second

5.2.3 Testing Apparatus and Test Specimens

A testing apparatus was designed and constructed for both parallel and perpendicular to grain testing. The apparatus was designed so that the samples could be easily placed and removed during the testing and was constructed from 1/4 in. A36 plate steel, as well as 1-1/4 in. and 3/4 in.

cold rolled dowel steel. The apparatus was designed with three main components, two of which were used for testing samples parallel to grain (upper and lower main connectors) and another piece that can be placed on the lower main connector piece to test perpendicular to grain.

The specimens that were prepared for testing parallel to grain consisted of two 5 in. x 10 in. pieces of sheathing connected to two 10-¼ in. long pieces of framing, as shown in Figure 5.2. The top half of each piece of sheathing was nailed to the top piece of lumber with two common nails. The bottom half of each piece of sheathing was fastened to the bottom piece of lumber with two common nails and one screw along with epoxy to produce a fixed condition. This enabled only the top four nails to deform under an imposed longitudinal displacement. The two pieces of framing were then placed in the top and bottom steel components and bolted in place using four ¾ in. pins.

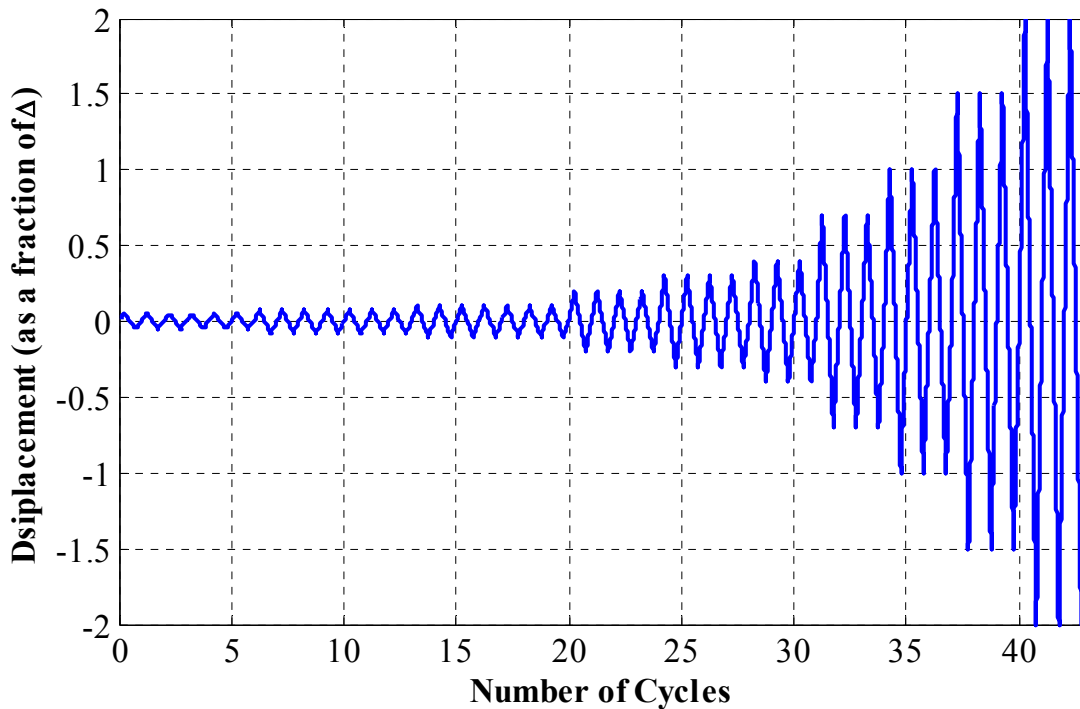


Figure 5.1: CUREe-Caltech Woodframe Project Simplified Cyclic Testing Protocol [3]

The specimens prepared for testing perpendicular to grain consisted of two 11 in. x 11-½ in. pieces of sheathing connected to an 11 in. long piece of framing with two common nails, as shown in Figure 5.2. The additional connector piece was placed over the lower main connector and was bolted into place using four ¾ in. pins. Spacers were also used in order to keep the apparatus centered. The specimens were bolted into place using two ¾ in. pins and spacers to keep the OSB centered and perpendicular to the wood framing, thereby preventing any in-plane rotation.

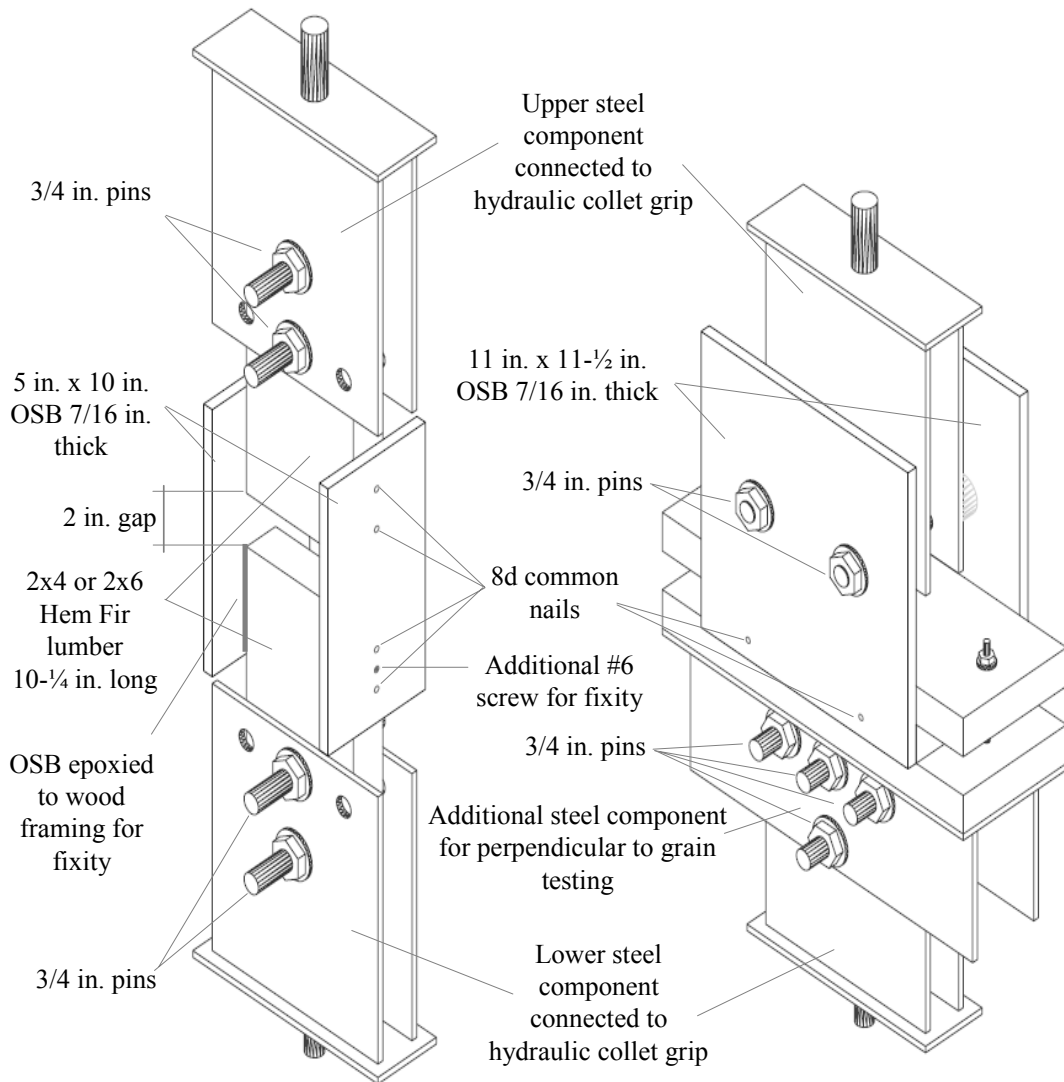


Figure 5.2: Test apparatus and specimen dimensions for testing parallel to grain (left) and perpendicular to grain (right)

5.2.4 Test Machine and Instrumentation

The testing machine used for all of the monotonic and cyclic tests was manufactured in 1984 by MTS Systems Corporation. The testing machine consists of a load frame, two hydraulic collet grips and a micro console, which are shown in Figure 5.3. The model numbers of the load frame, hydraulic collet grip and micro console are 309.40, 646.25A, and 458.10 respectively. The load frame has a capacity of 110 kips and each hydraulic collet grip has a capacity of 55 kips.

The load cell that was used in all tests was manufactured by Transducer Techniques (model number SWO-10K) with a capacity of 10 kips. The displacements were measured using two ± 2 in. linear potentiometers. Both sensors are shown in Figure 5.4.



Figure 5.3: MTS micro console (left) and MTS hydraulic collet grip (right)

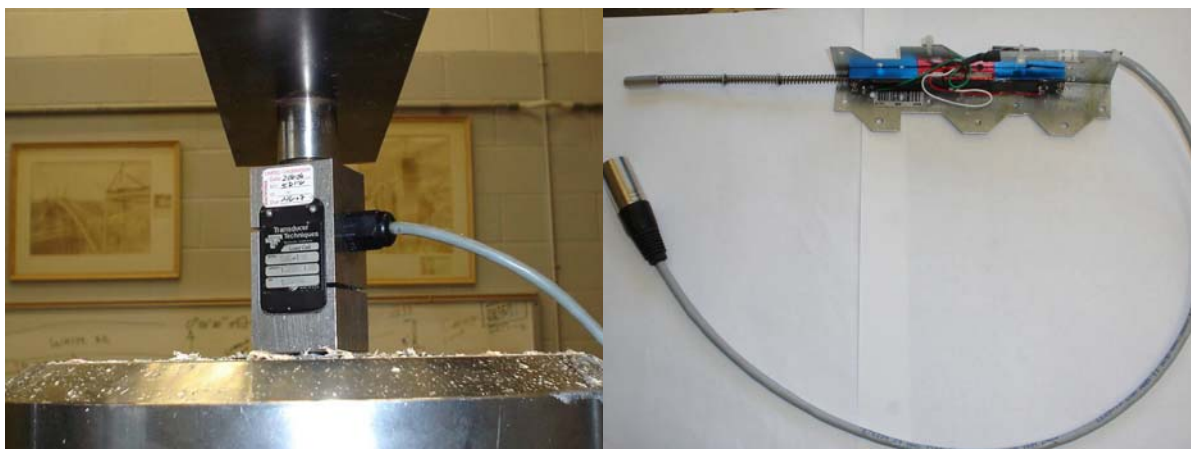


Figure 5.4: 10 kip load cell (left) and ± 2 in. linear potentiometer (right)

Figures 5.5 and 5.6 show the connection test setup during parallel and perpendicular to grain testing, respectively.



Figure 5.5: Parallel to grain connection test setup with 2x4 framing

Note that the potentiometers were installed directly on the specimen in order to measure the slip of the connection without the supplemental displacement caused by slipping of other connecting points.

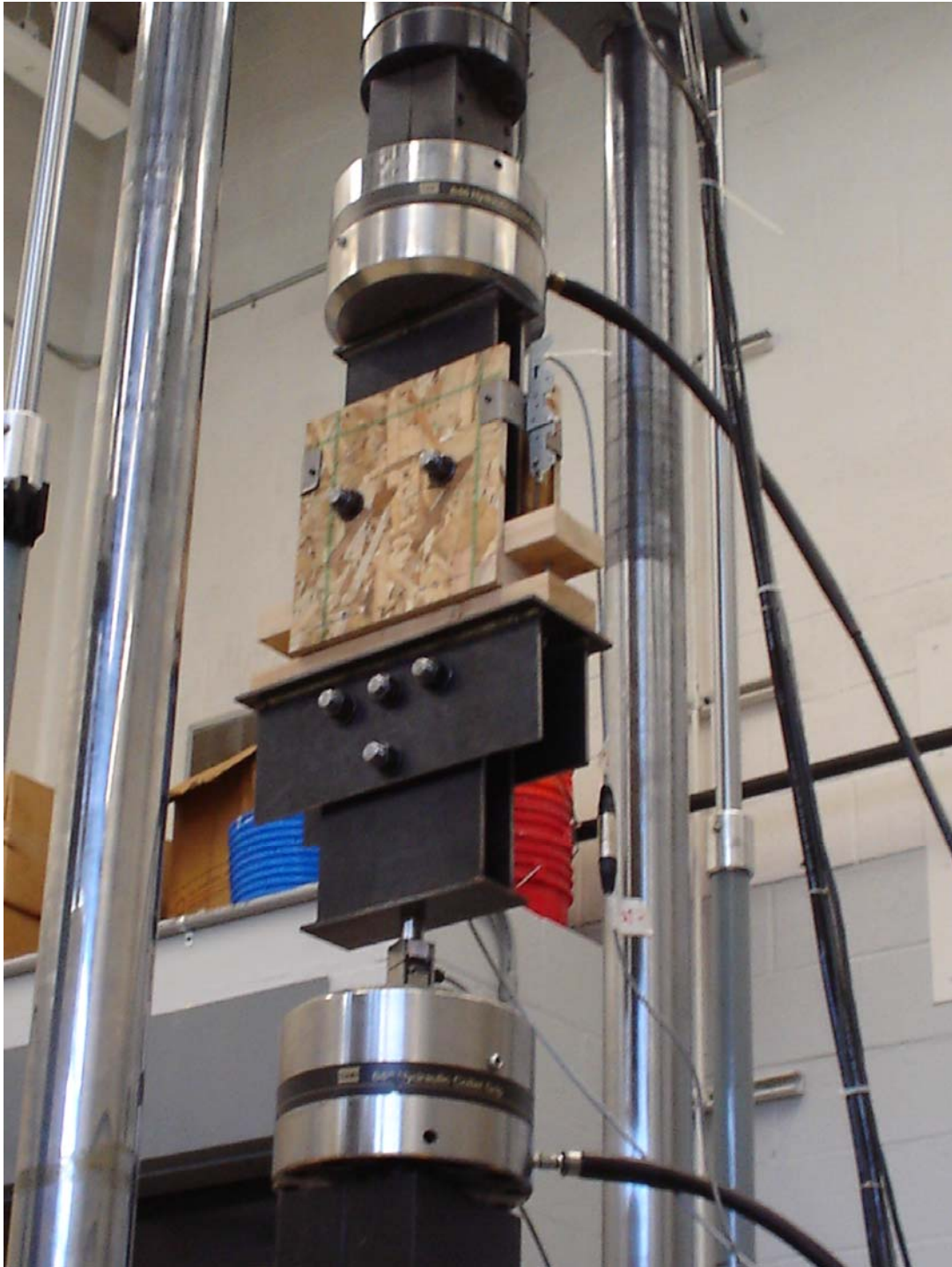


Figure 5.6: Perpendicular to grain connection test setup with 2x4 framing

5.2.5 Test Results and Parameter Identification

Appendix G shows plots of load versus deformation for the monotonic tests and load-deformation hysteresis loops for the cyclic tests of the sheathing-to-framing connection specimens. Tables 5.3 through 5.6 show the variability in the peak load and the corresponding deformation, for one nail connector, for each of the connection tests.

Table 5.3: Peak load and deformation at peak load for 2x4 parallel to grain connection tests

Loading	Specimen	Direction	Peak Load (lb)	Deformation at Peak Load (in)
Monotonic	1	N/A	217	0.11
	2	N/A	279	0.18
	3	N/A	363	0.63
	4	N/A	344	1.00
Cyclic	1	Positive	328	0.58
	1	Negative	-365	-0.49
	2	Positive	391	0.41
	2	Negative	-375	-0.36
	3	Positive	309	0.51
	3	Negative	-387	-0.50
	4	Positive	340	0.46
	4	Negative	-348	-0.38
	5	Positive	280	0.29
	5	Negative	-206	-0.67
	6	Positive	322	0.37
	6	Negative	-307	-0.29
	7	Positive	298	0.58
	7	Negative	-295	-0.43
	8	Positive	197	0.16
	8	Negative	-215	-0.33
	9	Positive	139	0.15
	9	Negative	-157	-0.15

Table 5.4: Peak load and deformation at peak load for 2x4 perpendicular to grain connection tests

Loading	Specimen	Direction	Peak Load (lb)	Deformation at Peak Load (in)
Monotonic	1	N/A	294	0.41
	2	N/A	285	0.42
	3	N/A	305	0.32
Cyclic	1	Positive	328	0.58
	1	Negative	-330	-0.43
	2	Positive	303	0.64
	2	Negative	-344	-0.40
	3	Positive	301	0.62
	3	Negative	-309	-0.41
	4	Positive	341	0.61
	4	Negative	-363	-0.39
	5	Positive	311	0.59
	5	Negative	-331	-0.62
	6	Positive	269	0.29
	6	Negative	-338	-0.61
	7	Positive	355	0.64
	7	Negative	-358	-0.61
	8	Positive	285	0.29
	8	Negative	-286	-0.24
	9	Positive	325	0.42
	9	Negative	-289	-0.61
	10	Positive	304	0.42
	10	Negative	-290	-0.39

The results presented in Tables 5.3 through 5.6 are summarized and plotted in Figure 5.7. The variability is quite high for both forces and displacements, but seems to be more pronounced for

the displacement at which the maximum load occurs. Lower load capacities are observed for the specimens tested parallel to grain compared to those tested perpendicular to grain.

A set of MATLAB routines was developed by Weichiang Pang [8], a post-doctoral research associate at Texas A&M University, to derive the optimal hysteretic parameters to be used with the SAWS hysteretic model described in [9]. The parameters are computed through an identification procedure that fits the numerical response in the experimental response minimizing

Table 5.5: Peak load and deformation at peak load for 2x6 parallel to grain connection tests

Loading	Specimen	Direction	Peak Load (lb)	Deformation at Peak Load (in)
Monotonic	1	N/A	282	0.92
	2	N/A	219	0.58
	3	N/A	342	0.89
	4	N/A	274	0.91
Cyclic	1	Positive	302	0.39
	1	Negative	-293	-0.40
	2	Positive	348	0.42
	2	Negative	-310	-0.36
	3	Positive	359	0.41
	3	Negative	-302	-0.39
	4	Positive	315	0.43
	4	Negative	-331	-0.62
	5	Positive	290	0.43
	5	Negative	-281	-0.58
	6	Positive	297	0.43
	6	Negative	-312	-0.60
	7	Positive	127	0.36
	7	Negative	-225	-0.41
	8	Positive	170	0.35
	8	Negative	-205	-0.22

Table 5.6: Peak load and deformation at peak load for 2x6 perpendicular to grain connection tests

Loading	Specimen	Direction	Peak Load (lb)	Deformation at Peak Load (in)
Monotonic	1	N/A	239	0.25
	2	N/A	278	0.38
	3	N/A	331	0.27
	4	N/A	283	0.34
Cyclic	1	Positive	321	0.49
	1	Negative	-311	-0.56
	2	Positive	255	0.55
	2	Negative	-315	-0.33
	3	Positive	276	0.53
	3	Negative	-328	-0.35
	4	Positive	325	0.53
	4	Negative	-342	-0.56
	5	Positive	274	0.57
	5	Negative	-321	-0.55
	6	Positive	287	0.56
	6	Negative	-328	-0.55
	7	Positive	295	0.56
	7	Negative	-322	-0.53
	8	Positive	296	0.55
	8	Negative	-332	-0.55
	9	Positive	305	0.58
	9	Negative	-345	-0.52

the differences in force and deformation. Figure 5.8 shows the SAWS hysteretic response of a sheathing-to framing nail connector and the associated parameters. Table 5.7 lists the fitted hysteretic parameters that were calculated by Pang, providing the average (Mean), sample

standard deviation (StD) and coefficient of variation (CoV) among the different test configurations. The final hysteretic parameters (average values from all tests) are identified with bold fonts. Figures 5.9 and 5.10 present the fitted models for two of the connection tests.

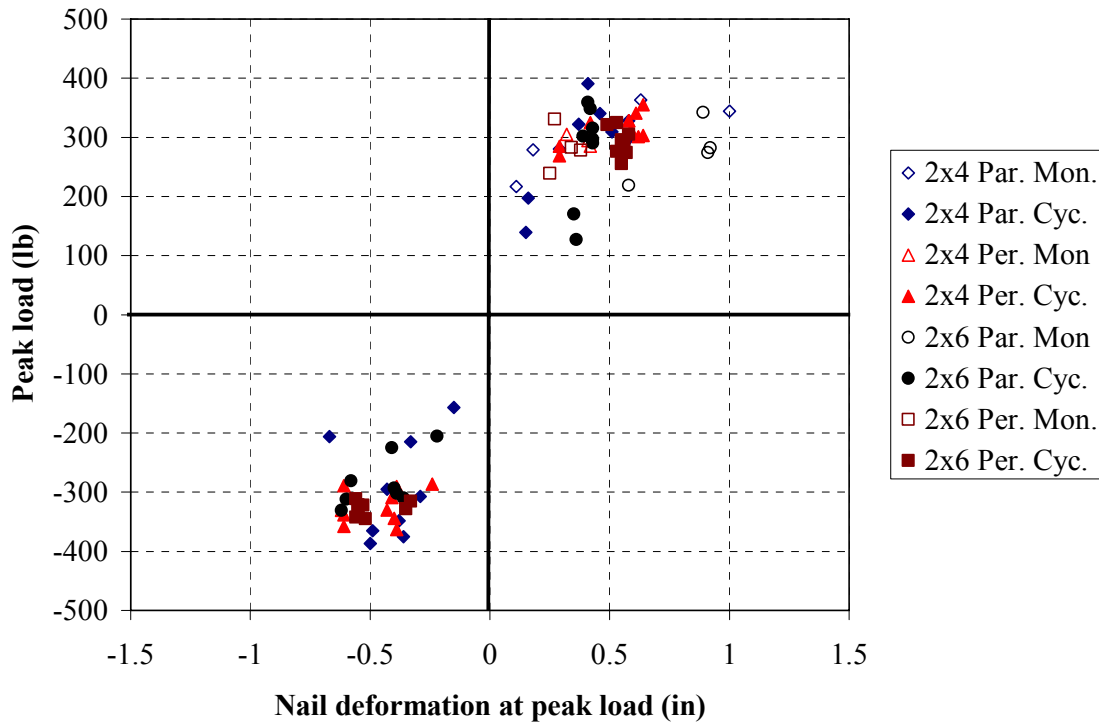


Figure 5.7: Variability of peak load and corresponding deformation from the connection tests

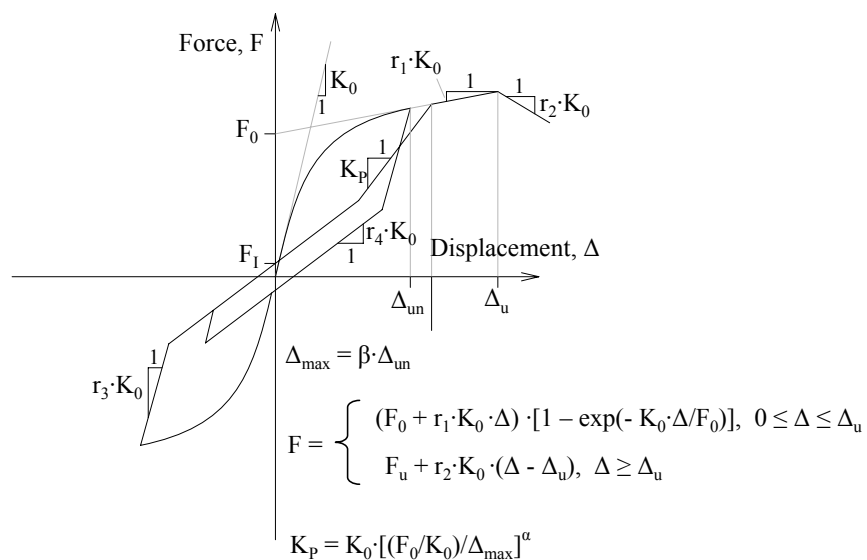


Figure 5.8: SAWS hysteretic response of a sheathing-to-framing connector

Table 5.7: Fitted hysteretic parameters for SAWS model

	K_0 (lbs/in)	r_1	r_2	r_3	r_4	F_0 (lbs)	F_1 (lbs)	Δ_u (in)	α	β
2x4 Hem Fir - 7/16 in. OSB - 8d common nails - loading parallel to grain										
Mean	8144.3	0.025	-0.027	1.028	0.005	242.4	35.0	0.470	0.77	1.24
Std	2208.6	0.015	0.018	0.046	0.002	50.3	5.6	0.118	0.08	0.08
CoV	0.271	0.626	0.660	0.045	0.435	0.208	0.160	0.251	0.102	0.065
2x4 Hem Fir - 7/16 in. OSB - 8d common nails - loading perpendicular to grain										
Mean	6063.8	0.026	-0.047	1.021	0.010	238.1	34.2	0.559	0.67	1.31
Std	1632.2	0.011	0.022	0.048	0.005	29.5	4.7	0.092	0.03	0.04
CoV	0.269	0.440	0.457	0.047	0.455	0.124	0.137	0.164	0.040	0.034
Mean of all 2x4 Hem Fir - 7/16 in. OSB - 8d common nails										
Mean	6920.5	0.025	-0.039	1.024	0.008	239.9	34.5	0.522	0.71	1.28
Std	2129.7	0.013	0.022	0.047	0.005	38.8	5.0	0.111	0.07	0.07
CoV	0.308	0.512	0.576	0.046	0.590	0.162	0.145	0.212	0.103	0.055
2x6 Hem Fir - 7/16 in. OSB - 8d common nails - loading parallel to grain										
Mean	6659.5	0.026	-0.026	1.021	0.004	203.2	25.7	0.448	0.75	1.30
Std	1225.3	0.011	0.013	0.042	0.002	33.4	5.6	0.098	0.11	0.09
CoV	0.184	0.407	0.520	0.041	0.488	0.164	0.218	0.218	0.147	0.066
2x6 Hem Fir - 7/16 in. OSB - 8d common nails - loading perpendicular to grain										
Mean	6039.9	0.026	-0.053	1.010	0.013	228.9	32.8	0.540	0.70	1.29
Std	1749.2	0.007	0.046	0.000	0.004	23.0	3.7	0.059	0.04	0.04
CoV	0.290	0.264	0.869	0.000	0.299	0.100	0.113	0.110	0.062	0.032
Mean of all 2x6 Hem Fir - 7/16 in. OSB - 8d common nails										
Mean	6349.7	0.026	-0.039	1.015	0.009	216.0	29.2	0.494	0.73	1.30
Std	1518.6	0.009	0.036	0.030	0.006	31.1	5.9	0.092	0.09	0.07
CoV	0.239	0.337	0.918	0.029	0.648	0.144	0.202	0.187	0.118	0.051
Mean of all tests - Hem Fir - 7/16 in. OSB - 8d common nails										
Mean	6643.8	0.026	-0.039	1.020	0.008	228.3	32.0	0.508	0.72	1.29
Std	1866.8	0.011	0.030	0.039	0.005	37.0	6.0	0.103	0.08	0.07
CoV	0.281	0.432	0.758	0.039	0.619	0.162	0.189	0.202	0.111	0.053

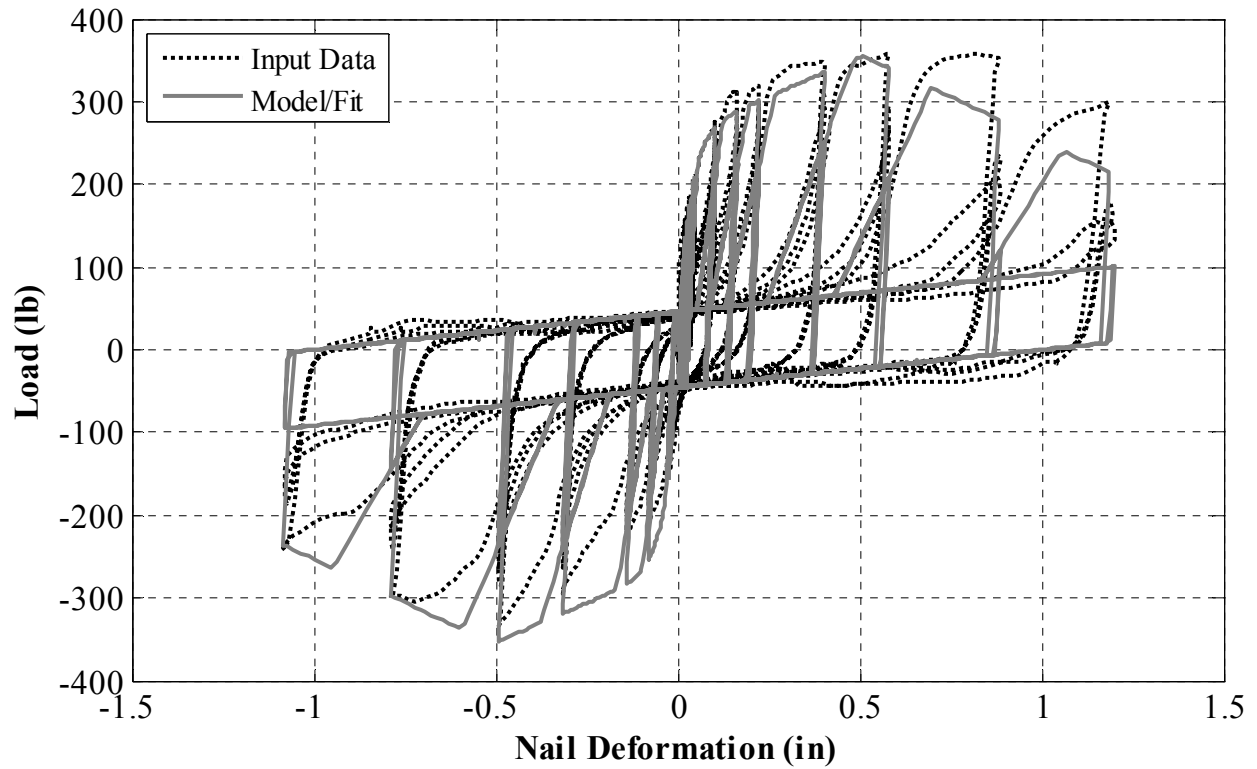


Figure 5.9: Hysteresis plot and fitted model for Specimen 1 of cyclic test of 2x4 parallel to grain

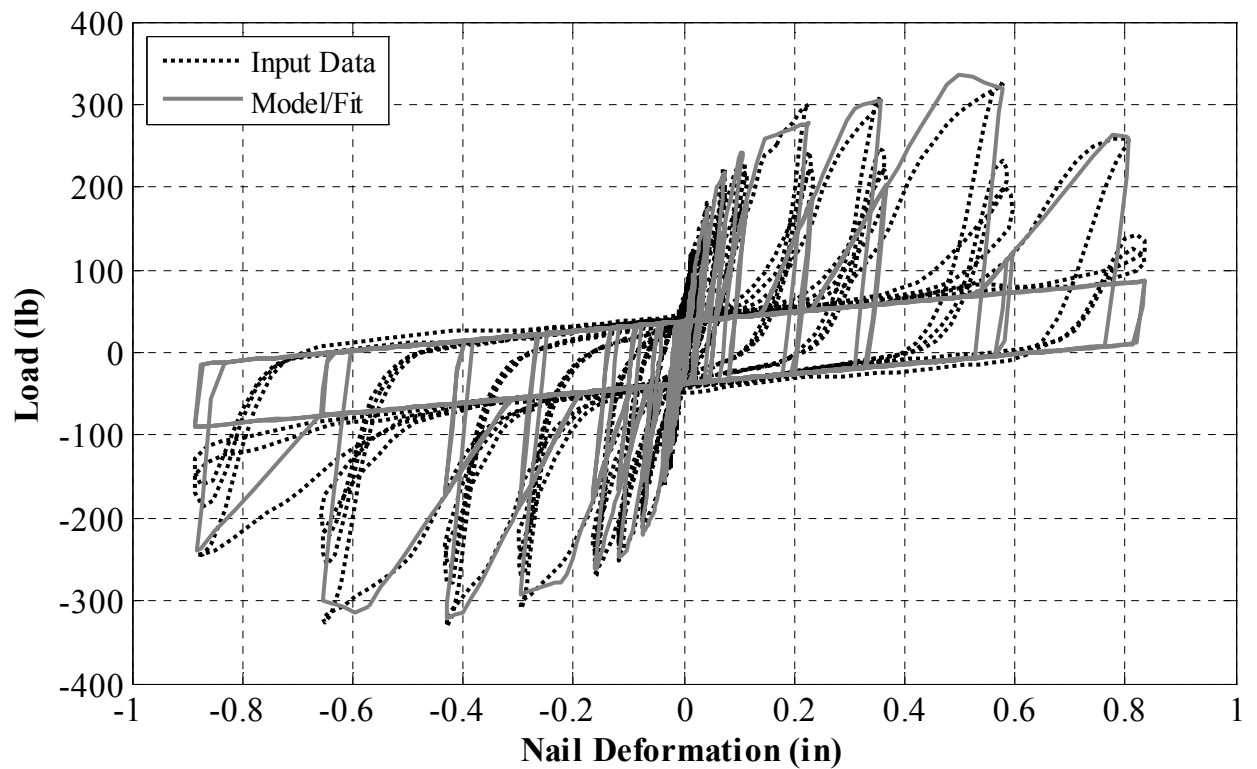


Figure 5.10: Hysteresis plot and fitted model for Specimen 1 of cyclic test of 2x4 perpendicular to grain

5.3 Compressive Strength of Exterior Stucco

This section presents the results from the uni-axial compressive tests of exterior stucco samples, which were conducted in order to define the peak strength σ_{\max} and the modulus of elasticity E of stucco. In preparations of Test Phase 5, stucco was applied to the exterior of the benchmark structure, in three separate coats. Different number of batches was prepared each day. Each batch was unique in quantity, but contained the same materials; Portland cement, lime, sand, and water. Three cubed samples of 2 in. were taken from each respective batch for testing.

The collection, curing, and compression testing of the stucco samples conformed to ASTM C109 Standards [10]. The mold used had three cubed compartments to which the stucco was placed. Shortly after a mix was complete, the soft stucco was placed in a mixing bowl. Next, the stucco was placed in the mold in a one inch layer, which is approximately one half the depth of the mold. The stucco was then tamped in the order shown in Figure 1 of ASTM C109 [10]. This tamping calls for sixteen adjacent, right angle strokes. Next, the mold was completely filled and another round of tamping was necessary. Sixteen more strokes, identical to the first round of tamping, proceeded. When this was done, it was important to have a little bit of stucco above the mold for leveling purposes. The stucco was then leveled out with a trowel and placed in a plastic box, which served the same purpose as a moisture room. The stucco samples were kept in the mold for twenty-four hours, after which they were removed and placed in a thin layer of saturated lime water to be tested. The samples were then tested in a compressive testing machine. The sample was wiped clean and placed on top of a stainless steel cylinder, and a constant load was applied. The load was applied until the sample failed, and then removed. The tests were relatively short, and rarely exceeded twenty seconds. Figure 5.11 shows a stress-strain curve from one of the compressive tests that were conducted.

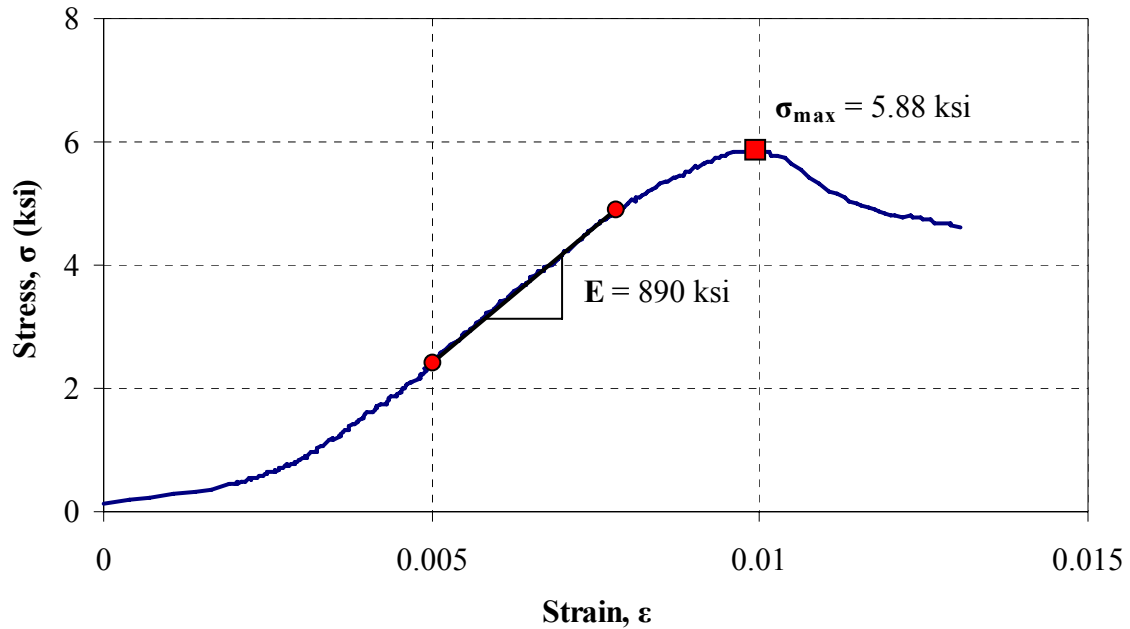


Figure 5.11: Stress-strain curve derived from the first sample of Specimen B-3

The modulus of elasticity E was computed from the slope of the linear range of the stress-strain curve, as shown in Figure 5.11. The peak stress is also indicated on that plot.

Table 5.8 lists the proportions of each component for some of the batches. The amount of water that was used for the first two coats varied, depending on the weather conditions and more specifically if it was raining before or during the mixing of each batch.

Table 5.9 identifies the stucco sampling locations as well as the date of sampling and the respective batch and specimen number. Table 5.10 summarizes the average peak stress and the average modulus of elasticity among the three samples of each specimen. These properties, computed by Jeremy Gworek, an undergraduate student at the University at Buffalo, were reported in [11].

The average strength of the first two coats was around 6.5 ksi and the average modulus of elasticity was around 1000 ksi. The third coat exhibited an average strength of 5.5 ksi and an average modulus of elasticity of 950 ksi.

Table 5.8: Stucco mix information

	Batch	Portland¹	Lime²	Sand³	Water
	#	(bags)	(bags)	(Shovels)	(gallons)
9/28/2006					
(First Coat)	1	2	1	40	15
	2	2	1	30	12
	3	2	1	30	12
9/29/2006					
	1	2	1	30	13
	2	2	1	30	12
	3	2	1	30	12-13
	4	2	1	30	12
	5	2	1	30	12
	6	2	1	30	12
	7	2	1	30	12
10/2/2006					
(Second Coat)	1	2	1	30	16
10/3/2006					
	1	2	1	30	12
10/11/2006					
(Third Coat)	1	1	1/2	18	7.5

¹ 1 bag of Portland Cement= 94 lb

² 1 bag of Limestone= 49.67 lb

³ 1 shovel of sand= 7538.3 g

Table 5.9: Exterior stucco sampling locations

Table Date	Time	Batch No.	Specimen No.	Notes (Locations applied)
9/28/2006	10:30 AM	1	A	*First coat* , Raining at mixing stations, X-Wall (SW)-top
	1:00 PM	2	B	Less sand, X-Wall (SW) bottom, atrium West, bottom
	2:00 PM	3	C	Atrium-Y West, top
9/29/2006	7:00 AM	1	D	Atrium- X
	8:00 AM	2	E	Atrium-Y (Line 4), A/2-4 (bottom)
	9:00 AM	3	F	A/2-4 (top, West) Line 2 (bottom), Line D (bottom)
	10:30 AM	4	G	A/2-4 (top East), Line D (bottom)
	11:00 AM	5	-	Skip sampling
	1:00 PM	6	H	Line D (top)
	1:45 PM	7	I	Line D (top)
10/2/2006	7:00 AM	1	A-2	Line D (top), Line 2 (top)
	8:30 AM	2	B-2	Line D (top), balcony (East), Roof ceiling (East)
	12:20 PM	5	C-2	Line D (top), Line 2 (top), Roof ceiling (East)
	2:10 PM	6	D-2	Line D (top), Line 2 (top)
	2:45 PM	7	E-2	*Second coat* , A/5-6 (top)
10/3/2006	7:30 AM	1	F-2	A/5-6
	8:30 AM	2	G-2	Line 5, *Raining
	10:00 AM	3	H-2	Line 4, Atrium-X
	1:45 PM	4	I-2	Line 4, A/2-4 (top)
	2:30 PM	5	J-2	A/2-4 (top)

Table 5.9: Exterior stucco sampling locations (cont'd)

Table Date	Time	Batch No.	Specimen No.	Notes (Locations applied)
10/4/2006	6:45 AM	1	A-3	Atrium-X
	7:30 AM	2	B-3	Line 6 (bottom), *Raining
	12:45 PM	4	C-3	Line 6 (top), balcony (West)
	2:00 PM	5	D-3	Line 2, balcony (East)
	4:00 PM	6	E-3	Line 2, Roof ceiling (East)
10/5/2006	6:45 AM	1	F-3	Line D
	8:00 AM	2	G-3	Line D, Line 2 (top)
	10:30 AM	4	H-3	Line D
	12:30 PM	5	I-3	Line D
	1:30 PM	6	J-3	Line D
10/6/2006	6:45 AM	1	A-4	Line 2 (top), Line D
	10:30 AM	2	B-4	Line 2 (top)
	1:00 PM	3	C-4	Line 2 (top)
10/11/2006	9:45 AM	1	A-5	*Third coat* , Line 6 (balcony), top
	11:30 AM	2	B-5	Line 6, *Raining
	1:00 PM	3	C-5	A/5-6 (top, bottom)
	1:50 PM	4	D-5	Line 5
	2:50 PM	5	E-5	Atrium-X, Line 4
	8:00 AM	1	F-5	Line D
10/12/2006	8:20 AM	2	G-5	Line D
	9:00 AM	3	H-5	Line D, *Raining
	12:45 PM	3	I-5	Atrium-X
	1:50 PM	3	J-5	Line A/2-4
10/17/2006	8:00	1	A-6	Line 2, *Raining

Table 5.10: Compressive strength and modulus of elasticity of exterior stucco

Specimen No.	Batch No.	Avg. Peak Stress (ksi)	Avg. E (ksi)
9/28/2006			
A	1	5.96	944
B	2	7.30	1150
C	3	6.75	1176
Average Values		6.67	1090
9/29/2006			
D	1	4.49	680
E	2	5.99	1165
F	3	6.34	1187
G	4	6.62	1053
H	6	7.37	1314
I	7	7.08	1183
Average Values		6.31	1097
10/2/2006			
A-2	1	7.93	1393
B-2	2	6.98	1074
C-2	5	6.75	1176
D-2	6	6.06	937
E-2	7	6.20	1129
Average Values		6.78	1142
10/3/2006-10/4/2006			
F-2	1	6.46	1027
G-2	2	7.24	1009
H-2	3	7.73	1070
I-2	4	5.60	850
J-2	5	5.42	899
A-3	1	6.65	1056
B-3	2	5.66	843
C-3	4	6.84	1001

Table 5.10: Compressive strength and modulus of elasticity of exterior stucco (cont'd)

Specimen No.	Batch No.	Avg. Peak Stress (ksi)	Avg. E (ksi)
10/3/2006-10/4/2006			
D-3	5	6.78	906
E-3	6	6.71	963
Average Values		6.51	963
10/5/2006-10/6/2006			
F-3	1	6.46	885
G-3	2	7.05	1045
H-3	4	5.83	912
I-3	5	6.59	1065
J-3	6	6.53	930
A-4	1	6.11	1066
B-4	2	7.28	1065
C-4	3	6.46	923
Average Values		6.54	986
10/11/2006-10/17/2006			
A-5	1	6.29	1069
B-5	2	5.15	937
C-5	3	6.98	1044
D-5	4	5.89	1016
E-5	5	6.33	1031
F-5	1	5.26	928
G-5	2	4.88	863
H-5	3	4.25	865
I-5	3	5.38	867
J-5	3	5.24	901
A-6	1	4.96	916
Average Values		5.51	949

Chapter 6 Results of System Identification Tests

This chapter presents the results derived from the data of the system identification tests. As discussed earlier, the main objective of those tests was to identify the dynamic characteristics of the test structure such as natural frequencies, associated mode shapes and modal damping ratios. The procedure that was followed to analyze the data and compute the aforementioned properties is discussed. The fundamental natural frequency results are presented in terms of the variation of fundamental periods and variation of normalized lateral stiffness. Appendix H summarizes all the results that were developed from the system identification tests.

6.1 Data Analysis

The input excitation of the system identification tests was a flat random noise, the properties of which are presented in Section 3.1.1. Only the recorded data from the accelerometers were utilized to calculate the dynamic properties of the test structure. More specifically, the natural frequencies, mode shapes and associated modal damping ratios were determined through the Transfer Functions (TFs) of the story acceleration response of the structure and the base motion. The TF is defined as an output structural response, normalized by a superimposed input base motion in the frequency domain, (i.e. the Fourier Transform of a story level acceleration time history, normalized by the Fourier Transform of the base acceleration time history). Thirty two horizontal accelerometers, located at the second floor diaphragm and the roof of the test building, as illustrated in Figure 6.1, as well as four accelerometers, located on the twin shake tables, were used to generate the TFs for each white noise test. The TFs were computed using a data analysis software (DADiSP 2002 [12]) that utilizes a script file, which has been developed by SEESL staff.

6.1.1 Identification of Natural Frequencies

The amplitude of the TF, when plotted with respect to frequency as shown in Figure 6.2, illustrates at which specific frequencies of the input signal the response of the structure is amplified (peak values). These frequencies correspond to the natural frequencies of the structure. For example, Figure 6.2 shows the amplitude of two TFs from two different identification white noise tests. Test NWP1W05 was conducted in the transverse (north-south) direction of the test structure and the black line corresponds to the amplitude of the TF between accelerometer A22,

located at the south-west corner of the roof (see Figure 6.1), and accelerometer A72, located on the east shake table. Both accelerometers record the motion in the transverse direction, as shown

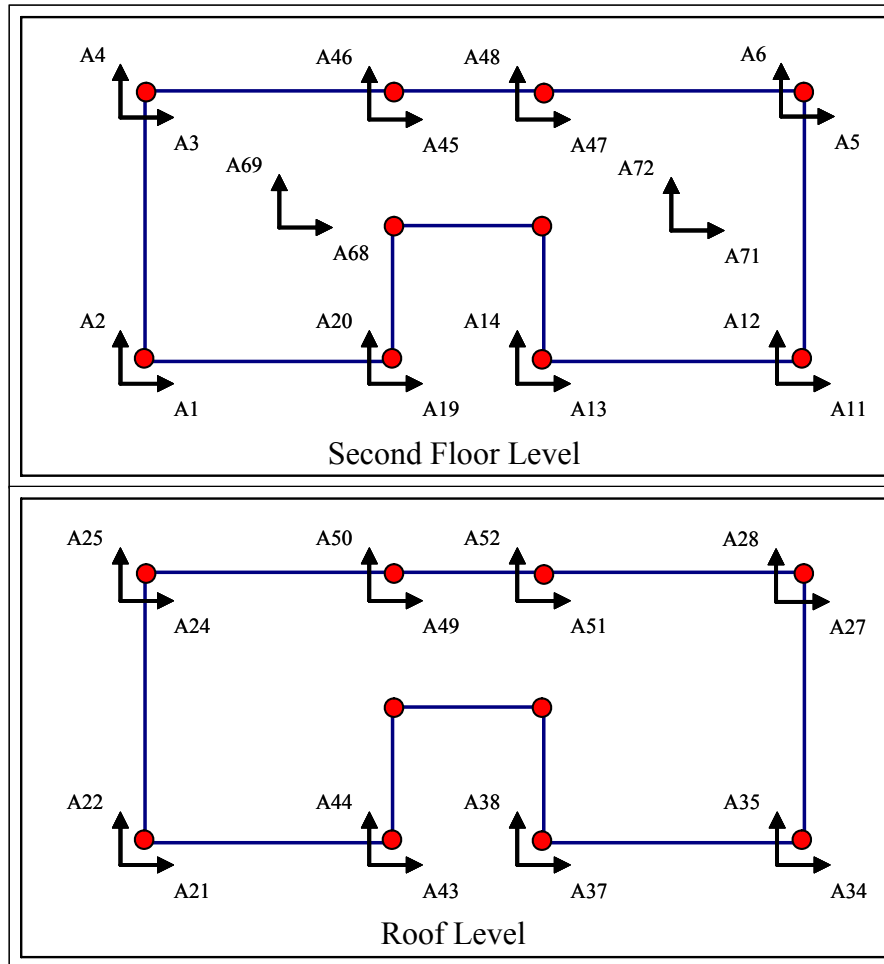


Figure 6.1: Accelerometers of the test structure used in the system identification

in Figure 6.1. The grey line corresponds to the amplitude of the TF between accelerometers A21 and A68 for Test NWP1W01 conducted in the longitudinal (east-west) direction. Both tests were conducted in Test Phase 1, before any seismic test. The first natural frequency (3.06Hz) is excited when the structure is shaken along the transverse direction, which is the shorter side of the test structure, compared to the longitudinal direction. The second and third natural frequencies (4.44Hz and 5.56Hz, respectively) are excited when the structure is shaken along the longitudinal direction. There are peaks in the TFs that show up in higher frequencies and

correspond to higher modes, however, only the first three modes of vibration were identified from the system identification tests.

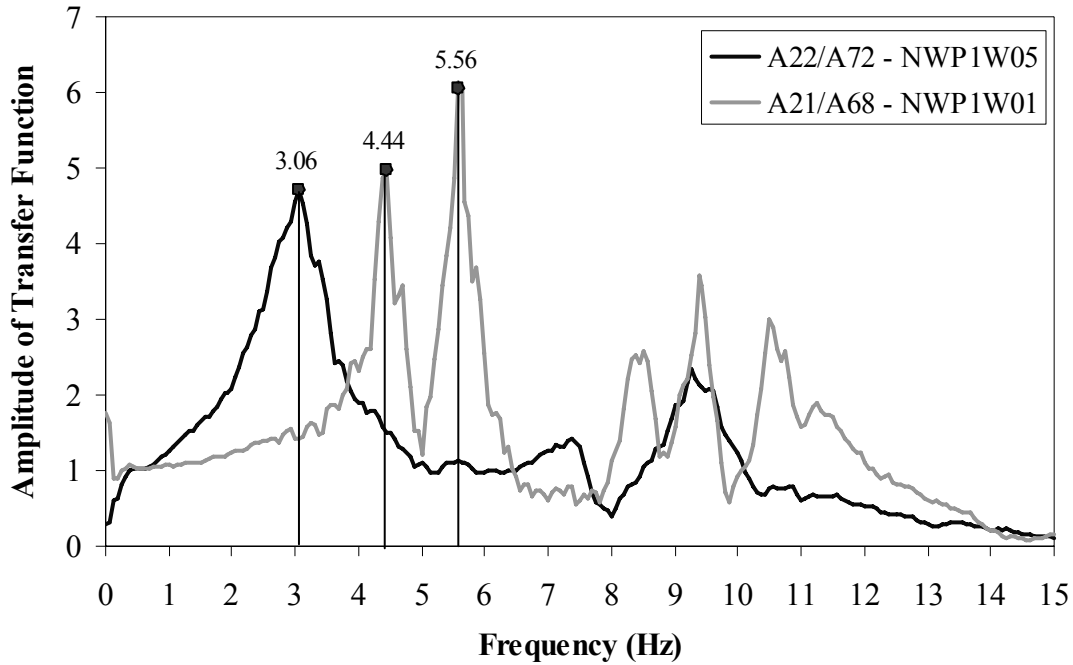


Figure 6.2: Transfer Functions from two white noise tests in the longitudinal and transverse directions

6.1.2 Calculation of Modal Damping Ratios

The equivalent viscous damping characteristics of the test structure can be determined from a TF using the well known half-power bandwidth method [13]. The damping ratio at a given natural frequency is determined from the frequencies at which the amplitude of the response is reduced by $(1/\sqrt{2})$ or the power input is half the input at resonance. Figure 6.3 and Eq. (6.1) show the numbers behind the calculation of the initial damping ratio ζ_1 of the first natural frequency of the test structure from Test NWP1W05.

$$\zeta_1 = \frac{f_b - f_a}{2 \cdot f_1} = \frac{3.50 - 2.56}{2 \cdot 3.06} = 0.154 = 15.4\% \quad (6.1)$$

Figure 6.4 shows the TF between accelerometers A21 and A68 for Test NWP3W13, which was conducted in the longitudinal direction following the bi-axial Level 1 test. When calculating the damping ratio for the second natural frequency, the half-power method cannot be directly applied because the third natural frequency is not well separated and the frequency bandwidth cannot be defined. In cases like these, the symmetric part of the TF (grey line) was considered to define the frequency bandwidth, as shown in Figure 6.4, and approximately determine the damping ratio ζ_2 of the second natural frequency for that particular white noise test.

$$\zeta_2 = \frac{5.15 - 3.97}{2 \cdot 4.56} = 0.129 = 12.9\% \quad (6.2)$$

6.1.3 Determination of Mode Shapes

The Transfer Functions (TFs) between the accelerometers that were installed on the test structure were also used to determine the mode shapes for each fundamental natural frequency. The input base acceleration time history is not necessary for the evaluation of the mode shapes, since what is of interest is the relative motion among the moving parts of the structure that are instrumented.

More specifically, if the Fourier Transform of each story level acceleration time history is normalized by the Fourier Transform of a single acceleration time history, for example accelerometer A1, then the amplitude of the resulting Transfer Functions at a specific natural frequency is linearly related to the amplitude of the motion of that part of the structure, in the direction of each accelerometer (see [14] for reference). Whether this motion is positive or negative, according to the sign convention specified, is determined from the phase angle of the TF at the given frequency. If the phase angle is close to 0 degrees, the two parts have the same sign, whereas, if the phase angle is close to 180 or -180 degrees the two parts have opposite signs.

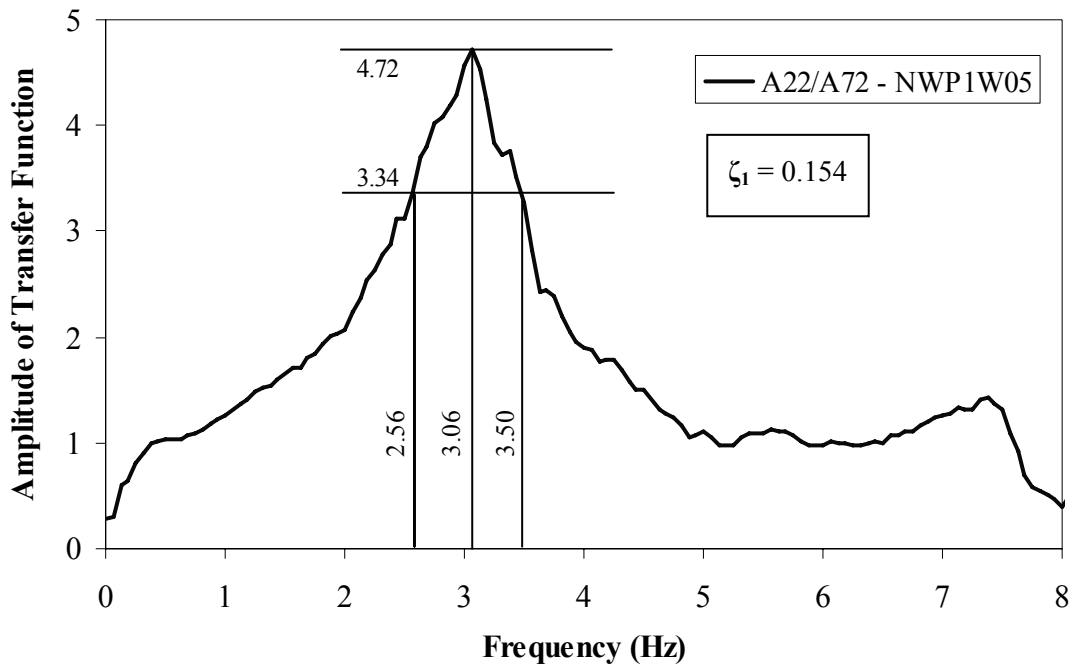


Figure 6.3: Application of half-power bandwidth method

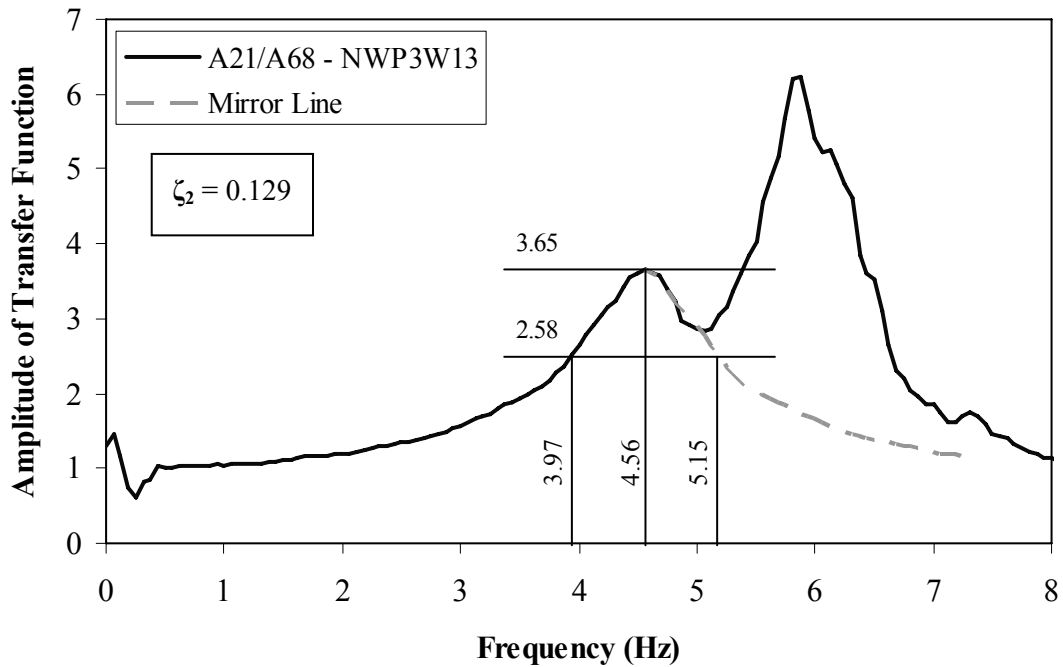


Figure 6.4: Use of symmetry on the application of half-power bandwidth method

Figure 6.5 shows the TFs (amplitude and phase angle) between the four accelerometers located on the north side of the roof along the transverse direction, from Test NWP1W04, which was conducted in the transverse direction prior to any seismic test, with an amplitude of 0.05g. Assuming that for A25 (west side) the amplitude of the motion is equal to 1 along the positive (north) direction, it is evident that the whole side is moving towards the same direction (phase angle equal to 0) and the amplitude of the motion is increasing towards the east side of the structure. The resulting mode shape for NWP1W04 is presented in Figure H.1a of Appendix H.

6.2 Initial Natural Periods and Damping Ratios

Following the procedures described in the previous sections, the natural periods and modal damping ratios of the test building were identified for each white noise identification test that was conducted during all test phases. The results are presented in Tables H.1 through H.7 of Appendix H. Tables 6.1 and 6.2 summarize the initial natural periods and damping ratios for each test phase, prior to any seismic test.

Table 6.1: Initial natural periods (sec)

Mode \ Phase	1	2	3	4	5
1	0.327	0.327	0.296	0.296	0.286
2	0.225	0.232	0.216	0.222	0.198
3	0.180	0.178	0.170	0.163	0.127

Table 6.2: Initial damping ratios (%)

Mode \ Phase	1	2	3	4	5
1	12.2	12.5	10.7	10.9	17.9
2	3.3	6.8	6.5	4.3	17.1
3	2.7	5.6	6.7	6.2	5.0

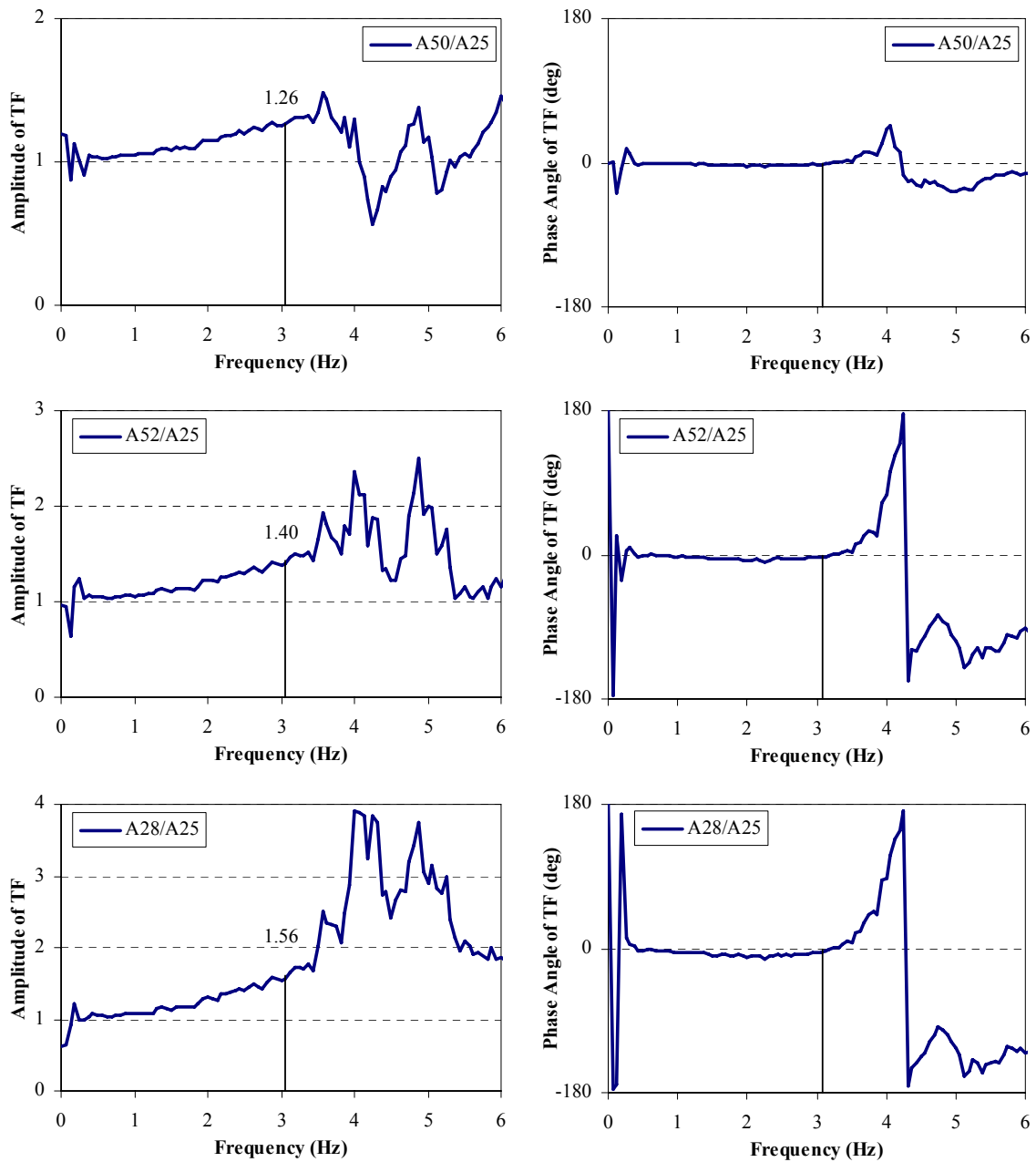


Figure 6.5: Transfer Functions of accelerometers on the north side of the roof of the test structure for Test NWP1S04

The fundamental periods for Test Phases 1 and 2 are almost the same, since the introduction of the damper-wall units did not affect the stiffness of the structure. The application of gypsum wallboard on the structural walls, on the contrary, in preparations of Test Phase 3, led to a reduction of the natural periods, as expected, due to the contribution of the gypsum to the stiffness of the structural members. The same trend was observed after the application of exterior stucco before Test Phase 5; the natural periods were decreased compared to Test Phase 3 and 4. The application of gypsum wallboard on partition walls and ceilings before Test Phase 4 did not affect the first natural period of the test structure. The second and third periods were slightly changed and this can be attributed to the change of these structural mode shapes, as it will be shown later in this chapter.

The equivalent viscous damping ratio of the first natural mode ranged around 11-12% for the first four test phases. The damping ratios of the second and third modes were around 3% for Test Phase 1 and were almost doubled for Test Phase 2, 3 and 4. The application of stucco led to an increase of the damping ratio of the first two natural modes above 17%.

6.3 Evolution of Natural Periods and Modal Damping Ratios

Figures 6.6 through 6.8 show the evolution of the first three natural periods of the structure during the test phases. Only the results from the identification tests that followed tri-directional (X-Y-Z) or bi-directional (X-Y) seismic tests are presented. This is the reason why the results from Test Phase 2 are not included in these figures. The horizontal axis in these plots denotes the seismic test (seismic level and direction) that was conducted before the identification test.

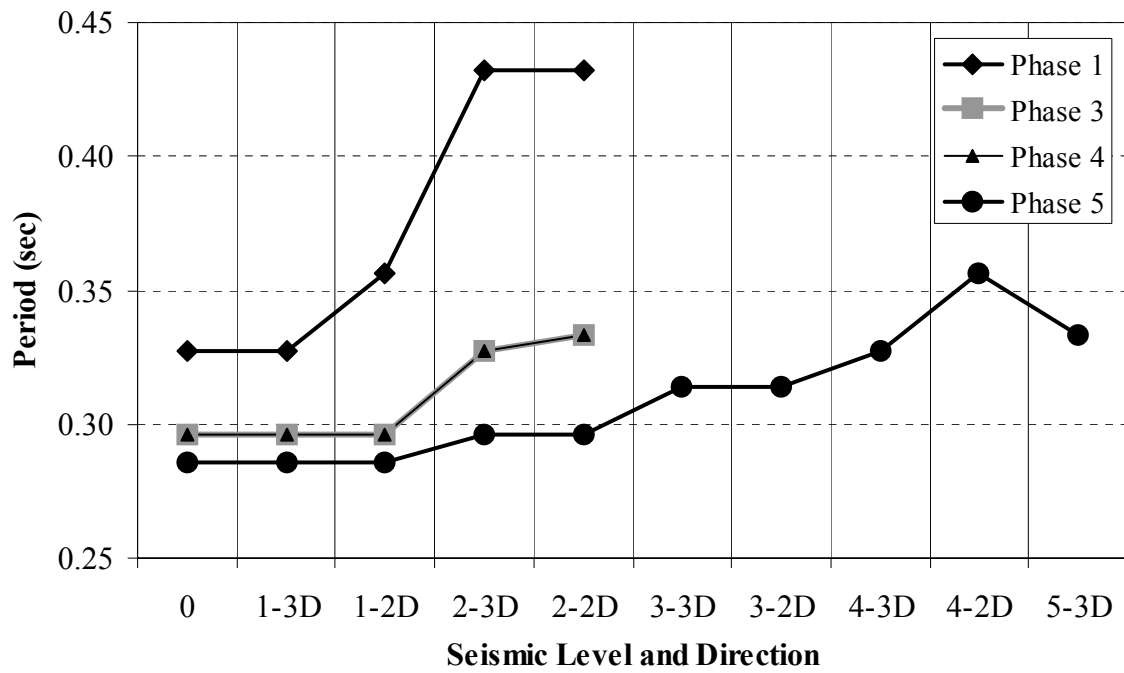


Figure 6.6: Evolution of the first natural period

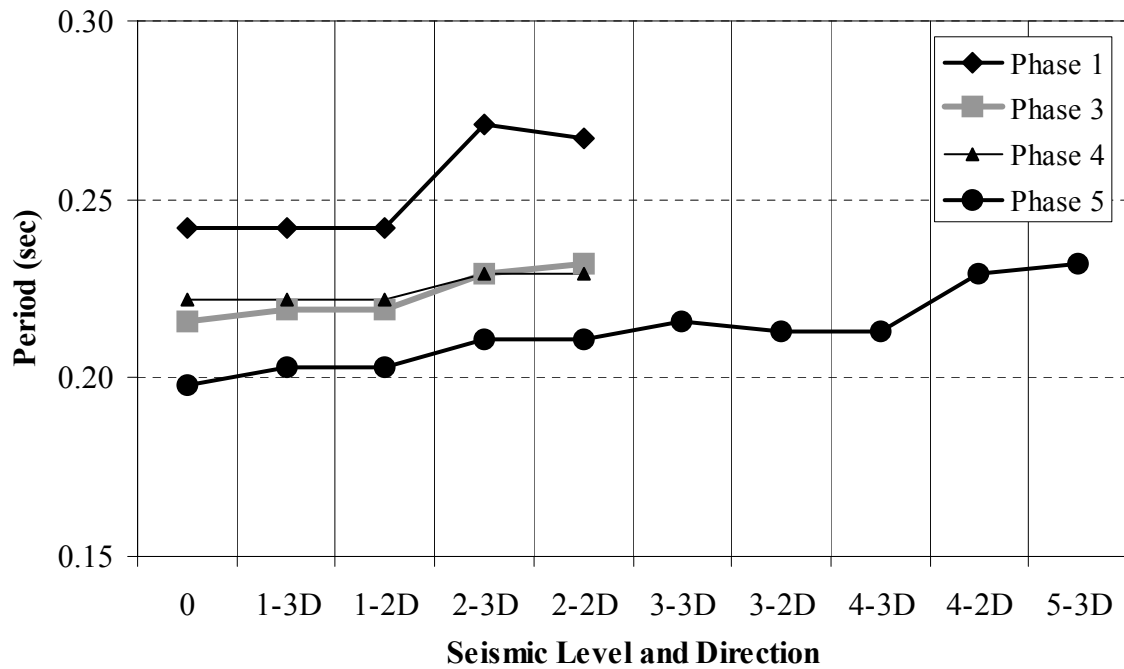


Figure 6.7: Evolution of the second natural period

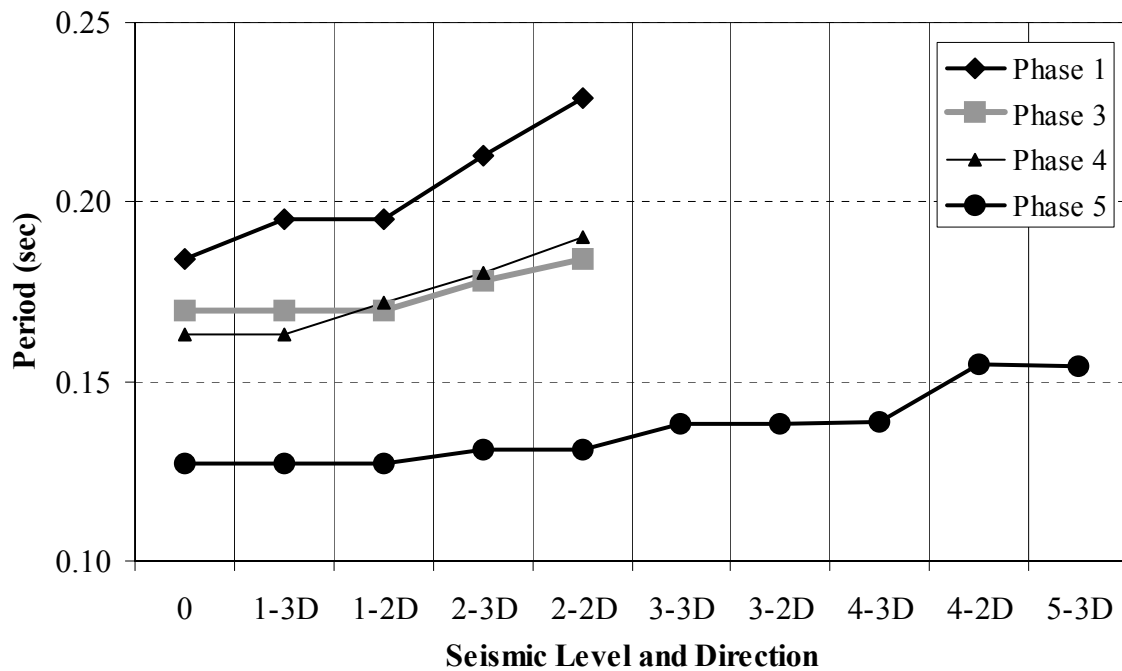


Figure 6.8: Evolution of the third natural period

As expected, the natural periods are increasing as the level of shaking increases. This is an indication of the level of damage that is induced in the structural members. The damage is more pronounced for the structure of Phase 1, which consists of the wood shear walls only, without any interior or exterior wall finish materials. The increase of the periods is observed after the tri-directional tests, for most of the cases, while a repetition of the same seismic level, excluding the vertical component, does not significantly affect the natural periods. The evolution of the natural periods for Test Phases 3 and 4 are very similar. Especially the first fundamental period is varied similarly throughout the seismic tests, which shows that the application of gypsum wallboard on non structural walls does not significantly affect the lateral stiffness of the structure at low response amplitude.

Figure 6.9 presents the deterioration of the lateral stiffness of the structure in the north-south direction, associated primarily with the first natural period, assuming a single-degree-of-freedom structure. Since the initial natural period \mathbf{T}_0 is known, as well as the period \mathbf{T}_i after each seismic test, the normalized stiffness \mathbf{k}_i , as a percentage of the initial stiffness \mathbf{k}_0 can be calculated as:

$$\frac{\mathbf{k}_i}{\mathbf{k}_0} = \left(\frac{\mathbf{T}_0}{\mathbf{T}_i} \right)^2 \cdot 100\% \quad (6.3)$$

As mentioned above, the deterioration of the lateral stiffness is more pronounced for the structure of Test Phase 1. The stiffness at the end of this phase dropped to less than 60% of the initial stiffness after test Level 2. The lateral stiffness for the structures of Test Phases 3 and 4 was above 80% of their initial stiffness after Level 2 test; the corresponding value for the Test Phase 5 structure was above 90%. Even after the DBE Seismic Level 4 test, the lateral stiffness of the Test Phase 5 structure remained above 75% of its initial lateral stiffness. The deterioration was smaller when wall finishes were applied for the same level of shaking. Note that the increase of the stiffness that is observed after the final tri-axial test of Seismic Level 5 of Test Phase 5 was due to the repair of damaged anchor bolts in the two walls on the west (garage wall) and east side of the first floor of the benchmark structure, prior to the conduction of the Level 5 tri-axial test, which resulted in a stiffer structure. Figures 6.10 through 6.12 show the evolution of the modal damping ratios.

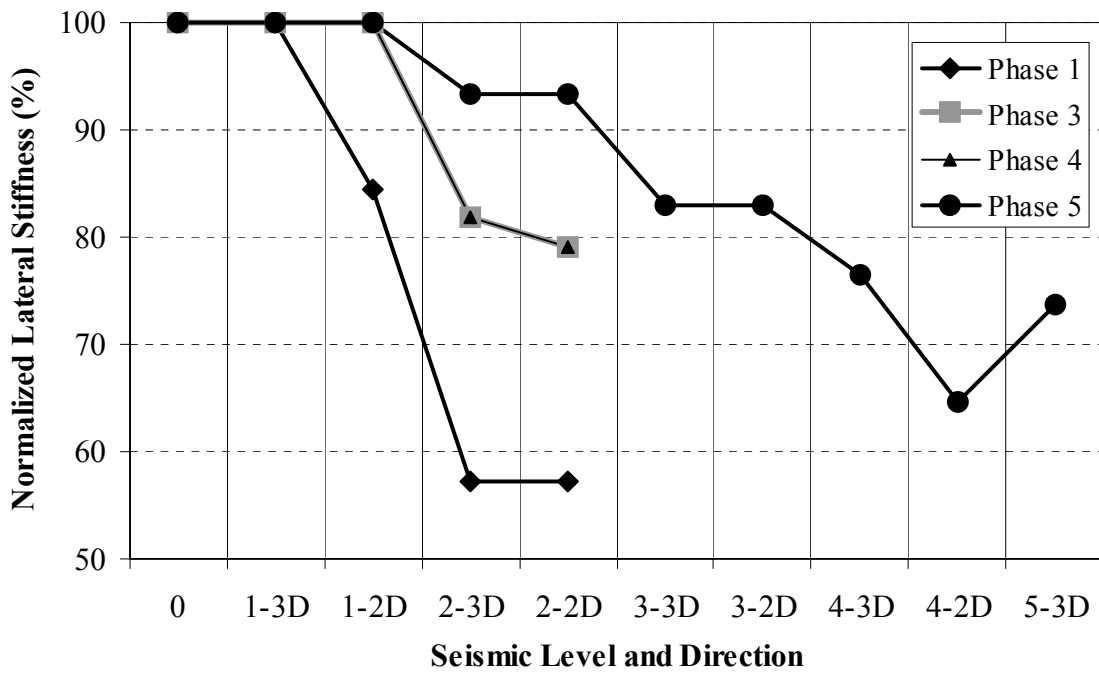


Figure 6.9: Variations of normalized lateral stiffness in the north-south direction

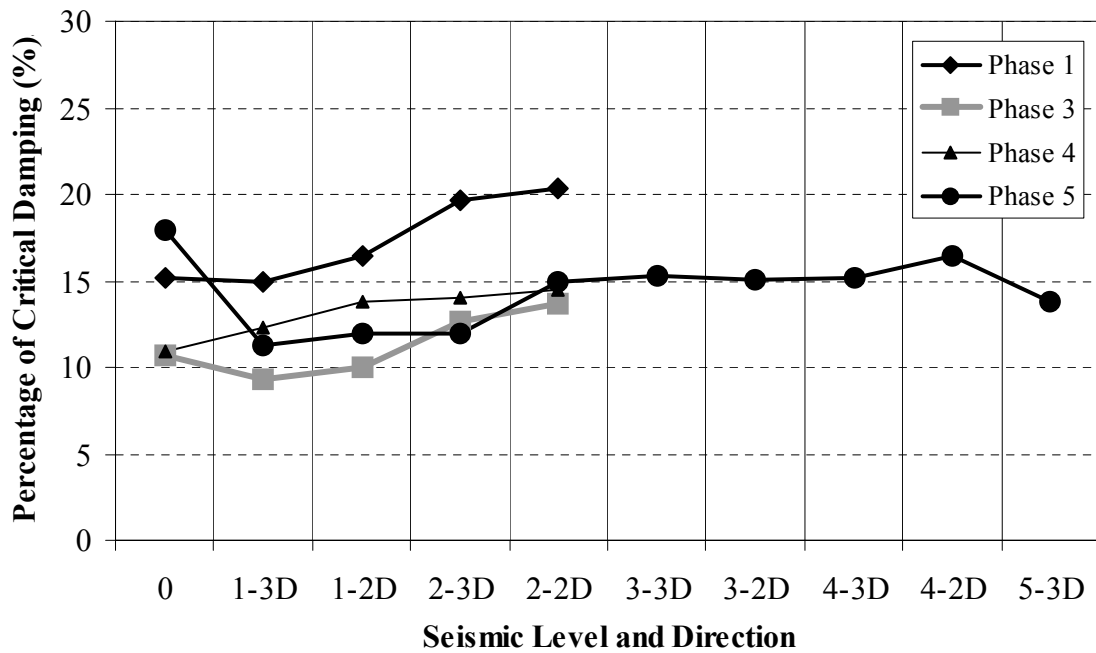


Figure 6.10: Evolution of the first modal damping ratio

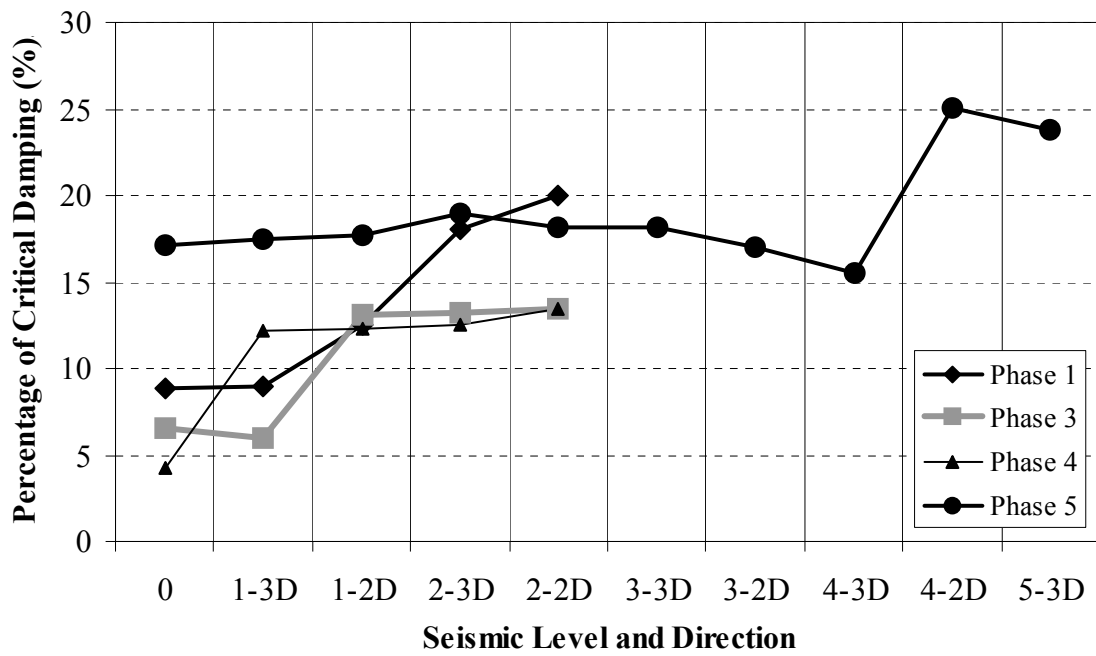


Figure 6.11: Evolution of the second modal damping ratio

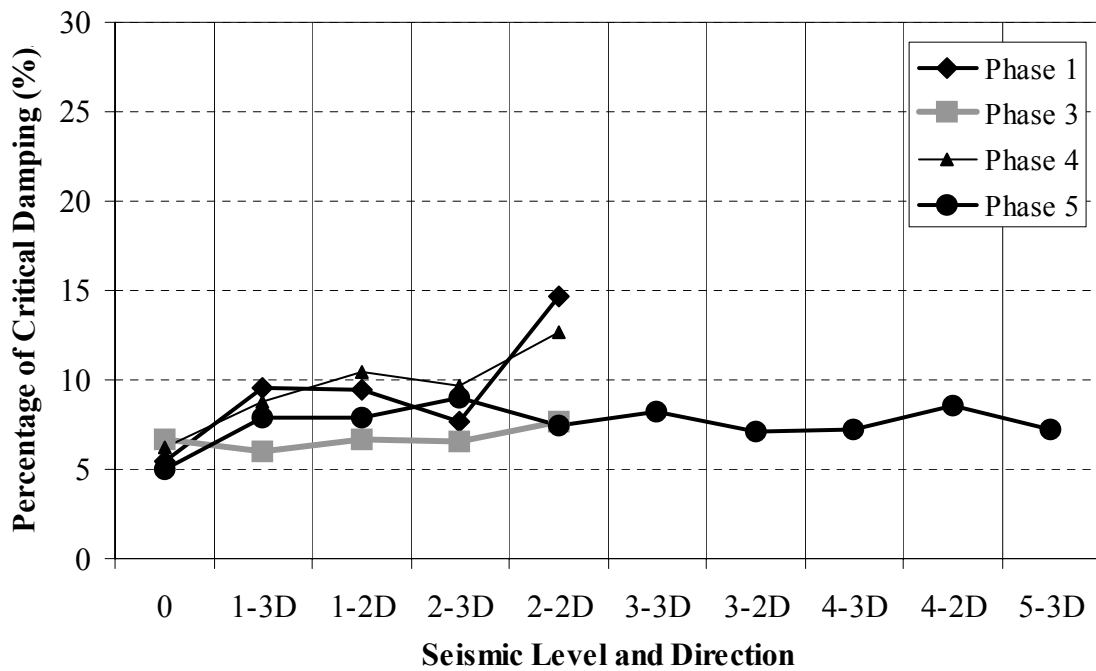


Figure 6.12: Evolution of the third modal damping ratio

The damping ratios of the first natural mode range from 10 to 20% of critical, with a mean value of around 15% of critical for all test phases. The variation of the second damping ratio is more significant and ranges from 5 to 20% of critical, with an exception of the last two seismic tests of Test Phase 5, after which the damping is increased to 25% of critical. The third modal damping ratio is mainly between 5 to 10% of critical. It is noted that a portion of the equivalent viscous damping comes from the nonlinear behavior associated with damage to the connections. Thus, although the fundamental damping ratios are high, they may, at least partially, be attributed to damage in the structure, albeit at low amplitudes of deformation.

6.4 Variation of Structural Mode Shapes

Figures H.1 through H.5 of Appendix H illustrate the initial structural mode shapes that were determined following the procedure described in Section 6.1.3. The mode shapes for Test Phases 3 and 4 are presented again below in Figures 6.13 and 6.14, respectively, for comparison purposes.

The mode shapes of these two phases summarize the basic characteristics that were observed from the mode shapes of all test phases. More specifically, the mode shapes of Test Phase 3 are very similar to the mode shapes of Test Phase 1 and 2. The first mode shape is along the transverse direction of the structure and the displacements between the floors are almost equally distributed. The east side of the roof is displaced slightly more than the west side, as shown by the grey line in Figure 6.13a. The second and third mode shapes are along the longitudinal direction, but there is also a torsional response that produces displacements along the transverse direction as well. This is attributed to the eccentricity between the center of mass and the center of stiffness along the longitudinal direction, because of the unsymmetrical shape of the benchmark structure. It is also evident that the central part of the structure has greater in plane

flexibility compared to the two main units of the house and behaves as a shear link between two stiffer diaphragms. This in-plane flexibility is expected due to the presence of the staircase opening that leads to the upper floor. Note that no wood staircase was incorporated in the test structure.

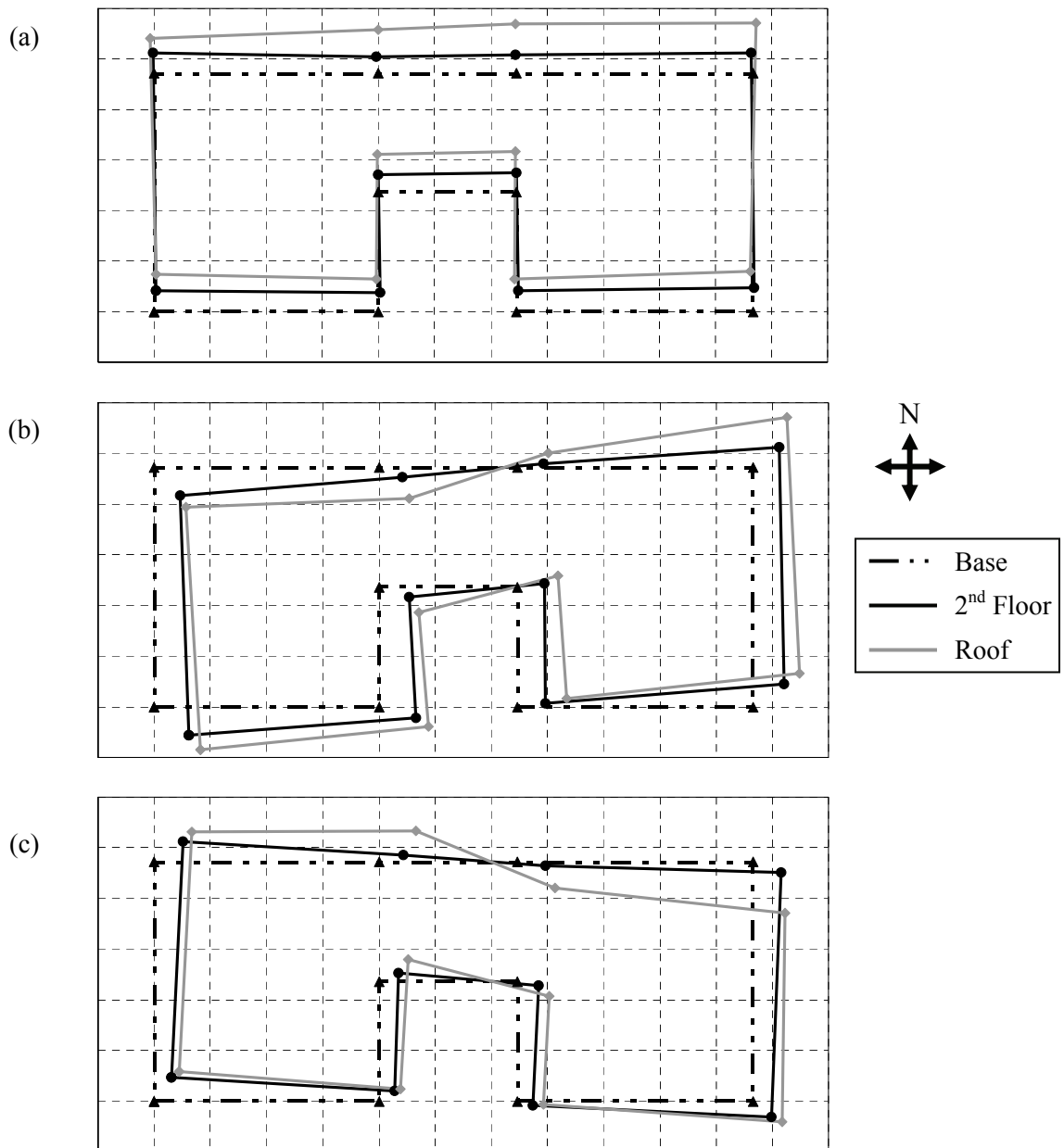


Figure 6.13: Mode shapes from Phase 3, (a) mode 1, $T_1 = 0.30$ sec, (b) mode 2, $T_2 = 0.22$ sec, (c) mode 3, $T_3 = 0.17$ sec

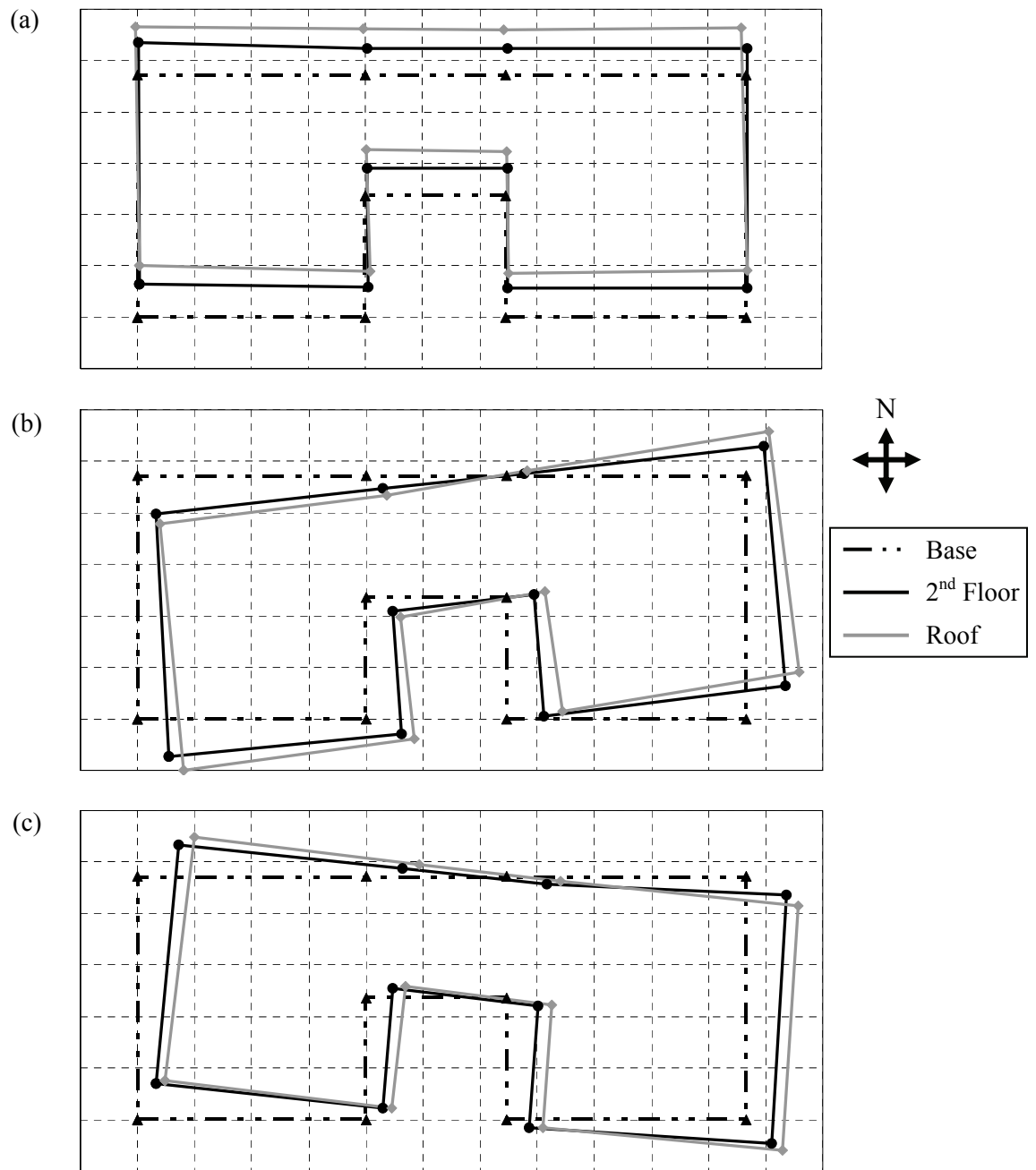


Figure 6.14: Mode shapes from Phase 4, (a) mode 1, $T_1 = 0.30$ sec, (b) mode 2, $T_2 = 0.22$ sec, (c) mode 3, $T_3 = 0.16$ sec

Comparing the mode shapes of Test Phase 3 and 4, there are some differences that can be readily observed. The first mode shape of Phase 4 is similar to the first mode shape of Phase 3 but does not exhibit higher displacements on the east side of the roof. However, mode shapes two and three of Phase 4 reveal that the application of gypsum board on the ceilings led to an increase of the diaphragm stiffness since each level floor is moving in unison without any shear deformations of the central part of the structure, at least for linear elastic response. This can explain the differences in the second and third natural frequencies between Test Phase 3 and 4. Moreover, a great portion of the total building motion takes place at the first story, where the inter-story displacement is much greater than the second inter-story displacement.

Chapter 7 Results of Seismic Tests

This chapter presents the results derived from the data of the seismic tests. As discussed earlier, the main objectives of those tests were to determine the performance of the benchmark structure under several levels of seismic shaking intensity as well as to observe the influence of interior and exterior wall finish materials on the seismic response of light-weight woodframe structures. This chapter concentrates on the effect of interior and exterior wall finishes on the seismic response of the test structure. Therefore, only the experimental results of Test Phases 1, 3, 4 and 5 are analyzed in detail in this chapter. A separate NEESWood Project Report will analyze the results of Test Phase 2 incorporating viscous fluid dampers within wood walls.

First, the shake table fidelity is discussed based on the correlation between the desired and the recorded shake table motions. The performance of the benchmark structure is then presented in terms of various recorded intensity measures, which have been incorporated in various appendices of this report. Selected comparative seismic responses among the different test phases are also included.

7.1 Shake Table Fidelity

One important aspect of shake table testing is the ability to accurately reproduce the simulated ground motions. It is significant to acquire a good match between the recorded and the desired shake table motions in the frequency range of interest, especially when input motions of different levels of shaking intensities are part of the testing program. Considering also that within the NEESWood Project, the benchmark structure was located on top of the twin shake tables and the connecting bridge structure, all of which were required to act as one large shake table, it was even more important to synchronize the motions of the two shake tables to minimize any potential hazard from different input base motions. Another challenging aspect was that the weight of the test structure was such that the shake tables had to perform close to their specified nominal performance limits in terms of the maximum test specimen weight and the maximum induced base overturning moment.

For these reasons, before the construction of the test structure, the two shake tables and the connecting bridge were subjected to the tri-axial Canoga Park and Rinaldi records scaled to the specified Seismic Levels 4 and 5, respectively. The mass of the structure was simulated by concrete blocks and steel plates of equal total weight that were strapped on the two extension frames. Figure 7.1 shows the configuration during those preliminary tests.

This procedure helps to correlate the drive and the achieved motions of the shake tables in the frequency domain. The Transfer Functions between the drive and the achieved motions show the frequencies at which the amplitude of the motions is amplified or reduced, assuming a rigid elastic test structure. This information helps to tune the shake tables and reproduce the desired motions with greater fidelity, neglecting however the flexibility as well as the stiffness deterioration of the test structure. Yet, tuning of the shake tables was also conducted between the seismic tests using the recorded data, including the effect of the flexibility of the test structure. The recorded acceleration time histories of the twin shake tables and the bridge in the three orthogonal directions were used to calculate the acceleration response spectra for each direction and compare it with the target acceleration response spectra of each specific seismic test. Appendix I contains plots of the 5% damped response spectra that were generated from the recorded motions of each table and the bridge (three spectra for every applicable direction), along with the desired response spectra of the given seismic test. Since the derived data from the seismic tests were filtered for frequencies greater than 10Hz, the spectral ordinates below 0.1sec in the plots of Appendix I are linear interpolations of the peak ground acceleration and the spectral ordinate at 0.1sec.



Figure 7.1: Ballast weights located on the shake tables and the connecting bridge

In general, the shake table fidelity was reasonable over the large number of seismic tests of different intensities that were part of the testing program throughout the five phases of the NEESWood Project benchmark testing. One general observation is that in most of the cases the motions of the tables and the bridge were very similar and the generated response spectra were very close to one another. This was not the case for the vertical components, however. For those tests including vertical excitation, the spectral ordinates from the records on the bridge structure were higher than the ones recorded on the shake tables, particularly in the vicinity of the peak spectral value at around 0.12sec. This is not surprising since the bridge structure was not hydraulically driven. The flexibility in the connections between the extension frames and the bridge structure might have amplified the transmitted motion, especially in the vertical direction for which the input has high frequency content. Figure 7.2 presents the generated response spectra from the tri-axial test of Level 2 of Phase 1 (Test NWP1S17).

A point worth to mention is that during Seismic Test NWP1S05, the tri-axial test of Level 2 of Phase 1, there was a synchronization malfunction that led to unsynchronized motions of the twin shake tables. In this test, the actuators of the east table, which was the “slave” table, did not receive the input motion from the west table and did not move. The test was promptly aborted, yet some of the anchor bolts located on the bridge structure failed in shear and were replaced. Figure I.5 of Appendix I shows the response spectra generated from this test.

Commenting on the shake table fidelity of the first four phases, it was observed that the response spectra of the recorded motions ranged slightly over the desired spectra for the two horizontal components and matched very well for the vertical component, independently of the seismic intensity, which did not exceed Level 2 for the tri-axial and bi-horizontal tests of Test Phases 1, 3 and 4. Regarding the longitudinal component, the peak spectral acceleration around 0.2sec was

usually higher than the desired value, while the peak spectral acceleration around 0.3sec was usually lower than the desired value, even for high seismic levels conducted during Test Phase 2. This result may be correlated with the second and third modes of vibrations of the test structure, which range around 0.2sec. It should also be noted that the accuracy of the shake table motions improved for seismic tests of Phase 4. This improvement can be attributed to the fact that the fundamental frequencies of the benchmark structure did not significantly change from Test Phase 3 and tuning of the shake tables based on the results of Phase 3 was more effective.

The same observations drawn previously apply also for Test Phase 5. Moreover, the significant increase in the stiffness of the test building, especially in the longitudinal direction, led to some discrepancies between the recorded and desired motion in this direction. More specifically, the table motion consistently overshoot around 0.12sec, for seismic tests of Levels 2, 3 and 4, which is close to the third natural frequency of the structure of Phase 5. The fidelity during the final tri-axial Level 5 test (NWP5S11) was reasonable over the range of natural periods of the test structure. Note that for this test the target amplitude was set to 85% of the actual Rinaldi record to account for overshooting, based on the results from the previous seismic test of 25% of the Rinaldi record (Test NWP5S09).

Another significant issue was the rocking response of the shake tables. Due to the high base overturning moment, which was close to the specified nominal limits, the rotational stiffness of the tables was not high enough to prevent them from rotating along both horizontal directions. Rocking was more pronounced during Test Phase 5, where the building was stiffer than previous phases and the seismic tri-axial and bi-axial tests exceeded Seismic Level 2. Moreover, rocking was greater along the transverse (north-south) direction of the structure because the stronger ground motion component was applied in this direction and the overturning moment was higher.

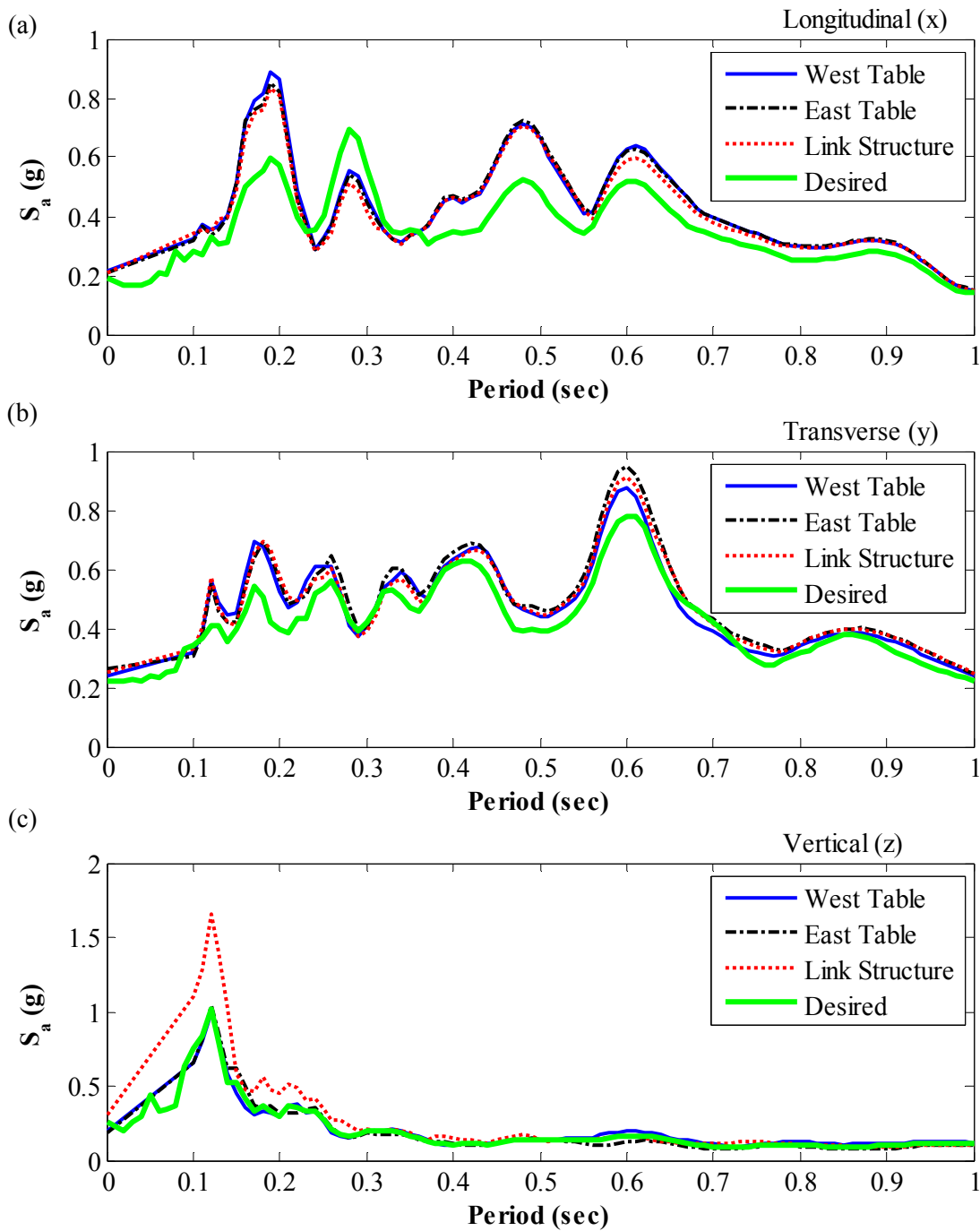


Figure 7.2: Acceleration response spectra of shake table motion for 5 % damping in (a) longitudinal, (b) transverse, and (c) vertical direction, for test NWP1S17

In addition, the shake tables and the bridge were connected along the longitudinal direction, thus, the overturning stiffness was much higher due to the composite action of the tables. Figure 7.3

presents the maximum angle of rotation in the transverse direction that was recorded from the feedback sensors on the tables, for the seismic tests of Test Phase 5 above Seismic Level 2. The vertical axis on the right is the equivalent maximum roof displacement at the height of the roof eaves H_{Roof} , equal to 206 in., assuming a rigid structure. Eq. (7.1) shows how the roof displacement D_{Roof} can be calculated for a base angle of rotation Φ of 0.6 deg. The maximum angle of rotation ranged from around 0.1deg for the Level 2 seismic tests up to almost 0.5 deg for the Level 5 final tri-axial test. The maximum angle of rotation was greater for the east table, than for the west table. This difference is attributed to the fact that the east table was supporting a greater portion of the test structure and the overturning moment was, therefore, greater than the overturning moment applied on the west table.

$$D_{\text{Roof}} = H_{\text{Roof}} \cdot \Phi = 206 \cdot (0.6 \cdot \pi / 180) = 2.16 \text{ in.} \quad (7.1)$$

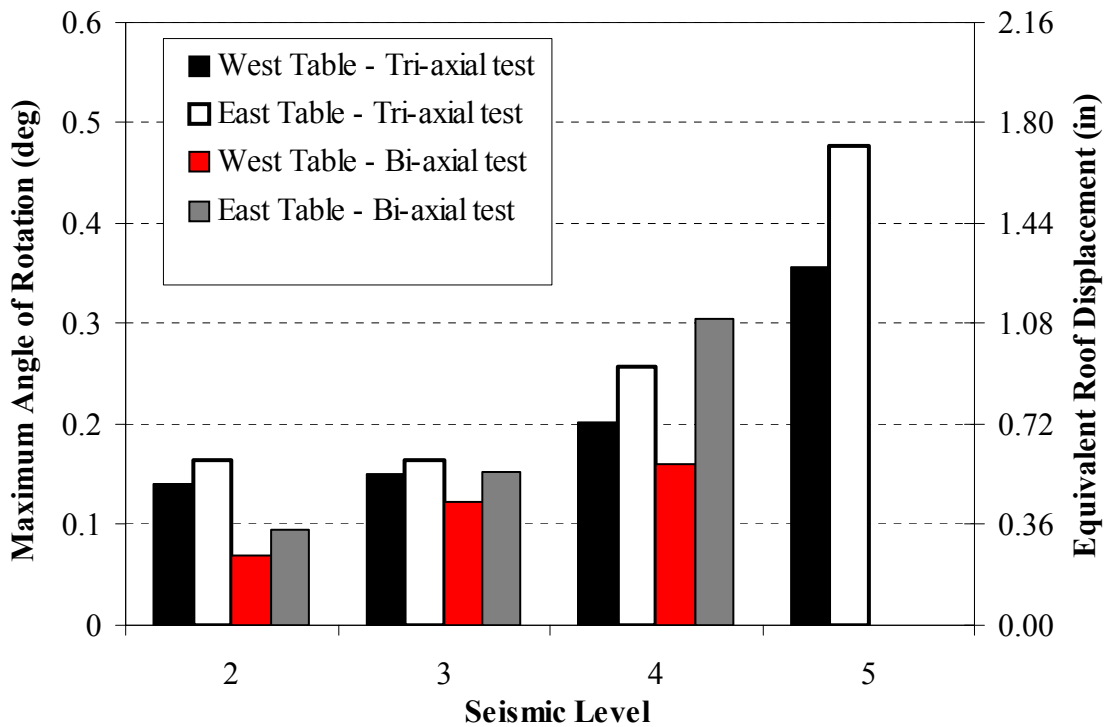


Figure 7.3: Maximum angle of rotation of the twin shake tables in the transverse direction for seismic tests of Test Phase 5

7.2 Visual Damage Observations

Visual damage observations were conducted almost after each seismic test. Appendix J contains selected visual damage identification photos that represent the major types of damage of the structural and non-structural members, which was identified in each test phase. Some of these photos are presented in Figure 7.4 in a smaller scale. Table 7.1 summarizes the types of damage observed in the three major components of the test structure: the wood shear walls that consisted of wood framing and OSB sheathing, the gypsum wallboard and the exterior stucco. Four different damage states are defined and correlated with the peak inter-story drift recorded near the damaged location. Damage states 1 to 3 occurred in the wood shear walls during the first two test phases, since the inter-story drift did not exceed 2% during those tests. Similarly, damage state 3 was observed on the gypsum wallboard applied on structural and partition walls during Test Phases 3 and 4. Finally, damage state 4 was observed on the stucco during Test Phase 5.

There were numerous occurrences of hairline cracking of sill plates even for small values of inter-story drifts. Since sill plates were not replaced during the different test phases, cracking propagated and led to significant splitting of the first floor sill plates, especially at the garage wall, following the tri-axial Level 5 test of Phase 5. Cracking was also propagated to hold-down vertical studs. Damage to gypsum wallboard was observed mainly in the form of diagonal cracking in wall openings, crushing of drywall corners and buckling of wallboard at higher drifts. A portion of the ceiling of the second floor hallway, connecting the two main rectangular units of the structure, failed under the Test Level 5 shaking. Damage to stucco was mostly concentrated at the garage wall line, where significant cracking and spalling was observed. Cracking of stucco was also visually identified around the periphery of the benchmark structure following the final tri-axial test of Phase 5.

Table 7.1: Damage chart based on the visual damage observations

Damage State	Peak Inter-story Drift (%)	Damage Description		
		Wood Framing and OSB Sheathing	Gypsum Wallboard (GWB)	Stucco
1	0.1-0.5	<ul style="list-style-type: none"> ✓ Minor splitting of sill plates ✓ Minor cracking of vertical studs 	<ul style="list-style-type: none"> ✓ Minor hairline cracking of GWB 	<ul style="list-style-type: none"> ✓ Minor cracking of stucco at bottom and top corners of garage wall opening
2	0.5-1.0	<ul style="list-style-type: none"> ✓ Partial nail pull-out (Fig. 7.4a) ✓ Minor splitting of top plates ✓ Propagation of sill plate splitting and cracking 	<ul style="list-style-type: none"> ✓ Cracking of GWB and diagonal crack propagation at door openings ✓ Partial screw pull-out ✓ Cracking of GWB at ceiling-wall connection 	<ul style="list-style-type: none"> ✓ Cracking and spalling of stucco at garage wall (Fig. 7.4h)
3	1.0-2.0	<ul style="list-style-type: none"> ✓ Permanent differential movement of adjacent panels (Fig. 7.4b) ✓ Sheathing pull-out at wall corners ✓ Major cracking and splitting of sill and top plates 	<ul style="list-style-type: none"> ✓ Crushing of GWB at wall corners (Fig. 7.4c) ✓ Tape cracking of GWB 	<ul style="list-style-type: none"> ✓ Significant crack propagation around garage wall ✓ Cracking of stucco on door and window openings
4	>2.0	<ul style="list-style-type: none"> ✓ Propagation of cracking and total splitting of sill plates at garage wall (1/2 in. wide) (Fig. 7.4e) ✓ Cracking of studs above anchor bolts (Fig. 7.4g) ✓ Possible failure of anchor bolts 	<ul style="list-style-type: none"> ✓ Separation of parts of GWB from the ceiling (Fig. 7.4d) ✓ Buckling of GWB at door openings (Fig. 7.4f) 	<ul style="list-style-type: none"> ✓ Cracking and spalling of stucco at the corners of the structure

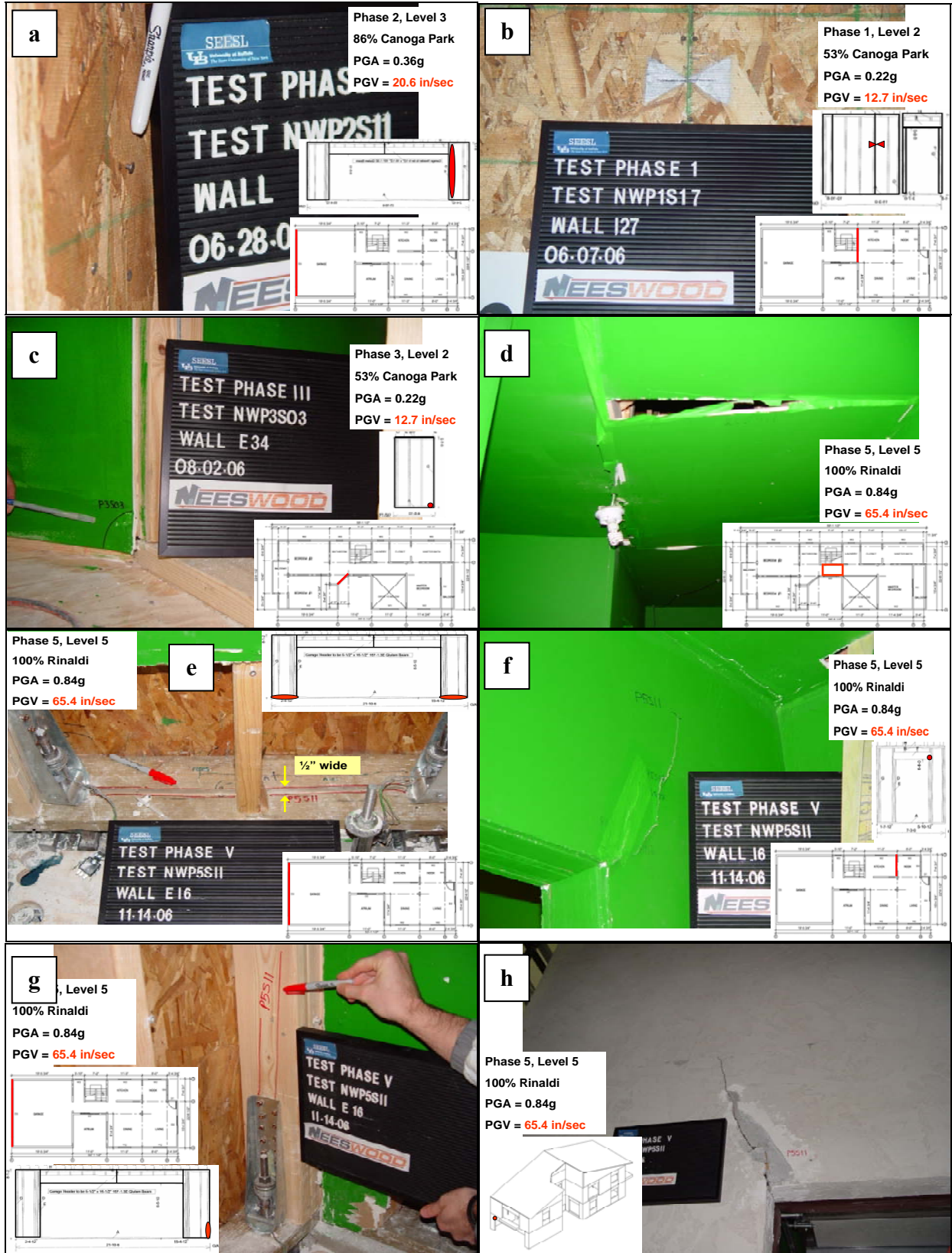


Figure 7.4: Selected visual damage identification photos

7.3 Inter-story Drift Measurements

The inter-story displacement time-histories of the benchmark structure, generated from the measurements of the linear string potentiometer installed along the north and west side of the townhouse, are presented in Appendix K, for each seismic test conducted. As indicated in these figures, the inter-story displacement time-histories for each building wall line were computed by subtracting the lower floor displacement from the top floor displacement, in the time domain. In addition, each displacement time-history was corrected to account for the rotation of the shake tables, since the linear string potentiometers were measuring the displacements of the floor levels with respect to a stationary reference system. For a given base angle of rotation and assuming that the structure was rigid, the string potentiometers would record a maximum displacement for each level equal to the maximum base rotation multiplied by the height of the given level, resulting in non-zero maximum inter-story displacements.

Figure 7.5 and Eqs. (7.2) and (7.3) present how the various displacement time-histories of the first and second floor levels, $\mathbf{D}_1(t)$ and $\mathbf{D}_2(t)$, respectively, were corrected to account for the shake table rotation $\Phi(t)$, with respect to the two orthogonal horizontal directions. Measurements from the west unit of the structure were corrected with table rotation data from the west table and, similarly, measurements from the east unit were corrected with rotation data from the east table.

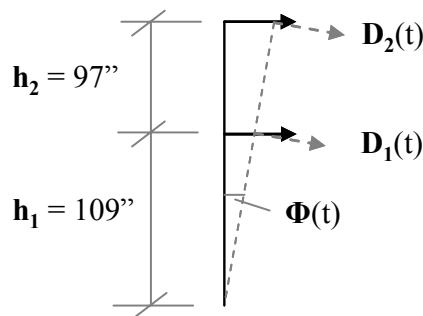


Figure 7.5: Correction of floor displacement time-histories for shake table rotation

$$\mathbf{D}_1(t)_c = \mathbf{D}_1(t) - \Phi(t) \cdot \mathbf{h}_1 \quad (7.2)$$

$$\mathbf{D}_2(t)_c = \mathbf{D}_2(t) - \Phi(t) \cdot (\mathbf{h}_1 + \mathbf{h}_2) \quad (7.3)$$

Figure 7.6 presents the maximum inter-story drifts, recorded along the six major building wall lines, for Level 2 tri-axial tests of Phases 1, 3, 4 and 5. The inter-story drift for each case was computed by dividing the maximum inter-story displacement by the floor height, which was equal to 97 in. for both floors. Note that in Figure 7.5 the first floor height includes the height of the floor joists, which was 12 in. Regarding the response at the first floor, higher drifts were consistently recorded along the garage wall line (Line 6), while maximum drifts were lower moving from the west to the east side of the structure (from Line 6 towards Line 2), for all test phases, as far as the transverse direction is concerned. In the longitudinal direction, the maximum drift of the south side (Line A) was slightly higher than the drift of the north side, except for Test Phase 3, but significantly lower than that recorded along the transverse direction. Note that only the south side of the west unit was instrumented with string potentiometers and there were no displacement measurements for the south side of the east unit. Therefore, results for Line A refer to the inter-story drifts of the west unit only. Inter-story drifts for the south side of the east unit were provided by the diagonal string potentiometers that measured the deformations of selected shear walls. These results are presented in Section 7.5.

At the second floor, along the transverse direction, maximum drifts were recorded on the internal wall Lines 4 and 5, while the drifts on the external wall lines were lower. This was not the case for Test Phase 5, for which the maximum drifts of the west unit of the benchmark structure was higher than the drifts of the east unit. Along the longitudinal direction, drifts were lower along Line A, compared to Line D, except for Test Phase 1.

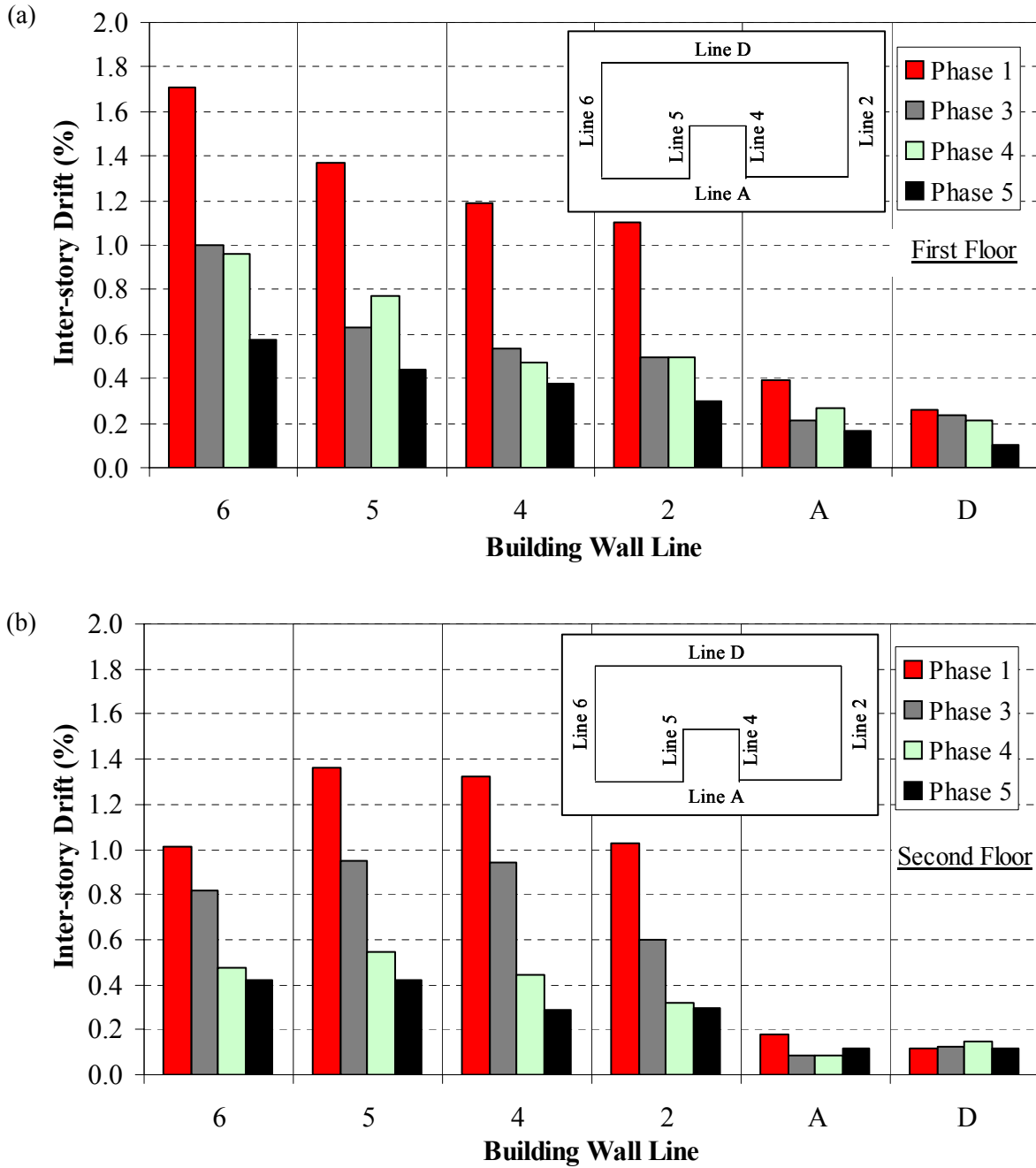


Figure 7.6: Maximum inter-story drifts for Seismic Level 2 tri-axial tests of Phases 1, 3, 4 and 5 for (a) first floor, and (b) second floor

Commenting on the variability of the response throughout the test phases, it is evident that the application of gypsum wallboard on the interior side of structural walls significantly reduced the

displacement response of both floors of the benchmark structure. The reduction of the maximum recorded inter-story drifts from Phase 1 to Phase 3, along the transverse direction, was of the order of 40-50%. The application of gypsum wallboard on the partition walls and the ceilings did not affect much the first floor drifts, but further reduced the drifts of the second floor. This is attributed to the fact that the first floor had few partition walls (none in the garage – west unit) and the stiffness and strength were not particularly affected. However, the effect was more pronounced at the second floor where the maximum reduction of drifts between Test Phase 4 and 1 was of the order of 60%.

Besides the stiffness contribution from the partition walls, the significant reduction of inter-story drifts on the second floor (from Phase 3 to Phase 4) can also be explained by the increase of diaphragm effect on the roof level. The in-plane stiffness of the roof diaphragm was increased because of the application of the gypsum wallboard to the bottom chords of the roof trusses. As a result, it also increased the load sharing effect between the transverse wall lines (Lines 2, 4, 5, and 6) and thus reduced the drifts on the second floor. On the other hand, the gypsum wallboard ceiling had minimal effect on the floor diaphragm since the structural floor system (plywood panels and the floor joists) alone provided enough in-plane stiffness to “act” as a rigid diaphragm.

The application of exterior stucco further reduced the maximum drifts at both floor levels. The reduction between Test Phase 5 and 1 was of the order of 70%.

Focusing on Test Phase 5, which included tests of all different seismic intensities, Figure 7.7 presents the maximum recorded drifts along the six major building wall lines, throughout the testing sequence.

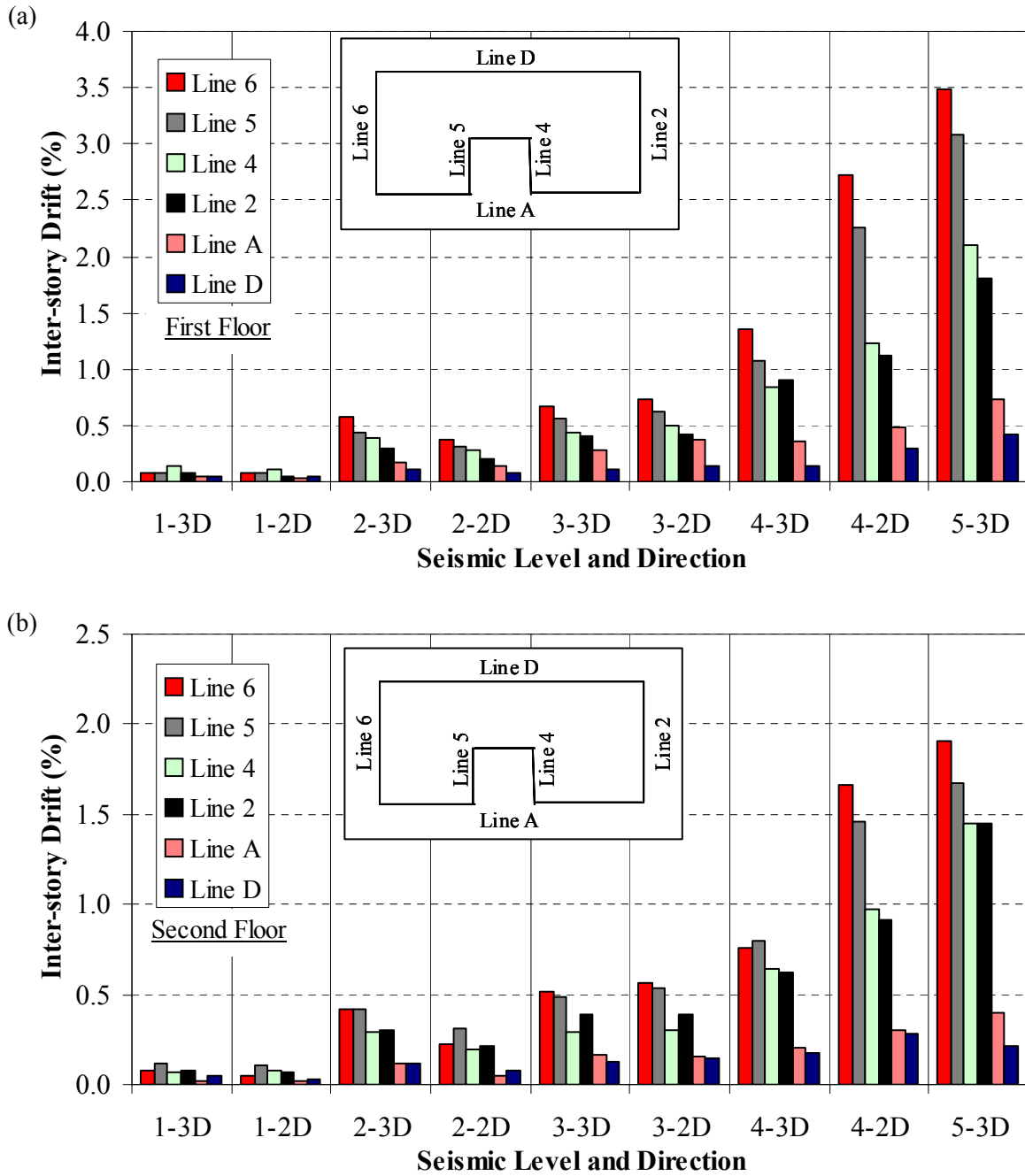


Figure 7.7: Maximum inter-story drifts for Phase 5 seismic tests for (a) first floor, and (b) second floor

The displacement profile was similar to that described previously for the tri-axial test of Level 2.

The maximum inter-story drift was consistently recorded along the garage wall line, while peak

drifts were lower moving from the west to the east side of the structure. It is interesting to note that the same profile was observed for the second floor as well. This observation is different from the response of the test structure during tests of Phases 1, 3 and 4, for which the internal wall lines of the second floor had higher drifts than the external ones, always along the transverse direction. This indicates the different effects of gypsum wallboard and exterior stucco. Application of drywall increases the stiffness and possibly the strength of a wood shear wall directly affecting only the properties of that particular structural element of the structure. On the other hand, due to the fact that stucco is applied continuously along the entire exterior face of the building, there is an increase of the stiffness and strength of the whole structure, independent of the floor levels. In fact, stucco acts as a single structural element that connects the base and the top of the building, being also attached to the intermediate floor levels. This effect forces the two floor levels, in the case of the benchmark structure, to move along a similar displacement profile.

An interesting observation is the distribution of the building drifts between the two floors of the test structure as its response increases with seismic intensity. This is graphically illustrated in Figure 7.8, where the ratios between the second floor peak drifts are normalized by the first floor peak drifts at the same wall lines and plotted for the seismic tests of Phase 5. Only the four building lines along the transverse direction are included in Figure 7.8. This graph shows that as the seismic intensity is amplified, the drift ratios are decreasing, which indicates that a greater portion of the total building displacement occurs at the first floor. Eventually, a first floor side-sway collapse mechanism would be the most probable scenario in case of a potentially very destructive earthquake. This conclusion verifies numerical studies that have focused on the seismic collapse analysis of two and three story woodframe buildings [15].

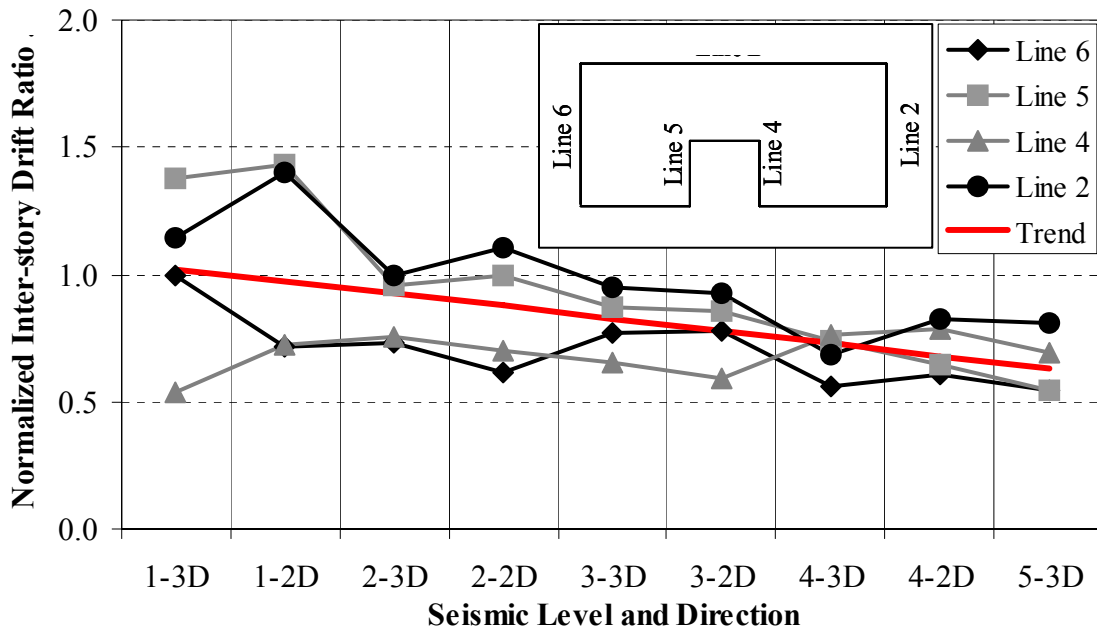


Figure 7.8: Second floor drift normalized by first floor drift of the same wall line along the transverse direction, for Test Phase 5

Concluding, the benchmark structure in general behaved well. Even for the Level 5 tri-axial test that represented an MCE event with a returning period of 2475 years (2% probability of exceedance in 50 years), the maximum drift at the garage wall was 3.5% (residual drift was 0.2%). The performance objective of collapse prevention was certainly achieved and there were no signs of the benchmark structure approaching the “collapse point”. Note that the FEMA 356 [16] uses 3% as the drift limit for collapse prevention.

Comparing the peak recorded drift at the garage wall for the tri-axial test of Seismic Level 4 (100% DBE) of Phase 5, which was less than 1.4%, with the peak drift at the same wall for the tri-axial test of Seismic Level 2 (44% DBE) of Phase 1, which was more than 1.7%, the significant contribution of wall finish materials in improving the seismic response of the test building is readily illustrated. The Phase 1 building, with no wall finish materials applied, almost

reached the 2% code drift limit under a seismic excitation that represented only 44% of the amplitude of the expected Design Basis Earthquake (DBE) event. On the other hand, the Phase 5 building, incorporating all structural and non-structural components and wall finish materials, demonstrated a better response under a 100% DBE event.

7.4 Absolute Acceleration Measurements

The absolute acceleration time-histories, recorded along the south and west side of the benchmark structure, are presented in Appendix L, for each seismic test conducted. Based on these measurements, the peak absolute acceleration values, measured for all wall lines during all test phases, are summarized in Figures 7.9 and 7.10.

Figure 7.9 presents the peak acceleration measurements from Level 2 tri-axial seismic tests that were conducted across Phases 1, 3, 4 and 5. Figure 7.10 summarizes the peak values recorded along the seismic tests of Test Phase 5, exclusively.

There is not a great variability between peak values recorded during the Seismic Level 2 tests across the different test phases. Maximum peak accelerations were observed at the garage wall (Line 6) for both floor levels. There is no clear trend to characterize the effect of different wall finish materials on the acceleration response of the structure. However, peak values are slightly higher for the Phase 1 building for most of the wall lines.

Regarding Phase 5 response, the peak accelerations were increased with increased level of intensity. Maximum second floor and roof level accelerations reached 1.3g for the final tri-axial Level 5 test. The peak acceleration during Phase 5, equal to 1.7g, was, however, recorded during the bi-axial Level 4 test, at the roof level along Line A.

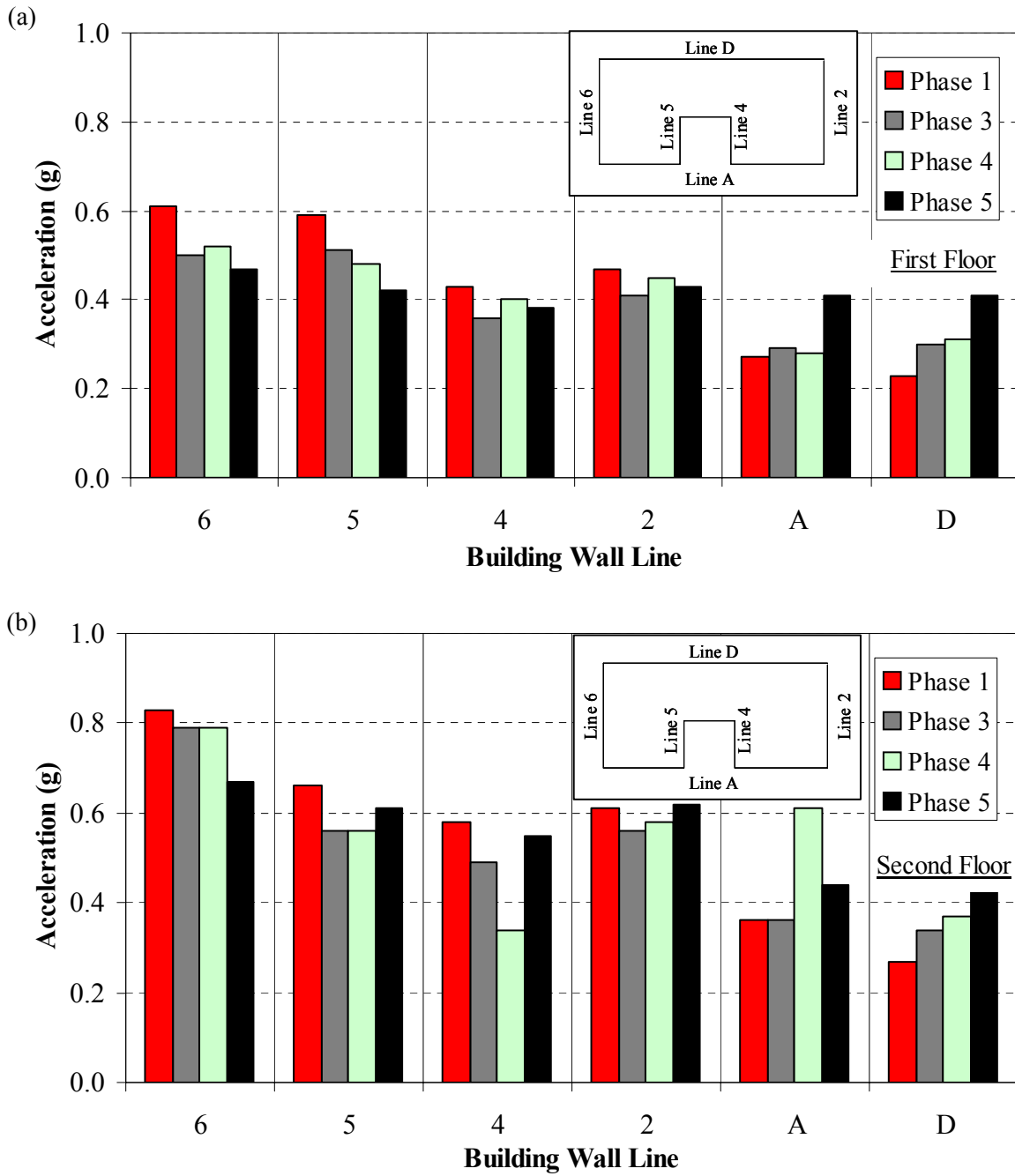


Figure 7.9: Maximum absolute acceleration measurements for Seismic Level 2 tri-axial tests of Phases 1, 3, 4 and 5 for (a) first floor, and (b) second floor

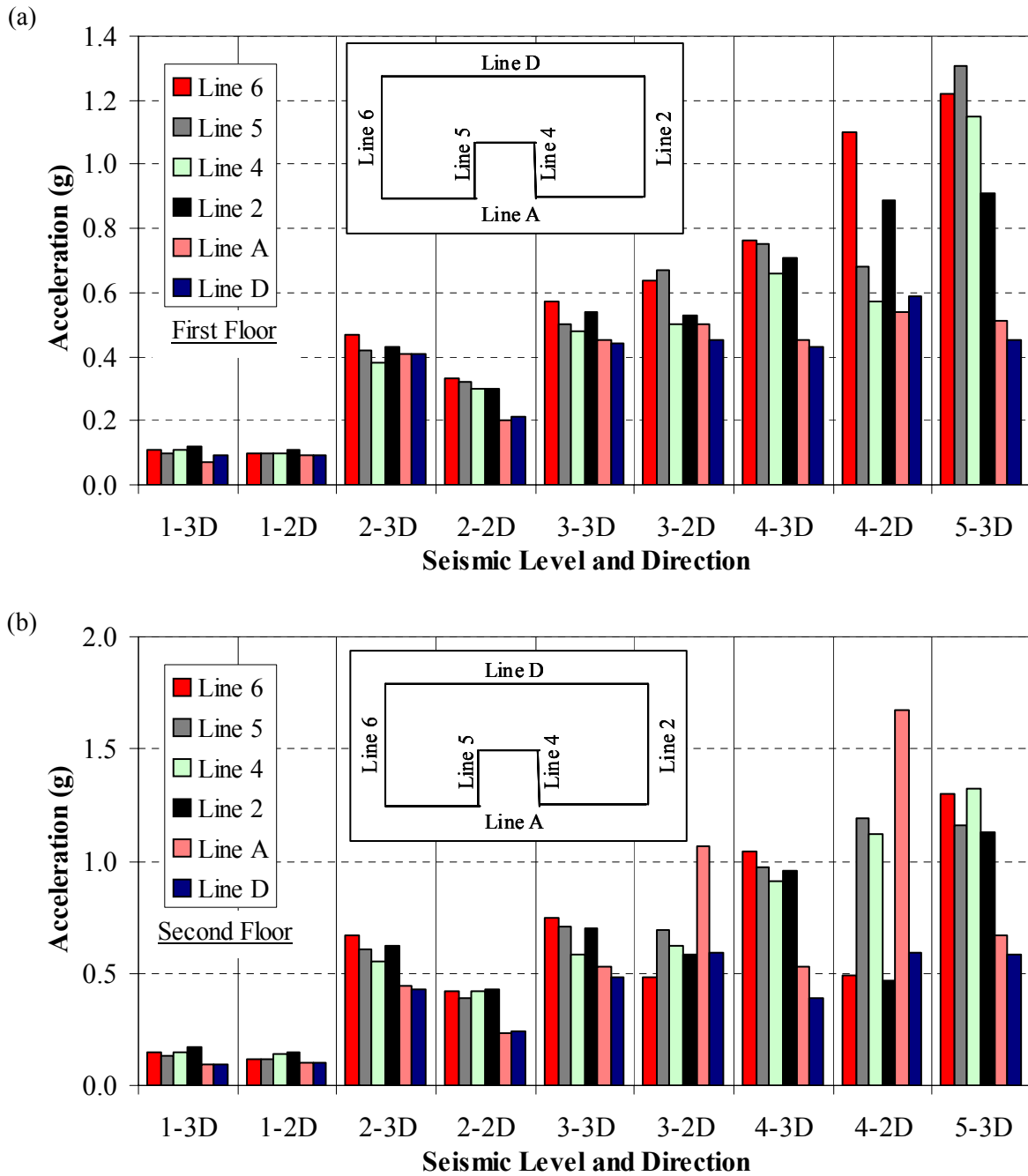


Figure 7.10: Maximum absolute acceleration measurements for Phase 5 seismic tests for (a) first floor, and (b) second floor

7.5 Wall Deformation Measurements

Appendix M presents the displacement time-histories derived from the diagonal string potentiometers that were installed across selected structural and partition walls of the test structure, for all seismic tests conducted. The recorded data were modified to transform the diagonal deformations of each instrumented wall, measured by the diagonally oriented string potentiometers, to the equivalent horizontal inter-story displacement. Table 7.2 contains the angle of inclination Φ of each diagonal potentiometer with respect to the horizontal direction, as shown in Figure 7.11, as well as the final scale factor **SF** that was applied to the test data to yield the correct horizontal displacement. Equation (7.4) shows how Φ and **SF** were computed based on the horizontal and vertical distances **L** and **H**, respectively, between the two ends of each string potentiometer. The potentiometers that measured the wall deformations were attached to the center of the top and bottom plates of the walls, while those measuring the displacement between story diaphragms were attached to the floor sheathing.

$$\mathbf{SF} = 1/\cos(\Phi) = 1/\cos(\tan^{-1}(\mathbf{H}/\mathbf{L})) \quad (7.4)$$

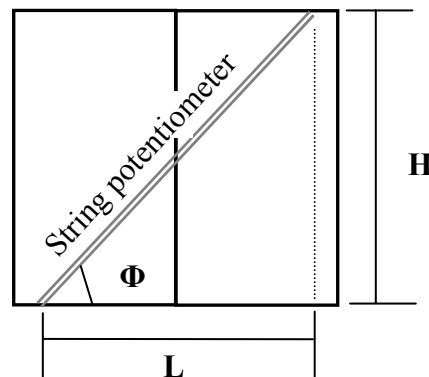


Figure 7.11: Typical configuration of a string potentiometer installed across a shear wall

Table 7.2: Angle of inclination and scale factor for each diagonal string potentiometer, throughout the testing phases

Test Phase 1, 2 and 3			Test Phase 4 and 5		
Nomenclature (see Table E.3)	Φ (deg)	Scale Factor SF	Nomenclature (see Table E.4)	Φ (deg)	Scale Factor SF
S1	73.8	3.58	S1	73.8	3.58
S2	26.9	1.12	S2	26.9	1.12
S3	50.1	1.56	S3	49.1	1.53
S4	64.4	2.31	S4	64.4	2.31
S5	52.4	1.64	S5	52.4	1.64
S6	76.5	4.27	S6	76.5	4.27
S7	49.1	1.53	S7	49.1	1.53
S8	38.7	1.28	S8	38.7	1.28
S9	26.1	1.11	S9	26.1	1.11
S10	59.2	1.95	S10	59.2	1.95
S11	33.3	1.20	S11	33.3	1.2
S12	64.4	2.31	S12	64.4	2.31
S13	56.0	1.79	S13	56	1.79
S14	40.1	1.31	S14	40.1	1.31
S15	49.1	1.53	S15	49.1	1.53
S16	47.0	1.47	S16	47	1.47
S17	50.1	1.56	S17	50.1	1.56
S18*	50.1	1.56	S18	48.3	1.5
S19*	49.3	1.53	S19	24.2	1.1
S20**	49.1	1.53	S20	38.3	1.27
S21**	48.3	1.50	S21	37.1	1.25
S22**	34.2	1.21			
S23**	32.8	1.19			

* Test Phase 1 and 3

** Test Phase 1 only

Figures 7.12 and 7.13 present the wall deformations measured during the Seismic Level 2 tri-axial tests of Phases 1, 3, 4 and 5, for the first and the second floor, respectively. The top graph

contains the peak wall deformations for each specific instrumented wall, as identified in the legend. The bottom graph presents the peak wall deformations, normalized by the corresponding peak inter-story deformation at the specific building wall line. The peak inter-story displacements were extracted either from the external linear string potentiometers (presented in Section 7.3), at those building wall lines where that data were available, or from the diagonal string potentiometers that were measuring the deformation between the adjacent floor levels. This explains why there are no wall-diaphragm deformation ratios presented for walls E9-10 and E24-25. These walls were located at the south side of the east unit, where no inter-story displacements were recorded.

The wall displacement measured by the diagonal potentiometers is associated primarily with the shear (racking) deformation of the wall, composed of shear in the sheathing panels, slipping of the nails, and bending deformations of the framing, which can be observed in walls with relatively high aspect (height over length) ratio. In cases where the lower end of the diagonal potentiometers originated from the bottom corner of a shear wall with a hold-down installed, such as the potentiometer installed on the garage wall (E16), the wall deformation included also any uplift of the hold-down stud from the sill plate. Components of the total inter-story displacements that are not measured by the diagonal potentiometers are the slipping of the bottom sill and the top plate and the uplift of the sill plate from the foundation.

String potentiometers across walls I2 and I12 were installed only in Phases 1 to 3, while across wall I21 only in Phases 4 and 5. It should also be noted that no peak wall deformation values are included in cases where the maximum displacement was less than 0.01 in. This is the case especially for the second floor walls.

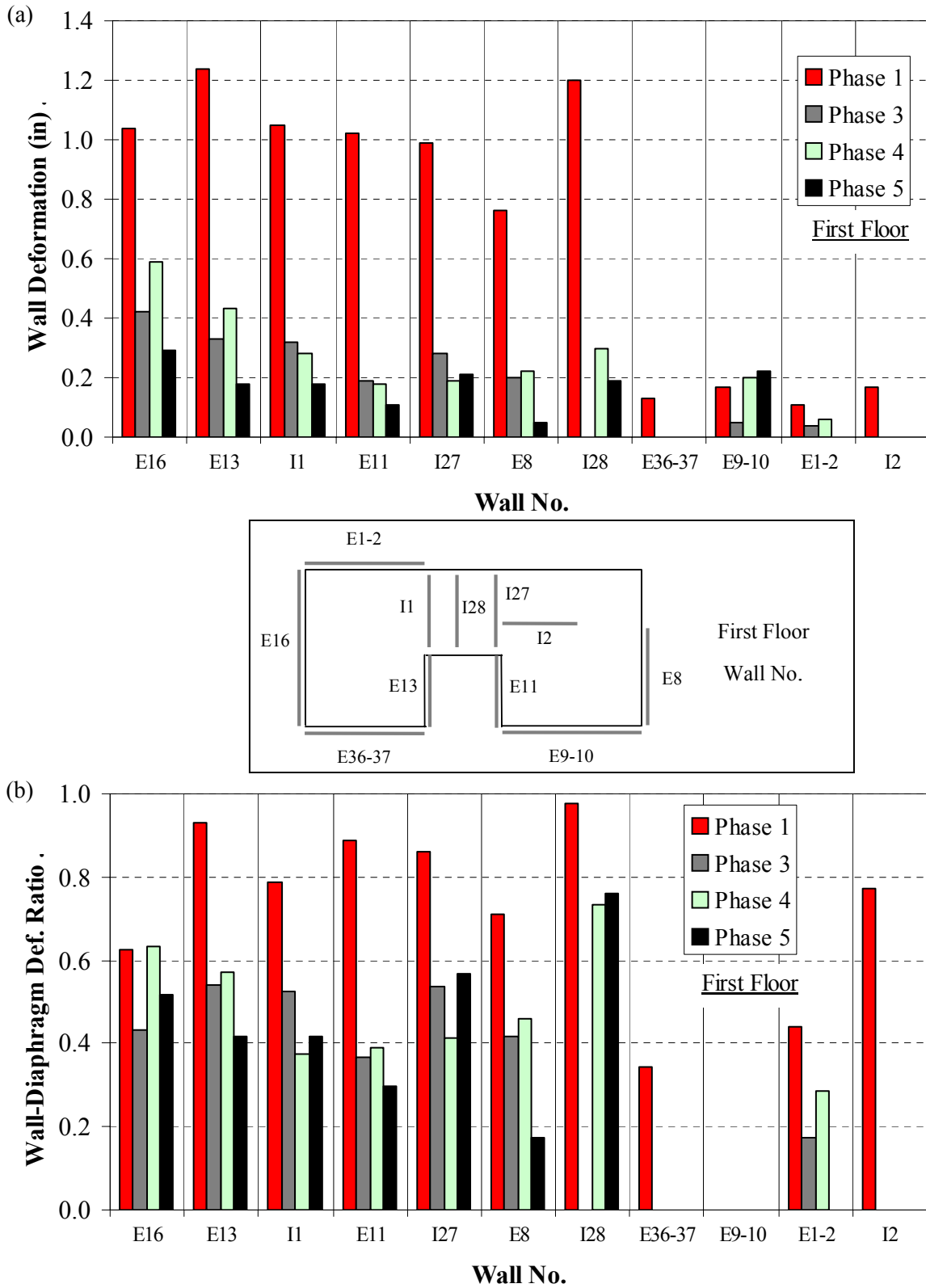


Figure 7.12: (a) Wall deformation, and (b) wall-diaphragm deformation ratio of first floor walls, for Seismic Level 2 tri-axial tests of Test Phase 1, 3, 4 and 5

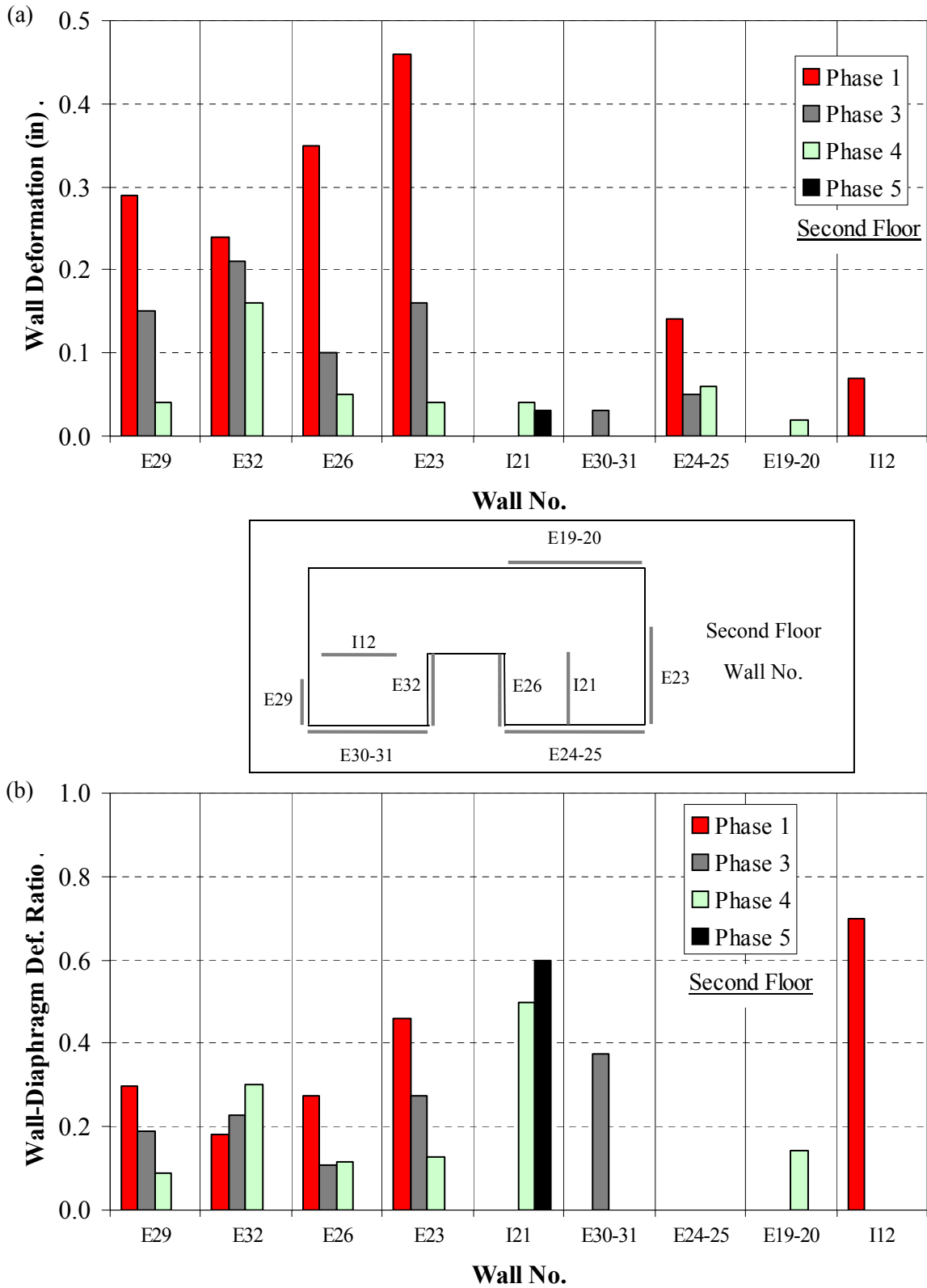


Figure 7.13: (a) Wall deformation, and (b) wall-diaphragm deformation ratio of second floor walls, for Seismic Level 2 tri-axial tests of Test Phase 1, 3, 4 and 5

From the recorded displacements of the first floor walls, it can be observed that the wall deformations during Test Phase 1 were much greater than what the walls experienced during the other test phases, especially for walls oriented in the transverse (north-south) direction. The displacement profile is similar to that of the inter-story displacements (see Fig. 7.6), which included higher deformations along the garage wall line. Moreover, the south side of the east unit (E9-10) experienced higher drifts than the south side of the west unit (E36-37). Similar trends were observed for the walls of the second floor, although what was particularly interesting is that the peak deformations during Test Phase 4 were lower than those of Test Phase 3. Also, during Test Phase 5, the second floor walls were deformed by less than 0.01 in., the latter showing that the application of exterior stucco significantly increased the in-plane stiffness of the second floor walls.

The wall-diaphragm deformation ratios for the first floor walls of Phase 1 building, along the transverse direction, ranged around 0.8, while the same ratios reduced further to 0.4-0.5 for the subsequent test phases. The second floor ratios further decreased to values around 0.3 for all test phases, which reveals that other components of deformation (top or bottom plate slippage or uplifting) were more pronounced for the second floor walls.

It was also observed that interior structural (I1 and I 27) or partition (I28, I2, I12 and I21) walls demonstrated a high wall-diaphragm deformation ratio, well above 0.5 for most of the cases. Especially regarding the second floor, the interior walls had the highest deformation ratios.

Similarly to the previous figures, Figures 7.14 and 7.15 present the wall deformation and corresponding ratios from the Phase 5 seismic tests, for the first and second floor, respectively. The results from the Seismic Level 1 tri-axial and bi-axial tests were not included, since the wall deformations were lower than 0.01 in. almost for all cases.

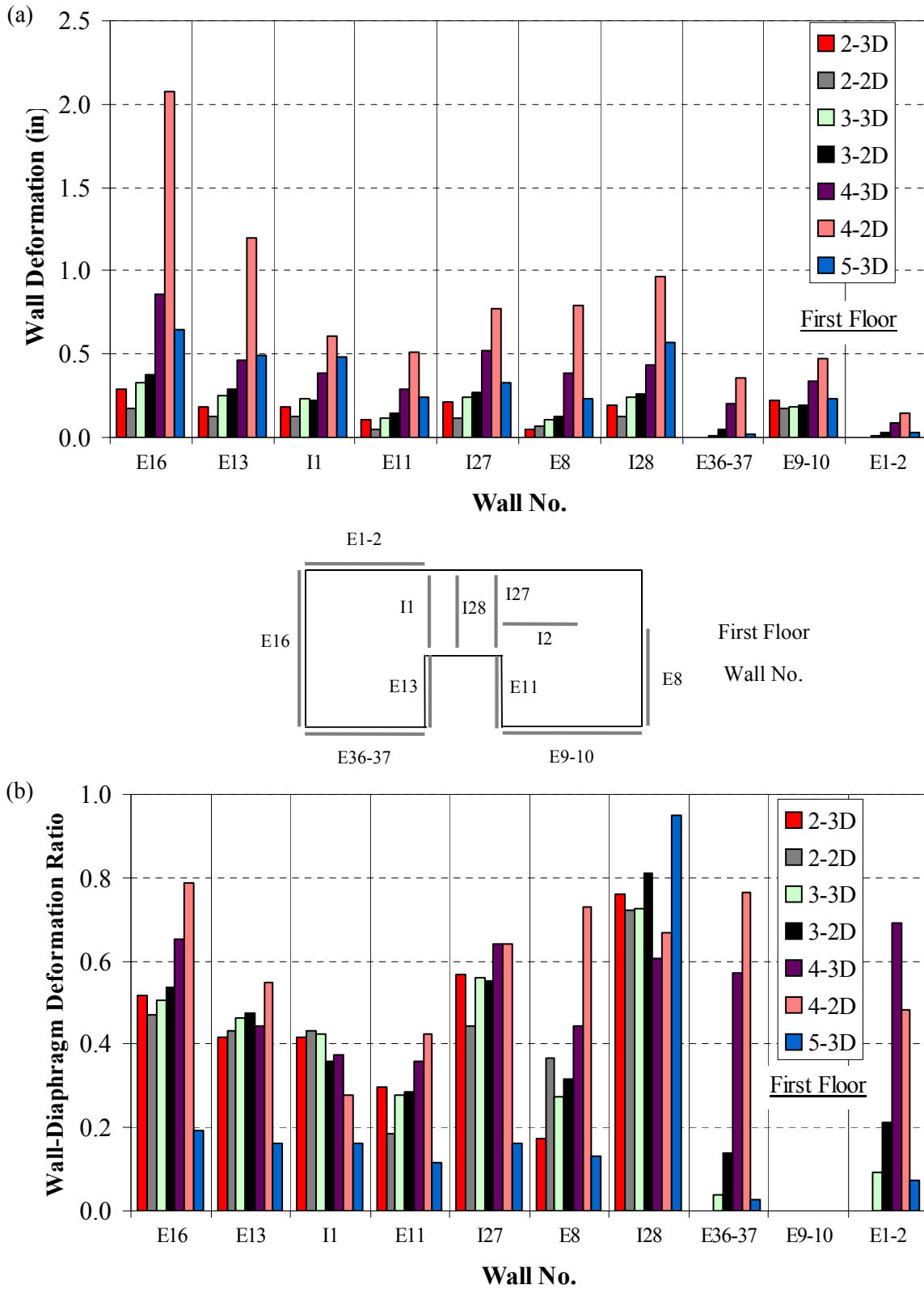


Figure 7.14: (a) Wall deformation, and (b) wall-diaphragm deformation ratio of first floor walls, for seismic tests of Test Phase 5

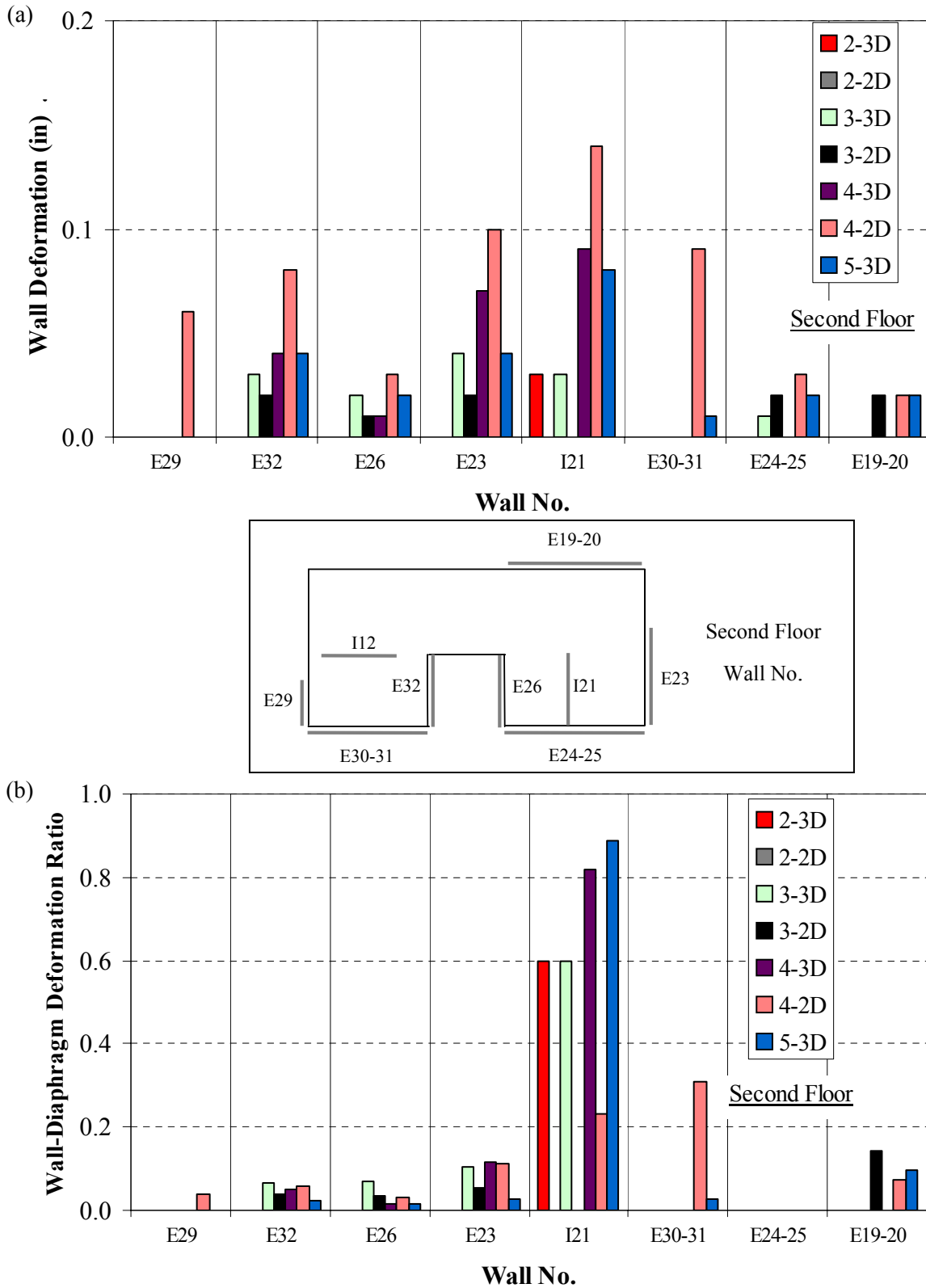


Figure 7.15: (a) Wall deformation, and (b) wall-diaphragm deformation ratio of second floor walls, for seismic tests of Test Phase 5

The maximum wall deformations were observed for the bi-axial Level 4 test, for both floor levels. Even while the peak inter-story drifts were higher during the final tri-axial Level 5 seismic test, the wall deformations were much lower compared to the bi-axial Level 4 test. This result can only be attributed to the significant rocking response of the benchmark structure during the final tri-axial test, a response which was even visually observed from the recorded videos. This resulted in very low deformation ratios, of the order of 0.2, for most of the first floor walls on the contrary to the ratios between 0.3 and 0.6 that were observed during previous seismic tests. No specific trend was identified to relate the deformation ratio with the excitation intensity, based on these particular test data. Similarly to what observed throughout the other test phases, the south side of the east unit was deformed more than the south side of the west unit, and both had higher displacements compared to the north side of the structure. Second floor wall deformations were only a small portion of the total inter-story displacements, of the order of 10%, for most of the cases.

It is important to note that the wall-diaphragm deformation ratios clearly indicate that only a portion of the inter-story drift between two adjacent floors is transmitted into wall racking deformations, particularly when wall finishes are included in the structural configuration. Therefore, results of racking (shear) tests of wall specimens must be interpreted carefully, since the behavior of the wall specimen, dictated by the tests, is different than the real behavior when the wall is incorporated in a structure.

Concluding, the wall deformations were identified throughout the significant bi-axial and tri-axial tests of Test Phases 1, 3, 4 and 5. It is important to identify the contribution of other deformation components, such as slipping and uplifting, of the walls before drawing safe

conclusions on the effect of wall finish materials and excitation intensity on the structural performance of wood shear walls.

7.6 Global Hysteretic Response

Appendix N presents the global hysteresis loops, in terms of base shear force and building roof central relative displacement, recorded along the two principal orthogonal directions, for all seismic tests conducted. Similarly, Appendix O contains the inter-story hysteresis loops, in terms of story shear force and story central relative displacement, recorded along the two principal directions, for all seismic tests conducted. The forces at each floor level were computed by multiplying the recorded absolute acceleration measurements by the tributary mass near the specific locations of the accelerometers (see Figure 6.1 and Table F.1 of Appendix F). This means that the calculated forces include both the resistant force generated by the wall deformation and the damping force that is inherent in the system. The displacements were calculated from the linear string potentiometers installed between the benchmark structure and an absolute reference, as described in Section 7.3. The central displacement along the transverse direction was computed as the average displacement of Wall Lines 4 and 5, while the central displacement along the longitudinal direction was calculated as the average displacement of Wall Lines A and D. The maximum and minimum force and displacement values are indicated on each figure of Appendices N and O by a black circle. Note that the maximum (or minimum) displacement and force may not occur at the same time, thus the point indicated by the circle may not be part of the data points.

Some of the global hysteresis loop plots that are included in Appendix N are repeated here for comparison purposes. Figure 7.16 presents the global hysteresis loops derived from the Seismic Level 2 tri-axial tests of Phases 1, 3, 4 and 5. Similarly, Figure 7.17 summarizes the global

hysteresis loops derived from the five tri-axial seismic tests of Phase 5. Both figures include loops in the two orthogonal directions of the benchmark structure.

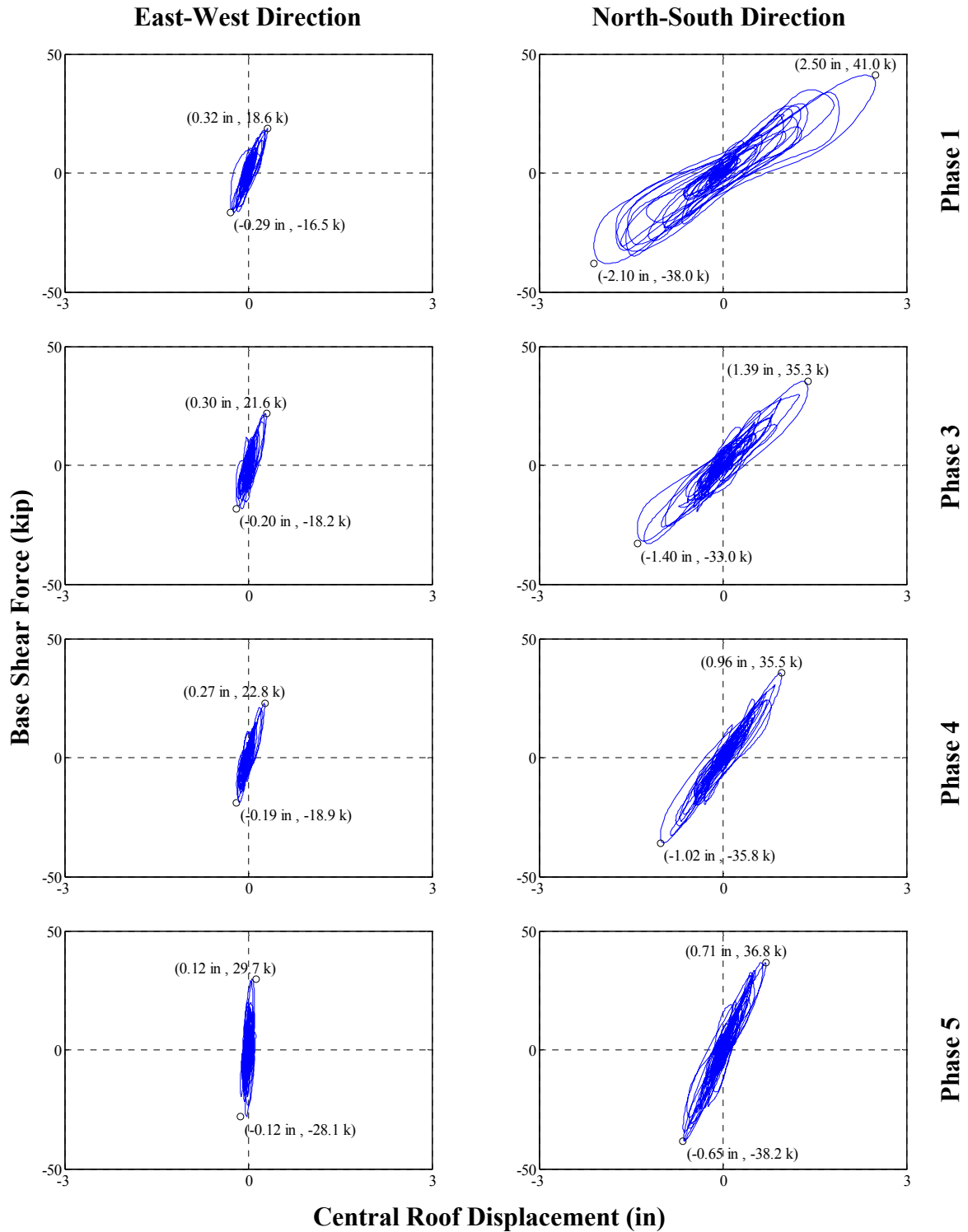


Figure 7.16: Global force-displacement hysteresis loops for Seismic Level 2 tri-axial tests of Phases 1, 3, 4 and 5

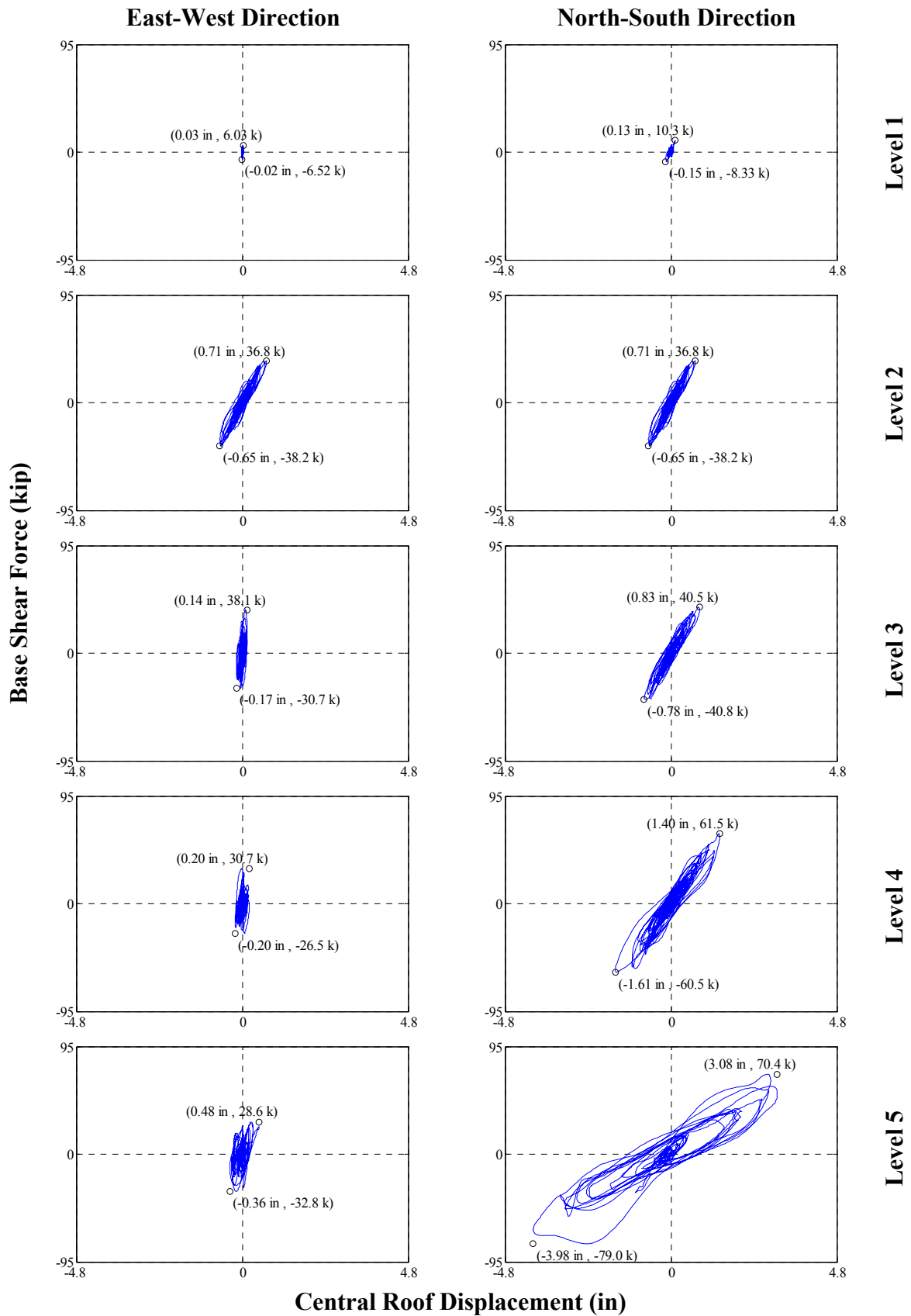


Figure 7.17: Global force-displacement hysteresis loops for the tri-axial tests of Phase 5

Observing Figure 7.16, the effects of the wall finish materials are clearly illustrated. The effective stiffness (defined as the slope of the line connecting the maximum and minimum depicted points) of the benchmark structure increased in both directions as gypsum wallboard and exterior stucco were applied at each test phase. This resulted in lower central displacements when the structure incorporated the wall finish materials, for the same level of seismic excitation, compared to the Phase 1 building. The hysteresis loops were also wider for the Phase 1 test, especially in the transverse direction, compared to the tests of the subsequent phases. This means that more energy was dissipated during that Phase 1 test. This result may be associated with the higher wall-diaphragm deformation ratio during Phase 1, as identified and presented in Section 7.5.

Figure 7.17 demonstrates the cumulative damage of the test structure for increasing level of seismic intensity, as this was translated in a degradation of the effective stiffness of the structure. Additionally, the transverse displacement demand for Level 5 (MCE event) seismic test was much greater than that of Level 4 (DBE event). It was observed that along the longitudinal direction, the maximum base shear force during Level 4 and 5 seismic tests was lower than the maximum base shear force during Level 3 tri-axial test. This can be explained by looking at the performance of the shake tables, as presented in Appendix I. Comparing the response spectra of the actual motion along the longitudinal direction, for the tri-axial tests of Levels 3, 4 and 5 (Figures I.46, I.48 and I.51, respectively), it can be seen that the response spectrum of the actual table motion during Level 3 test was higher than the desired spectrum, ranging around and above 1g. On the contrary, the spectra of the actual table motion during Level 4 and 5 tests were lower than desired and resulted in smaller spectral ordinates, compared to Level 3, on the vicinity of the fundamental periods of the benchmark structure. This effect can also be identified by

observing the peak recorded acceleration measurements along the longitudinal direction during these specific tests, as presented in Figure 7.10.

7.7 Wall Line Hysteresis Loops

This section presents hysteresis loop plots of the four wall lines of the benchmark structure that were located at the first floor in the transverse direction. The inter-story displacements and forces were computed as described in the previous section. Figure 7.18 contains the hysteresis loops derived from the tri-axial Level 2 tests of Phase 1, 3, 4 and 5, while Figure 7.19 presents the hysteresis loops derived from the tri-axial tests of Phase 5.

As discussed in Section 7.3, the peak inter-story displacements were maximum along Line 6 (the garage wall line) and were reducing from the west to the east side of the structure (from Line 6 towards Line 2). Wall line 5 had the highest stiffness among these four wall lines due to the fact that the external wall incorporated no openings and the internal wall was one of the two interior structural shear walls. Similar observations as in the previous section, such as the increase of stiffness along the test phases and the stiffness degradation with increasing intensity of seismic excitation, can also be seen from these two figures.

7.8 Experimental Capacity Spectra

Capacity spectra were developed for each phase of seismic testing, in the two principal directions, to compare the global response of the benchmark structure and to illustrate the evolution of the response along the different levels of testing. Only the data derived from the tri-axial seismic tests were included in the capacity spectra plots. The peak absolute central roof displacement and peak absolute base shear force, computed from each tri-axial seismic test, were converted into equivalent spectral displacement and acceleration ordinates.

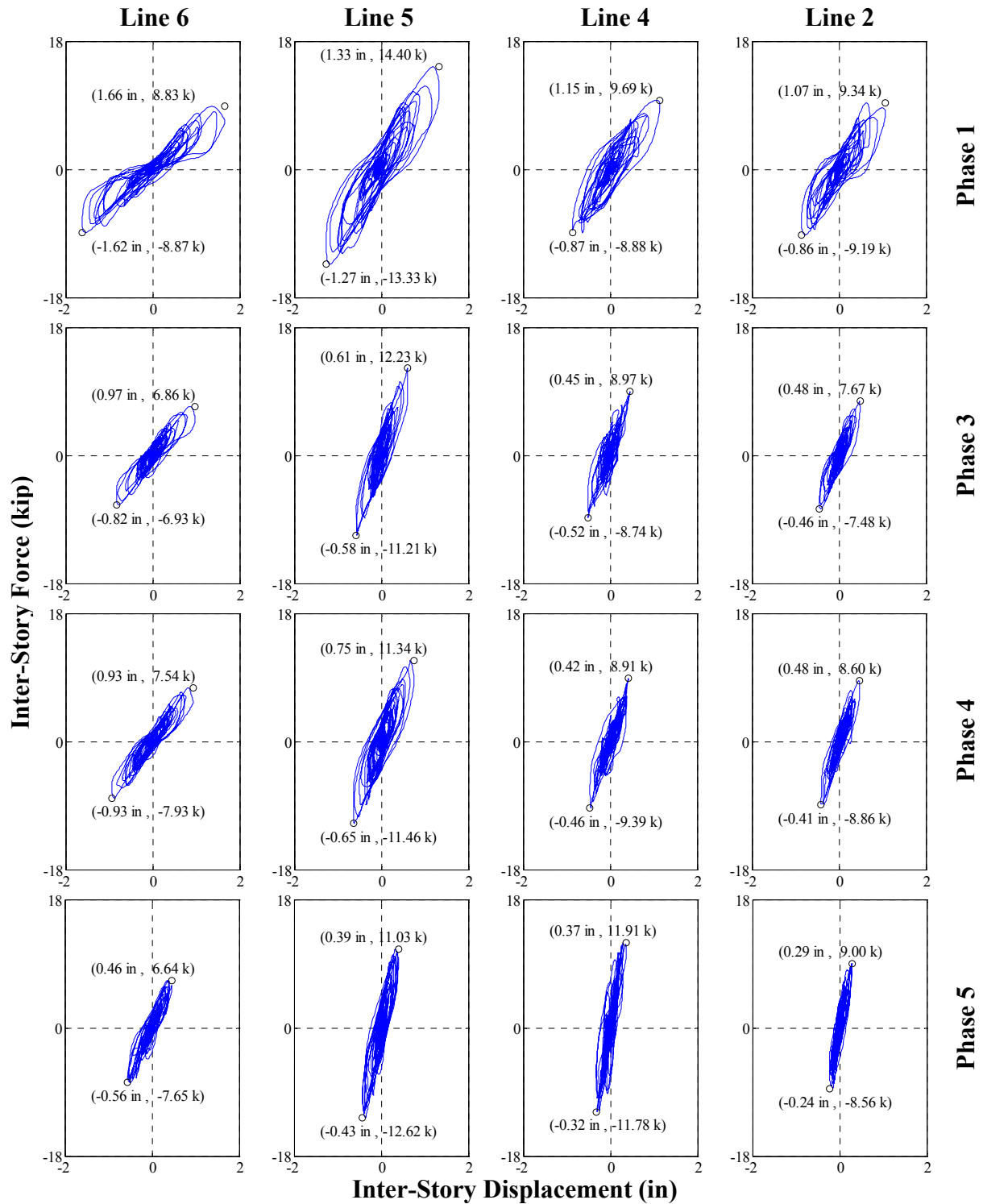


Figure 7.18: Transverse wall lines force-displacement hysteresis loops for Seismic Level 2 tri-axial tests of Phases 1, 3, 4 and 5

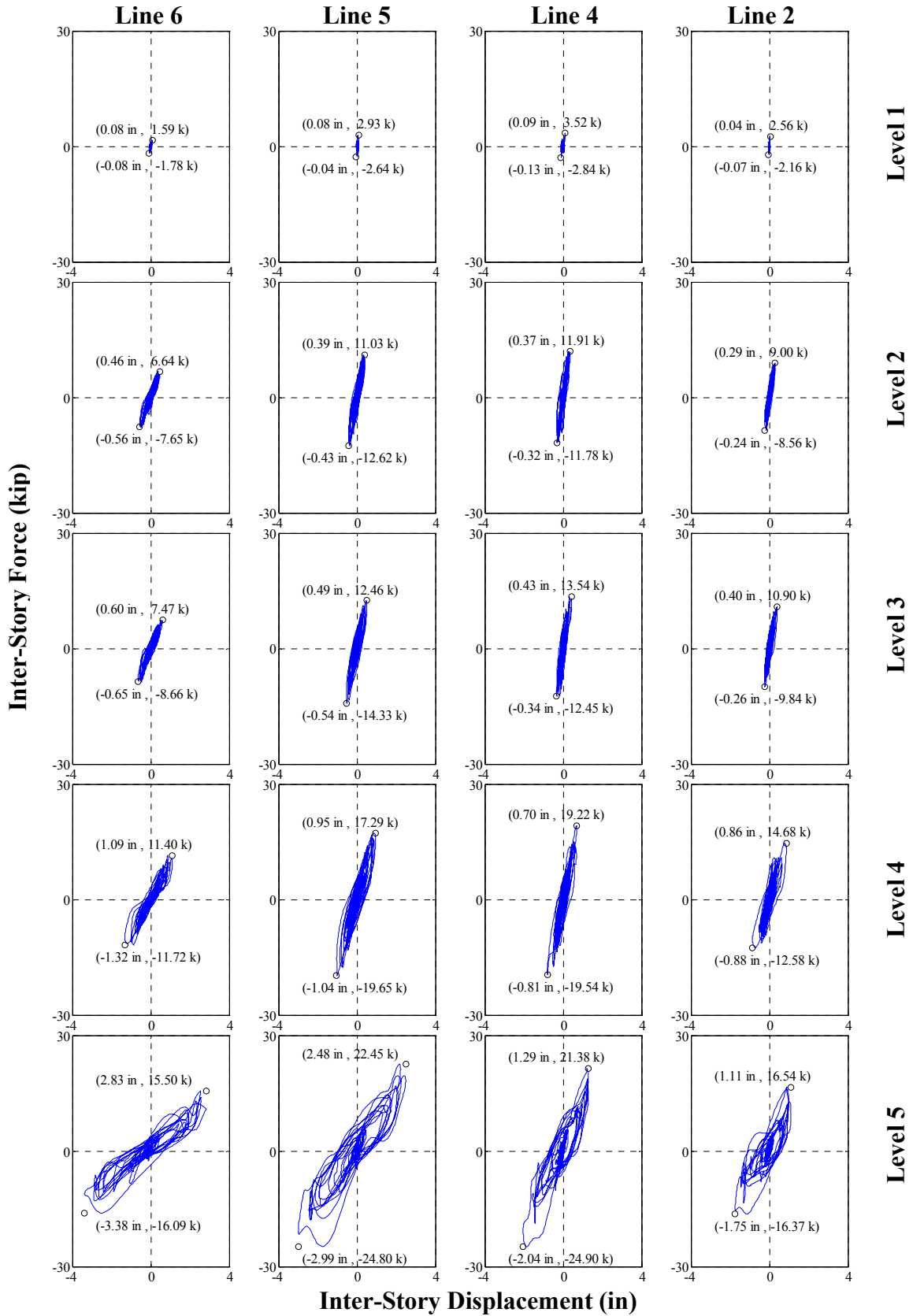


Figure 7.19: Transverse wall lines force-displacement loops for the tri-axial tests of Phase 5

For the calculation of the equivalent spectral displacements and acceleration ordinates, the modal participation factor Γ_n and the modal mass M_n of the first and second mode of the structure, defined for each test phase prior to any seismic test, were first calculated. The first and second mode shapes were used to calculate the equivalent spectral ordinates along the transverse and longitudinal directions, respectively. To illustrate the procedure, the following equations were used to calculate the spectral ordinates for the transverse direction, using the first mode shape of the test structure.

First, only the mode shape components in the transverse direction were taken into account. From sixteen accelerometers (eight in each floor in each direction) the mode shape $\{\Phi\}_1$ was first defined as an array of 16x1. The tributary mass at each accelerometer's location was calculated and a diagonal mass matrix $[M]$ (16x16) was populated. The modal mass M_1 and the modal participation factor Γ_1 are given by [17]:

$$M_1 = \{\Phi\}_1^T \cdot [M] \cdot \{\Phi\}_1 \quad (7.5)$$

$$\Gamma_1 = \frac{\{\Phi\}_1^T \cdot [M] \cdot \{r\}}{M_1} \quad (7.6)$$

where $\{r\}$ is a 16x1 array with all its elements equal to 1. The effective modal mass M_1^* , which is the mass contributing to this mode of deformation, is given by:

$$M_1^* = \Gamma_1^2 \cdot M_1 \quad (7.7)$$

If D_R is the peak central roof displacement and V the peak base shear force, then the equivalent spectral displacement and acceleration ordinates, S_d and S_a , respectively, are:

$$S_d = \frac{D_R}{\Gamma_1 \cdot \Phi_R} \quad (7.8)$$

$$S_a = \frac{V}{M_1^*} \quad (7.9)$$

where ϕ_R is the mode shape value at the roof, calculated similarly to the central roof displacement (average of mode shape value for Lines 4 and 5 for this case).

Figure 7.20 presents the experimental capacity spectra that were developed for each tri-axial seismic test, in the two principal directions. The response spectra of the actual recorded motions are also included. Level 2 response spectra were derived from the West Table motion recorded during Test Phase 1, while Level 5 spectra were derived from the West Table motion recorded during Test Phase 5. Based on the equivalent damping ratios that were computed in Chapter 6 (see Figure 6.10 for the first modal damping ratio), a damping ratio of 13% of critical was used for the calculation of the response spectra of Level 2 motion and a ratio of 15% for the calculation of the spectra of Level 5 motion.

The Phase 1 building demonstrated the higher flexibility and the Phase 5 building the higher stiffness. Phase 3 and 4 buildings had similar responses. It is interesting to note that the response spectra curves are close to the capacity data points, for the case of the response in both directions, for both Seismic Levels 2 and 5. This is not the case, however, for the Level 5 response in the longitudinal direction. Moreover, the drop in the S_a component for the Phase 5 building after the Level 3 test is attributed to the low intensity of the achieved table motion, as mentioned in the last paragraph of Section 7.6.

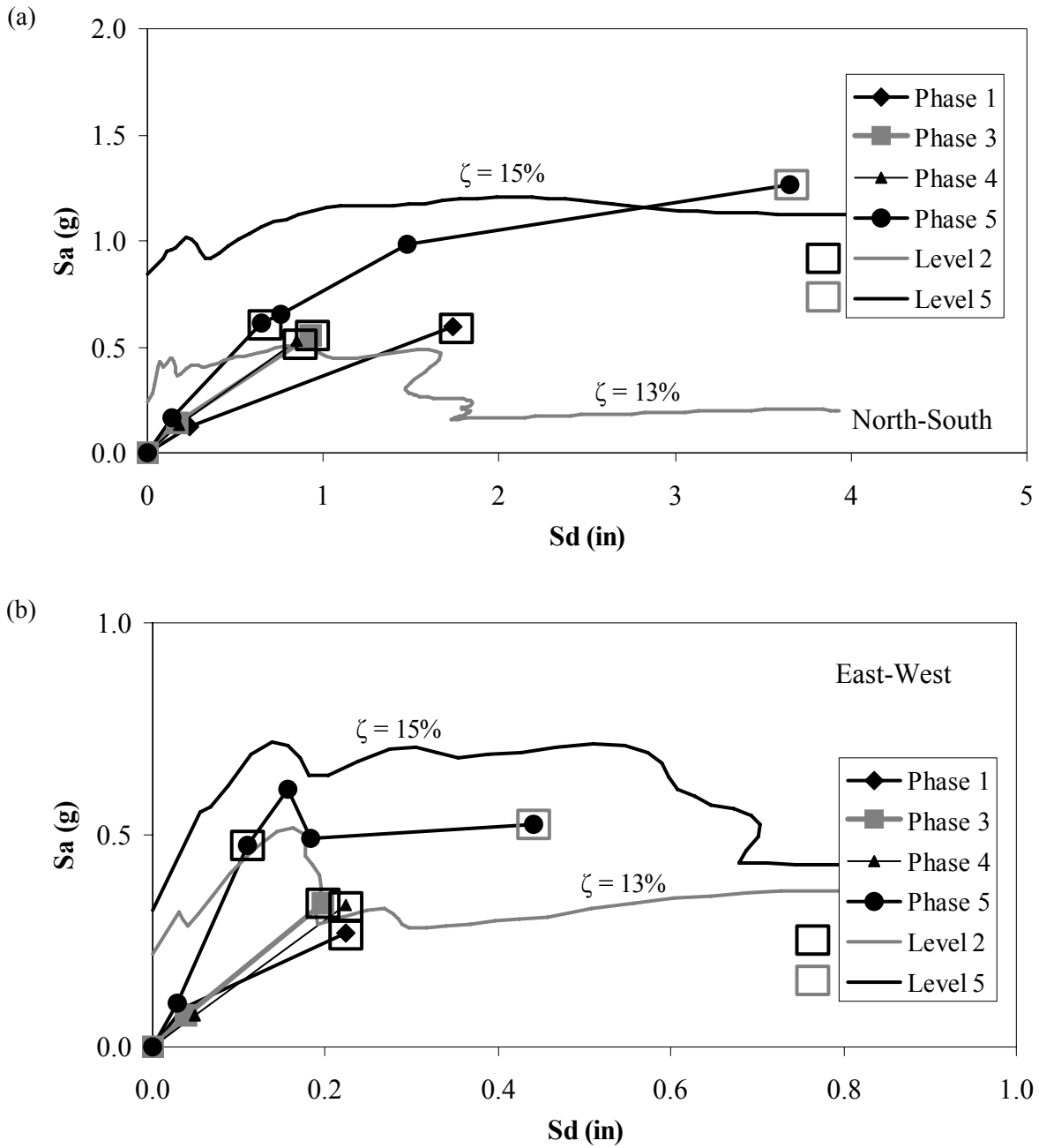


Figure 7.20: Experimental capacity spectra from the response of the benchmark structure (a) in the transverse direction, and (b) in the longitudinal direction

7.9 Energy Response

The relative input energy that was induced in the benchmark structure was estimated for most of the tri-axial tests of Phases 1, 3, 4 and 5. The relative input energy time-histories E_I were calculated by integrating (a) the force at each floor level, equal to the total mass m_i of that level multiplied by the ground acceleration α_g , over the relative displacement of that level with respect to the base of the structure x_i , and (b) the force at each floor level, equal to the total mass of that level m_i multiplied by the ground (table) rotational acceleration θ_g multiplied by the floor level height from the base h_i , over the relative displacement of that level with respect to the base of the structure x_i as well. The integration shown in Eq. (7.10) was executed for both horizontal directions (x and y) to yield the total relative input energy of the system. The last two terms in Eq. (7.10) are introduced based on the assumption that the structure is rotationally rigid and each floor diaphragm follows the rotation time-history of the shake tables.

$$E_I = \int_0^{x_1} m_1 \alpha_g dx_1 + \int_0^{x_2} m_2 \alpha_g dx_2 + \int_0^{x_1} m_1 h_1 \theta_g dx_1 + \int_0^{x_2} m_2 h_2 \theta_g dx_2 \quad (7.10)$$

Figure 7.21 presents the total relative input energy time-histories for the tri-axial Level 2 tests of Phases 1, 3, 4 and 5. Similarly, Figure 7.22 shows the total relative input energy time-histories for the tri-axial tests of Phase 5. Figure 7.21 indicates that the amount of energy associated with Phase 1 test was much higher than the other phases, ranging above 300 kip-in. The amount of energy associated with Test Phase 5 was the lowest, ranging around 120 kip-in, while the energy in Phases 3 and 4 was similar and slightly higher than Phase 5. This illustrates the effect of wall finish materials that increased the stiffness of the structure and resulted in lower amount of input energy, thus, lower amount of absorbed energy by the structural walls and eventually less damage in the structural and non-structural members. As expected, the amount of energy is

proportional to the shaking intensity. The higher is the level of shaking, the higher is the associated cumulative input energy (see Figure 7.22). The energy difference between Level 2 and Level 3 tri-axial tests was small, while the energy associated with Seismic Level 5 was much higher than any other test, reaching 900 kip-in.

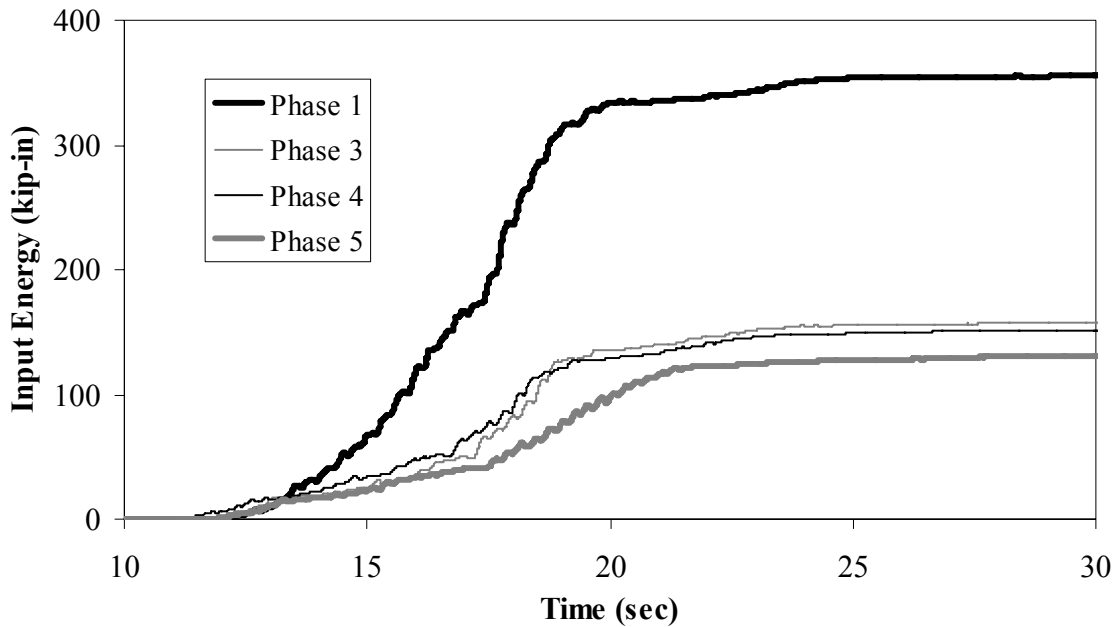


Figure 7.21: Relative input energy time-histories, for Seismic Level 2 tri-axial tests of Phases 1, 3, 4 and 5

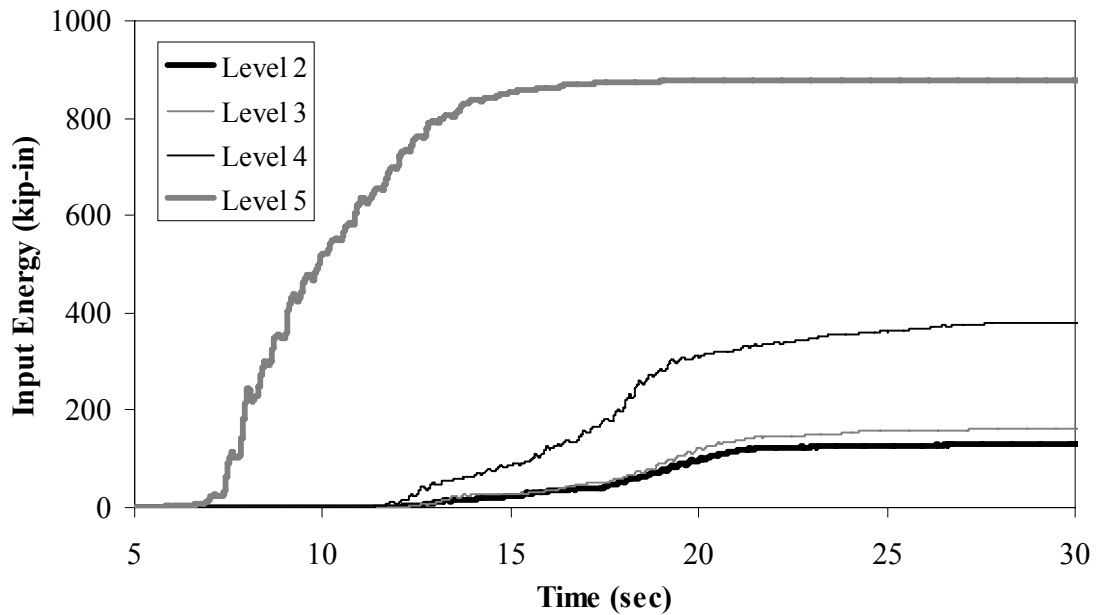


Figure 7.22: Relative input energy time-histories, for tri-axial tests of Phase 5

7.10 Sill Plate Slippage

Appendix P contains the sill plate slippage time-histories recorded at the base of a number of first floor shear walls during the seismic tests conducted. The maximum and minimum values of each individual measurement are also indicated on the plots. Figure 7.23a presents the absolute peak sill plate slippage recorded during the Seismic Level 2 tri-axial tests, while Figure 7.23b presents the ratio of the peak sill plate slippage with respect to the peak inter-story displacement at that particular wall line. Similarly, Figures 7.24a and 7.24b illustrate the same information mentioned above, but for the seismic tests of Phase 5. Note that the results from Level 1 tests were not included because the slippage of the sill plates was below 0.01 in.

The average peak sill plate slippage of the first floor walls, during the Seismic Level 2 tri-axial tests was below 0.05 in., across all test phases. Values larger than 0.05 in. were recorded along Lines A and 5 (SL1 and SL10, respectively). Not surprisingly, the walls along these two lines had no wall openings and demonstrated the highest lateral structural stiffness among all the wall lines, resisting a higher portion of the induced seismic load that resulted in higher sill plate slippage displacements. The average percentage of the inter-story displacement due to sill plate slippage was around 10%, considering all the sill plate measurements (note that there were no inter-story displacement data for SL7). Significantly higher ratios were observed for Test Phase 5 (see Fig. 23b). Regarding the variability of sill plate slippage with respect to the seismic level of intensity, there were no clear trends observed. However, Figure 7.24a shows that at lower levels of shaking, the values of peak sill plate slippage were low (below 0.1 in.), while at higher levels of shaking, peak values of slippage were around 0.5 in. for SL8, SL9 and SL10. The ratios of sill plate slippages with respect to the inter-story displacements ranged around 0.3, with high variability among the different sill plates and shaking intensities.

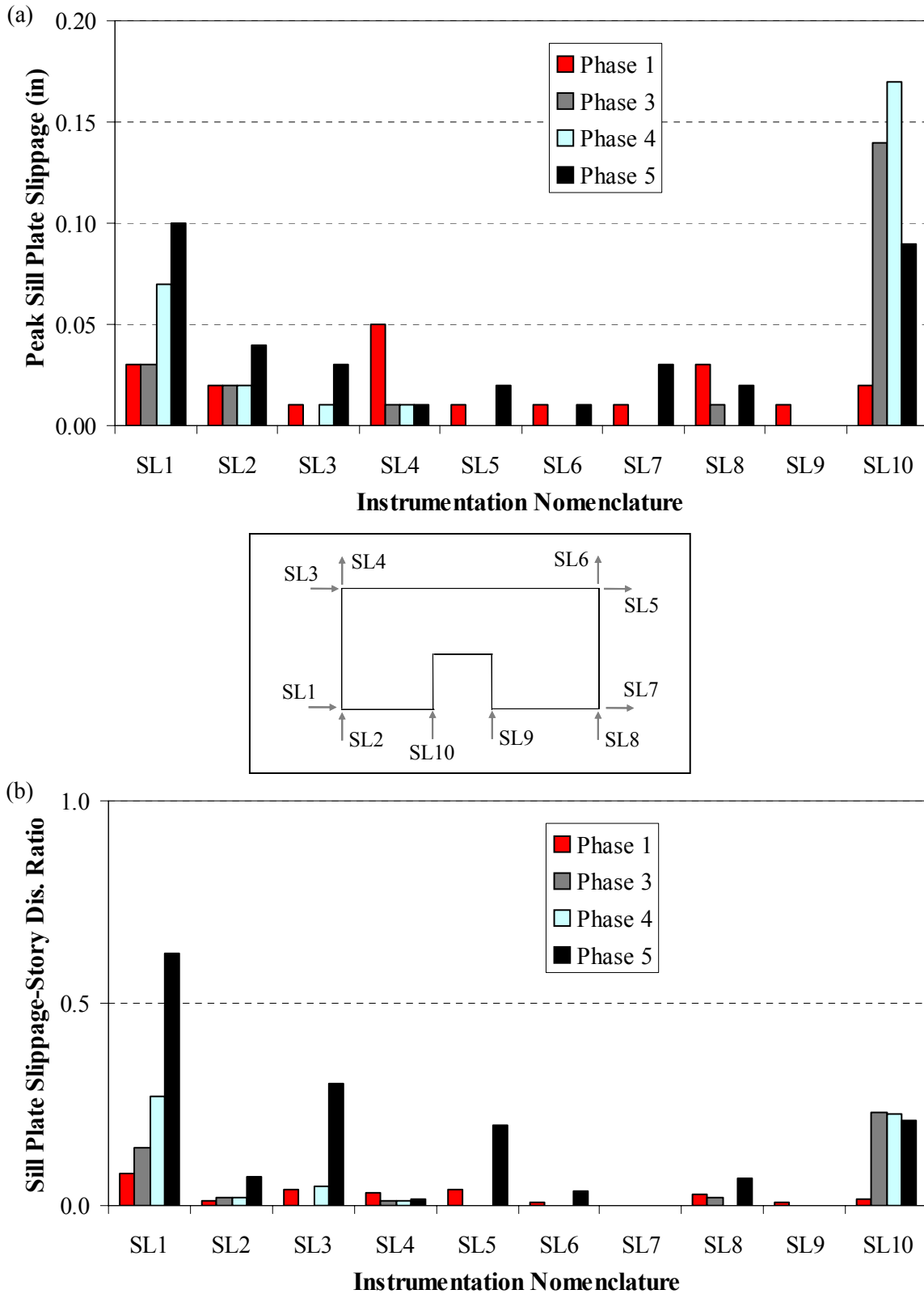


Figure 7.23: (a) Peak sill plate slippage, and (b) sill plate slippage over story displacement ratio, for Seismic Level 2 tri-axial tests of Phases 1, 3, 4 and 5

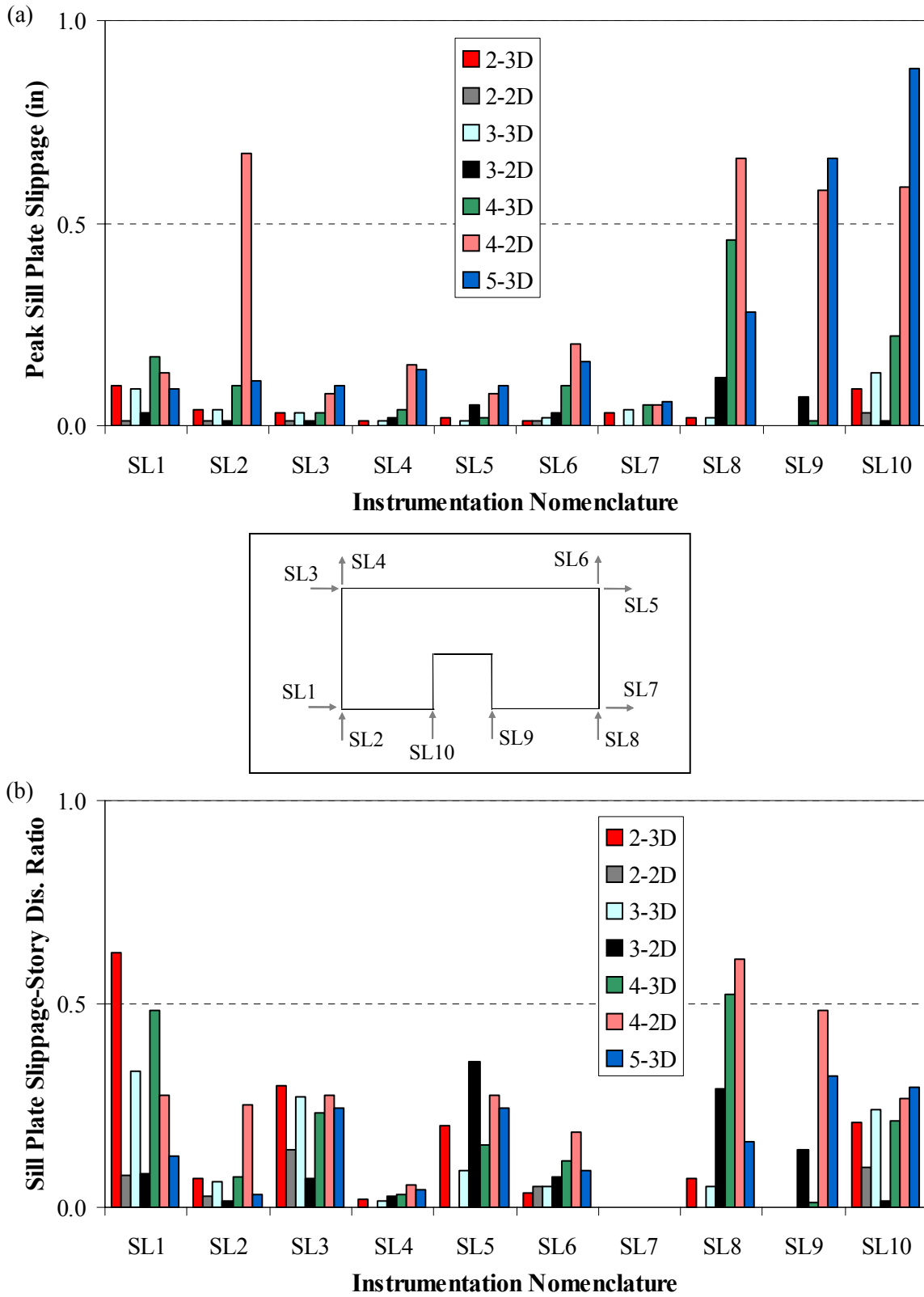


Figure 7.24: (a) Peak sill plate slippage, and (b) sill plate slippage over story displacement ratio, for seismic tests of Phase 5

7.11 Peak Holddown Forces

Appendix Q presents the peak holddown and anchor bolt forces recorded at the base of various first floor structural and partition walls, for all seismic tests conducted. Four holddowns were installed along each of Wall Lines 6, 4 and 2 of the benchmark structure. From the plots of Appendix Q, it can be observed that peak forces at holddown locations are much higher than peak forces at anchor bolt locations, for all seismic tests conducted.

Figure 7.25a presents the peak forces recorded across the four holddowns of Wall Lines 6, 4 and 2 of the benchmark structure for the Seismic Level 2 tri-axial tests of Phases 1, 3, 4 and 5. The peak recorded forces are then normalized by the nominal ultimate strength of the holddown devices and the resulting ratios are presented in Figure 7.25b. The ultimate strength was calculated based on the allowable tension load F_{all} that can be found in *Simpson Strong-Tie* website [18]. According to the 2005 National Design Specification for Wood Construction [19], the ultimate strength F_{ult} is the product of the allowable design load and a format conversion factor K_F , equal to $2.16/\phi$, where ϕ is the resistance factor, equal to 0.65. These values apply for wood connections. Holddowns of type PHD2 and PHD5 were installed in structural walls along Lines 4 and Lines 2 and 6, respectively (see Drawing S-6 of Appendix A). The allowable tension load specified by Simpson Strong-Tie was 3505 and 4030 lbs for PHD2 and PHD5, respectively, for Hem Fir structural lumber. The ultimate strength is:

$$F_{ult} = K_F \cdot F_{all} = 2.16/.65 \cdot F_{all} = 3.32 \cdot F_{all} = \begin{cases} 3.32 \cdot 3505 = 11637\text{lb, for PHD2} \\ 3.32 \cdot 4030 = 13380\text{lb, for PHD5} \end{cases} \quad (7.12)$$

Similarly to Figure 7.25, Figure 7.26a presents the peak recorded holddown forces along the same three wall lines for the tri-axial tests (above Level 1) of Phase 5 and Figure 7.26b shows the normalized ratio with the nominal ultimate strength of the devices.

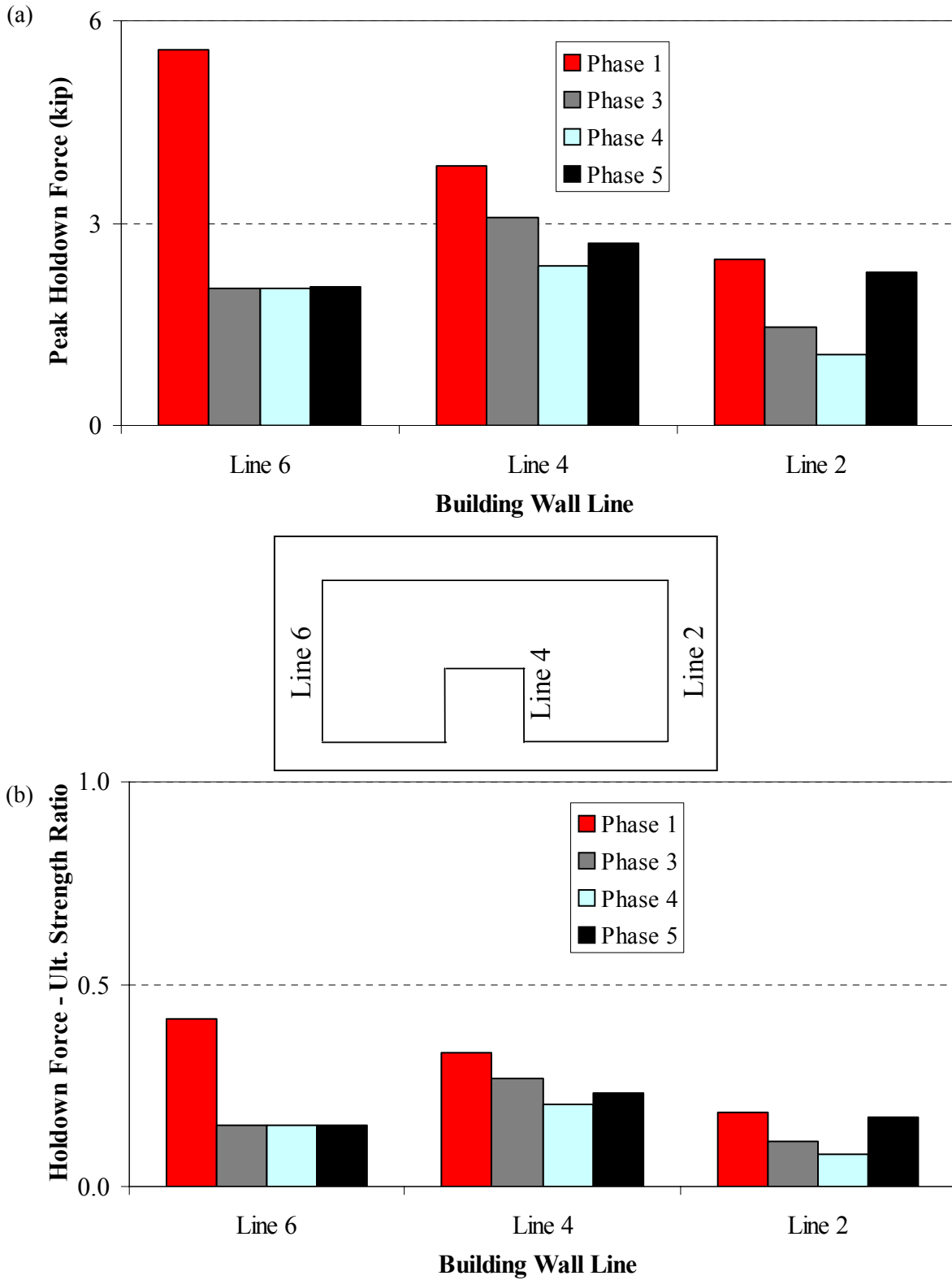


Figure 7.25: (a) Peak holdown force, and (b) peak holdown force to nominal ultimate strength ratio, for Seismic Level 2 tri-axial tests of Phases 1, 3, 4 and 5

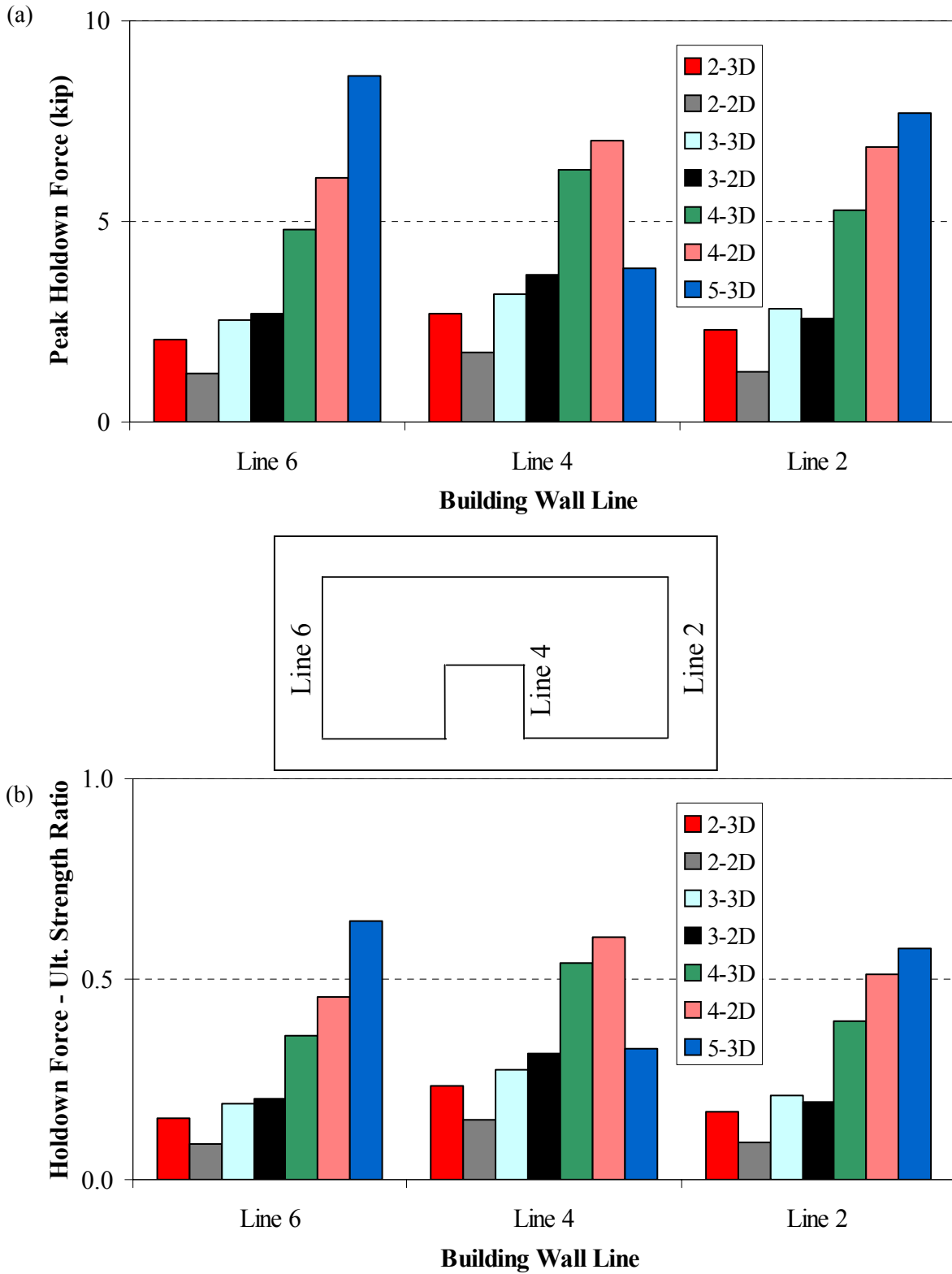


Figure 7.26: (a) Peak holdown force, and (b) peak holdown force to nominal ultimate strength ratio, for seismic tests of Phase 5

Comparing the peak holdown forces between the Level 2 tri-axial tests of different phases, the maximum force was recorded at the garage wall for the Phase 1 building and it was close to 6 kips. On average, the peak forces ranged below 3 kips for all holdowns installed and for all Level 2 tests. The differences between Phases 3, 4 and 5 were small compared to the differences with Phase 1 peak forces. The strength ratios were below 0.5 and averaged around 0.25, which means that a safety factor of 4 was applicable for this level of shaking.

As expected, the peak holdown forces increased with the increase of shaking level, throughout Test Phase 5. Maximum values were below 10 kips. For DBE and MCE levels of shaking (Levels 4 and 5, respectively) the strength ratios were around 0.5 to 0.6, which translates to a safety factor of 1.5 to 2.

7.12 Peak Sill Plate and Holdown Stud Uplift

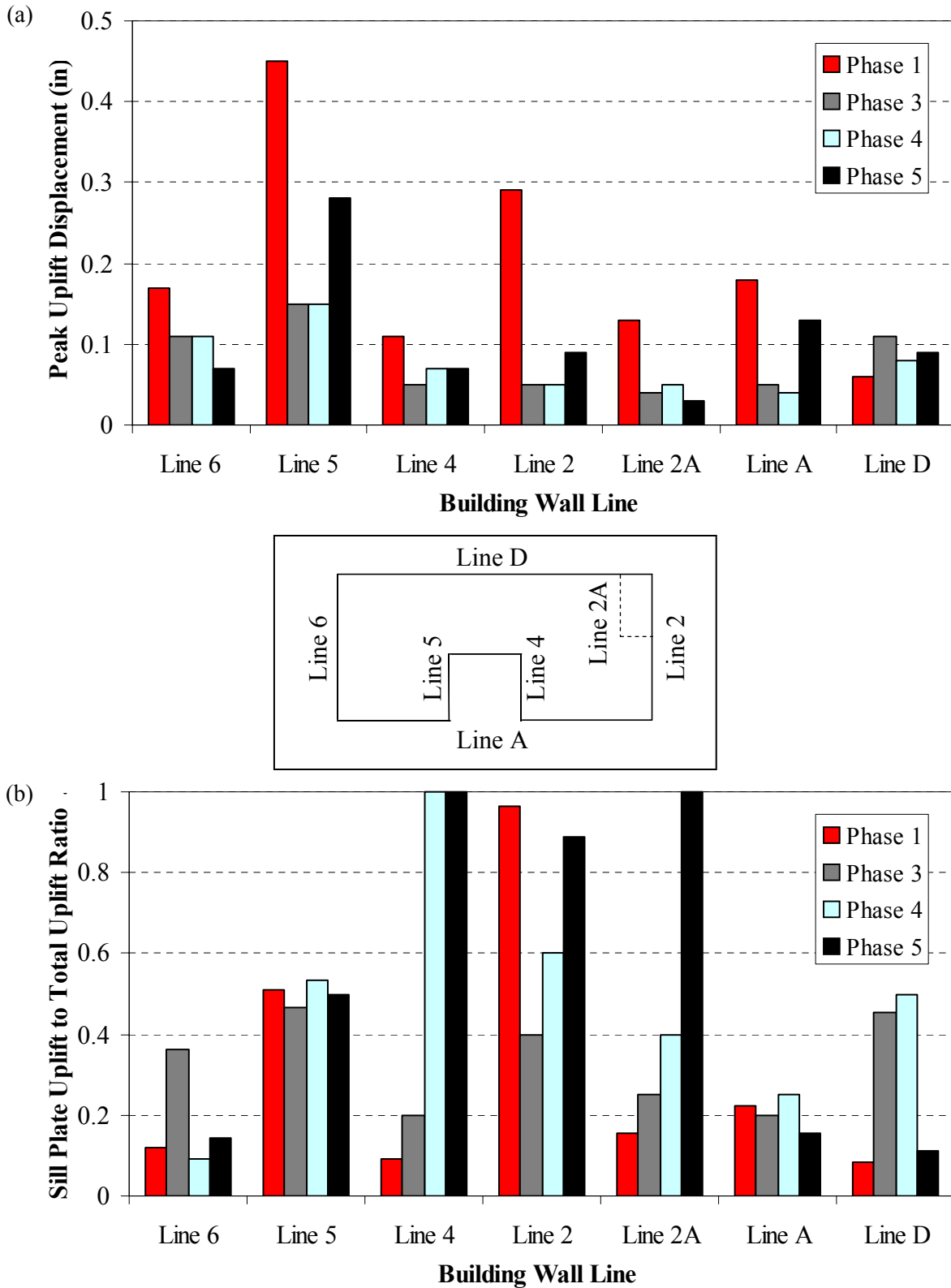
Appendix R presents the peak uplift displacements recorded at the end studs of various exterior first floor walls, for all seismic tests conducted. The total uplift displacement consisted of two components. The first component was the uplift displacement of the sill plate with respect to the foundation and the second part was the uplift of the end stud with respect to the sill plate. Both components were measured with two linear potentiometers at each desired location (see Fig. 4.4 and Fig 4.5). The time-histories recorded from each pair of potentiometers were summed to yield the total uplift displacement and the maximum positive value was identified as the peak uplift displacement (positive sign for uplift). At the same time instant, the uplift displacement of the sill plate to the ground was used to calculate the ratio of the sill plate uplift over the total uplift. Peak displacements for the sill plate uplift and the total uplift are indicated in Appendix R, for every location.

The stud-to-sill-plate uplift displacement time-histories were corrected to remove any small negative values that were recorded, considering that any negative values were artificially created by the rotation of the end stud with respect to the sill plate. The sill plate-to-foundation uplift displacement time-histories were not modified on the basis that crushing of the sill plate during cyclic response is possible to yield negative displacement values at some time instants.

Figure 7.27 summarizes the results for the tri-axial Level 2 seismic tests of Phases 1, 3, 4 and 5. The peak total uplift displacements at each of the main wall lines of the structure were identified and included in Figure 7.27a, while Figure 7.27b shows what percentage of the total uplift displacement was due to the sill plate uplift. Similarly, Figure 7.28 presents the same information for the seismic tests conducted as part of Phase 5 testing. Note that Wall Lines 2, 4 and 6 had holdowns installed while Wall Lines 5, 2A, A and D had typical anchor bolts.

Commenting on the results of the Level 2 tri-axial tests, the greatest uplift displacements were recorded for the Phase 1 building, reaching values of up to 0.3 in. and 0.45 in. at some wall lines. This is attributed mainly to the higher inter-story shear forces, compared to the other phases, which resulted in higher uplift forces. The peak uplift displacements for the Phase 3 and Phase 4 building were around 0.1 in., slightly lower than for the Phase 5 structure.

Figure 7.28a clearly indicates the significant increase of peak uplift displacements recorded during the bi-axial Level 4 and the final tri-axial Level 5 seismic tests of Phase 5. During the latter test, the peak displacements exceeded 0.5 in. at all wall lines and the maximum value (above 3 in.) was recorded at Wall Line 5.



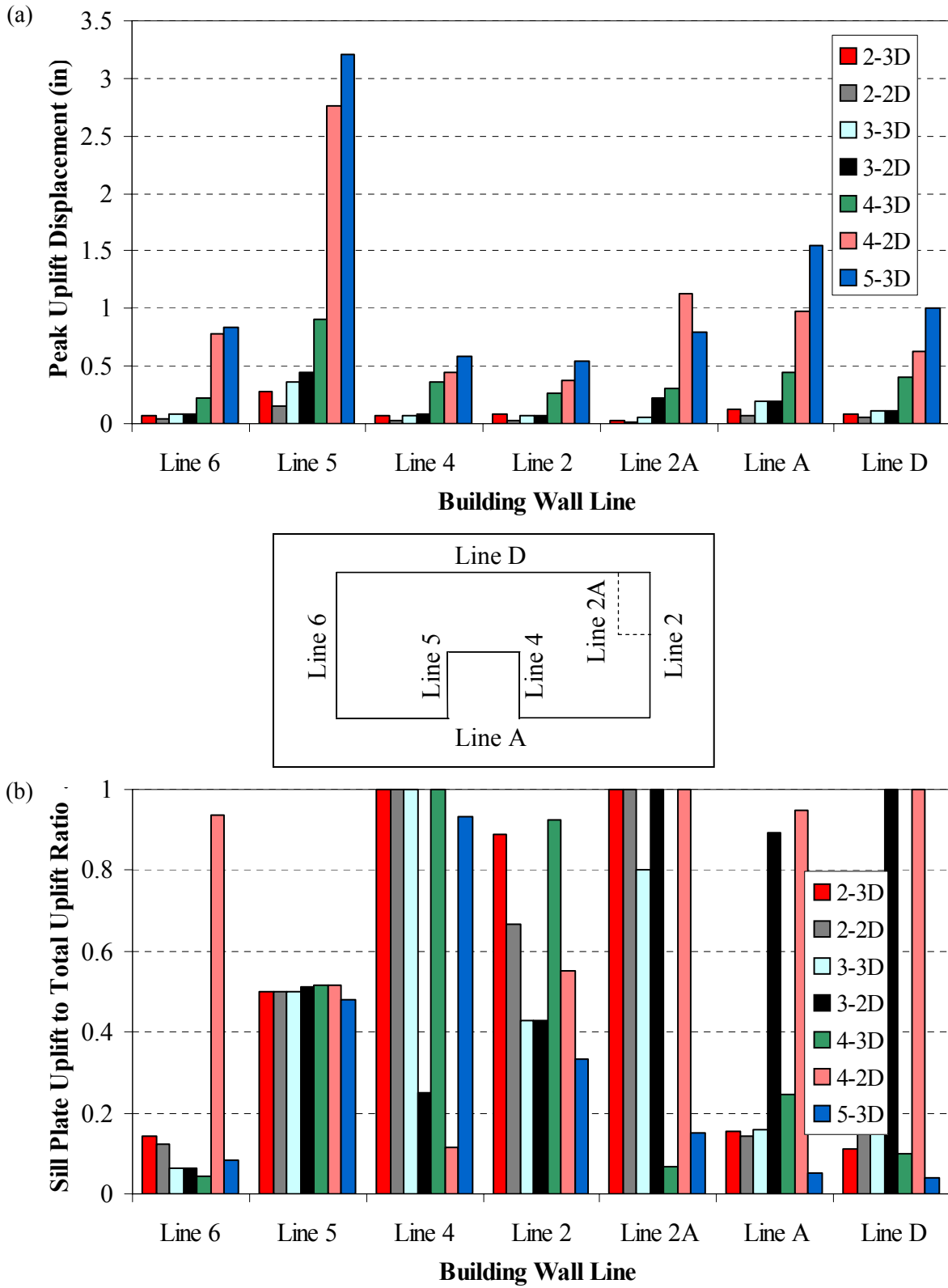


Figure 7.28: (a) Peak uplift displacement, and (b) sill plate uplift to total uplift ratio, for seismic tests of Phase 5

The ratio of sill plate uplift to total uplift exhibited a large variability for the different wall lines, the different test phases and the different seismic intensities. In general, this ratio depends on the ratio of the stiffness associated with each mode of deformation. Considering that the use of two vertical springs in series can model the uplifting behavior of a wood shear-wall, the bottom spring would represent the force-displacement relationship of the holdown (or anchor bolt) while the second would capture the local slipping of wood framing and the sheathing. Therefore, the ratio of the displacements depends on the type of anchoring (type of holdown or anchor bolt) as well as the nailing schedule of the shear wall, especially along the sill plate. This would intuitively suggest that the application of interior gypsum wallboard would increase this ratio, since the bottom screws of the gypsum boards are screwed in the sill plate. Figure 7.27b shows that this is the case for Lines 6, 4, 2A and D. No clear trend, however, was identified relating this ratio with the wall finish materials or the level of shaking, even when data from wall lines with holdowns were examined separately. Only Wall Line 5 exhibited a constant ratio of 0.5 for all the seismic tests conducted. This variability may arise from the fact that these ratios were extracted only from the location of the wall line where the peak uplift displacement was the maximum between at least two or not more than four end-stud locations. Perhaps the collection of more data from all the end studs could provide a better view.

7.13 Identification of Displacement Components

In this section, an attempt is made to decompose the first floor inter-story displacements of specific walls into different components, by combining in the time domain the recorded data from the wall deformations, the slippage of sill plates and the uplifting response of the end studs. Four exterior walls along the transverse direction were selected (E16, E13, E11 and E8 from Wall Lines 6, 5, 4 and 2, respectively), as shown in Figure 7.29a. Figure 7.29b illustrates the wall configurations, indicating the length of the wall or the wall panel that was instrumented and the locations of the holdowns, in three of the four walls.

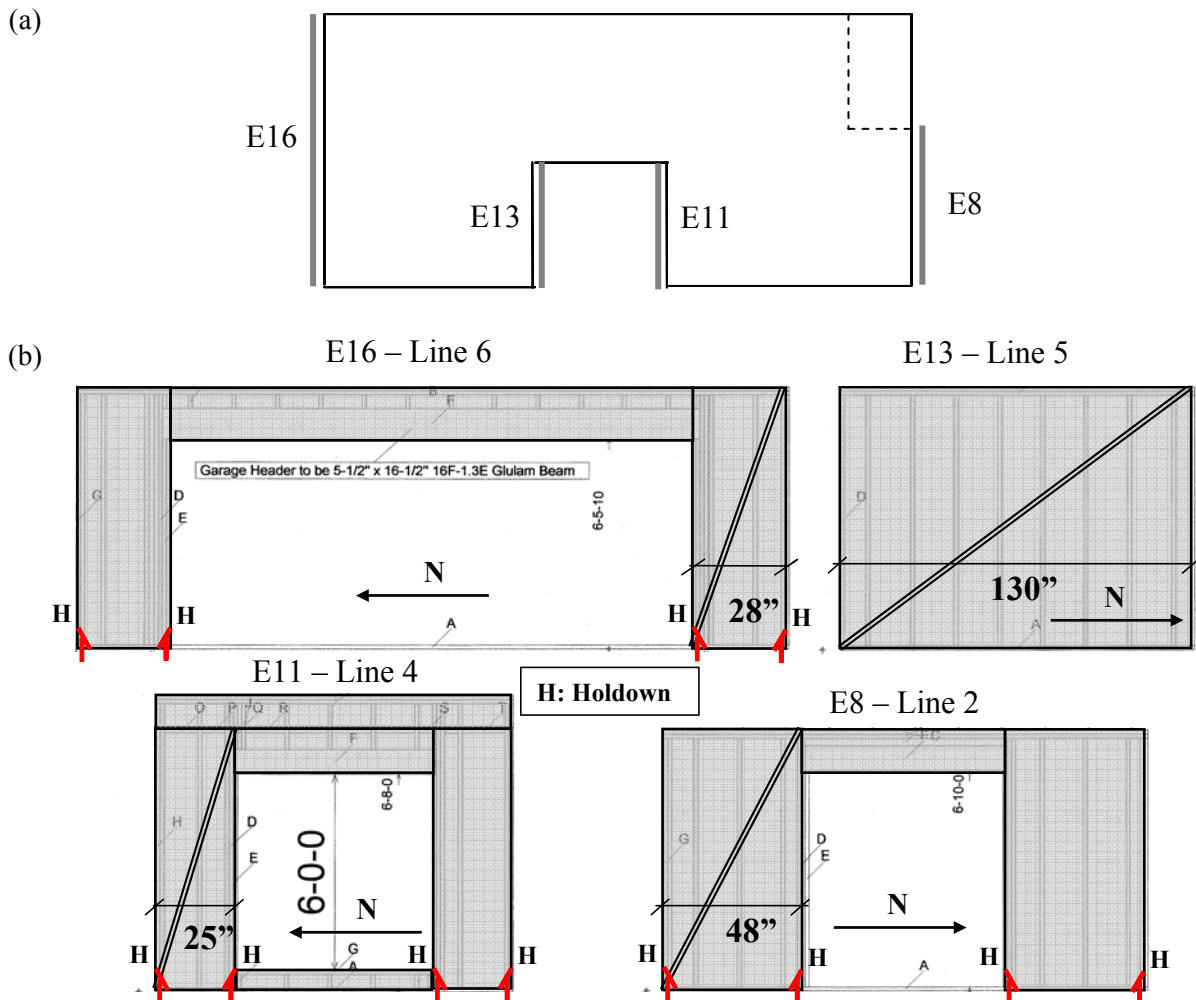


Figure 7.29: (a) Location and (b) configuration of the walls used for the displacement decomposition

The only displacement component that needed to be evaluated was that caused by the uplifting response of each wall. The displacement time-history at the top of a wall (or a wall panel) can be estimated when the uplift displacement time-histories at the two end studs are known, by defining a wall base angle of rotation and extrapolating the horizontal displacement at the top assuming a rigid body motion.

Figure 7.30 illustrates how the inter-story displacement due to uplifting response was estimated at the garage wall (E16) for the tri-axial Level 2 test of Phase 1 (Test NWP1S17). Figure 7.30a presents the sill-plate uplift displacement time-histories (UP2 and UP4) and Figure 7.30b shows the total uplift displacement time histories (UP1+UP2 and UP3+UP4), at the base corners of the south wall segment of the garage wall (see Table E.6 and Figure E.6 of Appendix E). Figure 7.30c plots the horizontal displacement time-histories, $\mathbf{d}_{U,S}$ and $\mathbf{d}_{U,S+S}$, due to the sill plate uplift and the sill-plate-plus-stud uplift, respectively, which are given by:

$$\mathbf{d}_{U,S}(t) = \frac{UP2(t) - UP4(t)}{L_{Wall}} \cdot \mathbf{h} \quad (7.11)$$

$$\mathbf{d}_{U,S+S}(t) = \frac{(UP1(t) + UP2(t)) - (UP3(t) + UP4(t))}{L_{Wall}} \cdot \mathbf{h} \quad (7.12)$$

where L_{Wall} is the length of the wall panel, equal to 28 in., and \mathbf{h} is the height of the first floor, equal to 109 in.

Displacements $\mathbf{d}_{U,S}$ and $\mathbf{d}_{U,S+S}$ were computed based on the assumption of rigid body rotation of the wall, which holds for narrow wall-piers with high height-to-length ratio, such as these in Walls E16 and E11. Yet, it is not clear if these displacement estimates are reliable in cases of low aspect ratio walls, such as Wall E13, or in cases where two wall panels can interact with each other, such as Walls E11 and E8.

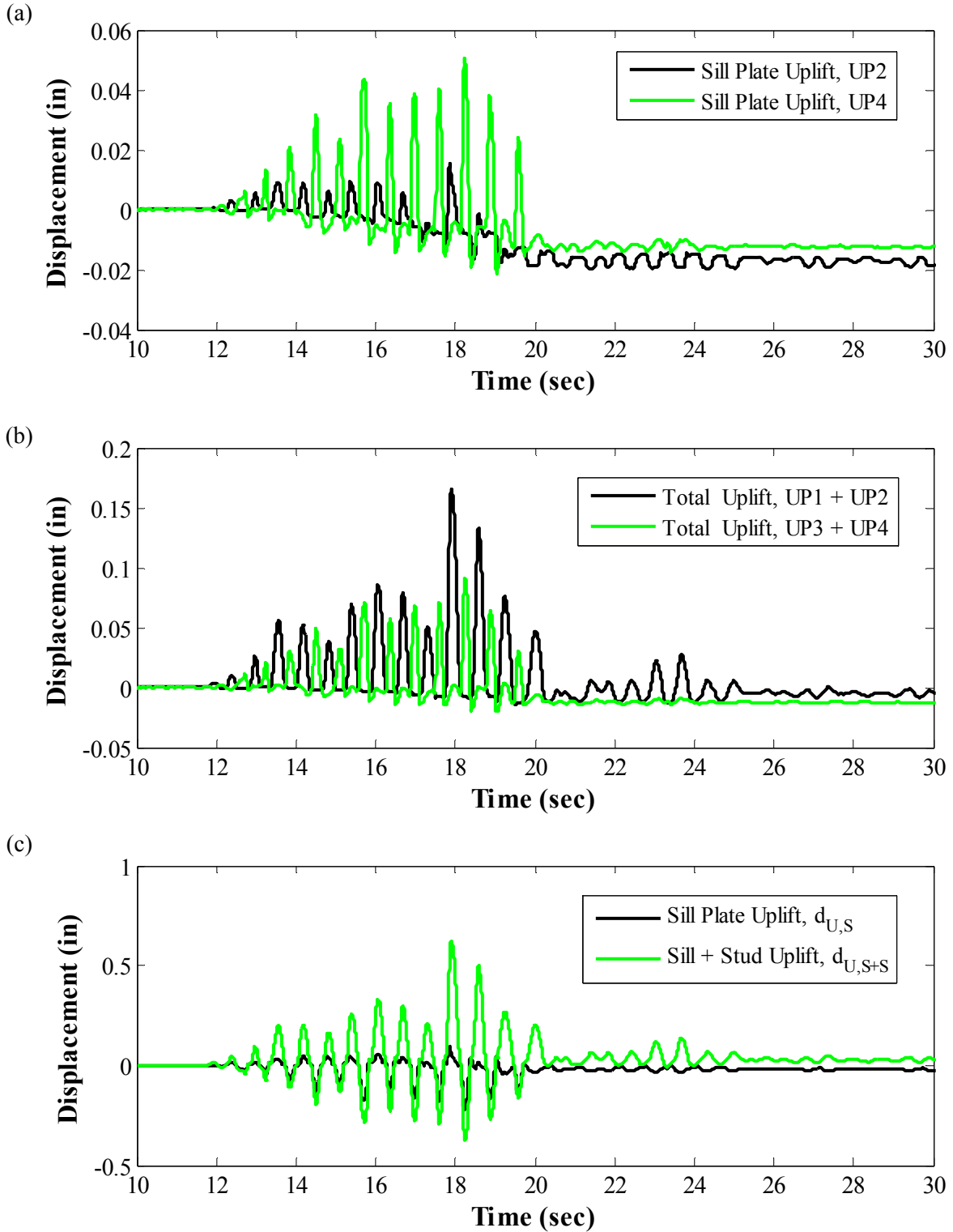


Figure 7.30: (a) Sill plate uplift displacements, (b) total uplift displacements, and (c) associated inter-story displacement estimates of the south segment of the garage wall, for Test NWP1S17

Moreover, it was mentioned in Section 7.5 that since the diagonal potentiometers were connected at the sill and top plates of the walls, it is expected that the horizontal displacement due to stud-to-sill-plate uplift should be already included in the wall deformation measurement, provided by the diagonal potentiometer, in cases where the rigid body assumption applies, such as the garage wall panels. However, due to associated uncertainty, the horizontal component due to stud uplift is explicitly computed and shown for each case. Figures 7.31a and 7.31b present the computed displacement components of Wall E16 for the tri-axial Level 2 tests of Phases 1 and 4, respectively.

In these plots, the inter-story displacement, measured between the floor diaphragms, is compared with the combined displacement at the wall and the sill plate slippage, including the effect only from the sill plate uplift response with respect to the foundation. The explicit effect of the stud uplift is also plotted with the dotted line. It is observed that the combined displacement time-history correlates well with the inter-story displacement time-history and is always smaller (in the absolute sense). The difference between these two lines is an unidentified displacement component, which can include the effect of stud uplift as well as other sources of displacements that are not measured, such as the slippage of the top plate with respect to the diaphragm and the deformation of the floor joists.

Figures 7.32 and 7.33 summarize the normalized displacement components at the time instant of the peak inter-story drift, for all the tri-axial Level 2 tests and the tri-axial tests of Phase 5, respectively. The peak inter-story displacement of each wall line is also indicated, for each test, in white fonts.

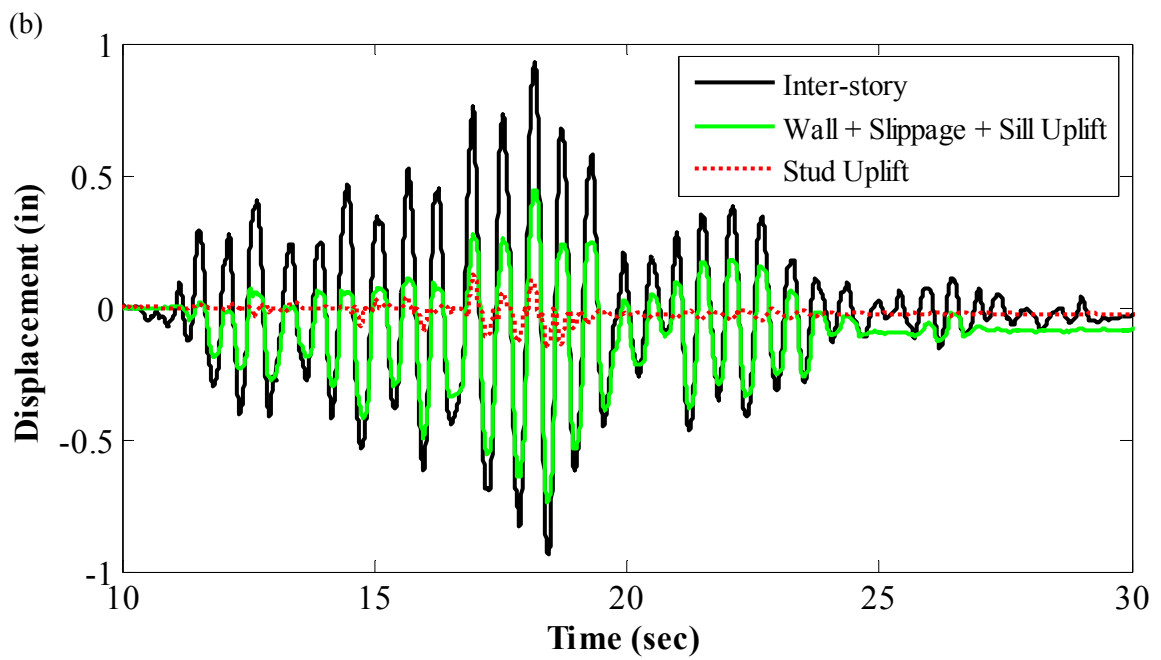
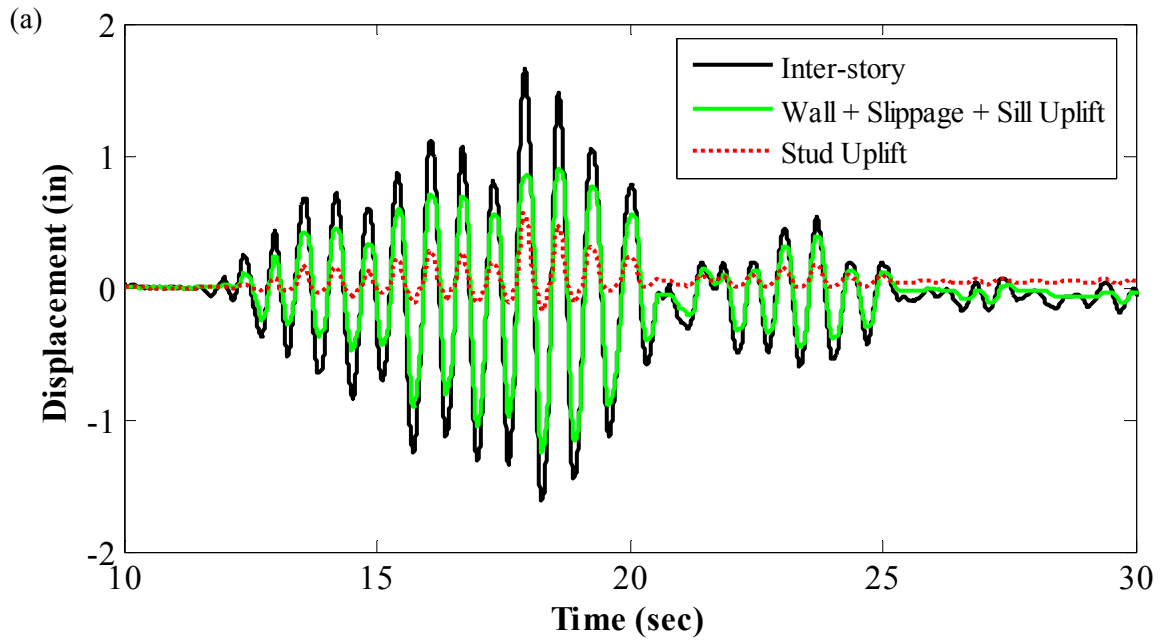


Figure 7.31: Displacement components of garage wall E16 for (a) Test NWP1S17 and (b) Test NWP4S03

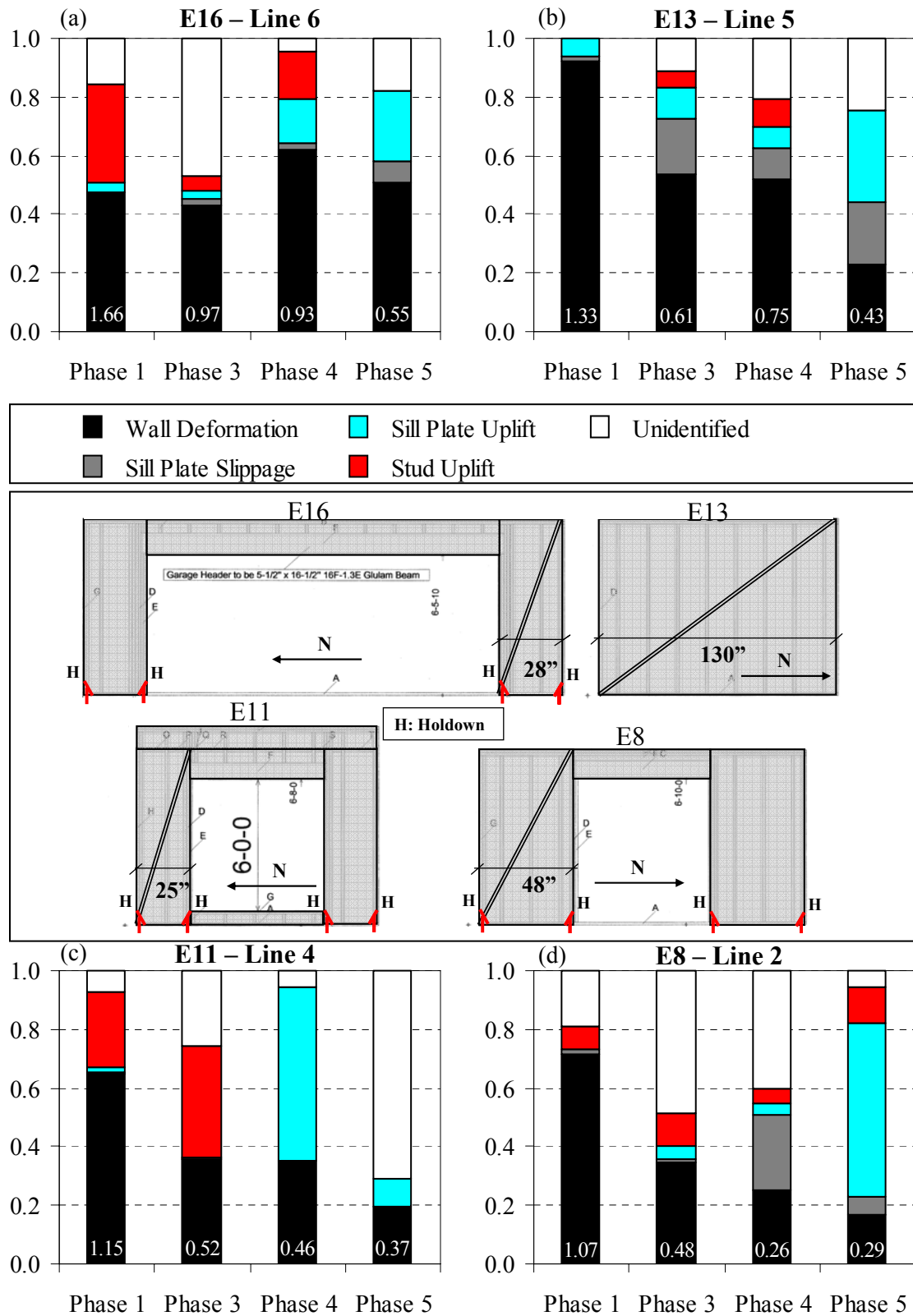


Figure 7.32: Displacement components at the peak inter-story drifts for the Seismic Level 2 tri-axial tests of Phases 1, 3, 4 and 5 and walls (a) E16, (b) E13, (c) E11, and (d) E8. Numerical values in each histogram indicate peak inter-story displacements

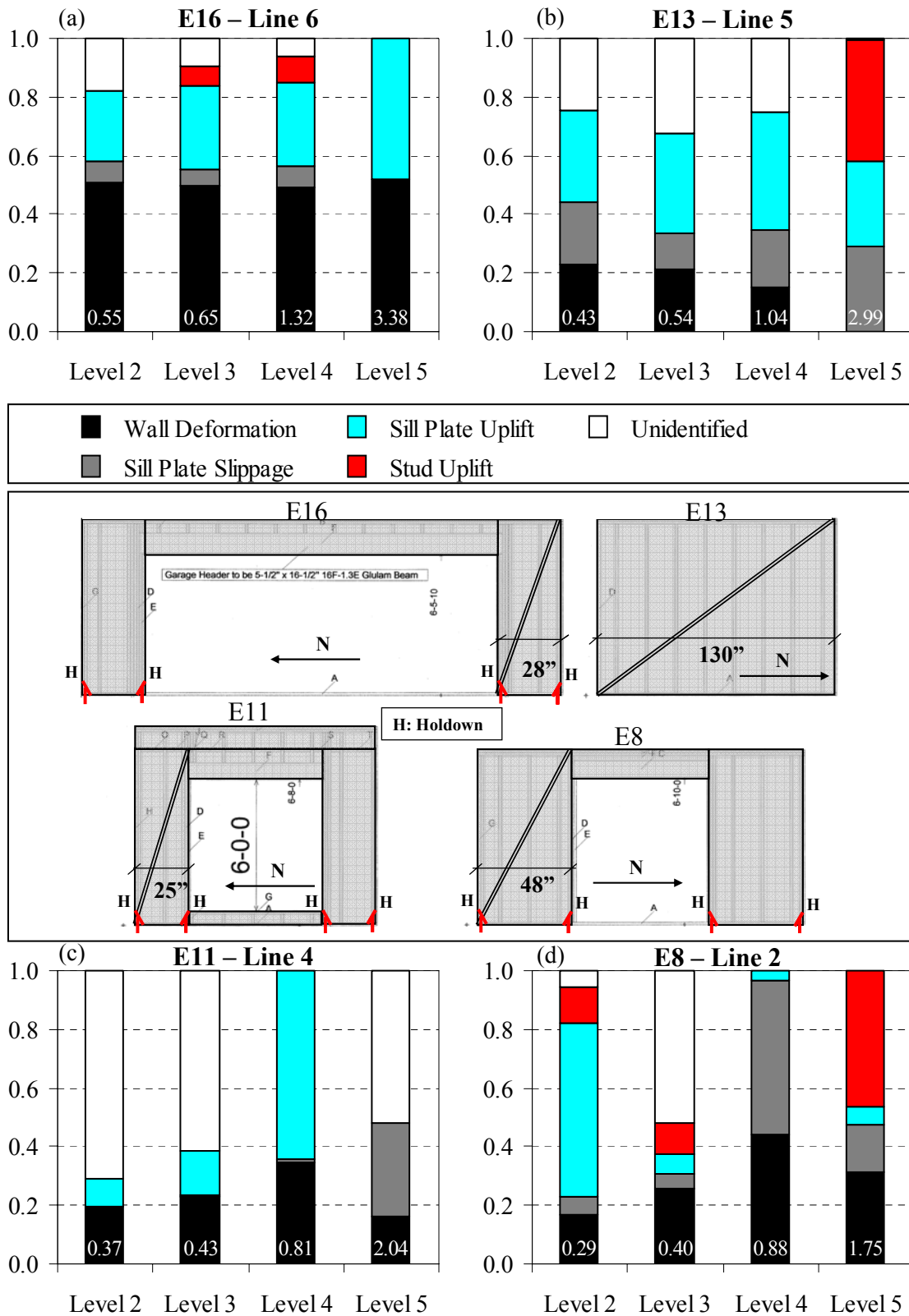


Figure 7.33: Displacement components at the peak inter-story drifts for the tri-axial seismic tests of Phase 5 and walls (a) E16, (b) E13, (c) E11, and (d) E8. Numerical values in each histogram indicate peak inter-story displacements

Figure 7.32 clearly indicates that the application of wall finish materials reduced the wall deformation ratio of three of the four walls, from high values of 0.8, observed for Phase 1, to as low as 0.2, observed for Phase 5. Consequently, the sill plate slippage and the sill plate uplift ratios were generally increased after the installation of wall finishes, and a greater portion of the total uplift was due to the sill plate uplift. The garage wall deformation ratio was around 0.5 for all the seismic tests evaluated. It was not affected either by the wall finishes or the level of shaking intensity and the level of deformation (Figs. 7.32a and 7.33a). Figure 7.33 shows that the wall deformation ratios remained quite low for all tri-axial tests of Phase 5. The unidentified component ratio varied between 0 and 0.7 and was higher for the Phase 5 displacement decomposition.

7.14 Effect of Vertical Input Excitation

The effect of vertical input excitation on the seismic response of the benchmark structure can be investigated by comparing the displacement amplitudes recorded between tri-axial and bi-axial tests of the same seismic level. Note that the bi-axial test, for a given phase and seismic level, was always conducted after the corresponding tri-axial tests. Therefore, the structural system was not intact before the start of the bi-axial test. For simplicity purposes, the building roof central displacement in the two orthogonal directions is used to compare the response and assess the effect of vertical input excitation.

Figures 7.34 and 7.35 contain the maximum recorded building central displacements for all tri-axial and bi-axial tests of Test Phases 1, 3, 4 and 5, for Seismic Levels 1 and 2, respectively. Furthermore, Figure 7.36 presents the maximum recorded building central displacements for the remaining tri-axial and bi-axial tests of Phase 5, which are those of Seismic Levels 3 and 4.

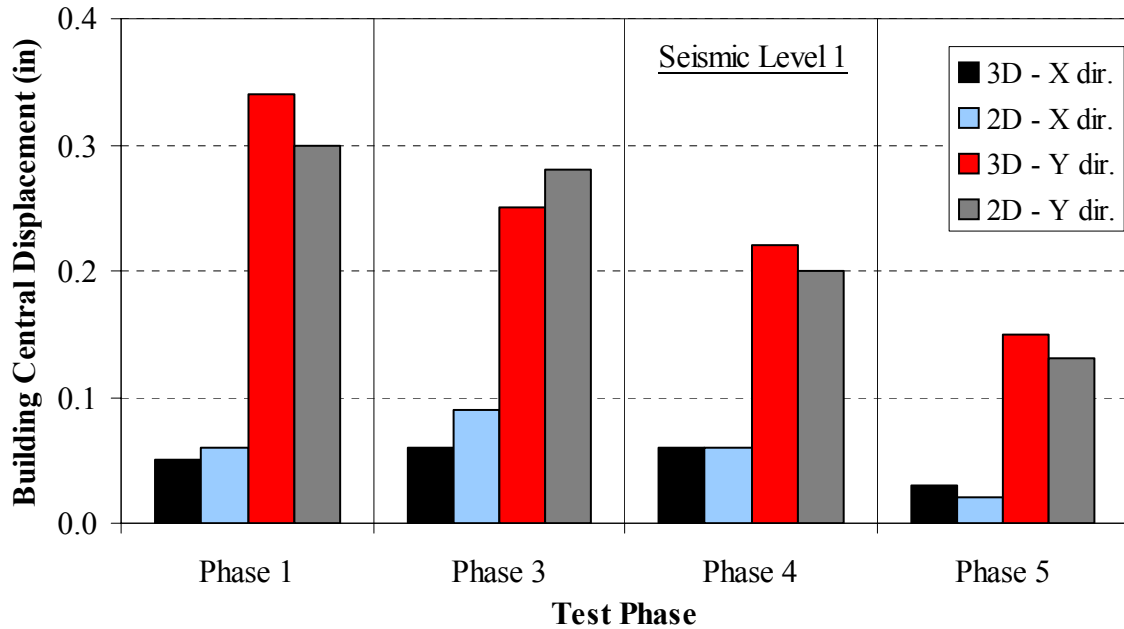


Figure 7.34: Building central displacements for Seismic Level 1 tri-axial and bi-axial tests of Phases 1, 3, 4, and 5

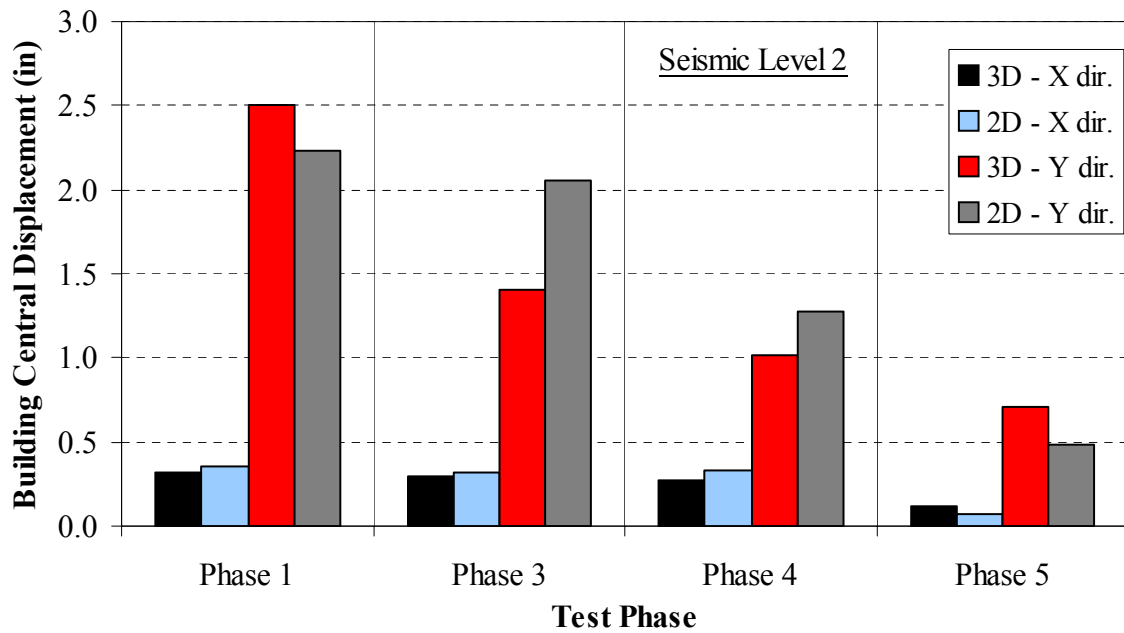


Figure 7.35: Building central displacements for Seismic Level 2 tri-axial and bi-axial tests of Phases 1, 3, 4, and 5

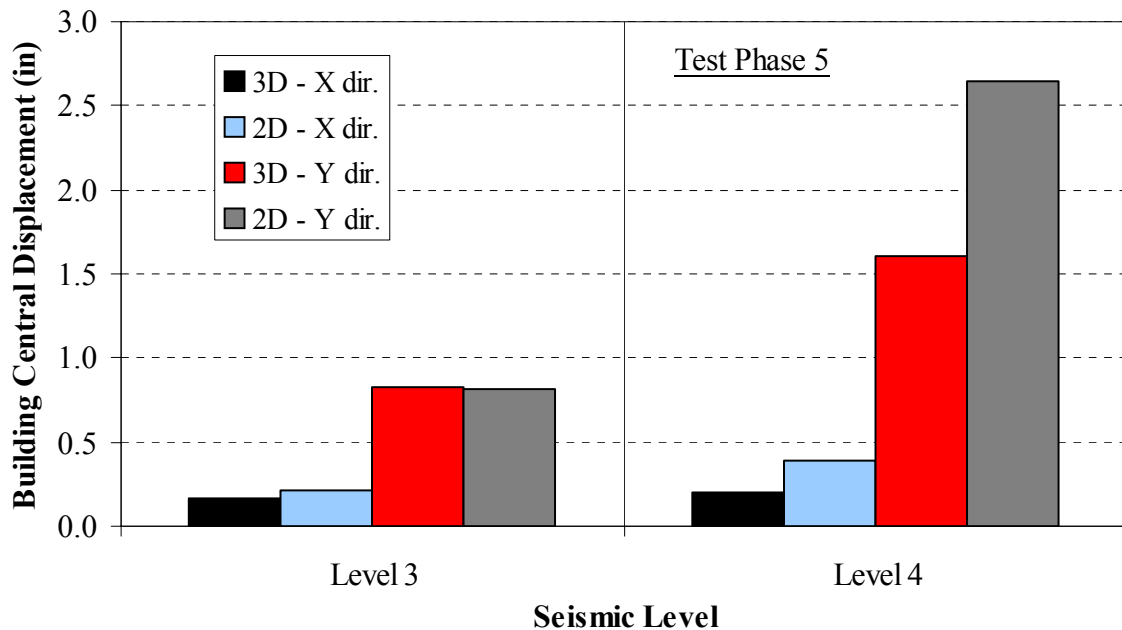


Figure 7.36: Building central displacements for Seismic Levels 3 and 4 tri-axial and bi-axial tests of Phase 5

The response of the structure during the Level 1 tests (Figure 7.34) was similar between tri-axial and bi-axial input excitation. Small differences of the order of 10% were observed mainly in the transverse (Y) direction.

Similar trends were identified for Level 2 tests (Figure 7.35), where the differences in peak transverse displacements between tri-axial and bi-axial tests were also of the order of 10%. However, at Test Phase 3, the maximum roof central displacement in the transverse direction during the bi-axial test was more than 25% greater than that recorded during the tri-axial test.

A similar difference in the central displacement along the transverse direction was also observed for Level 4 tests of Phase 5 (Figure 7.36), where the response during the bi-axial test was greater than that during the tri-axial test. In this case, the difference in the response can be attributed to the failure of some holdown welds along the garage wall during the execution of the bi-axial test,

which resulted in significant stiffness degradation along the transverse direction and increased the building displacements.

From the results obtained, no general trends were observed that relate the displacement response of the benchmark structure with the presence of vertical input excitation. On average, the responses between tri-axial and bi-axial tests of the same seismic level were similar. In some cases, the responses during the bi-axial tests were higher, while in some other cases the responses of the tri-axial tests were higher.

It has to be noted that the variation in the recorded peak displacements between tri-axial and bi-axial tests may be attributed to other reasons as well. One main reason is the modification of the dynamic characteristics of the structure due to the cumulative damage, induced during previously conducted tests. This means that a repetition of the same input excitation may lead to different response of the structure. A second reason is the potential difference in the performance of the shake tables between tri-axial and bi-axial tests, due to the fact that the shake tables were required to perform close to the specified nominal performance limits, as mentioned in Section 7.1.

Chapter 8 Summary and Conclusions

The benchmark shake table testing of a full-scale two-story woodframe townhouse building within the NEESWood project has provided an opportunity to study various parameters that influence the seismic response of woodframe structural systems.

The testing program focused on the various construction elements that have significant influence on the seismic response of woodframe buildings. Five different testing phases were conducted to investigate the influence of the following elements on the seismic behavior: Phase 1 - Engineered wood structural (shear) walls alone; Phase 2 - Wood structural walls incorporating viscous fluid dampers; Phase 3 - Installation of gypsum wallboard to engineered wood structural walls; Phase

4 - Installation of gypsum wallboard to interior partition walls and ceilings; and Phase 5 - Installation of stucco as exterior wall finish.

Two different types of tri-axial historical ground motions were used for the seismic tests: ordinary ground motions and near-field ground motions. The ordinary ground motions represented a Design Basis Earthquake (DBE) having a probability of exceedance of 10% in 50 years (10%/50 years), or equivalently, a return period of 475 years. The 1994 Northridge Earthquake ground motions recorded at Canoga Park, with an amplitude scaling factor of 1.20, were selected as the DBE (Seismic Level 4). The near-field ground motions represented a Maximum Credible Earthquake (MCE) having a probability of exceedance of 2% in 50 years (2%/ 50 years), or a return period of 2475 years. The unscaled 1994 Northridge Earthquake ground motions recorded at Rinaldi were selected as the MCE (Seismic Level 5).

In addition to the DBE and MCE hazard levels, the Canoga Park ground motions were scaled to simulate hazard levels of 99.9%/50 years (Seismic Level 1), 50%/50 years (Seismic Level 2) and 20%/50 years (Seismic Level 3). Note that during Test Phases 1, 3 and 4, only Seismic Test Levels 1 and 2 were conducted in order to limit the damage to a repairable level.

This report has concentrated on the effect of interior and exterior wall finishes on the seismic response of the test structure. Therefore, only the experimental results of Test Phases 1, 3, 4 and 5 were analyzed in detail. A separate NEESWood Project Report will analyze the results of Test Phase 2 incorporating viscous fluid dampers within wood walls.

Based on the experimental results obtained, it can be concluded that the installation of gypsum wallboard to the interior surfaces of structural walls improved substantially the seismic response of the test structure. The application of exterior stucco improved further the seismic response of

the test structure, particularly in its longitudinal direction, where the shear response of the wall piers dominated. The key results obtained in this study are summarized below:

- The application of gypsum wallboard on the interior surfaces of the structural walls caused a reduction of the initial natural periods of the test building. The same trend was observed after the application of exterior stucco finish. The application of gypsum wallboard on partition walls and ceilings, however, did not affect significantly the initial fundamental period of the test structure.
- The equivalent lateral stiffness of the wood-only Phase 1 test structure deteriorated more rapidly through the seismic tests than the other configurations. The transverse equivalent lateral stiffness of the Phase 1 test structure at the end of the Seismic Level 2 was reduced to less than 60% of its initial transverse stiffness. The transverse lateral stiffness for the structures of Test Phases 3 and 4, incorporating gypsum wallboard, was above 80% of their initial transverse stiffness at the end of the Seismic Level 2. The corresponding value for the Phase 5 test structure, incorporating stucco as exterior finish, is above 90%. Even after the DBE Seismic Level 4, the transverse lateral stiffness of the Test Phase 5 test structure remained above 75% of its initial transverse lateral stiffness.
- The fundamental damping ratios of the test structure ranged from 10% to 20% of critical, with a mean value of approximately 15% of critical for all test phases.
- For all test phases, the fundamental mode shape of the test structure was along the transverse direction. The second and third mode shapes of the test structure were along the longitudinal direction with various degrees of torsional coupling depending on the test phase configurations. For the Phase 1 test structure, the in-plane stiffness of the floor and roof diaphragms at the location of the stair case opening was lower than the rest of the structure. The application of gypsum wallboard on these diaphragms increased significantly the in-plane stiffness of the diaphragms. All mode shapes of the test structure were characterized by larger lateral inter-story displacements in the first story than in the second story.

- Hairline cracking occurred in the gypsum wallboard applied to the interior surfaces of the structural walls of the Phase 3 test structure during Seismic Level 2. This cracking occurred mainly at corners of the openings of the interior shear walls. This cracking propagated with increasing level of shaking.
- Ceiling damage was observed in the Phase 4 test structure. Cracking of the partition-to-ceiling connections in the transverse direction of the test building started occurring under Seismic Level 2. Ceiling damage increased in the Phase 5 test structure until a large portion of the ceiling gypsum failed under Seismic Level 5 (MCE). This failure occurred in the second level ceiling connecting the two main rectangular units of the test structure and can be attributed to the in-plane shear deformation of the ceiling diaphragm at that location.
- Hairline cracking of stucco in the Phase 5 test building started during Seismic Level 2. This cracking occurred mainly at corners of windows and door openings and propagated with increasing level of shaking. After Seismic Level 5 (MCE), significant spalling and cracking of stucco occurred around the garage door opening.
- The most significant damage observed in the Phase 5 test structure after Seismic Level 5 (MCE) was the splitting of the 2x4 and 2x6 sill plates around the entire perimeter of the building. In particular, the sill plate of the narrow wall piers of the garage separated by more than $\frac{1}{2}$ in. This damage would be very costly to repair in a real building.
- The largest inter-story drifts in the test structure were recorded in the transverse direction along the first level garage wall line. Generally, the first level inter-story drifts were lower on the East side of the test structure than on the West side. The drifts measured in the longitudinal direction of the test structure were significantly lower than the drifts measured in the transverse direction.
- The application of gypsum wallboard on the interior surfaces of the structural wood walls reduced significantly the displacement response of both floors of the test structure. The reduction of the maximum transverse inter-story drifts from Phase 1 to Phase 3 was of the order of 40% for Seismic Level 2. The application of gypsum wallboard on the partition

walls and the ceilings did not affect much the first level inter-story drifts of the test structure, but further reduced the drifts of the second floor. This is attributed to the fact that the first floor level had only few partition walls compared to the second level of the test structure. Besides the stiffness contribution from the partition walls, the significant reduction of inter-story drifts on the second floor was also explained by the increase of diaphragm effect on the roof level. The in-plane stiffness of the roof diaphragm was increased because of the application of the gypsum wallboard to the bottom chords of the roof trusses. On the other hand, the gypsum wallboard ceiling had minimal effect on the floor diaphragm since the structural floor system (plywood panels and the floor joists) alone provided enough in-plane stiffness to “act” as a rigid diaphragm. The application of stucco as exterior finish further reduced the inter-story drifts in both levels of the test structure.

- For the Phase 5 test structure, the portion of the total lateral building drift occurring in the first level increased with the intensity of the seismic shaking. This indicates that a first level side-sway mechanism would likely govern the collapse of the test structure.
- Under the Seismic Level 5 (MCE) tri-axial test, the Phase 5 test structure experienced a maximum inter-story drift of 3.5% in the first level garage wall line, thereby achieving the collapse prevention performance objective.
- Under Seismic Level 4 (DBE), the Phase 5 test structure experienced a maximum inter-story drift of 1.4% in the first level garage wall line, which is less than the corresponding maximum inter-story drift of 1.7% experienced by the Phase 1 test structure under Seismic Level 2 (44% DBE). This result suggests that the Phase 1 test structure may have collapsed under Seismic Level 5 (MCE).
- The peak horizontal accelerations measured during Seismic Level 2 did not vary greatly across the different test phases. Maximum peak horizontal accelerations were recorded at the garage wall line for both floor levels of the test structure.

- The racking deformations of the wood shear walls accounted for approximately 80% of the measured inter-story drifts for the Phase 1 test structure under Seismic Level 2. This ratio reduces to approximately 50% for the Phase 3, 4 and 5 test structures. These results indicate that only a portion of the inter-story drift translates directly into wall racking deformations, particularly when wall finishes are included. Therefore, results of racking (shear) tests of wall specimens must be interpreted carefully since the racking displacement in a shear wall test can not be directly associated with inter-story drift.
- The seismic energy inputted to the Phase 1 test structure under Seismic Level 2 was approximately three times higher than that of the Phase 5 test structure. The seismic energy inputted in the Phase 3 and 4 test structures was slightly higher than that of the Phase 5 test structure.
- The average peak sill plate slippage of the first floor walls recorded during Seismic Level 2 was below 0.05 in. across all test phases. The portion of inter-story displacement due to sill plate slippage was approximately 10% on average for Seismic Level 2.
- For Seismic Level 2, a maximum anchor bolt force of approximately 6 kips (approximately 40% of ultimate capacity), was recorded in a holdown device of the garage wall line of the Phase 1 test building. For the Phase 5 building under Seismic Level 5 (MCE), this same holdown device recorded a peak force of just below 10 kips (approximately 60% of ultimate capacity).
- For Seismic Level 2, the largest sill plate and end stud uplifts (0.3 in. to 0.45 in.) were recorded in the Phase 1 test structure. The peak uplifts for the Phase 3 and 4 test structures were approximately 0.1 in., slightly lower than for the Phase 5 test structure. The Phase 5 test structure, on the other hand, experienced peak uplifts over 3 in. during Seismic Level 5 (MCE).
- No significant effect of vertical input excitation on the seismic response of the benchmark structure was identified. On average, the responses between tri-axial and bi-axial tests of the same seismic level were similar (10% differences in peak building central displacements).

Further information on this benchmark project and on the overall research program of the NEESWood Project can be obtained at the following web site:

<http://www.engr.colostate.edu/NEESWood/>

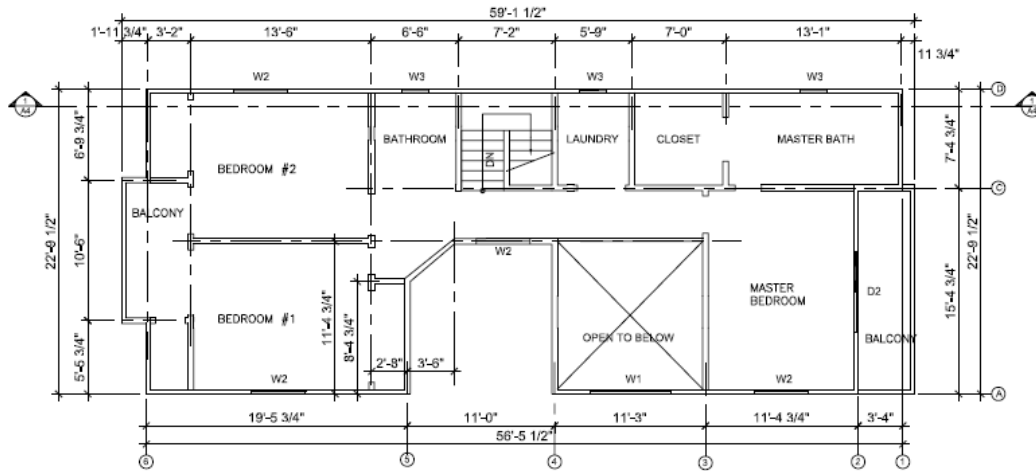
REFERENCES

- [1] Reitherman, R., Cobeen, K. and Serban, K., (2003). “Design Documentation of Woodframe Project Index Buildings,” Report No. W-29, *Consortium of Universities for Research in Earthquake Engineering*, Richmond, CA.
- [2] ICBO, (1988). *Uniform Building Code*, 1988 edition, International Conference of Building Officials, Whittier, California.
- [3] Krawinkler, H., Parisi, F., Ibarra, L., Ayoub, A. and Medina, R., (2003). “Development of a Testing Protocol for Woodframe Structures”, Report No. W-02, *Consortium of Universities for Research in Earthquake Engineering*, Richmond, CA.
- [4] Department of General Services, Division of the State Architect, (2005). *Guidelines for Earthquake Bracing of Residential Water Heaters*, 1102 “Q” Street, Suite 5100, Sacramento, CA, 12 p.
- [5] Governor’s Office of Emergency Services, Department of General Services, Division of the State Architect, Seismic Safety Commission and Department of Education (2003). *Guide and Checklist for Nonstructural Earthquake Hazards in California Schools*, 1102 “Q” Street, Suite 5100, Sacramento, CA, 56 p.
- [6] Fierro, E. A., Perry, C. L. and Freeman, S. A., (1994). *Reducing the Risks of Nonstructural Earthquake Damage: A Practical Guide*, FEMA 74, Third Edition, Federal Emergency Management Agency, 139 p.
- [7] Ekiert, C. and Hong, J., (2006). “Framing-to-Sheathing Connection Tests in Support of NEESWood Project”, Network of Earthquake Engineering Simulation Host Institution: State University of New York at University at Buffalo, Buffalo, NY, 28 p.
- [8] Pang, W., (2007). “guiMSTEWfit, MATLAB Code for Parameter Fitting of Connection Tests”, Personal Communication.
- [9] Folz, B. and Filiatrault, A., (2001). “Cyclic Analysis of Wood Shear Walls”, *ASCE Journal of Structural Engineering*, Vol. 127, No. 4, pp. 433-441.
- [10] ASTM C109, (2003). “Standard Test Method for Compressive Strength of Hydraulic Cement Mortars”, Vol. 04.01, *American Standards National Institute*.

- [11] Gworek, J., (2006). “NEESWood Project: Stucco Sample Data and Analysis”, State University of New York at University at Buffalo, Buffalo, NY, 13 p.
- [12] DADiSP 2002, (2006). DSP Development Corporation, Boston, MA 02284-7108.
- [13] Clough, R. W. and Penzien, J., (1975). “Dynamics of structures”, McGraw Hill Book Co., NY.
- [14] Bracci, J. M., Reinhorn, A. M. and Mander, J. B., (1992). “Seismic Resistance of Reinforced Concrete Frame Structures Designed Only for Gravity Loads: Part I - Design and Properties of a One-Third Scale Model Structure”, Technical Report [NCEER-92-0027](#), *National Center for Earthquake Engineering Research*, State University of New York at University at Buffalo, Buffalo, NY.
- [15] Christovasilis, I. P., Filiatrault, A., Wanitkorkul, A. and Constantinou, M. C., (2007). “Seismic Collapse Analysis of Woodframe Buildings”, *Earthquake Engineering and Structural Dynamics*, (submitted for publication, November 2007).
- [16] FEMA (2000). *Prestandard and Commentary for the Seismic Rehabilitation of Buildings*, FEMA 356, Federal emergency Management Agency, Washington, DC.
- [17] Chopra, A. K., (2001). “Dynamics of Structures. Theory and Applications to Earthquake Engineering”, Second Edition, Prentice Hall, New Jersey.
- [18] *Simpson Strong-Tie* website: <http://www.strongtie.com/products/connectors/PHD-HDQ8.html>.
- [19] ANSI/AF&PA, (2005). “2005 National Design Specification for Wood Construction”, *American Standards National Institute*.

Appendix A
Architectural and Structural Drawings
of Test Structure

Appendix A



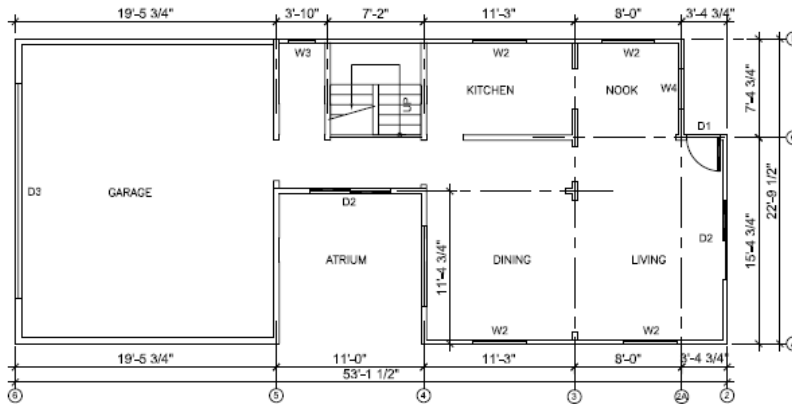
NOTE

DOORS:

- D1 - Prehung 2'6" x 6'8" solid core door
- D2 - 6' x 6'10" aluminum sliding glass door
- D3 - 16' x 7' hinged, wood double door

WINDOWS:

- W1 - 6' x 6' aluminum window, standard glazed
- W2 - 4' x 4' sliding aluminum window, standard glazed
- W3 - 2' x 2' sliding aluminum window, standard glazed
- W4 - 3' x 2'6" sliding aluminum window, standard glazed



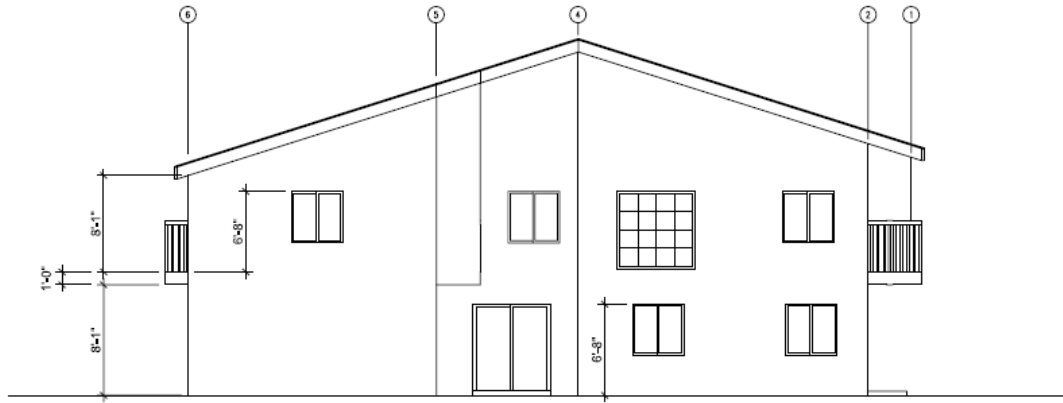
6	03/06/06	Final drawings for construction
3	01/02/06	Correct the North direction (according to the shake table)
2	12/06/05	Change location of W4 to center of the wall
1	10/26/05	Remove all interior doors, add windows at line A

REV. NO.	DATE	DESCRIPTIONS
		University at Buffalo
PROJECT: NEESWood Townhouse Building for Benchmark Testing		CONTENT: Floor Plans
DATE: 03/06/06		REV. NO.: 6
		SCALE: 1/8" = 1'

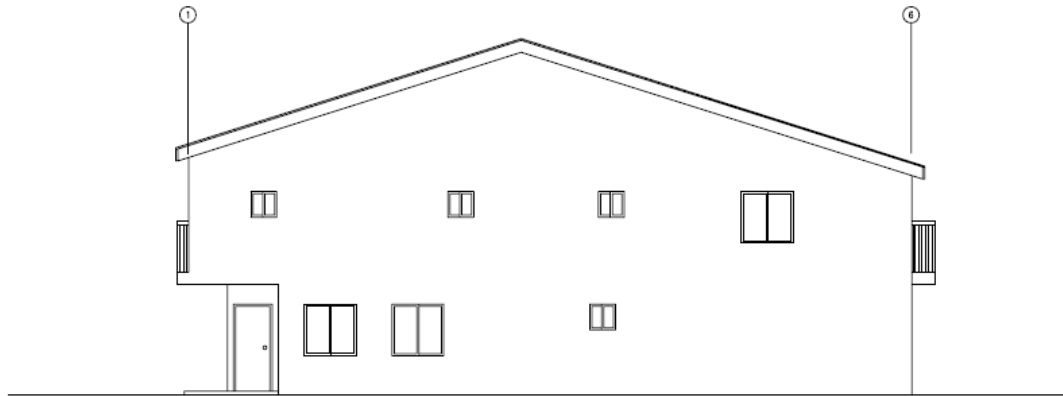
DWG. NO.
A-1

FOR CONSTRUCTION

Appendix A



SOUTH ELEVATION



NORTH ELEVATION

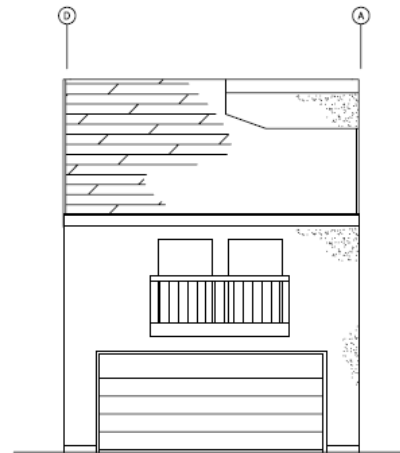
FOR CONSTRUCTION

6	03/06/06	Final drawings for construction	
REV. NO.	DATE	DESCRIPTIONS	
NEESWOOD		University at Buffalo	DWG. NO. A-2
PROJECT: NEESWood		CONTENT: Elevations	
Townhouse Building for Benchmark Testing		DATE: 03/06/06	REV. NO. 6
		SCALE: 1:100	

Appendix A




EAST ELEVATION

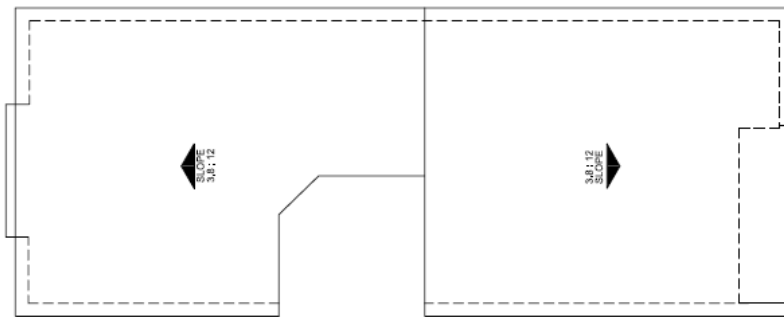
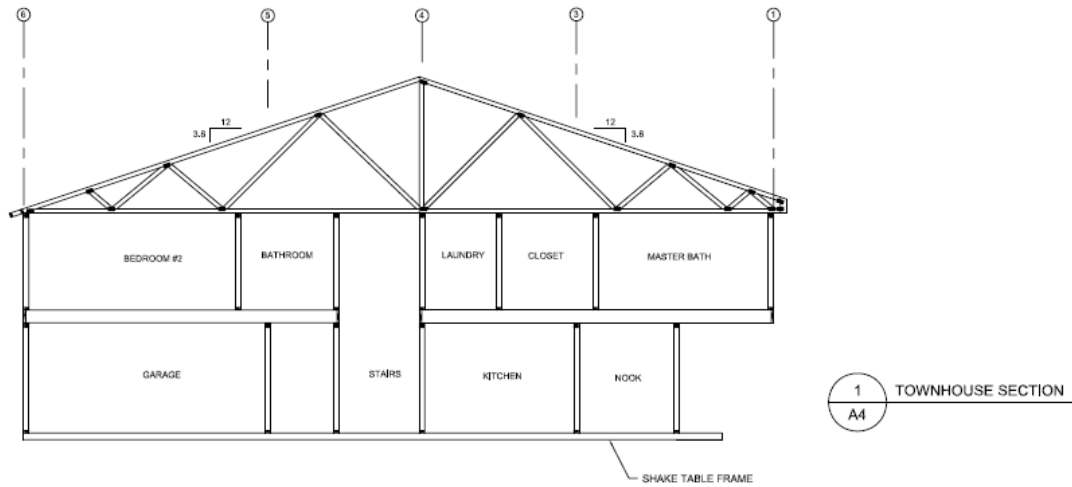


WEST ELEVATION

FOR CONSTRUCTION

6	03/06/06	Final drawings for construction
3	01/02/06	Correct the North direction (according to the shake table)
2	12/06/05	Change location of W4 to center of the wall
REV. NO.	DATE	DESCRIPTIONS
		University at Buffalo DWG. NO. A-3
PROJECT: NEESWOOD Townhouse Building for Benchmark Testing		CONTENT: Elevations DATE: 03/06/06 REV. NO. 6 SCALE: 1/8" = 1'

Appendix A



ROOF PLAN

FOR CONSTRUCTION

6	03/06/06	Final drawings for construction		
REV. NO.	DATE	DESCRIPTIONS		DWG. NO.
NEESWOOD		University at Buffalo		A-4
PROJECT: NEESWood		CONTENT: Roof Plan & Section		
Townhouse Building for Benchmark Testing		DATE: 03/06/06	REV. NO. 6	SCALE: 1:100

Appendix A

ABBREVIATIONS

ABBREVIATIONS

AB	ANCHOR BOLT	EXT	EXTERIOR	OPP	OPPOSITE
ADH	ADHESIVE	FNON	FOUNDATION	OPNG	OPENING
ALT	ALTERNATE	FIN FLR	FINISHED FLOOR	OSB	ORIENTED STRAND BOARD
ARCH	ARCHITECTURAL	FLR	FLOOR	P.D.F.	POWER DRIVEN FASTENER
AWS	AMERICAN WELDING SOCIETY	F.O.	FACE OF	PERP	PERPENDICULAR
Ø	AT	F.O.B.	FACE OF BLOCK	PERM	PERMETER
BLDG	BUILDING	F.O.C.	FACE OF CONCRETE	PL	PLATE
BLK	BLOCK	F.O.S.	FACE OF STEEL	PLWD	PLYWOOD
BLKG	BLOCKING	FRMG	FRAMING	POST TEN	POST TENSIONED
BM	BEAM	F.S.	FACE SIDE	PTDF	PRESSURE TREATED DOUGLAS FIR
B.O.	BOTTOM OF	FT	FOOT	REF	REFERENCE
B.O.C.	BOTTOM OF CONCRETE	FTG	FOOTING	REINF	REINFORCING
B.O.S.	BOTTOM OF STEEL	GA, ØB	GAGE	REQ'D	REQUIRED
BS	BOTH SIDES	GALV	GALVANIZED	ROOM	ROUGH OPENING
BRG	BEARING	G.E.T.	GABLE END TRUSS	R.O.	ROUGH OPENING
BOIT	BOTTOM	GR BM	GRADE BEAM	RWDW	REDWOOD
BTWN	BETWEEN	GL	GLULAM	S.A.D.	SEE ARCHITECTURAL DRAWINGS
CL	CENTER LINE	GYP BD	GYPNUM BOARD	SCHED	SCHEDULE
CLG	CEILING	HDR	HEADER	SEL STRUCT	SELECT STRUCTURAL
CLR	CLEAR	HDR	HANGER	SHT	SHEET
COL	COLUMN	HORIZ	HORIZONTAL	SHTG	SHEATHING
CONC	CONCRETE	H.P.	HIGH POINT	SM	SIMILAR
CONN	CONNECTION	H.S.B.	HIGH STRENGTH BOLT	SPEC	SPECIFICATIONS
CONSTR	CONSTRUCTION	INSUL	INSULATION	SO	SQUARE
CONT	CONTINUOUS	INT	INTERIOR	SS	STAINLESS STEEL
CP	COMPLETE PENETRATION	JNT	JOINT	STD	STANDARD
CTR	CENTER	JOST	JOIST	STRUCT	STRUCTURAL
DBL	DOUBLE	LOCN	LOCATION	T & B	TOP AND BOTTOM
DET	DETAIL	L.P.	LOW POINT	T & G	TONGUE AND GROOVE
DF	DOUGLAS FIR	MATL	MATERIAL	TH	TOE NAIL
DF /L	DOUGLAS FIR-LARCH	MAX	MAXIMUM	T.O.	TOP OF
DIA	DIAMETER	MC	MOISTURE CONTENT	T.O.C.	TOP OF CONCRETE
DIAG	DIAGONAL	MCH	MECHANICAL	T.O.S.	TOP OF STEEL
DIM	DIMENSION	MFG	MANUFACTURER	TS	TUBE STEEL
DWG	DRAWING	MN	MINIMUM	TSW	TOP SEAM WELD
(E)	EXISTING	MCL	MICRO LAM	TYP	TYPICAL
EA	EACH	MNL	MINILAM	UN	UNLESS OTHERWISE NOTED
EF	EACH FACE	(N)	NEW	VERT	VERTICAL
ELEC	ELECTRICAL	NA	NOT APPLICABLE	W.P.	WORKING POINT OR WATER PROOFING
ELEV, EL	ELEVATION	N.C.	NOT IN CONTRACT	WF	WELD
EN	EDGE NAIL	NO. #	NUMBER	W/W	WELDED WIRE FABRIC
EQUIP	EQUIPMENT	N.S.	NEAR SIDE	W/	WITH
EW	EACH WAY	N.T.S.	NOT TO SCALE	XS	EXTRA STRONG
EXP BOLT	EXPANSION BOLT	OC	ON CENTER		
EXP JNT	EXPANSION JOINT	O/	OVER		

GENERAL NOTES

SCOPE

These structural drawings are for the construction of a townhouse residence to be used for testing on two adjacent shake tables at the University at Buffalo as part of the NEESWood Project. Details of attachment to the testing frame are to be provided by others. The configuration shown in these drawings corresponds to the final stages of testing.

COORDINATION

Details shown are typical, similar details apply to similar conditions. Contractor shall review drawings as to layout, details, dimensions and elevations. All questions, discrepancies and conflicts shall be reported to the NEESWood Project for adjustment before proceeding with work. No substitutions shall be made without approval from the NEESWood Project.

TEMPORARY SHORES AND BRACING

The contractor shall provide temporary shores and bracing to rigidly and safely support structural elements during construction.

CUTTING AND PATCHING

Do not cut structural elements except as shown on the drawings, or as specially approved by the NEESWood Project.

CODE

Design is based on the Uniform Building Code, 1988 Edition except for foundation steel plate washers which conform to the more restrictive requirements of the 1997 UBC. Construction shall conform with applicable sections of the 1988 UBC except as specifically noted.

SEISMIC BASE SHEAR = 0.183W

STRUCTURAL NOTES

Drawing sheets A1-A4 and S1-S15 contain information describing the building. Sheets A1-A4 contain the architectural plans, while /Sheets S1-S15 contain typical details, notes, assembly and weight information.

SPECIES

Typical species for wall framing - Hem-Fir
Typical species for floor framing - Douglas-Fir NO. 2
Foundation sill plates - pressure treated Hem-Fir.
Roof trusses - could vary - assume SPF.

MOISTURE CONTENT

Moisture content for all solid sawn lumber should be "dry" (MC less than 19%)

STRUCTURAL GLUED LAMINATED WOOD MEMBERS (GLULAMS)

Design and construction shall conform to ANSI/AITC Standard A190.1-83 and ASTM Standard D3737-89a. "Glulams" (GL) shall be manufactured from species and grades of lumber which will produce design values equal to or exceeding the following, when loaded perpendicular to the wide faces of the laminations:

Bending (F _b) - tension on tension face	1600 PSI
- tension on compression face	825 PSI
Horizontal shear (F _v)	195 PSI
Compression perpendicular to the grain on the tension face (F _c perp)	315 PSI
Modulus of elasticity (E)	1,300,000 PSI

SHEATHING

Roof sheathing 7/16" OSB

8d common dimensions - ASTM F1667:
Flat head, diamond point, L=2.5", D=0.131" pneumatically installed at 6" supported edges, 12" other supports.

Floor sheathing shall be 3/4" T&G, Exposure 1, Span Rating 48/24. Lay face grain across joists, stagger sheets. Attach plywood to joists and blocking with adhesive in accordance with APA glued floor system.
10d common dimensions, L=3", D=0.148" pneumatically installed at 6" / 10".

Wall sheathing 7/16" OSB.

8d common. See shear wall schedule for edge nail spacing, 12" field spacing.

Gypsum wallboard sheathing - 1/2" sheathing - applied horizontally.

#8 Type A, sharp point screw 1-1/4" long.

For gypsum board wall sheathing these fasteners are at 7 inches on center over the height of each stud.

Gypsum board ceiling sheathing. The fasteners above are at 7 inches along the ceiling joists. The perimeter edges parallel to the joists should be nailed in order to provide proper vertical support. The edges perpendicular should not be nailed or blocked.

STUCCO

USC Tables 47B & C. 18 ga hexagonal woven wire, furred out from backing 1" nailed with 16 gauge staple, 7/8" minimum leg, spaced 6" maximum vertically, 16" horizontally, except at perimeter of wall 6" o.c. spacing.

ROOF DIAPHRAGM

2"x6" joists spaced at 24" on center with 7/16" OSB sheathing

FASTENERS

Nails called out in details are noted as #d, where #d is penny weight. N# denotes Simpson joist hanger nails. EN denotes plywood edge nailing. For schedule of other minimum nailing see Uniform Building Code Table 23-0. Where sinkers are detailed, they shall be green vinyl coated sinkers.

Framing nailing to be done with coated sinker nails. The following is the schedule of minimum fastening from the 1988 UBC. It needs to be kept in mind that much of the framing nailing was done with 16d sinker nails. Fastening noted as having multiple 8d nails were more likely to have one or two 16d sinker nails.

- Joist to sill or girder - toe nail 3-8d
- Bridging to joist - toe nail each end 2-8d
- Sole plate to joist or blocking - face nail 16d # 16"
- Top plate to stud - end nail 2-16d
- Stud to sole plate - end nail 2-16d or toe nail 2-16d or toe nail 4-8d
- Double studs - face nail 16d # 24"
- Doubled top plates - face nail 16d # 16"
- Ceiling joists - to plate - toe nail 3-8d
- Continuous header to stud - toe nail 4-8d
- Ceiling joists - laps over partitions face nail 3-16d
- Ceiling joists to parallel rafters face nail 3-16d
- Header to plate - toe nail 3-16d
- Corner studs and angles (built up corners) 16d # 24"
- Built-up corners and beams 20d # 32" at top and bottom staggered, 2-20d at ends and each splice.
- Sills to joists, interior partition walls 16d # 16"

OTHER WOOD FASTENERS

BOLTS. Bolts shall be ASTM A490. Bolts bearing on wood shall have standard plate washers under heads and nuts except where steel plate washers are detailed. Bolts in connections shall be re-tightened just prior to closing of the wall and/or floor.

Anchor bolts - per shear wall schedule at noted shear walls, otherwise 1/2" diameter at 6"-0" maximum on center.

CONNECTOR DEVICES. Connector devices, unless otherwise noted, are Simpson Strong Tie. Alternates may be submitted for consideration. Joist hangers are to be Simpson LUS, u.o.n.

REFERENCES

- Uniform Building Code, 1988 Edition
- ASTM F-1667-85 Standard Specification for Driven Fasteners: Nails, Spikes, Staples

6	03/06/06	Final drawings for construction
4	01/11/06	Add nailing schedule for int. walls (sills to joists)
2	12/06/05	Update structural notes and tiedown annotations
REV. NO.	DATE	DESCRIPTIONS
NEESWOOD		University at Buffalo
PROJECT: NEESWOOD		CONTENT: General & Structural Notes
Townhouse Building for Benchmark Testing		DATE: 03/06/06
		REV. NO. 6
		SCALE: NA
		DWG. NO. S-1

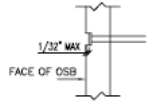
FOR CONSTRUCTION

Appendix A

SHEAR WALL SCHEDULE							
SYMBOL	ALLOWABLE SHEAR (PSF)	SHEATHING MATERIAL	MIN STUD AT ADJOINING PANEL EDGES	FOUNDATION SILL	SHEATHING EDGE NAILS (END (1))	SHEATHING INTERMEDIATE NAILS (1)	ANCHOR BOLTS (2)
⬡	260	7/16 OSB SHEATHING	2x	2x	8d@6"	8d@12"	1/2"Ø48"
⬢	380		2x	2x	8d@4"		1/2"Ø32"
⬣	490		2x	2x	8d@3"		1/2"Ø16"

SHEAR WALL NOTES

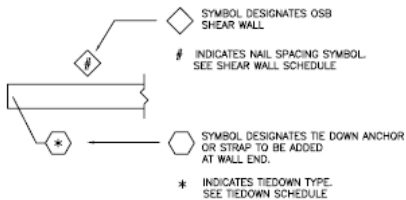
- See General Notes for nails. Common nails, substitutions must be approved by the NEESWood Project.
- Minimum two bolts per piece of sill plate.
- Locate tie down stud or post and provide plywood edge nailing to stud or post, as well as all panel edges.
- Nails shall be considered overdriven when the top of the head of the nail is more than 1/32" below the face of OSB sheathing. Replace each overdriven nail with a new nail.



Where more than 30 percent of edge nailing on any side of a shear wall is overdriven, remove sheathing, replace any split framing members, and add new sheathing.

- Edge nails at 4" or closer require double 2X studs at abutting panel edges.

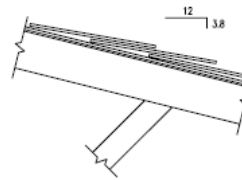
SHEAR WALL LEGEND



TIEDOWN SCHEDULE			
SYMBOL	TIEDOWN	ALLOWABLE UPLIFT (P)	ADJUSTED ALLOWABLE UPLIFT (P)
⊕	PH02	3375	NA
⊕	PH05	4380	NA
⊕	STR236	2475	1650

* ADJUSTMENT ONLY CONSIDERS NAILS FALLING IN POST ABOVE & BELOW. NAILS AT FLOOR DEPTH ARE DEDUCTED.

3.8 : 12 SLOPED ROOF



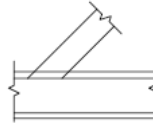
	PSE
CONC TILE	10.0
RE-ROOF	0.0
BUILDING PAPER	
7/16" OSB	1.5
2X6@24" TRUSS TOP CHORD	1.0
2X4@24" TRUSS WEB	0.6
SUB-TOTAL	13.1
ADJUST FOR SLOPE X1.049	13.7
MISC	0.3
TOTAL	14.0

EXTERIOR WALL



	PSE
7/8" 3 COAT STUCCO	8.8
2X4 STUDS@16"	1.1
PLATES	0.5
3/8" PLYWOOD-OSB	1.1
INT FINISH MIN 1/2" GYP	1.8
MISC.	0.2
TOTAL	13.4
1/4" GLAZING + FRAME ~ 4.0 PSF	
DOORS ~ 2.0 PSF	

CEILING



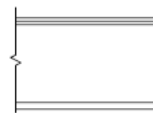
	PSE
2X6@24" BOTTOM CHORD	1.0
2X4@24" TRUSS WEB	0.6
FINISH MIN 1/2" GYP	1.8
MISC	0.2
TOTAL	3.6

INTERIOR WALL



	PSE
2X4 STUDS@16"	1.0
PLATES	0.5
FINISH - 2 X 1/2" GYPBD	3.6
MISC.	0.2
TOTAL	5.3

FLOOR

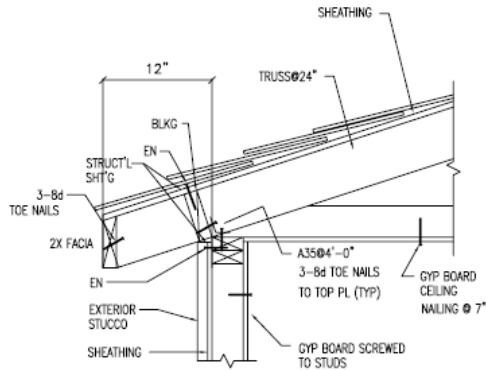


	PSE
3/4" T&G PLWD	2.2
2X12@16"	3.1
GYPBOARD	2.2
MISC.	0.5
TOTAL	8.0

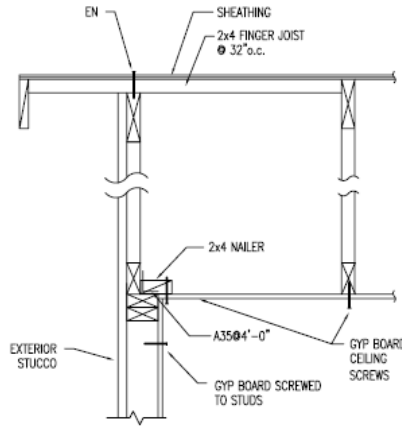
6	03/06/06	Final drawings for construction
4	01/11/06	Add nailing schedule for int. walls (sills to joists)
2	12/06/05	Update structural notes and tiedown annotations
REV. NO.	DATE	DESCRIPTIONS
NEESWOOD		University at Buffalo
PROJECT: NEESWOOD		CONTENT: Additional Notes
Townhouse Building for Benchmark Testing		DATE: 03/06/06
		REV. NO. 6
		DWG. NO. S-2
		SCALE: NA

FOR CONSTRUCTION

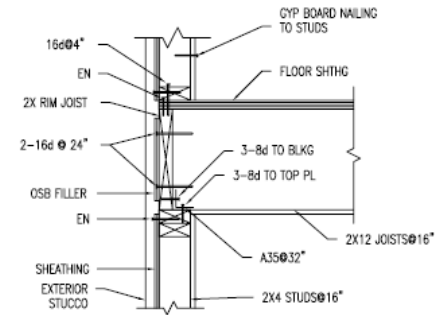
Appendix A



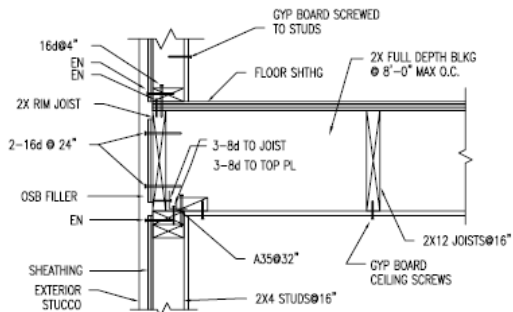
1 ROOF EAVE
S3



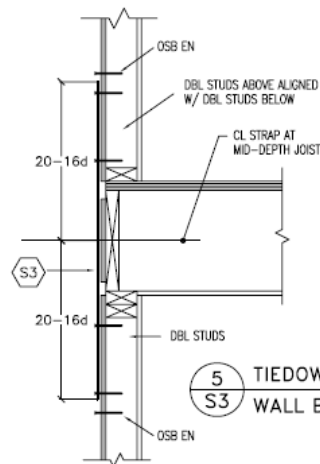
2 TYP. GABLE END ROOF
S3 HIGH CEILING



3 2ND FLOOR EXT. WALL
S3 PERP. TO JSTS



4 2ND FLOOR EXT. WALL
S3 PARALLEL TO JSTS

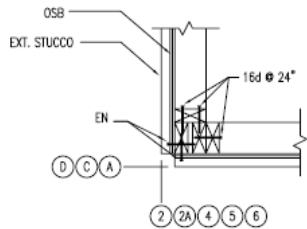


5 TIEDOWN STRAP TO
S3 WALL BELOW

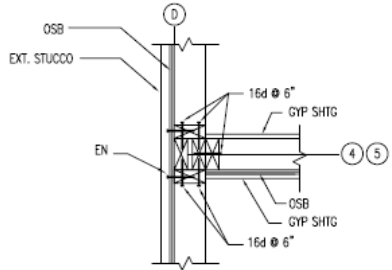
6	03/06/06	Final drawings for construction
3	01/02/06	Correct the North direction (according to shake table)
2	12/06/05	Add typ. corder details and typ. hold-down connection
1	10/26/05	Add non-shrink grout at foundation sill plates
REV. NO.	DATE	DESCRIPTIONS
		University at Buffalo DWG. NO. S-3
PROJECT: NEESWOOD Townhouse Building for Benchmark Testing		CONTENT: Structural Details DATE: 03/06/06 REV. NO. 6 SCALE: 1" : 1'

FOR CONSTRUCTION

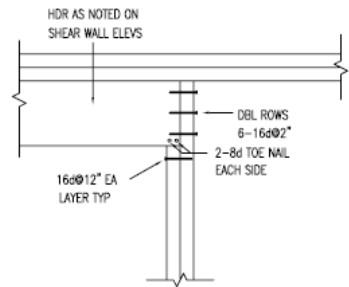
Appendix A



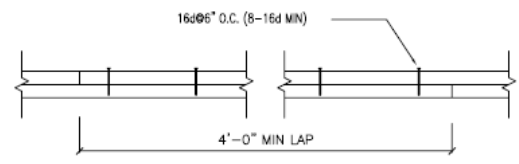
6 TYP. SHEAR TRANSFER AT CORNER
S4 PLAN VIEW



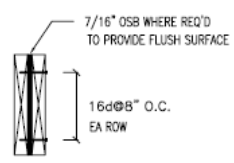
7 SHEAR TRANSFER AT T-JOINT
S4 PLAN VIEW



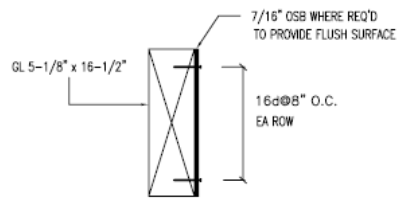
8 TYP. HEADER FRAMING
S4



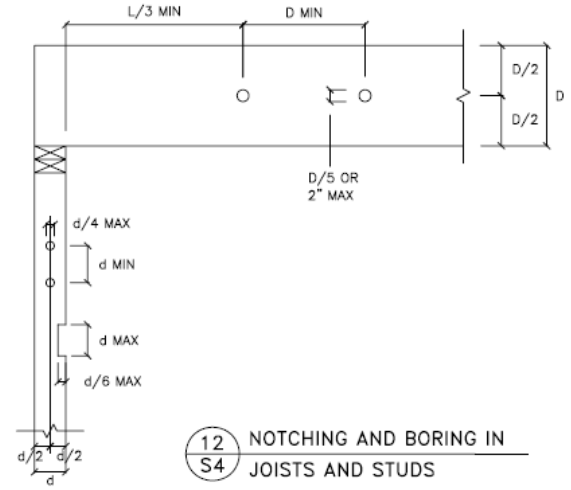
9 TYP TOP PLATE SPLICE
S4



10 TYP. BUILT UP HEADERS
S4 AND JOISTS



11 BUILT UP HEADER
S4 AT GARAGE

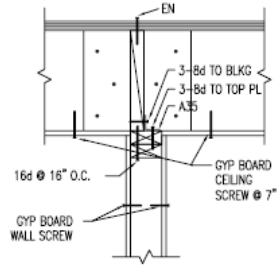


12 NOTCHING AND BORING IN
S4 JOISTS AND STUDS

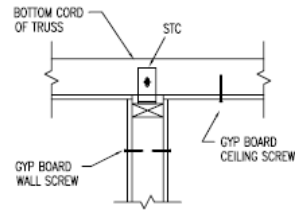
6	03/06/06	Final drawings for construction
3	01/02/06	Correct the North direction (according to shake table)
2	12/06/05	Add typ. corner details and typ. hold-down connection
1	10/26/05	Add non-shrink grout at foundation sill plates
REV. NO.	DATE	DESCRIPTIONS
NEESWOOD		University at Buffalo
PROJECT: NEESWOOD		CONTENT: Structural Details
Townhouse Building for Benchmark Testing		DATE: 03/06/06
		REV. NO. 6
		DWG. NO. S-4
		SCALE: 1" : 1'

FOR CONSTRUCTION

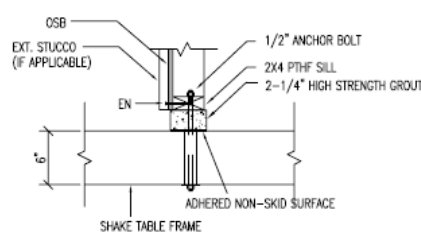
Appendix A



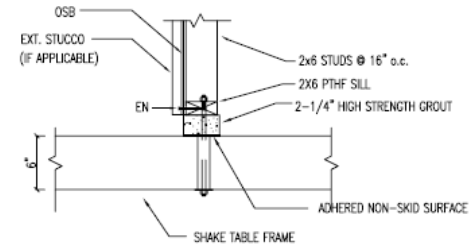
13 1ST FLOOR INTERIOR WALL
S5



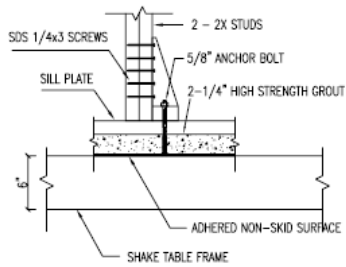
14 2ND FLOOR PARTITION WALL
S5 AT CEILING



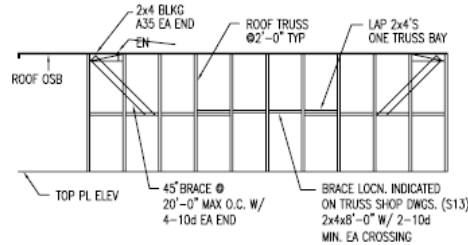
15 TYP. ANCHORAGE
S5



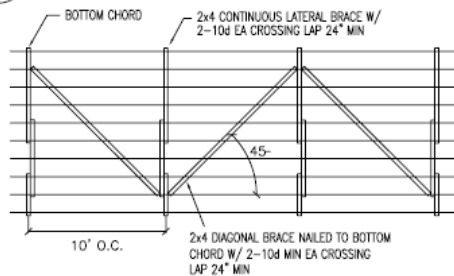
16 TYP. ANCHORAGE
S5 AT GARAGE



17 TYP. HOLD-DOWN CONNECTION
S5



18 BRACING OF ROOF TRUSS
S5 WEB MEMBERS NTS



19 BRACING OF ROOF TRUSS
S5 BOTTOM CHORDS NTS

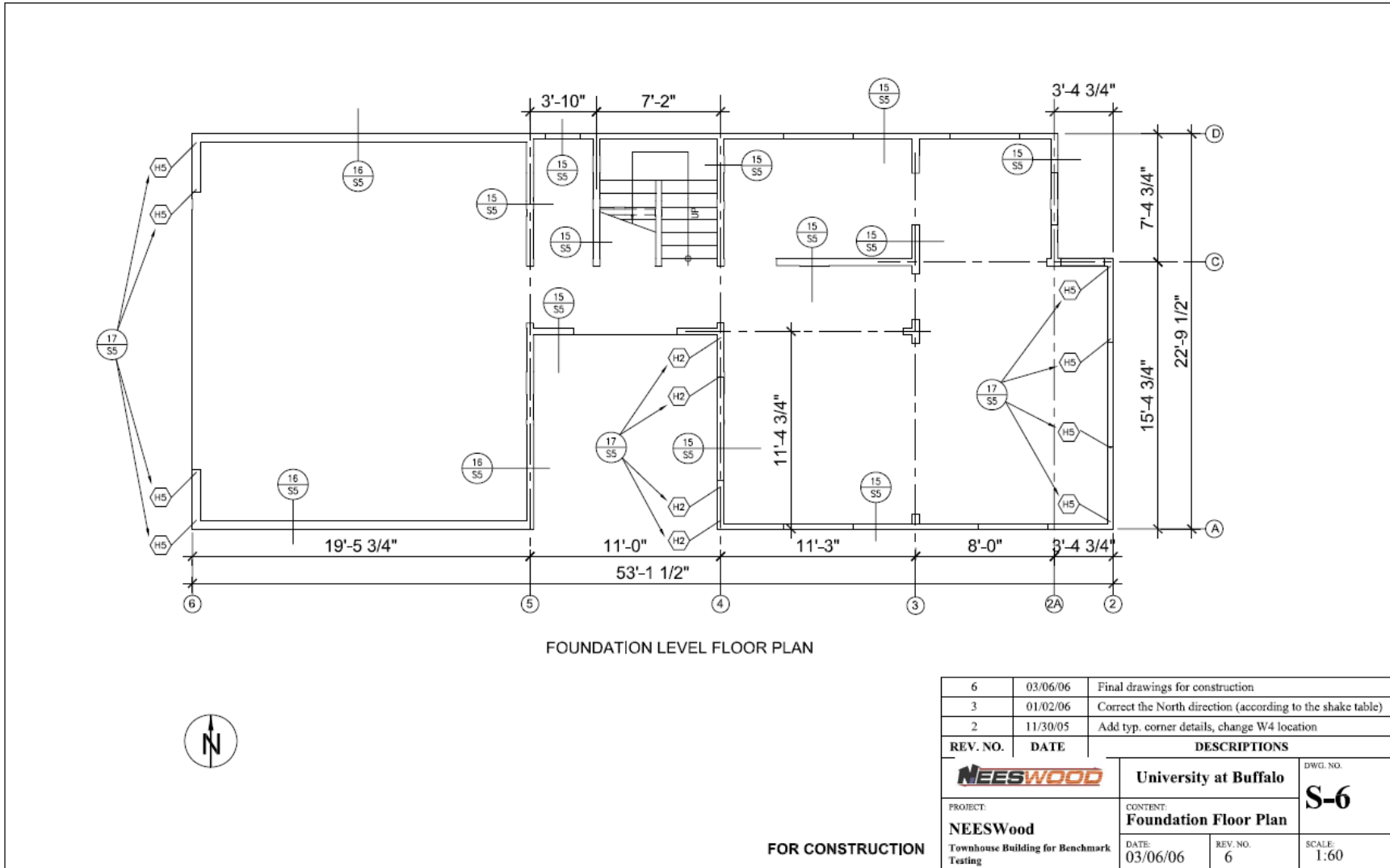
NOTE

Most of the testing will occur without the ceiling gypsum board on the truss bottom chord. The truss design shall accommodate this bottom chord condition. See 19/S5 for bottom chord bracing.

REV. NO.	DATE	DESCRIPTIONS
6	03/06/06	Final drawings for construction
3	01/02/06	Correct the North direction (according to shake table)
2	12/06/05	Add typ. corder details and typ. hold-down connection
1	10/26/05	Add non-shrink grout at foundation sill plates

	University at Buffalo		DWG. NO. S-5
	PROJECT: NEESWOOD Townhouse Building for Benchmark Testing	CONTENT: Structural Details	
FOR CONSTRUCTION		REV. NO. 6	SCALE: 1" : 1'

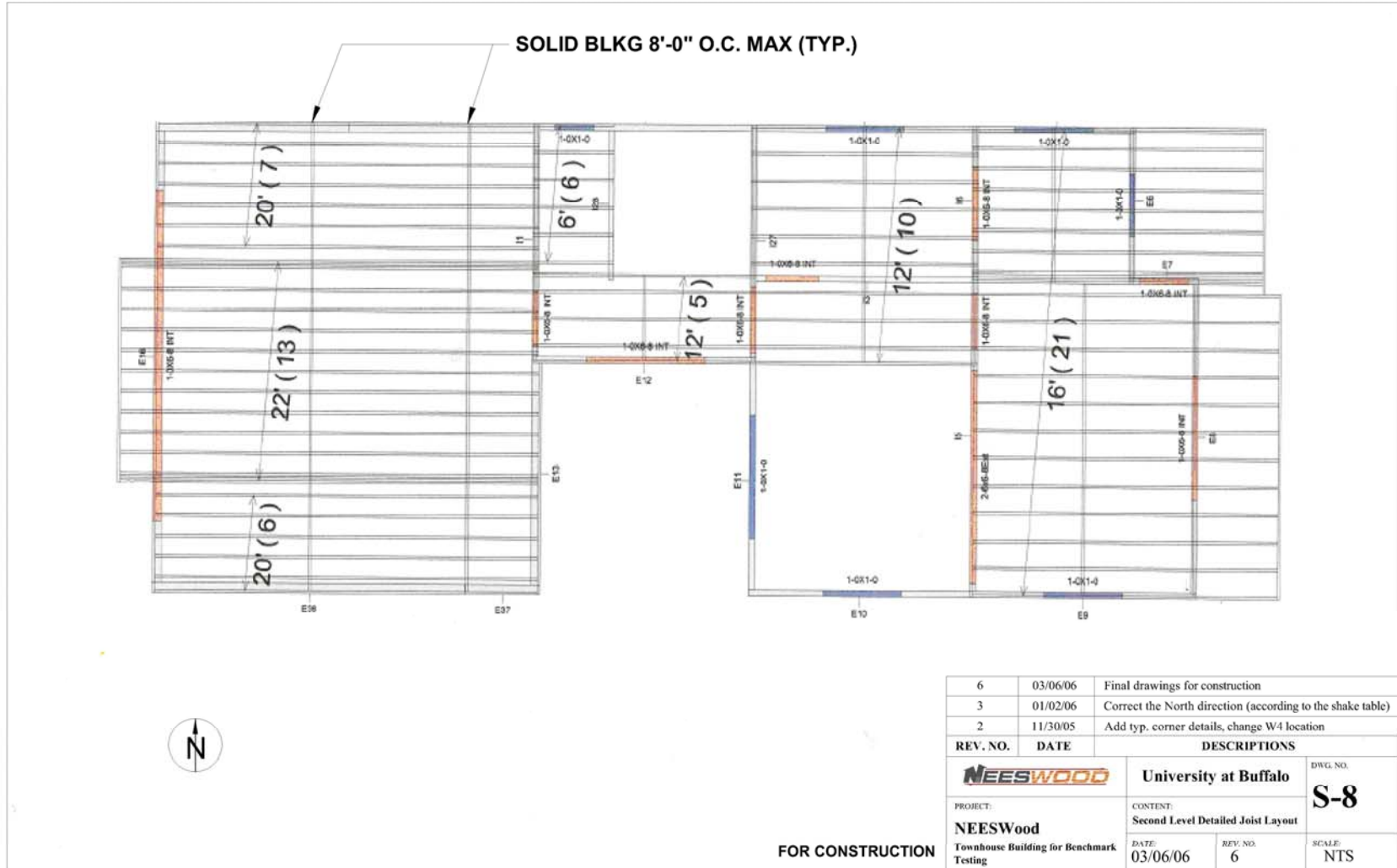
Appendix A



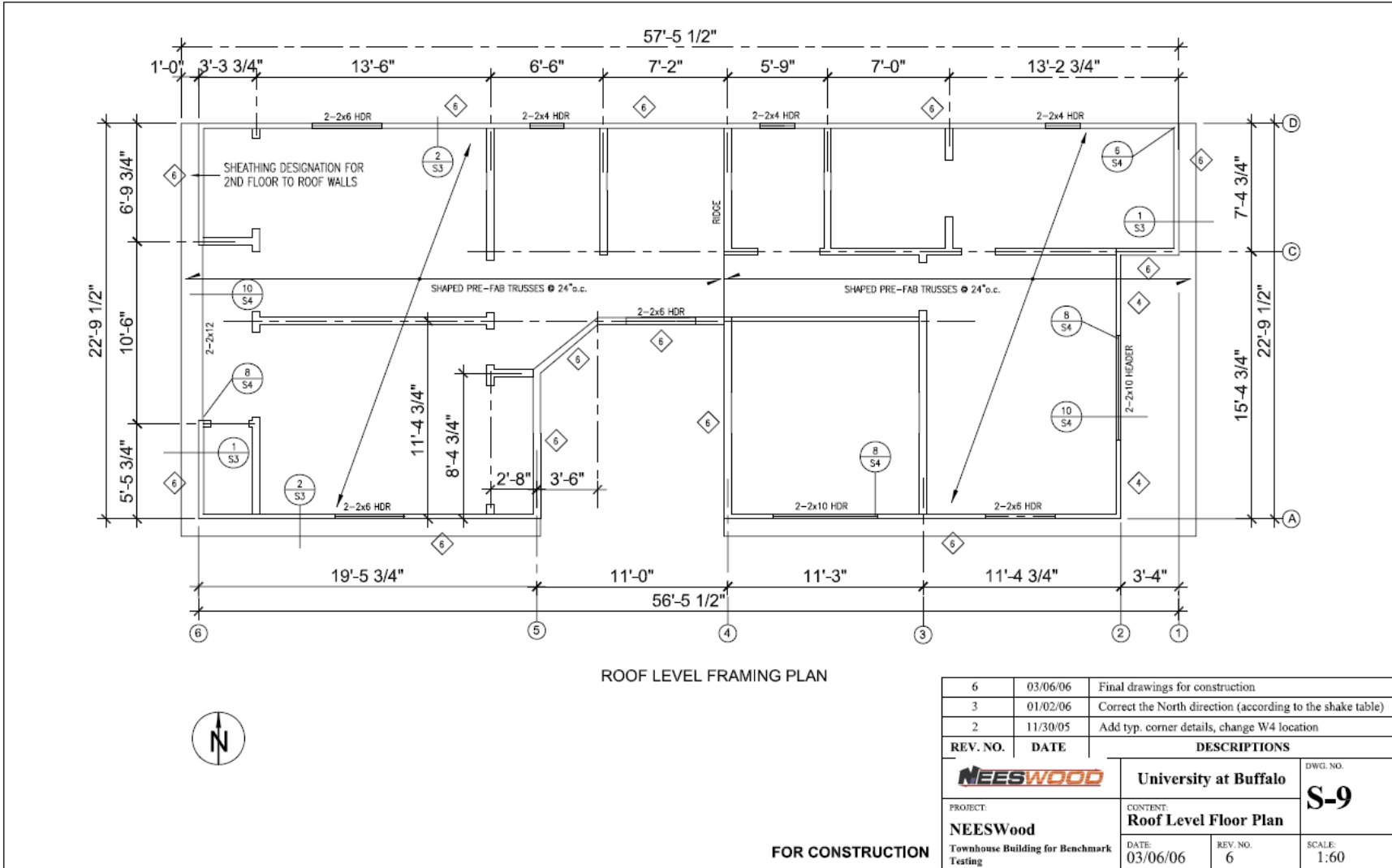
6	03/06/06	Final drawings for construction
3	01/02/06	Correct the North direction (according to the shake table)
2	11/30/05	Add typ. corner details, change W4 location
REV. NO.	DATE	DESCRIPTIONS
		University at Buffalo DWG. NO. S-6
PROJECT: NEESWood Townhouse Building for Benchmark Testing		CONTENT: Foundation Floor Plan DATE: 03/06/06 REV. NO. 6 SCALE: 1:60

FOR CONSTRUCTION

Appendix A



Appendix A

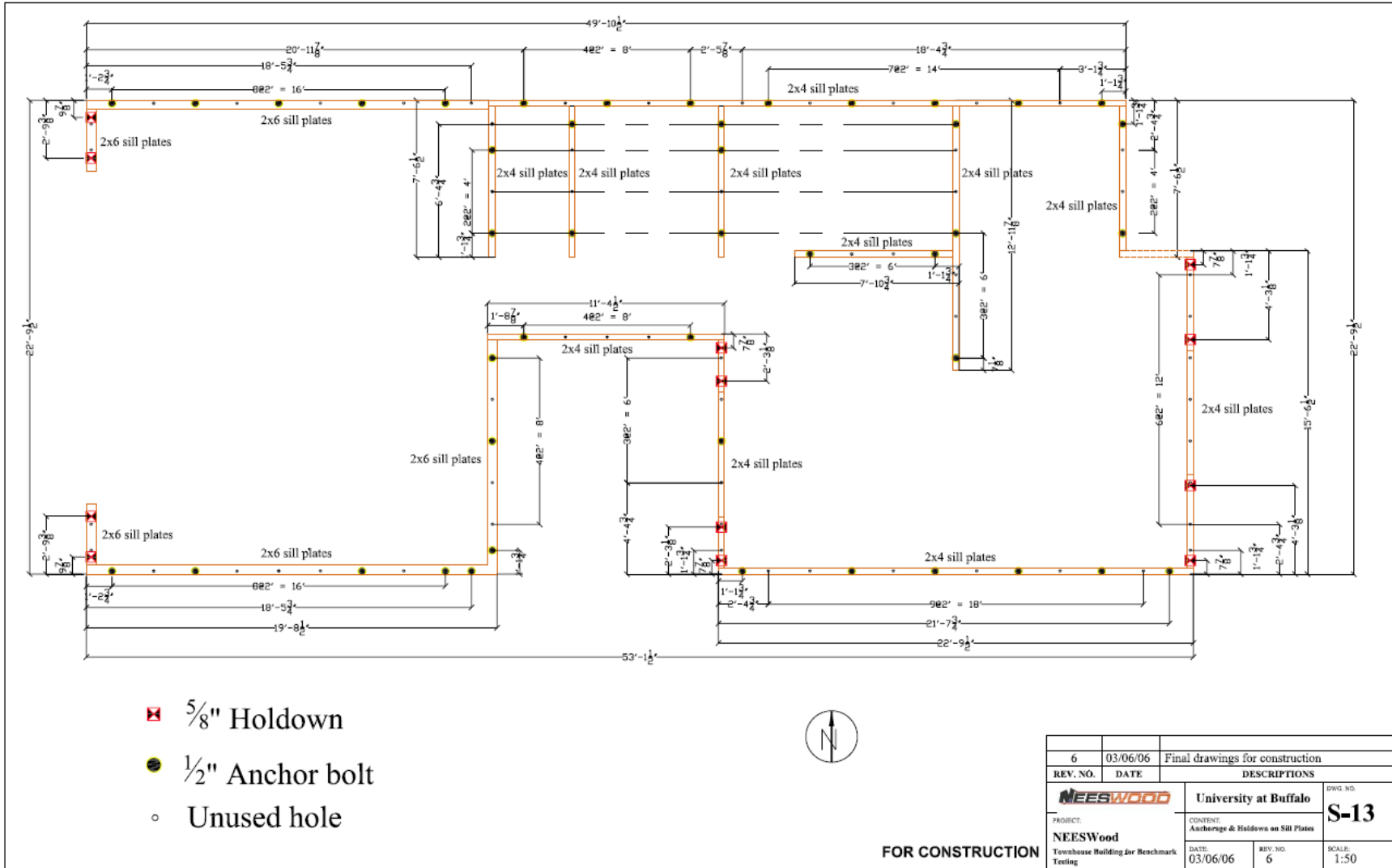


ROOF LEVEL FRAMING PLAN

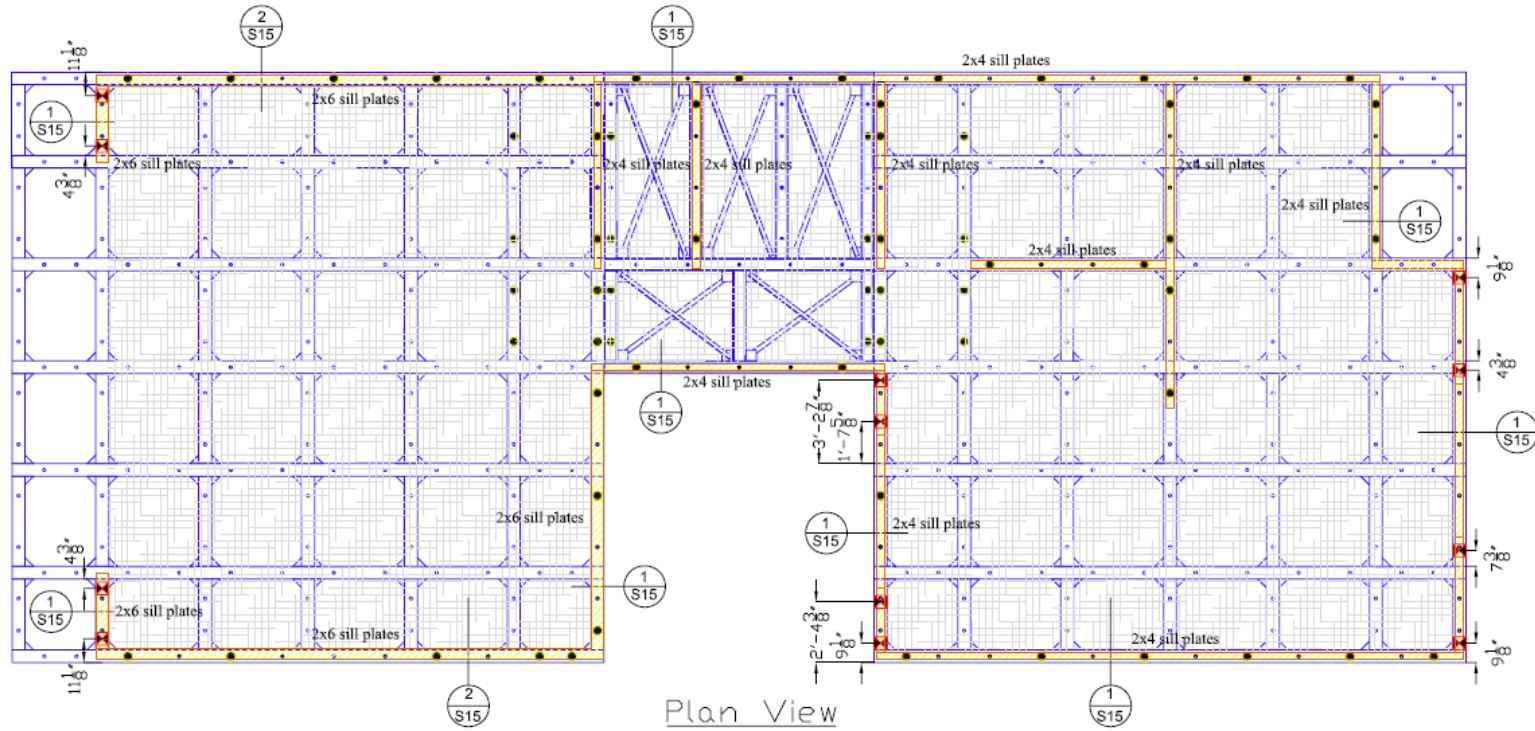
6	03/06/06	Final drawings for construction
3	01/02/06	Correct the North direction (according to the shake table)
2	11/30/05	Add typ. corner details, change W4 location
REV. NO.	DATE	DESCRIPTIONS
		University at Buffalo DWG. NO. S-9
PROJECT: NEESWood Townhouse Building for Benchmark Testing		CONTENT: Roof Level Floor Plan DATE: 03/06/06 REV. NO. 6 SCALE: 1:60

FOR CONSTRUCTION

Appendix A



Appendix A



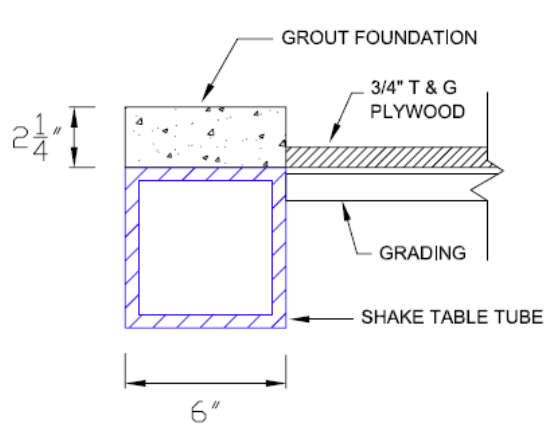
- Holdown (tack weld)
- Anchor bolts (with grout in the holes)
- Grout foundation
- Plywoods



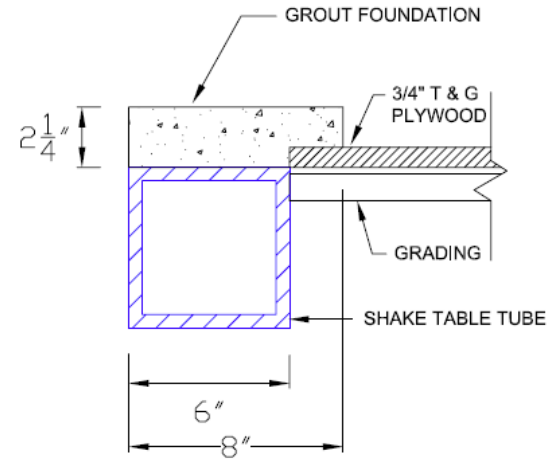
6	03/06/06	Final drawings for construction
4	01/11/06	Add anchorages for interior partition walls
3	01/02/06	Correct the North direction (according to the shake table)
REV. NO.	DATE	DESCRIPTIONS
		University at Buffalo PROJECT: NEESWood Townhouse Building for Benchmark Testing
CONTENT: Grout Foundation on Shake Table Extension Frame		DWG. NO. S-14
DATE:	03/06/06	REV. NO.: 6
		SCALE: 1:50

FOR CONSTRUCTION

Appendix A



1 TYP. GROUT FOUNDATION
S15

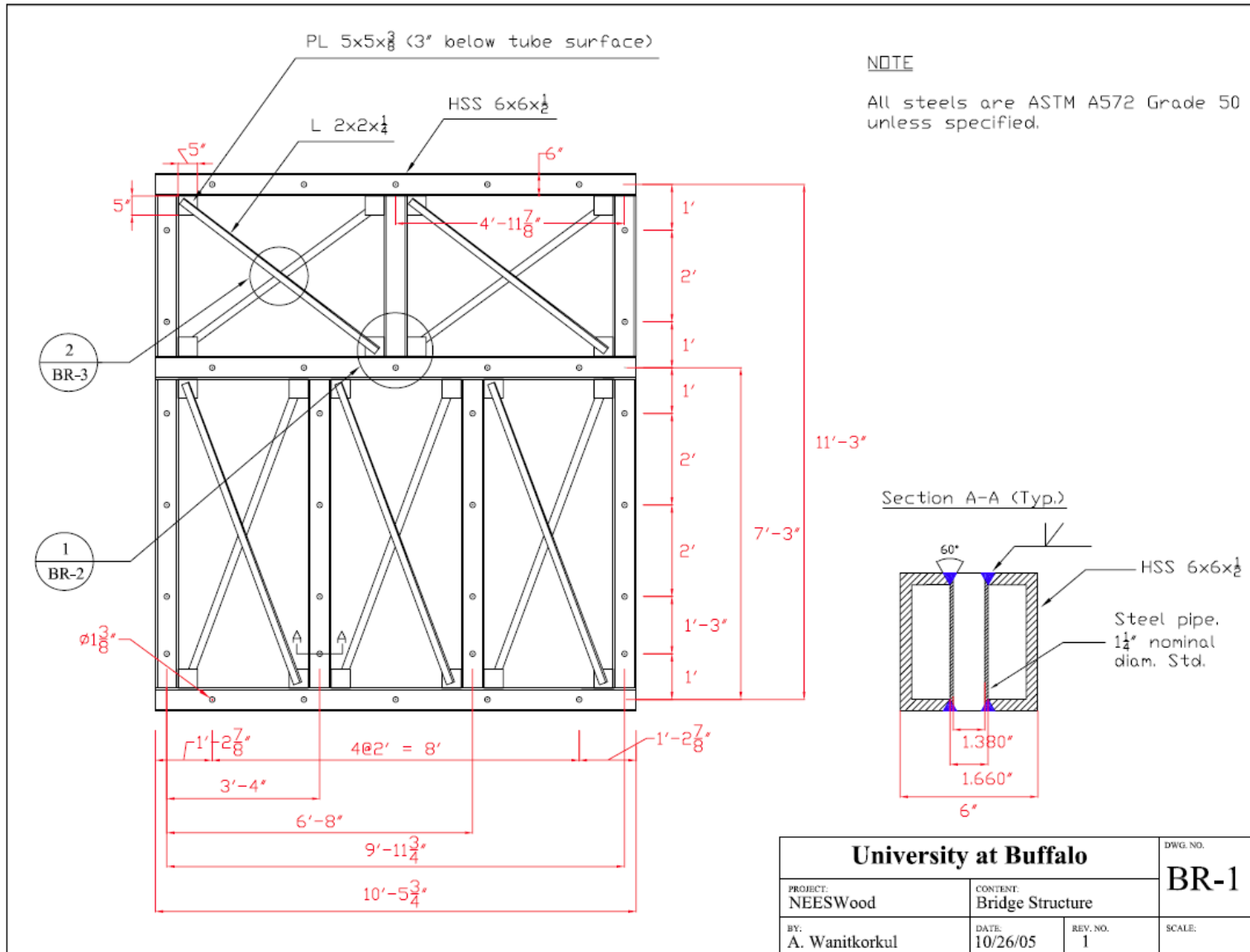


2 GROUT FOUNDATION
S15 AT GARAGE

6	03/06/06	Final drawings for construction	
4	01/11/06	Add anchorages for interior partition walls	
3	01/02/06	Correct the North direction (according to the shake table)	
REV. NO.	DATE	DESCRIPTIONS	
NEESWOOD		University at Buffalo	DWG. NO. S-15
PROJECT: NEESWood		CONTENT: Grout Foundation Details	
Townhouse Building for Benchmark Testing		DATE: 03/06/06	REV. NO. 6
		SCALE: 3" : 1'	

FOR CONSTRUCTION

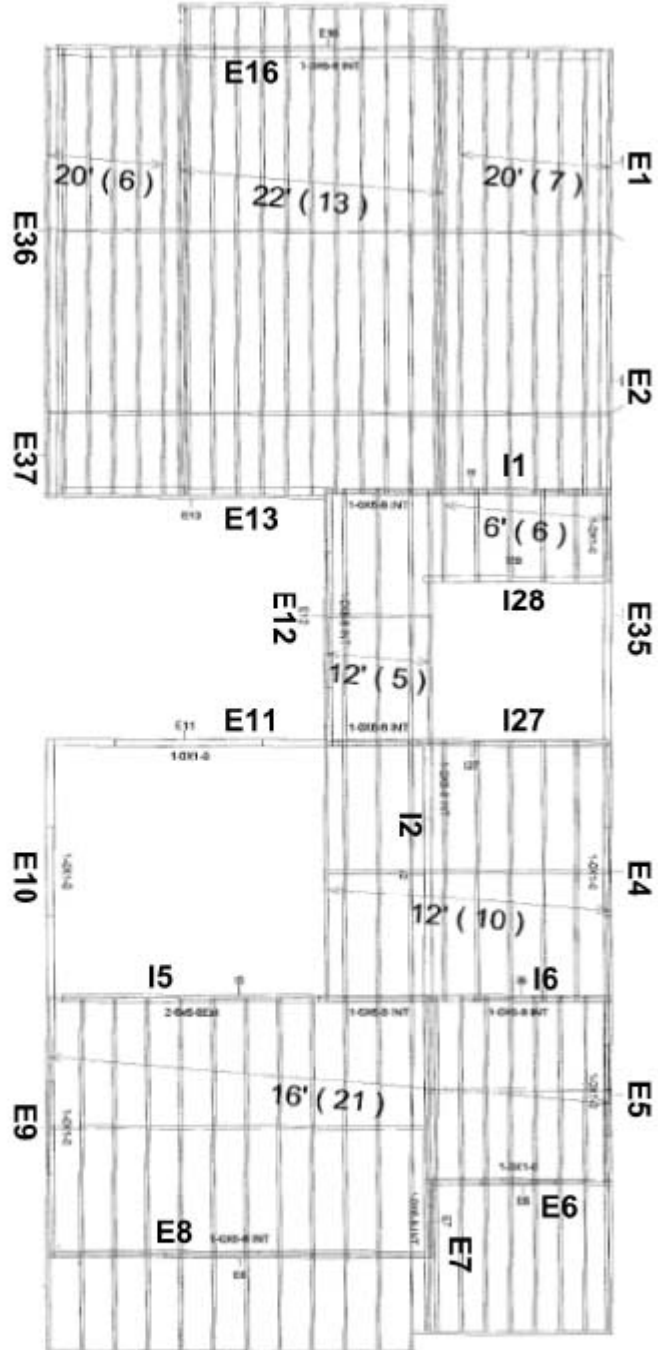
Appendix A



Appendix B
Structural Drawings of Wood
Shear Walls

Appendix B

First Floor Wood Shear Walls



FOR CONSTRUCTION

REV. NO.	DATE	DESCRIPTIONS
6	03/06/06	Final drawings for construction
3	01/02/06	Correct the North direction (according to the state table)
2	11/30/05	Add top corner details, change W4 location

NEESWOOD Engineering Building for Seneca Textile		PROJECT UNIVERSITY OF BUFFALO 1st Level Post-tensioned Wall Layout	DATE 03/06/06	REV. NO. 6	SHEET NO. S-10 SCALE N.T.S.
---	--	---	------------------	---------------	--------------------------------------

Appendix B

First Floor Wood Shear Walls

Job:O-UB3 Elevation Report

02/27/2006 10:11:48 AM

Bundle Name: N/A

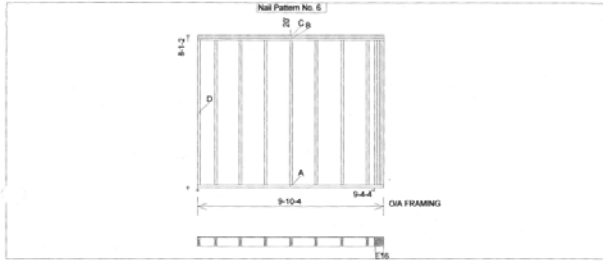
Panel:E1

Page: 1

Level Name: First Floor

Length=118-1/4 Stud Height=92-5/8 Width=5-1/2 Stud Spacing=16 Stud=6 X 2 SPF No.2 1st Stud=11
 T/Pt pitch, xLen, spring= 0, 118-1/4, 97-1/8
 B/Pt pitch, xLen, spring= 0, 118-1/4, 0
 Fire Block Hgt (Center) =
 VTP=118-1/4 Offset=0
 Sheathing=Plywood/OSB Structural L=0 R=0 T=-1-1/8
 L=0 R=0 T= B=

Nom.Lumber=126.0000BdF1



Cutting List

Label	Member	Description	Qty/Length	LElev	RElev	LPlan	RPlan
A	Bottom Plate	SPF 2 X 6 No.2 D T	(1) 118-1/4				
B	Top Plate	SPF 2 X 6 No.2 D	(1) 118-1/4				
C	VTP	SPF 2 X 6 No.2 D	(1) 118-1/4				
D	Stud	SPF 2 X 6 No.2 D	(12) 92-5/8				
E	Sheathing	Plywood/OSB Structural	(3) 96				

Job:O-UB3 Elevation Report

02/27/2006 10:11:48 AM

Bundle Name: N/A

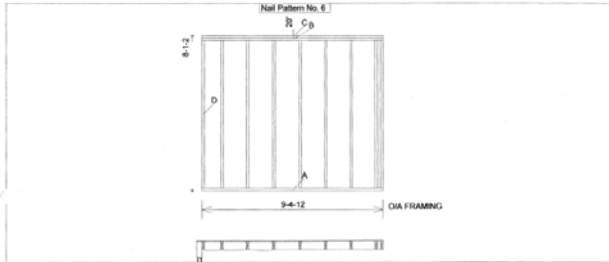
Panel:E2

Page: 2

Level Name: First Floor

Length=112-3/4 Stud Height=92-5/8 Width=5-1/2 Stud Spacing=16 Stud=6 X 2 SPF No.2 1st Stud=11-3/4
 T/Pt pitch, xLen, spring= 0, 112-3/4, 97-1/8
 B/Pt pitch, xLen, spring= 0, 112-3/4, 0
 Fire Block Hgt (Center) =
 VTP=112-3/4 Offset=0
 Sheathing=Plywood/OSB Structural L=3-1/2 R=0 T=-1-1/8
 L=0 R=0 T= B=

Nom.Lumber=132.0000BdF1



Cutting List

Label	Member	Description	Qty/Length	LElev	RElev	LPlan	RPlan
A	Bottom Plate	SPF 2 X 6 No.2 D T	(1) 112-3/4				
B	Top Plate	SPF 2 X 6 No.2 D	(1) 112-3/4				
C	VTP	SPF 2 X 6 No.2 D	(1) 112-3/4				
D	Stud	SPF 2 X 6 No.2 D	(9) 92-5/8				
F	Sheathing	Plywood/OSB Structural	(3) 96				

Job:O-UB3 Elevation Report

02/27/2006 10:11:48 AM

Bundle Name: N/A

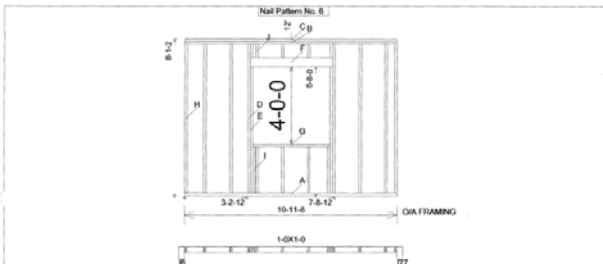
Panel:E4

Page: 3

Level Name: First Floor

Length=131-1/2 Stud Height=92-5/8 Width=3-1/2 Stud Spacing=16 Stud=4 X 2 SPF Stud 1st Stud=11-3/4
 T/Pt pitch, xLen, spring= 0, 131-1/2, 97-1/8
 B/Pt pitch, xLen, spring= 0, 131-1/2, 0
 Fire Block Hgt (Center) =
 VTP=131-1/2 Offset=0
 Sheathing=Plywood/OSB Structural L=3-1/2 R=3-1/2 T=-1-1/8
 L=0 R=0 T= B=

Nom.Lumber=112.4722BdF1



Cutting List

Label	Member	Description	Qty/Length	LElev	RElev	LPlan	RPlan
A	Bottom Plate	SPF 2 X 4 No.2 D T	(1) 131-1/2				
B	Top Plate	SPF 2 X 4 No.2 D	(1) 131-1/2				
C	VTP	SPF 2 X 4 No.2 D	(1) 131-1/2				
D	Jack Stud	SPF 2 X 4 Stud D	(2) 92-5/8				
E	Jack	SPF 2 X 4 Stud D	(2) 78-1/2				
F	Header	SPF 6 X 2 No.2 D	(2) 51				
G	Sill	SPF 2 X 4 Stud D	(1) 48				
H	Stud	SPF 2 X 4 Stud D	(8) 92-5/8				
I	Bottom Cripples	SPF 2 X 4 Stud D	(5) 29				
J	Top Cripples	SPF 2 X 4 Stud D	(5) 8-5/8				
K	Sheathing	Plywood/OSB Structural	(3) 96				

Job:O-UB3 Elevation Report

02/27/2006 10:11:48 AM

Bundle Name: N/A

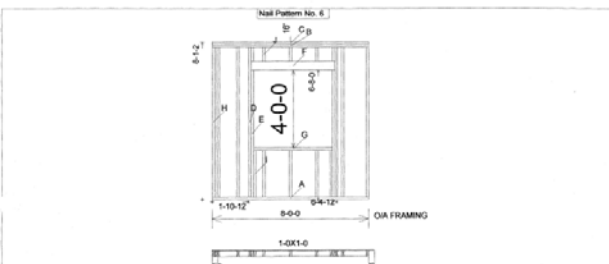
Panel:E5

Page: 4

Level Name: First Floor

Length=96 Stud Height=92-5/8 Width=3-1/2 Stud Spacing=16 Stud=4 X 2 SPF Stud 1st Stud=15-1/4
 T/Pt pitch, xLen, spring= 0, 96, 97-1/8
 B/Pt pitch, xLen, spring= 0, 96, 0
 Fire Block Hgt (Center) =
 VTP=96 Offset=0
 Sheathing=Plywood/OSB Structural L=0 R=3-1/2 T=-1-1/8
 L=0 R=0 T= B=

Nom.Lumber=107.8333BdF1



Cutting List

Label	Member	Description	Qty/Length	LElev	RElev	LPlan	RPlan
A	Bottom Plate	SPF 2 X 4 No.2 D T	(1) 96				
B	Top Plate	SPF 2 X 4 No.2 D	(1) 96				
C	VTP	SPF 2 X 4 No.2 D	(1) 96				
D	Jack Stud	SPF 2 X 4 Stud D	(2) 92-5/8				
E	Jack	SPF 2 X 4 Stud D	(2) 78-1/2				
F	Header	SPF 6 X 2 No.2 D	(2) 51				
G	Sill	SPF 2 X 4 Stud D	(1) 48				
H	Stud	SPF 2 X 4 Stud D	(6) 92-5/8				
I	Bottom Cripples	SPF 2 X 4 Stud D	(5) 29				
J	Top Cripples	SPF 2 X 4 Stud D	(5) 8-5/8				
K	Sheathing	Plywood/OSB Structural	(3) 96				

Appendix B

First Floor Wood Shear Walls

Job:O-UB3

Elevation Report

02/27/2006 10:11:48 AM

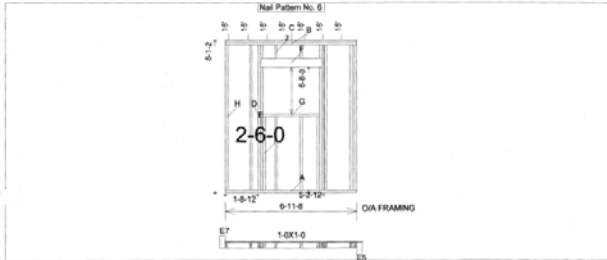
Bundle Name: N/A

Panel:E6

Level Name: First Floor

Page: 5

Length=83-1/2 Stud Height=92-5/8 Width=3-1/2 Stud Spacing=16 Studs=4 X 2 SPF Stud 1st Stud=15-1/4
 TPlt pitch, xLen, spring= 0, 83-1/2, 97-1/8
 BPtch pitch, xLen, spring= 0, 83-1/2, 0
 Fire Block Hgt (Center) =
 VTP=83-1/2 Offset=0
 Sheathing=Pywood/OSB Structural L=0 R=4 T=-1-1/8
 L=0 R=0 T= B=



Cutting List

Label	Member	Description	Qty/Length	LElev	RElev	LPlan	RPlan
A	Bottom Plate	SPF 2 X 4 No.2 D T	(1) 83-1/2				
B	Top Plate	SPF 2 X 4 No.2 D	(1) 83-1/2				
C	VTP	SPF 2 X 4 No.2 D	(1) 83-1/2				
D	Jack Stud	SPF 2 X 4 Stud D	(2) 92-5/8				
E	Jack	SPF 2 X 4 Stud D	(2) 78-1/2				
F	Header	SPF 6 X 2 No.2 D	(2) 39				
G	Sill	SPF 2 X 4 Stud D	(1) 30				
H	Stud	SPF 2 X 4 Stud D	(8) 92-5/8				
I	Bottom Cripples	SPF 2 X 4 Stud D	(4) 47				
J	Top Cripples	SPF 2 X 4 Stud D	(4) 8-5/8				
K	Sheathing	Pywood/OSB Structural	(2) 96				

Job:O-UB3

Elevation Report

02/27/2006 10:11:48 AM

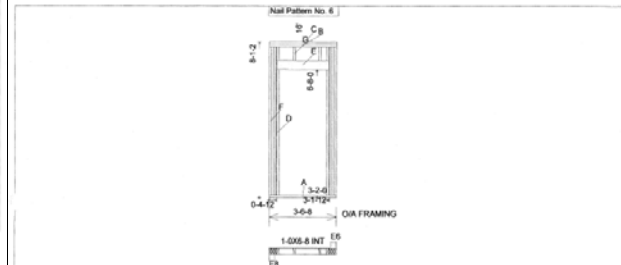
Bundle Name: N/A

Panel:E7

Level Name: First Floor

Page: 6

Length=42-1/2 Stud Height=92-5/8 Width=3-1/2 Stud Spacing=16 Studs=4 X 2 SPF Stud 1st Stud=15-1/4
 TPlt pitch, xLen, spring= 0, 42-1/2, 97-1/8
 BPtch pitch, xLen, spring= 0, 42-1/2, 0
 Fire Block Hgt (Center) =
 VTP=42-1/2 Offset=0
 Sheathing=Pywood/OSB Structural L=0 R=4 T=-1-1/8
 L=0 R=0 T= B=



Cutting List

Label	Member	Description	Qty/Length	LElev	RElev	LPlan	RPlan
A	Bottom Plate	SPF 2 X 4 No.2 D T	(1) 42-1/2				
B	Top Plate	SPF 2 X 4 No.2 D	(1) 42-1/2				
C	VTP	SPF 2 X 4 No.2 D	(1) 42-1/2				
D	Jack Stud	SPF 2 X 4 Stud D	(2) 78-1/2				
E	Header	SPF 6 X 2 No.2 D	(2) 39				
F	Stud	SPF 2 X 4 Stud D	(8) 92-5/8				
G	Top Cripples	SPF 2 X 4 Stud D	(4) 8-5/8				
H	Sheathing	Pywood/OSB Structural	(1) 96				

Job:O-UB3

Elevation Report

02/27/2006 10:11:48 AM

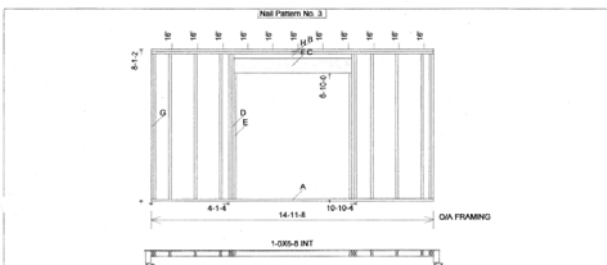
Bundle Name: N/A

Panel:E8

Level Name: First Floor

Page: 7

Length=179-1/2 Stud Height=92-5/8 Width=3-1/2 Stud Spacing=16 Studs=4 X 2 SPF Stud 1st Stud=11-1/4
 TPlt pitch, xLen, spring= 0, 179-1/2, 97-1/8
 BPtch pitch, xLen, spring= 0, 179-1/2, 0
 Fire Block Hgt (Center) =
 VTP=179-1/2 Offset=0
 Sheathing=Pywood/OSB Structural L=4 R=4 T=-1-1/8
 L=0 R=0 T= B=



Cutting List

Label	Member	Description	Qty/Length	LElev	RElev	LPlan	RPlan
A	Bottom Plate	SPF 2 X 4 No.2 D T	(1) 179-1/2				
B	Top Plate	SPF 2 X 4 No.2 D	(1) 179-1/2				
C	VTP	SPF 2 X 4 No.2 D	(1) 179-1/2				
D	Jack Stud	SPF 2 X 4 Stud D	(4) 92-5/8				
E	Jack	SPF 2 X 4 Stud D	(2) 83-1/2				
F	Header	SPF 10 X 2 No.2 D	(1) 75				
G	Stud	SPF 2 X 4 Stud D	(10) 92-5/8				
H	Pad	SPF 2 X 4 (0-2-14 x 0-3-8 Act) Stud D	(1) 75				
I	Sheathing	Pywood/OSB Structural	(4) 96				

Job:O-UB3

Elevation Report

02/27/2006 10:11:48 AM

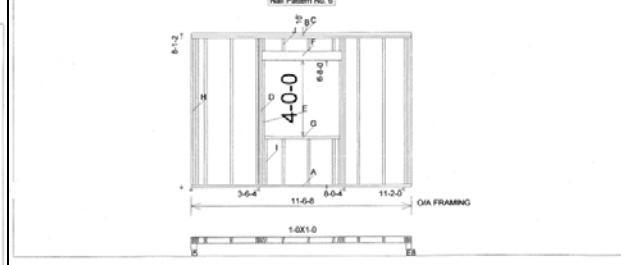
Bundle Name: N/A

Panel:E9

Level Name: First Floor

Page: 8

Length=138-1/2 Stud Height=92-5/8 Width=3-1/2 Stud Spacing=16 Studs=4 X 2 SPF Stud 1st Stud=8-1/4
 TPlt pitch, xLen, spring= 0, 138-1/2, 97-1/8
 BPtch pitch, xLen, spring= 0, 138-1/2, 0
 Fire Block Hgt (Center) =
 VTP=138-1/2 Offset=0
 Sheathing=Pywood/OSB Structural L=0 R=0 T=-1-1/8
 L=0 R=0 T= B=



Cutting List

Label	Member	Description	Qty/Length	LElev	RElev	LPlan	RPlan
A	Bottom Plate	SPF 2 X 4 No.2 D T	(1) 138-1/2				
B	Top Plate	SPF 2 X 4 No.2 D	(1) 138-1/2				
C	VTP	SPF 2 X 4 No.2 D	(1) 138-1/2				
D	Jack Stud	SPF 2 X 4 Stud D	(2) 92-5/8				
E	Jack	SPF 2 X 4 Stud D	(2) 78-1/2				
F	Header	SPF 6 X 2 No.2 D	(2) 51				
G	Sill	SPF 2 X 4 Stud D	(1) 48				
H	Stud	SPF 2 X 4 Stud D	(11) 92-5/8				
I	Bottom Cripples	SPF 2 X 4 Stud D	(5) 29				
J	Top Cripples	SPF 2 X 4 Stud D	(5) 8-5/8				
K	Sheathing	Pywood/OSB Structural	(3) 96				

Appendix B

First Floor Wood Shear Walls

Job:O-UB3

Elevation Report

02/27/2006 10:11:48 AM

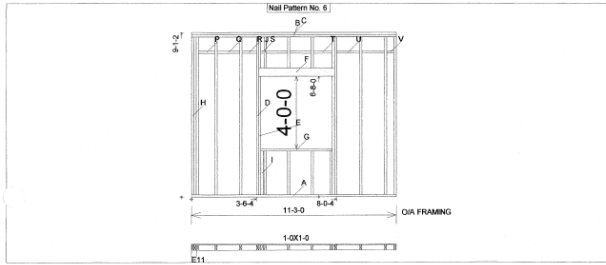
Bundle Name: N/A

Panel:E10

Level Name: First Floor

Page: 9

Length=135 Stud Height=104-5/8 Width=3-1/2 Stud Spacing=16 Studs=4 X 2 SPF Stud 1st Stud=15-14
 TPtch pitch, xLen, spring= 0, 135, 109-1/8
 BPtch pitch, xLen, spring= 0, 135, 0
 Fire Block Hgt (Center) =
 VTP=135 Offset=0
 Sheathing=Plywood/OSB Structural L=0 R=0 T=-1-1/8
 L=0 R=0 T= B=



Cutting List

Label	Member	Description	Qty/Length	LElev	RElev	LPlan	RPlan
A	Bottom Plate	SPF 2 X 4 No.2 D T	(1) 135				
B	Top Plate	SPF 2 X 4 No.2 D	(1) 135				
C	VTP	SPF 2 X 4 No.2 D	(1) 135				
D	Jack Stud	SPF 2 X 4 Stud D	(2) 104-5/8				
E	Jack	SPF 2 X 4 Stud D	(2) 78-1/2				
F	Header	SPF 6 X 2 No.2 D	(2) 51				
G	Sill	SPF 2 X 4 Stud D	(1) 48				
H	Stud	SPF 2 X 4 Stud D	(8) 104-5/8				
I	Bottom Cripples	SPF 2 X 4 Stud D	(5) 29				
J	Top Cripples	SPF 2 X 4 Stud D	(5) 29-5/8				
K	Sheathing	Plywood/OSB Structural	(4) 96				
L	Seam Block	SPF 2 X 4 Stud D	(1) 10-3/4				
M	Seam Block	SPF 2 X 4 Stud D	(4) 14-1/2				
N	Seam Block	SPF 2 X 4 Stud D	(1) 9-1/2				
O	Seam Block	SPF 2 X 4 Stud D	(1) 2				
P	Seam Block	SPF 2 X 4 Stud D	(1) 12-1/2				
Q	Seam Block	SPF 2 X 4 Stud D	(1) 15				
R	Seam Block	SPF 2 X 4 Stud D	(1) 4-3/4				

Job:O-UB3

Elevation Report

02/27/2006 10:11:48 AM

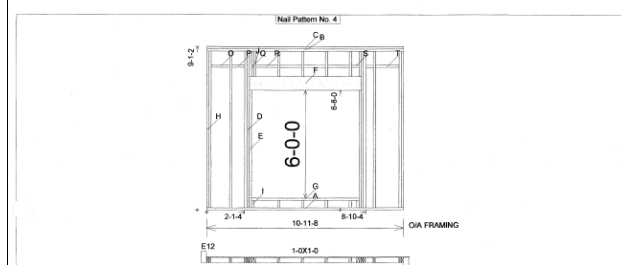
Bundle Name: N/A

Panel:E11

Level Name: First Floor

Page: 10

Length=131-1/2 Stud Height=104-5/8 Width=3-1/2 Stud Spacing=16 Studs=4 X 2 SPF Stud 1st Stud=15-14
 TPtch pitch, xLen, spring= 0, 131-1/2, 109-1/8
 BPtch pitch, xLen, spring= 0, 131-1/2, 0
 Fire Block Hgt (Center) =
 VTP=131-1/2 Offset=0
 Sheathing=Plywood/OSB Structural L=0 R=4 T=-1-1/8
 L=0 R=0 T= B=



Cutting List

Label	Member	Description	Qty/Length	LElev	RElev	LPlan	RPlan
A	Bottom Plate	SPF 2 X 4 No.2 D T	(1) 131-1/2				
B	Top Plate	SPF 2 X 4 No.2 D	(1) 131-1/2				
C	VTP	SPF 2 X 4 No.2 D	(1) 131-1/2				
D	Jack Stud	SPF 2 X 4 Stud D	(4) 104-5/8				
E	Jack	SPF 2 X 4 Stud D	(2) 78-1/2				
F	Header	SYP 10 X 2 No.2 D	(2) 75				
G	Sill	SPF 2 X 4 Stud D	(1) 72				
H	Stud	SPF 2 X 4 Stud D	(8) 104-5/8				
I	Bottom Cripples	SPF 2 X 4 Stud D	(6) 5				
J	Top Cripples	SPF 2 X 4 Stud D	(7) 16-7/8				
K	Sheathing	Plywood/OSB Structural	(4) 96				
L	Seam Block	SPF 2 X 4 Stud D	(1) 12-1/4				
M	Seam Block	SPF 2 X 4 Stud D	(1) 8-1/2				
N	Seam Block	SPF 2 X 4 Stud D	(1) 1-1/2				
O	Seam Block	SPF 2 X 4 Stud D	(4) 14-1/2				
P	Seam Block	SPF 2 X 4 Stud D	(2) 5				
Q	Seam Block	SPF 2 X 4 Stud D	(1) 15-3/4				

Job:O-UB3

Elevation Report

02/27/2006 10:11:48 AM

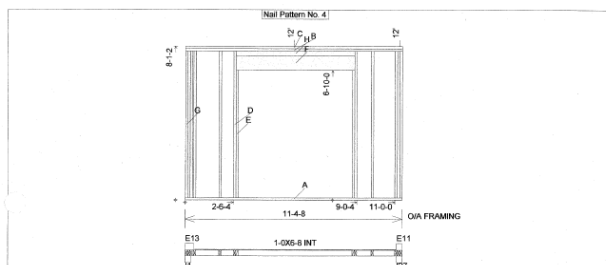
Bundle Name: N/A

Panel:E12

Level Name: First Floor

Page: 11

Length=136-1/2 Stud Height=92-5/8 Width=3-1/2 Stud Spacing=16 Studs=4 X 2 SPF Stud 1st Stud=5-1/4
 TPtch pitch, xLen, spring= 0, 136-1/2, 97-1/8
 BPtch pitch, xLen, spring= 0, 136-1/2, 0
 Fire Block Hgt (Center) =
 VTP=136-1/2 Offset=0
 Sheathing=Plywood/OSB Structural L=6 R=4 T=-1-1/8
 L=0 R=0 T= B=



Cutting List

Label	Member	Description	Qty/Length	LElev	RElev	LPlan	RPlan
A	Bottom Plate	SPF 2 X 4 No.2 D T	(1) 136-1/2				
B	Top Plate	SPF 2 X 4 No.2 D	(1) 136-1/2				
C	VTP	SPF 2 X 4 No.2 D	(1) 136-1/2				
D	Jack Stud	SPF 2 X 4 Stud D	(2) 92-5/8				
E	Jack	SPF 2 X 4 Stud D	(2) 80-1/2				
F	Header	SYP 10 X 2 No.2 D	(1) 75				
G	Sill	SPF 2 X 4 Stud D	(9) 92-5/8				
H	Stud	SPF 2 X 4 Stud D	(1) 75				
I	Bottom Cripples	SPF 2 X 4 Stud D	(3) 96				

Job:O-UB3

Elevation Report

02/27/2006 10:11:48 AM

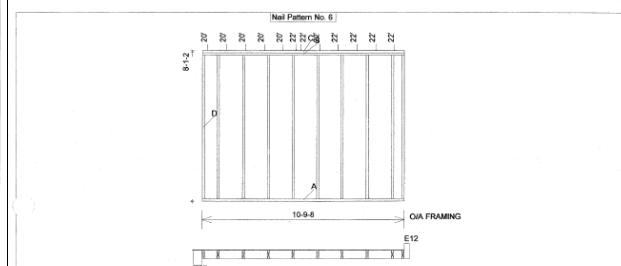
Bundle Name: N/A

Panel:E13

Level Name: First Floor

Page: 12

Length=129-1/2 Stud Height=92-5/8 Width=5-1/2 Stud Spacing=16 Studs=6 X 2 SPF No.2 1st Stud=9-1/4
 TPtch pitch, xLen, spring= 0, 129-1/2, 97-1/8
 BPtch pitch, xLen, spring= 0, 129-1/2, 0
 Fire Block Hgt (Center) =
 VTP=129-1/2 Offset=0
 Sheathing=Plywood/OSB Structural L=6 R=0 T=-1-1/8
 L=0 R=0 T= B=



Cutting List

Label	Member	Description	Qty/Length	LElev	RElev	LPlan	RPlan
A	Bottom Plate	SPF 2 X 6 No.2 D T	(1) 129-1/2				
B	Top Plate	SPF 2 X 6 No.2 D	(1) 129-1/2				
C	VTP	SPF 2 X 6 No.2 D	(1) 129-1/2				
D	Jack Stud	SPF 2 X 6 No.2 D	(10) 92-5/8				
E	Jack	Plywood/OSB Structural	(3) 96				

Appendix B

First Floor Wood Shear Walls

Job:O-UB3

Elevation Report

02/27/2006 10:11:48 AM

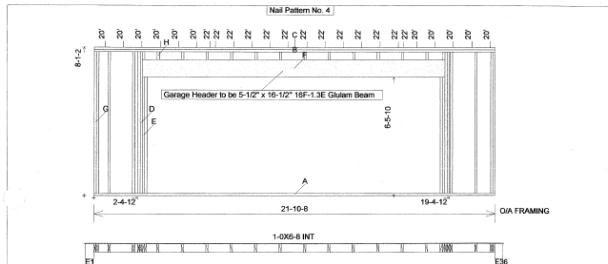
Bundle Name: N/A

Panel:E16

Level Name: First Floor

Page: 13

Length=262-1/2 Stud Height=92-5/8 Width=5-1/2 Stud Spacing=16 Studs=6 X 2 SPF No.2 1st Stud=9-1/4
 TPit pitch, xLen, spring= 0, 262-1/2, 97-1/8
 BPit pitch, xLen, spring= 0, 262-1/2, 0
 Fire Block Hgt (Center) =
 VTP=262-1/2 Offset=0
 Sheathing=Plywood/OSB Structural L=6 R=6 T=-1-1/8
 L=0 R=0 T= B=



Cutting List

Label	Member	Description	Qty/Length	LElev	RElev	LPlan	RPlan
A	Bottom Plate	SPF 2 X 6 No.2 D T	(1) 262-1/2				
B	Top Plate	SPF 2 X 6 No.2 D	(1) 262-1/2				
C	VTP	SPF 2 X 6 No.2 D	(1) 262-1/2				
D	Jack Stud	SPF 2 X 6 No.2 D	(4) 92-5/8				
E	Jack	SPF 2 X 6 No.2 D	(4) 76-1/8				
F	Header	SYP 12 X 2 No.2 D	(1) 198				
G	Stud	SPF 2 X 6 No.2 D	(6) 92-5/8				
H	Top Cripples	SPF 2 X 6 No.2 D	(14) 5-1/4				
I	Sheathing	Plywood/OSB Structural	(6) 96				

Job:O-UB3

Elevation Report

02/27/2006 10:11:48 AM

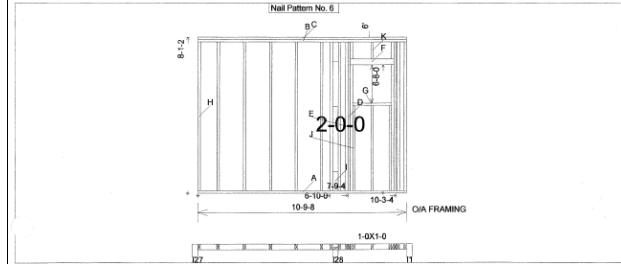
Bundle Name: N/A

Panel:E35

Level Name: First Floor

Page: 32

Length=129-1/2 Stud Height=92-5/8 Width=3-1/2 Stud Spacing=16 Studs=4 X 2 SPF Stud 1st Stud=11-3/4
 TPit pitch, xLen, spring= 0, 129-1/2, 97-1/8
 BPit pitch, xLen, spring= 0, 129-1/2, 0
 Fire Block Hgt (Center) =
 VTP=129-1/2 Offset=0



Cutting List

Label	Member	Description	Qty/Length	LElev	RElev	LPlan	RPlan
A	Bottom Plate	SPF 2 X 4 No.2 D T	(1) 129-1/2				
B	Top Plate	SPF 2 X 4 No.2 D	(1) 129-1/2				
C	VTP	SPF 2 X 4 No.2 D	(1) 129-1/2				
D	Jack Stud	SPF 2 X 4 Stud D	(2) 92-5/8				
E	Jack	SPF 2 X 4 Stud D	(2) 76-1/2				
F	Header	SPF 4 X 2 No.2 D	(2) 27				
G	SB	SPF 2 X 4 Stud D	(1) 24				
H	Stud	SPF 2 X 4 Stud D	(11) 92-5/8				
I	Block	SPF 4 X 2 No.2 D	(3) 12				
J	Bottom Cripples	SPF 2 X 4 Stud D	(3) 53				
K	Top Cripples	SPF 2 X 4 Stud D	(3) 10-5/8				

Job:O-UB3

Elevation Report

02/27/2006 10:11:48 AM

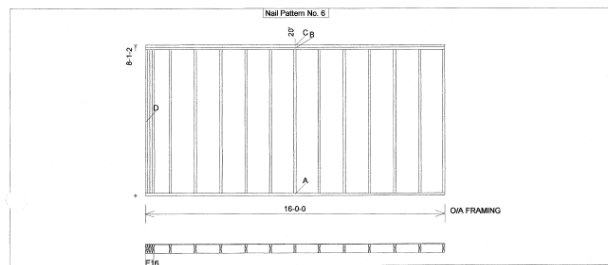
Bundle Name: N/A

Panel:E36

Level Name: First Floor

Page: 33

Length=192 Stud Height=92-5/8 Width=5-1/2 Stud Spacing=16 Studs=6 X 2 SPF No.2 1st Stud=15-1/4
 TPit pitch, xLen, spring= 0, 192, 97-1/8
 BPit pitch, xLen, spring= 0, 192, 0
 Fire Block Hgt (Center) =
 VTP=192 Offset=0
 Sheathing=Plywood/OSB Structural L=0 R=0 T=-1-1/8
 L=0 R=0 T= B=



Cutting List

Label	Member	Description	Qty/Length	LElev	RElev	LPlan	RPlan
A	Bottom Plate	SPF 2 X 6 No.2 D T	(1) 192				
B	Top Plate	SPF 2 X 6 No.2 D	(1) 192				
C	VTP	SPF 2 X 6 No.2 D	(1) 192				
D	Stud	SPF 2 X 6 No.2 D	(16) 92-5/8				
E	Sheathing	Plywood/OSB Structural	(4) 96				

Job:O-UB3

Elevation Report

02/27/2006 10:11:48 AM

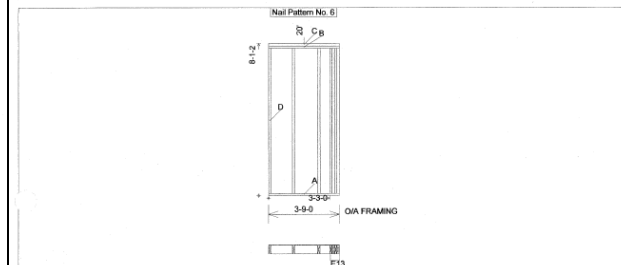
Bundle Name: N/A

Panel:E37

Level Name: First Floor

Page: 34

Length=45 Stud Height=92-5/8 Width=5-1/2 Stud Spacing=16 Studs=6 X 2 SPF No.2 1st Stud=15-1/4
 TPit pitch, xLen, spring= 0, 45, 97-1/8
 BPit pitch, xLen, spring= 0, 45, 0
 Fire Block Hgt (Center) =
 VTP=45 Offset=0
 Sheathing=Plywood/OSB Structural L=0 R=0 T=-1-1/8
 L=0 R=0 T= B=



Cutting List

Label	Member	Description	Qty/Length	LElev	RElev	LPlan	RPlan
A	Bottom Plate	SPF 2 X 6 No.2 D T	(1) 45				
B	Top Plate	SPF 2 X 6 No.2 D	(1) 45				
C	VTP	SPF 2 X 6 No.2 D	(1) 45				
D	Stud	SPF 2 X 6 No.2 D	(7) 92-5/8				
E	Sheathing	Plywood/OSB Structural	(1) 96				

Appendix B

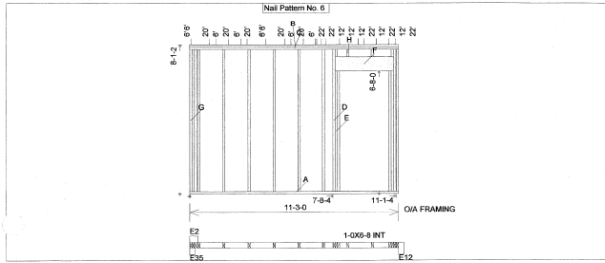
First Floor Wood Shear Walls

Job:O-UB3
Elevation Report
 02/27/2008 10:11:48 AM

Bundle Name: N/A

Panel:I1 Page: 35
 Level Name: First Floor

Length=135 Stud Height=92-5/8 Width=3-1/2 Stud Spacing=16 Studs=4 X 2 SPF Stud 1st Stud=5-1/4
 TPit pitch, xLen, spring= 0, 135, 97-1/8
 BPit pitch, xLen, spring= 0, 135, 0
 Fire Block Hgt (Center) =
 Nom.Lumber=118.58338BfI
 VTP=135 Offset=0



Cutting List

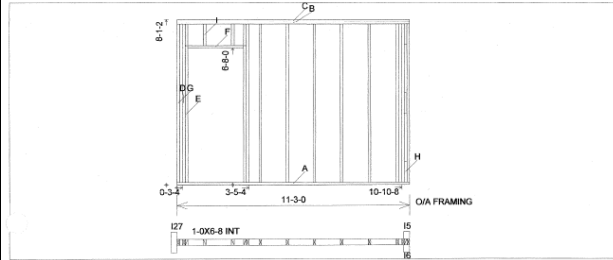
Label	Member	Description	Qty/Length	LElev	RElev	LPlan	RPlan
A	Bottom Plate	SPF 2 X 4 No.2 D T	(1) 135				
B	Top Plate	SPF 2 X 4 No.2 D	(1) 135				
C	VTP	SPF 2 X 4 No.2 D	(1) 135				
D	Jack Stud	SPF 2 X 4 Stud D	(2) 92-5/8				
E	Jack	SPF 2 X 4 Stud D	(4) 78-1/2				
F	Header	SYP 10 X 2 No.2 D	(1) 38				
G	Stud	SPF 2 X 4 Stud D	(10) 92-5/8				
H	Top Cripples	SPF 2 X 4 Stud D	(4) 4-7/8				

Job:O-UB3
Elevation Report
 02/27/2008 10:11:48 AM

Bundle Name: N/A

Panel:I2 Page: 36
 Level Name: First Floor

Length=135 Stud Height=92-5/8 Width=3-1/2 Stud Spacing=16 Studs=4 X 2 SPF Stud 1st Stud=15-1/4
 TPit pitch, xLen, spring= 0, 135, 97-1/8
 BPit pitch, xLen, spring= 0, 135, 0
 Fire Block Hgt (Center) =
 Nom.Lumber=119.43758BfI
 VTP=135 Offset=0



Cutting List

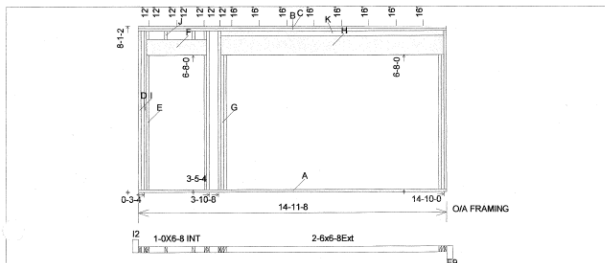
Label	Member	Description	Qty/Length	LElev	RElev	LPlan	RPlan
A	Bottom Plate	SPF 2 X 4 No.2 D T	(1) 135				
B	Top Plate	SPF 2 X 4 No.2 D	(1) 135				
C	VTP	SPF 2 X 4 No.2 D	(1) 135				
D	Jack Stud	SPF 2 X 4 Stud D	(2) 92-5/8				
E	Jack	SPF 2 X 4 Stud D	(2) 80				
F	Trimmer	SPF 2 X 4 Stud D	(1) 32				
G	Stud	SPF 2 X 4 Stud D	(9) 92-5/8				
H	Block	SPF 2 X 4 No.2 D	(3) 12				
I	Top Cripples	SPF 2 X 4 Stud D	(4) 12-5/8				

Job:O-UB3
Elevation Report
 02/27/2008 10:11:48 AM

Bundle Name: N/A

Panel:I5 Page: 37
 Level Name: First Floor

Length=179-1/2 Stud Height=92-5/8 Width=3-1/2 Stud Spacing=16 Studs=4 X 2 SPF Stud 1st Stud=15-1/4
 TPit pitch, xLen, spring= 0, 179-1/2, 97-1/8
 BPit pitch, xLen, spring= 0, 179-1/2, 0
 Fire Block Hgt (Center) =
 Nom.Lumber=134.92368BfI
 VTP=179-1/2 Offset=0



Cutting List

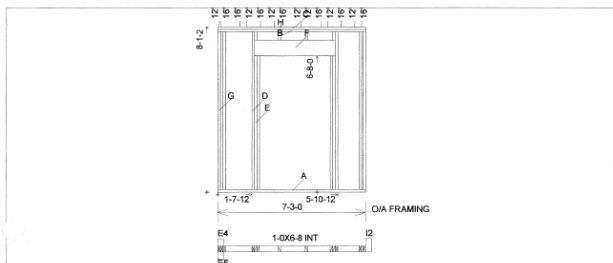
Label	Member	Description	Qty/Length	LElev	RElev	LPlan	RPlan
A	Bottom Plate	SPF 2 X 4 No.2 D T	(1) 179-1/2				
B	Top Plate	SPF 2 X 4 No.2 D	(1) 179-1/2				
C	VTP	SPF 2 X 4 No.2 D	(1) 179-1/2				
D	Jack Stud	SPF 2 X 4 Stud D	(5) 92-5/8				
E	Jack	SPF 2 X 4 Stud D	(2) 78-1/2				
F	Header	SYP 10 X 2 No.2 D	(1) 35				
G	Jack	SPF 2 X 4 No.2 D	(4) 78-1/2				
H	Header	DF 12 X 2 No.2 D	(1) 130				
I	Stud	SPF 2 X 4 Stud D	(2) 92-5/8				
J	Top Cripples	SPF 2 X 4 Stud D	(4) 4-7/8				
K	Pad	SPF 2 X 4 (0-2-14 x 0-3-8 Act)	(1) 130				

Job:O-UB3
Elevation Report
 02/27/2008 10:11:48 AM

Bundle Name: N/A

Panel:I6 Page: 38
 Level Name: First Floor

Length=87 Stud Height=92-5/8 Width=3-1/2 Stud Spacing=16 Studs=4 X 2 SPF Stud 1st Stud=3-1/4
 TPit pitch, xLen, spring= 0, 87, 97-1/8
 BPit pitch, xLen, spring= 0, 87, 0
 Fire Block Hgt (Center) =
 Nom.Lumber=87.52088BfI
 VTP=87 Offset=0



Cutting List

Label	Member	Description	Qty/Length	LElev	RElev	LPlan	RPlan
A	Bottom Plate	SPF 2 X 4 No.2 D T	(1) 87				
B	Top Plate	SPF 2 X 4 No.2 D	(1) 87				
C	VTP	SPF 2 X 4 No.2 D	(1) 87				
D	Jack Stud	SPF 2 X 4 Stud D	(2) 92-5/8				
E	Jack	SPF 2 X 4 Stud D	(4) 78-1/2				
F	Header	SYP 10 X 2 No.2 D	(1) 48				
G	Stud	SPF 2 X 4 Stud D	(5) 92-5/8				
H	Top Cripples	SPF 2 X 4 Stud D	(4) 4-7/8				

Appendix B

First Floor Wood Shear Walls

Job:O-UB3 Elevation Report

02/27/2008 10:11:48 AM

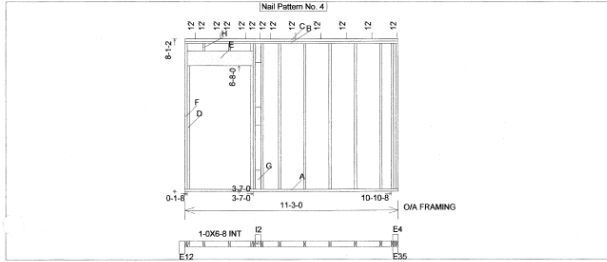
Bundle Name: N/A

Panel:127

Level Name: First Floor

Page: 54

Length=135 Stud Height=92-5/8 Width=3-1/2 Stud Spacing=16 Studs=4 X 2 SPF Stud 1st Stud=11-1/4
 TPit pitch, xLen, spring= 0, 135, 97-1/8
 BPit pitch, xLen, spring= 0, 135, 0
 Fire Block Hgt (Center) =
 VTP=135 Offset=0
 Nom.Lumber=122.1042BdF1



Cutting List

Label	Member	Description	Qty/Length	LElev	RElev	LPlan	RPlan
A	Bottom Plate	SPF 2 X 4 No.2 D T	(1) 135				
B	Top Plate	SPF 2 X 4 No.2 D	(1) 135				
C	VTP	SPF 2 X 4 No.2 D	(1) 135				
D	Jack	SPF 2 X 4 Stud D	(2) 78-1/2				
E	Header	SYP 10 X 2 No.2 D	(1) 41-1/2				
F	Stud	SPF 2 X 4 Stud D	(11) 92-5/8				
G	Block	SPF 4 X 2 No.2 D	(3) 12				
H	Top Cripples	SPF 2 X 4 Stud D	(3) 4-7/8				

Job:O-UB3 Elevation Report

02/27/2008 10:11:48 AM

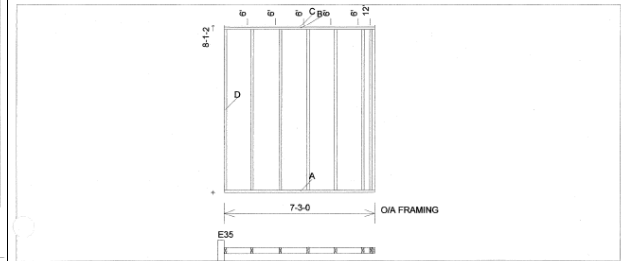
Bundle Name: N/A

Panel:128

Level Name: First Floor

Page: 55

Length=87 Stud Height=92-5/8 Width=3-1/2 Stud Spacing=16 Studs=4 X 2 SPF Stud 1st Stud=15-1/4
 TPit pitch, xLen, spring= 0, 87, 97-1/8
 BPit pitch, xLen, spring= 0, 87, 0
 Fire Block Hgt (Center) =
 VTP=87 Offset=0
 Nom.Lumber=58.3333BdF1

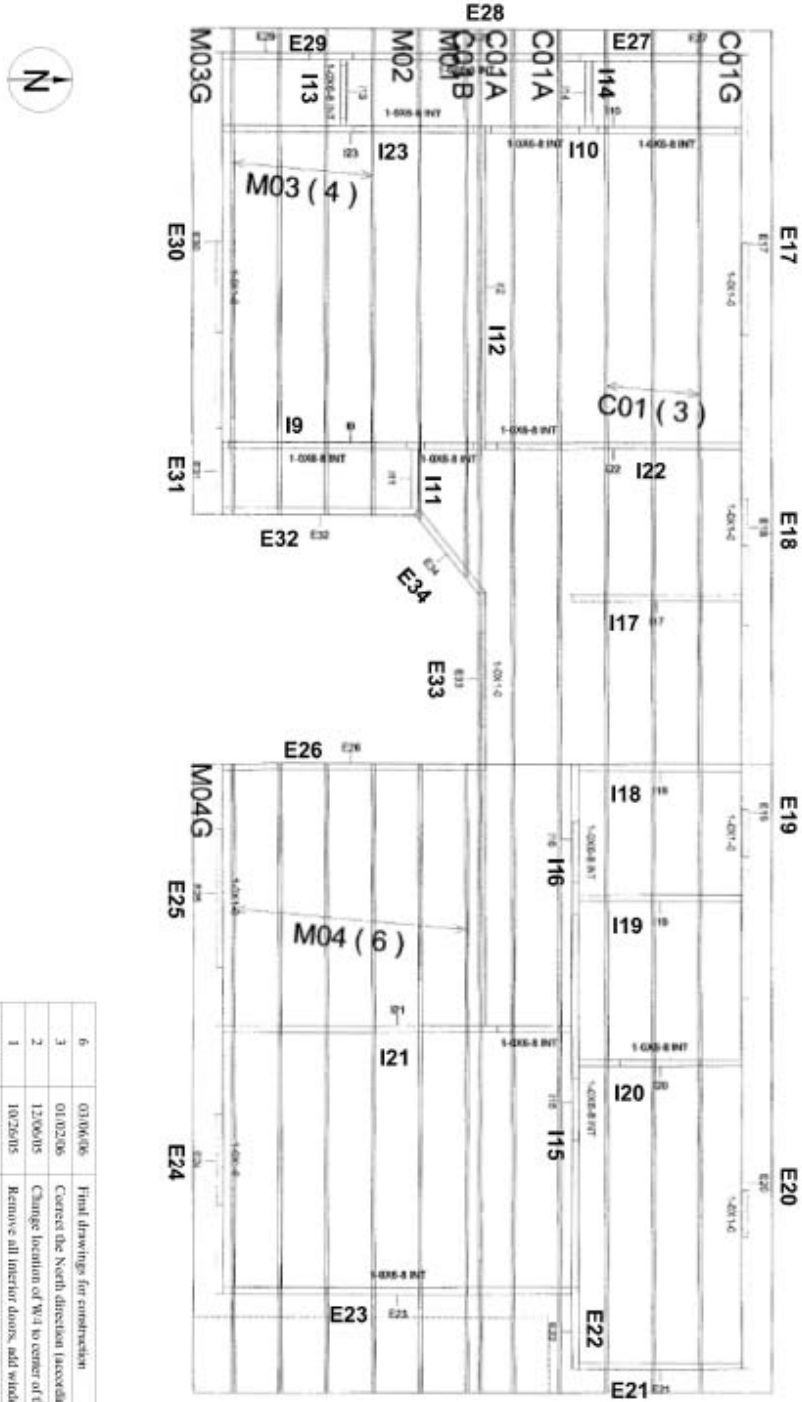


Cutting List

Label	Member	Description	Qty/Length	LElev	RElev	LPlan	RPlan
A	Bottom Plate	SPF 2 X 4 No.2 D T	(1) 87				
B	Top Plate	SPF 2 X 4 No.2 D	(1) 87				
C	VTP	SPF 2 X 4 No.2 D	(1) 87				
D	Stud	SPF 2 X 4 Stud D	(8) 92-5/8				

Appendix B

Second Floor Wood Shear Walls



REV. NO.	DATE	DESCRIPTIONS
6	03/06/06	Final drawings for construction
3	01/02/06	Correct the North direction (according to the stake table)
2	12/06/05	Change location of W-1 to center of the wall
1	10/26/05	Remove all interior doors, add windows at line A

NEESWOOD		UNIVERSITY OF BUFFALO	DATE: 03/06/06	REV. NO.: 6	SCALE: NTS
PROJECT: NEESWOOD Teaching Building for Bandmark Testing		COURTNEY 2nd Level Pre-Industrialized Wall Layout			

FOR CONSTRUCTION

Appendix B

Second Floor Wood Shear Walls

Job:O-UB3

Elevation Report

02/27/2006 10:11:48 AM

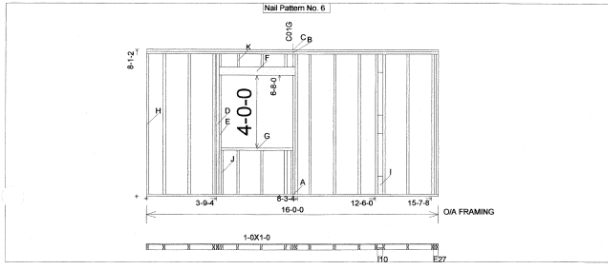
Bundle Name: N/A

Panel:E17

Level Name: Second Floor

Page: 14

Length=192 Stud Height=92-5/8 Width=3-1/2 Stud Spacing=16 Studs=4 X 2 SPF Stud 1st Stud=10-3/4
 TPit pitch, xLen, spring= 0, 192, 97-1/8
 BPit pitch, xLen, spring= 0, 192, 0
 Fire Block Hgt (Center) =
 Nom.Lumber=169.18768dF1
 VTP=192 Offset=0
 Sheathing=Plywood/OSB Structural L=0 R=0 T=-1-1/8
 L=0 R=0 T= B=



Cutting List

Label	Member	Description	Qty/Length	LElev	RElev	LPlan	RPlan
A	Bottom Plate	SPF 2 X 4 No.2 D	(1) 192				
B	Top Plate	SPF 2 X 4 No.2 D	(1) 192				
C	VTP	SPF 2 X 4 No.2 D	(1) 192				
D	Jack Stud	SPF 2 X 4 Stud D	(2) 92-5/8				
E	Jack	SPF 2 X 4 Stud D	(2) 78-1/2				
F	Header	SPF 6 X 2 No.2 D	(1) 51				
G	Sill	SPF 2 X 4 Stud D	(1) 48				
H	Stud	SPF 2 X 4 Stud D	(13) 92-5/8				
I	Block	SPF 4 X 2 No.2 D	(3) 12				
J	Bottom Cripples	SPF 2 X 4 Stud D	(5) 29				
K	Top Cripples	SPF 2 X 4 Stud D	(5) 8-5/8				
L	Sheathing	Plywood/OSB Structural	(4) 96				

Job:O-UB3

Elevation Report

02/27/2006 10:11:48 AM

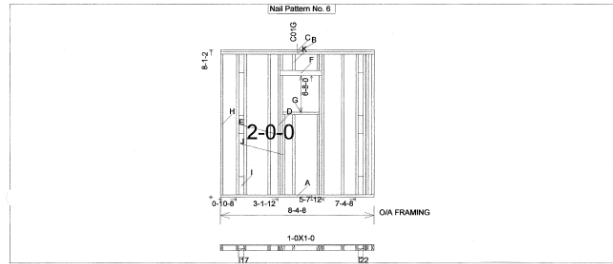
Bundle Name: N/A

Panel:E18

Level Name: Second Floor

Page: 15

Length=100-1/2 Stud Height=92-5/8 Width=3-1/2 Stud Spacing=16 Studs=4 X 2 SPF Stud 1st Stud=15-1/4
 TPit pitch, xLen, spring= 0, 100-1/2, 97-1/8
 BPit pitch, xLen, spring= 0, 100-1/2, 0
 Fire Block Hgt (Center) =
 Nom.Lumber=152.60428dF1
 VTP=100-1/2 Offset=0
 Sheathing=Plywood/OSB Structural L=0 R=0 T=-1-1/8
 L=0 R=0 T= B=



Cutting List

Label	Member	Description	Qty/Length	LElev	RElev	LPlan	RPlan
A	Bottom Plate	SPF 2 X 4 No.2 D	(1) 100-1/2				
B	Top Plate	SPF 2 X 4 No.2 D	(1) 100-1/2				
C	VTP	SPF 2 X 4 No.2 D	(1) 100-1/2				
D	Jack Stud	SPF 2 X 4 Stud D	(2) 92-5/8				
E	Jack	SPF 2 X 4 Stud D	(2) 78-1/2				
F	Header	SPF 4 X 2 No.2 D	(1) 27				
G	Sill	SPF 2 X 4 Stud D	(1) 24				
H	Stud	SPF 2 X 4 Stud D	(9) 92-5/8				
I	Block	SPF 4 X 2 No.2 D	(8) 12				
J	Bottom Cripples	SPF 2 X 4 Stud D	(3) 53				
K	Top Cripples	SPF 2 X 4 Stud D	(4) 10-5/8				
L	Sheathing	Plywood/OSB Structural	(3) 96				

Job:O-UB3

Elevation Report

02/27/2006 10:11:48 AM

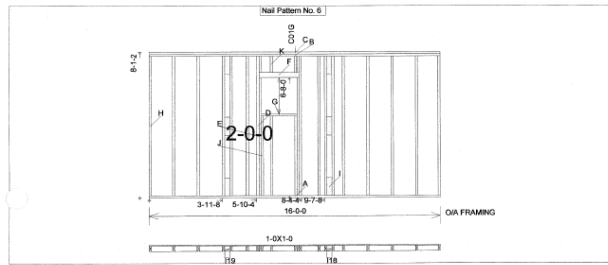
Bundle Name: N/A

Panel:E19

Level Name: Second Floor

Page: 16

Length=192 Stud Height=92-5/8 Width=3-1/2 Stud Spacing=16 Studs=4 X 2 SPF Stud 1st Stud=15-1/4
 TPit pitch, xLen, spring= 0, 192, 97-1/8
 BPit pitch, xLen, spring= 0, 192, 0
 Fire Block Hgt (Center) =
 Nom.Lumber=197.00008dF1
 VTP=192 Offset=0
 Sheathing=Plywood/OSB Structural L=0 R=0 T=-1-1/8
 L=0 R=0 T= B=



Cutting List

Label	Member	Description	Qty/Length	LElev	RElev	LPlan	RPlan
A	Bottom Plate	SPF 2 X 4 No.2 D	(1) 192				
B	Top Plate	SPF 2 X 4 No.2 D	(1) 192				
C	VTP	SPF 2 X 4 No.2 D	(1) 192				
D	Jack Stud	SPF 2 X 4 Stud D	(2) 92-5/8				
E	Jack	SPF 2 X 4 Stud D	(2) 78-1/2				
F	Header	SPF 4 X 2 No.2 D	(2) 27				
G	Sill	SPF 2 X 4 Stud D	(1) 24				
H	Stud	SPF 2 X 4 Stud D	(14) 92-5/8				
I	Block	SPF 4 X 2 No.2 D	(8) 12				
J	Bottom Cripples	SPF 2 X 4 Stud D	(3) 53				
K	Top Cripples	SPF 2 X 4 Stud D	(4) 10-5/8				
L	Sheathing	Plywood/OSB Structural	(4) 96				

Job:O-UB3

Elevation Report

02/27/2006 10:11:48 AM

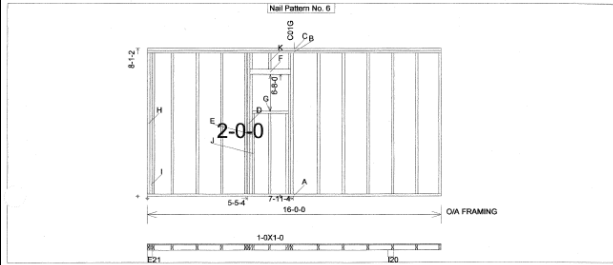
Bundle Name: N/A

Panel:E20

Level Name: Second Floor

Page: 17

Length=192 Stud Height=92-5/8 Width=3-1/2 Stud Spacing=16 Studs=4 X 2 SPF Stud 1st Stud=15-1/4
 TPit pitch, xLen, spring= 0, 192, 97-1/8
 BPit pitch, xLen, spring= 0, 192, 0
 Fire Block Hgt (Center) =
 Nom.Lumber=180.14588dF1
 VTP=192 Offset=0
 Sheathing=Plywood/OSB Structural L=0 R=0 T=-1-1/8
 L=0 R=0 T= B=



Cutting List

Label	Member	Description	Qty/Length	LElev	RElev	LPlan	RPlan
A	Bottom Plate	SPF 2 X 4 No.2 D	(1) 192				
B	Top Plate	SPF 2 X 4 No.2 D	(1) 192				
C	VTP	SPF 2 X 4 No.2 D	(1) 192				
D	Jack Stud	SPF 2 X 4 Stud D	(2) 92-5/8				
E	Jack	SPF 2 X 4 Stud D	(2) 78-1/2				
F	Header	SPF 4 X 2 No.2 D	(2) 27				
G	Sill	SPF 2 X 4 Stud D	(1) 24				
H	Stud	SPF 2 X 4 Stud D	(15) 92-5/8				
I	Block	SPF 4 X 2 No.2 D	(3) 12				
J	Bottom Cripples	SPF 2 X 4 Stud D	(3) 53				
K	Top Cripples	SPF 2 X 4 Stud D	(3) 10-5/8				
L	Sheathing	Plywood/OSB Structural	(4) 96				

Appendix B

Second Floor Wood Shear Walls

Job:O-UB3

Elevation Report

02/27/2006 10:11:48 AM

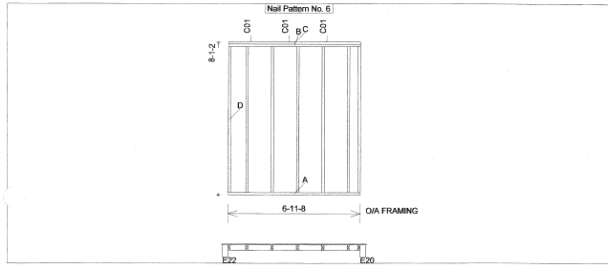
Bundle Name: N/A

Panel:E21

Level Name: Second Floor

Page: 18

Length=83-1/2 Stud Height=92-5/8 Width=3-1/2 Stud Spacing=16 Studs=4 X 2 SPF Stud 1st Stud=11-1/4
 TPit pitch, xLen, spring= 0, 83-1/2, 97-1/8
 BPit pitch, xLen, spring= 0, 83-1/2, 0
 Fire Block Hgt (Center) =
 VTP=83-1/2 Offset=0
 Sheathing=Plywood/OSB Structural L=4 R=4 T=-1-1/8
 L=0 R=0 T= B=



Cutting List

Label	Member	Description	Qty/Length	LElev	RElev	LPlan	RPlan
A	Bottom Plate	SPF 2 X 4 No.2 D	(1) 83-1/2				
B	Top Plate	SPF 2 X 4 No.2 D	(1) 83-1/2				
C	VTP	SPF 2 X 4 No.2 D	(1) 83-1/2				
D	Stud	SPF 2 X 4 Stud D	(7) 92-5/8				
E	Sheathing	Plywood/OSB Structural	(2) 96				

Job:O-UB3

Elevation Report

02/27/2006 10:11:48 AM

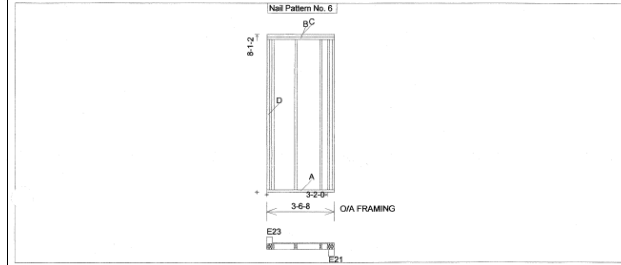
Bundle Name: N/A

Panel:E22

Level Name: Second Floor

Page: 19

Length=42-1/2 Stud Height=92-5/8 Width=3-1/2 Stud Spacing=16 Studs=4 X 2 SPF Stud 1st Stud=1-1/4
 TPit pitch, xLen, spring= 0, 42-1/2, 97-1/8
 BPit pitch, xLen, spring= 0, 42-1/2, 0
 Fire Block Hgt (Center) =
 VTP=42-1/2 Offset=0
 Sheathing=Plywood/OSB Structural L=4 R=0 T=-1-1/8
 L=0 R=0 T= B=



Cutting List

Label	Member	Description	Qty/Length	LElev	RElev	LPlan	RPlan
A	Bottom Plate	SPF 2 X 4 No.2 D	(1) 42-1/2				
B	Top Plate	SPF 2 X 4 No.2 D	(1) 42-1/2				
C	VTP	SPF 2 X 4 No.2 D	(1) 42-1/2				
D	Stud	SPF 2 X 4 Stud D	(8) 92-5/8				
E	Sheathing	Plywood/OSB Structural	(1) 96				

Job:O-UB3

Elevation Report

02/27/2006 10:11:48 AM

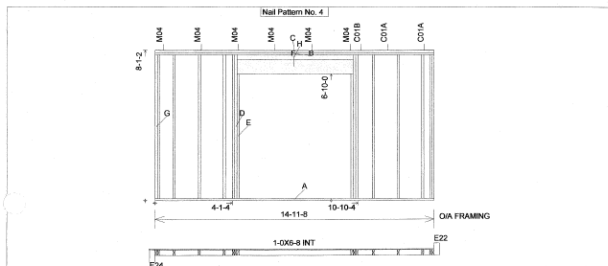
Bundle Name: N/A

Panel:E23

Level Name: Second Floor

Page: 20

Length=179-1/2 Stud Height=92-5/8 Width=3-1/2 Stud Spacing=16 Studs=4 X 2 SPF Stud 1st Stud=11-1/4
 TPit pitch, xLen, spring= 0, 179-1/2, 97-1/8
 BPit pitch, xLen, spring= 0, 179-1/2, 0
 Fire Block Hgt (Center) =
 VTP=179-1/2 Offset=0
 Sheathing=Plywood/OSB Structural L=4 R=0 T=-1-1/8
 L=0 R=0 T= B=



Cutting List

Label	Member	Description	Qty/Length	LElev	RElev	LPlan	RPlan
A	Bottom Plate	SPF 2 X 4 No.2 D	(1) 179-1/2				
B	Top Plate	SPF 2 X 4 No.2 D	(1) 179-1/2				
C	VTP	SPF 2 X 4 No.2 D	(1) 179-1/2				
D	Jack Stud	SPF 2 X 4 Stud D	(4) 92-5/8				
E	Jack	SPF 2 X 4 Stud D	(2) 89-1/2				
F	Header	SYP 10 X 2 No.2 D	(2) 75				
G	Stud	SPF 2 X 4 Stud D	(16) 92-5/8				
H	Pad	SPF 2 X 4 (0-2-14 x 0-3-8 Act) Stud D	(1) 75				
I	Sheathing	Plywood/OSB Structural	(4) 96				

Job:O-UB3

Elevation Report

02/27/2006 10:11:48 AM

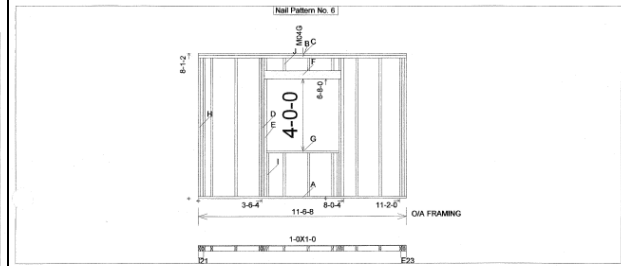
Bundle Name: N/A

Panel:E24

Level Name: Second Floor

Page: 21

Length=138-1/2 Stud Height=92-5/8 Width=3-1/2 Stud Spacing=16 Studs=4 X 2 SPF Stud 1st Stud=8-1/4
 TPit pitch, xLen, spring= 0, 138-1/2, 97-1/8
 BPit pitch, xLen, spring= 0, 138-1/2, 0
 Fire Block Hgt (Center) =
 VTP=138-1/2 Offset=0
 Sheathing=Plywood/OSB Structural L=0 R=0 T=-1-1/8
 L=0 R=0 T= B=



Cutting List

Label	Member	Description	Qty/Length	LElev	RElev	LPlan	RPlan
A	Bottom Plate	SPF 2 X 4 No.2 D	(1) 138-1/2				
B	Top Plate	SPF 2 X 4 No.2 D	(1) 138-1/2				
C	VTP	SPF 2 X 4 No.2 D	(1) 138-1/2				
D	Jack Stud	SPF 2 X 4 Stud D	(2) 92-5/8				
E	Jack	SPF 2 X 4 Stud D	(2) 78-1/2				
F	Header	SPF 6 X 2 No.2 D	(2) 51				
G	Sill	SPF 2 X 4 Stud D	(1) 48				
H	Stud	SPF 2 X 4 Stud D	(11) 92-5/8				
I	Bottom Cripples	SPF 2 X 4 Stud D	(5) 29				
J	Top Cripples	SPF 2 X 4 Stud D	(5) 8-5/8				
K	Sheathing	Plywood/OSB Structural	(3) 96				

Appendix B

Second Floor Wood Shear Walls

Job:O-UB3

Elevation Report

02/27/2006 10:11:48 AM

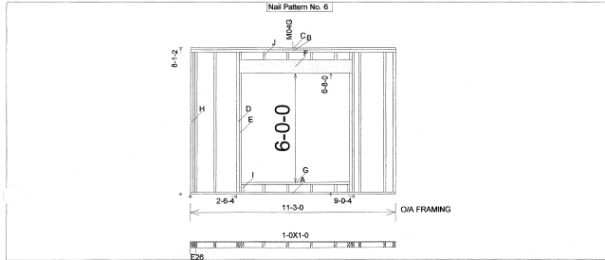
Bundle Name: N/A

Panel:E25

Level Name: Second Floor

Page: 22

Length=135 Stud Height=92-5/8 Width=3-1/2 Stud Spacing=16 Studs=4 X 2 SPF Stud 1st Stud=15-1/4
 TPitch, xLen, spring= 0, 135, 97-1/8
 BPitch, xLen, spring= 0, 135, 0
 Fire Block Hgt (Center) =
 Nom.Lumber=130.9792BdFt
 VTP=135 Offset=0
 Sheathing=Plywood/OSB Structural L=0 R=0 T=-1-1/8
 L=0 R=0 T= B=



Cutting List

Label	Member	Description	Qty/Length	LElev	RElev	LPlan	RPlan
A	Bottom Plate	SPF 2 X 4 No.2 D	(1) 135				
B	Top Plate	SPF 2 X 4 No.2 D	(1) 135				
C	VTP	SPF 2 X 4 No.2 D	(1) 135				
D	Jack Stud	SPF 2 X 4 Stud D	(2) 92-5/8				
E	Jack	SPF 2 X 4 Stud D	(2) 78-1/2				
F	Header	SYP 10 X 2 No.2 D	(2) 75				
G	Sill	SPF 2 X 4 Stud D	(1) 72				
H	Stud	SPF 2 X 4 Stud D	(7) 92-5/8				
I	Bottom Cripples	SPF 2 X 4 Stud D	(8) 5				
J	Top Cripples	SPF 2 X 4 Stud D	(8) 4-7/8				
K	Sheathing	Plywood/OSB Structural	(3) 96				

Job:O-UB3

Elevation Report

02/27/2006 10:11:48 AM

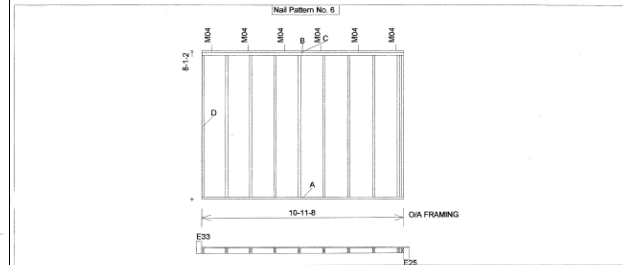
Bundle Name: N/A

Panel:E26

Level Name: Second Floor

Page: 23

Length=131-1/2 Stud Height=92-5/8 Width=3-1/2 Stud Spacing=16 Studs=4 X 2 SPF Stud 1st Stud=15-1/4
 TPitch, xLen, spring= 0, 131-1/2, 97-1/8
 BPitch, xLen, spring= 0, 131-1/2, 0
 Fire Block Hgt (Center) =
 Nom.Lumber=75.4583BdFt
 VTP=131-1/2 Offset=0
 Sheathing=Plywood/OSB Structural L=0 R=4 T=-1-1/8
 L=0 R=0 T= B=



Cutting List

Label	Member	Description	Qty/Length	LElev	RElev	LPlan	RPlan
A	Bottom Plate	SPF 2 X 4 No.2 D	(1) 131-1/2				
B	Top Plate	SPF 2 X 4 No.2 D	(1) 131-1/2				
C	VTP	SPF 2 X 4 No.2 D	(1) 131-1/2				
D	Stud	SPF 2 X 4 Stud D	(10) 92-5/8				
E	Sheathing	Plywood/OSB Structural	(3) 96				

Job:O-UB3

Elevation Report

02/27/2006 10:11:48 AM

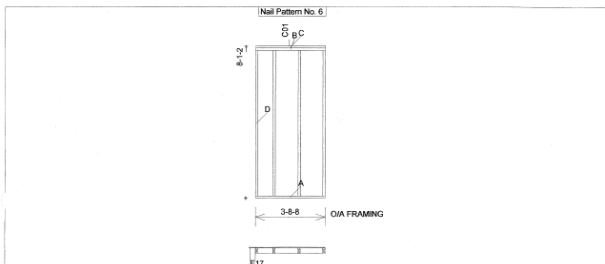
Bundle Name: N/A

Panel:E27

Level Name: Second Floor

Page: 24

Length=44-1/2 Stud Height=92-5/8 Width=3-1/2 Stud Spacing=16 Studs=4 X 2 SPF Stud 1st Stud=11-1/4
 TPitch, xLen, spring= 0, 44-1/2, 97-1/8
 BPitch, xLen, spring= 0, 44-1/2, 0
 Fire Block Hgt (Center) =
 Nom.Lumber=40.5838BdFt
 VTP=44-1/2 Offset=0
 Sheathing=Plywood/OSB Structural L=4 R=0 T=-1-1/8
 L=0 R=0 T= B=



Cutting List

Label	Member	Description	Qty/Length	LElev	RElev	LPlan	RPlan
A	Bottom Plate	SPF 2 X 4 No.2 D	(1) 44-1/2				
B	Top Plate	SPF 2 X 4 No.2 D	(1) 44-1/2				
C	VTP	SPF 2 X 4 No.2 D	(1) 44-1/2				
D	Stud	SPF 2 X 4 Stud D	(4) 92-5/8				
E	Sheathing	Plywood/OSB Structural	(2) 96				

Job:O-UB3

Elevation Report

02/27/2006 10:11:48 AM

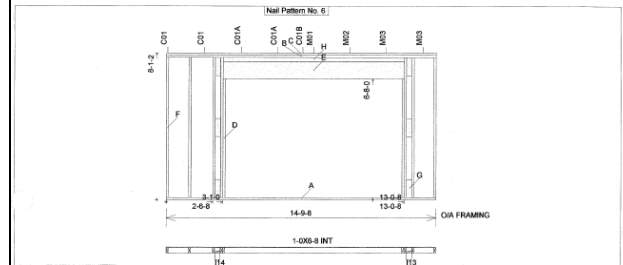
Bundle Name: N/A

Panel:E28

Level Name: Second Floor

Page: 25

Length=177-1/2 Stud Height=92-5/8 Width=3-1/2 Stud Spacing=16 Studs=4 X 2 SPF Stud 1st Stud=14-3/4
 TPitch, xLen, spring= 0, 177-1/2, 97-1/8
 BPitch, xLen, spring= 0, 177-1/2, 0
 Fire Block Hgt (Center) =
 Nom.Lumber=143.9007BdFt
 VTP=177-1/2 Offset=0
 Sheathing=Plywood/OSB Structural L=0 R=0 T=-1-1/8
 L=0 R=0 T= B=



Cutting List

Label	Member	Description	Qty/Length	LElev	RElev	LPlan	RPlan
A	Bottom Plate	SPF 2 X 4 No.2 D	(1) 177-1/2				
B	Top Plate	SPF 2 X 4 No.2 D	(1) 177-1/2				
C	VTP	SPF 2 X 4 No.2 D	(1) 177-1/2				
D	Jack	SPF 2 X 4 Stud D	(2) 78-1/2				
E	Header	DF 12 X 2 No.2 D	(1) 119-1/2				
F	Stud	SPF 2 X 4 Stud D	(7) 92-5/8				
G	Block	SPF 4 X 2 No.2 D	(6) 12				
H	Pad	SPF 2 X 4 (D-2-14 X D-3-8 Act)	(1) 119-1/2				
I	Sheathing	Plywood/OSB Structural	(4) 96				

Appendix B

Second Floor Wood Shear Walls

Job:O-UB3 Elevation Report

02/27/2006 10:11:46 AM

Bundle Name: N/A

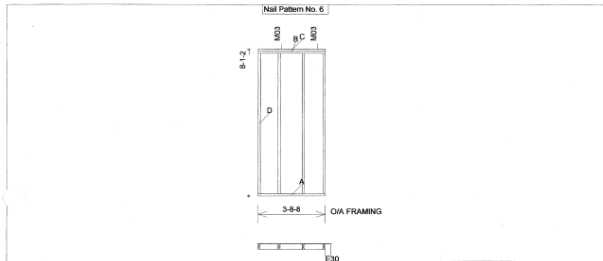
Panel:E29

Page: 26

Level Name: Second Floor

Length=44-1/2 Stud Height=92-5/8 Width=3-1/2 Stud Spacing=16 Studs=4 X 2 SPF Stud 1st Stud=13-1/4
 T/Pt pitch, xLen, spring= 0, 44-1/2, 97-1/8
 B/Pt pitch, xLen, spring= 0, 44-1/2, 0
 Fire Block Hgt (Center) =
 VTP=44-1/2 Offset=0
 Sheathing=Plywood/OSB Structural L=0 R=4 T=-1-1/8
 L=0 R=0 T= B=

Nom.Lumber=40.5833BdFt



Cutting List

Label	Member	Description	Qty/Length	LElev	RElev	LPlan	RPlan
A	Bottom Plate	SPF 2 X 4 No.2 D	(1) 44-1/2				
B	Top Plate	SPF 2 X 4 No.2 D	(1) 44-1/2				
C	VTP	SPF 2 X 4 No.2 D	(1) 44-1/2				
D	Stud	SPF 2 X 4 Stud D	(4) 92-5/8				
E	Sheathing	Plywood/OSB Structural	(2) 96				

Job:O-UB3

Elevation Report

02/27/2006 10:11:46 AM

Bundle Name: N/A

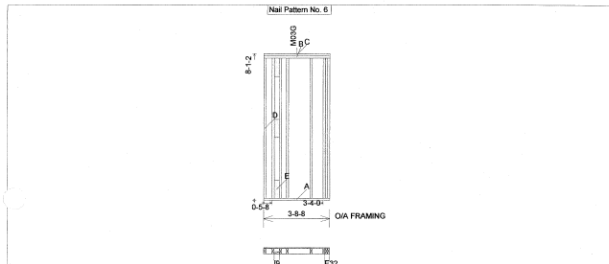
Panel:E31

Page: 28

Level Name: Second Floor

Length=44-1/2 Stud Height=92-5/8 Width=3-1/2 Stud Spacing=16 Studs=4 X 2 SPF Stud 1st Stud=15-1/4
 T/Pt pitch, xLen, spring= 0, 44-1/2, 97-1/8
 B/Pt pitch, xLen, spring= 0, 44-1/2, 0
 Fire Block Hgt (Center) =
 VTP=44-1/2 Offset=0
 Sheathing=Plywood/OSB Structural L=0 R=0 T=-1-1/8
 L=0 R=0 T= B=

Nom.Lumber=61.1667BdFt



Cutting List

Label	Member	Description	Qty/Length	LElev	RElev	LPlan	RPlan
A	Bottom Plate	SPF 2 X 4 No.2 D	(1) 44-1/2				
B	Top Plate	SPF 2 X 4 No.2 D	(1) 44-1/2				
C	VTP	SPF 2 X 4 No.2 D	(1) 44-1/2				
D	Stud	SPF 2 X 4 Stud D	(8) 92-5/8				
E	Block	SPF 4 X 2 No.2 D	(3) 12				
F	Sheathing	Plywood/OSB Structural	(1) 96				

Job:O-UB3

Elevation Report

02/27/2006 10:11:48 AM

Bundle Name: N/A

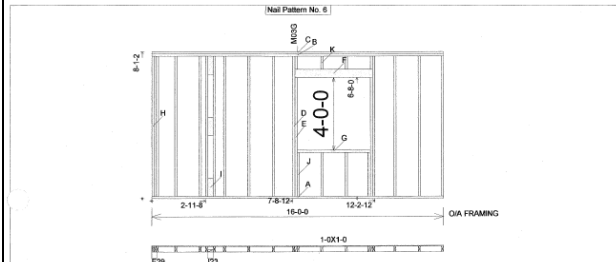
Panel:E30

Page: 27

Level Name: Second Floor

Length=192 Stud Height=92-5/8 Width=3-1/2 Stud Spacing=16 Studs=4 X 2 SPF Stud 1st Stud=15-1/4
 T/Pt pitch, xLen, spring= 0, 192, 97-1/8
 B/Pt pitch, xLen, spring= 0, 192, 0
 Fire Block Hgt (Center) =
 VTP=192 Offset=0
 Sheathing=Plywood/OSB Structural L=0 R=0 T=-1-1/8
 L=0 R=0 T= B=

Nom.Lumber=173.1675BdFt



Cutting List

Label	Member	Description	Qty/Length	LElev	RElev	LPlan	RPlan
A	Bottom Plate	SPF 2 X 4 No.2 D	(1) 192				
B	Top Plate	SPF 2 X 4 No.2 D	(1) 192				
C	VTP	SPF 2 X 4 No.2 D	(1) 192				
D	Jack Stud	SPF 2 X 4 Stud D	(2) 92-5/8				
E	Jack	SPF 2 X 4 Stud D	(2) 78-1/2				
F	Header	SPF 6 X 2 No.2 D	(2) 51				
G	Sill	SPF 2 X 4 Stud D	(1) 48				
H	Stud	SPF 2 X 4 Stud D	(13) 92-5/8				
I	Block	SPF 4 X 2 No.2 D	(3) 12				
J	Bottom Cripples	SPF 2 X 4 Stud D	(4) 29				
K	Top Cripples	SPF 2 X 4 Stud D	(4) 9-5/8				
L	Sheathing	Plywood/OSB Structural	(4) 96				

Job:O-UB3

Elevation Report

02/27/2006 10:11:48 AM

Bundle Name: N/A

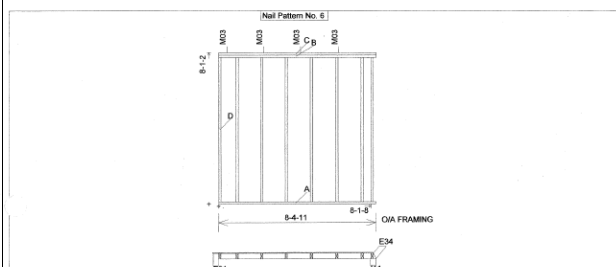
Panel:E32

Page: 29

Level Name: Second Floor

Length=100-11/16 Stud Height=92-5/8 Width=3-1/2 Stud Spacing=16 Studs=4 X 2 SPF Stud 1st Stud=11-1/4
 T/Pt pitch, xLen, spring= 0, 100-11/16, 97-1/8
 B/Pt pitch, xLen, spring= 0, 100-11/16, 0
 Fire Block Hgt (Center) =
 VTP=100-11/16 Offset=0
 Sheathing=Plywood/OSB Structural L=4 R=0-1/4 T=-1-1/8
 L=0 R=0 T= B=

Nom.Lumber=61.1667BdFt



Cutting List

Label	Member	Description	Qty/Length	LElev	RElev	LPlan	RPlan
A	Bottom Plate	SPF 2 X 4 No.2 D	(1) 100-11/16				25.5
B	Top Plate	SPF 2 X 4 No.2 D	(1) 100-11/16				25.5
C	VTP	SPF 2 X 4 No.2 D	(1) 100-11/16				25.5
D	Stud	SPF 2 X 4 Stud D	(8) 92-5/8				
E	Sheathing	Plywood/OSB Structural	(3) 96				

Appendix B

Second Floor Wood Shear Walls

Job:O-UB3

Elevation Report

02/27/2006 10:11:48 AM

Bundle Name: NA

Panel:E33

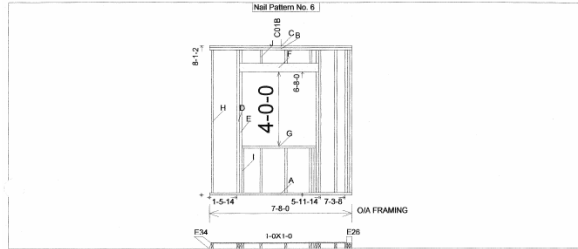
Level Name: Second Floor

Page: 30

Length=92 Stud Height=92-5/8 Width=3-1/2 Stud Spacing=16 Studs=4 X 2 SPF Stud 1st Stud=15-7/16
 TPI pitch, xLen, spring= 0, 92, 97-1/8
 BPI pitch, xLen, spring= 0, 92, 0
 Fire Block Hgt (Center) = Non.Lumber=104.02088dP1

VTP=92 Offset=-1-1/4

Sheathing=Plywood/OSB Structural L=0-3/16 R=4 T=1-1/8
 L=0 R=0 T= B=



Cutting List

Label	Member	Description	Qty/Length	LElev	RElev	LPlan	RPlan
A	Bottom Plate	SPF 2 X 4 No.2 D	(1) 92			119.5	
B	Top Plate	SPF 2 X 4 No.2 D	(1) 92			119.5	
C	VTP	SPF 2 X 4 No.2 D	(1) 92			119.5	
D	Jack Stud	SPF 2 X 4 Stud D	(2) 92-5/8				
E	Jack	SPF 2 X 4 Stud D	(2) 78-1/2				
F	Header	SPF 6 X 2 No.2 D	(2) 51				
G	Sill	SPF 2 X 4 Stud D	(1) 48				
H	Stud	SPF 2 X 4 Stud D	(5) 92-5/8				
I	Bottom Cripples	SPF 2 X 4 Stud D	(5) 29				
J	Top Cripples	SPF 2 X 4 Stud D	(5) 8-5/8				
K	Sheathing	Plywood/OSB Structural	(2) 96				

Job:O-UB3

Elevation Report

02/27/2006 10:11:48 AM

Bundle Name: NA

Panel:E34

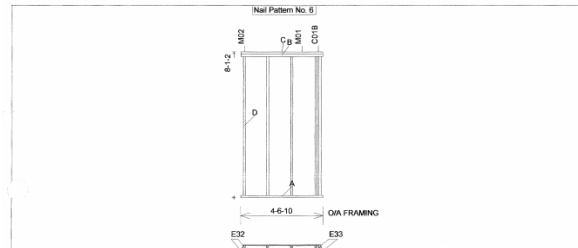
Level Name: Second Floor

Page: 31

Length=54-5/8 Stud Height=92-5/8 Width=3-1/2 Stud Spacing=16 Studs=4 X 2 SPF Stud 1st Stud=15-1/2
 TPI pitch, xLen, spring= 0, 54-5/8, 97-1/8
 BPI pitch, xLen, spring= 0, 54-5/8, 0
 Fire Block Hgt (Center) = Non.Lumber=45.72928dP1

VTP=54-5/8 Offset=-1-11/16

Sheathing=Plywood/OSB Structural L=0-1/4 R=0-3/16 T=1-1/8
 L=0 R=0 T= B=



Cutting List

Label	Member	Description	Qty/Length	LElev	RElev	LPlan	RPlan
A	Bottom Plate	SPF 2 X 4 No.2 D	(1) 54-5/8			125.5	119.5
B	Top Plate	SPF 2 X 4 No.2 D	(1) 54-5/8			125.5	119.5
C	VTP	SPF 2 X 4 No.2 D	(1) 54-5/8			125.5	119.5
D	Stud	SPF 2 X 4 Stud D	(5) 92-5/8				
E	Sheathing	Plywood/OSB Structural	(2) 96				

Appendix B

Second Floor Wood Shear Walls

Job:O-UB3

Elevation Report

02/27/2008 10:11:48 AM

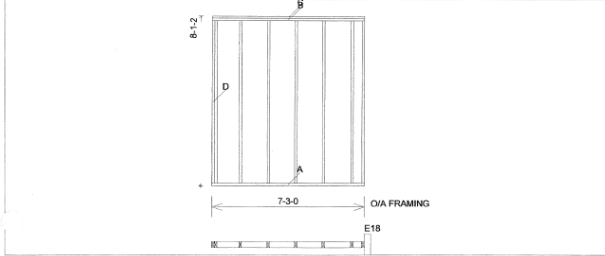
Bundle Name: N/A

Panel:I17

Level Name: Second Floor

Page: 47

Length=87 Stud Height=92-5/8 Width=3-1/2 Stud Spacing=16 Studs=4 X 2 SPF Stud 1st Stud=15-1/4
 TPit pitch, xLen, spring= 0, 87, 97-1/8
 BPit pitch, xLen, spring= 0, 87, 0
 Fire Block Hgt (Center) =
 VTP=87 Offset=0
 Nom Lumber=61.16678BF1



Cutting List

Label	Member	Description	Qty/Length	LElev	RElev	LPlan	RPlan
A	Bottom Plate	SPF 2 X 4 No.2 D	(1) 87				
B	Top Plate	SPF 2 X 4 No.2 D	(1) 87				
C	VTP	SPF 2 X 4 No.2 D	(1) 87				
D	Stud	SPF 2 X 4 Stud D	(8) 92-5/8				

Job:O-UB3

Elevation Report

02/27/2008 10:11:48 AM

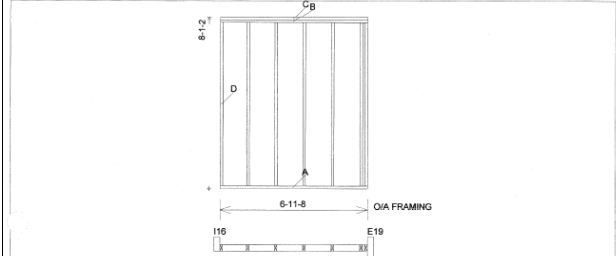
Bundle Name: N/A

Panel:I18

Level Name: Second Floor

Page: 48

Length=83-1/2 Stud Height=92-5/8 Width=3-1/2 Stud Spacing=16 Studs=4 X 2 SPF Stud 1st Stud=15-1/4
 TPit pitch, xLen, spring= 0, 83-1/2, 97-1/8
 BPit pitch, xLen, spring= 0, 83-1/2, 0
 Fire Block Hgt (Center) =
 VTP=83-1/2 Offset=0
 Nom Lumber=56.02088BF1



Cutting List

Label	Member	Description	Qty/Length	LElev	RElev	LPlan	RPlan
A	Bottom Plate	SPF 2 X 4 No.2 D	(1) 83-1/2				
B	Top Plate	SPF 2 X 4 No.2 D	(1) 83-1/2				
C	VTP	SPF 2 X 4 No.2 D	(1) 83-1/2				
D	Stud	SPF 2 X 4 Stud D	(7) 92-5/8				

Job:O-UB3

Elevation Report

02/27/2008 10:11:48 AM

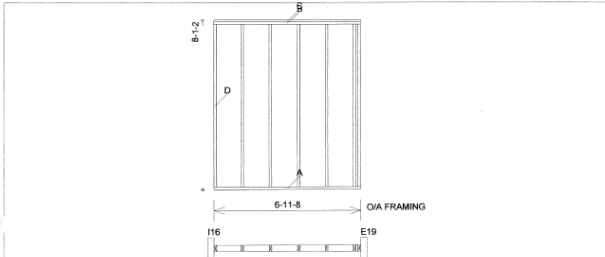
Bundle Name: N/A

Panel:I19

Level Name: Second Floor

Page: 49

Length=83-1/2 Stud Height=92-5/8 Width=3-1/2 Stud Spacing=16 Studs=4 X 2 SPF Stud 1st Stud=15-1/4
 TPit pitch, xLen, spring= 0, 83-1/2, 97-1/8
 BPit pitch, xLen, spring= 0, 83-1/2, 0
 Fire Block Hgt (Center) =
 VTP=83-1/2 Offset=0
 Nom Lumber=56.02088BF1



Cutting List

Label	Member	Description	Qty/Length	LElev	RElev	LPlan	RPlan
A	Bottom Plate	SPF 2 X 4 No.2 D	(1) 83-1/2				
B	Top Plate	SPF 2 X 4 No.2 D	(1) 83-1/2				
C	VTP	SPF 2 X 4 No.2 D	(1) 83-1/2				
D	Stud	SPF 2 X 4 Stud D	(7) 92-5/8				

Job:O-UB3

Elevation Report

02/27/2008 10:11:48 AM

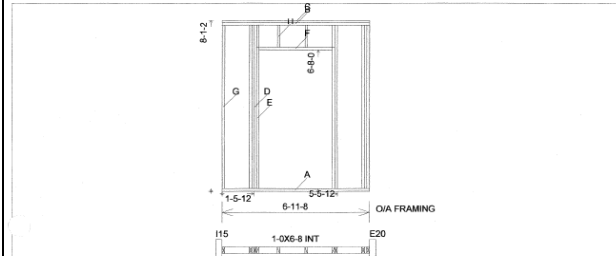
Bundle Name: N/A

Panel:I20

Level Name: Second Floor

Page: 50

Length=83-1/2 Stud Height=92-5/8 Width=3-1/2 Stud Spacing=16 Studs=4 X 2 SPF Stud 1st Stud=15-1/4
 TPit pitch, xLen, spring= 0, 83-1/2, 97-1/8
 BPit pitch, xLen, spring= 0, 83-1/2, 0
 Fire Block Hgt (Center) =
 VTP=83-1/2 Offset=0
 Nom Lumber=70.87508BF1



Cutting List

Label	Member	Description	Qty/Length	LElev	RElev	LPlan	RPlan
A	Bottom Plate	SPF 2 X 4 No.2 D	(1) 83-1/2				
B	Top Plate	SPF 2 X 4 No.2 D	(1) 83-1/2				
C	VTP	SPF 2 X 4 No.2 D	(1) 83-1/2				
D	Jack Stud	SPF 2 X 4 Stud D	(2) 92-5/8				
E	Jack	SPF 2 X 4 Stud D	(2) 80				
F	Trimmer	SPF 2 X 4 Stud D	(1) 42				
G	Stud	SPF 2 X 4 Stud D	(4) 92-5/8				
H	Top Cripples	SPF 2 X 4 Stud D	(4) 12-5/8				

Appendix B

Second Floor Wood Shear Walls

Job:O-UB3 Elevation Report

02/27/2006 10:11:48 AM

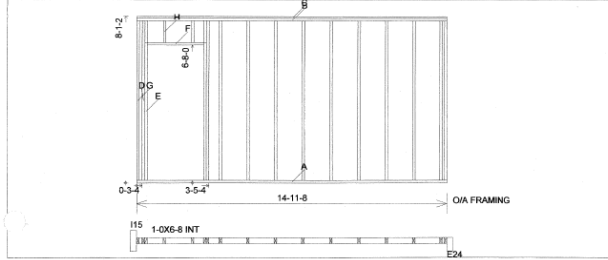
Bundle Name: N/A

Panel:I21

Level Name: Second Floor

Page: 51

Length=179-1/2 Stud Height=92-5/8 Width=3-1/2 Stud Spacing=16 Studs=4 X 2 SPF Stud 1st Stud=15-14
 TPft pitch, xLen, spring= 0, 179-1/2, 97-1/8
 BPft pitch, xLen, spring= 0, 179-1/2, 0
 Fire Block Hgt (Center) =
 VTP=179-1/2 Offset=0
 Nom Lumber=118.229286F1



Cutting List

Label	Member	Description	Qty/Length	LElev	RElev	LPlan	RPlan
A	Bottom Plate	SPF 2 X 4 No.2 D	(1) 179-1/2				
B	Top Plate	SPF 2 X 4 No.2 D	(1) 179-1/2				
C	VTP	SPF 2 X 4 No.2 D	(1) 179-1/2				
D	Jack Stud	SPF 2 X 4 Stud D	(2) 92-5/8				
E	Jack	SPF 2 X 4 Stud D	(2) 80				
F	Trimmer	SPF 2 X 4 Stud D	(1) 32				
G	Stud	SPF 2 X 4 Stud D	(11) 92-5/8				
H	Top Cripples	SPF 2 X 4 Stud D	(4) 12-5/8				

Job:O-UB3 Elevation Report

02/27/2006 10:11:48 AM

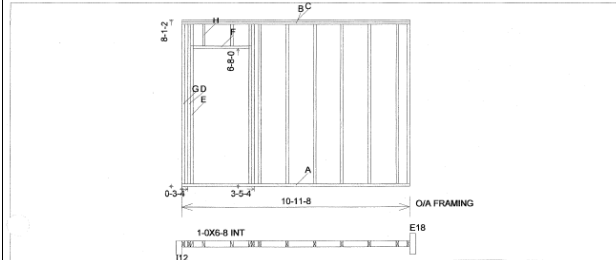
Bundle Name: N/A

Panel:I22

Level Name: Second Floor

Page: 52

Length=131-1/2 Stud Height=92-5/8 Width=3-1/2 Stud Spacing=16 Studs=4 X 2 SPF Stud 1st Stud=11-3/4
 TPft pitch, xLen, spring= 0, 131-1/2, 97-1/8
 BPft pitch, xLen, spring= 0, 131-1/2, 0
 Fire Block Hgt (Center) =
 VTP=131-1/2 Offset=0
 Nom Lumber=94.791765F1



Cutting List

Label	Member	Description	Qty/Length	LElev	RElev	LPlan	RPlan
A	Bottom Plate	SPF 2 X 4 No.2 D	(1) 131-1/2				
B	Top Plate	SPF 2 X 4 No.2 D	(1) 131-1/2				
C	VTP	SPF 2 X 4 No.2 D	(1) 131-1/2				
D	Jack Stud	SPF 2 X 4 Stud D	(2) 92-5/8				
E	Jack	SPF 2 X 4 Stud D	(2) 80				
F	Trimmer	SPF 2 X 4 Stud D	(1) 32				
G	Stud	SPF 2 X 4 Stud D	(8) 92-5/8				
H	Top Cripples	SPF 2 X 4 Stud D	(4) 12-5/8				

Job:O-UB3 Elevation Report

02/27/2006 10:11:48 AM

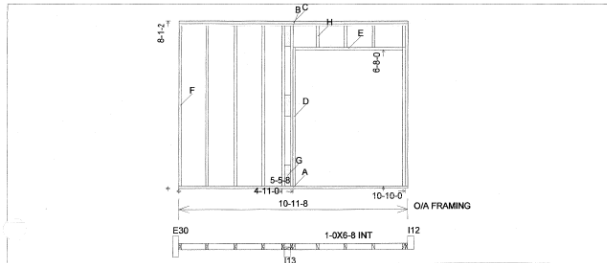
Bundle Name: N/A

Panel:I23

Level Name: Second Floor

Page: 53

Length=131-1/2 Stud Height=92-5/8 Width=3-1/2 Stud Spacing=16 Studs=4 X 2 SPF Stud 1st Stud=15-1/4
 TPft pitch, xLen, spring= 0, 131-1/2, 97-1/8
 BPft pitch, xLen, spring= 0, 131-1/2, 0
 Fire Block Hgt (Center) =
 VTP=131-1/2 Offset=0
 Nom Lumber=101.354286F1

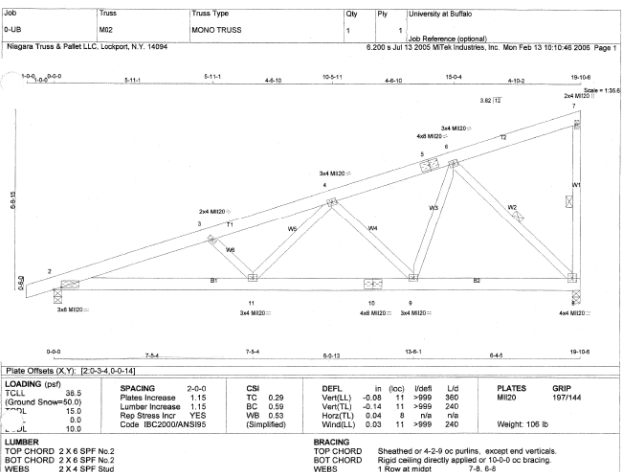
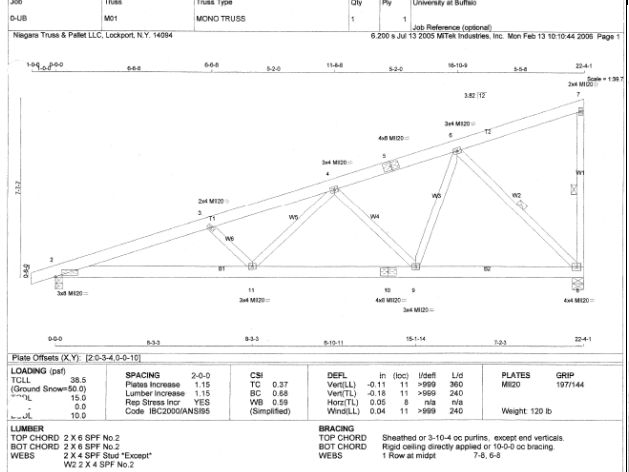
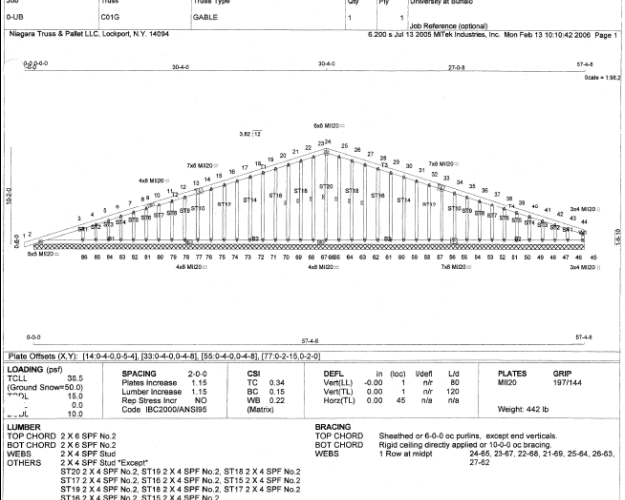
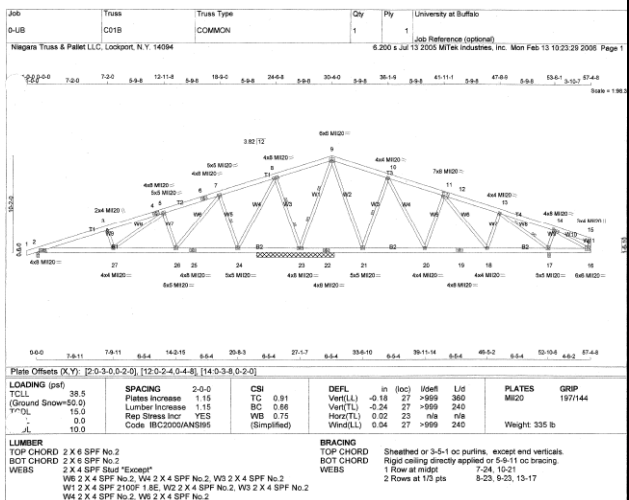
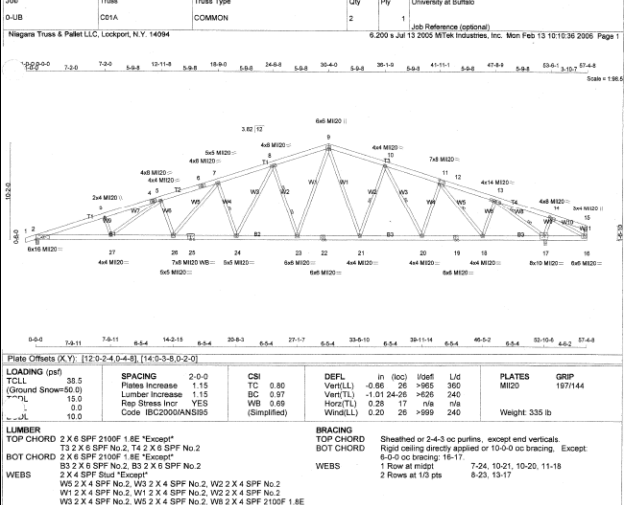
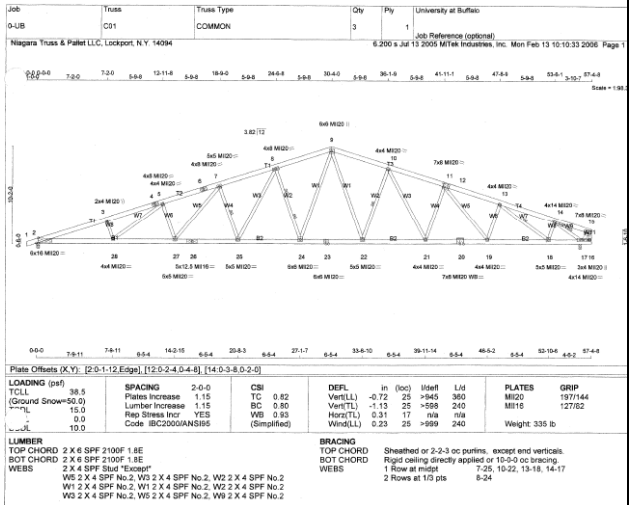


Cutting List

Label	Member	Description	Qty/Length	LElev	RElev	LPlan	RPlan
A	Bottom Plate	SPF 2 X 4 No.2 D	(1) 131-1/2				
B	Top Plate	SPF 2 X 4 No.2 D	(1) 131-1/2				
C	VTP	SPF 2 X 4 No.2 D	(1) 131-1/2				
D	Jack	SPF 2 X 4 Stud D	(2) 80				
E	Trimmer	SPF 2 X 4 Stud D	(1) 61-1/2				
F	Stud	SPF 2 X 4 Stud D	(7) 92-5/8				
G	Block	SPF 4 X 2 No.2 D	(3) 12				
H	-Top Cripples	SPF 2 X 4 Stud D	(4) 12-5/8				

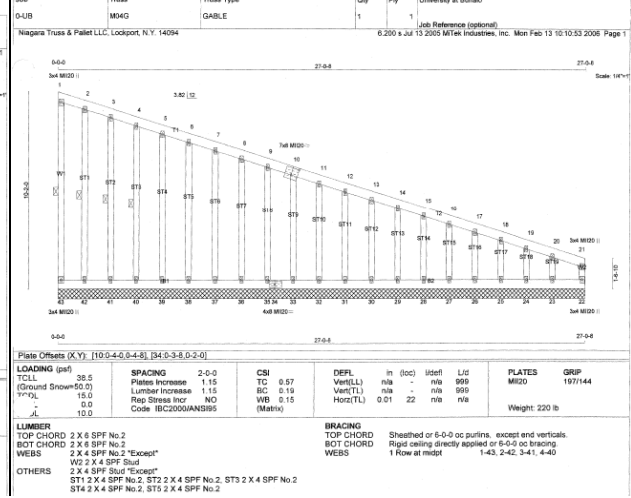
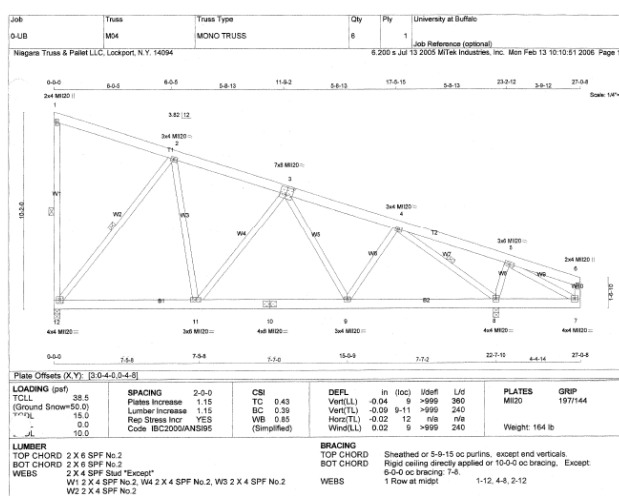
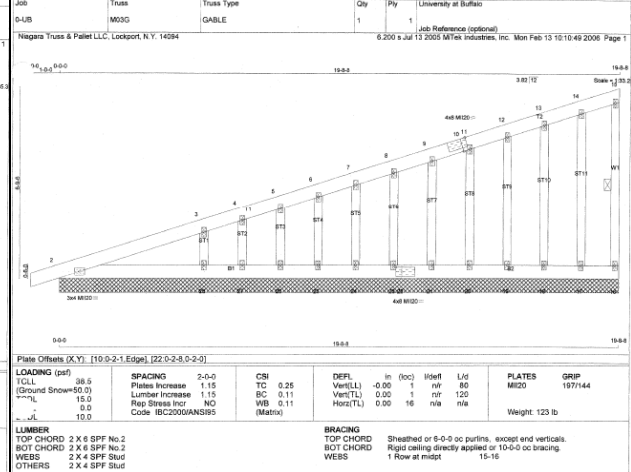
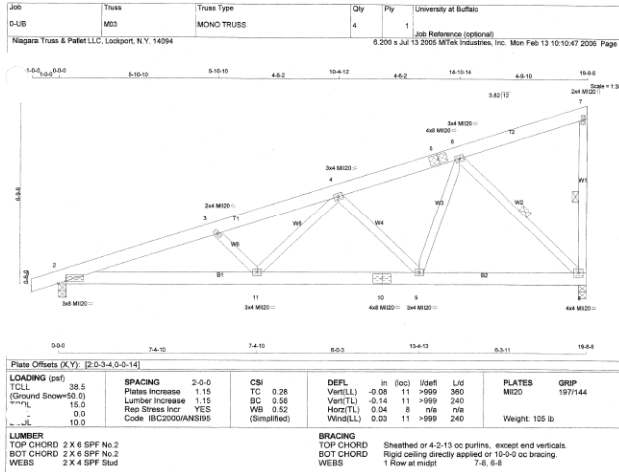
Appendix B

Roof Trusses



Appendix B

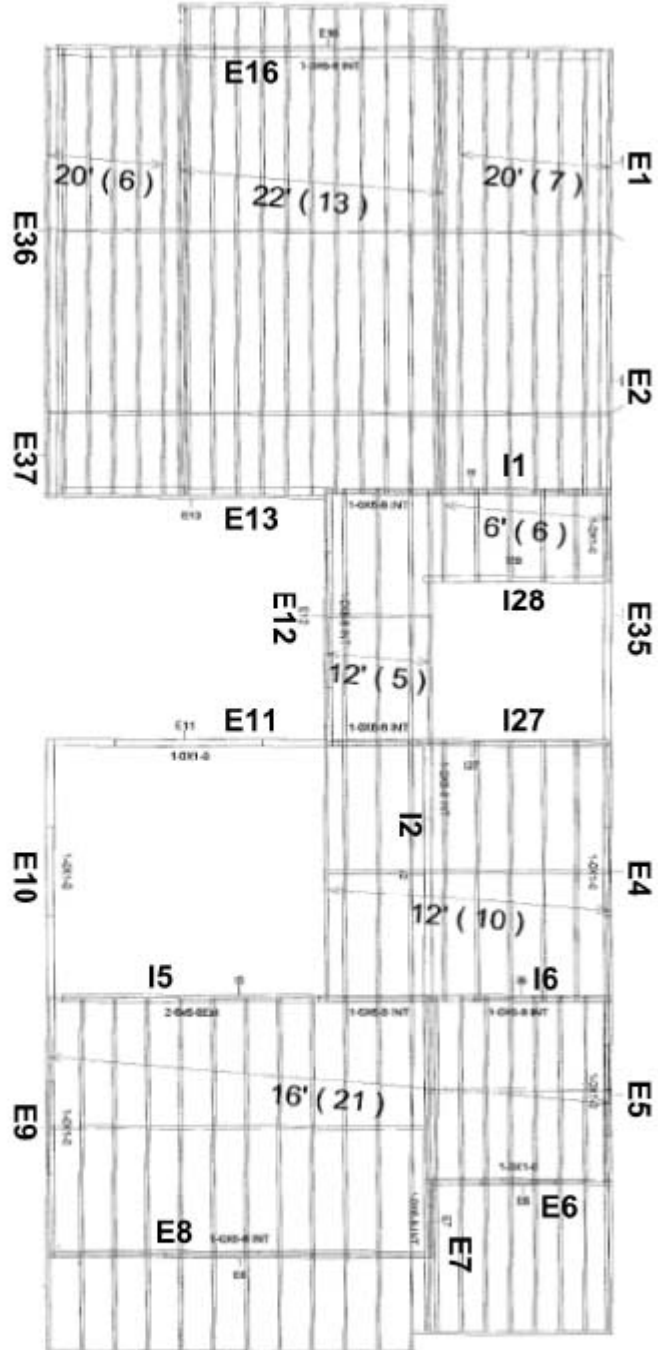
Roof Trusses



Appendix C
As-Built Sheathing Cutout and Nail
Schedule for Wood Shear Walls

Appendix C

First Floor Wood Shear Walls



FOR CONSTRUCTION

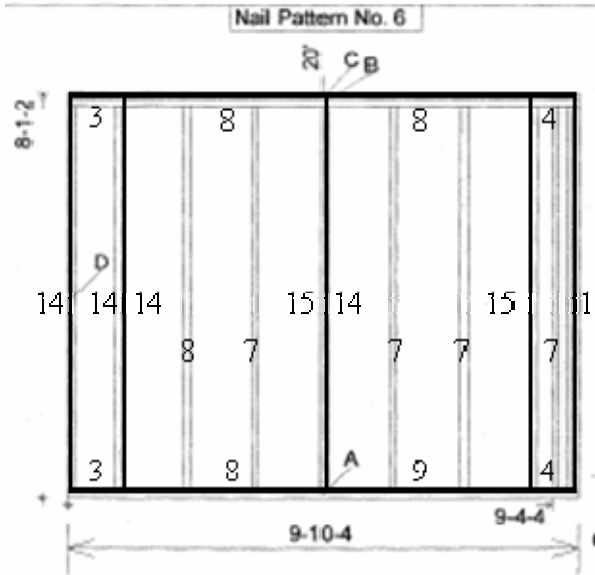
REV. NO.	DATE	DESCRIPTIONS
6	03/06/06	Final drawings for construction
3	01/02/06	Correct the North direction (according to the state table)
2	11/30/05	Add top corner details, change W4 location

NEESWOOD Engineering Building for Benchmark Textile		PROJECT UNIVERSITY OF BUFFALO 1st Level Post-tensioned Wall Layout	DATE 03/06/06	REV. NO. 6	SCALE NTS
--	--	---	------------------	---------------	--------------

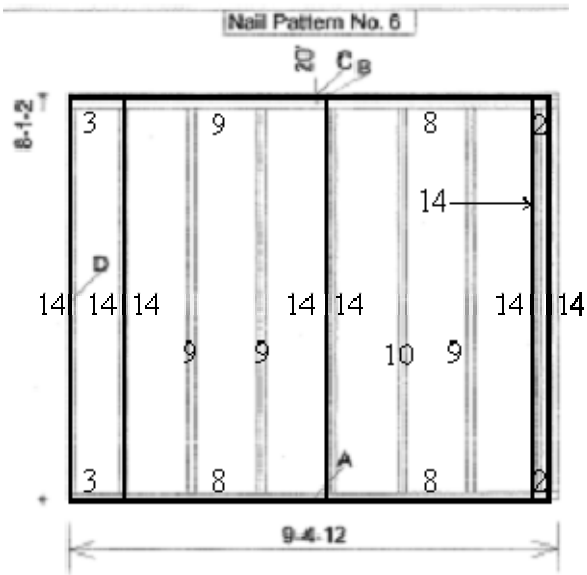
Appendix C

First Floor Wood Shear Walls

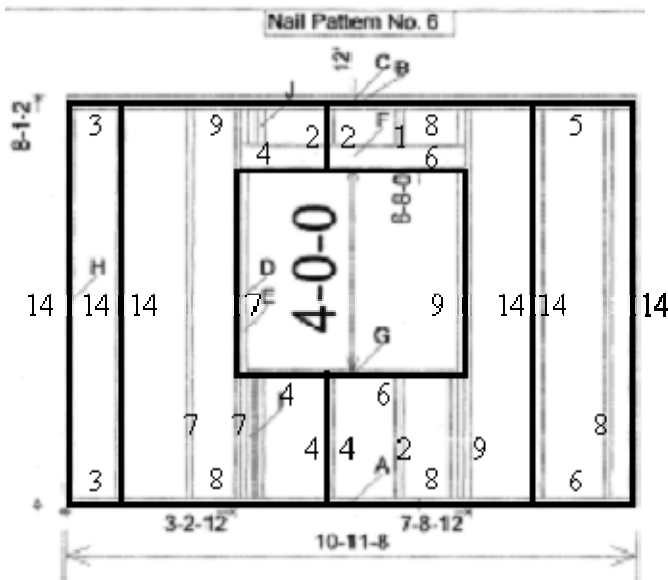
Panel E1



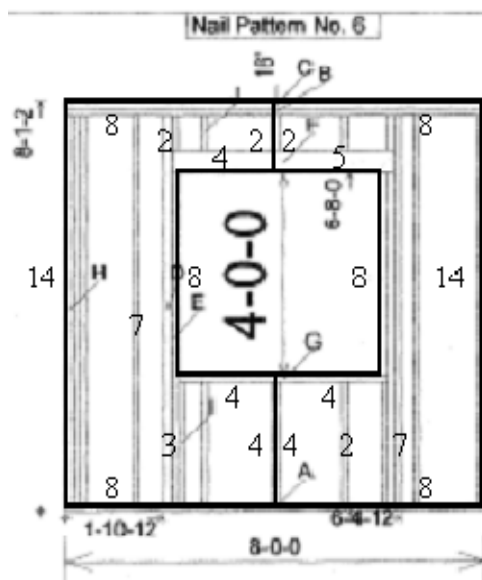
Panel E2



Panel E4



Panel E5

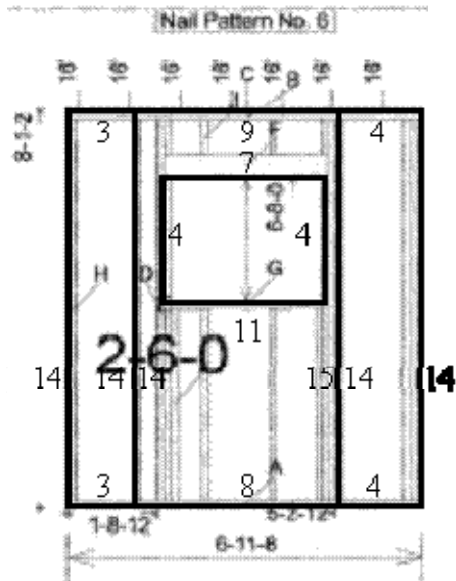


Note: Numbers shown represent the number of nails used for the construction of the wall. Horizontal nails should be applied first along the full length. Vertical nails should then be applied excluding the corner nails to avoid overlapping.

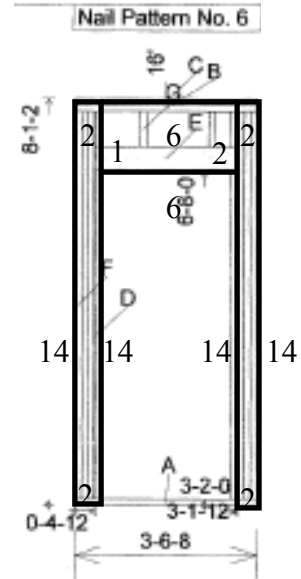
Appendix C

First Floor Wood Shear Walls

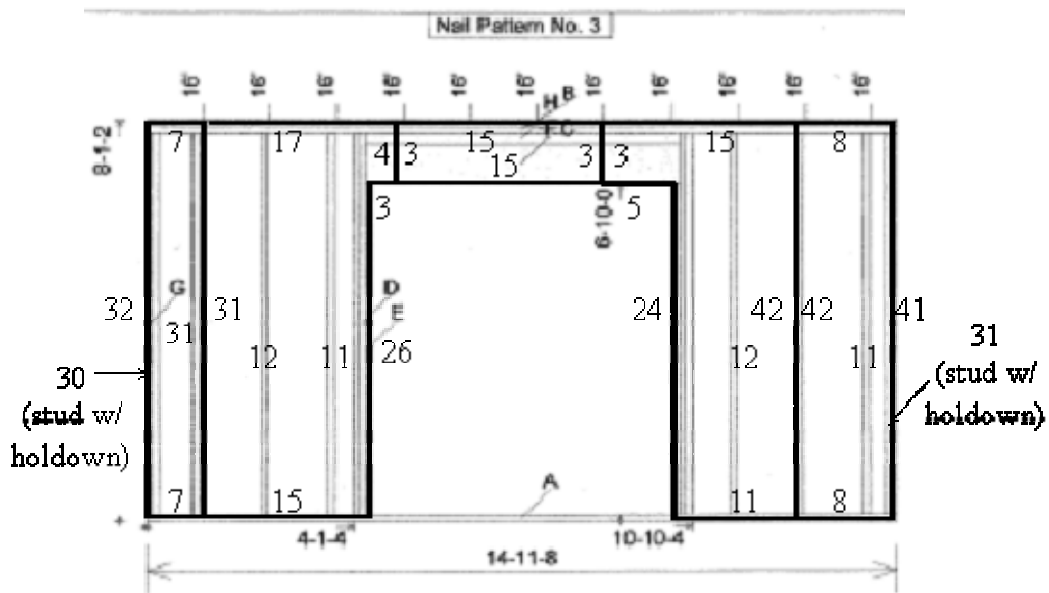
Panel E6



Panel E7



Panel E8

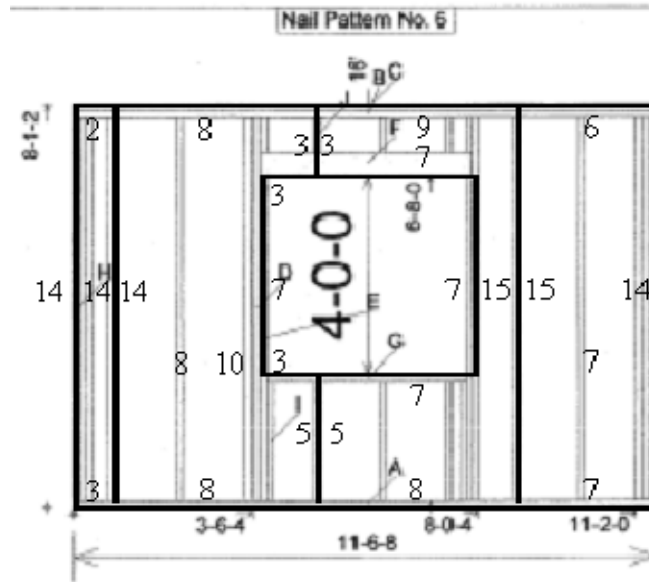


Note: Numbers shown represent the number of nails used for the construction of the wall. Horizontal nails should be applied first along the full length. Vertical nails should then be applied excluding the corner nails to avoid overlapping.

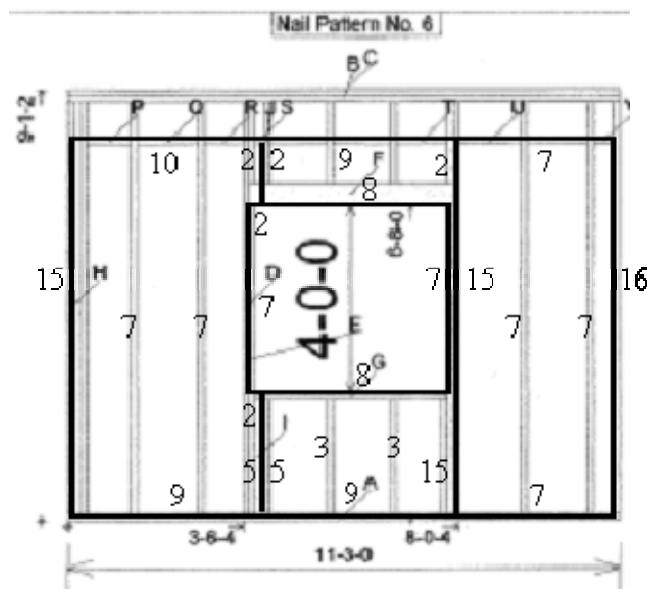
Appendix C

First Floor Wood Shear Walls

Panel E9



Panel E10

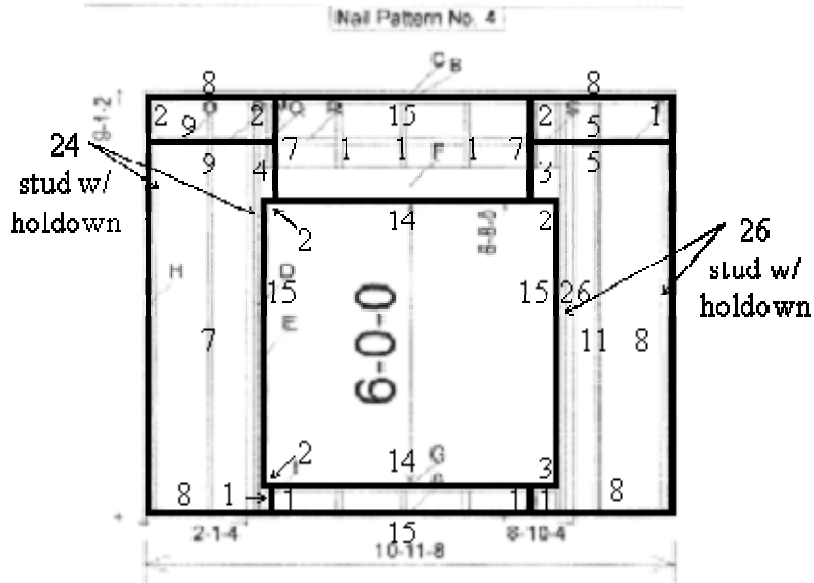


Note: Numbers shown represent the number of nails used for the construction of the wall. Horizontal nails should be applied first along the full length. Vertical nails should then be applied excluding the corner nails to avoid overlapping.

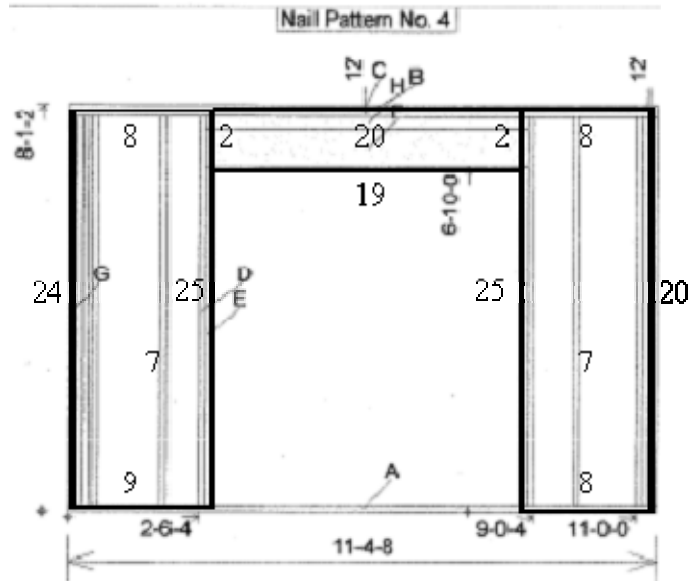
Appendix C

First Floor Wood Shear Walls

Panel E11



Panel E12

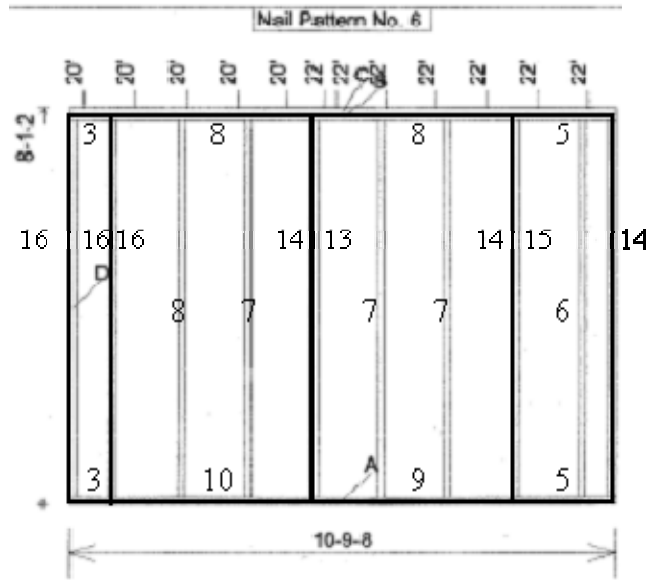


Note: Numbers shown represent the number of nails used for the construction of the wall. Horizontal nails should be applied first along the full length. Vertical nails should then be applied excluding the corner nails to avoid overlapping.

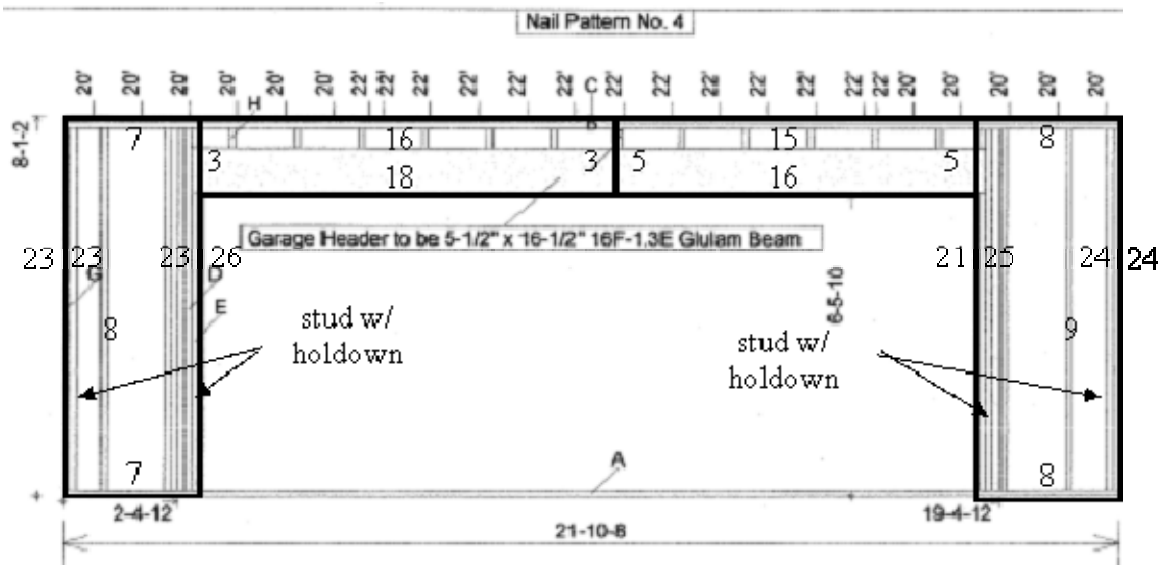
Appendix C

First Floor Wood Shear Walls

Panel E13



Panel E16

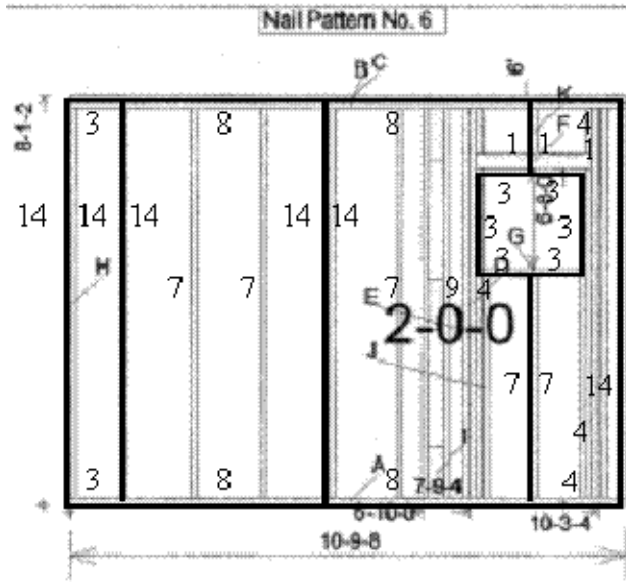


Note: Numbers shown represent the number of nails used for the construction of the wall. Horizontal nails should be applied first along the full length. Vertical nails should then be applied excluding the corner nails to avoid overlapping.

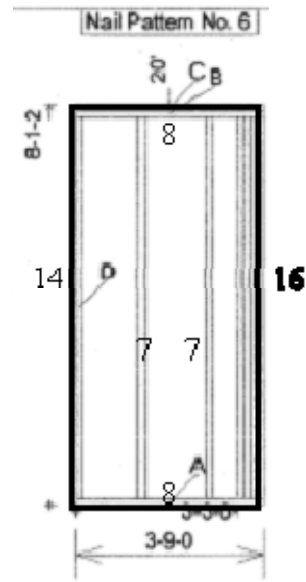
Appendix C

First Floor Wood Shear Walls

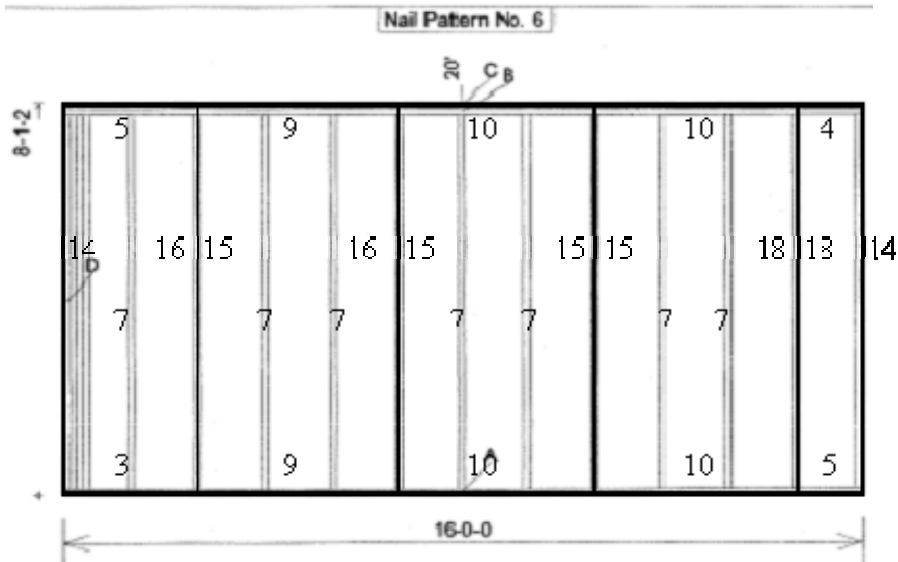
Panel E35



Panel 37



Panel E36

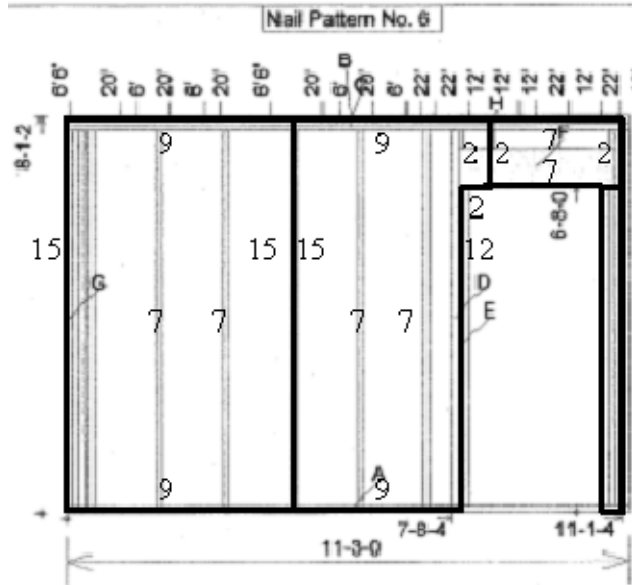


Note: Numbers shown represent the number of nails used for the construction of the wall. Horizontal nails should be applied first along the full length. Vertical nails should then be applied excluding the corner nails to avoid overlapping.

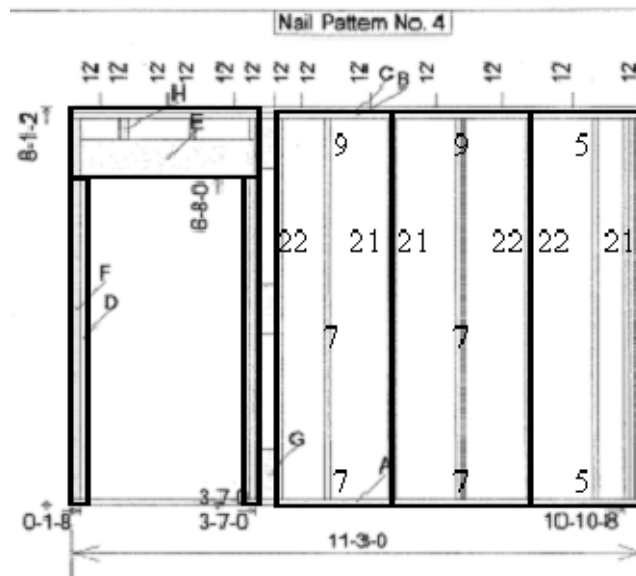
Appendix C

First Floor Wood Shear Walls

Panel I1



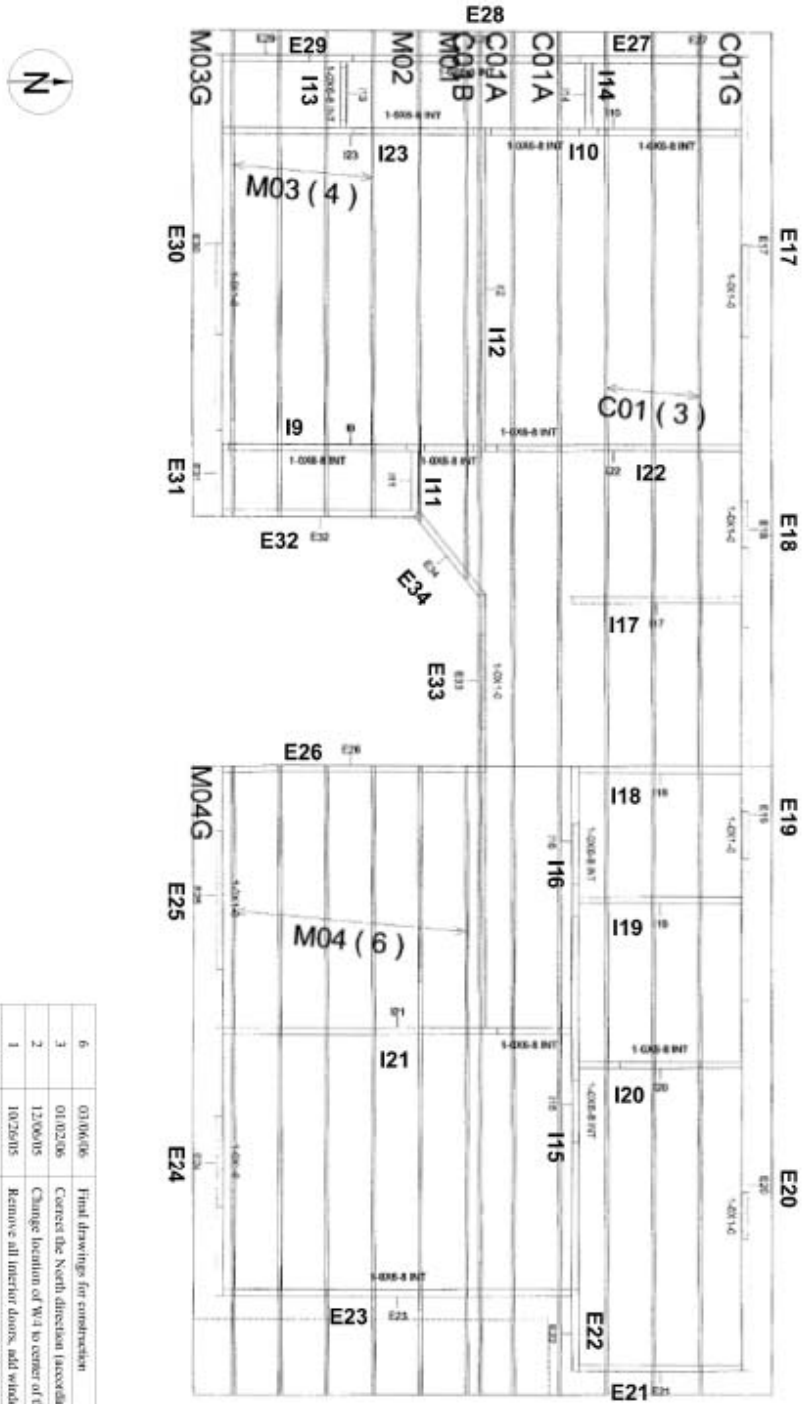
Panel I27



Note: Numbers shown represent the number of nails used for the construction of the wall. Horizontal nails should be applied first along the full length. Vertical nails should then be applied excluding the corner nails to avoid overlapping.

Appendix C

Second Floor Wood Shear Walls



REV. NO.	DATE	DESCRIPTIONS
6	03/06/06	Final drawings for construction
3	01/02/06	Correct the North direction (according to the stake table)
2	12/06/05	Change location of W.1 to center of the wall
1	10/26/05	Remove all interior doors, add windows at line A

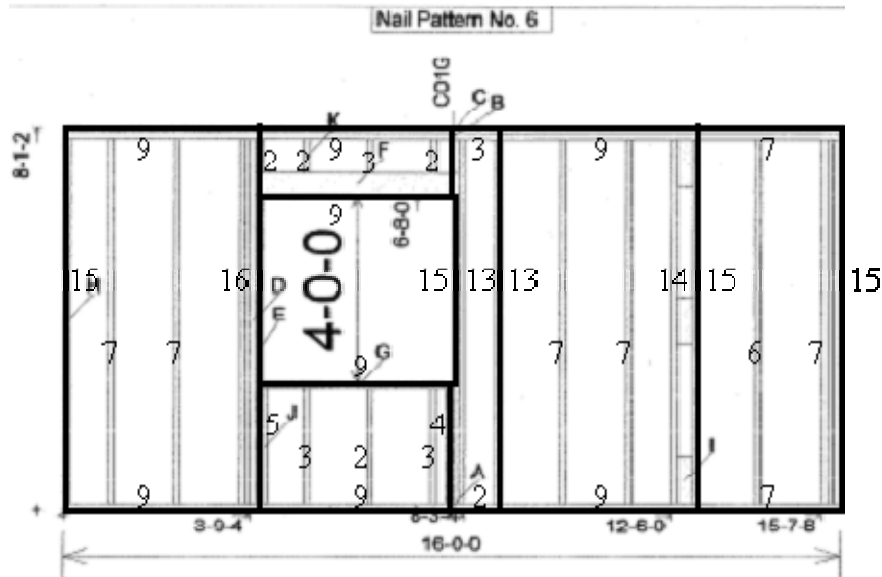
NEESWOOD		UNIVERSITY OF BUFFALO	DATE: 03/06/06	REV. NO.: 6	SCALE: NTS
PROJECT: NEESWOOD Teaching Building for Student Testing		COURTNEY 2nd Level Pre-Industrialized Wall Layout			

FOR CONSTRUCTION

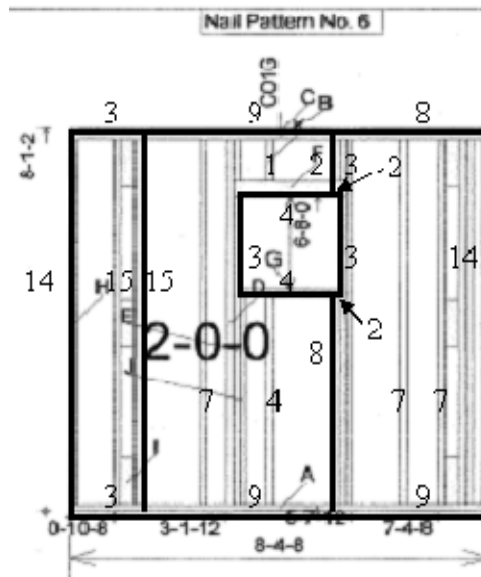
Appendix C

Second Floor Wood Shear Walls

Panel E17



Panel E18

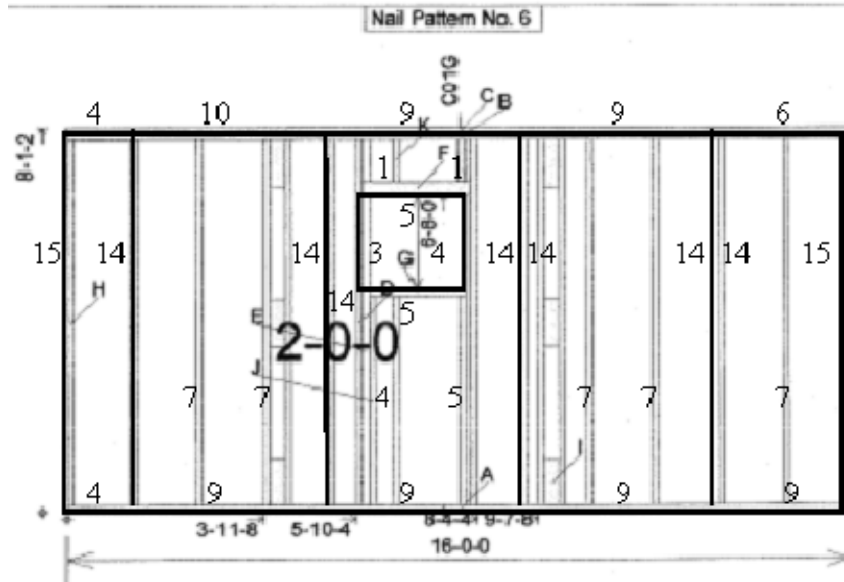


Note: Numbers shown represent the number of nails used for the construction of the wall. Horizontal nails should be applied first along the full length. Vertical nails should then be applied excluding the corner nails to avoid overlapping.

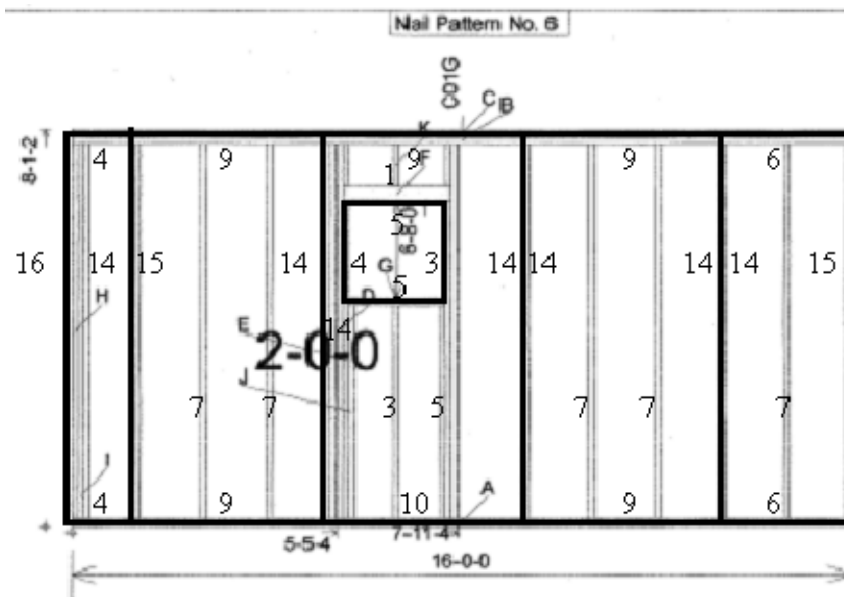
Appendix C

Second Floor Wood Shear Walls

Panel E19



Panel E20

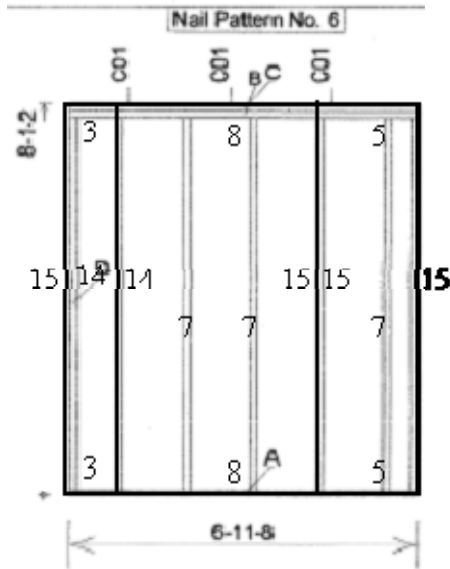


Note: Numbers shown represent the number of nails used for the construction of the wall. Horizontal nails should be applied first along the full length. Vertical nails should then be applied excluding the corner nails to avoid overlapping.

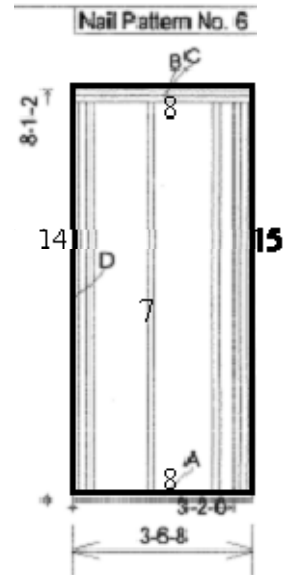
Appendix C

Second Floor Wood Shear Walls

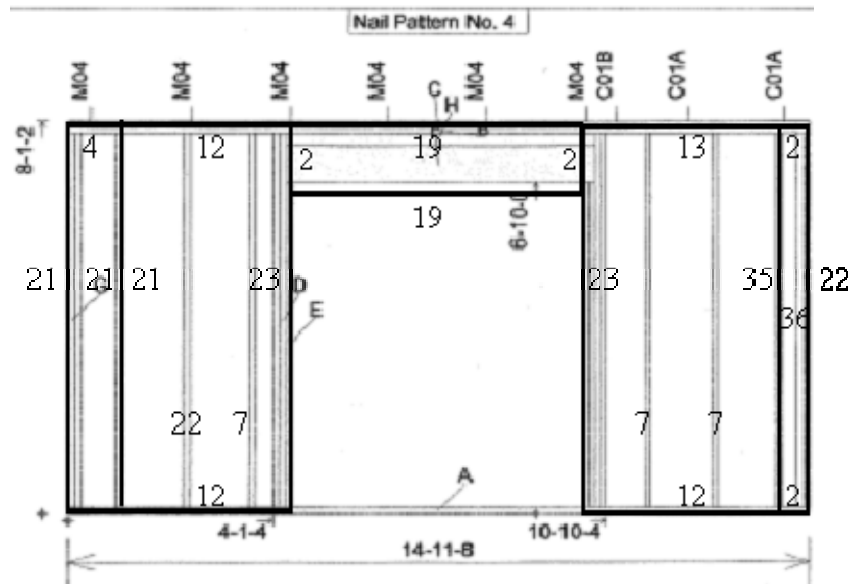
Panel E21



Panel E22



Panel E23

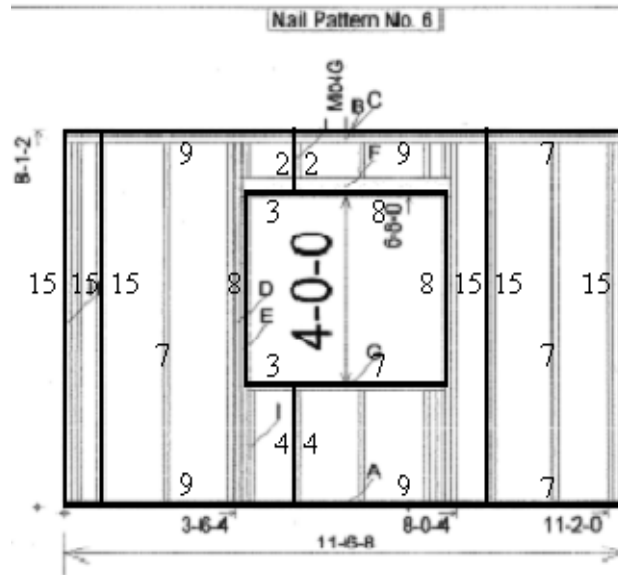


Note: Numbers shown represent the number of nails used for the construction of the wall. Horizontal nails should be applied first along the full length. Vertical nails should then be applied excluding the corner nails to avoid overlapping.

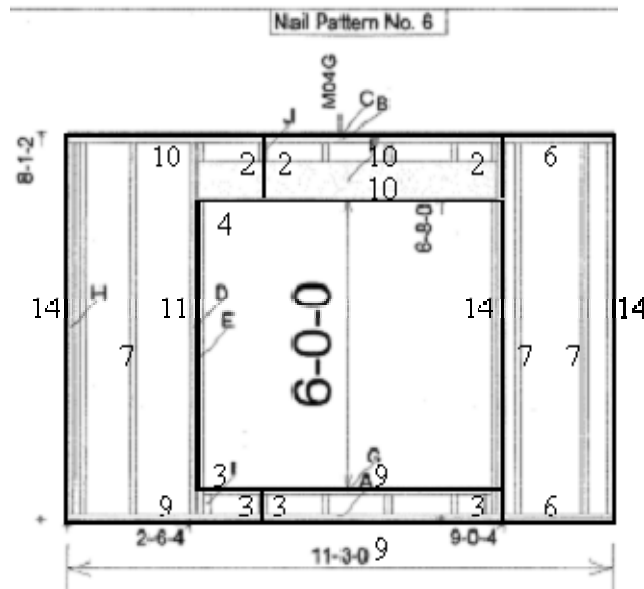
Appendix C

Second Floor Wood Shear Walls

Panel E24



Panel E25

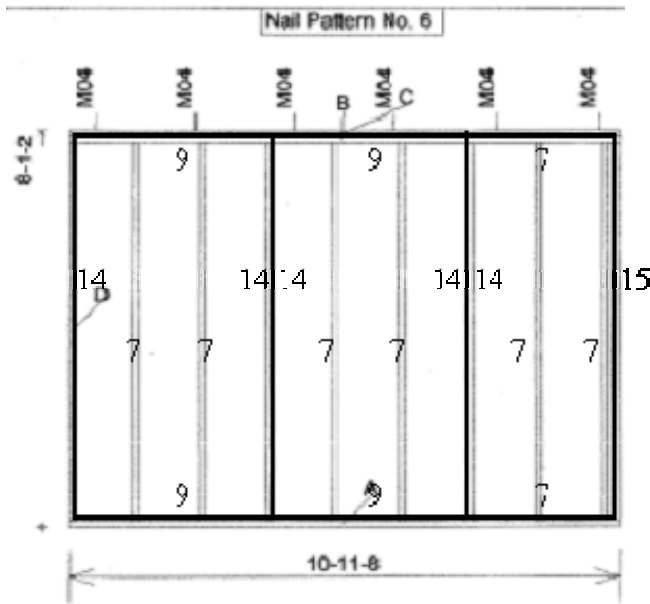


Note: Numbers shown represent the number of nails used for the construction of the wall. Horizontal nails should be applied first along the full length. Vertical nails should then be applied excluding the corner nails to avoid overlapping.

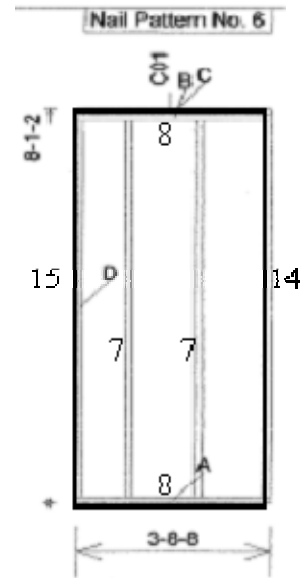
Appendix C

Second Floor Wood Shear Walls

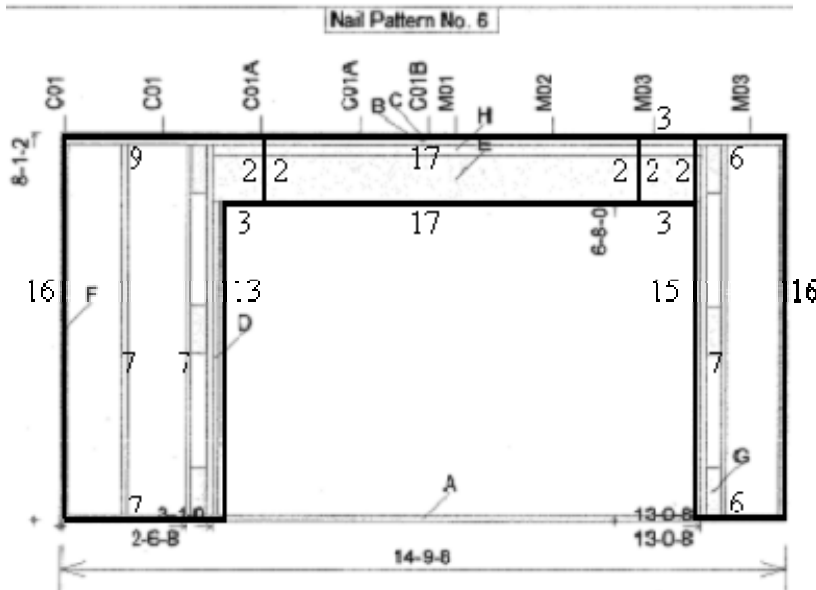
Panel E26



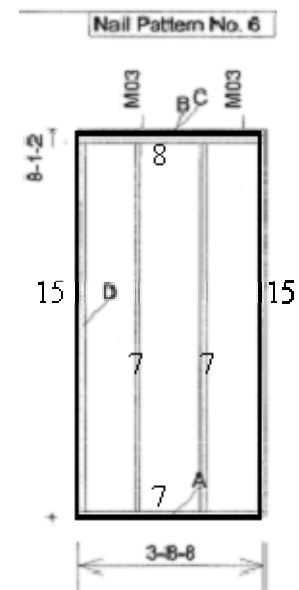
Panel 27



Panel E28



Panel 29

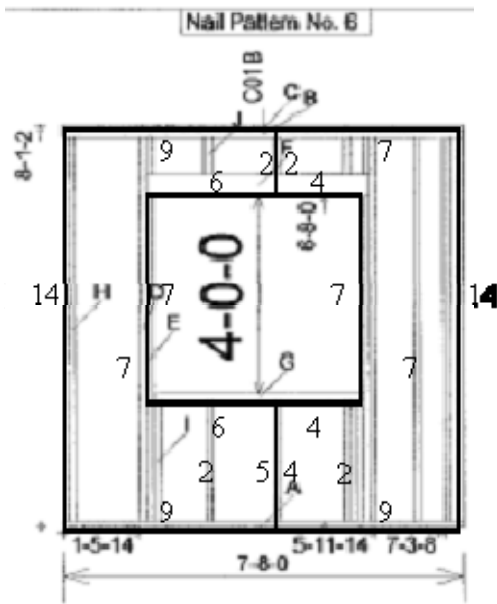


Note: Numbers shown represent the number of nails used for the construction of the wall. Horizontal nails should be applied first along the full length. Vertical nails should then be applied excluding the corner nails to avoid overlapping.

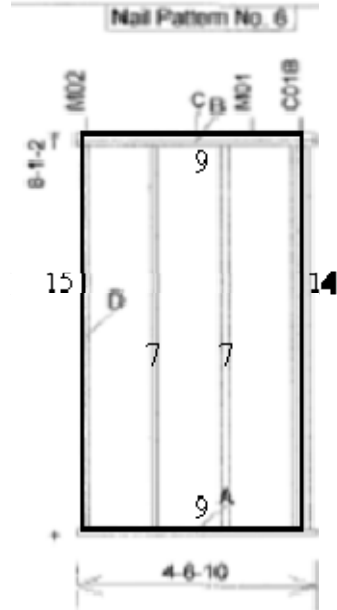
Appendix C

Second Floor Wood Shear Walls

Panel E33



Panel E34



Note: Numbers shown represent the number of nails used for the construction of the wall. Horizontal nails should be applied first along the full length. Vertical nails should then be applied excluding the corner nails to avoid overlapping.

Appendix D

Description of Shake Table Tests

Appendix D

Table D.1: Phase 1 test sequence, June 6 – 8, 2006

Test No.	Test Type	Test Level	PGA (g)			Description/Remarks
			X (E-W)	Y (N-S)	Z (Vert.)	
NWP1W01	White Noise	N/A	0.05	0	0	
NWP1W02	White Noise	N/A	0.10	0	0	
NWP1W04	White Noise	N/A	0	0.05	0	
NWP1W05	White Noise	N/A	0	0.10	0	
NWP1W07	White Noise	N/A	0	0	0.05	
NWP1S01	Seismic	1	0.04	0.05	0.06	
NWP1W10	White Noise	N/A	0	0.10	0	
NWP1W11	White Noise	N/A	0	0	0.10	
NWP1S02	Seismic	1	0.04	0.05	0	
NWP1W12	White Noise	N/A	0	0.10	0	
NWP1W13	White Noise	N/A	0	0	0.10	
NWP1S03	Seismic	1	0.04	0	0	
NWP1W14	White Noise	N/A	0	0.10	0	
NWP1W15	White Noise	N/A	0	0	0.10	
NWP1S04	Seismic	1	0	0.05	0	
NWP1W16	White Noise	N/A	0	0.10	0	
NWP1W17	White Noise	N/A	0	0	0.10	
NWP1S05	Seismic	2	0.19	0.22	0.26	Aborted
NWP1W20	White Noise	N/A	0.05	0	0	
NWP1W21	White Noise	N/A	0	0.05	0	
NWP1W44	White Noise	N/A	0	0.10	0	
NWP1W45	White Noise	N/A	0	0	0.10	
NWP1S17	Seismic	2	0.19	0.22	0.26	Repeated
NWP1W46	White Noise	N/A	0	0.10	0	
NWP1W47	White Noise	N/A	0	0	0.10	
NWP1W48	White Noise	N/A	0.05	0	0	
NWP1W49	White Noise	N/A	0	0.05	0	
NWP1S07	Seismic	2	0.19	0	0	
NWP1W24	White Noise	N/A	0	0.10	0	
NWP1W25	White Noise	N/A	0	0	0.10	
NWP1S06	Seismic	2	0.19	0.22	0	
NWP1W22	White Noise	N/A	0	0.10	0	
NWP1W23	White Noise	N/A	0	0	0.10	
NWP1S10	Seismic	3	0.31	0	0	
NWP1W30	White Noise	N/A	0	0.10	0	
NWP1W31	White Noise	N/A	0	0	0.10	

Appendix D

Table D.2: Phase 2 test sequence, June 26 – 28 and July 7, 2006

Test No.	Test Type	Test Level	PGA (g)			Description/Remarks
			X (E-W)	Y (N-S)	Z (Vert.)	
NWP2W01	White Noise	N/A	0.05	0	0	
NWP2W02	White Noise	N/A	0.10	0	0	
NWP2W03	White Noise	N/A	0	0.05	0	
NWP2S01	Seismic	1	0.04	0	0.06	
NWP2W05	White Noise	N/A	0.10	0	0	
NWP2S02	Seismic	1	0.04	0	0	
NWP2W06	White Noise	N/A	0.10	0	0	
NWP2S03	Seismic	2	0.19	0	0.26	
NWP2W07	White Noise	N/A	0.10	0	0	
NWP2W27	White Noise	N/A	0.10	0	0	After 1 st retrofit of dampers
NWP2S21	Seismic	2	0.19	0	0.26	Repeated
NWP2W28	White Noise	N/A	0.10	0	0	
NWP2S04	Seismic	2	0.19	0	0	
NWP2W08	White Noise	N/A	0.10	0	0	
NWP2S05	Seismic	3	0.31	0	0.42	
NWP2W09	White Noise	N/A	0.10	0	0	
NWP2W29	White Noise	N/A	0.10	0	0	After 2 nd retrofit of dampers
NWP2S24	Seismic	2	0.19	0	0.26	
NWP2W32	White Noise	N/A	0.10	0	0	
NWP2S25	Seismic	2	0.19	0	0	Repeated
NWP2W33	White Noise	N/A	0.10	0	0	
NWP2S26	Seismic	3	0.31	0	0.42	Repeated
NWP2W34	White Noise	N/A	0.10	0	0	
NWP2S06	Seismic	3	0.31	0	0	
NWP2W10	White Noise	N/A	0.10	0	0	
NWP2W11	White Noise	N/A	0.10	0	0	After 3 rd retrofit of dampers
NWP2S07	Seismic	1	0.04	0	0.06	
NWP2W12	White Noise	N/A	0.10	0	0	
NWP2S08	Seismic	1	0.04	0	0	
NWP2W13	White Noise	N/A	0.10	0	0	
NWP2S09	Seismic	2	0.19	0	0.26	
NWP2W14	White Noise	N/A	0.10	0	0	
NWP2S10	Seismic	2	0.19	0	0	
NWP2W15	White Noise	N/A	0.10	0	0	
NWP2S11	Seismic	3	0.31	0	0.42	
NWP2W16	White Noise	N/A	0.10	0	0	
NWP2S12	Seismic	3	0.31	0	0	
NWP2W17	White Noise	N/A	0.10	0	0	

Appendix D

Table D.2: Phase 2 test sequence, June 26 – 28 and July 7, 2006 (cont'd)

Test No.	Test Type	Test Level	PGA (g)			Description/Remarks
			X (E-W)	Y (N-S)	Z (Vert.)	
NWP2S13	Seismic	4	0.43	0	0.59	
NWP2W18	White Noise	N/A	0.10	0	0	
NWP2S14	Seismic	4	0.43	0	0	
NWP2W19	White Noise	N/A	0.10	0	0	
NWP2S17	Seismic	4	0.43	0	0.59	Repeated
NWP2W23	White Noise	N/A	0.10	0	0	
NWP2S16	Seismic	5	0.47	0	0	
NWP2W21	White Noise	N/A	0.10	0	0	
NWP2W22	White Noise	N/A	0	0.10	0	
NWP2W35	White Noise	N/A	0.10	0	0	Media day
NWP2S27	Seismic	4	0.43	0	0.59	
NWP2W36	White Noise	N/A	0.10	0	0	
NWP2W40	White Noise	N/A	0.10	0	0	Dampers disconnected
NWP2S28	Seismic	3	0.31	0	0	
NWP2W37	White Noise	N/A	0.10	0	0	
NWP2S29	Seismic	4	0.43	0	0	
NWP2W38	White Noise	N/A	0.10	0	0	
NWP2W39	White Noise	N/A	0	0.10	0	
NWP2S30	Seismic	5	0.47	0	0	
NWP2W41	White Noise	N/A	0.10	0	0	
NWP2W42	White Noise	N/A	0	0.10	0	

Appendix D

Table D.3: Phase 3 test sequence, August 2 – 3, 2006

Test No.	Test Type	Test Level	PGA (g)			Description/Remarks
			X (E-W)	Y (N-S)	Z (Vert.)	
NWP3W01	White Noise	N/A	0.10	0	0	Before installation of drywall, garage door open
NWP3W02	White Noise	N/A	0	0.10	0	
NWP3W03	White Noise	N/A	0.10	0	0	Before installation of drywall, garage door closed
NWP3W04	White Noise	N/A	0	0.10	0	
NWP3W05	White Noise	N/A	0.05	0	0	After installation of drywall, garage door open
NWP3W06	White Noise	N/A	0	0.05	0	
NWP3W07	White Noise	N/A	0	0	0.05	
NWP3S01	Seismic	1	0.04	0.05	0.06	
NWP3W11	White Noise	N/A	0.05	0	0	
NWP3W12	White Noise	N/A	0	0.05	0	
NWP3S02	Seismic	1	0.04	0.05	0	
NWP3W13	White Noise	N/A	0.05	0	0	
NWP3W14	White Noise	N/A	0	0.05	0	
NWP3S03	Seismic	2	0.19	0.22	0.26	
NWP3W15	White Noise	N/A	0.05	0	0	
NWP3W16	White Noise	N/A	0	0.05	0	
NWP3S04	Seismic	2	0.19	0.22	0	
NWP3W17	White Noise	N/A	0.05	0	0	
NWP3W18	White Noise	N/A	0	0.05	0	

Appendix D

Table D.4: Phase 4 test sequence, August 29 – 30, 2006

Test No.	Test Type	Test Level	PGA (g)			Description/Remarks
			X (E-W)	Y (N-S)	Z (Vert.)	
NWP4W01	White Noise	N/A	0.05	0	0	
NWP4W02	White Noise	N/A	0	0.05	0	
NWP4W03	White Noise	N/A	0	0	0.05	
NWP4S01	Seismic	1	0.04	0.05	0.06	
NWP4W04	White Noise	N/A	0.05	0	0	
NWP4W05	White Noise	N/A	0	0.05	0	
NWP4S02	Seismic	1	0.04	0.05	0	
NWP4W06	White Noise	N/A	0.05	0	0	
NWP4W07	White Noise	N/A	0	0.05	0	
NWP4S03	Seismic	2	0.19	0.22	0.26	
NWP4W08	White Noise	N/A	0.05	0	0	
NWP4W09	White Noise	N/A	0	0.05	0	
NWP4S04	Seismic	2	0.19	0.22	0	
NWP4W10	White Noise	N/A	0.05	0	0	
NWP4W11	White Noise	N/A	0	0.05	0	

Appendix D

Table D.5: Phase 5 test sequence, November 6 – 8 and 14, 2006

Test No.	Test Type	Test Level	PGA (g)			Description/Remarks
			X (E-W)	Y (N-S)	Z (Vert.)	
NWP5W01	White Noise	N/A	0.05	0	0	
NWP5W02	White Noise	N/A	0	0.05	0	
NWP5W03	White Noise	N/A	0	0	0.05	
NWP5S01	Seismic	1	0.04	0.05	0.06	
NWP5W04	White Noise	N/A	0.05	0	0	
NWP5W05	White Noise	N/A	0	0.05	0	
NWP5S02	Seismic	1	0.04	0.05	0	
NWP5W06	White Noise	N/A	0.05	0	0	
NWP5W07	White Noise	N/A	0	0.05	0	
NWP5S03	Seismic	2	0.19	0.22	0.26	
NWP5W08	White Noise	N/A	0.05	0	0	
NWP5W09	White Noise	N/A	0	0.05	0	
NWP5S04	Seismic	2	0.19	0.22	0	
NWP5W10	White Noise	N/A	0.05	0	0	
NWP5W11	White Noise	N/A	0	0.05	0	
NWP5S05	Seismic	3	0.31	0.36	0.42	
NWP5W12	White Noise	N/A	0.05	0	0	
NWP5W13	White Noise	N/A	0	0.05	0	
NWP5S06	Seismic	3	0.31	0.36	0	
NWP5W14	White Noise	N/A	0.05	0	0	
NWP5W15	White Noise	N/A	0	0.05	0	
NWP5S07	Seismic	4	0.43	0.50	0.59	
NWP5W16	White Noise	N/A	0.05	0	0	
NWP5W17	White Noise	N/A	0	0.05	0	Repair of broken holdowns
NWP5S08	Seismic	4	0.43	0.50	0	
NWP5W18	White Noise	N/A	0.05	0	0	
NWP5W19	White Noise	N/A	0	0.05	0	
NWP5S09	Seismic	N/A	0.12	0.21	0.21	25 % of level 5
NWP5W20	White Noise	N/A	0.05	0	0	
NWP5W21	White Noise	N/A	0	0.05	0	
NWP5W27	White Noise	N/A	0.05	0	0	Media day
NWP5W28	White Noise	N/A	0	0.05	0	
NWP5S11	Seismic	N/A	0.47	0.84	0.85	Span set at 80 % to consider overshoot
NWP5W29	White Noise	N/A	0.05	0	0	
NWP5W30	White Noise	N/A	0	0.05	0	

Appendix E

Instrumentation Setup of the Test Structure

Appendix E

Table E.1: List of accelerometers for all test phases

No.	Nomenclature	Direction	Location / Notes
1	A1	X	Corner, A-6, 2nd floor diaphragm
2	A2	Y	Corner, A-6, 2nd floor diaphragm
3	A3	X	Corner, D-6, 2nd floor diaphragm
4	A4	Y	Corner, D-6, 2nd floor diaphragm
5	A5	X	Corner, D-2 & 3, 2nd floor diaphragm
6	A6	Y	Corner, D-2 & 3, 2nd floor diaphragm
7	A7	X	Corner, C-2 & 3, 2nd floor diaphragm
8	A8	Y	Corner, C-2 & 3, 2nd floor diaphragm
9	A9	X	Corner, C-2, 2nd floor diaphragm
10	A10	Y	Corner, C-2, 2nd floor diaphragm
11	A11	X	Corner, A-2, 2nd floor diaphragm
12	A12	Y	Corner, A-2, 2nd floor diaphragm
13	A13	X	Corner, A-4, 2nd floor diaphragm
14	A14	Y	Corner, A-4, 2nd floor diaphragm
16	A16	Y	Roof ridge
17	A17	X	Roof sheathing (center, East side)
18	A18	Y	Roof sheathing (center, East side)
19	A19	X	Corner, A-5, 2nd floor diaphragm
20	A20	Y	Corner, A-5, 2nd floor diaphragm
21	A21	X	Corner, A-6, 2nd floor ceiling
22	A22	Y	Corner, A-6, 2nd floor ceiling
24	A24	X	Corner, D-6, 2nd floor ceiling
25	A25	Y	Corner, D-6, 2nd floor ceiling
27	A27	X	Corner, D-2 & 3, 2nd floor ceiling
28	A28	Y	Corner, D-2 & 3, 2nd floor ceiling
30	A30	X	Corner, C-2 & 3, 2nd floor ceiling
31	A31	Y	Corner, C-2 & 3, 2nd floor ceiling
32	A32	X	Corner, C-2, 2nd floor ceiling
33	A33	Y	Corner, C-2, 2nd floor ceiling
34	A34	X	Corner, A-2, 2nd floor ceiling
35	A35	Y	Corner, A-2, 2nd floor ceiling
37	A37	X	Corner, A-4, 2nd floor ceiling
38	A38	Y	Corner, A-4, 2nd floor ceiling
39	A39	X	Roof ridge
40	A40	Y	Roof ridge, *malfunctioned in Test Phase 5

Appendix E

Table E.1: List of accelerometers for all test phases (cont'd)

41	A41	X	Roof sheathing (center, West side)
42	A42	Y	Roof sheathing (center, West side)
43	A43	X	Corner, A-5, 2nd floor ceiling
44	A44	Y	Corner, A-5, 2nd floor ceiling
45	A45	X	Interior shear wall, Line 5, 2nd floor diaphragm level
46	A46	Y	Interior shear wall, Line 5, 2nd floor diaphragm level
47	A47	X	Interior shear wall, Line 4, 2nd floor diaphragm level
48	A48	Y	Interior shear wall, Line 4, 2nd floor diaphragm level
49	A49	X	Interior shear wall, Line 5, 2nd floor ceiling level
50	A50	Y	Interior shear wall, Line 5, 2nd floor ceiling level
51	A51	X	Interior shear wall, Line 4, 2nd floor ceiling level
52	A52	Y	Interior shear wall, Line 4, 2nd floor ceiling level
53	A53	Z	Corner, A-6, Base level
54	A54	Z	Corner, D-6, Base level
55	A55	Z	Corner, D-2 & 3, Base level
56	A56	Z	Corner, C-2 & 3, Base level
57	A57	Z	Corner, C-2, Base level
58	A58	Z	Corner, A-2, Base level
59	A59	Z	Corner, A-4, Base level
60	A60	Z	Corner, B-4, Base level
61	A61	Z	Corner, B-5, Base level
62	A62	Z	Corner, A-5, Base level
63	A63	Z	Bedroom 1
64	A64	Z	Bedroom 2
65	A65	Z	Master bathroom
66	A66	Z	Master bedroom
67	A67	Z	Walk way, 2nd floor
68	A68	X	West, Table extension frame
69	A69	Y	West, Table extension frame
70	A70	Z	West, Table extension frame
71	A71	X	East, Table extension frame
72	A72	Y	East, Table extension frame
73	A73	Z	East, Table extension frame
74	A74	X	Bridge structure
75	A75	Y	Bridge structure
76	A76	Z	Bridge structure

Appendix E

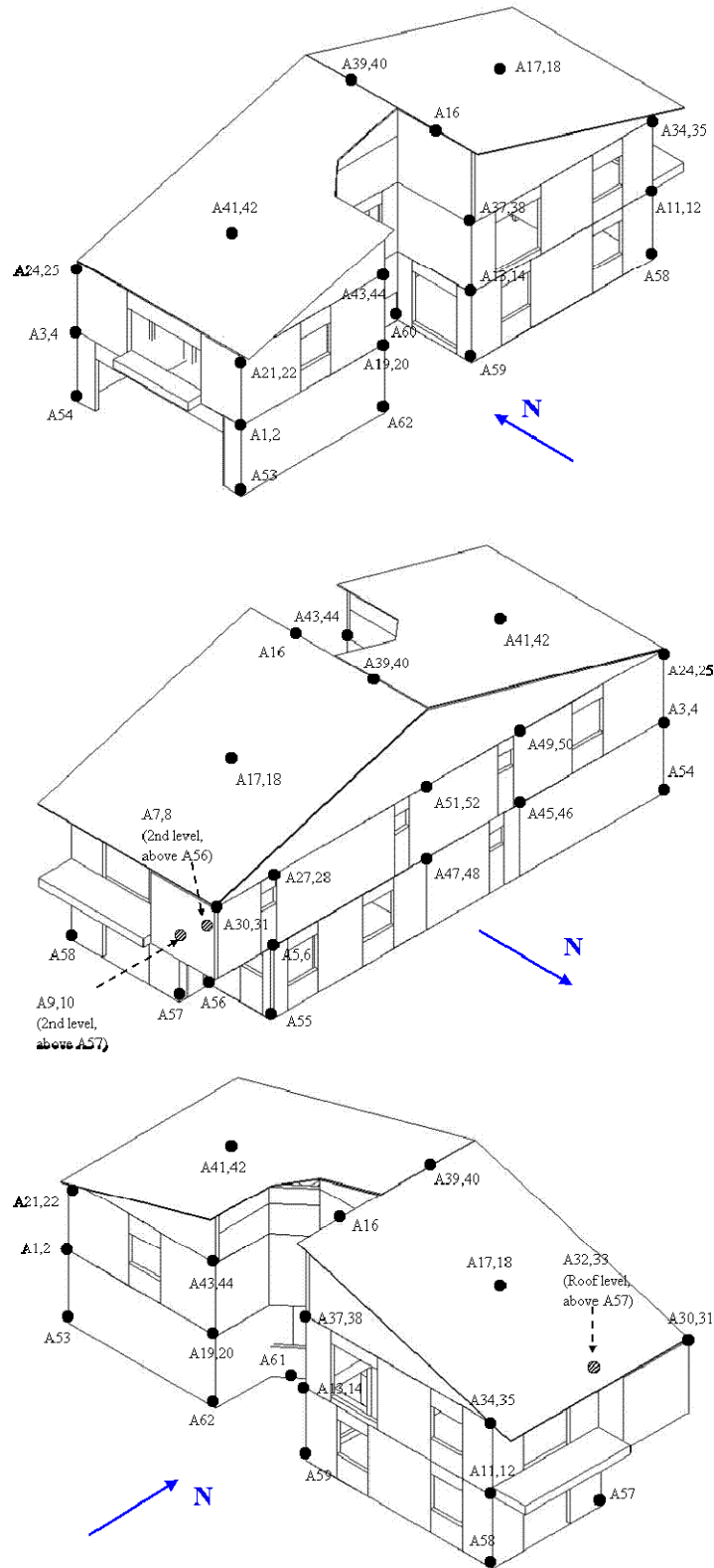


Figure E.1: Locations of accelerometers for all test phases

Appendix E

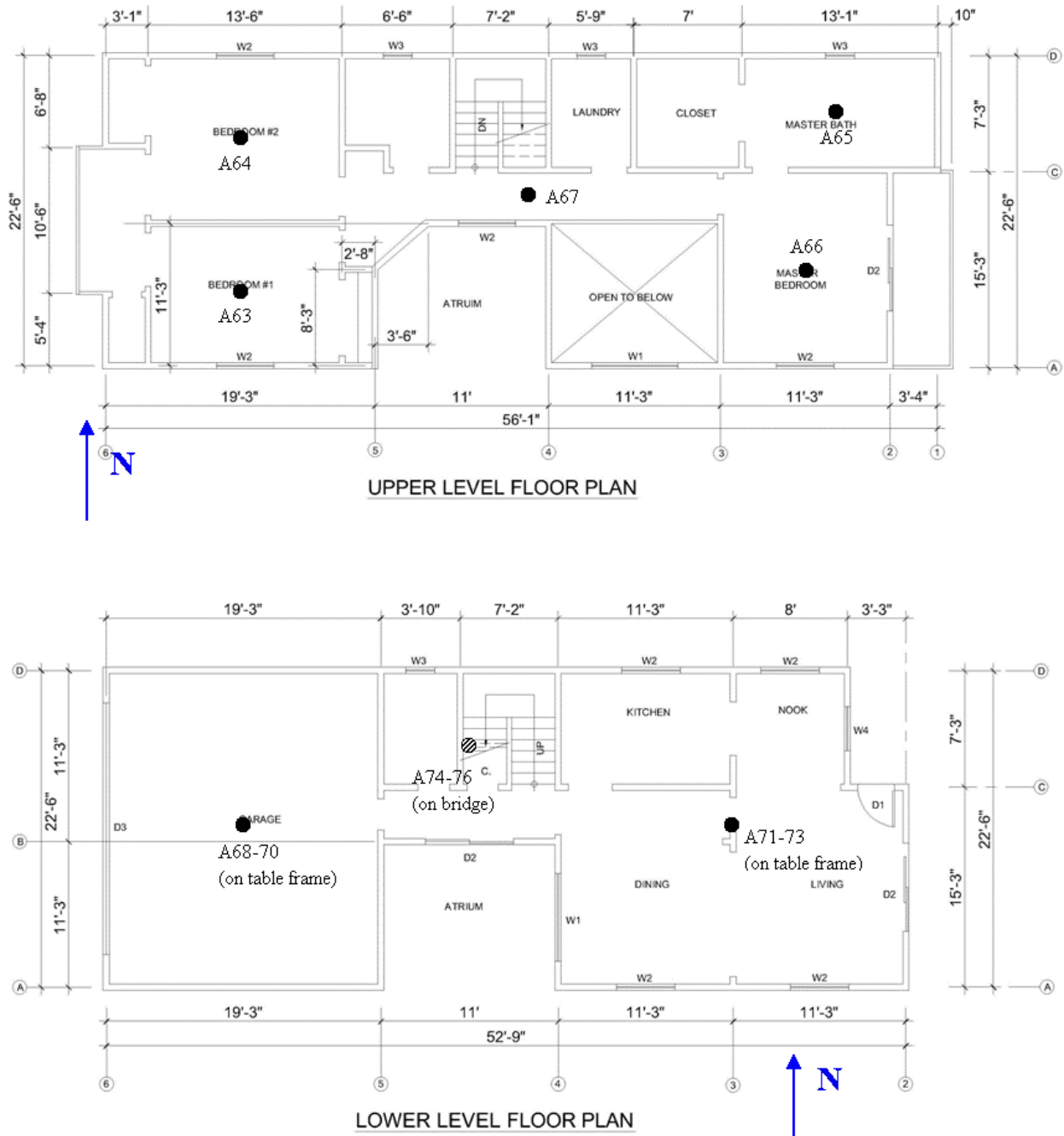


Figure E.1: Locations of accelerometers for all test phases (cont'd)

Appendix E

Table E.2: List of string potentiometers measuring absolute displacements for all test phases

No.	Nomenclature	Direction	Location / Notes
1	D1	X	West table frame, South-West corner
2	D2	X	West table frame, North-West corner
3	D3	Y	West table frame, North-West corner
4	D4	Y	West table frame, North-East corner
5	D5	Y	East table frame, North-West corner
6	D6	Y	East table frame, North-East corner
7	D7	Z	West table, Vertical
8	D8	X	Corner, A-6, 2nd floor diaphragm
9	D9	X	Corner, D-6, 2nd floor diaphragm
10	D10	Y	Corner, D-6, 2nd floor diaphragm
11	D11	Y	Interior shear wall, B & D-5, 2nd floor diaphragm
12	D12	Y	Interior shear wall, B & D-4, 2nd floor diaphragm
13	D13	Y	Corner, D-2 & 3, 2nd floor diaphragm
14	D14	Y	Corner, C-2, 2nd floor diaphragm
15	D15	X	Corner, A-6, 2nd floor ceiling level
16	D16	X	Corner, D-6, 2nd floor ceiling level
17	D17	Y	Corner, D-6, 2nd floor ceiling level
18	D18	Y	Interior shear wall, B & D-5, 2nd floor ceiling level
19	D19	Y	Interior shear wall, B & D-4, 2nd floor ceiling level
20	D20	Y	Corner, D-2 & 3, 2nd floor ceiling level
21	D21	Z	East table, Vertical

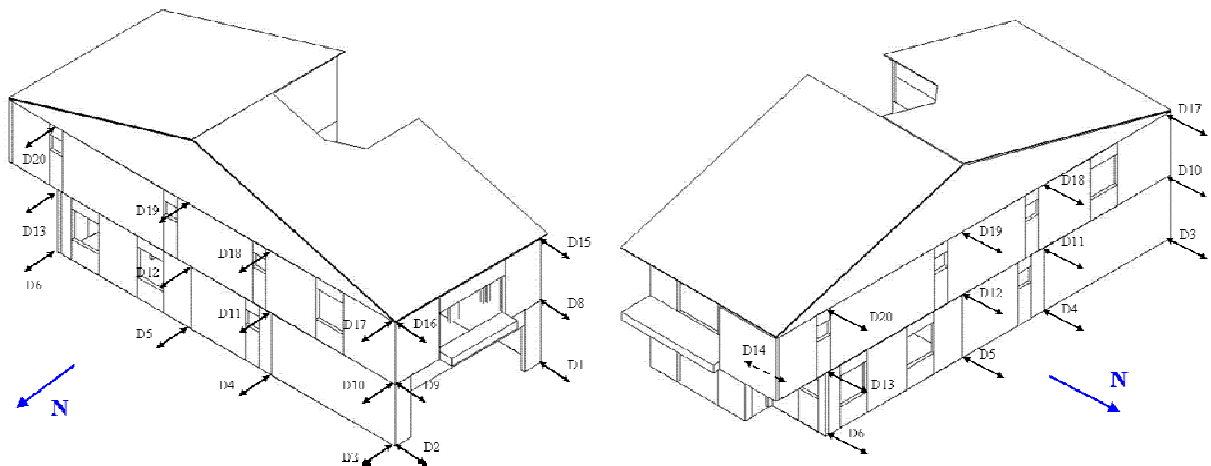


Figure E.2: Locations of string potentiometers measuring absolute displacements for all test phases

Appendix E

Table E.3: List of string potentiometers measuring shear deformations for Test Phases 1, 2 and 3

No.	Nomenclature	Direction	Location / Notes
1	S1	Shear	Shear wall, Line A & D-6, Base level
2	S2	Shear	Shear wall, Line D-2 & 6, Base level
3	S3	Shear	Shear wall, Line C & D-2 & 3, Base level
4	S4	Shear	Shear wall, Line A & C-2, Base level
5	S5	Shear	Shear wall, Line A-2 & 4, Base level
6	S6	Shear	Shear wall, Line A & B-4, Base level
7	S7	Shear	Shear wall, Line C & D-5, Base level (OSB side)
8	S8	Shear	Shear wall, Line A & B-5, Base level
9	S9	Shear	Shear wall, Line A-5 & 6, Base level
10	S10	Shear	Shear wall, Line A & D-6, 2nd level
11	S11	Shear	Shear wall, Line D-2 & 6, 2nd level
12	S12	Shear	Shear wall, Line A & C-2, 2nd level
13	S13	Shear	Shear wall, Line A-2 & 4, 2nd level
14	S14	Shear	Shear wall, Line A & B-4, 2nd level
15	S15	Shear	Shear wall, Line C & D-4, Base level (OSB side)
16	S16	Shear	Shear wall, Line A & B-5, 2nd level
17	S17	Shear	Shear wall, Line A-5 & 6, 2nd level
18	S18 ¹	Shear	Gypsum wall, Line C-3 & 4, Base level
19	S19 ¹	Shear	Parallel to #18, but connect between floor diaphragms
20	S20 ^{1,2}	Shear	Gypsum wall, Line C & D-4 & 5, Base level
21	S21 ^{1,2}	Shear	Parallel to #20, but connect between floor diaphragms
22	S22 ^{1,2}	Shear	Gypsum wall, Line B-5 & 6, 2nd level
23	S23 ^{1,2}	Shear	Parallel to #22, but connect between floor diaphragms

¹ Removed in Test Phase 2. Channels used for damper walls

² Removed in Test Phase 3

Appendix E

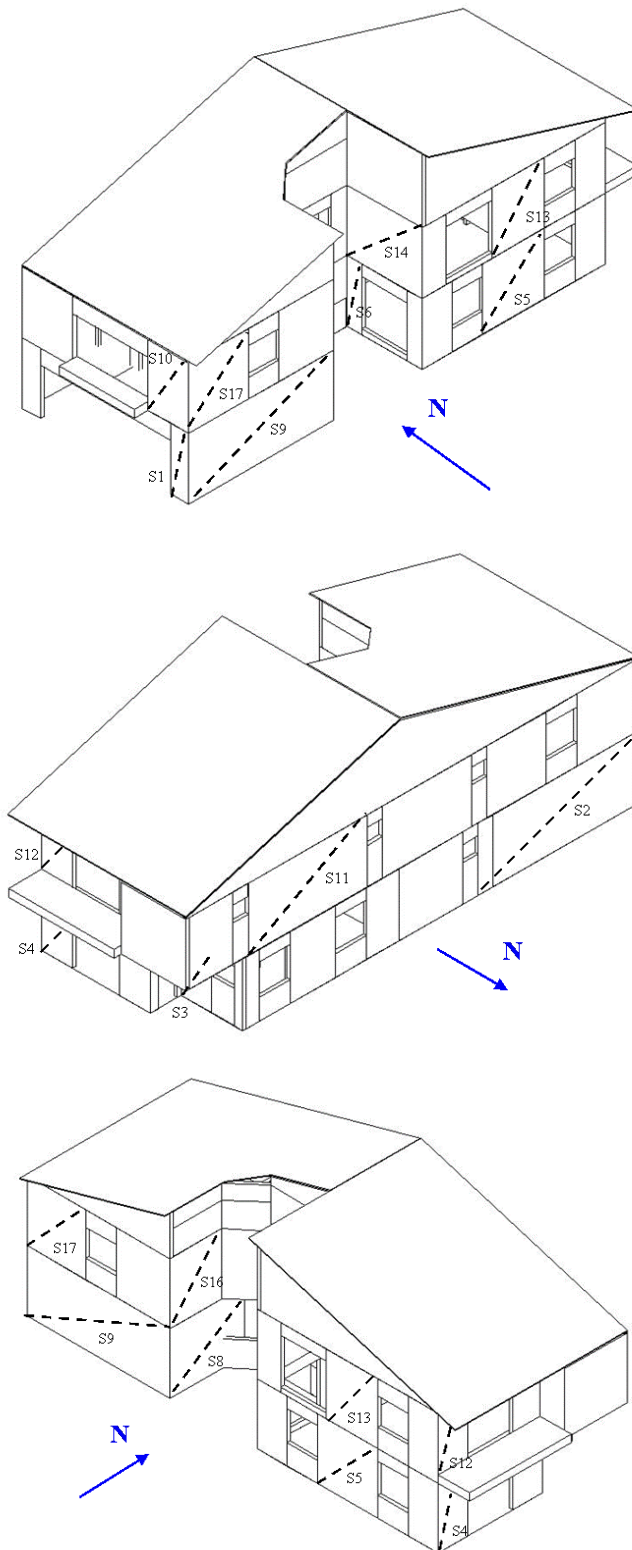


Figure E.3: Locations of string potentiometers measuring shear deformations for Test Phases 1, 2 and 3

Appendix E

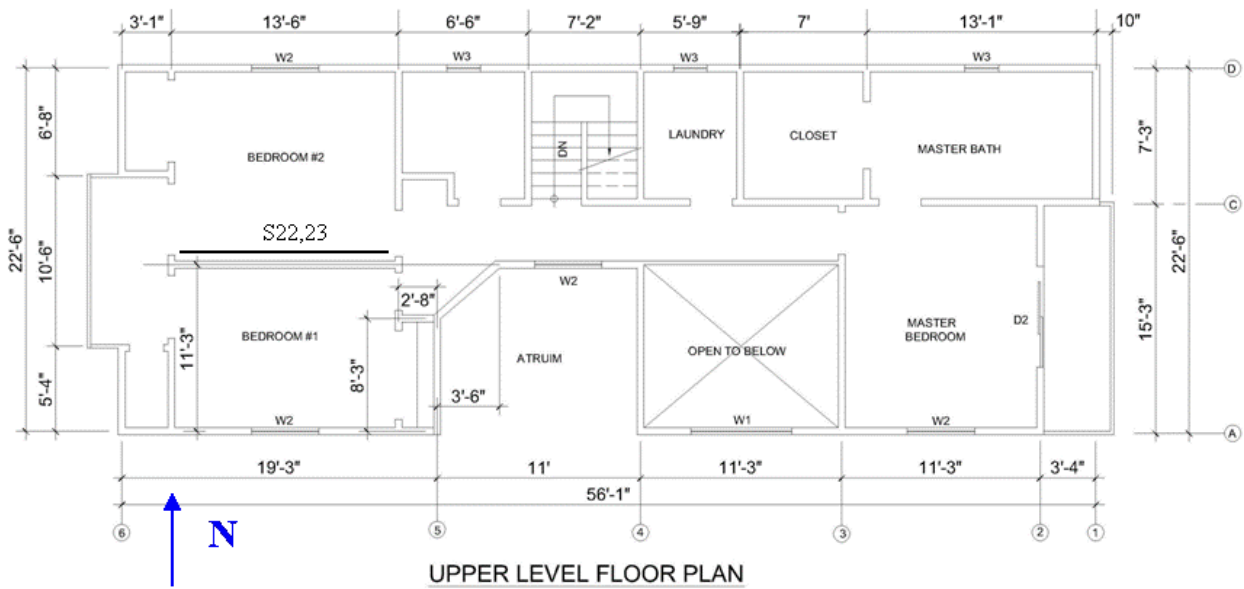
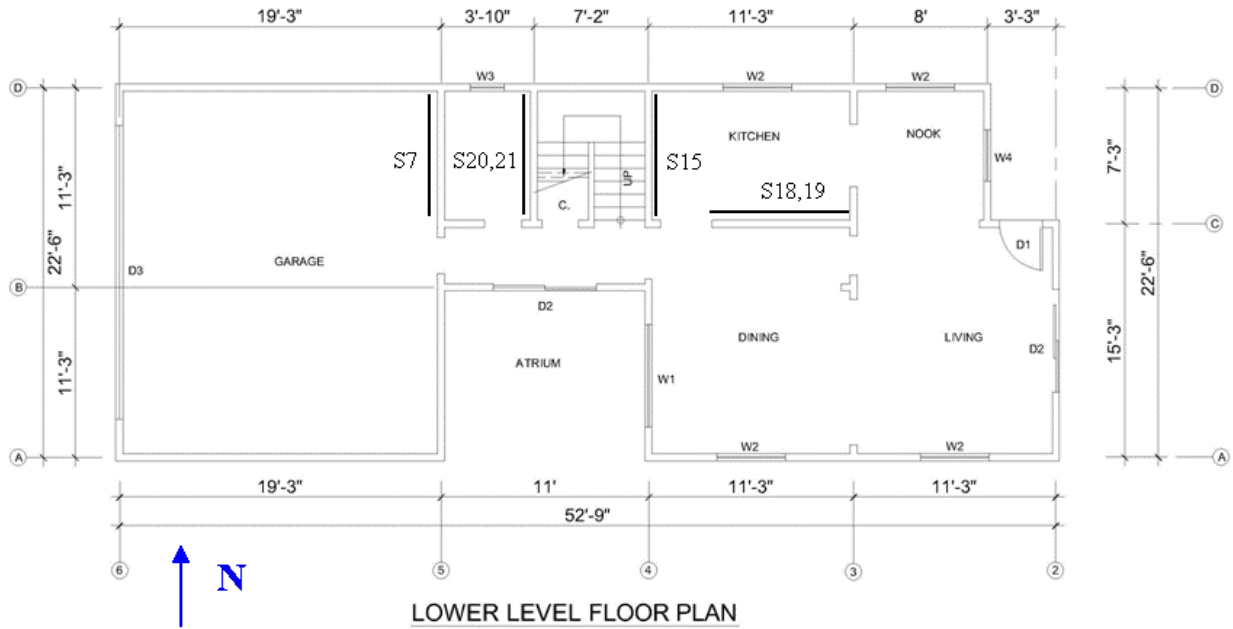


Figure E.3: Locations of string potentiometers measuring shear deformations for Test Phases 1, 2 and 3 (cont'd)

Appendix E

Table E.4: List of string potentiometers measuring shear deformations for Test Phases 4 and 5

No.	Nomenclature	Direction	Location / Notes
1	S1	Shear	Shear wall, Line A & D-6, Base level
2	S2	Shear	Shear wall, Line D-2 & 6, Base level
3	S3	Shear	Partition wall in stair well, Base level
4	S4	Shear	Shear wall, Line A & C-2, Base level
5	S5	Shear	Shear wall, Line A-2 & 4, Base level
6	S6	Shear	Shear wall, Line A & B-4, Base level
7	S7	Shear	Shear wall, Line C & D-5, Base level (OSB side)
8	S8	Shear	Shear wall, Line A & B-5, Base level, <u>* malfunctioned at media day of Test Phase 5</u>
9	S9	Shear	Shear wall, Line A-5 & 6, Base level
10	S10	Shear	Shear wall, Line A & D-6, 2nd level
11	S11	Shear	Shear wall, Line D-2 & 6, 2nd level
12	S12	Shear	Shear wall, Line A & C-2, 2nd level
13	S13	Shear	Shear wall, Line A-2 & 4, 2nd level
14	S14	Shear	Shear wall, Line A & B-4, 2nd level
15	S15	Shear	Shear wall, Line C & D-4, Base level (OSB side)
16	S16	Shear	Shear wall, Line A & B-5, 2nd level
17	S17	Shear	Shear wall, Line A-5 & 6, 2nd level
18	S18	Shear	Connect between floor diaphragms in the middle between #7 and #15
19	S19	Shear	Parallel to #9, but connect between floor diaphragms
20	S20	Shear	Partition wall in master bedroom, 2nd level
21	S21	Shear	Parallel to #20, but connect between floor diaphragms

Appendix E

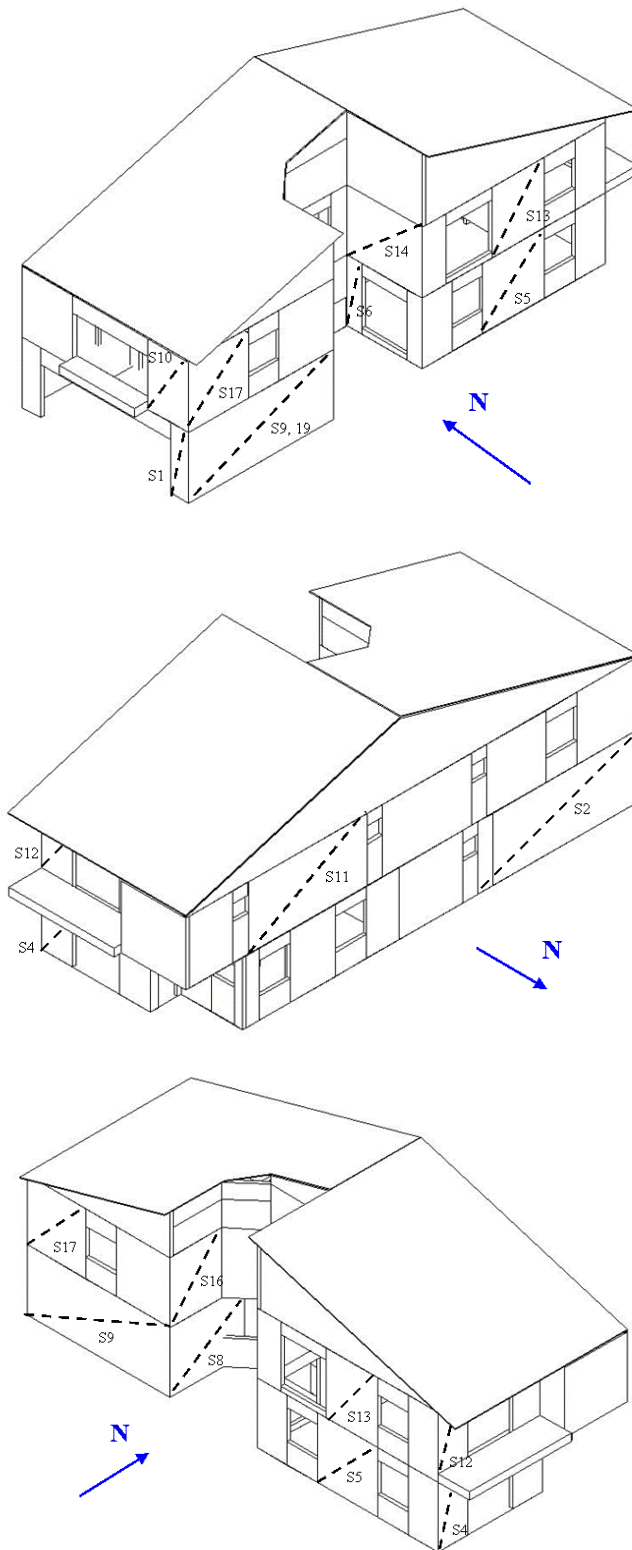


Figure E.4: Locations of string potentiometers measuring shear deformations for Test Phases 4 and 5

Appendix E

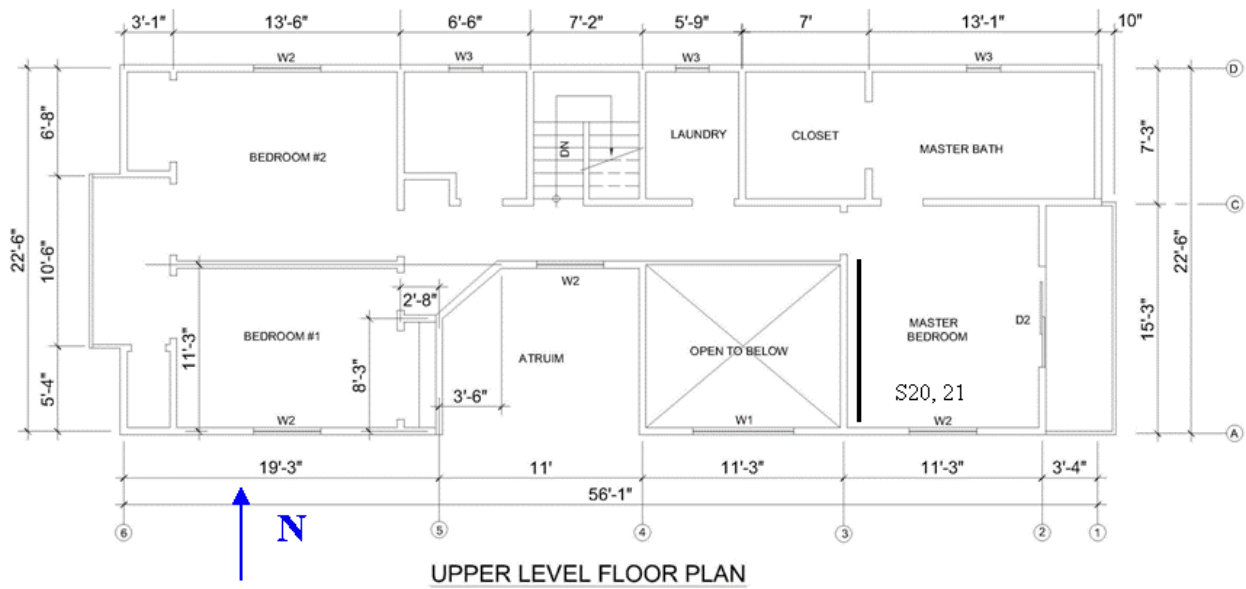
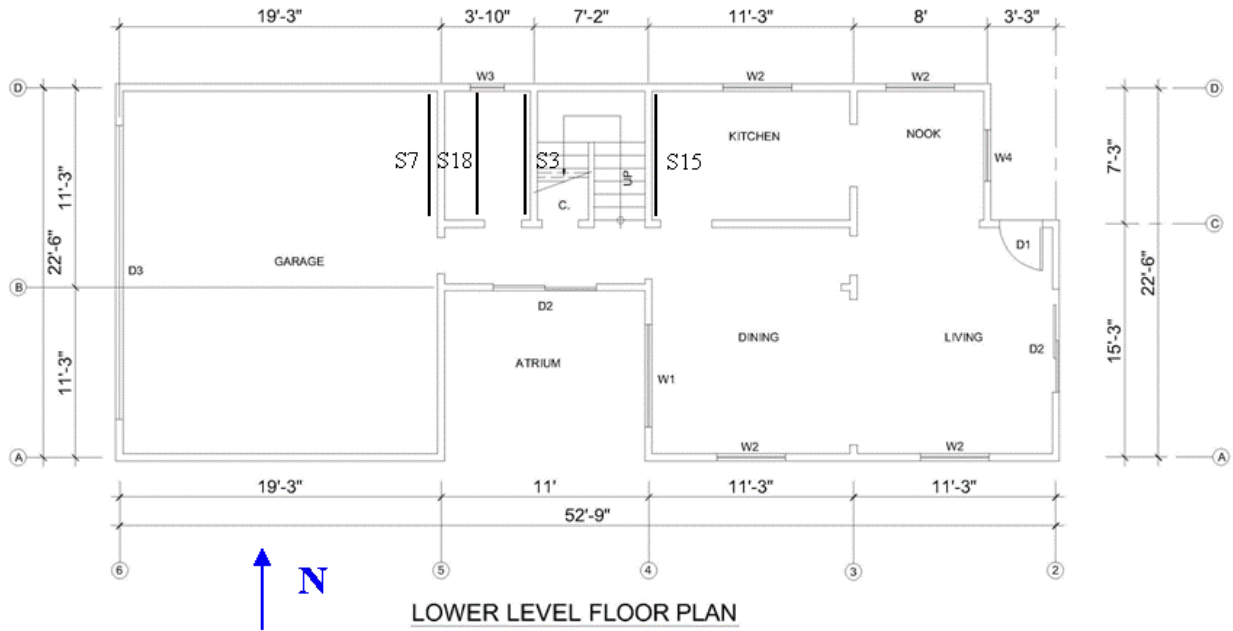


Figure E.4: Locations of string potentiometers measuring shear deformations for Test Phases 4 and 5 (cont'd)

Appendix E

Table E.5: List of displacement transducers measuring sill plate slippage for all test phases

No.	Nomenclature	Direction	Location / Notes
1	SL1	X	Sill plate, Corner, A-6
2	SL2	Y	Sill plate, Corner, A-6
3	SL3	X	Sill plate, Corner, D-6
4	SL4 ¹	Y	Sill plate, Corner, D-7
5	SL5	X	Sill plate, Corner, D-2 & 3
6	SL6	Y	Sill plate, Corner, D-2 & 3
7	SL7	X	Sill plate, Corner, A-2
8	SL8	Y	Sill plate, Corner, A-2
9	SL9	X	Sill plate, Corner, A-4
10	SL10 ¹	Y	Sill plate, Corner, A-5

¹ Removed in Test Phase 2 after Test NWP2S13. Channel used to measure displacement at first floor dampers

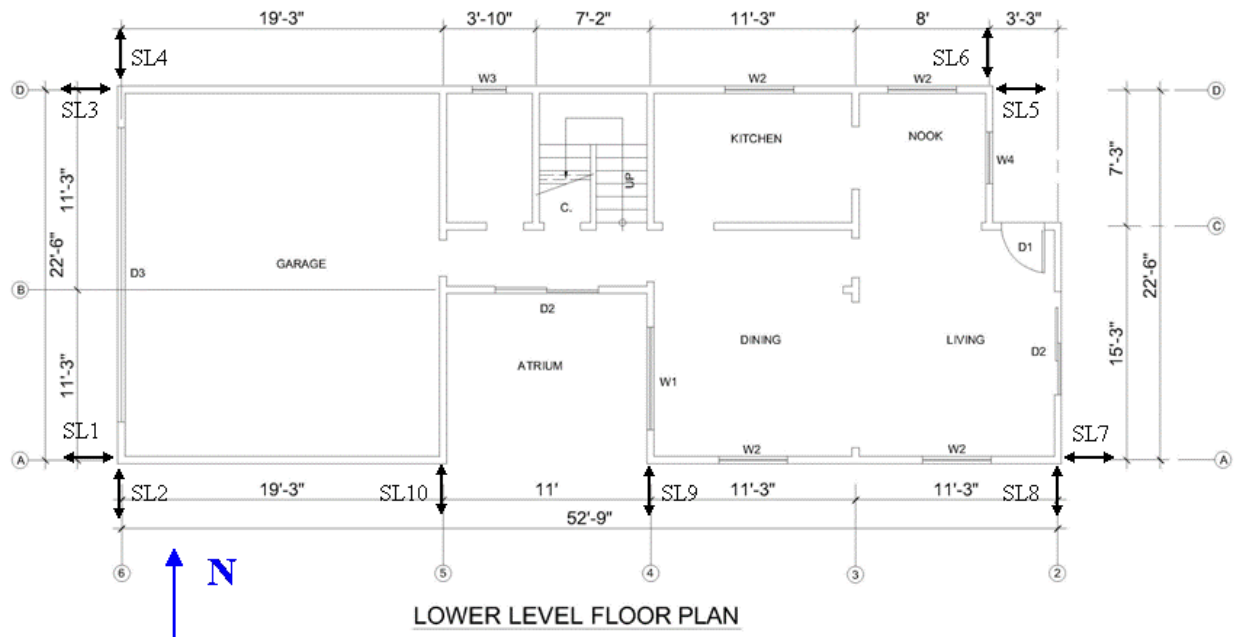


Figure E.5: Locations of displacement transducers measuring sill plate slippage for all test phases

Appendix E

Table E.6: List of displacement transducers measuring sill plate uplift for all test phases

No.	Nomenclature	Direction	Location / Notes
1	UP1	Z	Stud to sill plate
2	UP2	Z	Sill plate to table frame
3	UP3	Z	Stud to sill plate
4	UP4	Z	Sill plate to table frame
5	UP5	Z	Stud to sill plate
6	UP6	Z	Sill plate to table frame
7	UP7	Z	Stud to sill plate
8	UP8	Z	Sill plate to table frame
9	UP9	Z	Stud to sill plate
10	UP10	Z	Sill plate to table frame
11	UP11	Z	Stud to sill plate
12	UP12	Z	Sill plate to table frame
13	UP13	Z	Stud to sill plate
14	UP14	Z	Sill plate to table frame
15	UP15	Z	Stud to sill plate
16	UP16	Z	Sill plate to table frame
17	UP17	Z	Stud to sill plate
18	UP18	Z	Sill plate to table frame
19	UP19	Z	Stud to sill plate
20	UP20	Z	Sill plate to table frame
21	UP21	Z	Stud to sill plate
22	UP22	Z	Sill plate to table frame
23	UP23	Z	Stud to sill plate
24	UP24	Z	Sill plate to table frame
25	UP25	Z	Stud to sill plate
26	UP26	Z	Sill plate to table frame
27	UP27	Z	Stud to sill plate
28	UP28	Z	Sill plate to table frame
29	UP29	Z	Stud to sill plate
30	UP30	Z	Sill plate to table frame
31	UP31	Z	Stud to sill plate
32	UP32	Z	Sill plate to table frame
33	UP33	Z	Stud to sill plate
34	UP34	Z	Sill plate to table frame

Appendix E

Table E.6: List of displacement transducers measuring sill plate uplift for all test phases (cont'd)

35	UP35	Z	Stud to sill plate
36	UP36	Z	Sill plate to table frame
37	UP37	Z	Stud to sill plate
38	UP38	Z	Sill plate to table frame
39	UP39	Z	Stud to sill plate
40	UP40	Z	Sill plate to table frame
41	UP41	Z	Stud to sill plate
42	UP42	Z	Sill plate to table frame
43	UP43	Z	Stud to sill plate
44	UP44	Z	Sill plate to table frame
45	UP45	Z	Stud to sill plate
46	UP46	Z	Sill plate to table frame
47	UP47	Z	Stud to sill plate
48	UP48	Z	Sill plate to table frame
49	UP49	Z	Stud to sill plate
50	UP50	Z	Sill plate to table frame
51	UP51	Z	Stud to sill plate
52	UP52	Z	Sill plate to table frame

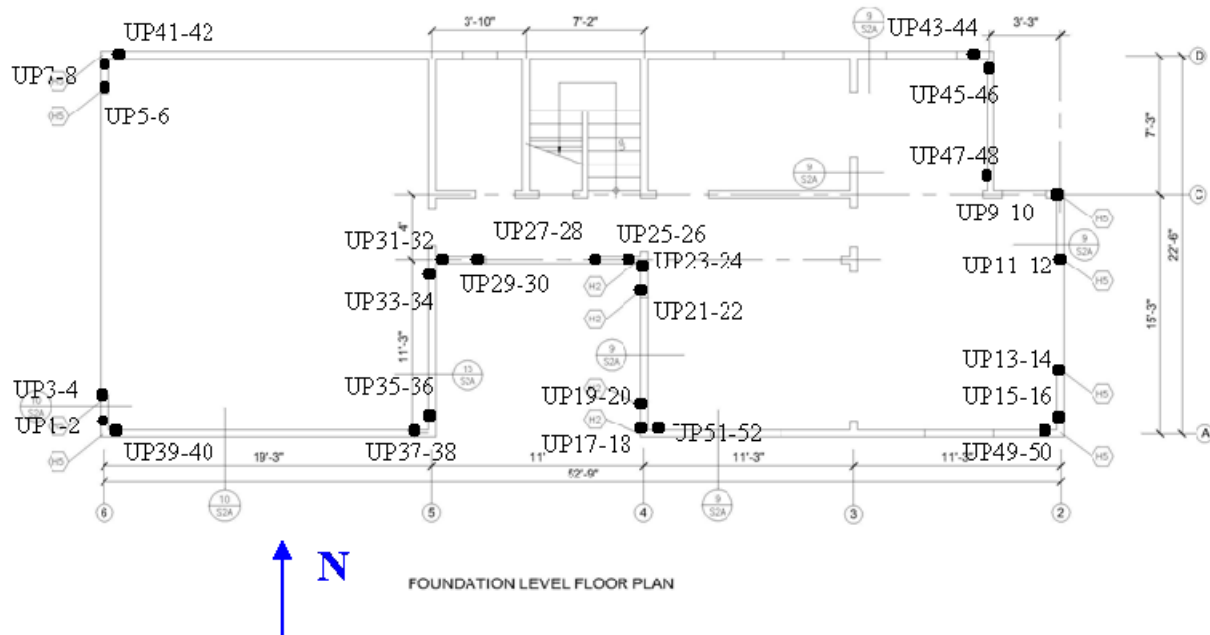


Figure E.6: Locations of displacement transducers measuring sill plate uplift for all test phases

Appendix E

Table E.7: List of load cells for all test phases

No.	Nomenclature	Direction	Location / Notes
1	LC1	Z	Holddown
2	LC2	Z	Holddown
3	LC3	Z	Holddown
4	LC4	Z	Holddown
5	LC5	Z	Anchor bolt
6	LC6	Z	Anchor bolt
7	LC7	Z	Anchor bolt
8	LC8	Z	Anchor bolt
9	LC9	Z	Anchor bolt
10	LC10	Z	Anchor bolt
11	LC11	Z	Anchor bolt, <u>*malfunctioned in Phase 5 except for Test NWP5S11</u>
12	LC12	Z	Anchor bolt
13	LC13	Z	Anchor bolt
14	LC14	Z	Anchor bolt
15	LC15	Z	Anchor bolt
16	LC16	Z	Anchor bolt
17	LC17	Z	Anchor bolt
18	LC18	Z	Anchor bolt
19	LC19	Z	Anchor bolt
20	LC20	Z	Holddown
21	LC21	Z	Holddown
22	LC22	Z	Holddown
23	LC23	Z	Holddown
24	LC24	Z	Anchor bolt
25	LC25	Z	Anchor bolt
26	LC26	Z	Anchor bolt
27	LC27	Z	Anchor bolt
28	LC28	Z	Anchor bolt
29	LC29	Z	Anchor bolt
30	LC30	Z	Holddown
31	LC31	Z	Holddown
32	LC32	Z	Anchor bolt
33	LC33	Z	Holddown
34	LC34	Z	Holddown

Appendix E

Table E.7: List of load cells for all test phases (cont'd)

35	LC35	Z	Anchor bolt
36	LC36	Z	Anchor bolt
37	LC37	Z	Anchor bolt
38	LC38	Z	Anchor bolt
39	LC39	Z	Anchor bolt
40	LC40	Z	Anchor bolt
41	LC41	Z	Anchor bolt
42	LC42	Z	Anchor bolt
43	LC43	Z	Anchor bolt
44	LC44	Z	Anchor bolt
45	LC45	Z	Anchor bolt
46	LC46	Z	Anchor bolt
47	LC47 ²	Z	Anchor bolt
48	LC48 ¹	Z	Anchor bolt
49	LC49 ²	Z	Anchor bolt
51	LC51	Z	Anchor bolt
52	LC52	Z	Anchor bolt
53	LC53	Z	Anchor bolt
54	LC54 ³	Z	Anchor bolt
55	LC55 ³	Z	Anchor bolt
56	LC56	Z	Anchor bolt
57	LC57 ²	Z	Anchor bolt
58	LC58	Z	Anchor bolt

¹ Not applicable to Test Phases 1 and 2

² Not applicable to Test Phases 1, 2 and 3

³ Removed in Test Phase 2. Channels used for damper walls

Appendix E

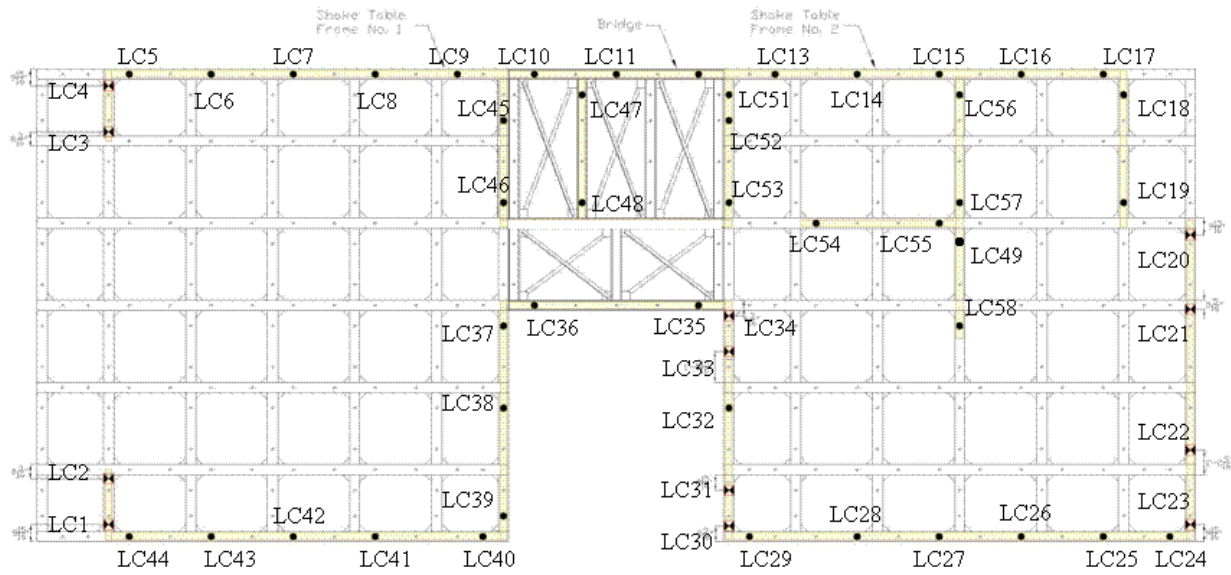


Figure E.7: Locations of load cells for all test phases

Appendix E

Table E.8: List of instrumentation for damper walls used during Test Phase 2

No.	Nomenclature	Direction	Type	Location / Notes
1	DD1	X	Displ.	1st floor, North
2	DF1	X	Force	1st floor, North
3	DD2	X	Displ.	1st floor, South
4	DF2	X	Force	1st floor, South
5	DD3	X	Displ.	2nd floor, North
6	DF3	X	Force </td <td>2nd floor, North</td>	2nd floor, North
7	DD4	X	Displ.	2nd floor, South
8	DF4	X	Force	2nd floor, South
9	SL4 ¹	X	Displ.	1 st floor, North
10	SL10 ¹	X	Displ.	1 st floor, South

¹ Channels added after Test NWP2S13

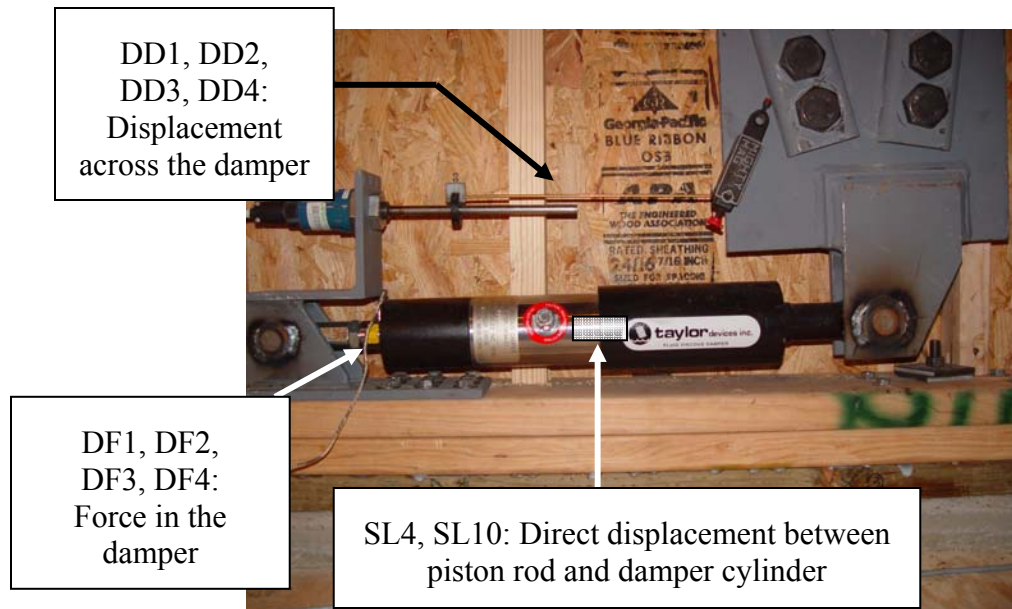


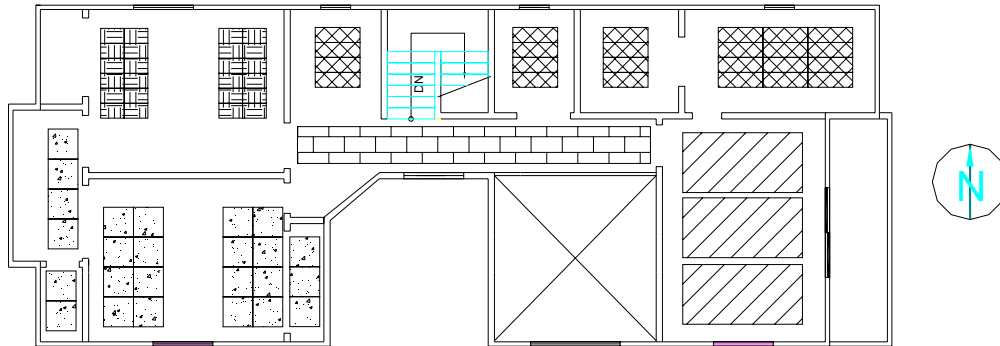
Figure E.8: Locations of displacement and force sensors for damper walls used during Test Phase 2

Appendix F
Supplemental Weight Layouts and
Total Weight of Benchmark Structure

Appendix F

Supplemental Weight Layout for Phases 1 and 2

Structure description: wood shear walls only, no wall finishes.



Total Supplemental Weight = 39.8 kips


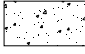


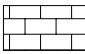
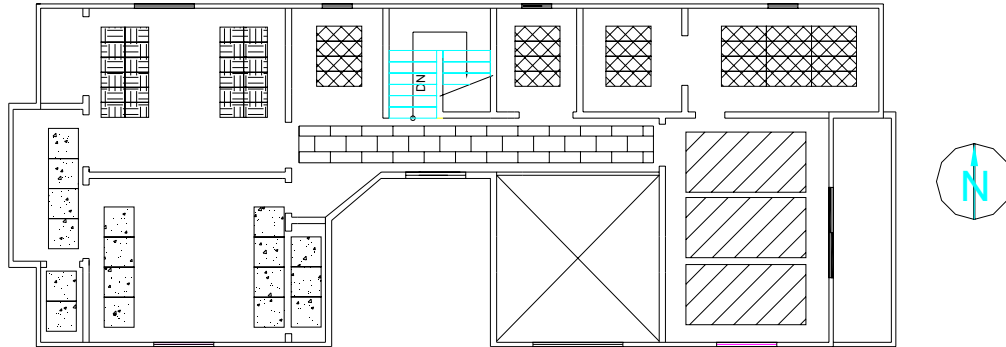
SYMBOL	DESCRIPTIONS
	GYPSUM BOARDS Stack of 49 gypsum boards Total = 147 sheets (9.4 kips)
	CONCRETE PAVERS Stack of 4 concrete pavers Total = 112 pavers (10.0 kips)
	QUICK CRETE Stack of 2 bags of Quick Crete Total = 84 bags (7.1 kips)
	ROOF SHINGLES Stack of 4 bundles of roof shingles Total = 96 bundles (7.2 kips)
	PAVER BRICKS 4 layers of paver bricks Total = 800 bricks (6.1 kips)

Figure F.1: Layout of supplemental weights for Test Phases 1 and 2

Appendix F

Supplemental Weight Layout for Phase 3

Structure description: wood shear walls and drywall on internal sides of shear walls.



Total Supplemental Weight = 33.3 kips

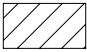
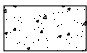


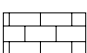
SYMBOL	DESCRIPTIONS
	GYPSUM BOARDS Remove 48 sheets from Phase 1 Total left = 99 sheets (6.3 kips)
	CONCRETE PAVERS Remove 38 pavers from Phase 1 Total left = 74 pavers (6.6 kips)
	QUICK CRETE No change from Phase 1 Total = 84 bags (7.1 kips)
	ROOF SHINGLES No change from Phase 1 Total = 96 bundles (7.2 kips)
	PAVER BRICKS No change from Phase 1 Total = 800 bricks (6.1 kips)

Figure F.2: Layout of supplemental weights for Test Phase 3

Appendix F

Supplemental Weight Layout for Phase 4

Structure description: wood shear walls and drywall on internal sides of shear and partition walls.







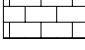
SYMBOL	DESCRIPTIONS
	<p>GYPSUM BOARDS Remove all sheets Total left = 0 sheets</p>
	<p>CONCRETE PAVERS Remove 6 pavers from Phase 3 Total = 68 pavers (6.1 kips)</p>
	<p>QUICK CRETE Remove 3 bags from Phase 4 Total left = 81 bags (6.8 kips)</p>
	<p>ROOF SHINGLES Remove 4 bundles from Phase 3 Total left = 92 bundles (6.9 kips)</p>
	<p>PAVER BRICKS Re-locate to master bedroom Total = 800 bricks (6.1 kips)</p>

Figure F.3: Layout of supplemental weights for Test Phase 4

Appendix F

Total Weight of Benchmark Structure

Table F.1: Tributary weight (self and supplemental) near the specific locations of the associated accelerometers (see Table E.1 and Figure E.1 of Appendix E for accelerometers' nomenclature)

	Location	Associated Accelerometers		Test Phase			
		East-West	North-South	1	3	4	5
	West Table	A68	A69	0.75	1.23	1.52	3.93
	East Table	A71	A72	0.92	1.51	1.86	4.81
	Total Weight on Tables			1.67	2.74	3.38	8.74
Second Floor Level	Line A & 6	A1	A2	6.61	5.20	5.16	3.56
	Line A & 5	A19	A20	6.67	5.30	5.29	3.87
	Line A & 4	A13	A14	0.56	0.91	1.16	2.90
	Line A & 2	A11	A12	8.06	6.30	8.43	3.88
	Line D & 6	A3	A4	5.13	5.40	5.45	3.40
	Line D & 5	A45	A46	9.15	9.39	6.93	3.60
	Line D & 4	A47	A48	8.20	8.49	4.93	4.05
	Line D & 2	A5	A6	8.74	8.11	6.16	4.74
	Total Weight of Second Floor Level			53.12	49.10	43.51	30.00
Roof of Second Floor Level	Line A & 6	A21	A22	0.86	1.02	1.43	2.70
	Line A & 5	A43	A44	0.97	1.15	1.61	3.05
	Line A & 4	A37	A38	1.03	1.23	1.71	3.24
	Line A & 2	A34	A35	0.92	1.09	1.53	2.90
	Line D & 6	A24	A25	0.80	0.96	1.33	2.53
	Line D & 5	A49	A50	0.73	0.86	1.20	2.28
	Line D & 4	A51	A52	0.84	1.00	1.40	2.65
	Line D & 2	A27	A28	1.20	1.43	2.00	3.79
	Total Weight of Roof of Second Floor Level			7.35	8.74	12.21	23.14
Roof Level	Center of West Roof	A41	A42	4.62	4.62	4.62	5.36
	Center of East Roof	A39	A16	6.93	6.93	6.93	8.04
	Center of Structure	A17	A18	4.62	4.62	4.62	5.36
	Total Weight of Roof Level			16.17	16.17	16.17	18.76
Total Weight of Structure [kips]				78.31	76.75	75.27	80.64

Appendix G
Sheathing-to-Framing Connection
Test Results

Appendix G

Monotonic Testing Data (2x4, parallel)

Loading: Monotonic

Direction: Parallel to grain

Framing: 2x4 Hem Fir

Sheathing: 7/16" OSB

Nailing: 8d common nails (load data represents one nail connector)

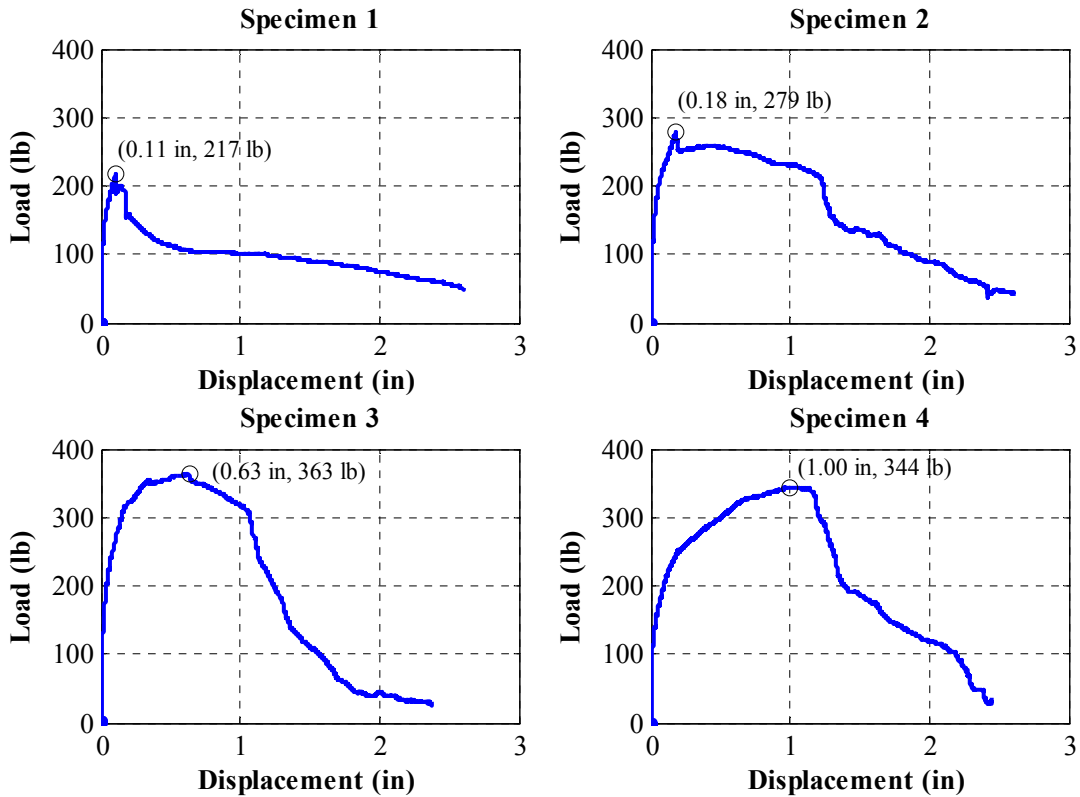


Figure G.1: Plots of load-displacement curves from monotonic pushover tests for 2x4 studs and OSB oriented parallel to grain

Appendix G

Monotonic Testing Data (2x4, perpendicular)

Loading: Monotonic

Direction: Perpendicular to grain

Framing: 2x4 Hem Fir

Sheathing: 7/16" OSB

Nailing: 8d common nails (load data represents one nail connector)

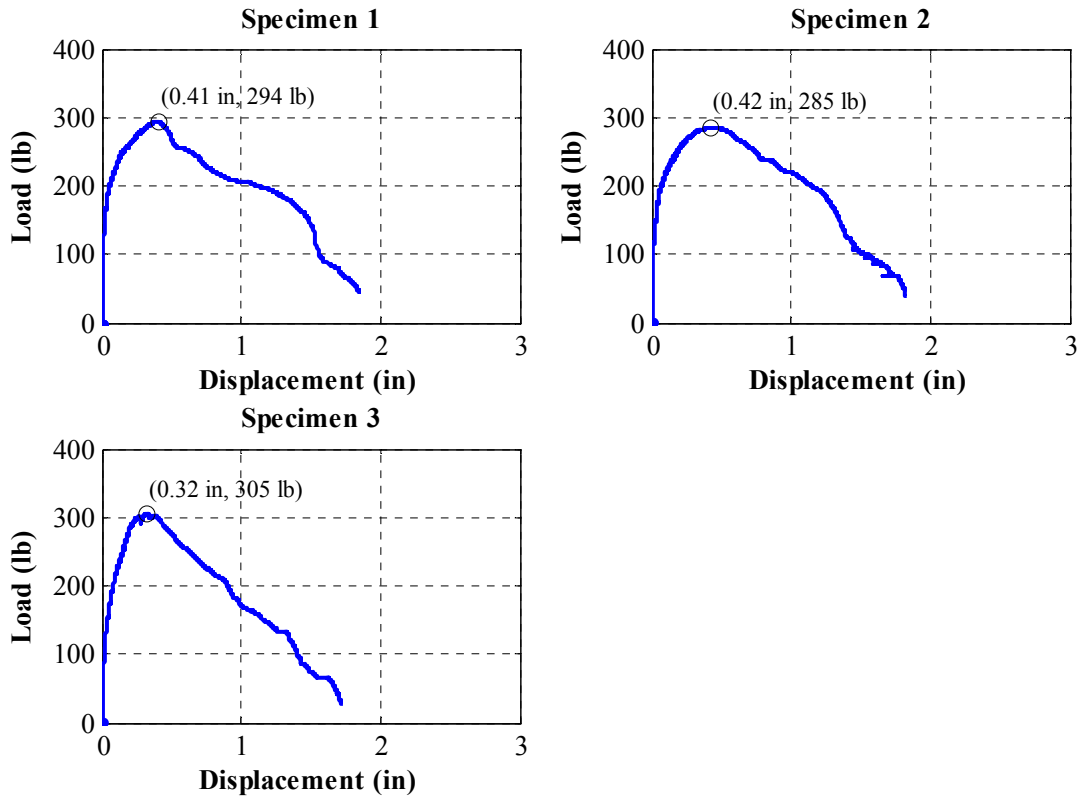


Figure G.2: Plots of load-displacement curves from monotonic pushover tests for 2x4 studs and OSB oriented perpendicular to grain

Appendix G

Monotonic Testing Data (2x6, parallel)

Loading: Monotonic

Direction: Parallel to grain

Framing: 2x6 Hem Fir

Sheathing: 7/16" OSB

Nailing: 8d common nails (load data represents one nail connector)

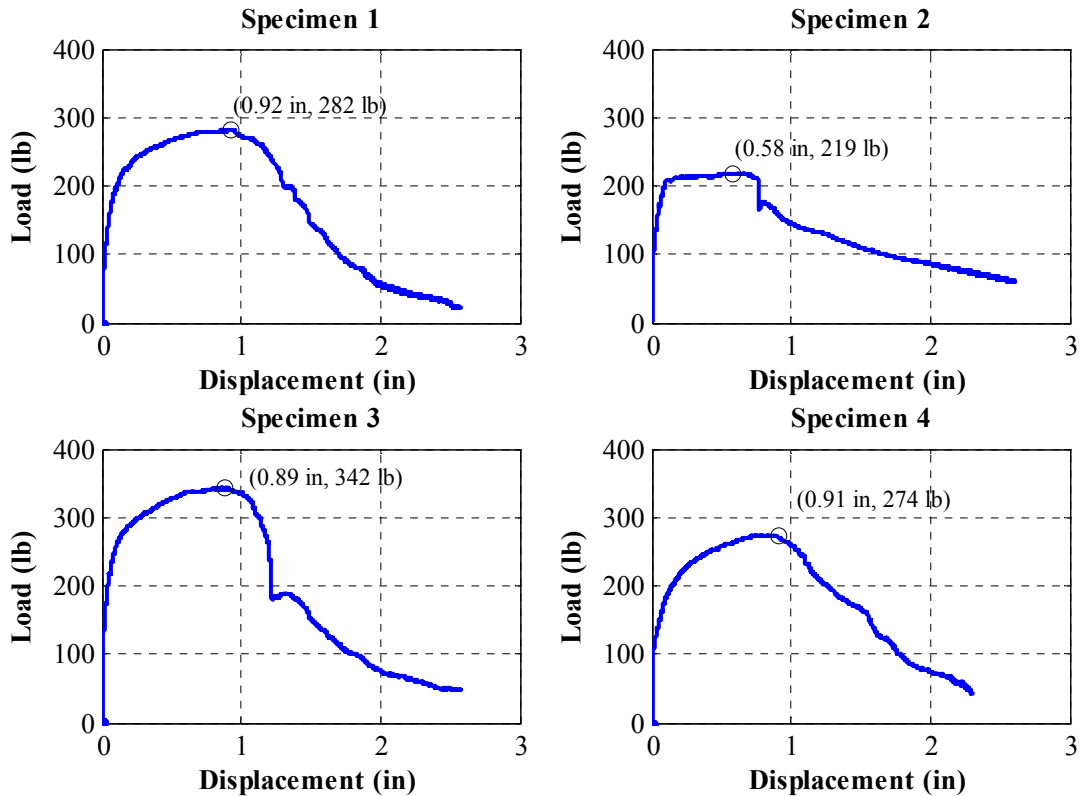


Figure G.3: Plots of load-displacement curves from monotonic pushover tests for 2x6 studs and OSB oriented parallel to grain

Appendix G

Monotonic Testing Data (2x6, perpendicular)

Loading: Monotonic

Direction: Perpendicular to grain

Framing: 2x6 Hem Fir

Sheathing: 7/16" OSB

Nailing: 8d common nails (load data represents one nail connector)

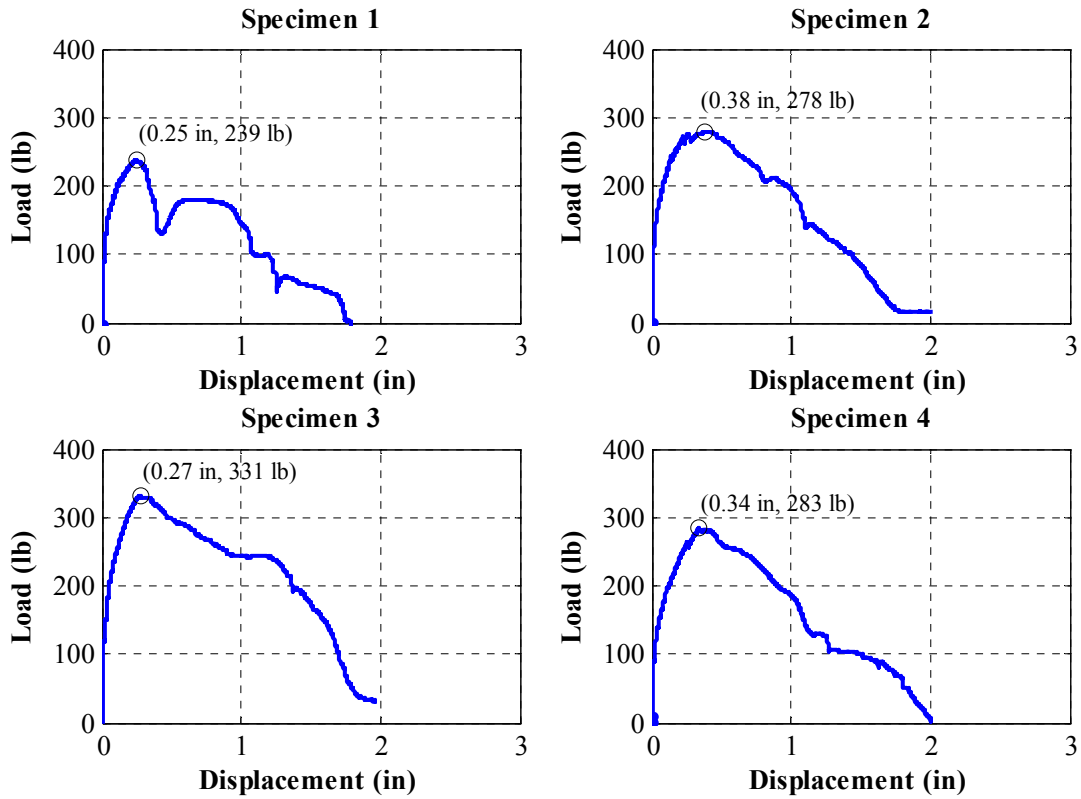


Figure G.4: Plots of load-displacement curves from monotonic pushover tests for 2x4 studs and OSB oriented perpendicular to grain

Appendix G

Cyclic Testing Data (2x4, parallel)

Loading: Cyclic

Direction: Parallel to grain

Framing: 2x4 Hem Fir

Sheathing: 7/16" OSB

Nailing: 8d common nails (load data represents one nail connector)

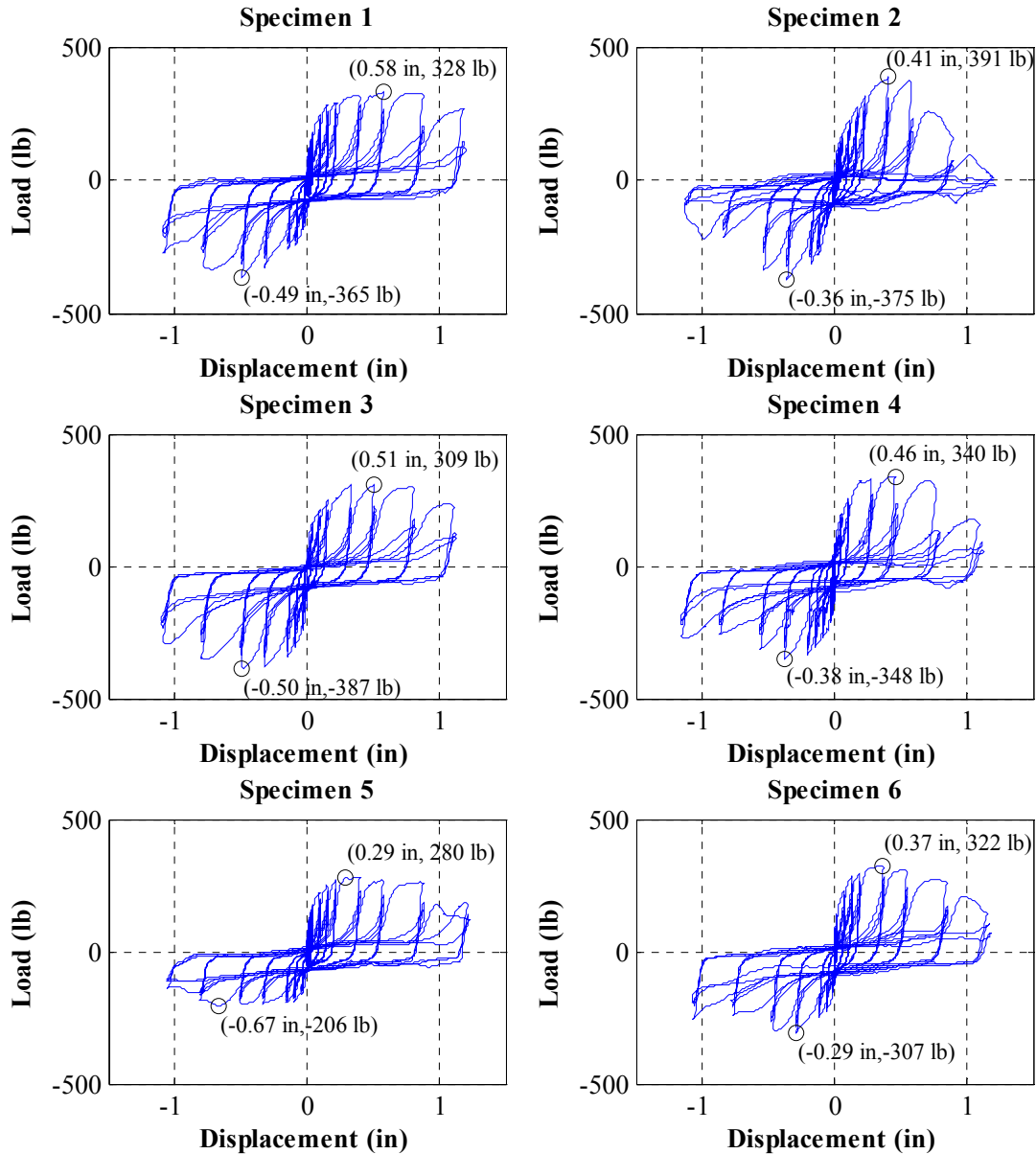


Figure G.5: Plots of load-displacement curves from cyclic pushover tests for 2x4 studs and OSB oriented parallel to grain

Appendix G

Cyclic Testing Data (2x4, parallel)

Loading: Cyclic

Direction: Parallel to grain

Framing: 2x4 Hem Fir

Sheathing: 7/16" OSB

Nailing: 8d common nails (load data represents one nail connector)

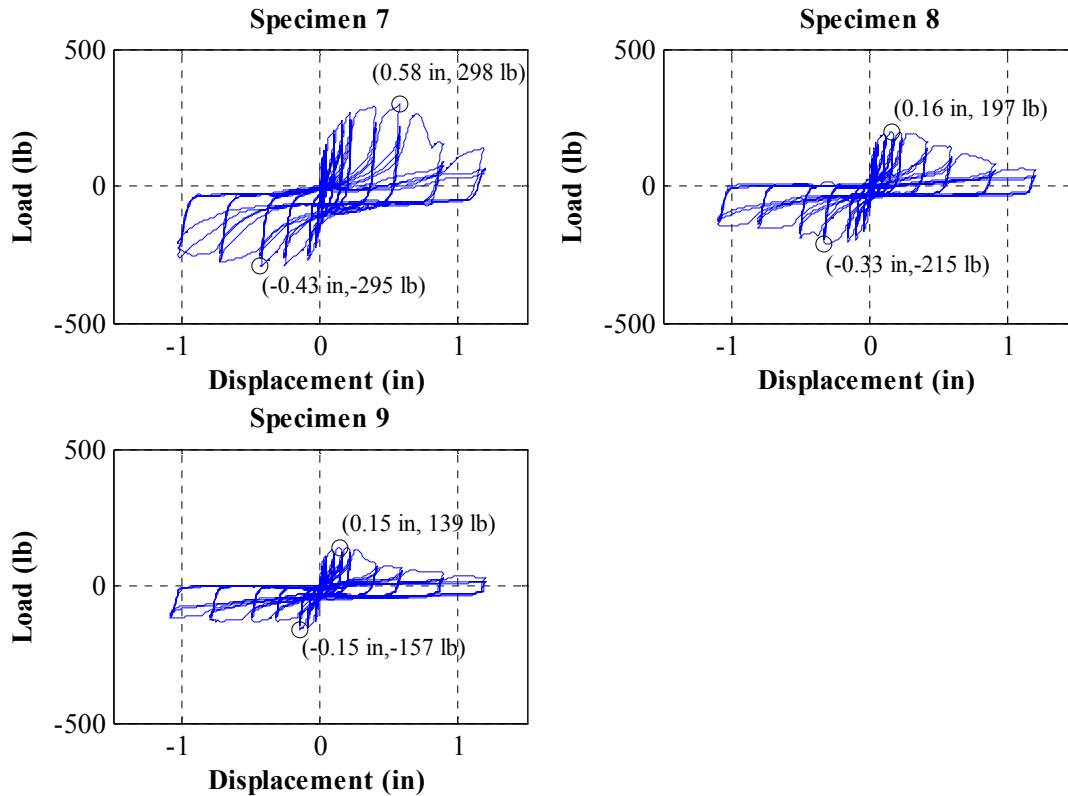


Figure G.5: Plots of load-displacement curves from cyclic pushover tests for 2x4 studs and OSB oriented parallel to grain (cont'd)

Appendix G

Cyclic Testing Data (2x4, perpendicular)

Loading: Cyclic

Direction: Perpendicular to grain

Framing: 2x4 Hem Fir

Sheathing: 7/16" OSB

Nailing: 8d common nails (load data represents one nail connector)

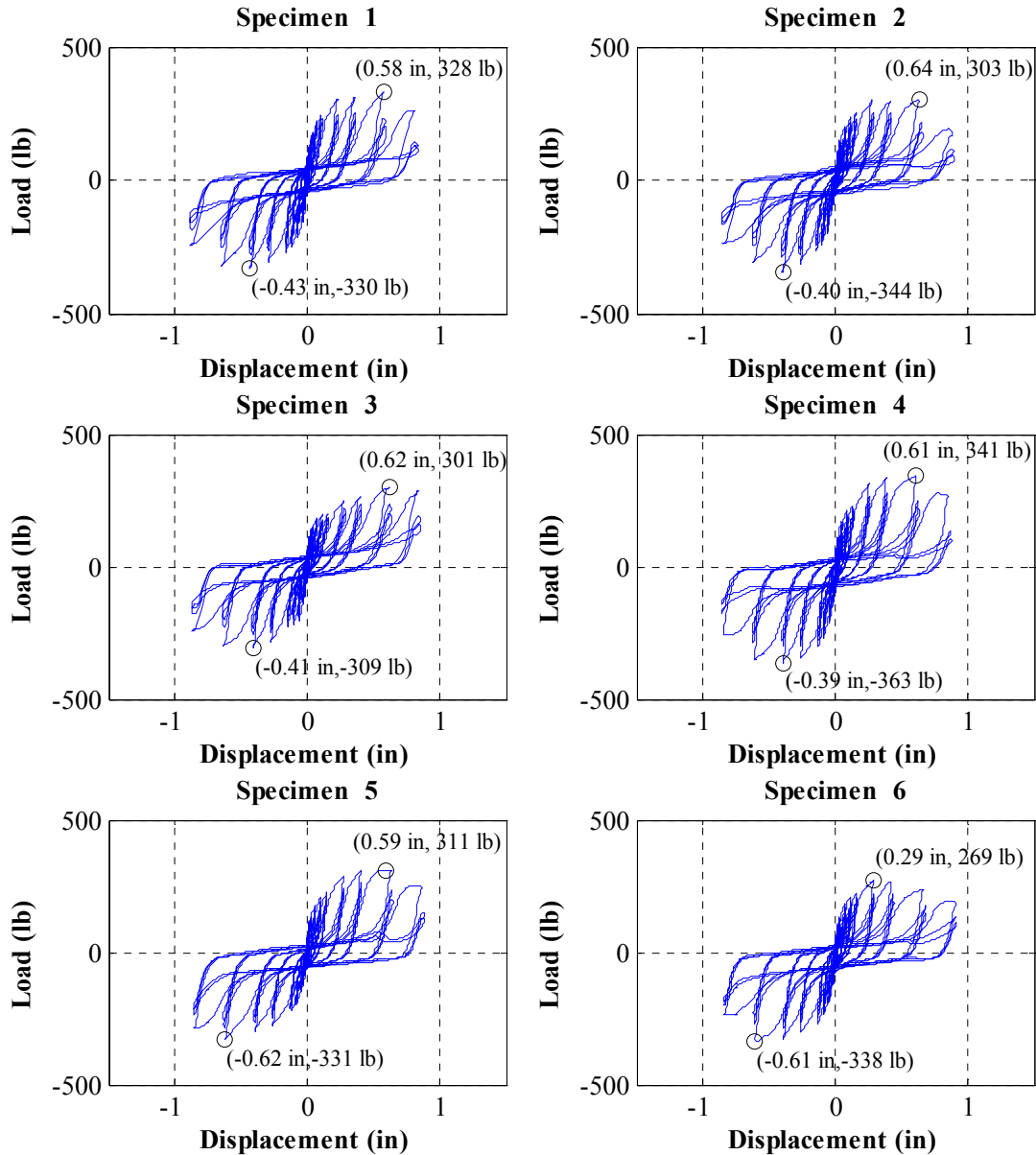


Figure G.6: Plots of load-displacement curves from cyclic pushover tests for 2x4 studs and OSB oriented perpendicular to grain

Appendix G

Cyclic Testing Data (2x4, perpendicular)

Loading: Cyclic

Direction: Perpendicular to grain

Framing: 2x4 Hem Fir

Sheathing: 7/16" OSB

Nailing: 8d common nails (load data represents one nail connector)

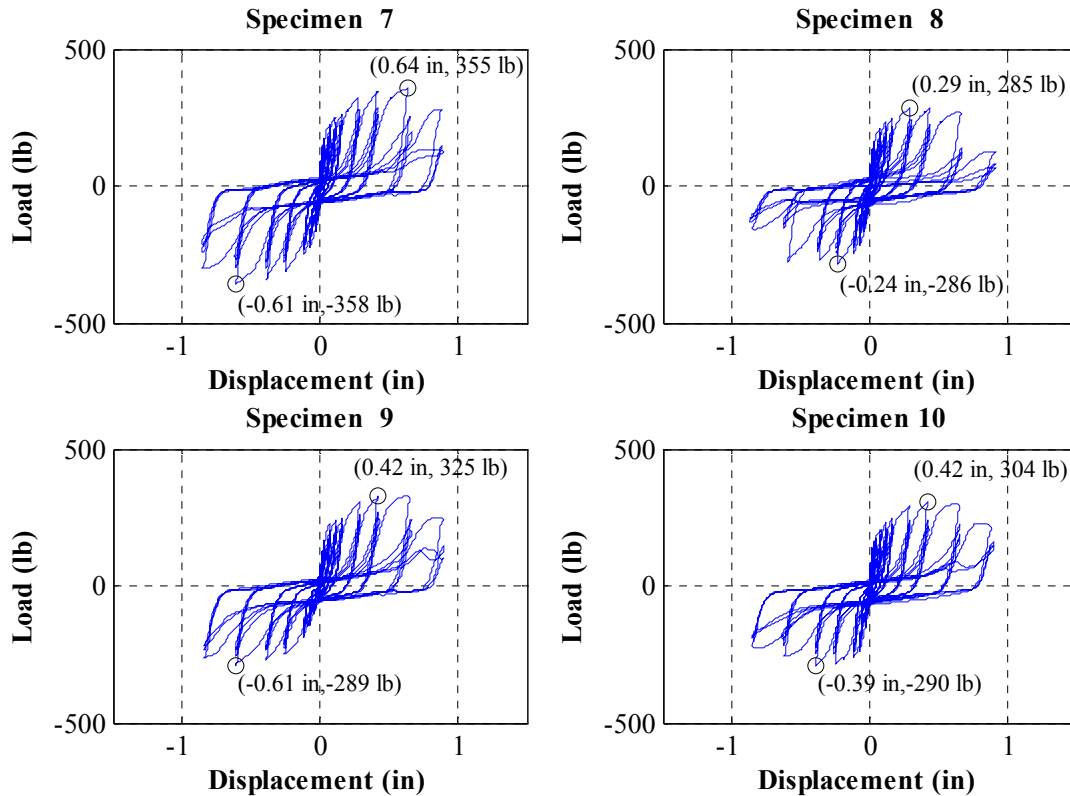


Figure G.6: Plots of load-displacement curves from cyclic pushover tests for 2x4 studs and OSB oriented perpendicular to grain (cont'd)

Appendix G

Cyclic Testing Data (2x6, parallel)

Loading: Cyclic

Direction: Parallel to grain

Framing: 2x6 Hem Fir

Sheathing: 7/16" OSB

Nailing: 8d common nails (load data represents one nail connector)

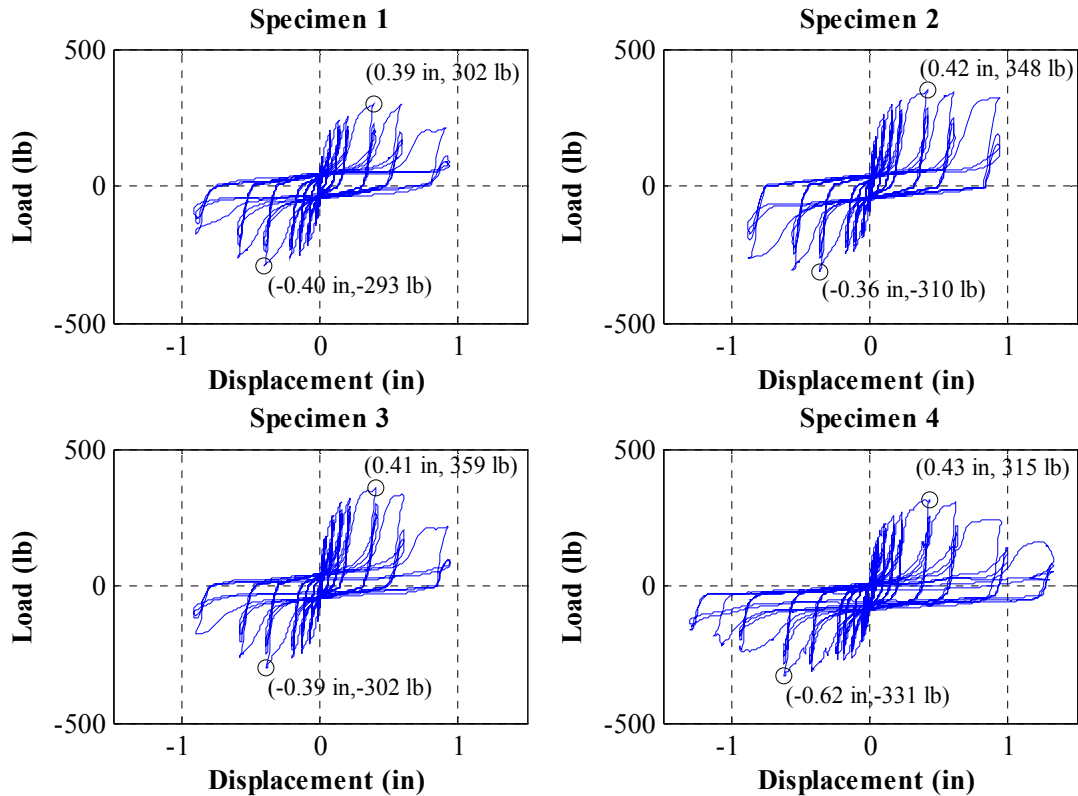


Figure G.7: Plots of load-displacement curves from cyclic pushover tests for 2x6 studs and OSB oriented parallel to grain

Appendix G

Cyclic Testing Data (2x6, parallel)

Loading: Cyclic

Direction: Parallel to grain

Framing: 2x6 Hem Fir

Sheathing: 7/16" OSB

Nailing: 8d common nails (load data represents one nail connector)

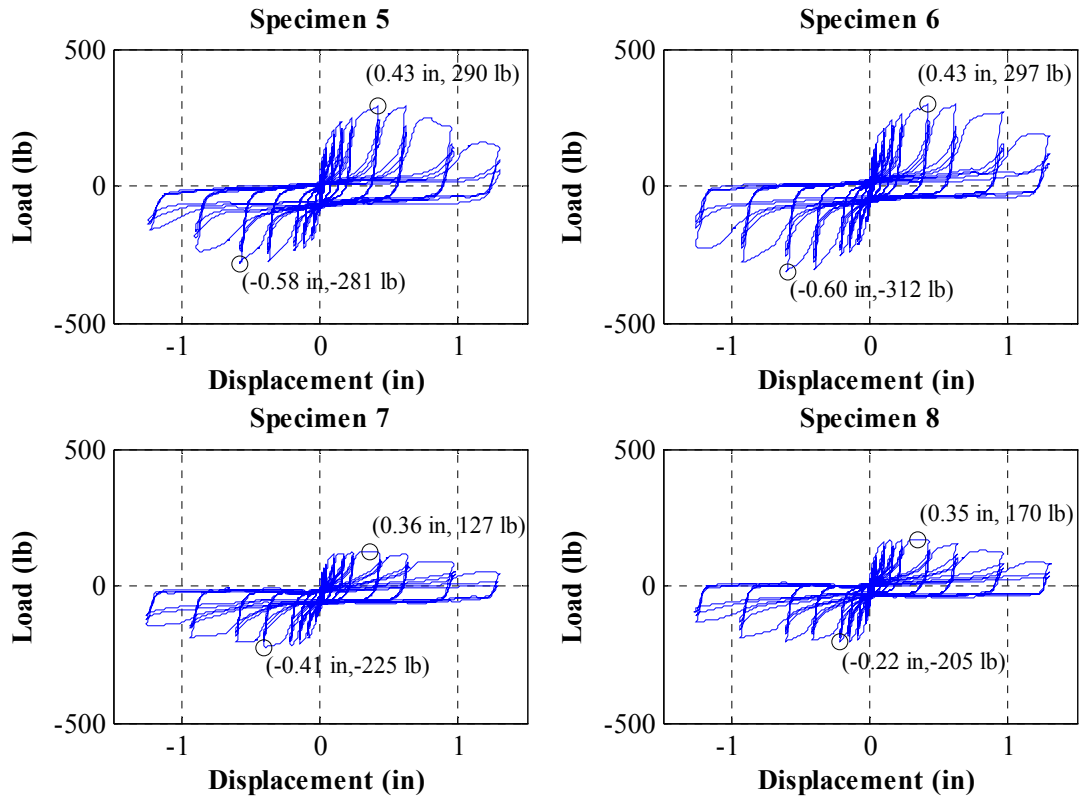


Figure G.7: Plots of load-displacement curves from cyclic pushover tests for 2x6 studs and OSB oriented parallel to grain (cont'd)

Appendix G

Cyclic Testing Data (2x6, perpendicular)

Loading: Cyclic

Direction: Perpendicular to grain

Framing: 2x6 Hem Fir

Sheathing: 7/16" OSB

Nailing: 8d common nails (load data represents one nail connector)

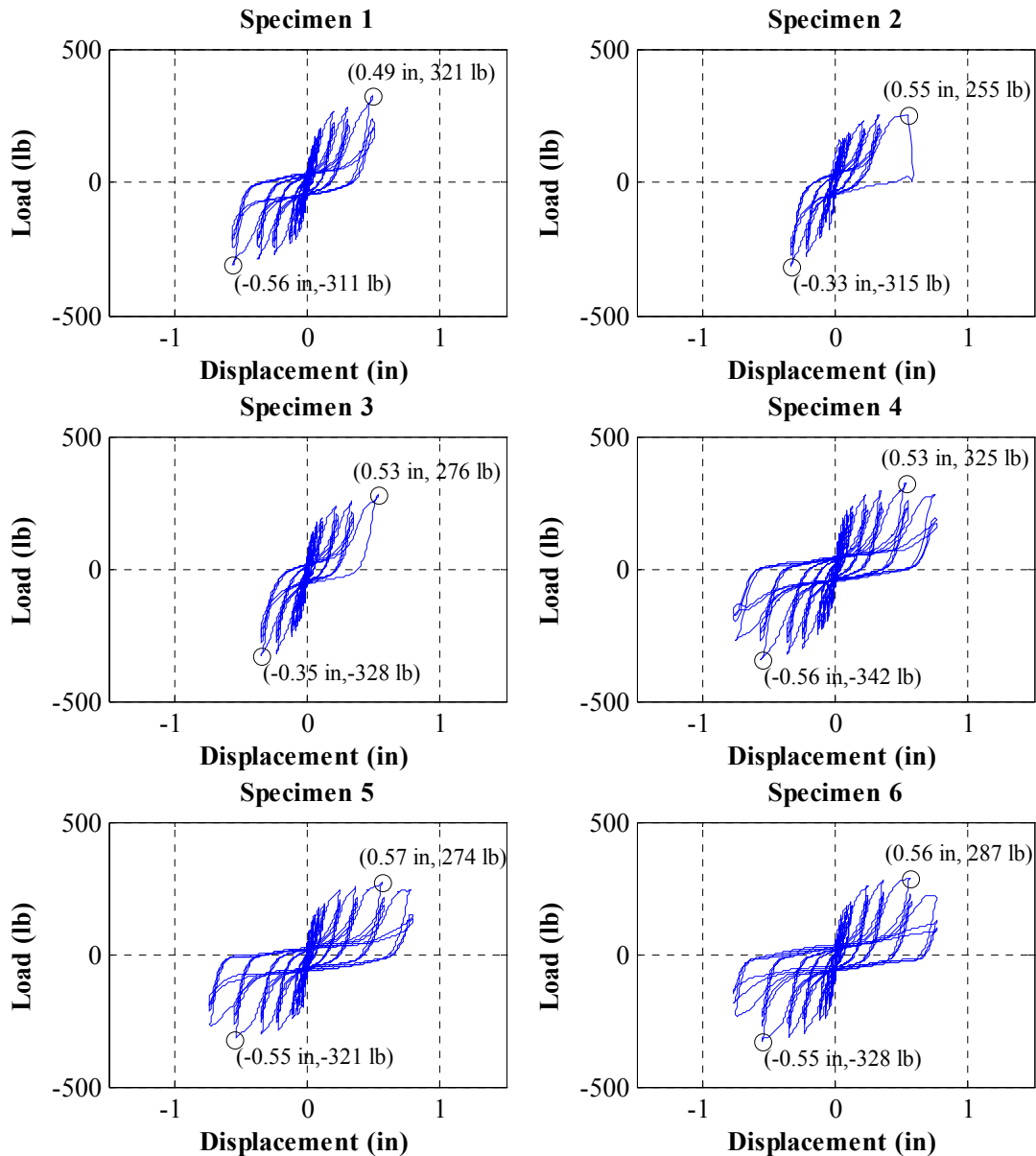


Figure G.8: Plots of load-displacement curves from cyclic pushover tests for 2x6 studs and OSB oriented perpendicular to grain

Appendix G

Cyclic Testing Data (2x6, perpendicular)

Loading: Cyclic

Direction: Perpendicular to grain

Framing: 2x6 Hem Fir

Sheathing: 7/16" OSB

Nailing: 8d common nails (load data represents one nail connector)

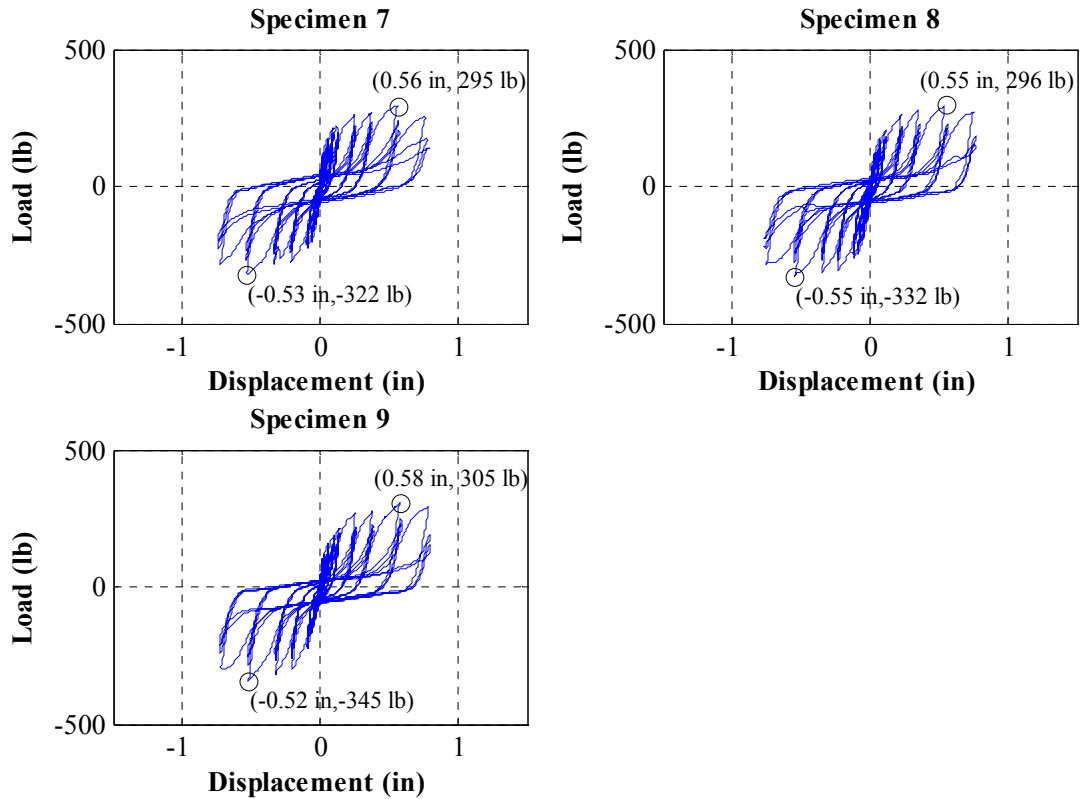


Figure G.8: Plots of load-displacement curves from cyclic pushover tests for 2x6 studs and OSB oriented perpendicular to grain (cont'd)

Appendix G

SAWS Model Hysteretic Parameters

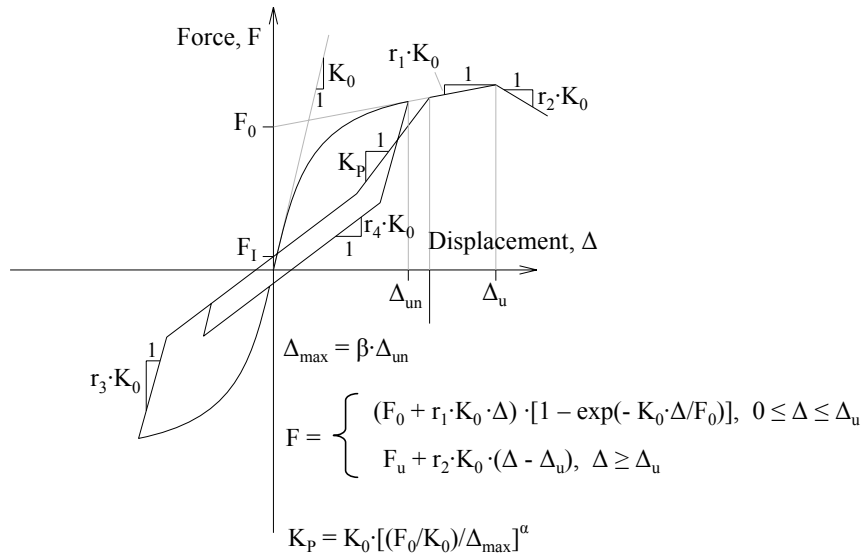


Figure G.9: Hysteretic response of a sheathing-to-framing connector based on SAWS model

Table G.1: Final benchmark hysteretic parameters for SAWS model

Parameters	Mean of 2x4			Mean of 2x6			Mean for all tests
	Parallel	Perpen- dicular	All tests	Parallel	Perpen- dicular	All tests	
F_I (lbs)	35.0	34.2	34.5	25.7	32.8	29.2	32.0
F₀ (lbs)	242.4	238.1	239.9	203.2	228.9	216.0	228.3
Δ_u (in)	0.470	0.559	0.522	0.448	0.540	0.494	0.508
K₀ (lbs/in)	8144.3	6063.8	6920.5	6659.5	6039.9	6349.7	6643.8
r₁	0.025	0.026	0.025	0.026	0.026	0.026	0.026
r₂	-0.027	-0.047	-0.039	-0.026	-0.053	-0.039	-0.039
r₃	1.028	1.021	1.024	1.021	1.010	1.015	1.020
r₄	0.005	0.010	0.008	0.004	0.013	0.009	0.008
α	0.77	0.67	0.71	0.75	0.70	0.73	0.72
β	1.24	1.31	1.28	1.30	1.29	1.30	1.29

Appendix H

System Identification Test Results

Appendix H

Initial Natural Periods and Damping of Test Structure

Initial natural periods and damping of the first three mode shapes of the test structure calculated from 0.05 g amplitude (0.5-50 Hz) white noise identification tests prior to any seismic test.

Table H.1: Initial natural periods (sec)

Mode \ Phase	1	2	3	4	5
1	0.327	0.327	0.296	0.296	0.286
2	0.225	0.232	0.216	0.222	0.198
3	0.180	0.178	0.170	0.163	0.127

Table H.2: Initial damping ratios (%)

Mode \ Phase	1	2	3	4	5
1	12.2	12.5	10.7	10.9	17.9
2	3.3	6.8	6.5	4.3	17.1
3	2.7	5.6	6.7	6.2	5.0

Evolution of Natural Periods and Damping of Test Structure

Evolution of natural periods T and damping ζ of the first three mode shapes of the test structure during each of the five test phases. Damping ratios are computed measuring the half-power bandwidth of transfer functions between recorded acceleration time-histories.

Table H.3: Evolution of natural periods and damping ratios for Test Phase 1

Description	Ampl. (g)	Mode 1 (Transverse)		Mode 2 (Coupled Longitud.-Torsional)		Mode 3	
		T (sec)	ζ (%)	T (sec)	ζ (%)	T (sec)	ζ (%)
Initial, prior to any seismic test	0.05	0.327	12.2	0.225	3.3	0.180	2.7
	0.10	0.327	15.2	0.242	8.8	0.184	5.4
Following level 1 X-Y-Z	0.10	0.327	15.0	0.242	9.0	0.195	9.6
Following level 1 X-Y	0.10	0.356	16.4	0.242	12.5*	0.195	9.5*
Following level 1 X	0.10	0.356	16.3	0.242	13.1*	0.195	9.4*
Following level 1 Y	0.10	0.356	16.6	0.242	13.0*	0.195	9.0*
Following aborted level 2 X-Y-Z due to table synchronization issue	0.05	0.327	11.1	0.235	6.2	0.190	5.4
	0.10	0.356	14.3	0.250	12.2*	0.211	10.8*
Following repeated level 2 X-Y-Z	0.10	0.432	19.6	0.271	18.1*	0.213	7.7*
	0.05	0.381	12.1	0.250	11.1*	0.203	8.9
Following level 2 X	0.10	0.421	18.2	0.271	16.6*	0.213	7.8*
Following level 2 X-Y	0.10	0.432	20.4	0.267	20.0*	0.229	14.7*
Following level 3 X	0.10	0.432	19.5	0.271	21.2*	0.242	18.0*

* Denotes the use of symmetry for the calculation of the half-power bandwidth

Appendix H

Table H.4: Evolution of natural periods and damping ratios for Test Phase 2

Description	Ampl. (g)	Mode 1 (Transverse)		Mode 2 (Coupled Longitud.-Torsional)		Mode 3	
		T (sec)	ζ (%)	T (sec)	ζ (%)	T (sec)	ζ (%)
Initial, prior to any seismic test	0.05	0.327	12.5	0.232	6.8	0.178	5.6
	0.10	N/A	N/A	0.250	18.5*	0.203	8.8*
Following level 1 X-Z	0.10	N/A	N/A	0.250	18.3*	0.203	12.0*
Following level 1 X	0.10	N/A	N/A	0.250	17.6*	0.203	13.0*
Following level 2 X-Z	0.10	N/A	N/A	0.250	16.3*	0.203	13.0*
Retrofit of dampers to prevent out of plane motion							
Following 1st retrofit	0.10	N/A	N/A	0.250	18.2*	0.203	8.9*
Following repeated level 2 X-Z	0.10	N/A	N/A	0.250	17.5*	0.203	9.9*
Following repeated level 2 X	0.10	N/A	N/A	0.250	19.0*	0.203	9.6*
Following repeated level 3 X-Z	0.10	N/A	N/A	0.250	17.7*	0.203	8.7*
Welding of the pinned connections of the dampers							
Following 2nd retrofit	0.10	N/A	N/A	0.250	17.8*	0.203	8.5*
Following repeated level 2 X-Z	0.10	N/A	N/A	0.250	18.1*	0.205	11.0*
Following repeated level 2 X	0.10	N/A	N/A	0.250	17.9*	0.203	8.6*
Following repeated level 3 X-Z	0.10	N/A	N/A	0.250	17.1*	0.205	9.9*
Following level 3 X	0.10	N/A	N/A	0.250	17.8*	0.205	9.6*
Retrofit of dampers to provide an overturning moment restraint system							
Following 3rd retrofit	0.10	N/A	N/A	0.250	17.6*	0.205	9.8*
Following repeated level 1 X-Z	0.10	N/A	N/A	0.250	17.9*	0.205	9.8*
Following repeated level 1 X	0.10	N/A	N/A	0.250	17.4*	0.205	10.5*
Following repeated level 2 X-Z	0.10	N/A	N/A	0.250	17.7*	0.205	10.6*
Following repeated level 2 X	0.10	N/A	N/A	0.250	17.5*	0.205	11.2*
Following repeated level 3 X-Z	0.10	N/A	N/A	0.250	18.2*	0.205	10.1*
Following repeated level 3 X	0.10	N/A	N/A	0.250	14.0*	0.205	14.1*
Following level 4 X-Z	0.10	N/A	N/A	0.250	15.5*	0.213	13.8*
Following level 4 X	0.10	N/A	N/A	0.250	17.7*	0.213	10.5*
Following repeated level 4 X-Z	0.10	N/A	N/A	0.250	19.1*	0.213	9.7*
Following level 5 X	0.10	0.364	14.7	0.267	15.5*	0.242	8.9*
Media day							
Initial of media day	0.10	N/A	N/A	0.267	14.6*	0.242	16.8*
Following repeated level 4 X-Z	0.10	N/A	N/A	0.267	16.9*	0.242	10.5*
Dampers disconnected through pressure release							
Following disconnection	0.10	N/A	N/A	0.267	16.7*	0.242	8.1*
Following repeated level 3 X	0.10	N/A	N/A	0.267	15.9*	0.242	8.2*
Following repeated level 4 X	0.10	N/A	N/A	0.267	16.9*	0.246	9.6*
Following repeated level 5 X	0.10	0.381	12.8	0.267	17.9*	0.250	10.3*

* Denotes the use of symmetry for the calculation of the half-power bandwidth

Appendix H

Table H.5: Evolution of natural periods and damping ratios for Test Phase 3

		Mode 1 (Transverse)		Mode 2 (Coupled Longitud.-Torsional)		Mode 3	
Description	Ampl. (g)	T (sec)	ζ (%)	T (sec)	ζ (%)	T (sec)	ζ (%)
Initial, prior to any seismic test	0.05	0.296	10.7	0.216	6.5	0.170	6.7
Following level 1 X-Y-Z	0.05	0.296	9.3	0.219	6.0	0.170	6.0
Following level 1 X-Y	0.05	0.296	10.0	0.219	13.1*	0.170	6.7
Following level 2 X-Y-Z	0.05	0.327	12.7	0.229	13.2*	0.178	6.6
Following level 2 X-Y	0.05	0.333	13.7	0.232	13.4*	0.184	7.7

* Denotes the use of symmetry for the calculation of the half-power bandwidth

Table H.6: Evolution of natural periods and damping ratios for Test Phase 4

		Mode 1 (Transverse)		Mode 2 (Coupled Longitud.-Torsional)		Mode 3	
Description	Ampl. (g)	T (sec)	ζ (%)	T (sec)	ζ (%)	T (sec)	ζ (%)
Initial, prior to any seismic test	0.05	0.296	10.9	0.222	4.3	0.163	6.2
Following level 1 X-Y-Z	0.05	0.296	12.3	0.222	12.2	0.163	8.8
Following level 1 X-Y	0.05	0.296	13.8	0.222	12.3*	0.172	10.4
Following level 2 X-Y-Z	0.05	0.327	14.0	0.229	12.5*	0.180	9.7*
Following level 2 X-Y	0.05	0.333	14.5	0.229	13.5*	0.190	12.7*

* Denotes the use of symmetry for the calculation of the half-power bandwidth

Appendix H

Table H.7: Evolution of natural periods and damping ratios for Test Phase 5

		Mode 1		Mode 2		Mode 3	
		(Transverse)		(Coupled Longitud.-Torsional)			
Description	Ampl. (g)	T (sec)	ζ (%)	T (sec)	ζ (%)	T (sec)	ζ (%)
Initial, prior to any seismic test	0.05	0.286	17.9	0.198	17.1	0.127	5.0
Following level 1 X-Y-Z	0.05	0.286	11.3	0.203	17.5	0.127	7.9
Following level 1 X-Y	0.05	0.286	12.0	0.203	17.7	0.127	7.9
Following level 2 X-Y-Z	0.05	0.296	12.0	0.211	19.0	0.131	9.0
Following level 2 X-Y	0.05	0.296	15.0	0.211	18.2	0.131	7.5
Following level 3 X-Y-Z	0.05	0.314	15.3	0.216	18.2	0.138	8.2
Following level 3 X-Y	0.05	0.314	15.1	0.213	17.0	0.138	7.1
Following level 4 X-Y-Z	0.05	0.327	15.2	0.213	15.5	0.139	7.2
Following level 4 X-Y	0.05	0.356	16.4	0.229	25.1*	0.155	8.6
Following 25 % of level 5 X-Y-Z	0.05	0.356	16.9	0.229	25.0*	0.154	8.4
Media day							
Initial of media day	0.05	0.327	16.2	0.222	28.1*	0.148	11.0
Following level 5 X-Y-Z	0.05	0.333	13.8	0.232	23.8*	0.154	7.2

* Denotes the use of symmetry for the calculation of the half-power bandwidth

Appendix H

Initial Mode Shapes from Phase 1 White Noise Tests

Structure description: wood shear walls only, no wall finishes.

White noise tests: NWP1W01 and NWP1W04.

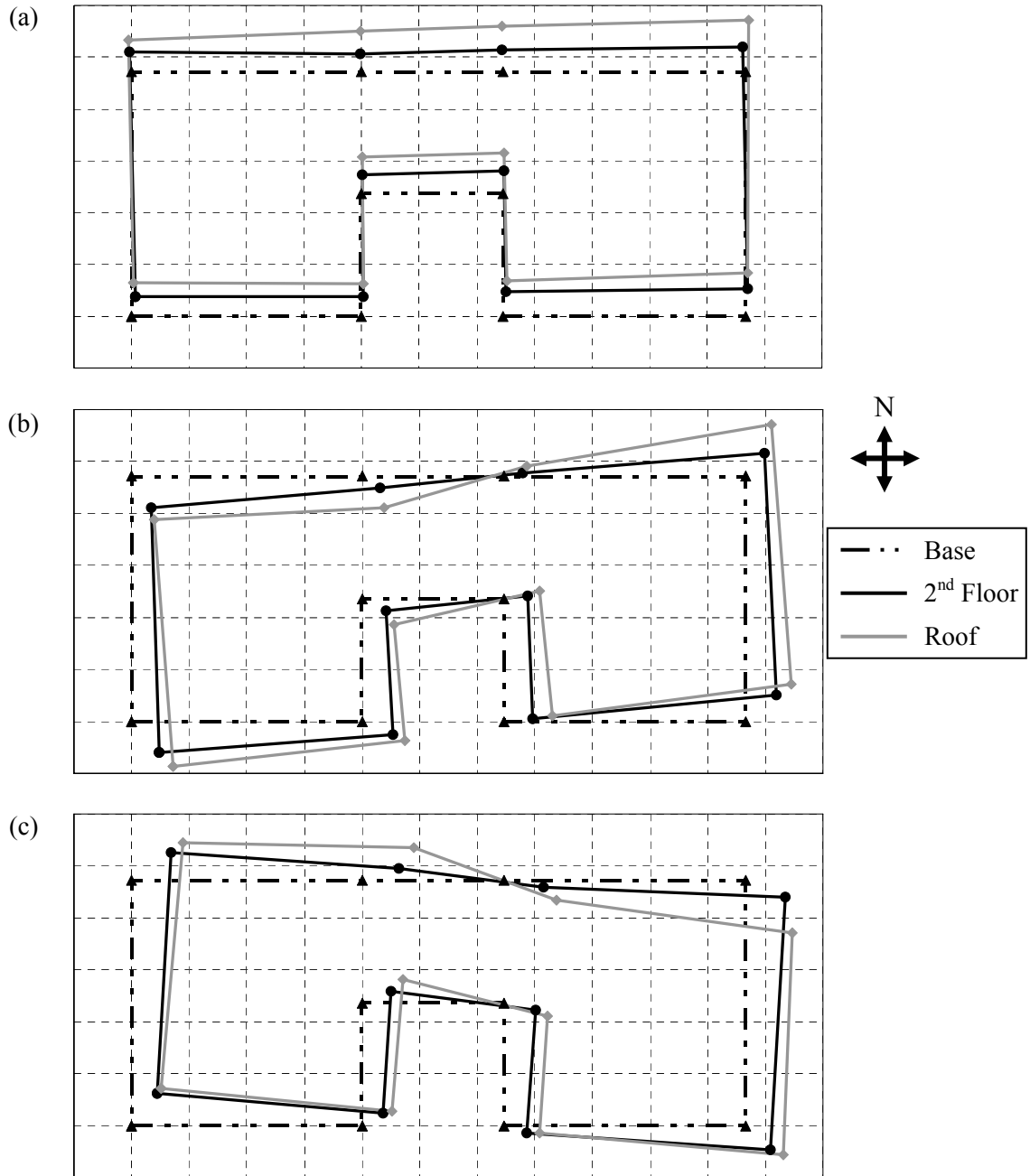


Figure H.1: Mode shapes from Test Phase 1, (a) mode 1, $T_1 = 0.33$ sec, (b) mode 2, $T_2 = 0.23$ sec, (c) mode 3, $T_3 = 0.18$ sec

Appendix H

Initial Mode Shapes from Phase 2 White Noise Tests

Structure description: wood shear walls with viscous dampers, no wall finishes.

White noise tests: NWP2W01 and NWP2W03.

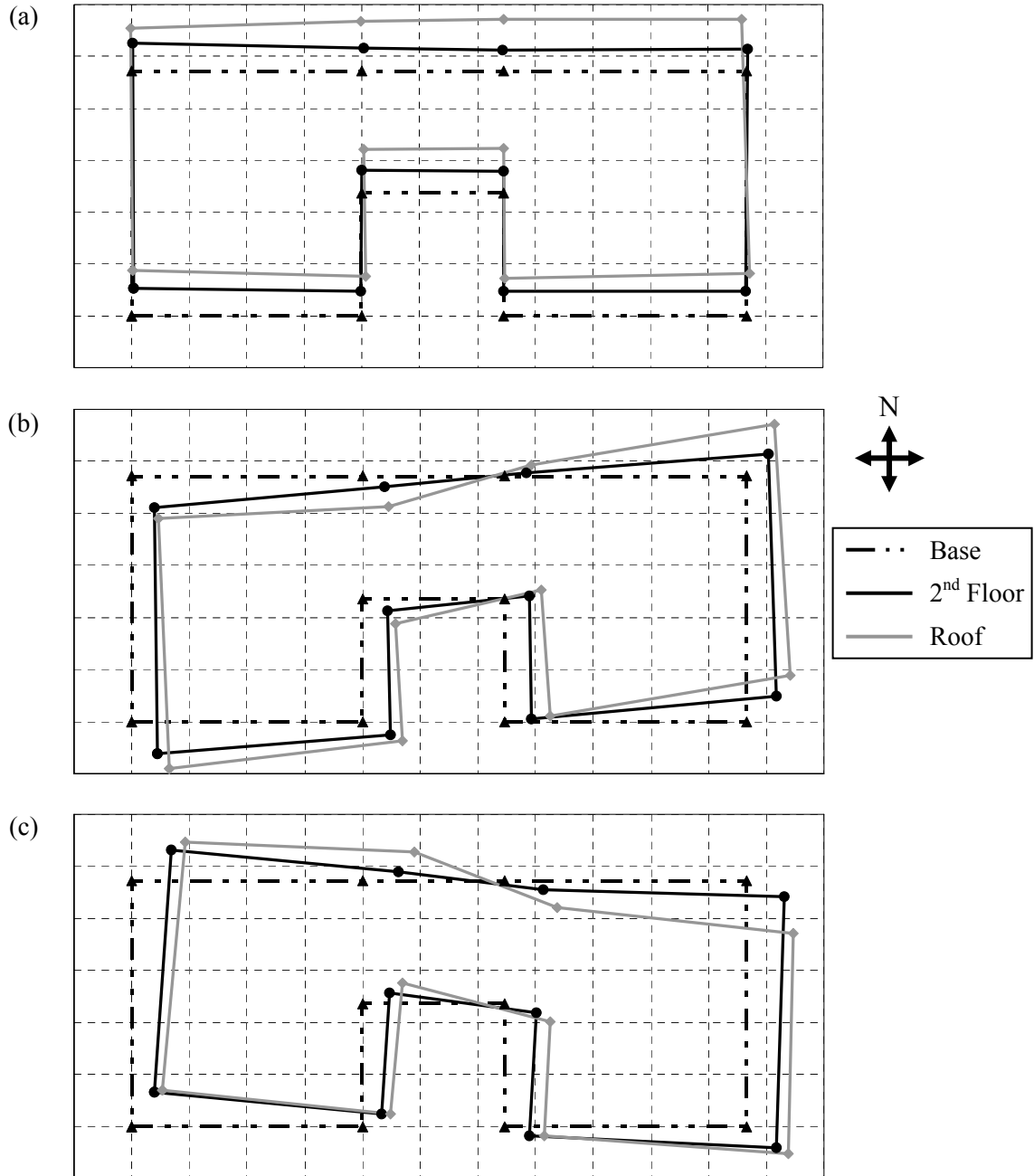


Figure H.2: Mode shapes from Test Phase 2, (a) mode 1, $T_1 = 0.33$ sec, (b) mode 2, $T_2 = 0.23$ sec, (c) mode 3, $T_3 = 0.18$ sec

Appendix H

Initial Mode Shapes from Phase 3 White Noise Tests

Structure description: wood shear walls and drywall on internal sides of shear walls.

White noise tests: NWP3W05 and NWP3W06.

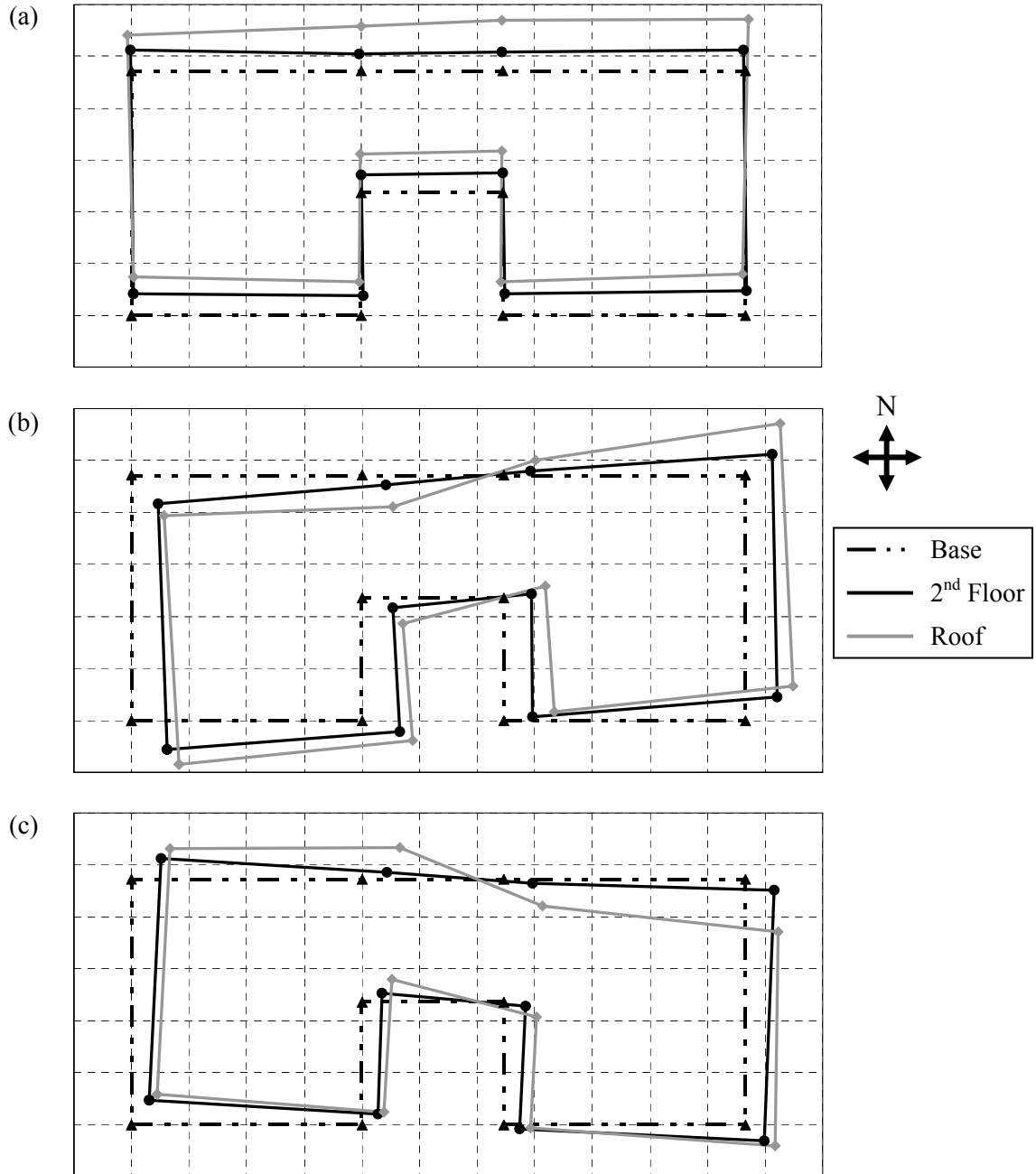


Figure H.3: Mode shapes from Test Phase 3, (a) mode 1, $T_1 = 0.30$ sec, (b) mode 2, $T_2 = 0.22$ sec, (c) mode 3, $T_3 = 0.17$ sec

Appendix H

Initial Mode Shapes from Phase 4 White Noise Tests

Structure description: wood shear walls and drywall on internal sides of shear and partition walls.

White noise tests: NWP4W01 and NWP4W02.

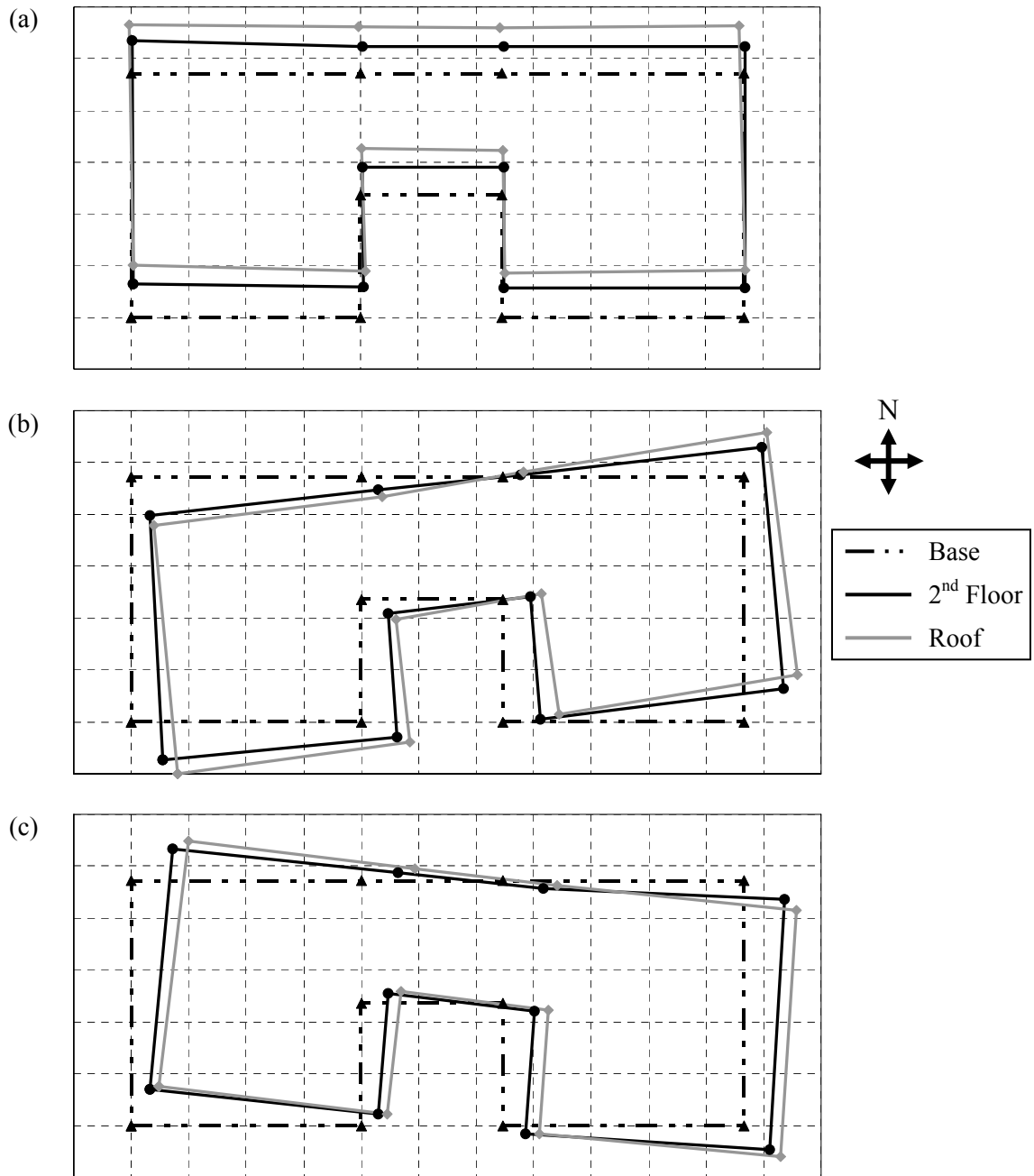


Figure H.4: Mode shapes from Test Phase 4, (a) mode 1, $T_1 = 0.30$ sec, (b) mode 2, $T_2 = 0.22$ sec, (c) mode 3, $T_3 = 0.16$ sec

Appendix H

Initial Mode Shapes from Phase 5 White Noise Tests

Structure description: wood shear walls, stucco on external sides of shear walls and drywall on internal sides of shear and partition walls.

White noise tests: NWP5W01 and NWP5W02.

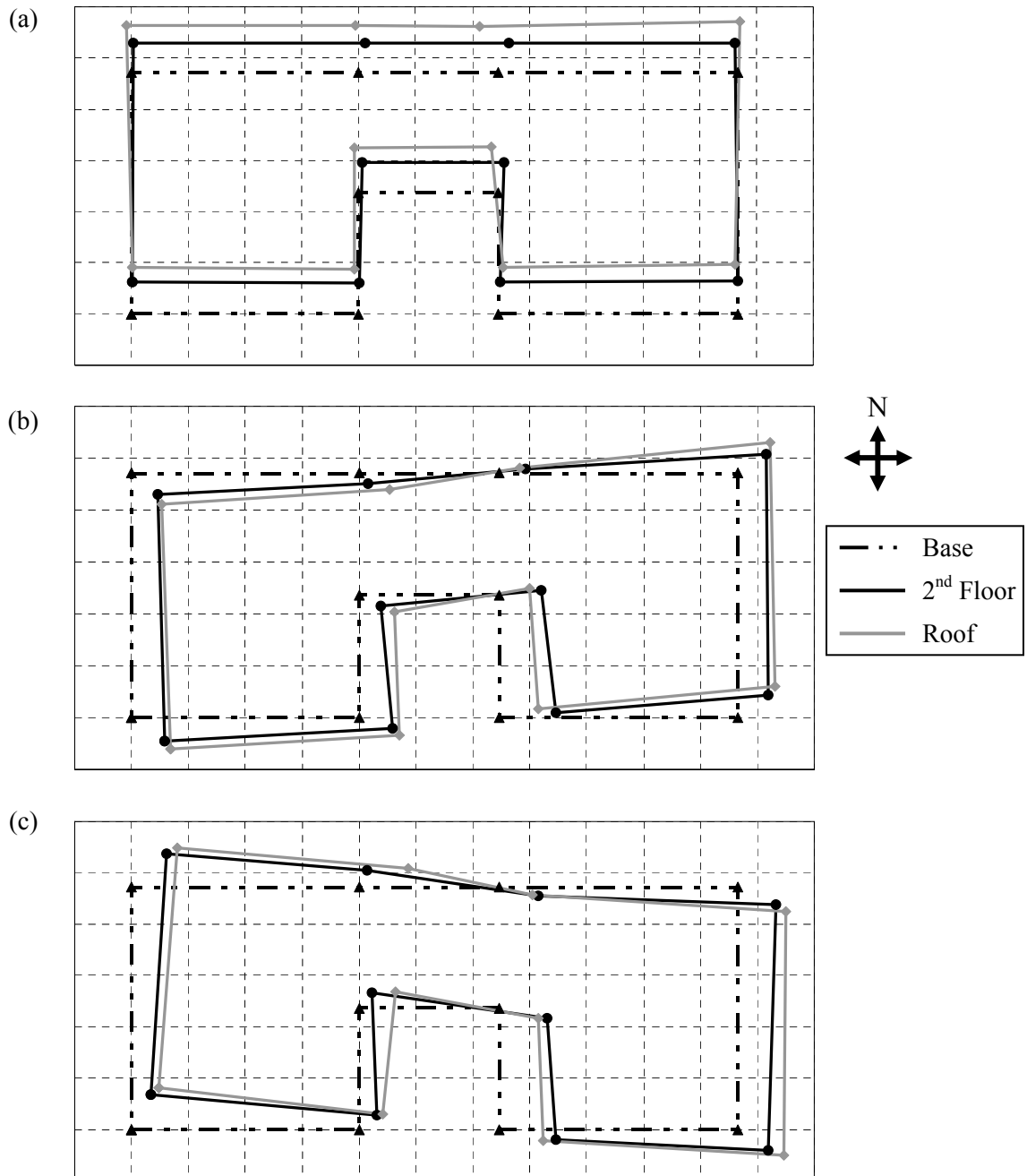


Figure H.5: Mode shapes from Test Phase 5, (a) mode 1, $T_1 = 0.29$ sec, (b) mode 2, $T_2 = 0.20$ sec, (c) mode 3, $T_3 = 0.13$ sec

Appendix I

Fidelity of Shake Table Motion

Appendix I

Phase 1, NWP1S01 Seismic Test

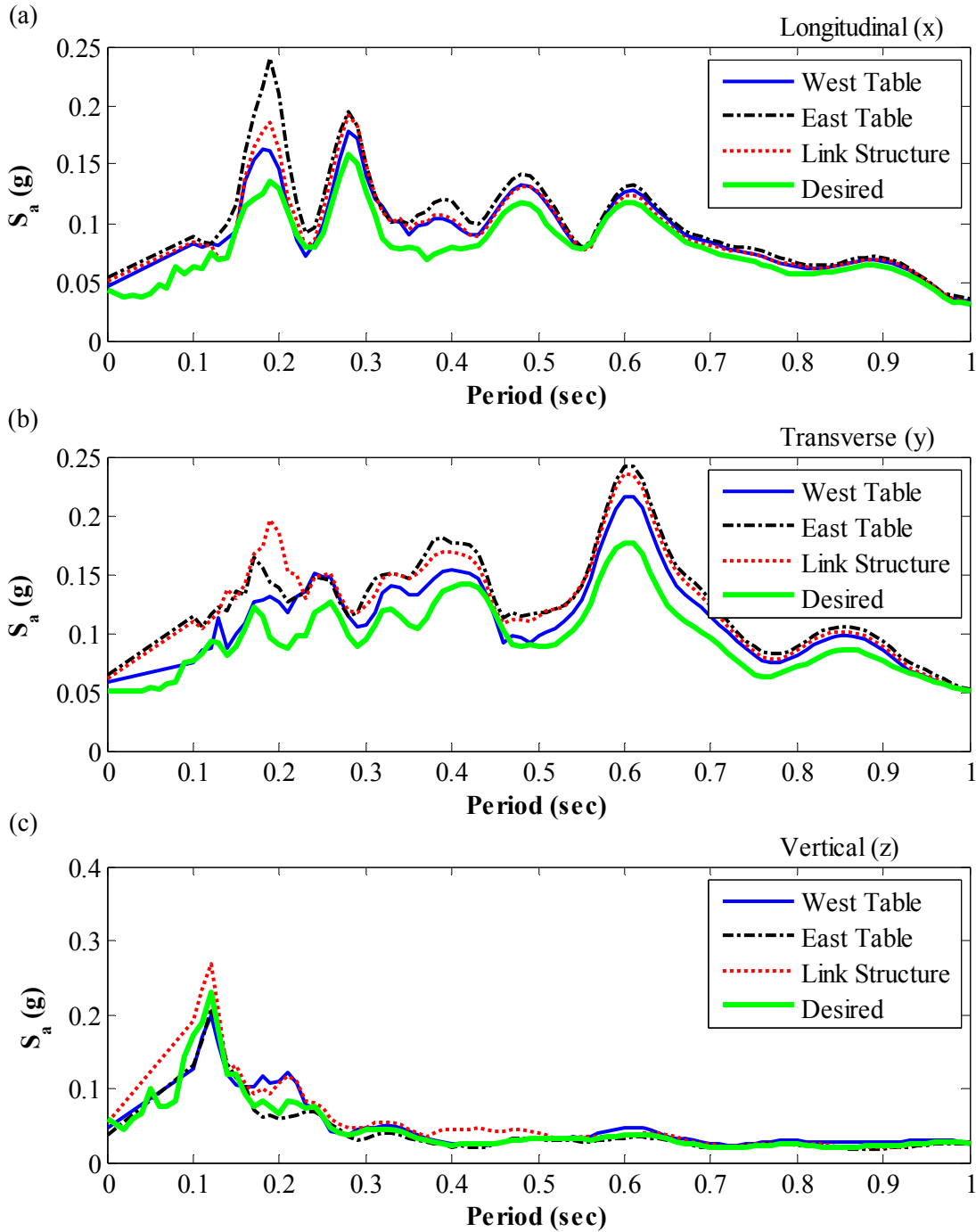


Figure I.1: Acceleration response spectra of shake table motion for 5 % damping in (a) longitudinal, (b) transverse, and (c) vertical direction, for Test NWP1S01

Appendix I

Phase 1, NWP1S02 Seismic Test

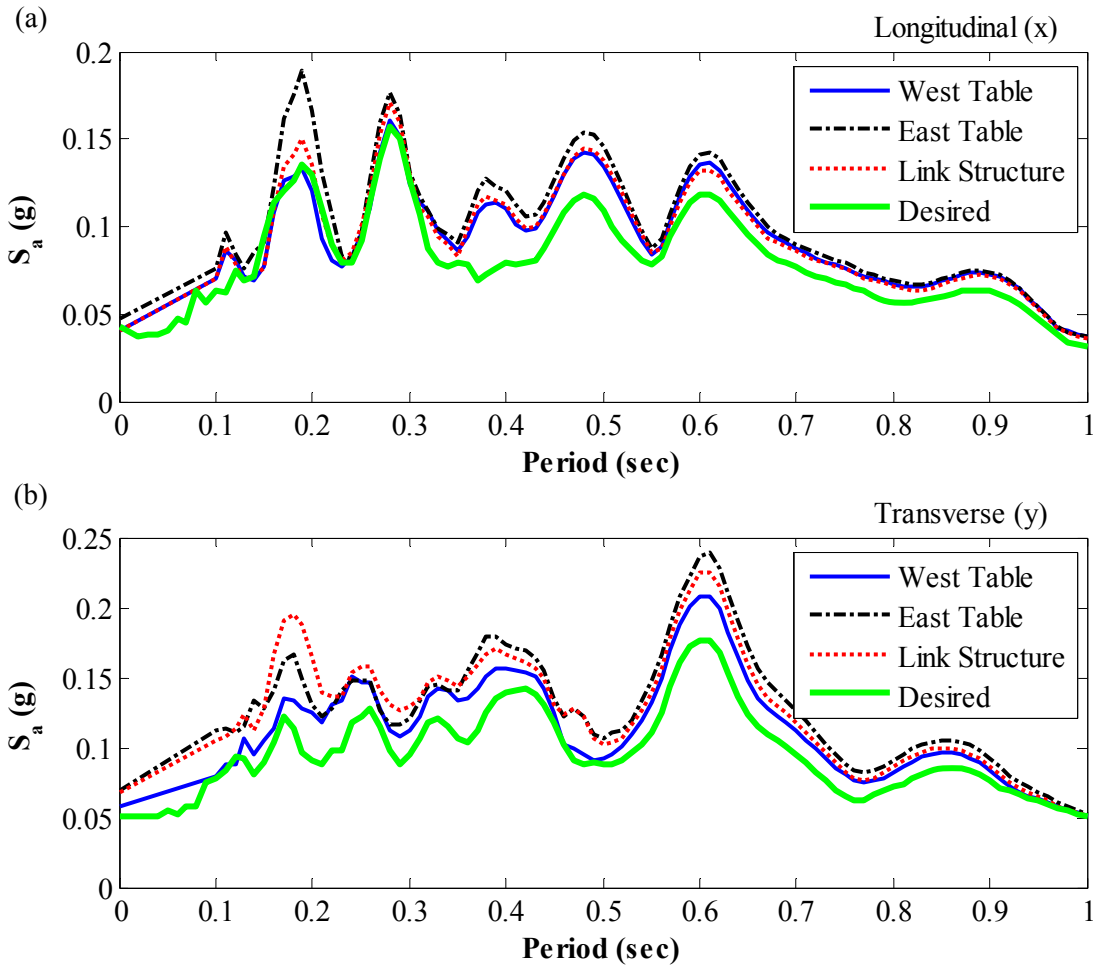


Figure I.2: Acceleration response spectra of shake table motion for 5 % damping in (a) longitudinal, and (b) transverse direction, for Test NWP1S02

Appendix I

Phase 1, NWP1S03 Seismic Test

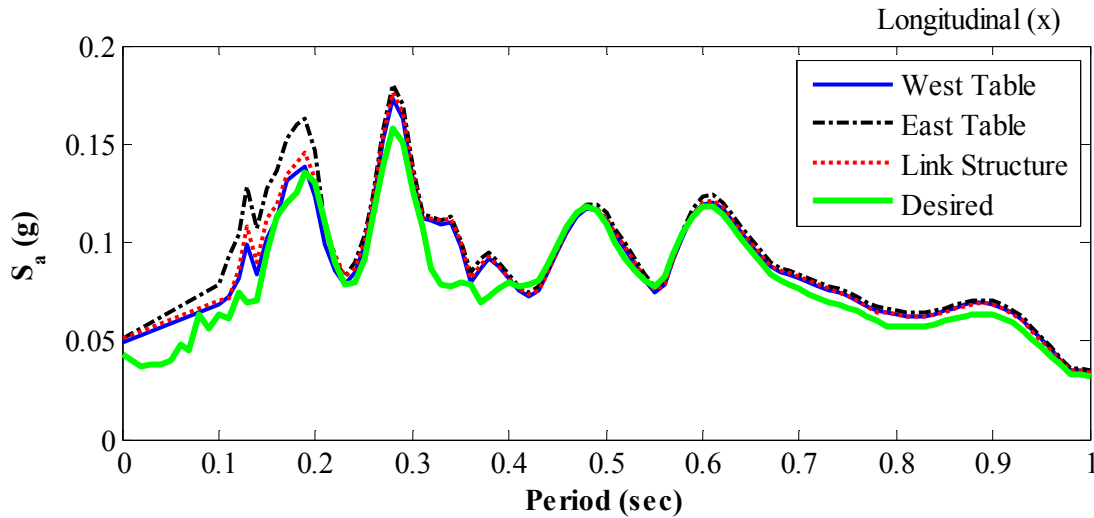


Figure I.3: Acceleration response spectra of shake table motion for 5 % damping in longitudinal direction, for Test NWP1S03

Phase 1, NWP1S04 Seismic Test

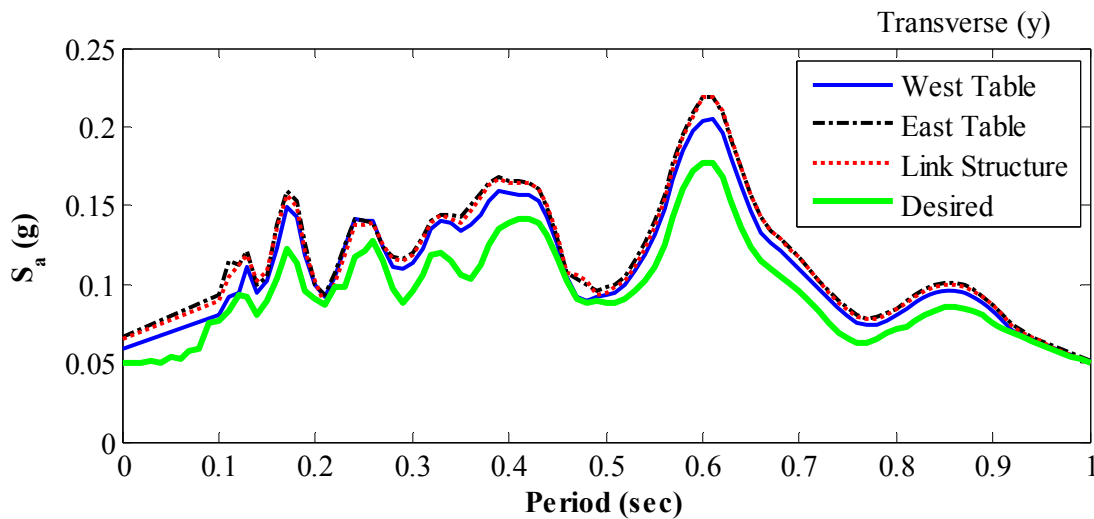


Figure I.4: Acceleration response spectra of shake table motion for 5 % damping in transverse direction, for Test NWP1S04

Appendix I

Phase 1, NWP1S05 Seismic Test

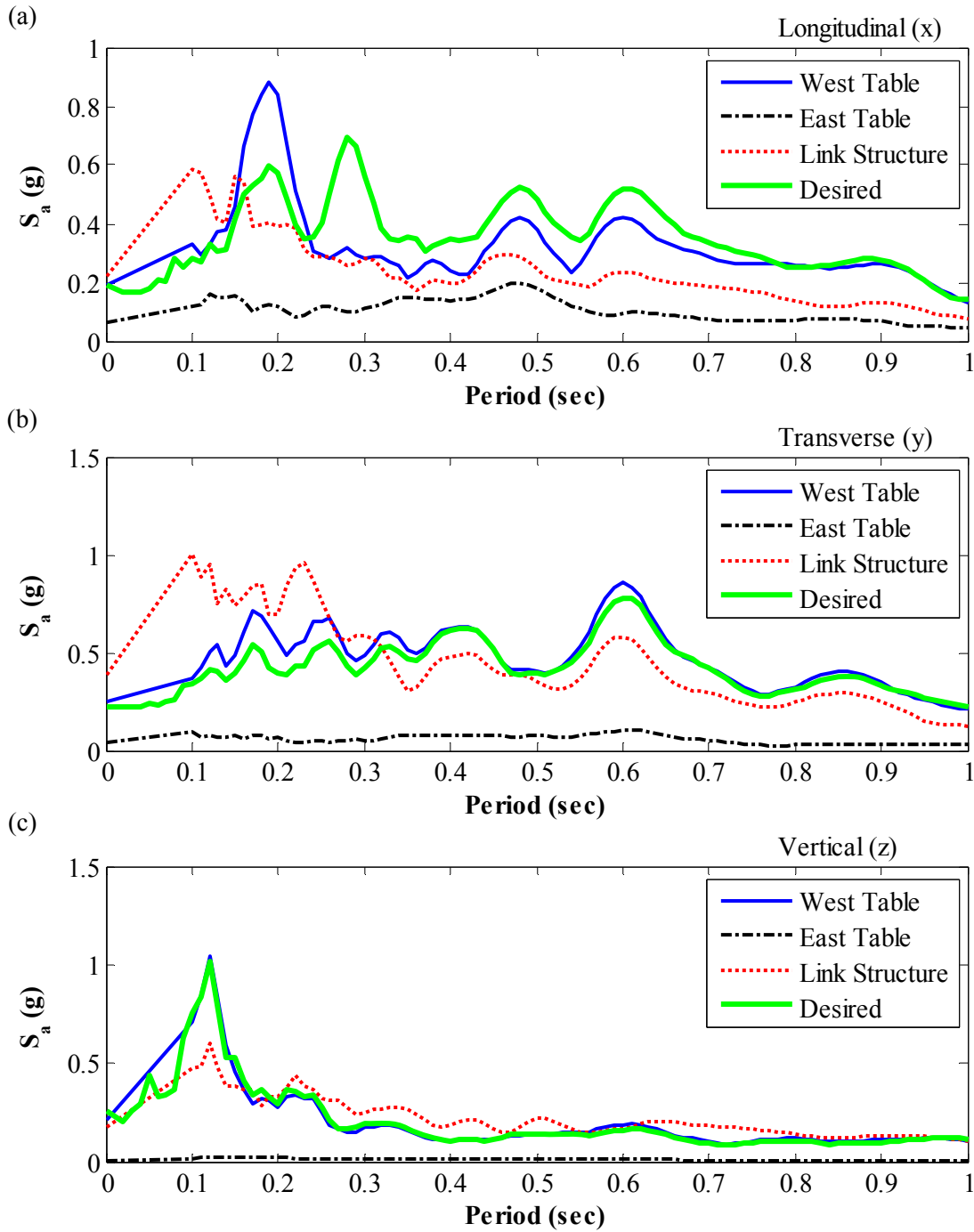


Figure I.5: Acceleration response spectra of shake table motion for 5 % damping in (a) longitudinal, (b) transverse, and (c) vertical direction, for Test NWP1S05

Appendix I

Phase 1, NWP1S17 Seismic Test

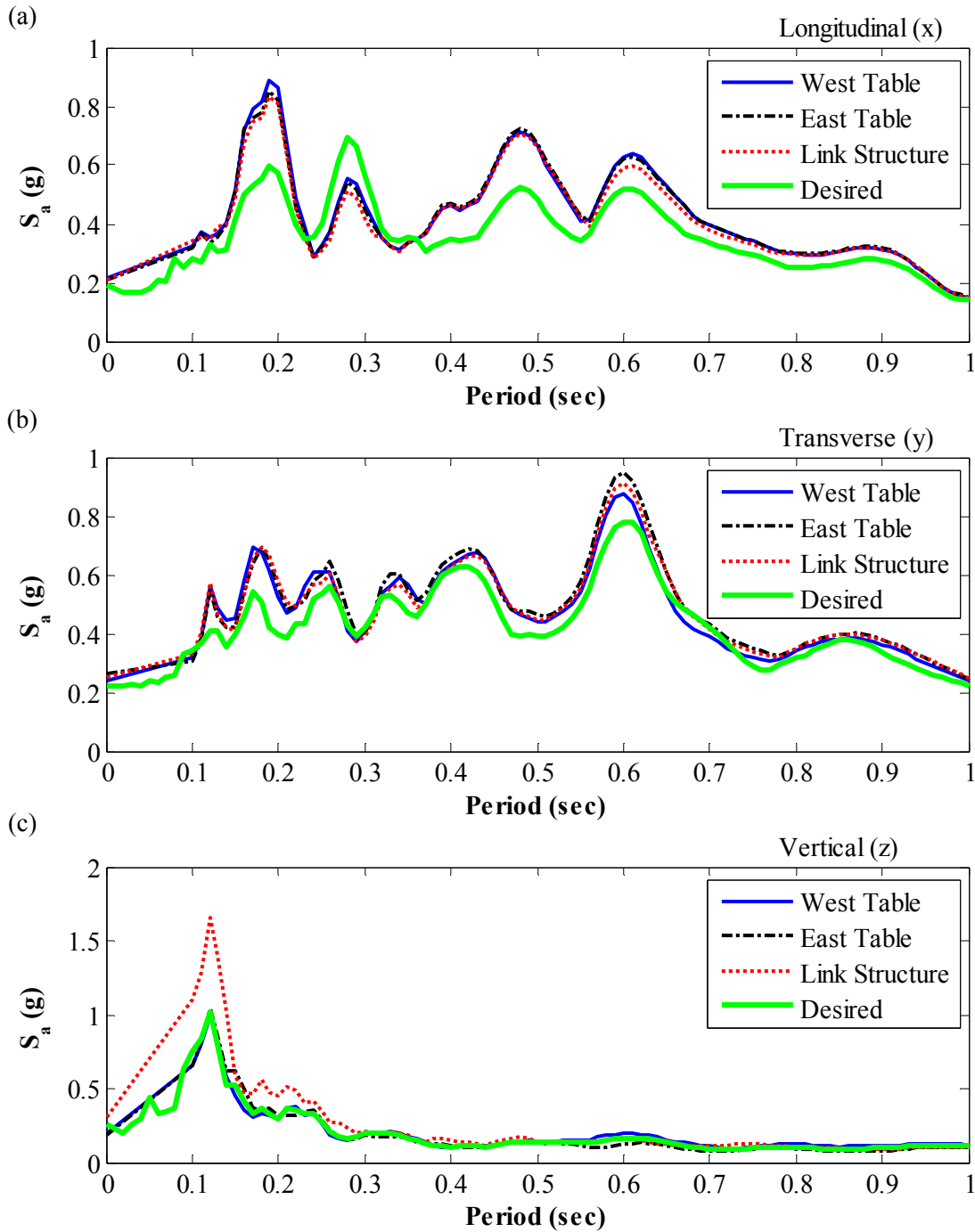


Figure I.6: Acceleration response spectra of shake table motion for 5 % damping in (a) longitudinal, (b) transverse, and (c) vertical direction, for Test NWP1S17

Appendix I

Phase 1, NWP1S06 Seismic Test

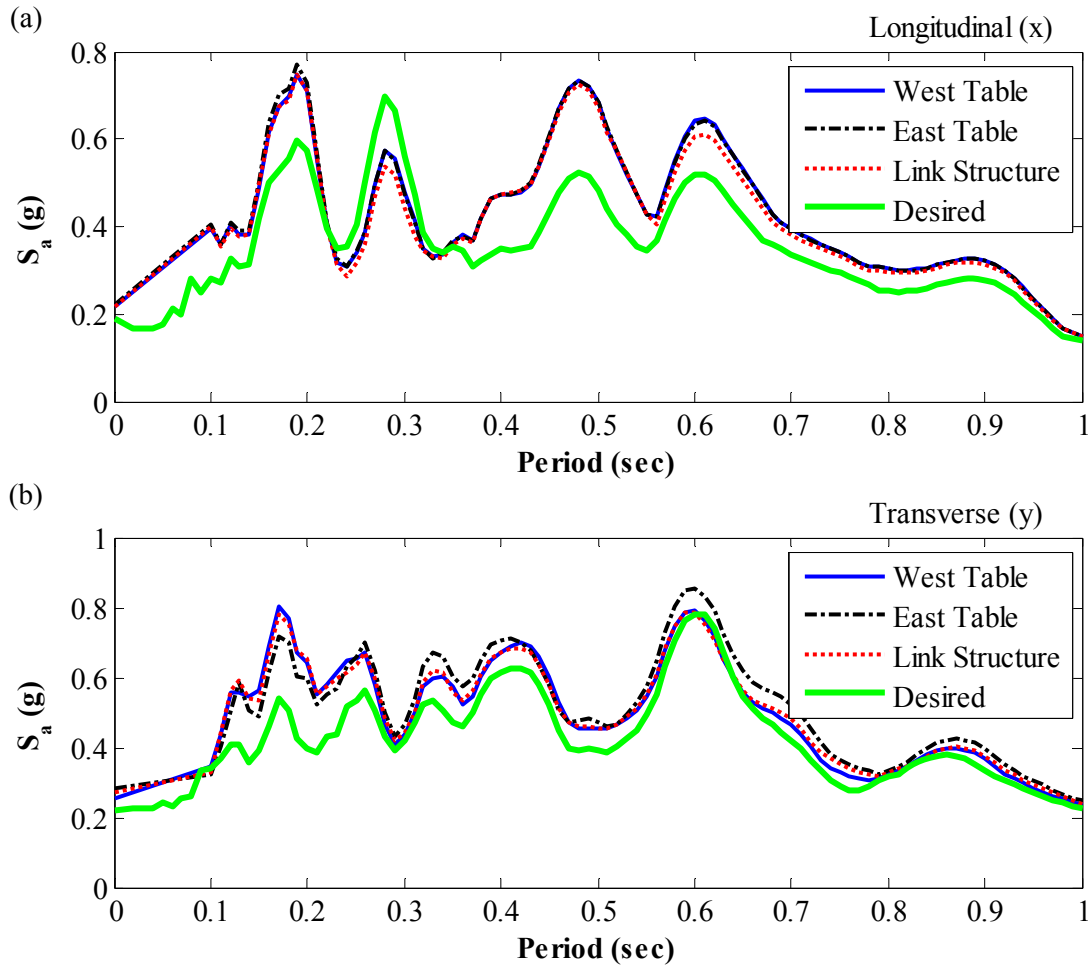


Figure I.7: Acceleration response spectra of shake table motion for 5 % damping in (a) longitudinal, and (b) transverse direction, for Test NWP1S06

Appendix I

Phase 1, NWP1S07 Seismic Test

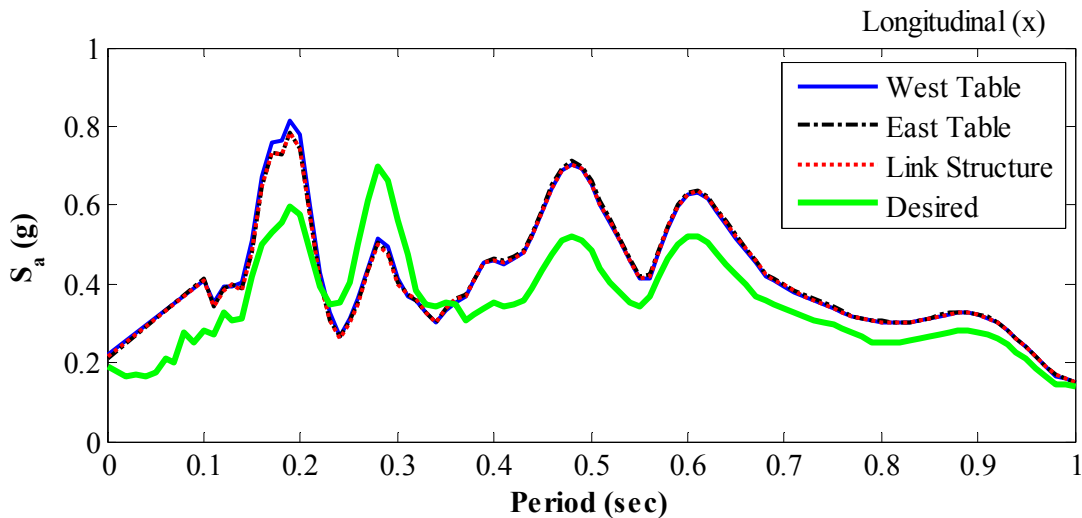


Figure I.8: Acceleration response spectra of shake table motion for 5 % damping in longitudinal direction, for Test NWP1S07

Phase 1, NWP1S10 Seismic Test

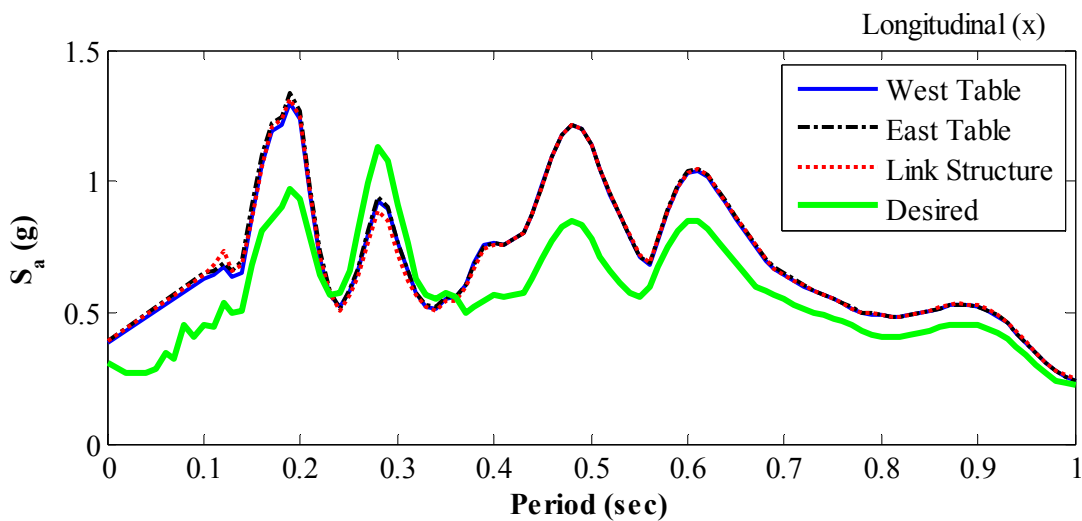


Figure I.9: Acceleration response spectra of shake table motion for 5 % damping in longitudinal direction, for Test NWP1S10

Appendix I

Phase 2, NWP2S01 Seismic Test

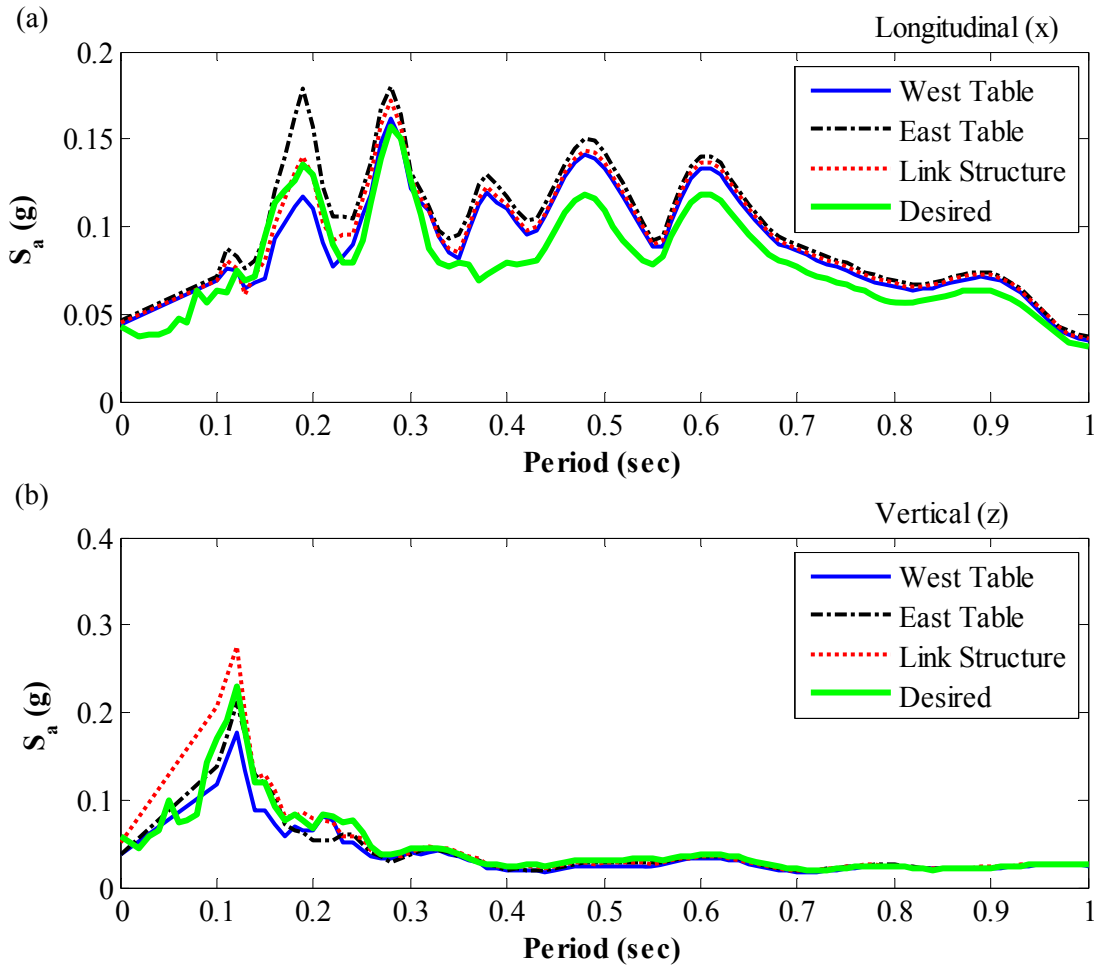


Figure I.10: Acceleration response spectra of shake table motion for 5 % damping in (a) longitudinal, and (b) vertical direction, for Test NWP2S01

Appendix I

Phase 2, NWP2S03 Seismic Test

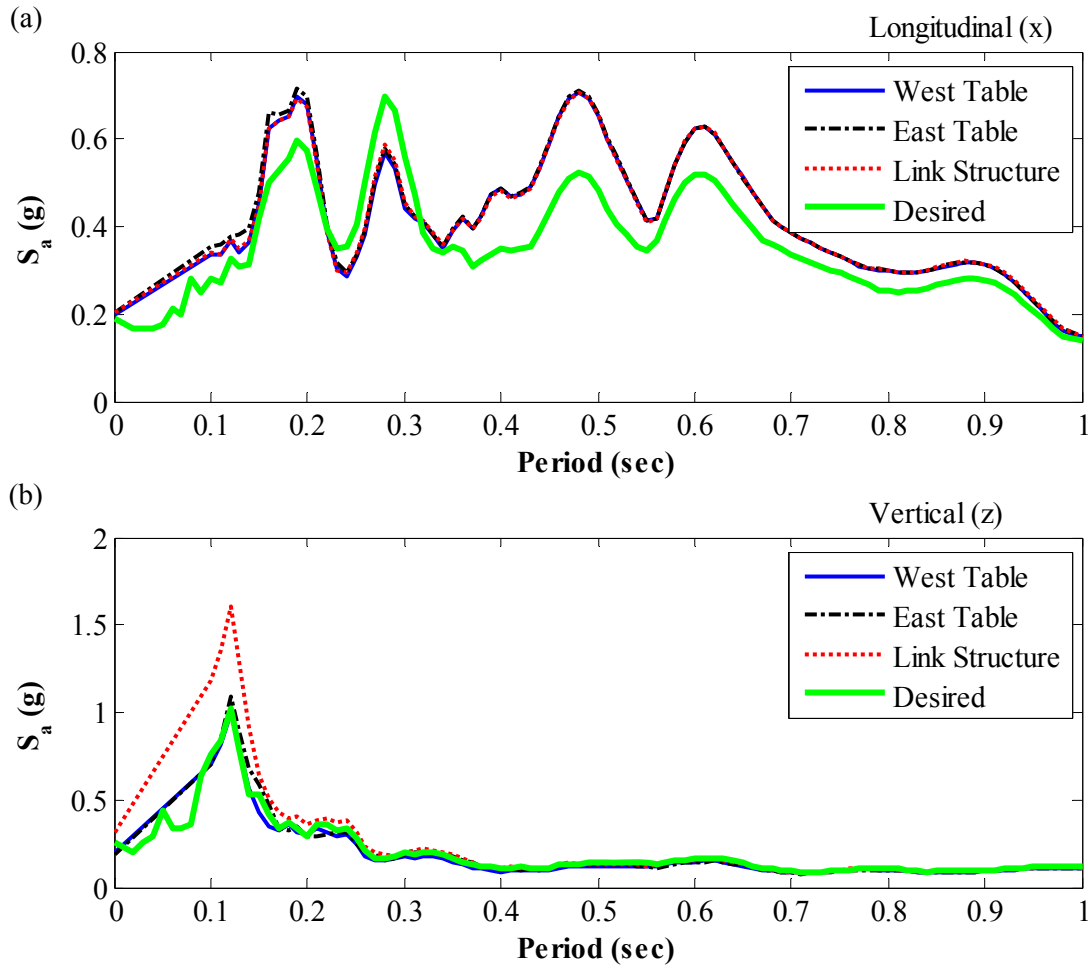


Figure I.11: Acceleration response spectra of shake table motion for 5 % damping in (a) longitudinal, and (b) vertical direction, for Test NWP2S03

Appendix I

Phase 2, NWP2S21 Seismic Test

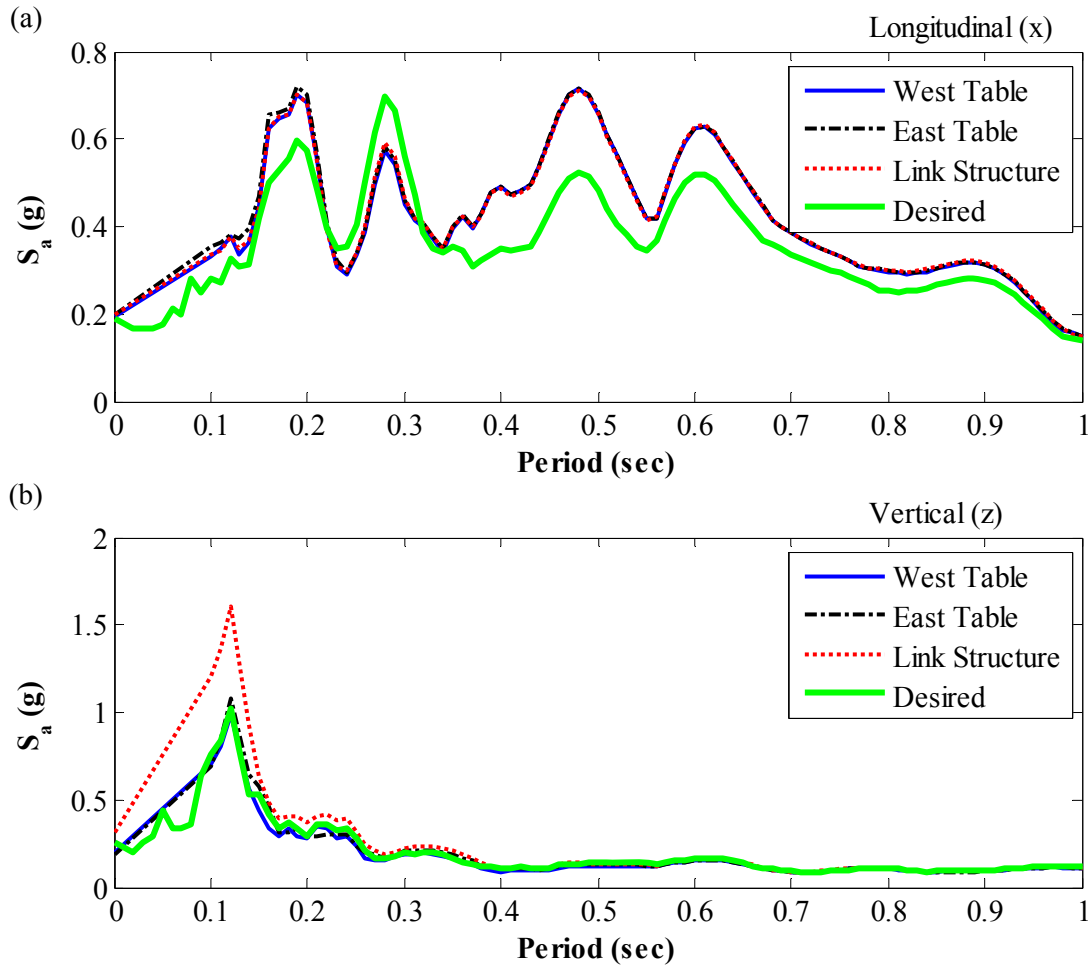


Figure I.12: Acceleration response spectra of shake table motion for 5 % damping in (a) longitudinal, and (b) vertical direction, for Test NWP2S21

Appendix I

Phase 2, NWP2S02 Seismic Test

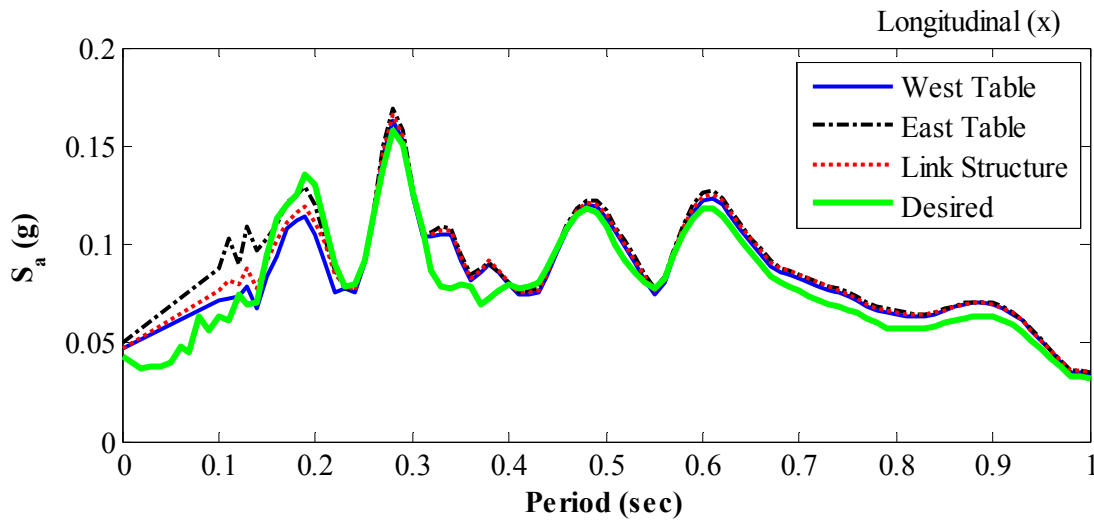


Figure I.13: Acceleration response spectra of shake table motion for 5 % damping in longitudinal direction, for Test NWP2S02

Phase 2, NWP2S04 Seismic Test

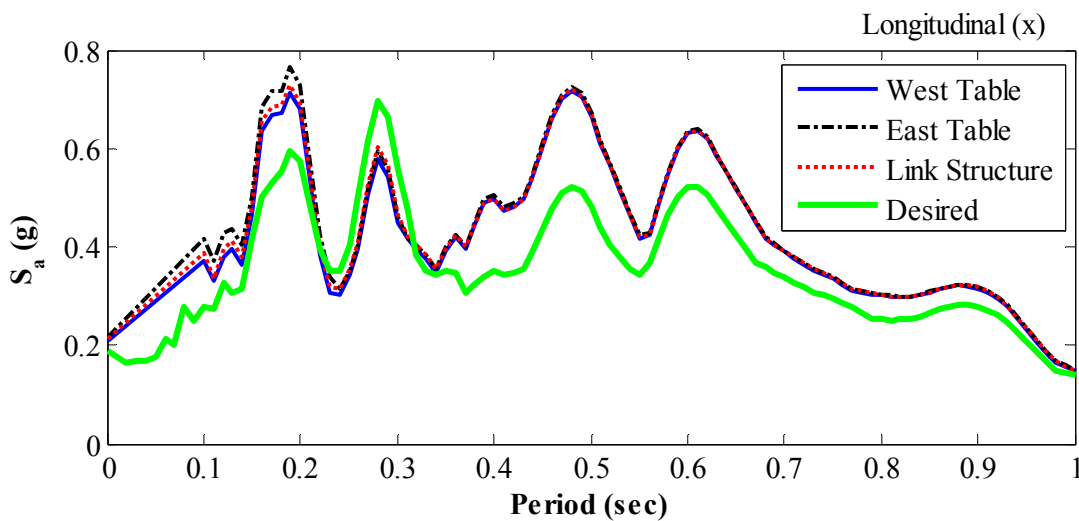


Figure I.14: Acceleration response spectra of shake table motion for 5 % damping in longitudinal direction, for Test NWP2S04

Appendix I

Phase 2, NWP2S05 Seismic Test

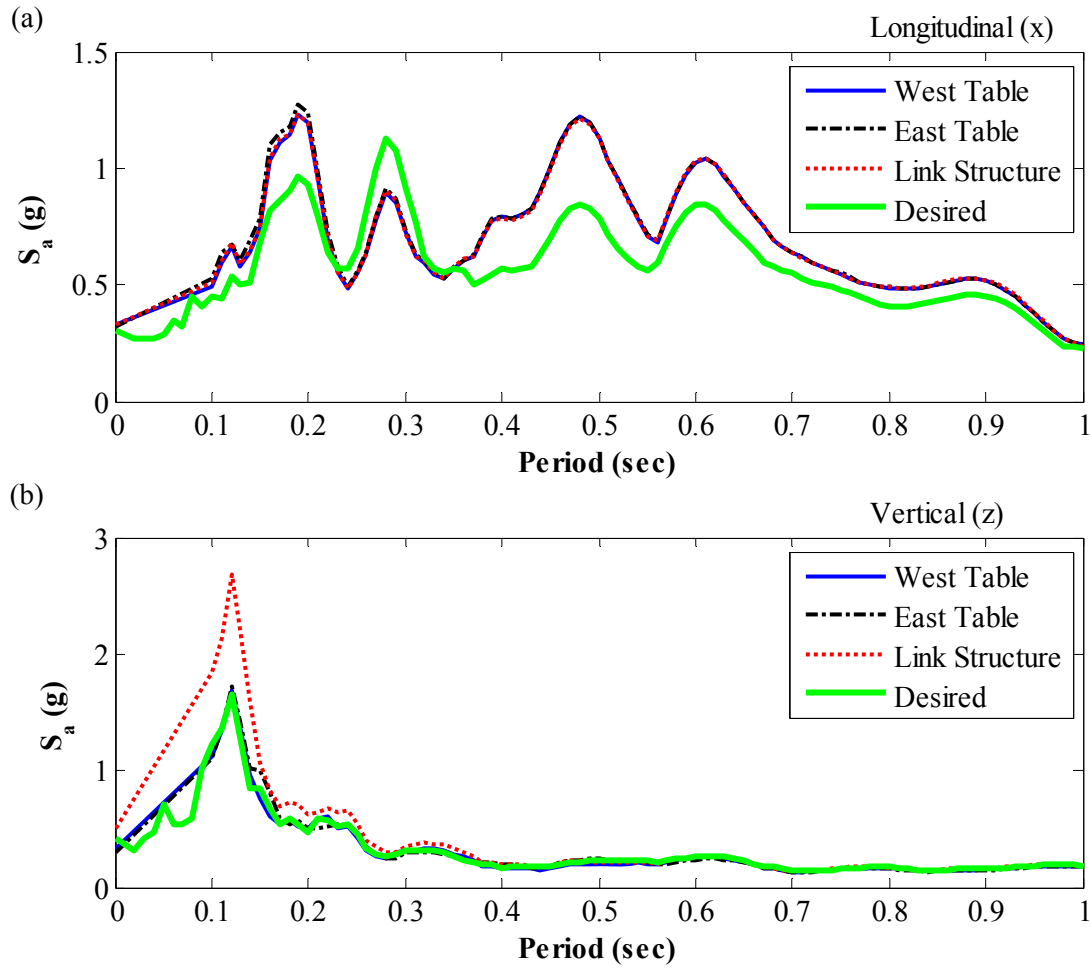


Figure I.15: Acceleration response spectra of shake table motion for 5 % damping in (a) longitudinal, and (b) vertical direction, for Test NWP2S05

Appendix I

Phase 2, NWP2S24 Seismic Test

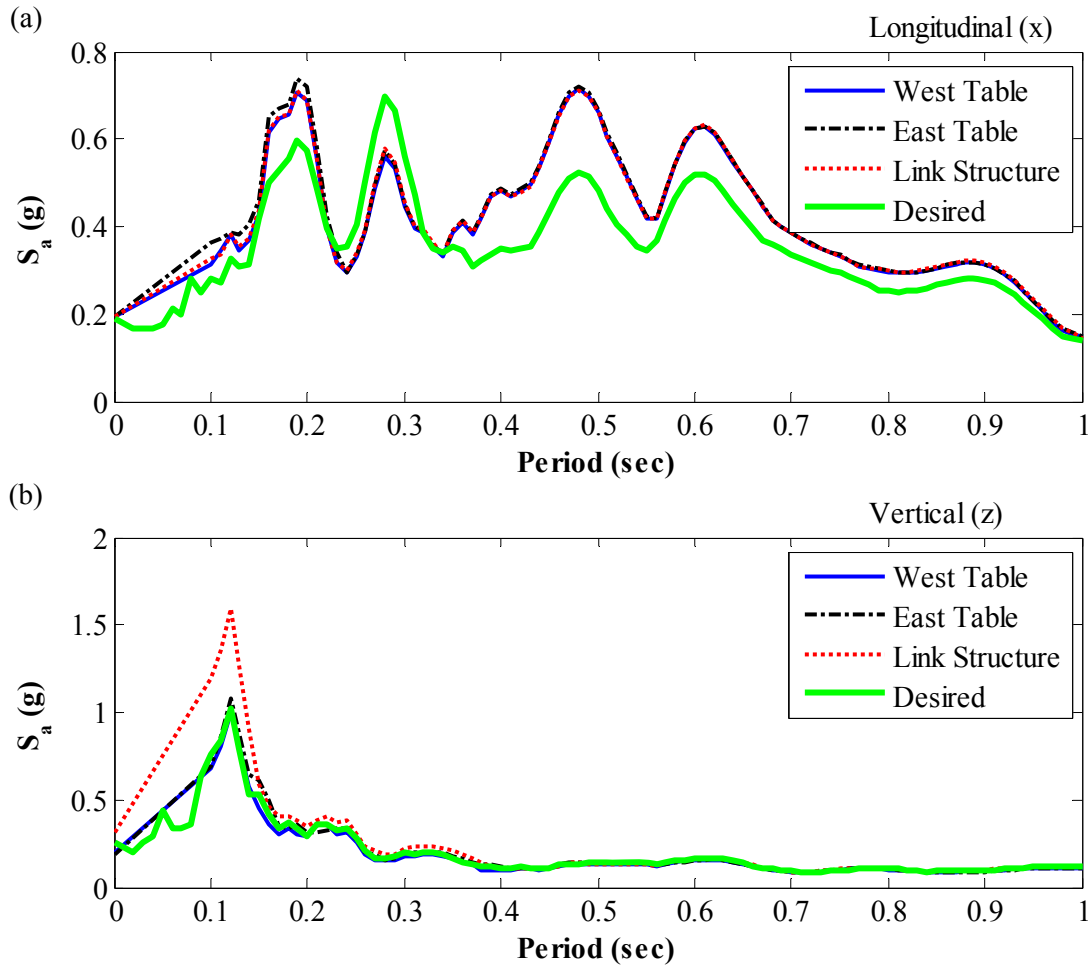


Figure I.16: Acceleration response spectra of shake table motion for 5 % damping in (a) longitudinal, and (b) vertical direction, for Test NWP2S24

Appendix I

Phase 2, NWP2S26 Seismic Test

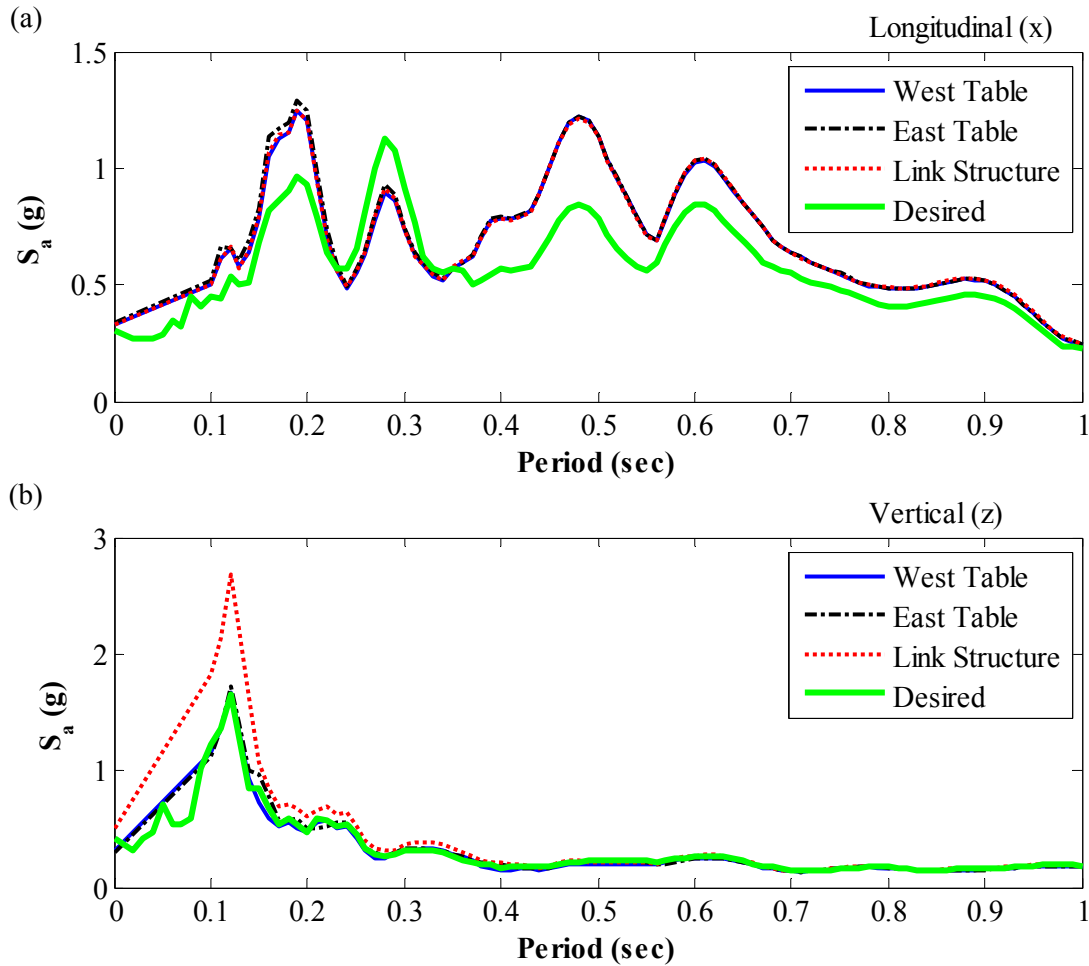


Figure I.17: Acceleration response spectra of shake table motion for 5 % damping in (a) longitudinal, and (b) vertical direction, for Test NWP2S26

Appendix I

Phase 2, NWP2S25 Seismic Test

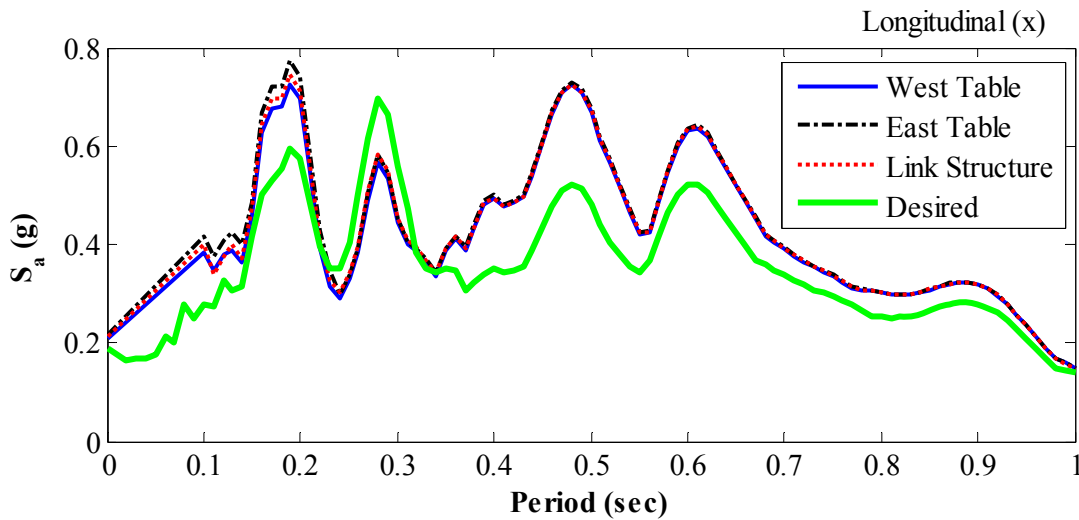


Figure I.18: Acceleration response spectra of shake table motion for 5 % damping in longitudinal direction, for Test NWP2S25

Phase 2, NWP2S06 Seismic Test

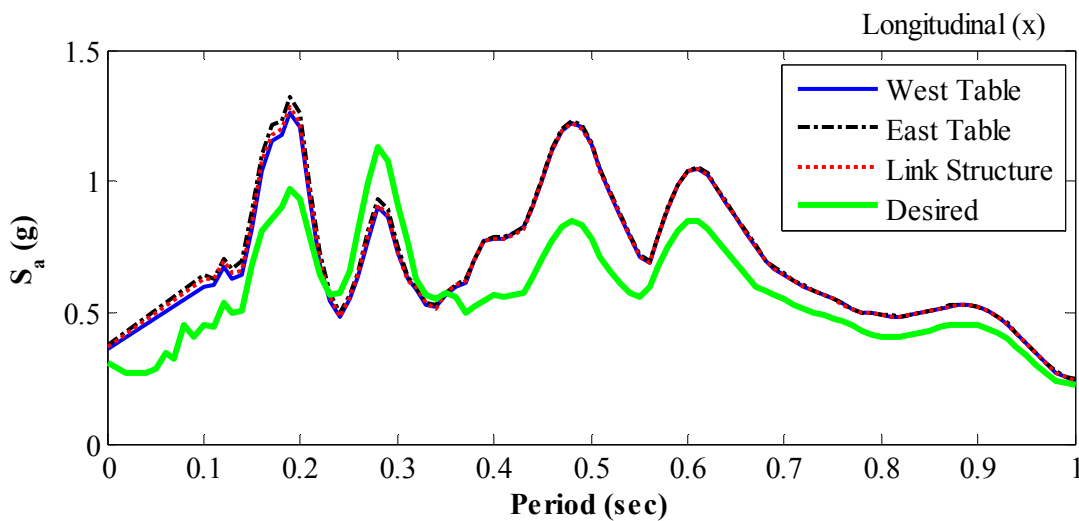


Figure I.19: Acceleration response spectra of shake table motion for 5 % damping in longitudinal direction, for Test NWP2S06

Appendix I

Phase 2, NWP2S07 Seismic Test

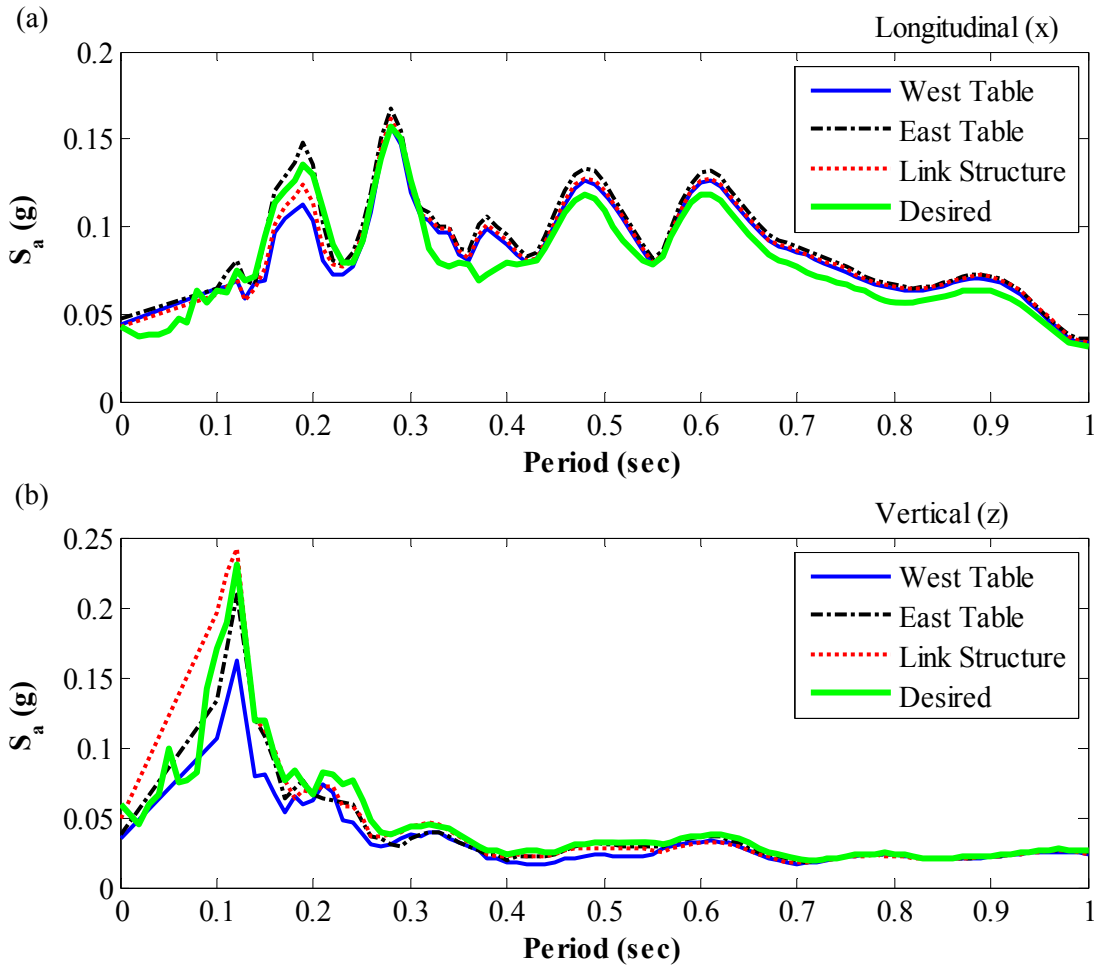


Figure I.20: Acceleration response spectra of shake table motion for 5 % damping in (a) longitudinal, and (b) vertical direction, for Test NWP2S07

Appendix I

Phase 2, NWP2S09 Seismic Test

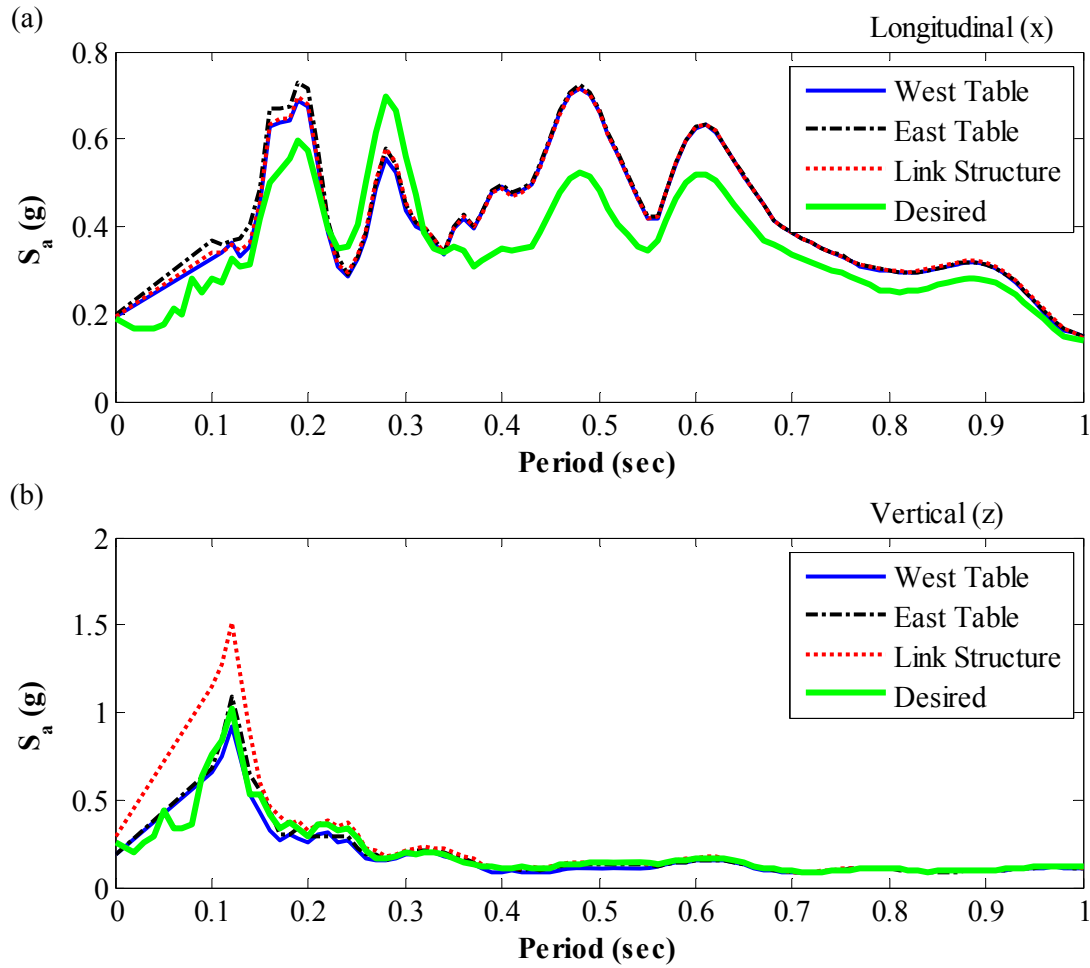


Figure I.21: Acceleration response spectra of shake table motion for 5 % damping in (a) longitudinal, and (b) vertical direction, for Test NWP2S09

Appendix I

Phase 2, NWP2S08 Seismic Test

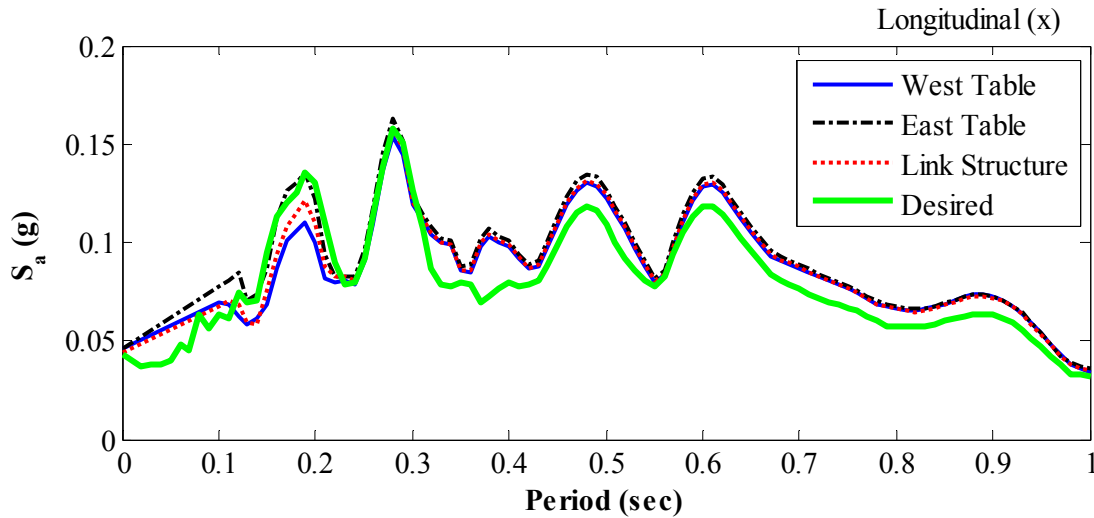


Figure I.22: Acceleration response spectra of shake table motion for 5 % damping in longitudinal direction, for Test NWP2S08

Phase 2, NWP2S10 Seismic Test

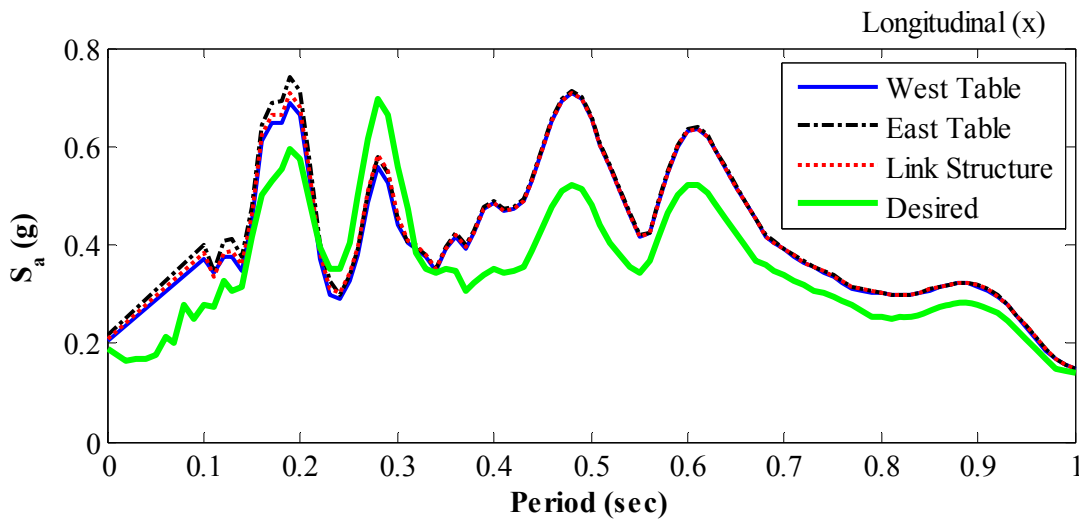


Figure I.23: Acceleration response spectra of shake table motion for 5 % damping in longitudinal direction, for Test NWP2S10

Appendix I

Phase 2, NWP2S11 Seismic Test

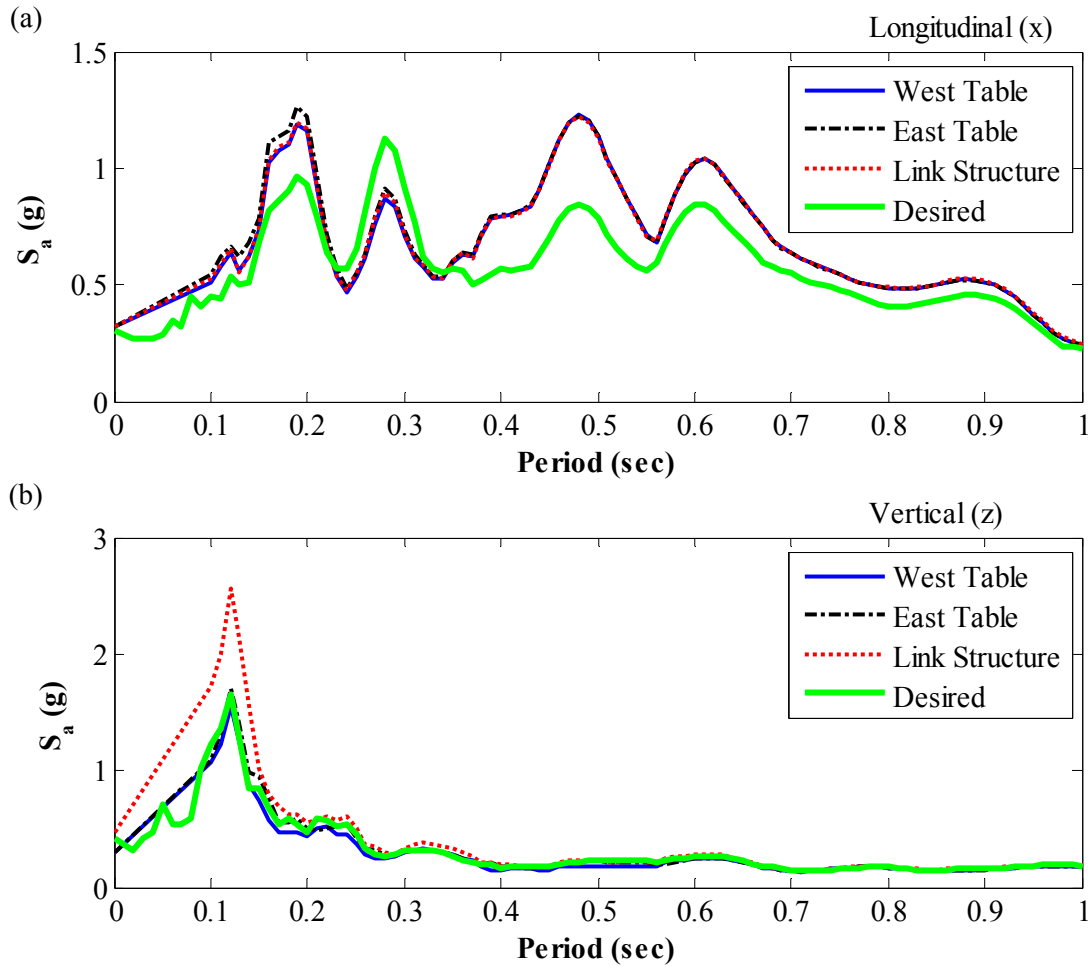


Figure I.24: Acceleration response spectra of shake table motion for 5 % damping in (a) longitudinal, and (b) vertical direction, for Test NWP2S11

Appendix I

Phase 2, NWP2S13 Seismic Test

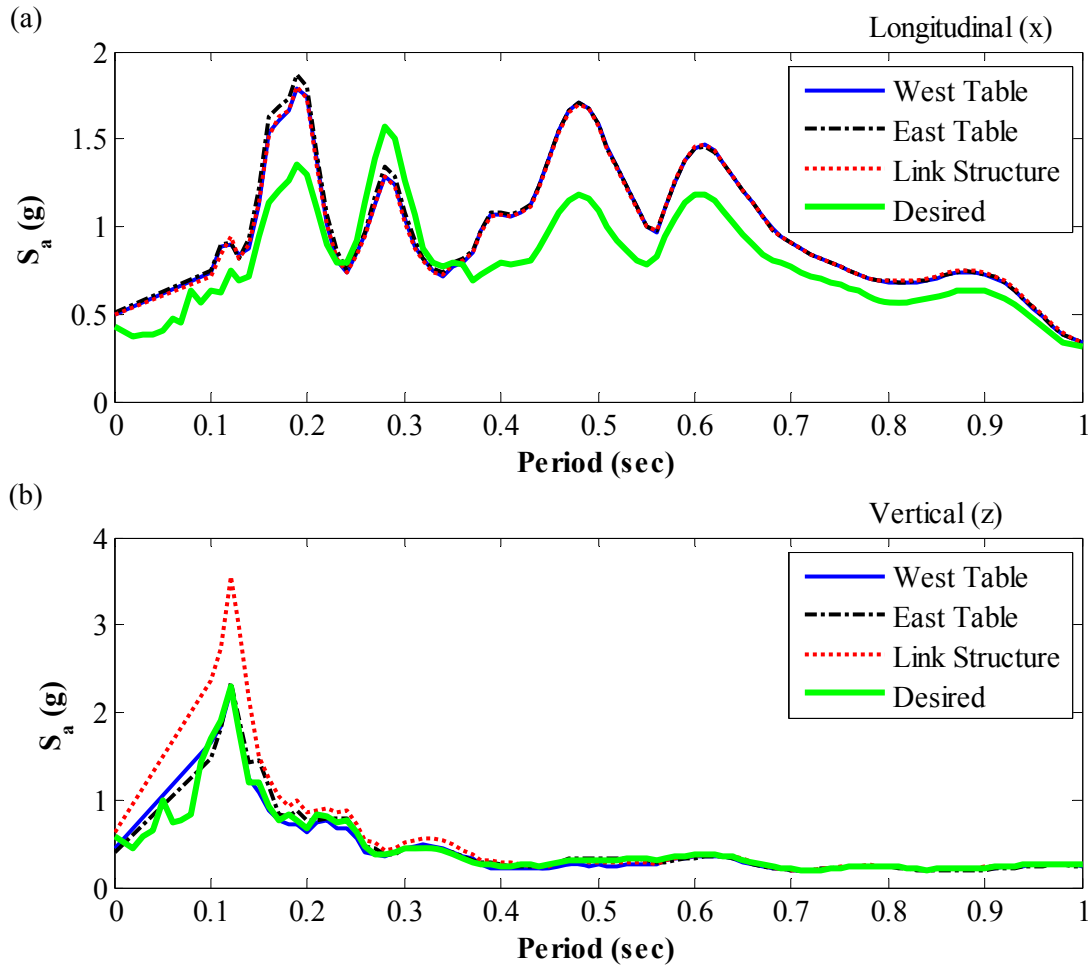


Figure I.25: Acceleration response spectra of shake table motion for 5 % damping in (a) longitudinal, and (b) vertical direction, for Test NWP2S13

Appendix I

Phase 2, NWP2S12 Seismic Test

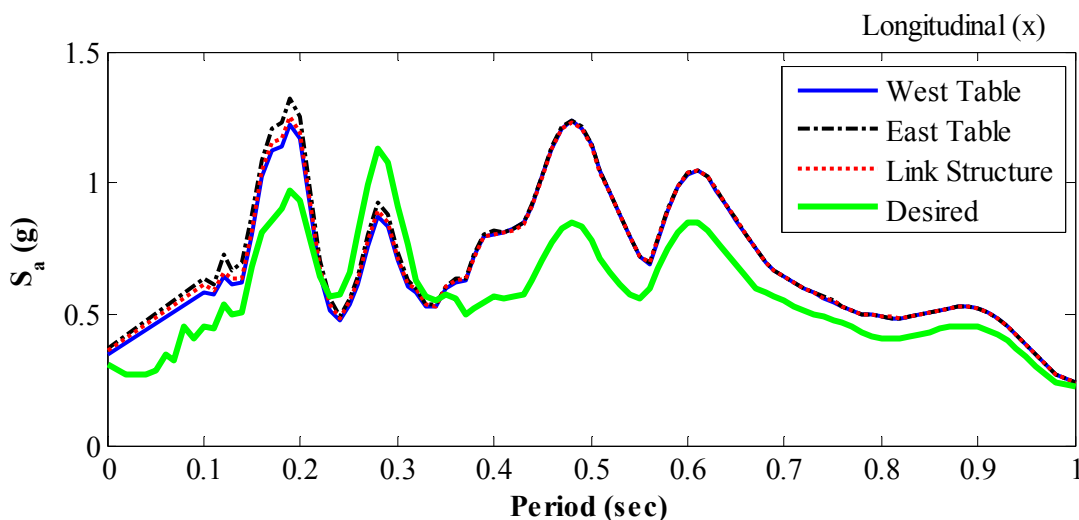


Figure I.26: Acceleration response spectra of shake table motion for 5 % damping in longitudinal direction, for Test NWP2S12

Phase 2, NWP2S14 Seismic Test

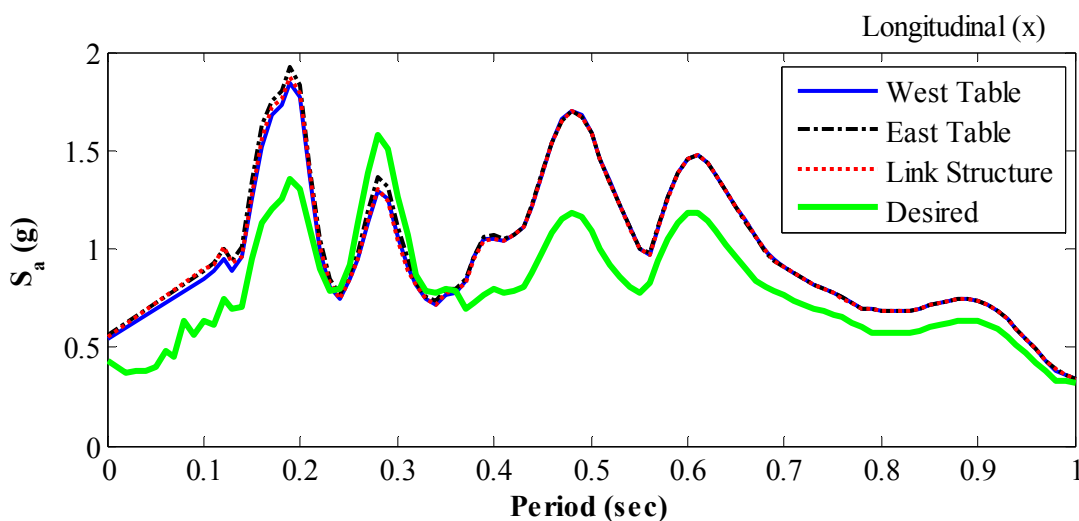


Figure I.27: Acceleration response spectra of shake table motion for 5 % damping in longitudinal direction, for Test NWP2S14

Appendix I

Phase 2, NWP2S17 Seismic Test

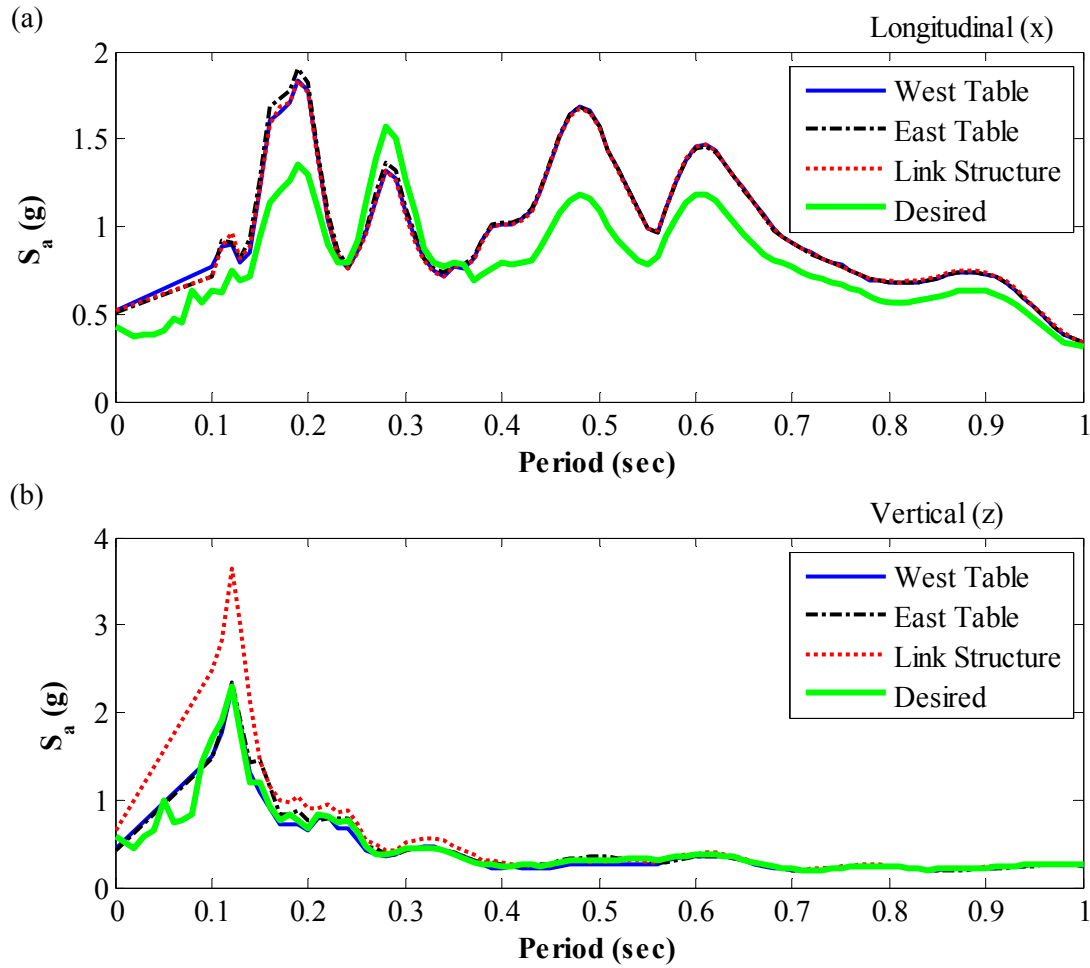


Figure I.28: Acceleration response spectra of shake table motion for 5 % damping in (a) longitudinal, and (b) vertical direction, for Test NWP2S17

Appendix I

Phase 2, NWP2S27 Seismic Test

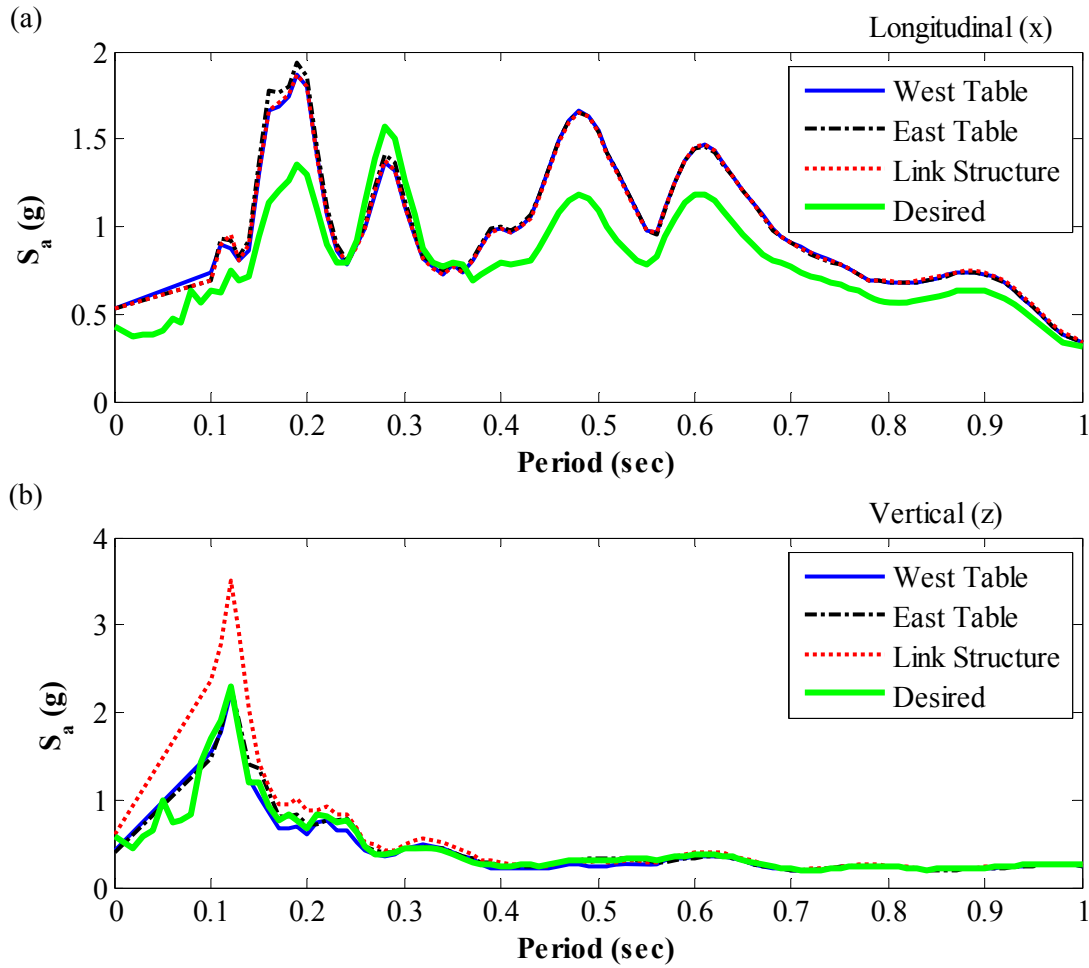


Figure I.29: Acceleration response spectra of shake table motion for 5 % damping in (a) longitudinal, and (b) vertical direction, for Test NWP2S27

Appendix I

Phase 2, NWP2S16 Seismic Test

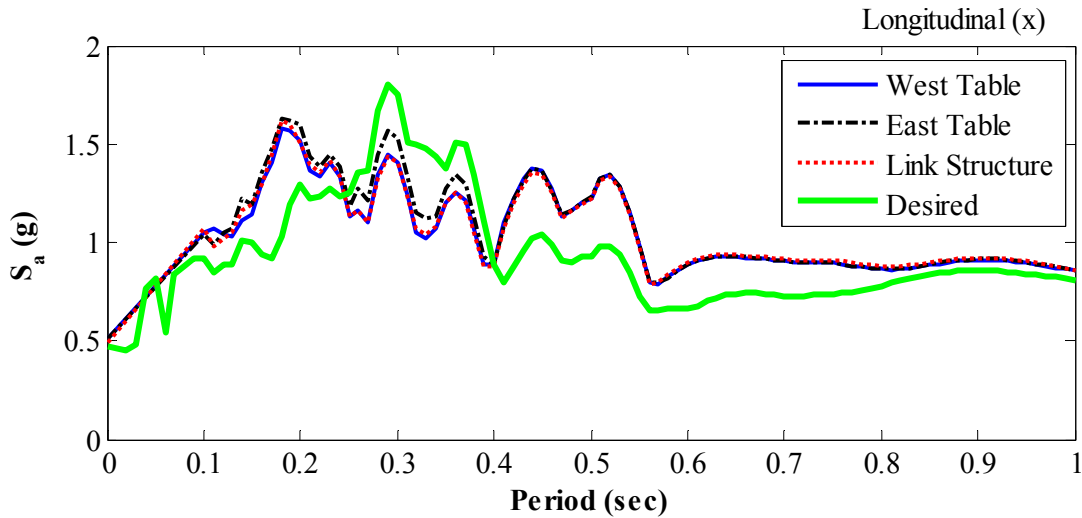


Figure I.30: Acceleration response spectra of shake table motion for 5 % damping in longitudinal direction, for Test NWP2S16

Phase 2, NWP2S28 Seismic Test

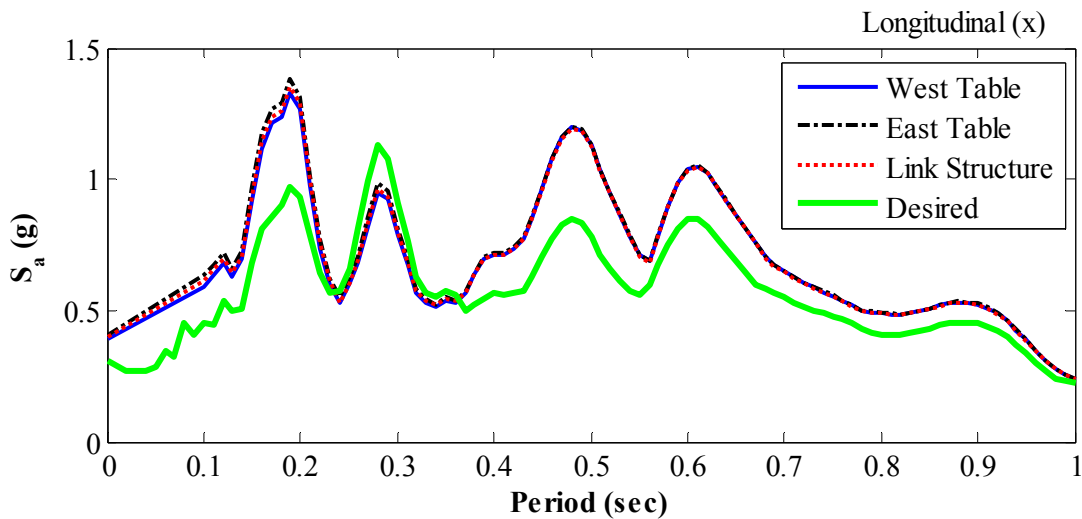


Figure I.31: Acceleration response spectra of shake table motion for 5 % damping in longitudinal direction, for Test NWP2S28

Appendix I

Phase 2, NWP2S29 Seismic Test

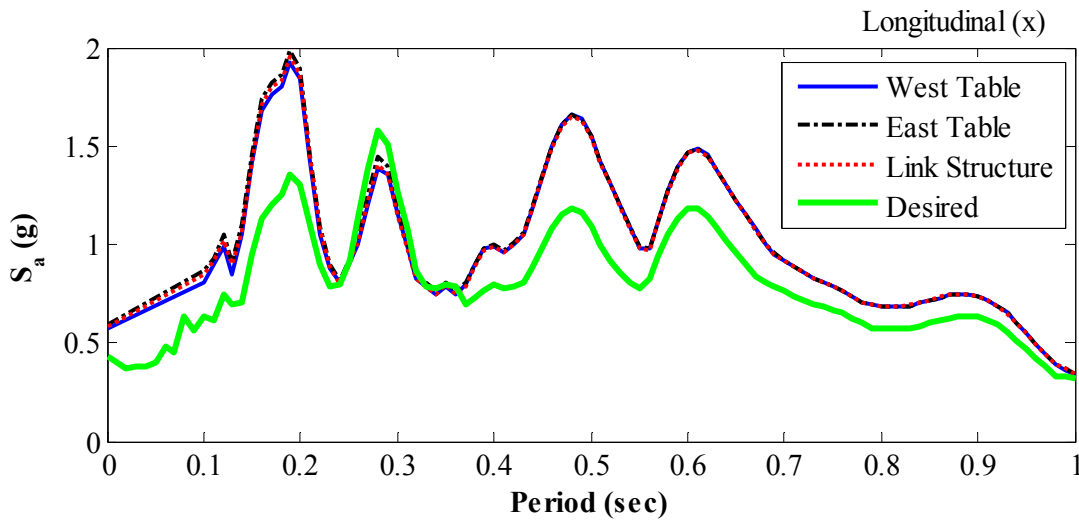


Figure I.32: Acceleration response spectra of shake table motion for 5 % damping in longitudinal direction, for Test NWP2S29

Phase 2, NWP2S30 Seismic Test

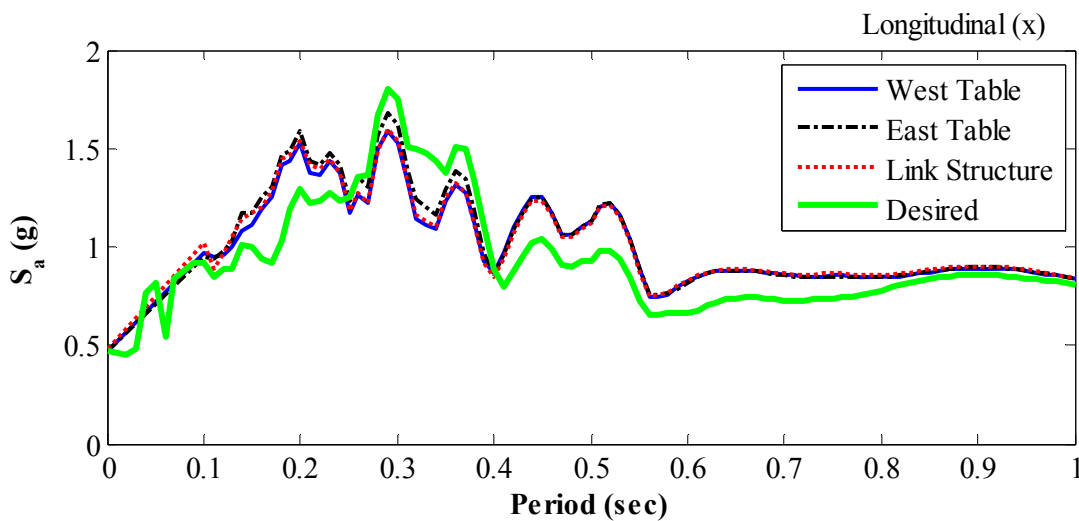


Figure I.33: Acceleration response spectra of shake table motion for 5 % damping in longitudinal direction, for Test NWP2S30

Appendix I

Phase 3, NWP3S01 Seismic Test

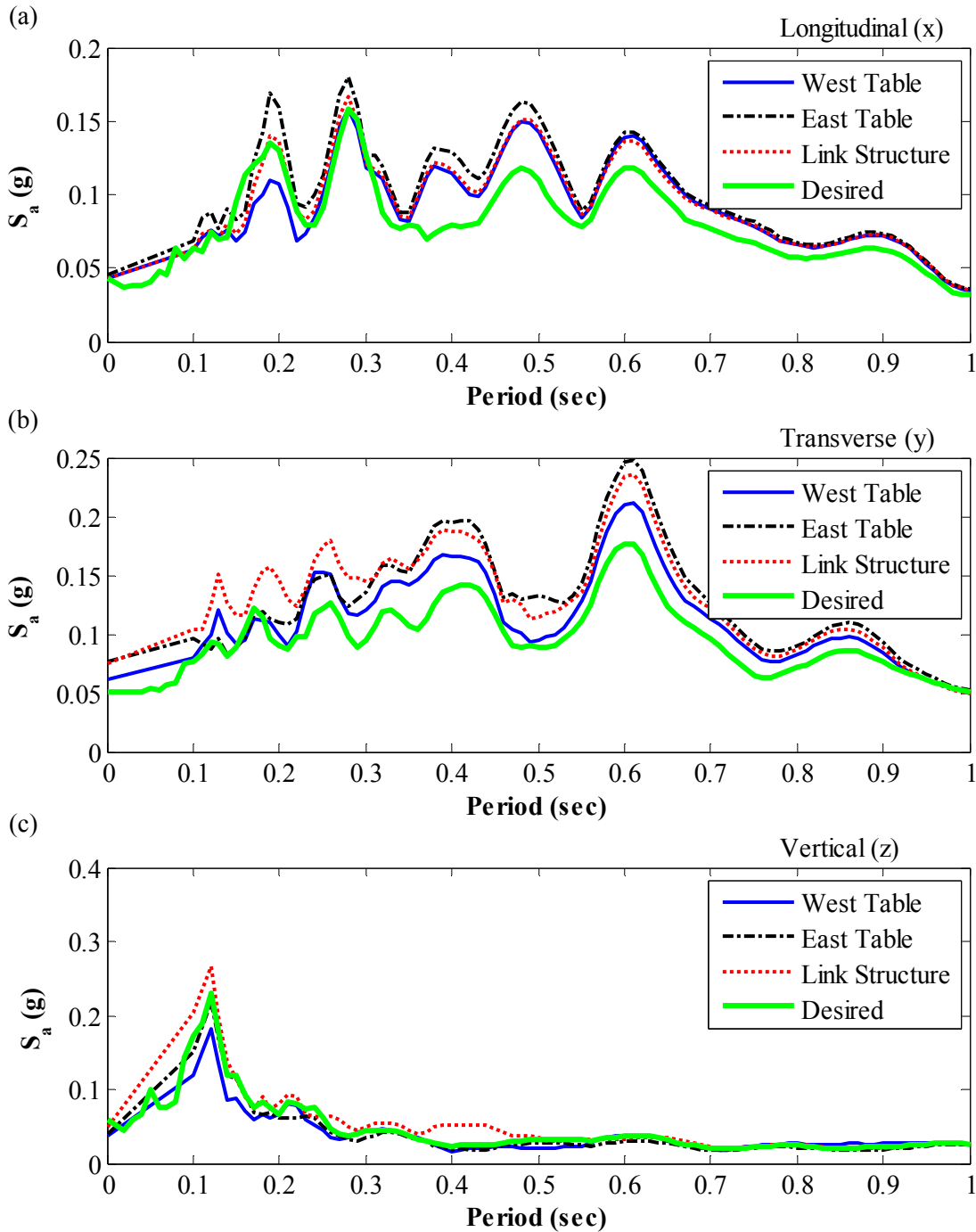


Figure I.34: Acceleration response spectra of shake table motion for 5 % damping in (a) longitudinal, (b) transverse, and (c) vertical direction, for Test NWP3S01

Appendix I

Phase 3, NWP3S02 Seismic Test

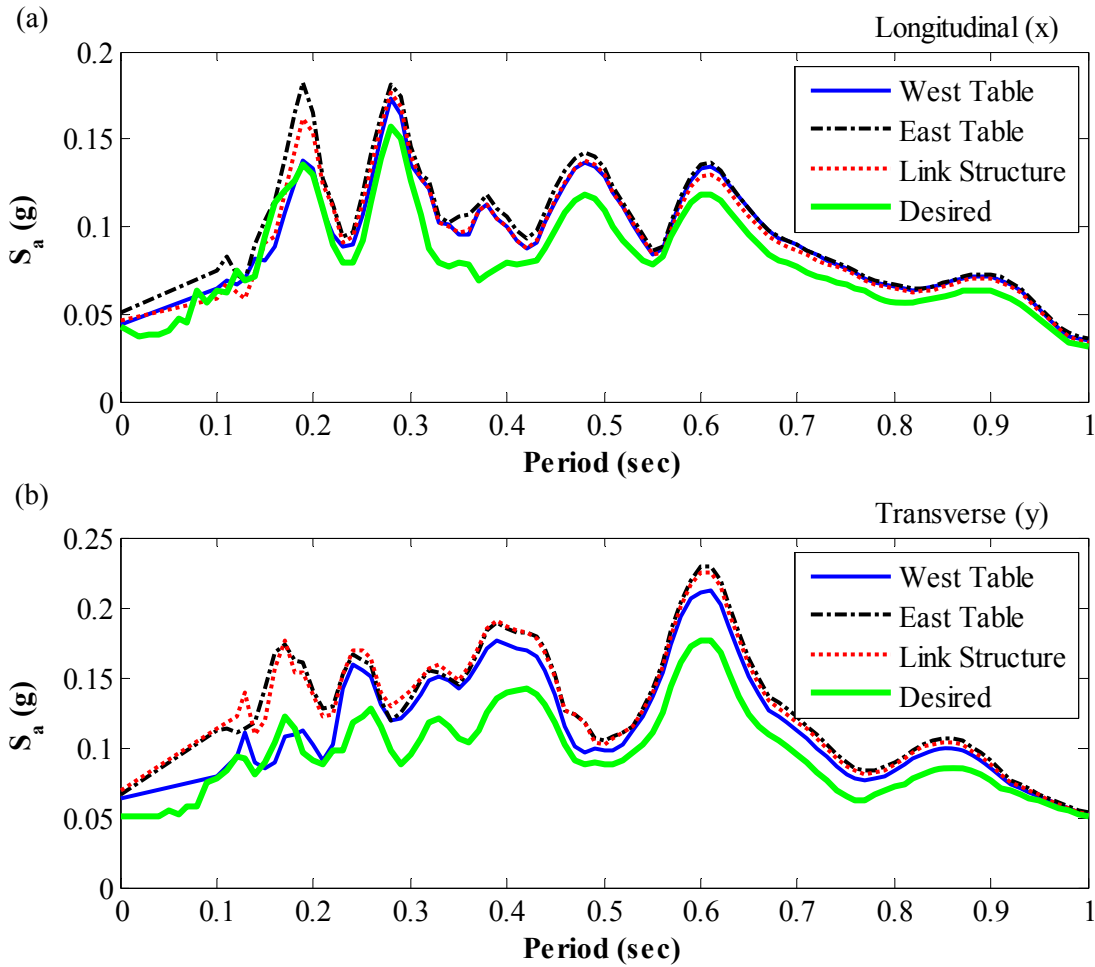


Figure I.35: Acceleration response spectra of shake table motion for 5 % damping in (a) longitudinal, and (b) transverse direction, for Test NWP3S02

Appendix I

Phase 3, NWP3S03 Seismic Test

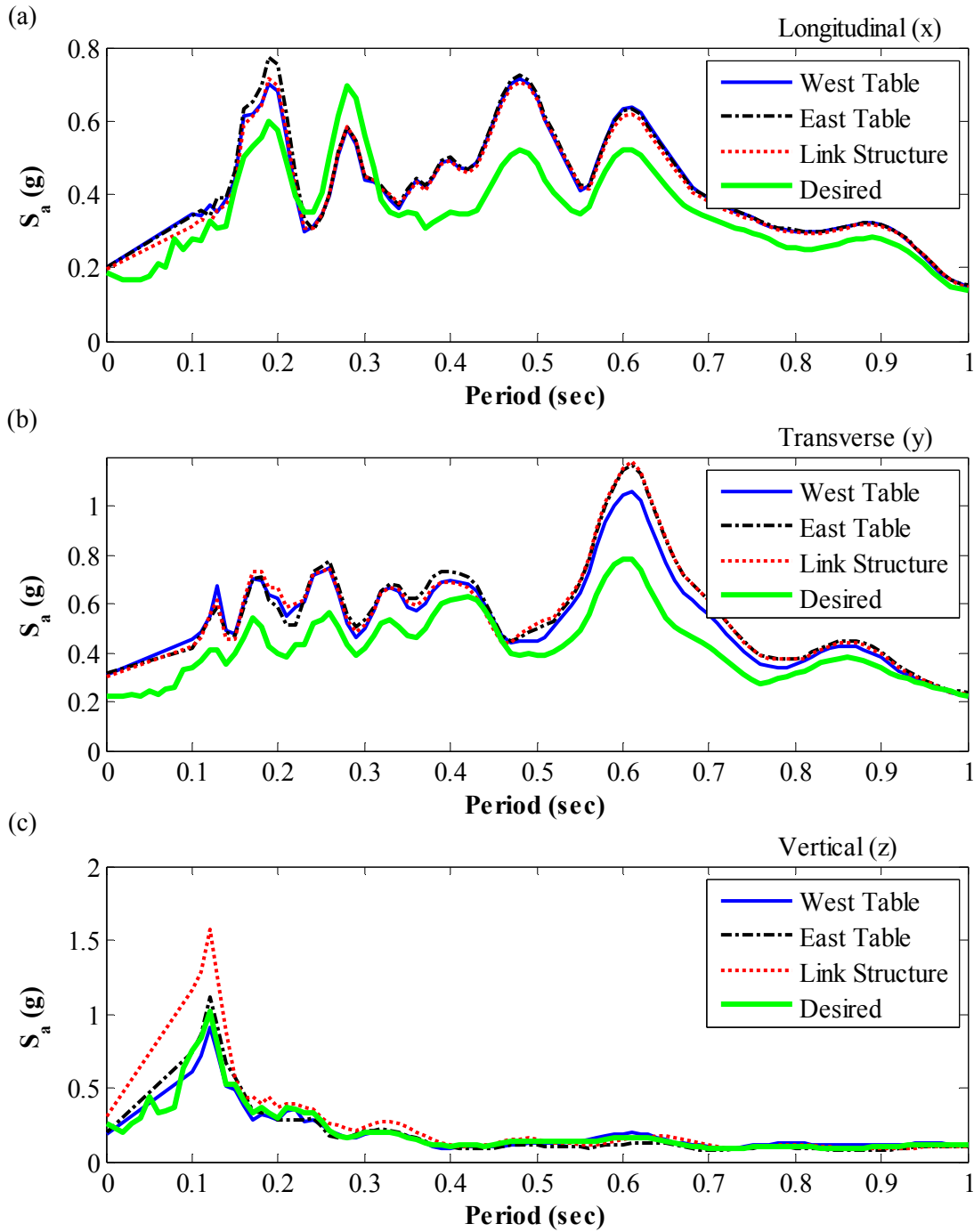


Figure I.36: Acceleration response spectra of shake table motion for 5 % damping in (a) longitudinal, (b) transverse, and (c) vertical direction, for Test NWP3S03

Appendix I

Phase 3, NWP3S04 Seismic Test

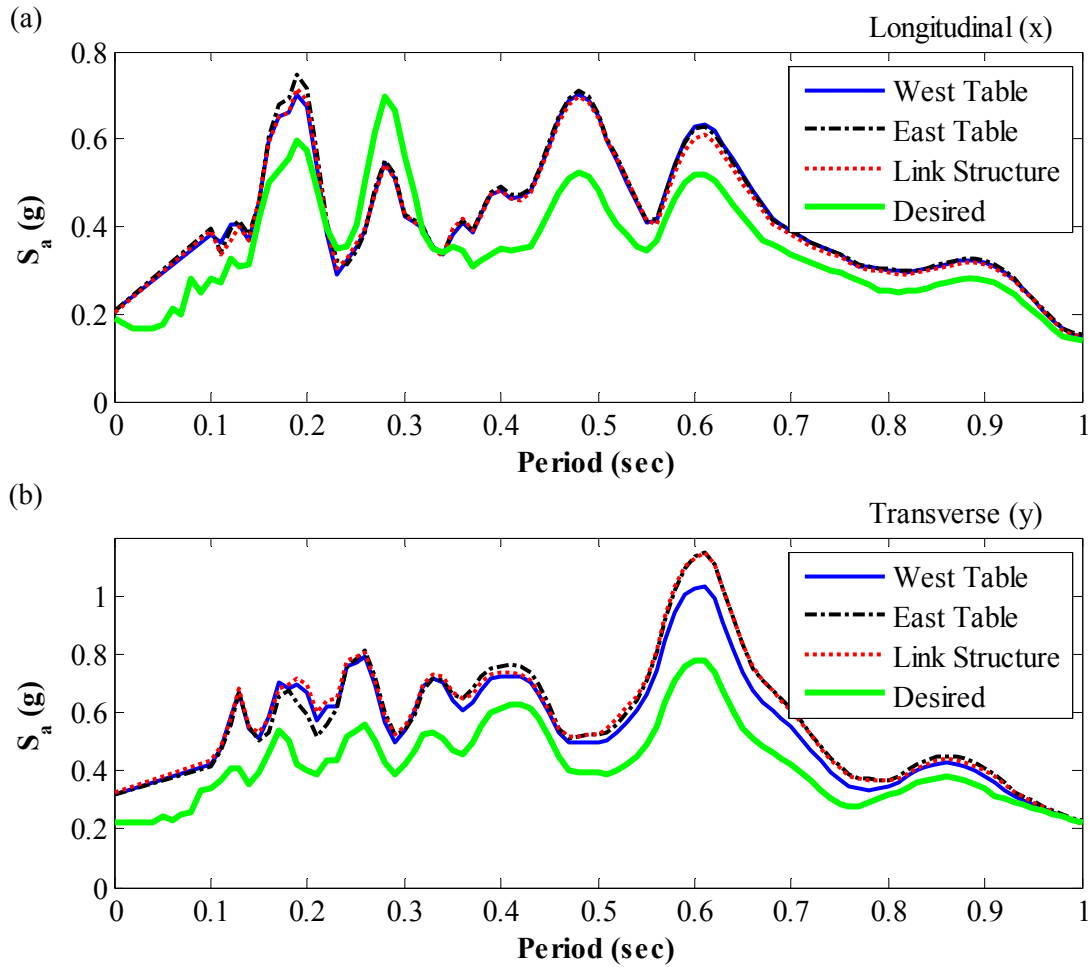


Figure I.37: Acceleration response spectra of shake table motion for 5 % damping in (a) longitudinal, and (b) transverse direction, for Test NWP3S04

Appendix I

Phase 4, NWP4S01 Seismic Test

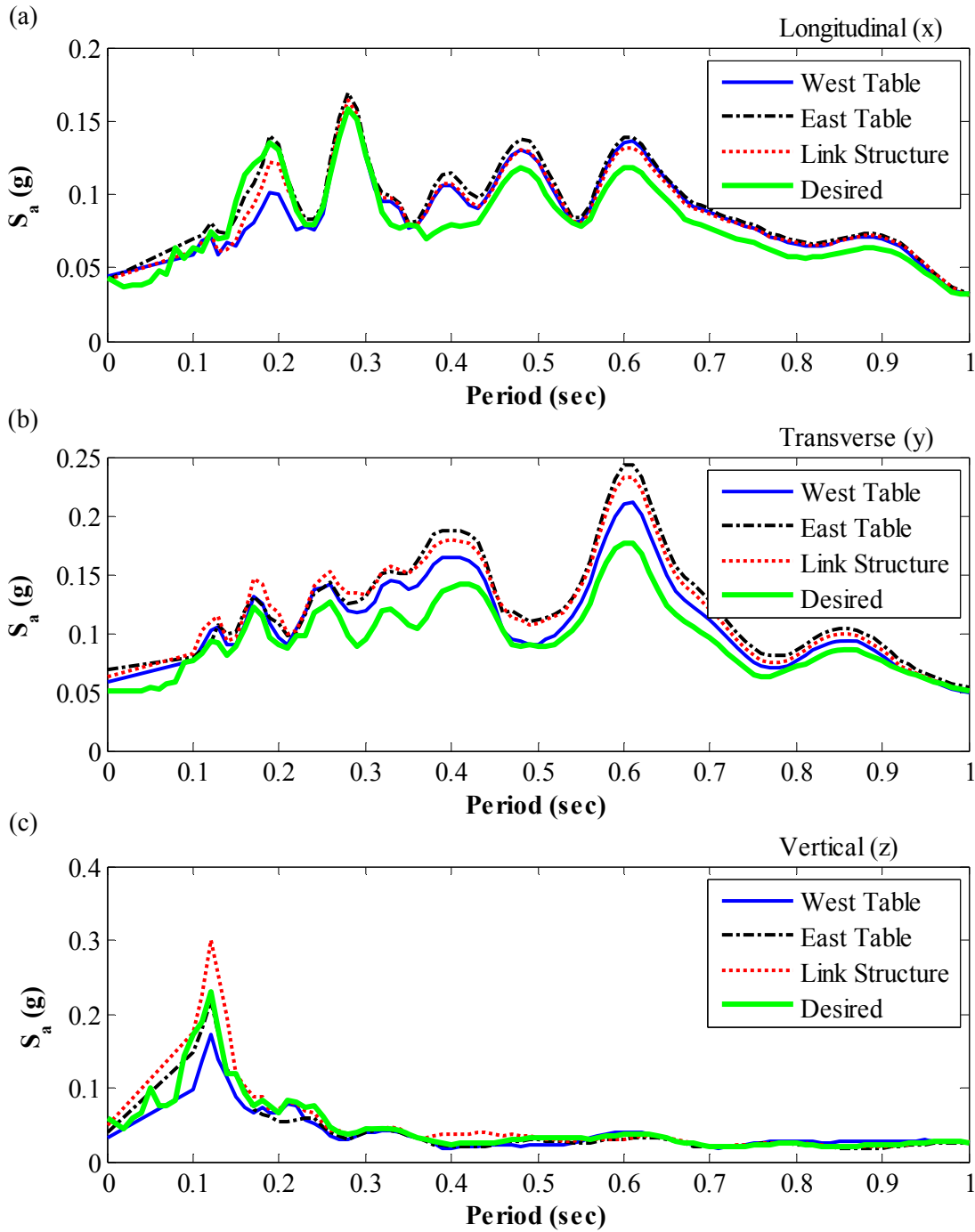


Figure I.38: Acceleration response spectra of shake table motion for 5 % damping in (a) longitudinal, (b) transverse, and (c) vertical direction, for Test NWP4S01

Appendix I

Phase 4, NWP4S02 Seismic Test

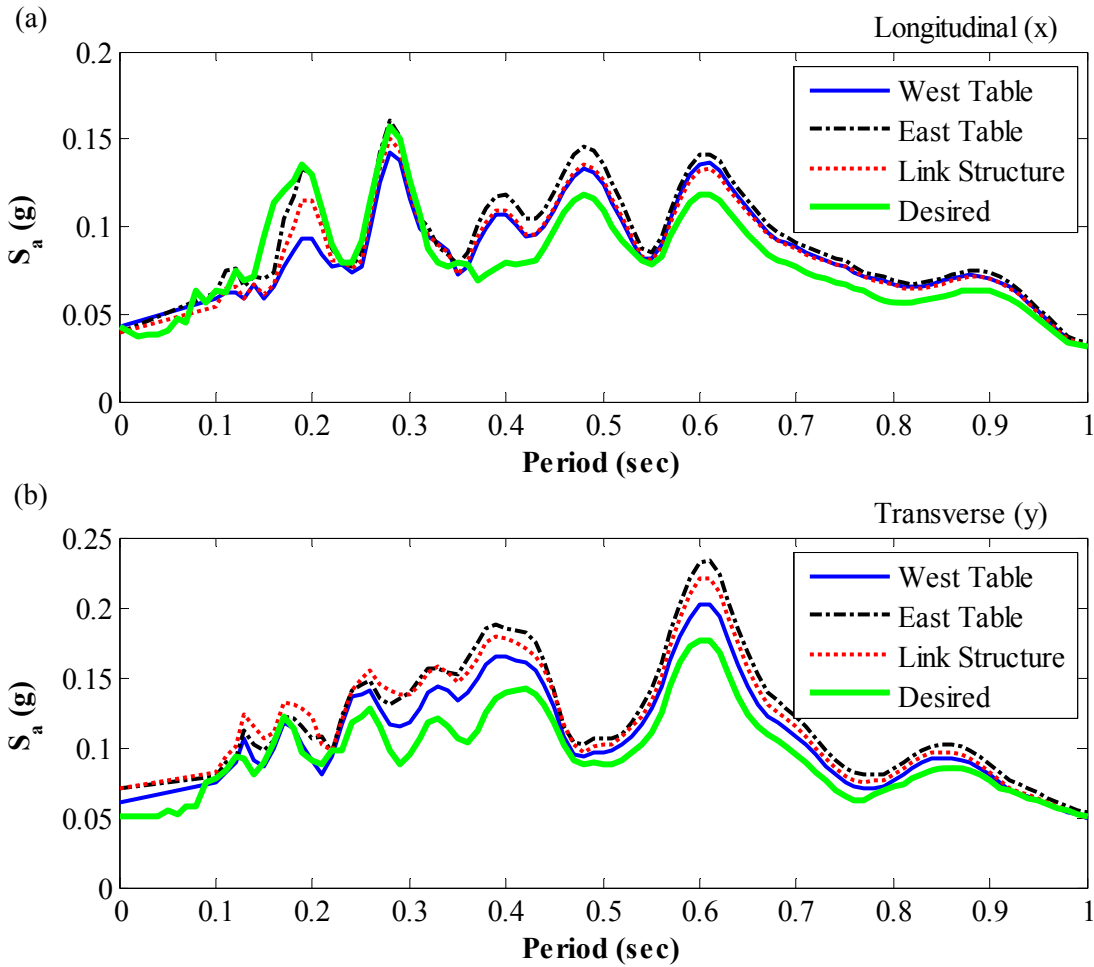


Figure I.39: Acceleration response spectra of shake table motion for 5 % damping in (a) longitudinal, and (b) transverse direction, for Test NWP4S02

Appendix I

Phase 4, NWP4S03 Seismic Test

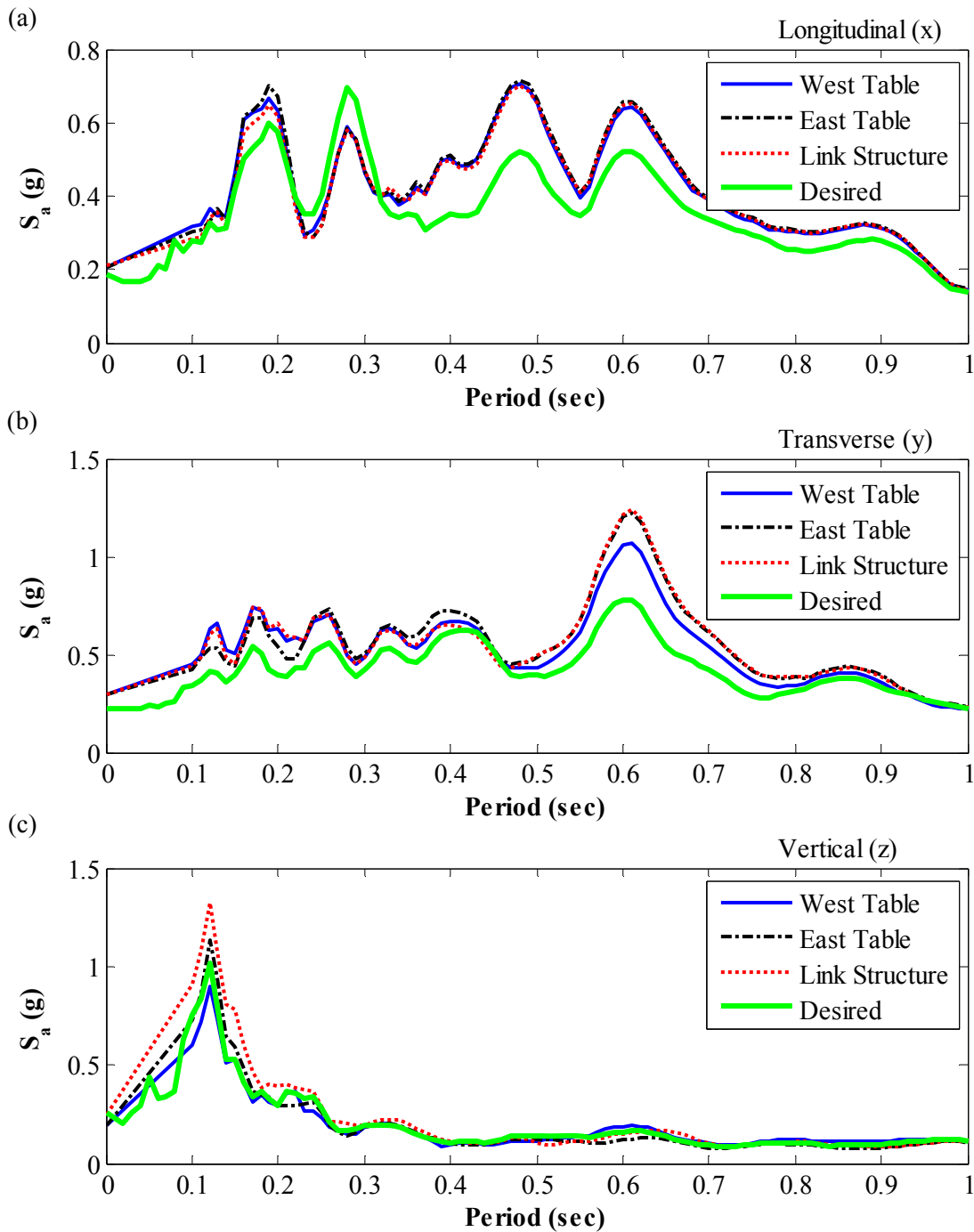


Figure I.40: Acceleration response spectra of shake table motion for 5 % damping in (a) longitudinal, (b) transverse, and (c) vertical direction, for Test NWP4S03

Appendix I

Phase 4, NWP4S04 Seismic Test

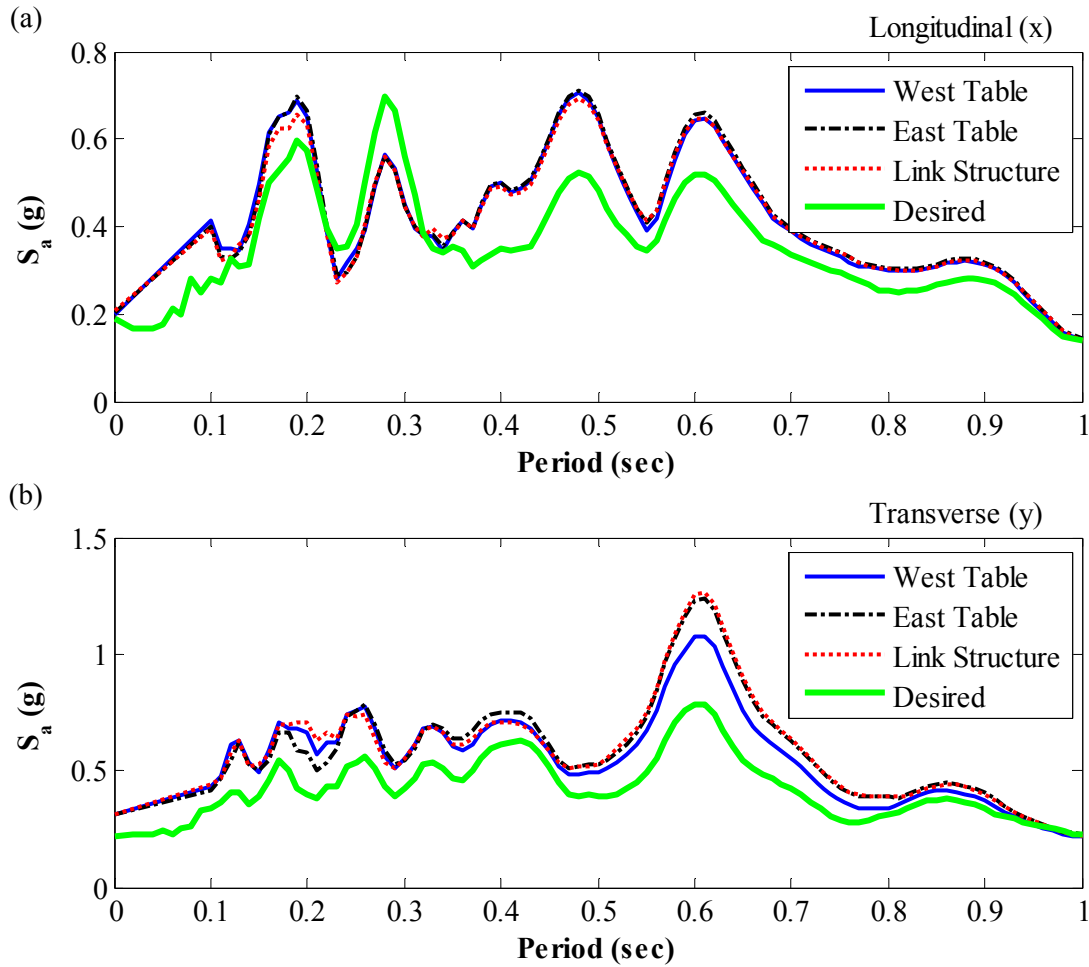


Figure I.41: Acceleration response spectra of shake table motion for 5 % damping in (a) longitudinal, and (b) transverse direction, for Test NWP4S04

Appendix I

Phase 5, NWP5S01 Seismic Test

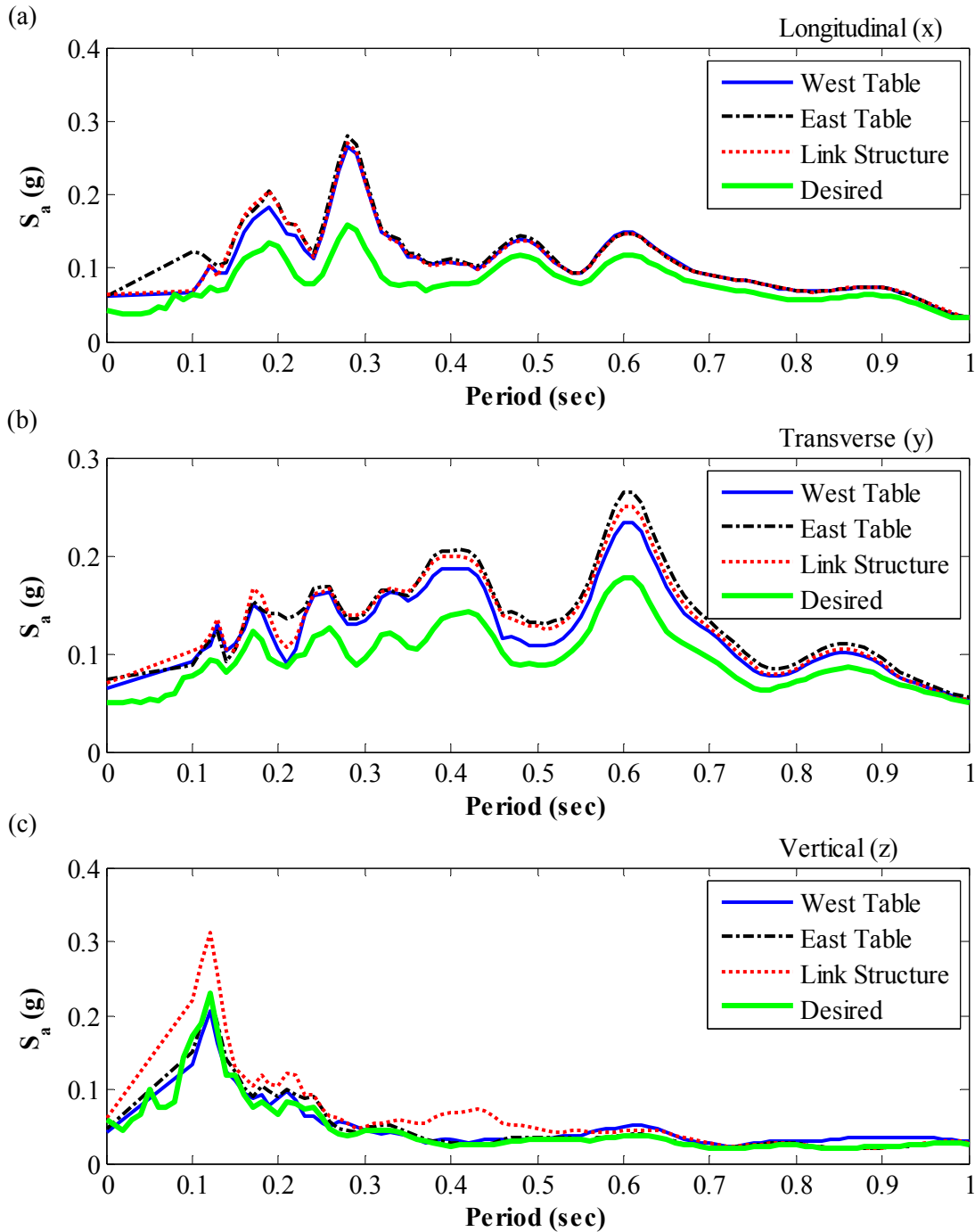


Figure I.42: Acceleration response spectra of shake table motion for 5 % damping in (a) longitudinal, (b) transverse, and (c) vertical direction, for Test NWP5S01

Appendix I

Phase 5, NWP5S02 Seismic Test

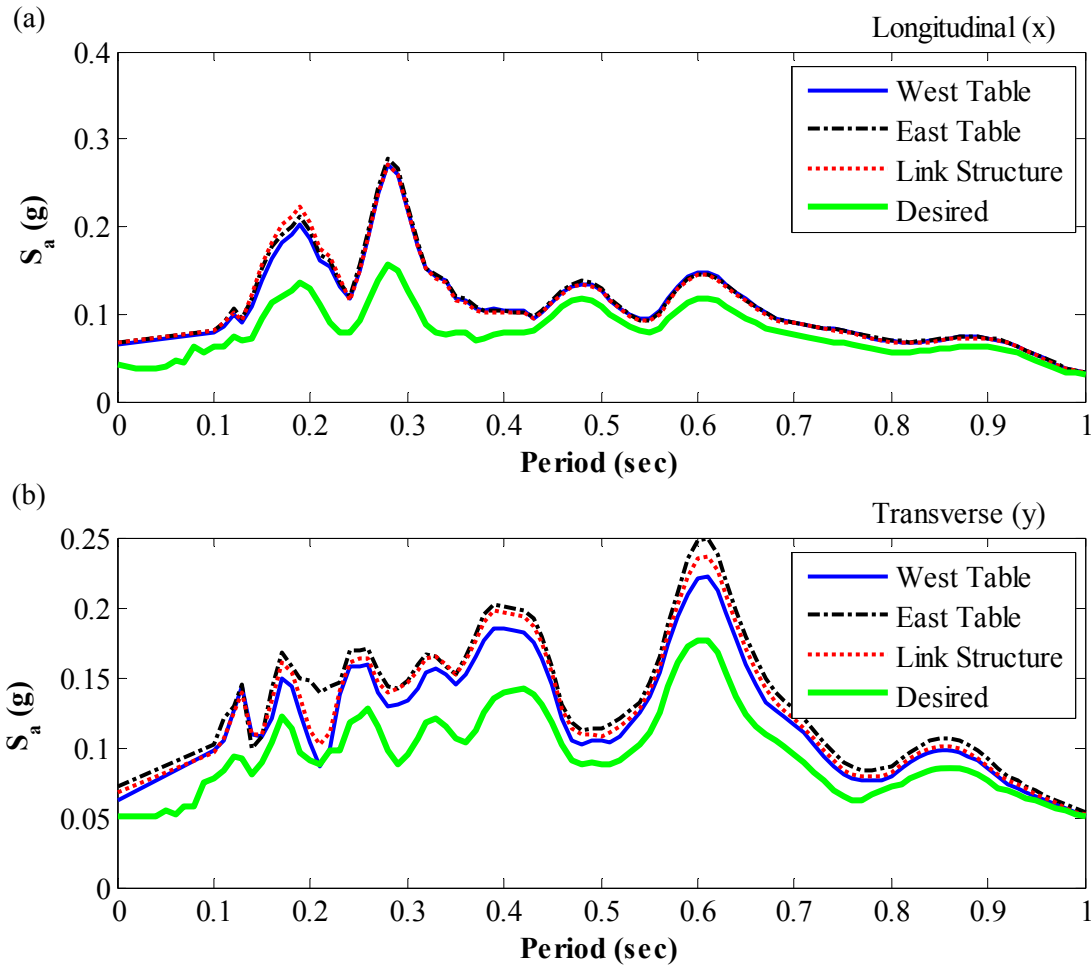


Figure I.43: Acceleration response spectra of shake table motion for 5 % damping in (a) longitudinal, and (b) transverse direction, for Test NWP5S02

Appendix I

Phase 5, NWP5S03 Seismic Test

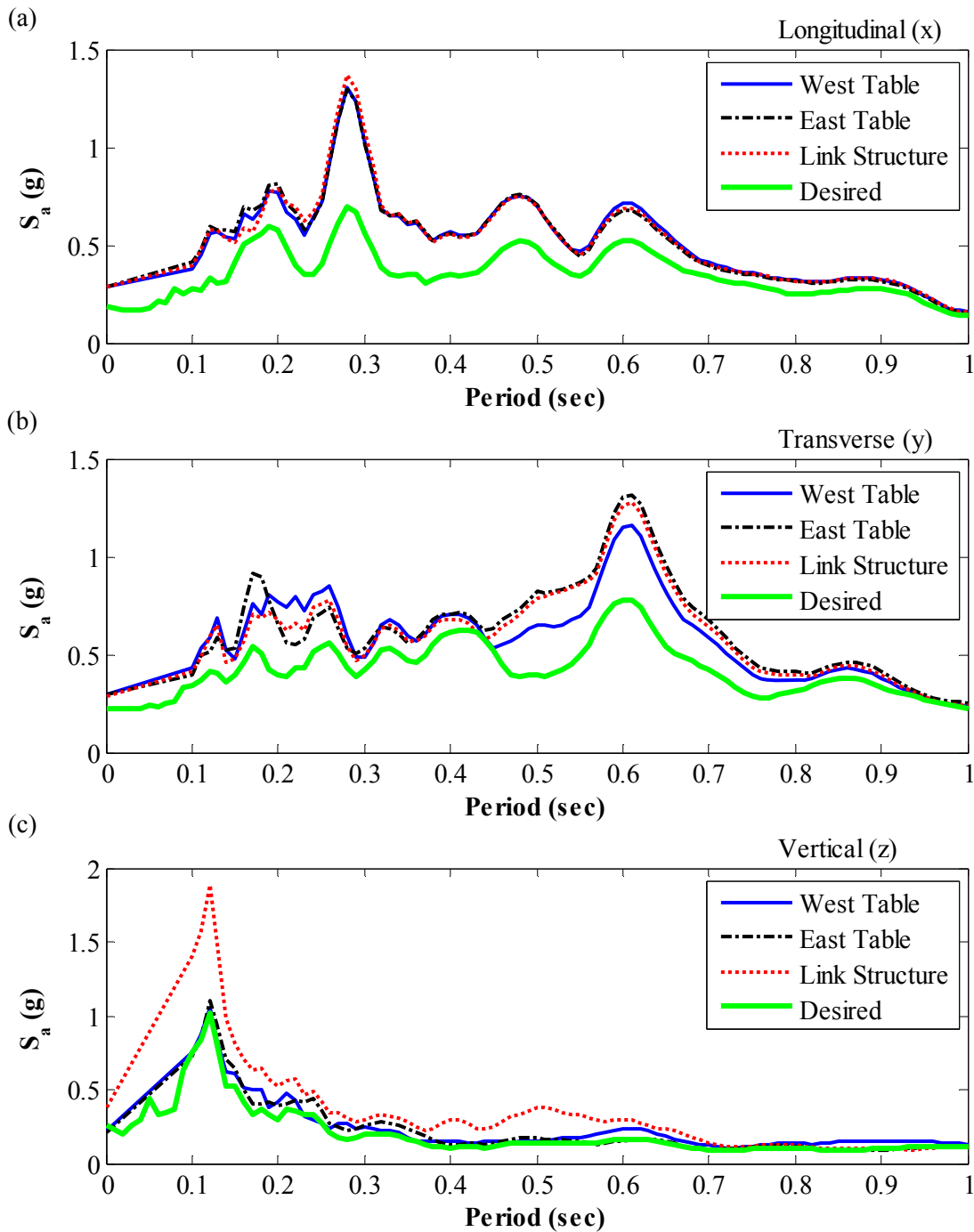


Figure I.44: Acceleration response spectra of shake table motion for 5 % damping in (a) longitudinal, (b) transverse, and (c) vertical direction, for Test NWP5S03

Appendix I

Phase 5, NWP5S04 Seismic Test

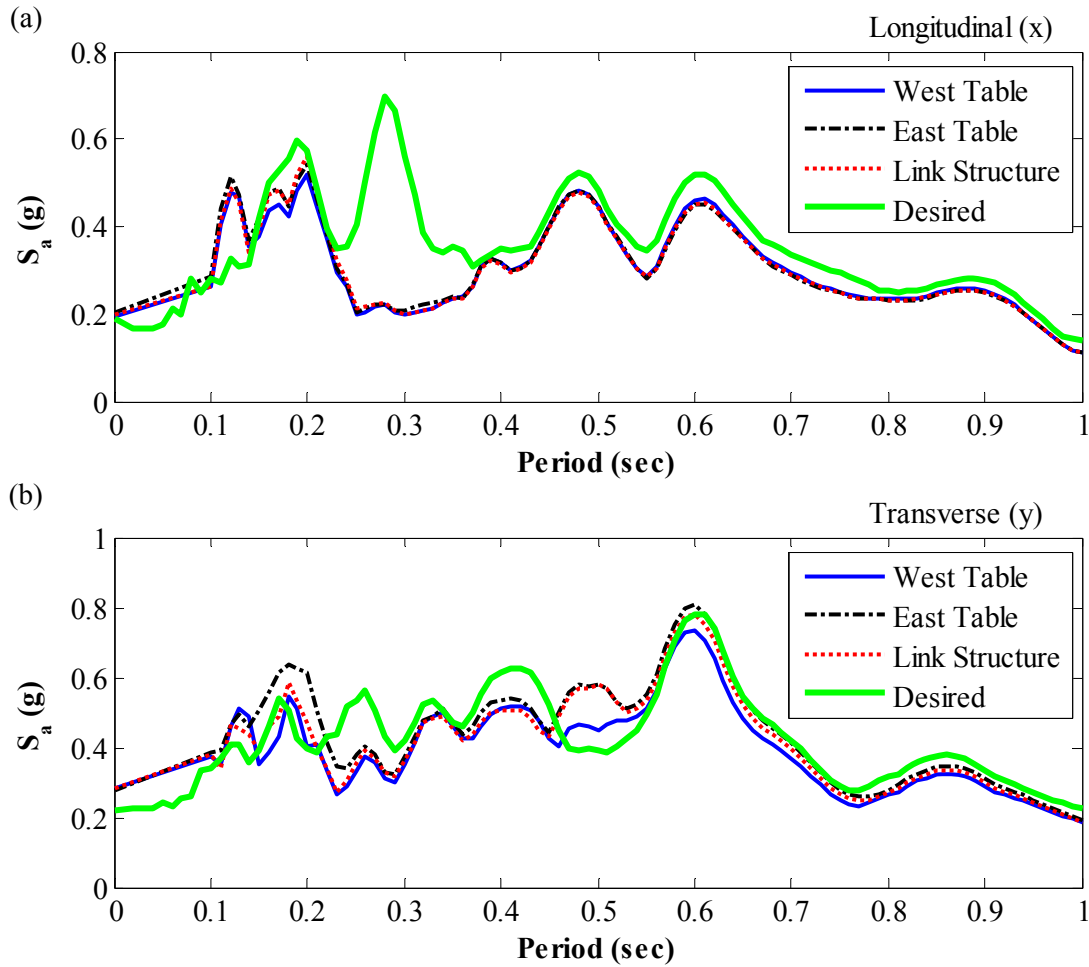


Figure I.45: Acceleration response spectra of shake table motion for 5 % damping in (a) longitudinal, and (b) transverse direction, for Test NWP5S04

Appendix I

Phase 5, NWP5S05 Seismic Test

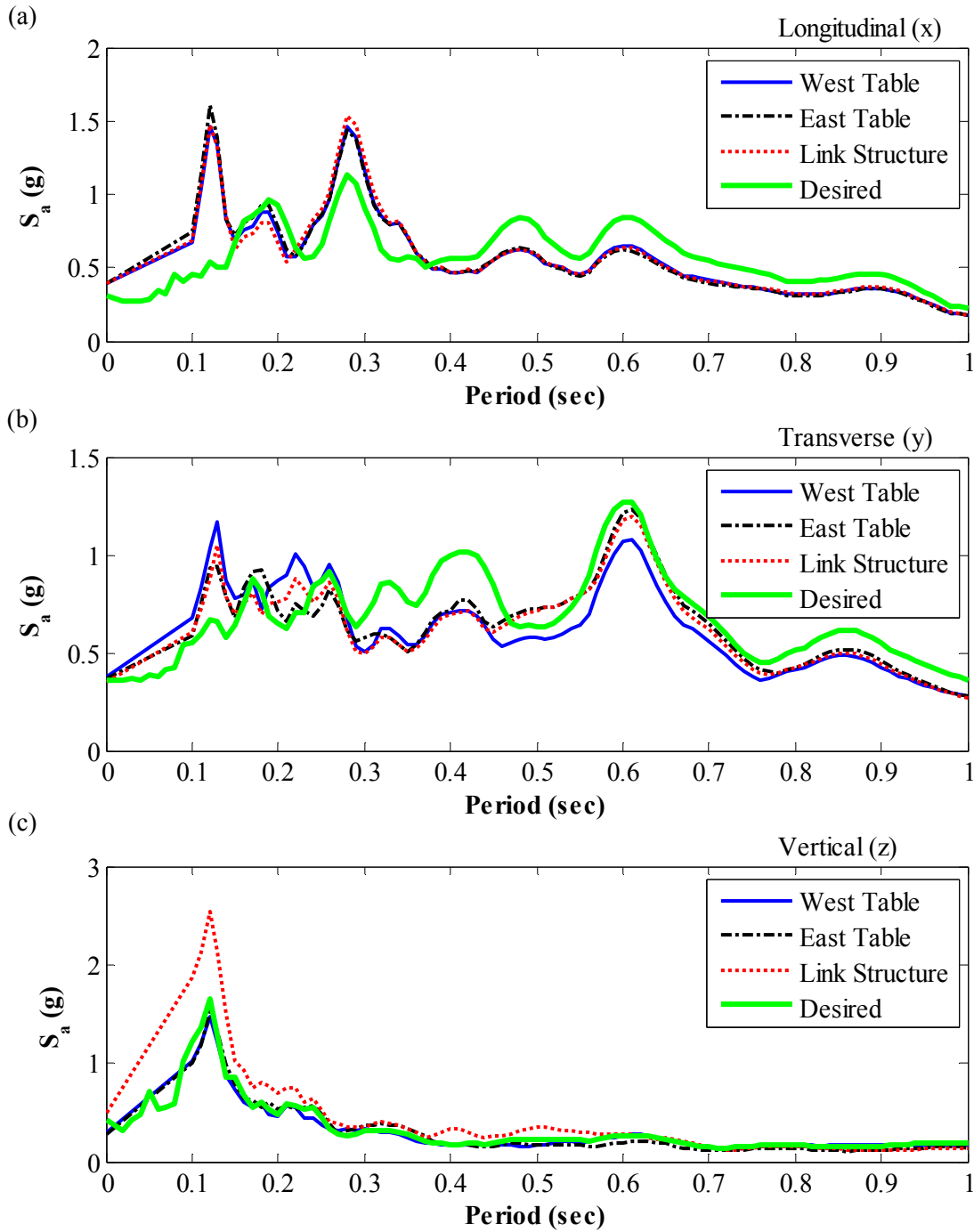


Figure I.46: Acceleration response spectra of shake table motion for 5 % damping in (a) longitudinal, (b) transverse, and (c) vertical direction, for Test NWP5S05

Appendix I

Phase 5, NWP5S06 Seismic Test

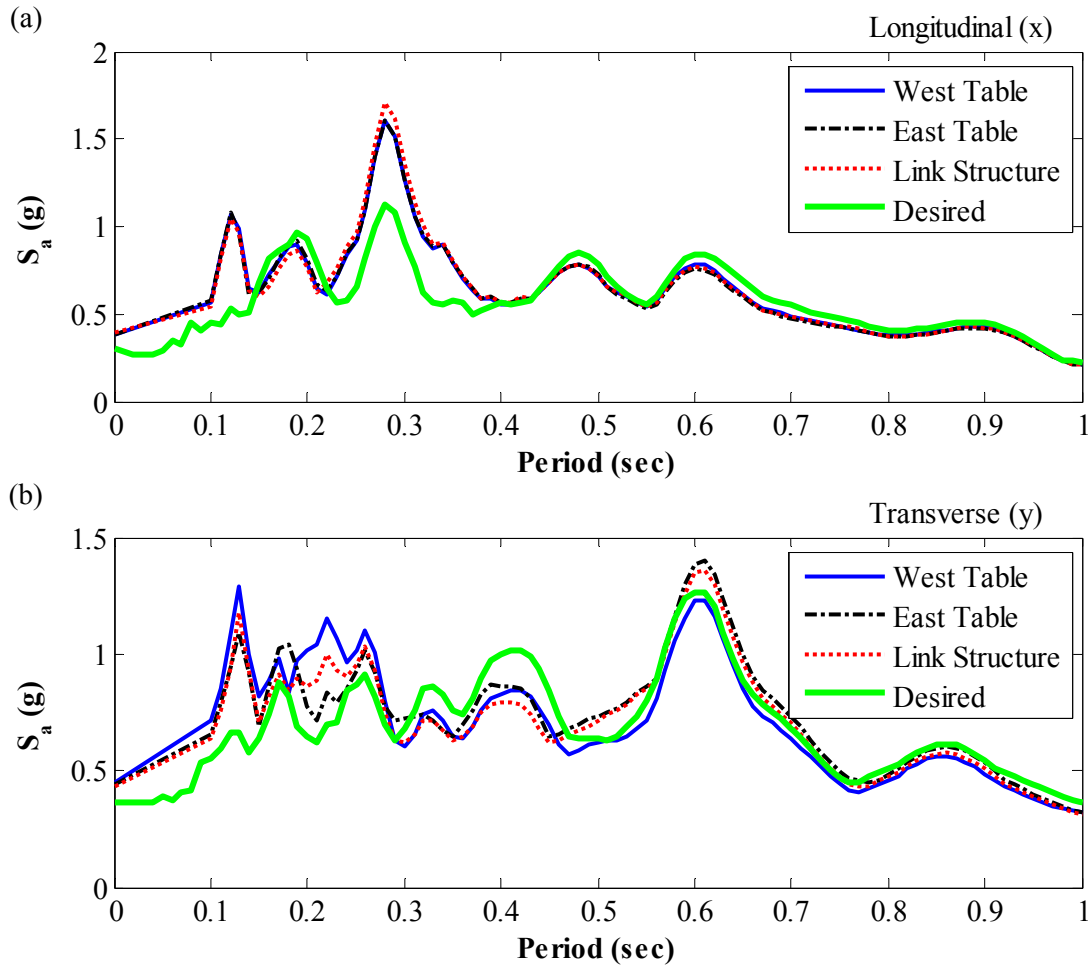


Figure I.47: Acceleration response spectra of shake table motion for 5 % damping in (a) longitudinal, and (b) transverse direction, for Test NWP5S06

Appendix I

Phase 5, NWP5S07 Seismic Test

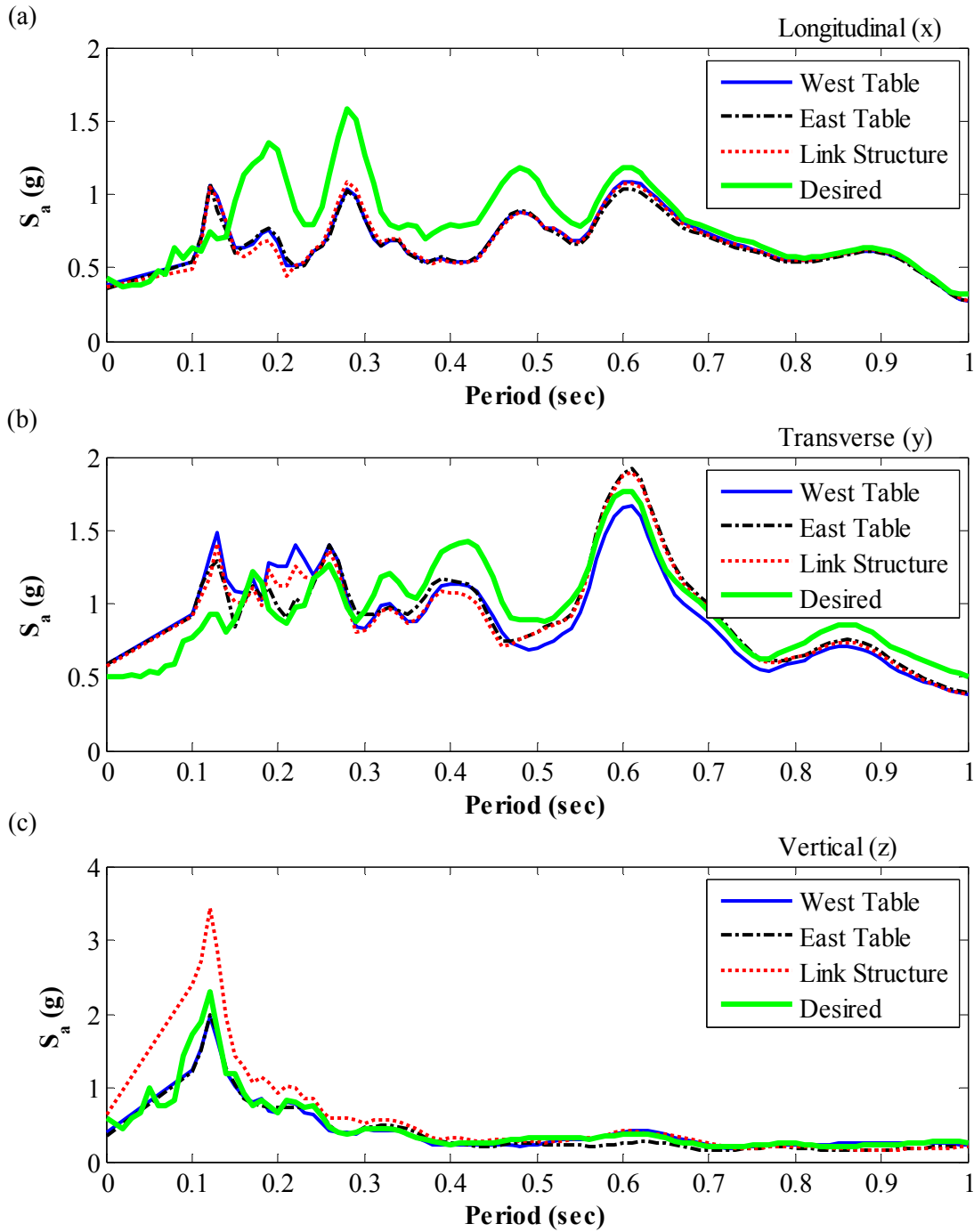


Figure I.48: Acceleration response spectra of shake table motion for 5 % damping in (a) longitudinal, (b) transverse, and (c) vertical direction, for Test NWP5S07

Appendix I

Phase 5, NWP5S08 Seismic Test

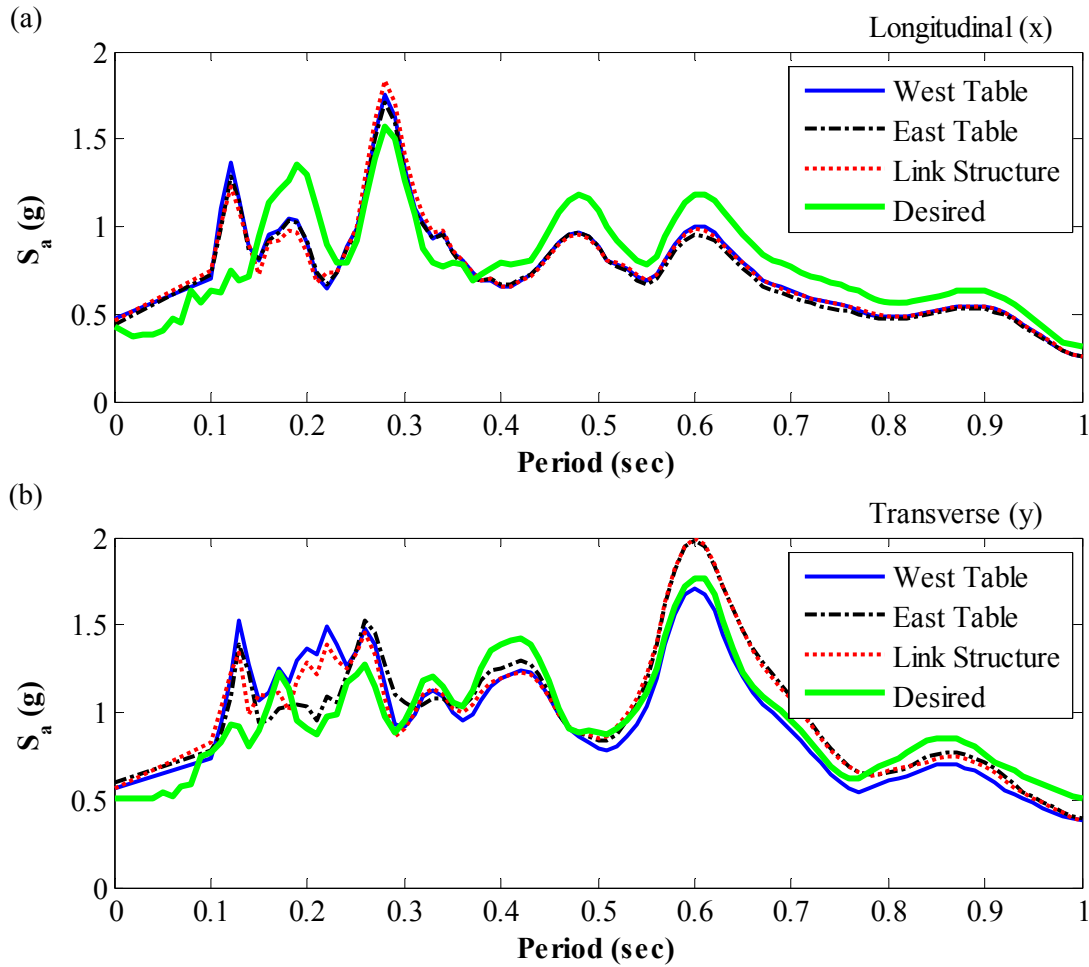


Figure I.49: Acceleration response spectra of shake table motion for 5 % damping in (a) longitudinal, and (b) transverse direction, for Test NWP5S08

Appendix I

Phase 5, NWP5S09 Seismic Test

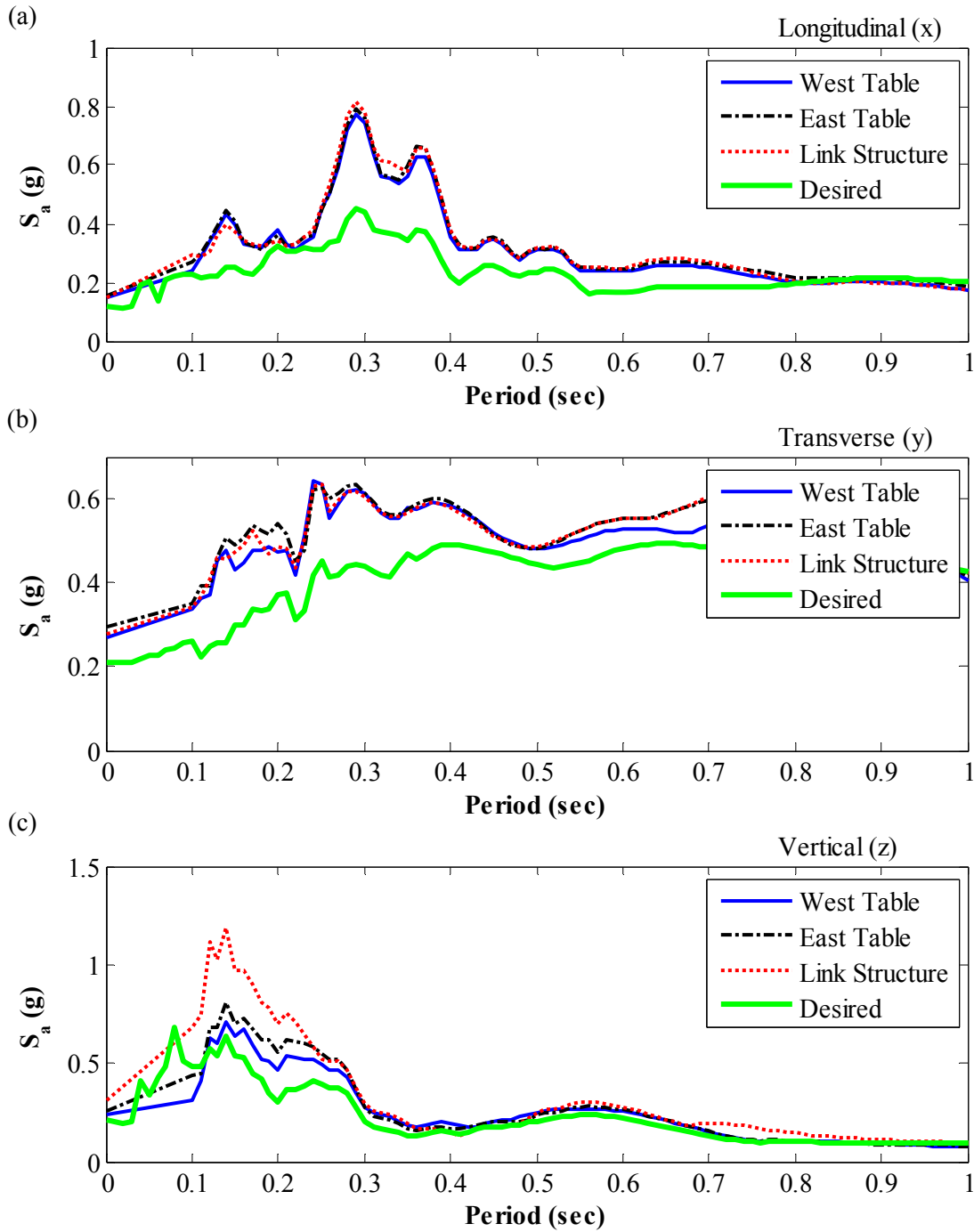


Figure I.50: Acceleration response spectra of shake table motion for 5 % damping in (a) longitudinal, (b) transverse, and (c) vertical direction, for Test NWP5S09

Appendix I

Phase 5, NWP5S11 Seismic Test

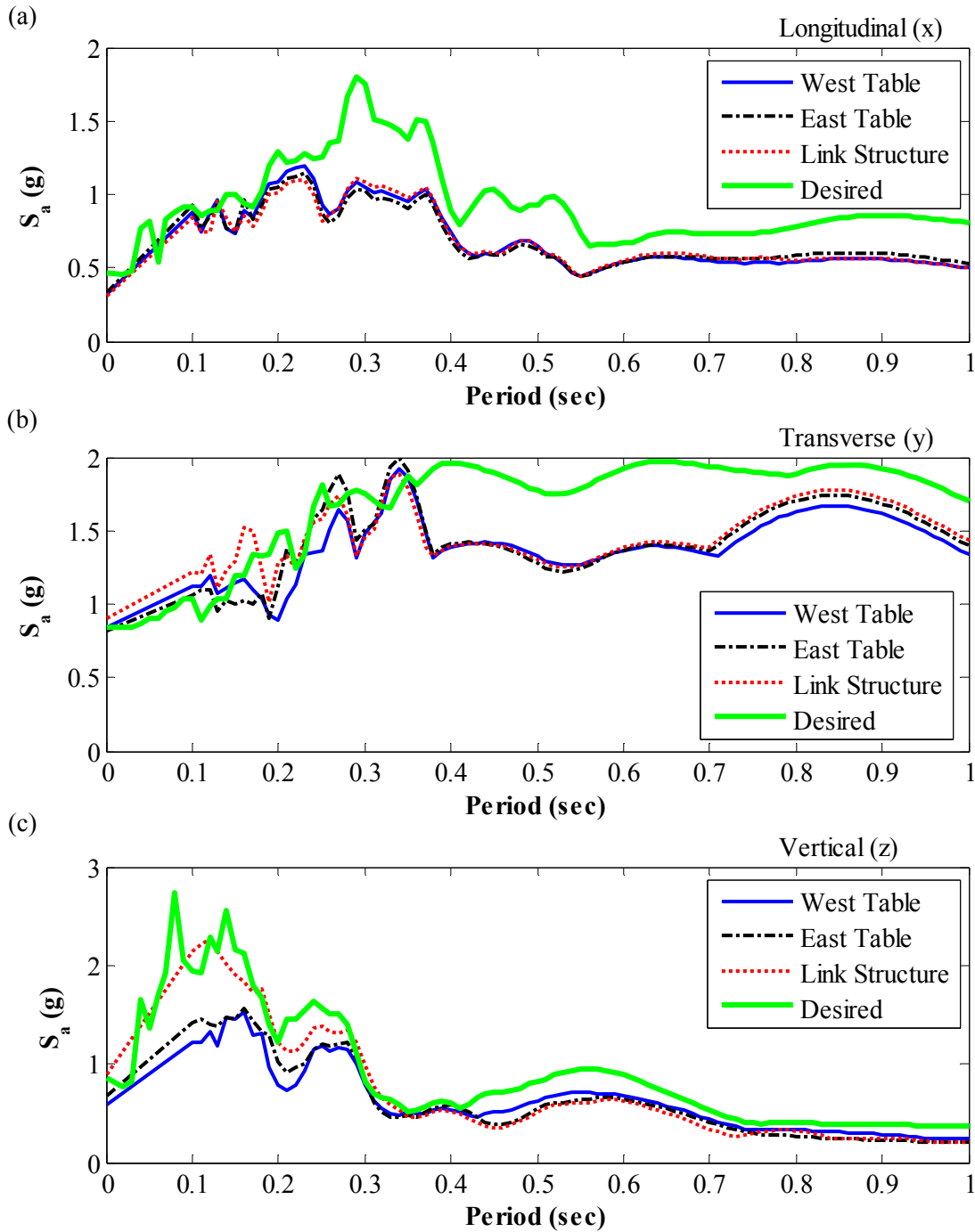
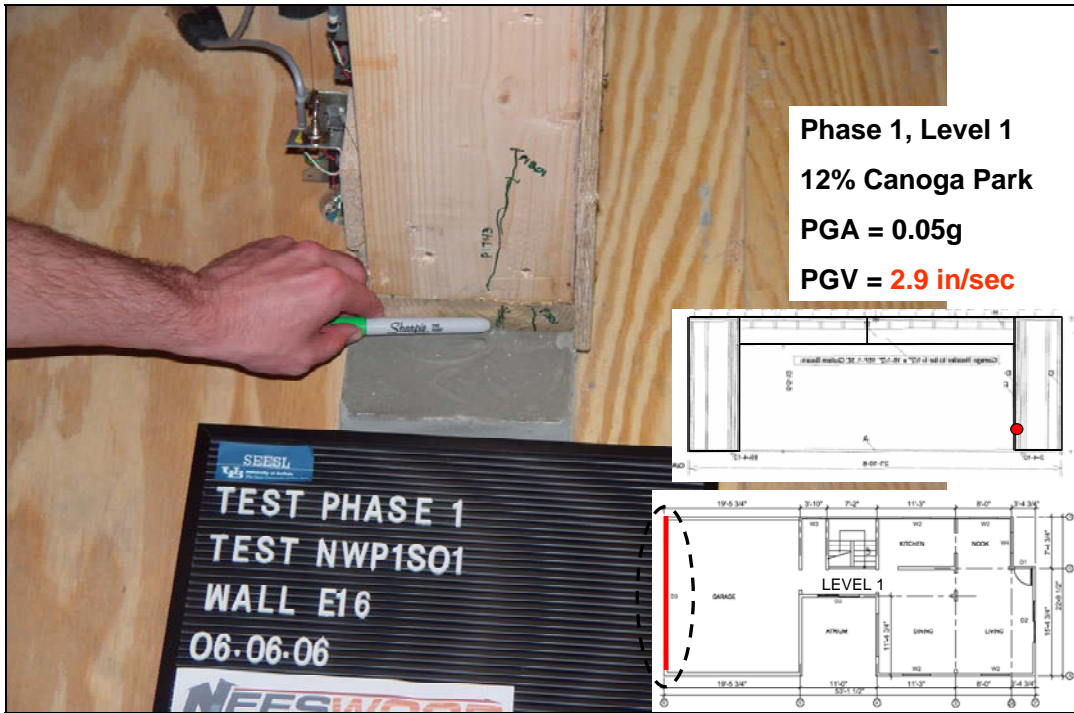


Figure I.51: Acceleration response spectra of shake table motion for 5 % damping in (a) longitudinal, (b) transverse, and (c) vertical direction, for Test NWP5S11

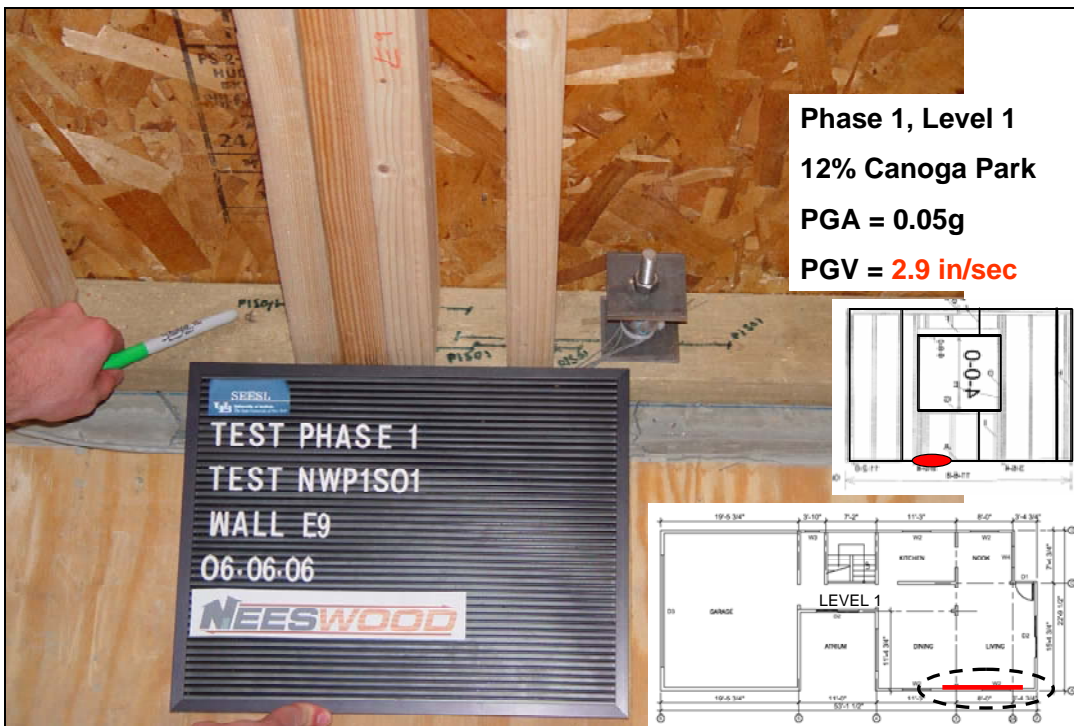
**Appendix J
Selected Visual Damage
Identification Photos**

Appendix J

Test Phase 1



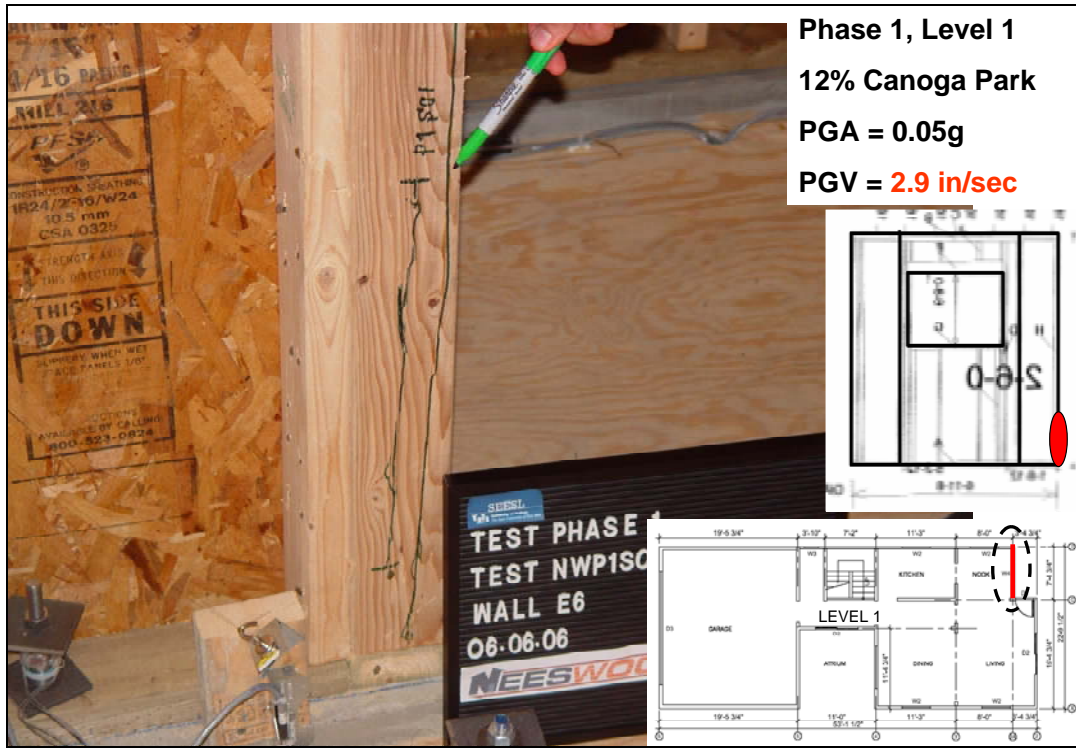
Splitting of garage wall sill plate



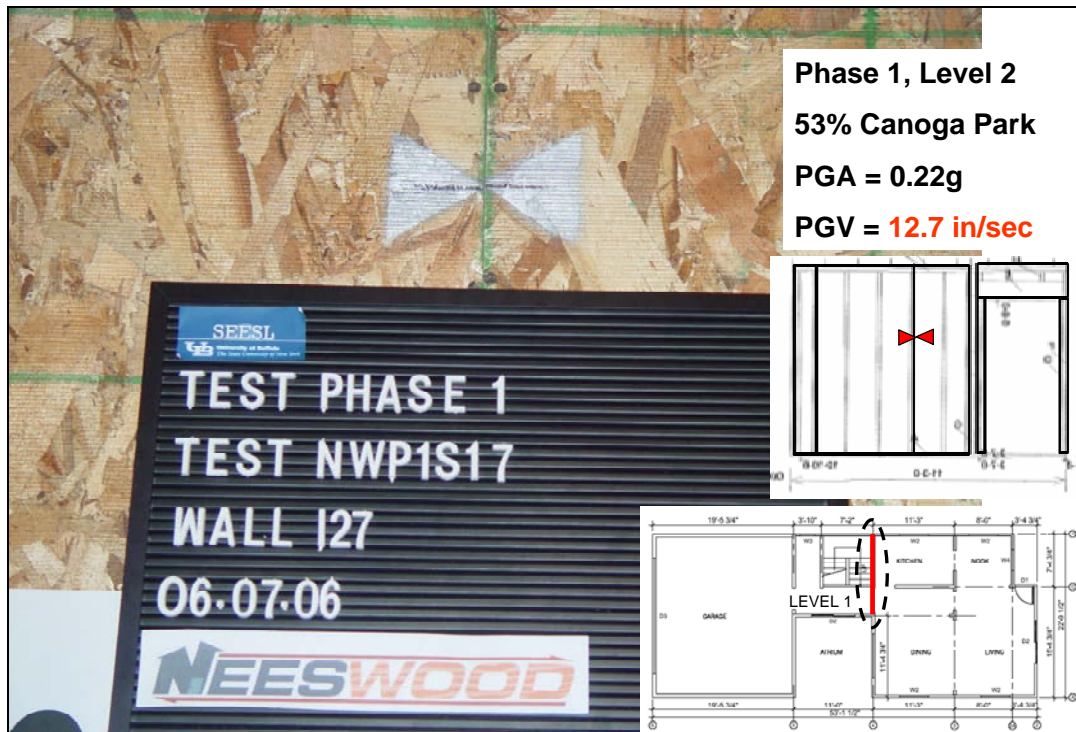
Splitting of sill plate

Appendix J

Test Phase 1



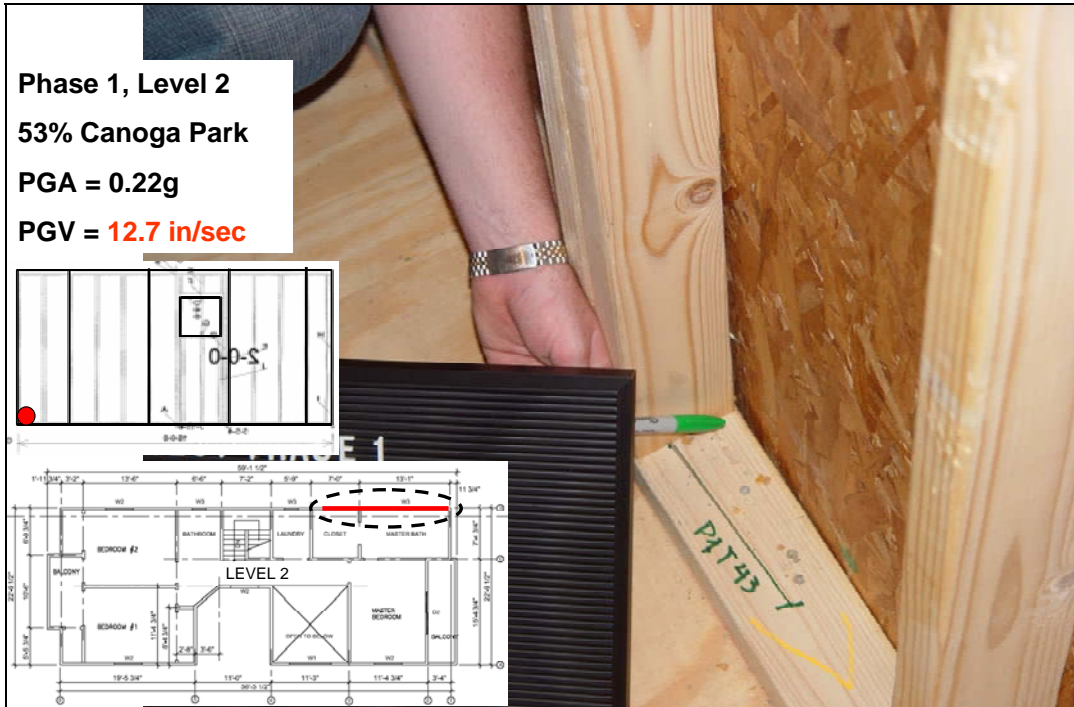
Splitting near bottom of back door frame



Permanent differential movement of two adjacent sheathing panels

Appendix J

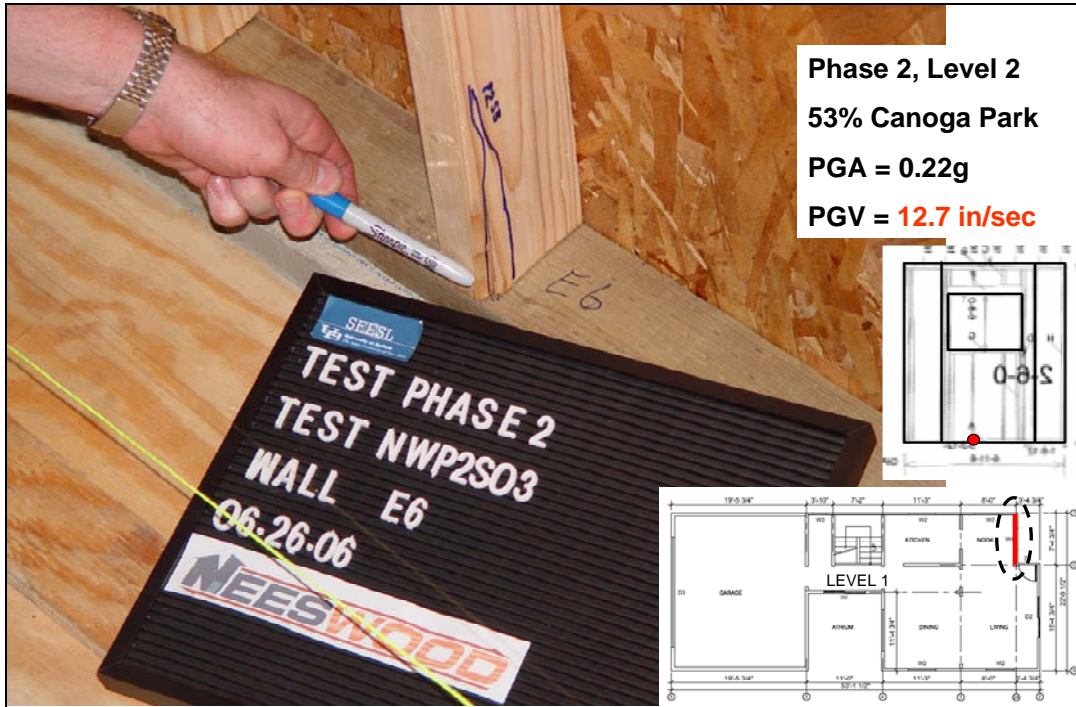
Test Phase 1



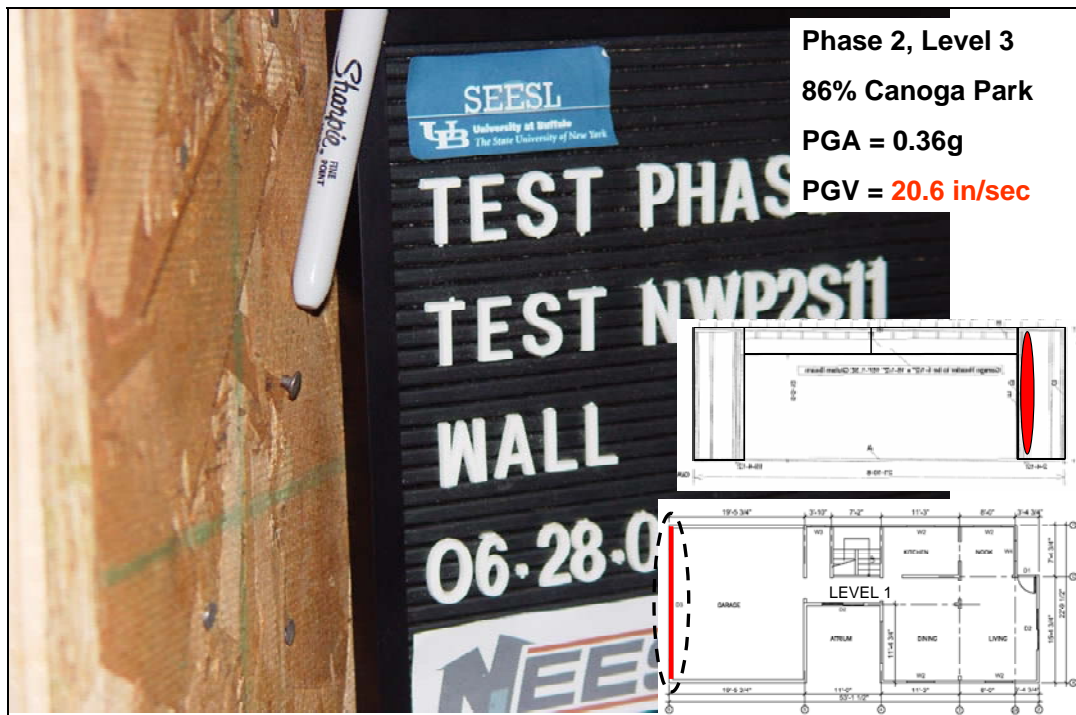
Sheathing pull-out at bottom corner of second floor shear wall

Appendix J

Test Phase 2



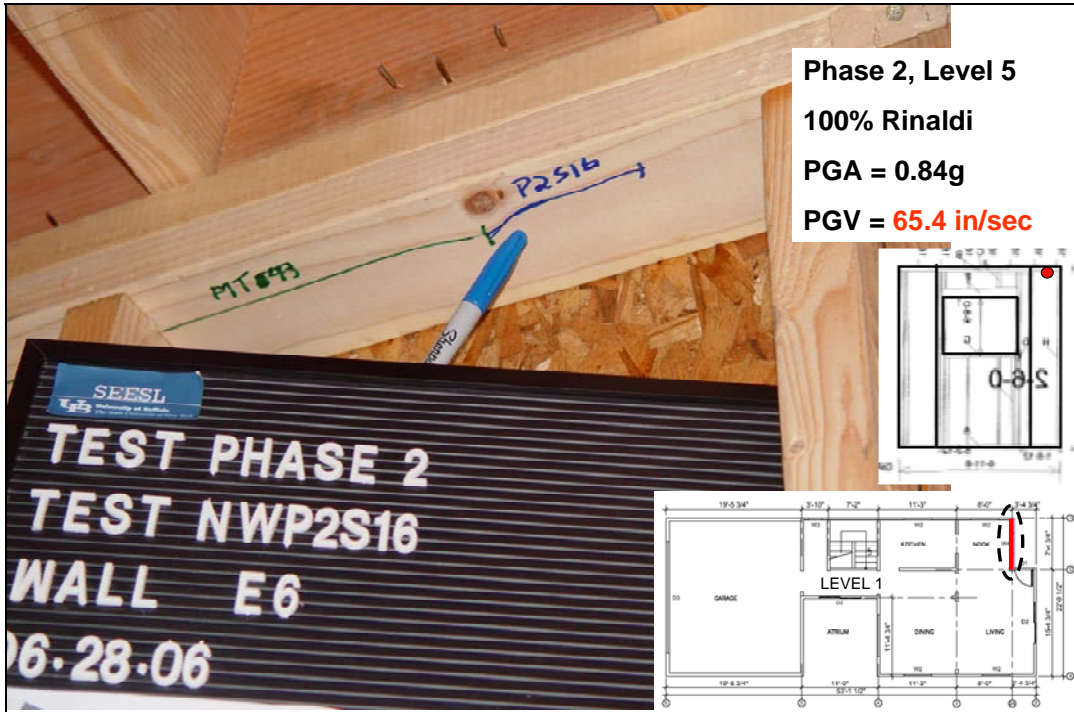
Cracking of vertical stud at connection with sill plate



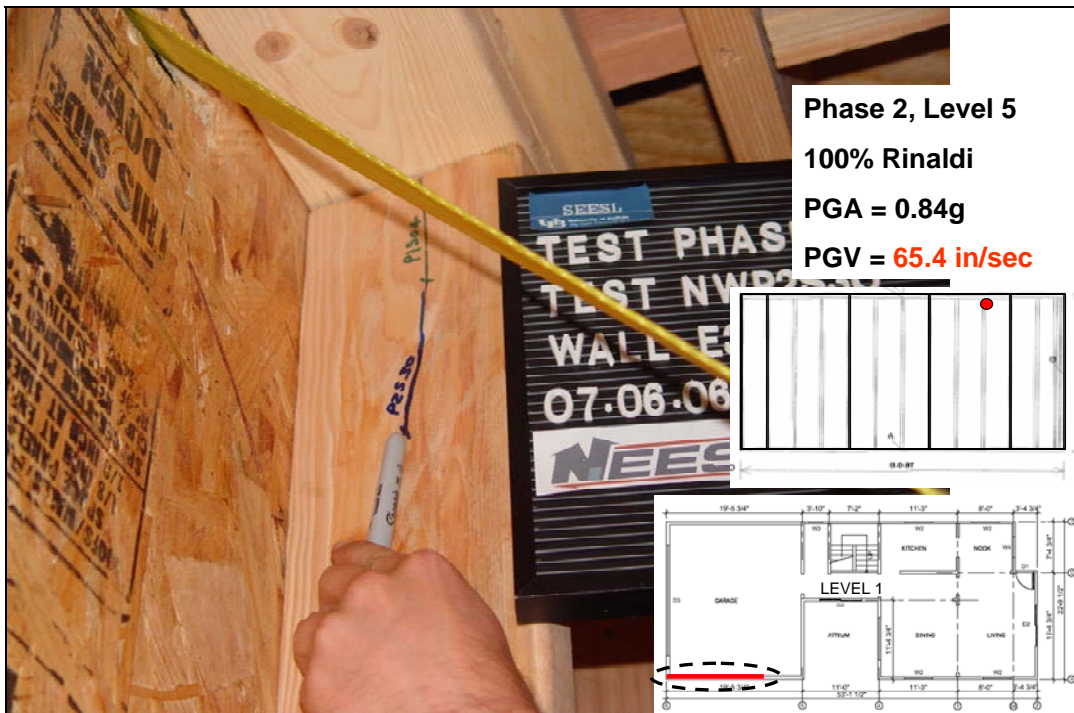
Nail partial pull-out at garage wall

Appendix J

Test Phase 2



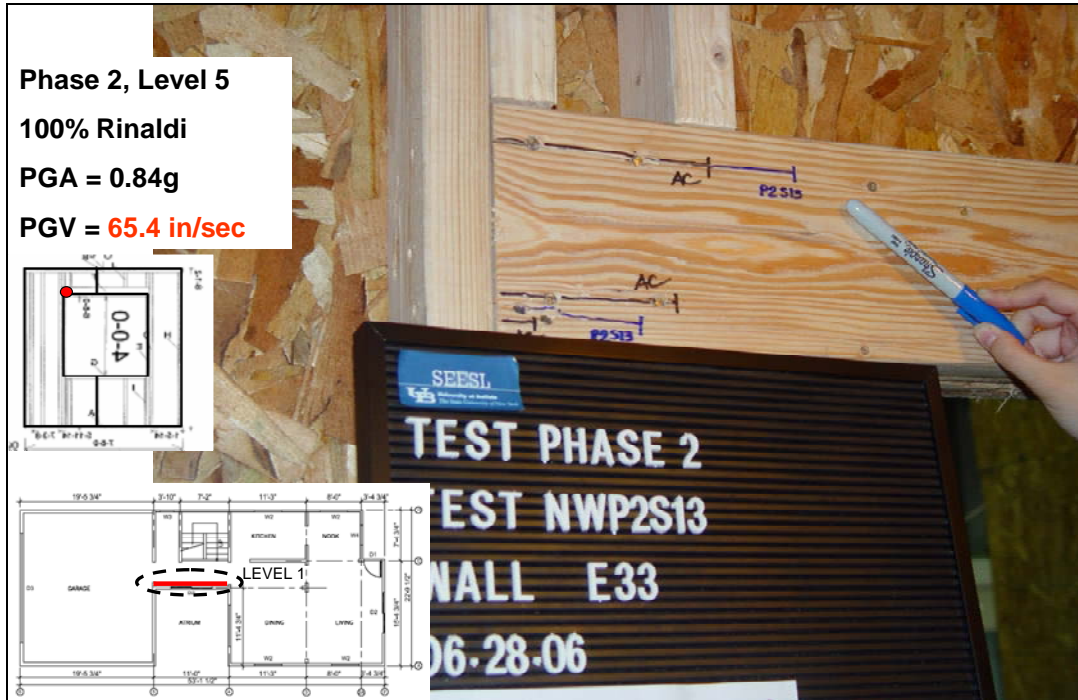
Splitting of top plate



Cracking of vertical stud near connection with top plate

Appendix J

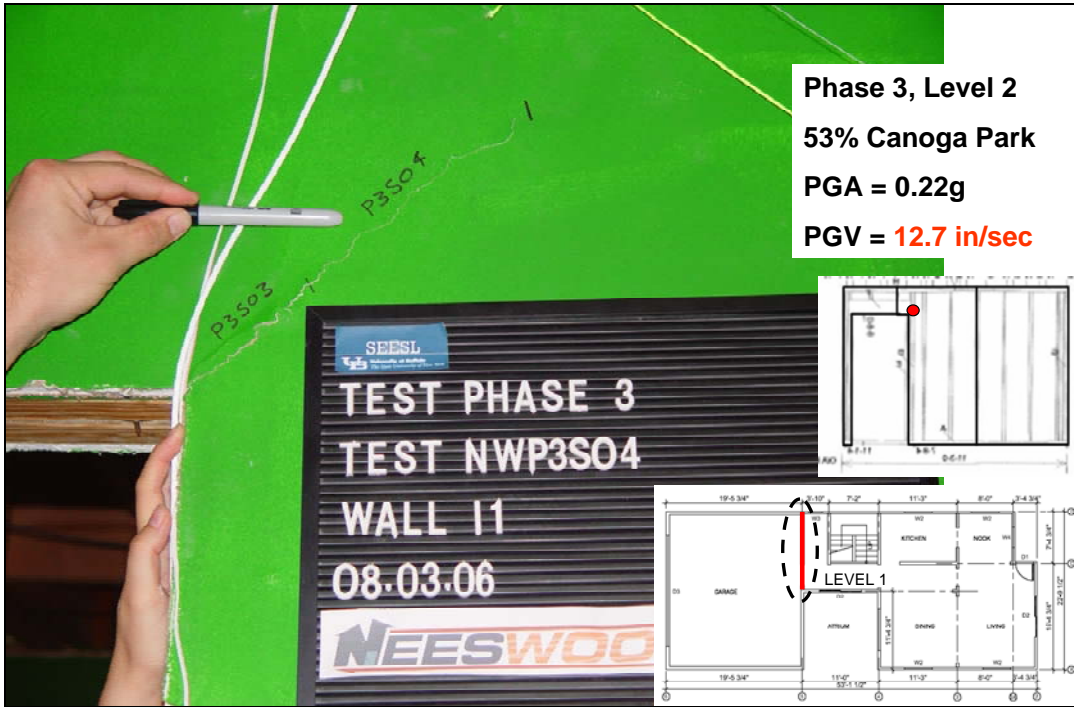
Test Phase 2



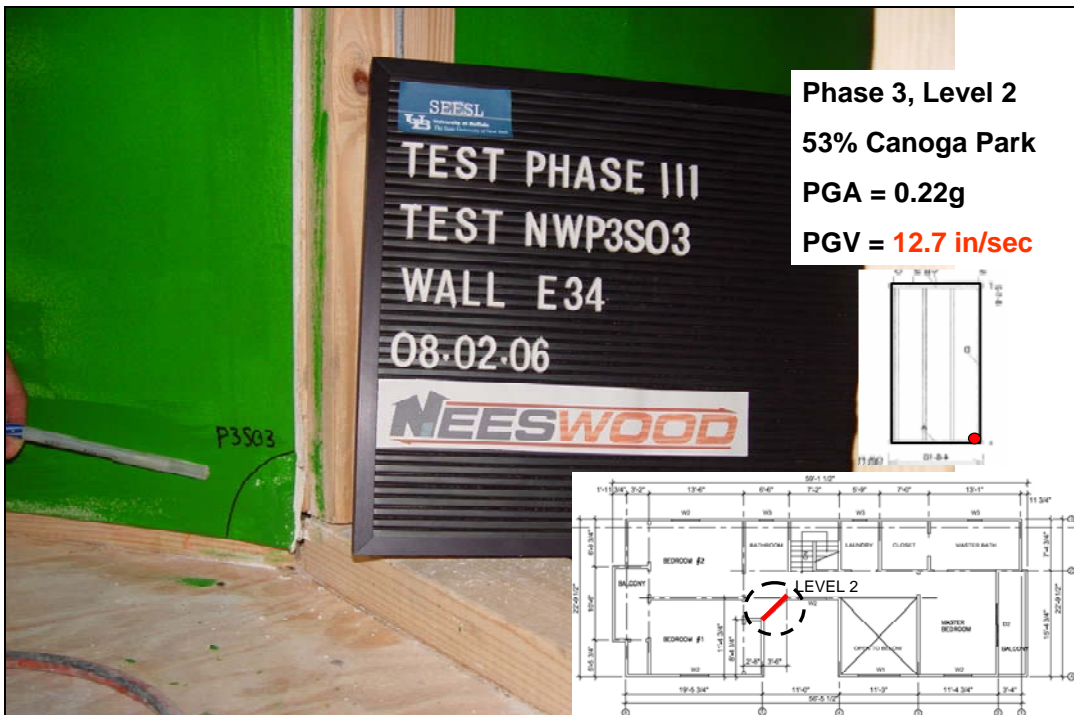
Splitting of window frame

Appendix J

Test Phase 3



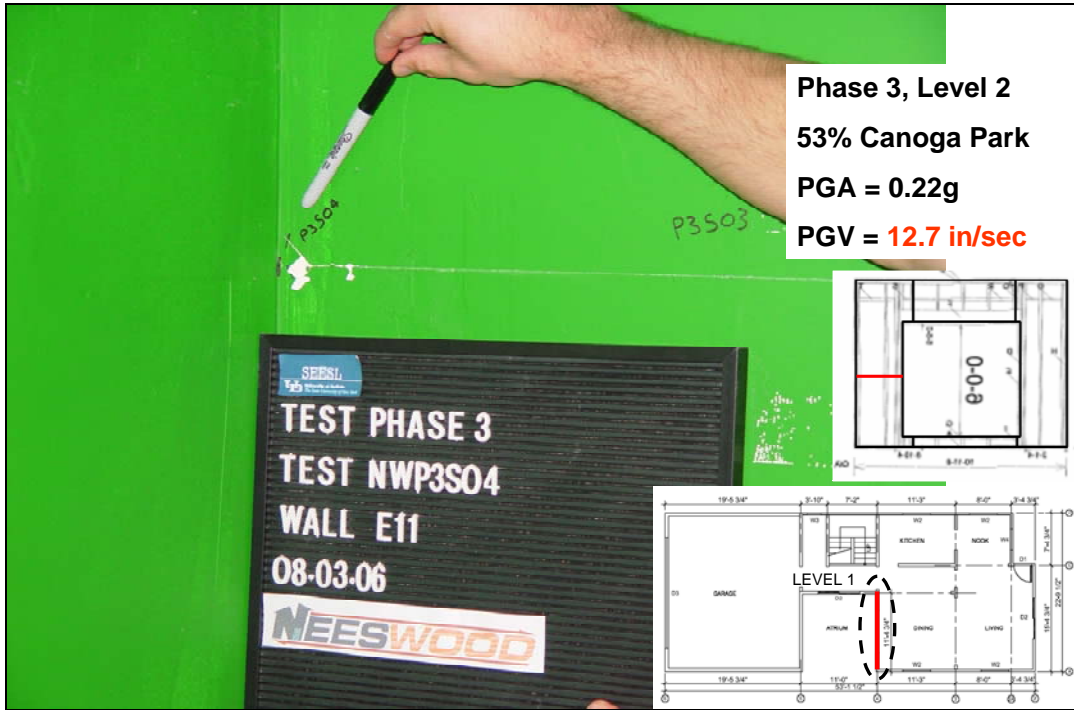
Cracking of gypsum wallboard and diagonal crack propagation at door frame



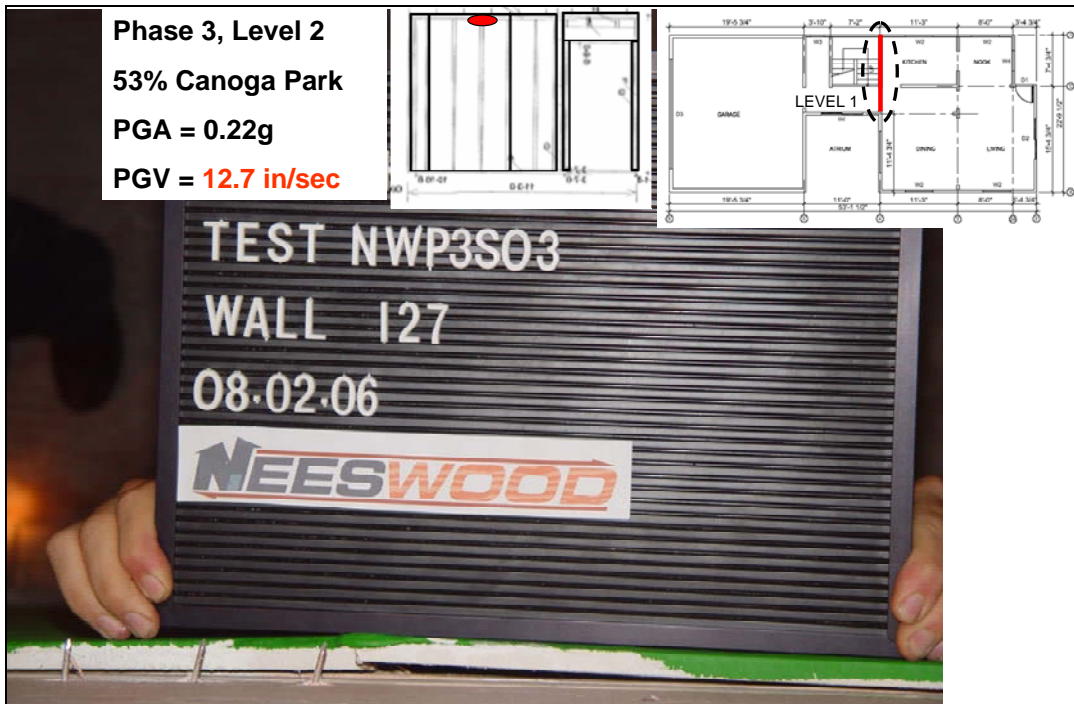
Crushing of gypsum wallboard at wall bottom corner

Appendix J

Test Phase 3



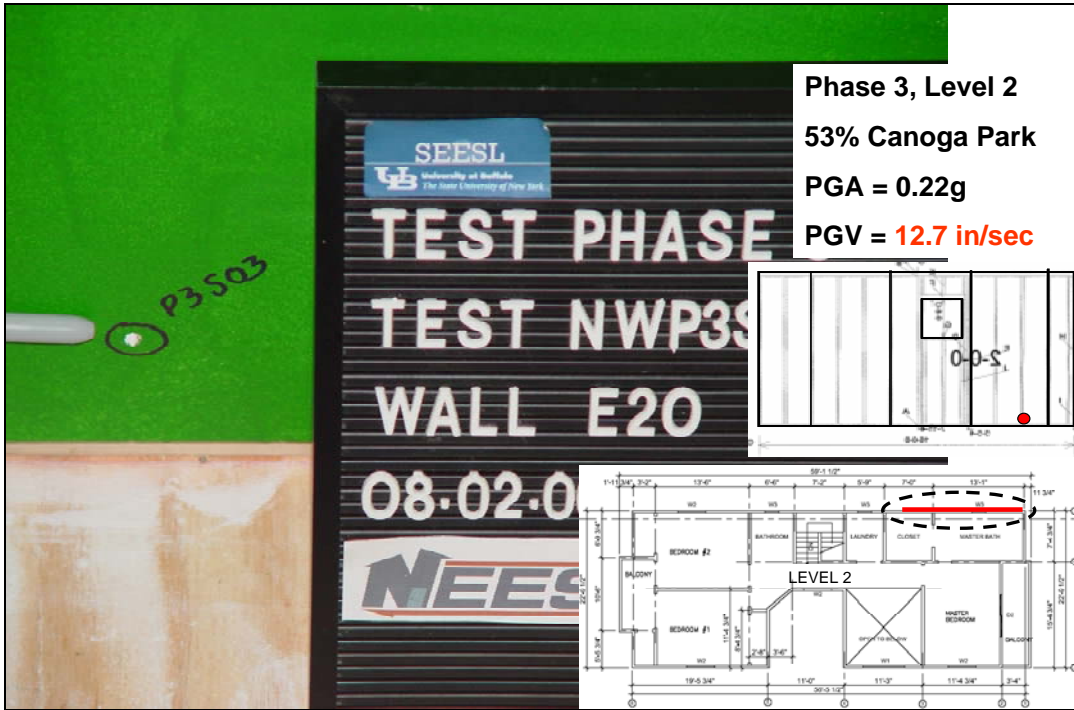
Tape cracking of gypsum wallboard at wall mid height



Screw pull-out and gypsum wall board cracking

Appendix J

Test Phase 3



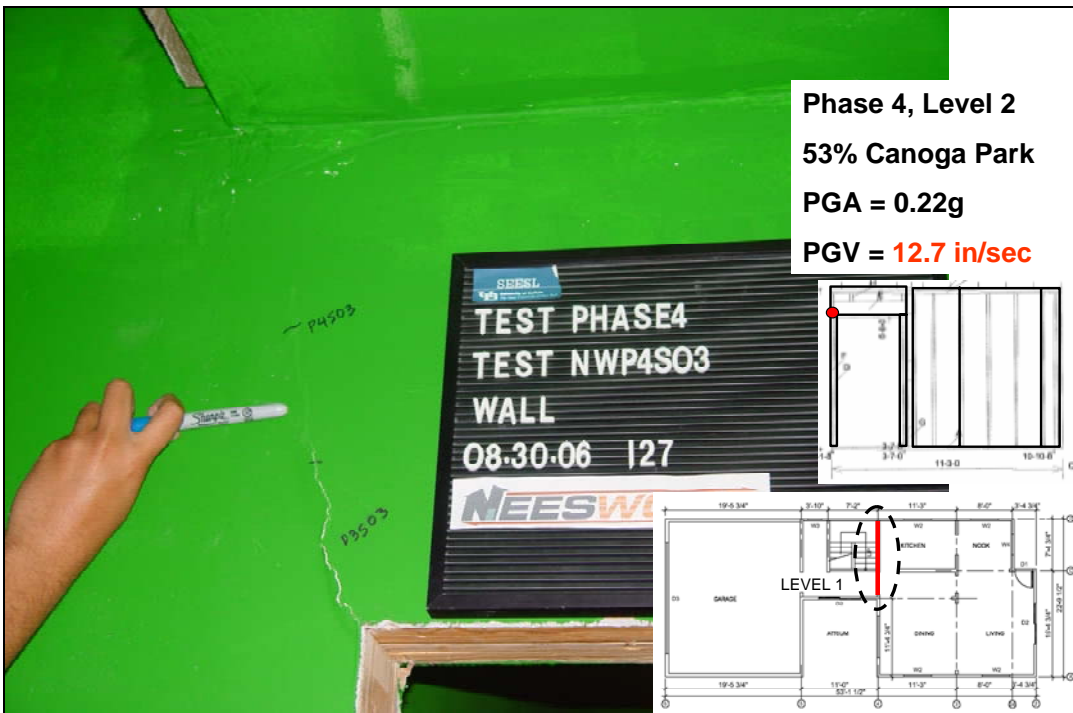
Screw pull-out in gypsum wallboard

Appendix J

Test Phase 4



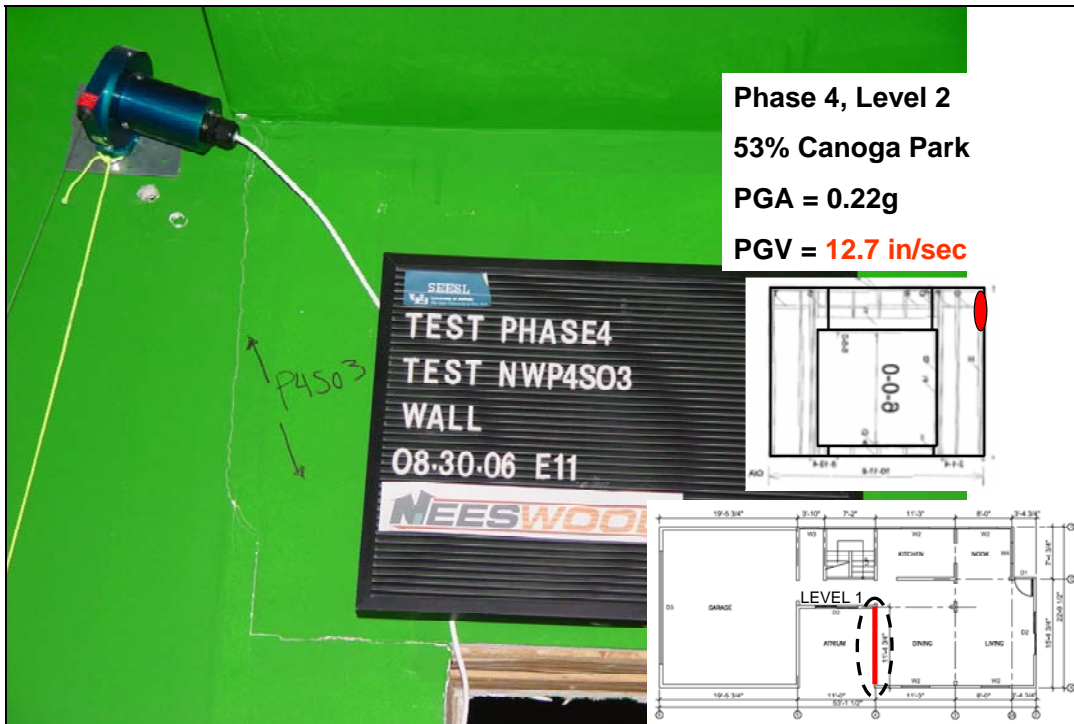
Cracking of gypsum wallboard at ceiling-wall connection



Cracking of gypsum wallboard and diagonal crack propagation at door corner

Appendix J

Test Phase 4



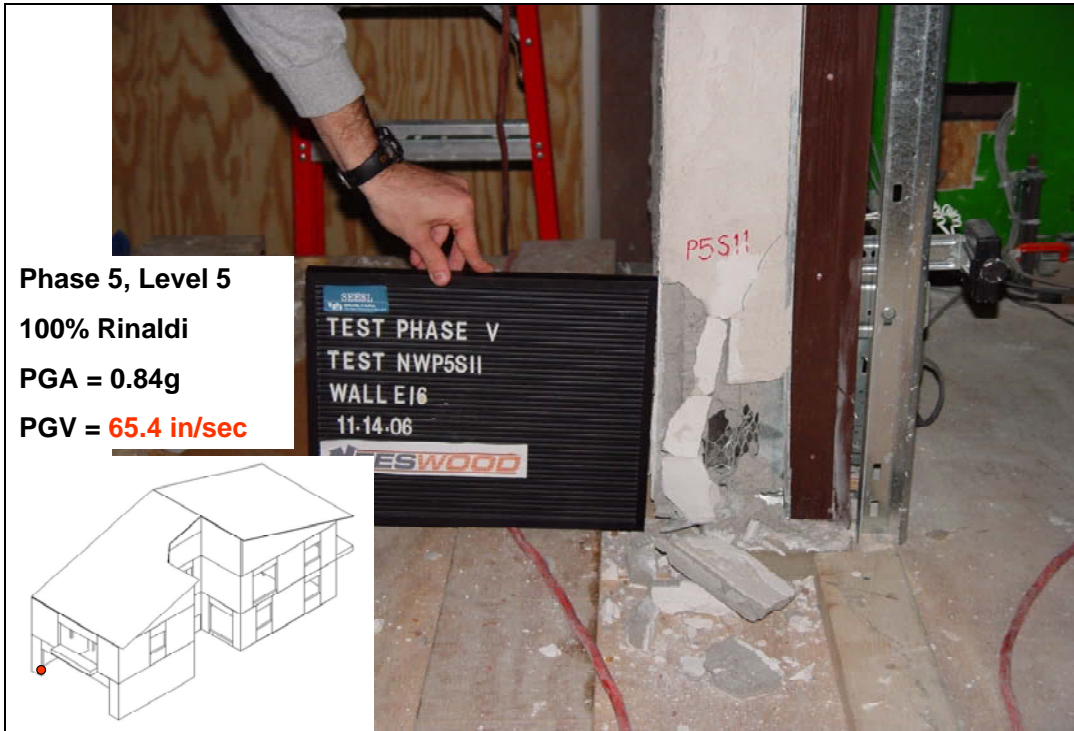
Cracking of gypsum wallboard and crack propagation at door corner



Screw pull-out in gypsum wallboard

Appendix J

Test Phase 5



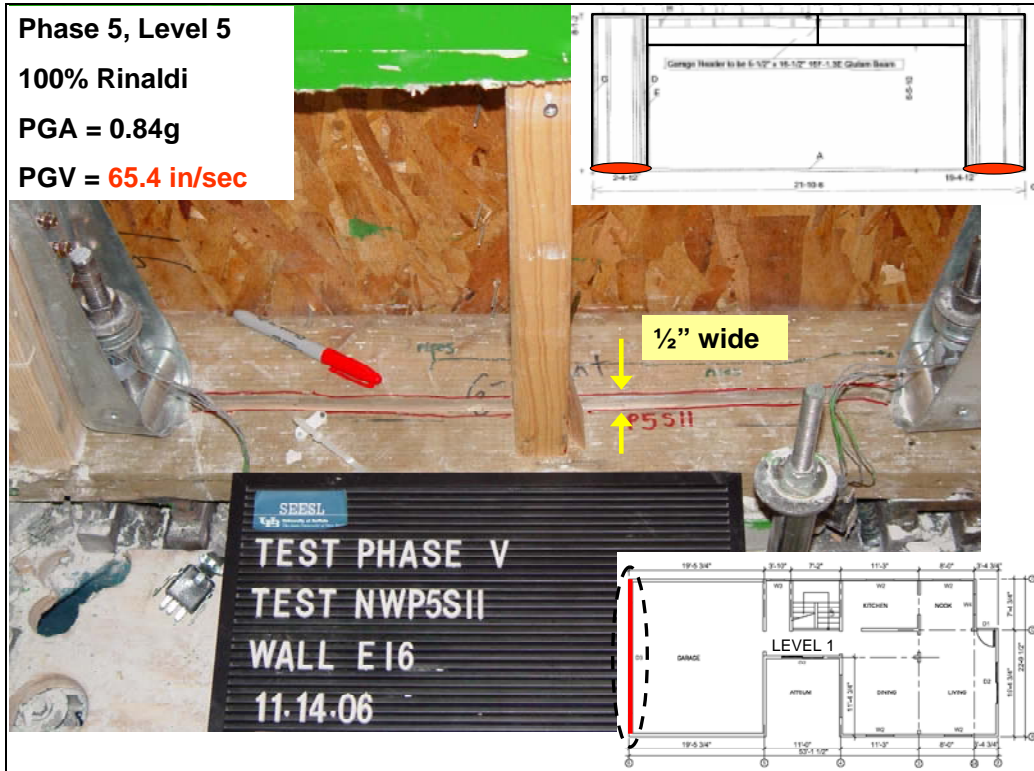
Cracking and spalling of stucco at bottom of garage wall



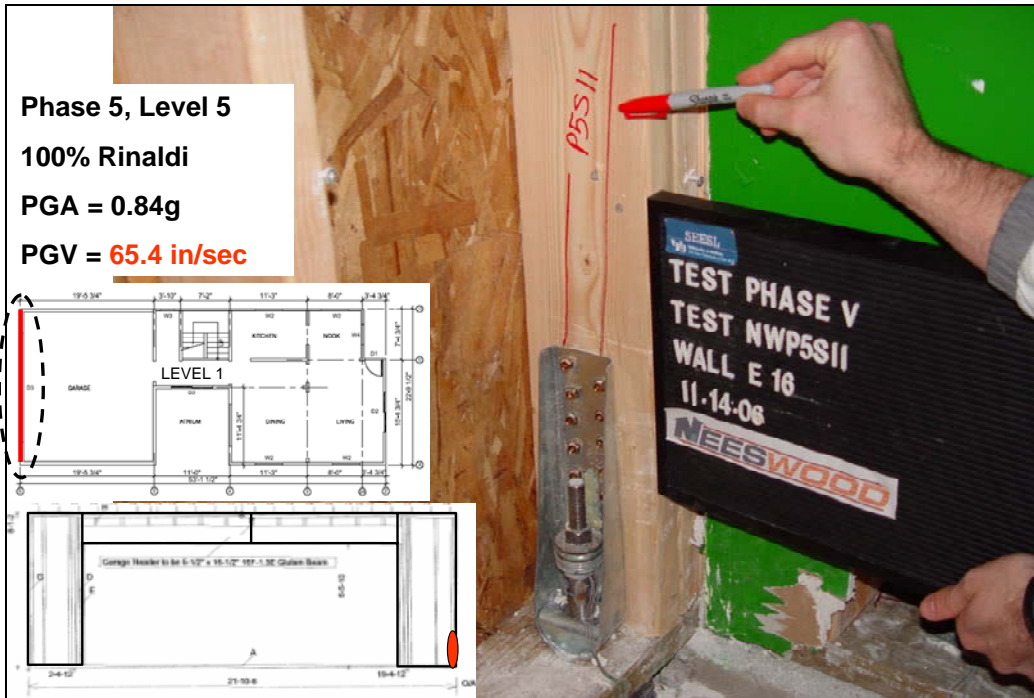
Cracking and spalling of stucco at corner of garage wall opening

Appendix J

Test Phase 5



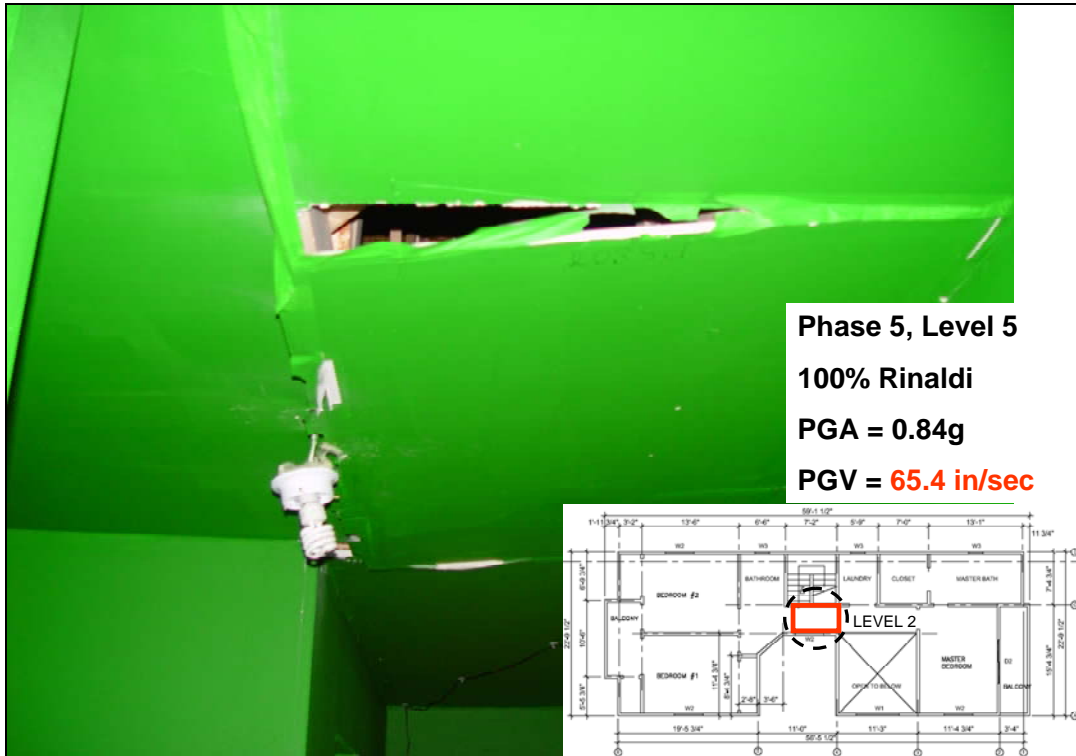
Cracking and separation of sill plate through entire length of garage narrow wall piers



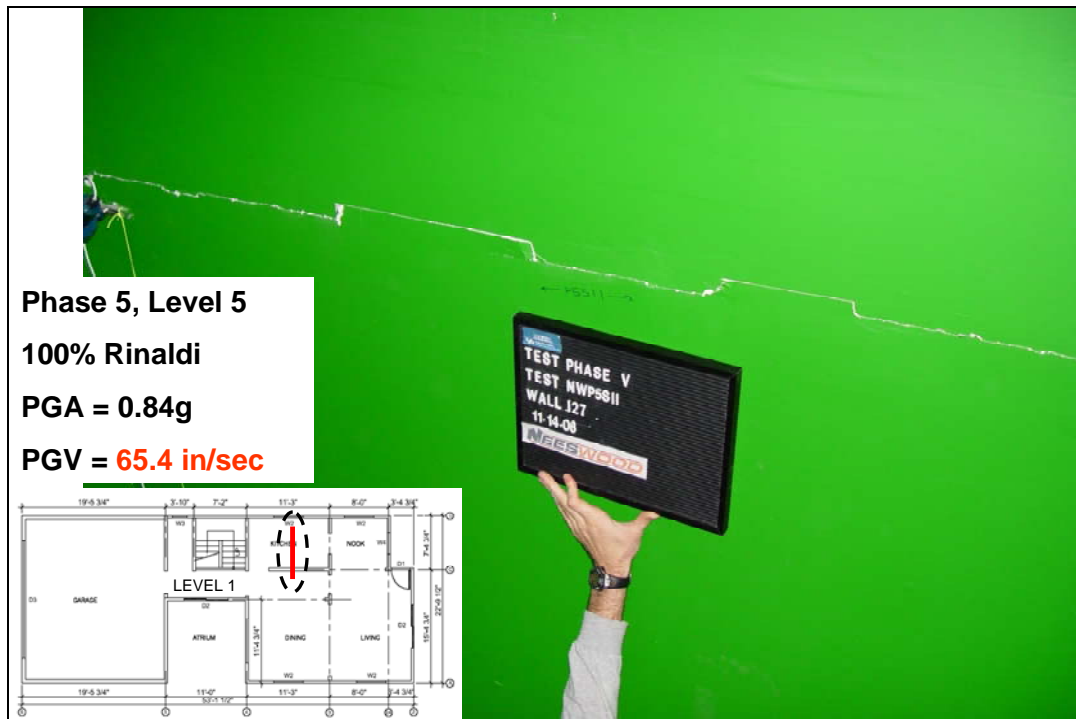
Cracking of stud above hold-down anchor

Appendix J

Test Phase 5



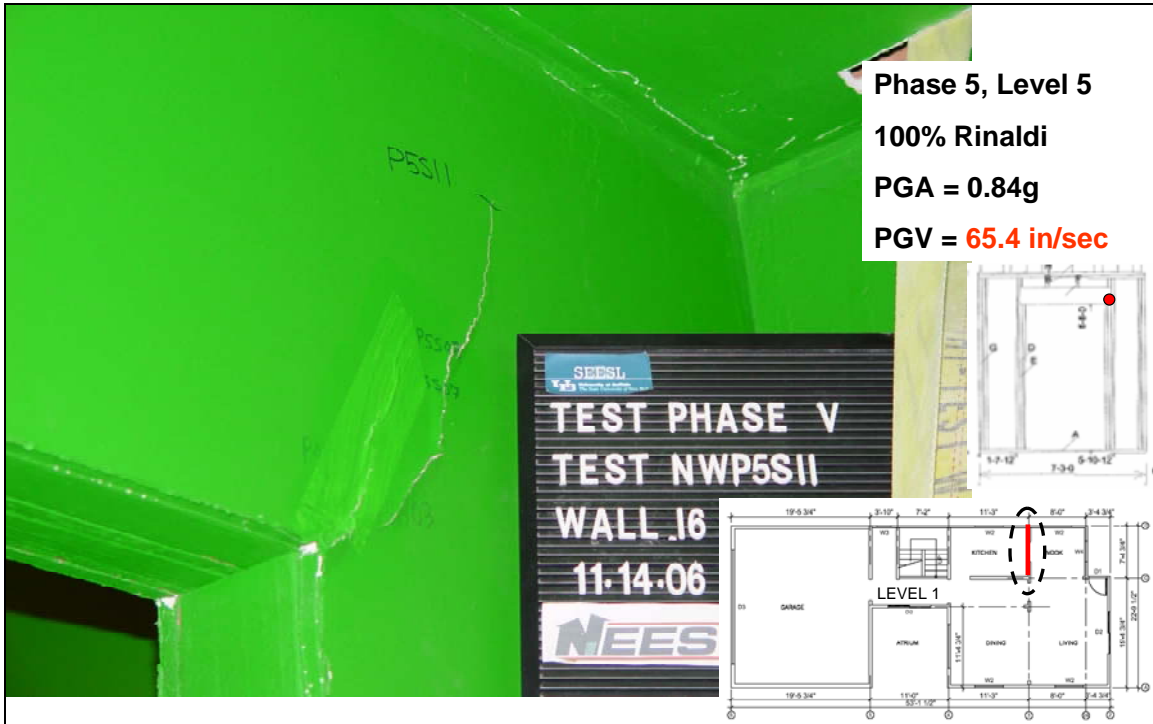
Separation of parts of gypsum wallboard from the ceiling



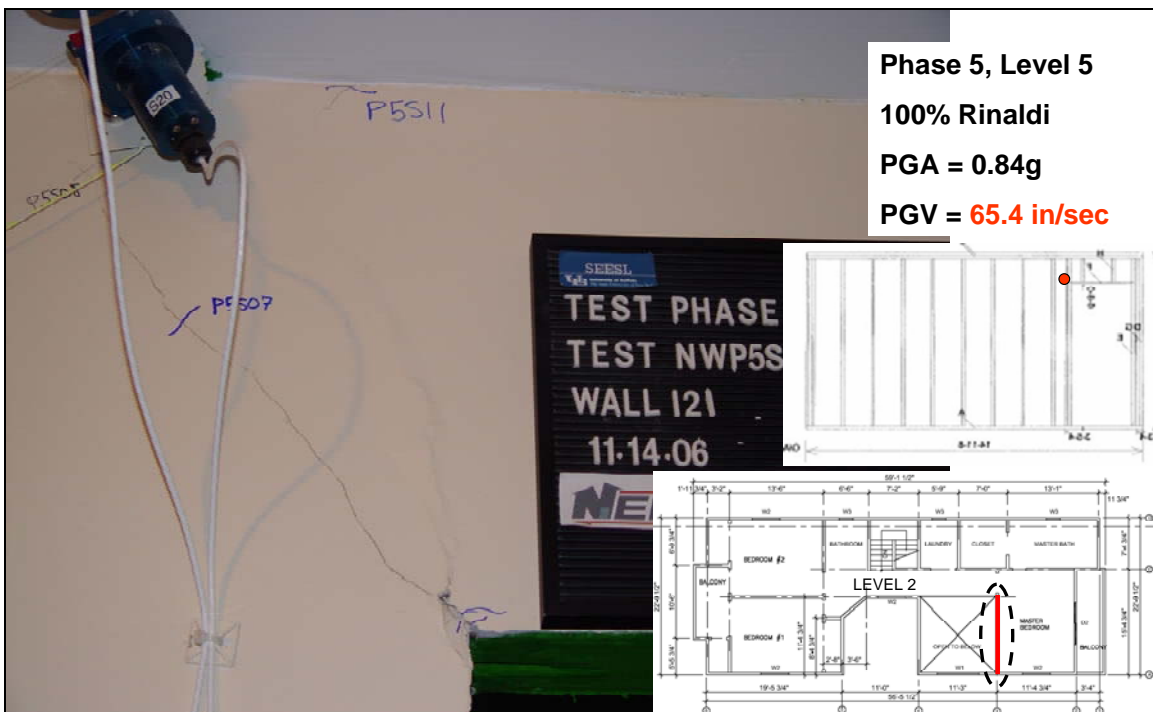
Horizontal cracking of gypsum wallboard at second floor level

Appendix J

Test Phase 5



Cracking and buckling of gypsum wallboard at door opening



Cracking of gypsum wallboard at door opening

Appendix J

Test Phase 5



Dining and living rooms before Test NWP5S11



Dining and living rooms after Test NWP5S11

Appendix J

Test Phase 5



Nook before Test NWP5S11



Nook after Test NWP5S11

Appendix J

Test Phase 5



Garage before Test NWP5S11



Garage after Test NWP5S11

Appendix J

Test Phase 5



Master bedroom before Test NWP5S11



Master bedroom after Test NWP5S11

Appendix J

Test Phase 5



Bedroom #1 before Test NWP5S11



Bedroom #1 after Test NWP5S11

Appendix J

Test Phase 5



Bedroom #2 before Test NWP5S11



Bedroom #2 after Test NWP5S11

Appendix K
Selected Seismic Results:
Relative Interstory Drift
Time Histories

Appendix K

Phase 1, NWP1S01 Seismic Test

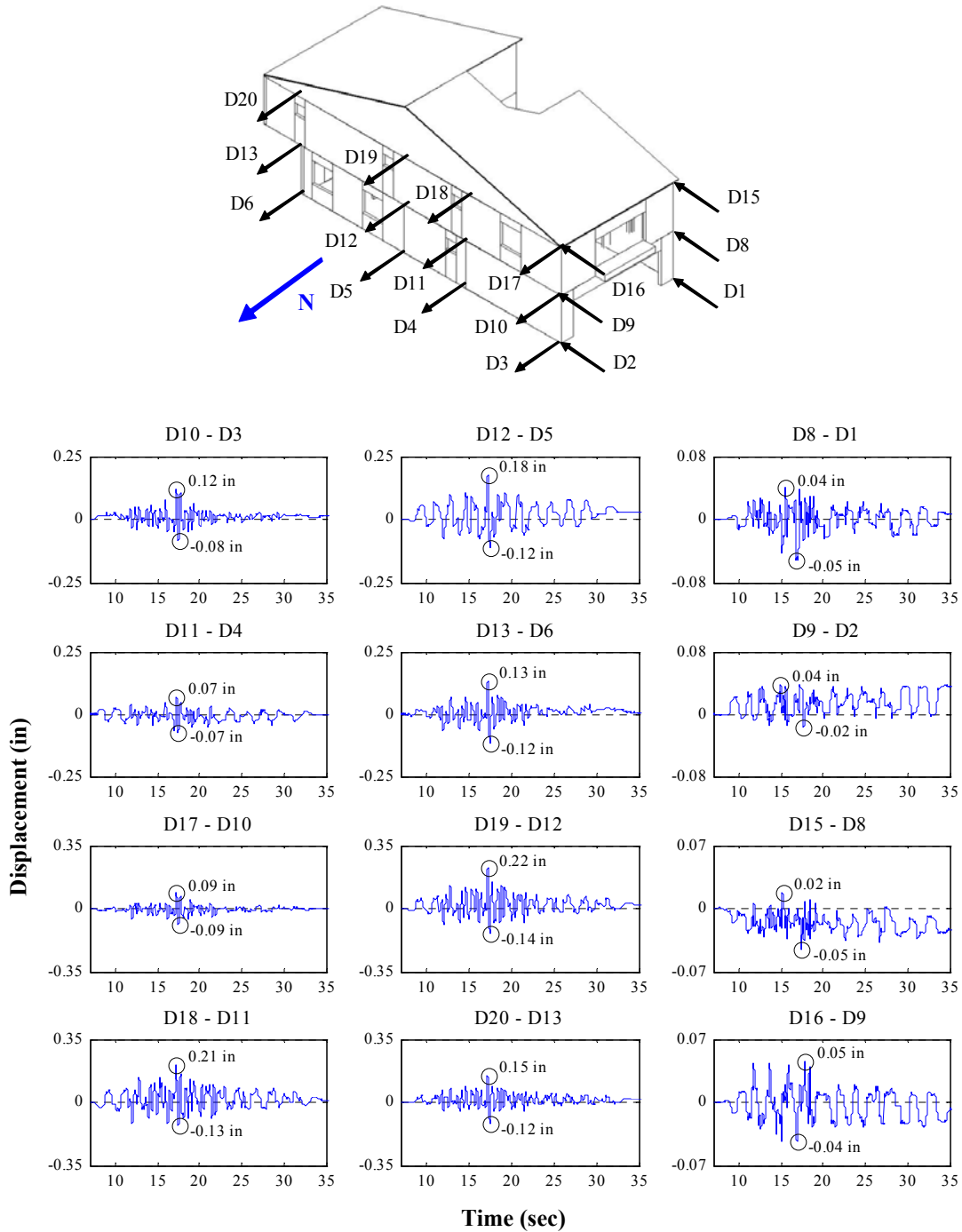


Figure K.1: Relative interstory drift time histories for Test NWP1S01

* Data not corrected to exclude the effect of shake table rotations due to data unavailability

Appendix K

Phase 1, NWP1S02 Seismic Test

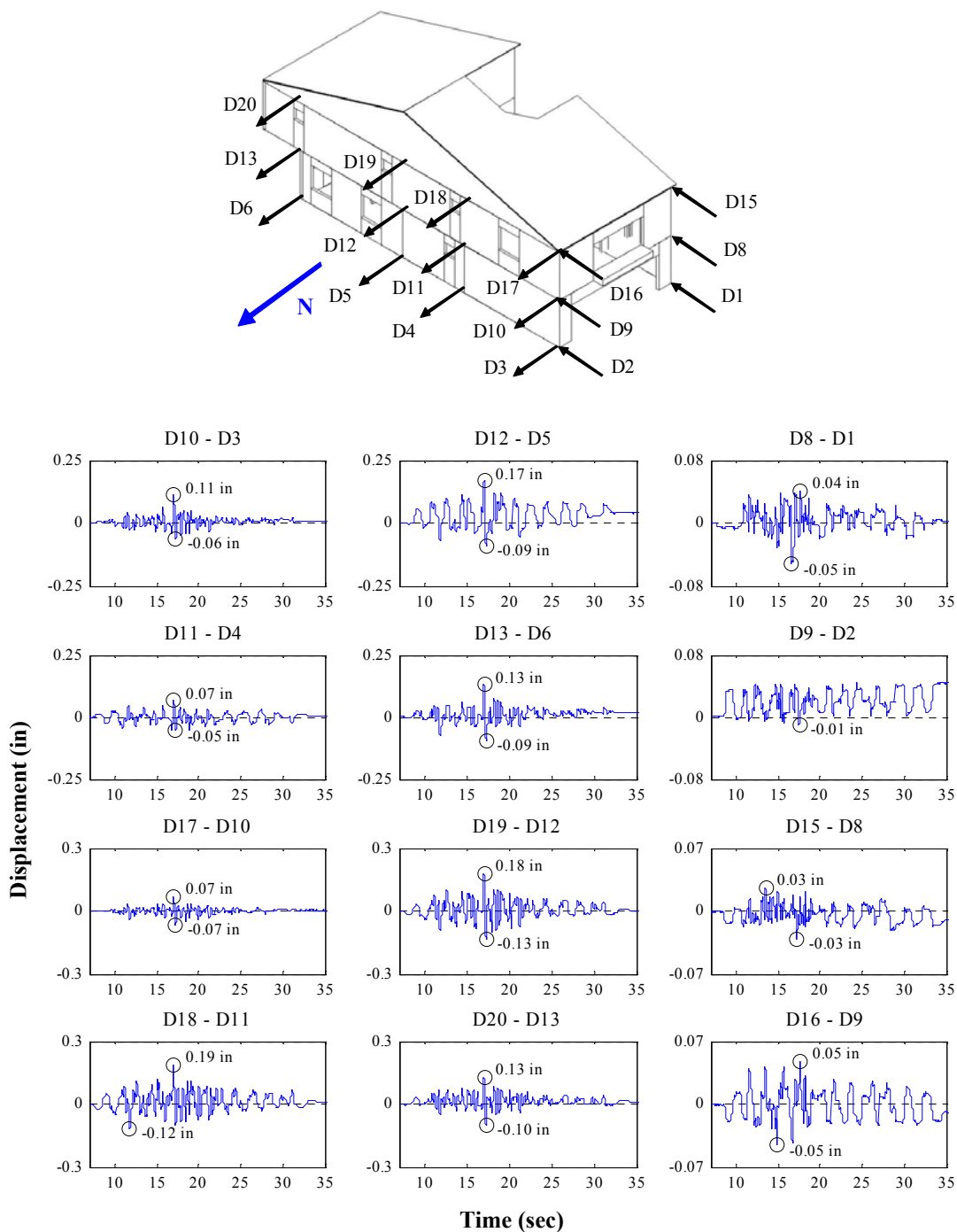


Figure K.2: Relative interstory drift time histories for Test NWP1S02

* Data not corrected to exclude the effect of shake table rotations due to data unavailability

Appendix K

Phase 1, NWP1S03 Seismic Test

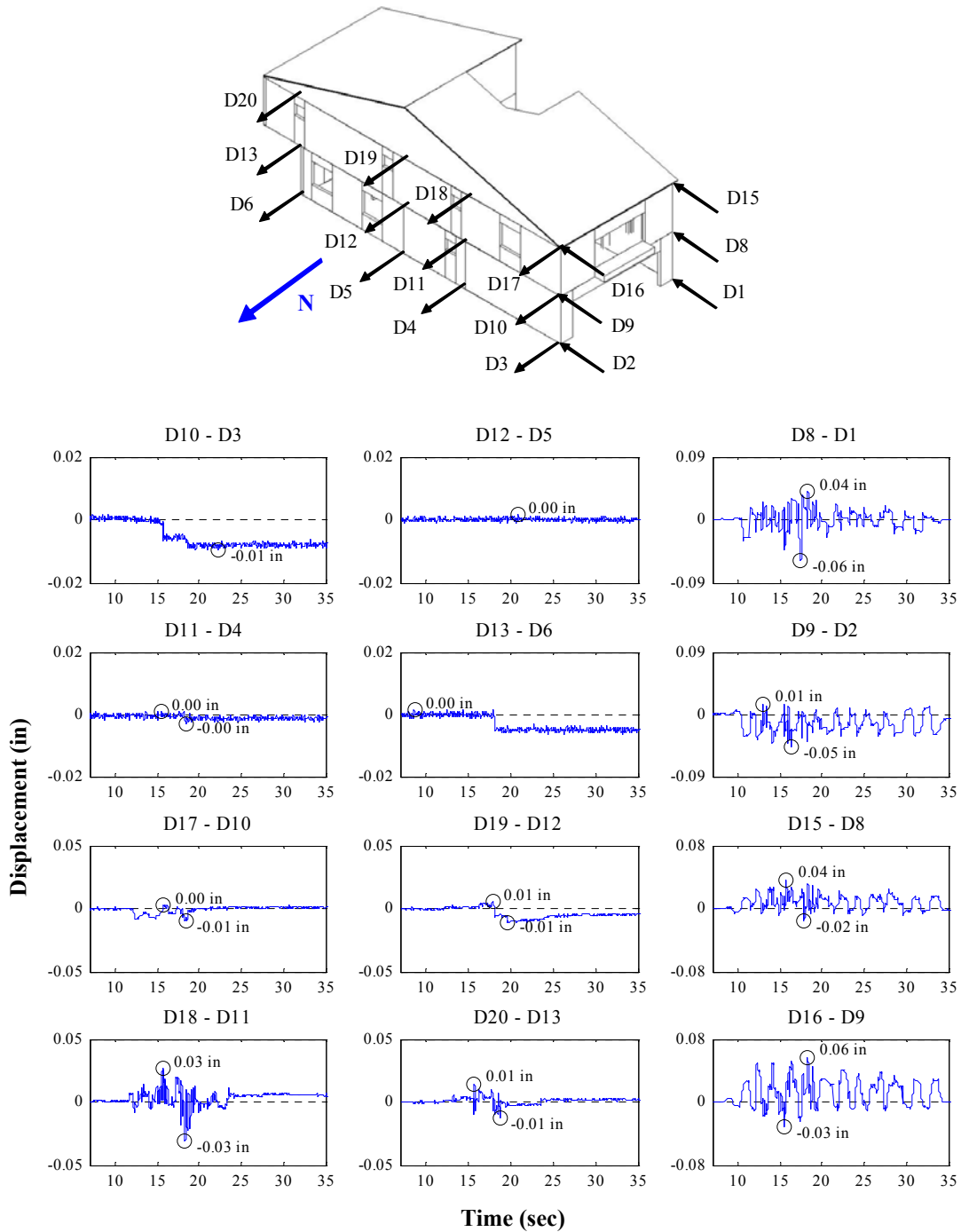


Figure K.3: Relative interstory drift time histories for Test NWP1S03

* Data not corrected to exclude the effect of shake table rotations due to data unavailability

Appendix K

Phase 1, NWP1S04 Seismic Test

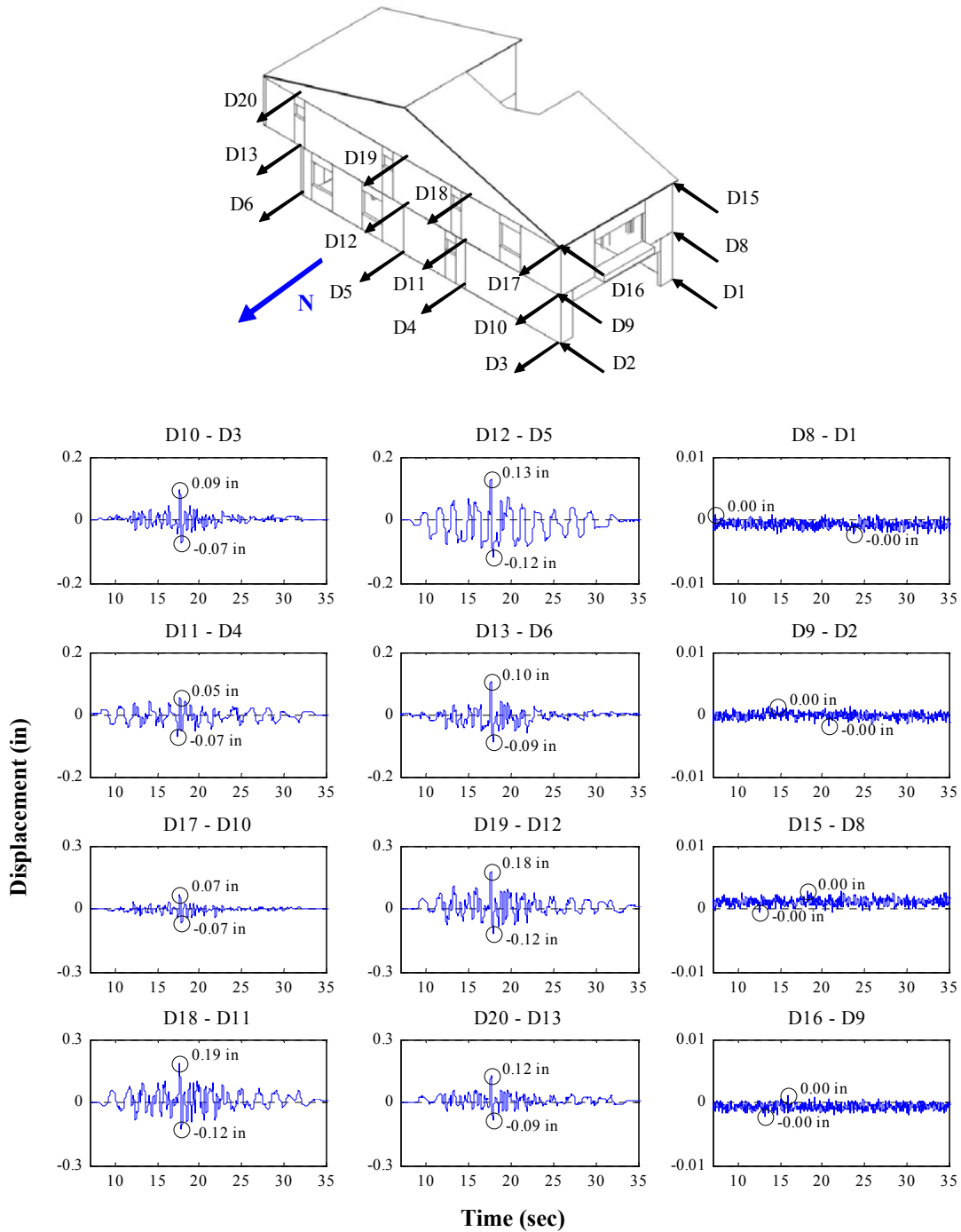


Figure K.4: Relative interstory drift time histories for Test NWP1S04

* Data not corrected to exclude the effect of shake table rotations due to data unavailability

Appendix K

Phase 1, NWP1S05 Seismic Test

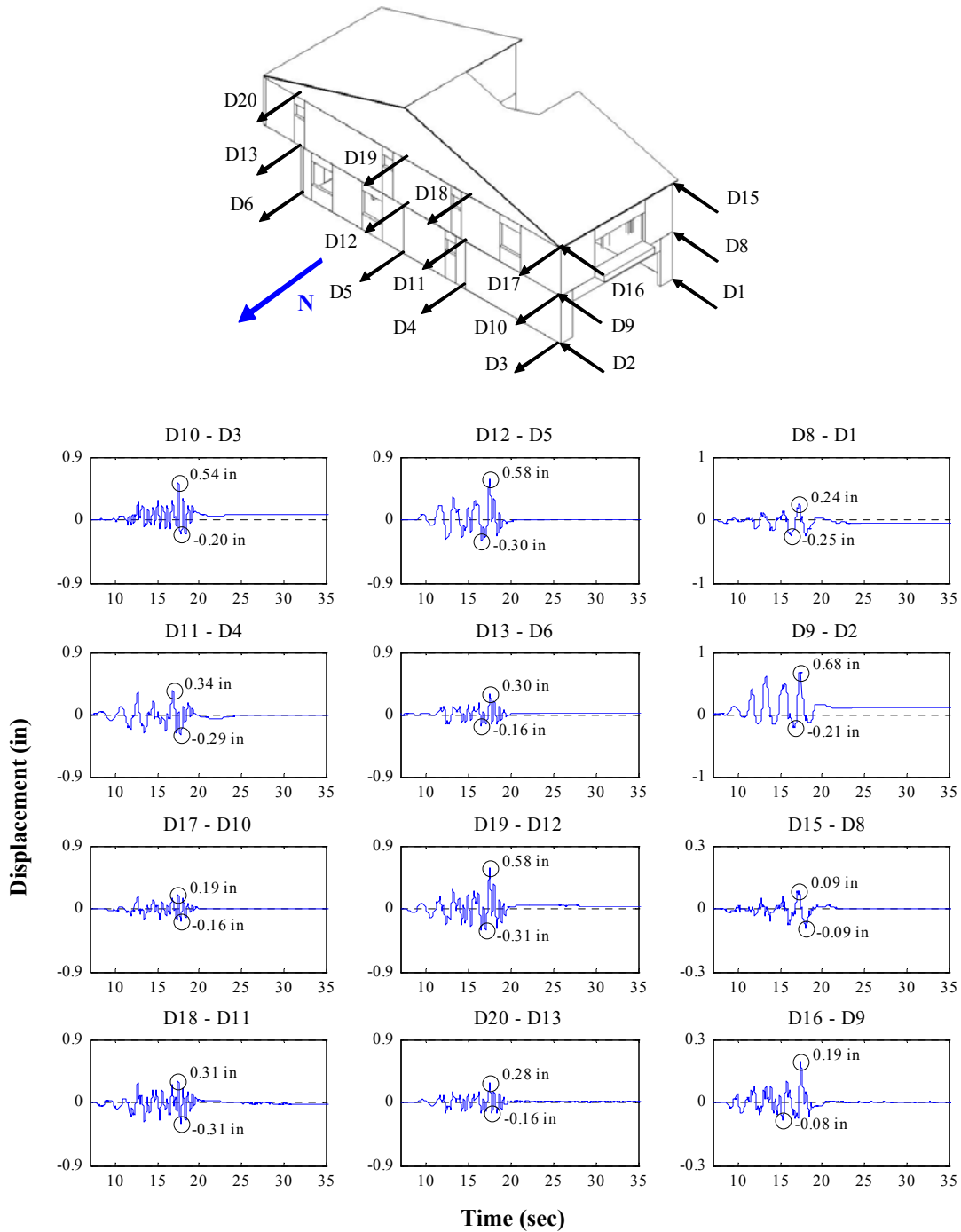


Figure K.5: Relative interstory drift time histories for Test NWP1S05

* Actual data are corrected to exclude the effect of shake table rotations

Appendix K

Phase 1, NWP1S17 Seismic Test

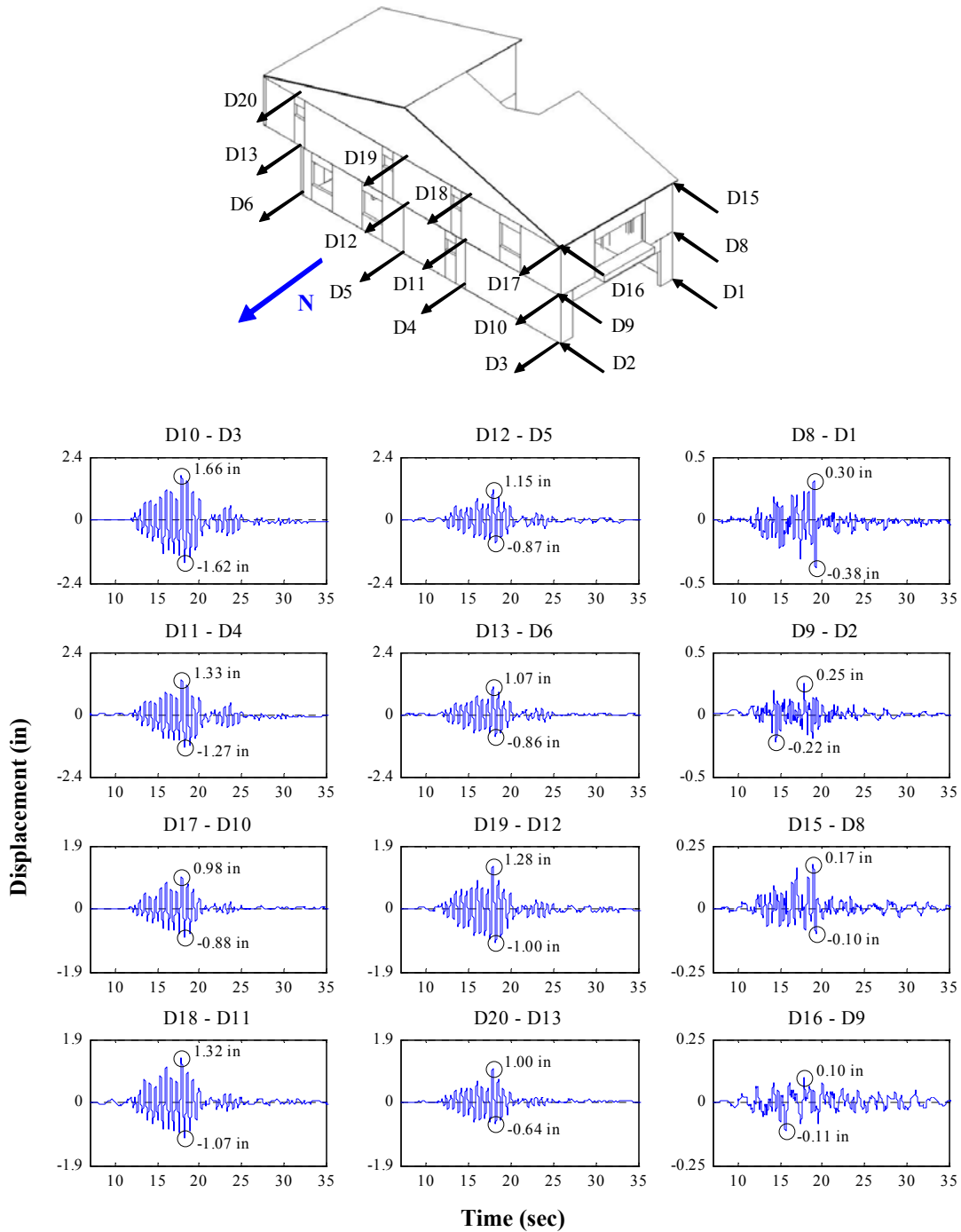


Figure K.6: Relative interstory drift time histories for Test NWP1S17

* Actual data are corrected to exclude the effect of shake table rotations

Appendix K

Phase 1, NWP1S07 Seismic Test

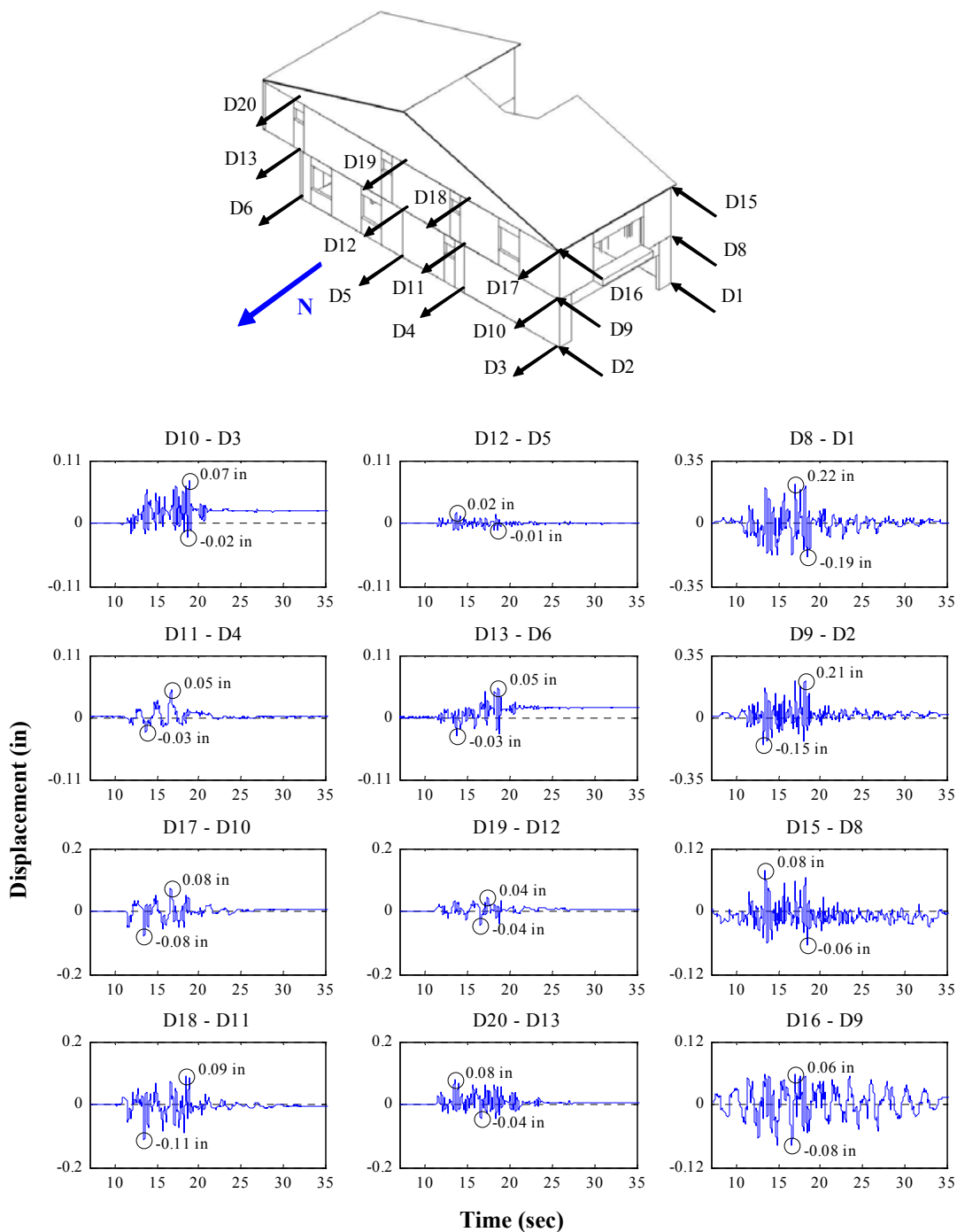


Figure K.7: Relative interstory drift time histories for Test NWP1S07

* Actual data are corrected to exclude the effect of shake table rotations

Appendix K

Phase 1, NWP1S06 Seismic Test

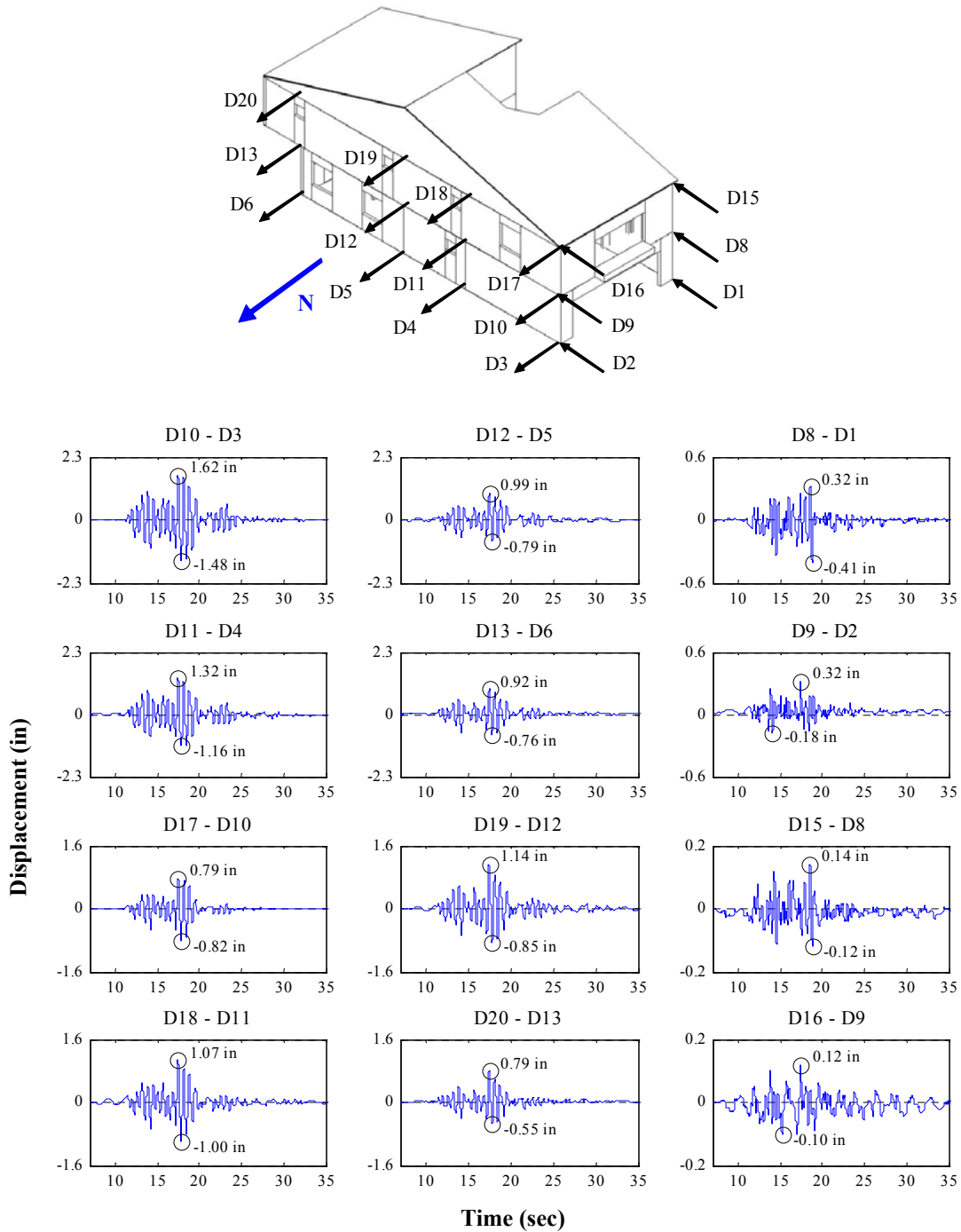


Figure K.8: Relative interstory drift time histories for Test NWP1S06

* Actual data are corrected to exclude the effect of shake table rotations

Appendix K

Phase 1, NWP1S10 Seismic Test

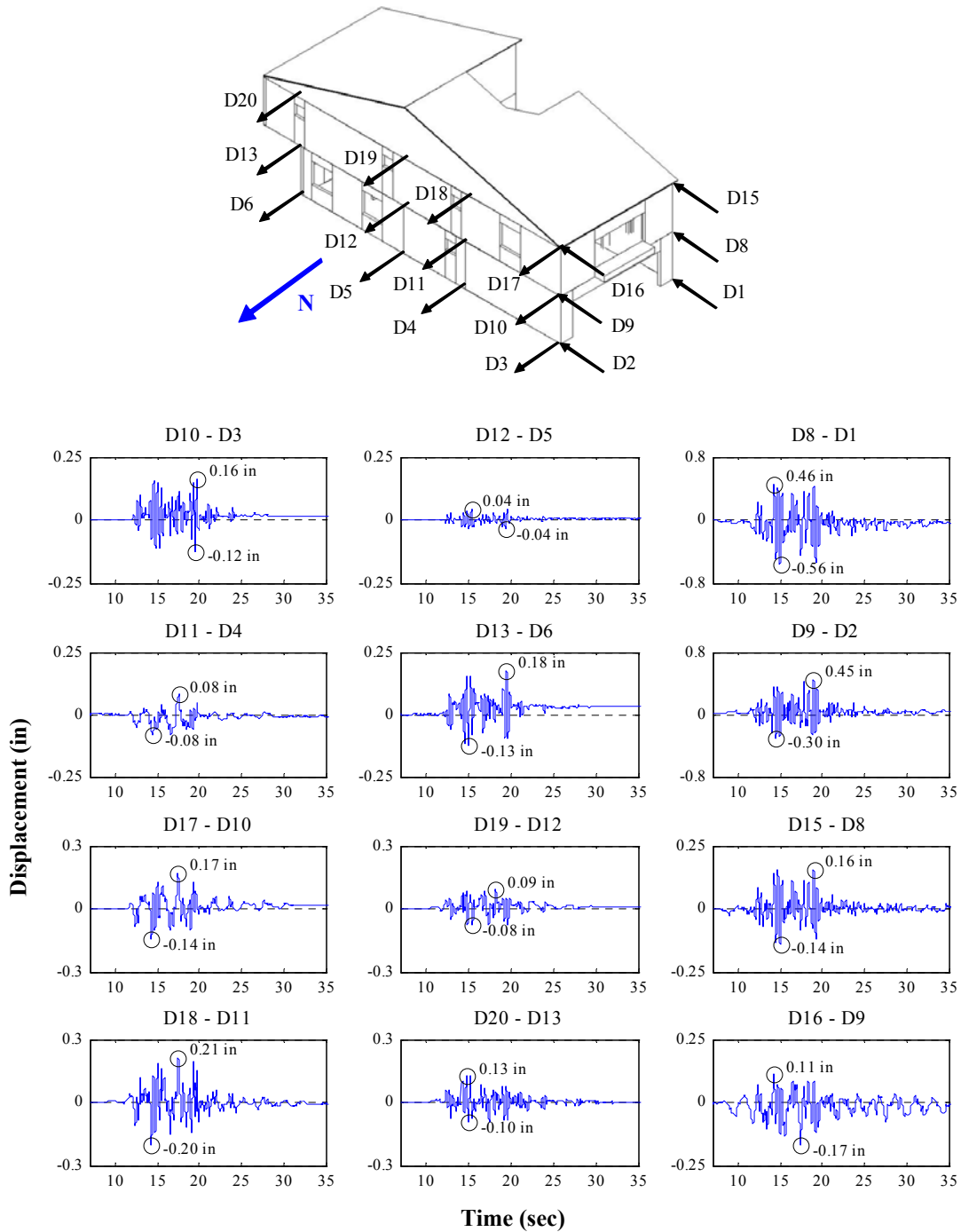


Figure K.9: Relative interstory drift time histories for Test NWP1S10

* Actual data are corrected to exclude the effect of shake table rotations

Appendix K

Phase 2, NWP2S01 Seismic Test

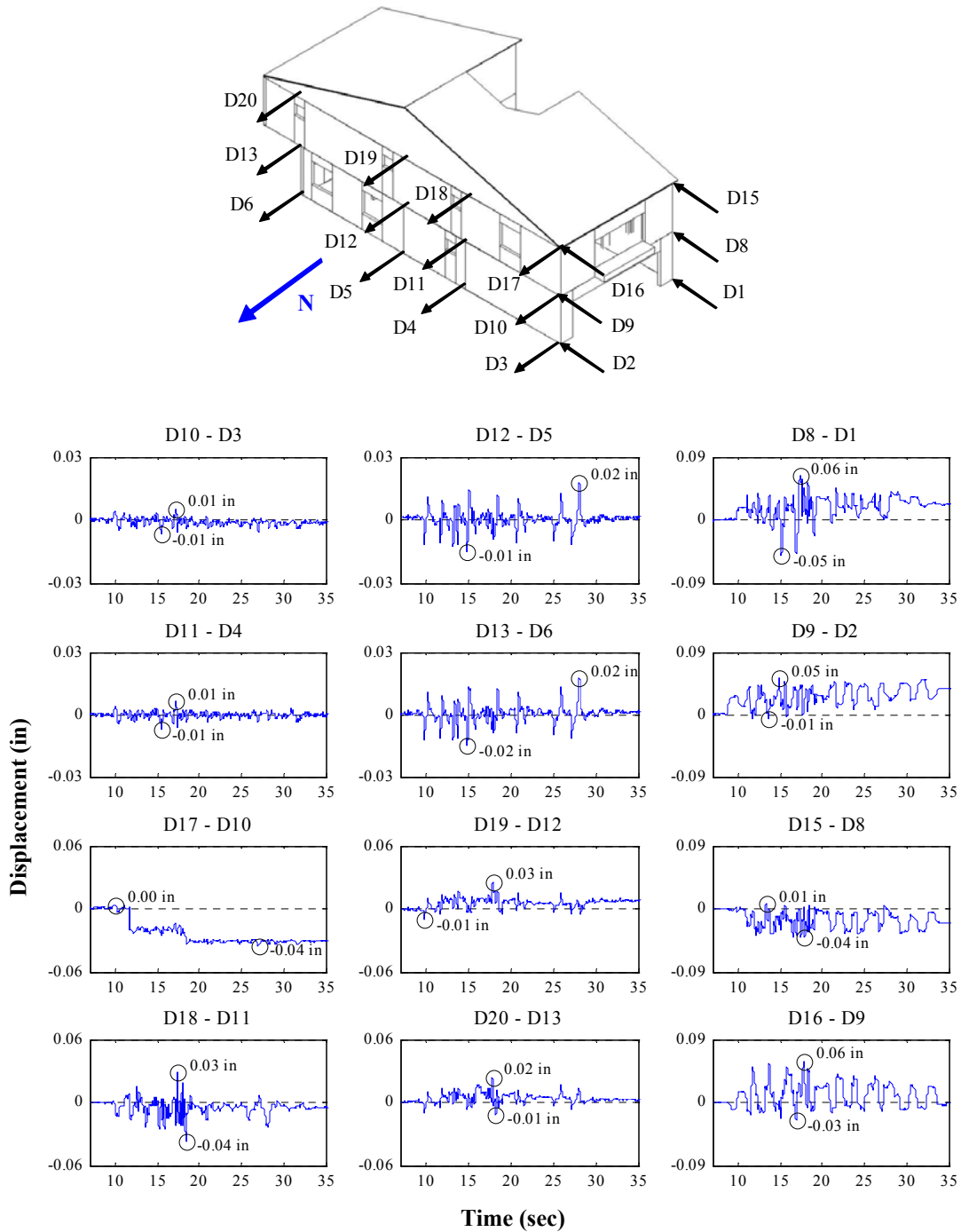


Figure K.10: Relative interstory drift time histories for Test NWP2S01

* Actual data are corrected to exclude the effect of shake table rotations

Appendix K

Phase 2, NWP2S02 Seismic Test

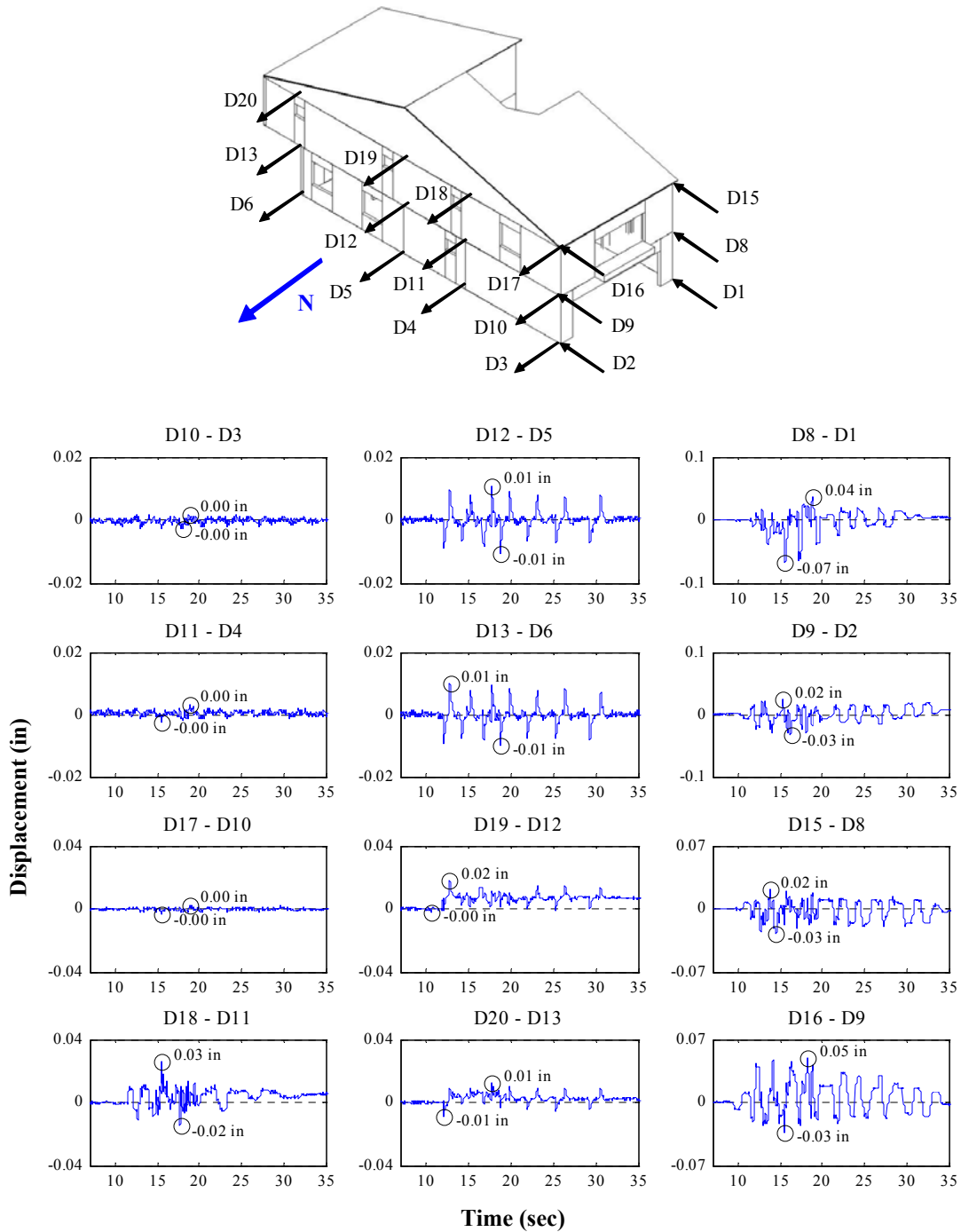


Figure K.11: Relative interstory drift time histories for Test NWP2S02

* Actual data are corrected to exclude the effect of shake table rotations

Appendix K

Phase 2, NWP2S03 Seismic Test

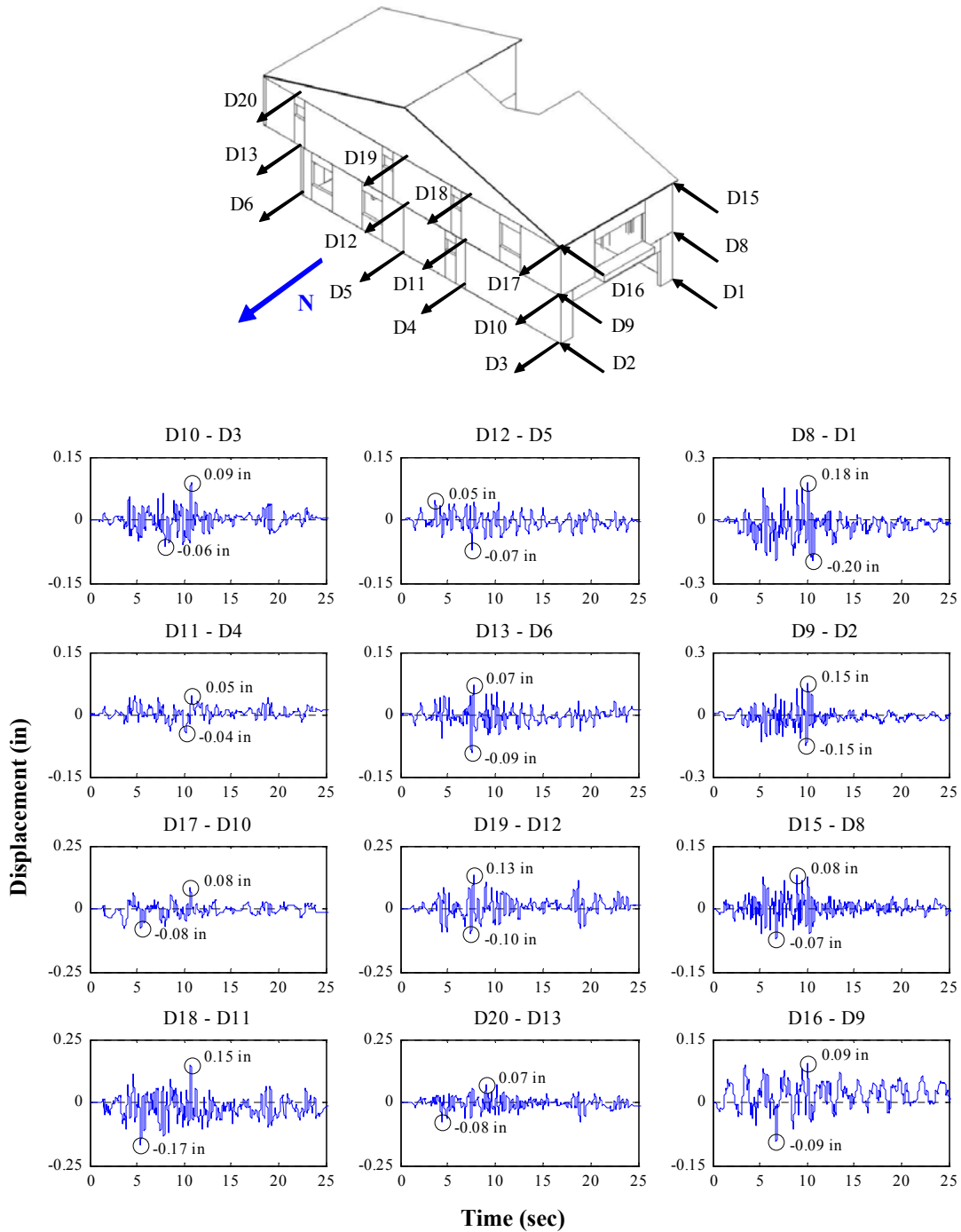


Figure K.12: Relative interstory drift time histories for Test NWP2S03

* Actual data are corrected to exclude the effect of shake table rotations

Appendix K

Phase 2, NWP2S04 Seismic Test

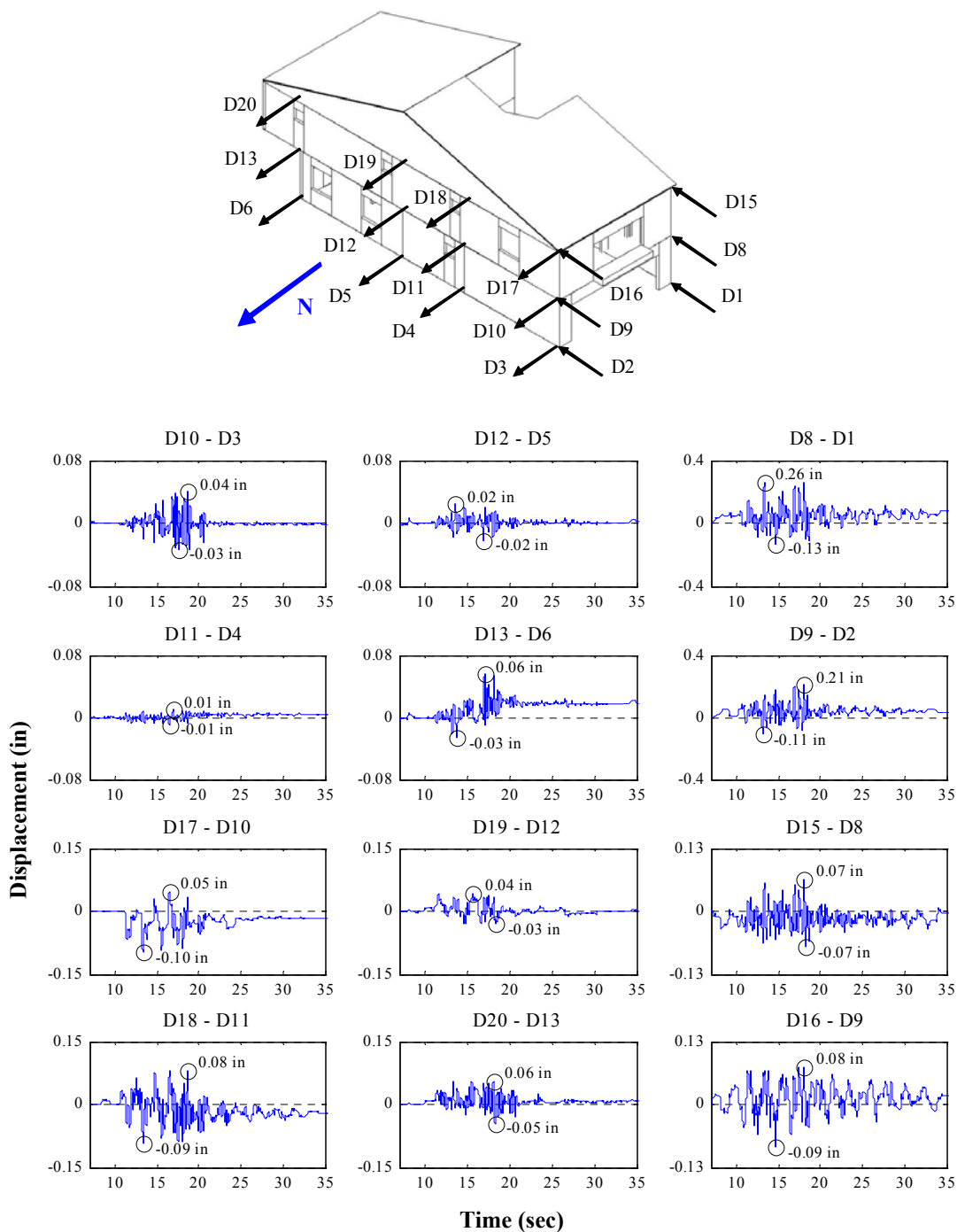


Figure K.13: Relative interstory drift time histories for Test NWP2S04

* Actual data are corrected to exclude the effect of shake table rotations

Appendix K

Phase 2, NWP2S05 Seismic Test

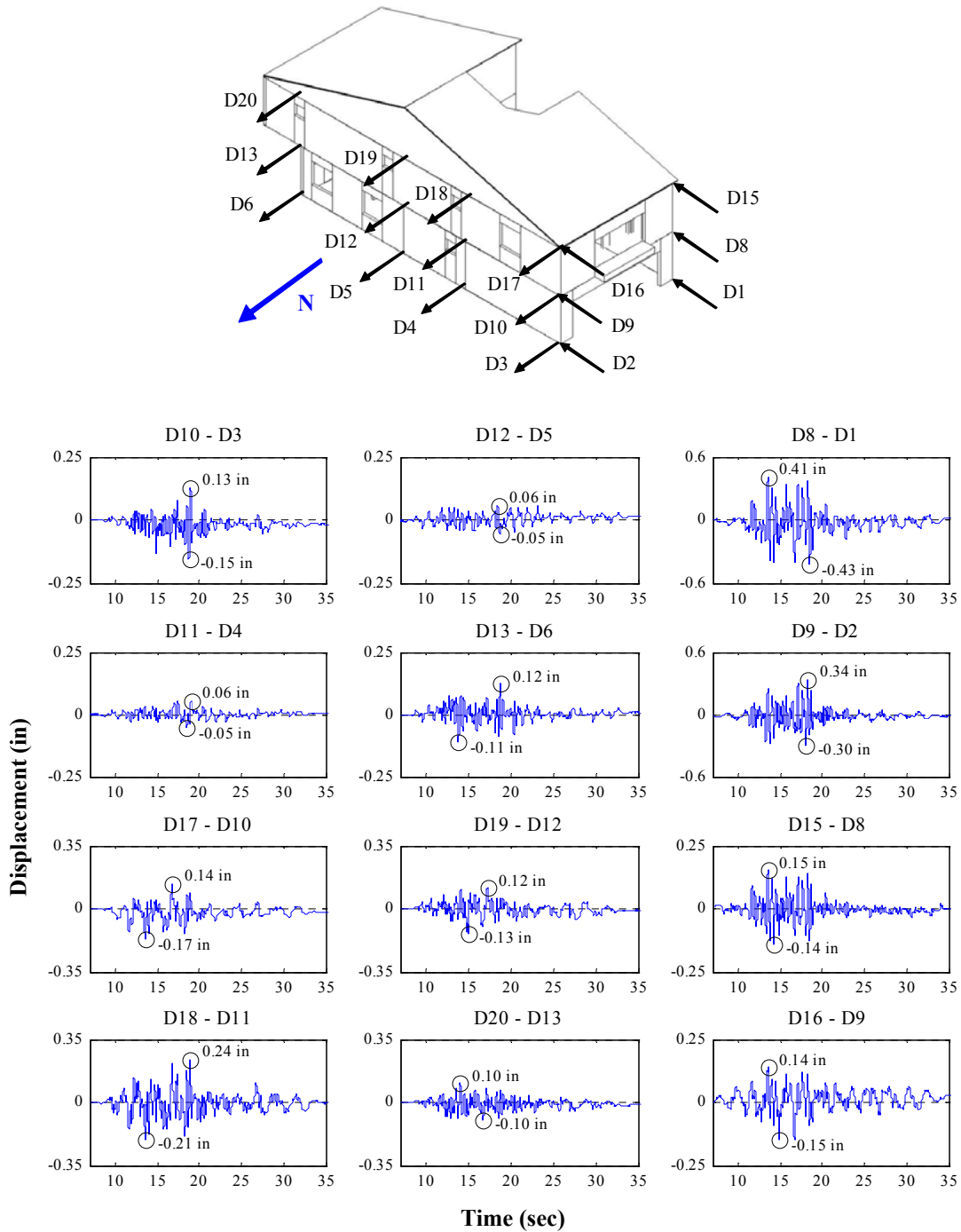


Figure K.14: Relative interstory drift time histories for Test NWP2S05

* Actual data are corrected to exclude the effect of shake table rotations

Appendix K

Phase 2, NWP2S06 Seismic Test

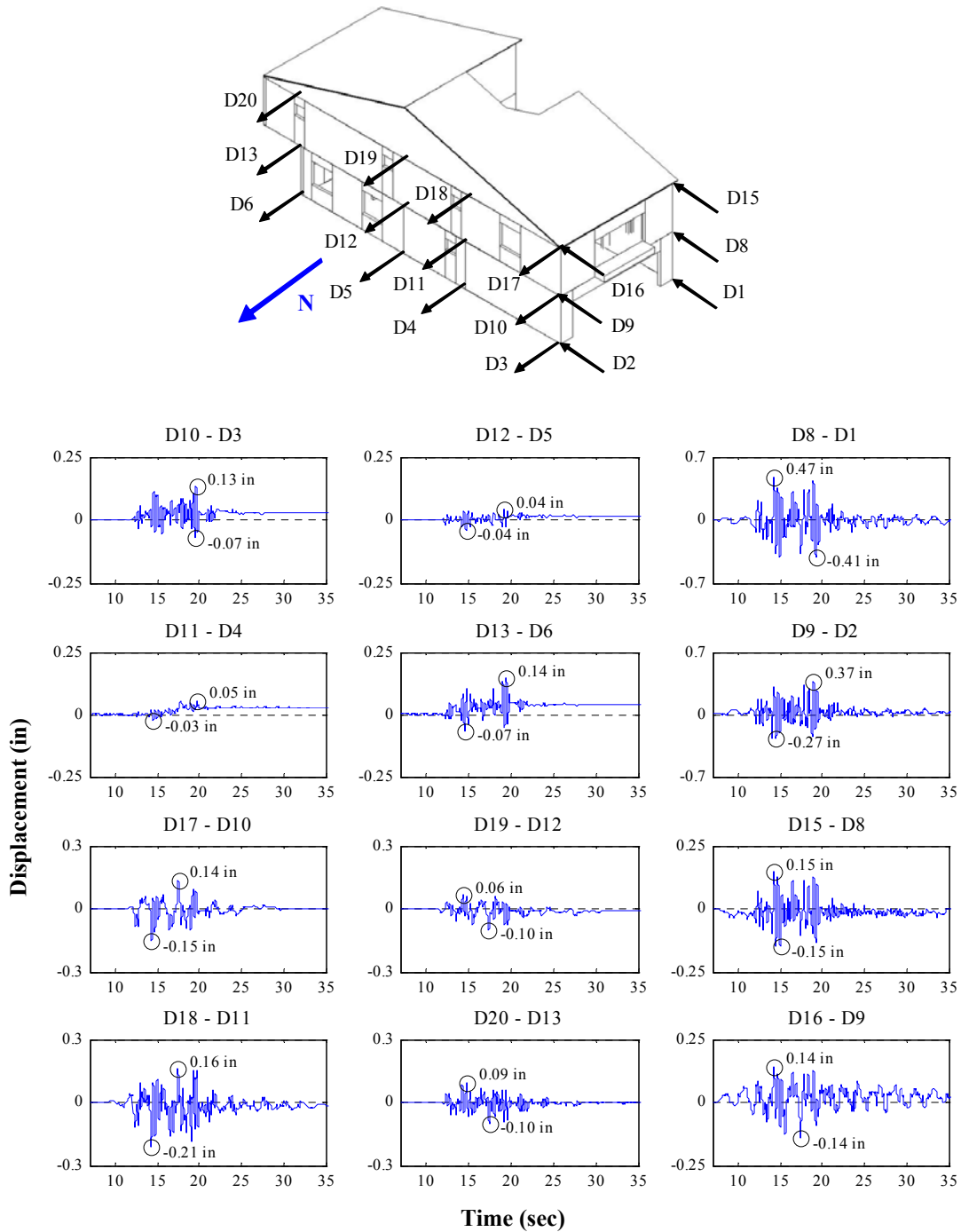


Figure K.15: Relative interstory drift time histories for Test NWP2S06

* Actual data are corrected to exclude the effect of shake table rotations

Appendix K

Phase 2, NWP2S07 Seismic Test

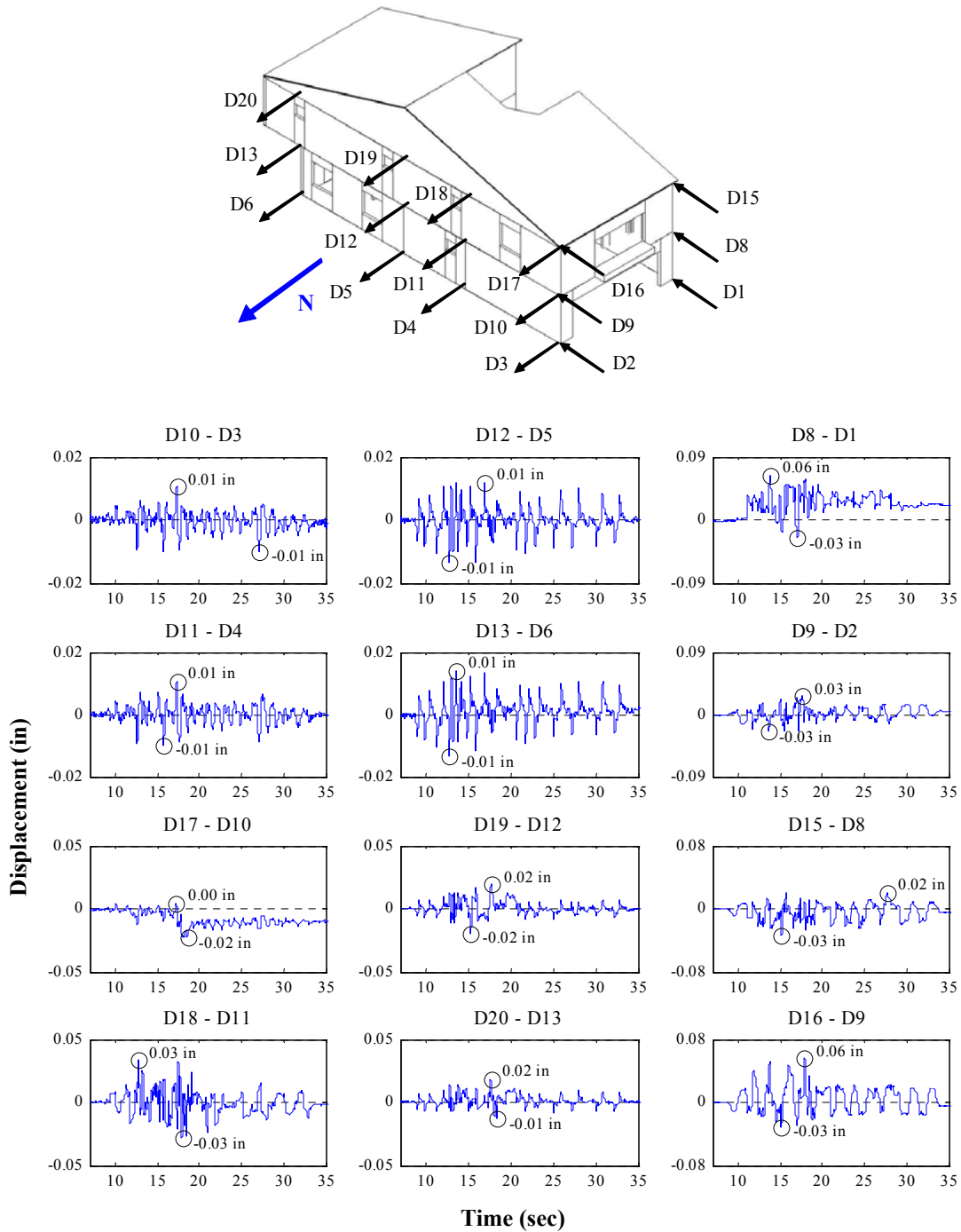


Figure K.16: Relative interstory drift time histories for Test NWP2S07

* Actual data are corrected to exclude the effect of shake table rotations

Appendix K

Phase 2, NWP2S08 Seismic Test

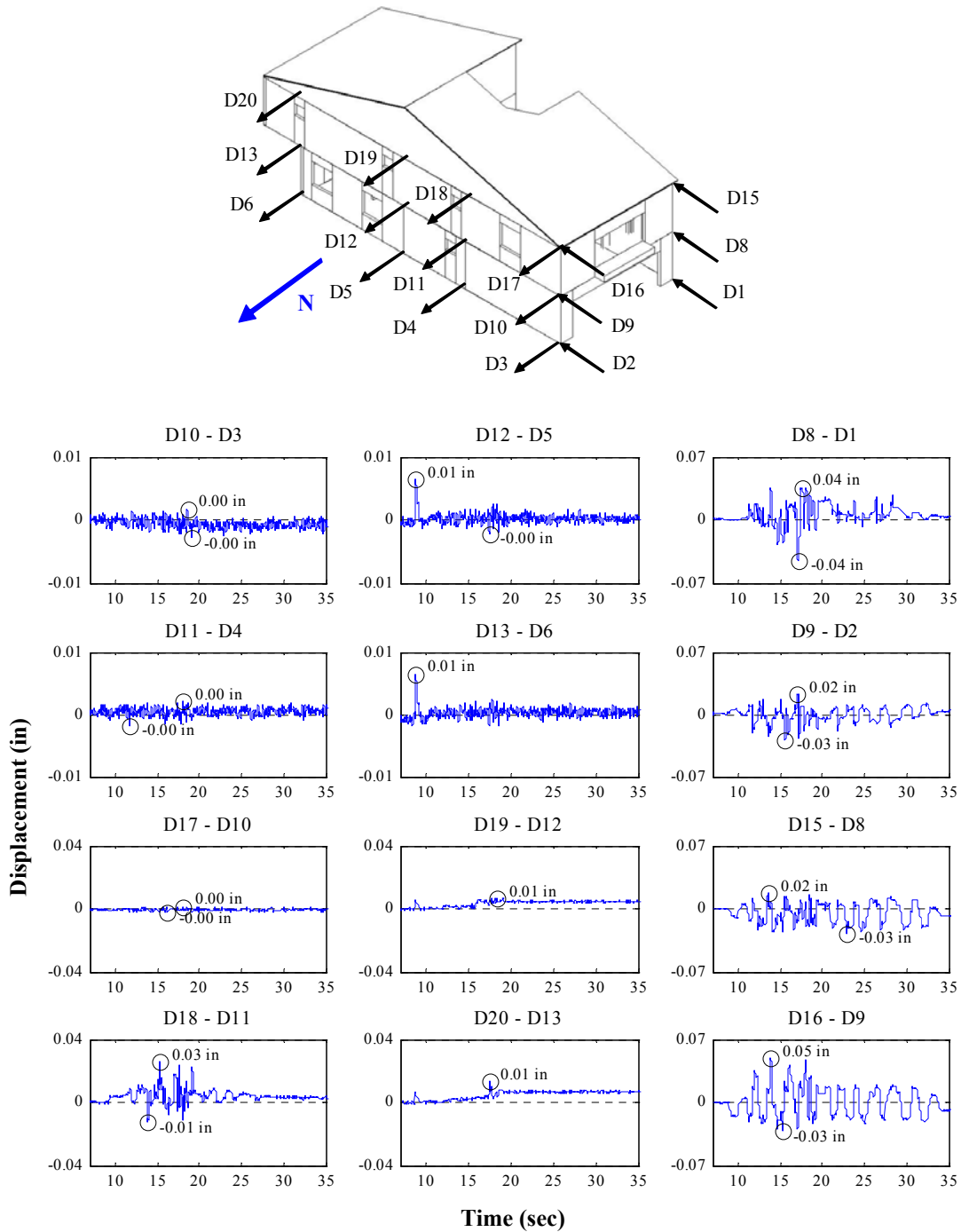


Figure K.17: Relative interstory drift time histories for Test NWP2S08

* Actual data are corrected to exclude the effect of shake table rotations

Appendix K

Phase 2, NWP2S09 Seismic Test

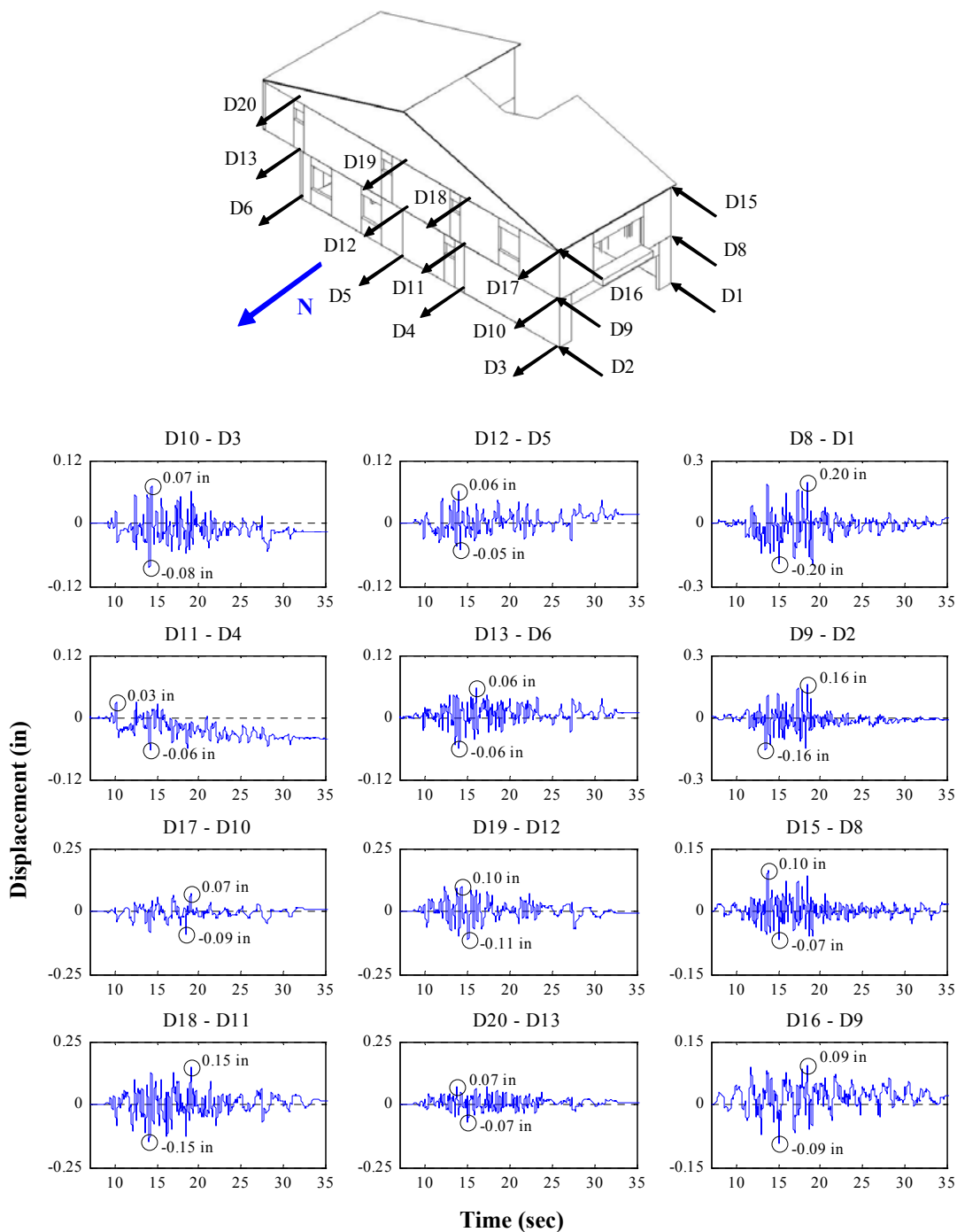


Figure K.18: Relative interstory drift time histories for Test NWP2S09

* Actual data are corrected to exclude the effect of shake table rotations

Appendix K

Phase 2, NWP2S10 Seismic Test

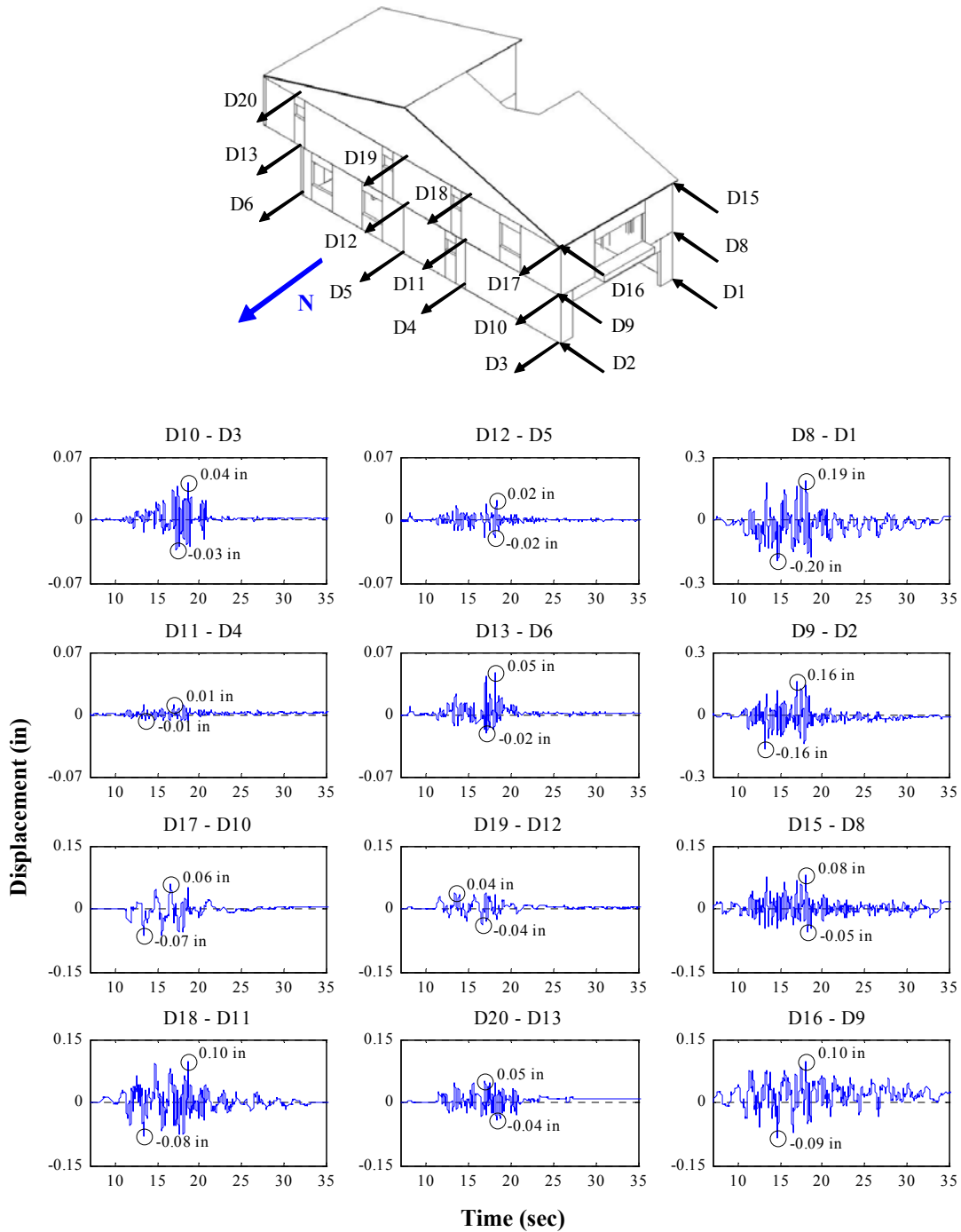


Figure K.19: Relative interstory drift time histories for Test NWP2S10

* Actual data are corrected to exclude the effect of shake table rotations

Appendix K

Phase 2, NWP2S11 Seismic Test

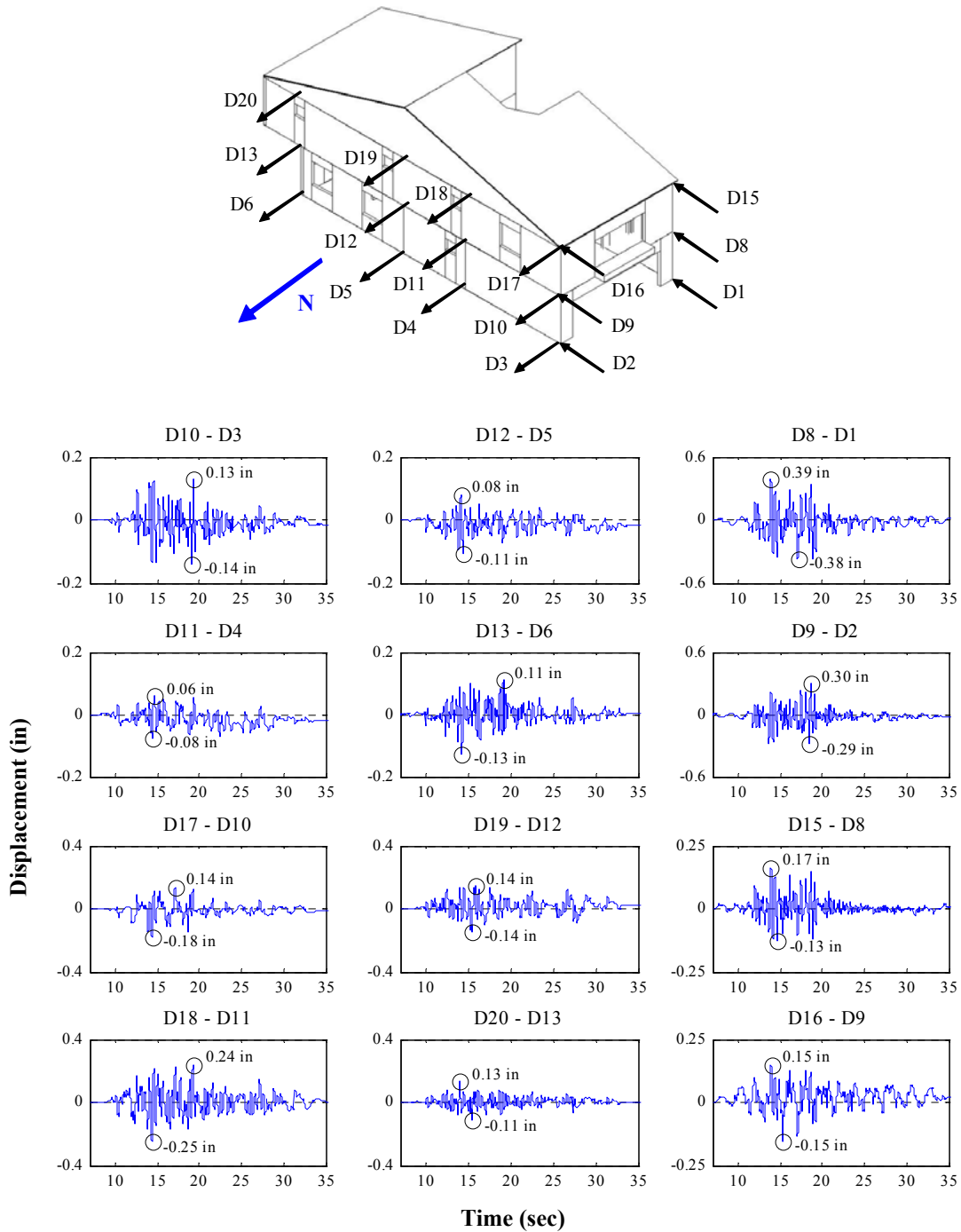


Figure K.20: Relative interstory drift time histories for Test NWP2S11

* Actual data are corrected to exclude the effect of shake table rotations

Appendix K

Phase 2, NWP2S12 Seismic Test

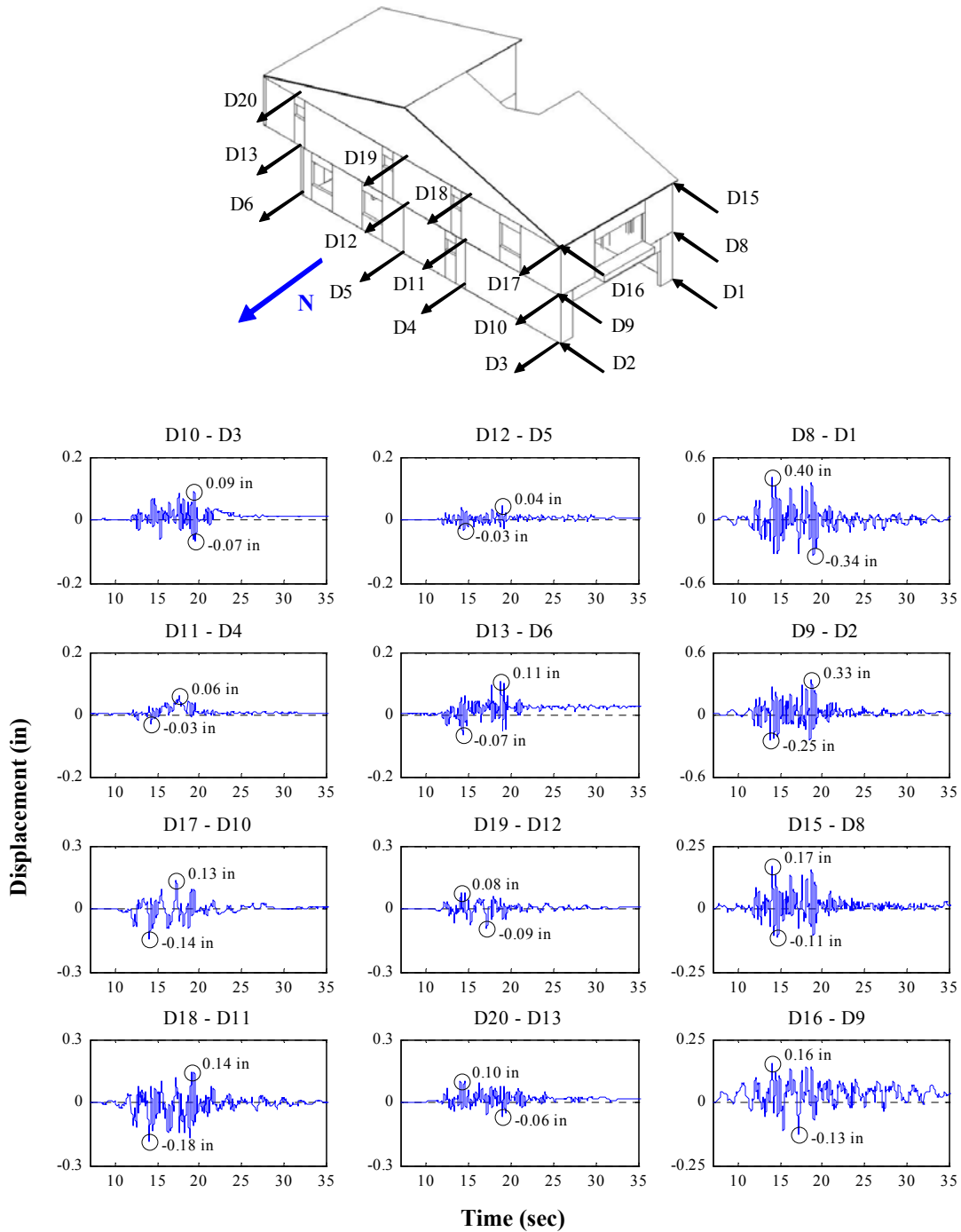


Figure K.21: Relative interstory drift time histories for Test NWP2S12

* Actual data are corrected to exclude the effect of shake table rotations

Appendix K

Phase 2, NWP2S13 Seismic Test

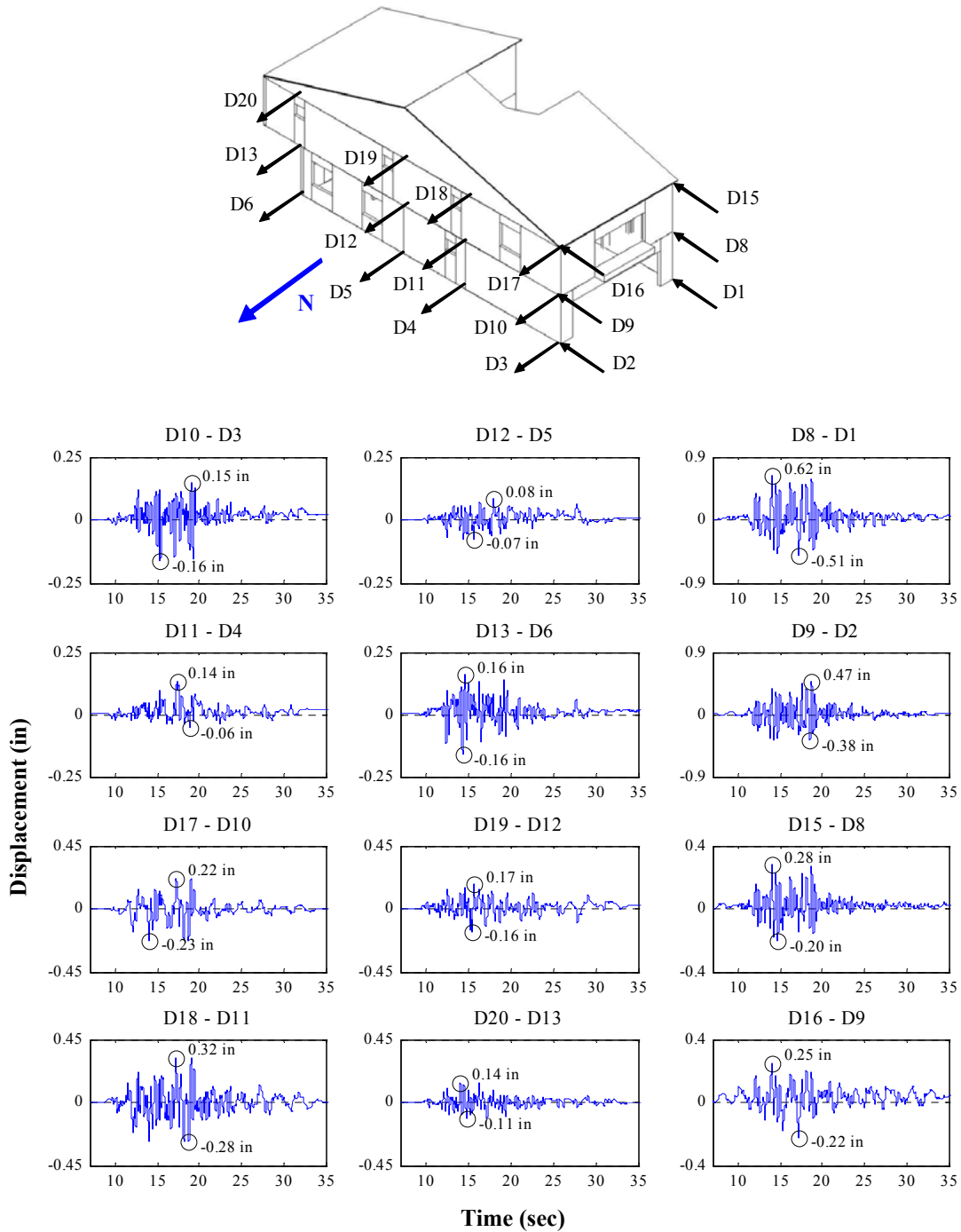


Figure K.22: Relative interstory drift time histories for Test NWP2S13

* Actual data are corrected to exclude the effect of shake table rotations

Appendix K

Phase 2, NWP2S14 Seismic Test

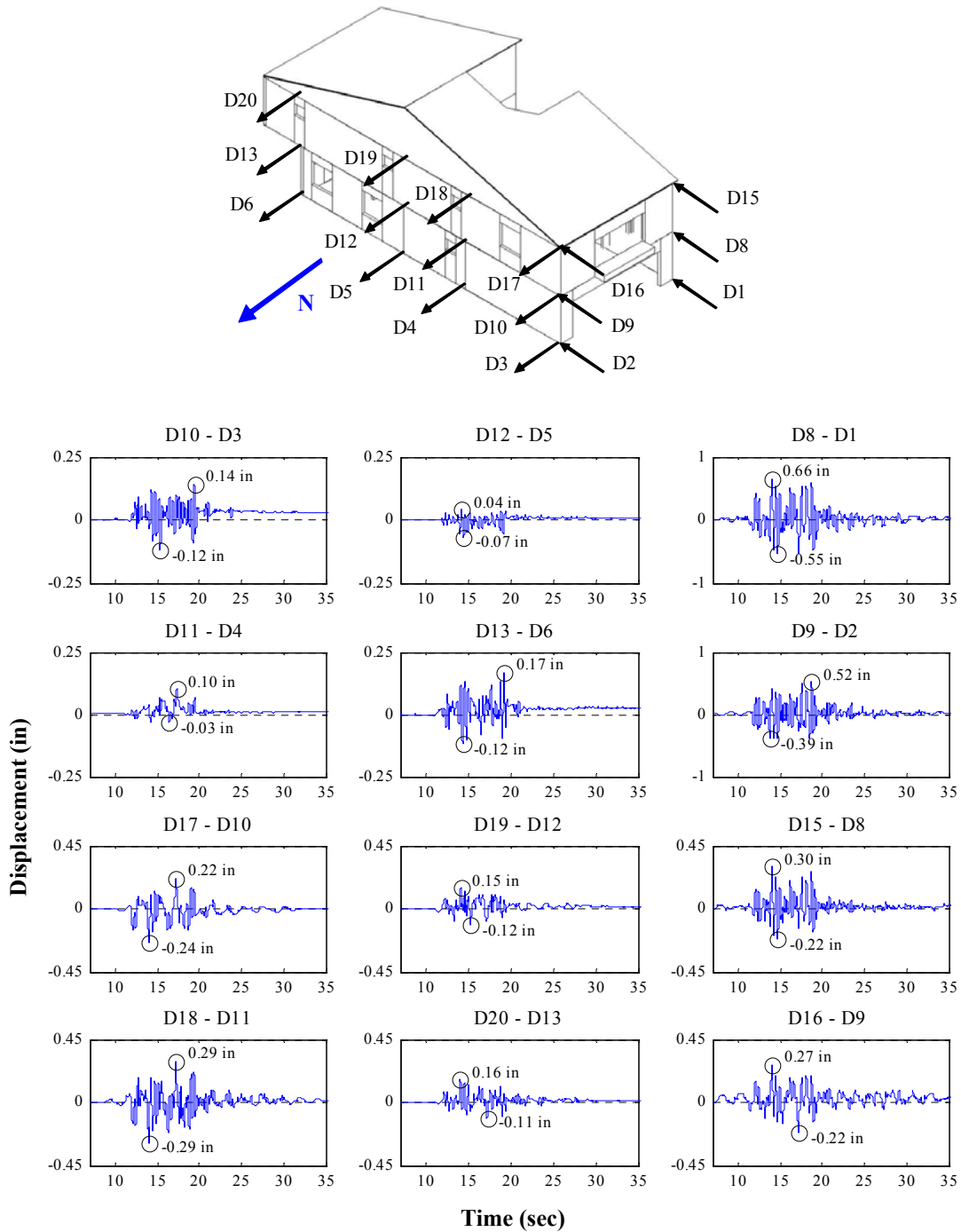


Figure K.23: Relative interstory drift time histories for Test NWP2S14

* Actual data are corrected to exclude the effect of shake table rotations

Appendix K

Phase 2, NWP2S16 Seismic Test

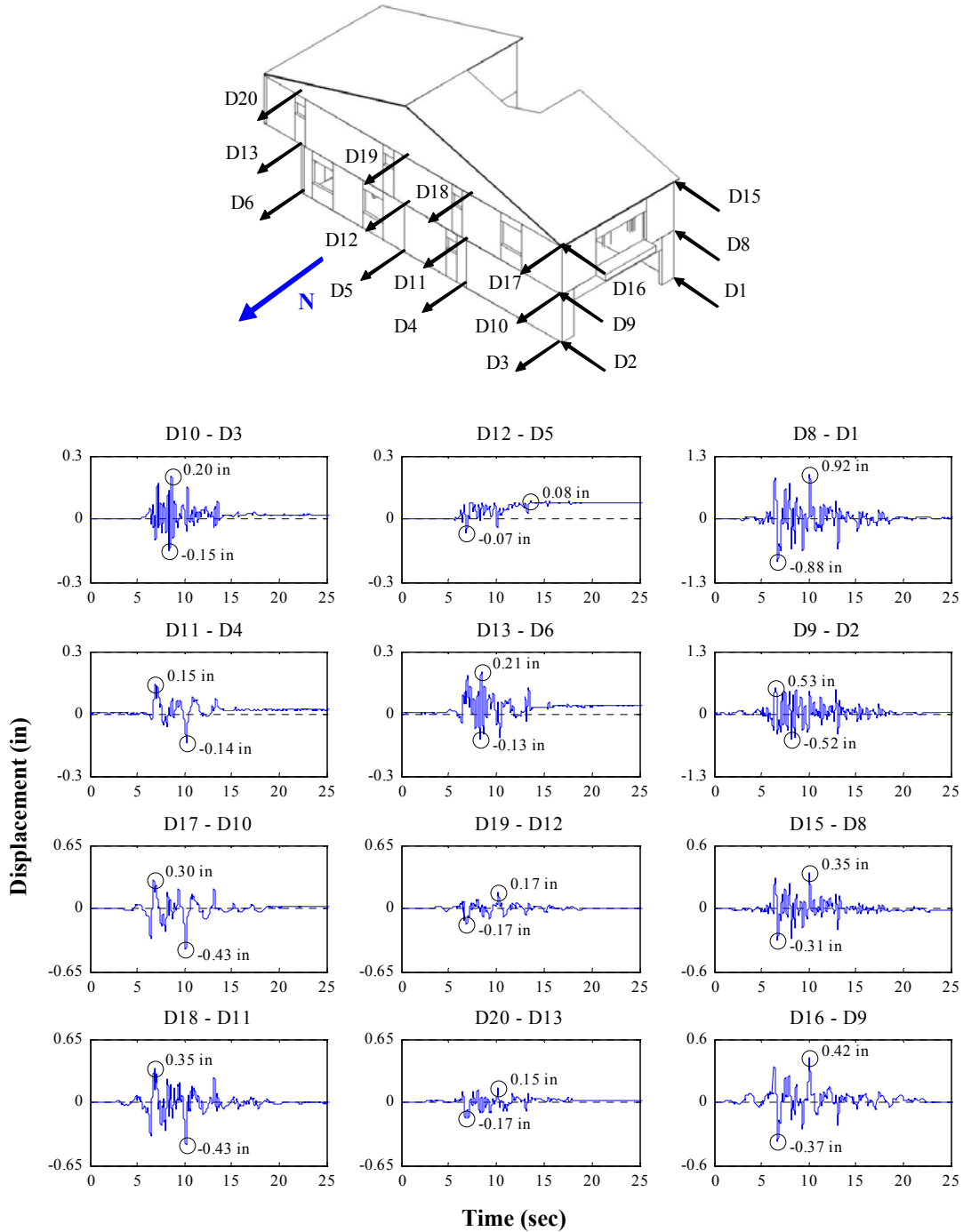


Figure K.24: Relative interstory drift time histories for Test NWP2S16

* Actual data are corrected to exclude the effect of shake table rotations

Appendix K

Phase 2, NWP2S17 Seismic Test

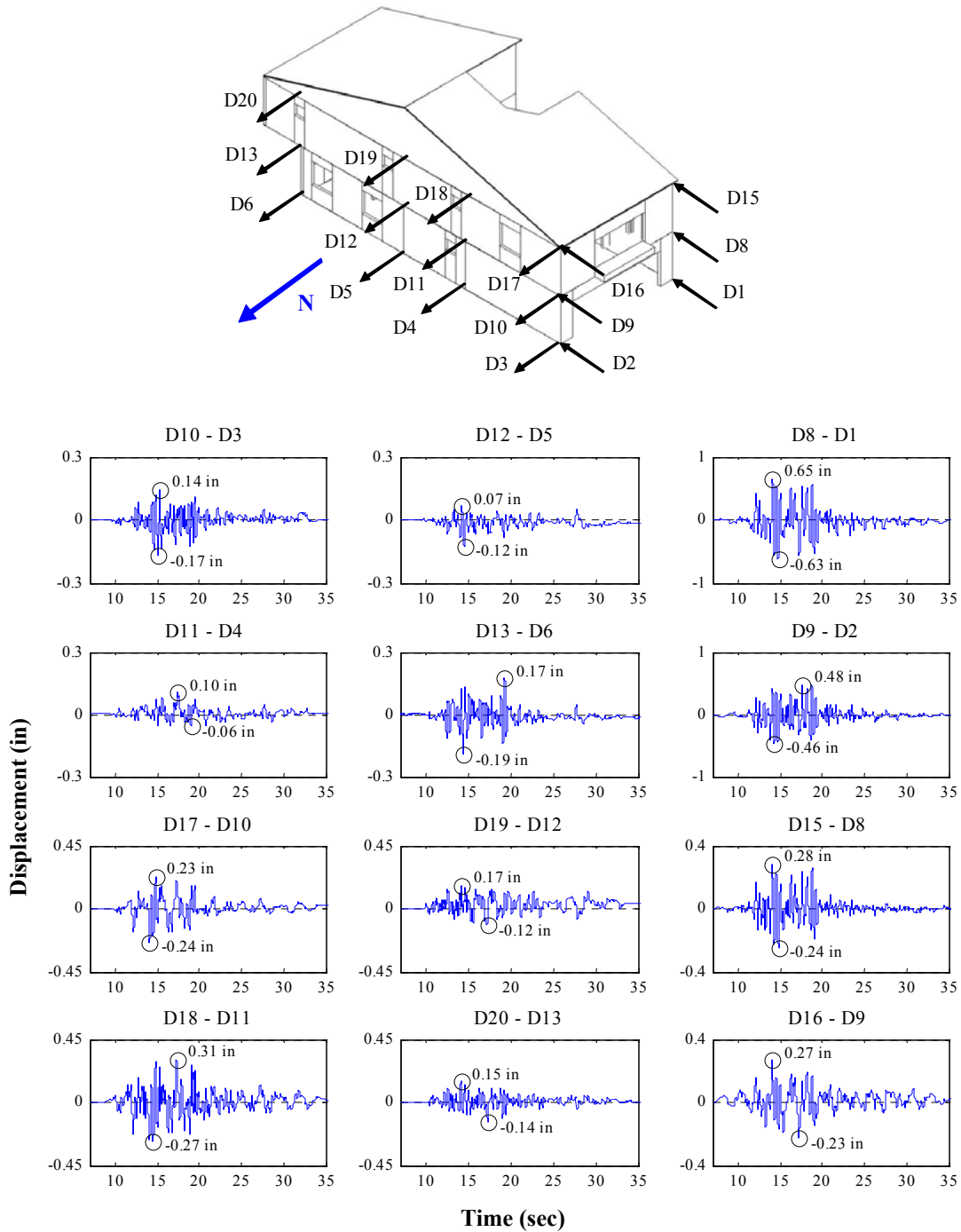


Figure K.25: Relative interstory drift time histories for Test NWP2S17

* Actual data are corrected to exclude the effect of shake table rotations

Appendix K

Phase 2, NWP2S21 Seismic Test

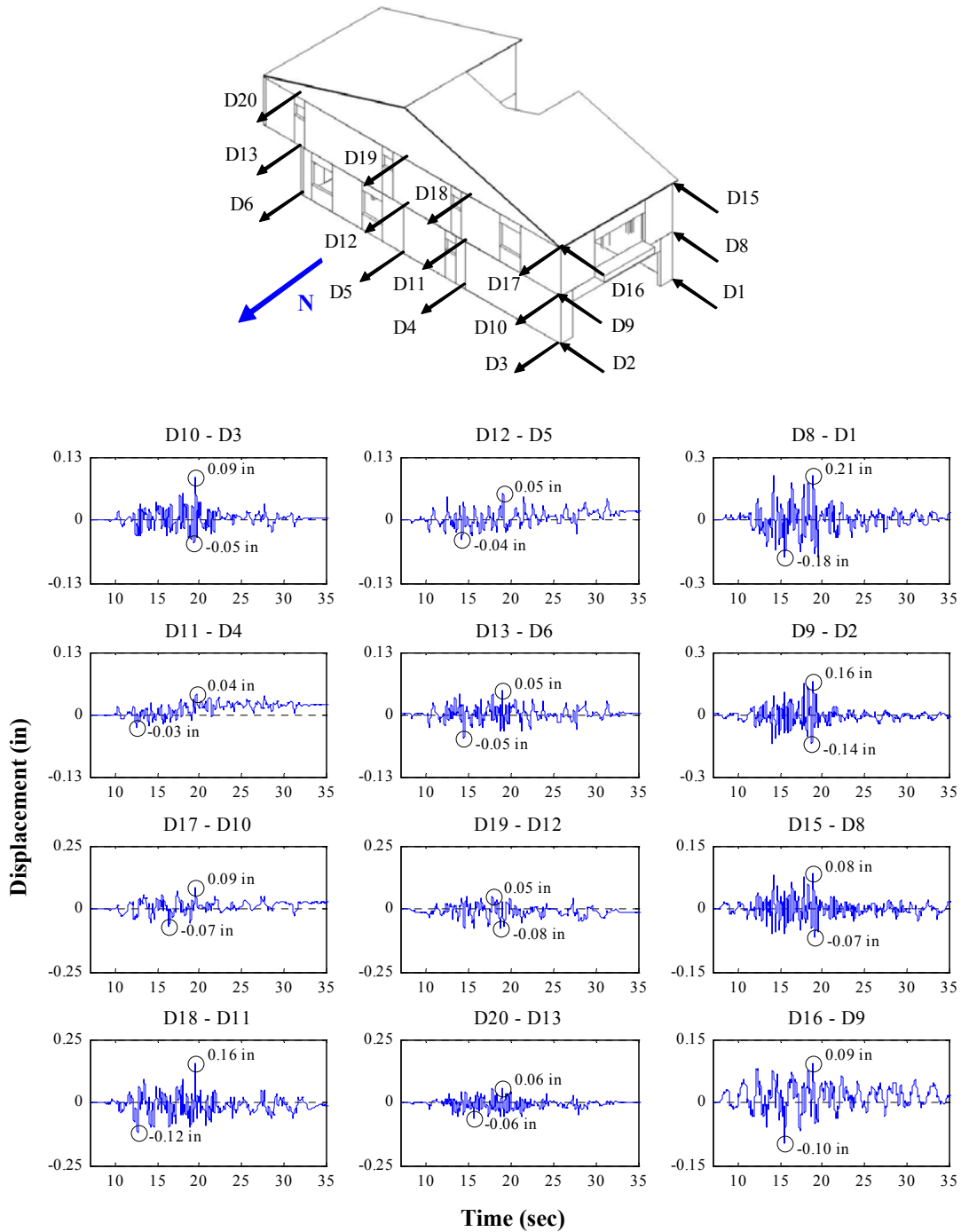


Figure K.26: Relative interstory drift time histories for Test NWP2S21

* Actual data are corrected to exclude the effect of shake table rotations

Appendix K

Phase 2, NWP2S24 Seismic Test

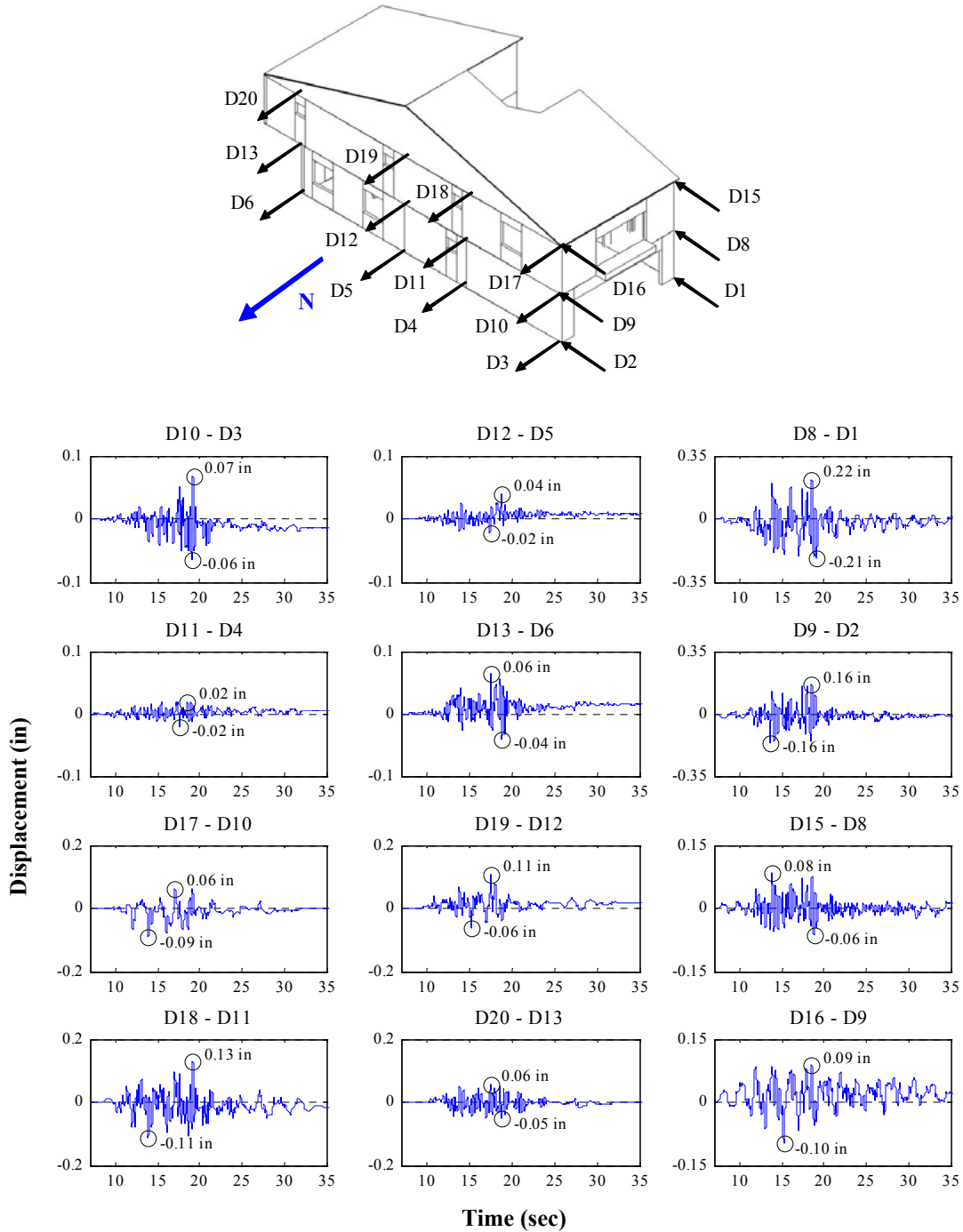


Figure K.27: Relative interstory drift time histories for Test NWP2S24

* Actual data are corrected to exclude the effect of shake table rotations

Appendix K

Phase 2, NWP2S25 Seismic Test

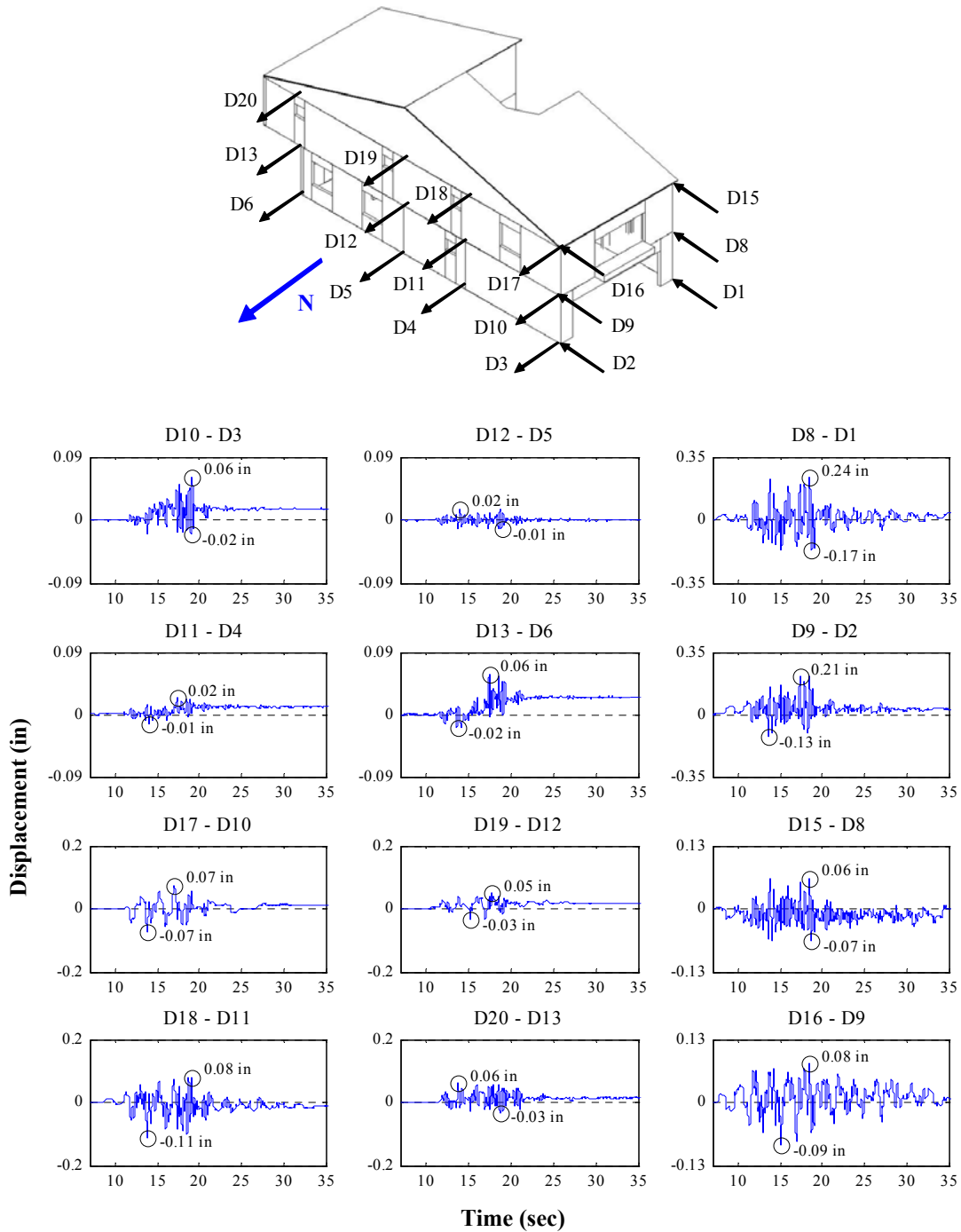


Figure K.28: Relative interstory drift time histories for Test NWP2S25

* Actual data are corrected to exclude the effect of shake table rotations

Appendix K

Phase 2, NWP2S26 Seismic Test

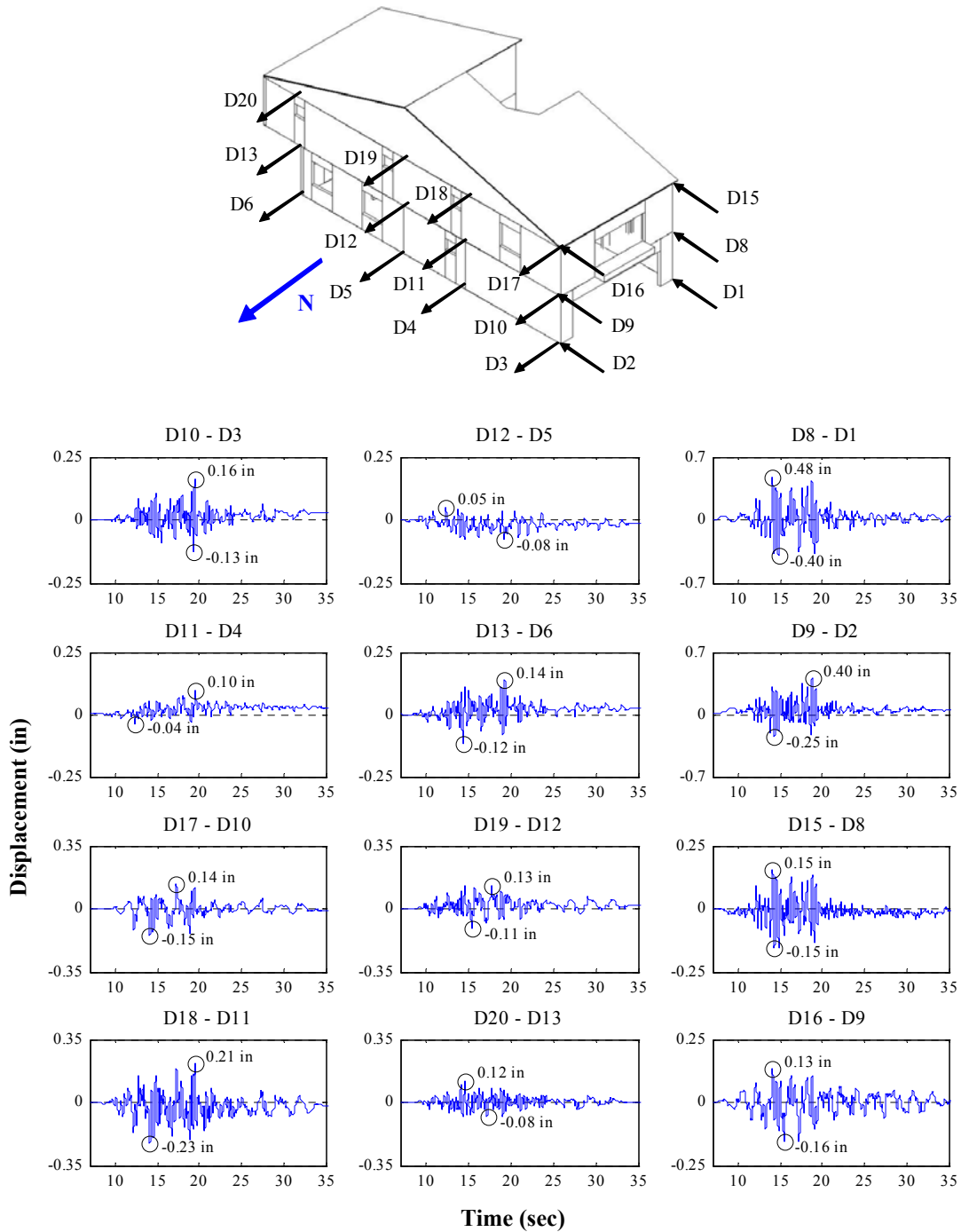


Figure K.29: Relative interstory drift time histories for Test NWP2S26

* Actual data are corrected to exclude the effect of shake table rotations

Appendix K

Phase 2, NWP2S27 Seismic Test

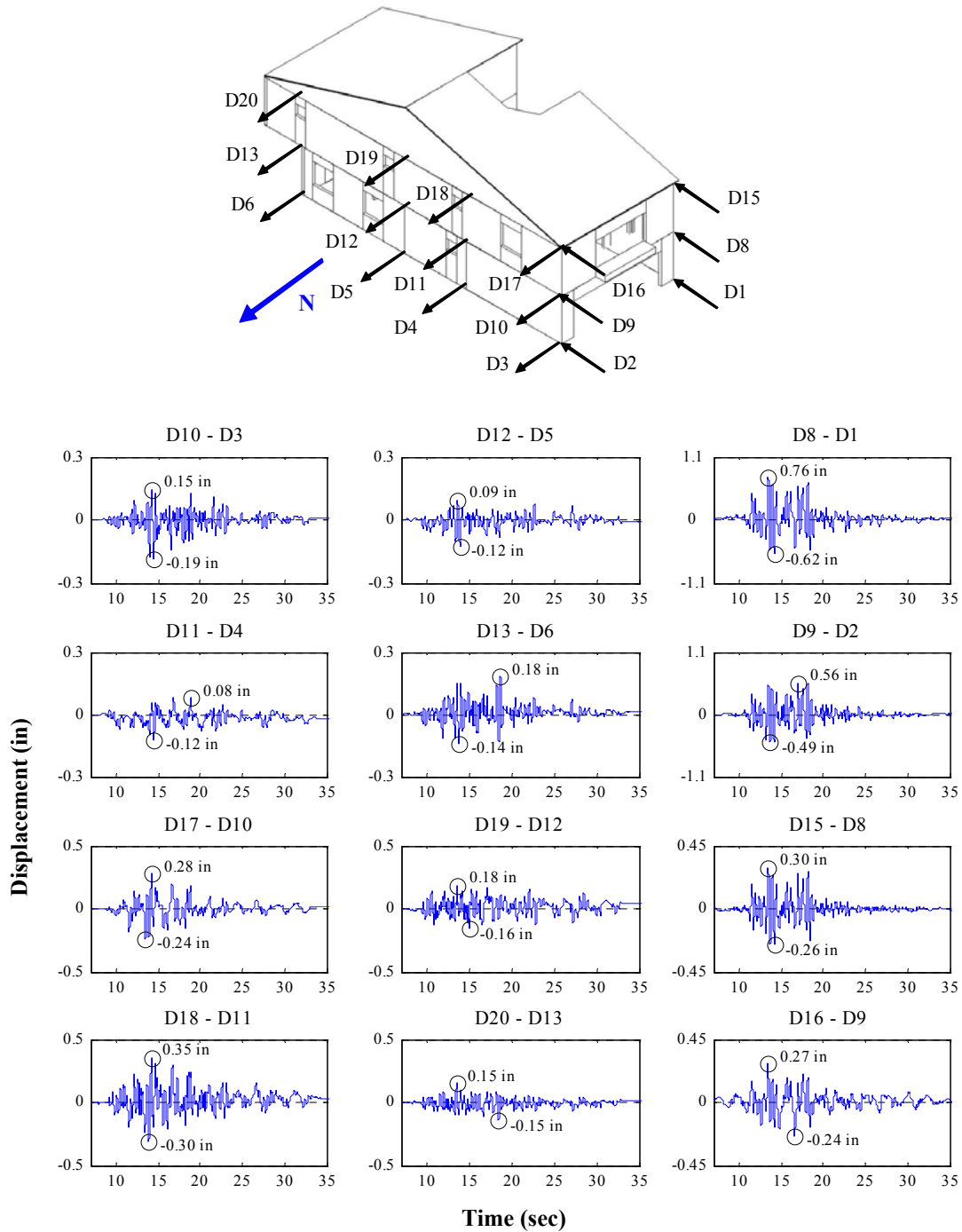


Figure K.30: Relative interstory drift time histories for Test NWP2S27

* Actual data are corrected to exclude the effect of shake table rotations

Appendix K

Phase 2, NWP2S28 Seismic Test

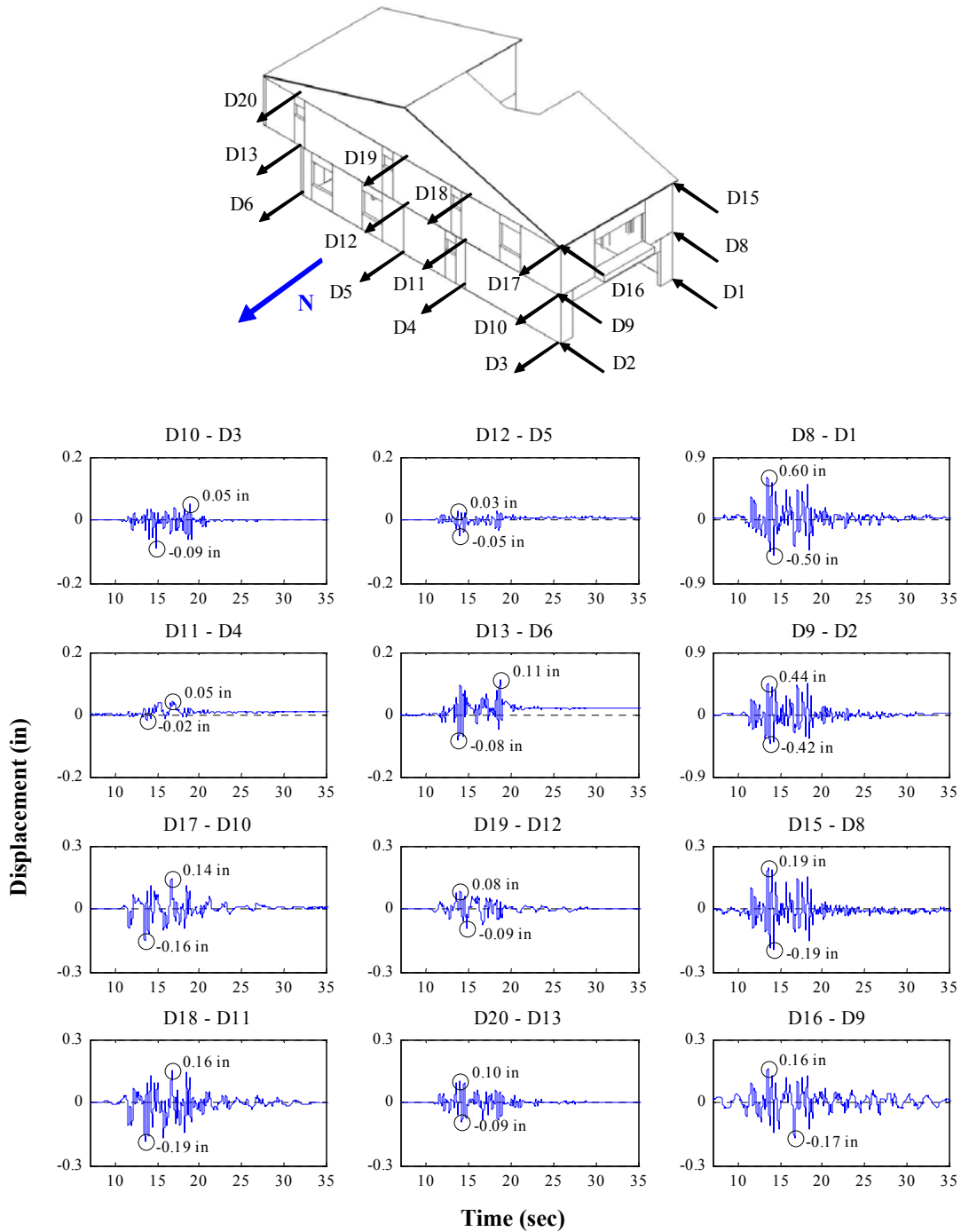


Figure K.31: Relative interstory drift time histories for Test NWP2S28

* Actual data are corrected to exclude the effect of shake table rotations

Appendix K

Phase 2, NWP2S29 Seismic Test

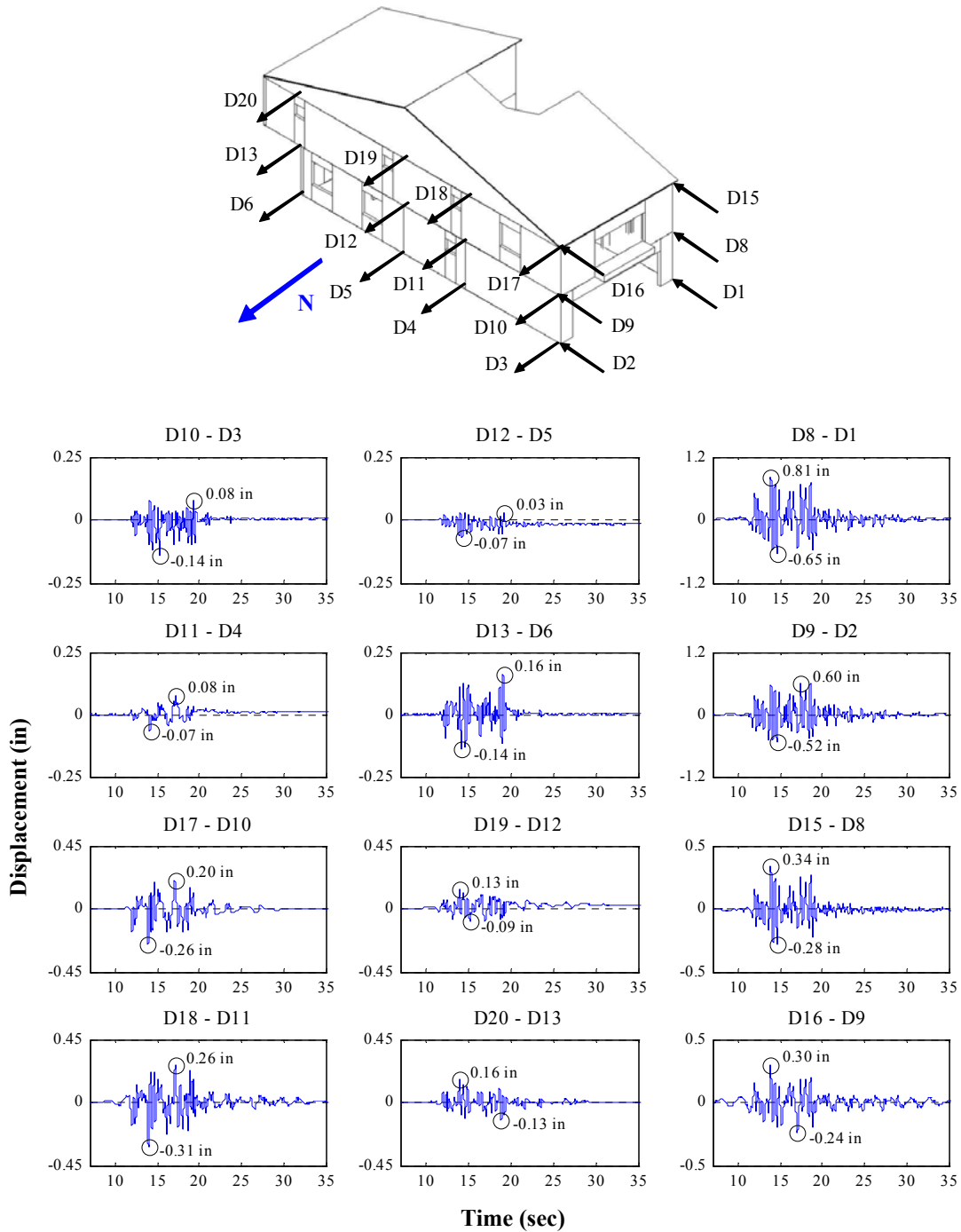


Figure K.32: Relative interstory drift time histories for Test NWP2S29

* Actual data are corrected to exclude the effect of shake table rotations

Appendix K

Phase 2, NWP2S30 Seismic Test

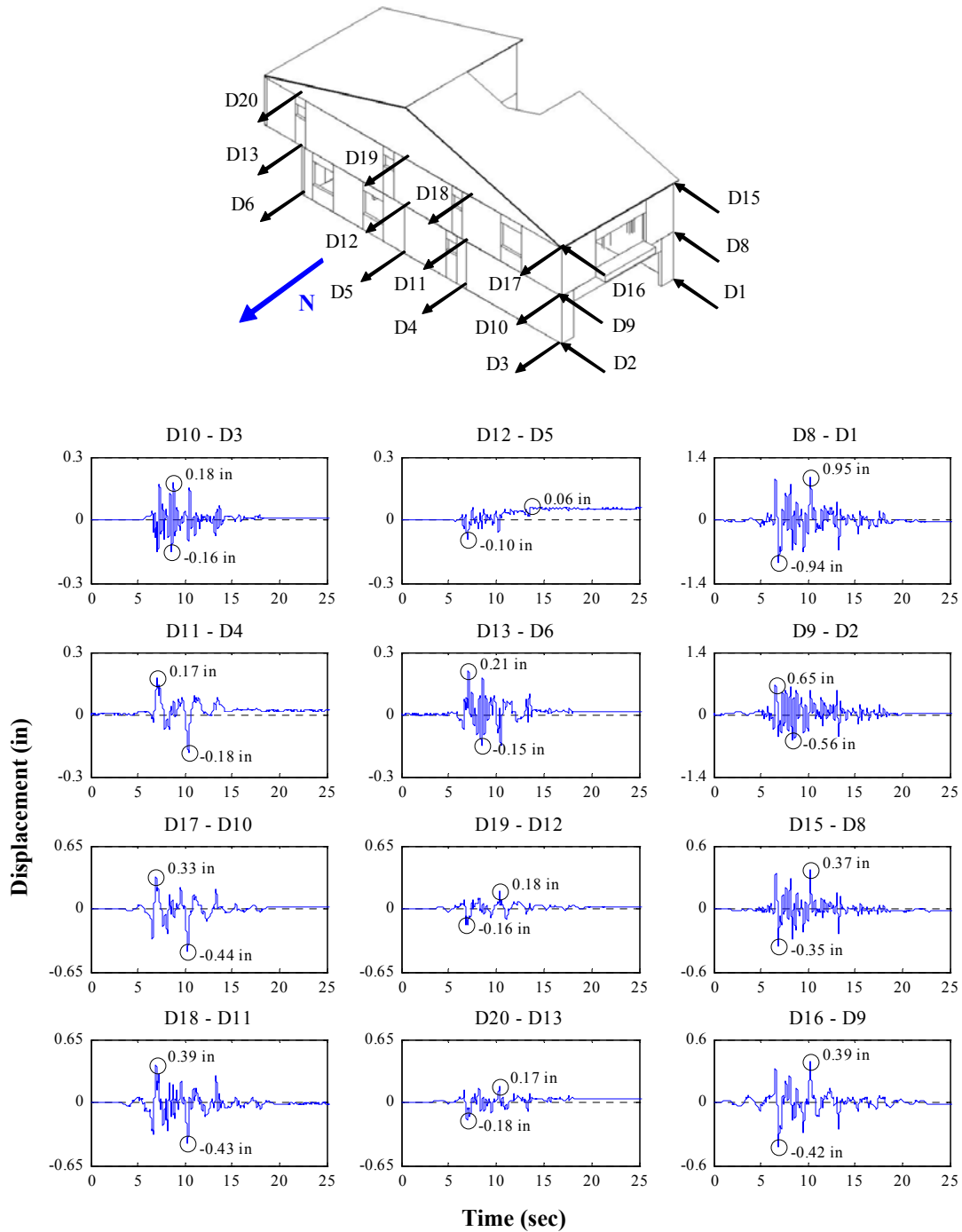


Figure K.33: Relative interstory drift time histories for Test NWP2S30

* Actual data are corrected to exclude the effect of shake table rotations

Appendix K

Phase 3, NWP3S01 Seismic Test

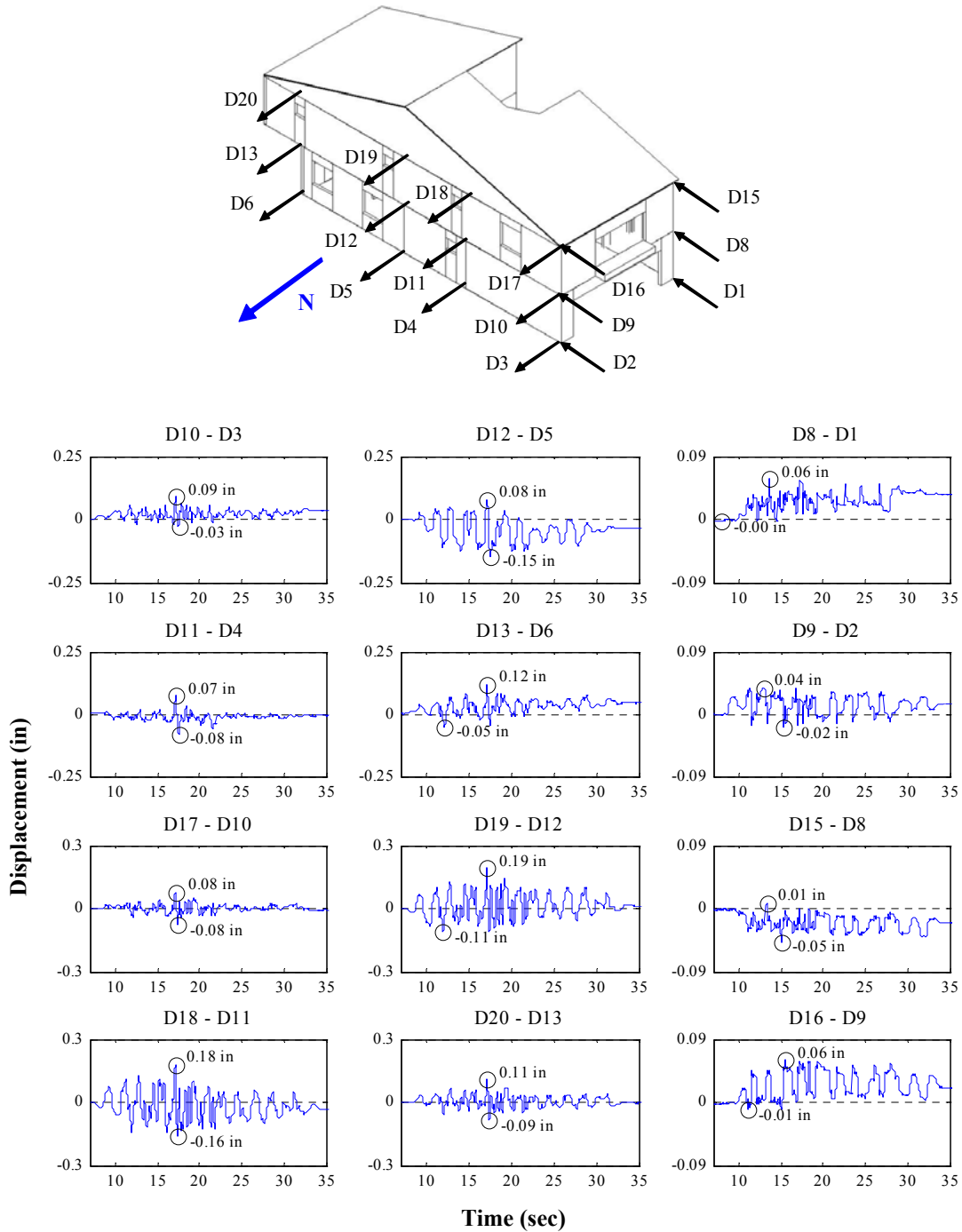


Figure K.34: Relative interstory drift time histories for Test NWP3S01

* Actual data are corrected to exclude the effect of shake table rotations

Appendix K

Phase 3, NWP3S02 Seismic Test

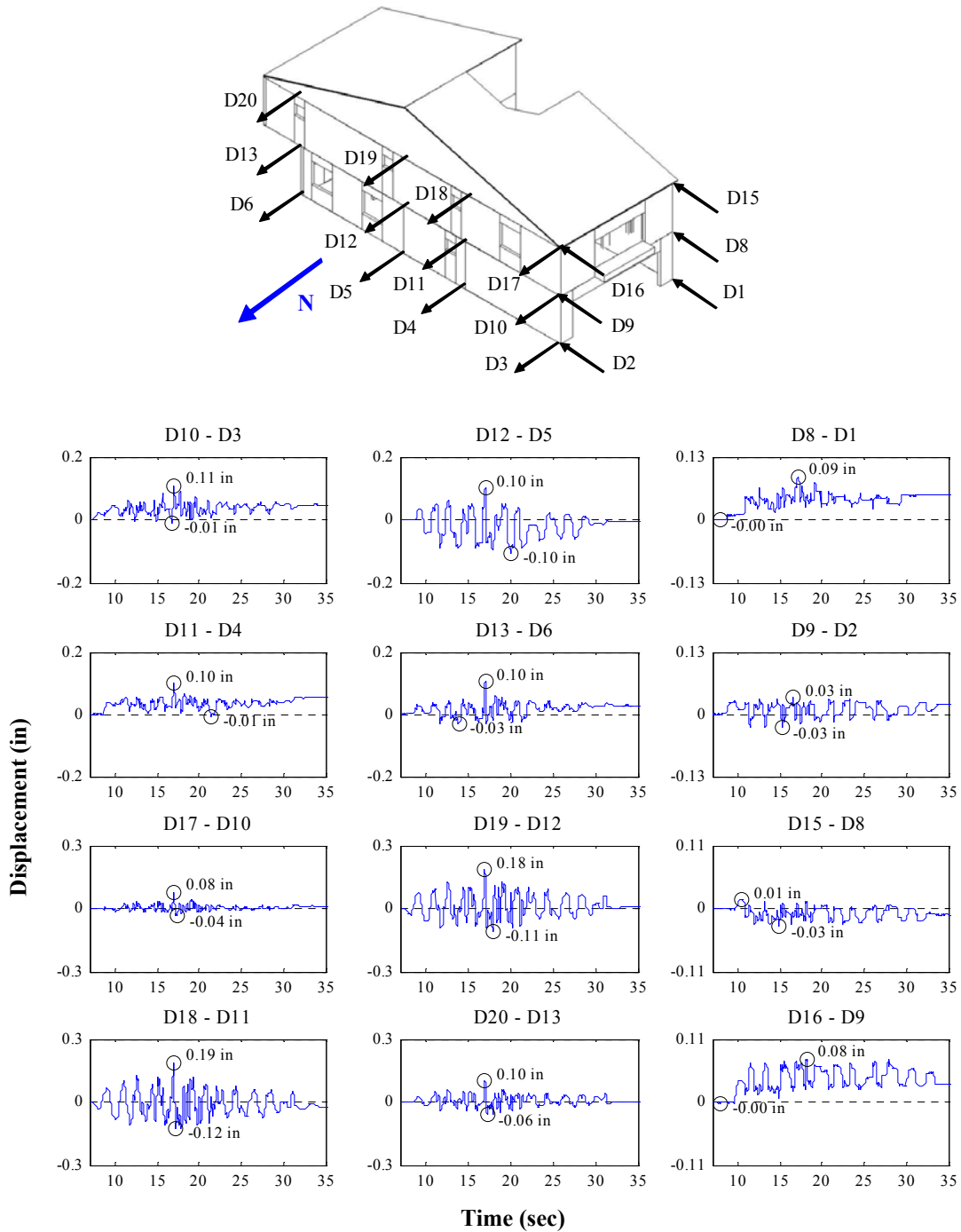


Figure K.35: Relative interstory drift time histories for Test NWP3S02

* Actual data are corrected to exclude the effect of shake table rotations

Appendix K

Phase 3, NWP3S03 Seismic Test

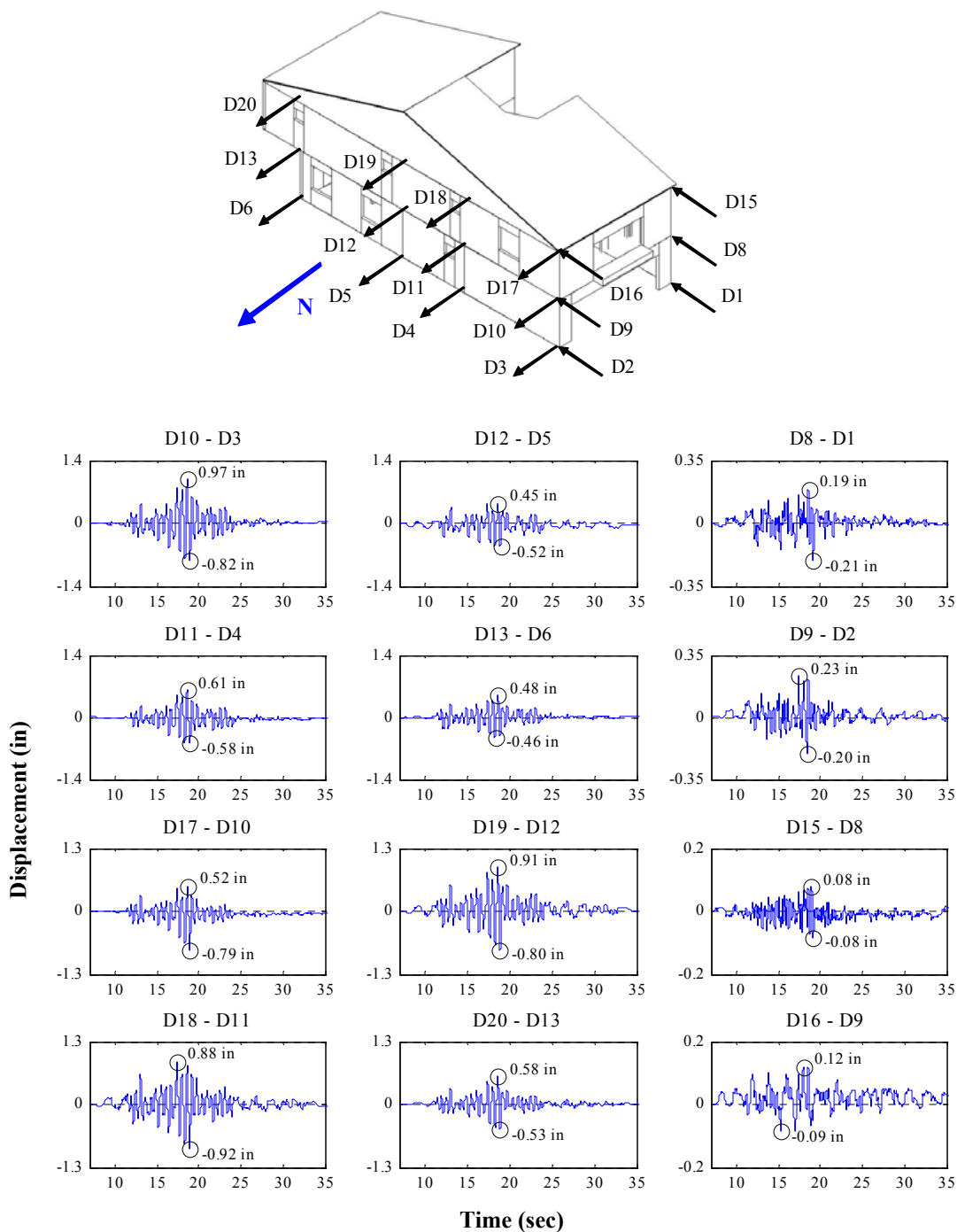


Figure K.36: Relative interstory drift time histories for Test NWP3S03

* Actual data are corrected to exclude the effect of shake table rotations

Appendix K

Phase 3, NWP3S04 Seismic Test

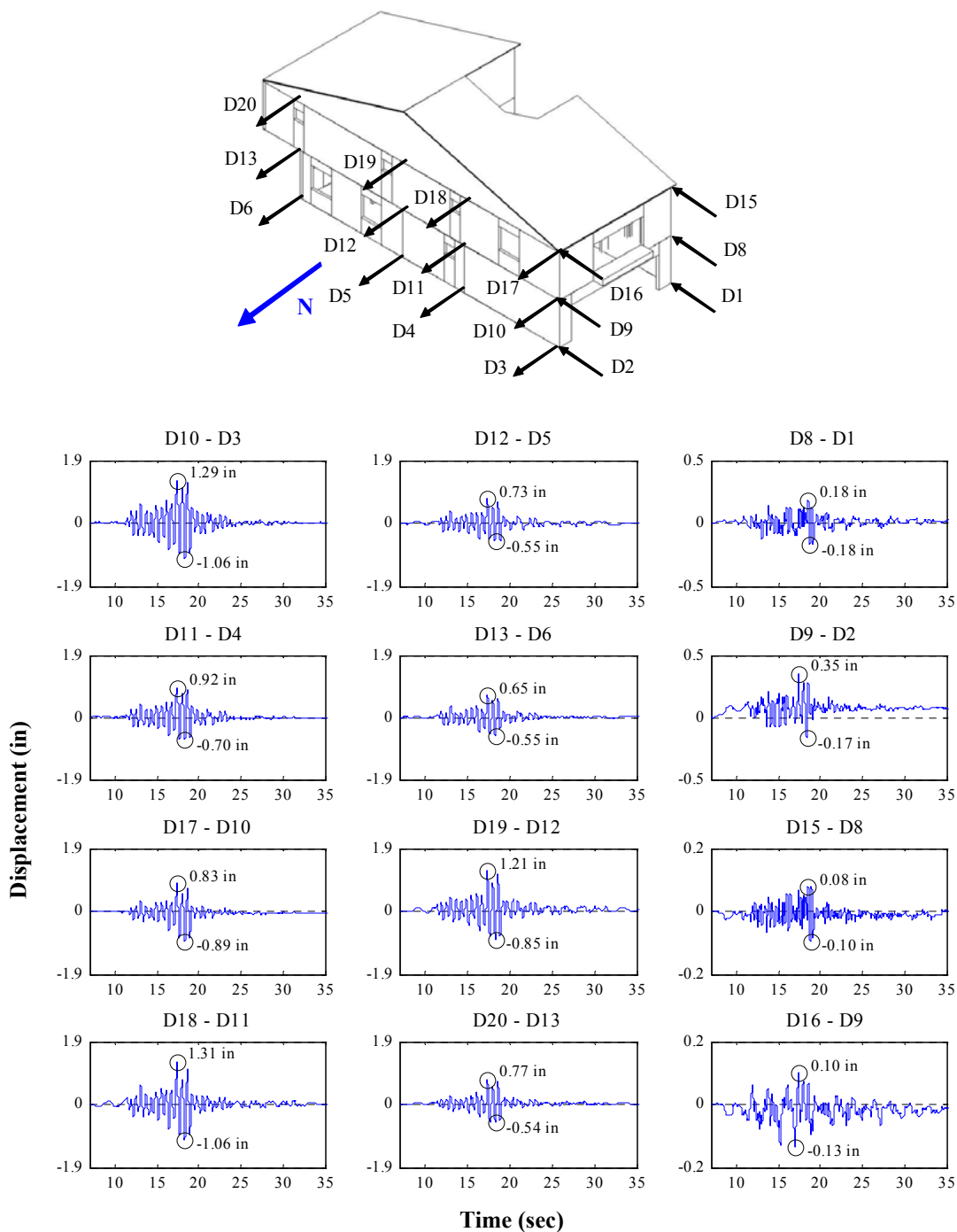


Figure K.37: Relative interstory drift time histories for Test NWP3S04

* Actual data are corrected to exclude the effect of shake table rotations

Appendix K

Phase 4, NWP4S01 Seismic Test

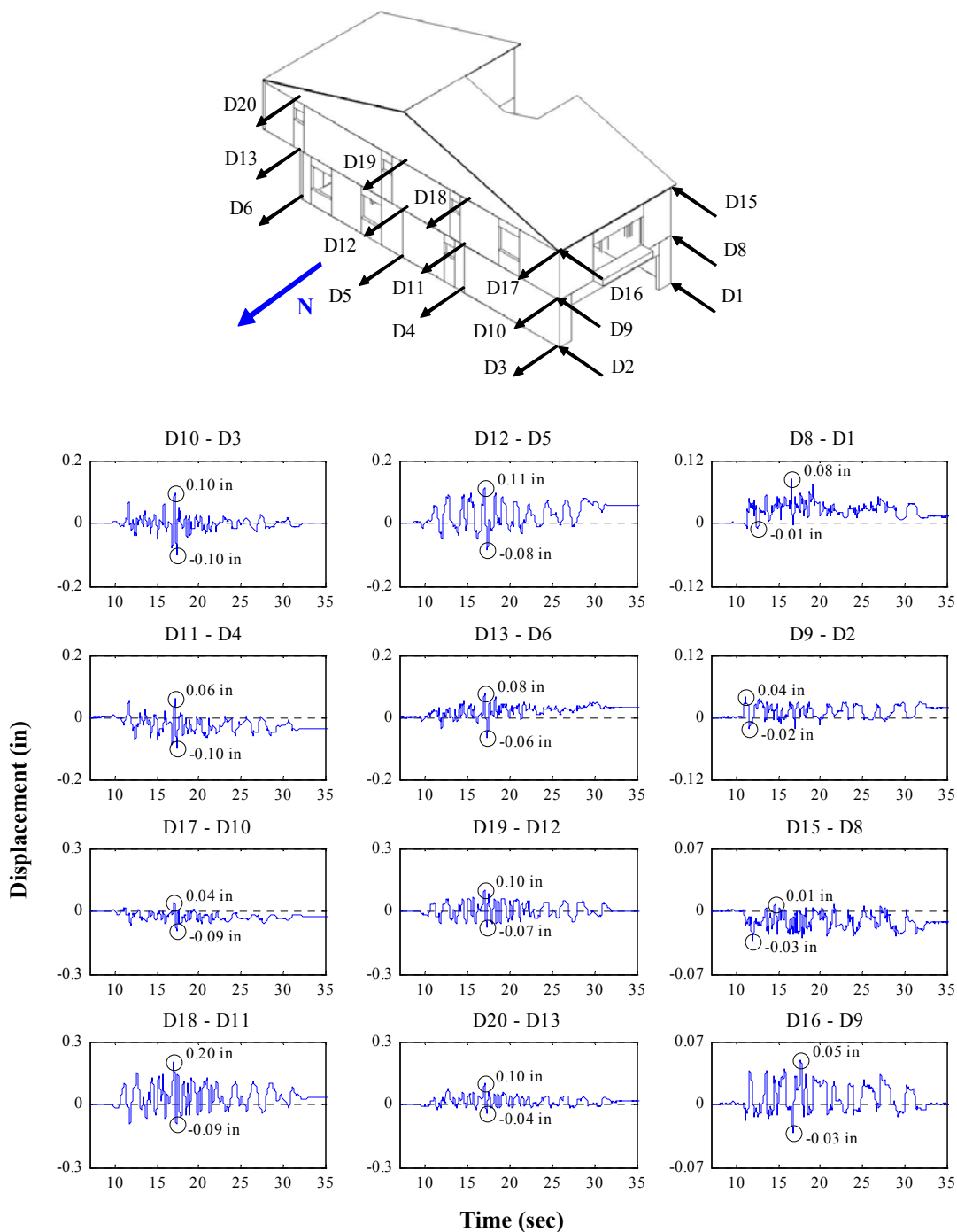


Figure K.38: Relative interstory drift time histories for Test NWP4S01

* Actual data are corrected to exclude the effect of shake table rotations

Appendix K

Phase 4, NWP4S02 Seismic Test

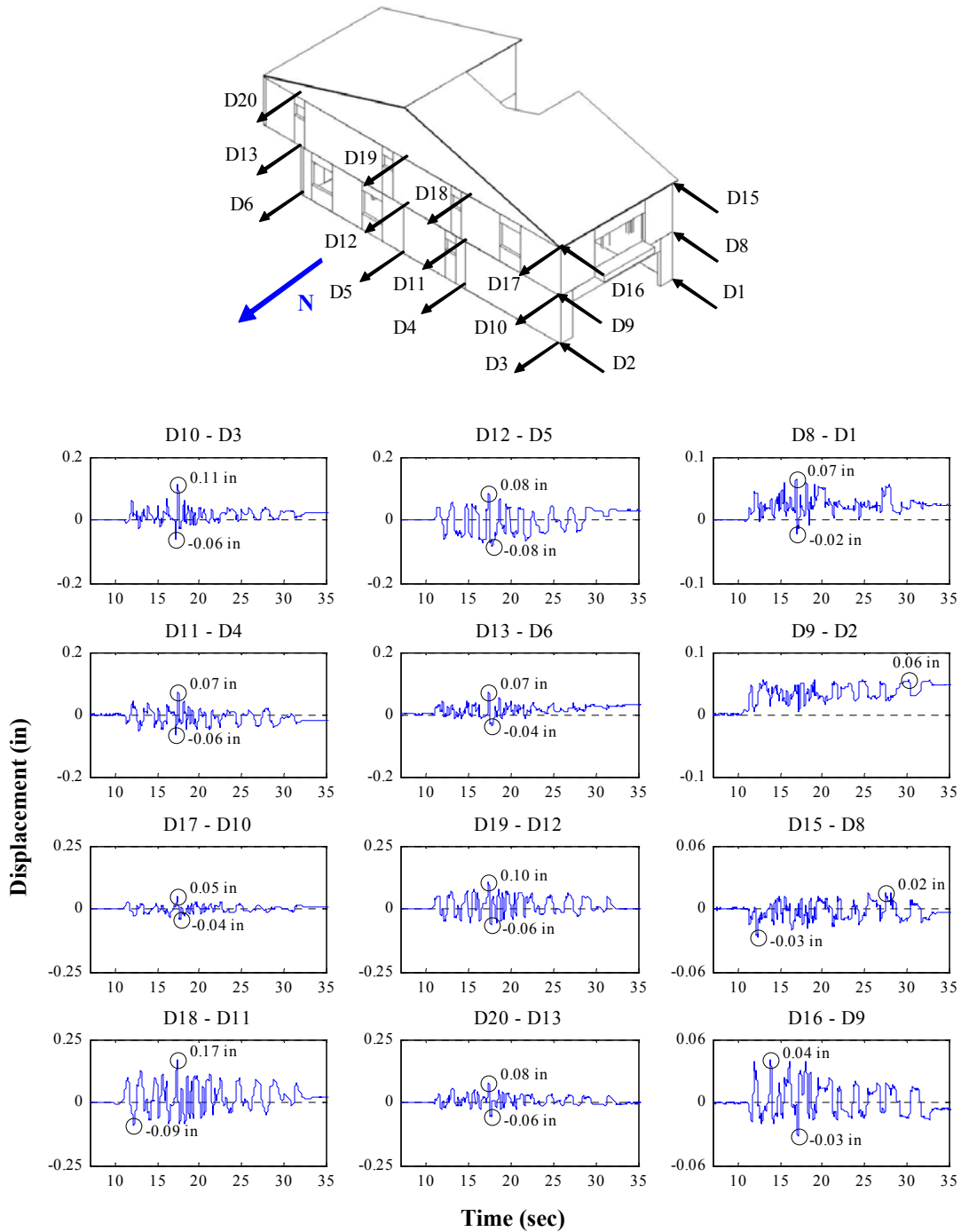


Figure K.39: Relative interstory drift time histories for Test NWP4S02

* Actual data are corrected to exclude the effect of shake table rotations

Appendix K

Phase 4, NWP4S03 Seismic Test

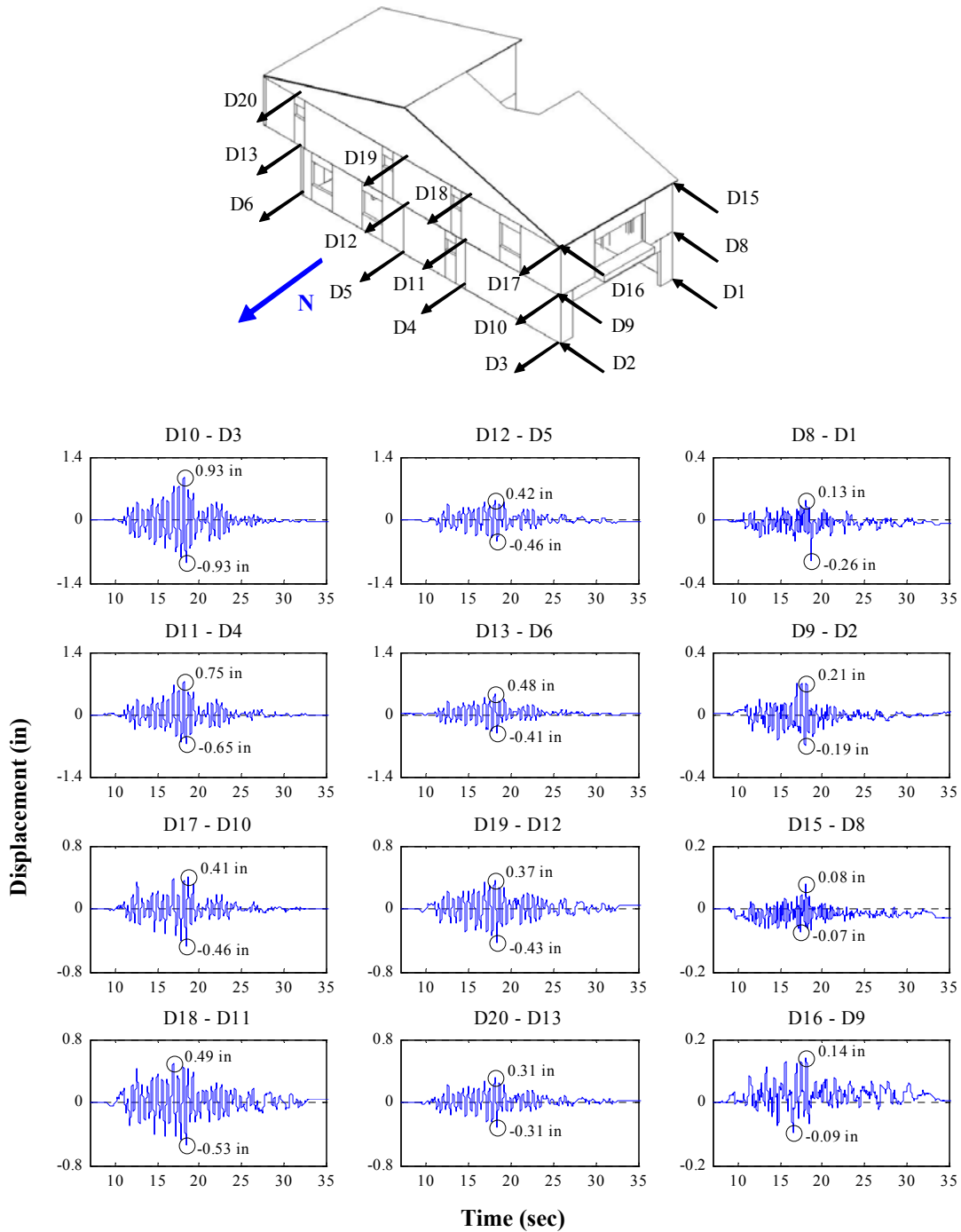


Figure K.40: Relative interstory drift time histories for Test NWP4S03

* Actual data are corrected to exclude the effect of shake table rotations

Appendix K

Phase 4, NWP4S04 Seismic Test

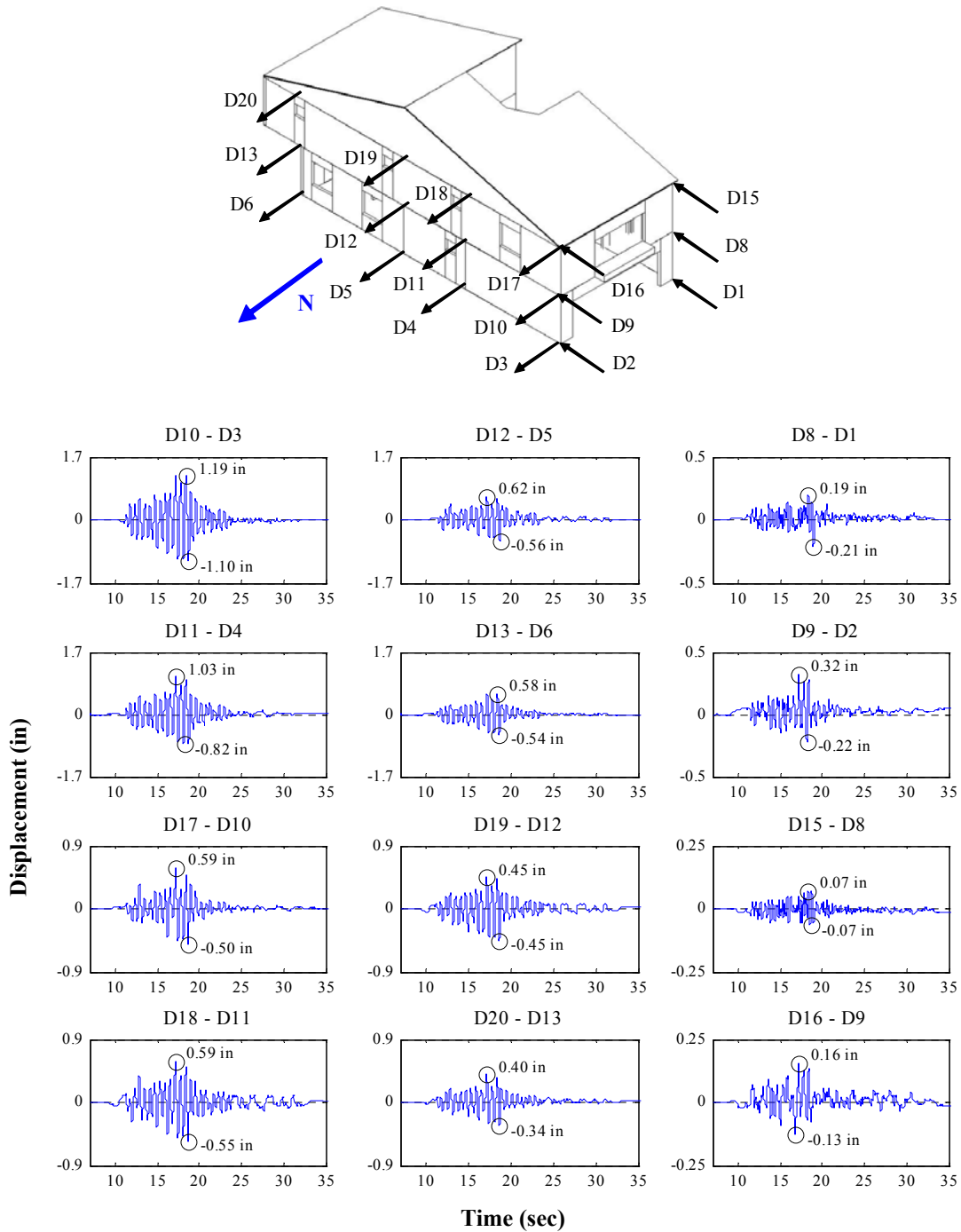


Figure K.41: Relative interstory drift time histories for Test NWP4S04

* Actual data are corrected to exclude the effect of shake table rotations

Appendix K

Phase 5, NWP5S01 Seismic Test

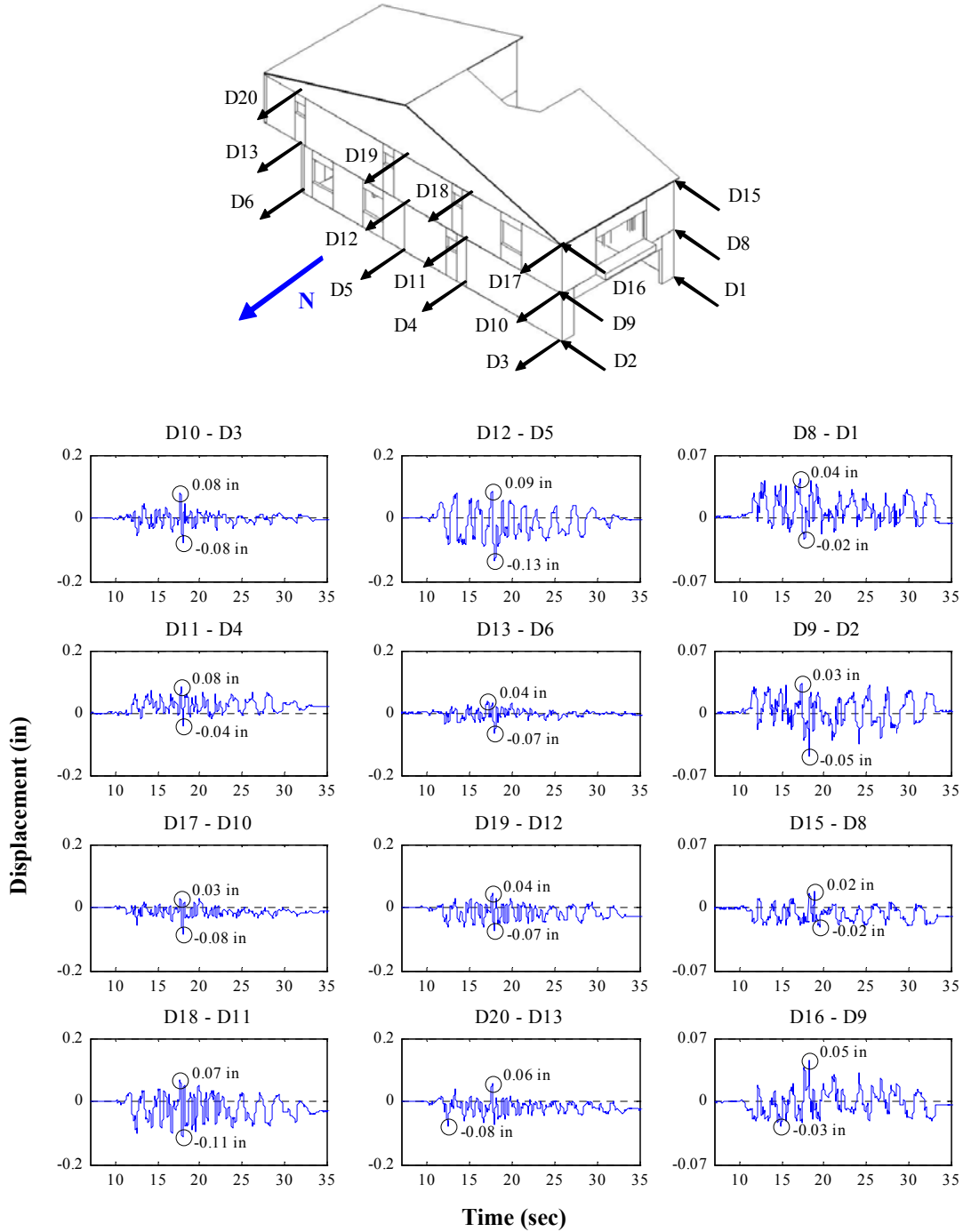


Figure K.42: Relative interstory drift time histories for Test NWP5S01

* Actual data are corrected to exclude the effect of shake table rotations

Appendix K

Phase 5, NWP5S02 Seismic Test

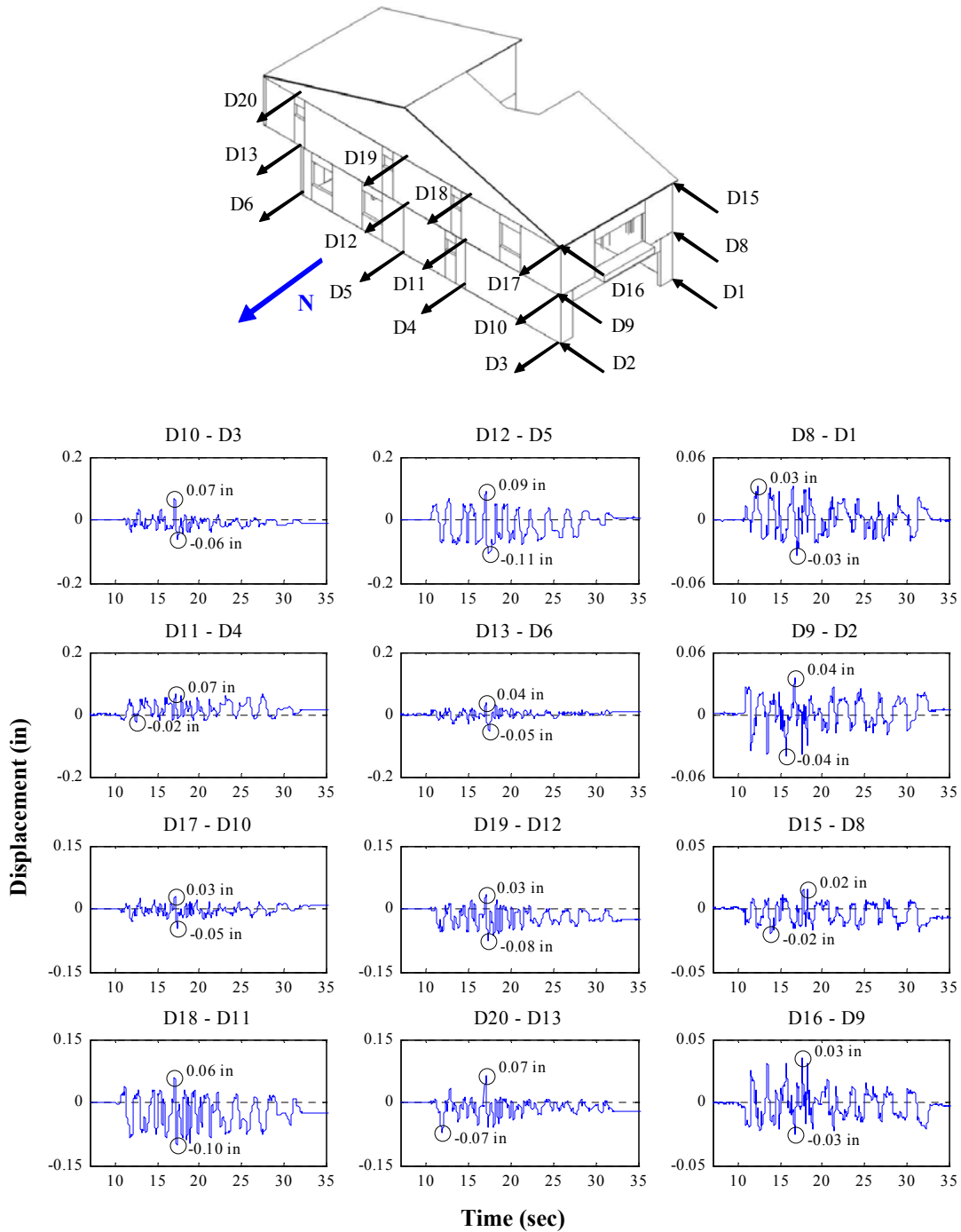


Figure K.43: Relative interstory drift time histories for Test NWP5S02

* Actual data are corrected to exclude the effect of shake table rotations

Appendix K

Phase 5, NWP5S03 Seismic Test

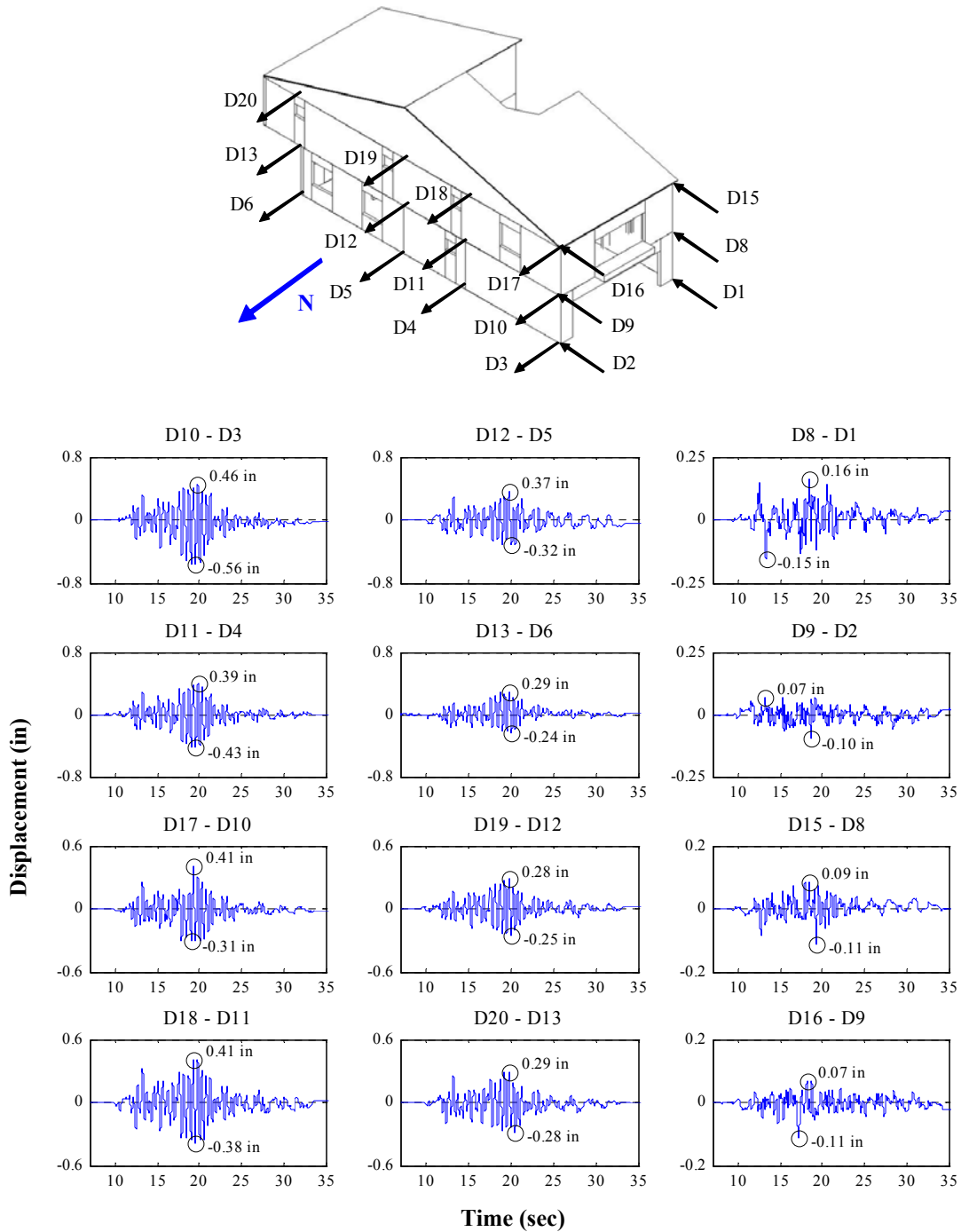


Figure K.44: Relative interstory drift time histories for Test NWP5S03

* Actual data are corrected to exclude the effect of shake table rotations

Appendix K

Phase 5, NWP5S04 Seismic Test

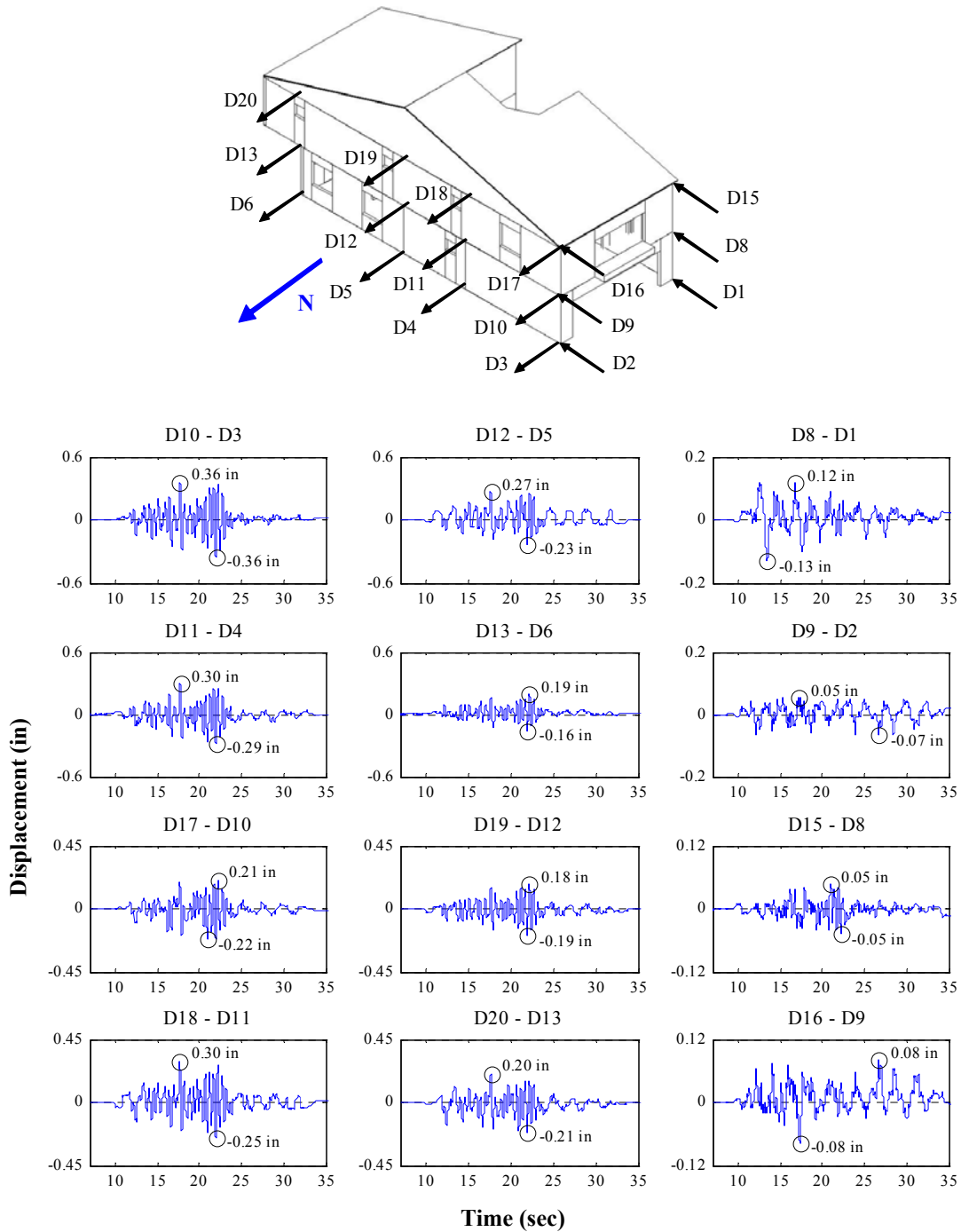


Figure K.45: Relative interstory drift time histories for Test NWP5S04

* Actual data are corrected to exclude the effect of shake table rotations

Appendix K

Phase 5, NWP5S05 Seismic Test

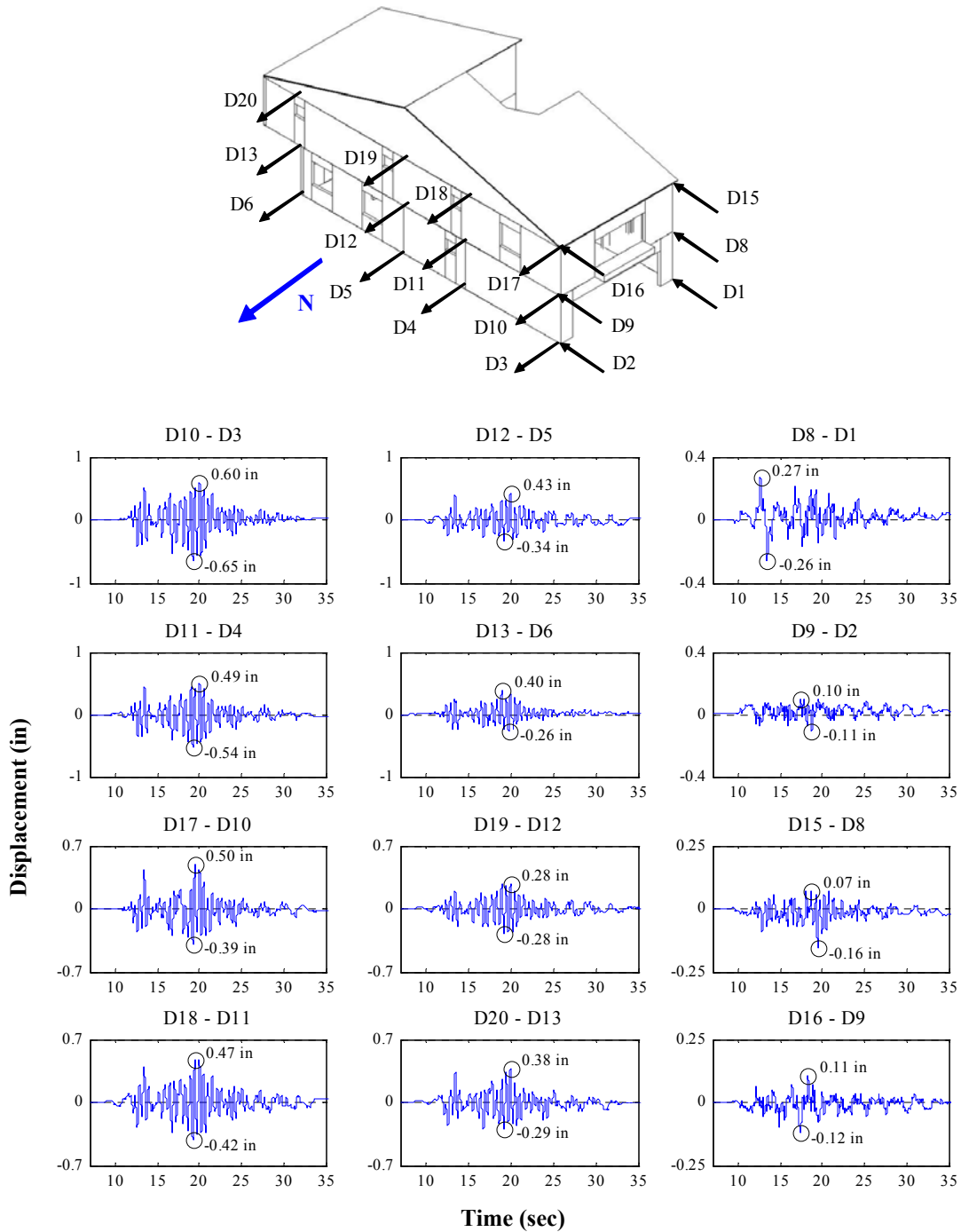


Figure K.46: Relative interstory drift time histories for Test NWP5S05

* Actual data are corrected to exclude the effect of shake table rotations

Appendix K

Phase 5, NWP5S06 Seismic Test

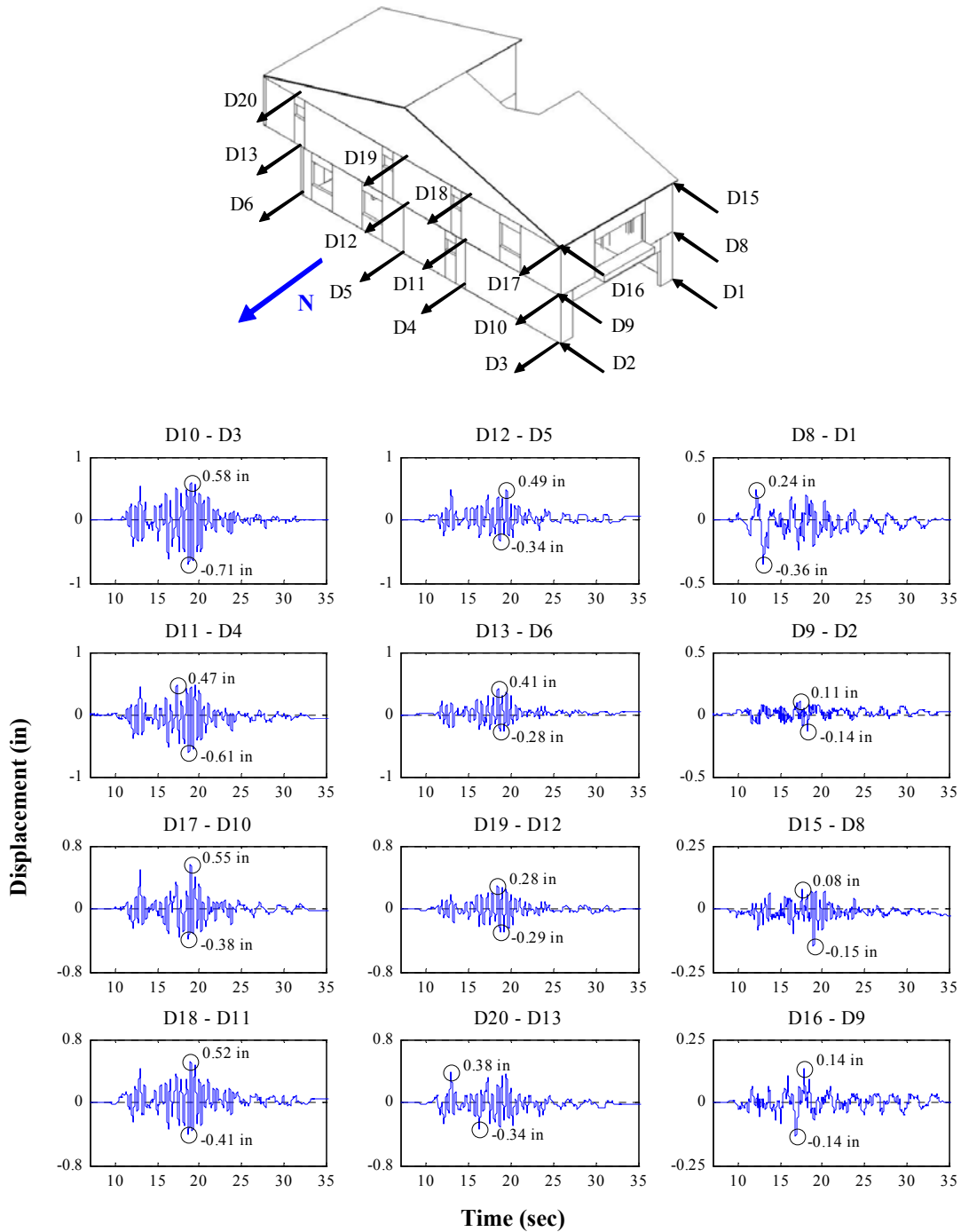


Figure K.47: Relative interstory drift time histories for Test NWP5S06

* Actual data are corrected to exclude the effect of shake table rotations

Appendix K

Phase 5, NWP5S07 Seismic Test

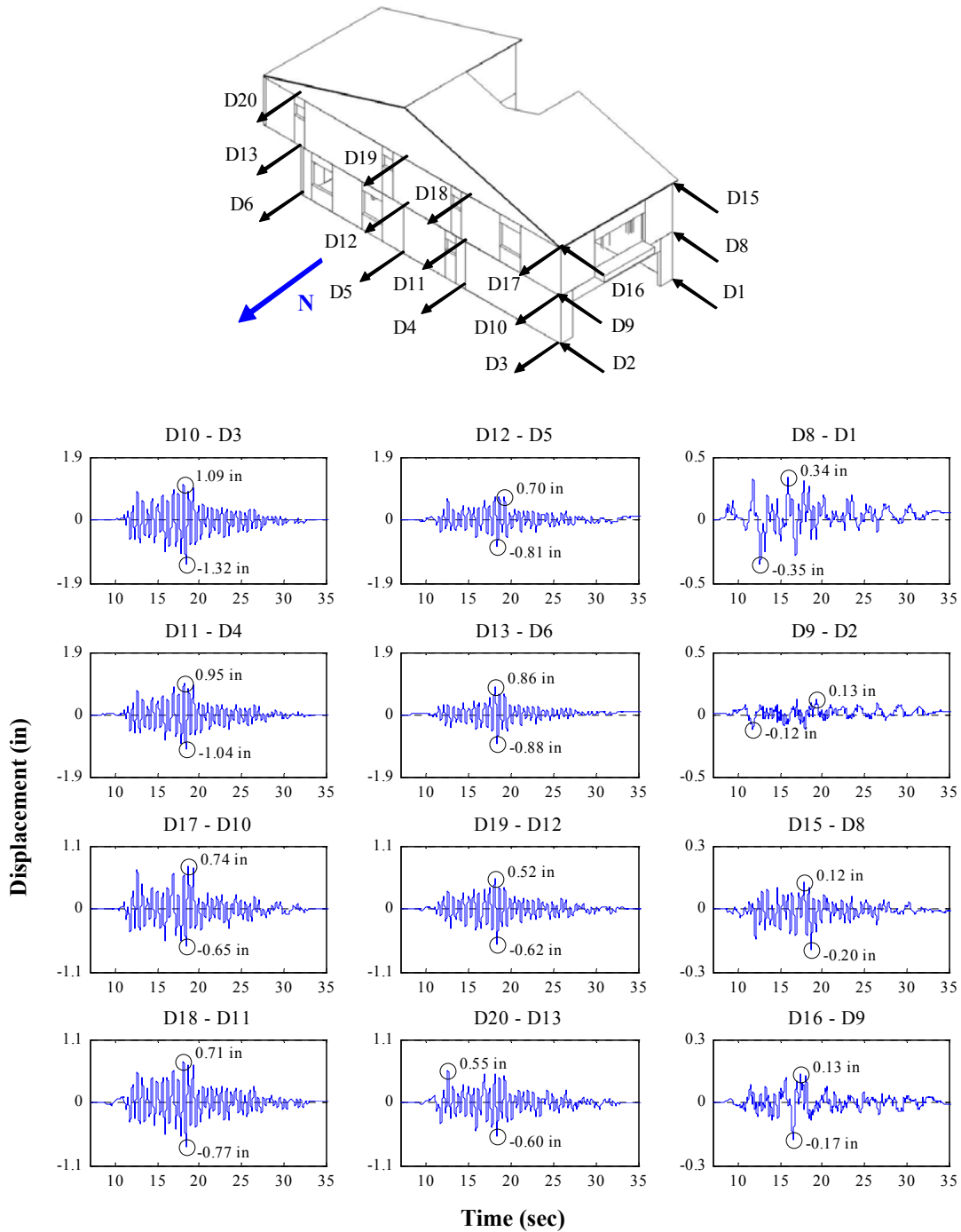


Figure K.48: Relative interstory drift time histories for Test NWP5S07

* Actual data are corrected to exclude the effect of shake table rotations

Appendix K

Phase 5, NWP5S08 Seismic Test

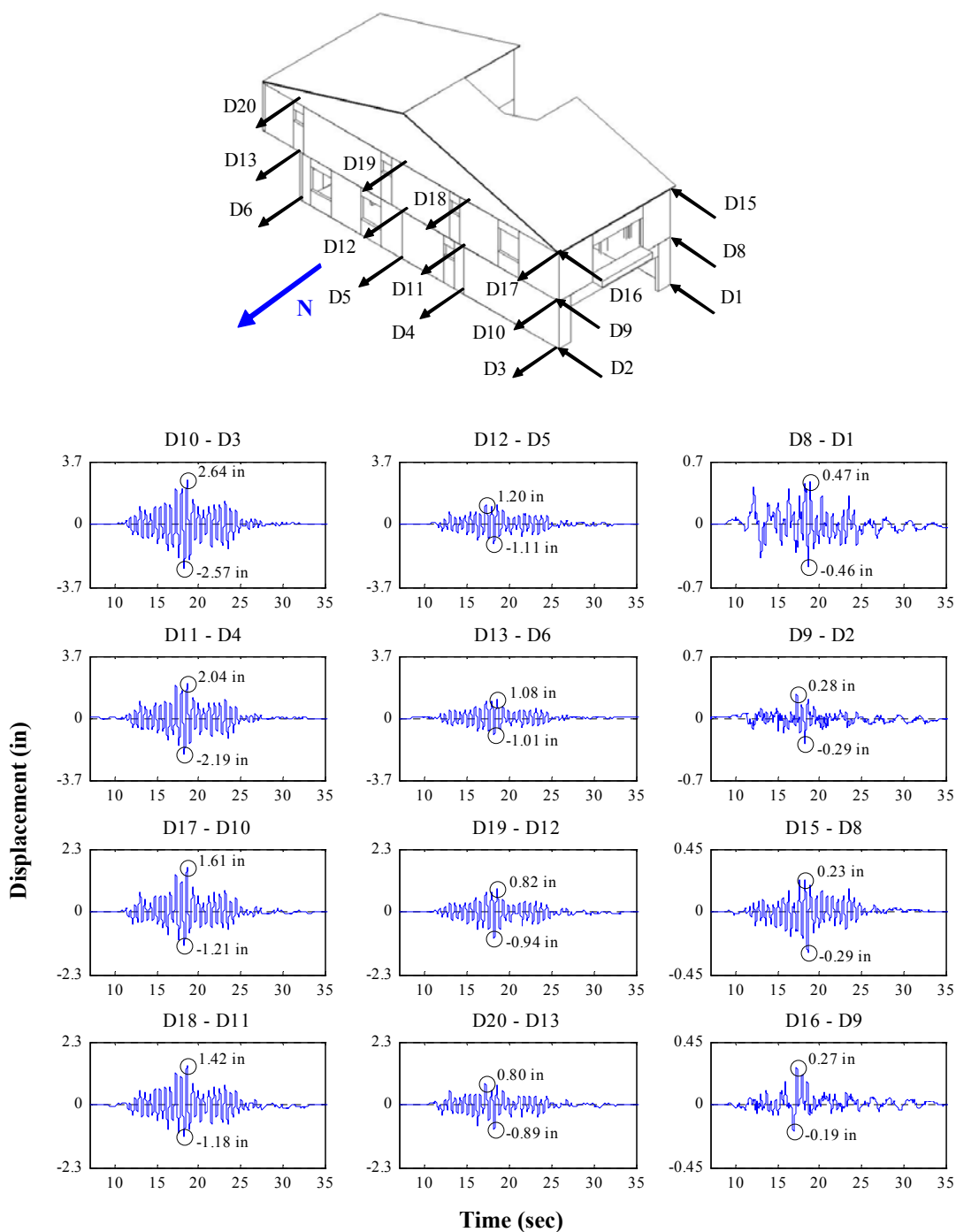


Figure K.49: Relative interstory drift time histories for Test NWP5S08

* Actual data are corrected to exclude the effect of shake table rotations

Appendix K

Phase 5, NWP5S09 Seismic Test

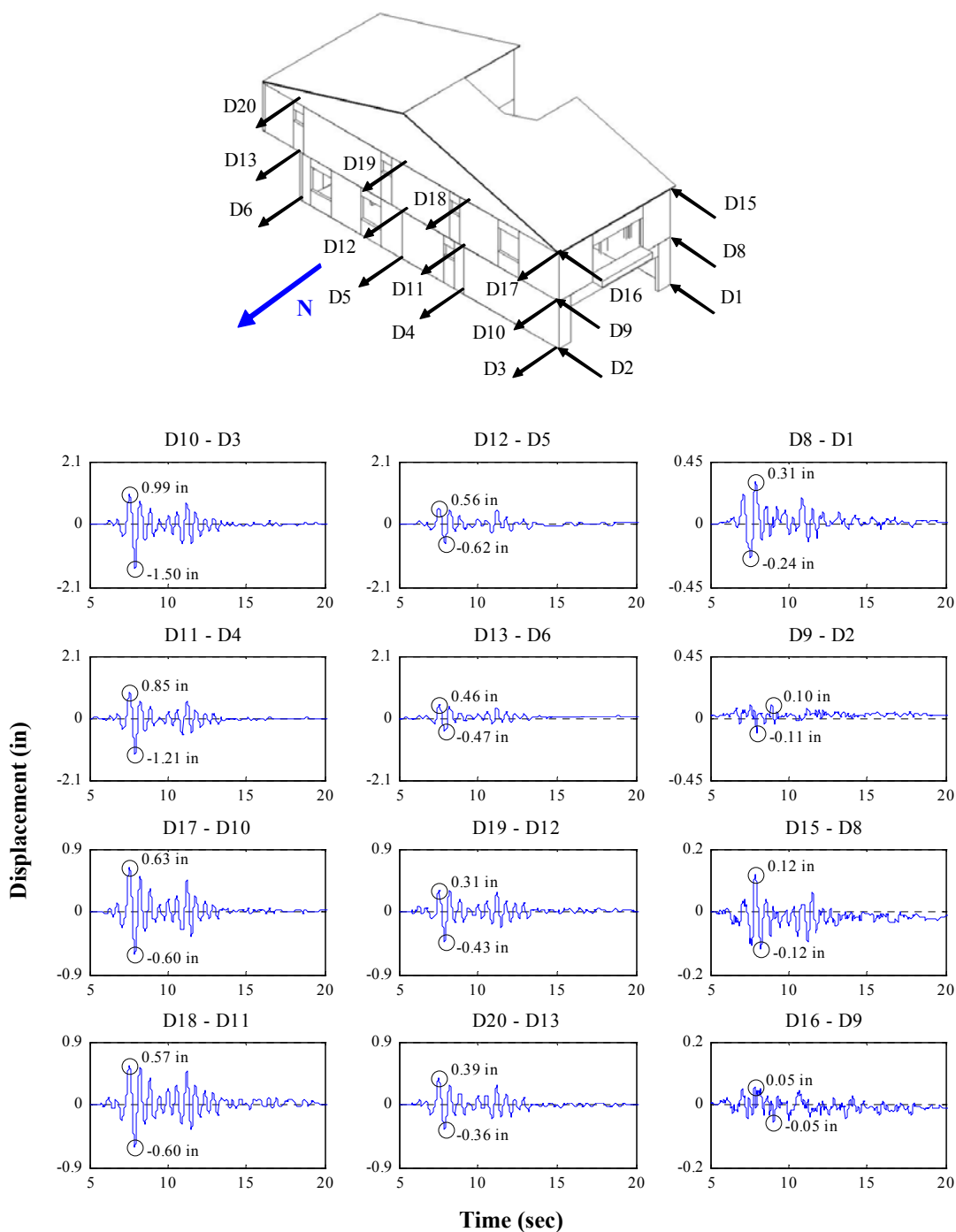


Figure K.50: Relative interstory drift time histories for Test NWP5S09

* Actual data are corrected to exclude the effect of shake table rotations

Appendix K

Phase 5, NWP5S11 Seismic Test

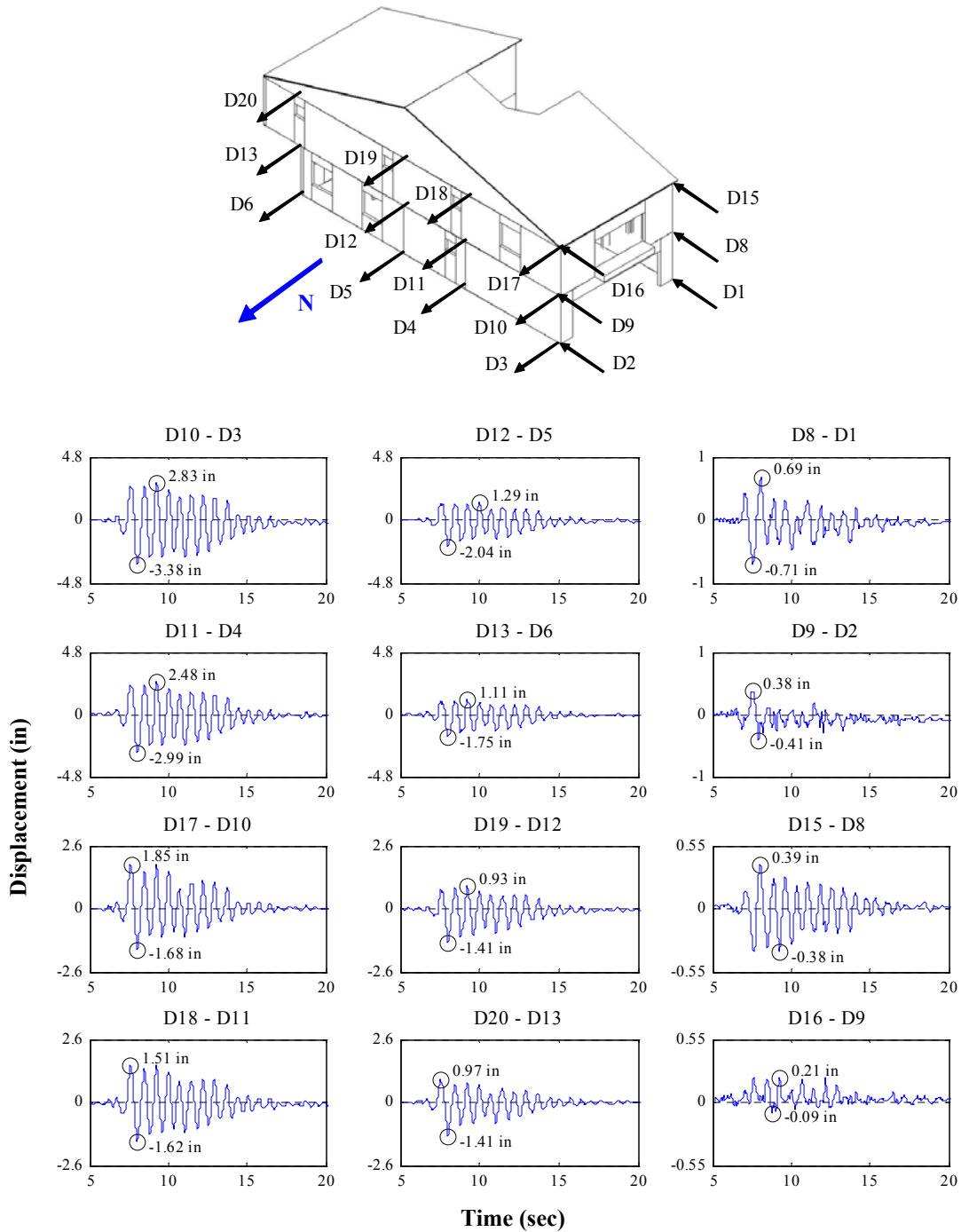


Figure K.51: Relative interstory drift time histories for Test NWP5S11

* Actual data are corrected to exclude the effect of shake table rotations

Appendix L
Selected Seismic Results:
Absolute Acceleration
Time Histories

Appendix L

Phase 1, NWP1S01 Seismic Test

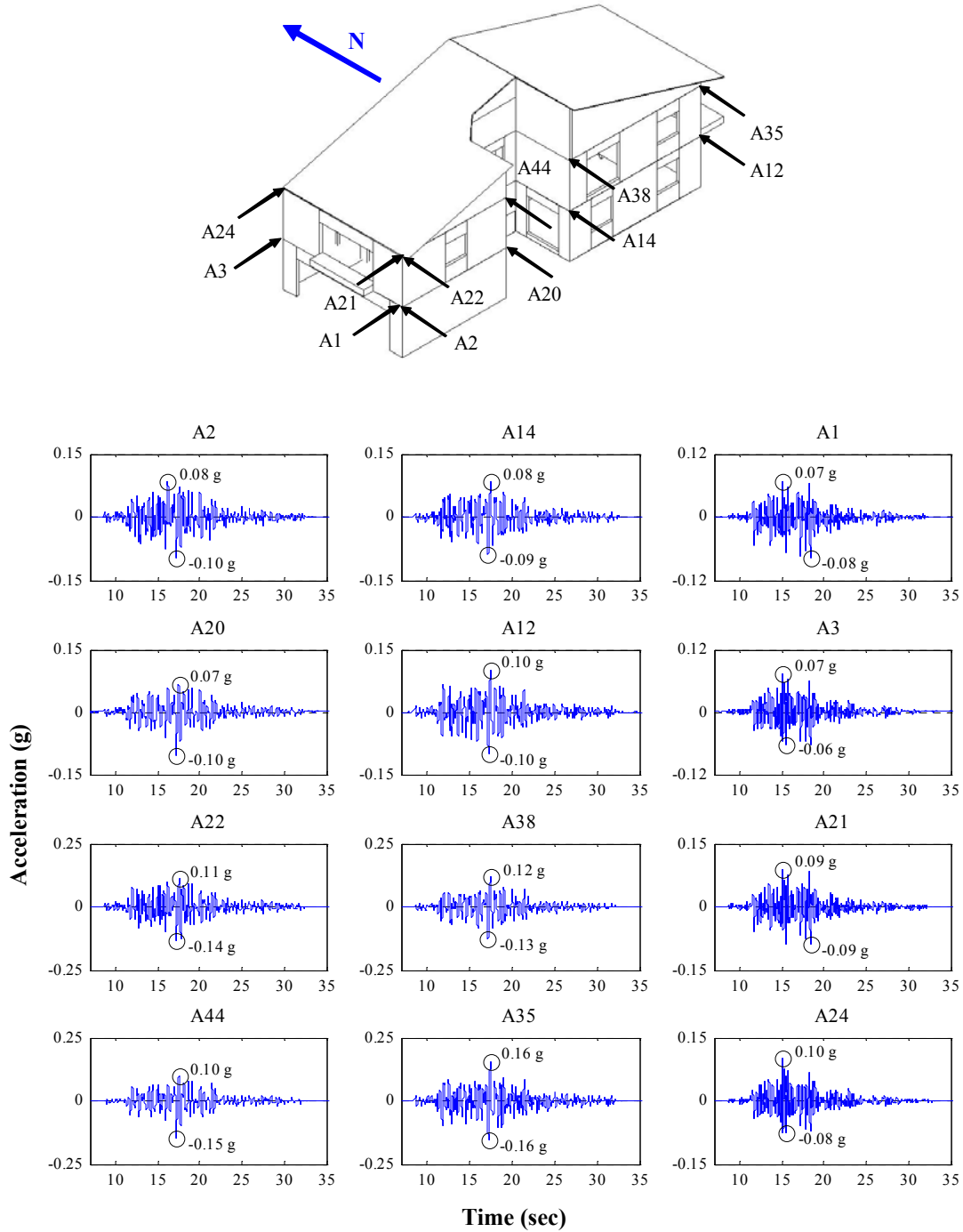


Figure L.1: Absolute acceleration time histories for Test NWP1S01

Appendix L

Phase 1, NWP1S02 Seismic Test

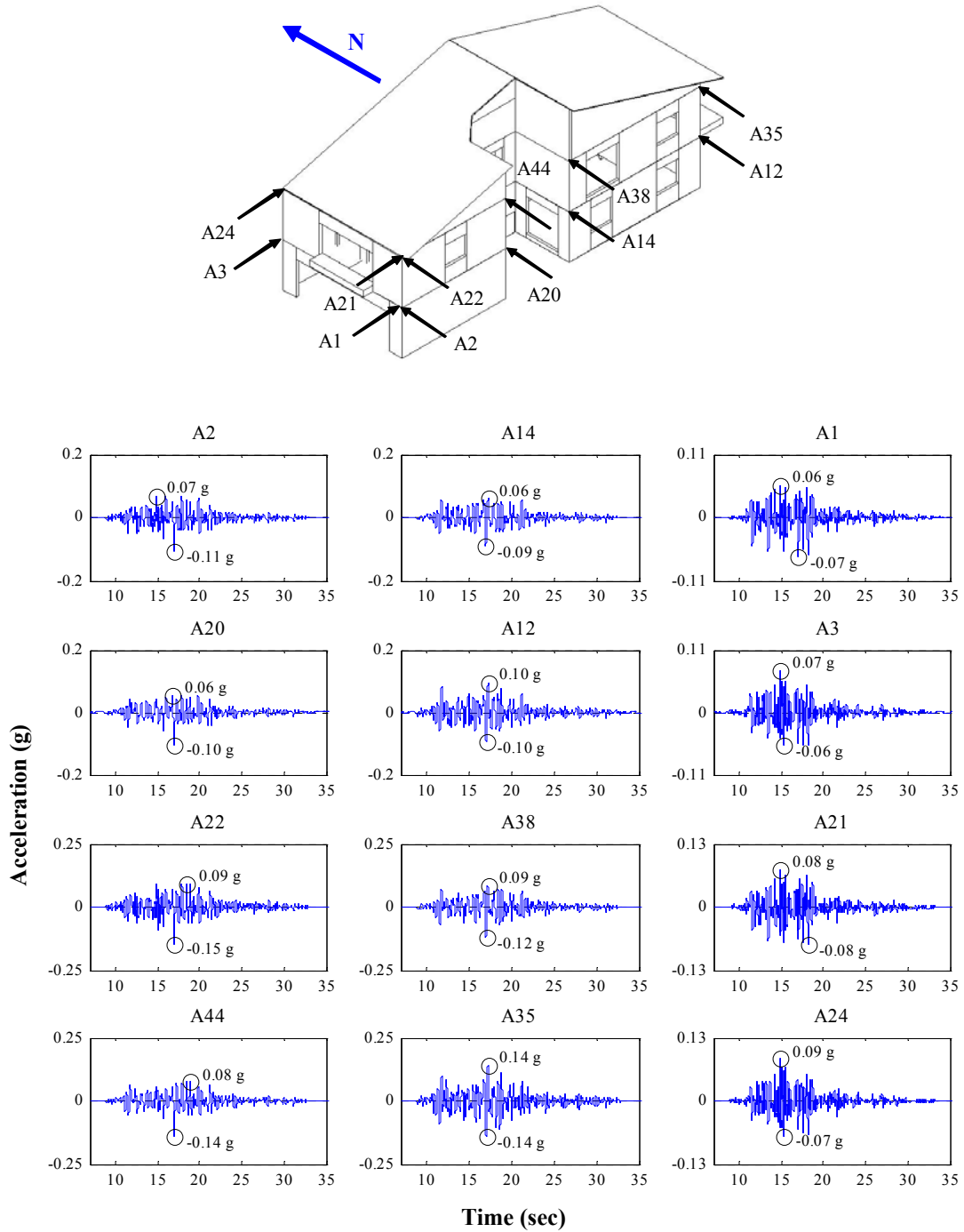


Figure L.2: Absolute acceleration time histories for Test NWP1S02

Appendix L

Phase 1, NWP1S03 Seismic Test

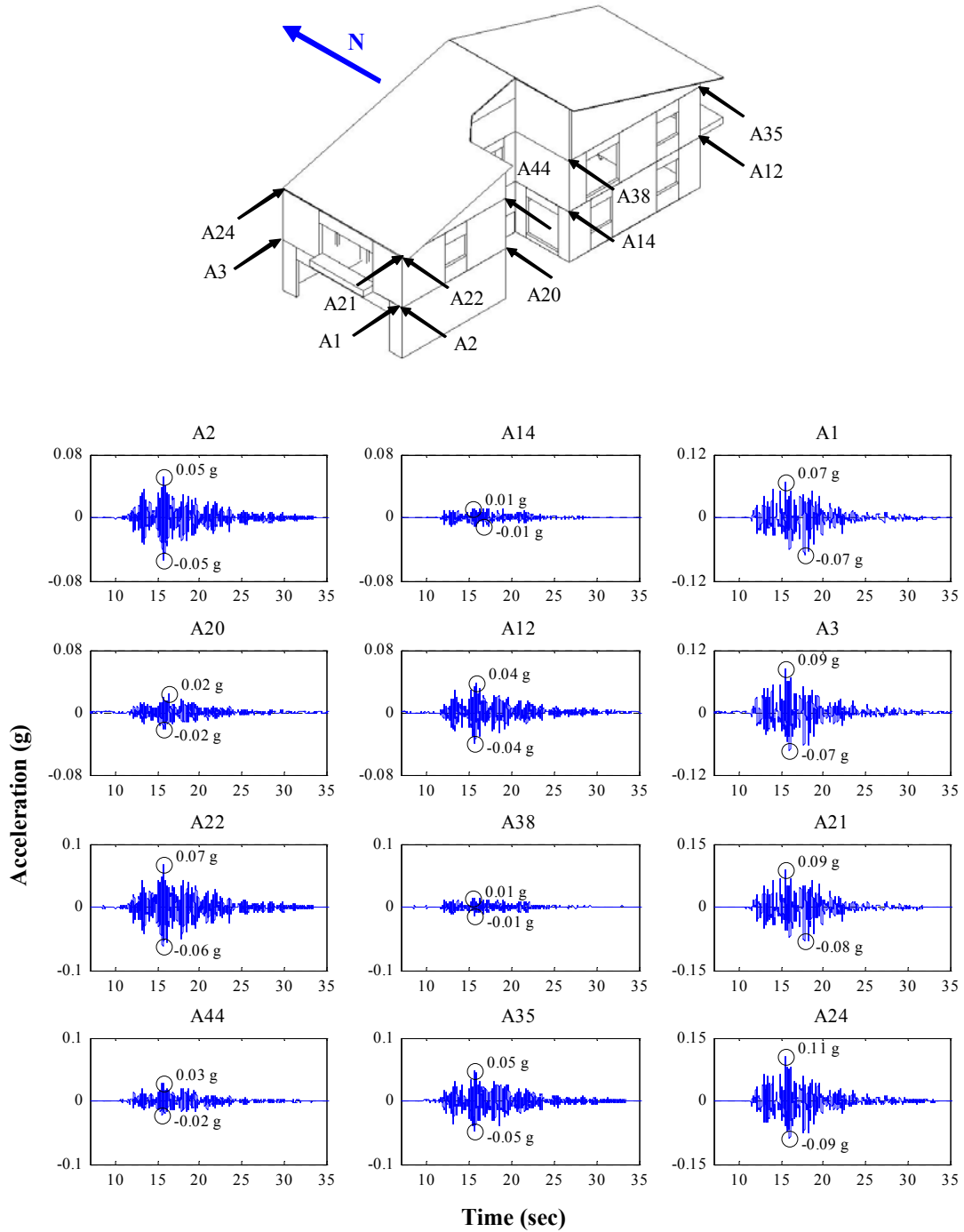


Figure L.3: Absolute acceleration time histories for Test NWP1S03

Appendix L

Phase 1, NWP1S04 Seismic Test

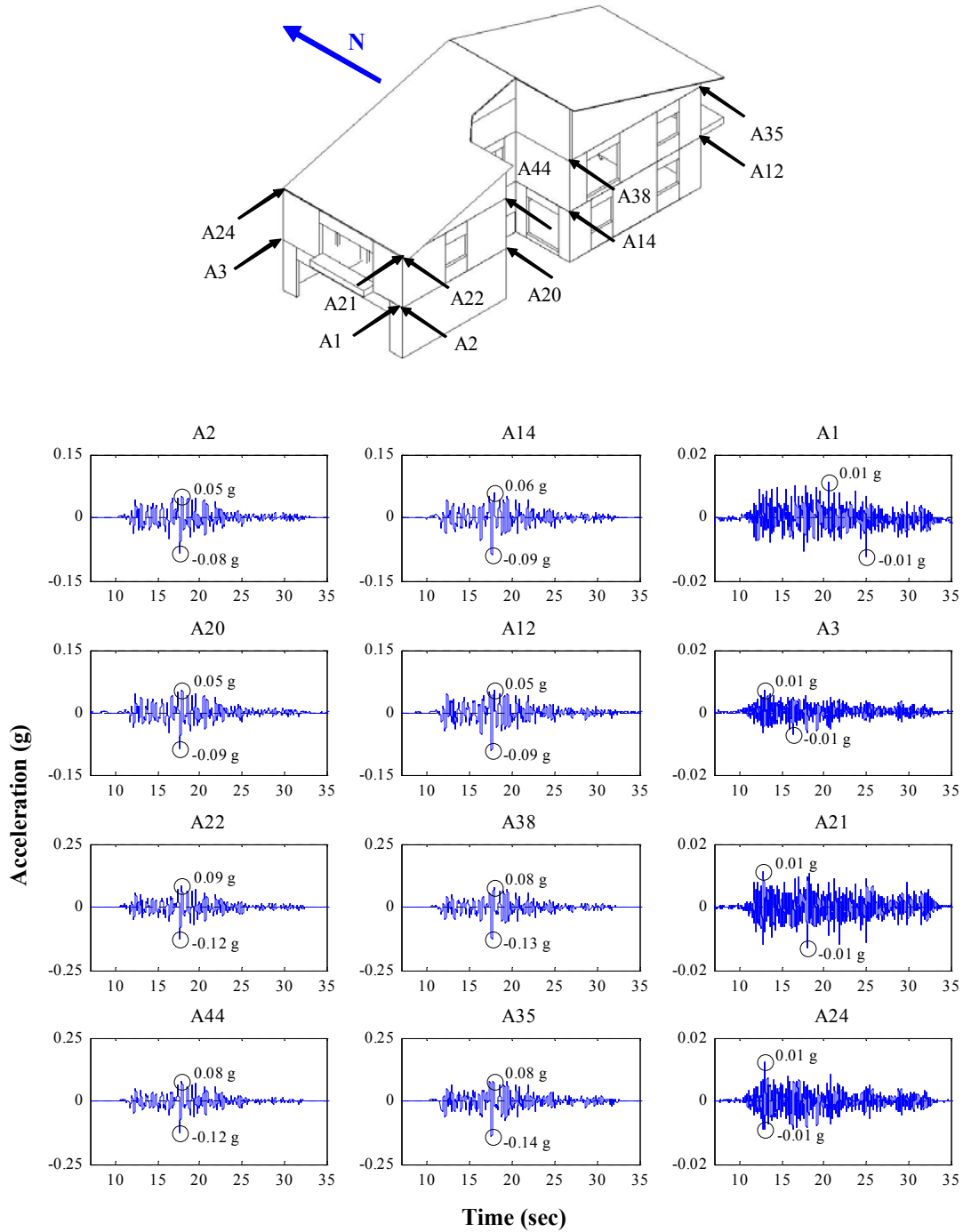


Figure L.4: Absolute acceleration time histories for Test NWP1S04

Appendix L

Phase 1, NWP1S05 Seismic Test

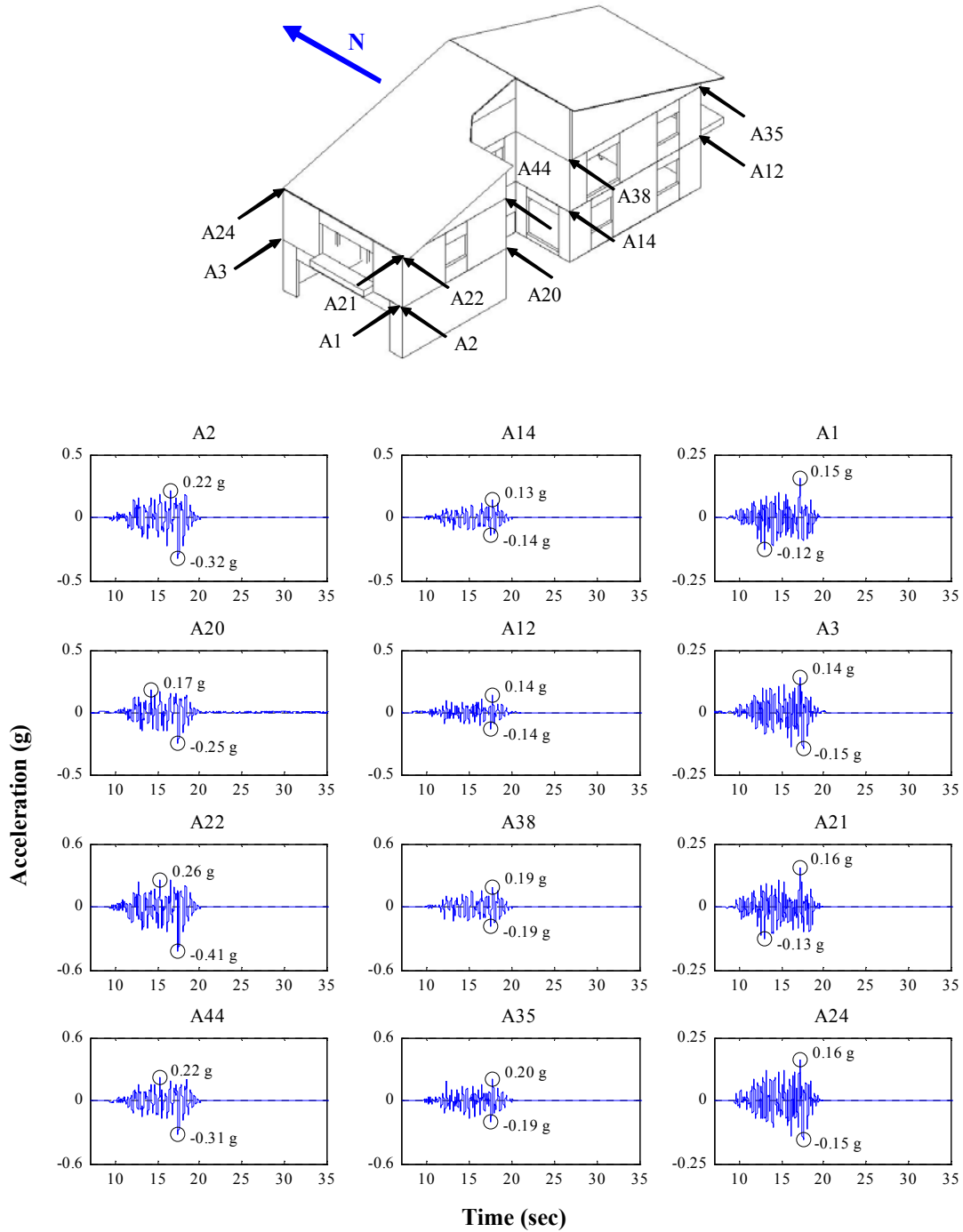


Figure L.5: Absolute acceleration time histories for Test NWP1S05

Appendix L

Phase 1, NWP1S17 Seismic Test

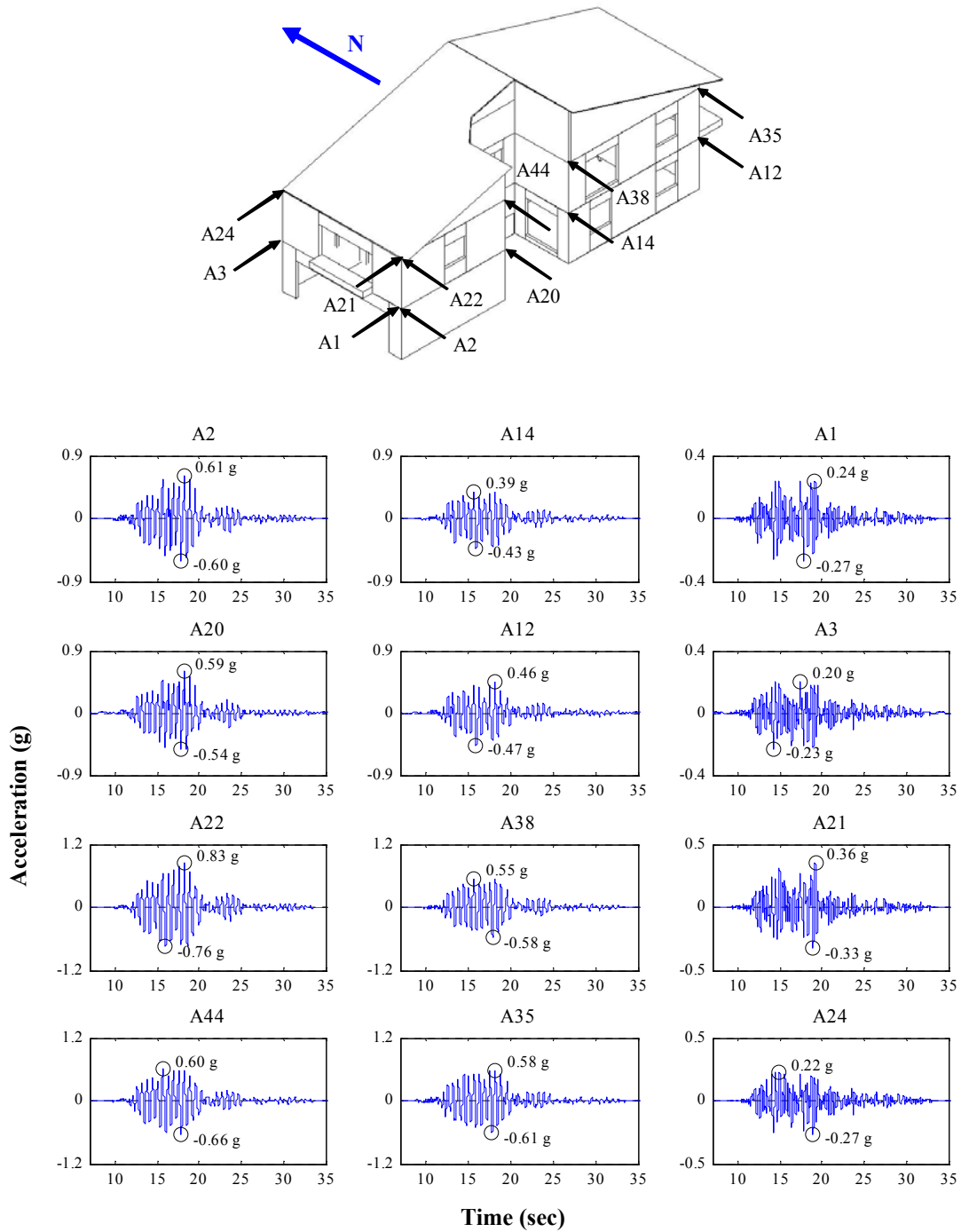


Figure L.6: Absolute acceleration time histories for Test NWP1S17

Appendix L

Phase 1, NWP1S07 Seismic Test

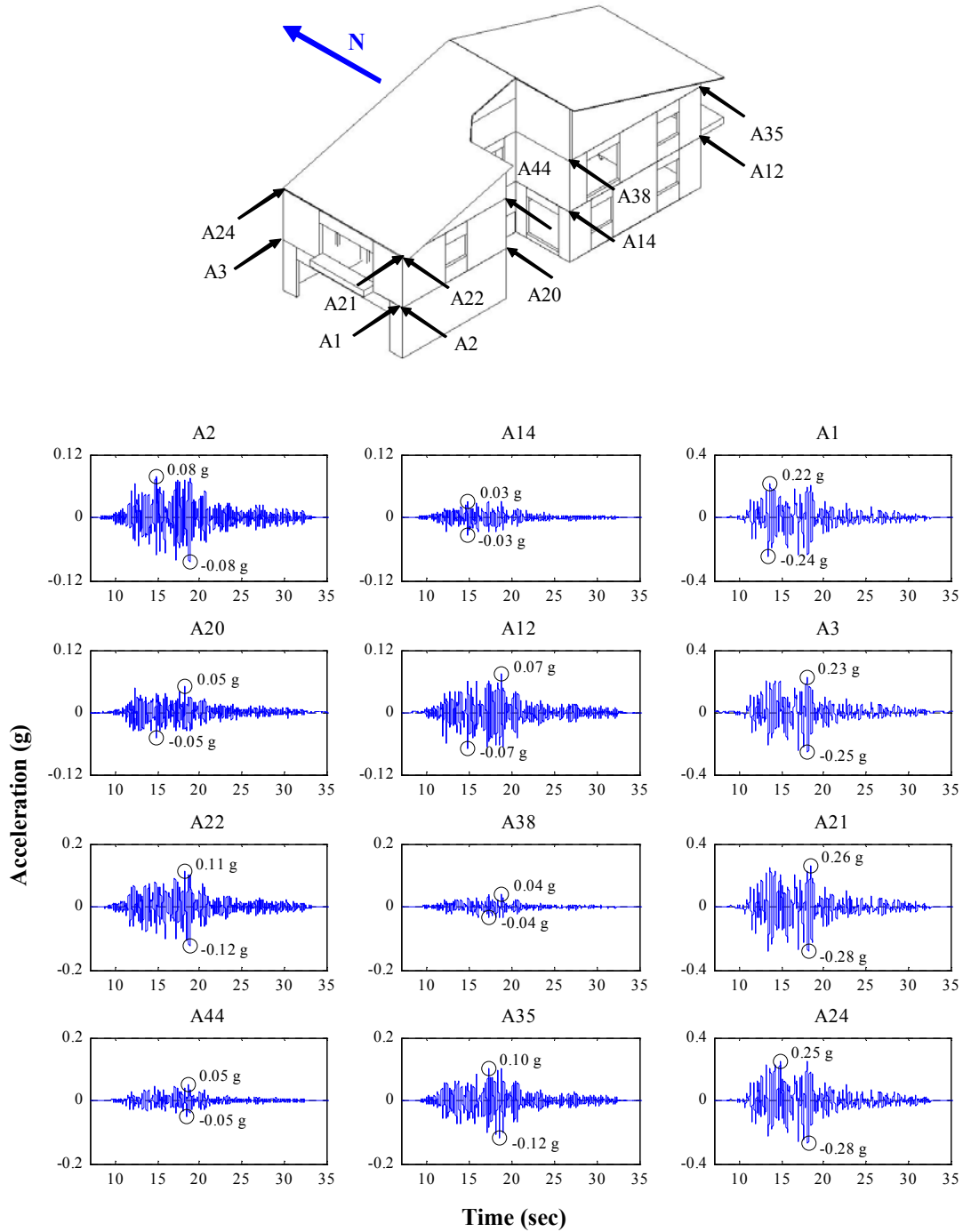


Figure L.7: Absolute acceleration time histories for Test NWP1S07

Appendix L

Phase 1, NWP1S06 Seismic Test

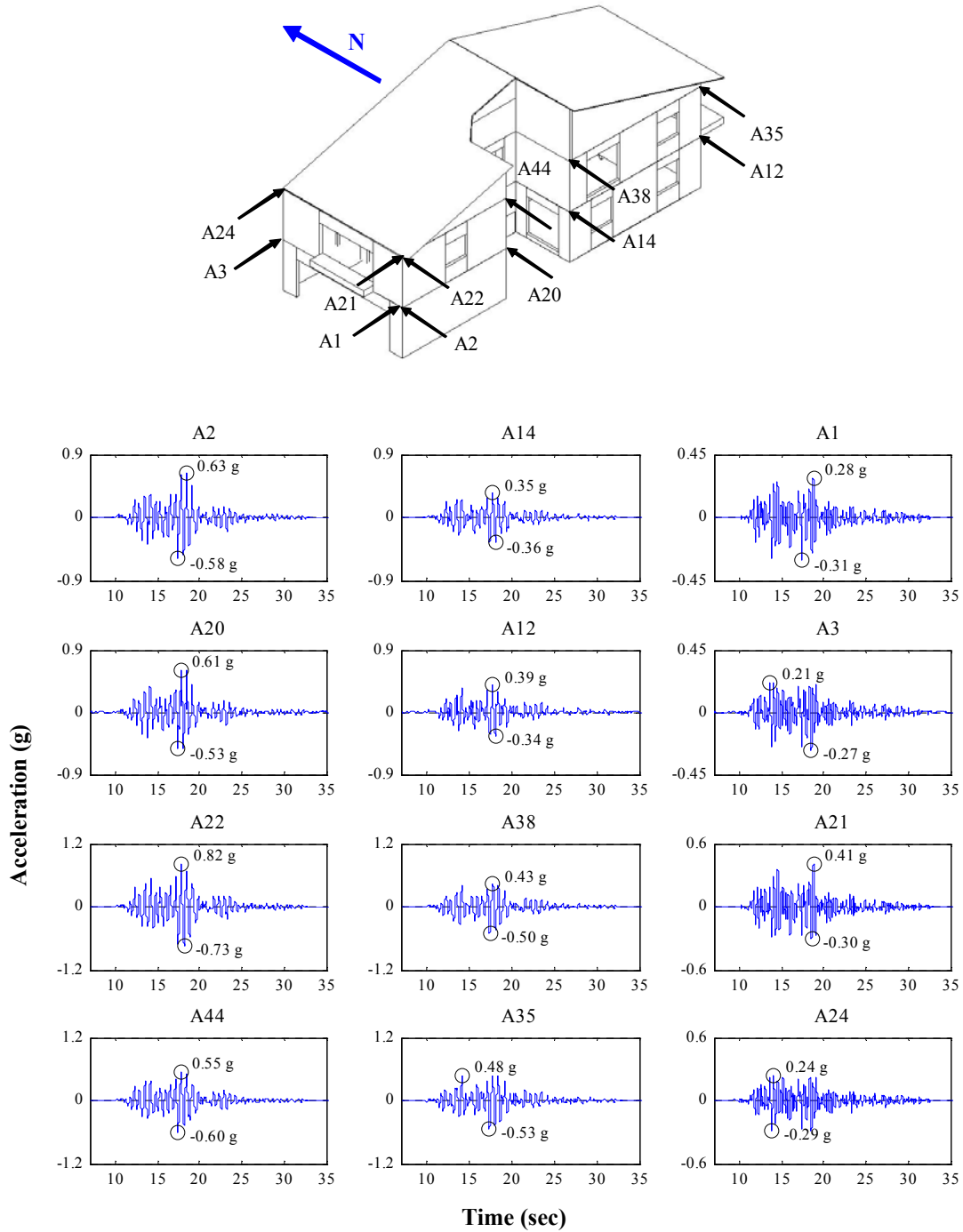


Figure L.8: Absolute acceleration time histories for Test NWP1S06

Appendix L

Phase 1, NWP1S10 Seismic Test

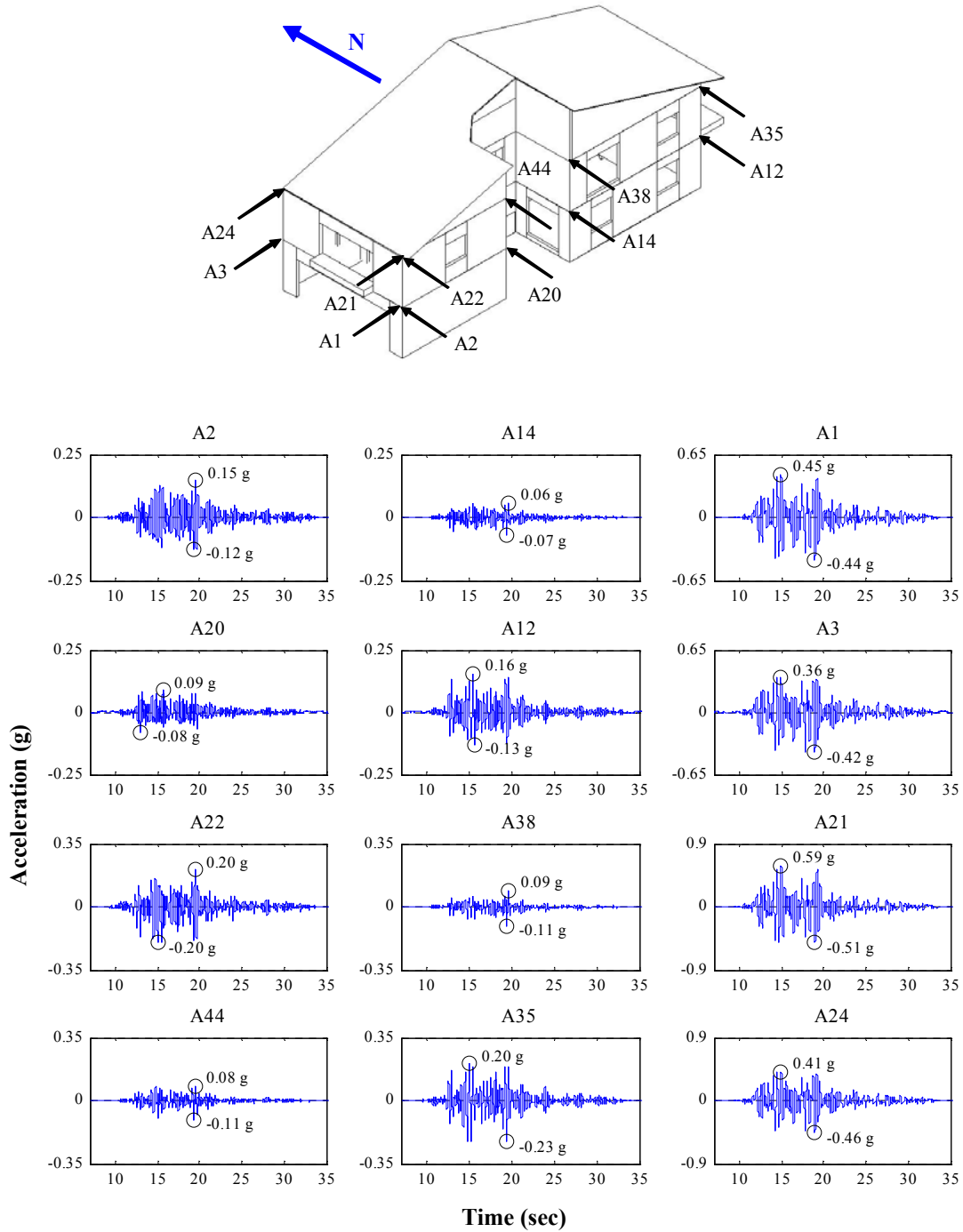


Figure L.9: Absolute acceleration time histories for Test NWP1S10

Appendix L

Phase 2, NWP2S01 Seismic Test

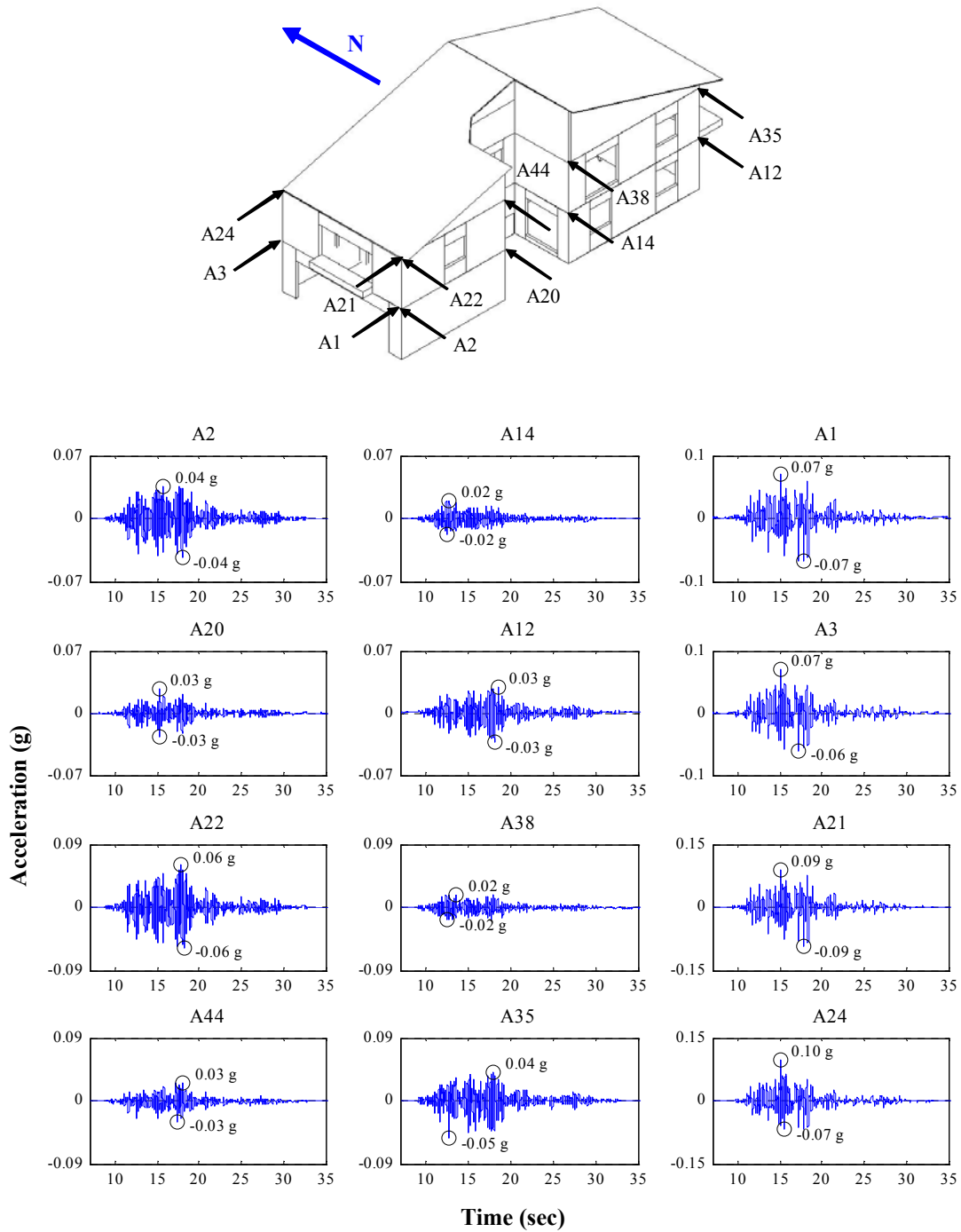


Figure L.10: Absolute acceleration time histories for Test NWP2S01

Appendix L

Phase 2, NWP2S02 Seismic Test

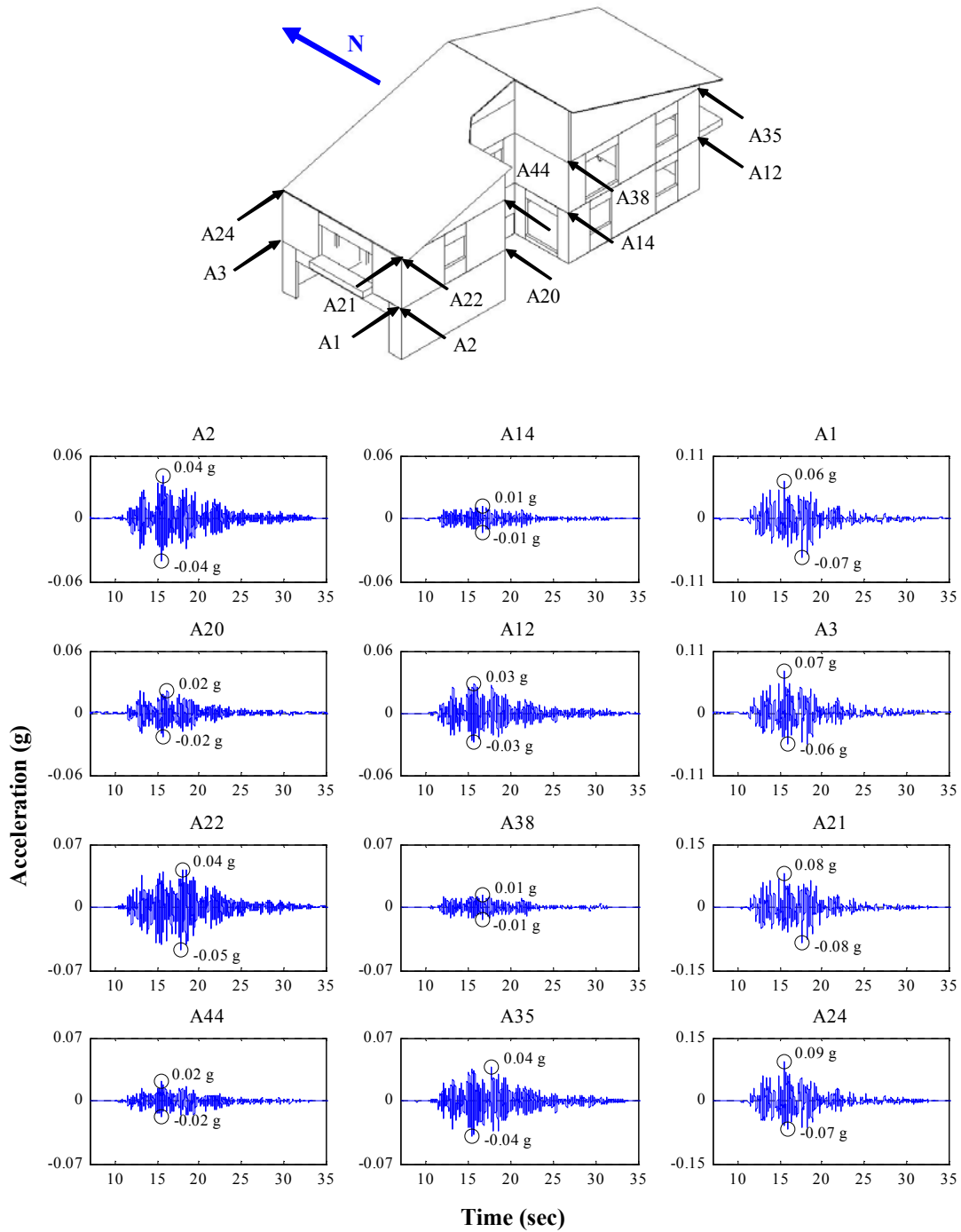


Figure L.11: Absolute acceleration time histories for Test NWP2S02

Appendix L

Phase 2, NWP2S03 Seismic Test

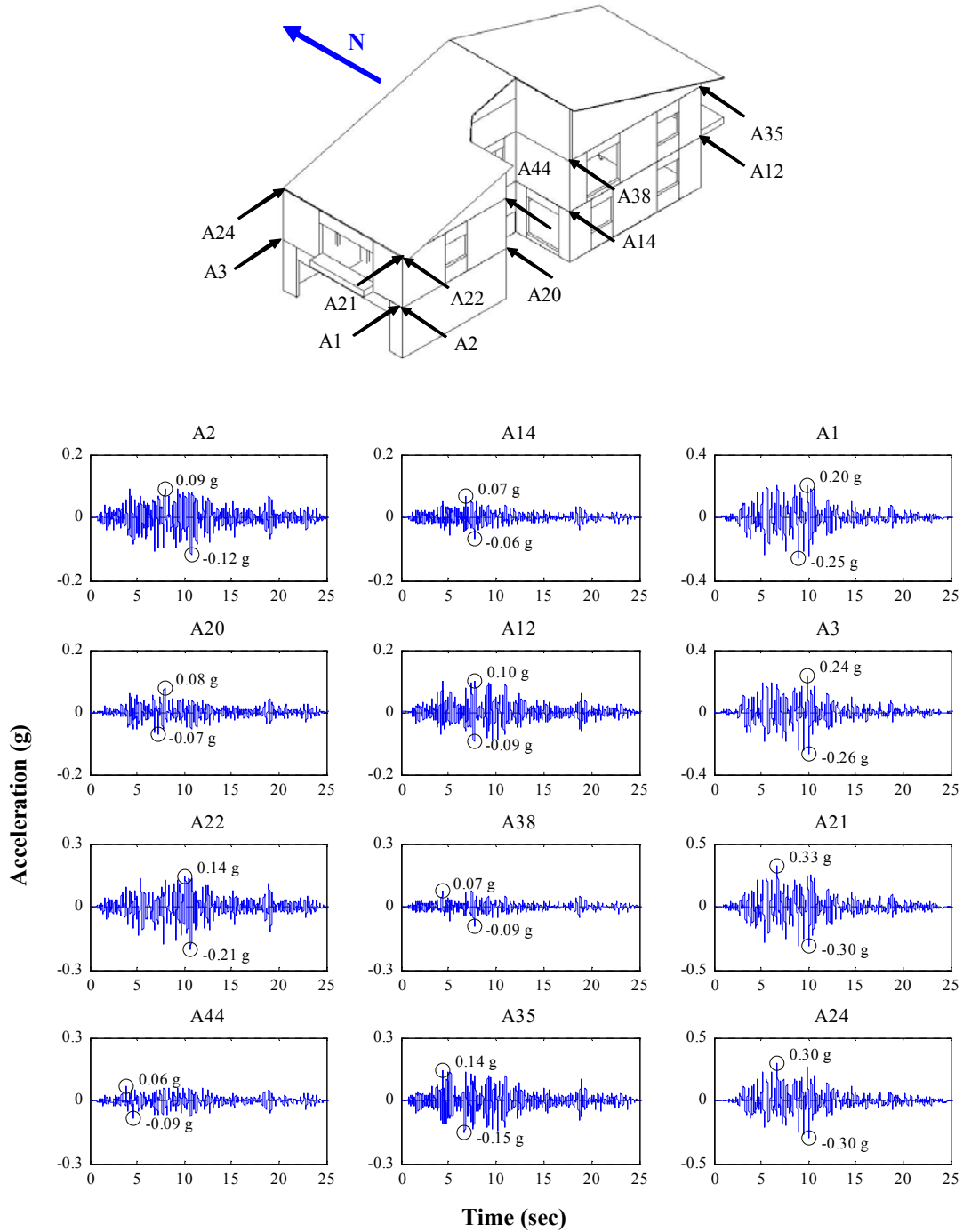


Figure L.12: Absolute acceleration time histories for Test NWP2S03

Appendix L

Phase 2, NWP2S04 Seismic Test

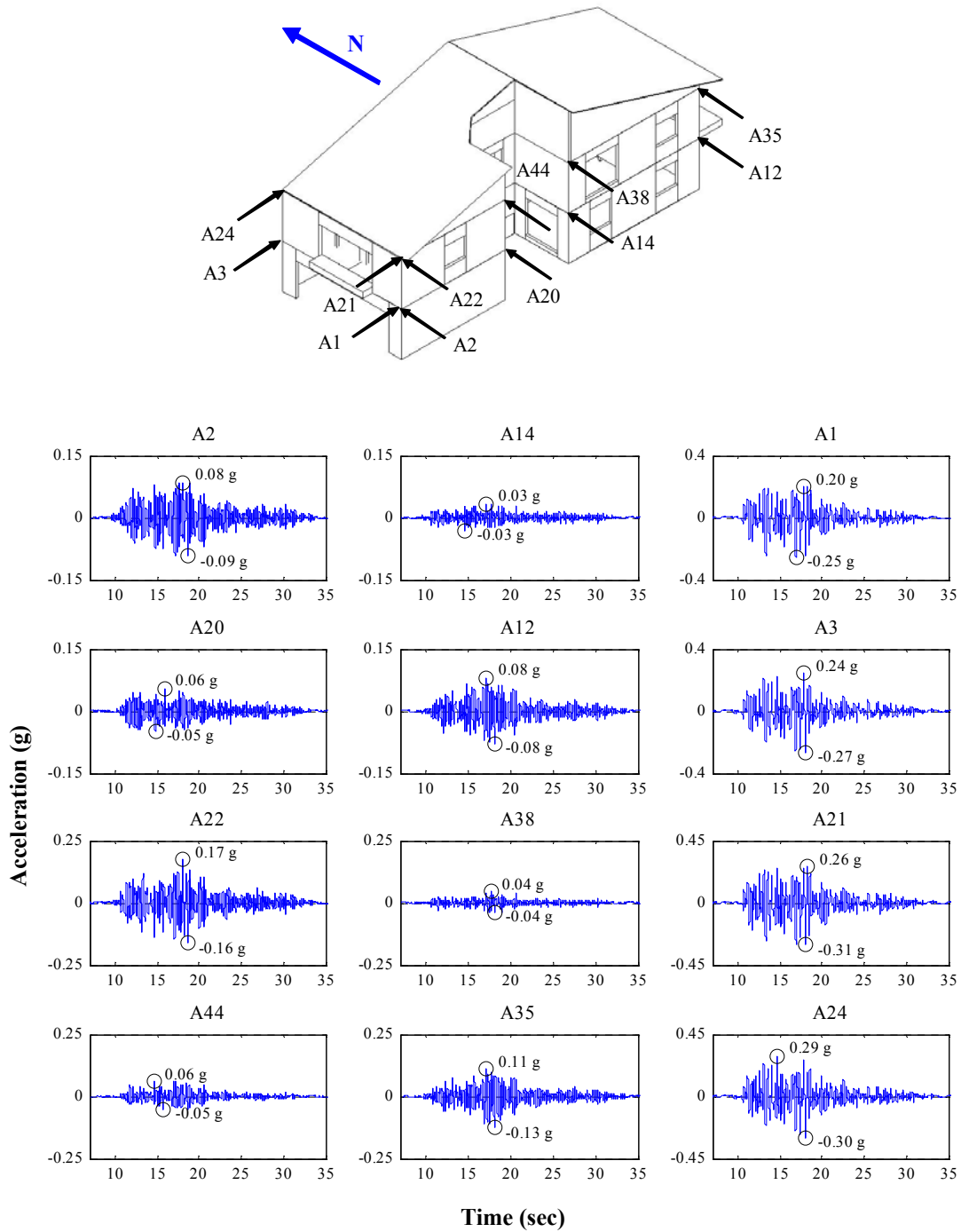


Figure L.13: Absolute acceleration time histories for Test NWP2S04

Appendix L

Phase 2, NWP2S05 Seismic Test

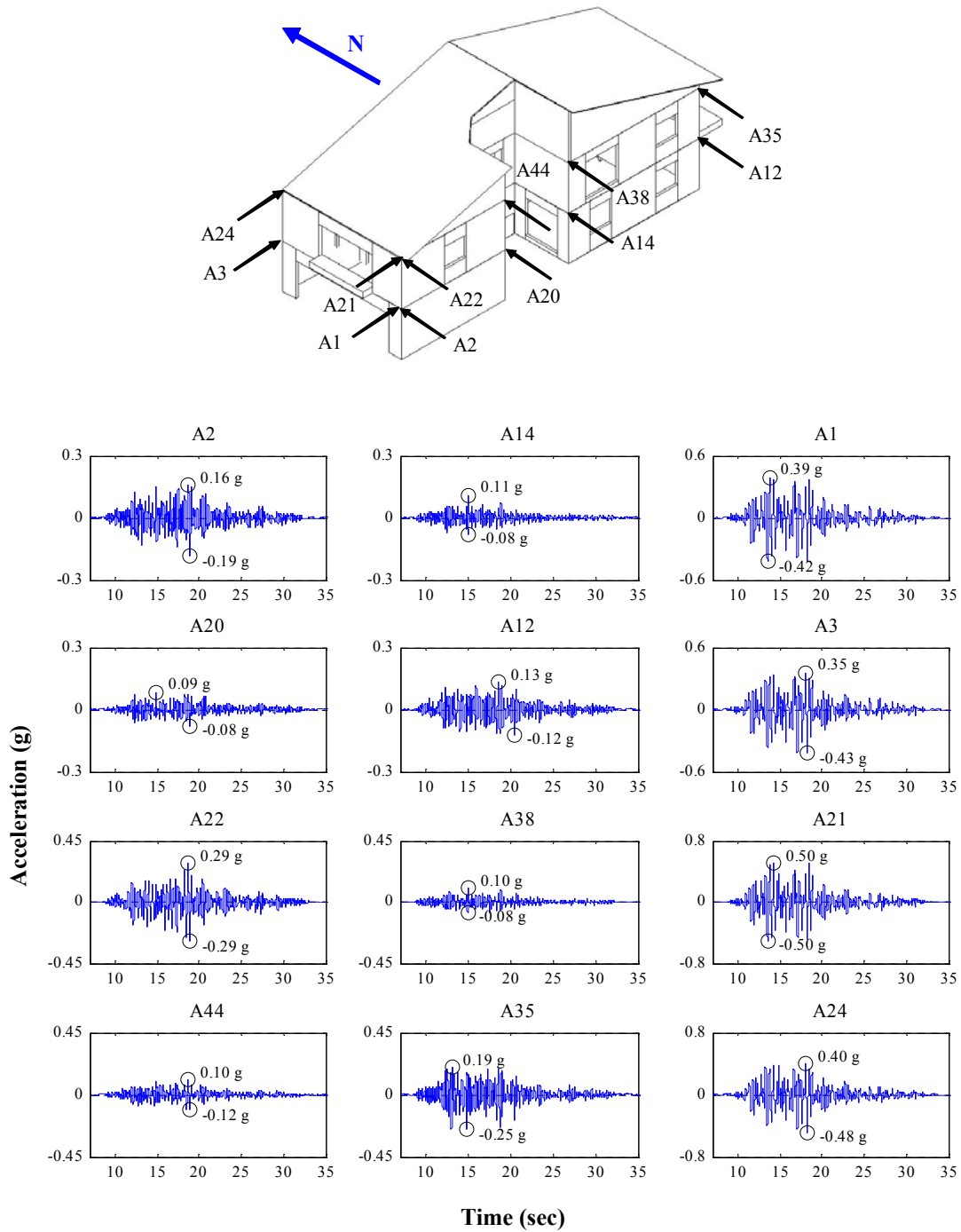


Figure L.14: Absolute acceleration time histories for Test NWP2S05

Appendix L

Phase 2, NWP2S06 Seismic Test

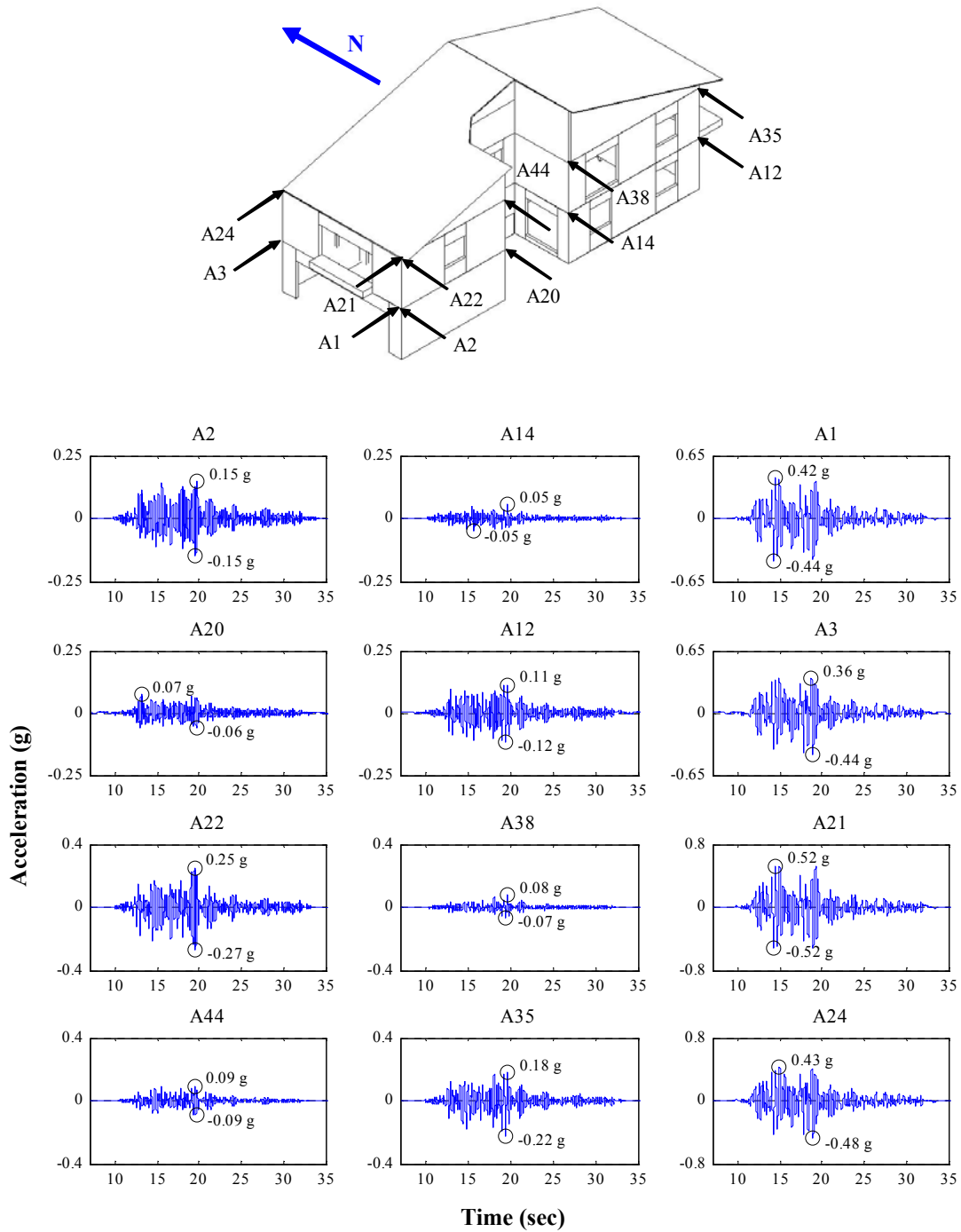


Figure L.15: Absolute acceleration time histories for Test NWP2S06

Appendix L

Phase 2, NWP2S07 Seismic Test

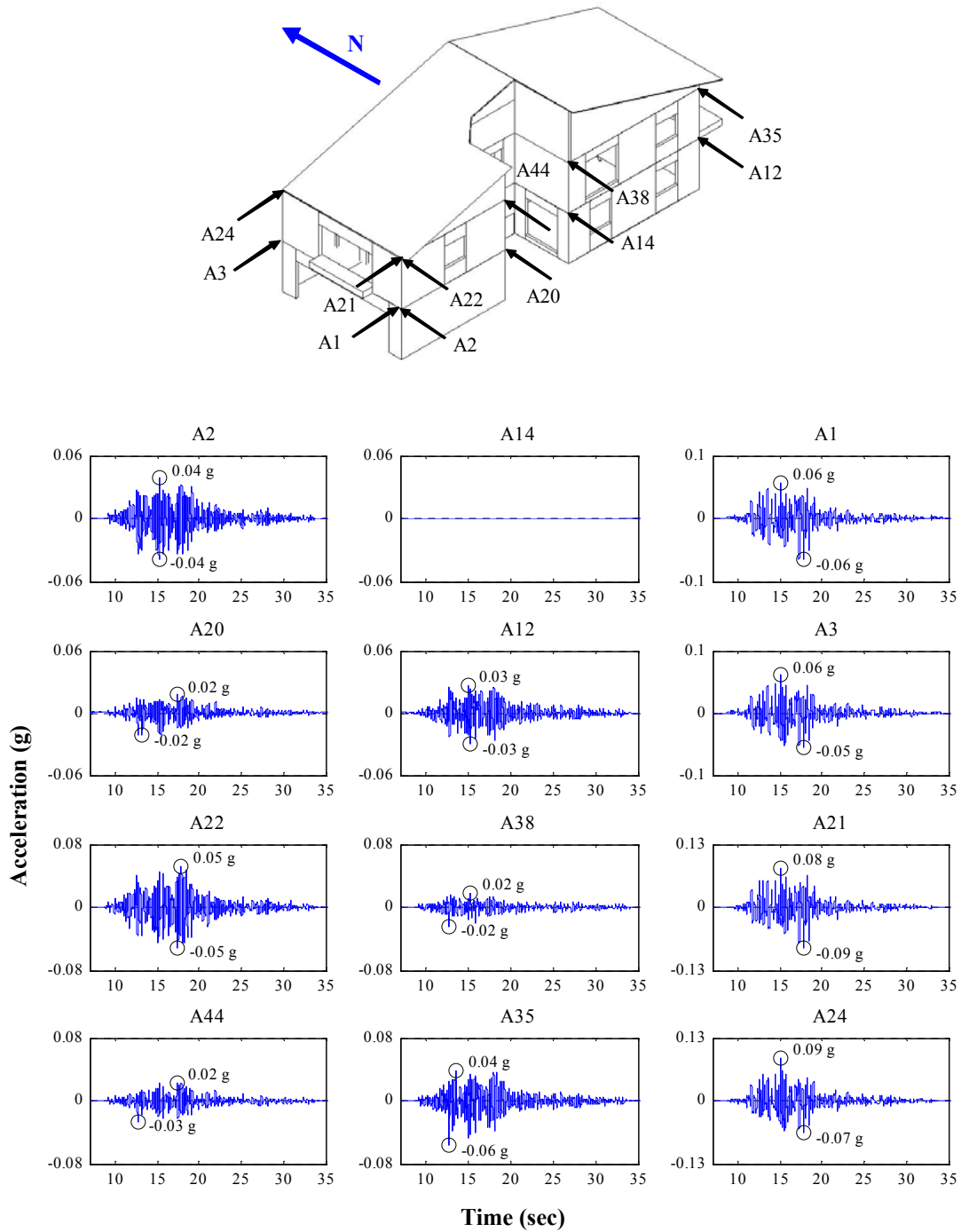


Figure L.16: Absolute acceleration time histories for Test NWP2S07

Appendix L

Phase 2, NWP2S08 Seismic Test

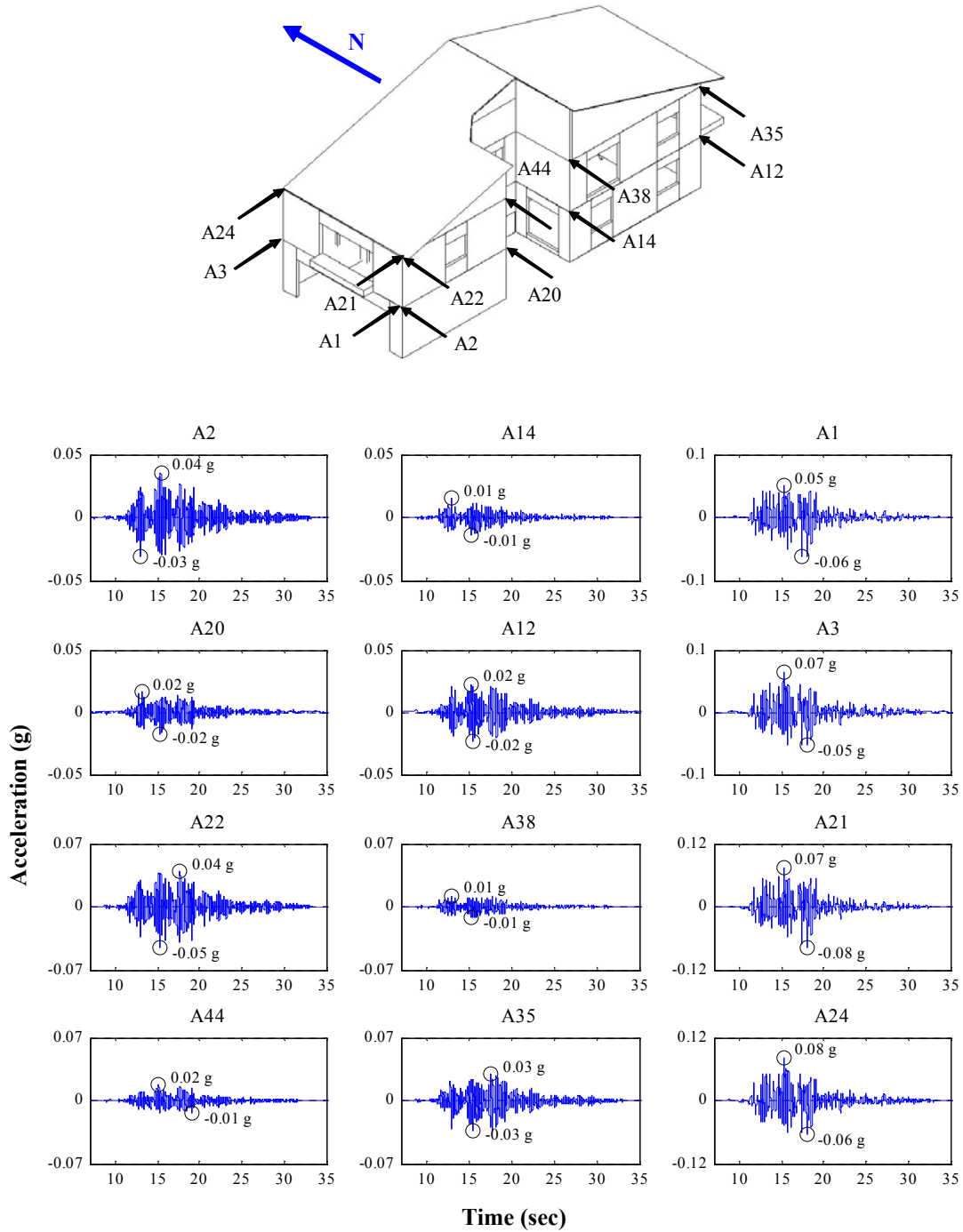


Figure L.17: Absolute acceleration time histories for Test NWP2S08

Appendix L

Phase 2, NWP2S09 Seismic Test

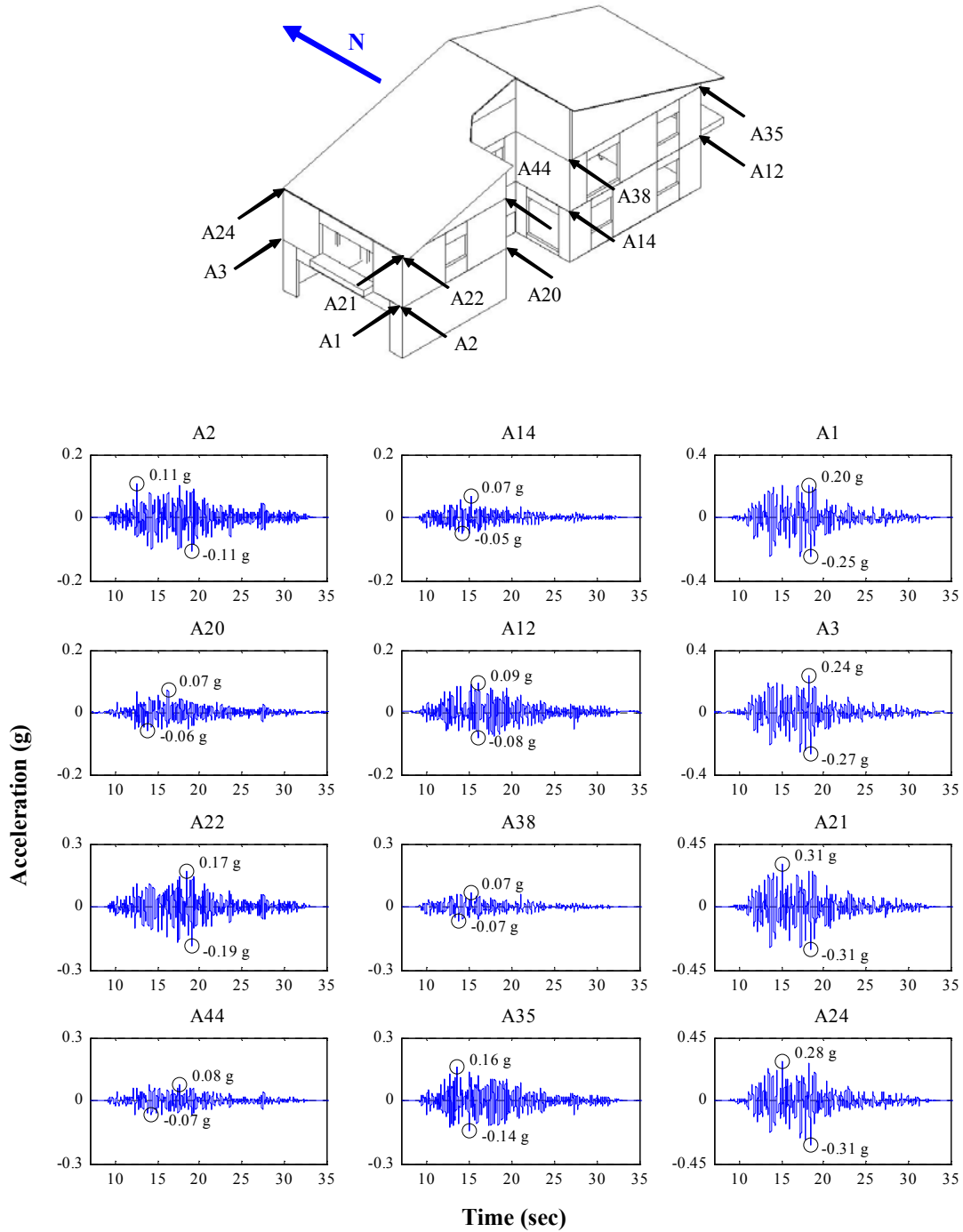


Figure L.18: Absolute acceleration time histories for Test NWP2S09

Appendix L

Phase 2, NWP2S10 Seismic Test

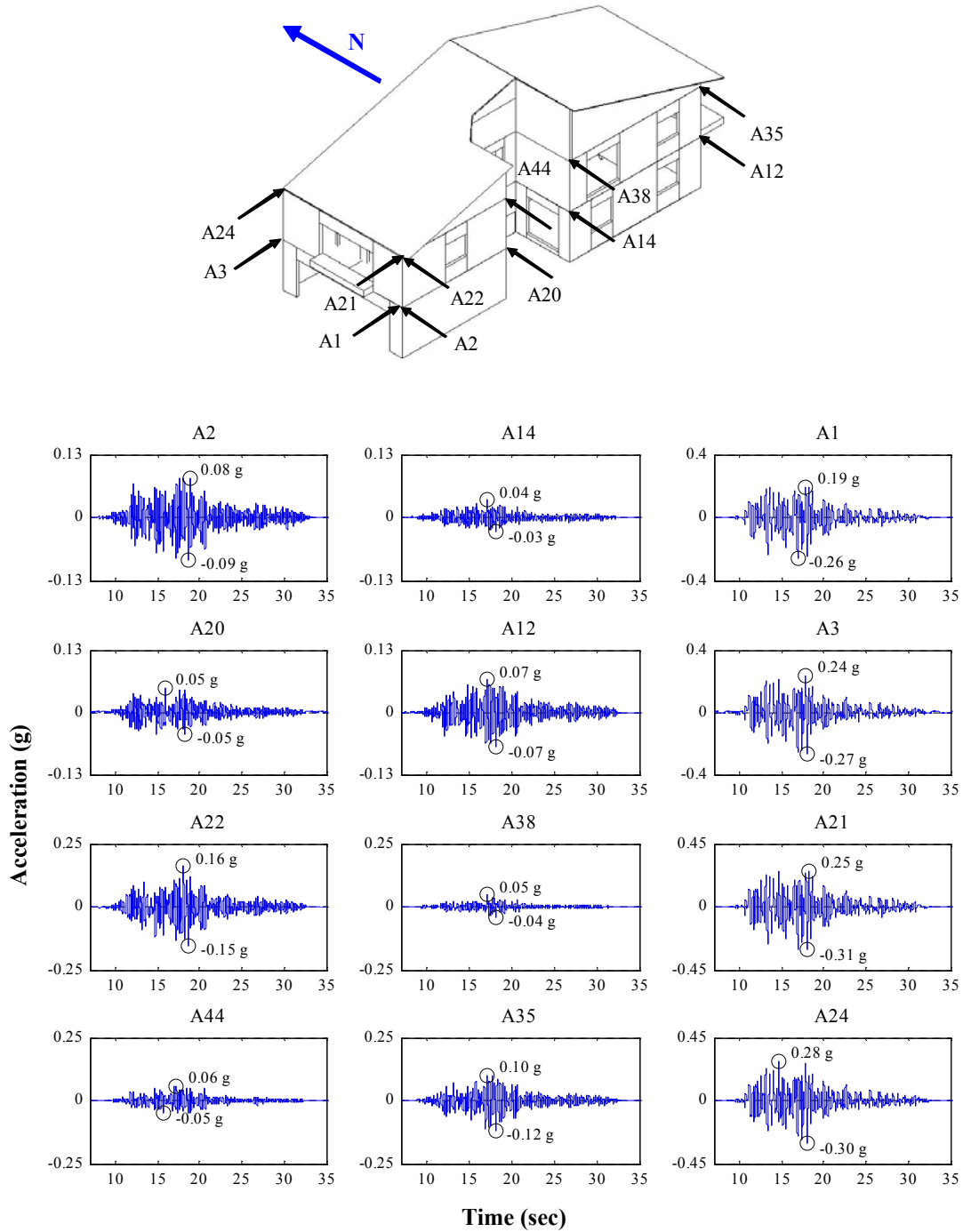


Figure L.19: Absolute acceleration time histories for Test NWP2S10

Appendix L

Phase 2, NWP2S11 Seismic Test

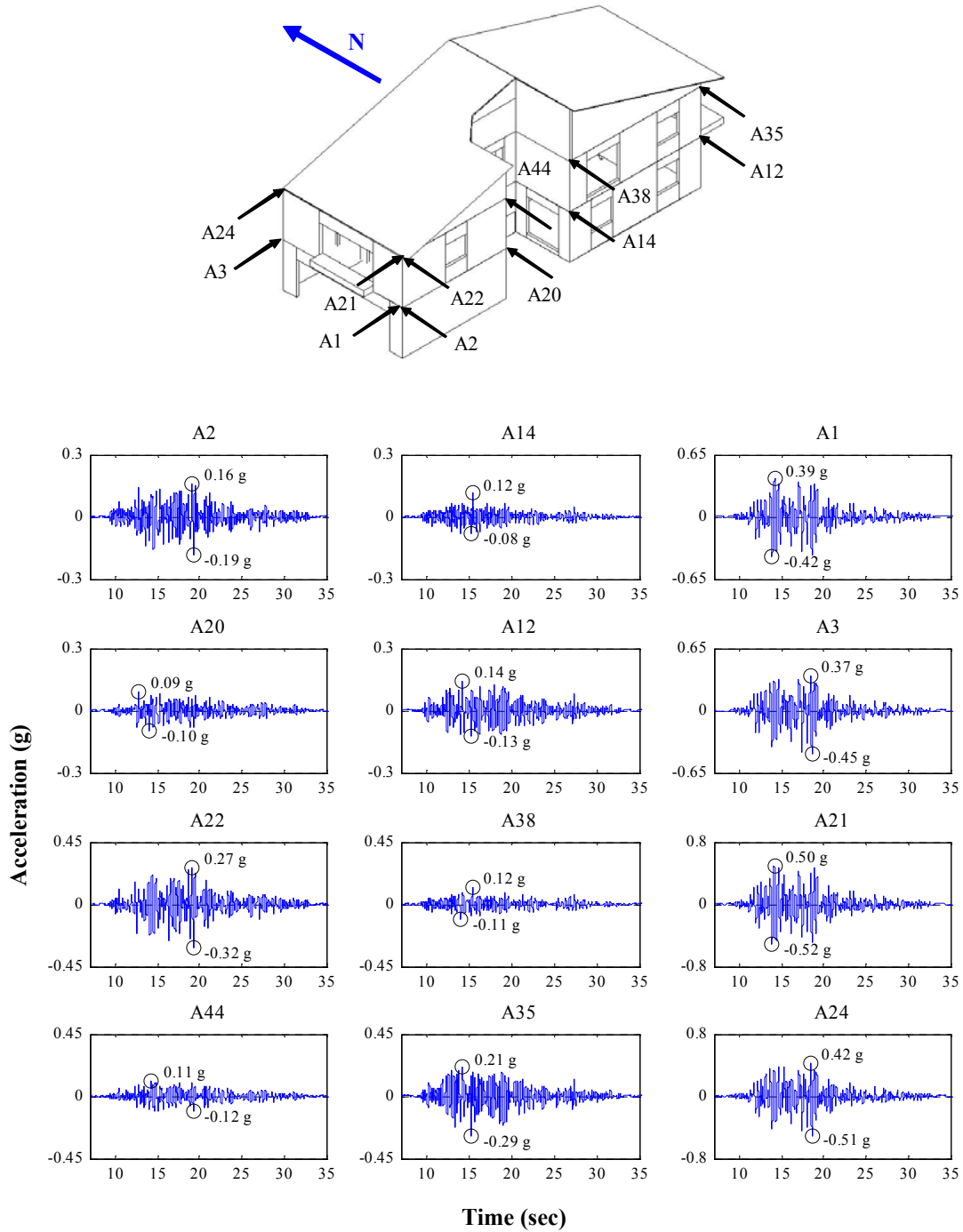


Figure L.20: Absolute acceleration time histories for Test NWP2S11

Appendix L

Phase 2, NWP2S12 Seismic Test

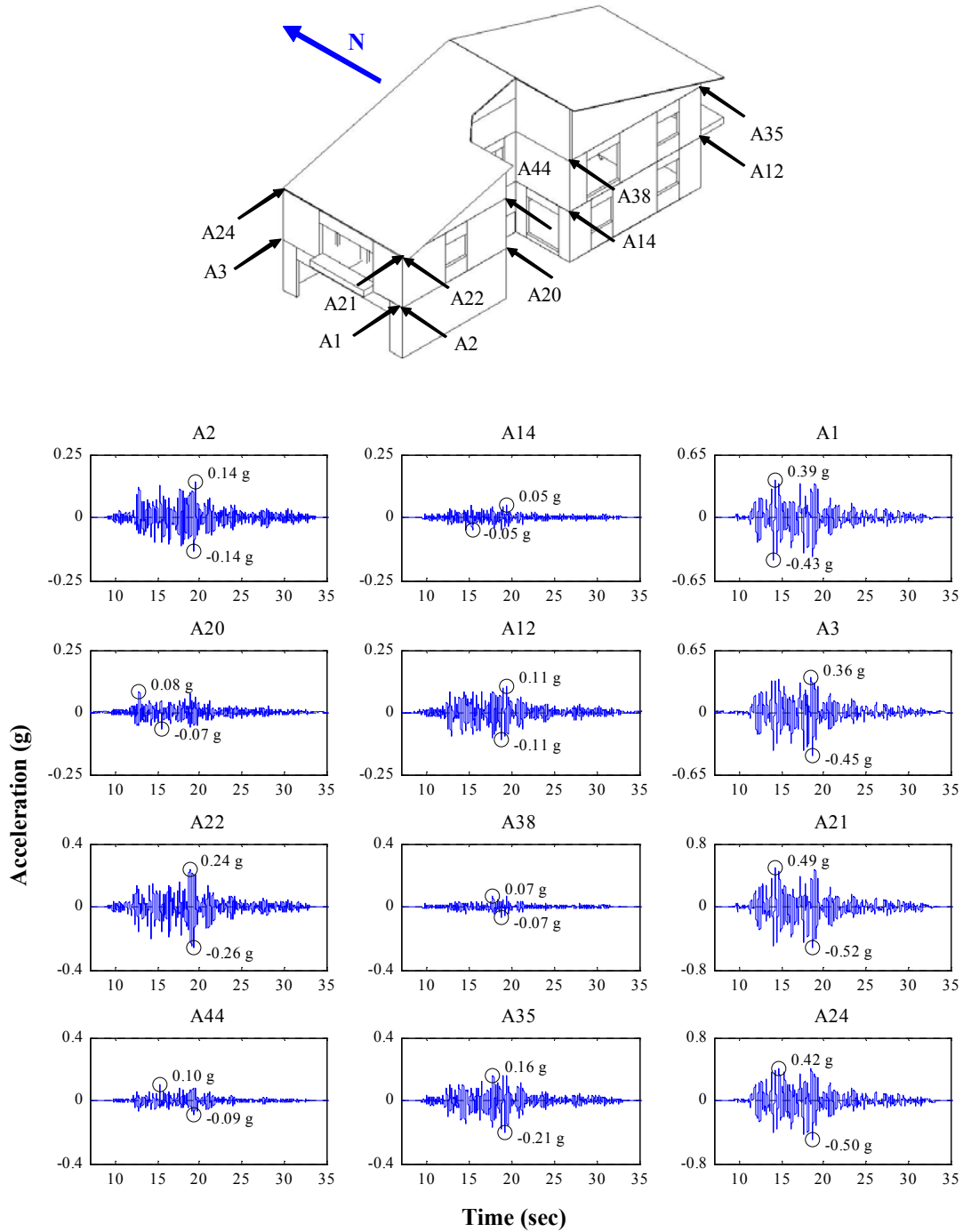


Figure L.21: Absolute acceleration time histories for Test NWP2S12

Appendix L

Phase 2, NWP2S13 Seismic Test

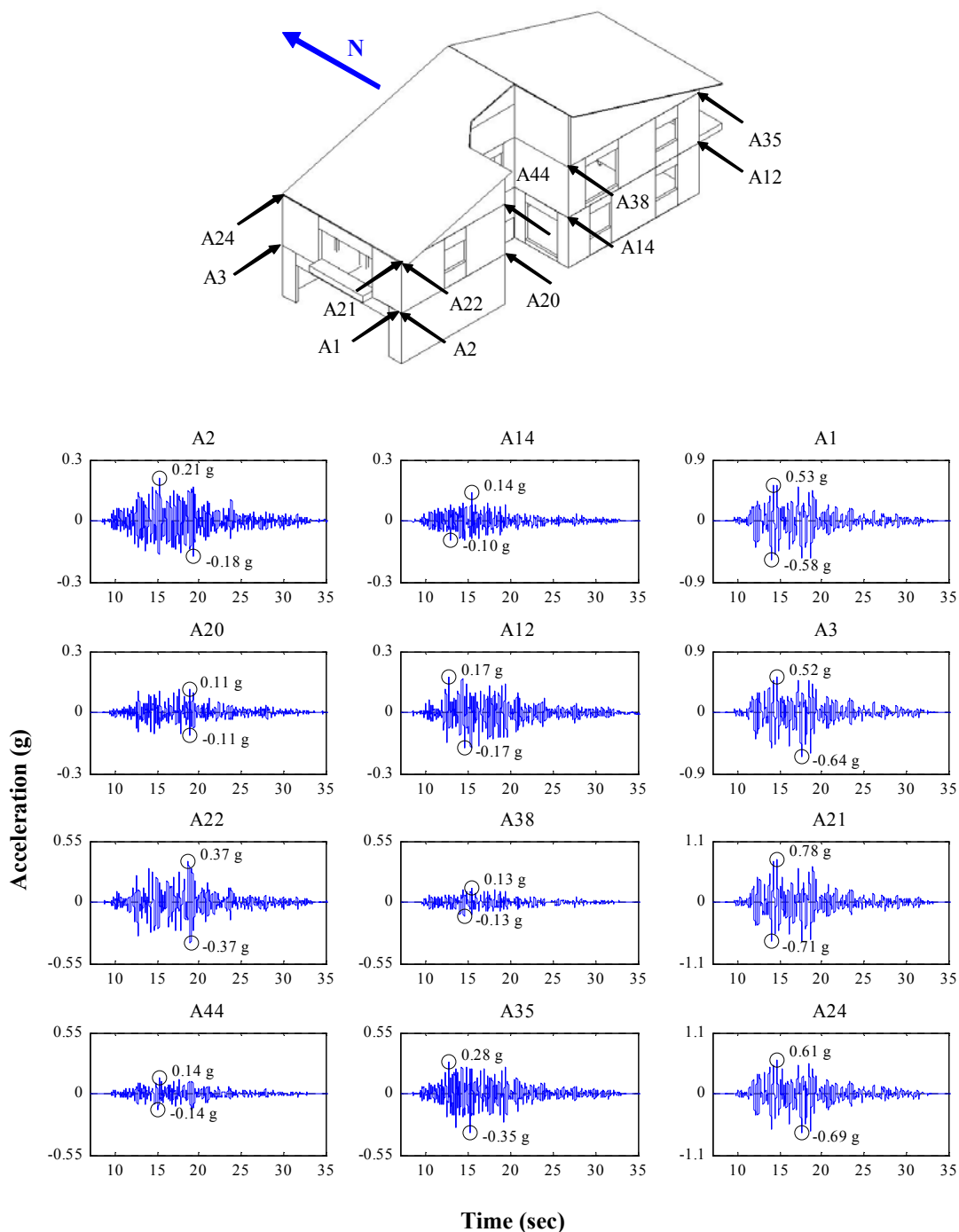


Figure L.22: Absolute acceleration time histories for Test NWP2S13

Appendix L

Phase 2, NWP2S14 Seismic Test

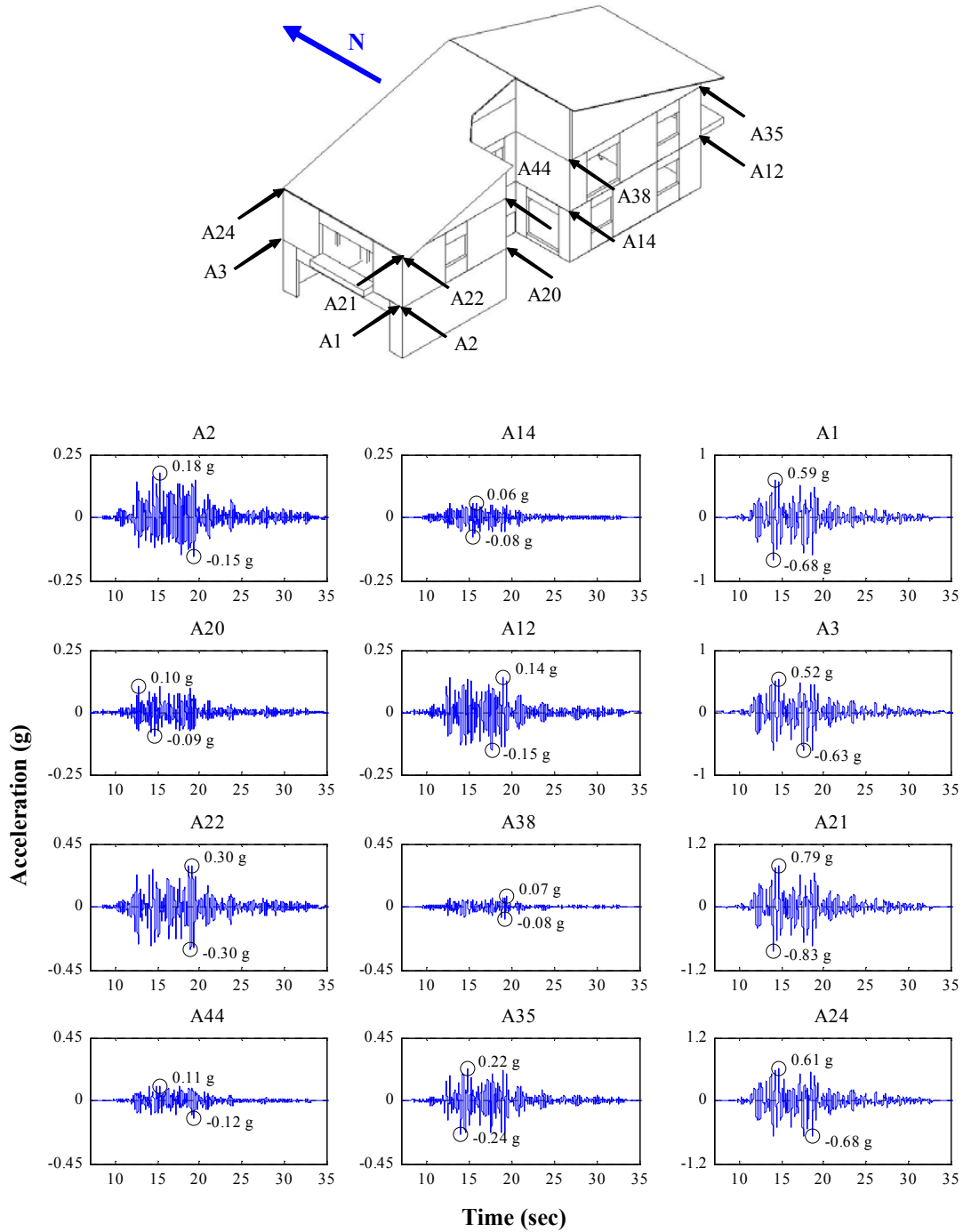


Figure L.23: Absolute acceleration time histories for Test NWP2S14

Appendix L

Phase 2, NWP2S16 Seismic Test

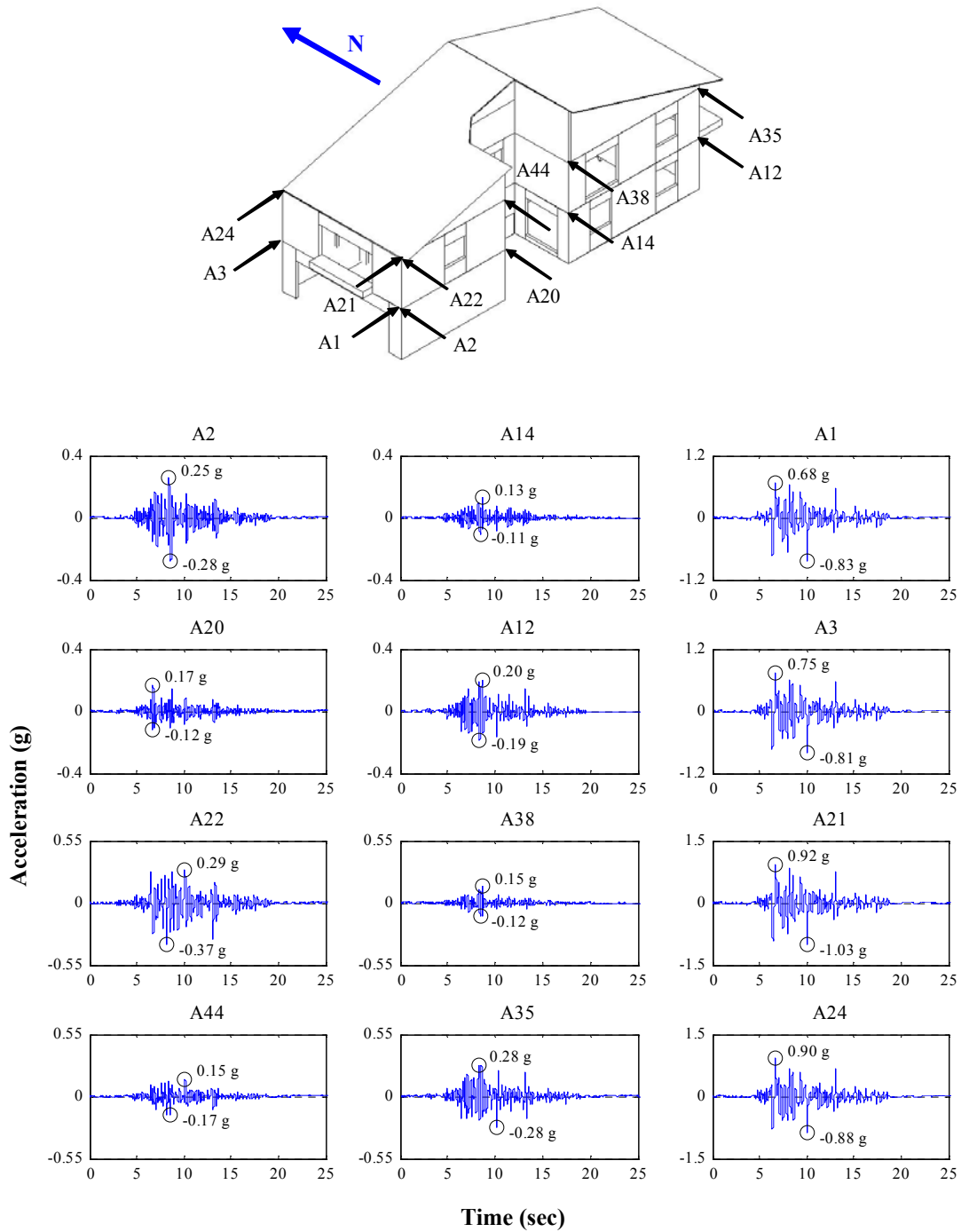


Figure L.24: Absolute acceleration time histories for Test NWP2S16

Appendix L

Phase 2, NWP2S17 Seismic Test

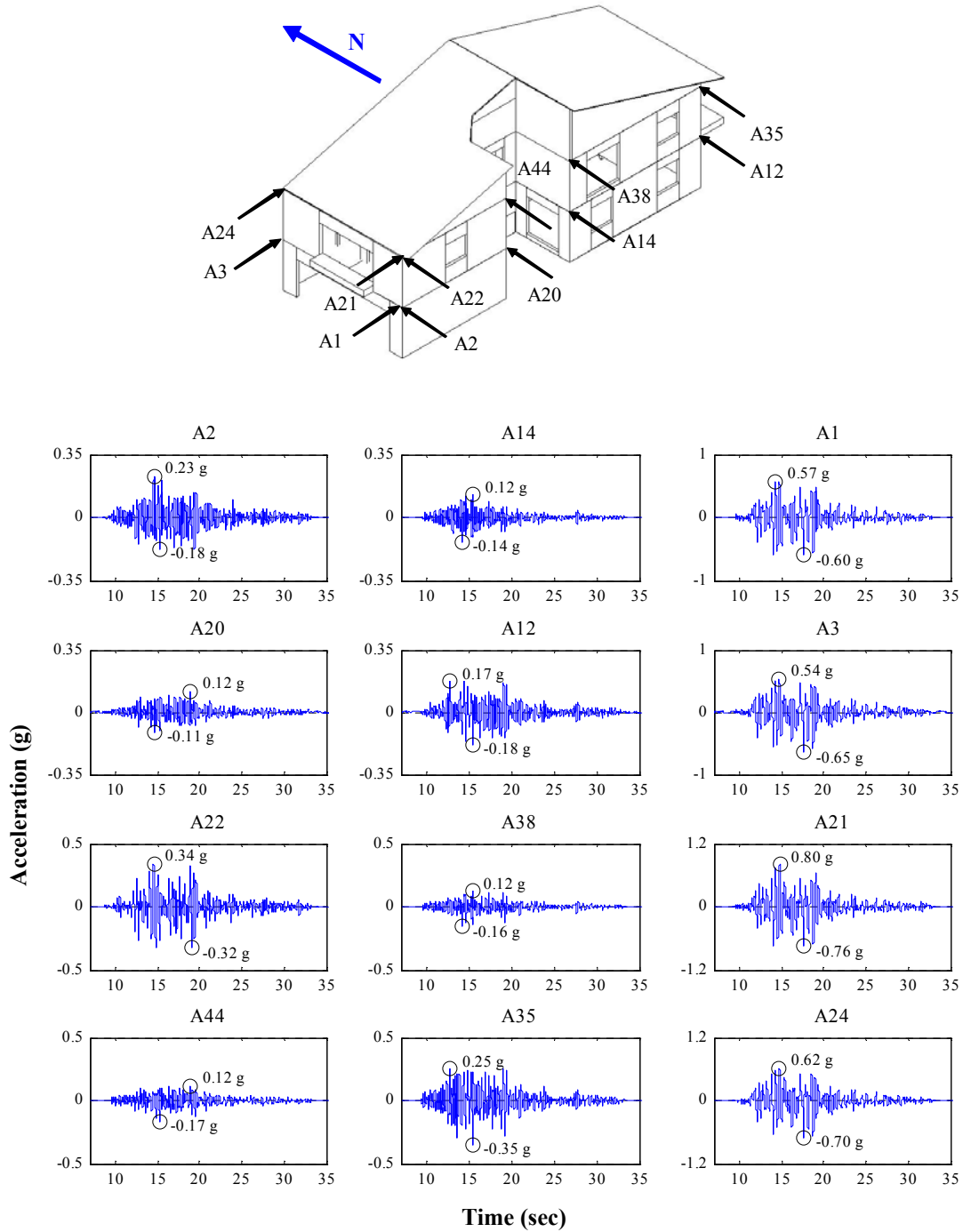


Figure L.25: Absolute acceleration time histories for Test NWP2S17

Appendix L

Phase 2, NWP2S21 Seismic Test

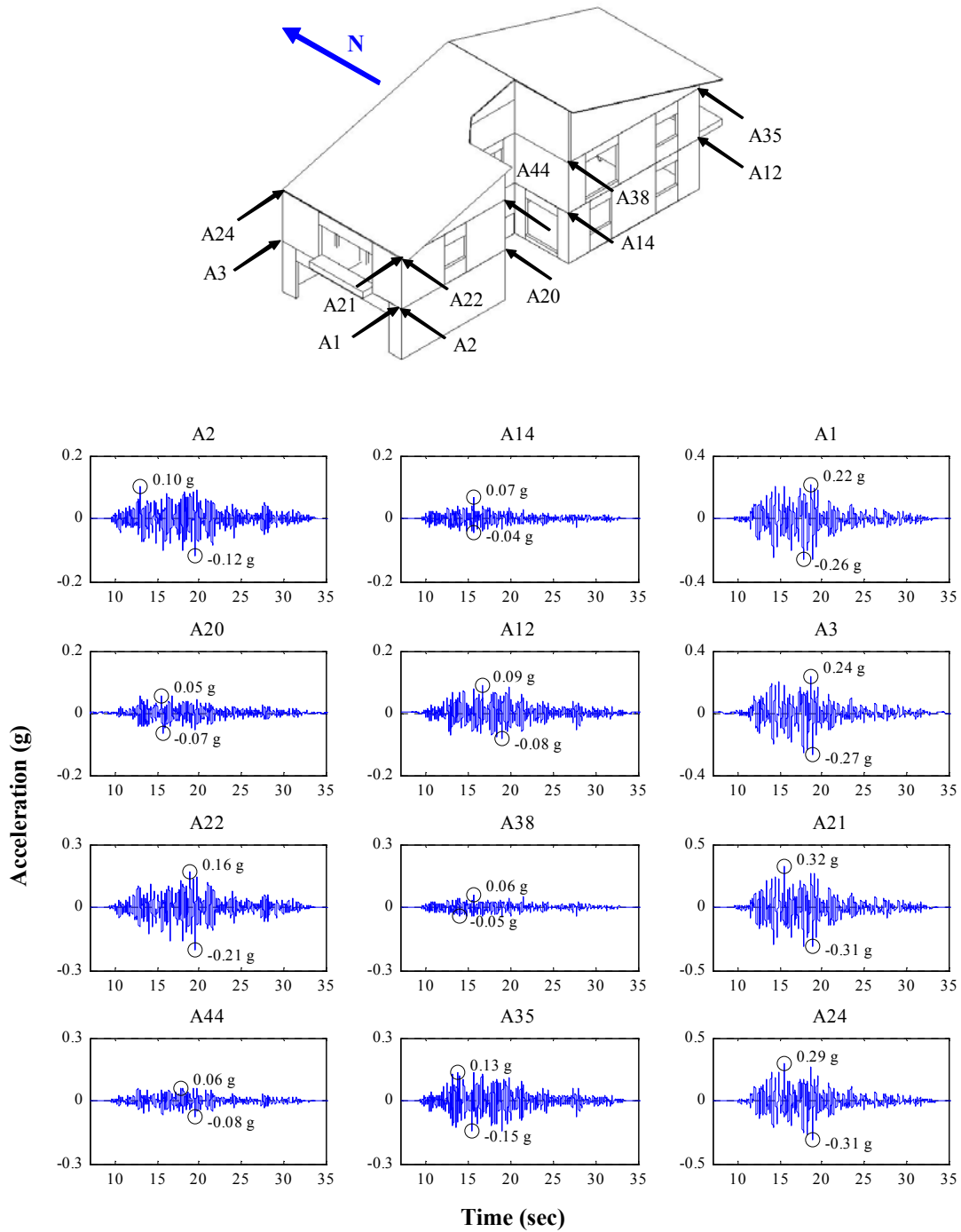


Figure L.26: Absolute acceleration time histories for Test NWP2S21

Appendix L

Phase 2, NWP2S24 Seismic Test

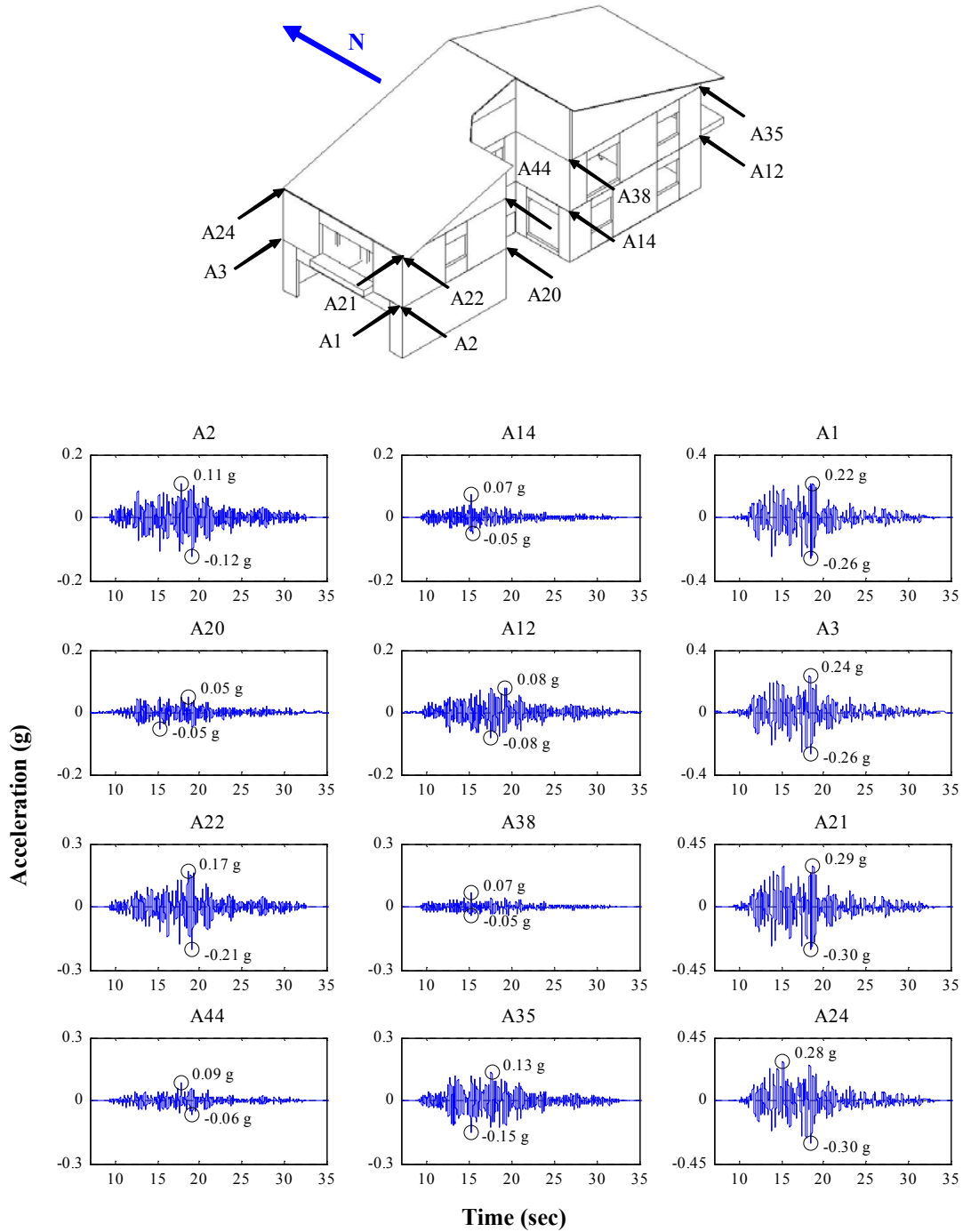


Figure L.27: Absolute acceleration time histories for Test NWP2S24

Appendix L

Phase 2, NWP2S25 Seismic Test

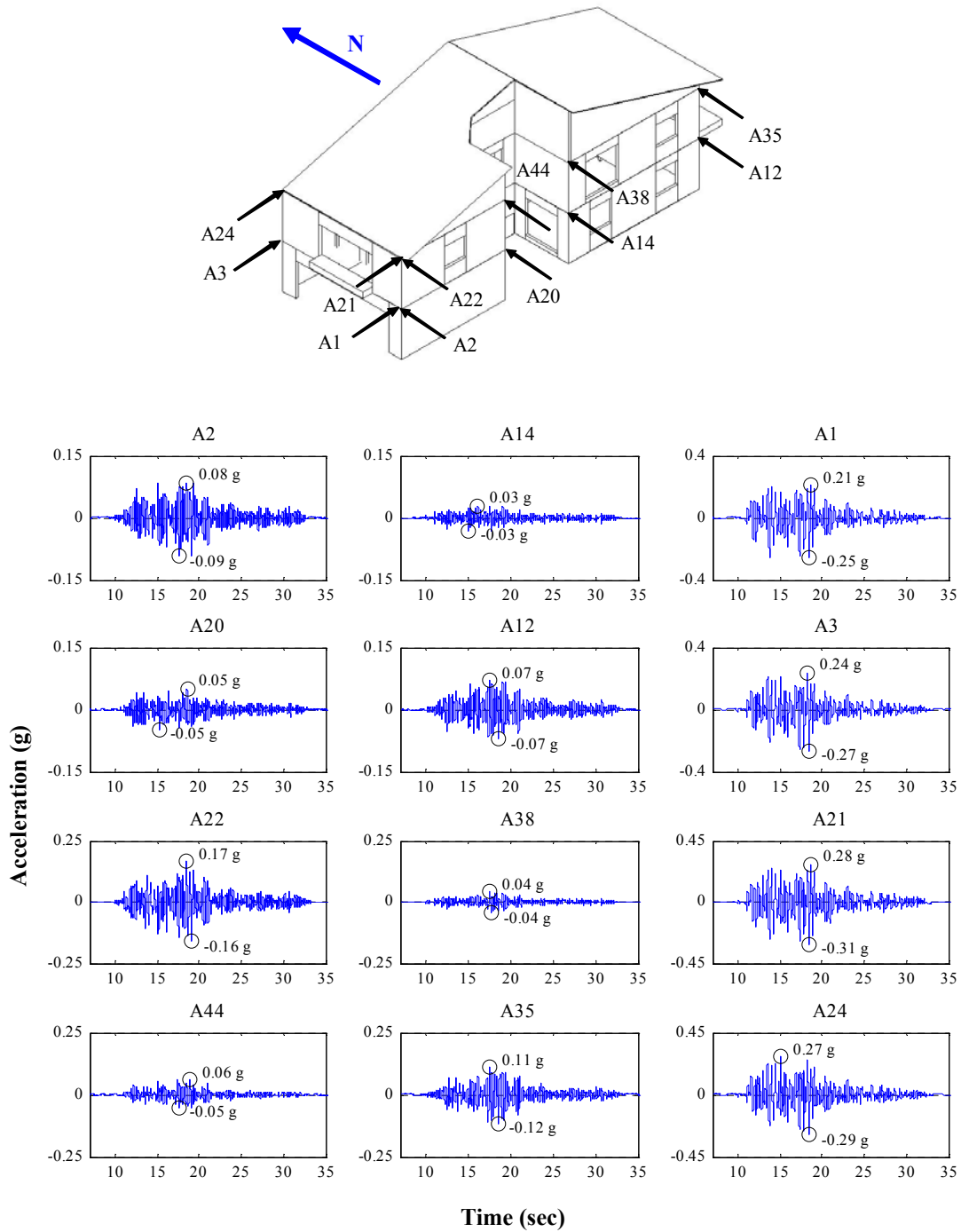


Figure L.28: Absolute acceleration time histories for Test NWP2S25

Appendix L

Phase 2, NWP2S26 Seismic Test

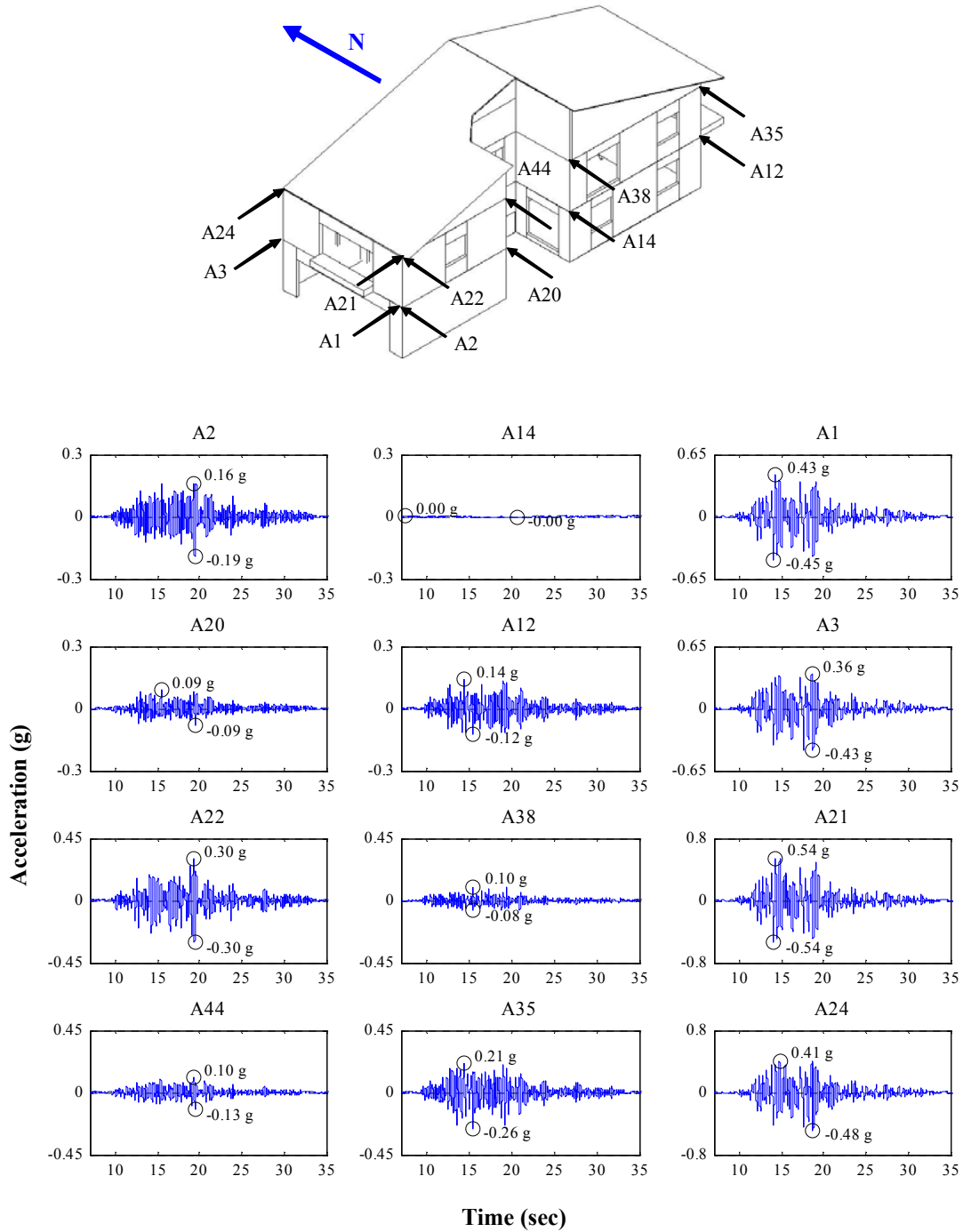


Figure L.29: Absolute acceleration time histories for Test NWP2S26

Appendix L

Phase 2, NWP2S27 Seismic Test

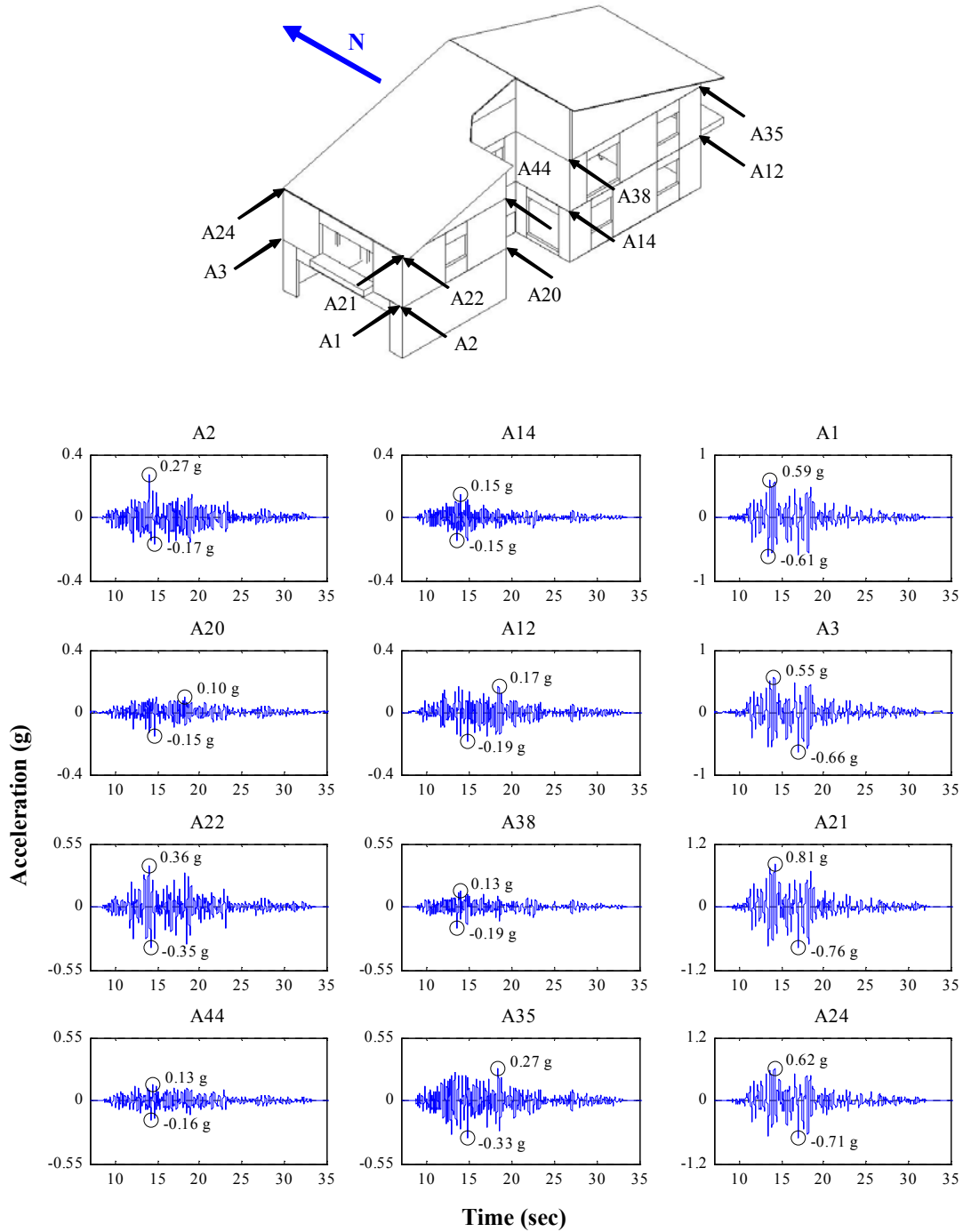


Figure L.30: Absolute acceleration time histories for Test NWP2S27

Appendix L

Phase 2, NWP2S28 Seismic Test

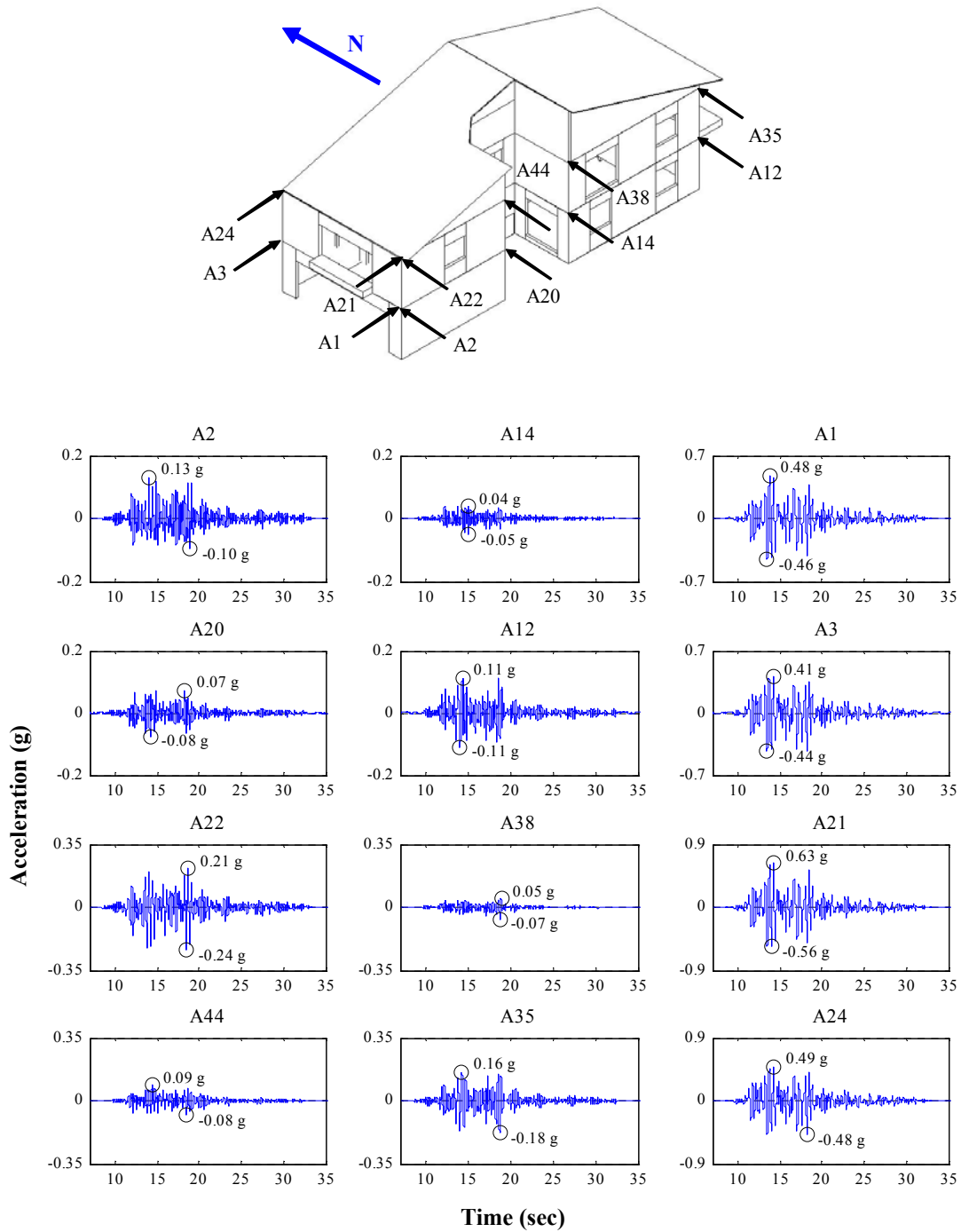


Figure L.31: Absolute acceleration time histories for Test NWP2S28

Appendix L

Phase 2, NWP2S29 Seismic Test

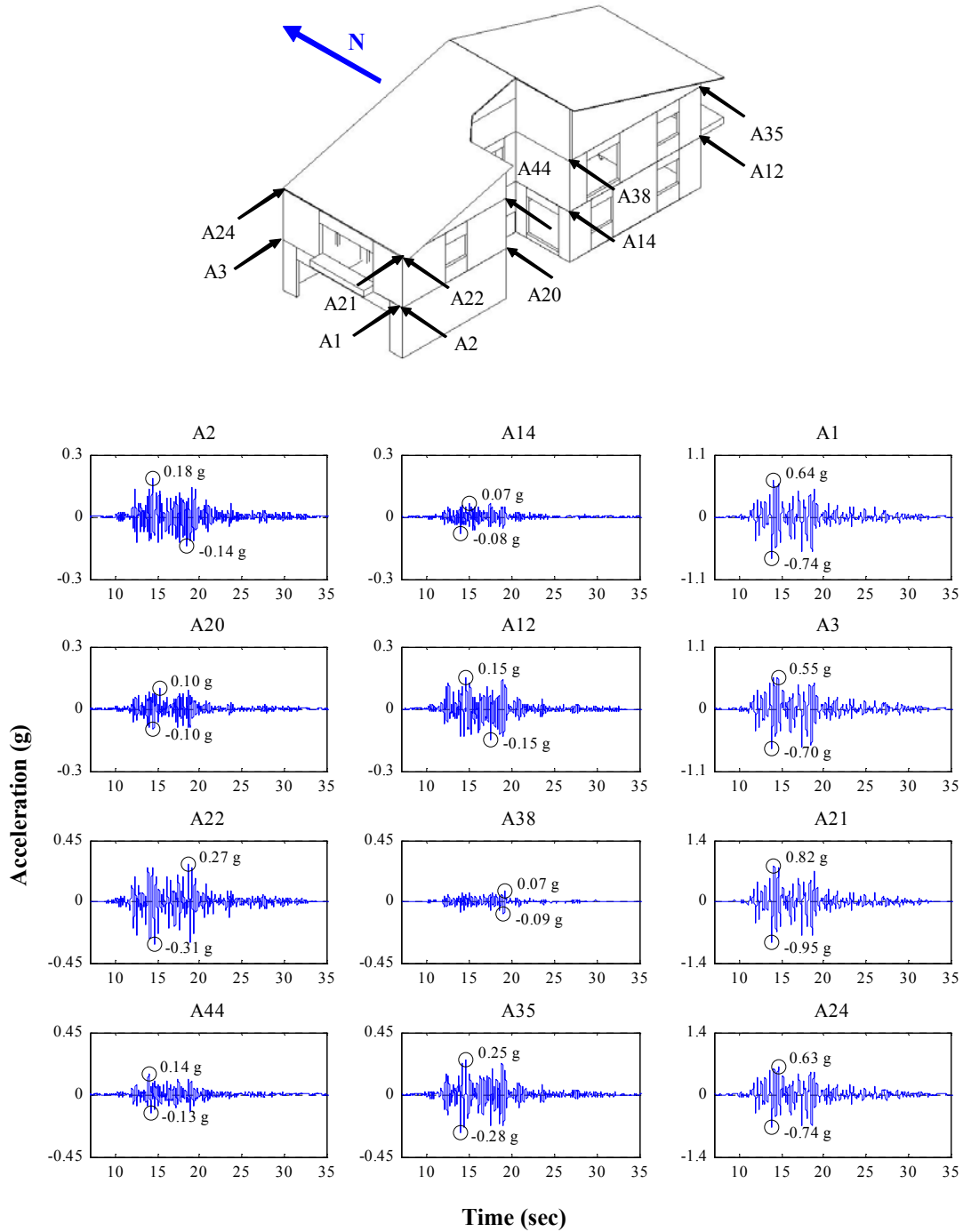


Figure L.32: Absolute acceleration time histories for Test NWP2S29

Appendix L

Phase 2, NWP2S30 Seismic Test

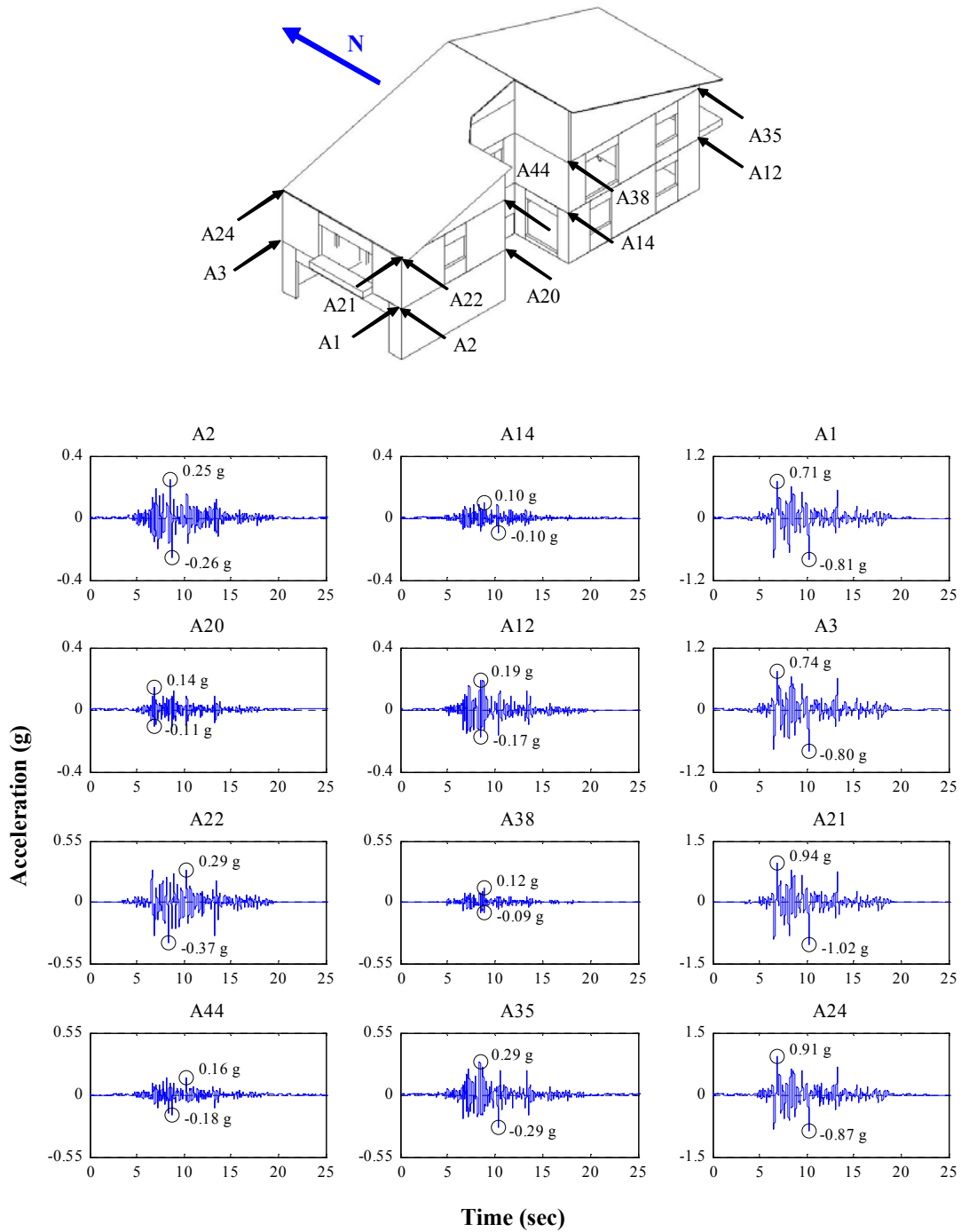


Figure L.33: Absolute acceleration time histories for Test NWP2S30

Appendix L

Phase 3, NWP3S01 Seismic Test

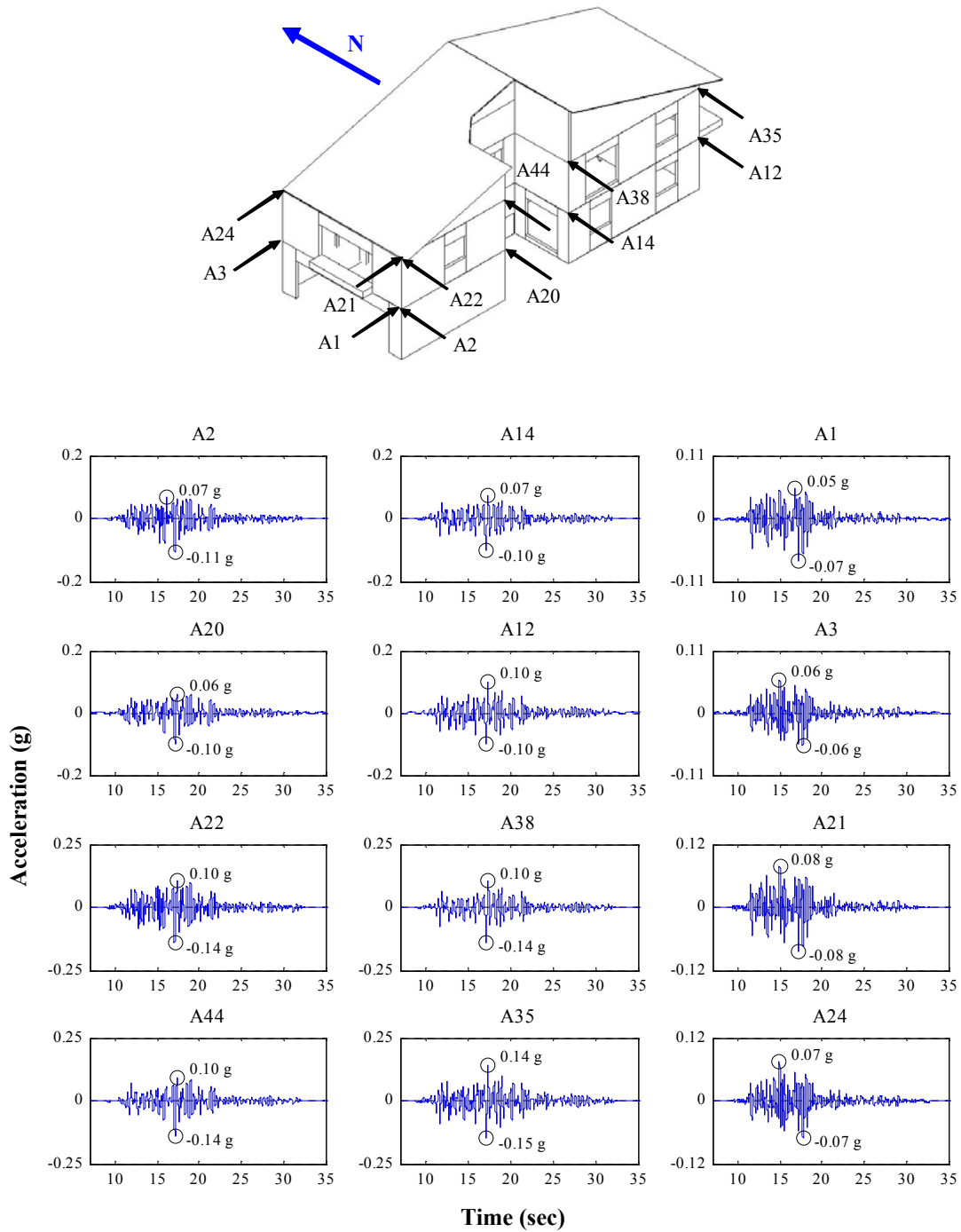


Figure L.34: Absolute acceleration time histories for Test NWP3S01

Appendix L

Phase 3, NWP3S02 Seismic Test

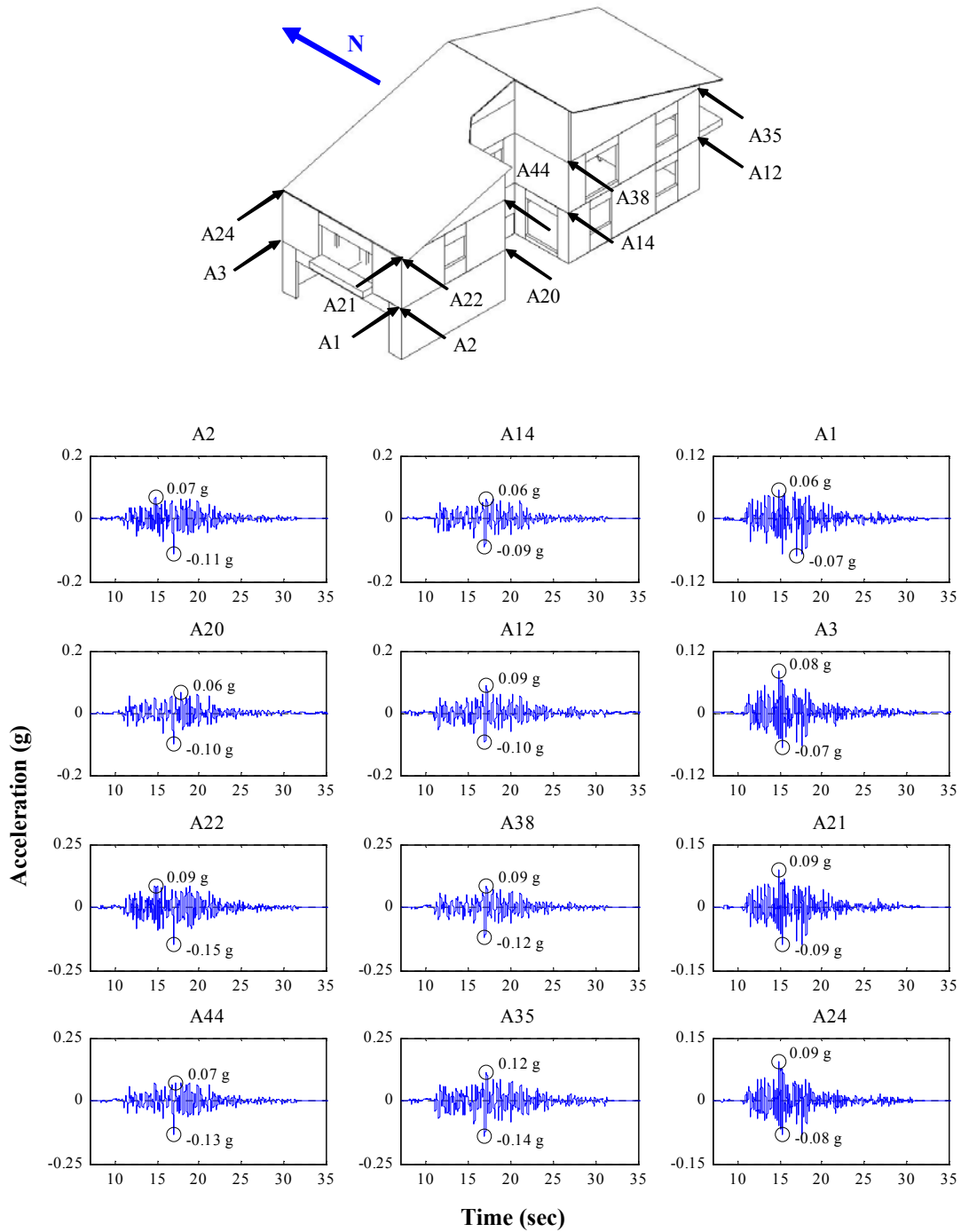


Figure L.35: Absolute acceleration time histories for Test NWP3S02

Appendix L

Phase 3, NWP3S03 Seismic Test

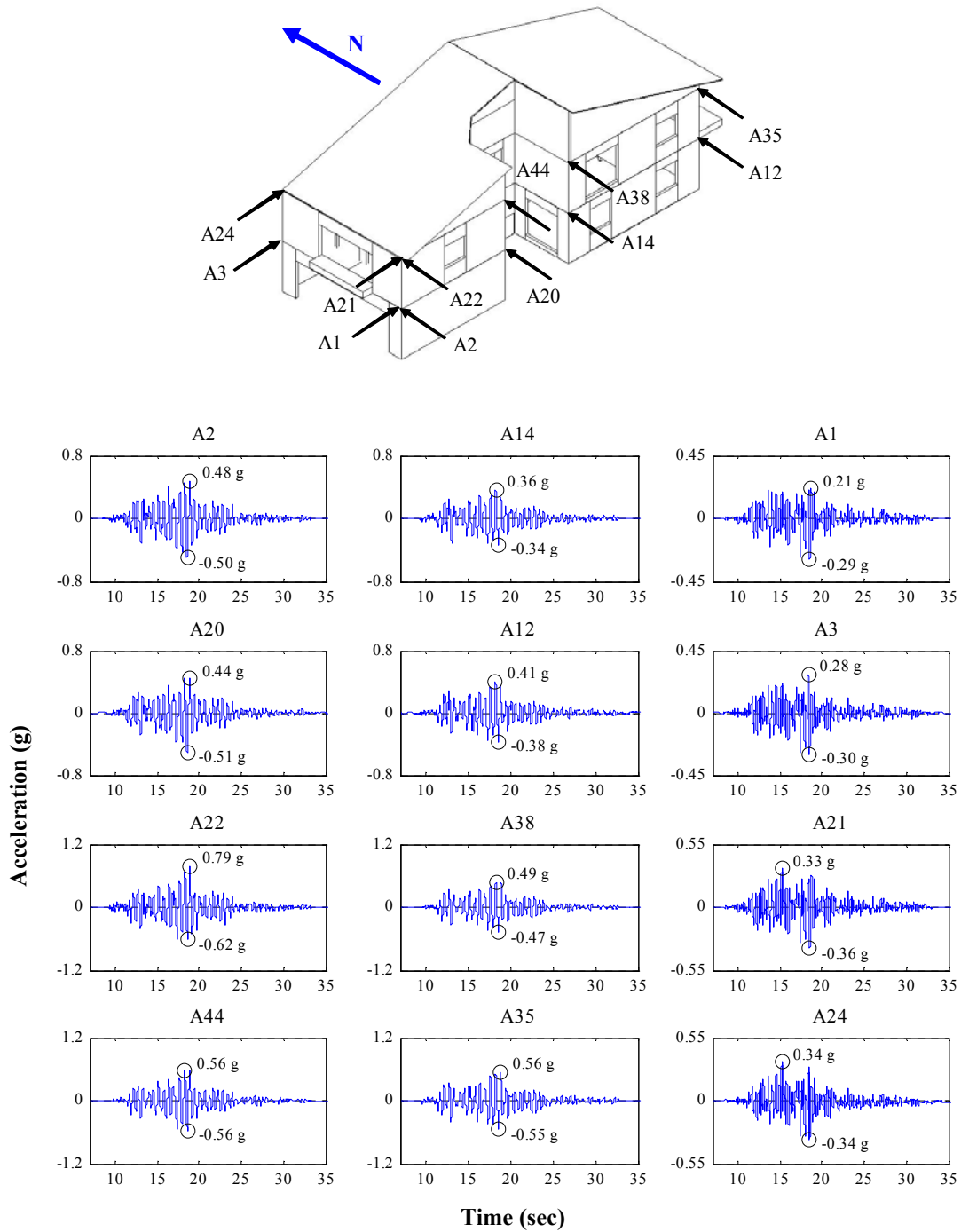


Figure L.36: Absolute acceleration time histories for Test NWP3S03

Appendix L

Phase 3, NWP3S04 Seismic Test

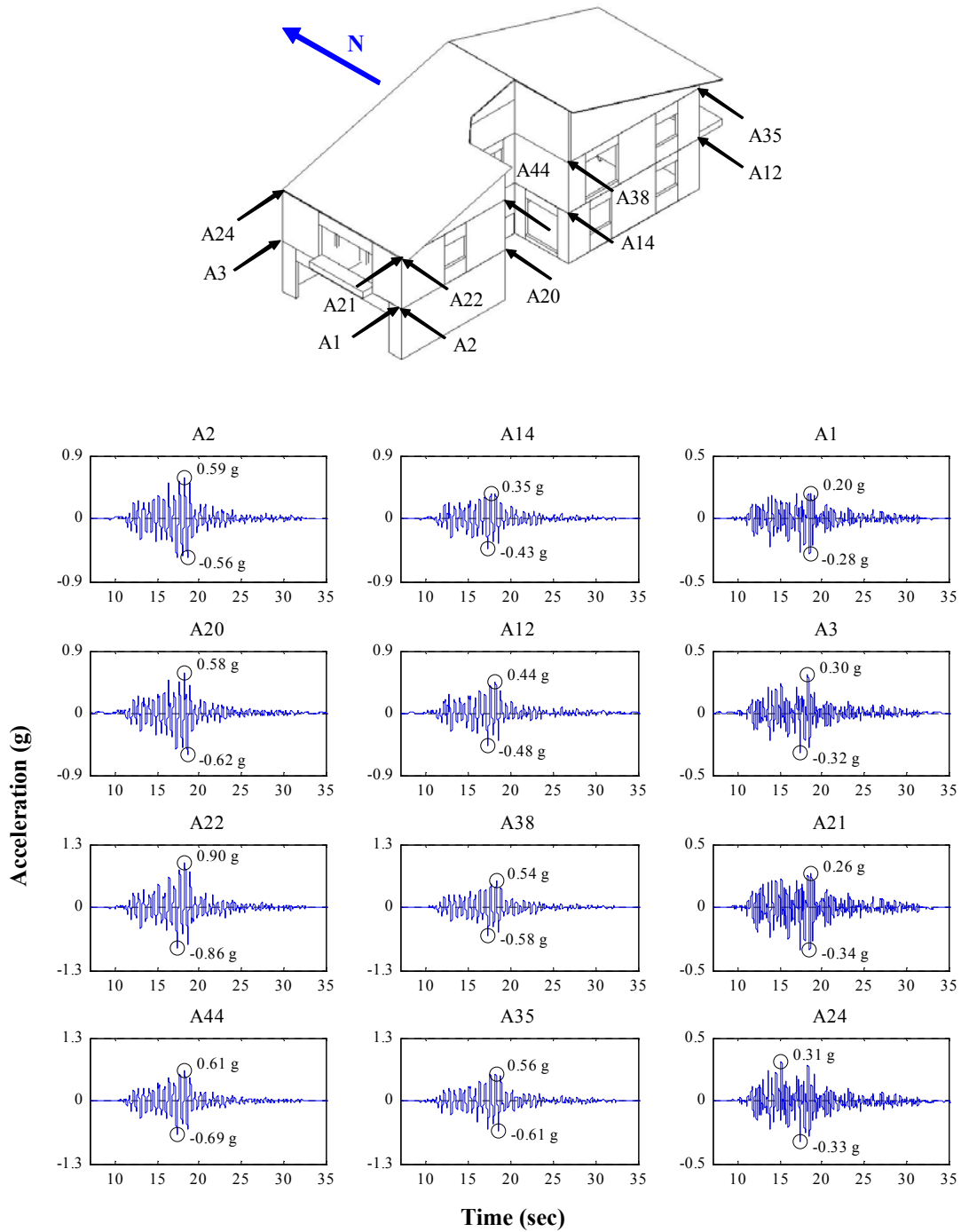


Figure L.37: Absolute acceleration time histories for Test NWP3S04

Appendix L

Phase 4, NWP4S01 Seismic Test

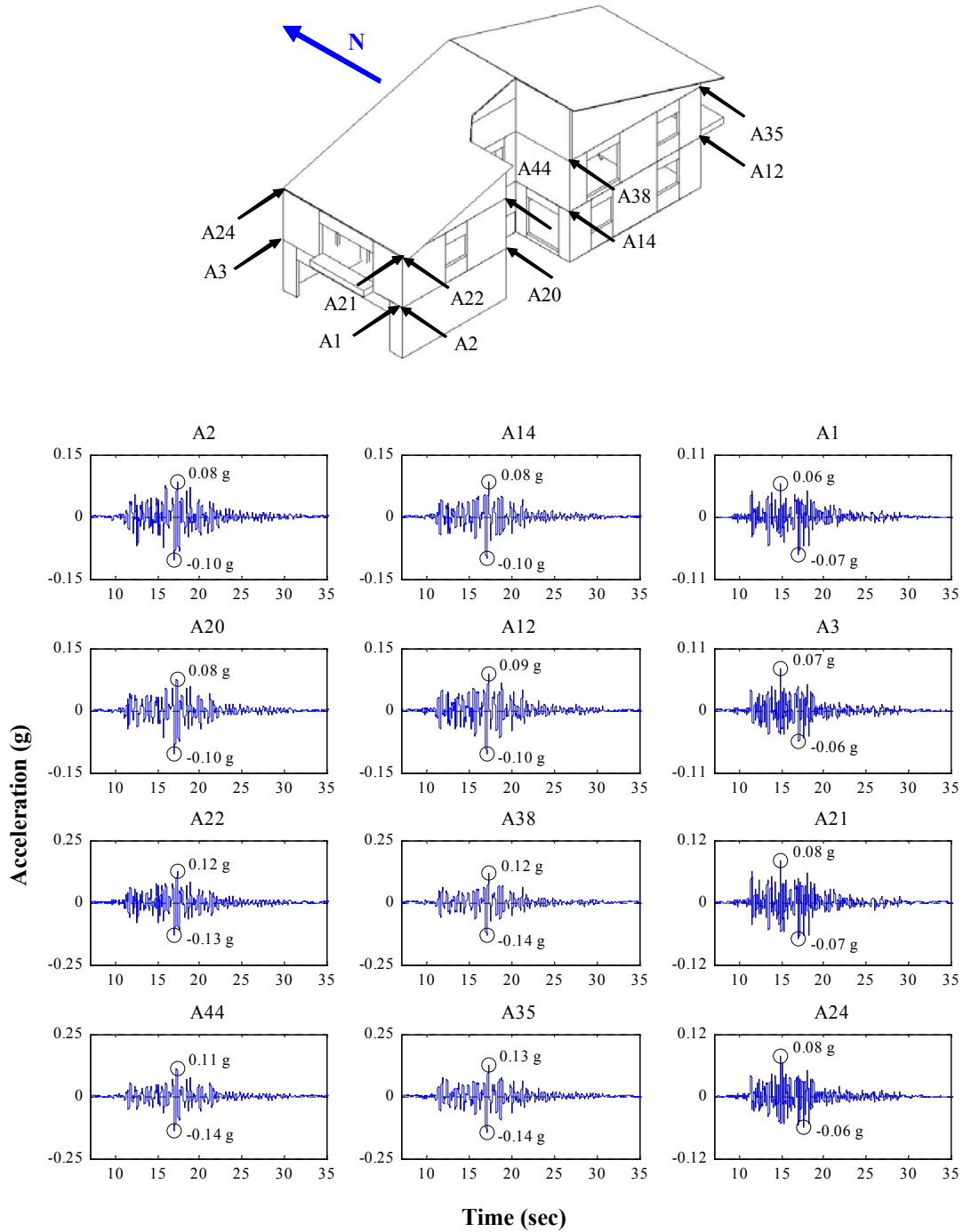


Figure L.38: Absolute acceleration time histories for Test NWP4S01

Appendix L

Phase 4, NWP4S02 Seismic Test

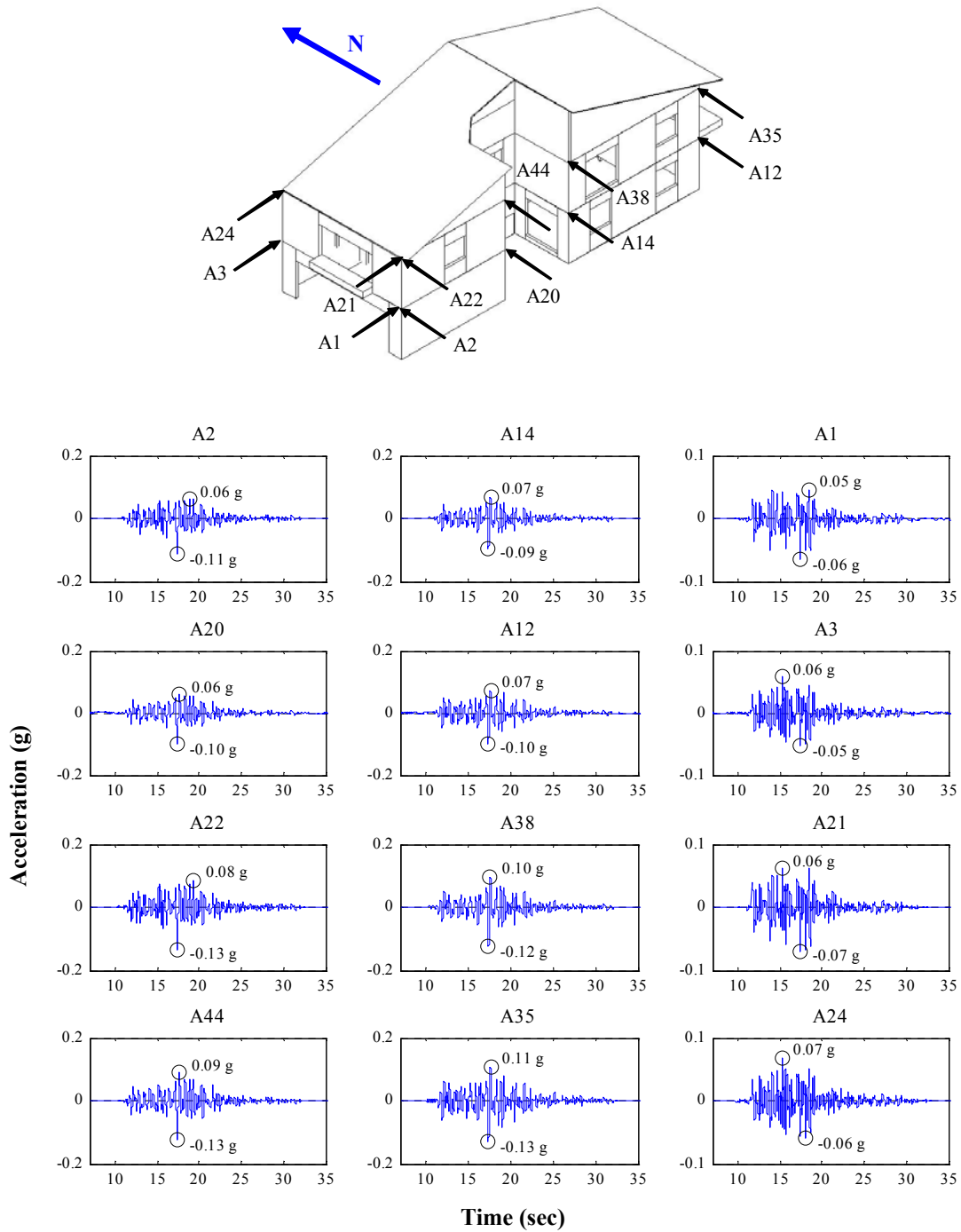


Figure L.39: Absolute acceleration time histories for Test NWP4S02

Appendix L

Phase 4, NWP4S03 Seismic Test

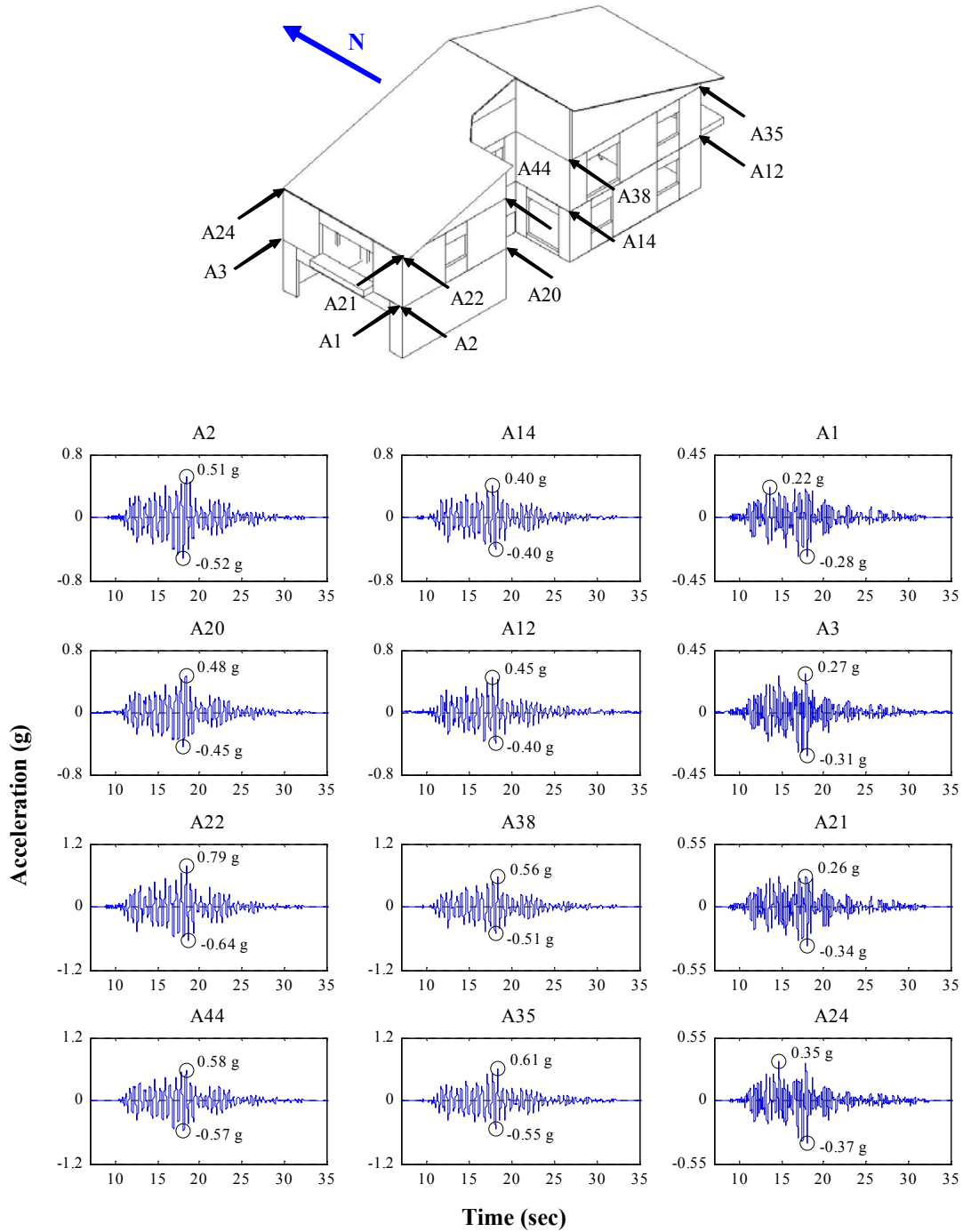


Figure L.40: Absolute acceleration time histories for Test NWP4S03

Appendix L

Phase 4, NWP4S04 Seismic Test

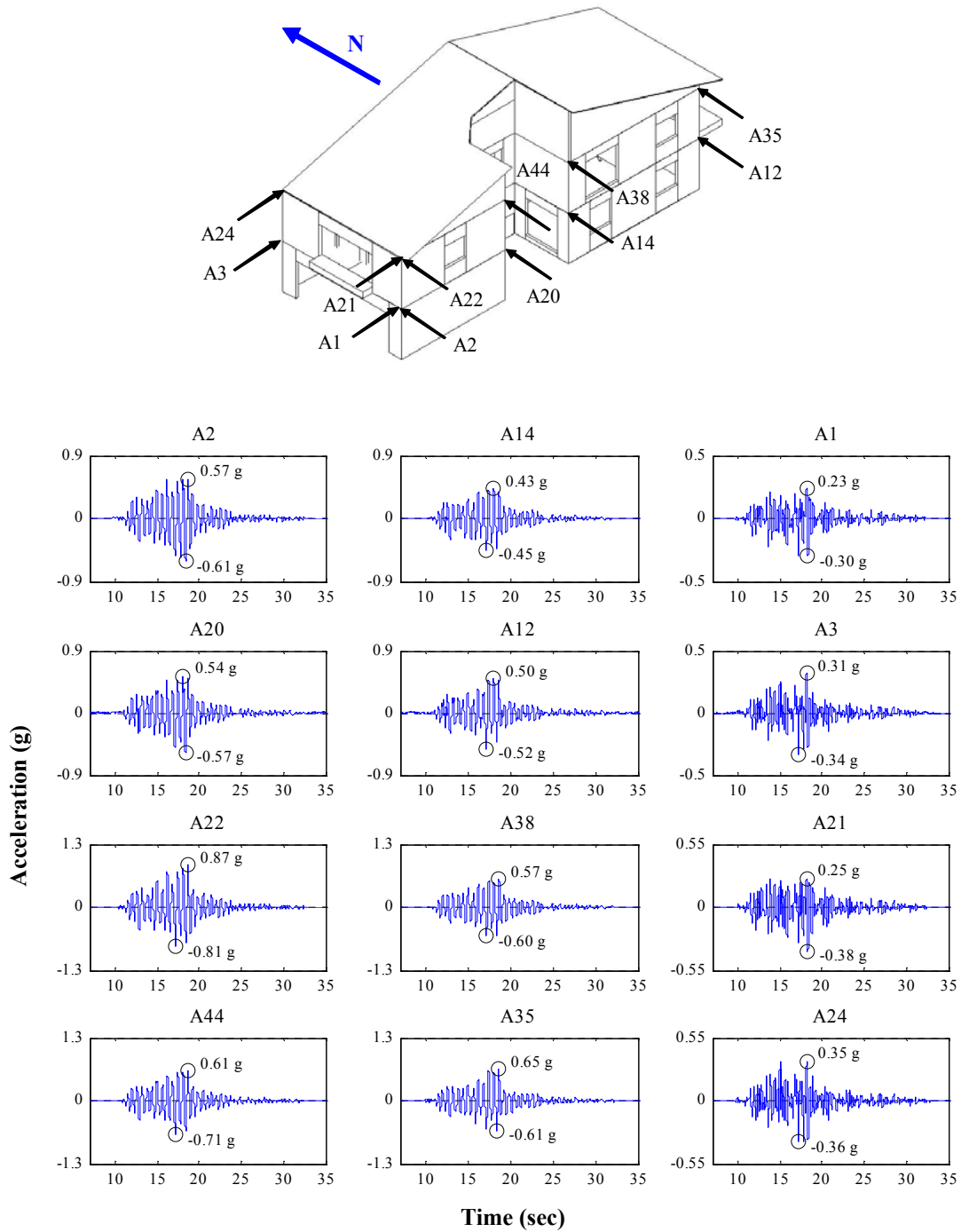


Figure L.41: Absolute acceleration time histories for Test NWP4S04

Appendix L

Phase 5, NWP5S01 Seismic Test

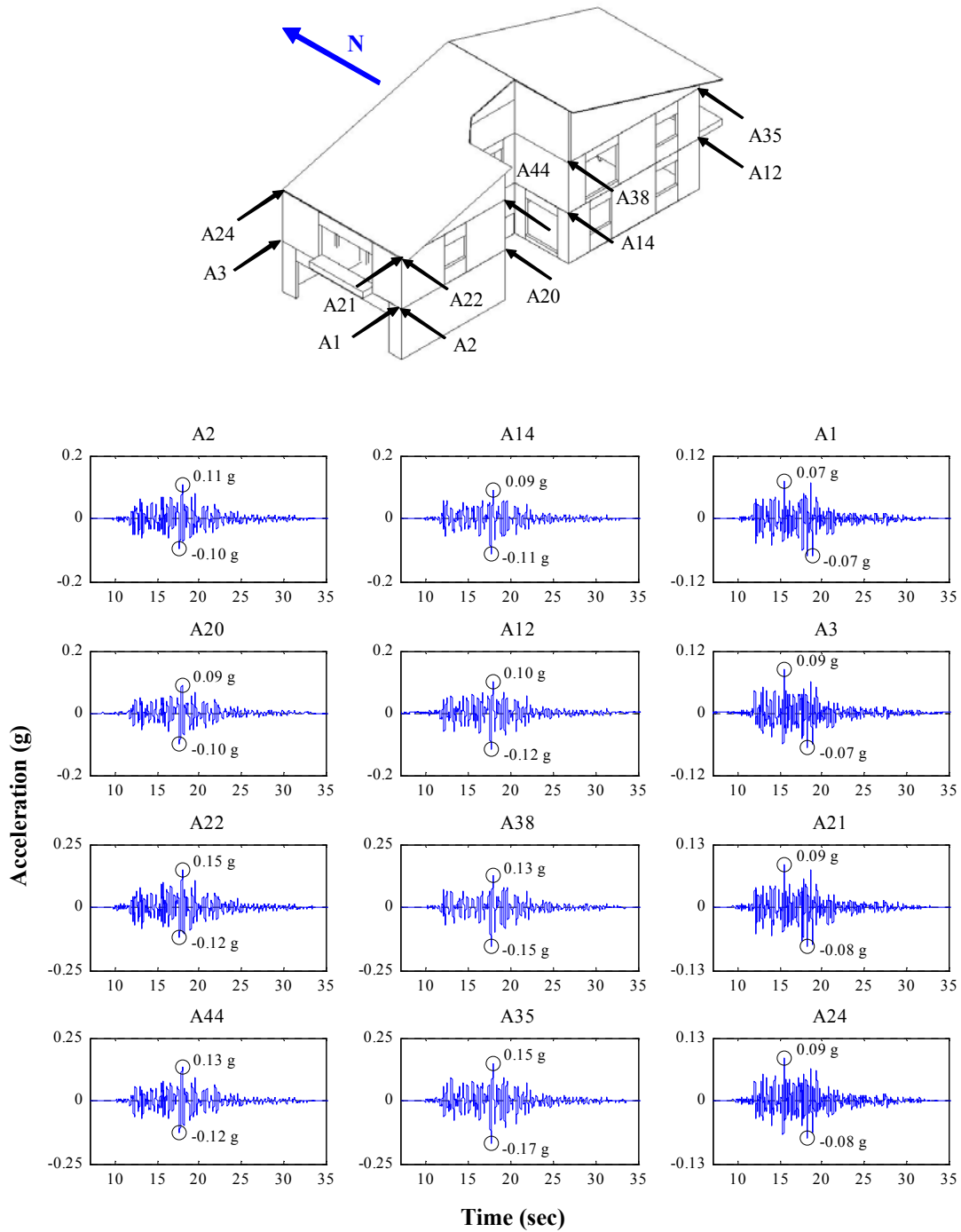


Figure L.42: Absolute acceleration time histories for Test NWP5S01

Appendix L

Phase 5, NWP5S02 Seismic Test

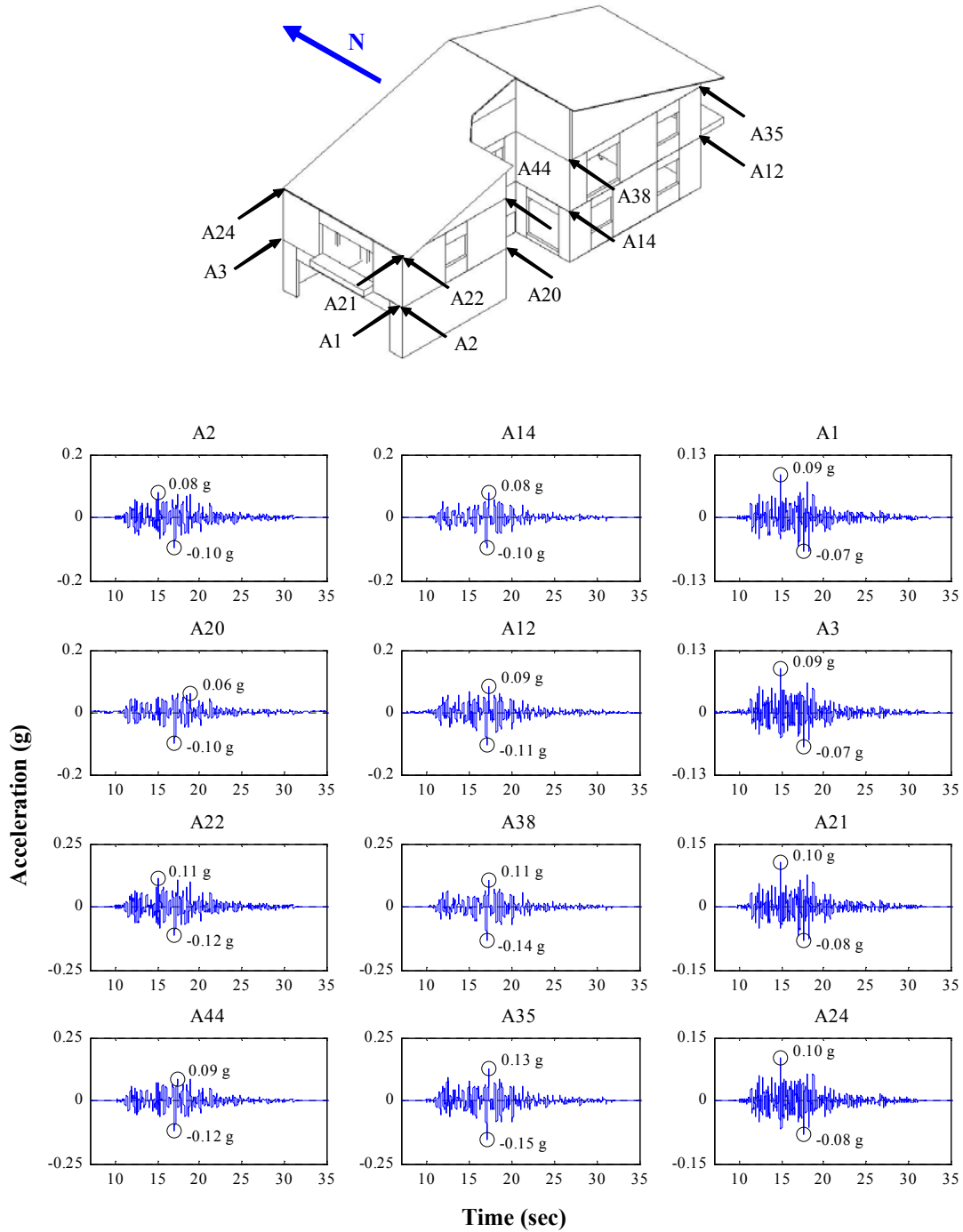


Figure L.43: Absolute acceleration time histories for Test NWP5S02

Appendix L

Phase 5, NWP5S03 Seismic Test

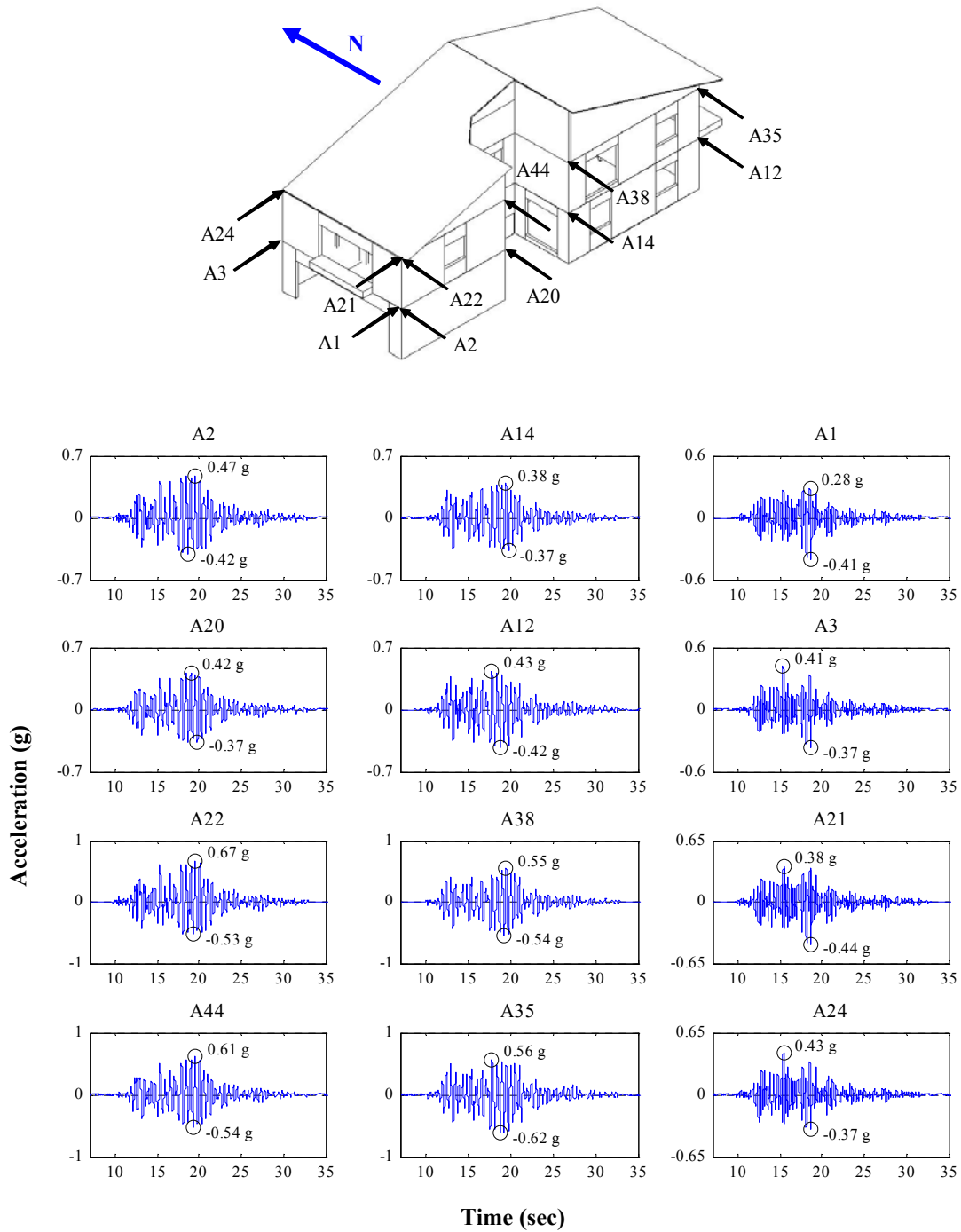


Figure L.44: Absolute acceleration time histories for Test NWP5S03

Appendix L

Phase 5, NWP5S04 Seismic Test

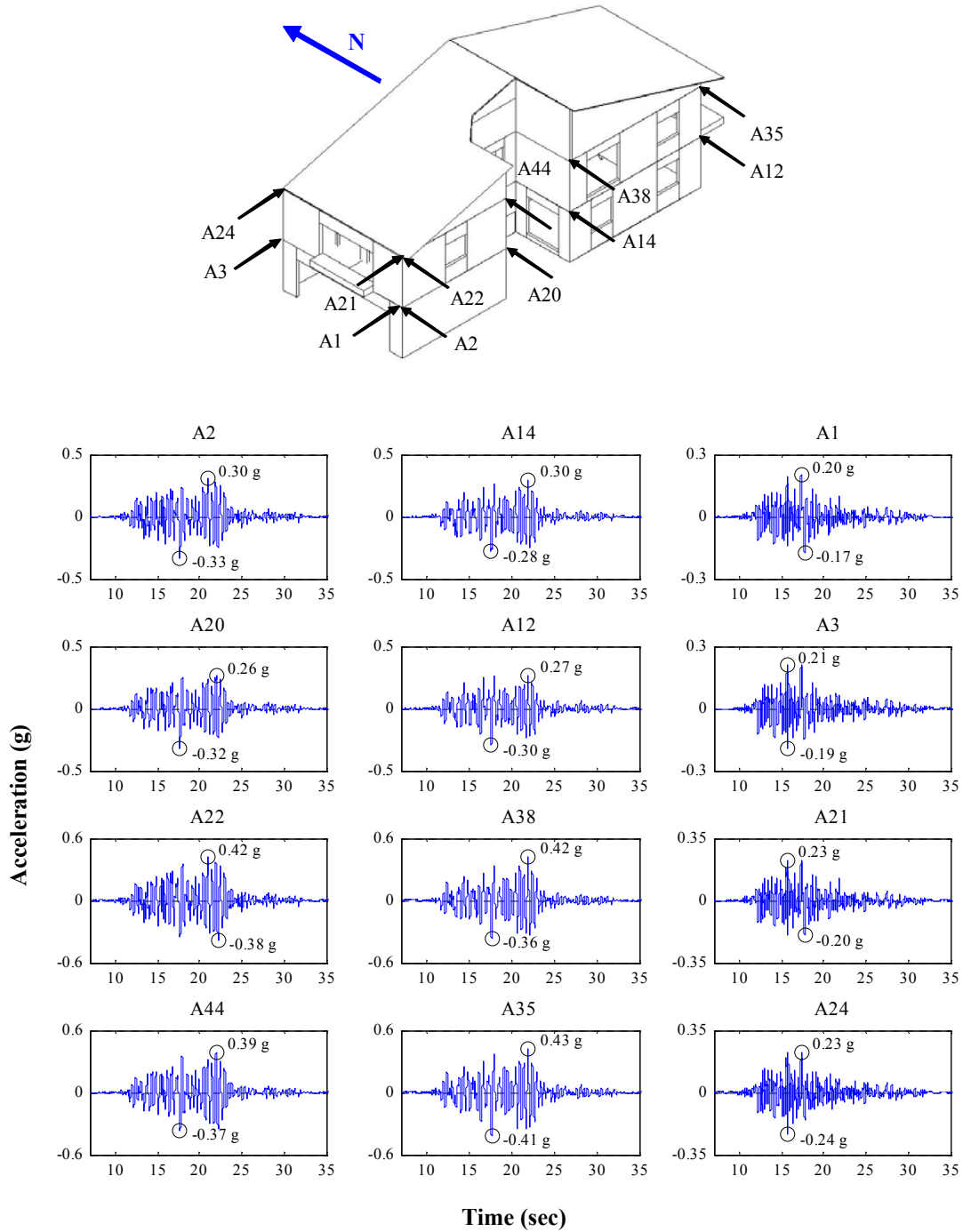


Figure L.45: Absolute acceleration time histories for Test NWP5S04

Appendix L

Phase 5, NWP5S05 Seismic Test

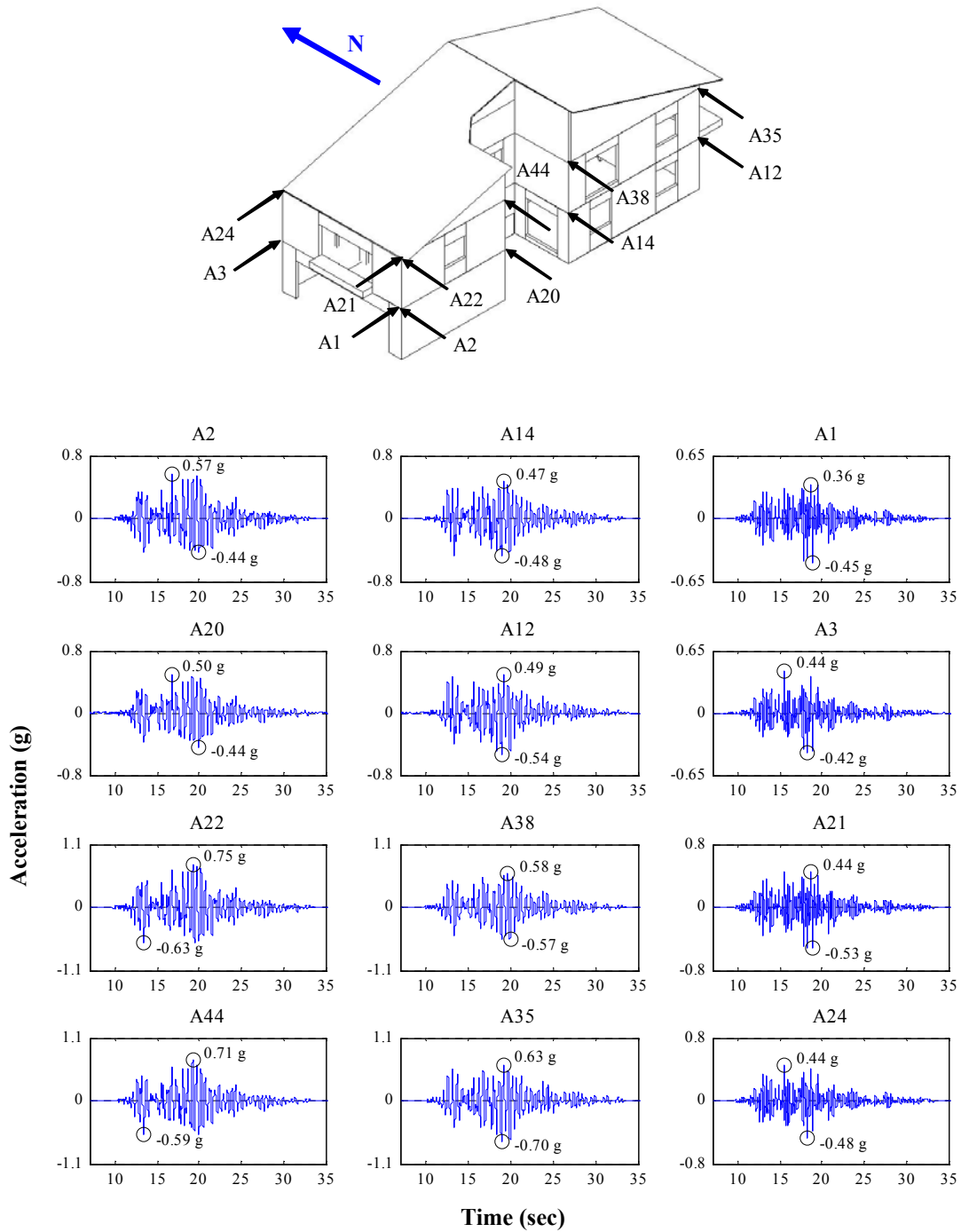


Figure L.46: Absolute acceleration time histories for Test NWP5S05

Appendix L

Phase 5, NWP5S06 Seismic Test

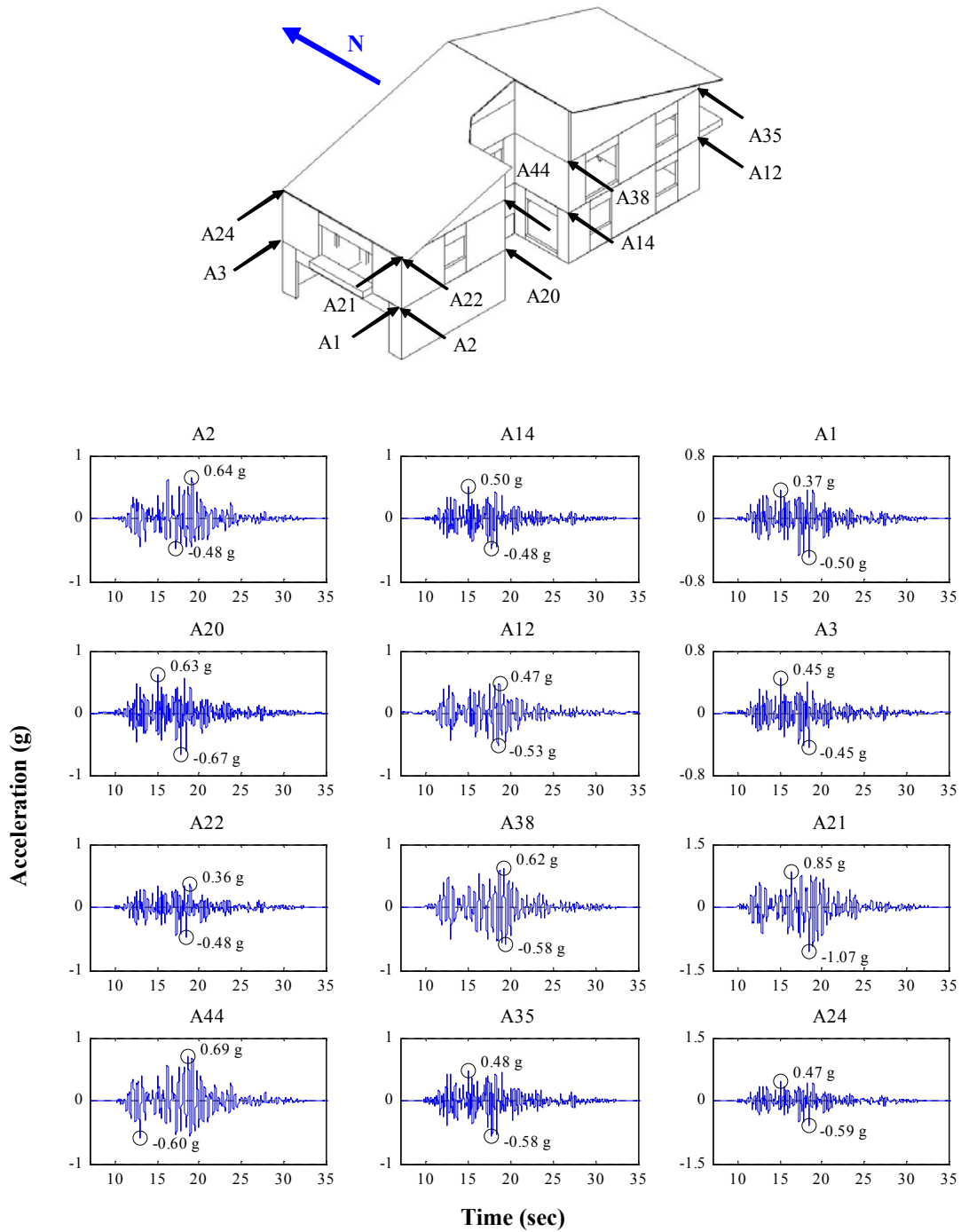


Figure L.47: Absolute acceleration time histories for Test NWP5S06

Appendix L

Phase 5, NWP5S07 Seismic Test

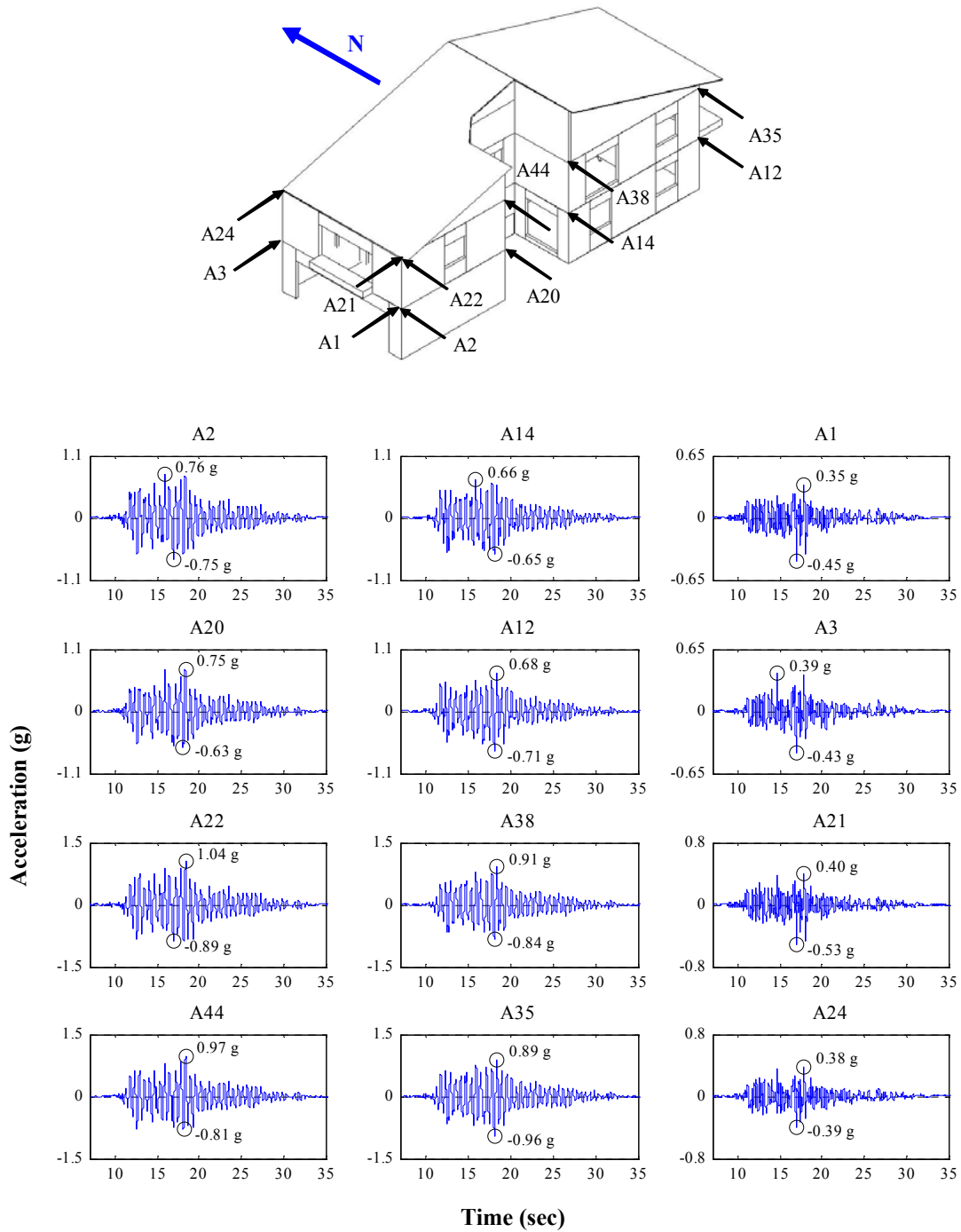


Figure L.48: Absolute acceleration time histories for Test NWP5S07

Appendix L

Phase 5, NWP5S08 Seismic Test

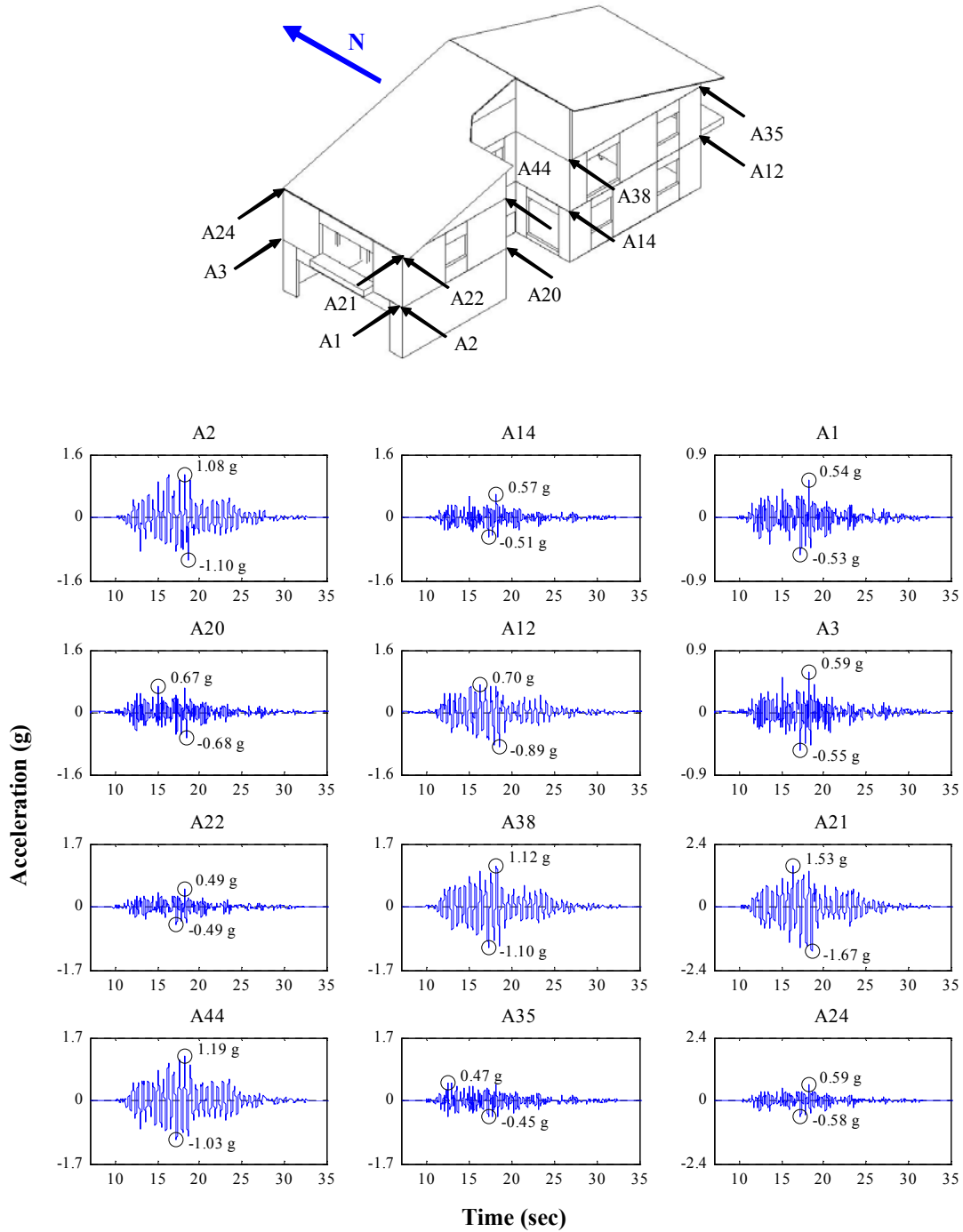


Figure L.49: Absolute acceleration time histories for Test NWP5S08

Appendix L

Phase 5, NWP5S09 Seismic Test

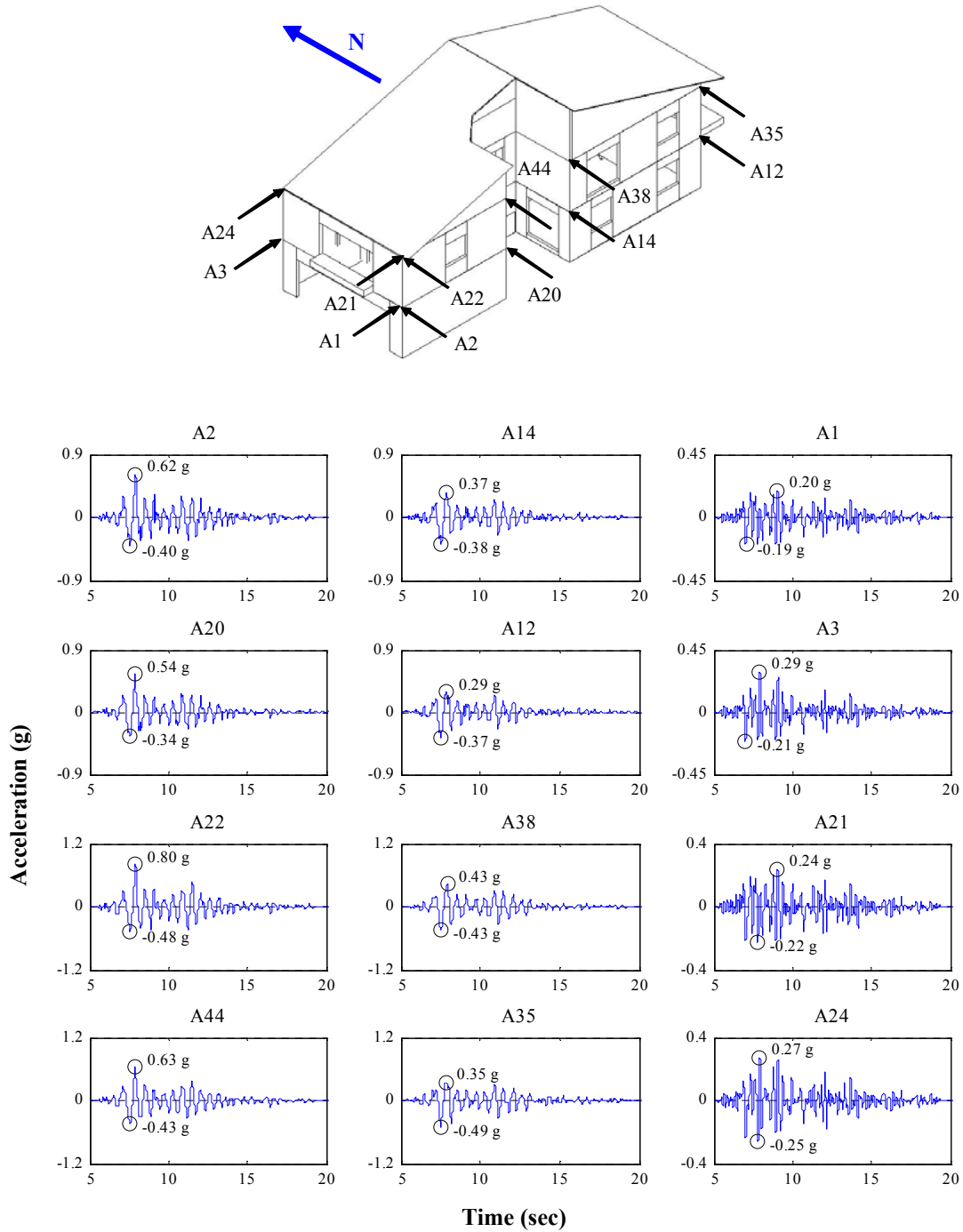


Figure L.50: Absolute acceleration time histories for Test NWP5S09

Appendix L

Phase 5, NWP5S11 Seismic Test

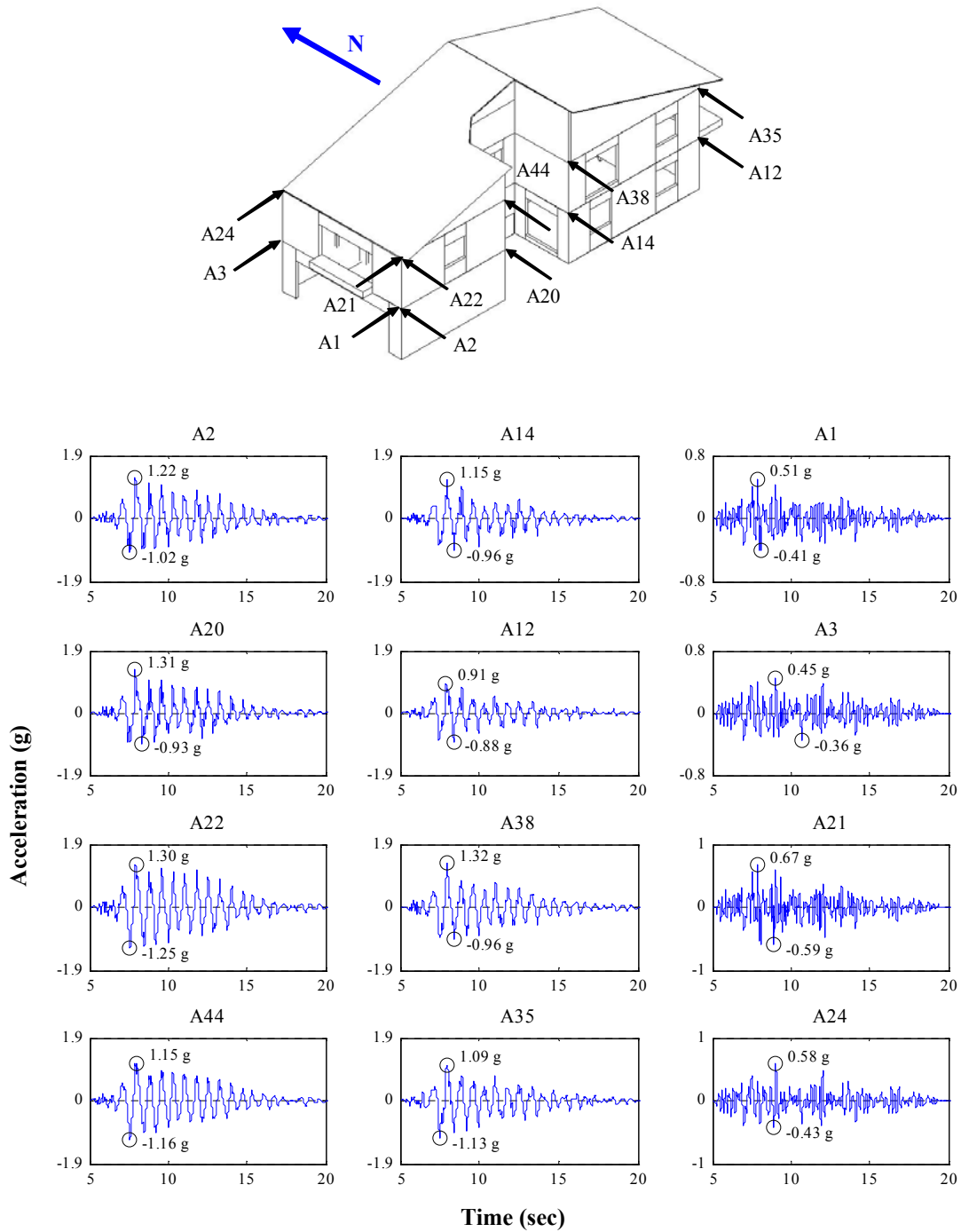


Figure L.51: Absolute acceleration time histories for Test NWP5S11

Appendix M
Selected Seismic Results:
Wall Deformations from Diagonal
String Potentiometers

Appendix M

Phase 1, NWP1S01 Seismic Test, North-South, External Walls

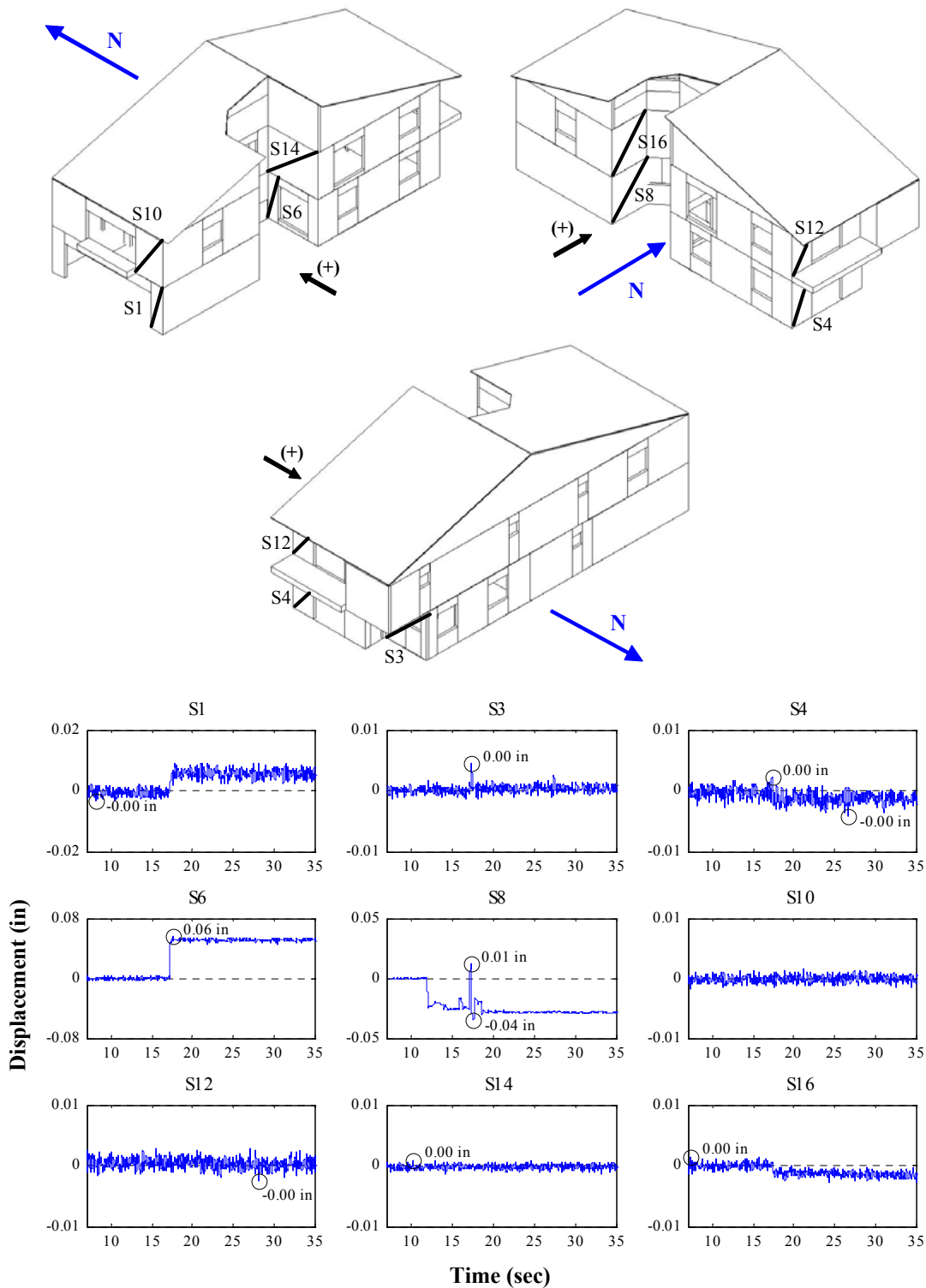


Figure M.1: Wall deformations of north-south external walls for Test NWP1S01

Appendix M

Phase 1, NWP1S01 Seismic Test, East-West, External Walls

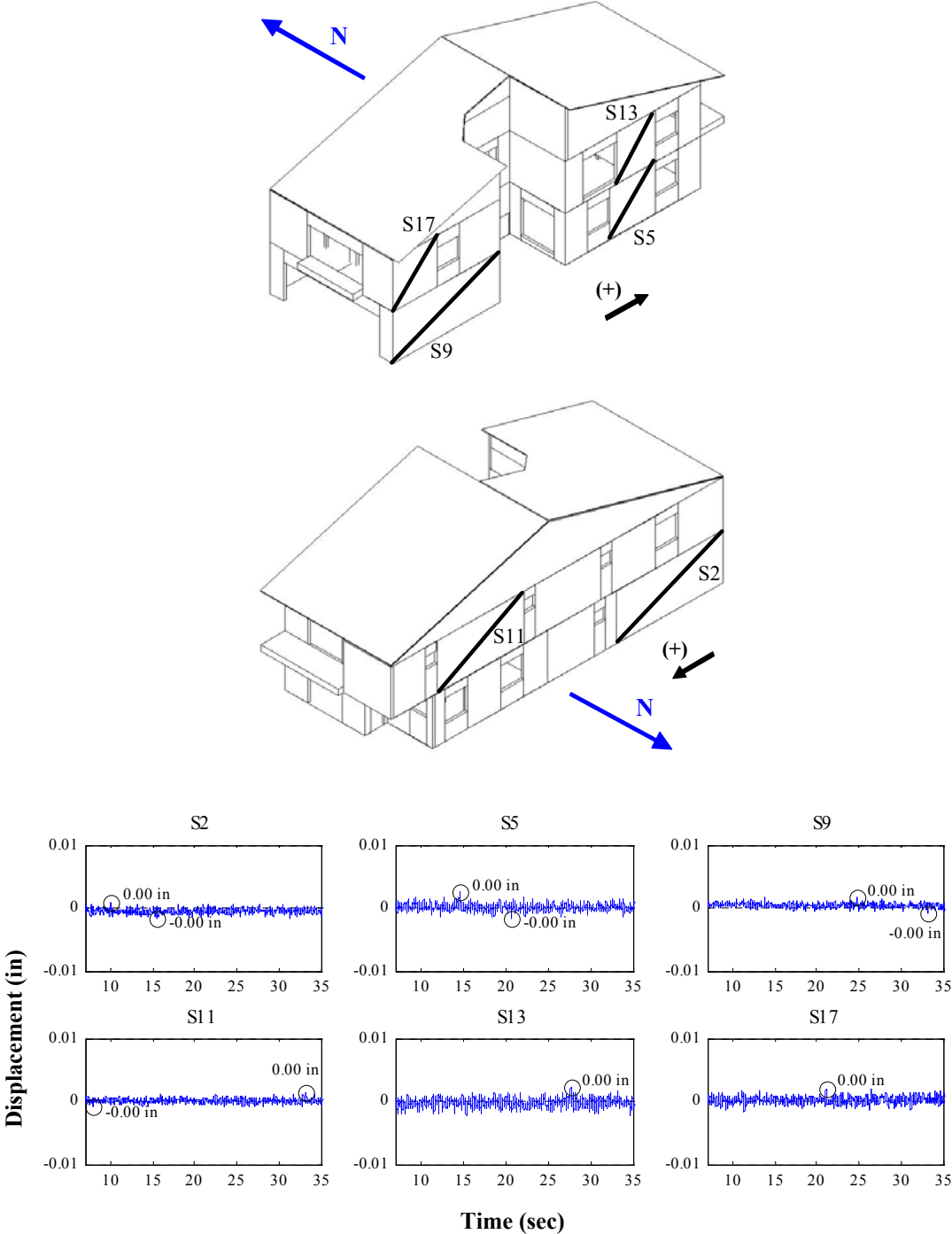


Figure M.2: Wall deformations of east-west external walls for Test NWP1S01

Appendix M

Phase 1, NWP1S01 Seismic Test, Internal Walls

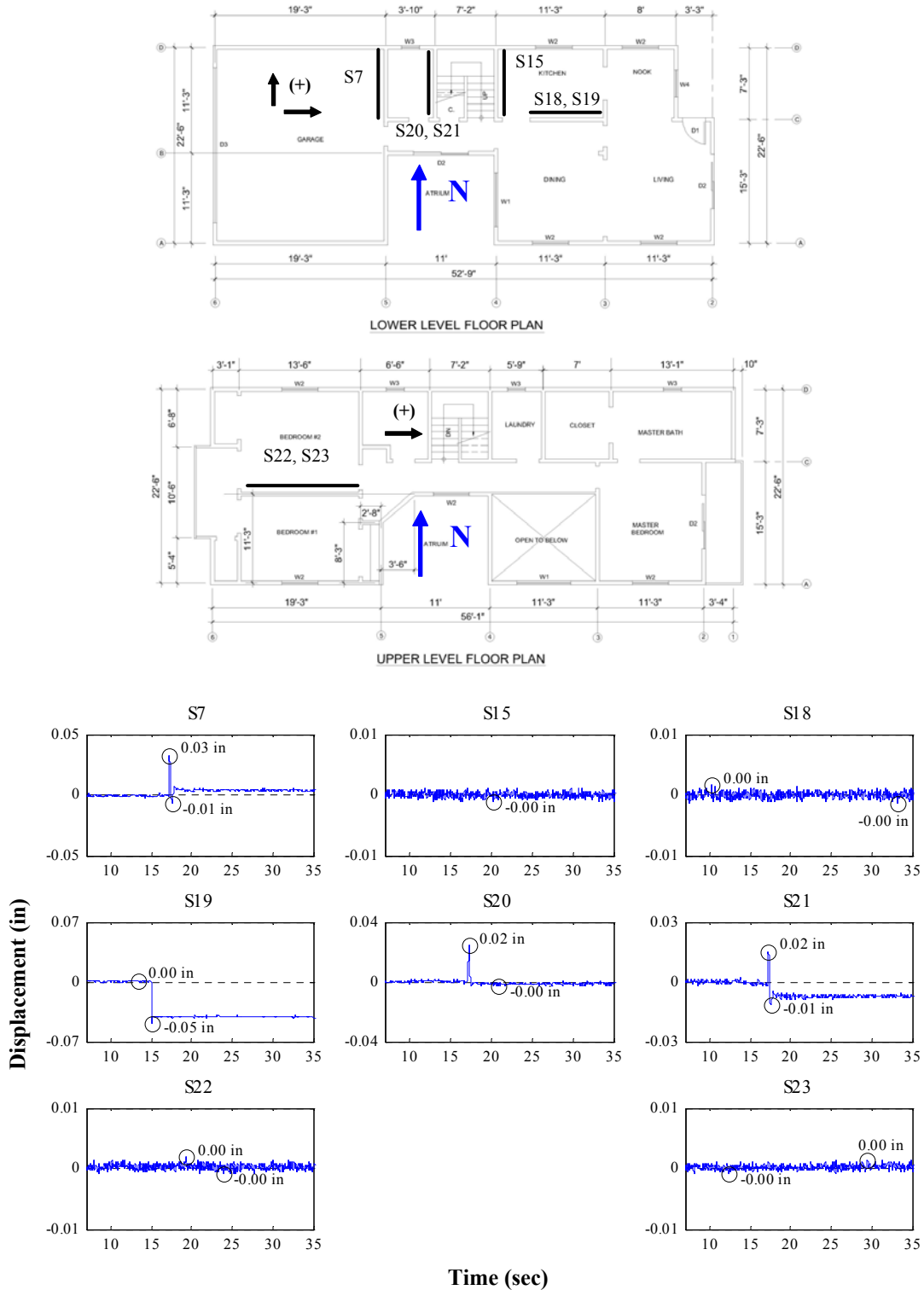


Figure M.3: Wall deformations of internal walls for Test NWP1S01

Appendix M

Phase 1, NWP1S02 Seismic Test, North-South, External Walls

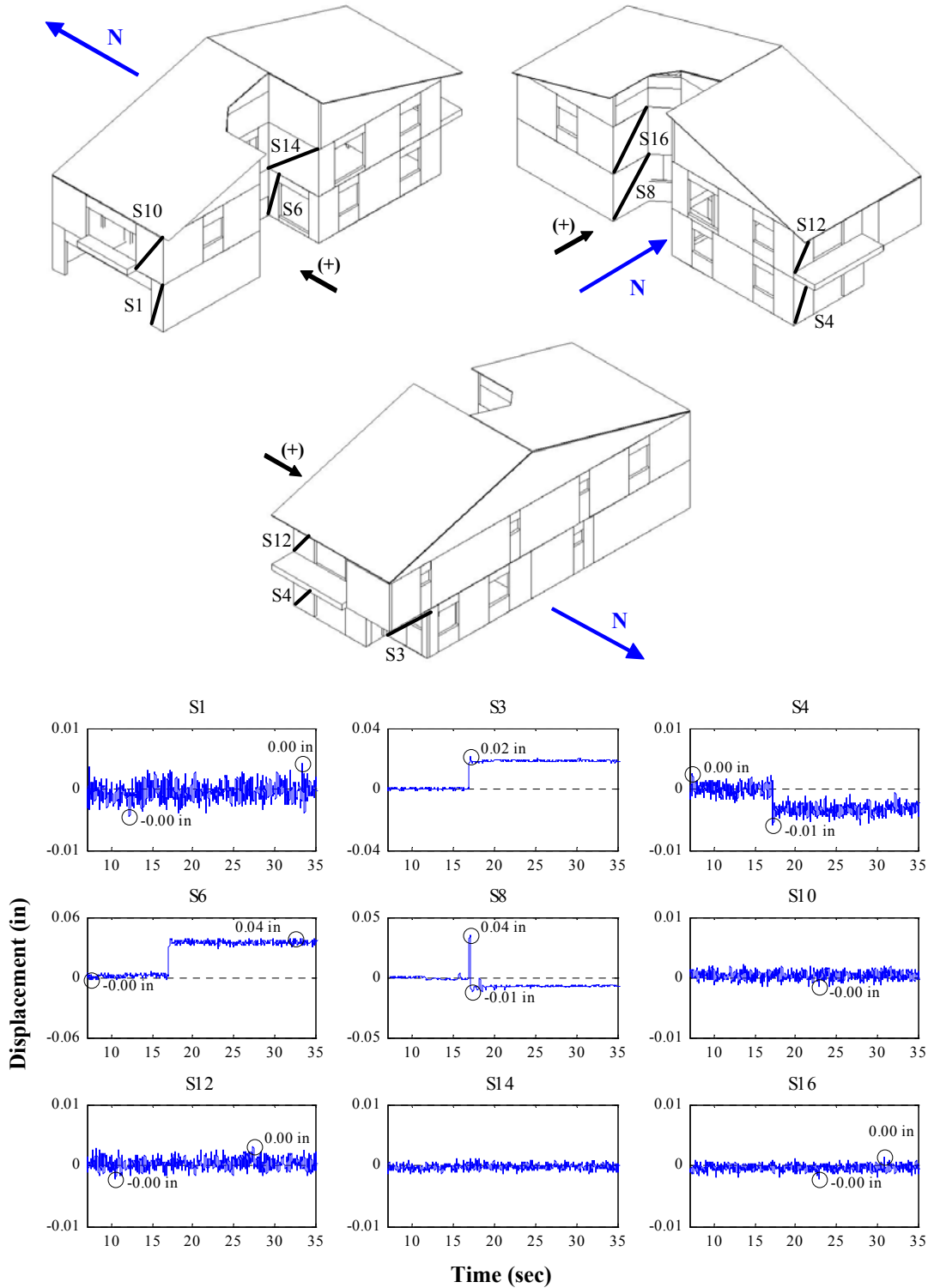


Figure M.4: Wall deformations of north-south external walls for Test NWP1S02

Appendix M

Phase 1, NWP1S02 Seismic Test, East-West, External Walls

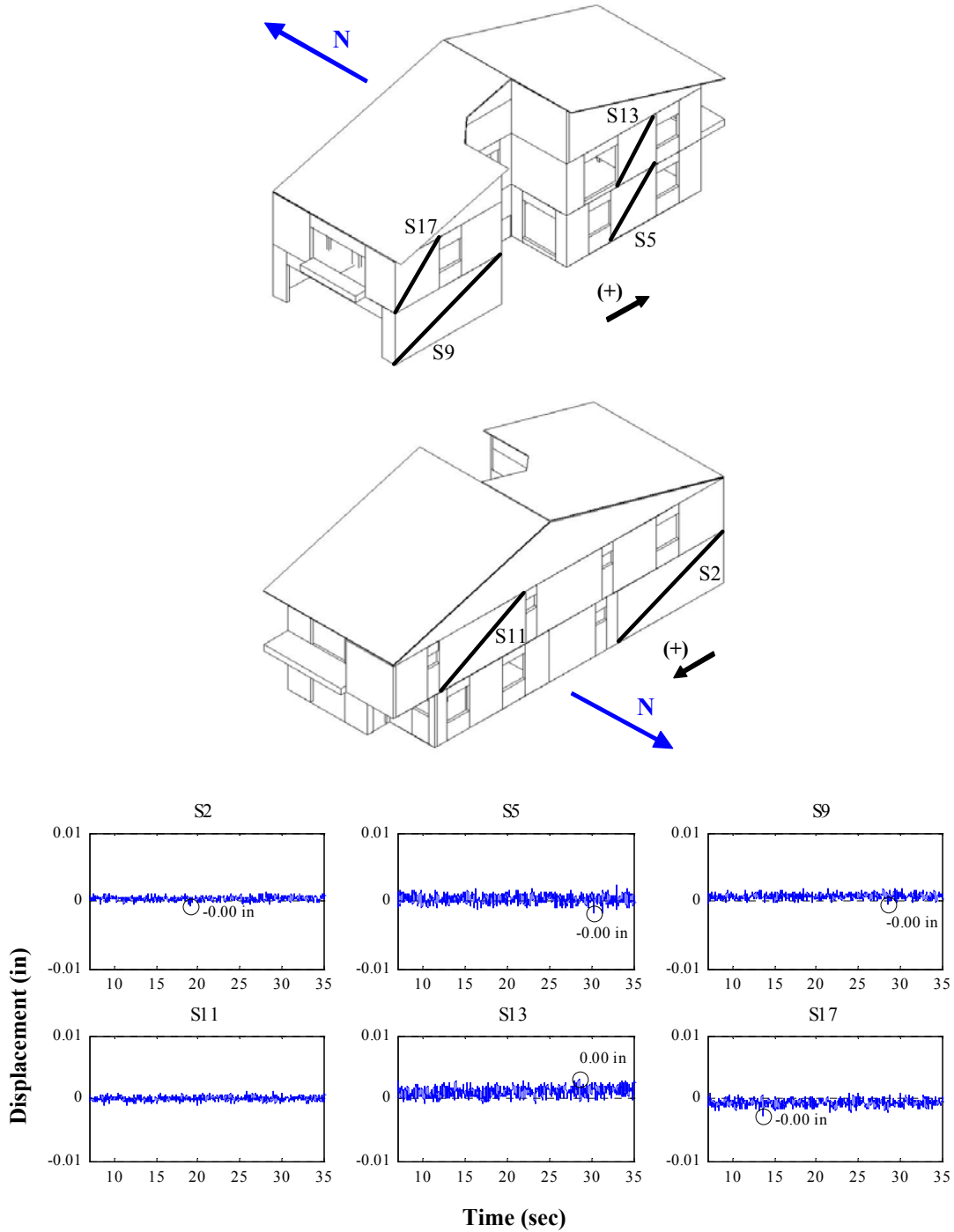


Figure M.5: Wall deformations of east-west external walls for Test NWP1S02

Appendix M

Phase 1, NWP1S02 Seismic Test, Internal Walls

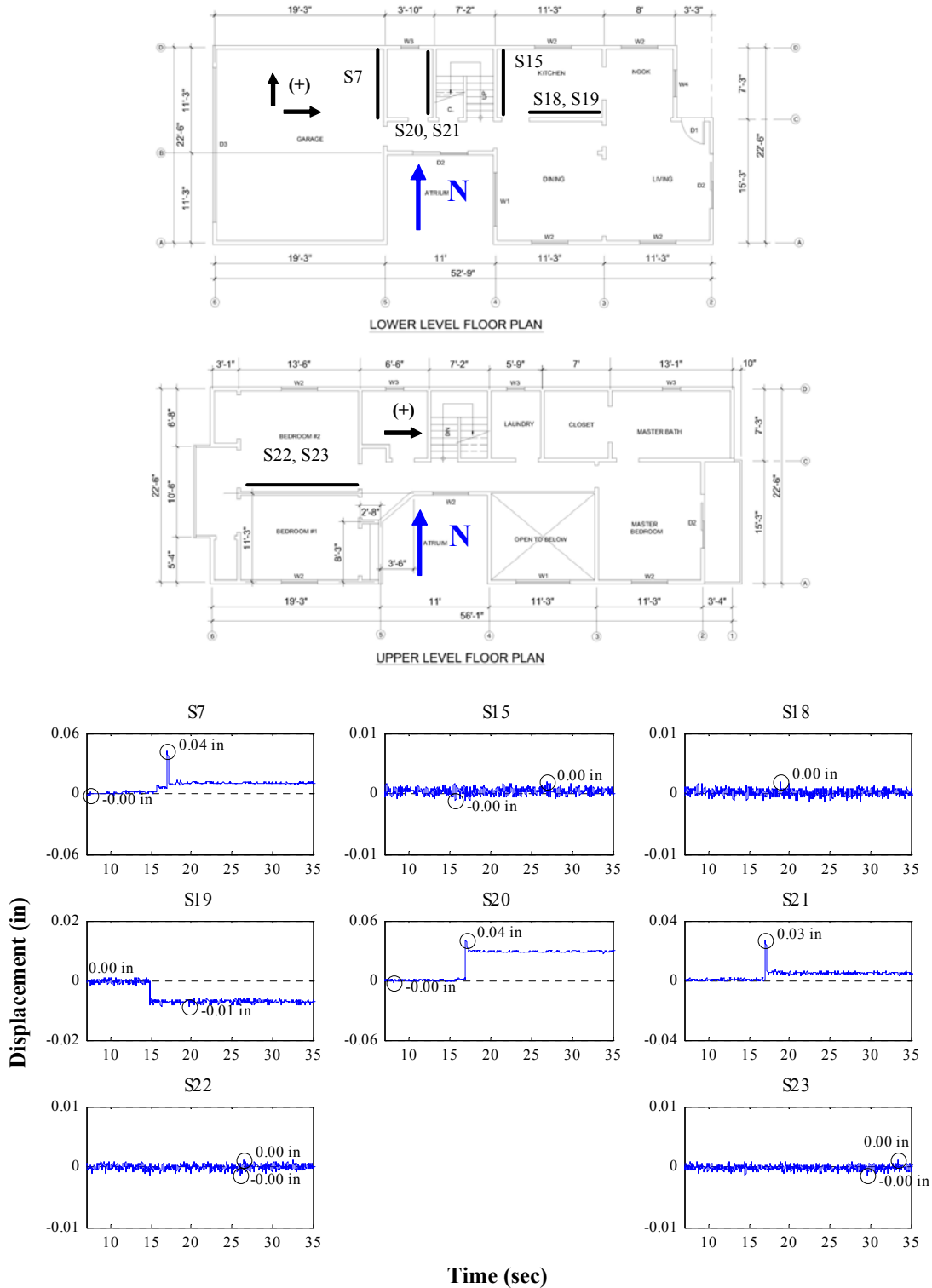


Figure M.6: Wall deformations of internal walls for Test NWP1S02

Appendix M

Phase 1, NWP1S03 Seismic Test, North-South, External Walls

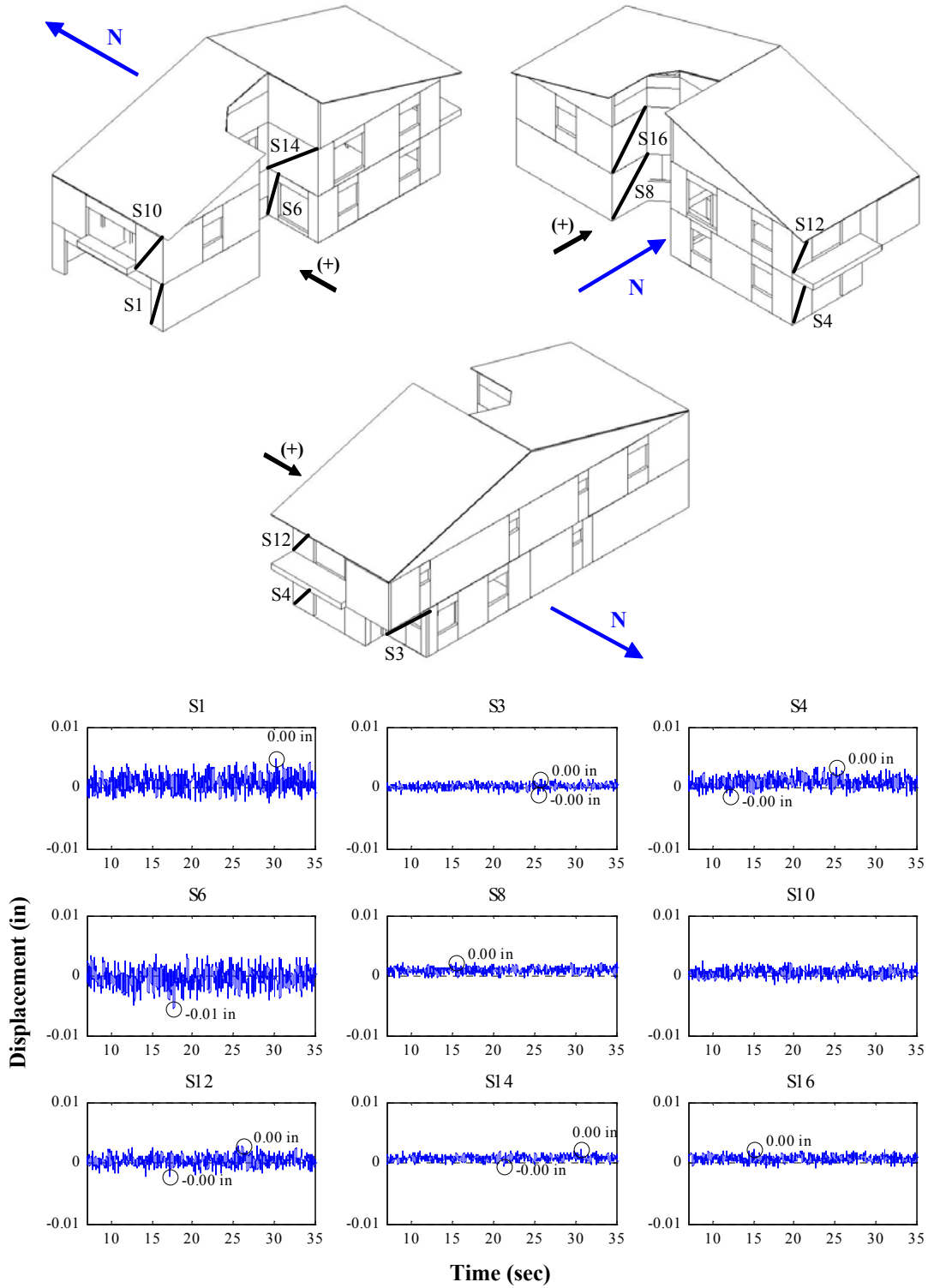


Figure M.7: Wall deformations of north-south external walls for Test NWP1S03

Appendix M

Phase 1, NWP1S03 Seismic Test, East-West, External Walls

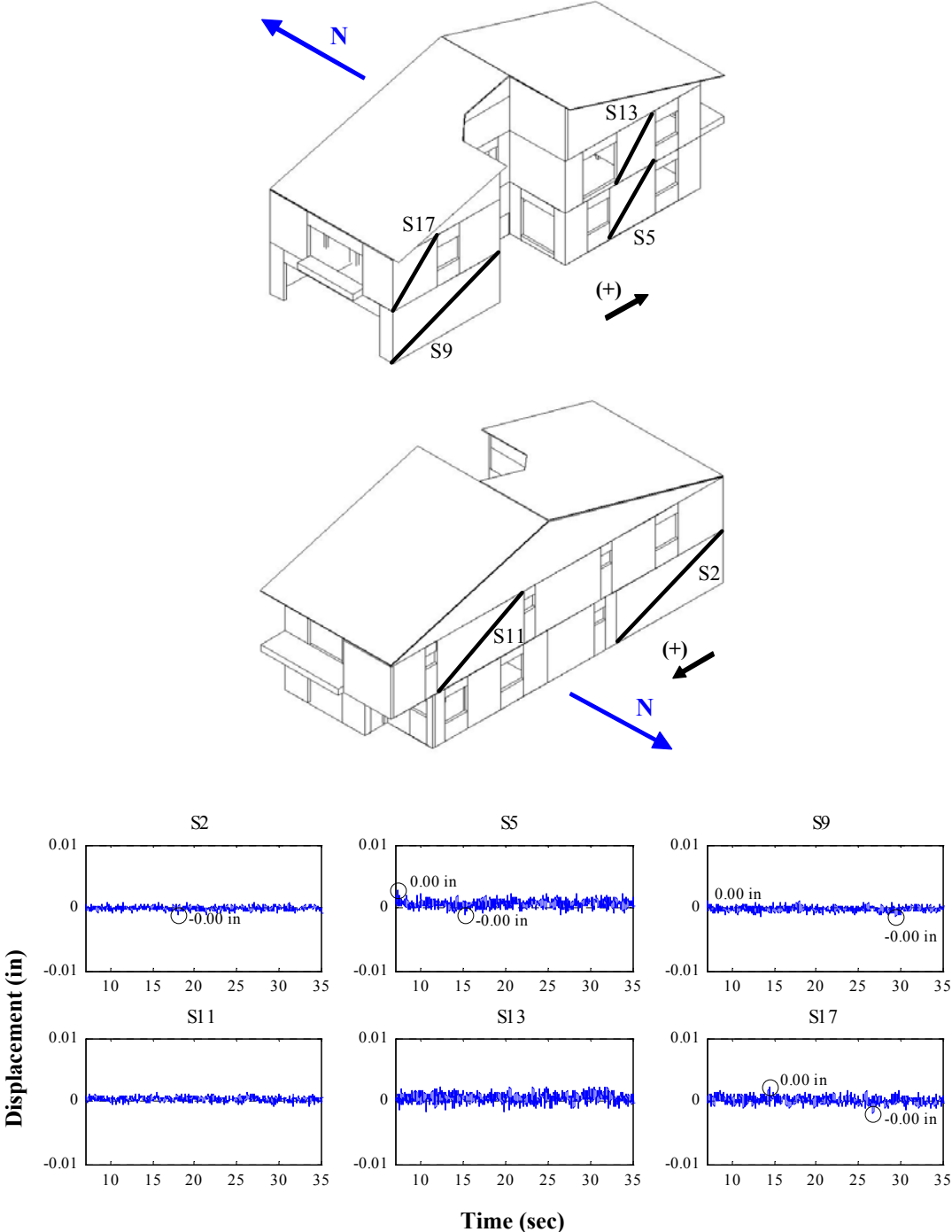


Figure M.8: Wall deformations of east-west external walls for Test NWP1S03

Appendix M

Phase 1, NWP1S03 Seismic Test, Internal Walls

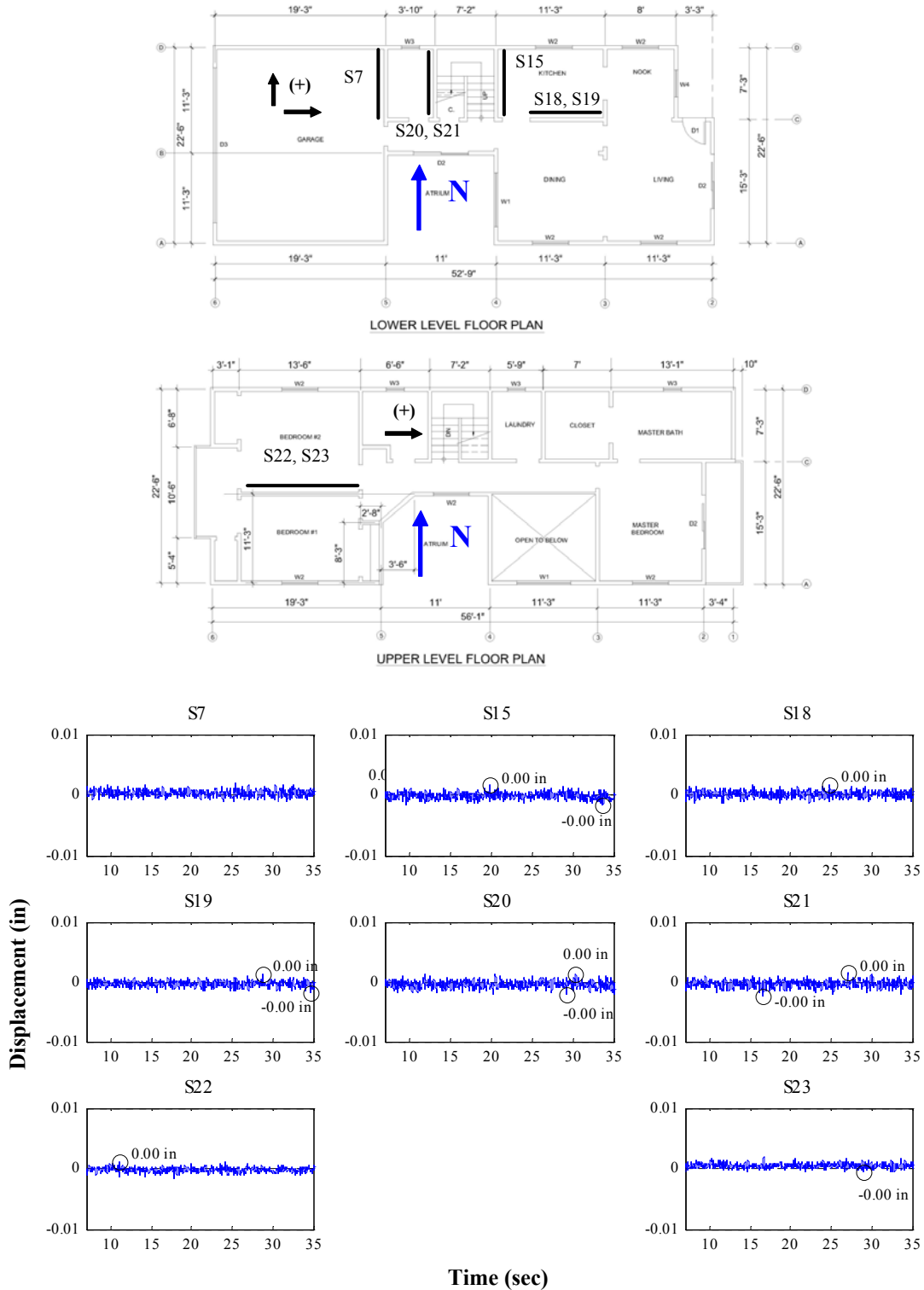


Figure M.9: Wall deformations of internal walls for Test NWP1S03

Appendix M

Phase 1, NWP1S04 Seismic Test, North-South, External Walls

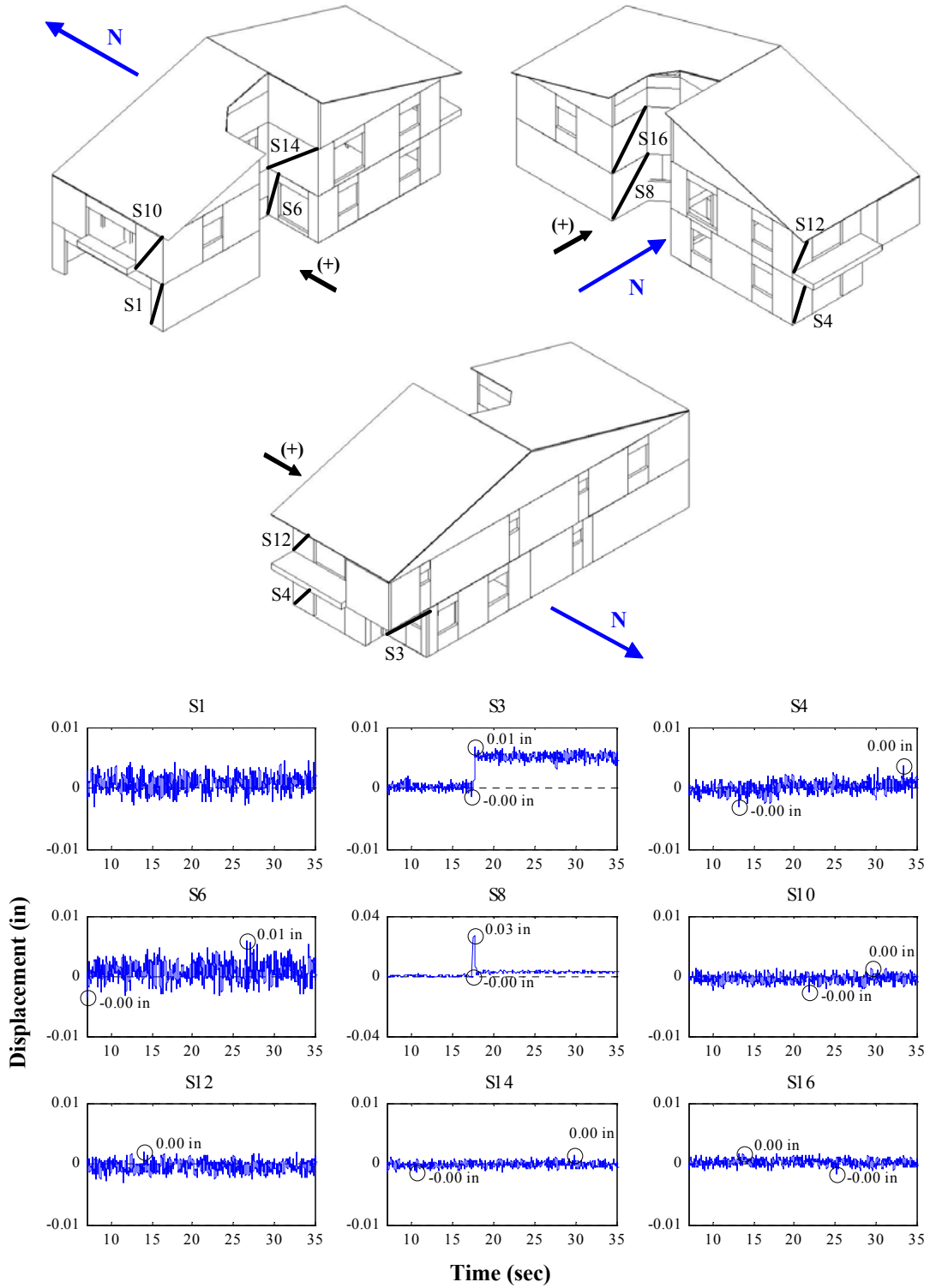


Figure M.10: Wall deformations of north-south external walls for Test NWP1S04

Appendix M

Phase 1, NWP1S04 Seismic Test, East-West, External Walls

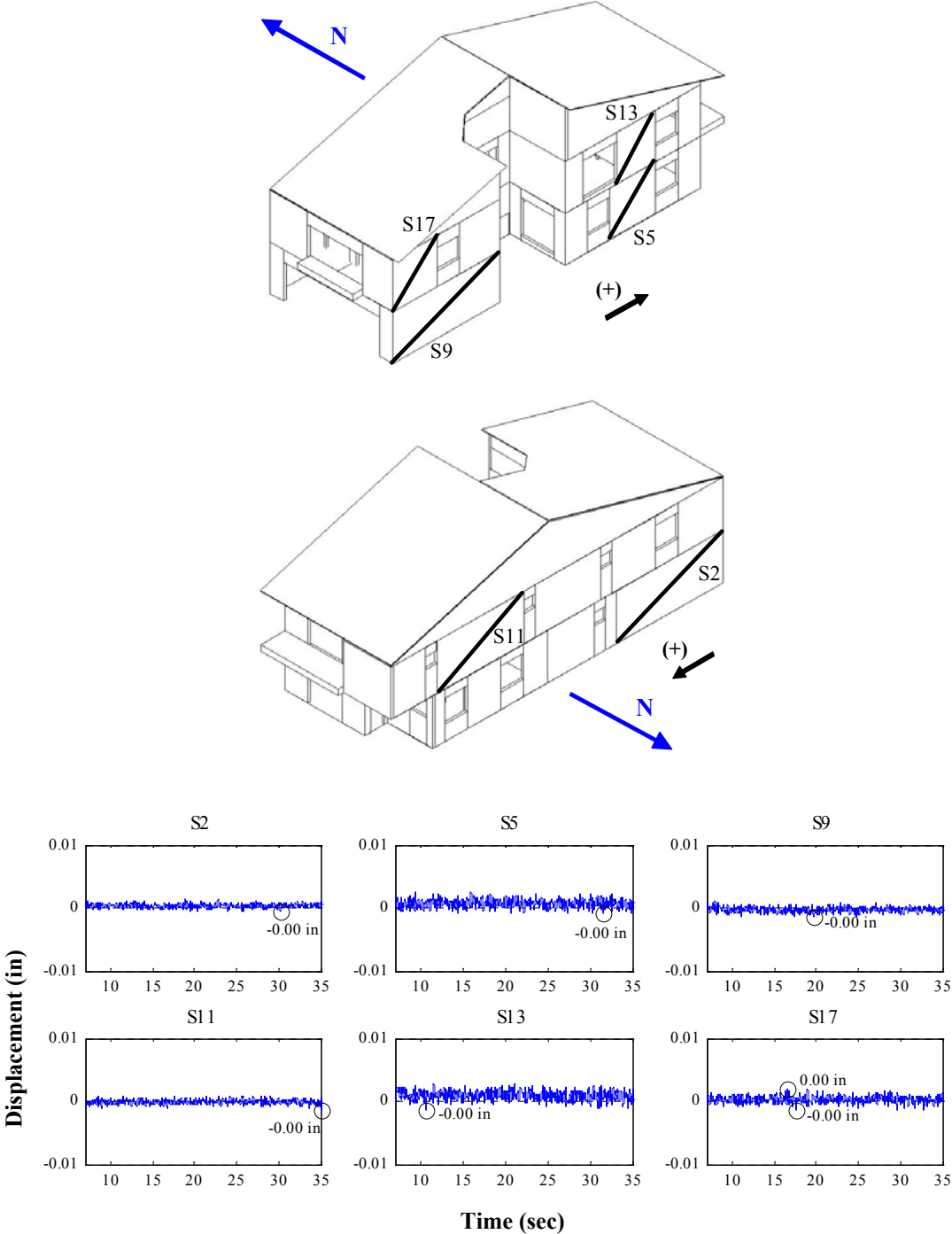


Figure M.11: Wall deformations of east-west external walls for Test NWP1S04

Appendix M

Phase 1, NWP1S04 Seismic Test, Internal Walls

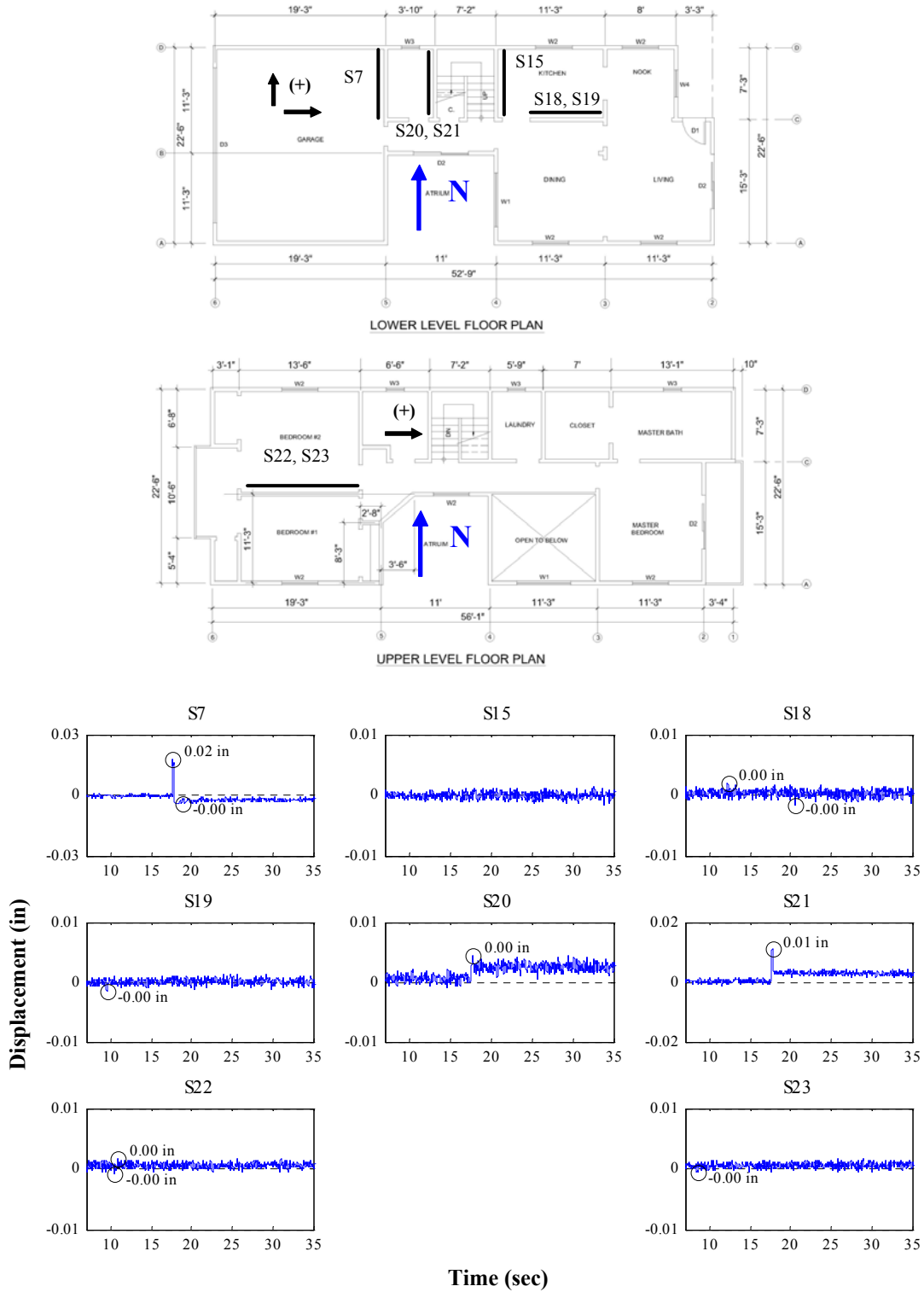


Figure M.12: Wall deformations of internal walls for Test NWP1S04

Appendix M

Phase 1, NWP1S05 Seismic Test, North-South, External Walls

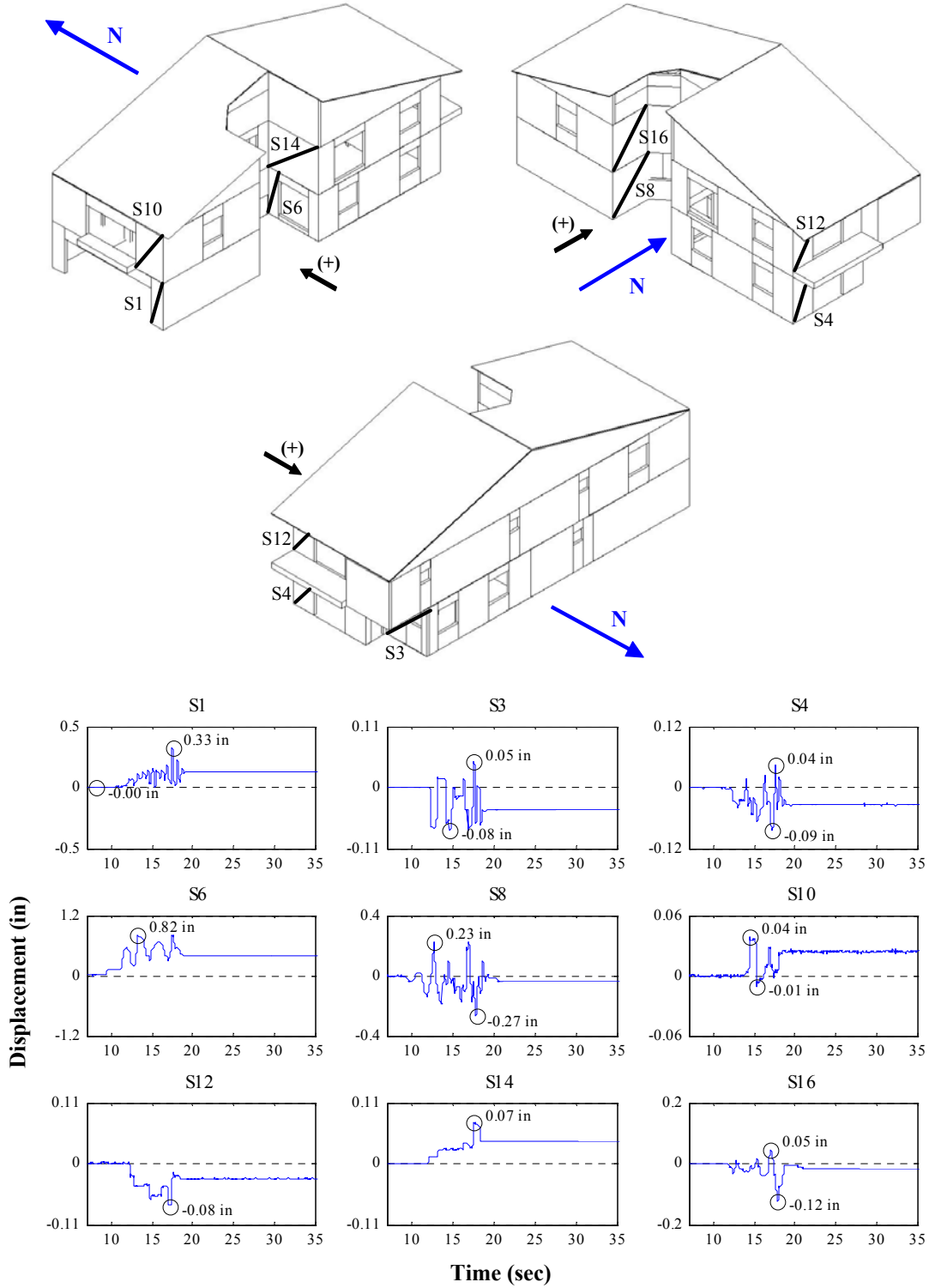


Figure M.13: Wall deformations of north-south external walls for Test NWP1S05

Appendix M

Phase 1, NWP1S05 Seismic Test, East-West, External Walls

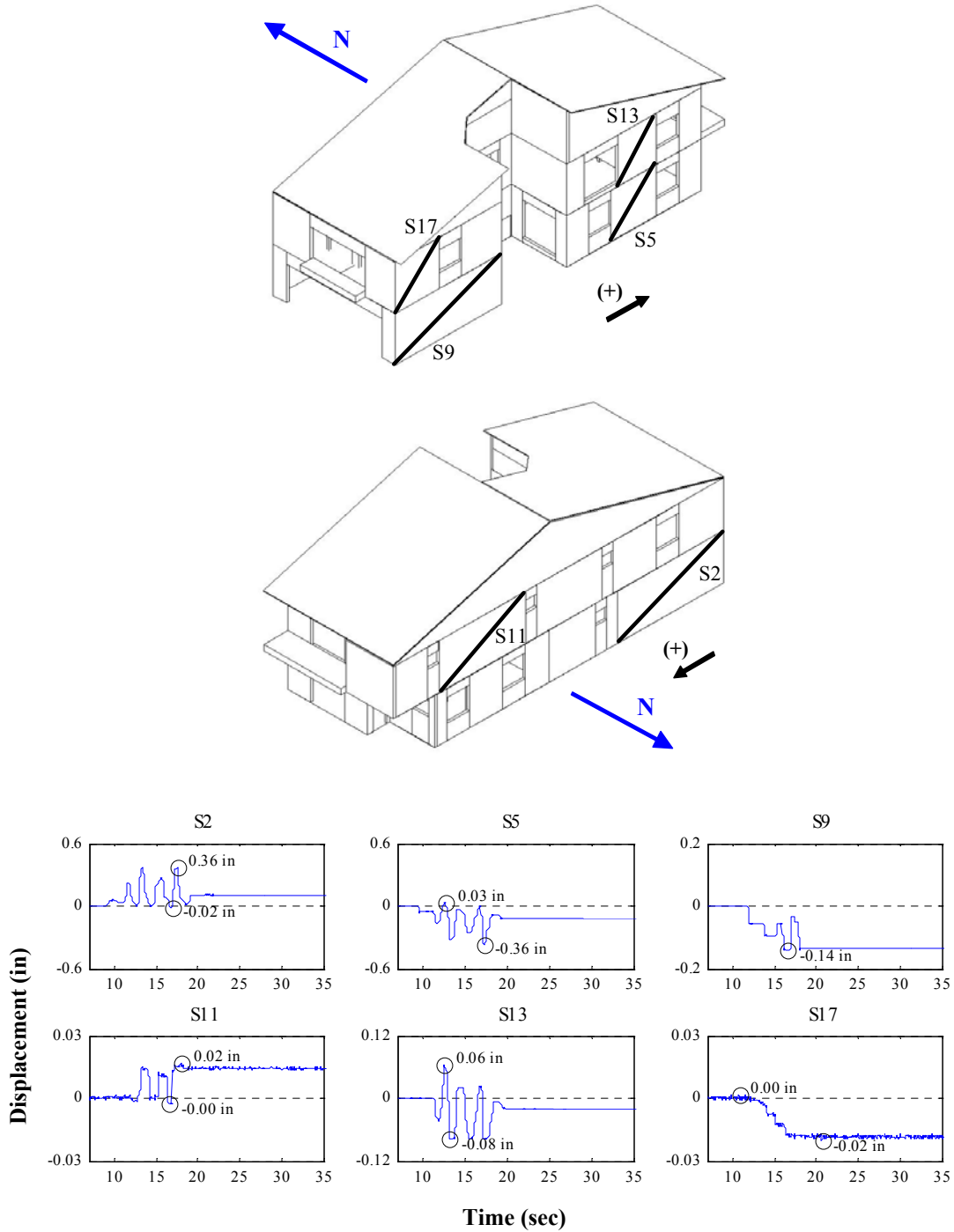


Figure M.14: Wall deformations of east-west external walls for Test NWP1S05

Appendix M

Phase 1, NWP1S05 Seismic Test, Internal Walls

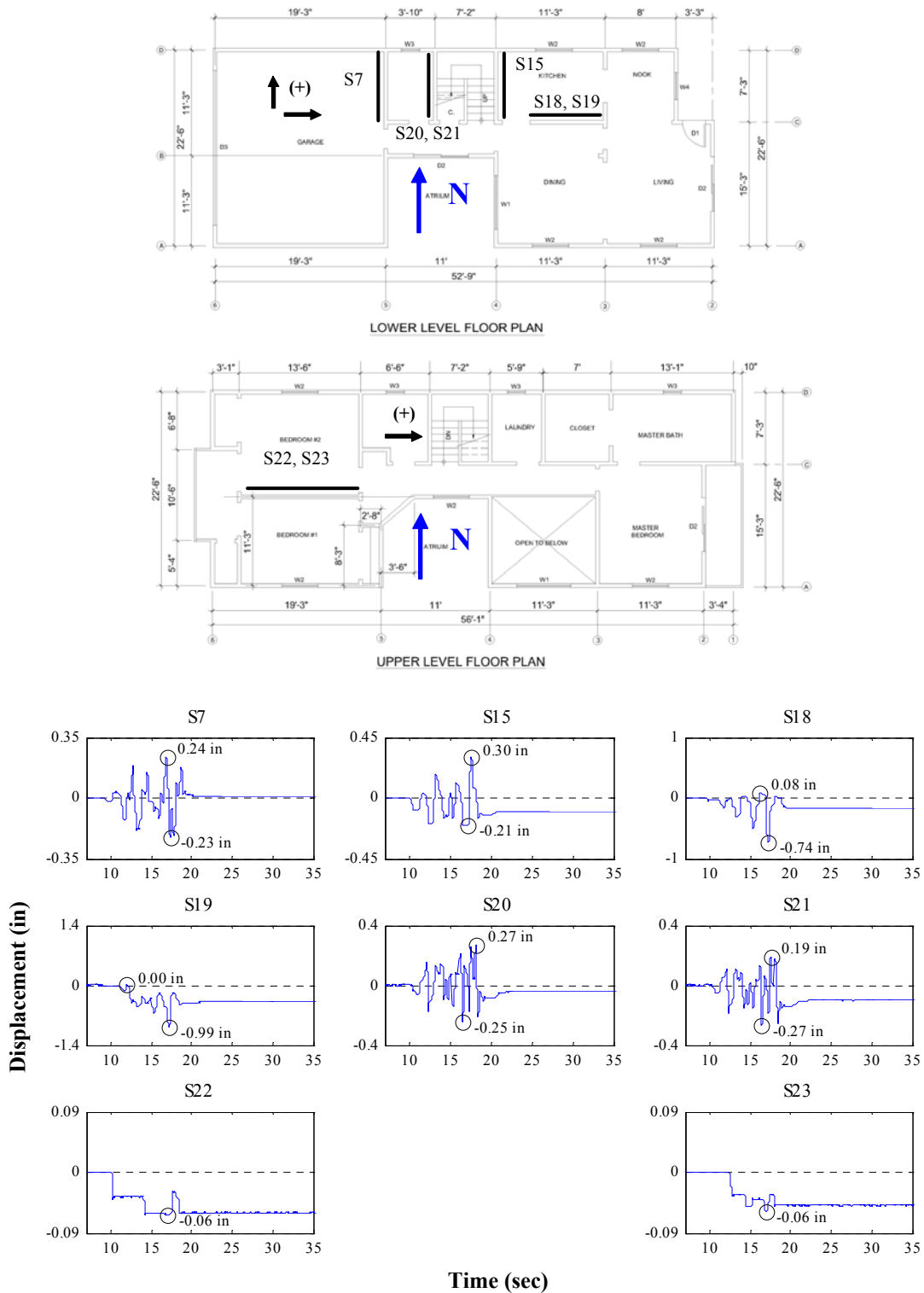


Figure M.15: Wall deformations of internal walls for Test NWP1S05

Appendix M

Phase 1, NWP1S017 Seismic Test, North-South, External Walls

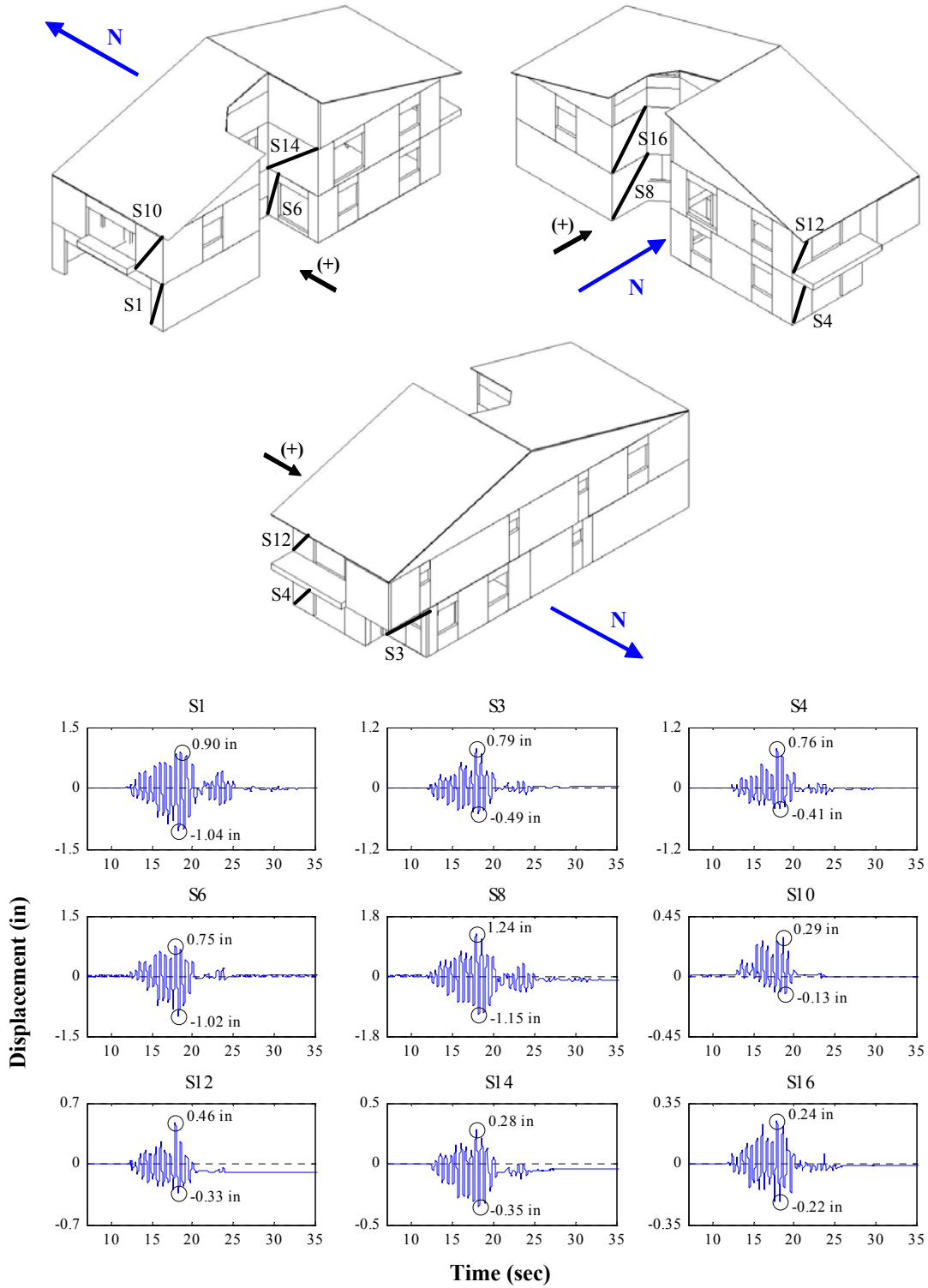


Figure M.16: Wall deformations of north-south external walls for Test NWP1S017

Appendix M

Phase 1, NWP1S017 Seismic Test, East-West, External Walls

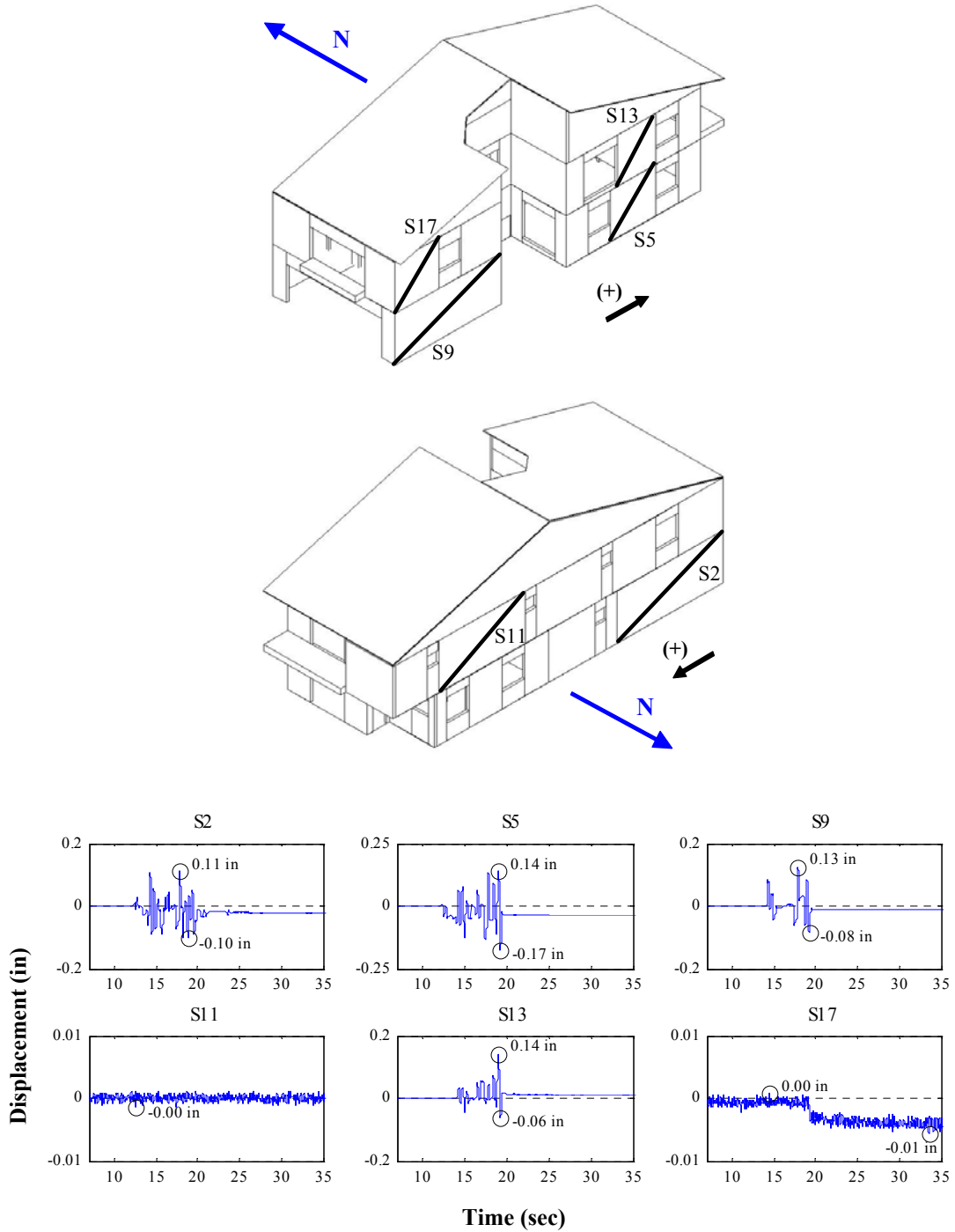


Figure M.17: Wall deformations of east-west external walls for Test NWP1S017

Appendix M

Phase 1, NWP1S017 Seismic Test, Internal Walls

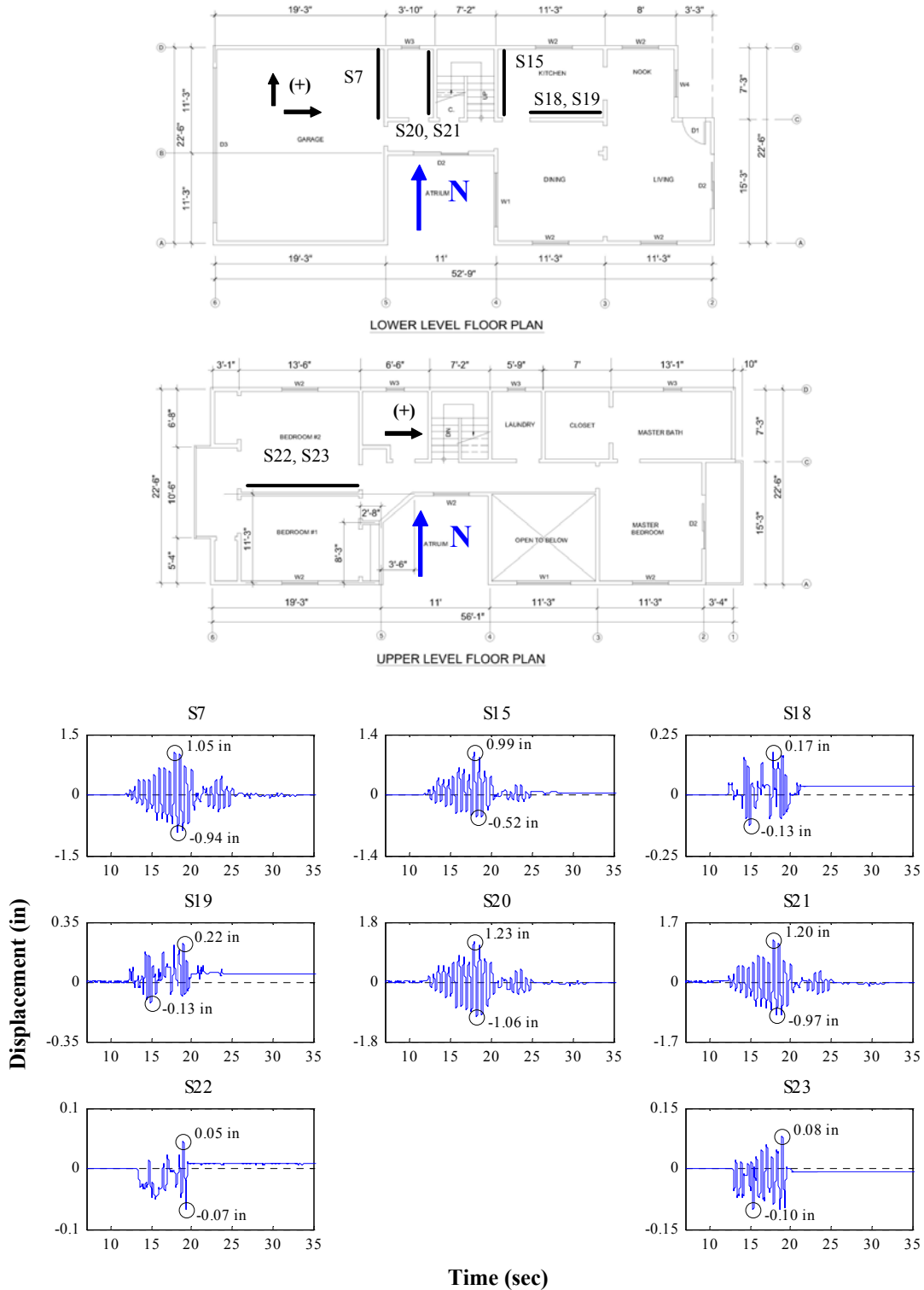


Figure M.18: Wall deformations of internal walls for Test NWP1S017

Appendix M

Phase 1, NWP1S07 Seismic Test, North-South, External Walls

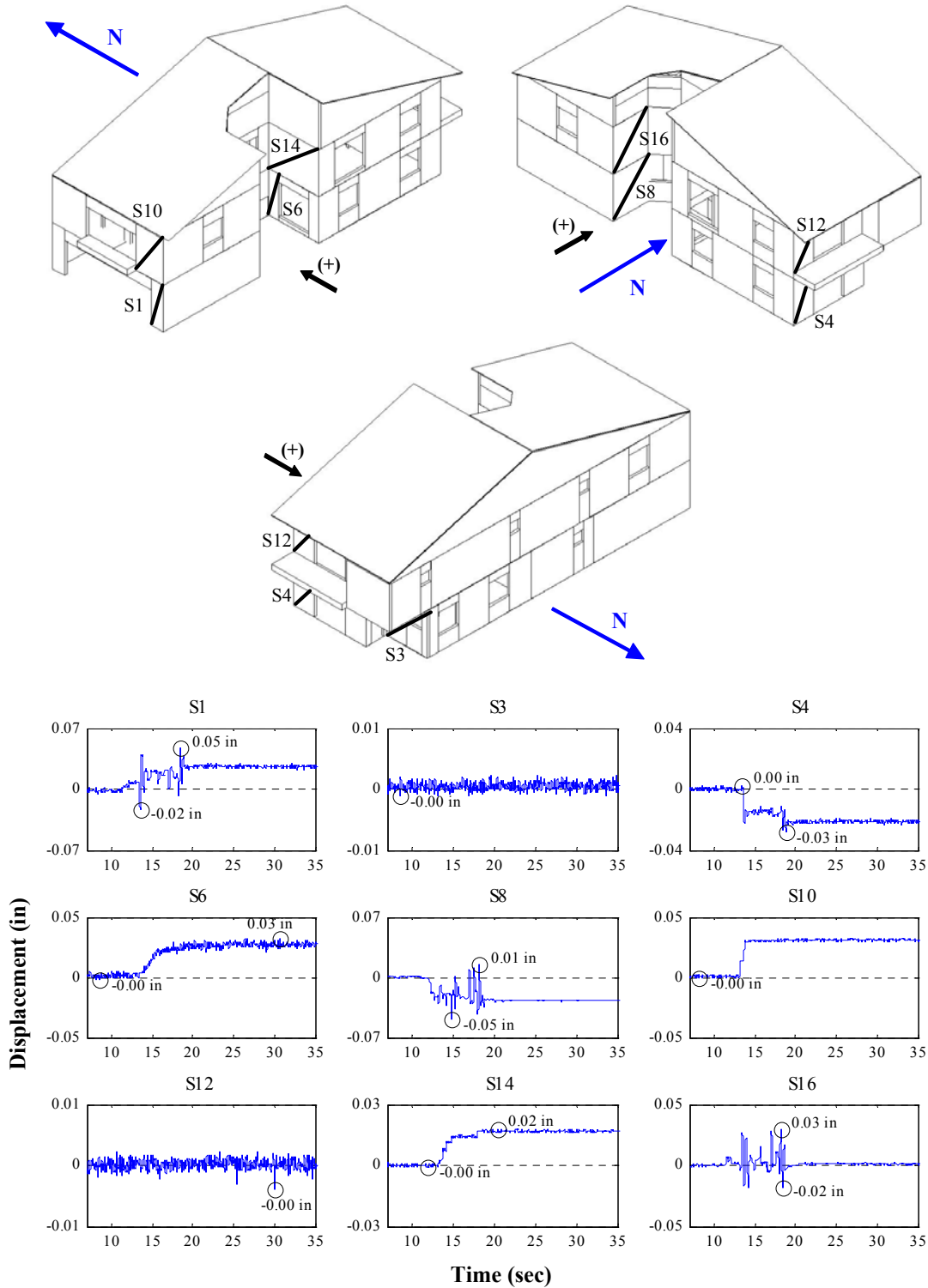


Figure M.19: Wall deformations of north-south external walls for Test NWP1S07

Appendix M

Phase 1, NWP1S07 Seismic Test, East-West, External Walls

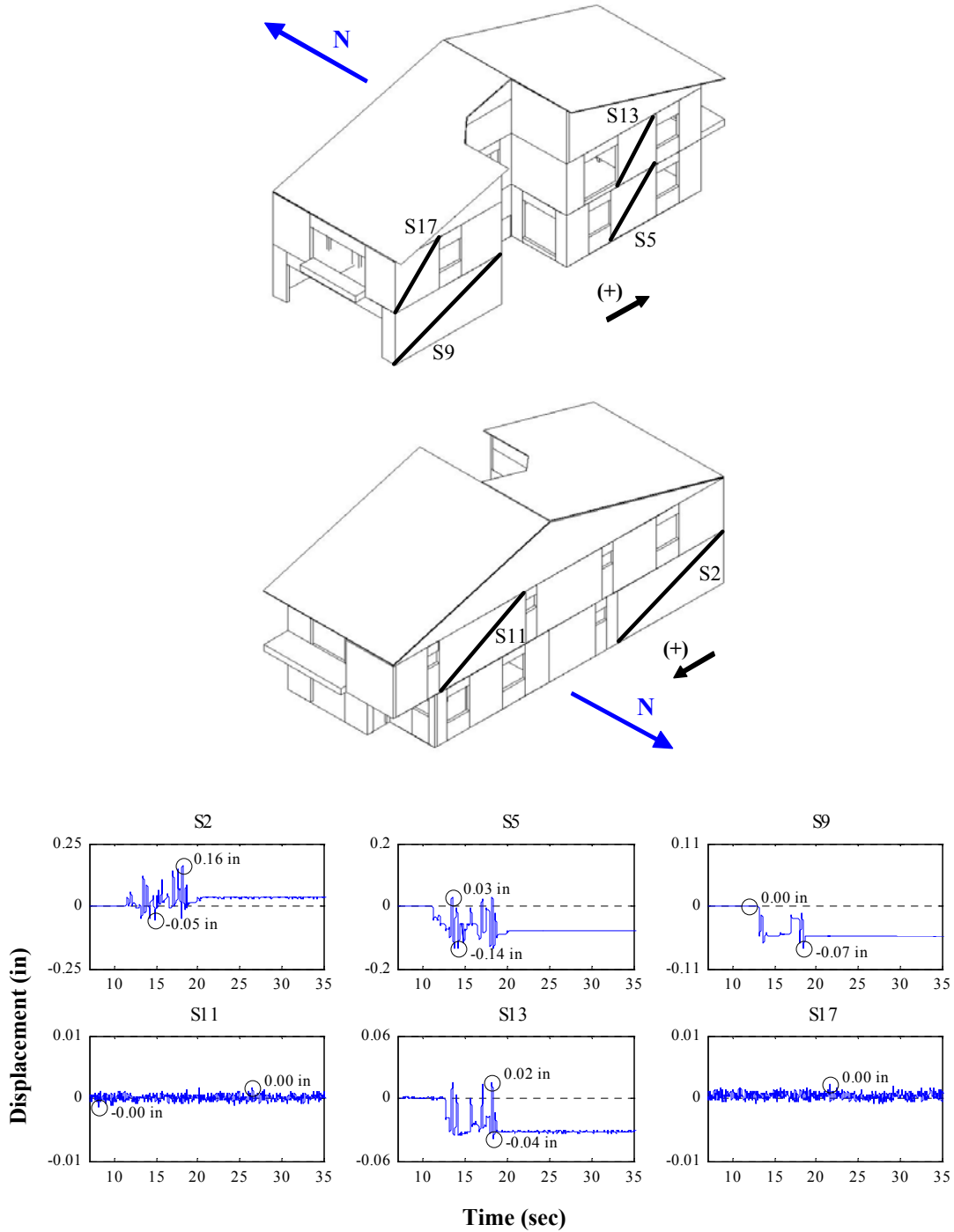


Figure M.20: Wall deformations of east-west external walls for Test NWP1S07

Appendix M

Phase 1, NWP1S07 Seismic Test, Internal Walls

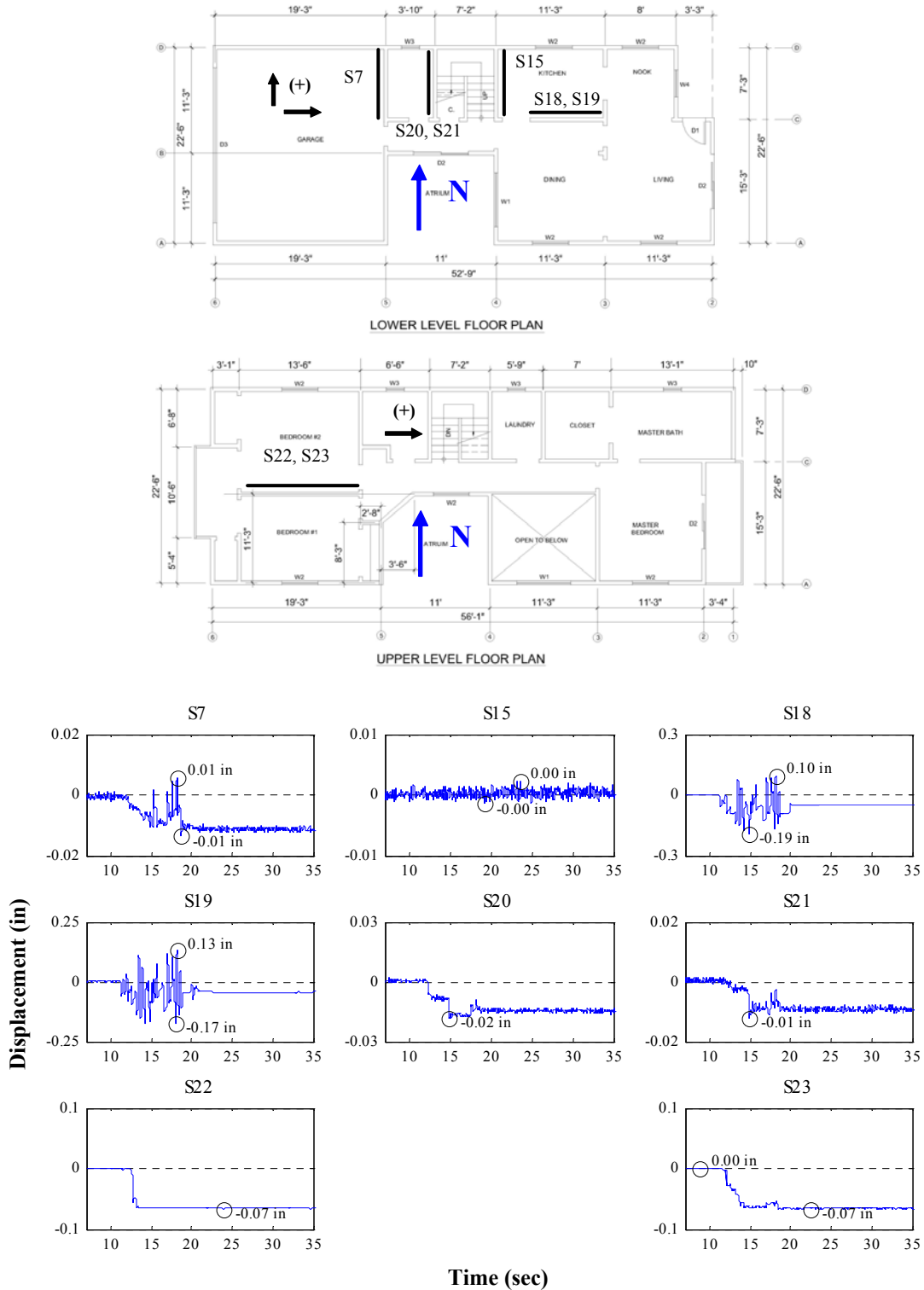


Figure M.21: Wall deformations of internal walls for Test NWP1S07

Appendix M

Phase 1, NWP1S06 Seismic Test, North-South, External Walls

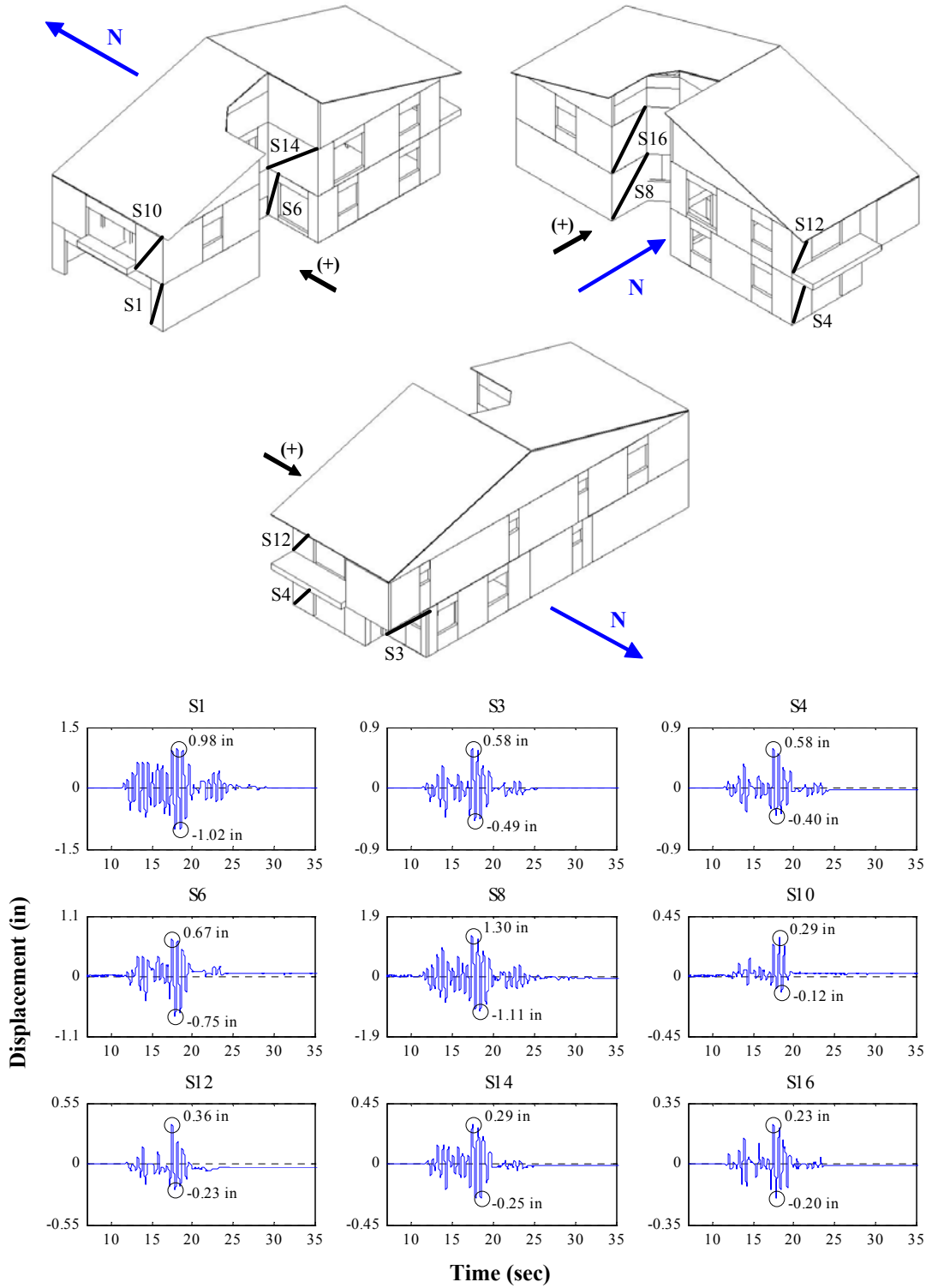


Figure M.22: Wall deformations of north-south external walls for Test NWP1S06

Appendix M

Phase 1, NWP1S06 Seismic Test, East-West, External Walls

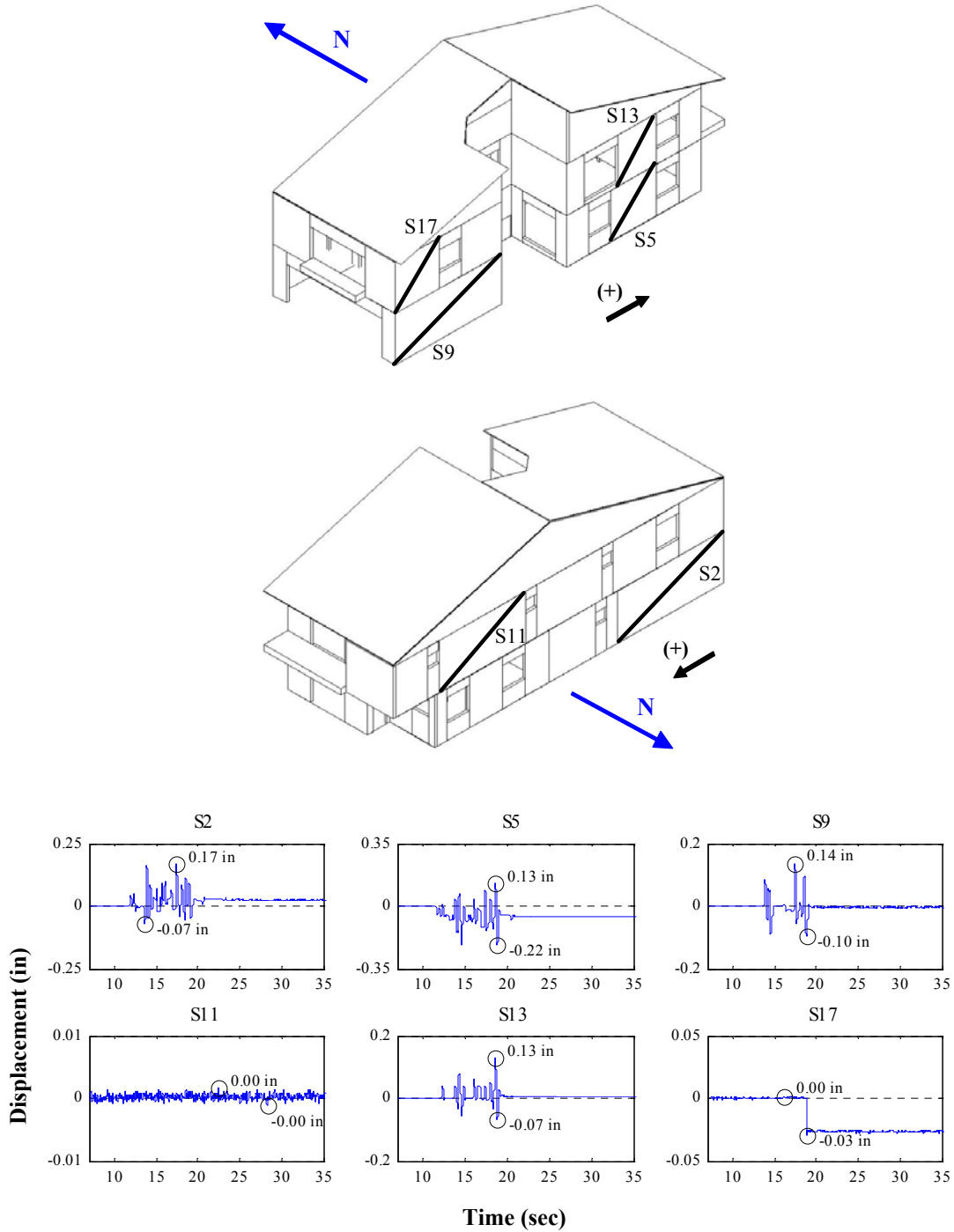


Figure M.23: Wall deformations of east-west external walls for Test NWP1S06

Appendix M

Phase 1, NWP1S06 Seismic Test, Internal Walls

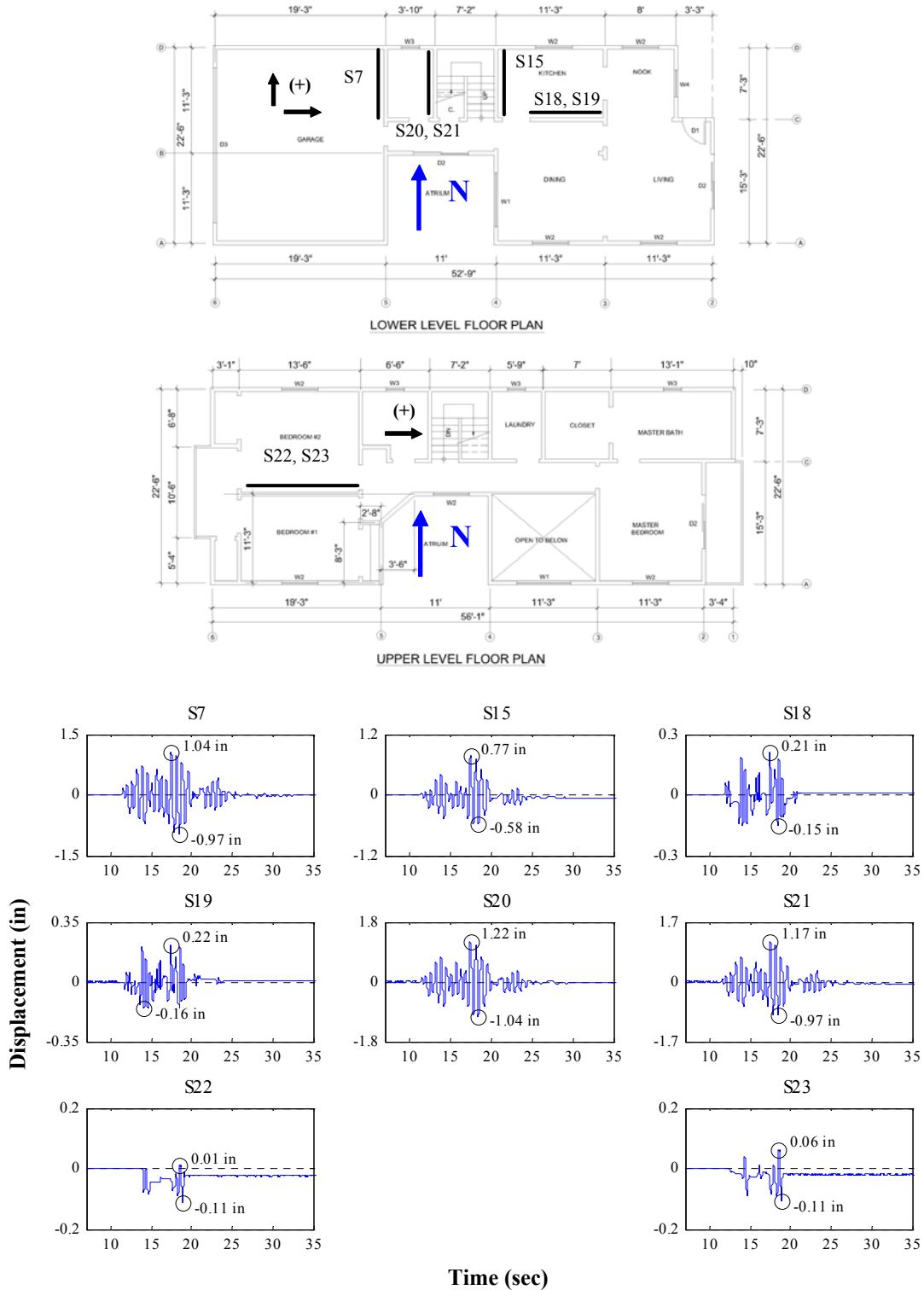


Figure M.24: Wall deformations of internal walls for Test NWP1S06

Appendix M

Phase 1, NWP1S10 Seismic Test, North-South, External Walls

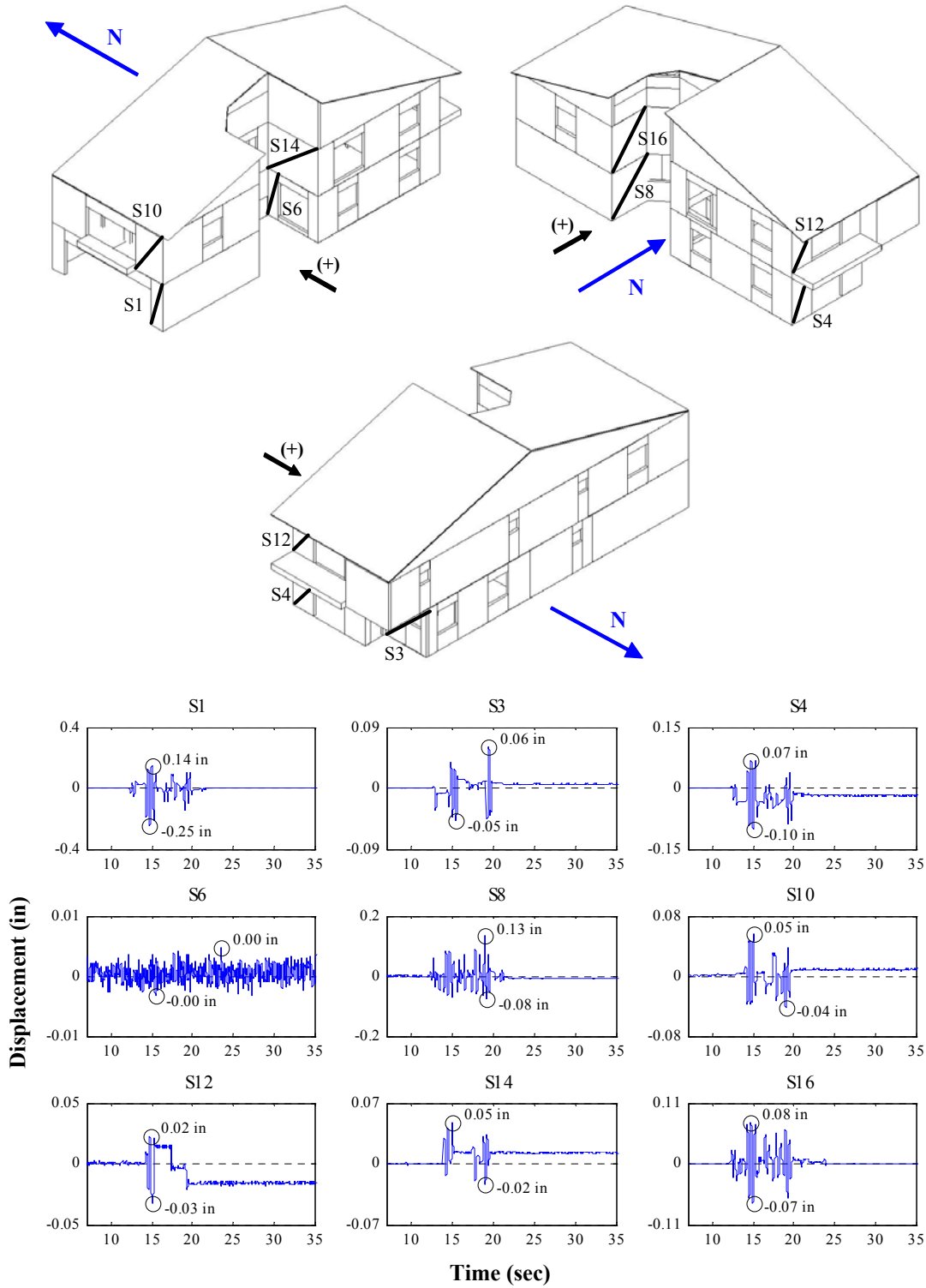


Figure M.25: Wall deformations of north-south external walls for Test NWP1S10

Appendix M

Phase 1, NWP1S10 Seismic Test, East-West, External Walls

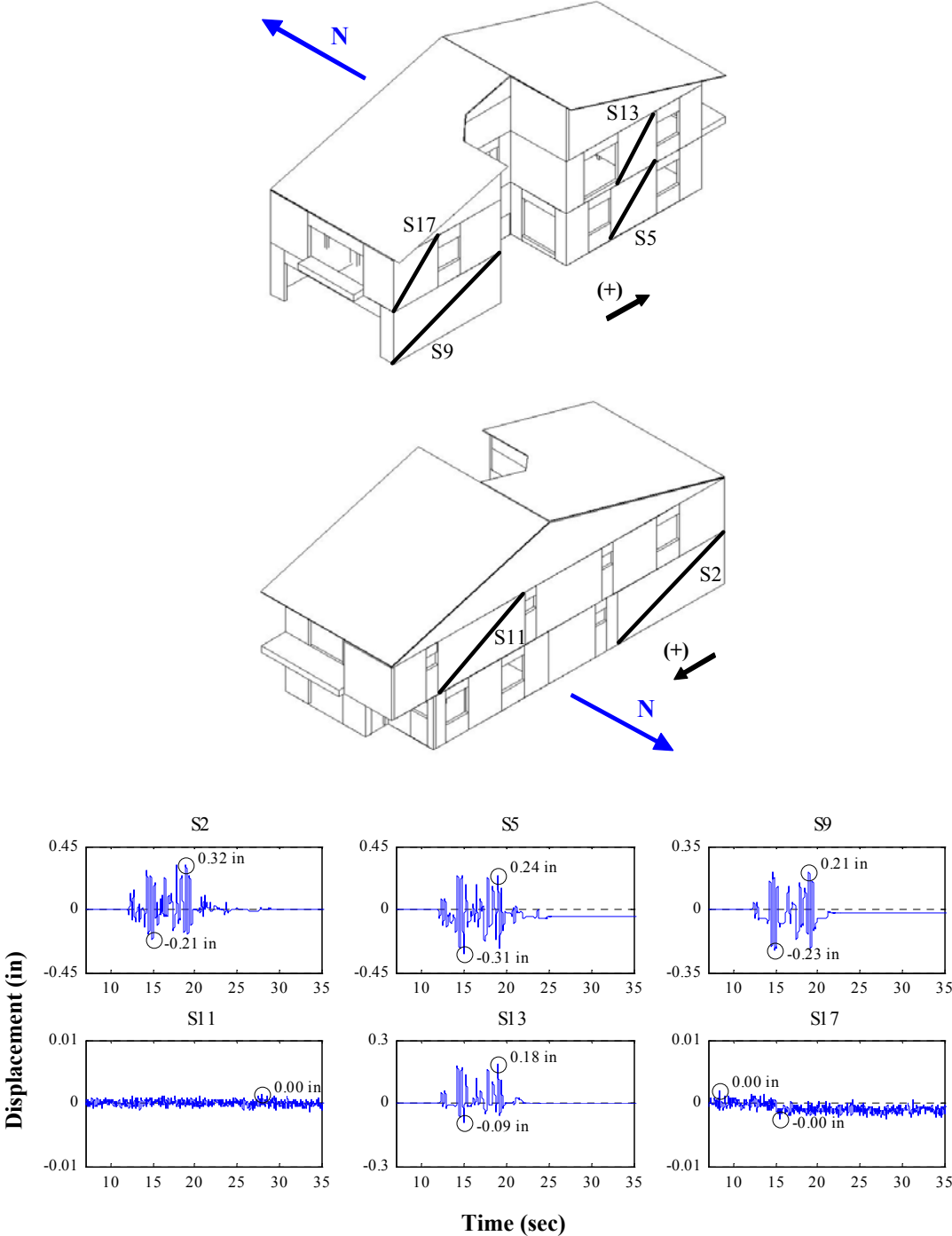


Figure M.26: Wall deformations of east-west external walls for Test NWP1S10

Appendix M

Phase 1, NWP1S10 Seismic Test, Internal Walls

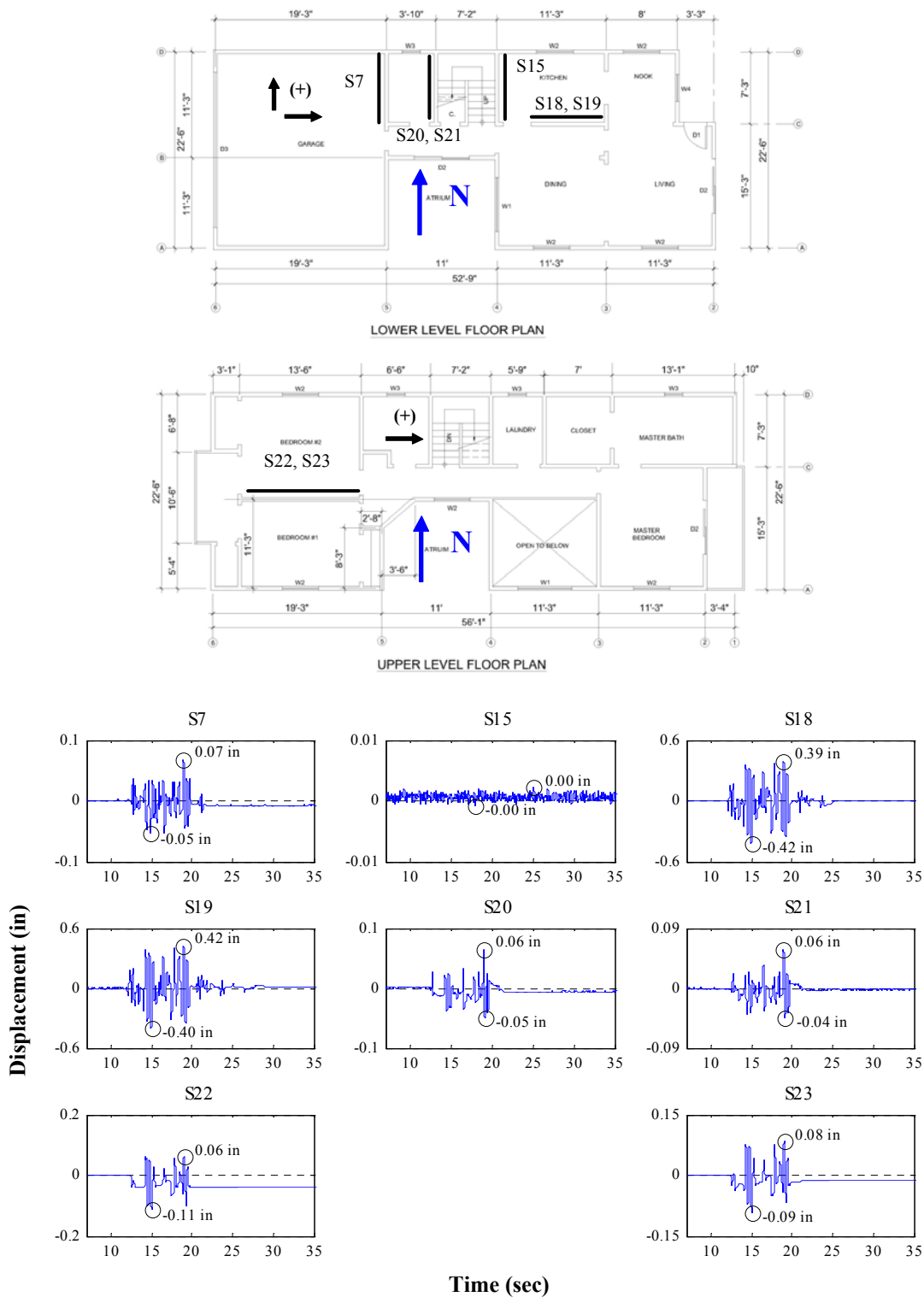


Figure M.27: Wall deformations of internal walls for Test NWP1S10

Appendix M

Phase 2, NWP2S01 Seismic Test, North-South, External Walls

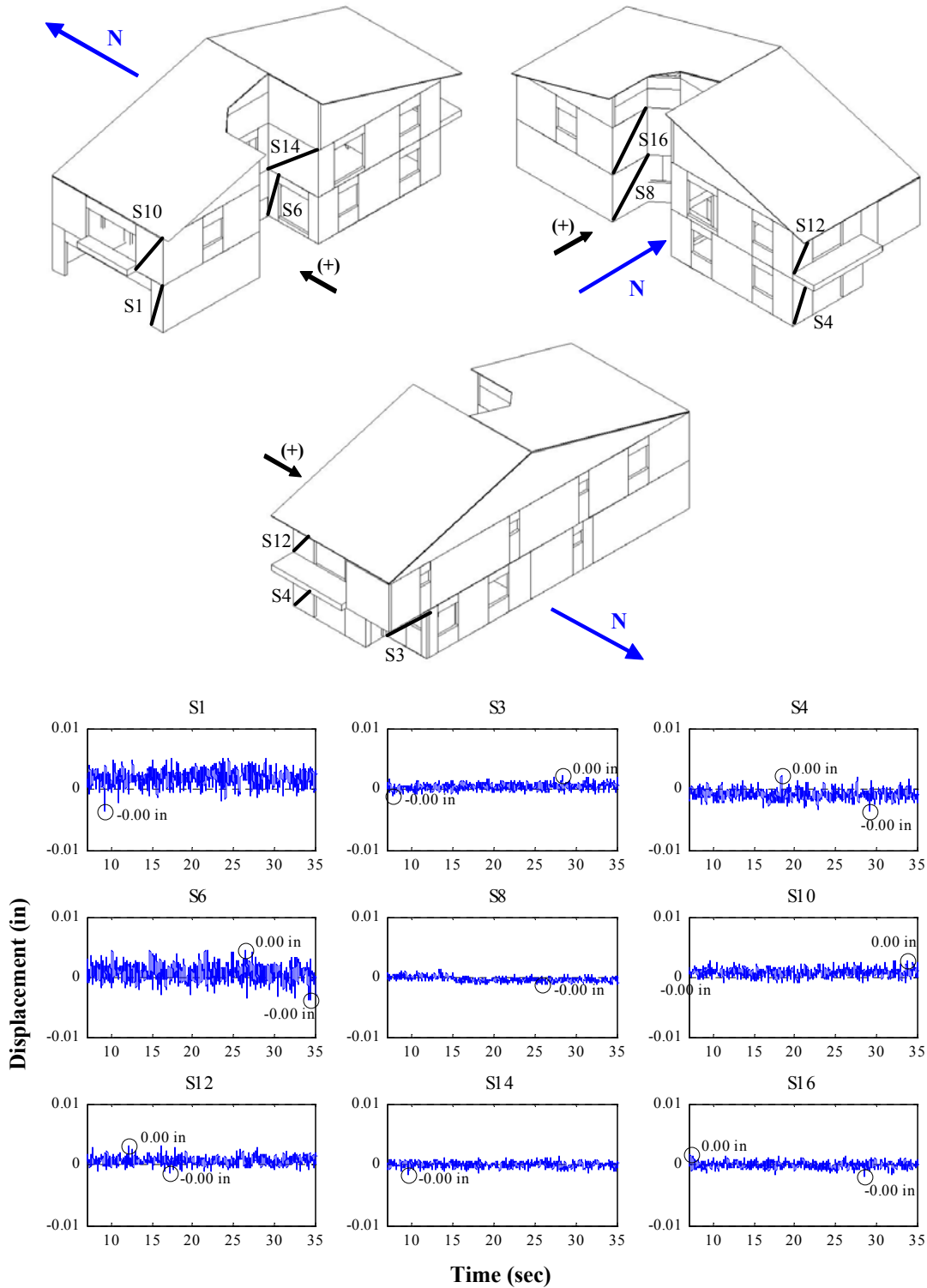


Figure M.28: Wall deformations of north-south external walls for Test NWP2S01

Appendix M

Phase 2, NWP2S01 Seismic Test, East-West, External Walls

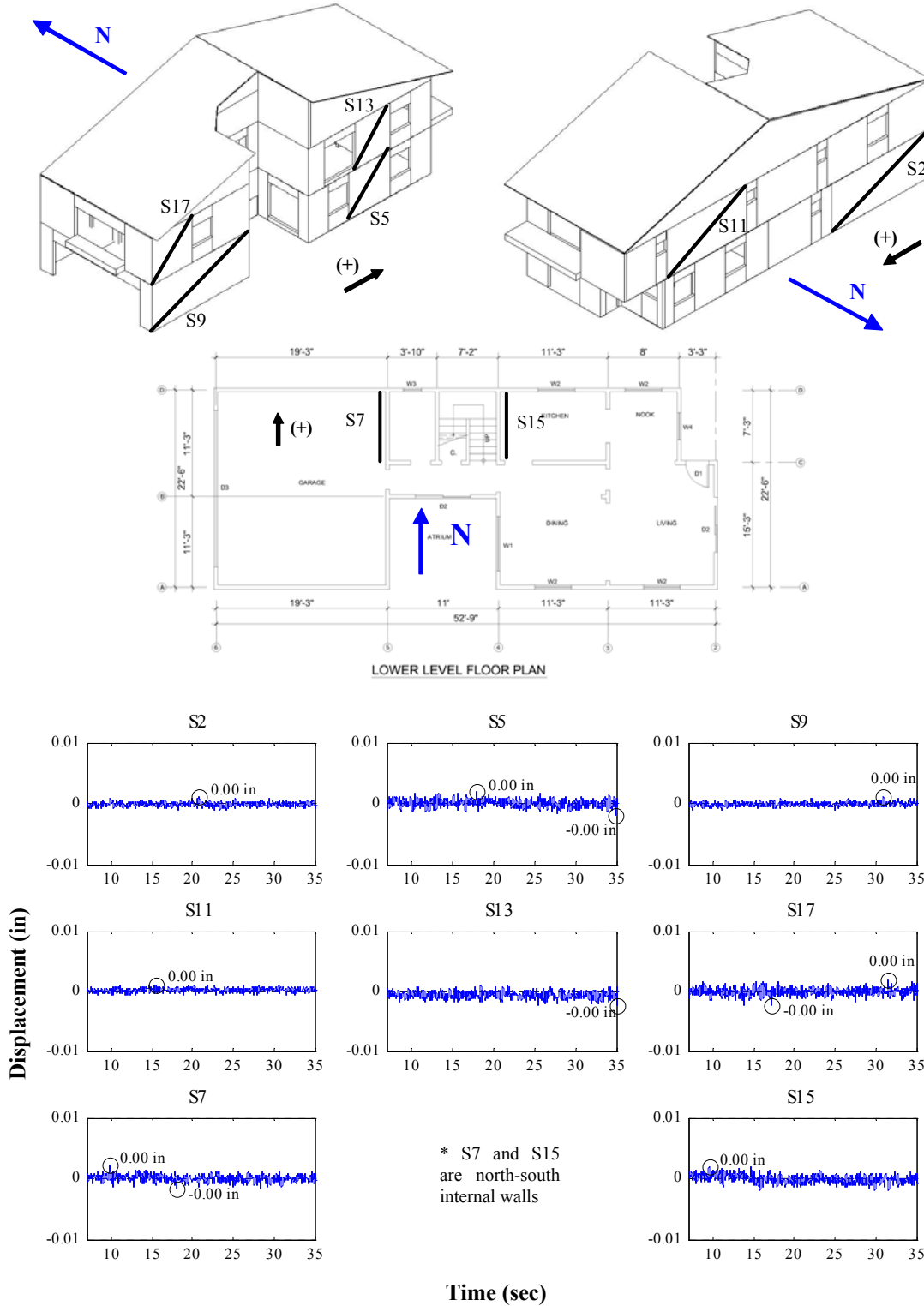


Figure M.29: Wall deformations of east-west internal walls for Test NWP2S01

Appendix M

Phase 2, NWP2S02 Seismic Test, North-South, External Walls

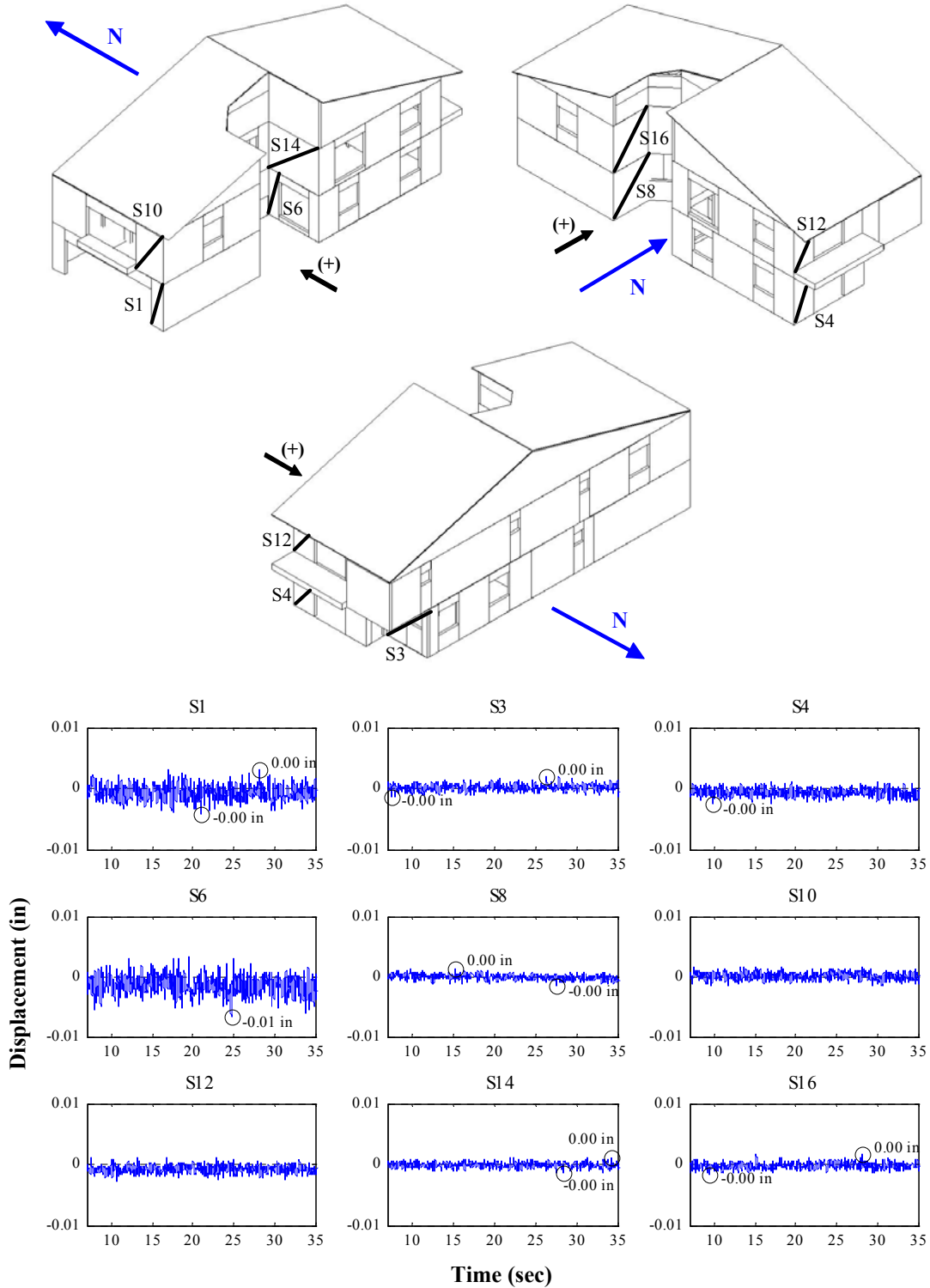


Figure M.30: Wall deformations of north-south external walls for Test NWP2S02

Appendix M

Phase 2, NWP2S02 Seismic Test, East-West, External Walls

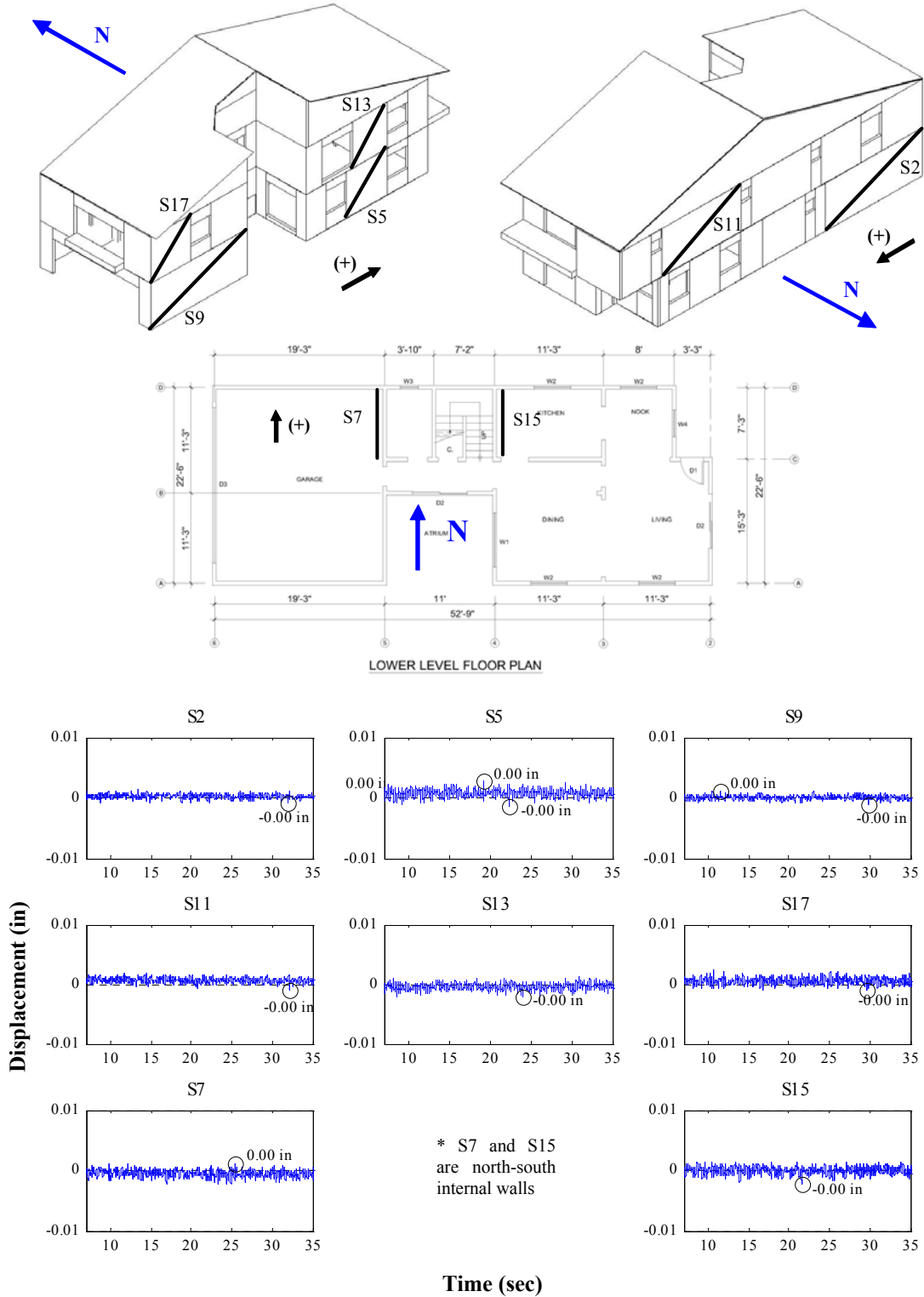


Figure M.31: Wall deformations of east-west internal walls for Test NWP2S02

Appendix M

Phase 2, NWP2S03 Seismic Test, North-South, External Walls

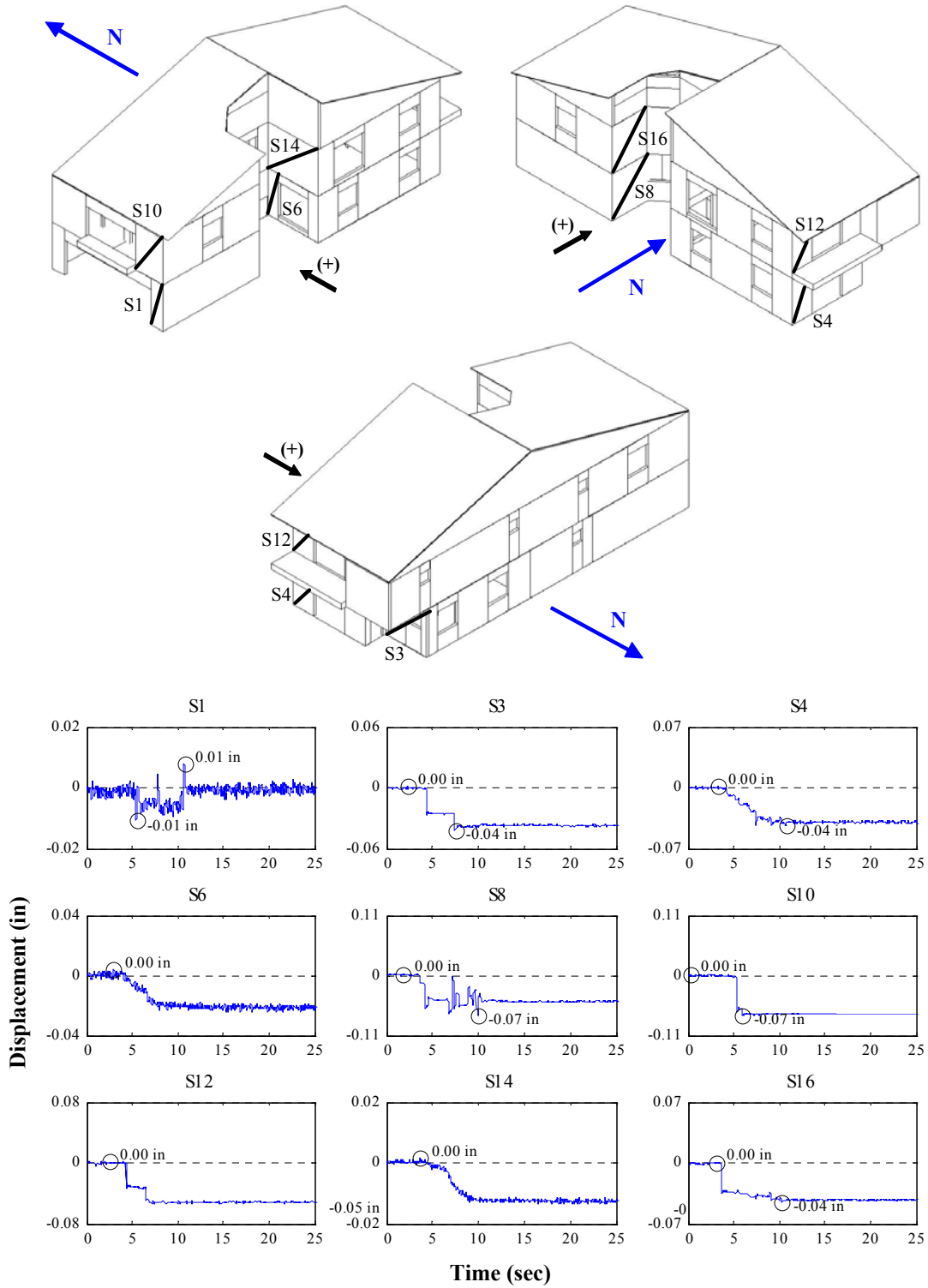


Figure M.32: Wall deformations of north-south external walls for Test NWP2S03

Appendix M

Phase 2, NWP2S03 Seismic Test, East-West, External Walls

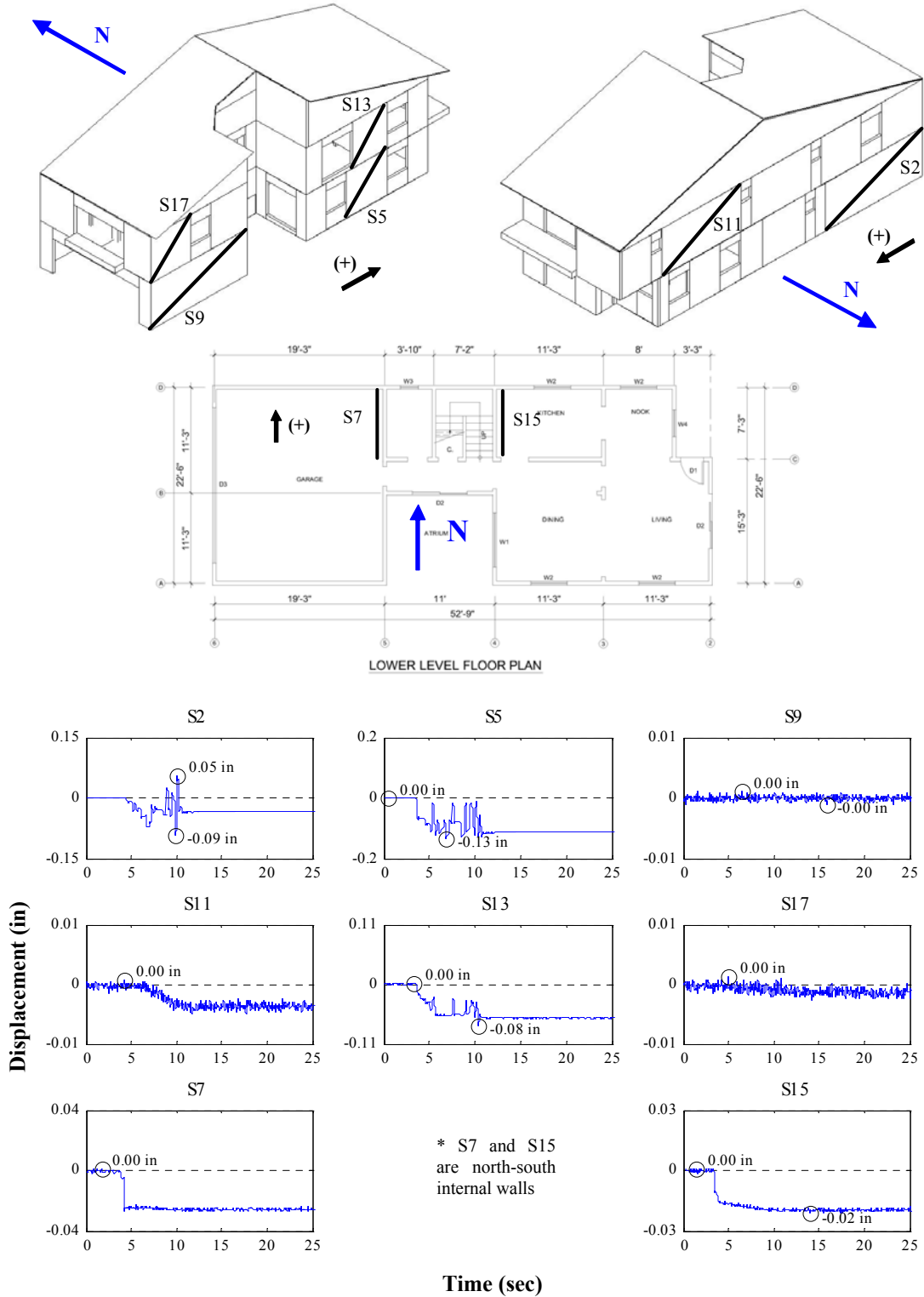


Figure M.33: Wall deformations of east-west internal walls for Test NWP2S03

Appendix M

Phase 2, NWP2S04 Seismic Test, North-South, External Walls

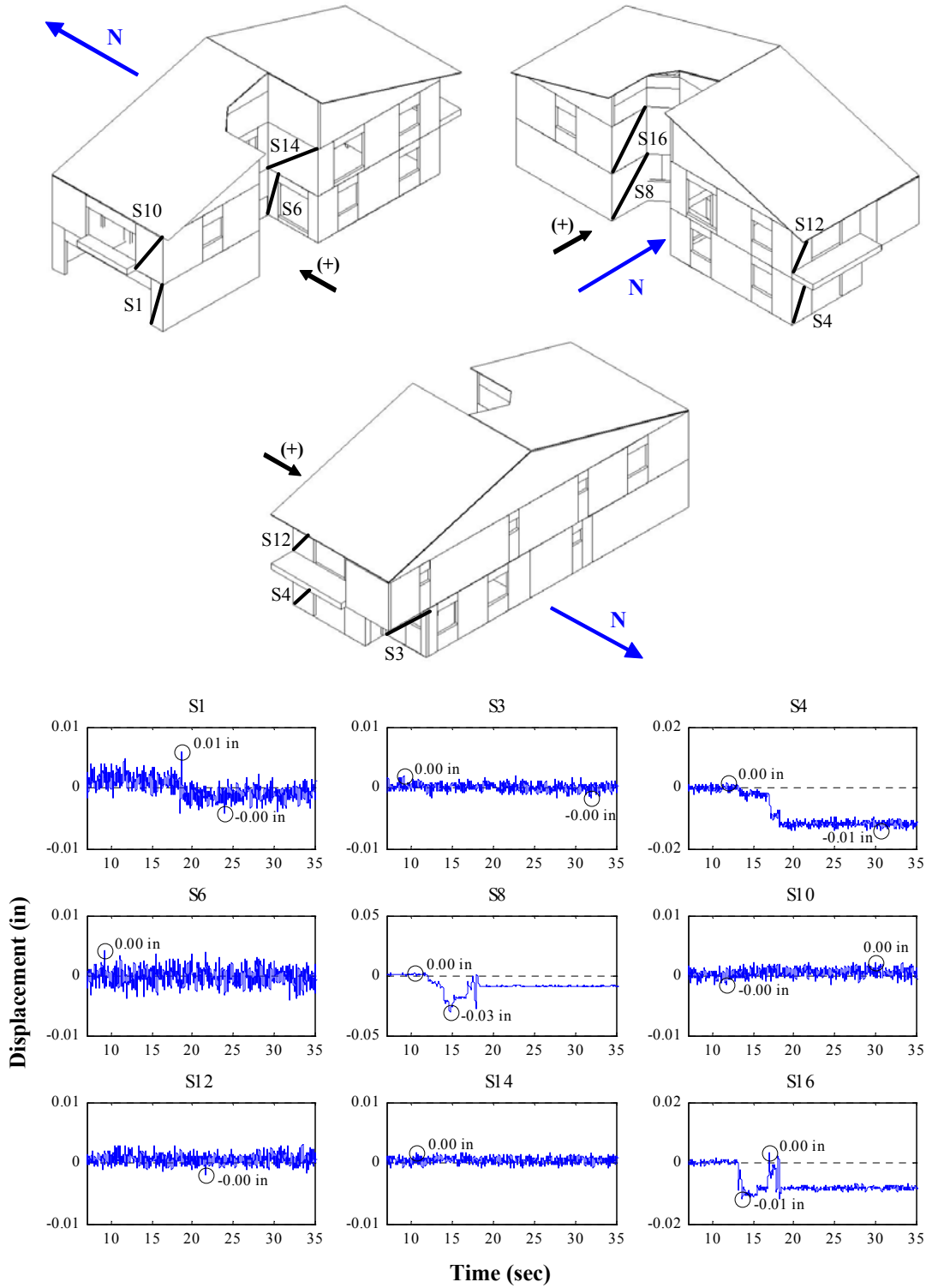


Figure M.34: Wall deformations of north-south external walls for Test NWP2S04

Appendix M

Phase 2, NWP2S04 Seismic Test, East-West, External Walls

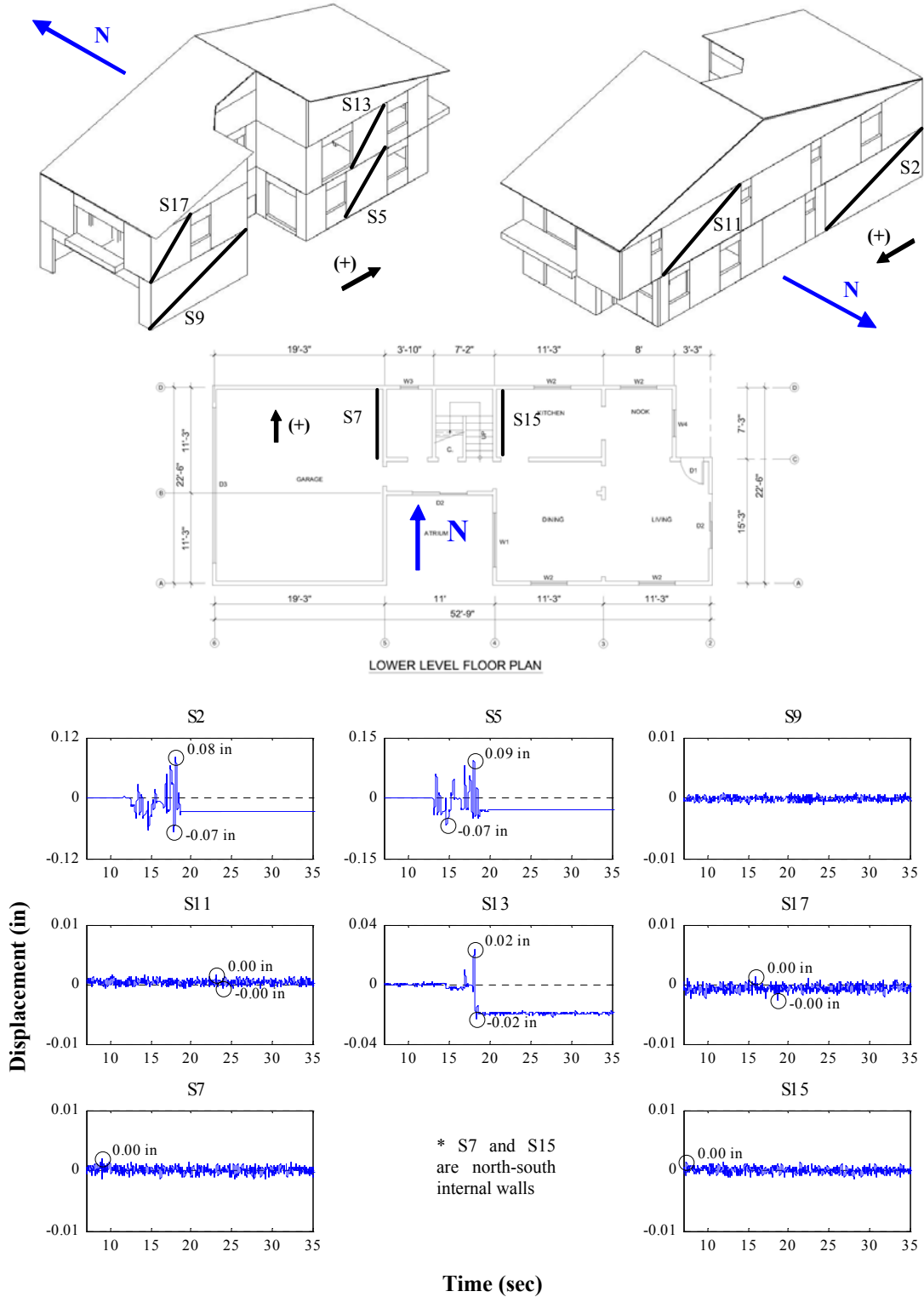


Figure M.35: Wall deformations of east-west internal walls for Test NWP2S04

Appendix M

Phase 2, NWP2S05 Seismic Test, North-South, External Walls

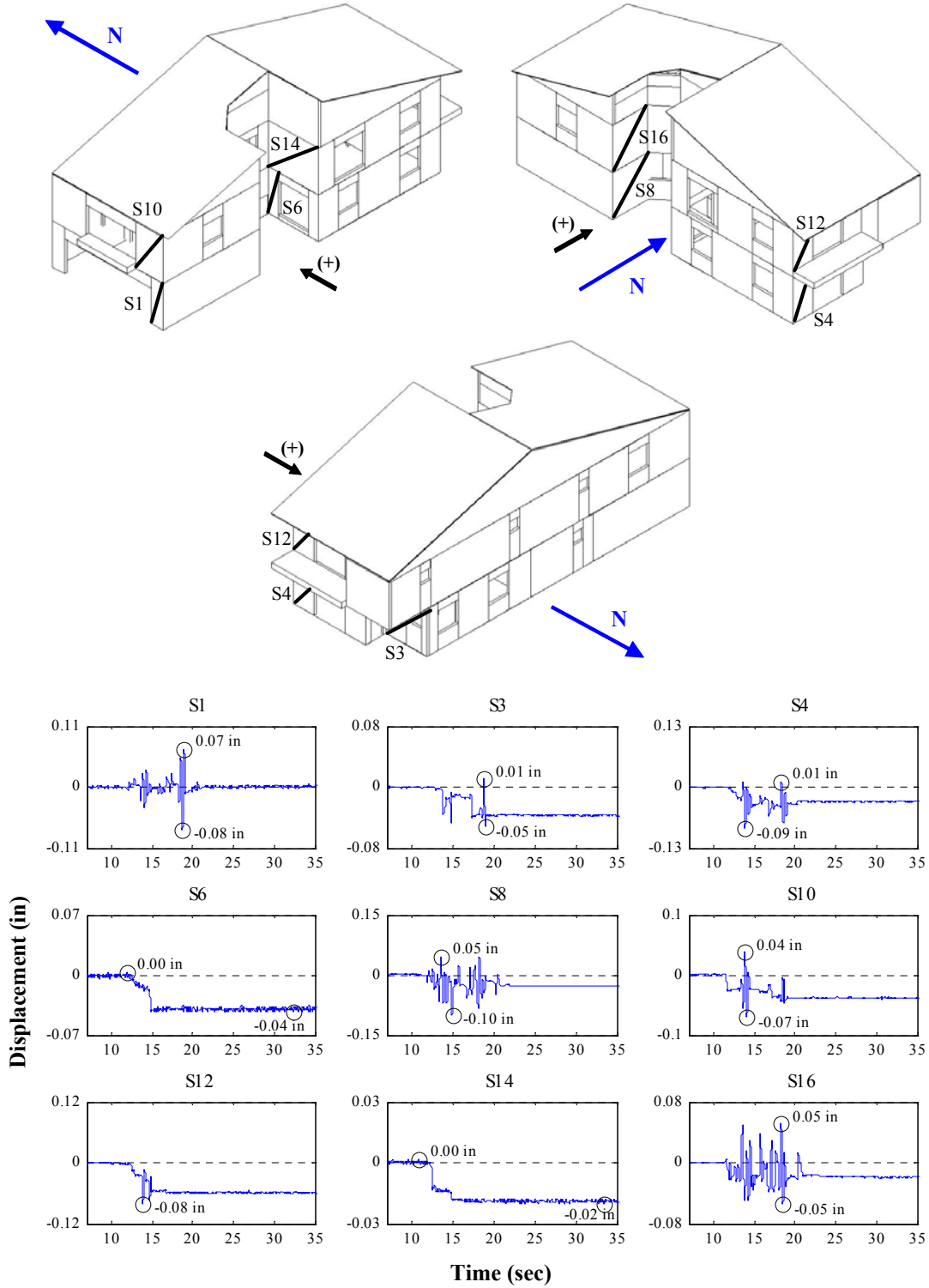


Figure M.36: Wall deformations of north-south external walls for Test NWP2S05

Appendix M

Phase 2, NWP2S05 Seismic Test, East-West, External Walls

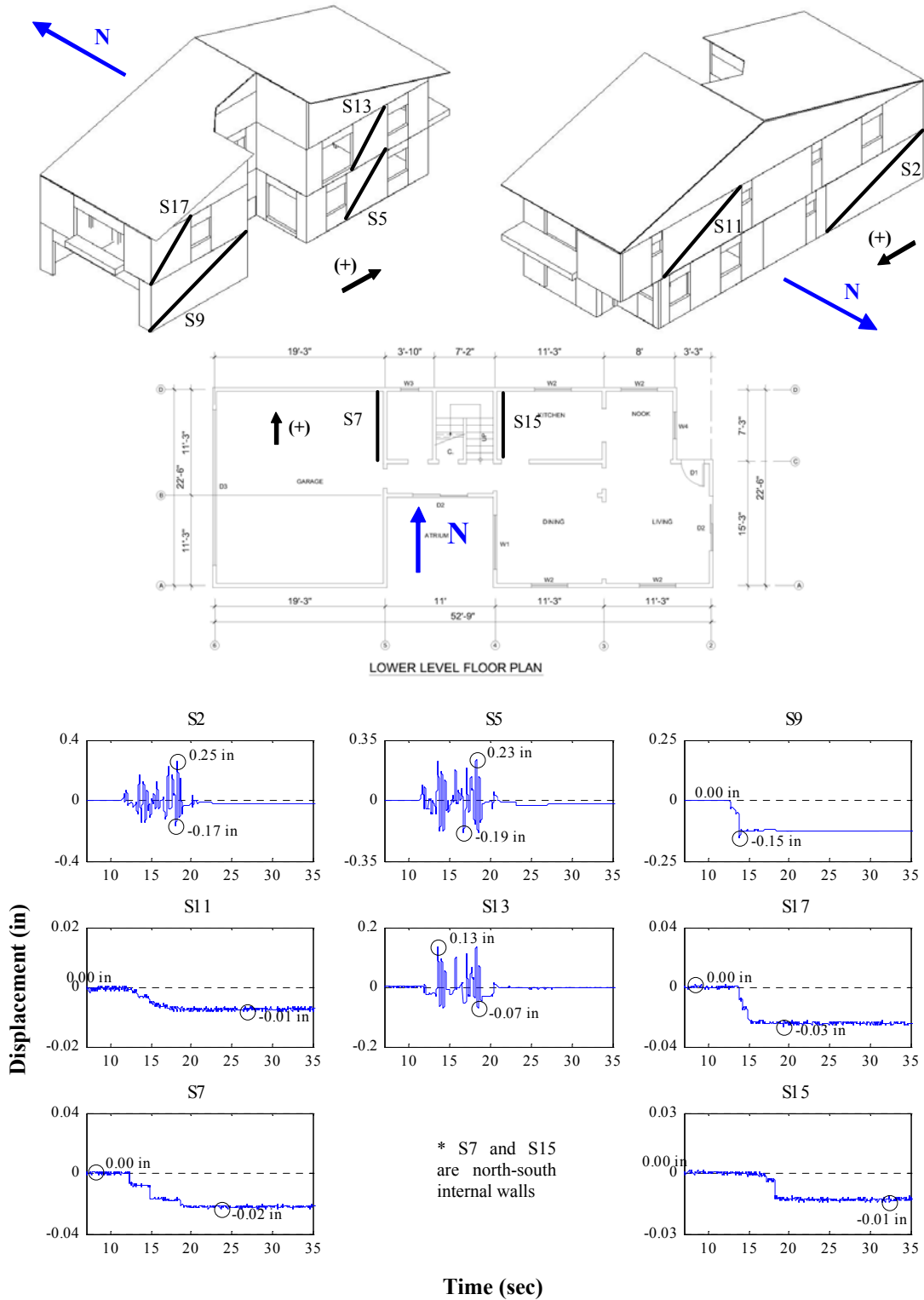


Figure M.37: Wall deformations of east-west internal walls for Test NWP2S05

Appendix M

Phase 2, NWP2S06 Seismic Test, North-South, External Walls

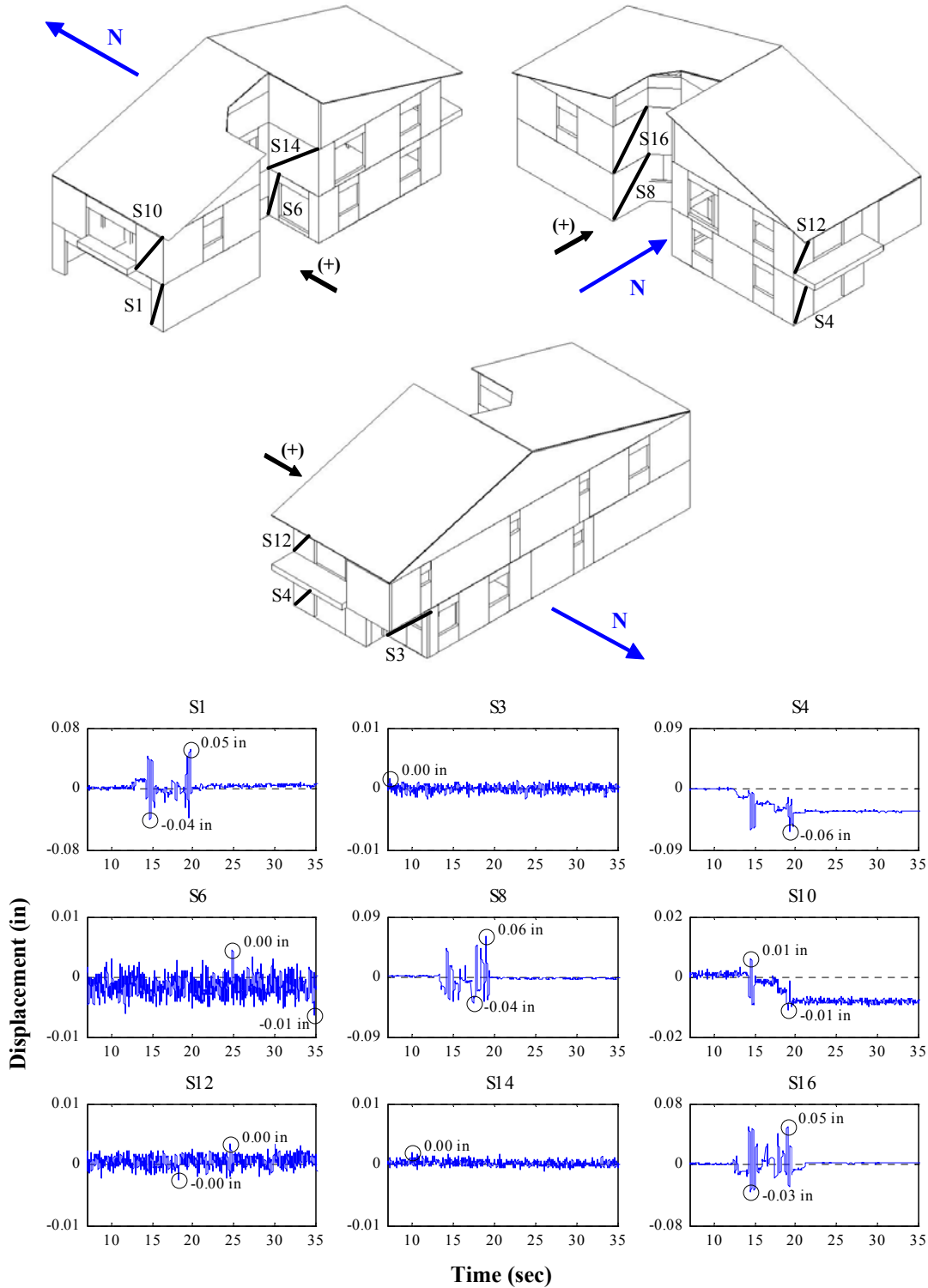


Figure M.38: Wall deformations of north-south external walls for Test NWP2S06

Appendix M

Phase 2, NWP2S06 Seismic Test, East-West, External Walls

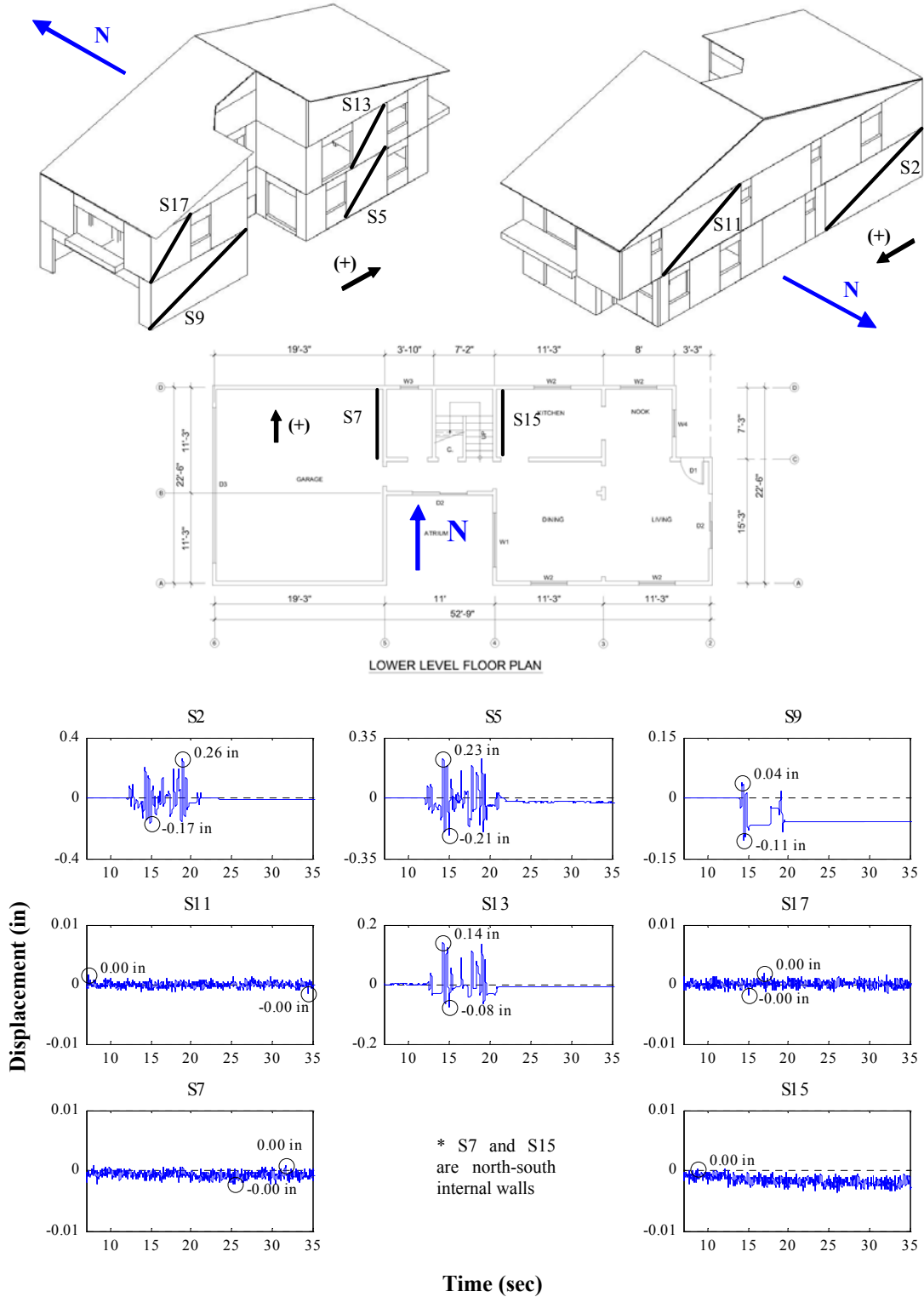


Figure M.39: Wall deformations of east-west internal walls for Test NWP2S06

Appendix M

Phase 2, NWP2S07 Seismic Test, North-South, External Walls

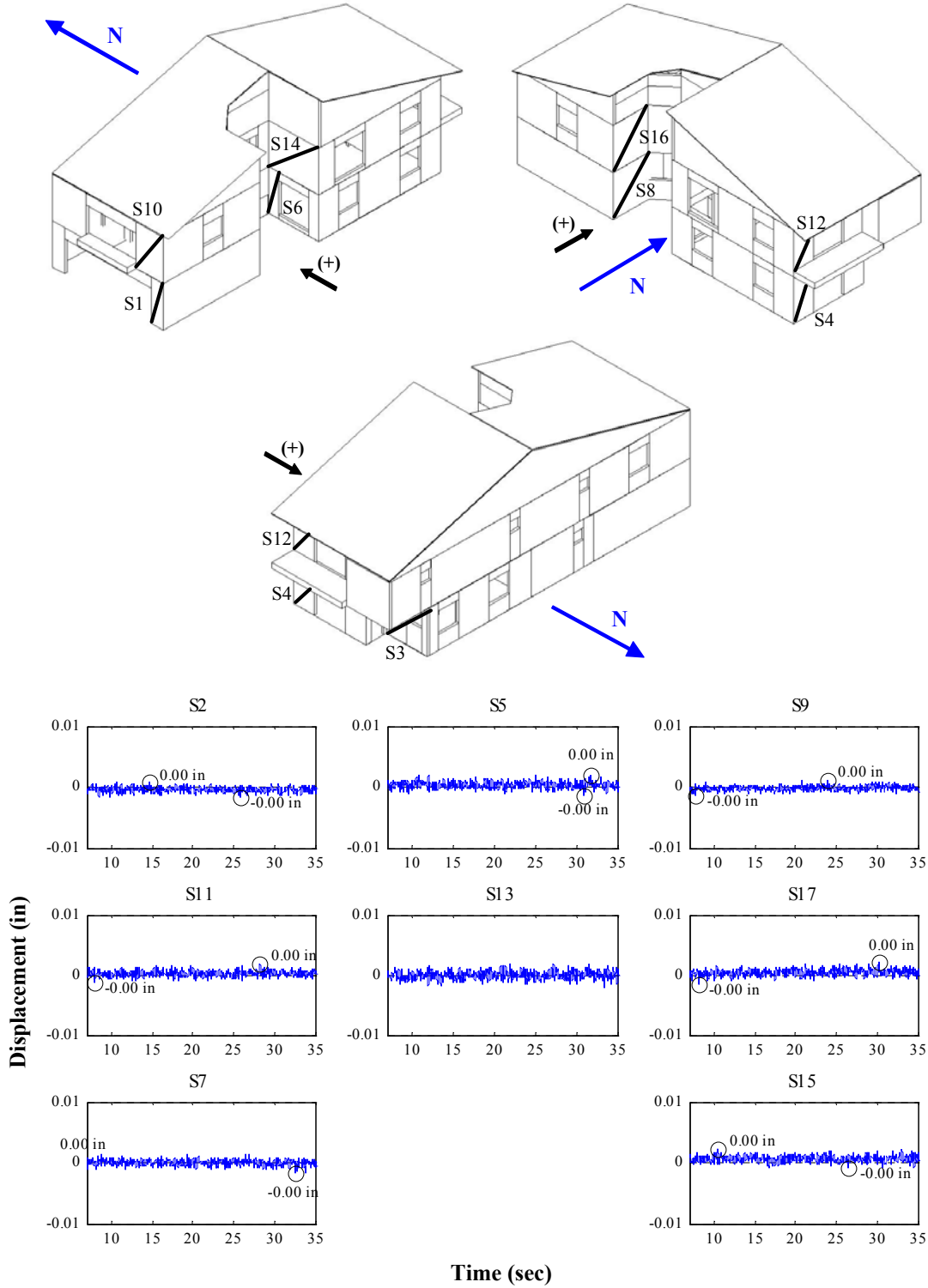


Figure M.40: Wall deformations of north-south external walls for Test NWP2S07

Appendix M

Phase 2, NWP2S07 Seismic Test, East-West, External Walls

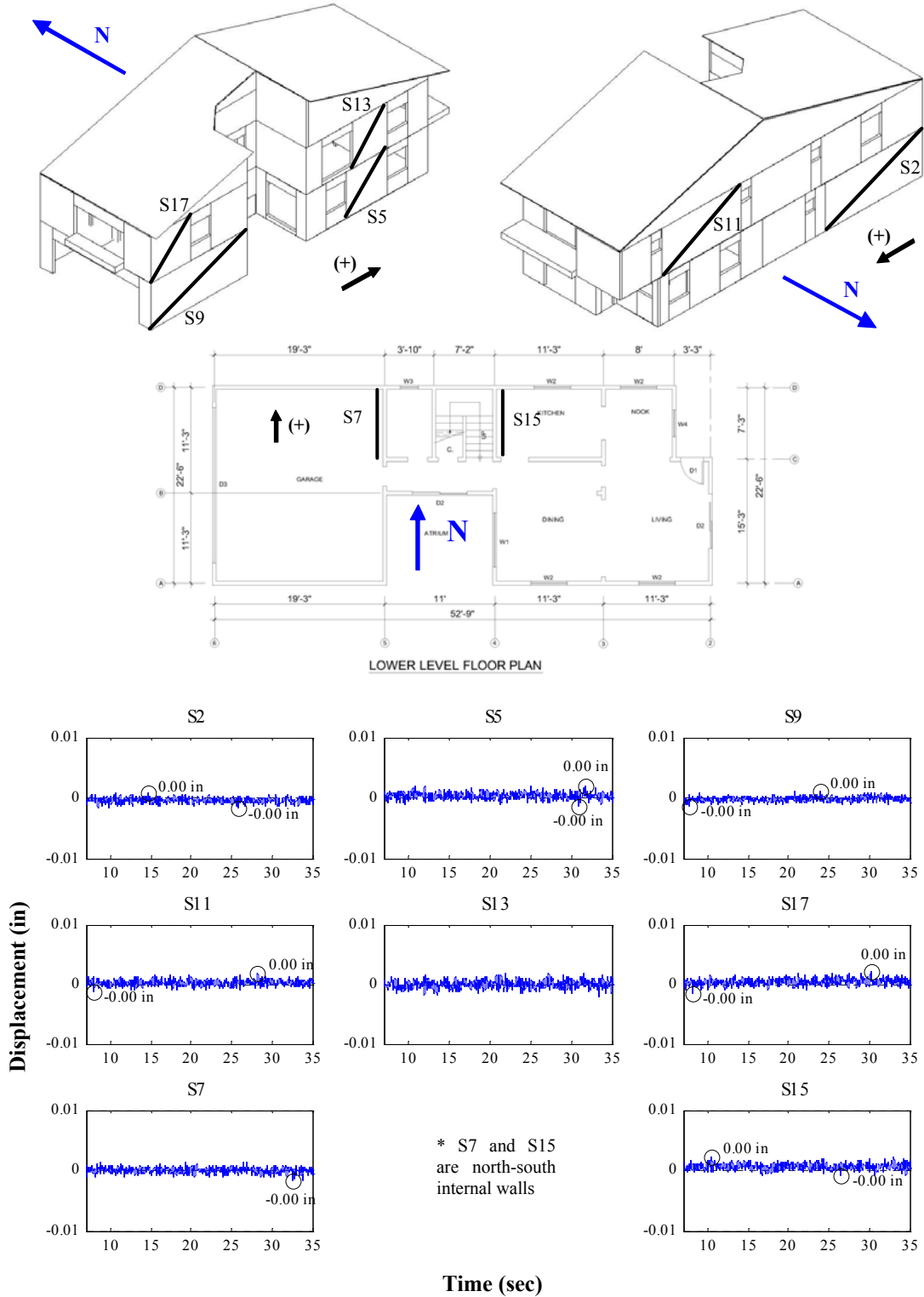


Figure M.41: Wall deformations of east-west internal walls for Test NWP2S07

Appendix M

Phase 2, NWP2S08 Seismic Test, North-South, External Walls

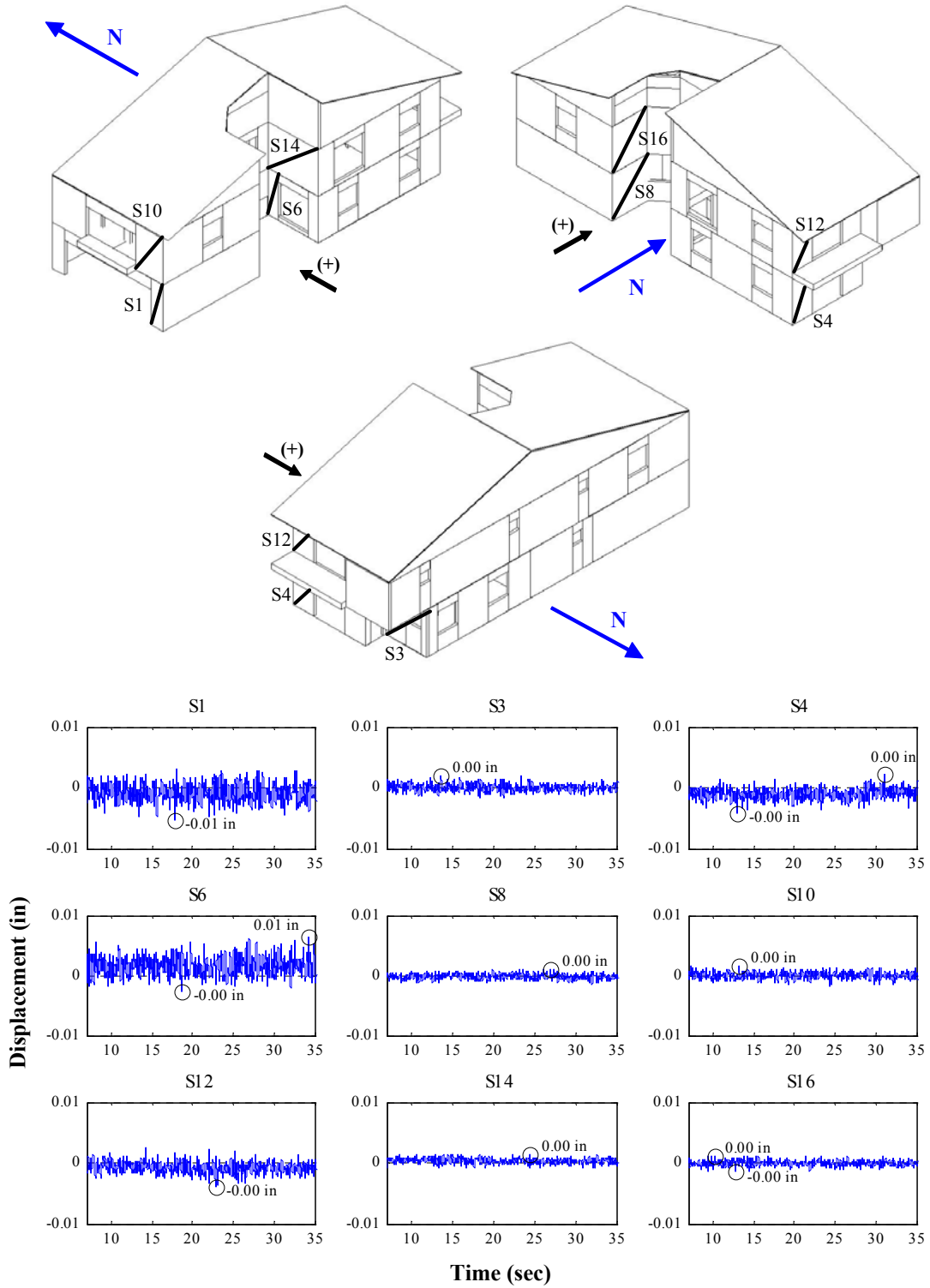


Figure M.42: Wall deformations of north-south external walls for Test NWP2S08

Appendix M

Phase 2, NWP2S08 Seismic Test, East-West, External Walls

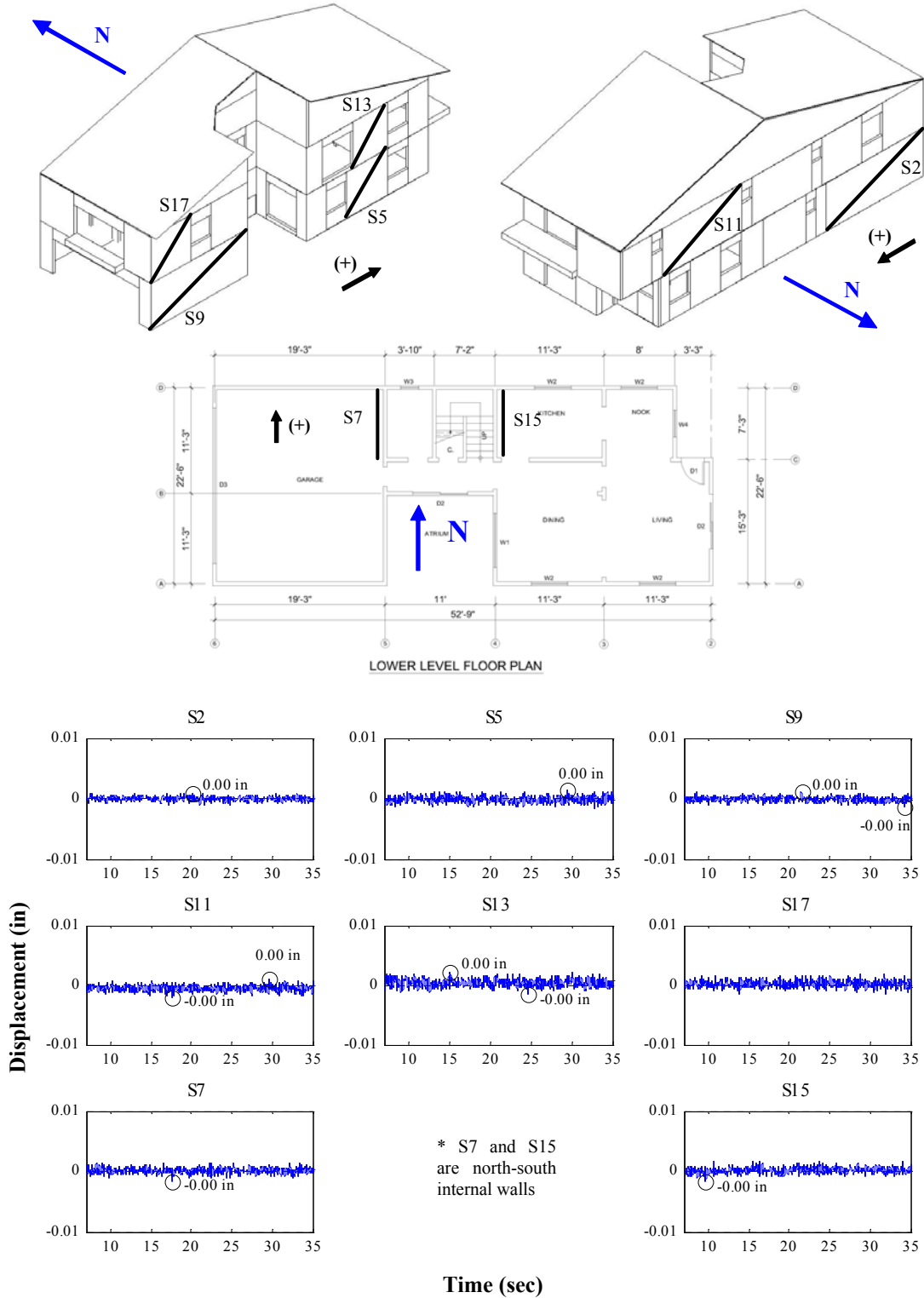


Figure M.43: Wall deformations of east-west internal walls for Test NWP2S08

Appendix M

Phase 2, NWP2S09 Seismic Test, North-South, External Walls

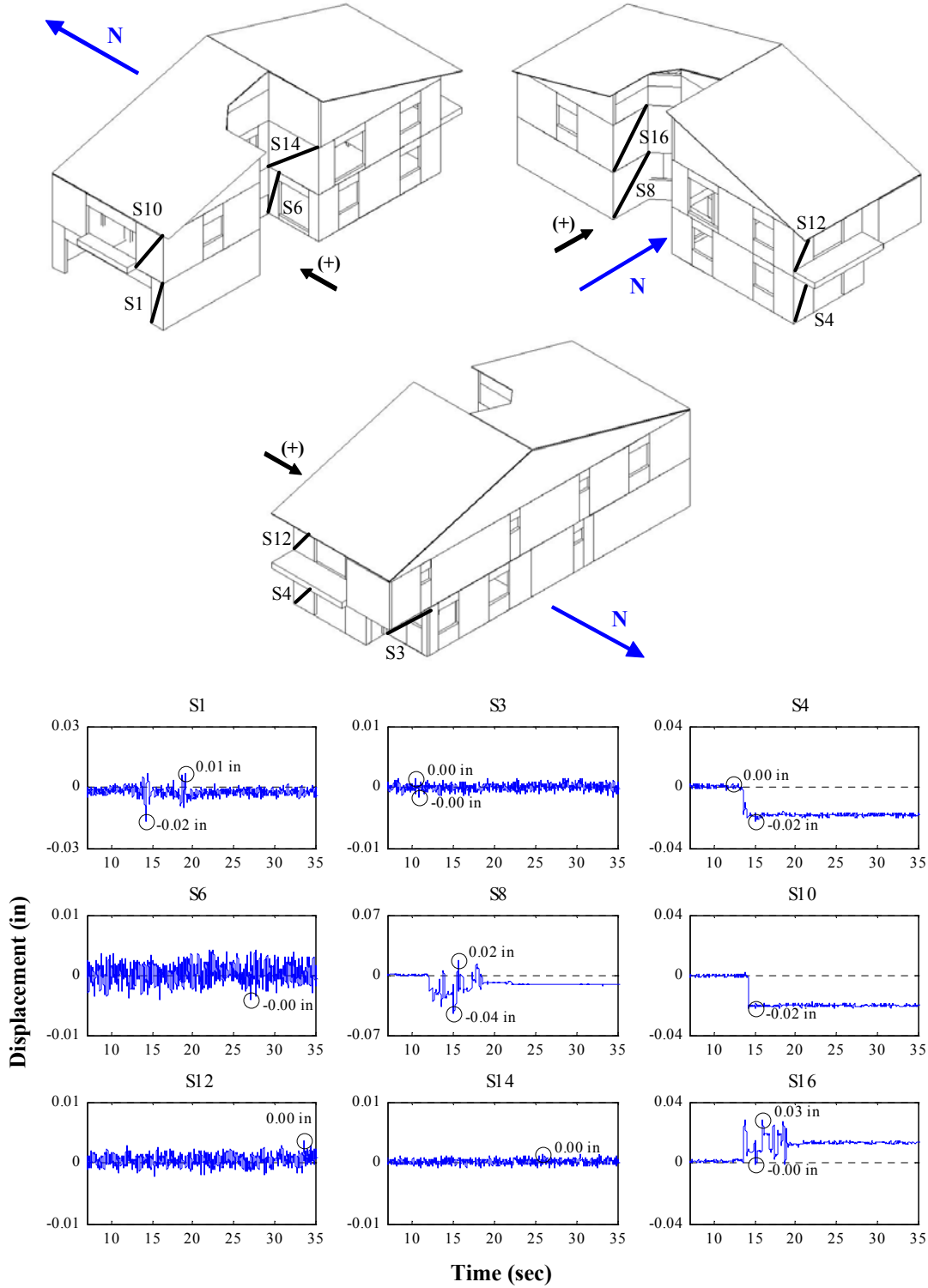


Figure M.44: Wall deformations of north-south external walls for Test NWP2S09

Appendix M

Phase 2, NWP2S09 Seismic Test, East-West, External Walls

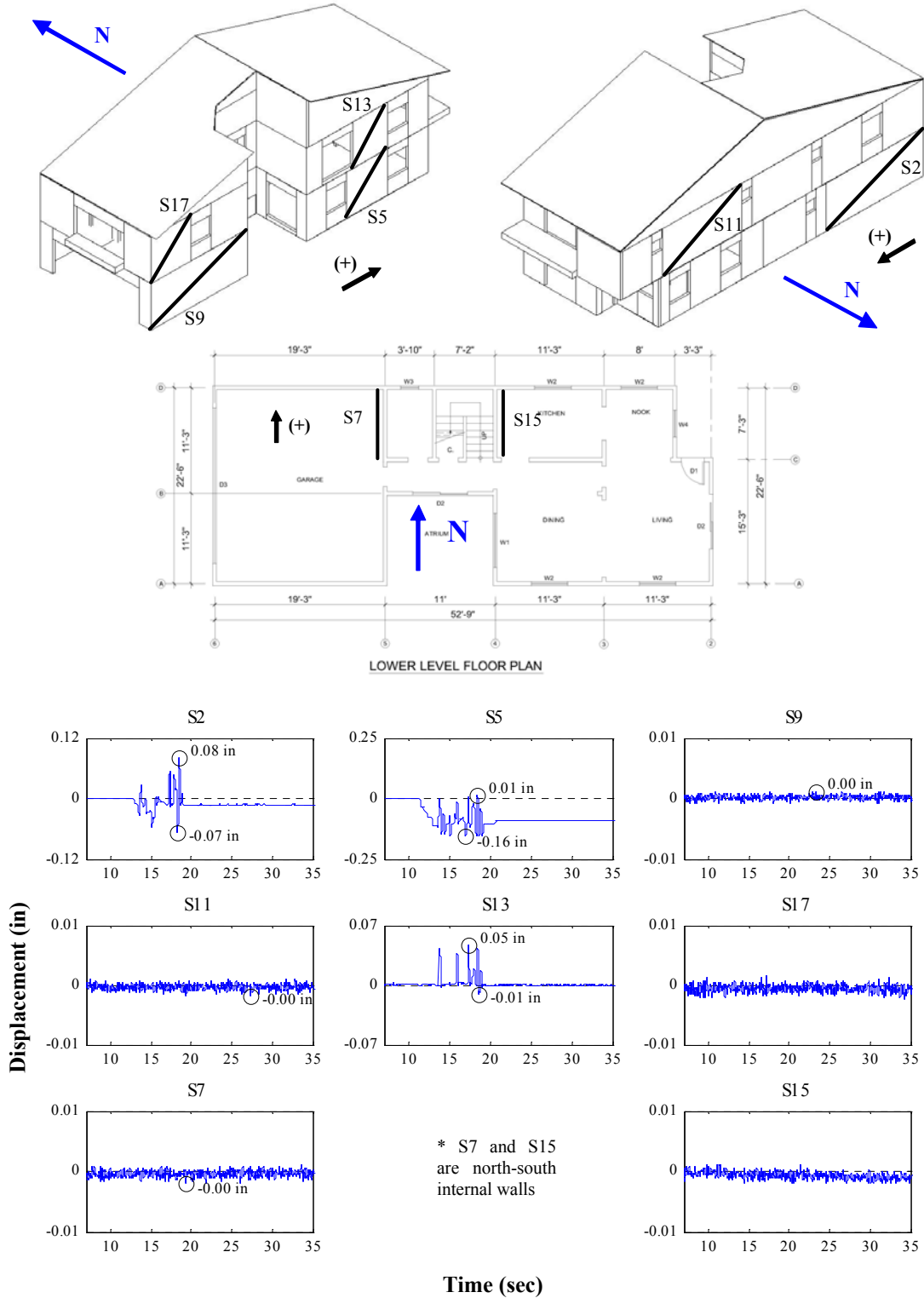


Figure M.45: Wall deformations of east-west internal walls for Test NWP2S09

Appendix M

Phase 2, NWP2S10 Seismic Test, North-South, External Walls

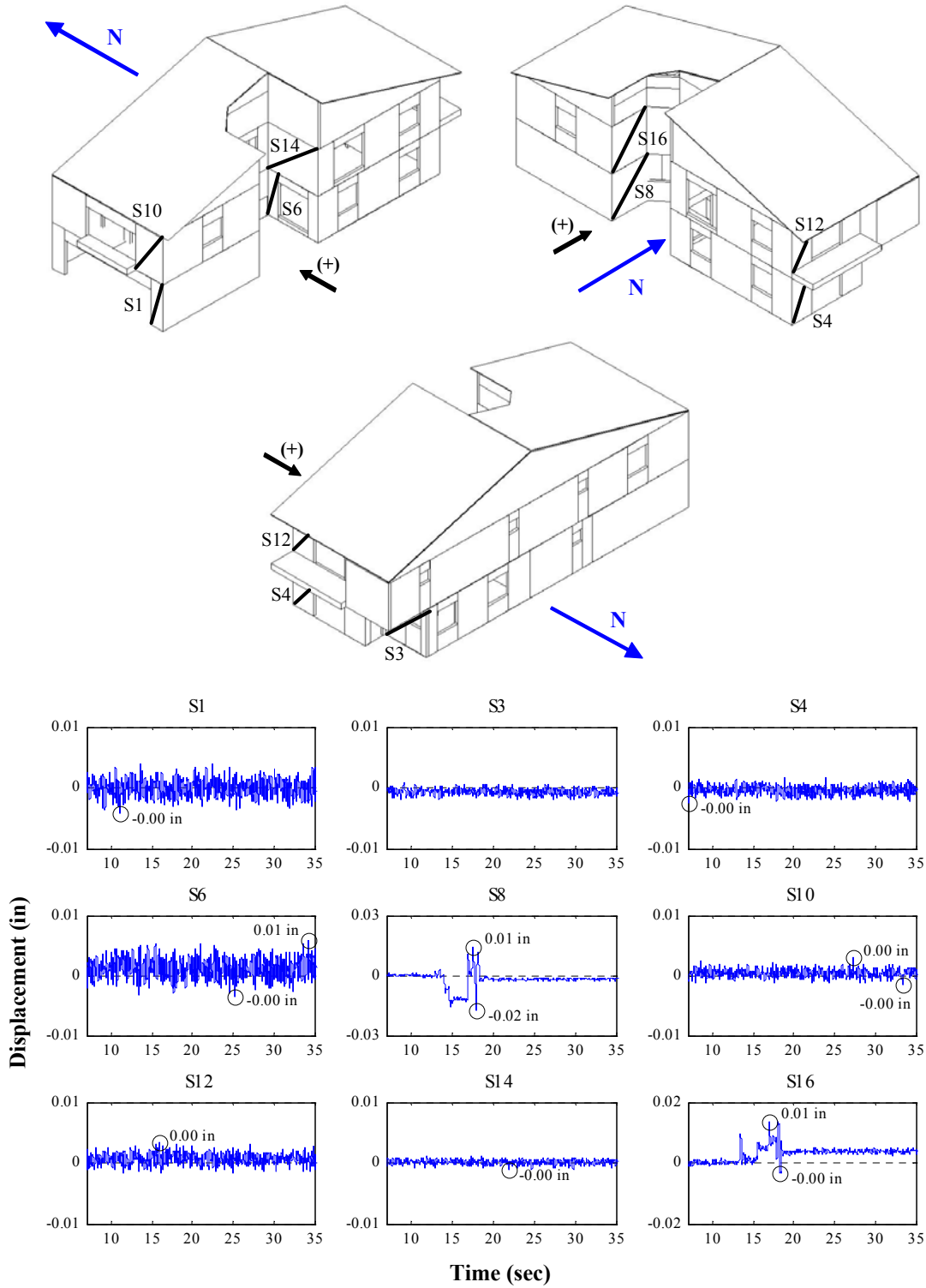


Figure M.46: Wall deformations of north-south external walls for Test NWP2S10

Appendix M

Phase 2, NWP2S10 Seismic Test, East-West, External Walls

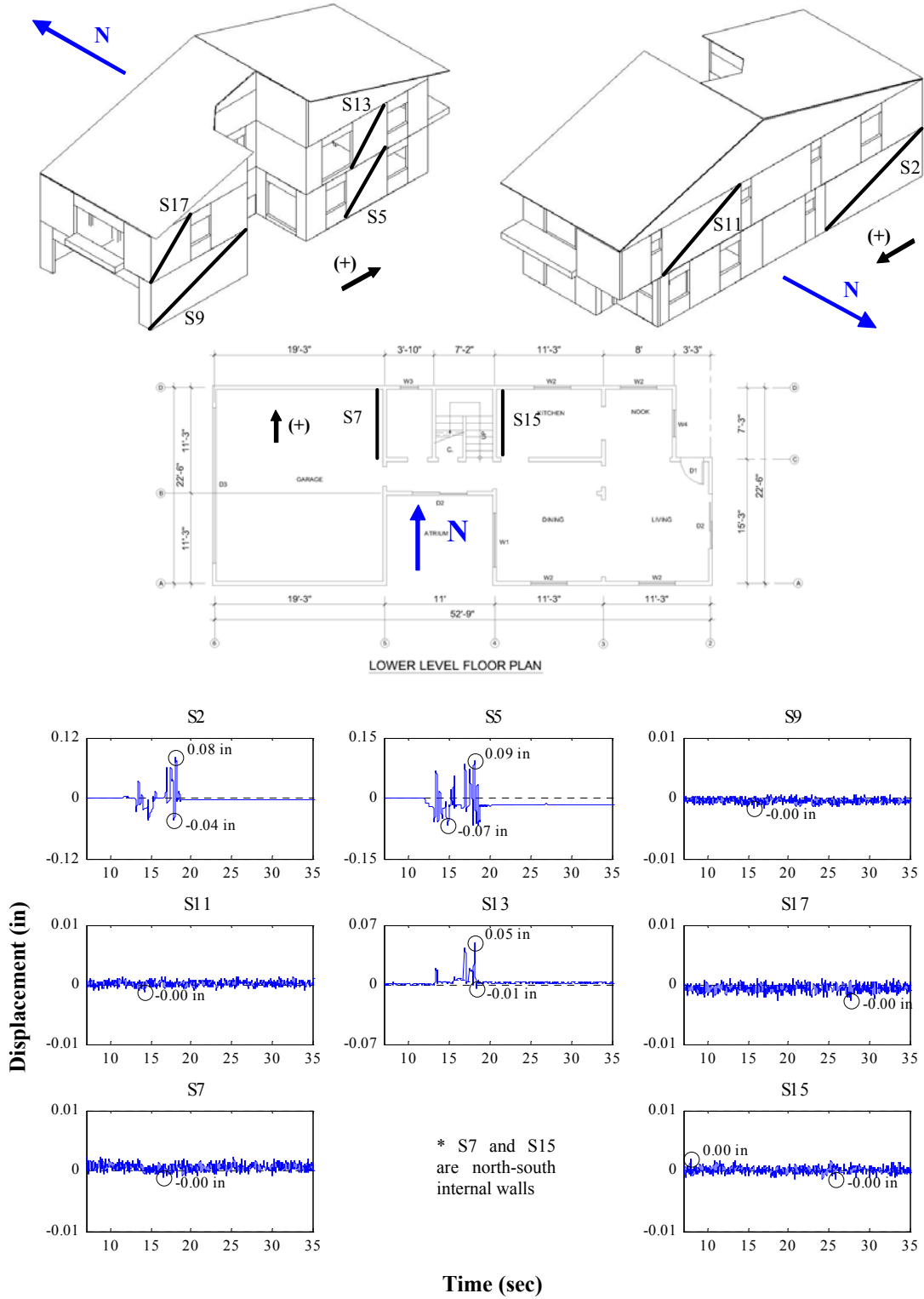


Figure M.47: Wall deformations of east-west internal walls for Test NWP2S10

Appendix M

Phase 2, NWP2S11 Seismic Test, North-South, External Walls

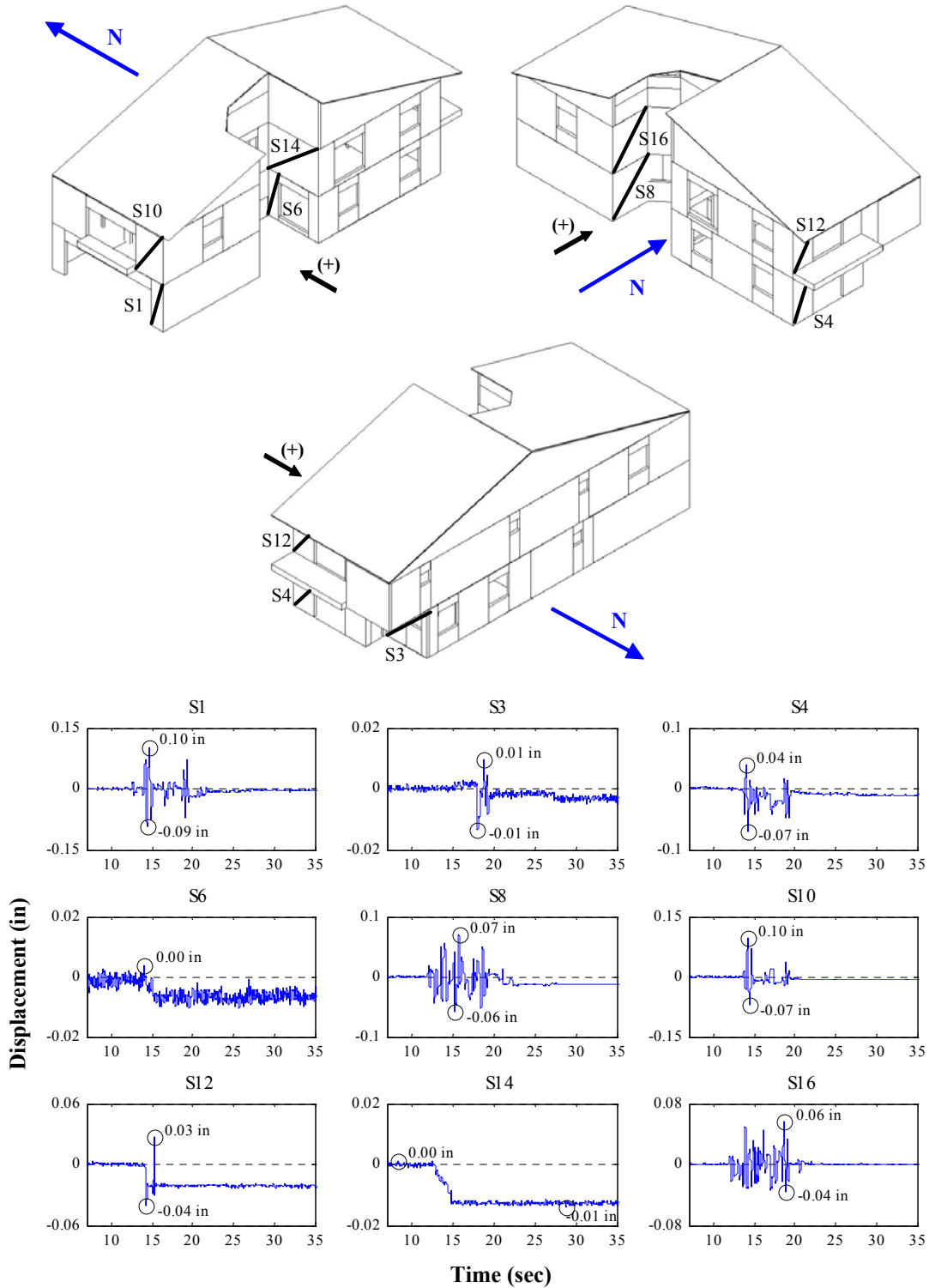


Figure M.48: Wall deformations of north-south external walls for Test NWP2S11

Appendix M

Phase 2, NWP2S11 Seismic Test, East-West, External Walls

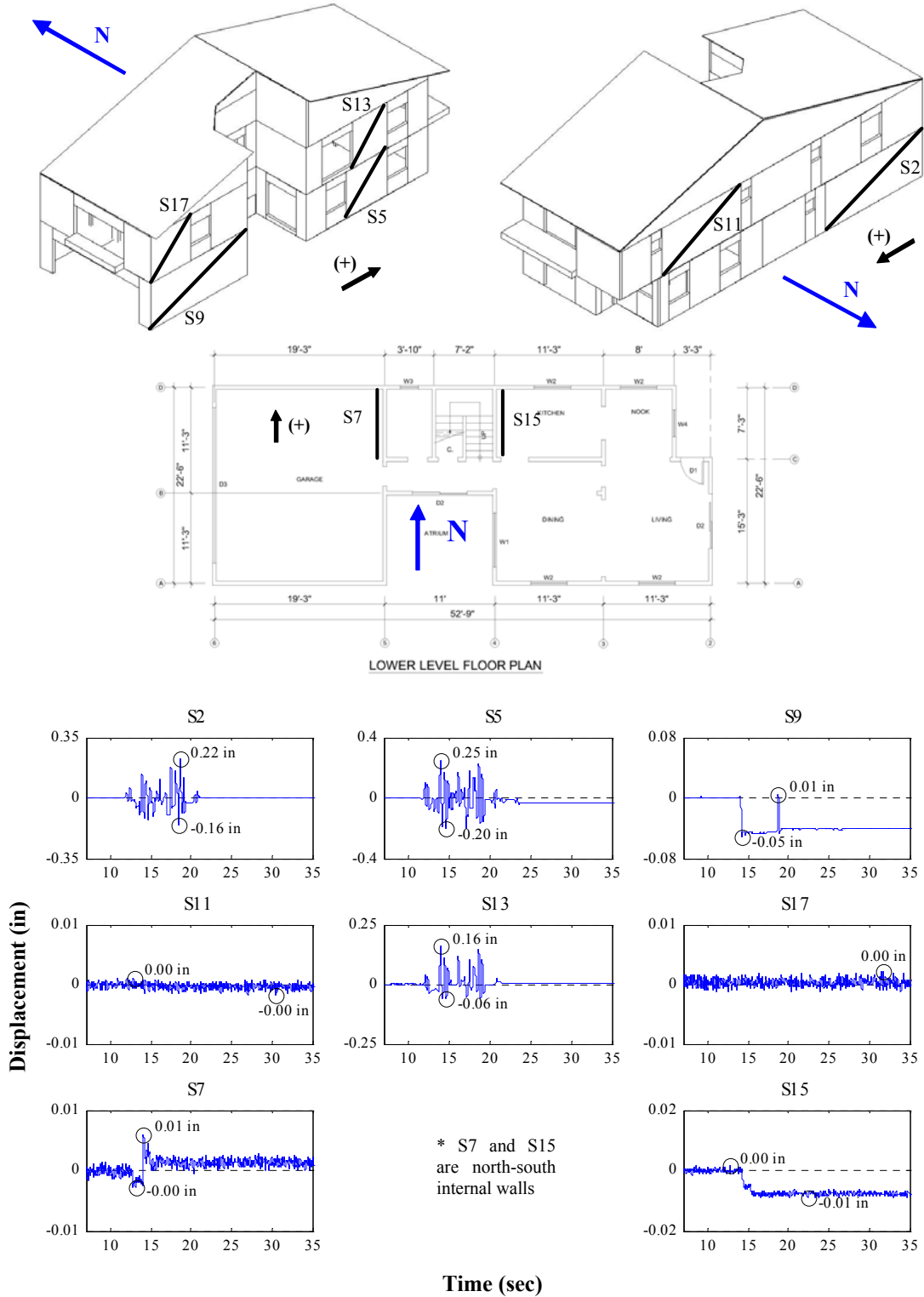


Figure M.49: Wall deformations of east-west internal walls for Test NWP2S11

Appendix M

Phase 2, NWP2S12 Seismic Test, North-South, External Walls

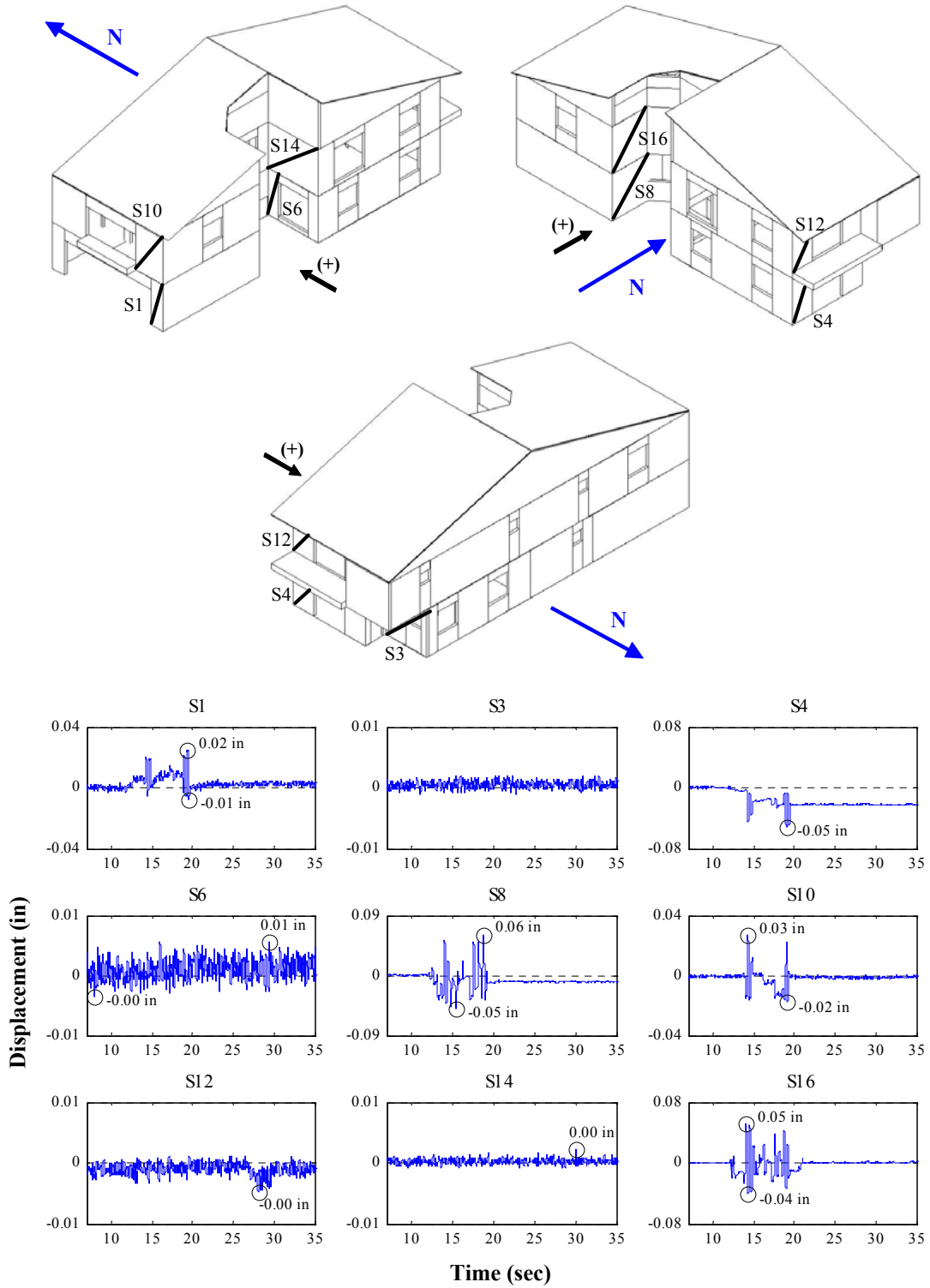


Figure M.50: Wall deformations of north-south external walls for Test NWP2S12

Appendix M

Phase 2, NWP2S12 Seismic Test, East-West, External Walls

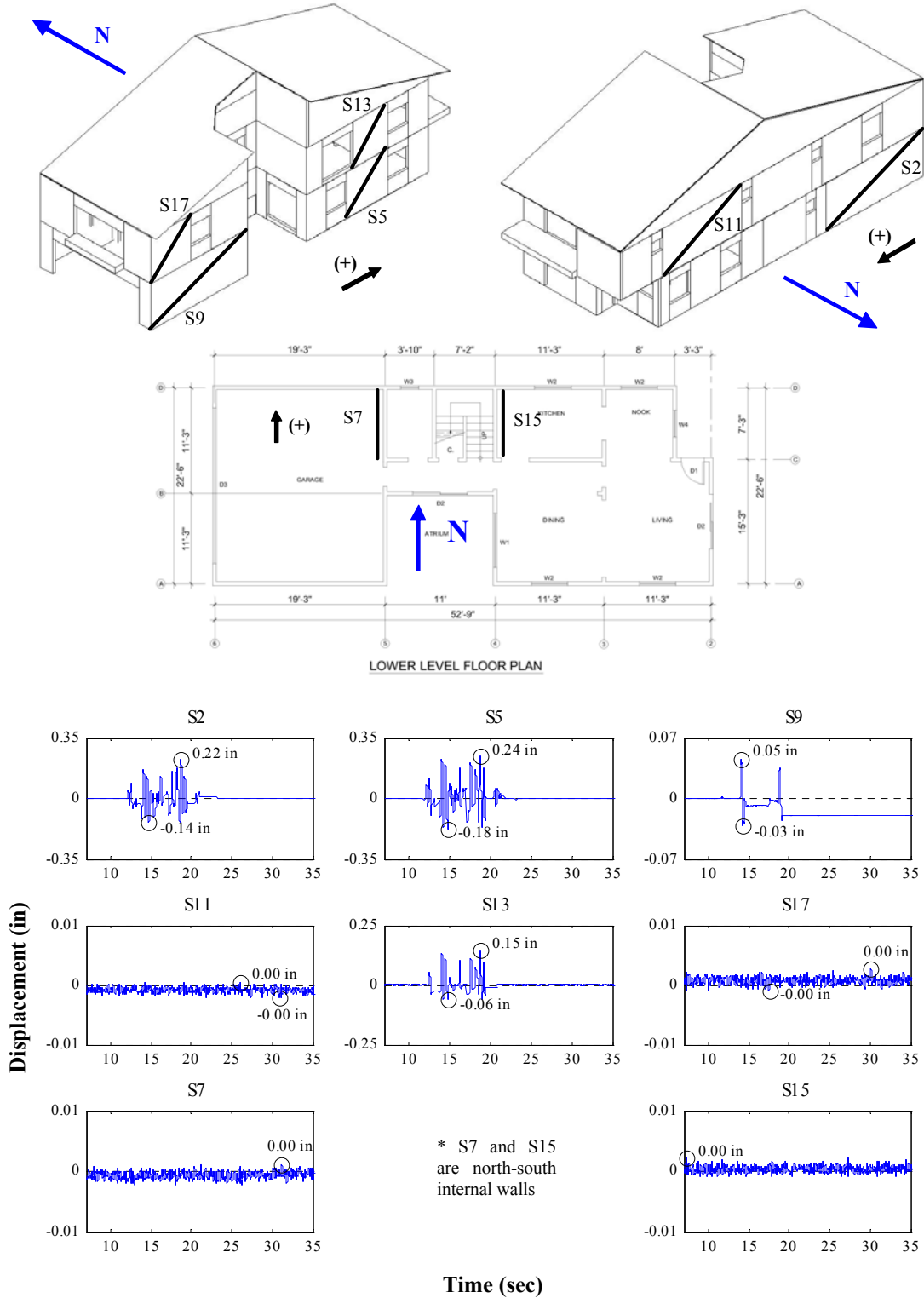


Figure M.51: Wall deformations of east-west internal walls for Test NWP2S12

Appendix M

Phase 2, NWP2S13 Seismic Test, North-South, External Walls

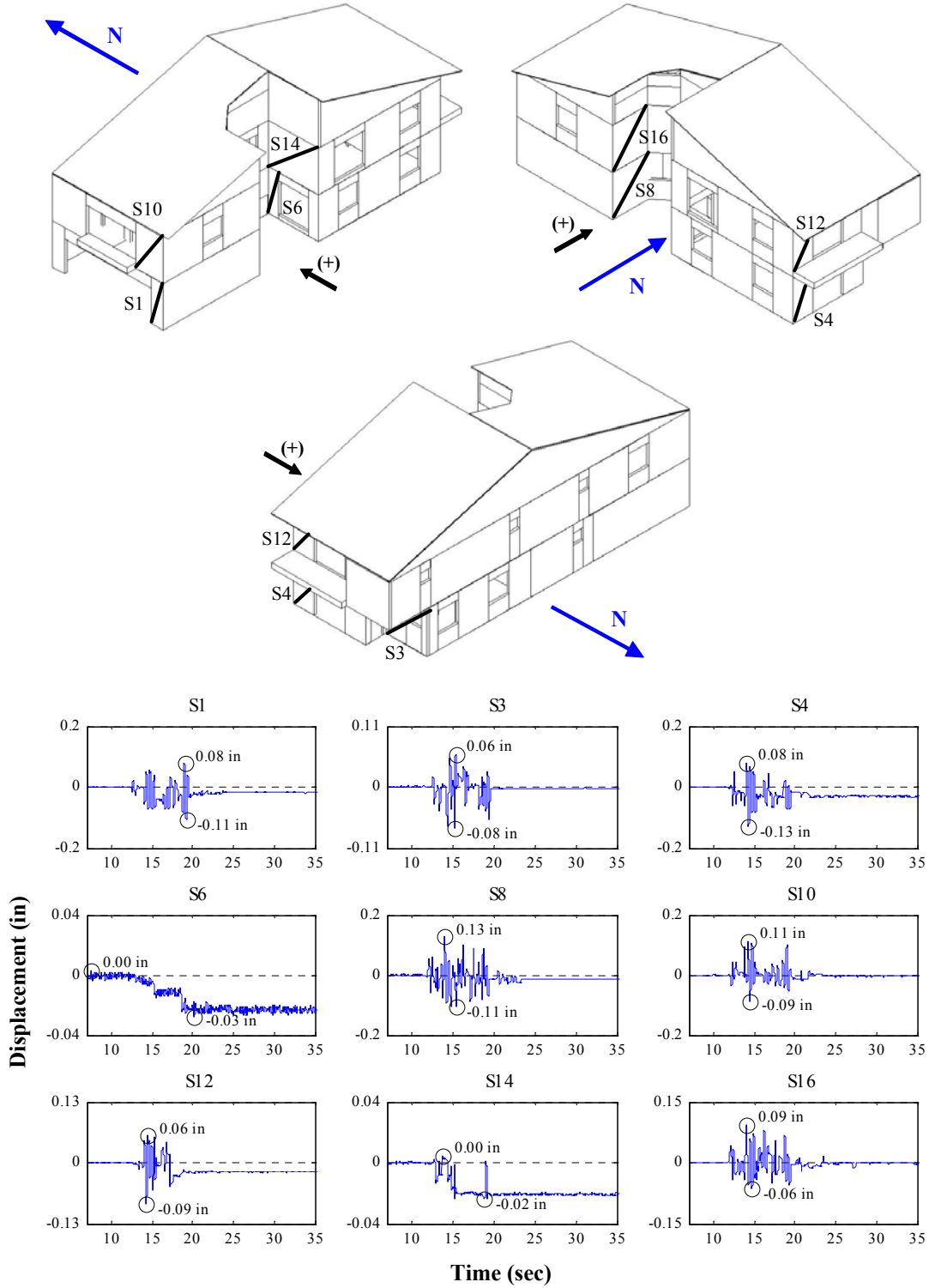


Figure M.52: Wall deformations of north-south external walls for Test NWP2S13

Appendix M

Phase 2, NWP2S13 Seismic Test, East-West, External Walls

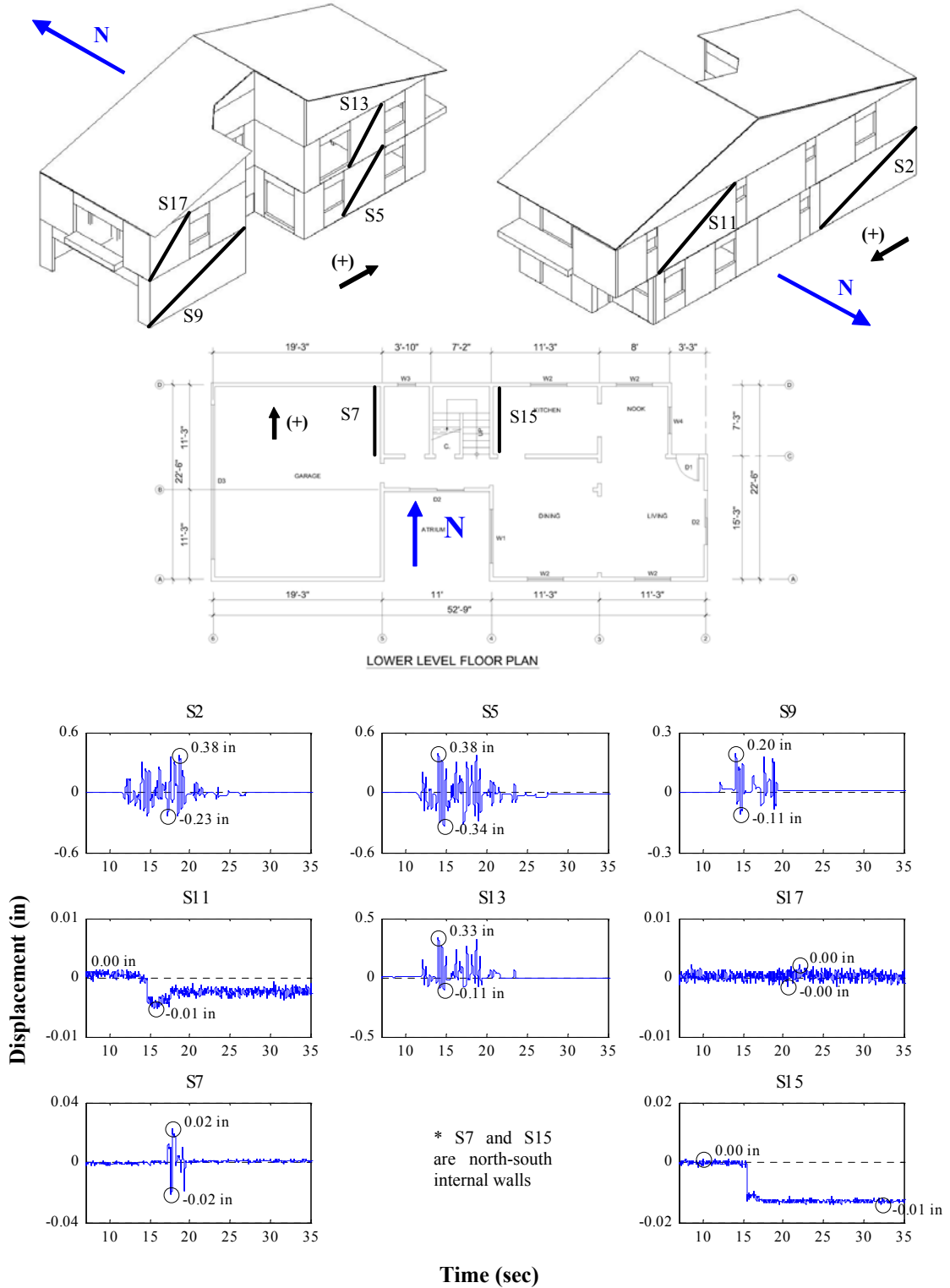


Figure M.53: Wall deformations of east-west internal walls for Test NWP2S13

Appendix M

Phase 2, NWP2S14 Seismic Test, North-South, External Walls

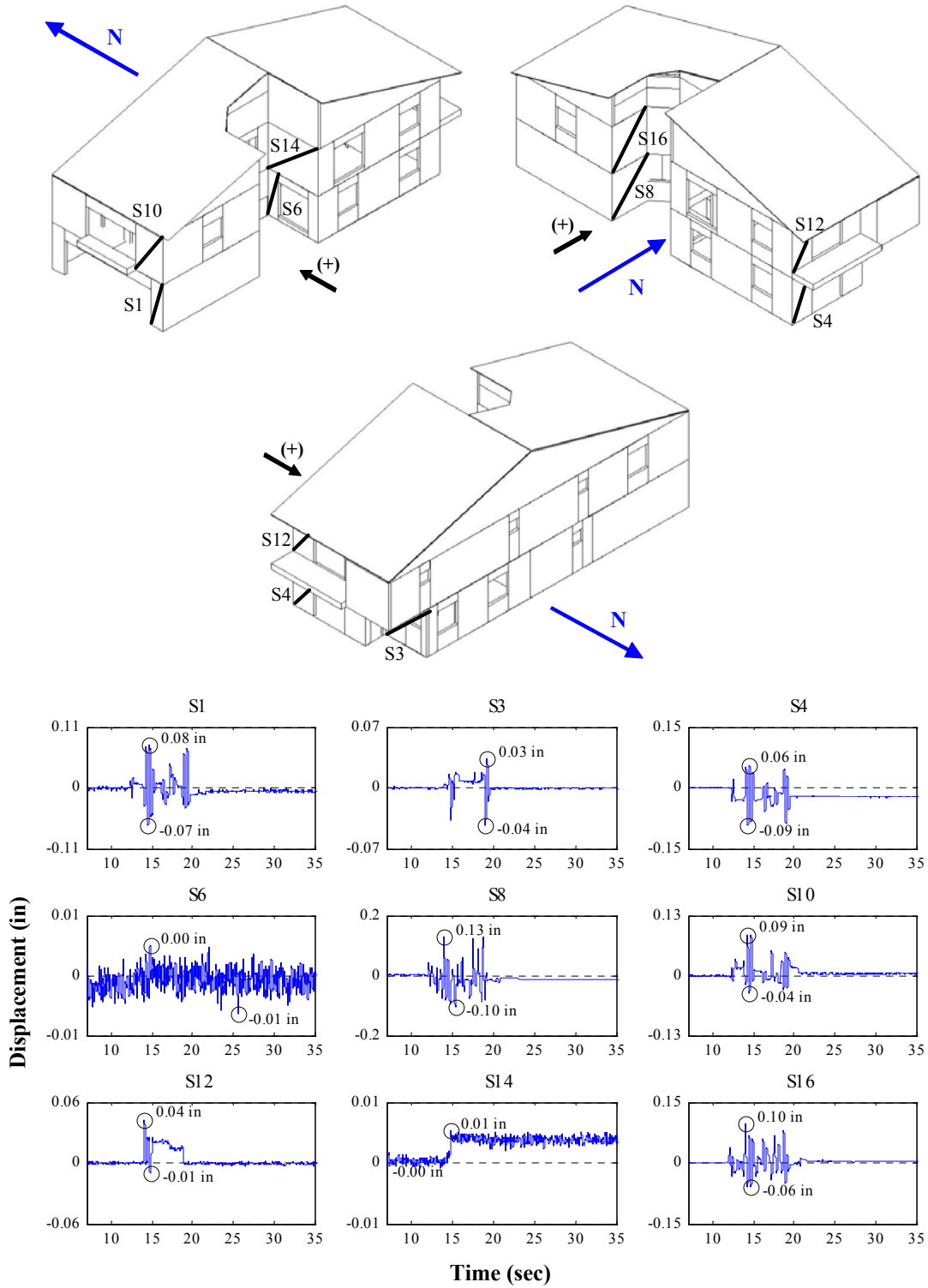


Figure M.54: Wall deformations of north-south external walls for Test NWP2S14

Appendix M

Phase 2, NWP2S14 Seismic Test, East-West, External Walls

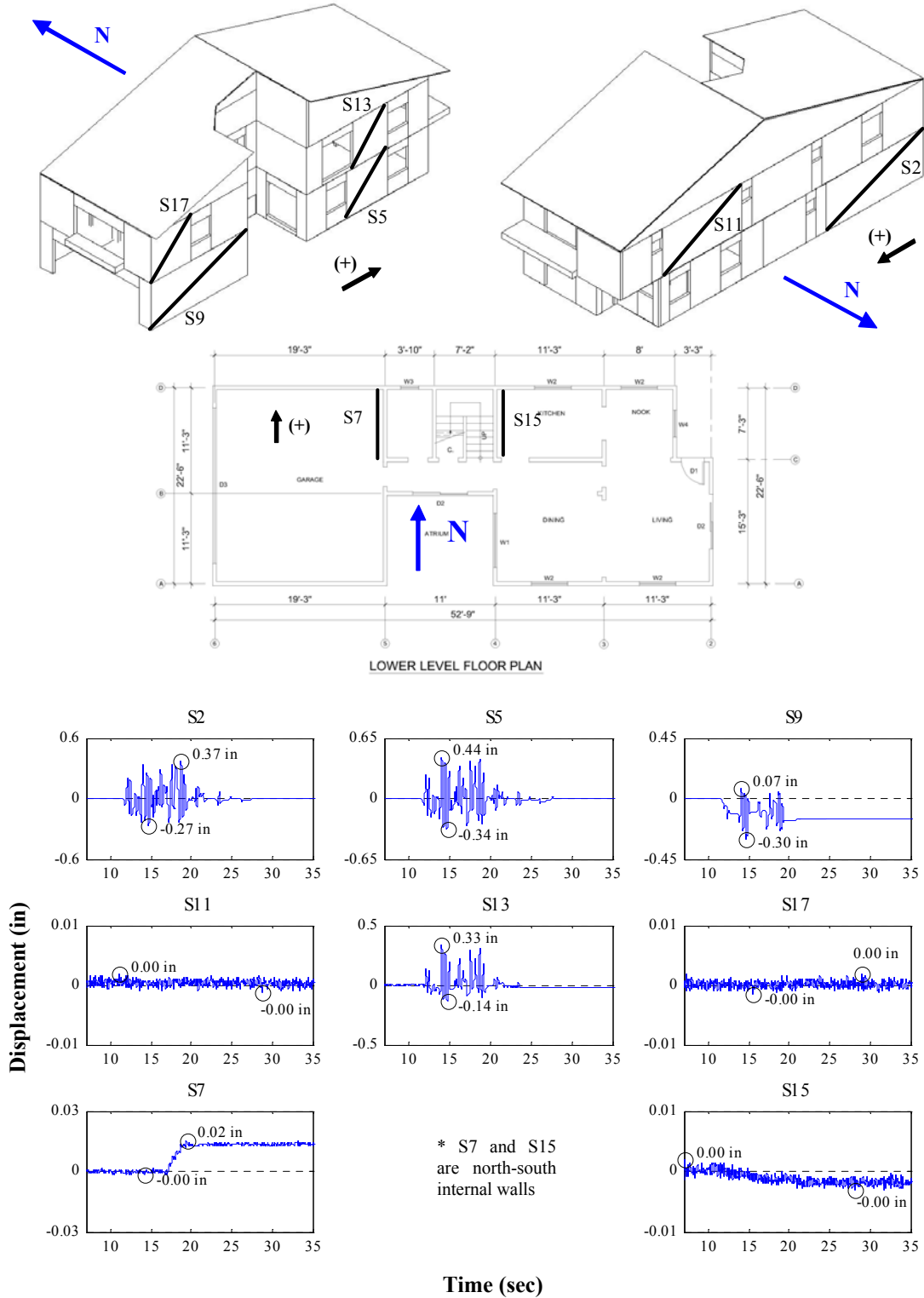


Figure M.55: Wall deformations of east-west internal walls for Test NWP2S14

Appendix M

Phase 2, NWP2S16 Seismic Test, North-South, External Walls

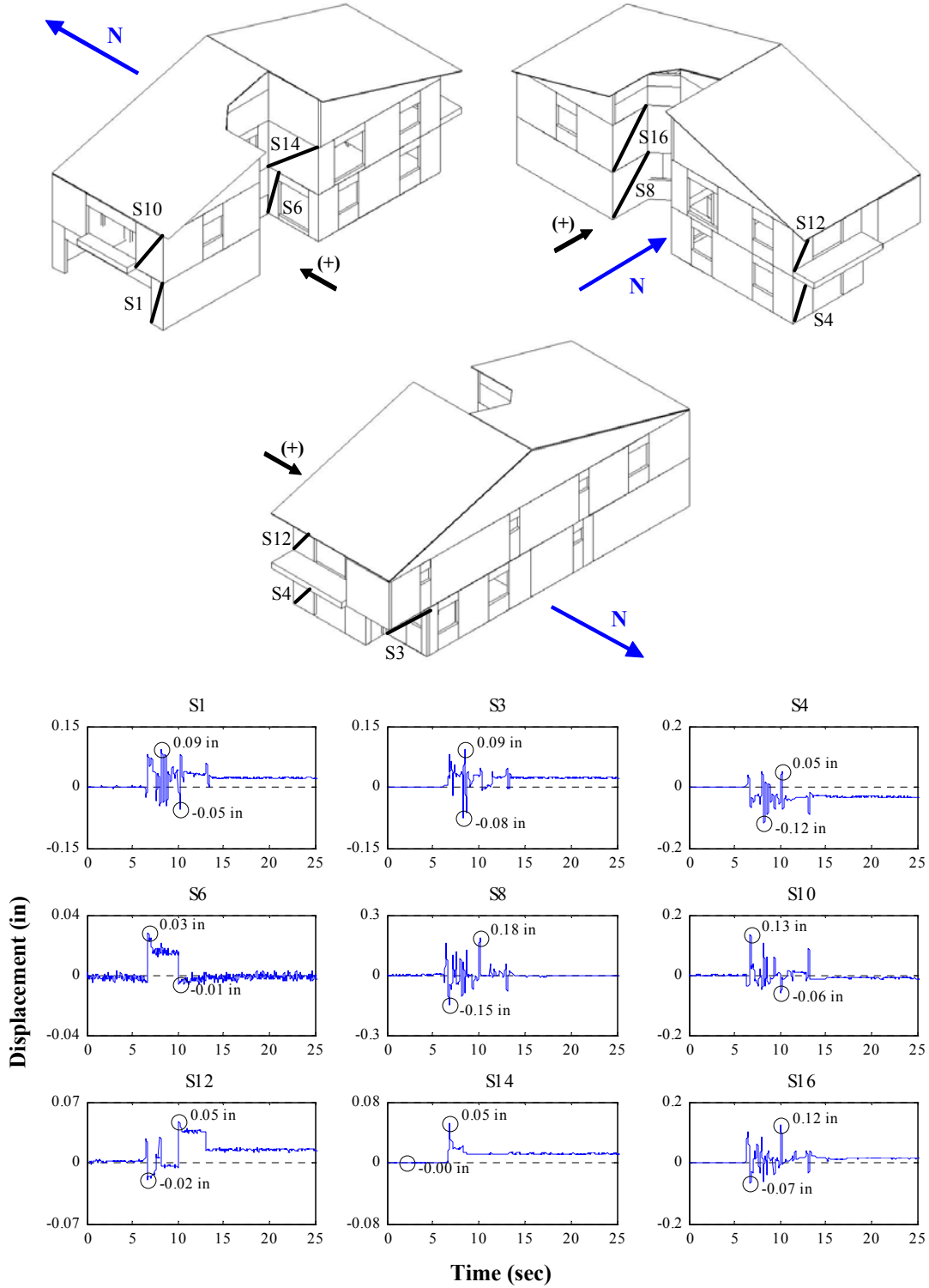


Figure M.56: Wall deformations of north-south external walls for Test NWP2S16

Appendix M

Phase 2, NWP2S16 Seismic Test, East-West, External Walls

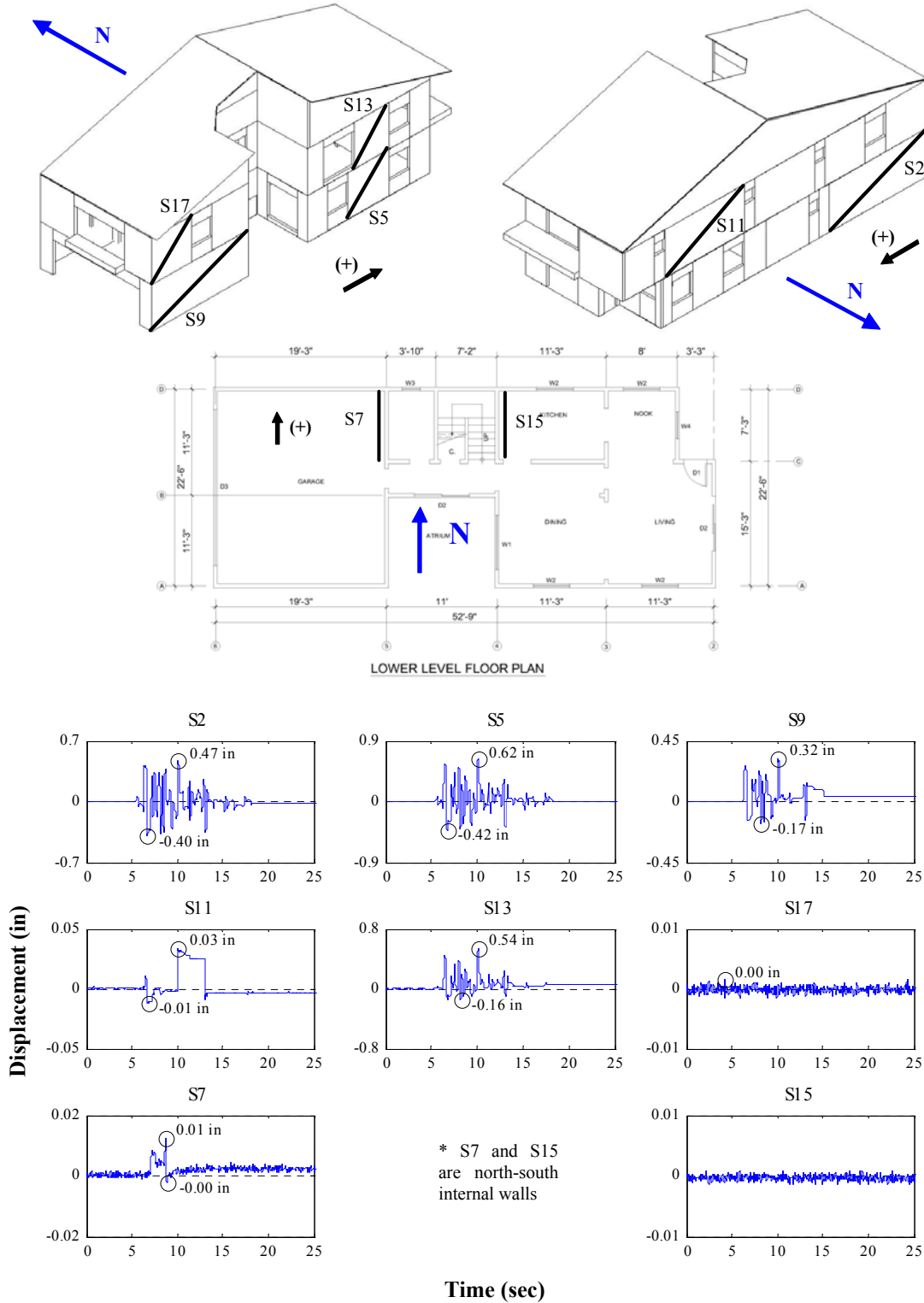


Figure M.57: Wall deformations of east-west internal walls for Test NWP2S16

Appendix M

Phase 2, NWP2S17 Seismic Test, North-South, External Walls

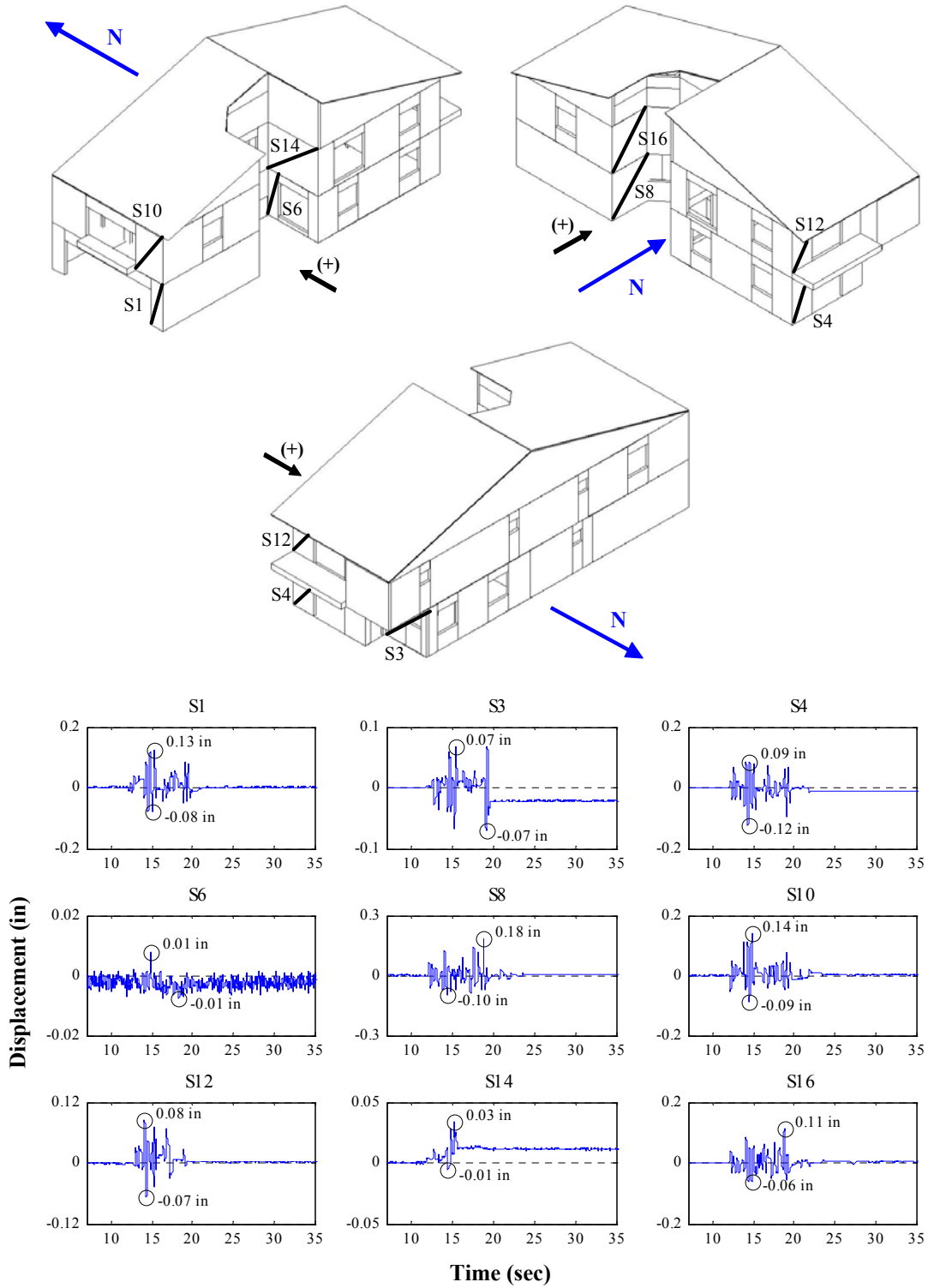


Figure M.58: Wall deformations of north-south external walls for Test NWP2S17

Appendix M

Phase 2, NWP2S17 Seismic Test, East-West, External Walls

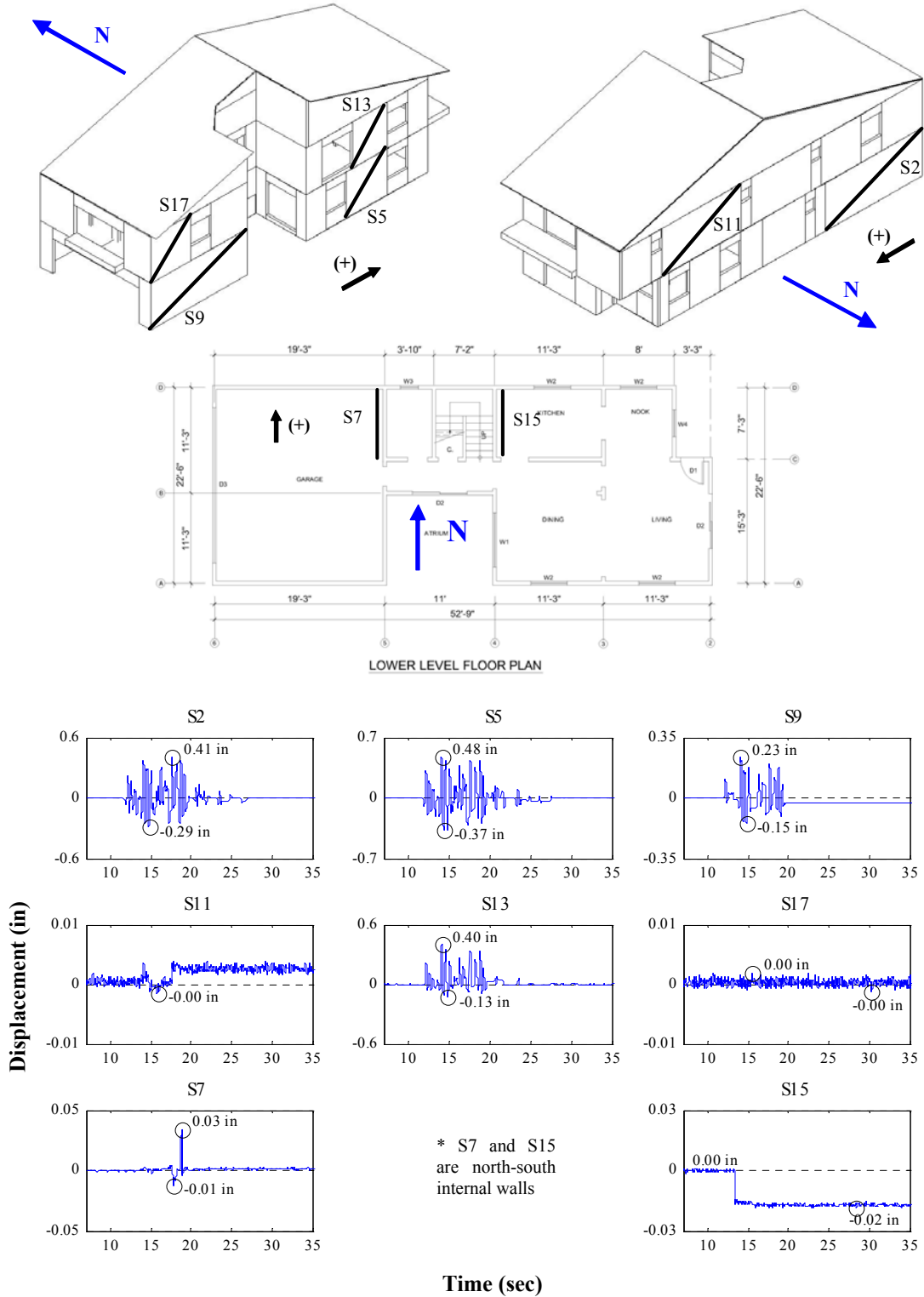


Figure M.59: Wall deformations of east-west internal walls for Test NWP2S17

Appendix M

Phase 2, NWP2S21 Seismic Test, North-South, External Walls

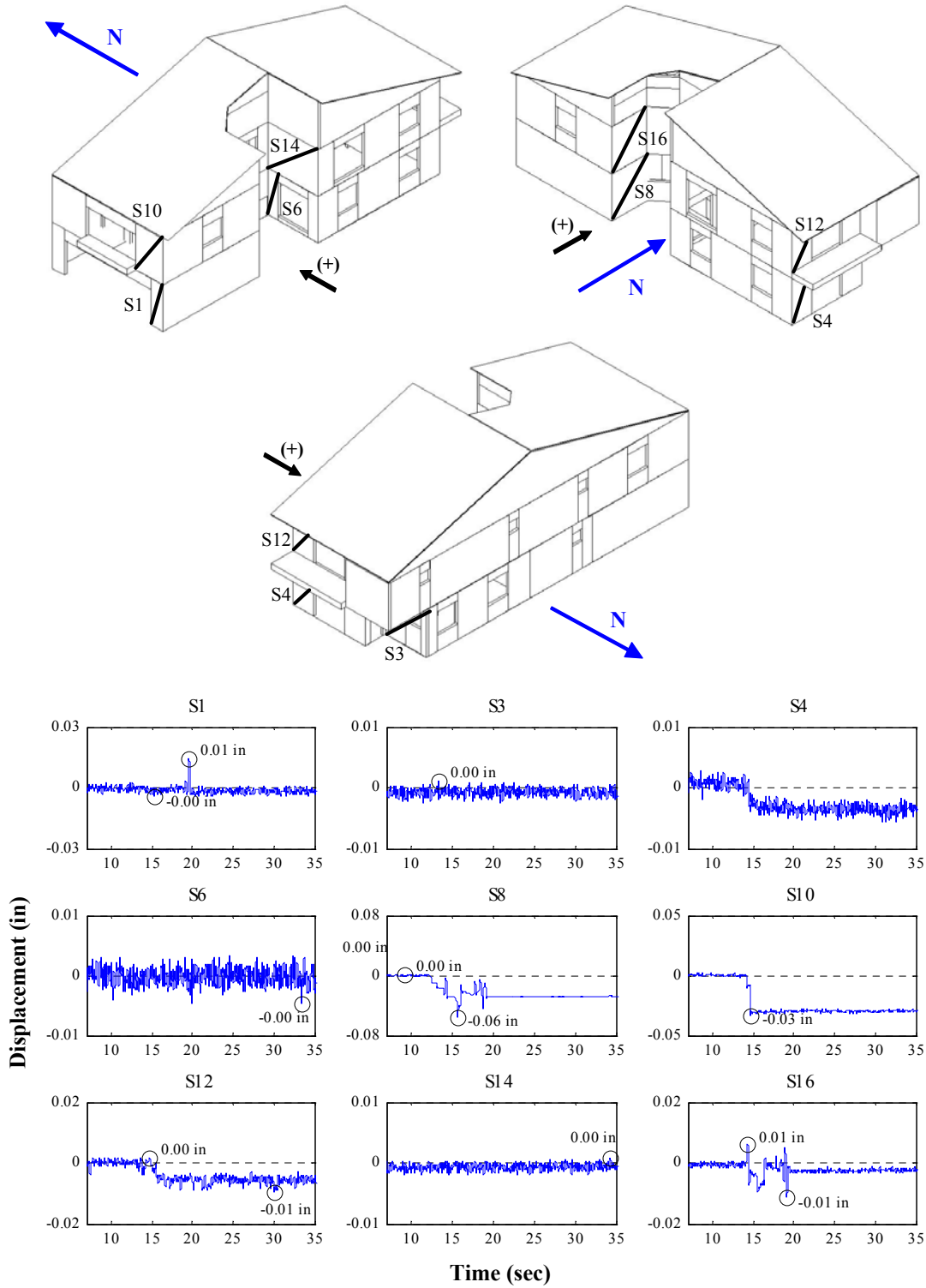


Figure M.60: Wall deformations of north-south external walls for Test NWP2S21

Appendix M

Phase 2, NWP2S21 Seismic Test, East-West, External Walls

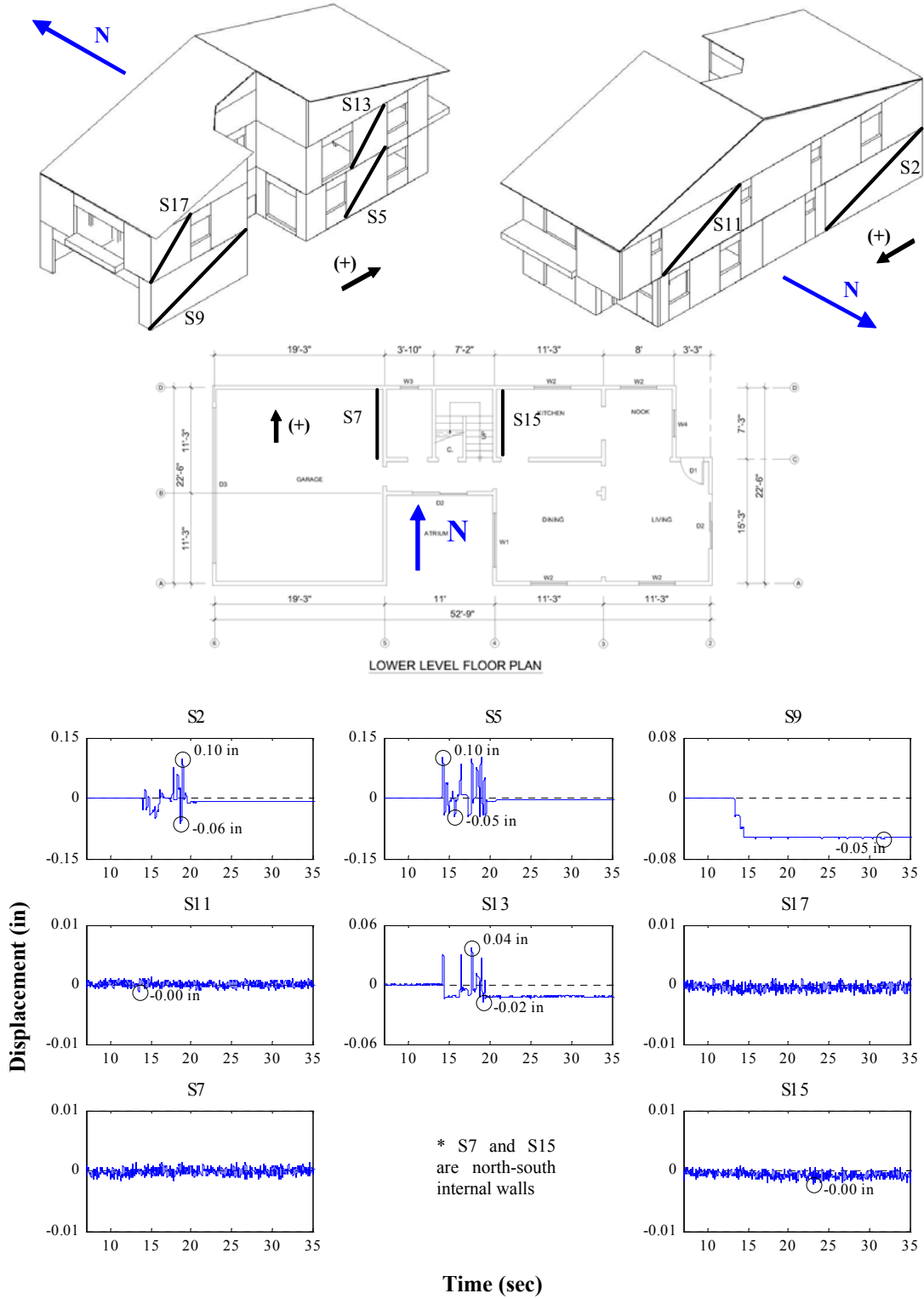


Figure M.61: Wall deformations of east-west internal walls for Test NWP2S21

Appendix M

Phase 2, NWP2S24 Seismic Test, North-South, External Walls

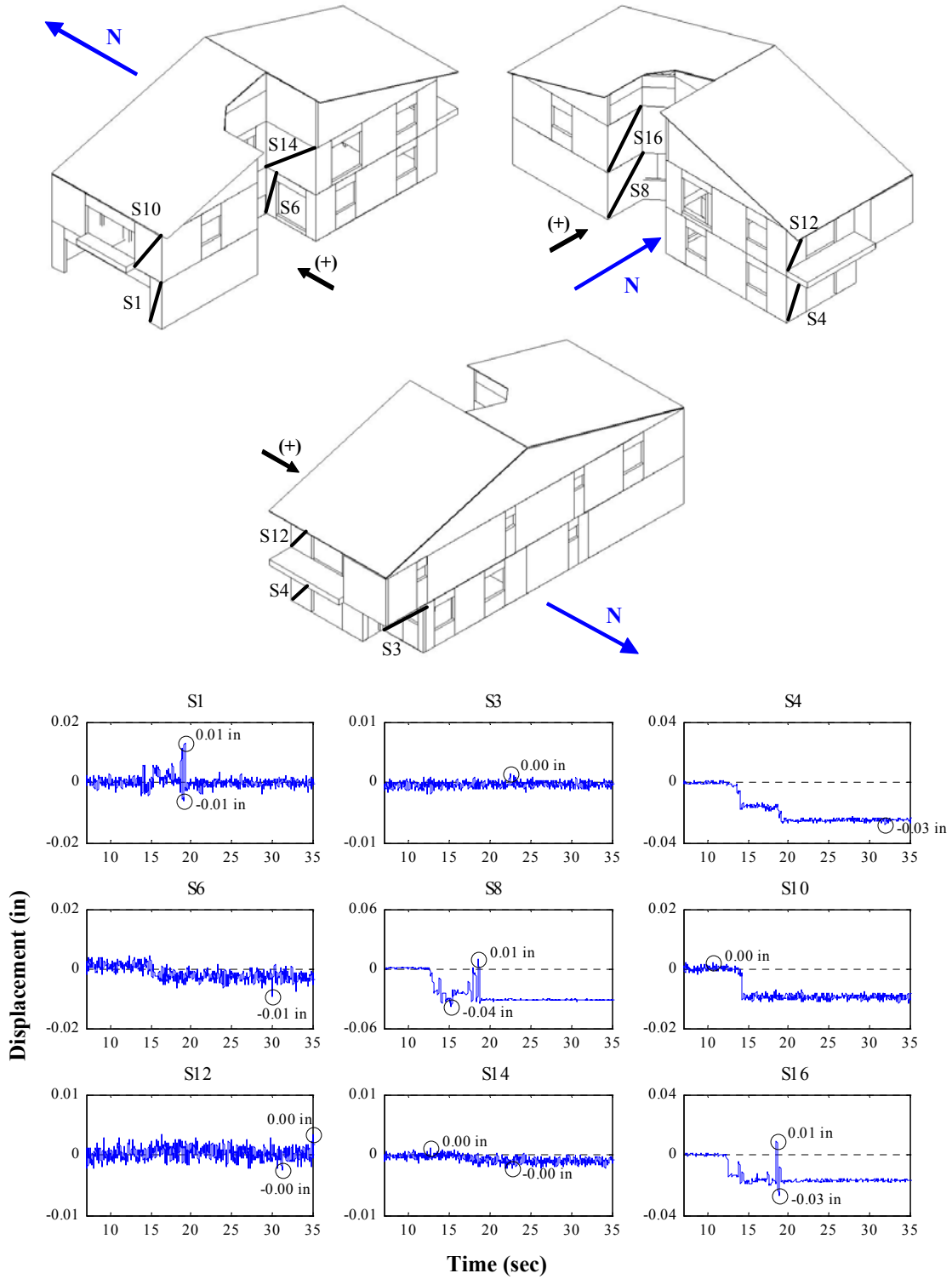


Figure M.62: Wall deformations of north-south external walls for Test NWP2S24

Appendix M

Phase 2, NWP2S24 Seismic Test, East-West, External Walls

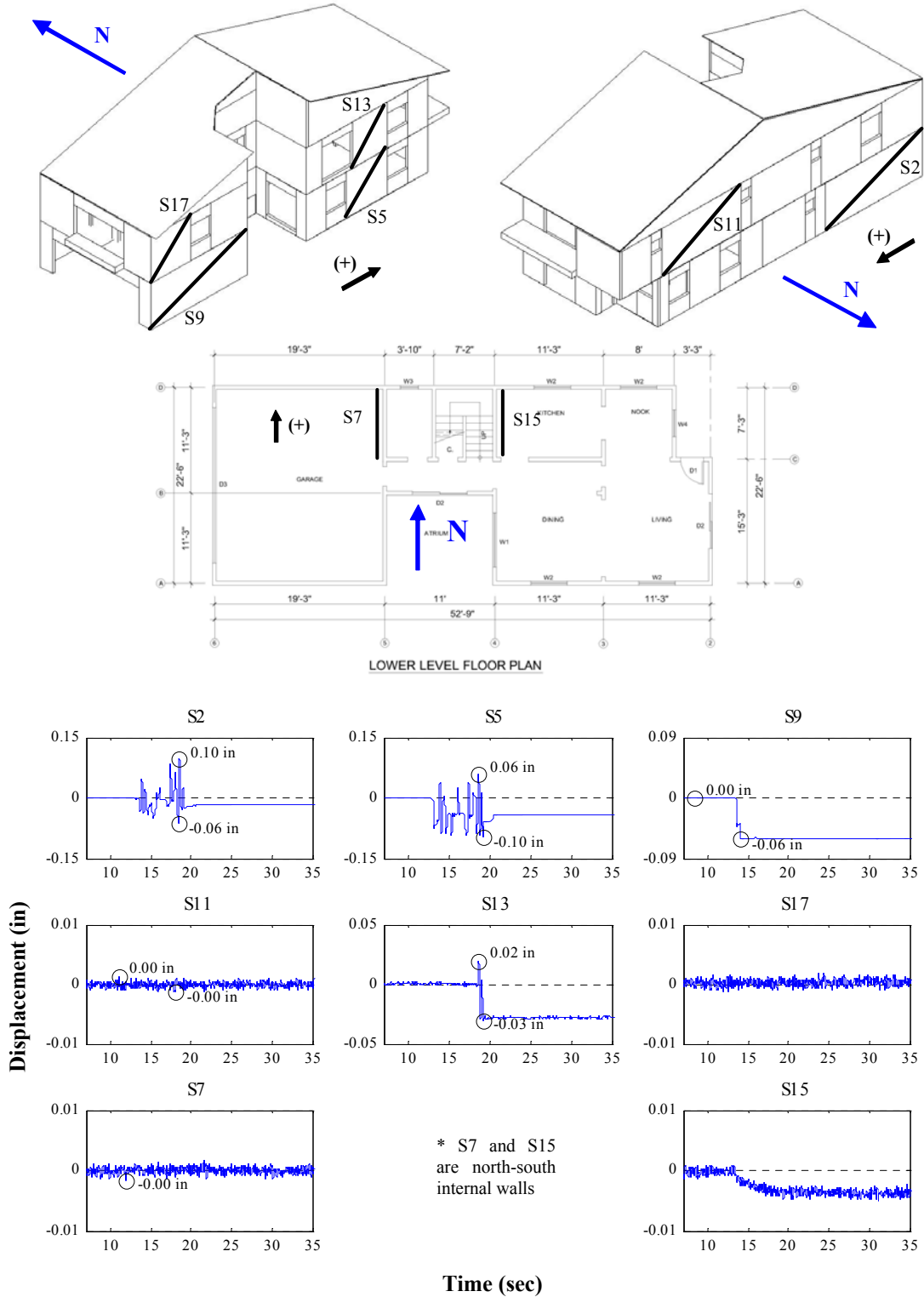


Figure M.63: Wall deformations of east-west internal walls for Test NWP2S24

Appendix M

Phase 2, NWP2S25 Seismic Test, North-South, External Walls

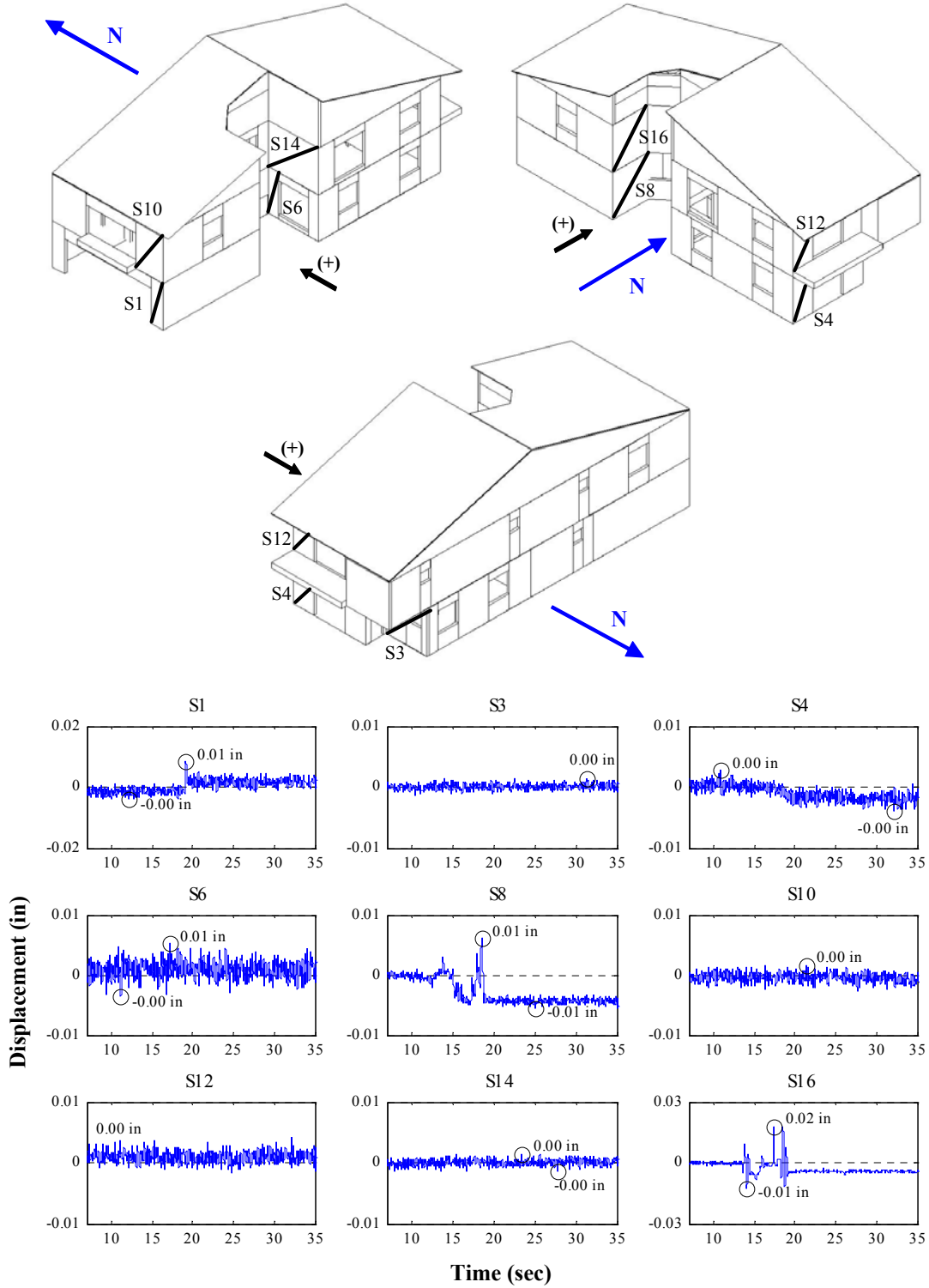


Figure M.64: Wall deformations of north-south external walls for Test NWP2S25

Appendix M

Phase 2, NWP2S25 Seismic Test, East-West, External Walls

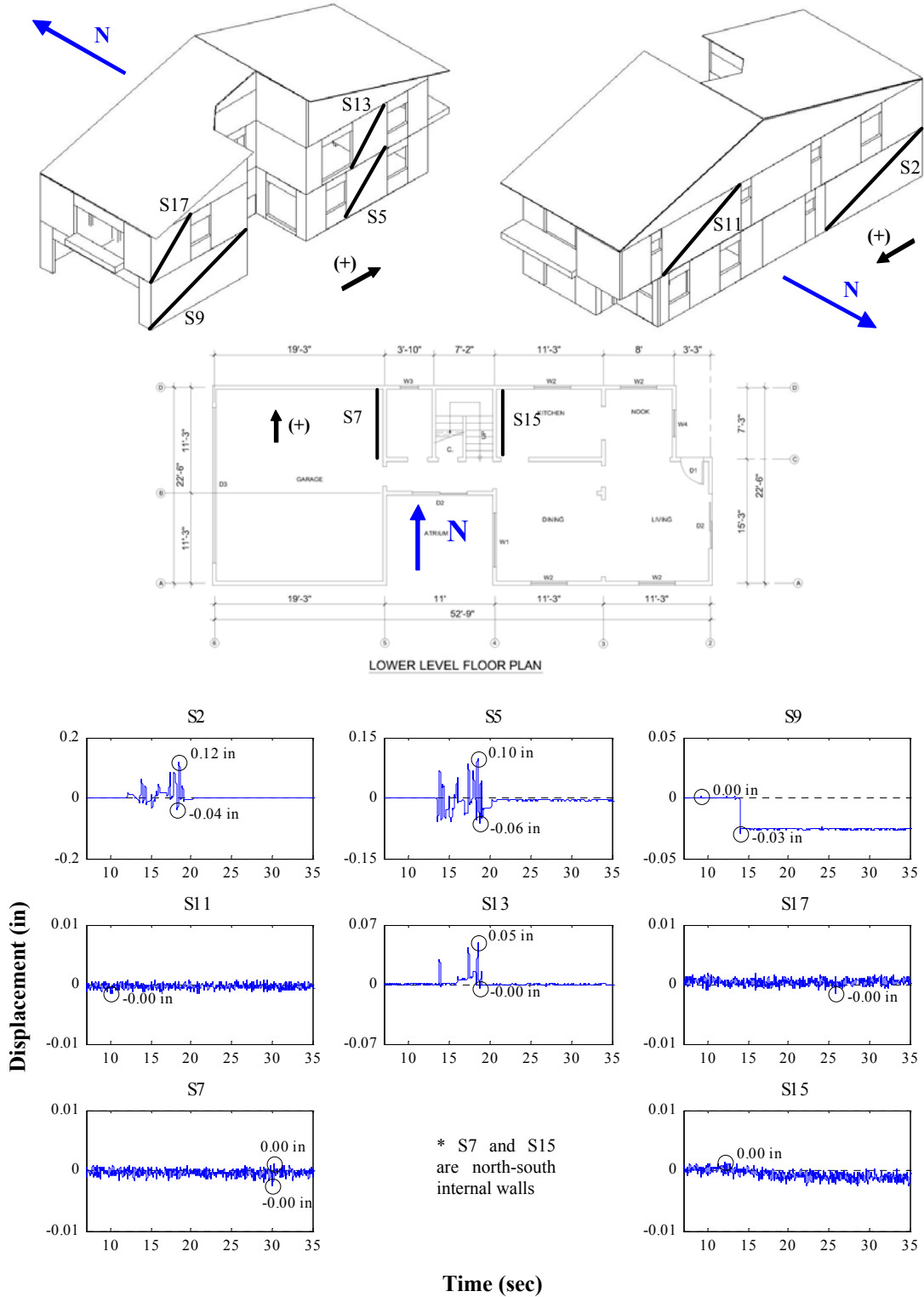


Figure M.65: Wall deformations of east-west internal walls for Test NWP2S25

Appendix M

Phase 2, NWP2S26 Seismic Test, North-South, External Walls

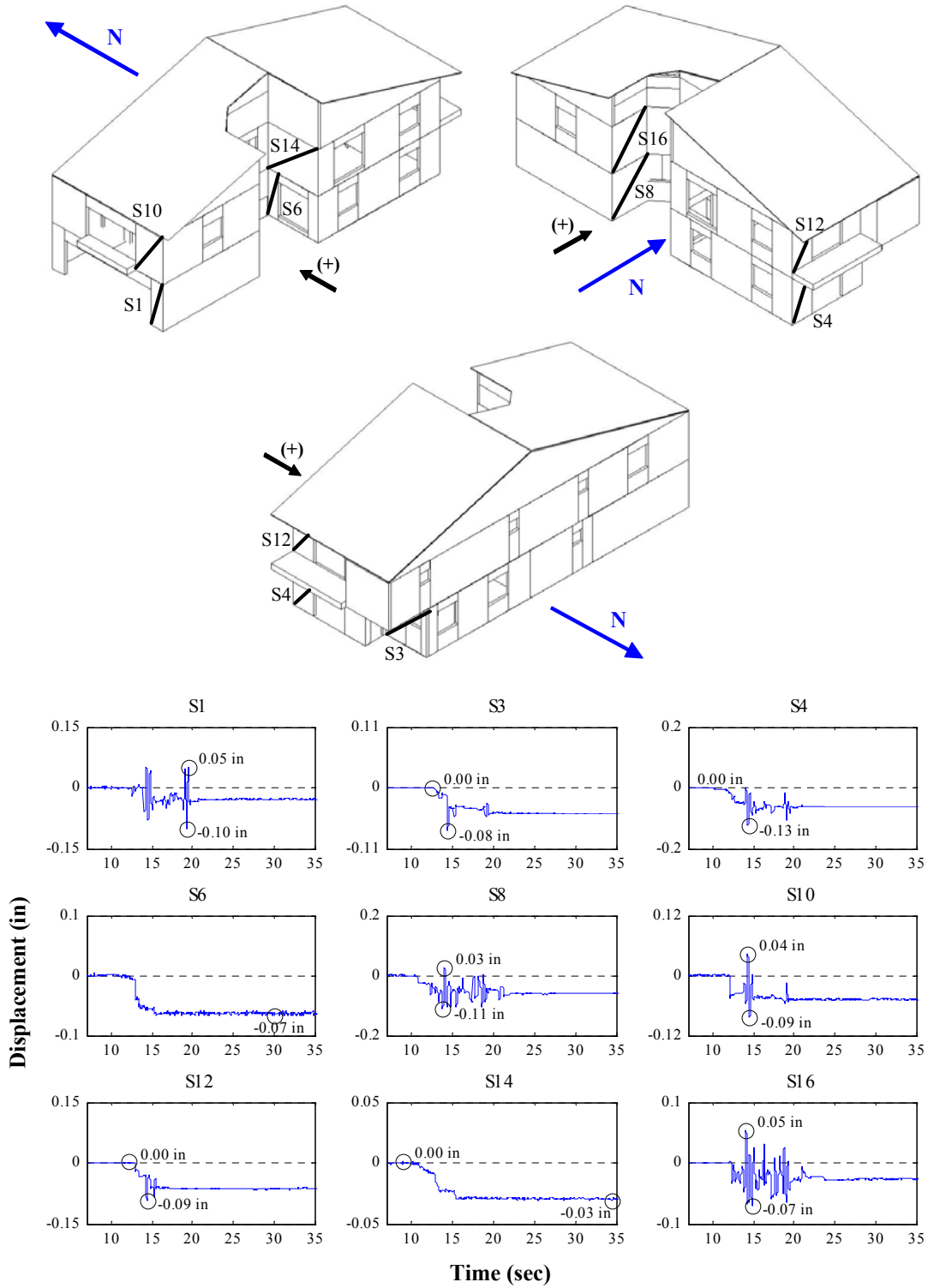


Figure M.66: Wall deformations of north-south external walls for Test NWP2S26

Appendix M

Phase 2, NWP2S26 Seismic Test, East-West, External Walls

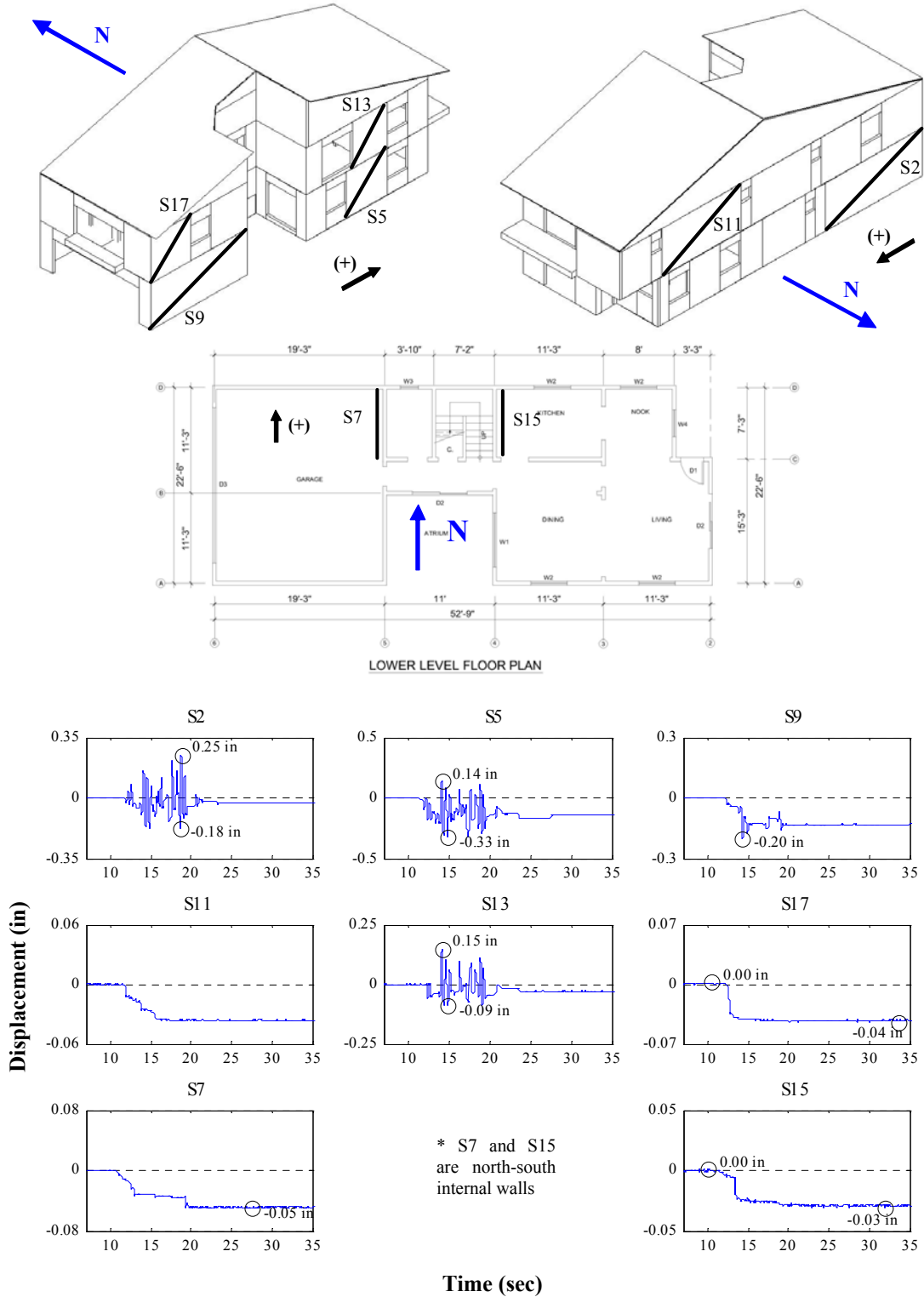


Figure M.67: Wall deformations of east-west internal walls for Test NWP2S26

Appendix M

Phase 2, NWP2S27 Seismic Test, North-South, External Walls

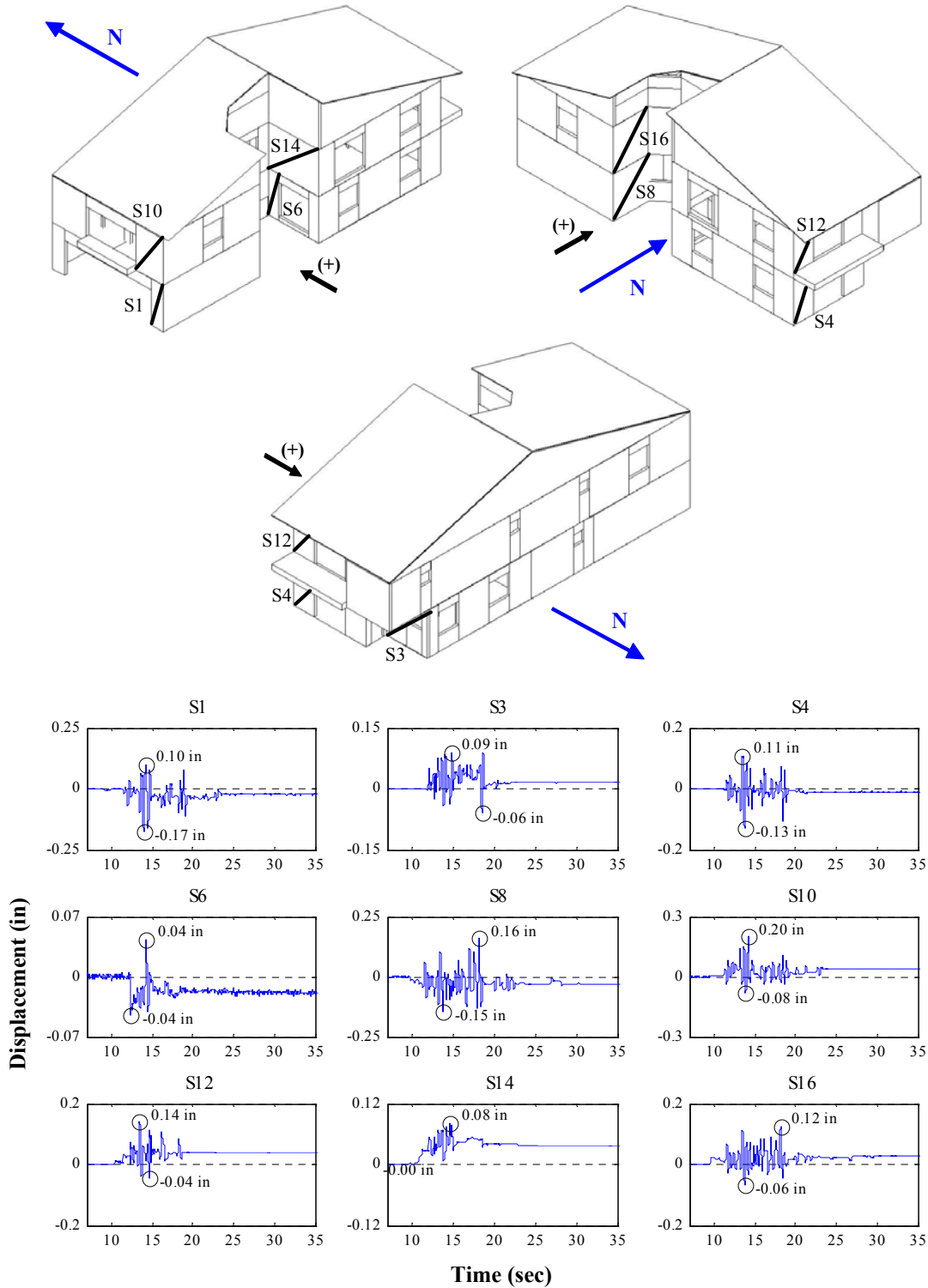


Figure M.68: Wall deformations of north-south external walls for Test NWP2S27

Appendix M

Phase 2, NWP2S27 Seismic Test, East-West, External Walls

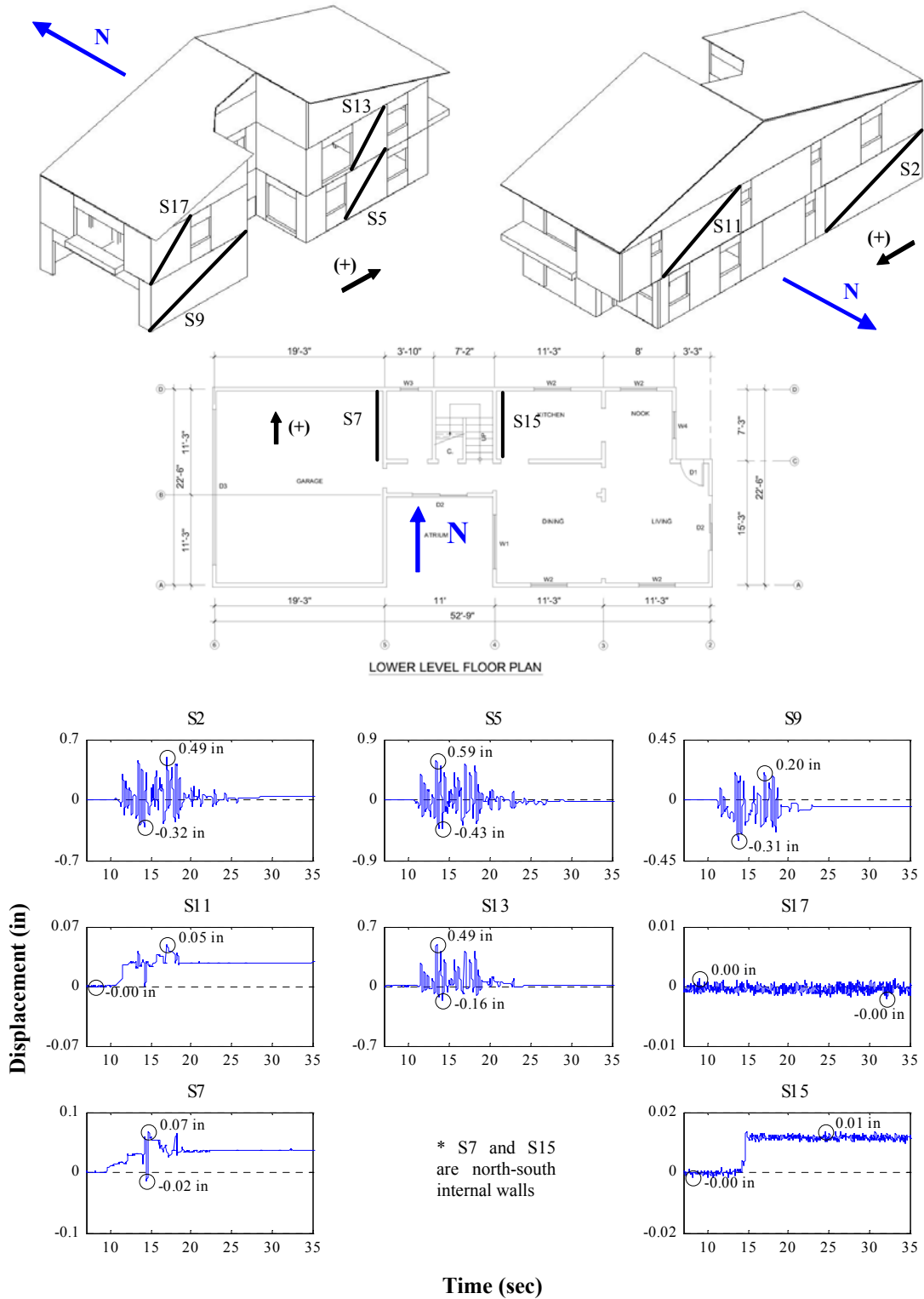


Figure M.69: Wall deformations of east-west internal walls for Test NWP2S27

Appendix M

Phase 2, NWP2S28 Seismic Test, North-South, External Walls

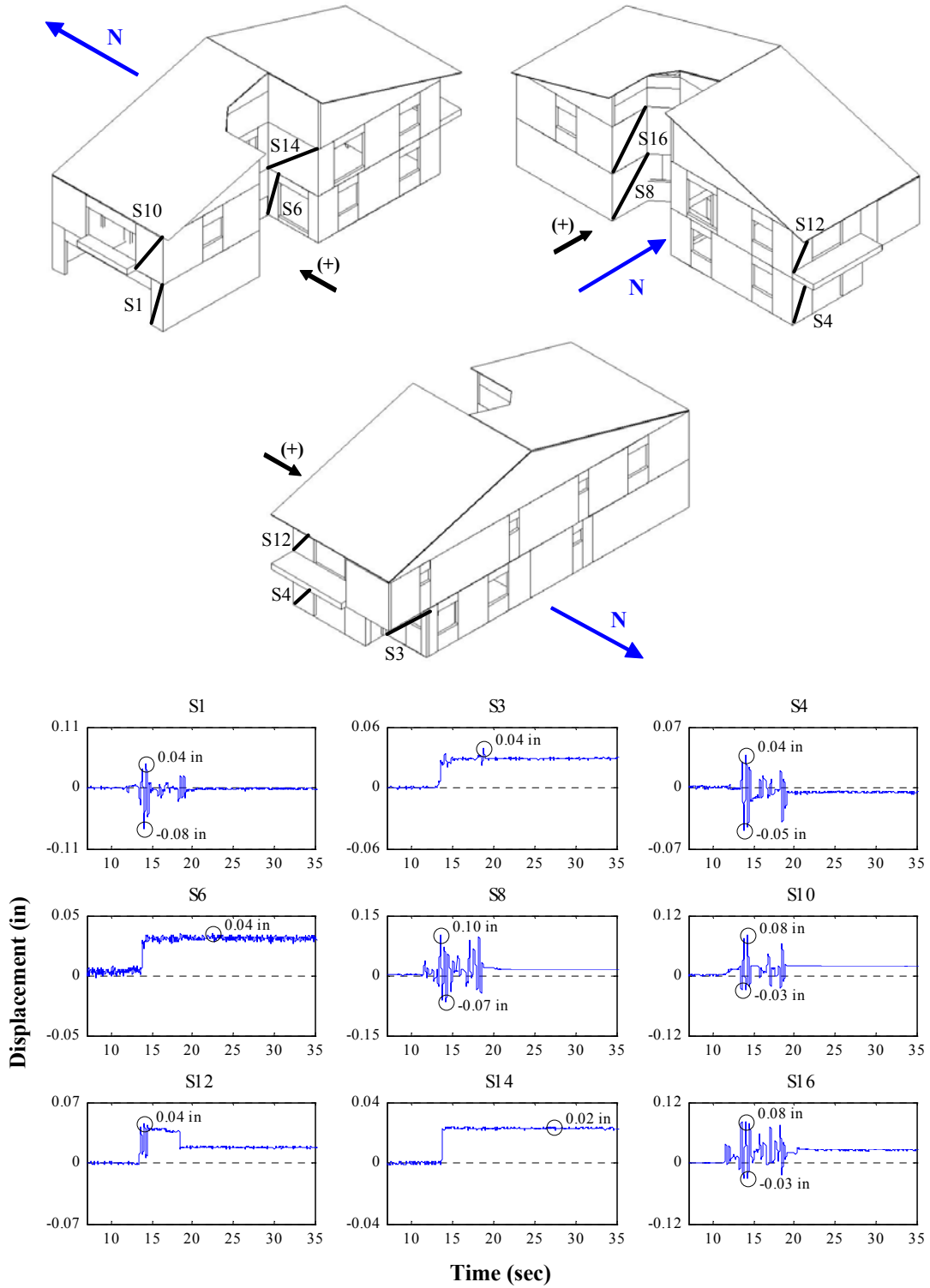


Figure M.70: Wall deformations of north-south external walls for Test NWP2S28

Appendix M

Phase 2, NWP2S28 Seismic Test, East-West, External Walls

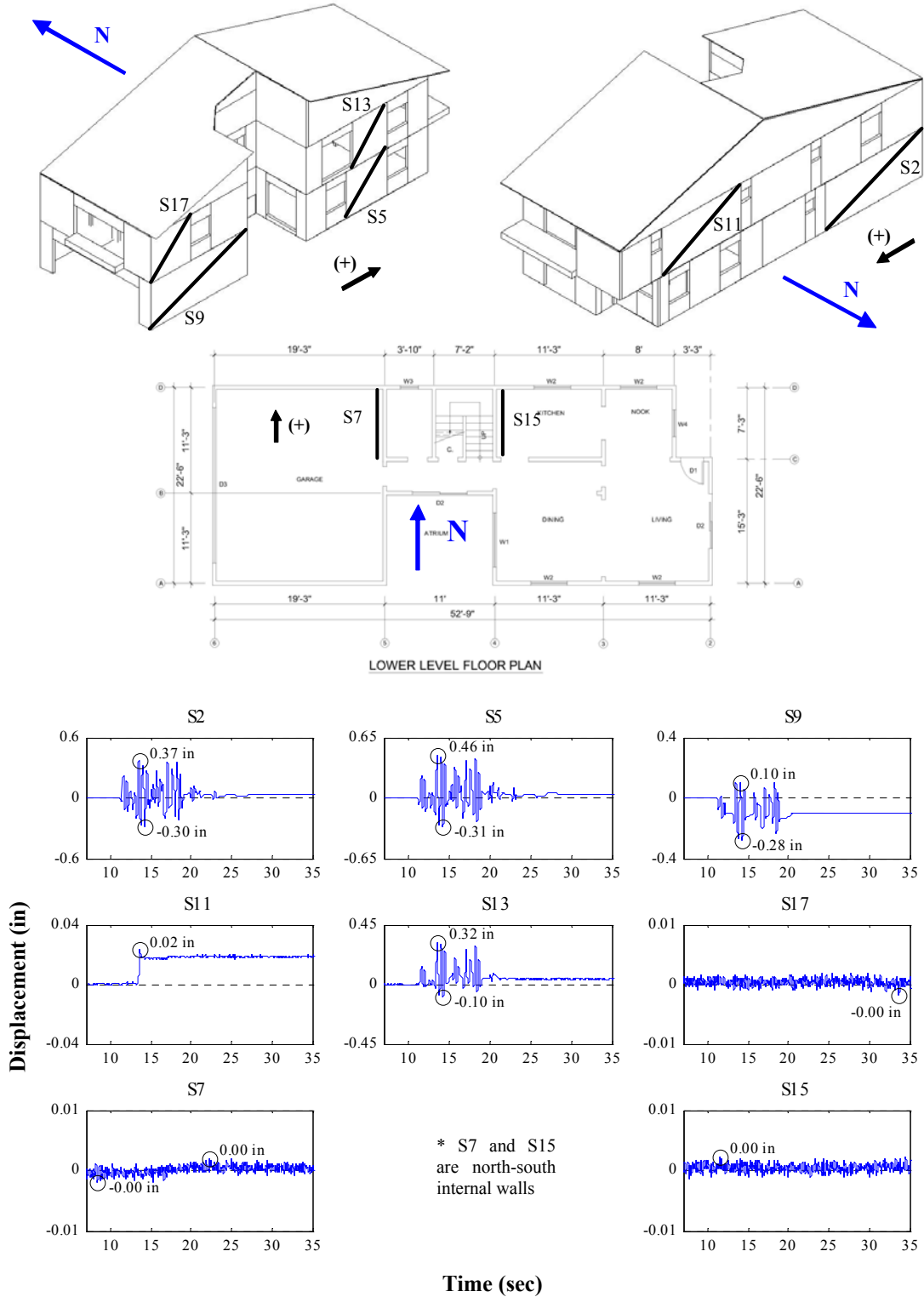


Figure M.71: Wall deformations of east-west internal walls for Test NWP2S28

Appendix M

Phase 2, NWP2S29 Seismic Test, North-South, External Walls

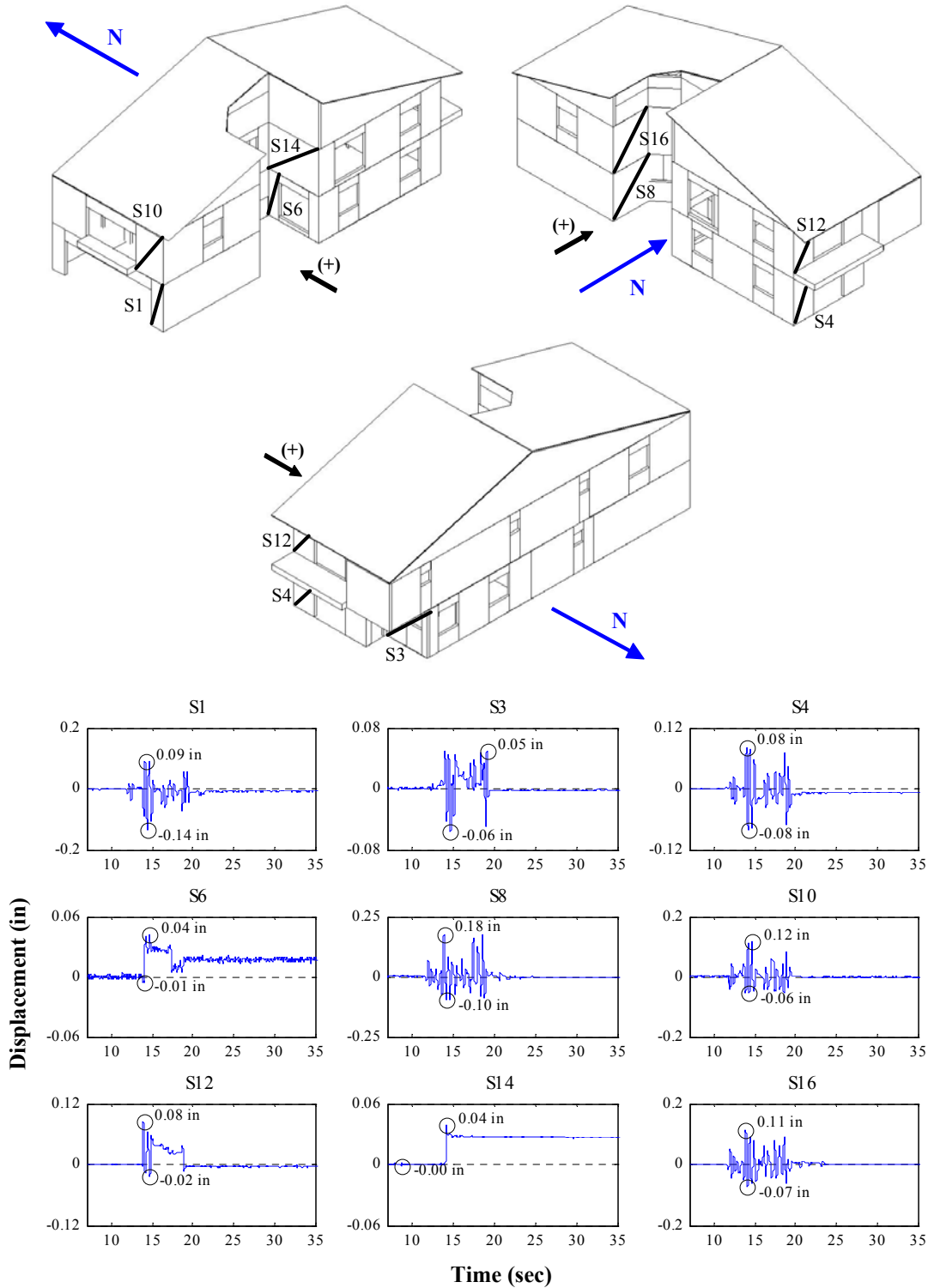


Figure M.72: Wall deformations of north-south external walls for Test NWP2S29

Appendix M

Phase 2, NWP2S29 Seismic Test, East-West, External Walls

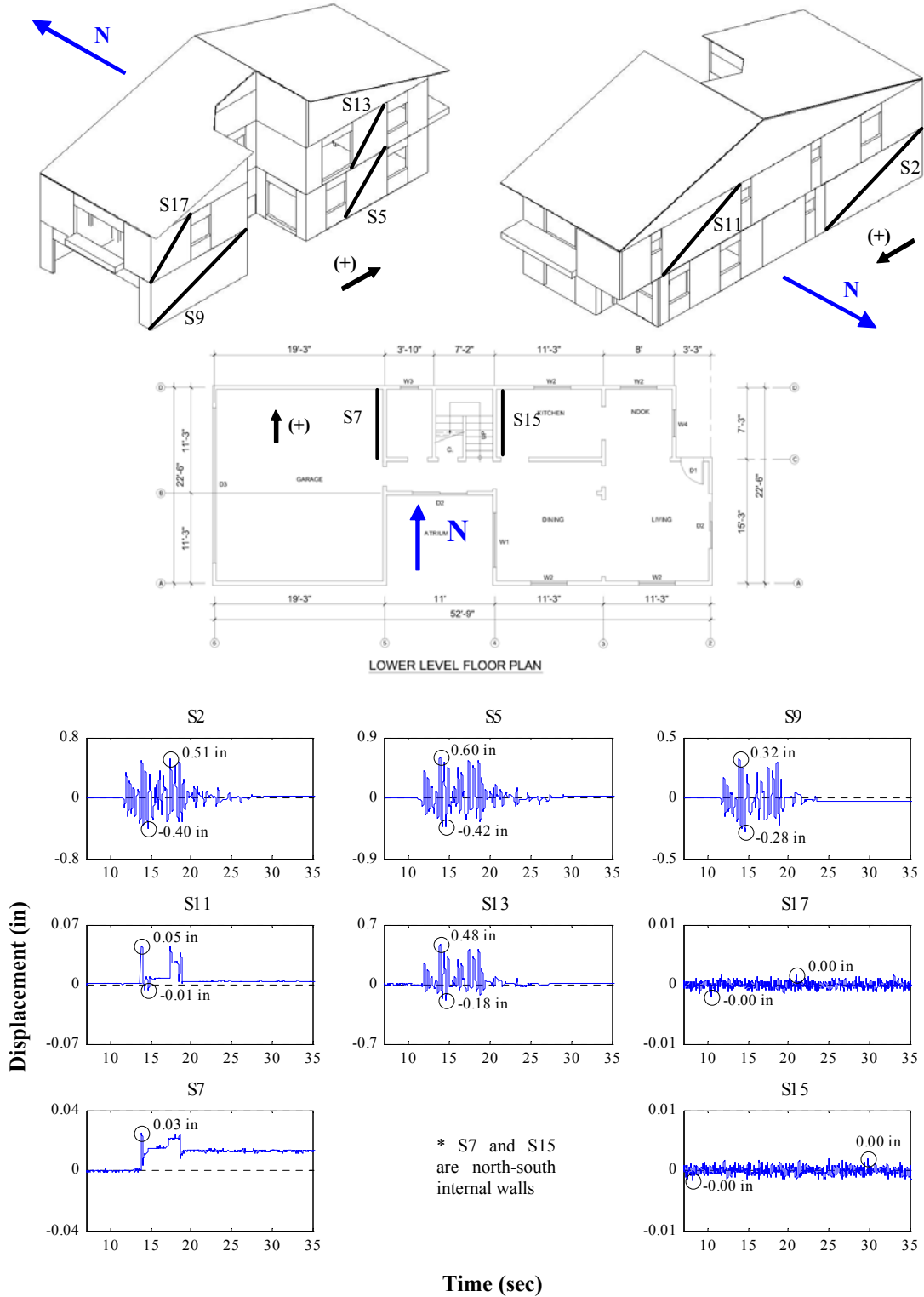


Figure M.73: Wall deformations of east-west internal walls for Test NWP2S29

Appendix M

Phase 2, NWP2S30 Seismic Test, North-South, External Walls

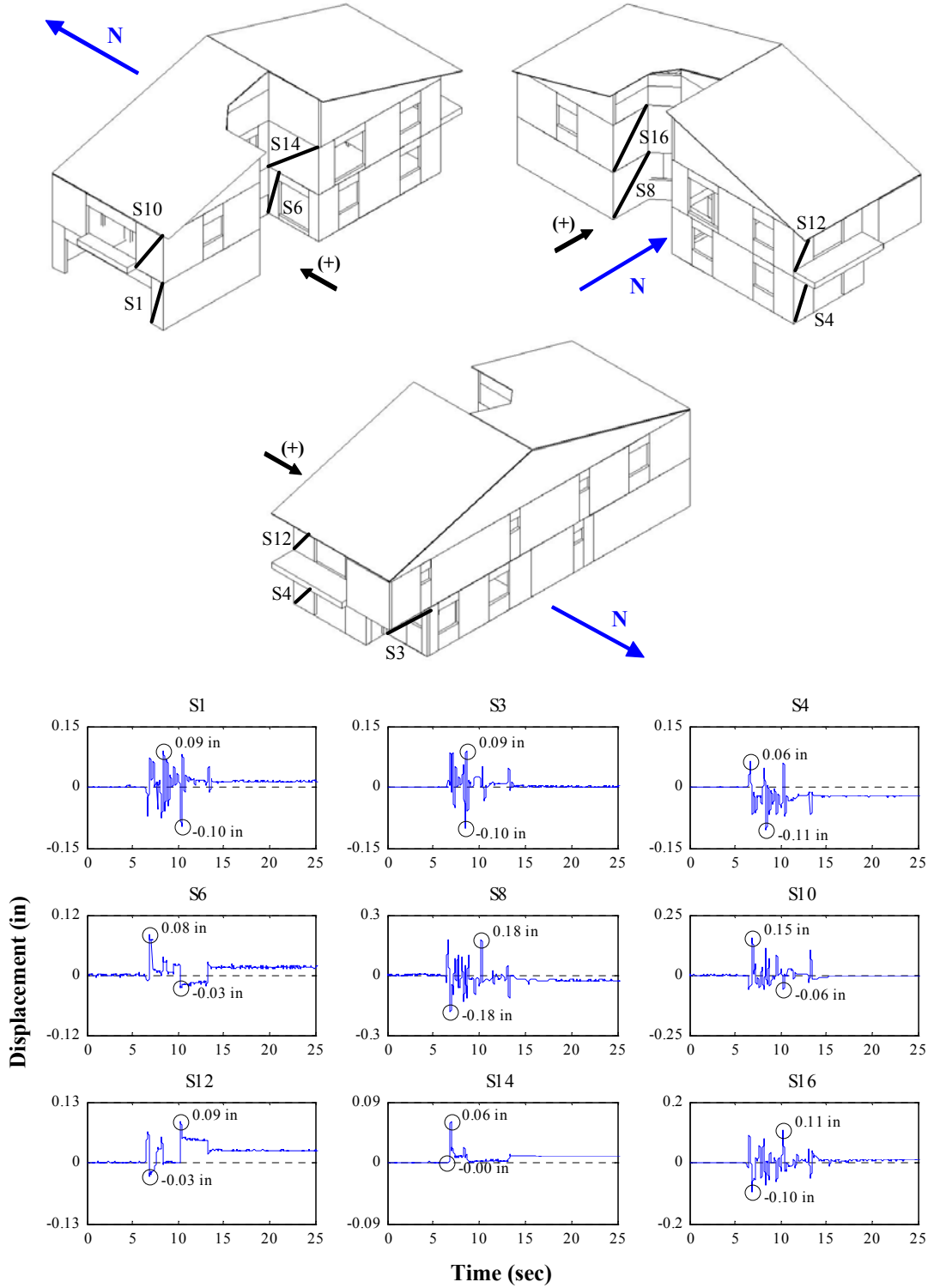


Figure M.74: Wall deformations of north-south external walls for Test NWP2S30

Appendix M

Phase 2, NWP2S30 Seismic Test, East-West, External Walls

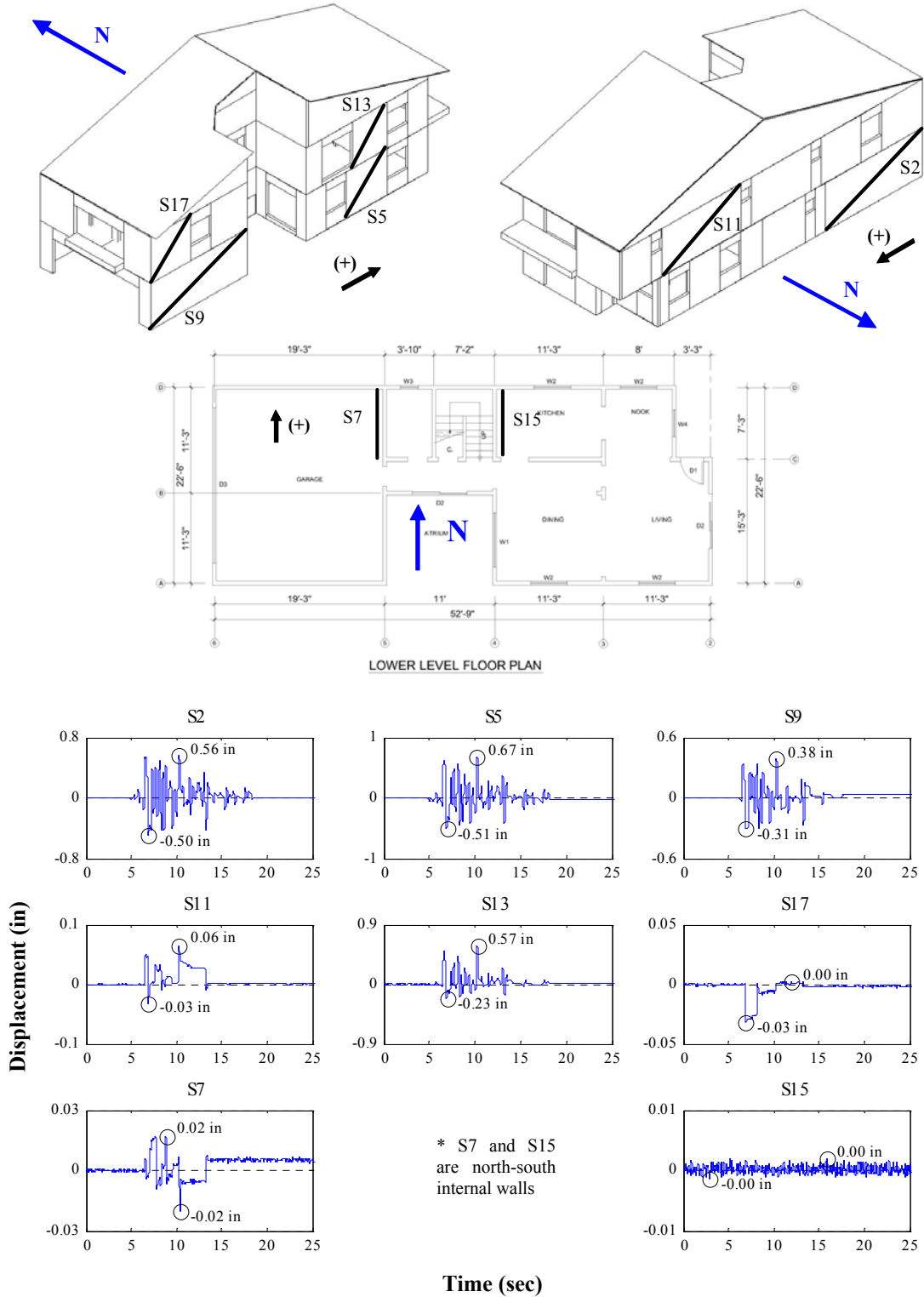


Figure M.75: Wall deformations of east-west internal walls for Test NWP2S30

Appendix M

Phase 3, NWP3S01 Seismic Test, North-South, External Walls

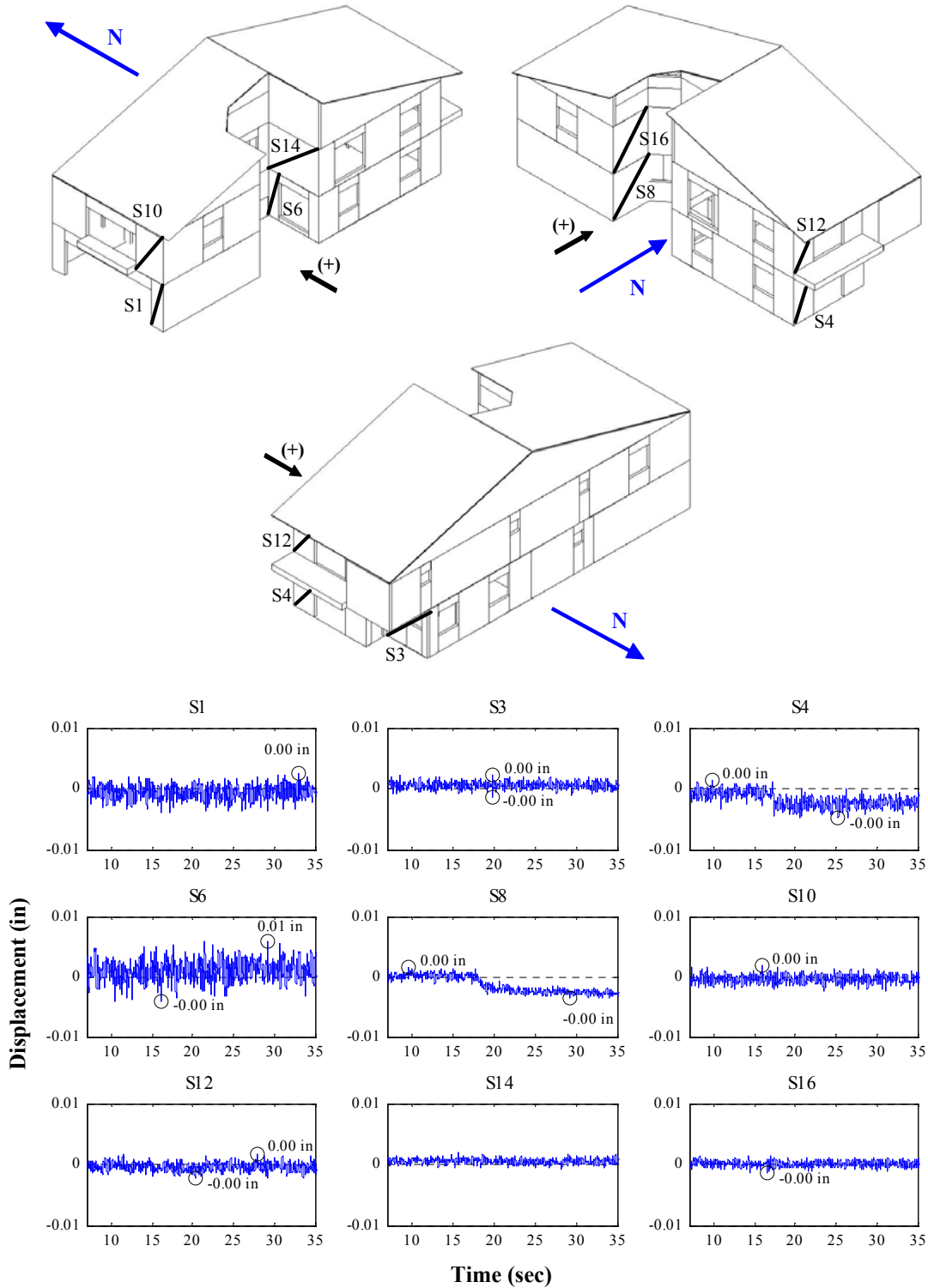


Figure M.76: Wall deformations of north-south external walls for Test NWP3S01

Appendix M

Phase 3, NWP3S01 Seismic Test, East-West, External Walls

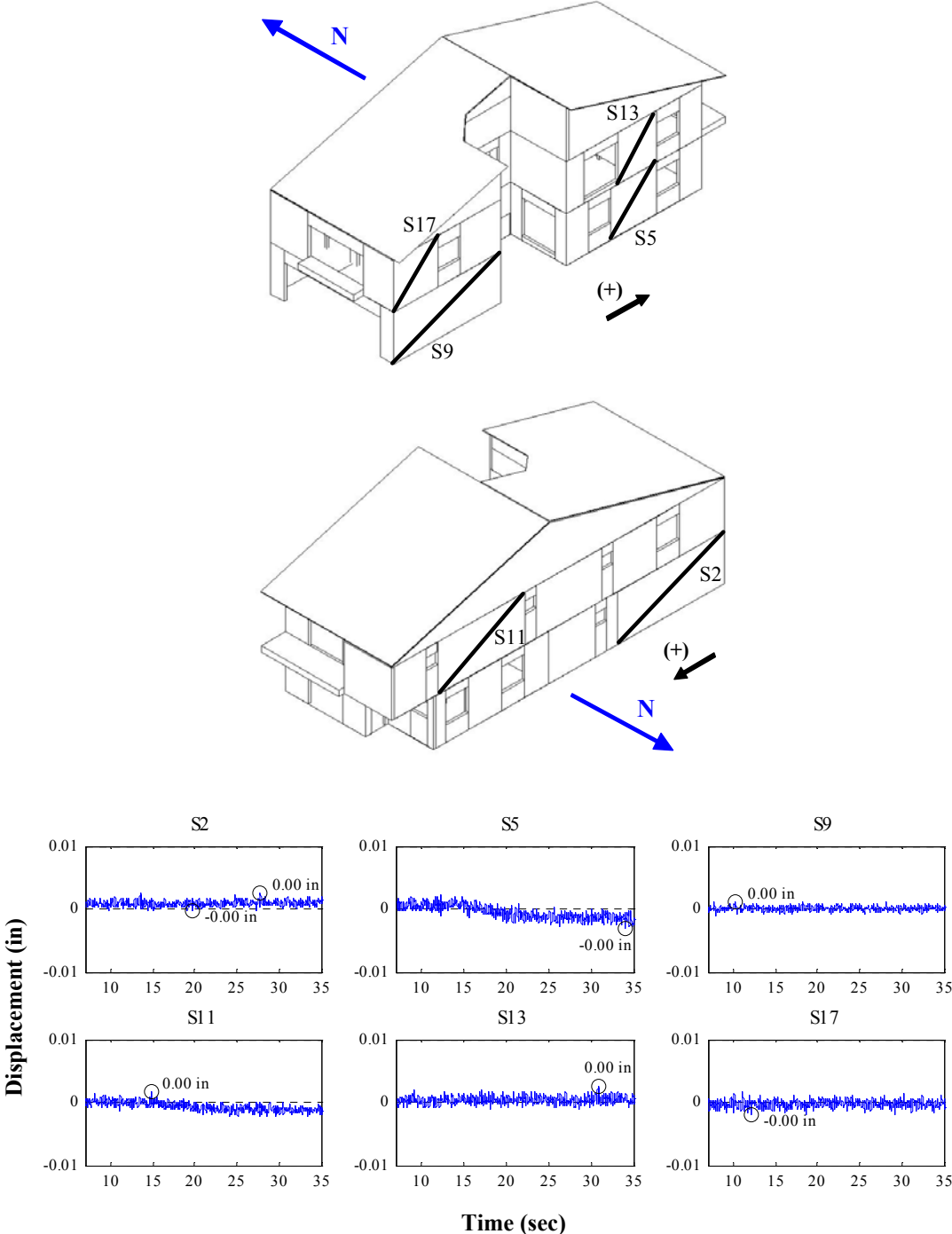


Figure M.77: Wall deformations of east-west external walls for Test NWP3S01

Appendix M

Phase 3, NWP3S01 Seismic Test, Internal Walls

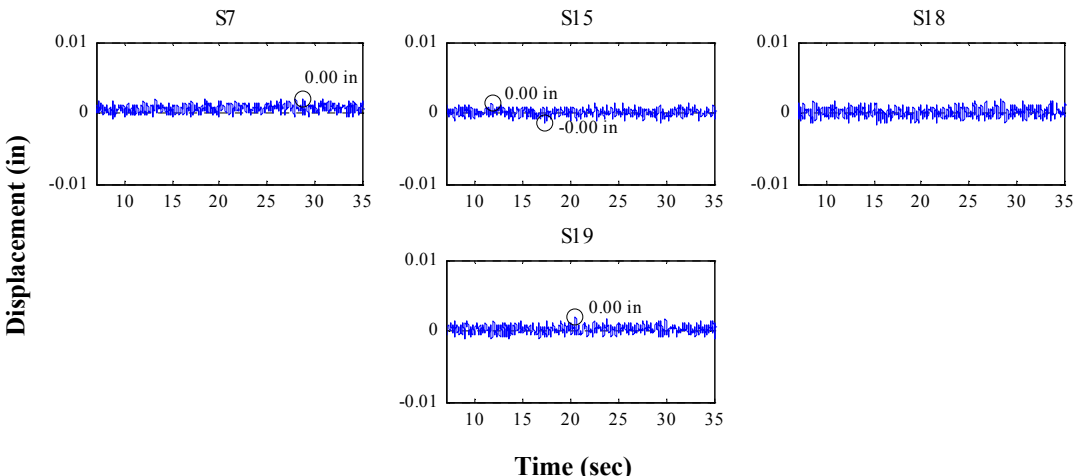
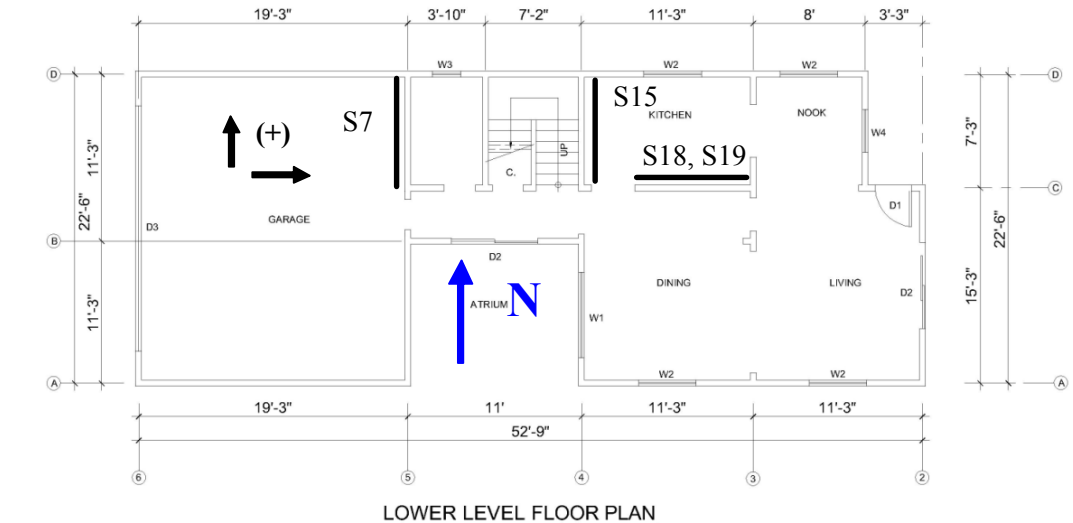


Figure M.78: Wall deformations of internal walls for Test NWP3S01

Appendix M

Phase 3, NWP3S02 Seismic Test, North-South, External Walls

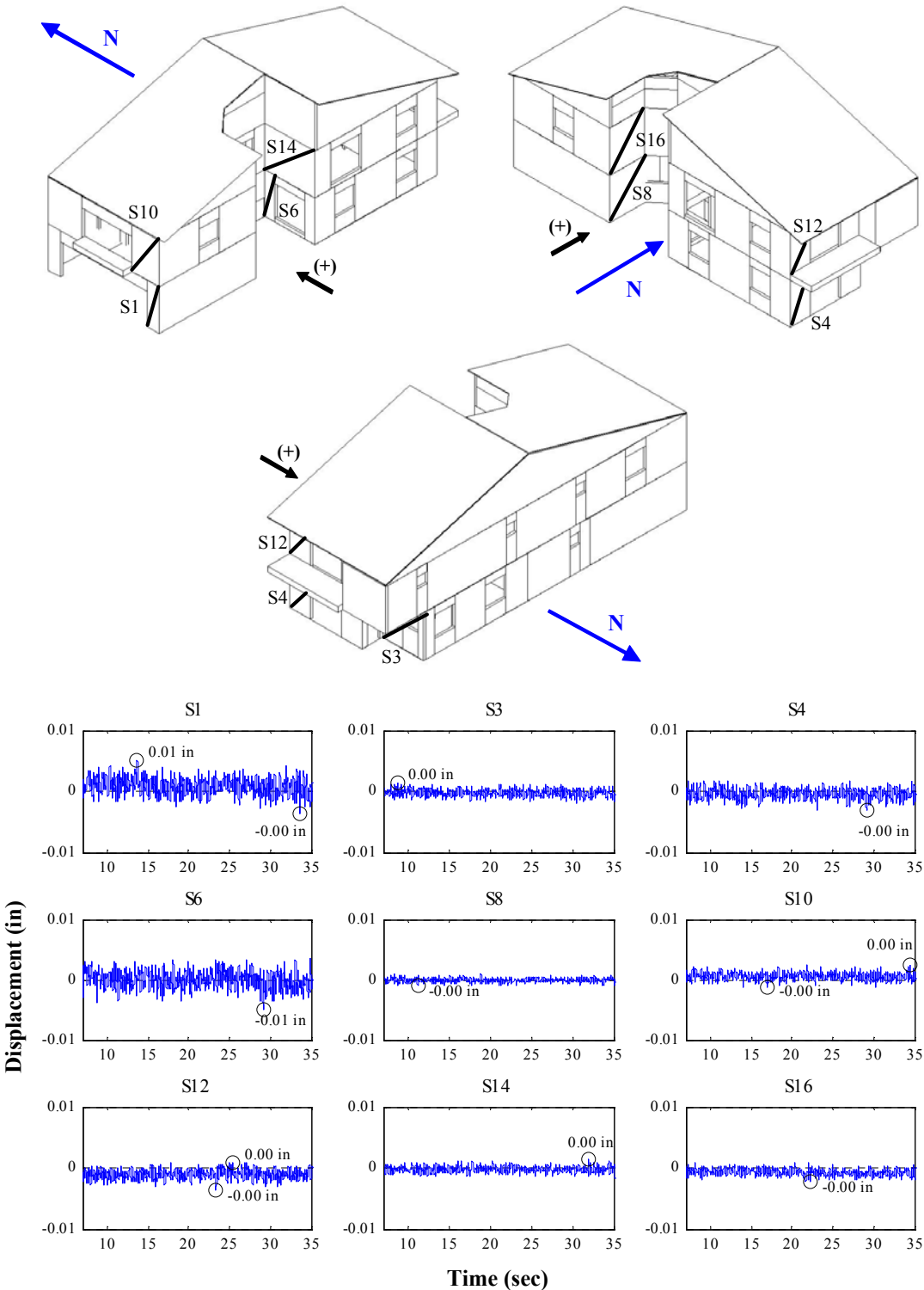


Figure M.79: Wall deformations of north-south external walls for Test NWP3S02

Appendix M

Phase 3, NWP3S02 Seismic Test, East-West, External Walls

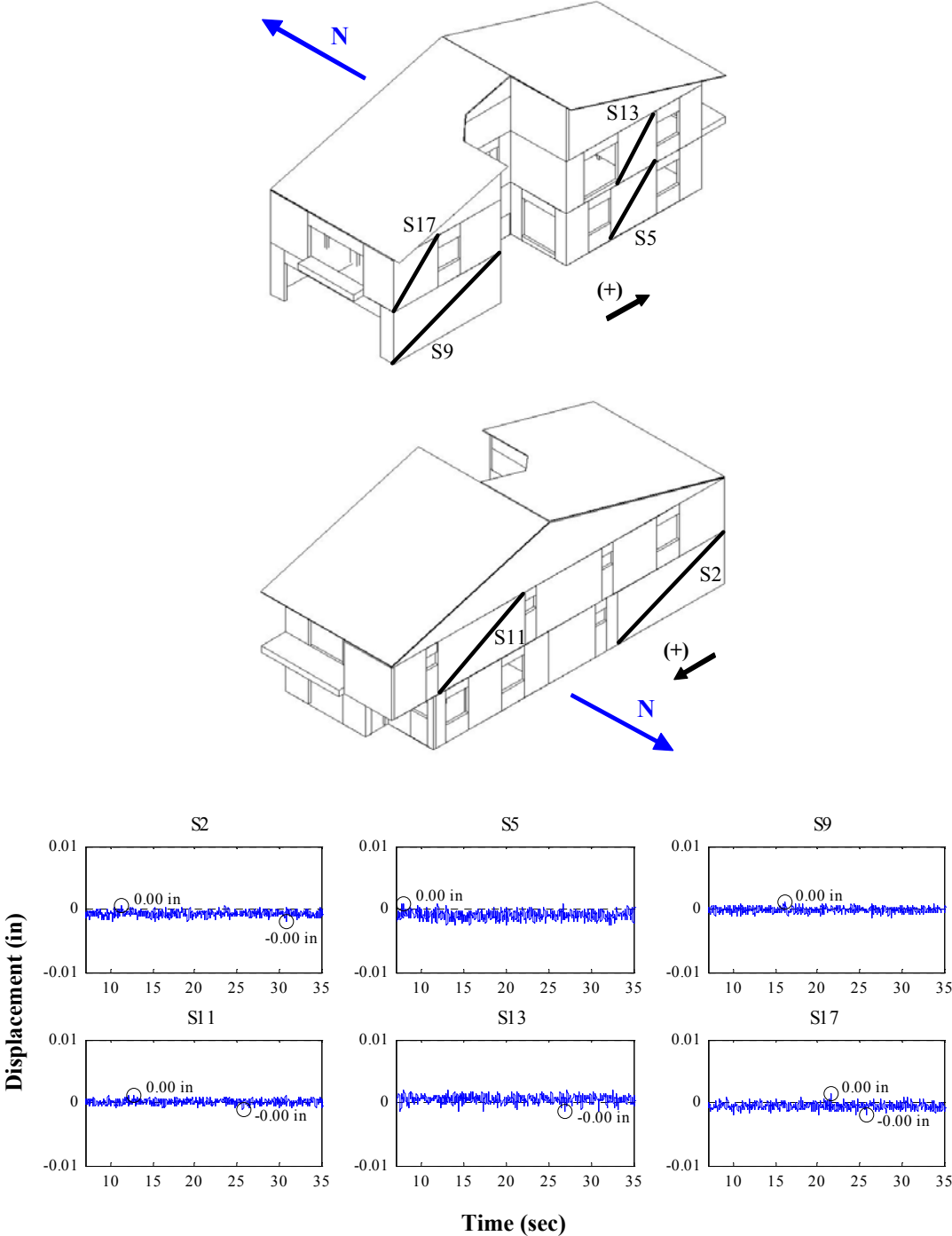


Figure M.80: Wall deformations of east-west external walls for Test NWP3S02

Appendix M

Phase 3, NWP3S02 Seismic Test, Internal Walls

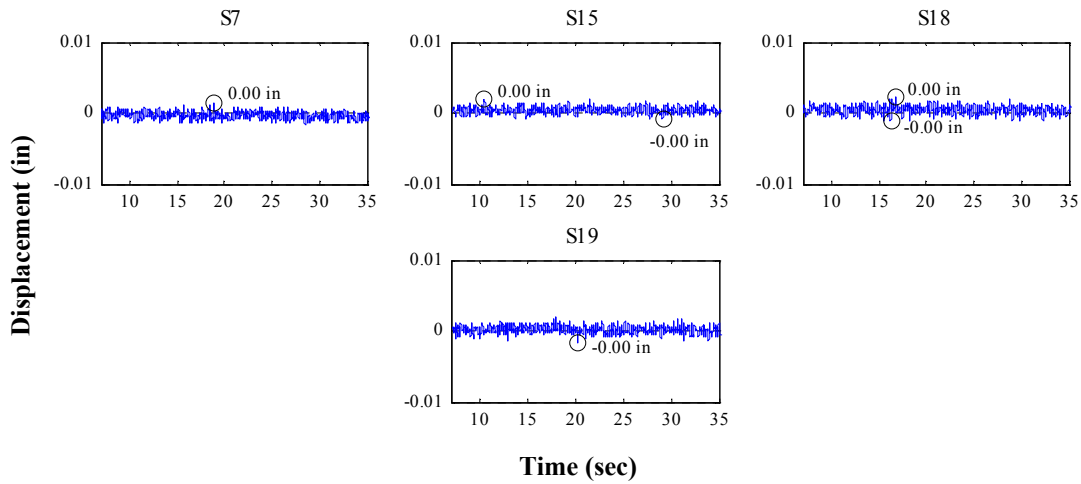
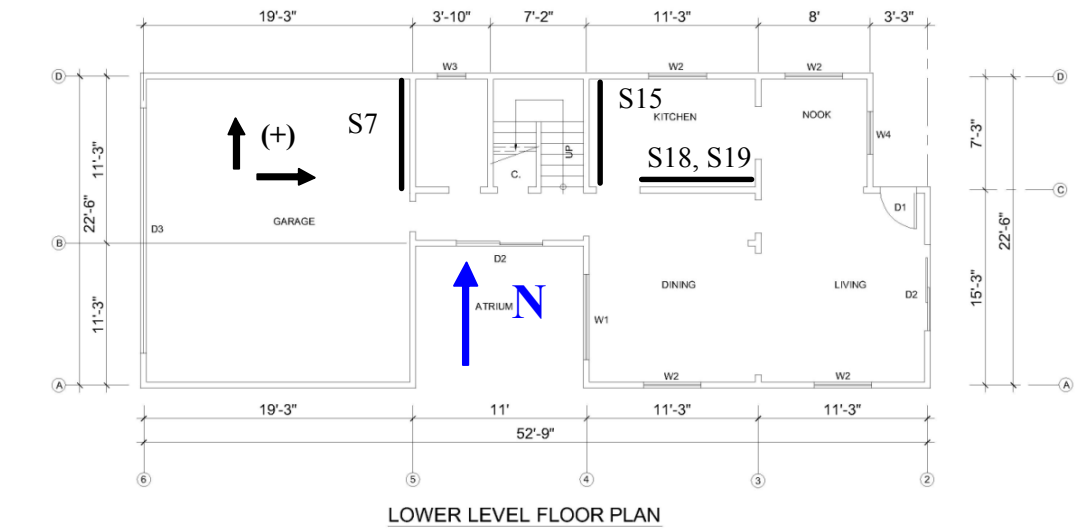


Figure M.81: Wall deformations of internal walls for Test NWP3S02

Appendix M

Phase 3, NWP3S03 Seismic Test, North-South, External Walls

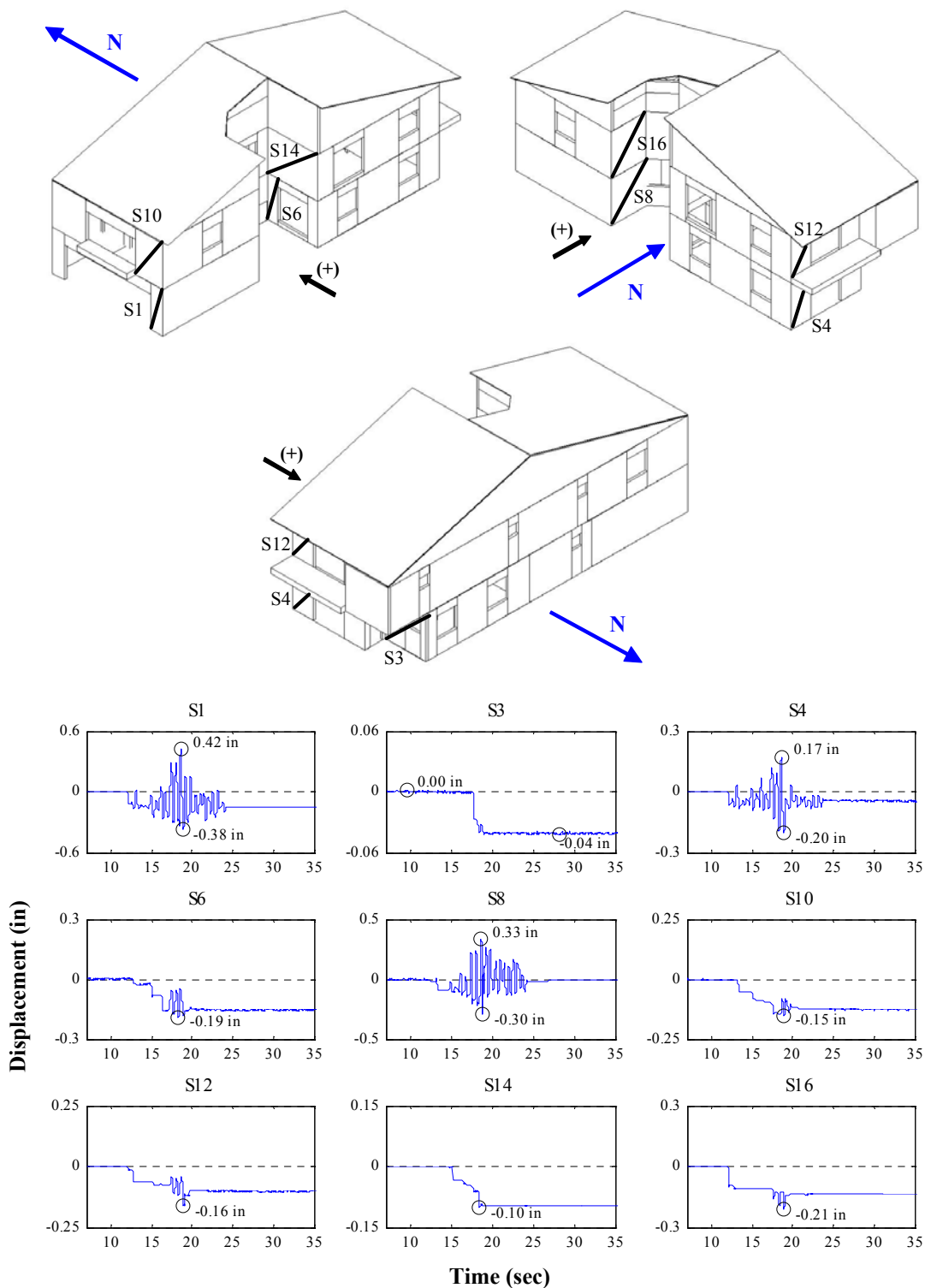


Figure M.82: Wall deformations of north-south external walls for Test NWP3S03

Appendix M

Phase 3, NWP3S03 Seismic Test, East-West, External Walls

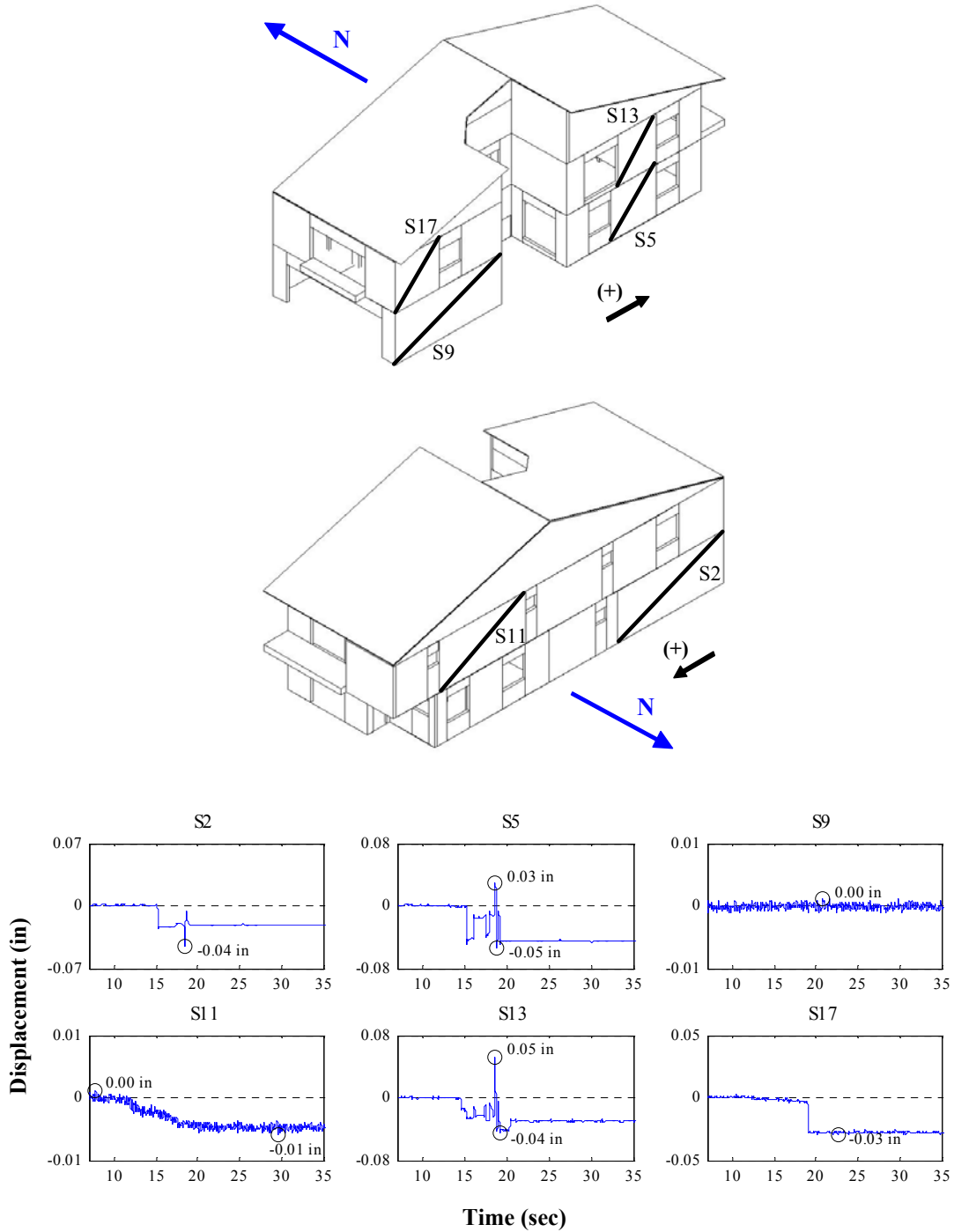


Figure M.83: Wall deformations of east-west external walls for Test NWP3S03

Appendix M

Phase 3, NWP3S03 Seismic Test, Internal Walls

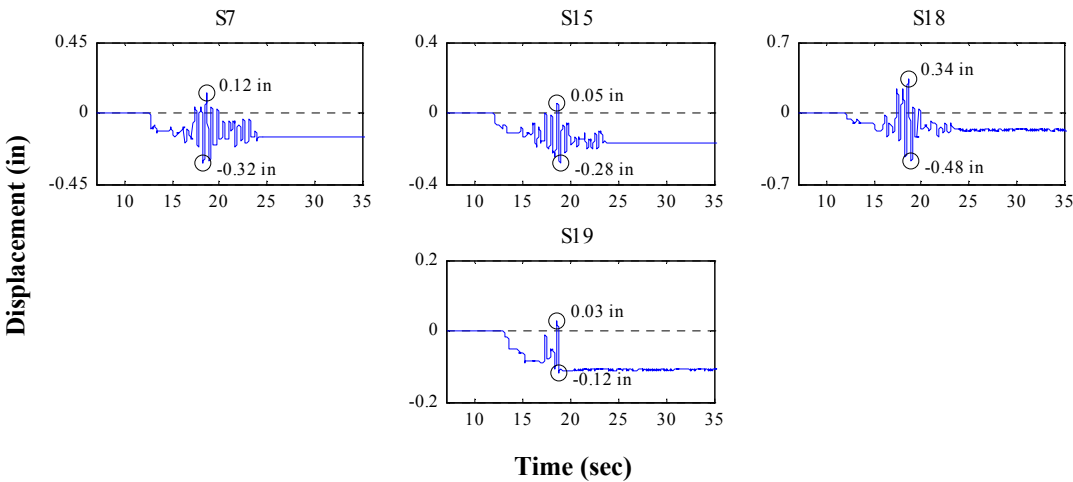
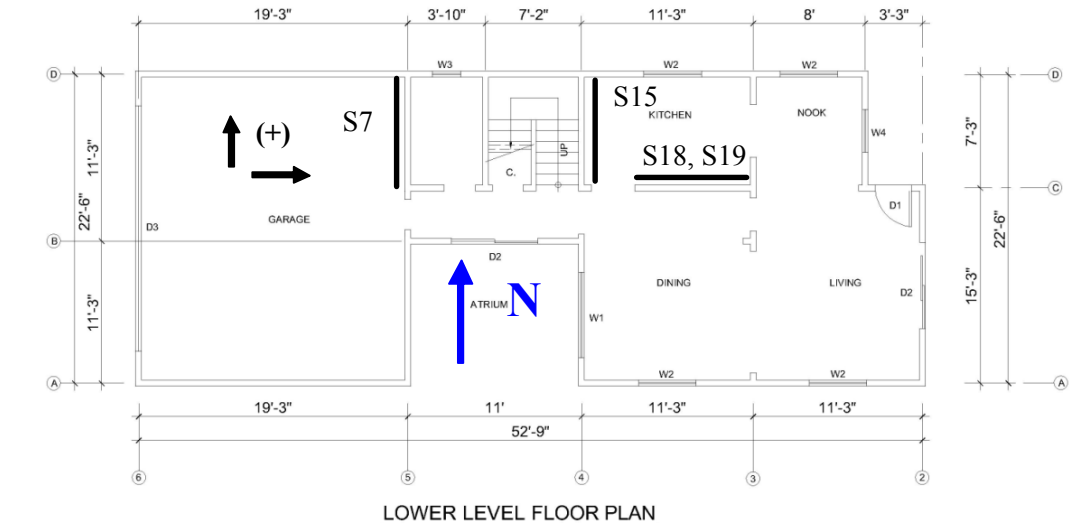


Figure M.84: Wall deformations of internal walls for Test NWP3S03

Appendix M

Phase 3, NWP3S04 Seismic Test, North-South, External Walls

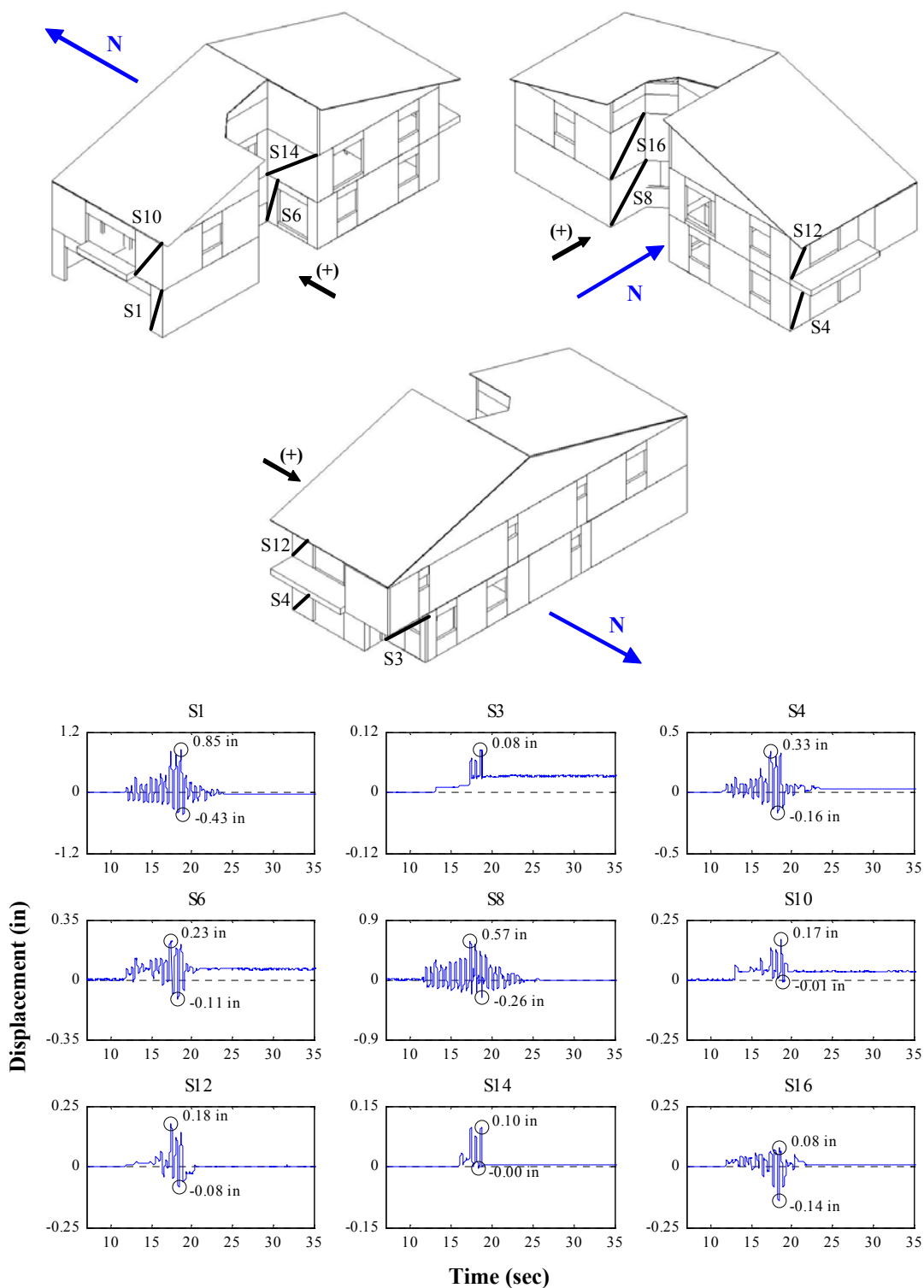


Figure M.85: Wall deformations of north-south external walls for Test NWP3S04

Appendix M

Phase 3, NWP3S04 Seismic Test, East-West, External Walls

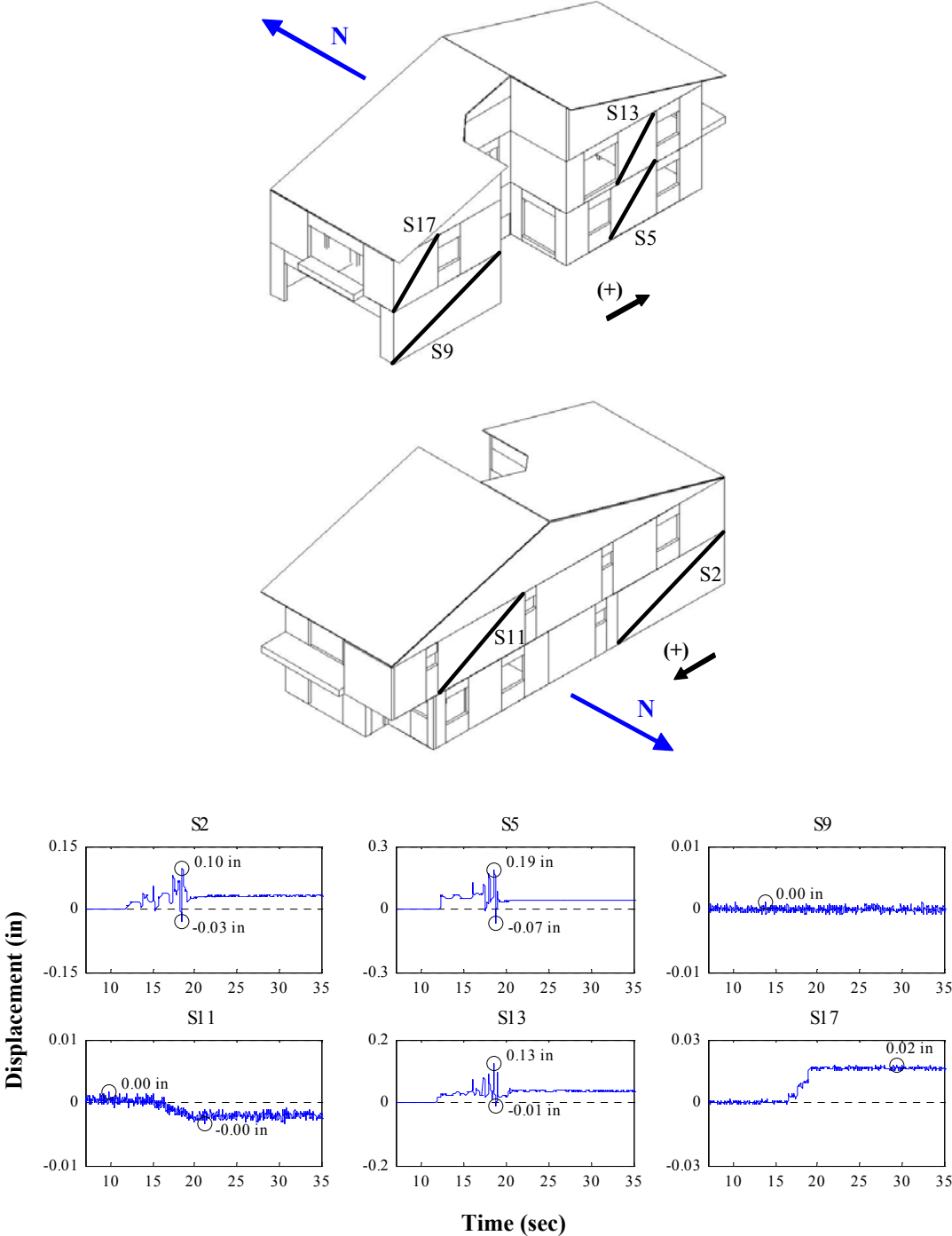


Figure M.86: Wall deformations of east-west external walls for Test NWP3S04

Appendix M

Phase 3, NWP3S04 Seismic Test, Internal Walls

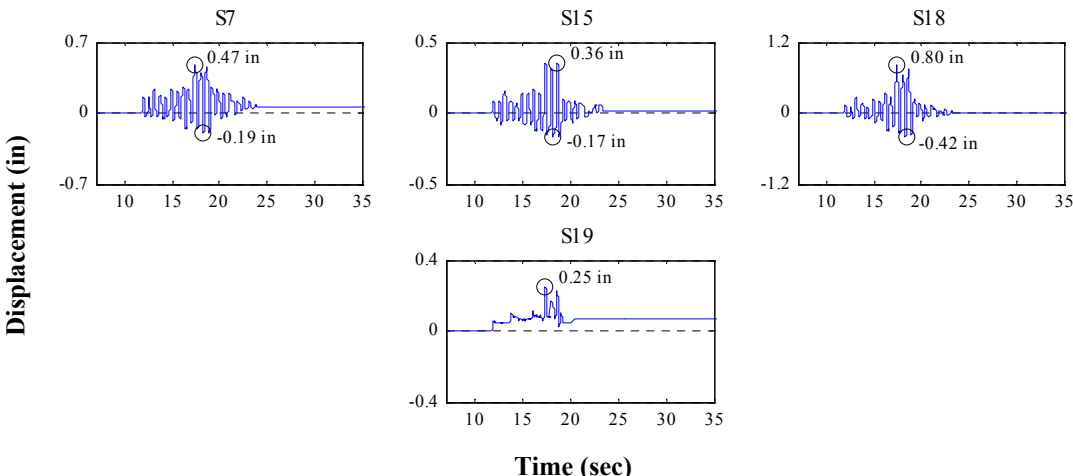
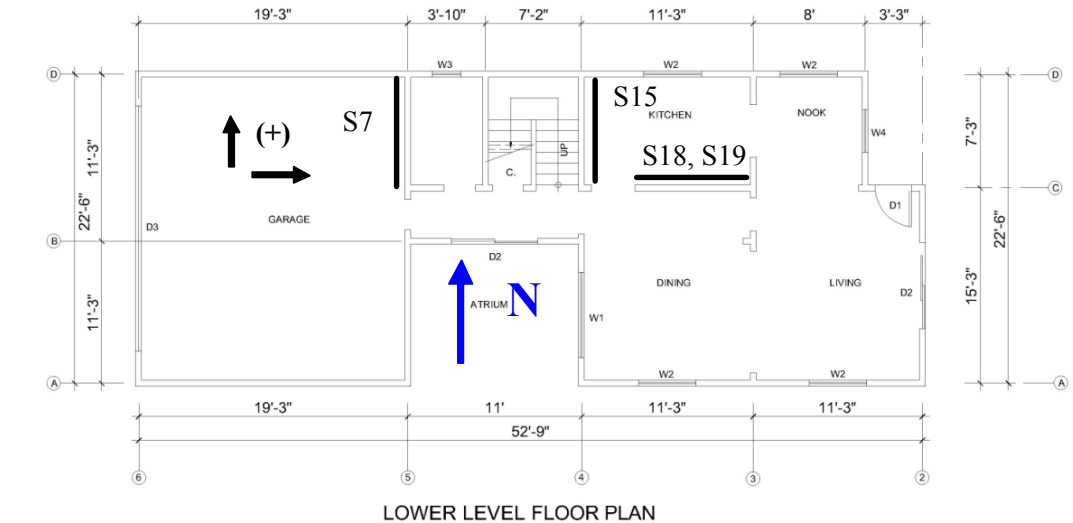


Figure M.87: Wall deformations of internal walls for Test NWP3S04

Appendix M

Phase 4, NWP4S01 Seismic Test, North-South, External Walls

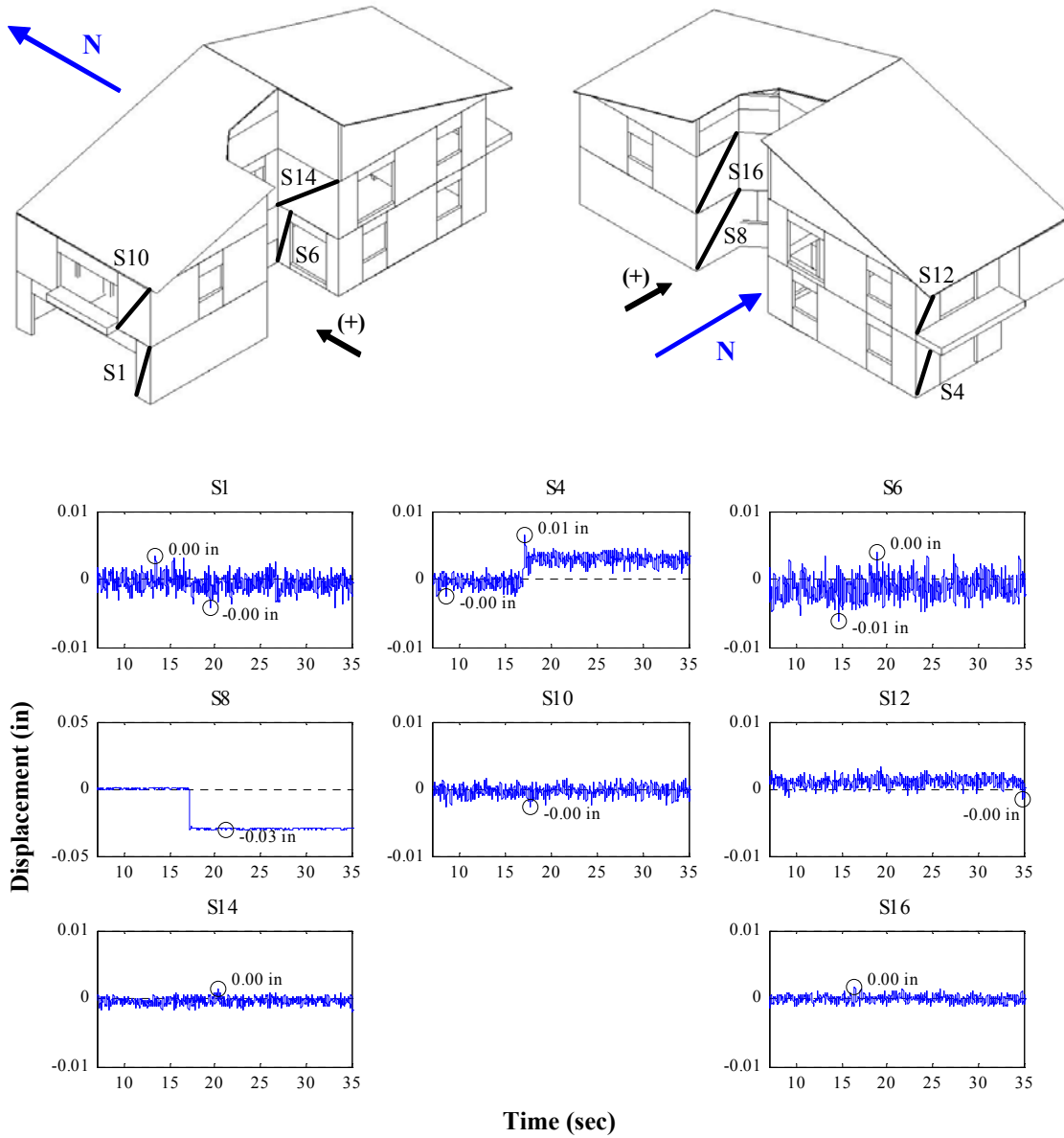


Figure M.88: Wall deformations of north-south external walls for Test NWP4S01

Appendix M

Phase 4, NWP4S01 Seismic Test, East-West, External Walls

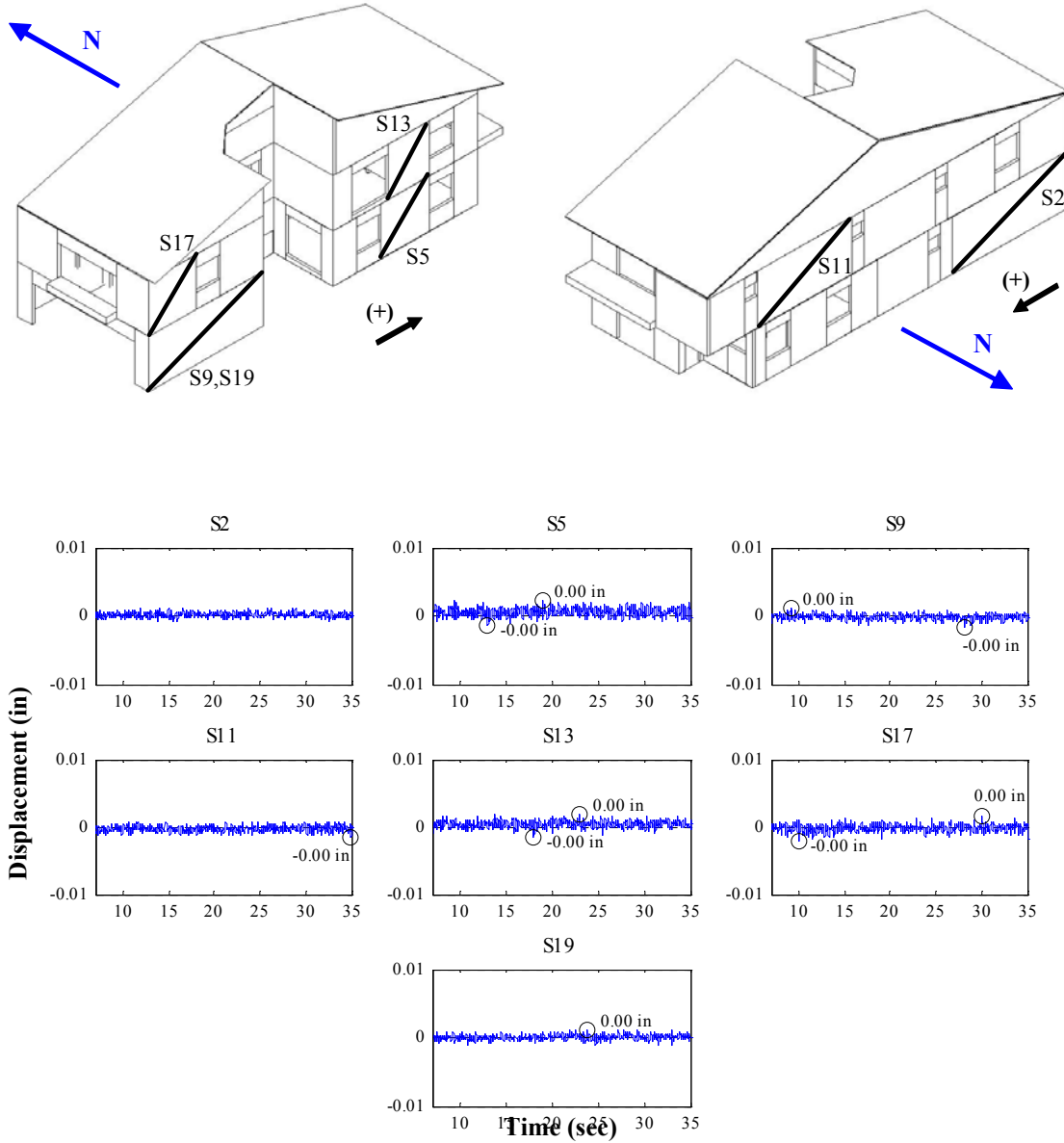


Figure M.89: Wall deformations of east-west external walls for Test NWP4S01

Appendix M

Phase 4, NWP4S01 Seismic Test, Internal Walls

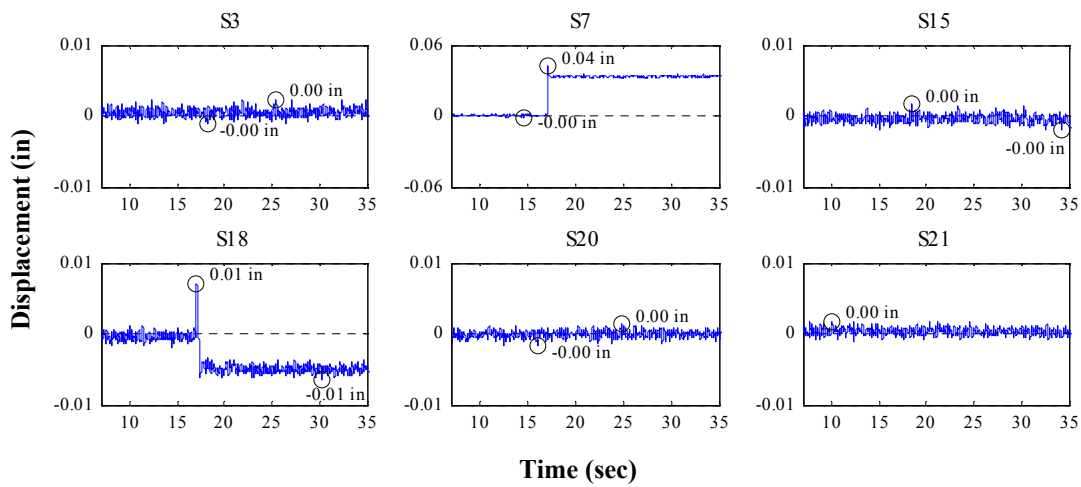
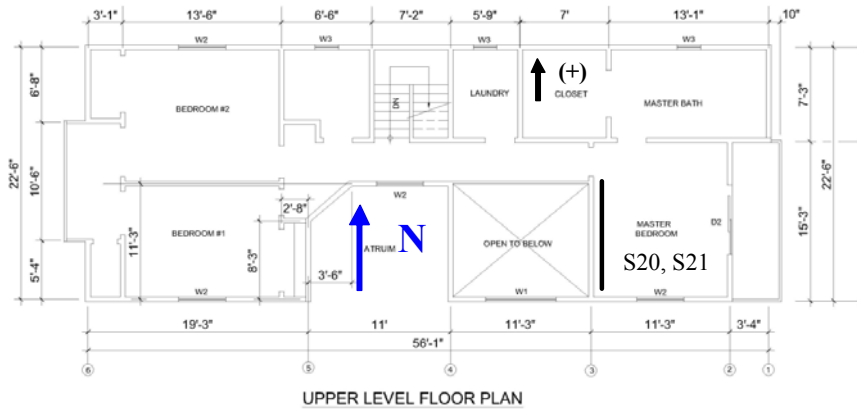
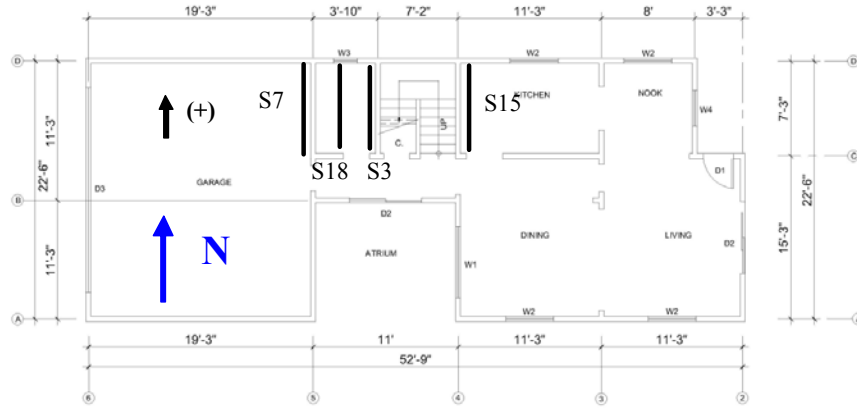


Figure M.90: Wall deformations of internal walls for Test NWP4S01

Appendix M

Phase 4, NWP4S02 Seismic Test, North-South, External Walls

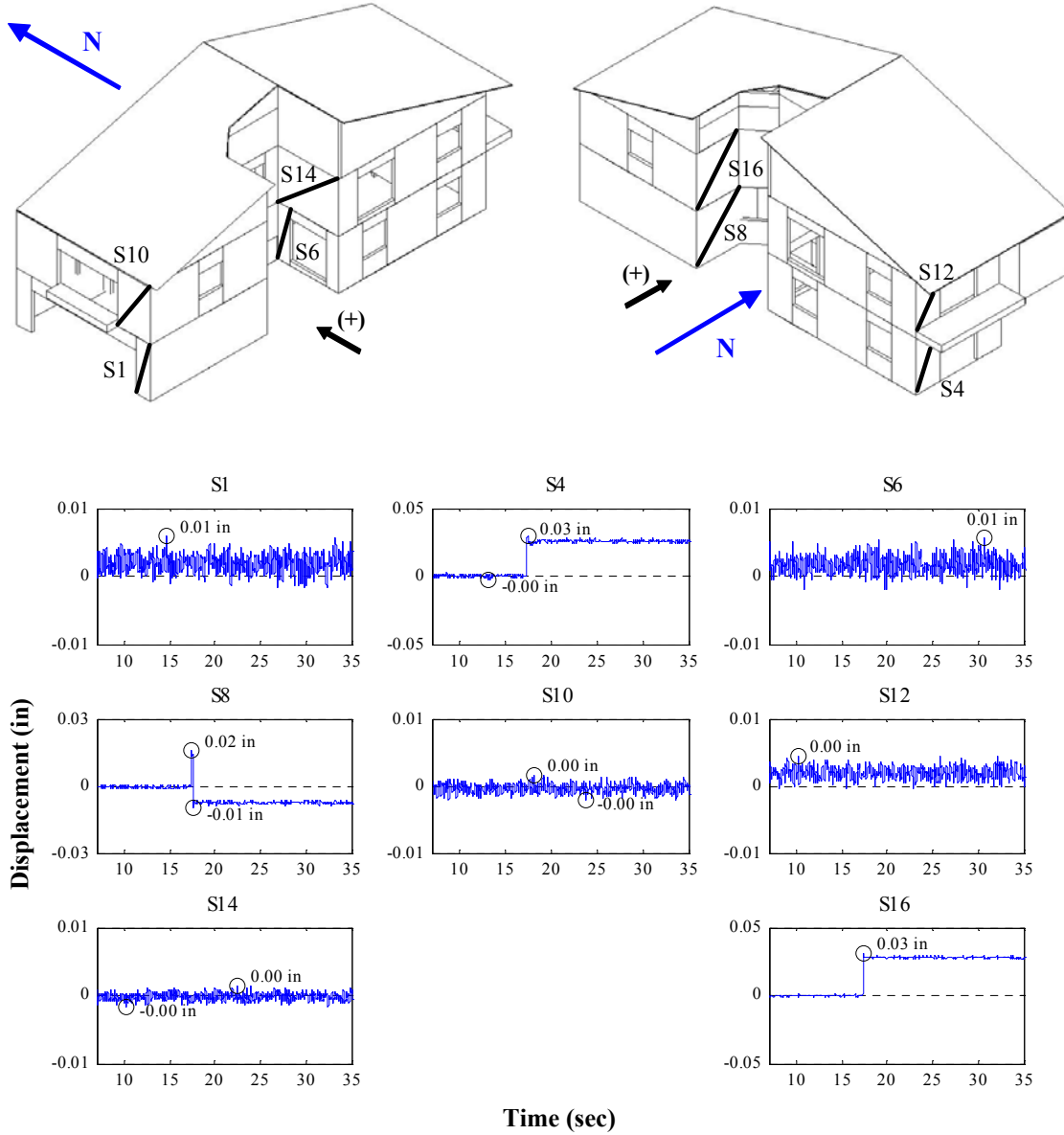


Figure M.91: Wall deformations of north-south external walls for Test NWP4S02

Appendix M

Phase 4, NWP4S02 Seismic Test, East-West, External Walls

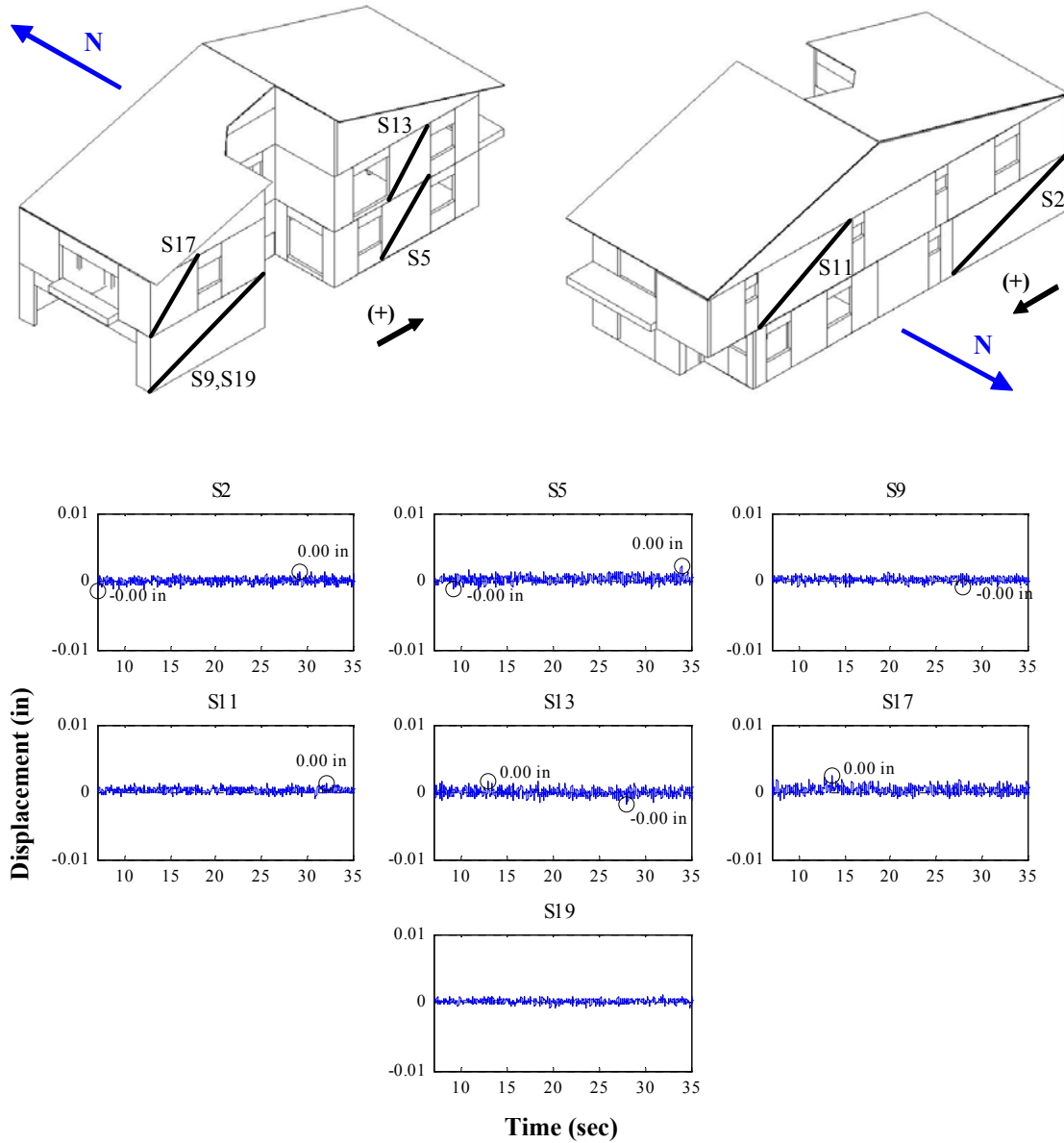


Figure M.92: Wall deformations of east-west external walls for Test NWP4S02

Appendix M

Phase 4, NWP4S02 Seismic Test, Internal Walls

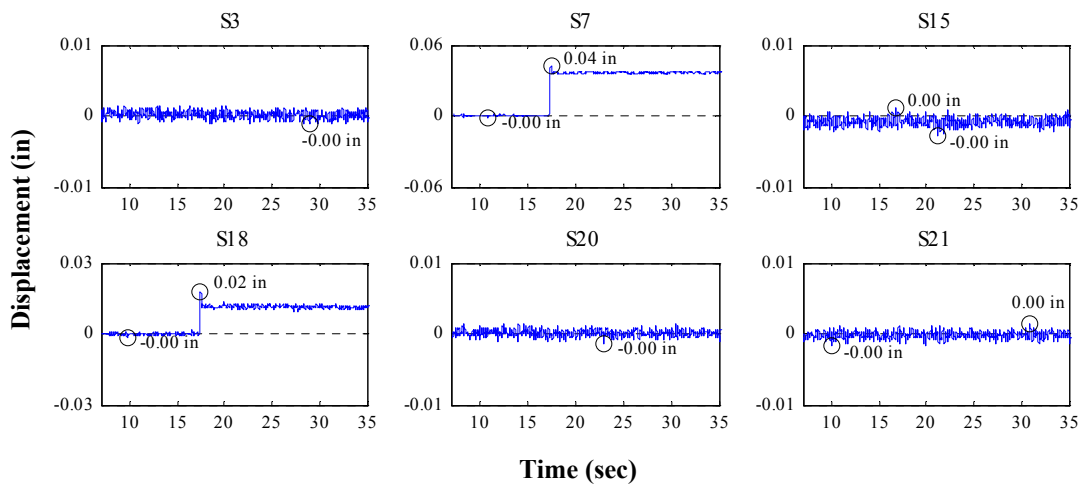
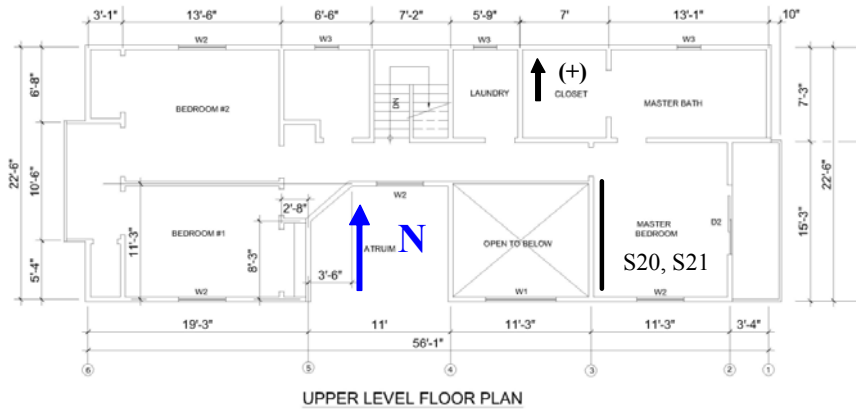
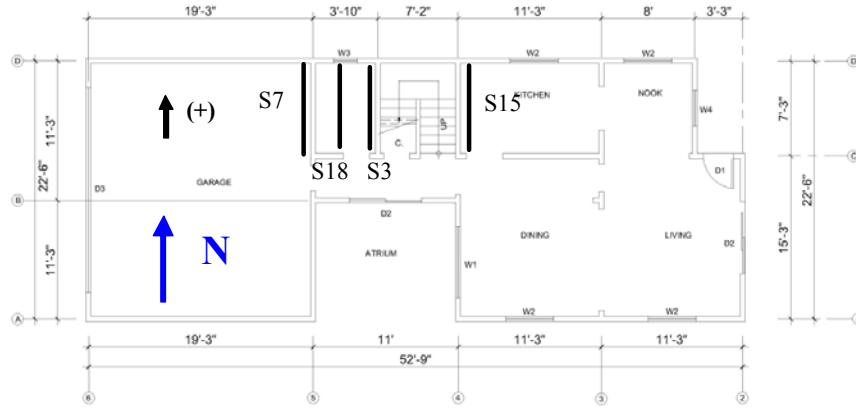


Figure M.93: Wall deformations of internal walls for Test NWP4S02

Appendix M

Phase 4, NWP4S03 Seismic Test, North-South, External Walls

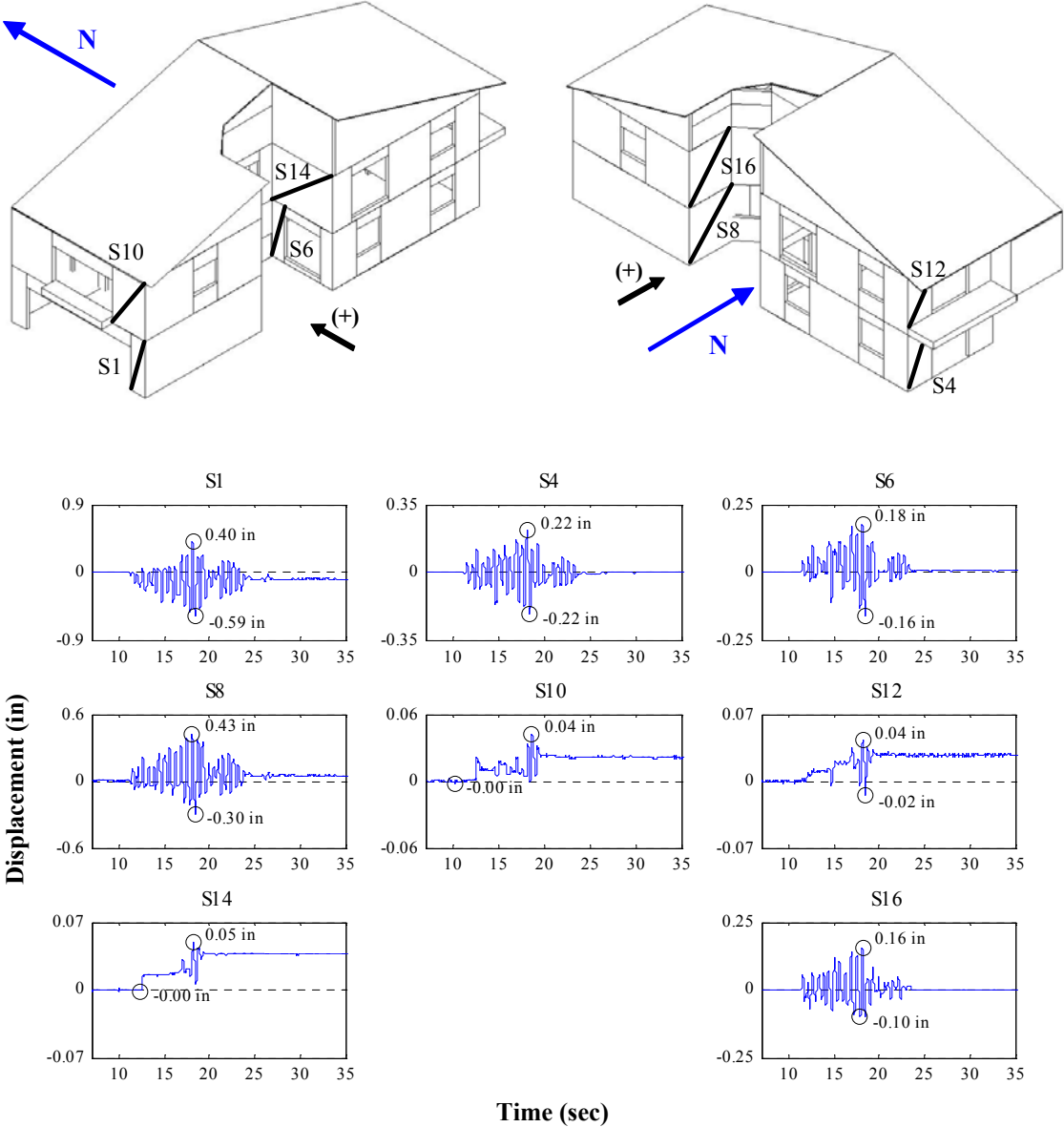


Figure M.94: Wall deformations of north-south external walls for Test NWP4S03

Appendix M

Phase 4, NWP4S03 Seismic Test, East-West, External Walls

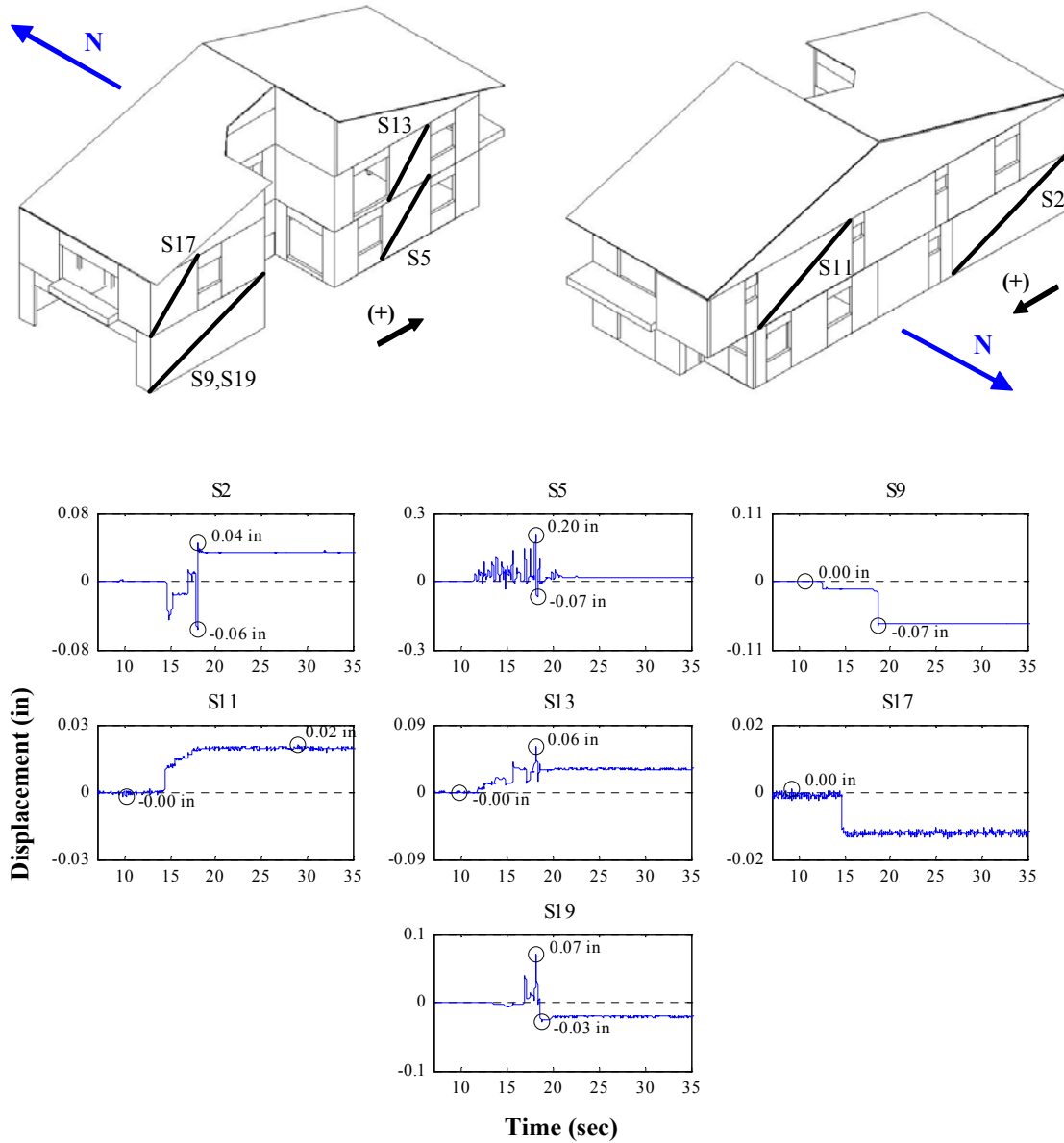


Figure M.95: Wall deformations of east-west external walls for Test NWP4S03

Appendix M

Phase 4, NWP4S03 Seismic Test, Internal Walls

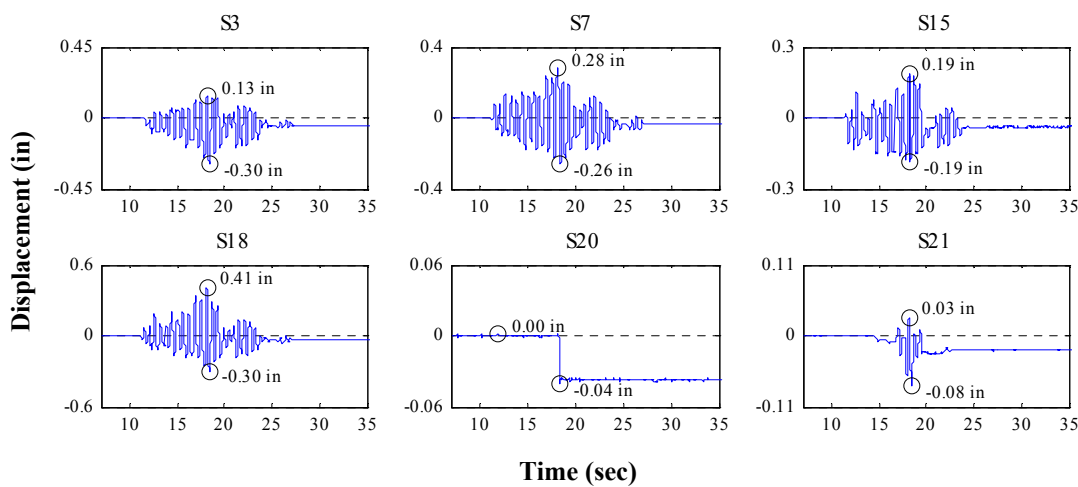
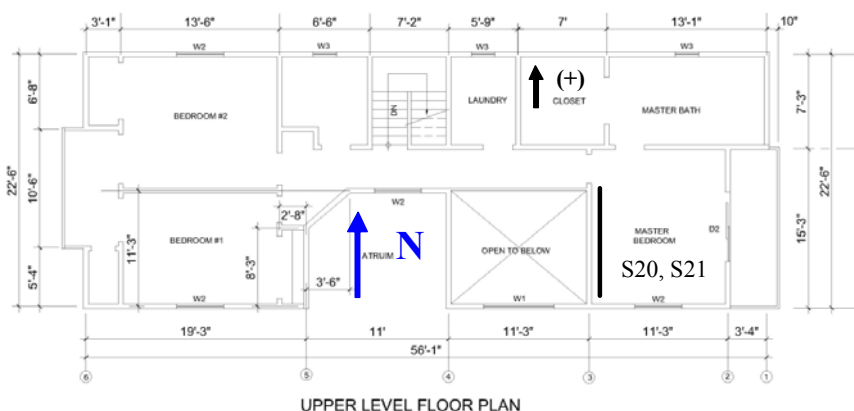
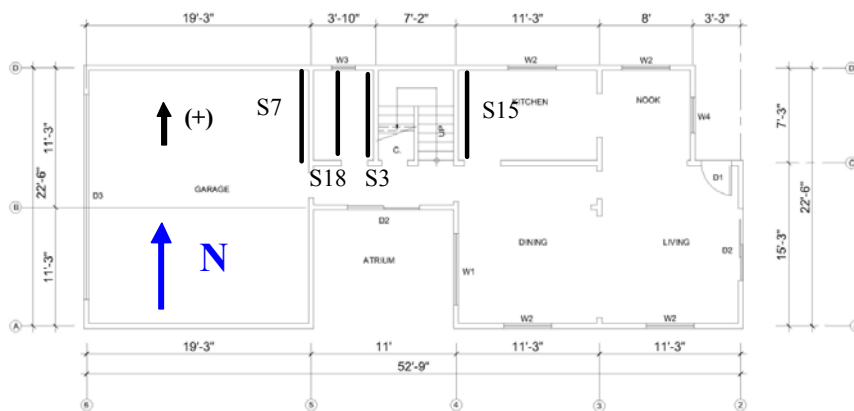


Figure M.96: Wall deformations of internal walls for Test NWP4S03

Appendix M

Phase 4, NWP4S04 Seismic Test, North-South, External Walls

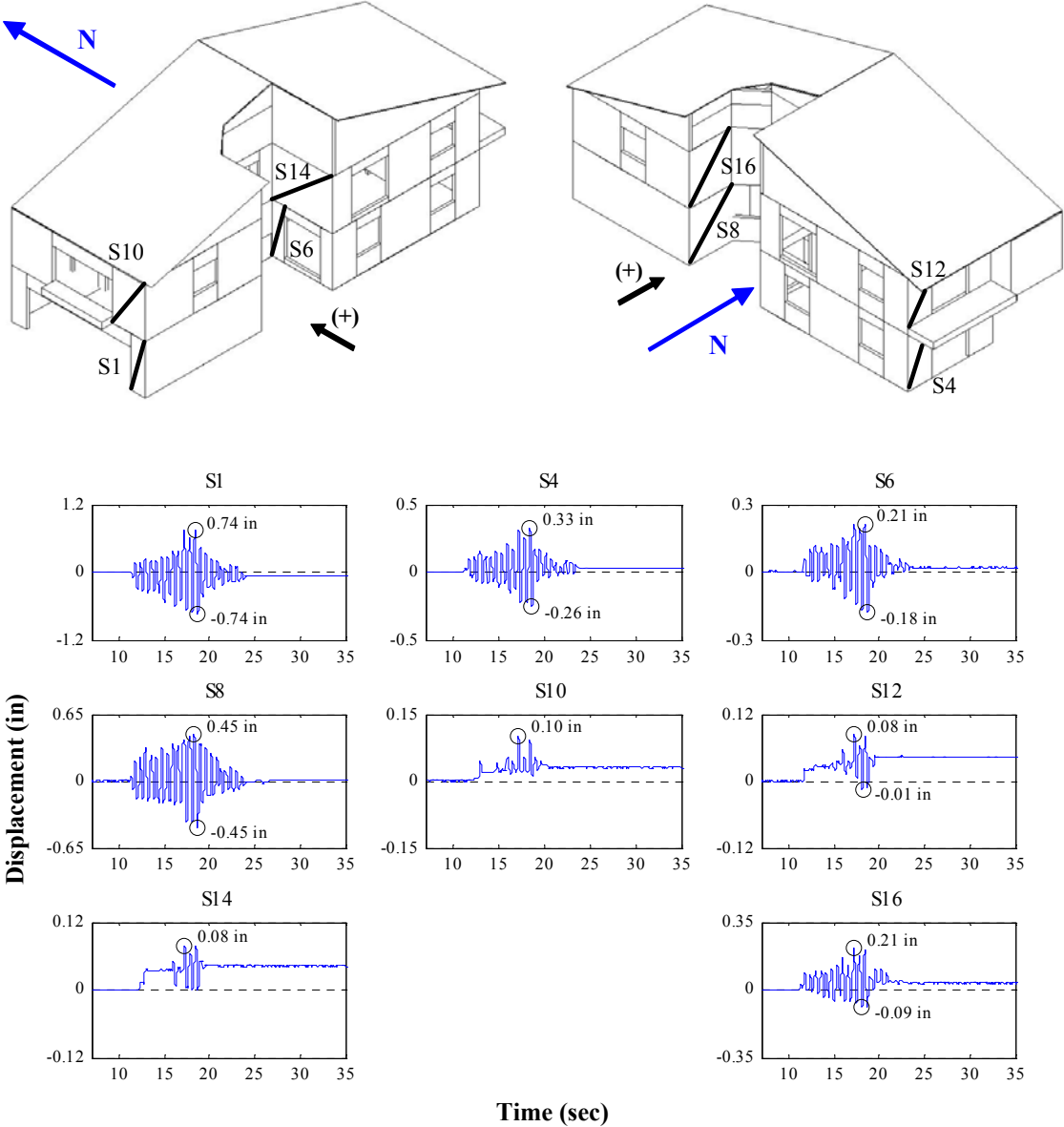


Figure M.97: Wall deformations of north-south external walls for Test NWP4S04

Appendix M

Phase 4, NWP4S04 Seismic Test, East-West, External Walls

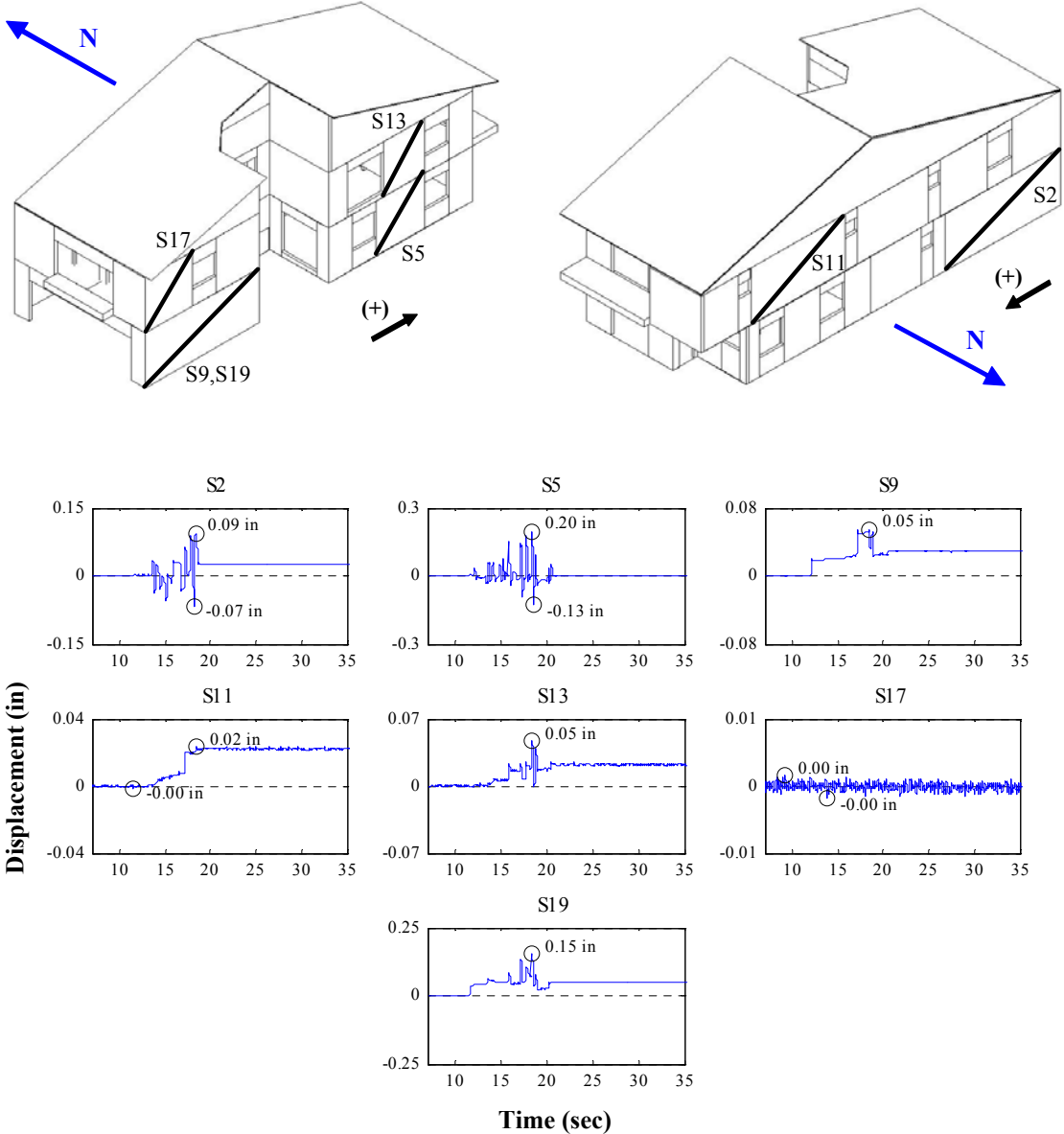


Figure M.98: Wall deformations of east-west external walls for Test NWP4S04

Appendix M

Phase 4, NWP4S04 Seismic Test, Internal Walls

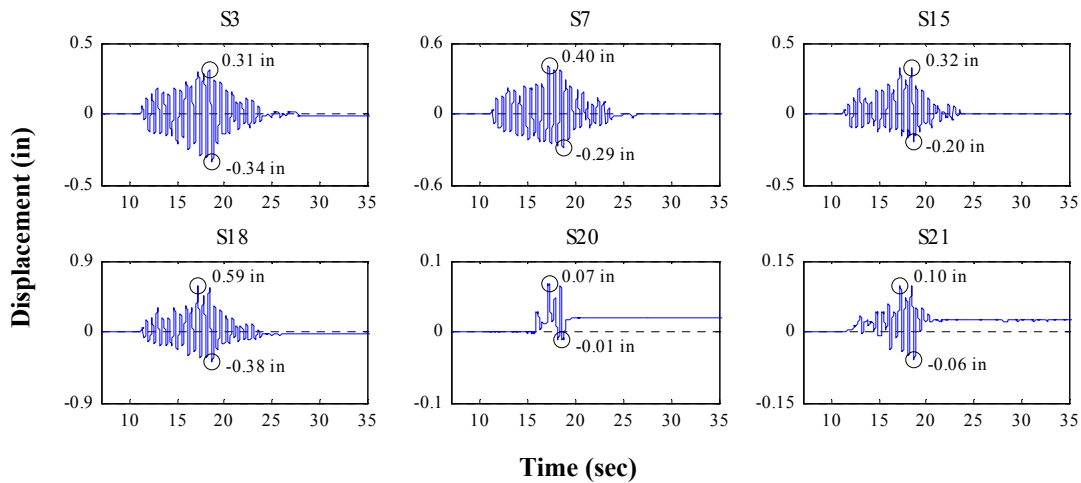
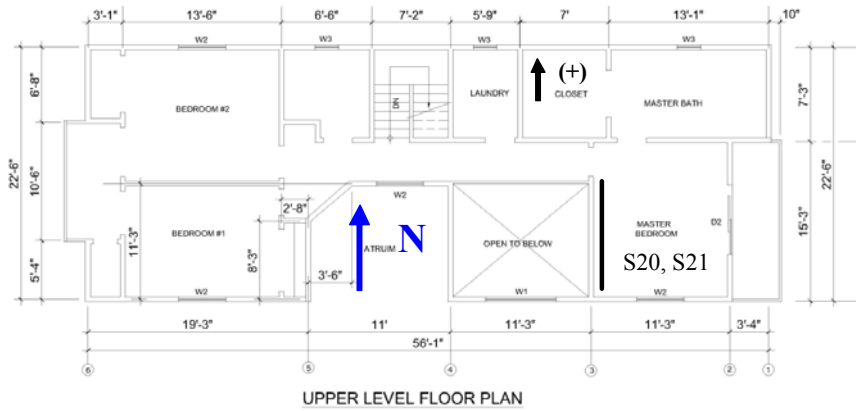
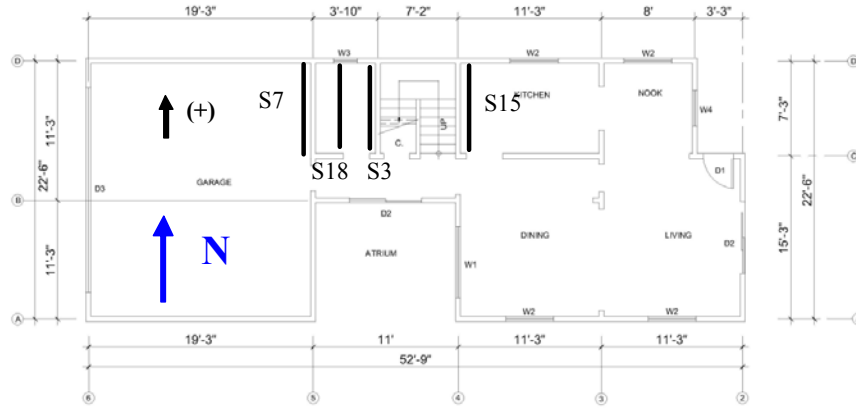


Figure M.99: Wall deformations of internal walls for Test NWP4S04

Appendix M

Phase 5, NWP5S01 Seismic Test, North-South, External Walls

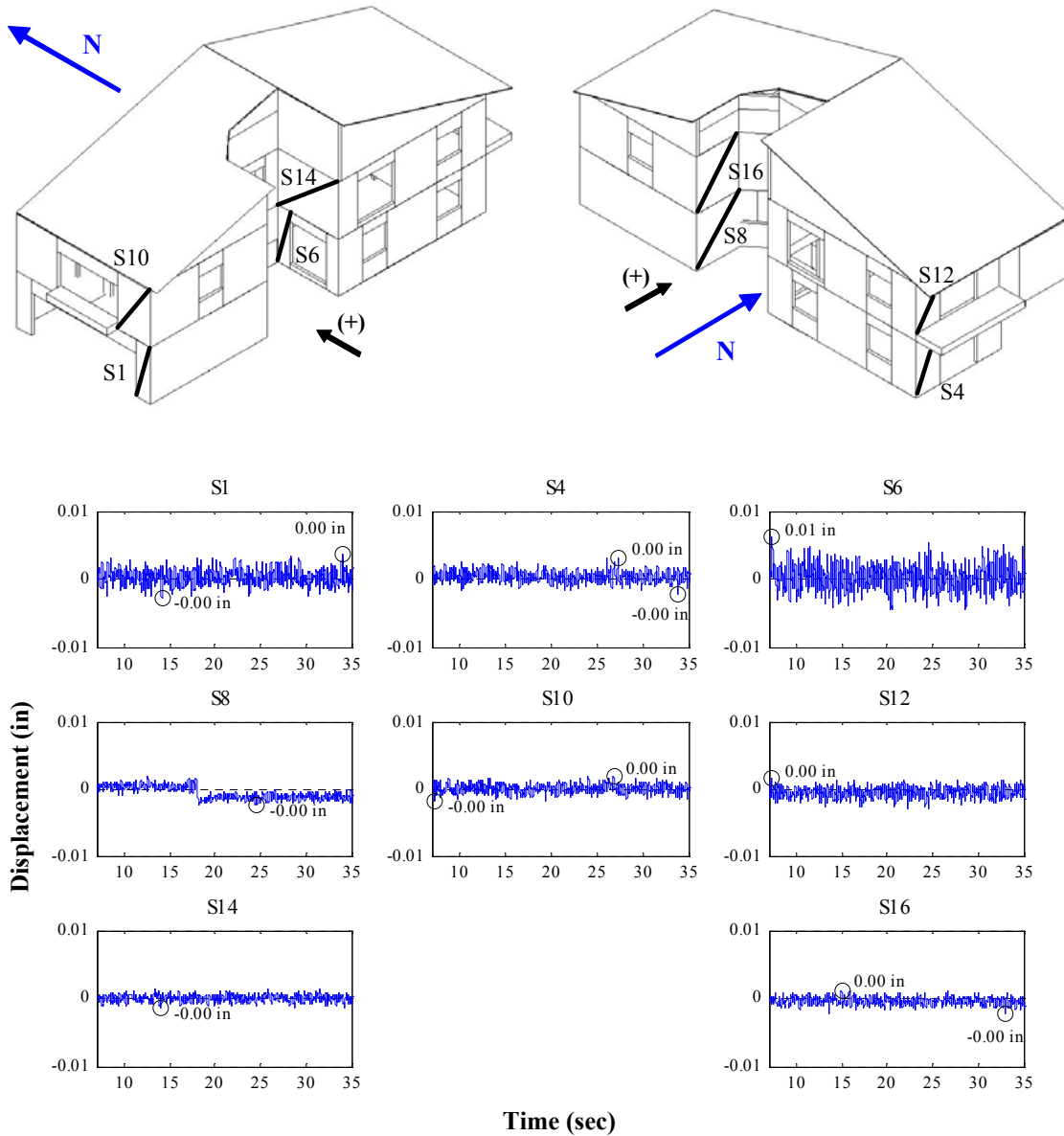


Figure M.100: Wall deformations of north-south external walls for Test NWP5S01

Appendix M

Phase 5, NWP5S01 Seismic Test, East-West, External Walls

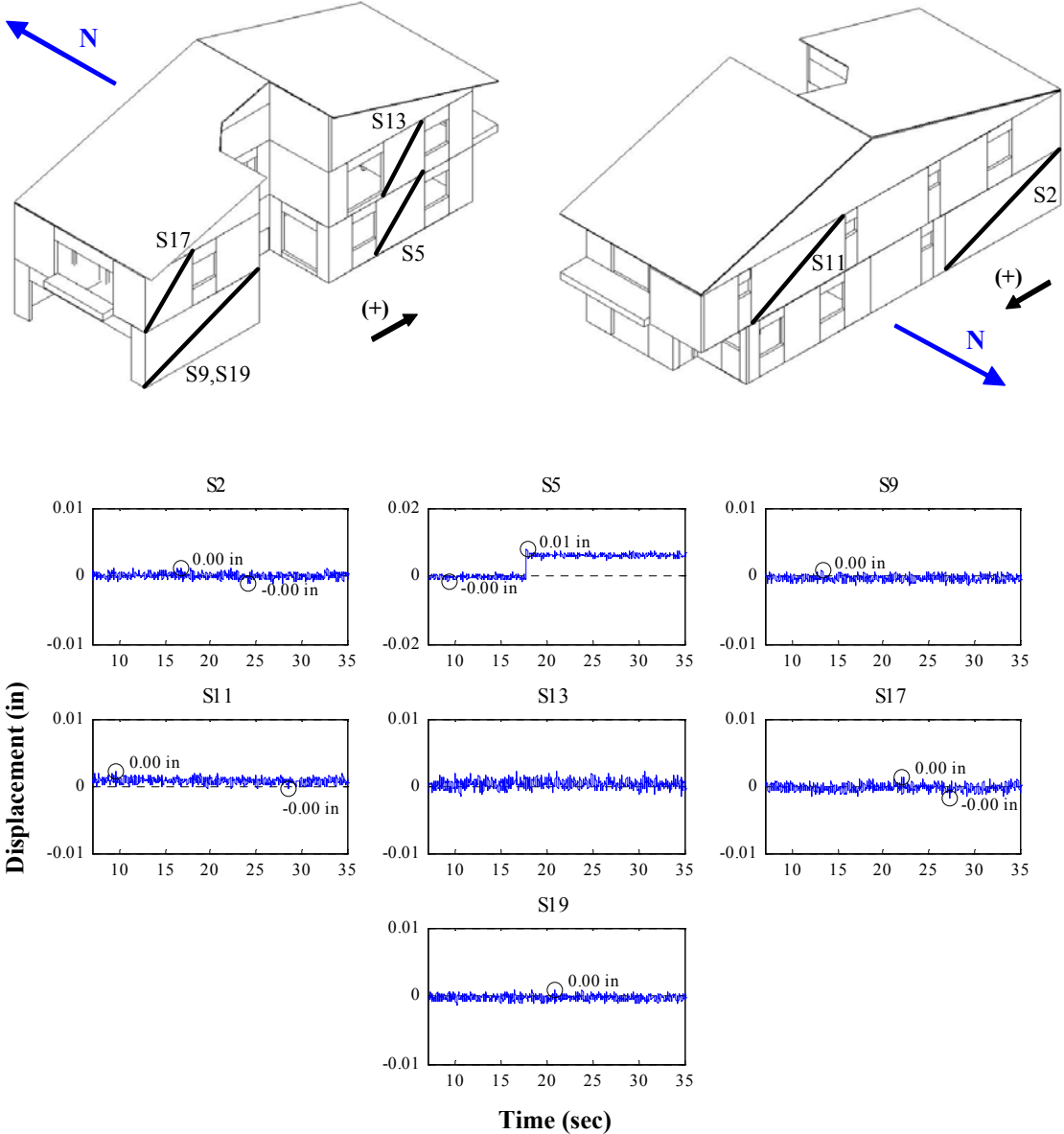


Figure M.101: Wall deformations of east-west external walls for Test NWP5S01

Appendix M

Phase 5, NWP5S01 Seismic Test, Internal Walls

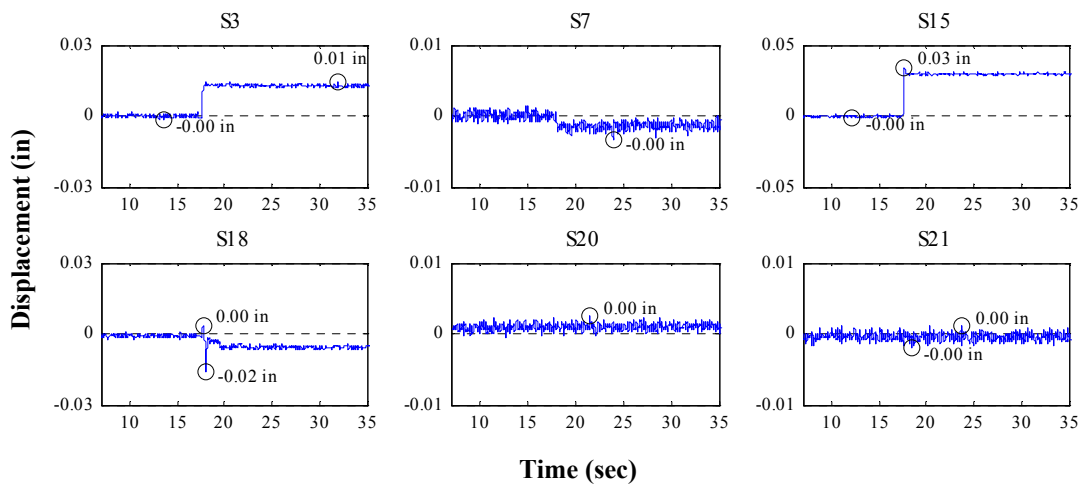
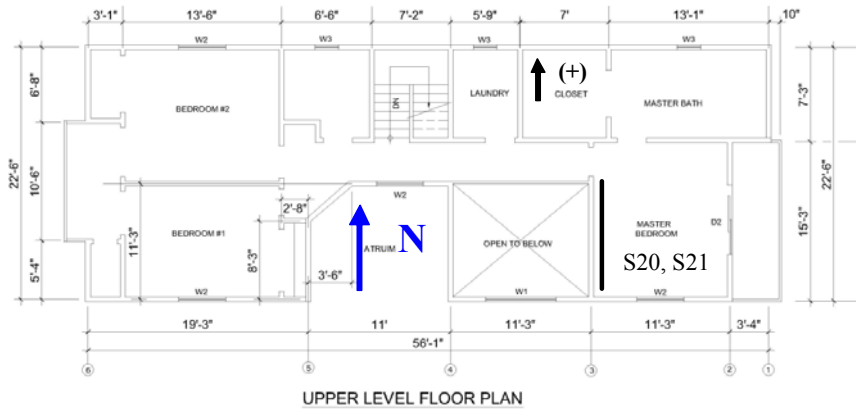
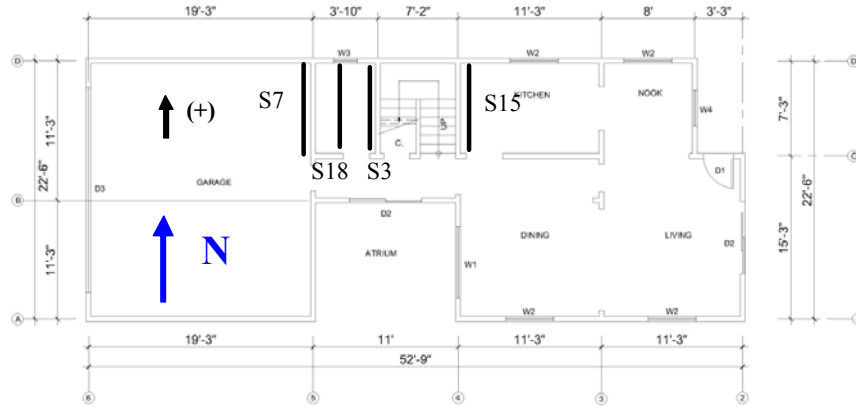


Figure M.102: Wall deformations of internal walls for Test NWP5S01

Appendix M

Phase 5, NWP5S02 Seismic Test, North-South, External Walls

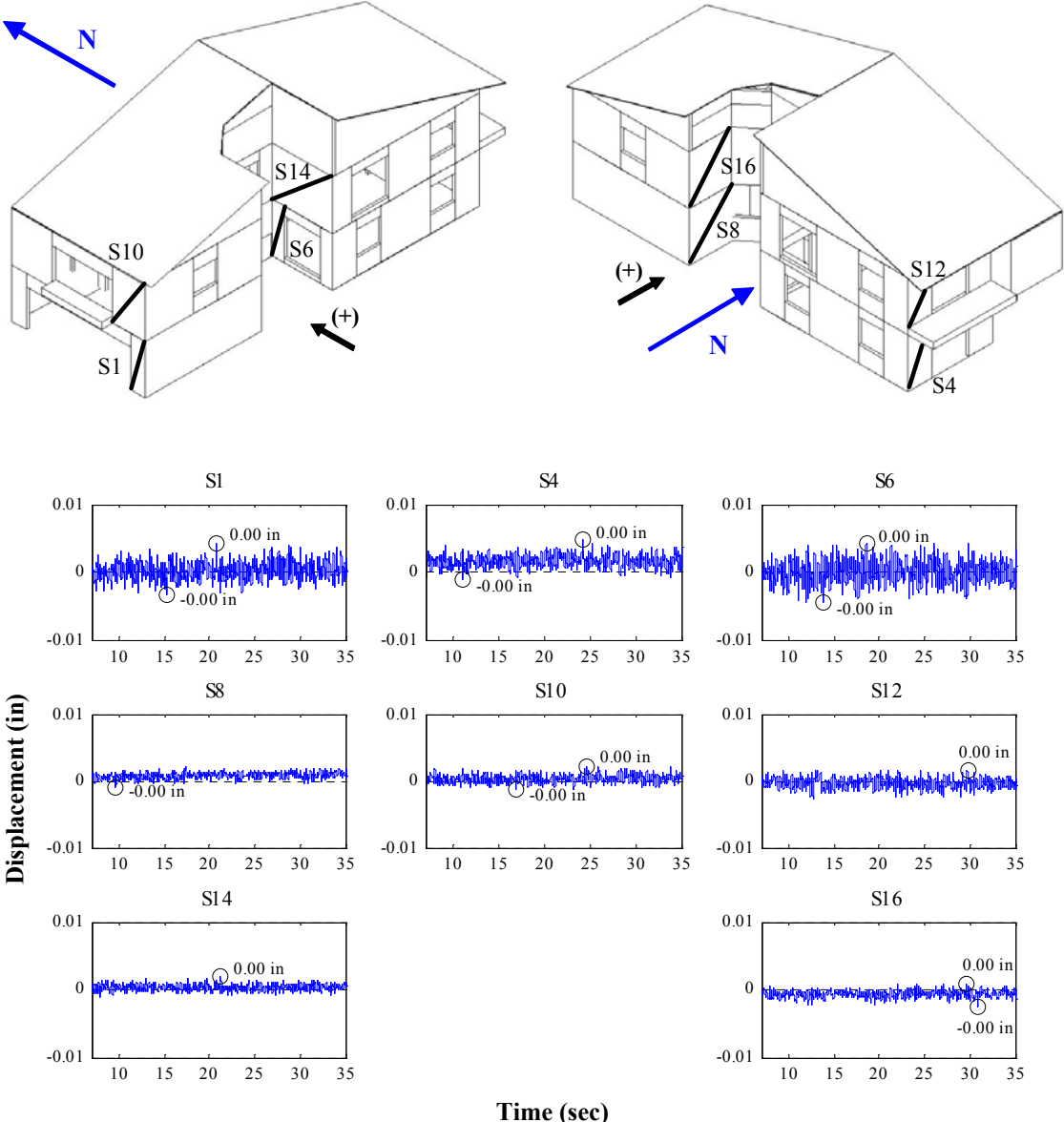


Figure M.103: Wall deformations of north-south external walls for Test NWP5S02

Appendix M

Phase 5, NWP5S02 Seismic Test, East-West, External Walls

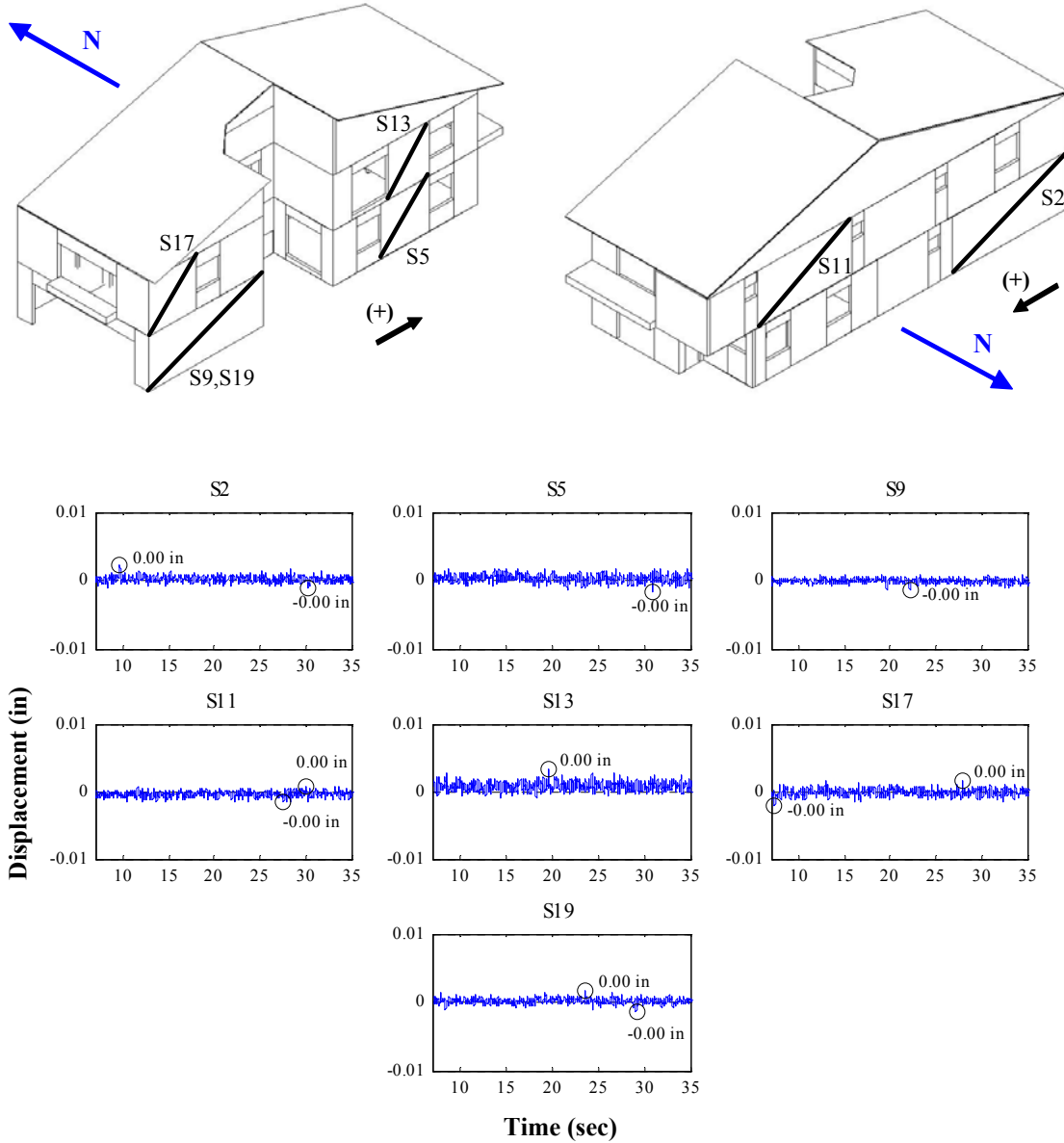


Figure M.104: Wall deformations of east-west external walls for Test NWP5S02

Appendix M

Phase 5, NWP5S02 Seismic Test, Internal Walls

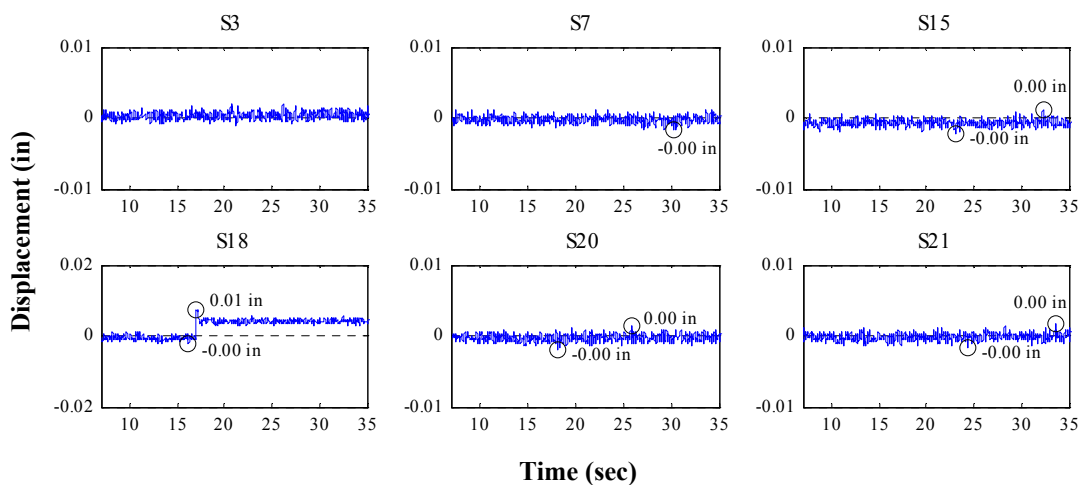
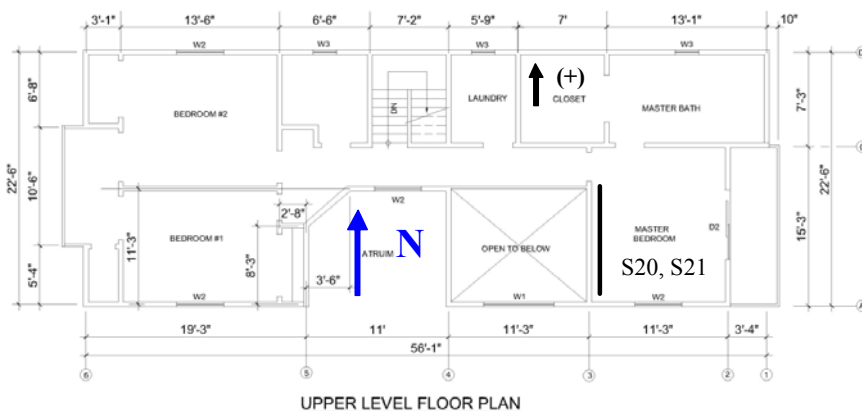
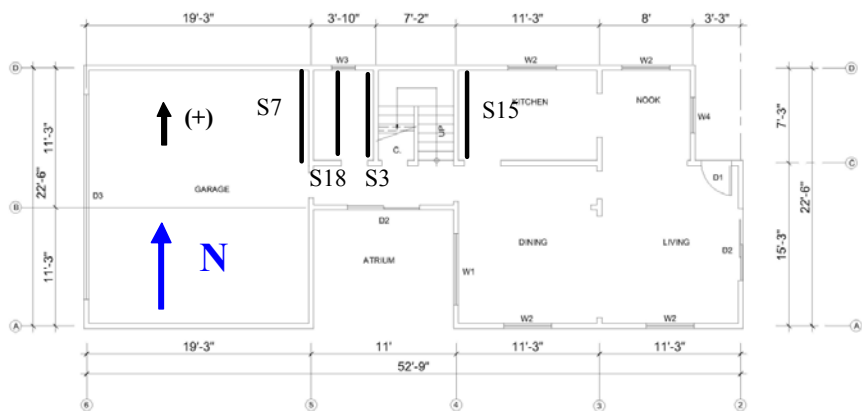


Figure M.105: Wall deformations of internal walls for Test NWP5S02

Appendix M

Phase 5, NWP5S03 Seismic Test, North-South, External Walls

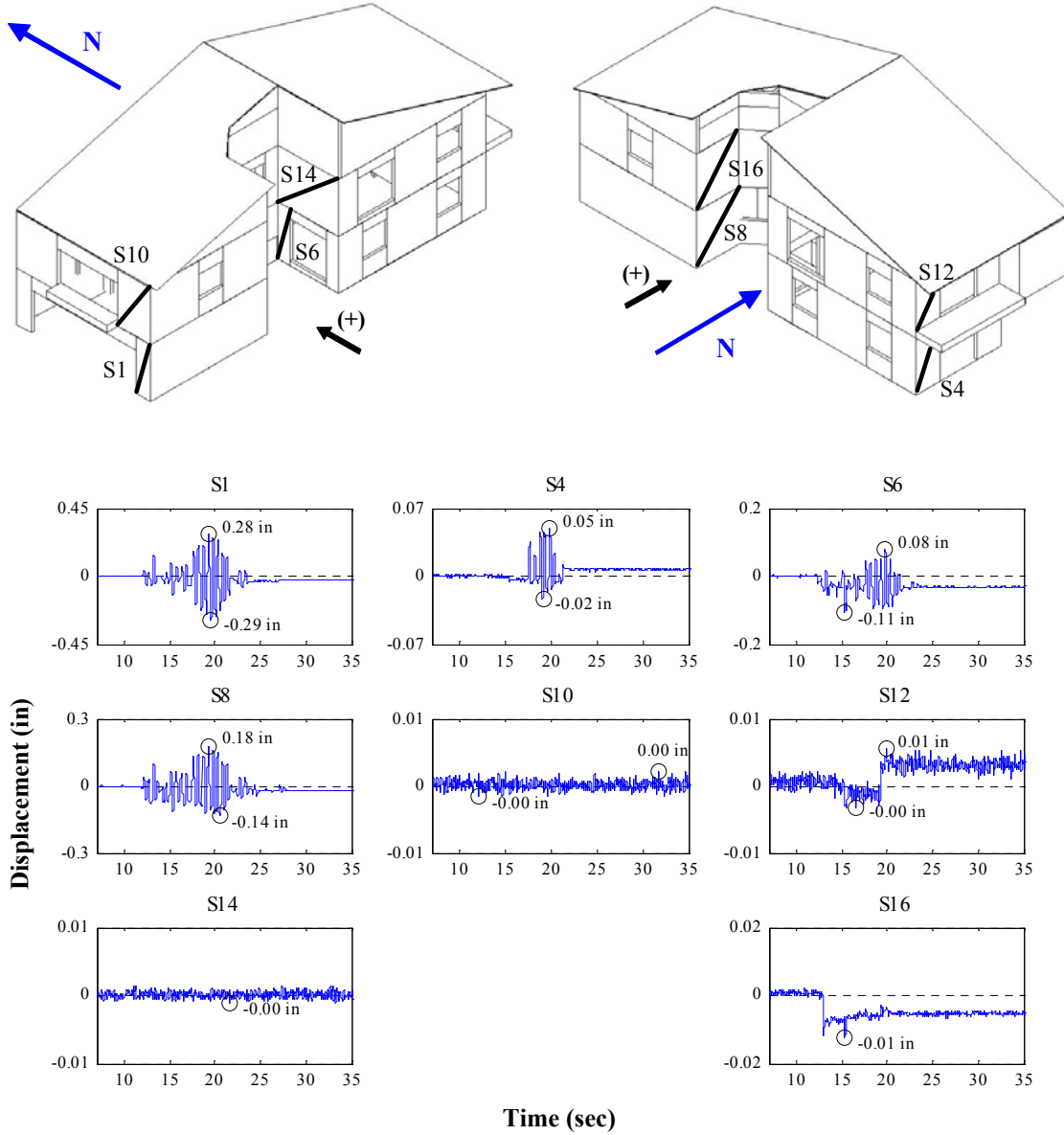


Figure M.106: Wall deformations of north-south external walls for Test NWP5S03

Appendix M

Phase 5, NWP5S03 Seismic Test, East-West, External Walls

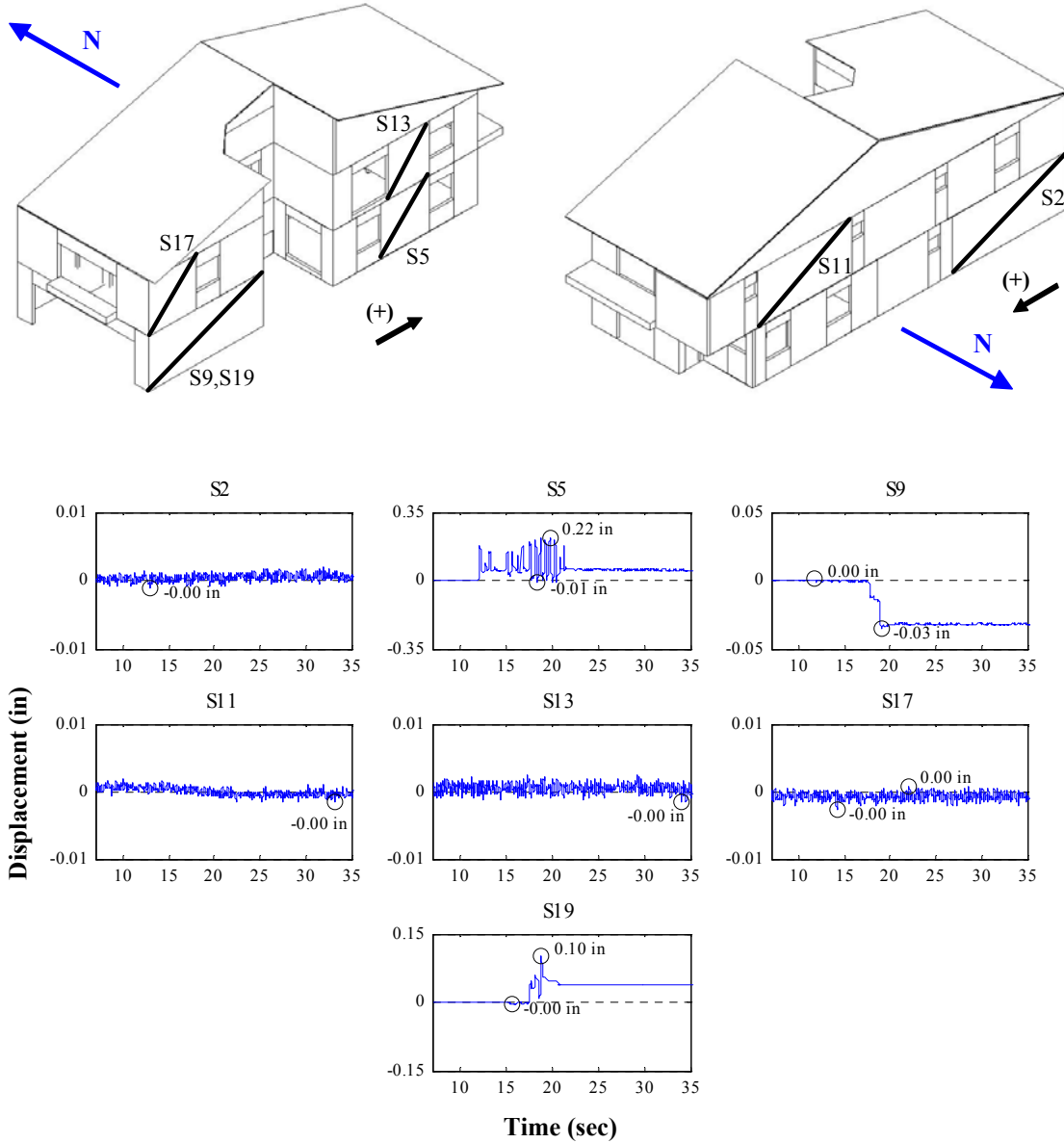


Figure M.107: Wall deformations of east-west external walls for Test NWP5S03

Appendix M

Phase 5, NWP5S03 Seismic Test, Internal Walls

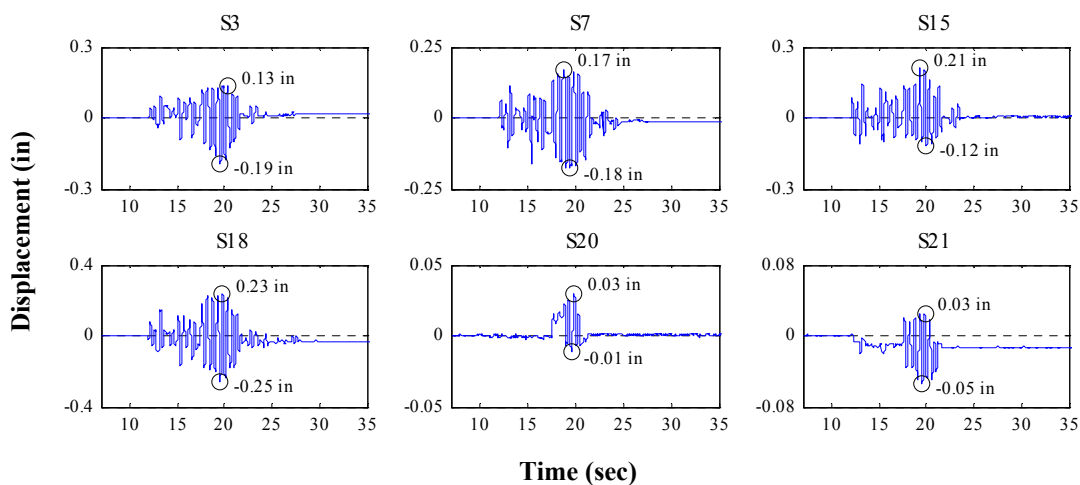
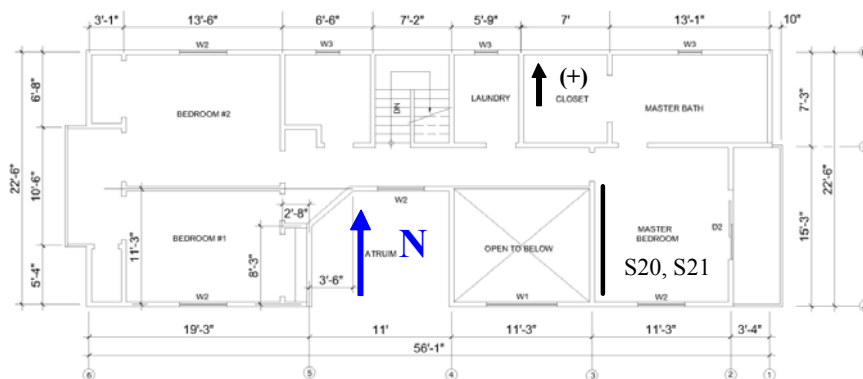
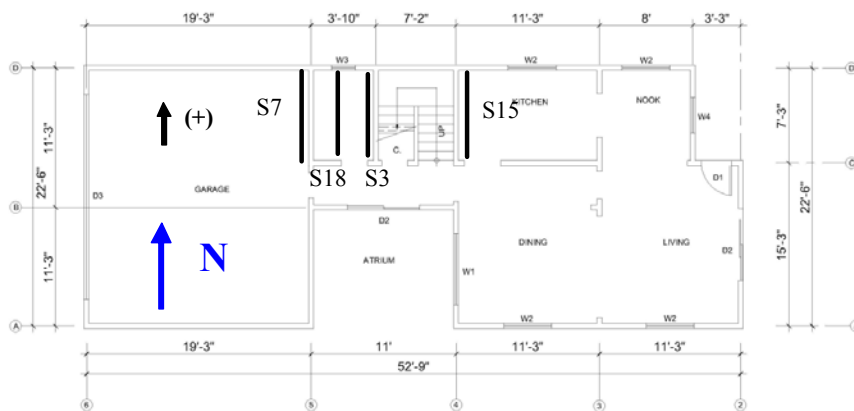


Figure M.108: Wall deformations of internal walls for Test NWP5S03

Appendix M

Phase 5, NWP5S04 Seismic Test, North-South, External Walls

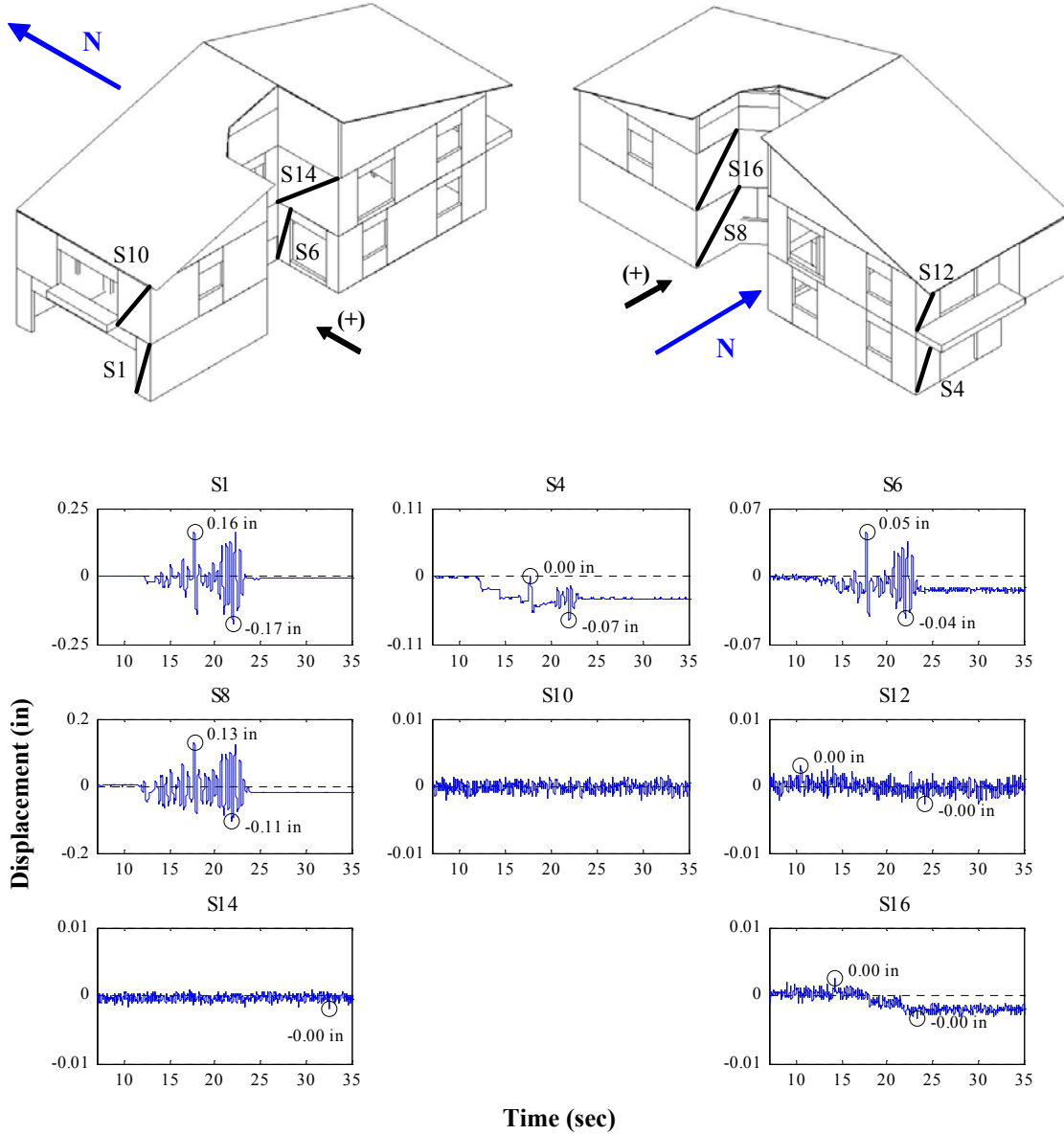


Figure M.109: Wall deformations of north-south external walls for Test NWP5S04

Appendix M

Phase 5, NWP5S04 Seismic Test, East-West, External Walls

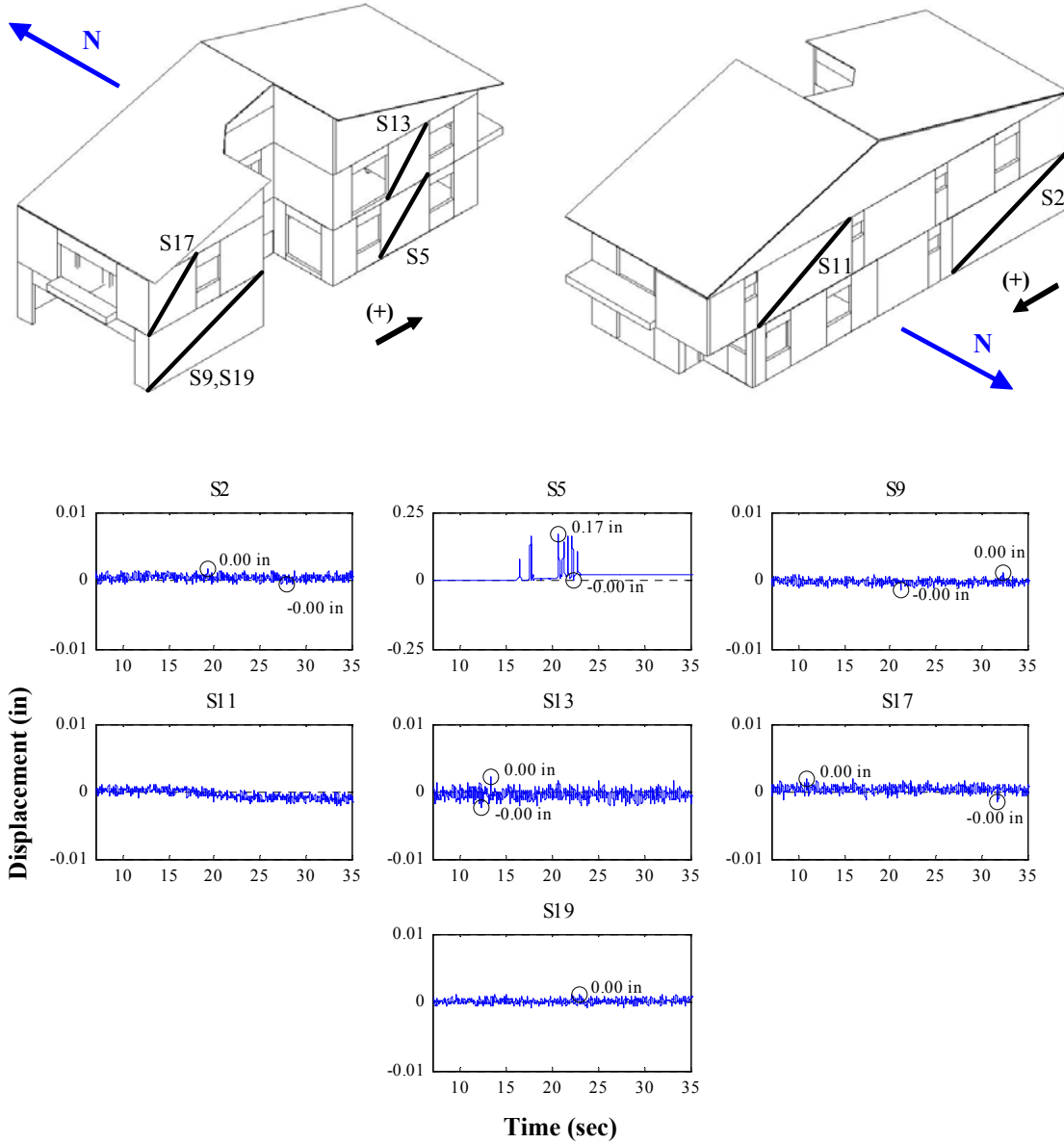


Figure M.110: Wall deformations of east-west external walls for Test NWP5S04

Appendix M

Phase 5, NWP5S04 Seismic Test, Internal Walls

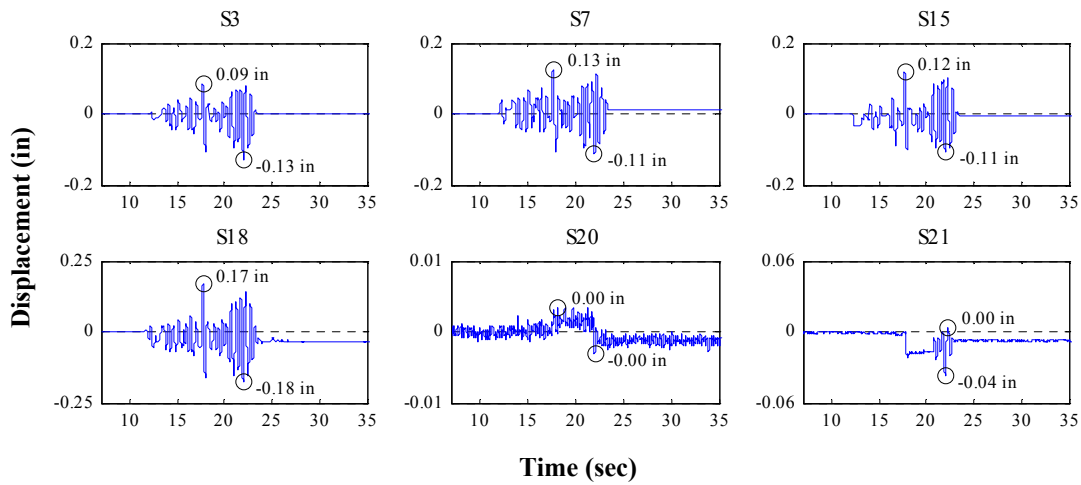
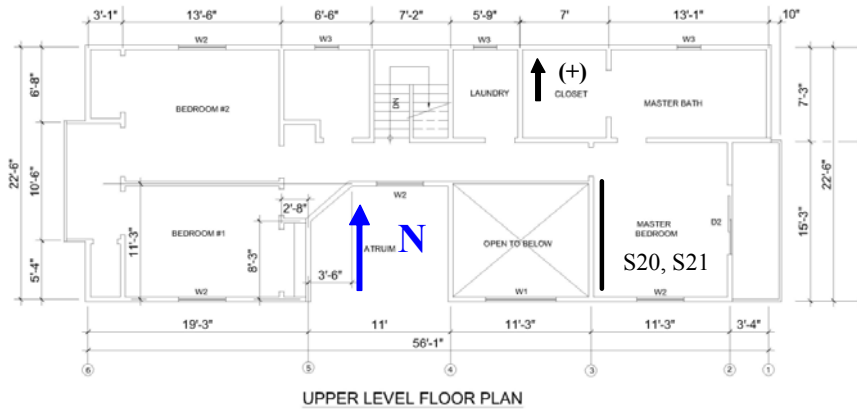
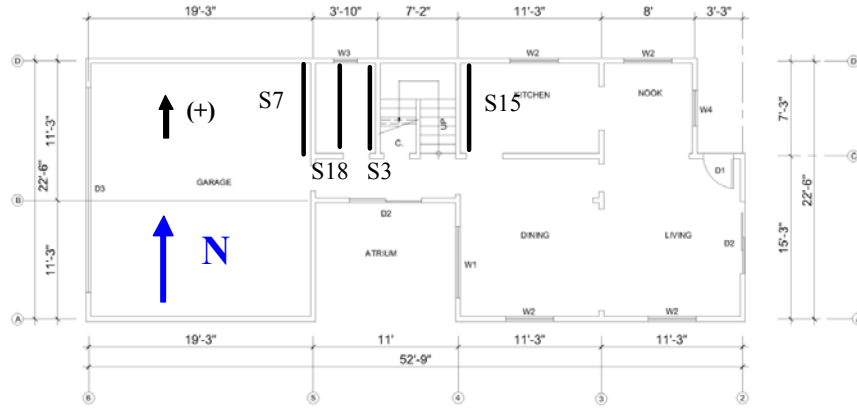


Figure M.111: Wall deformations of internal walls for Test NWP5S04

Appendix M

Phase 5, NWP5S05 Seismic Test, North-South, External Walls

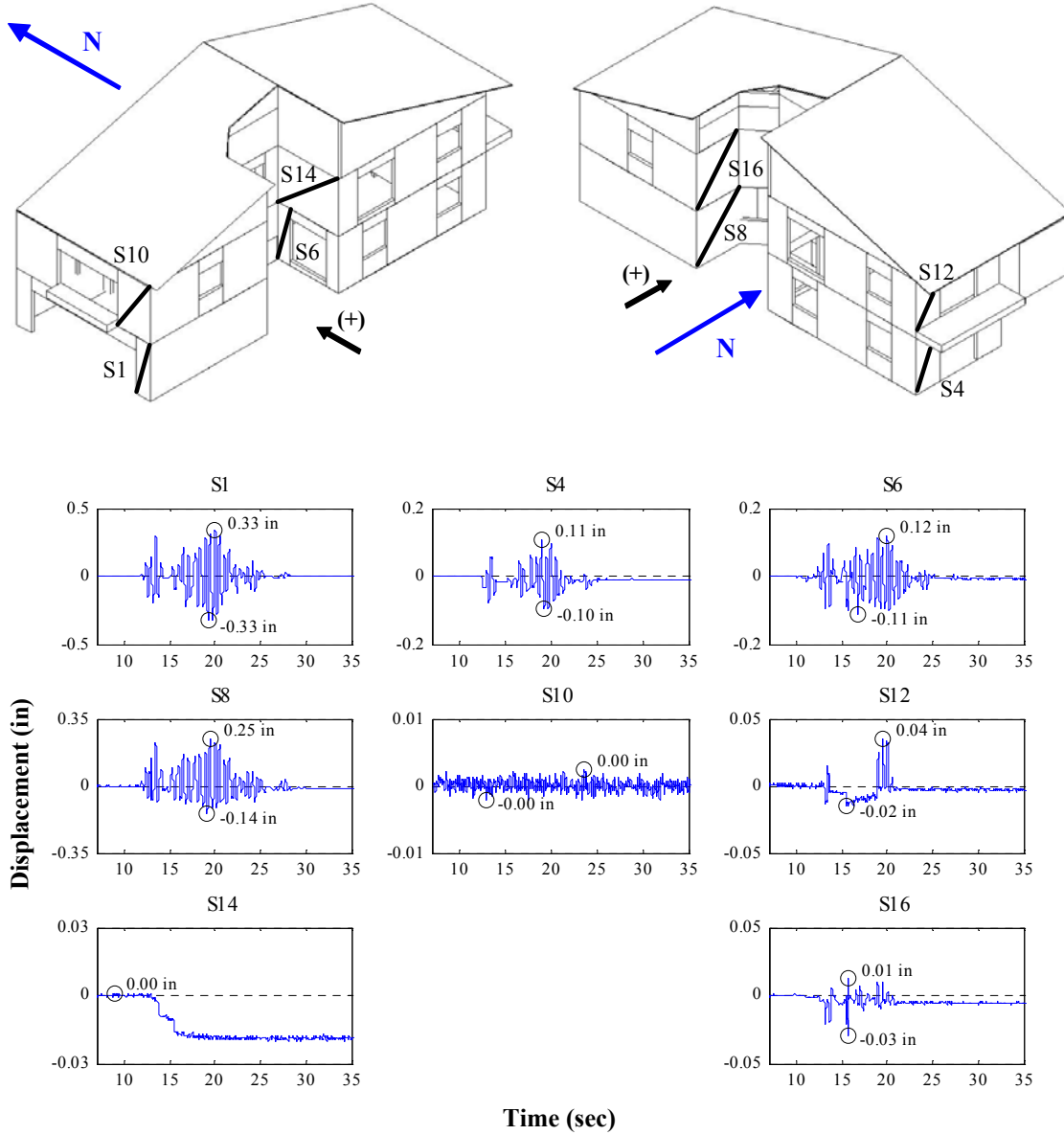


Figure M.112: Wall deformations of north-south external walls for Test NWP5S05

Appendix M

Phase 5, NWP5S05 Seismic Test, East-West, External Walls

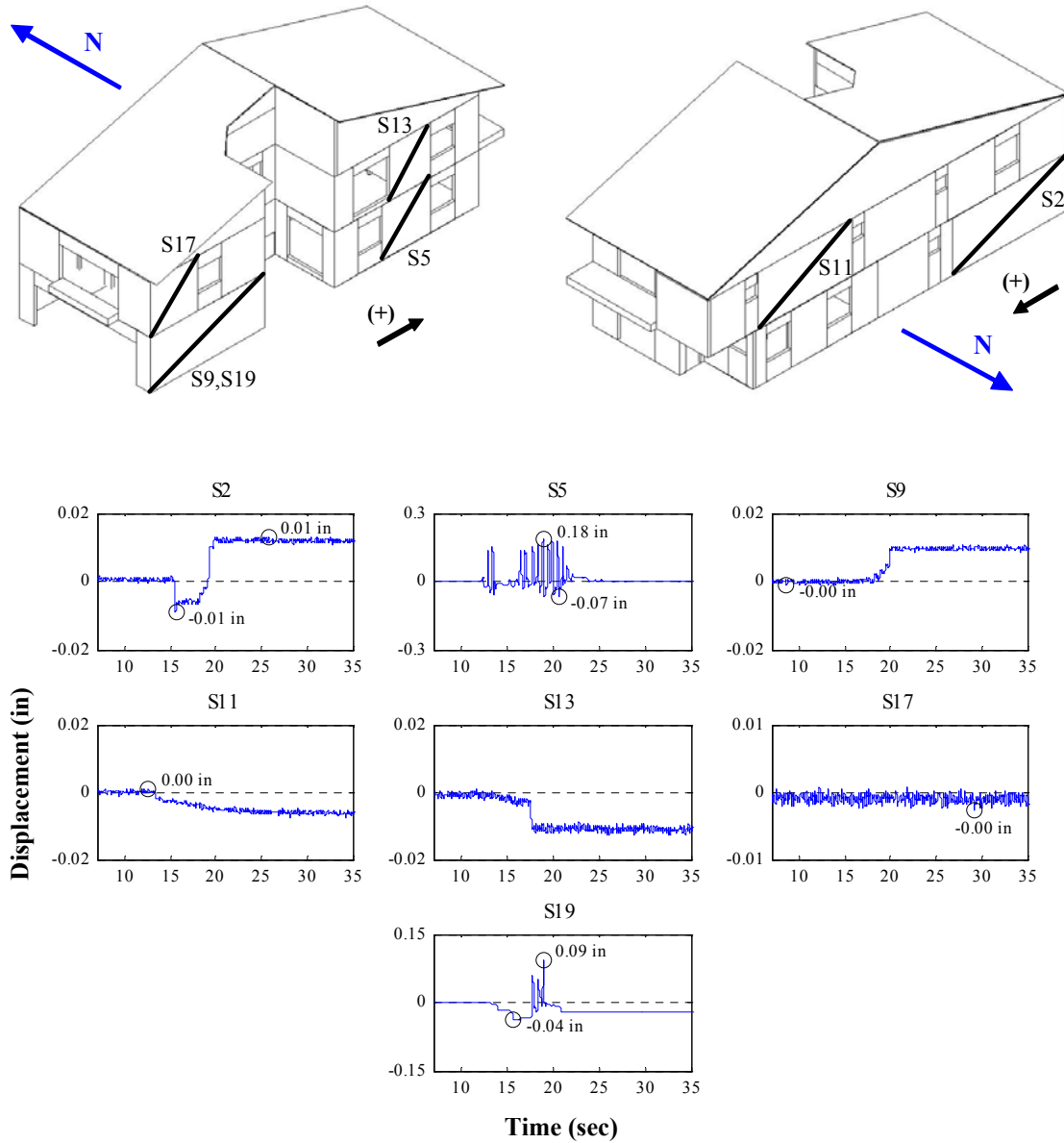


Figure M.113: Wall deformations of east-west external walls for Test NWP5S05

Appendix M

Phase 5, NWP5S05 Seismic Test, Internal Walls

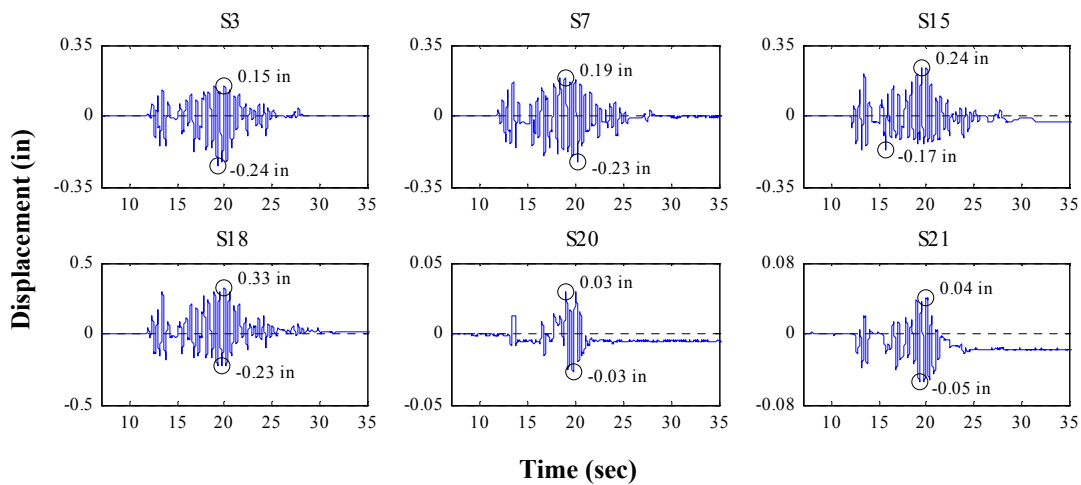
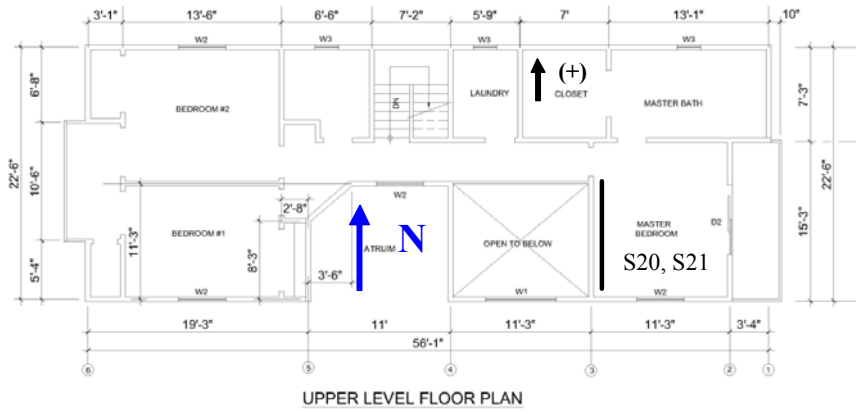
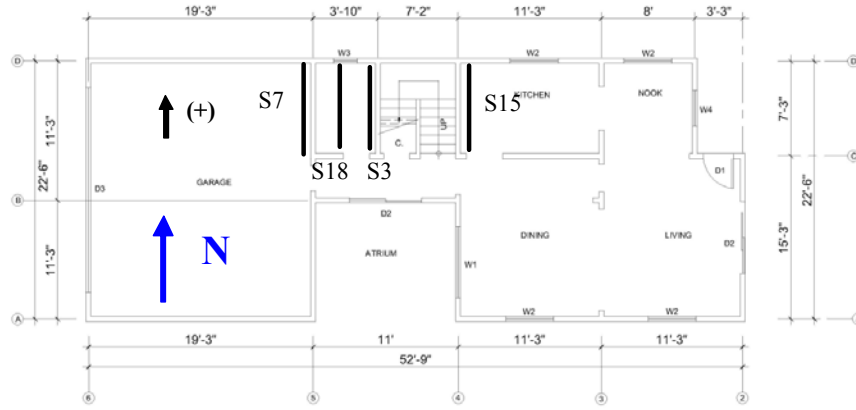


Figure M.114: Wall deformations of internal walls for Test NWP5S05

Appendix M

Phase 5, NWP5S06 Seismic Test, North-South, External Walls

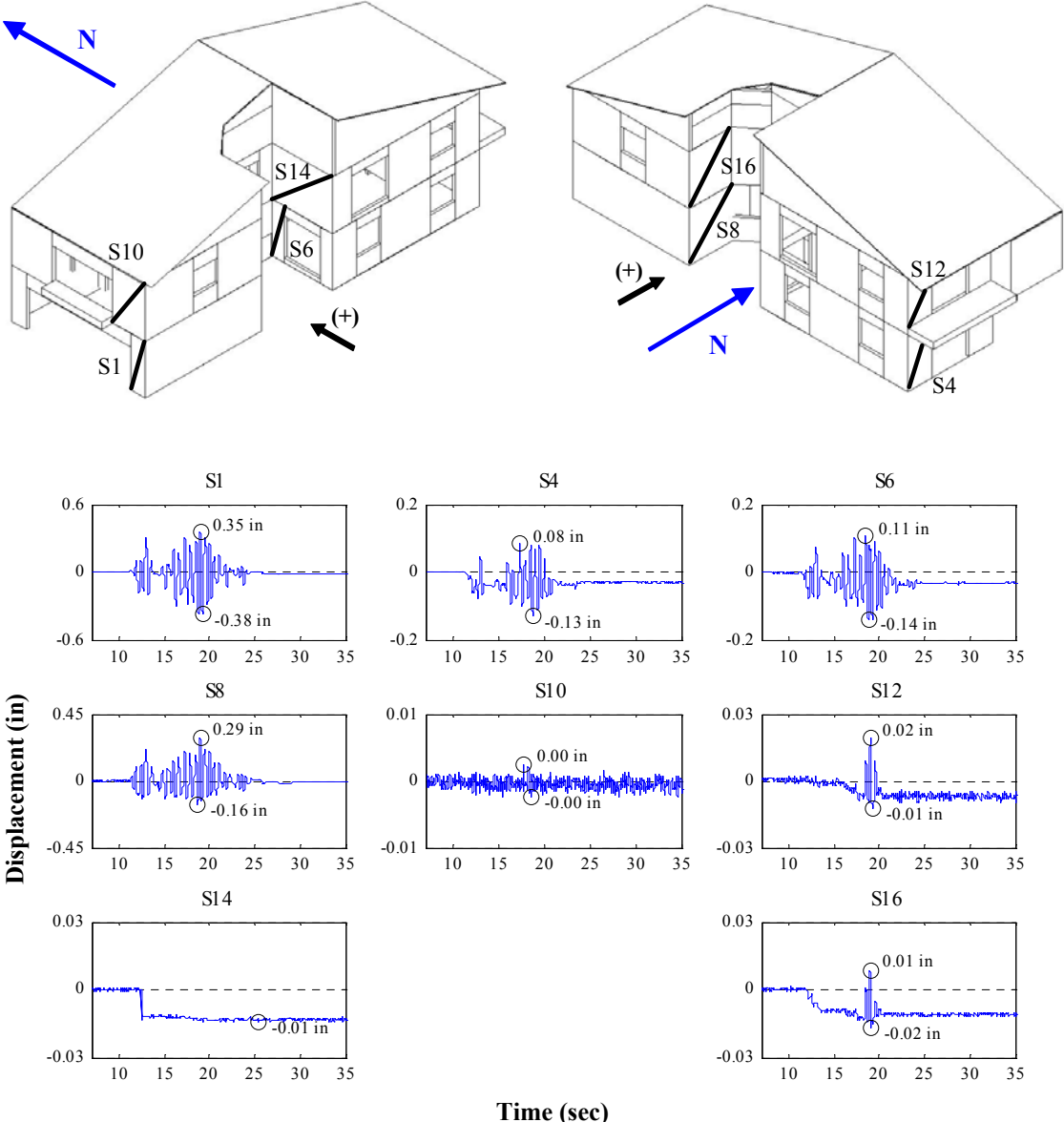


Figure M.115: Wall deformations of north-south external walls for Test NWP5S06

Appendix M

Phase 5, NWP5S06 Seismic Test, East-West, External Walls

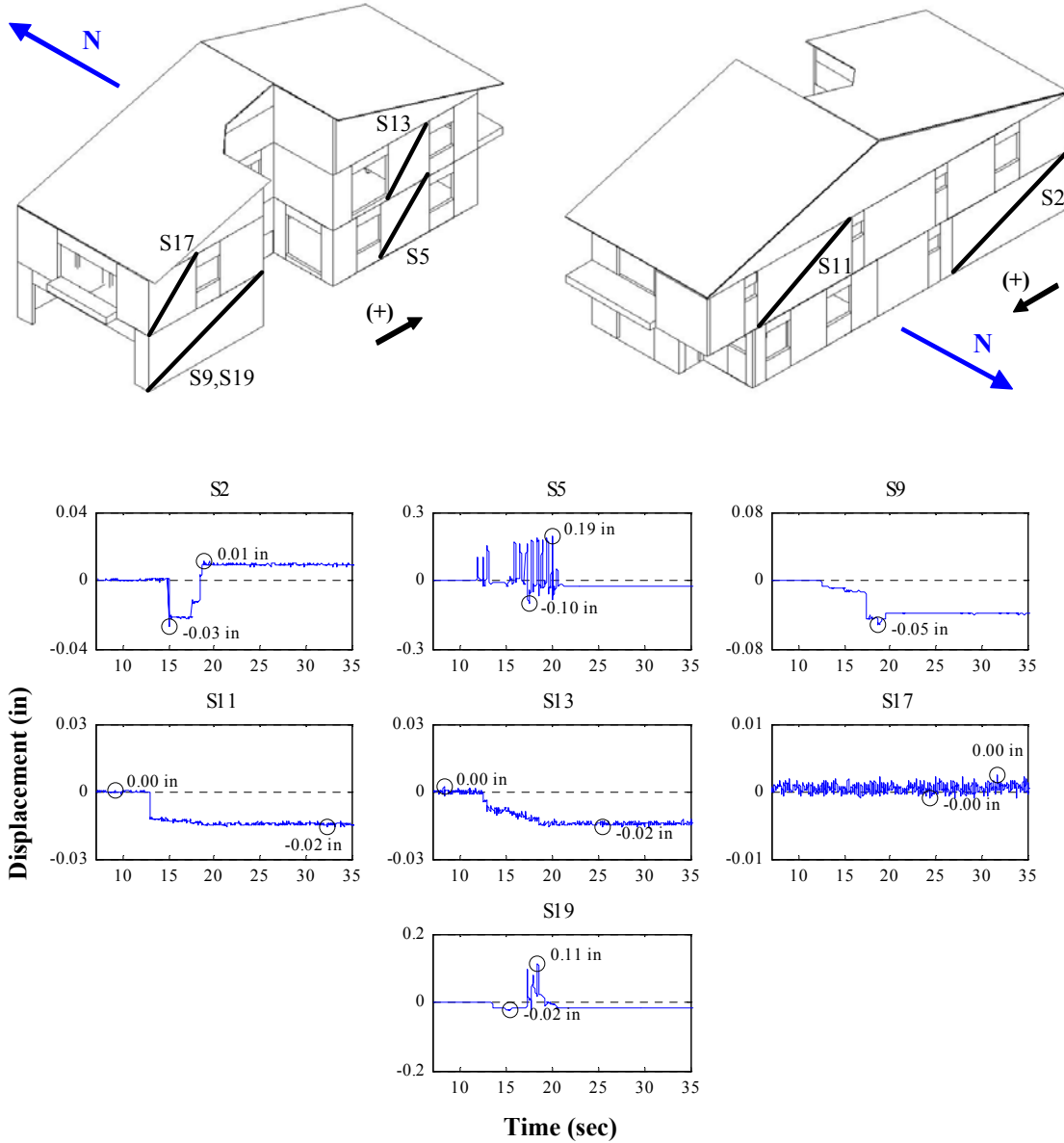


Figure M.116: Wall deformations of east-west external walls for Test NWP5S06

Appendix M

Phase 5, NWP5S06 Seismic Test, Internal Walls

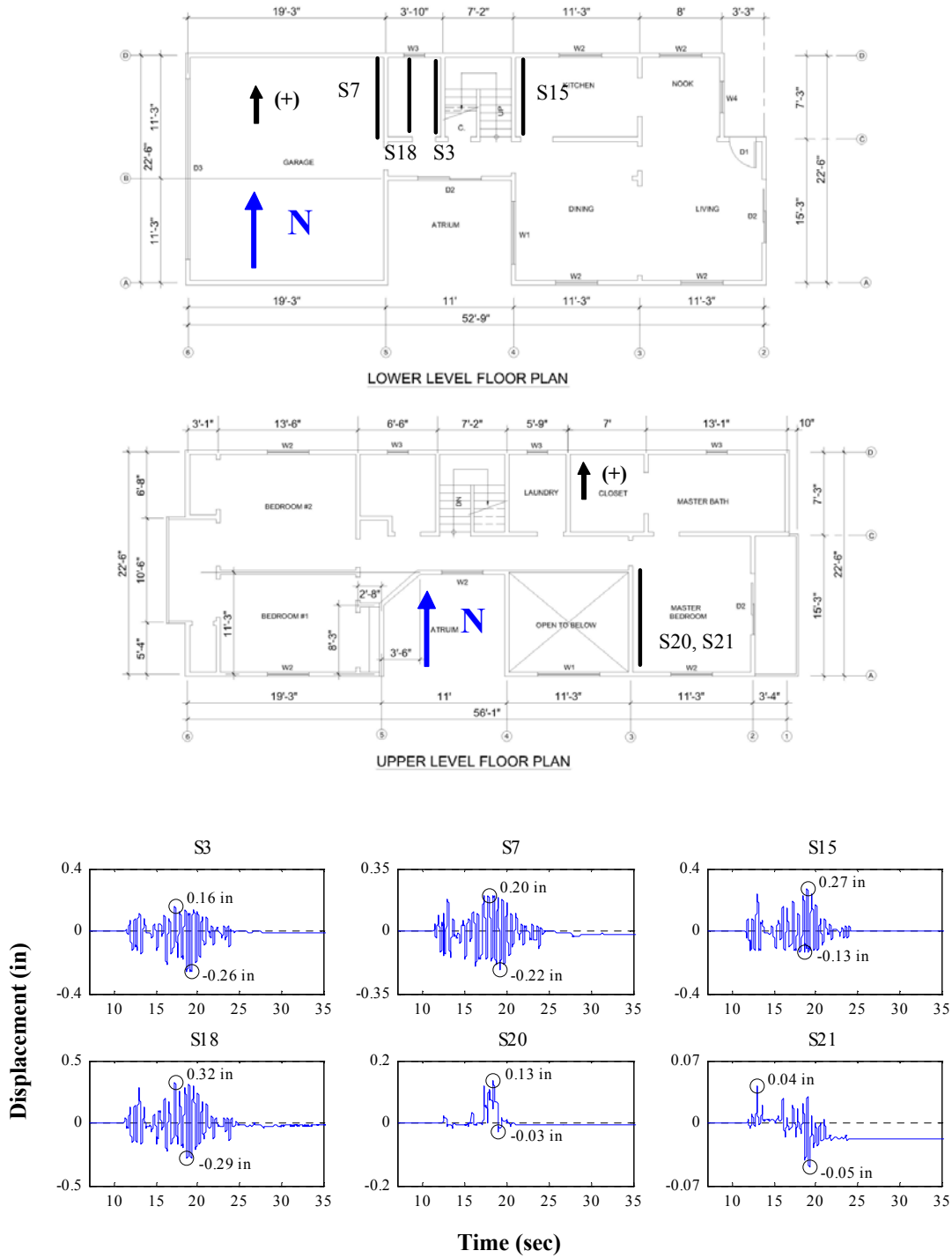


Figure M.117: Wall deformations of internal walls for Test NWP5S06

Appendix M

Phase 5, NWP5S07 Seismic Test, North-South, External Walls

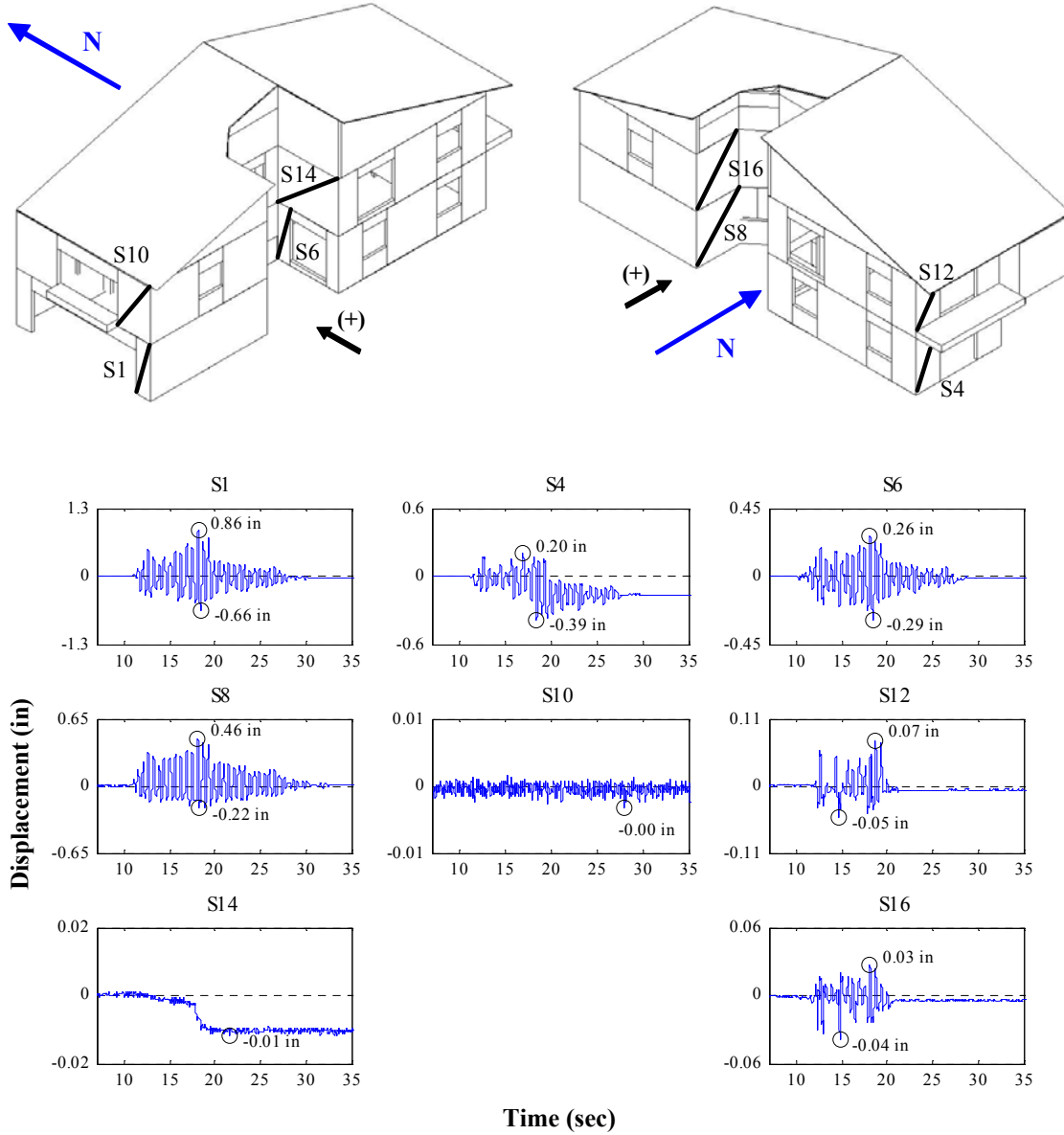


Figure M.118: Wall deformations of north-south external walls for Test NWP5S07

Appendix M

Phase 5, NWP5S07 Seismic Test, East-West, External Walls

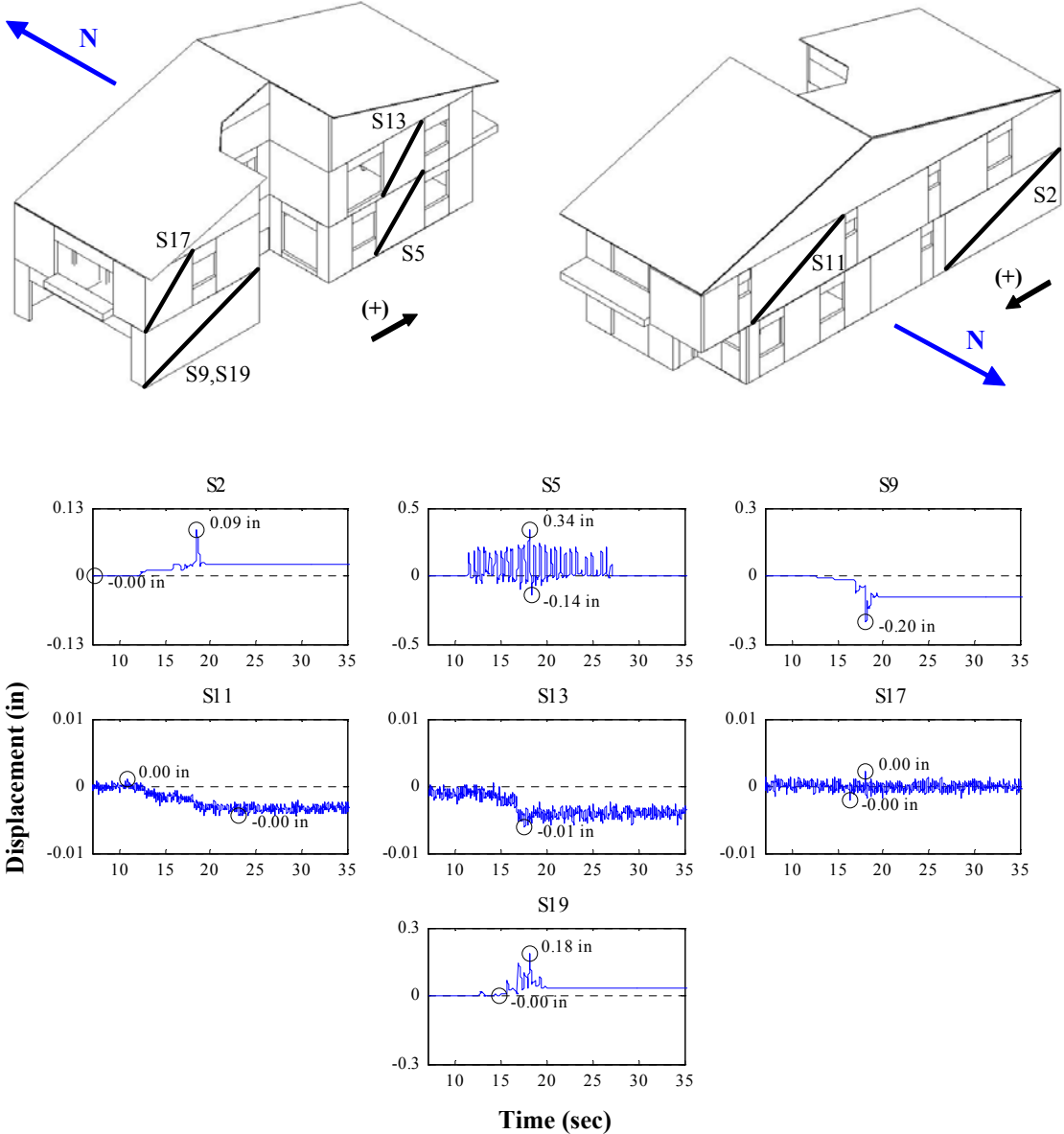


Figure M.119: Wall deformations of east-west external walls for Test NWP5S07

Appendix M

Phase 5, NWP5S07 Seismic Test, Internal Walls

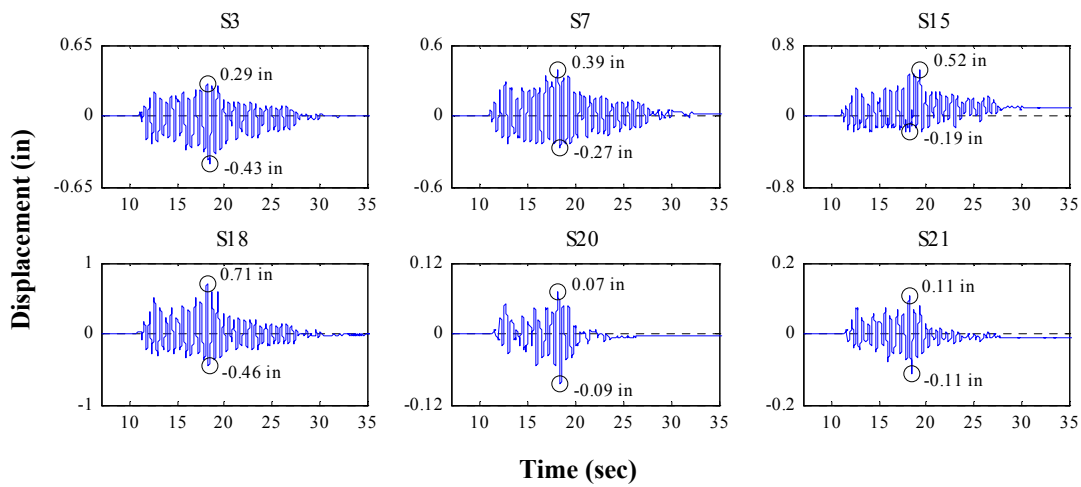
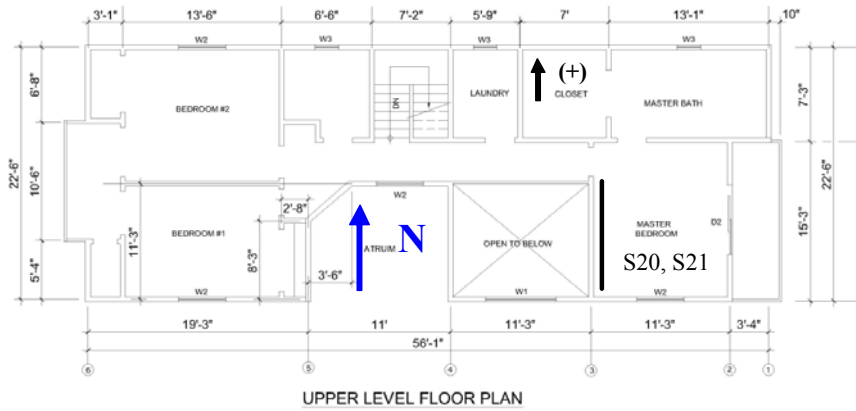
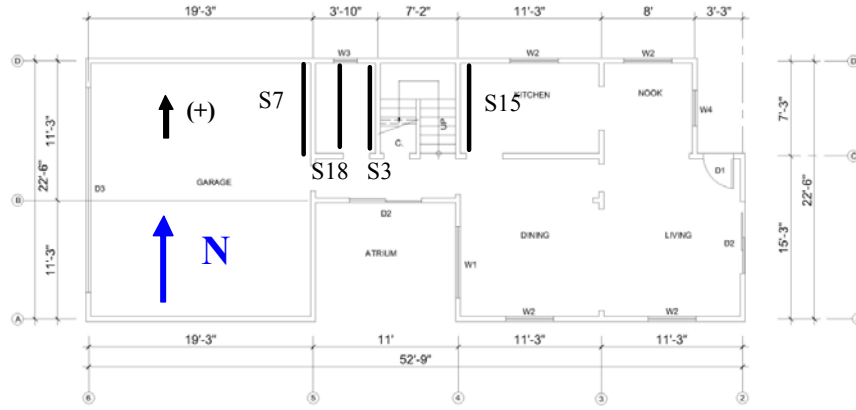


Figure M.120: Wall deformations of internal walls for Test NWP5S07

Appendix M

Phase 5, NWP5S08 Seismic Test, North-South, External Walls

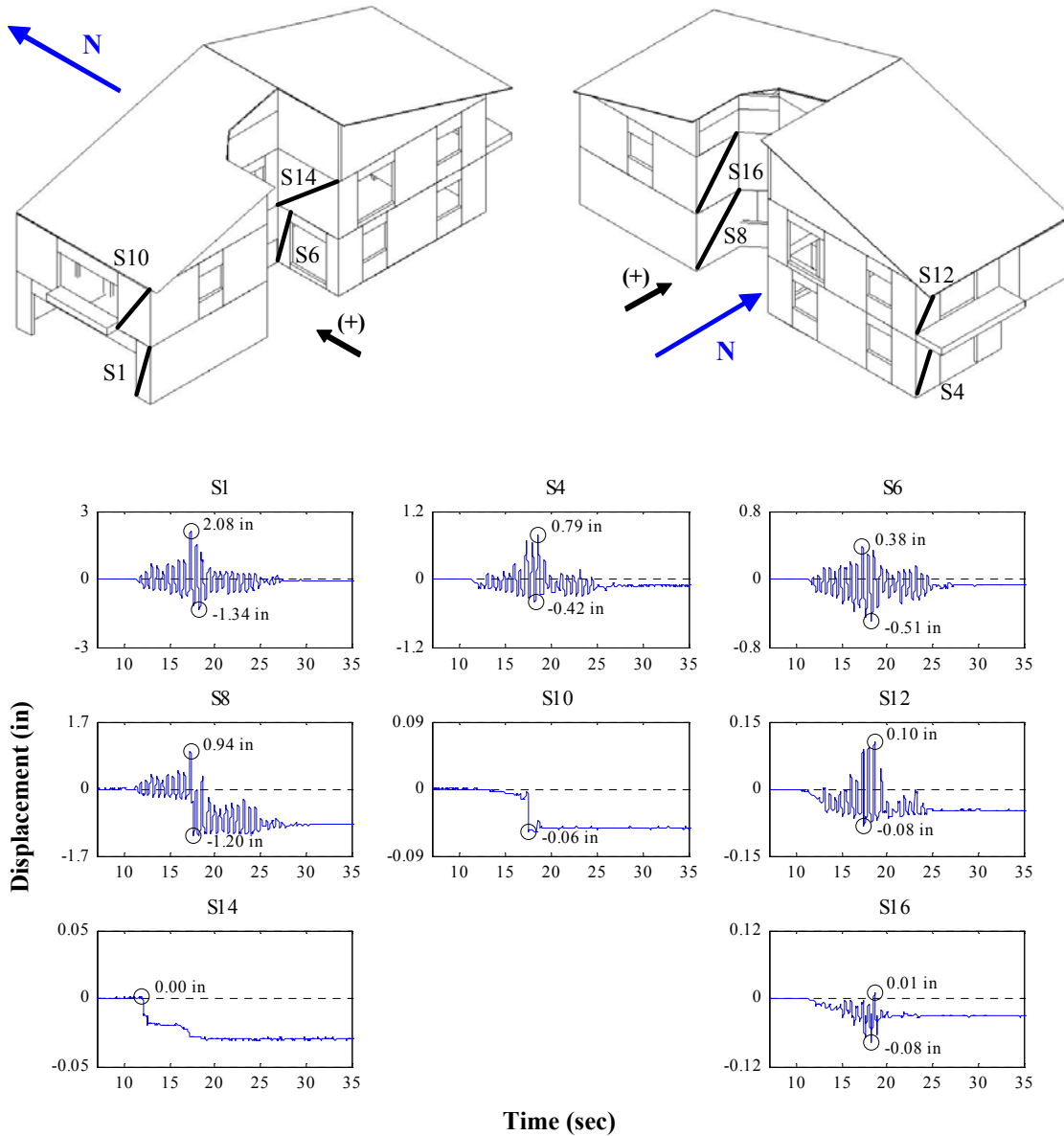


Figure M.121: Wall deformations of north-south external walls for Test NWP5S08

Appendix M

Phase 5, NWP5S08 Seismic Test, East-West, External Walls

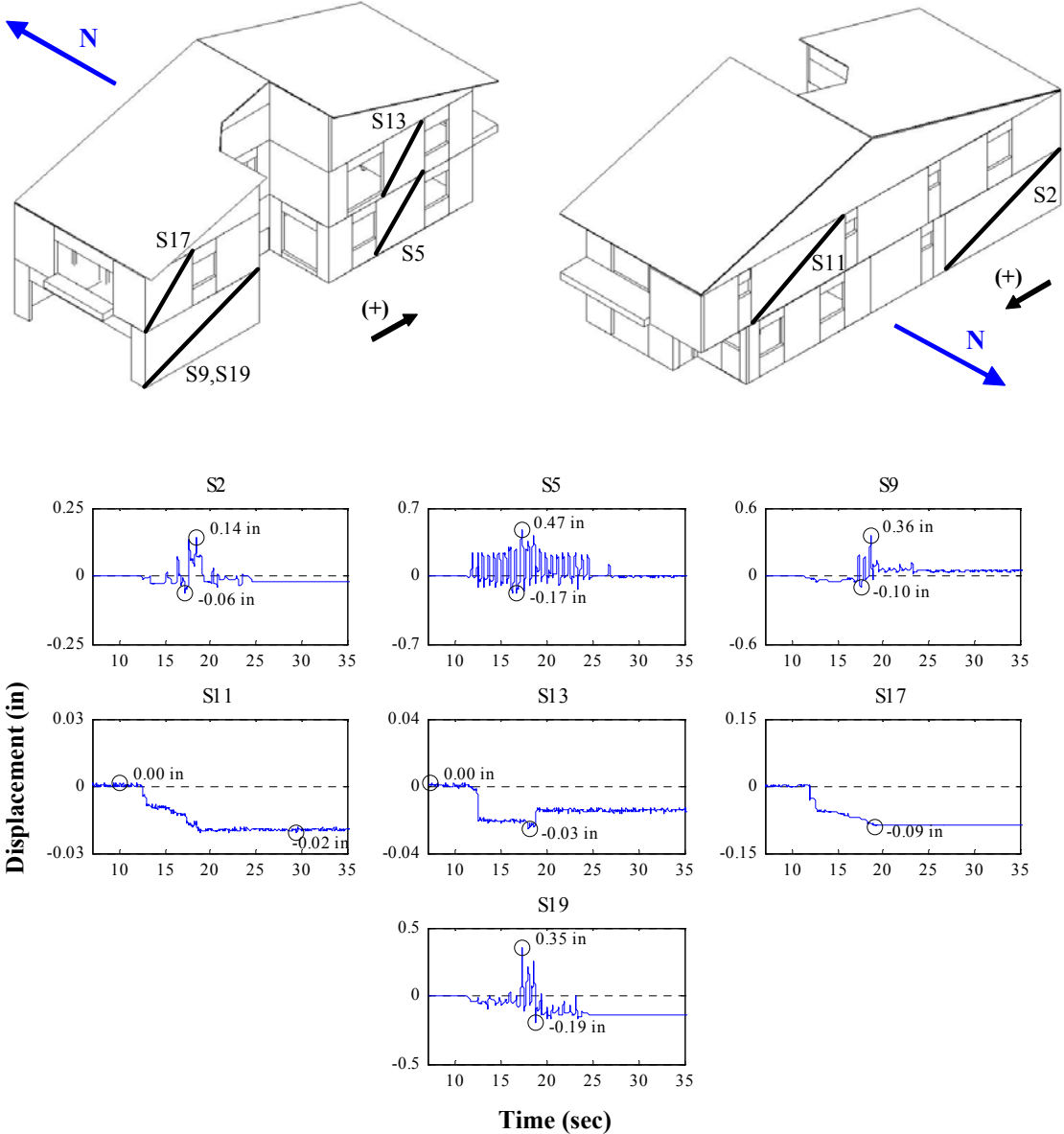


Figure M.122: Wall deformations of east-west external walls for Test NWP5S08

Appendix M

Phase 5, NWP5S08 Seismic Test, Internal Walls

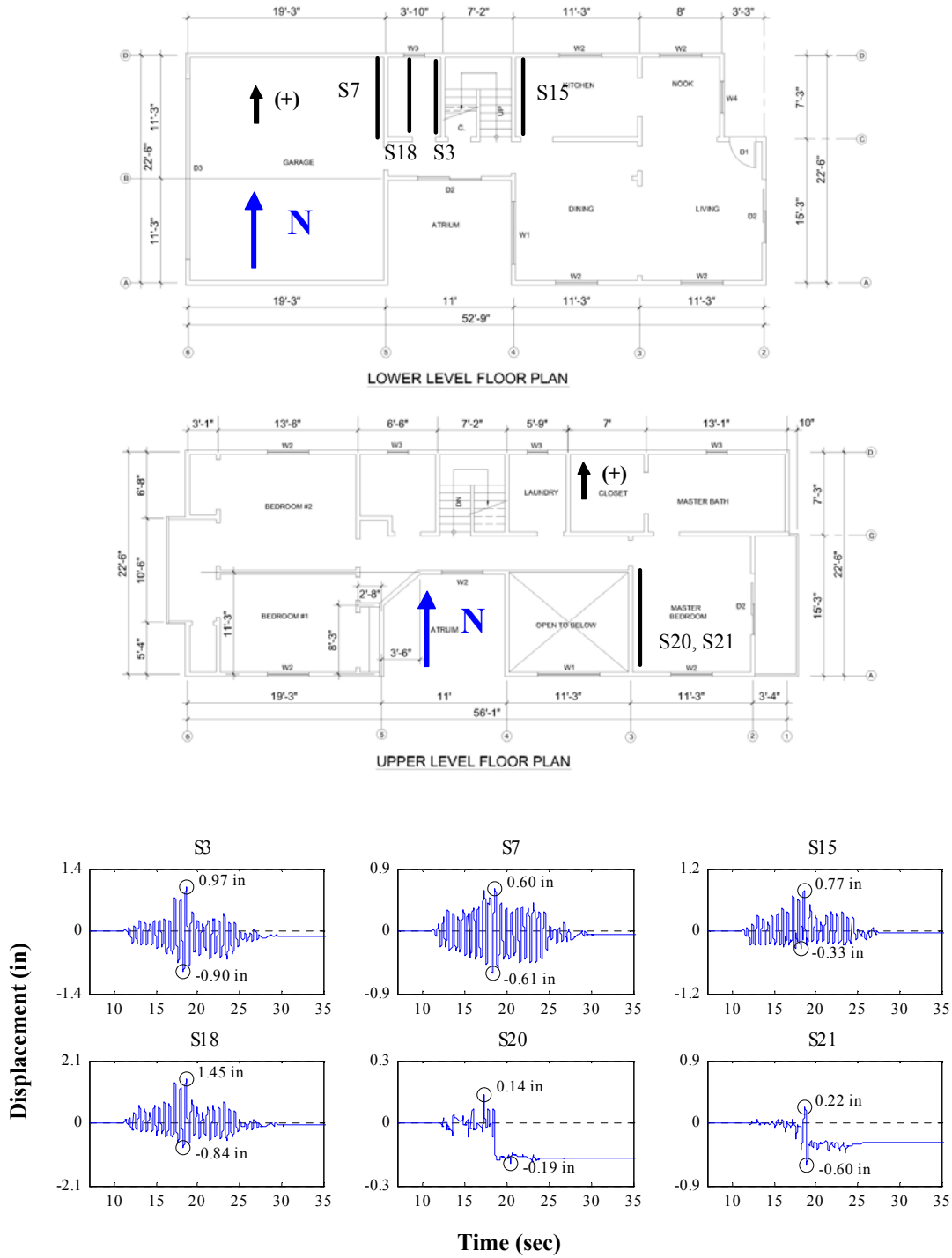


Figure M.123: Wall deformations of internal walls for Test NWP5S08

Appendix M

Phase 5, NWP5S09 Seismic Test, North-South, External Walls

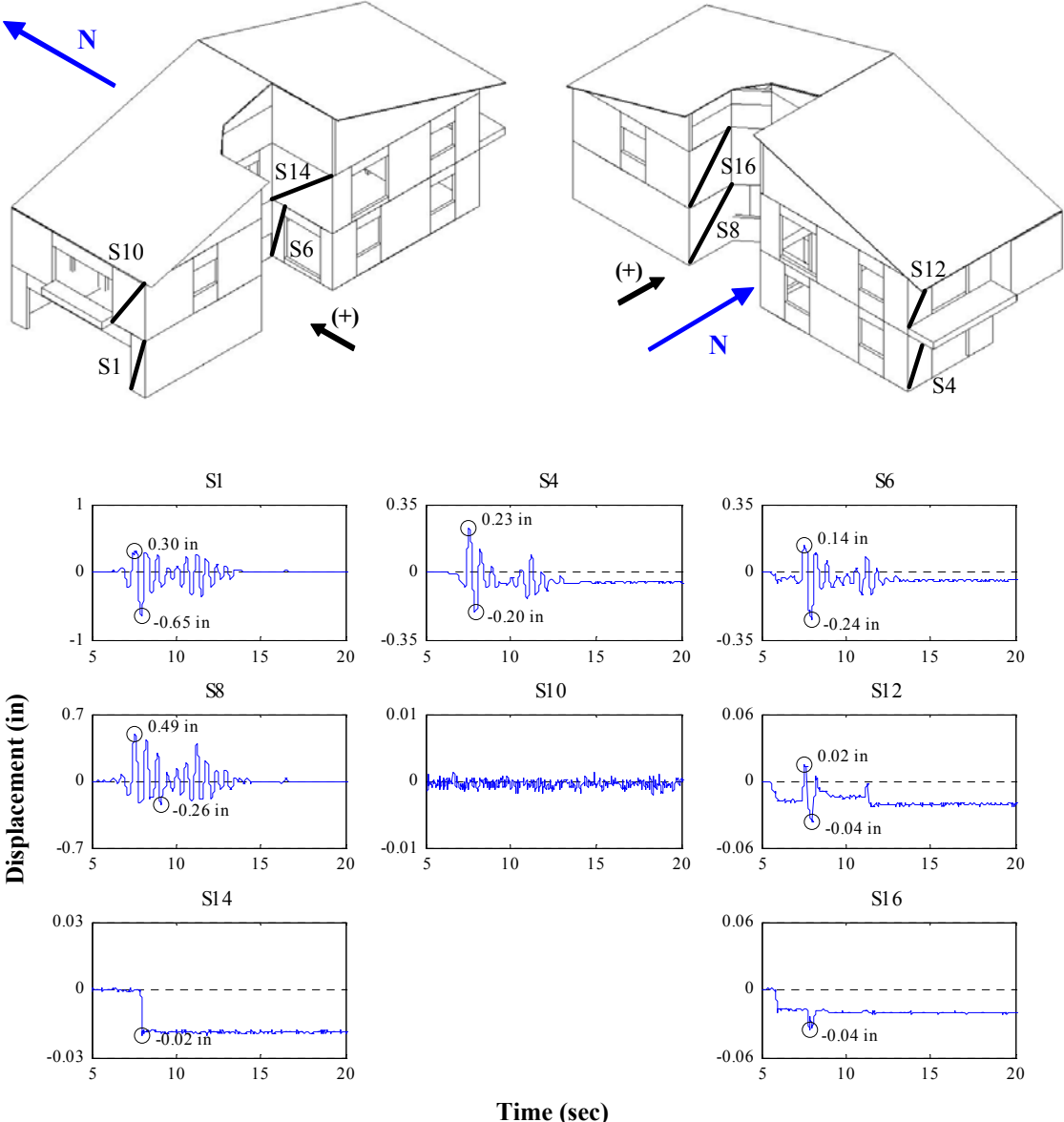


Figure M.124: Wall deformations of north-south external walls for Test NWP5S09

Appendix M

Phase 5, NWP5S09 Seismic Test, East-West, External Walls

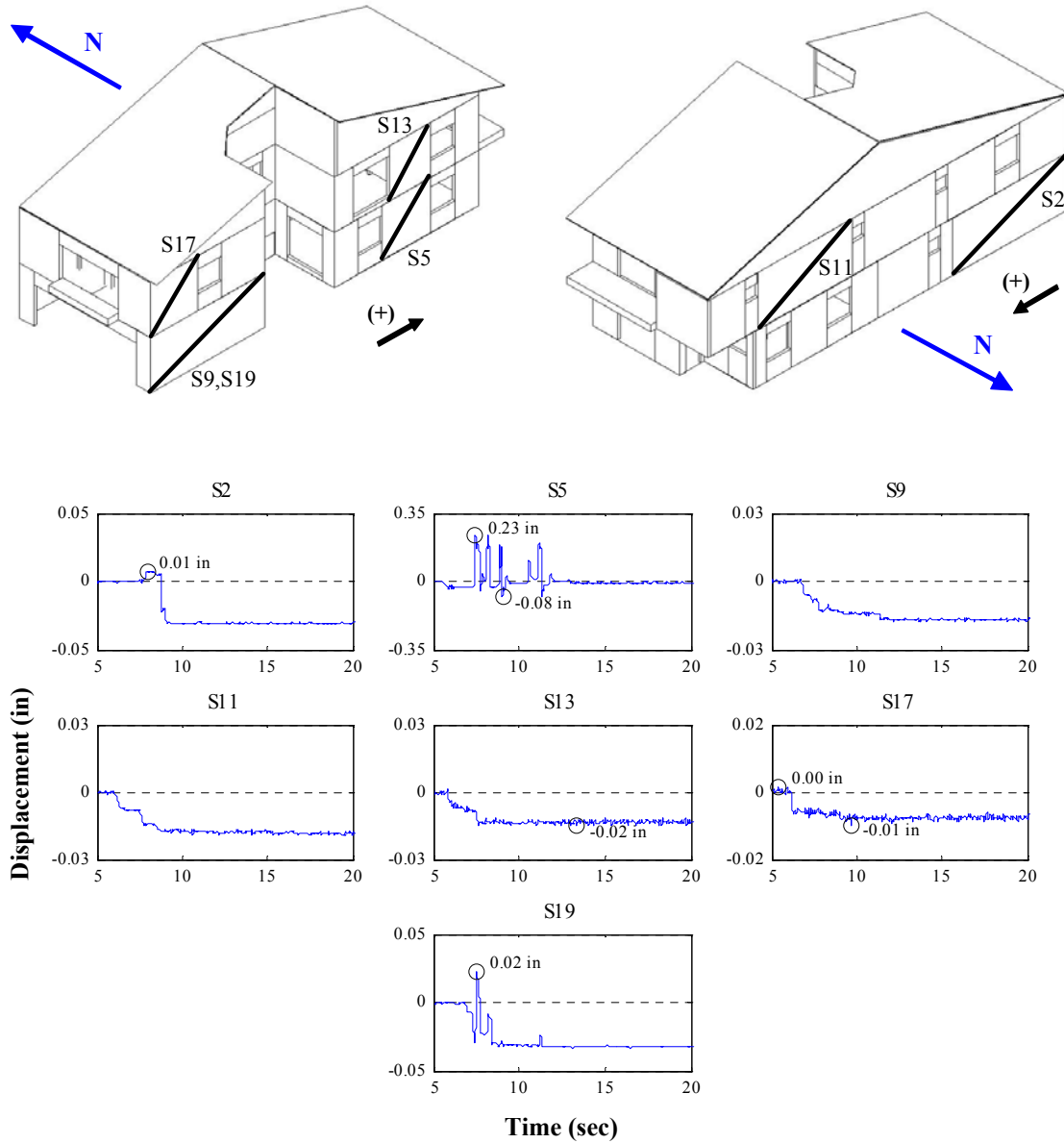


Figure M.125: Wall deformations of east-west external walls for Test NWP5S09

Appendix M

Phase 5, NWP5S09 Seismic Test, Internal Walls

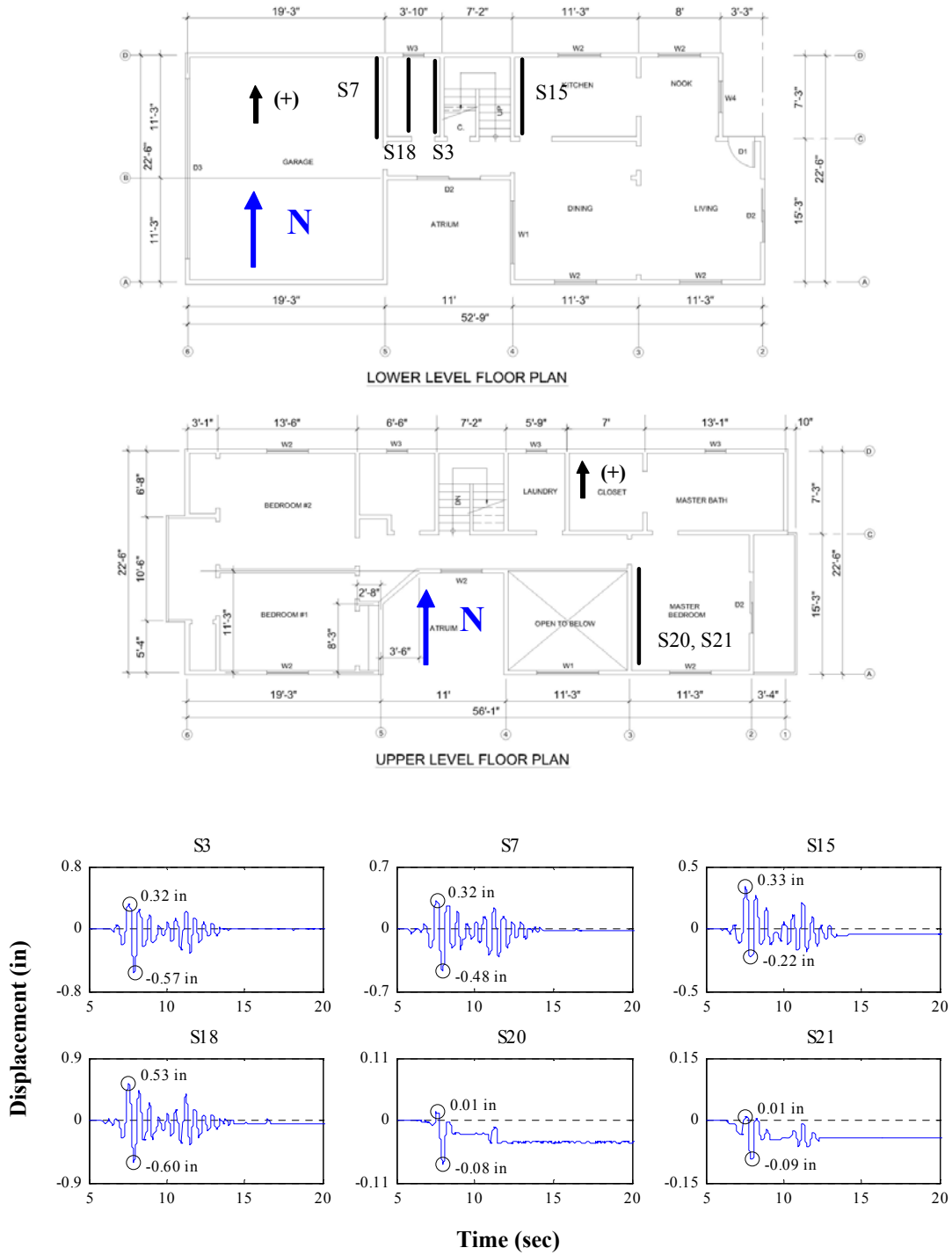


Figure M.126: Wall deformations of internal walls for Test NWP5S09

Appendix M

Phase 5, NWP5S11 Seismic Test, North-South, External Walls

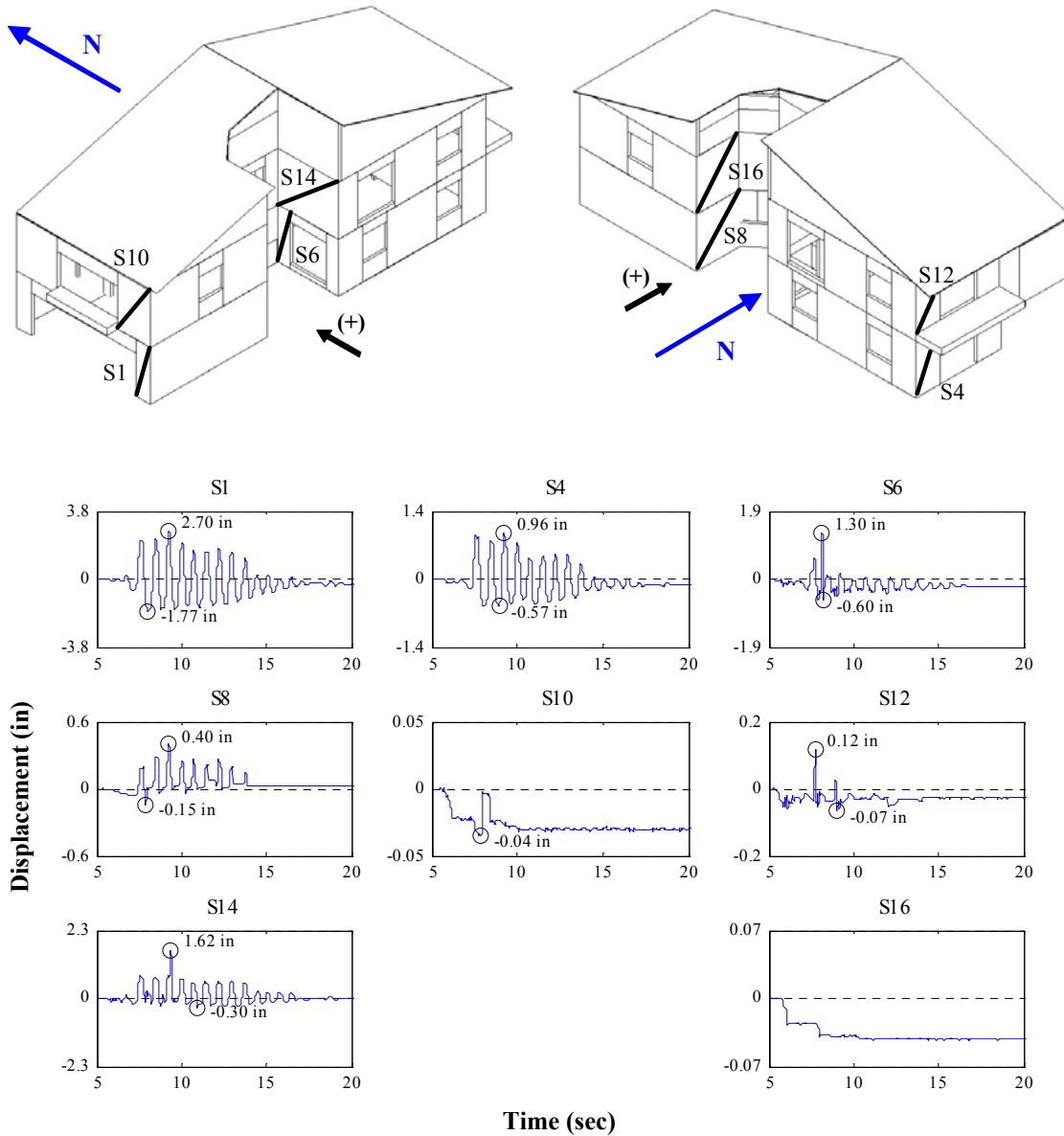


Figure M.127: Wall deformations of north-south external walls for Test NWP5S11

Appendix M

Phase 5, NWP5S11 Seismic Test, East-West, External Walls

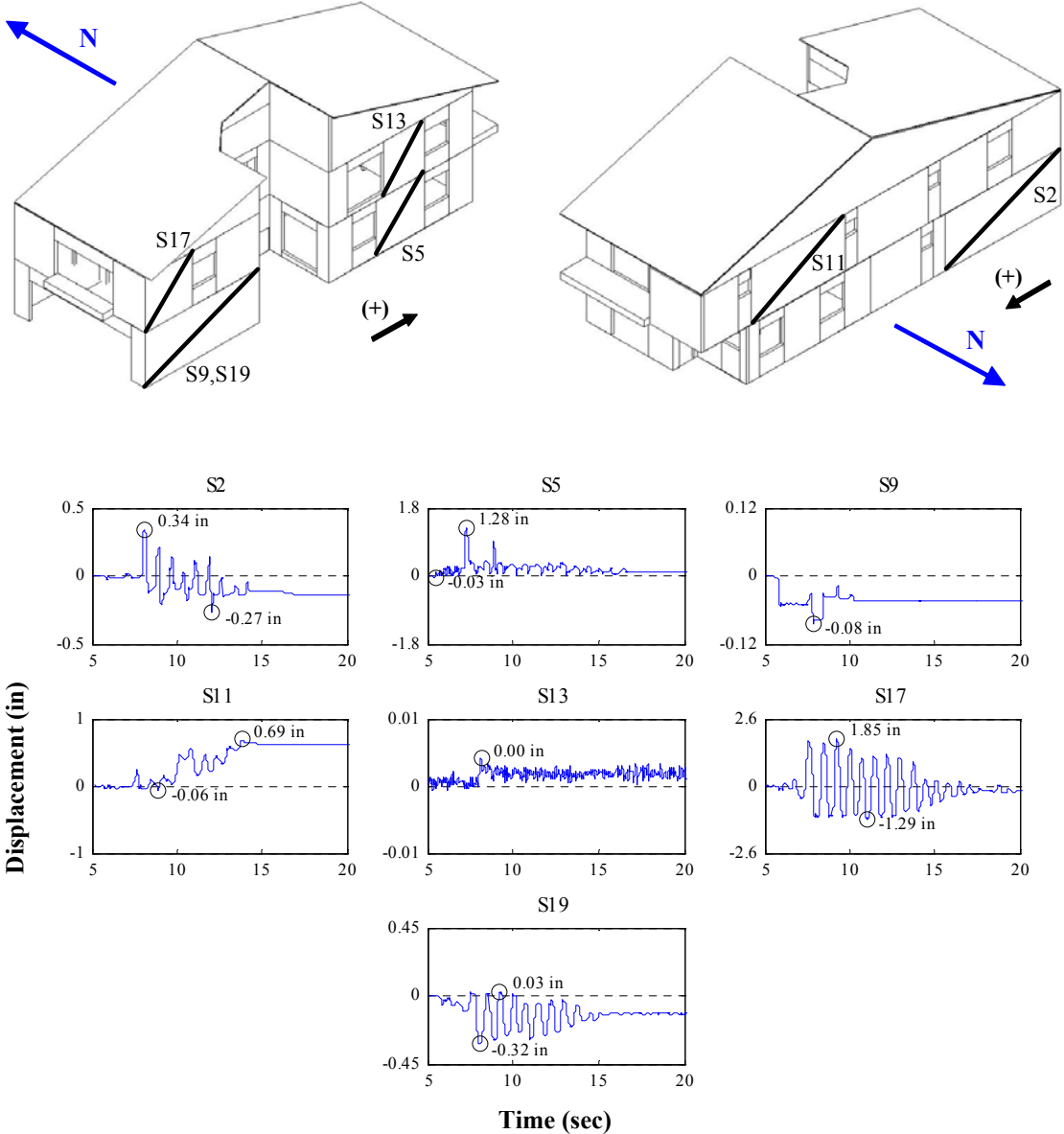


Figure M.128: Wall deformations of east-west external walls for Test NWP5S11

Appendix M

Phase 5, NWP5S11 Seismic Test, Internal Walls

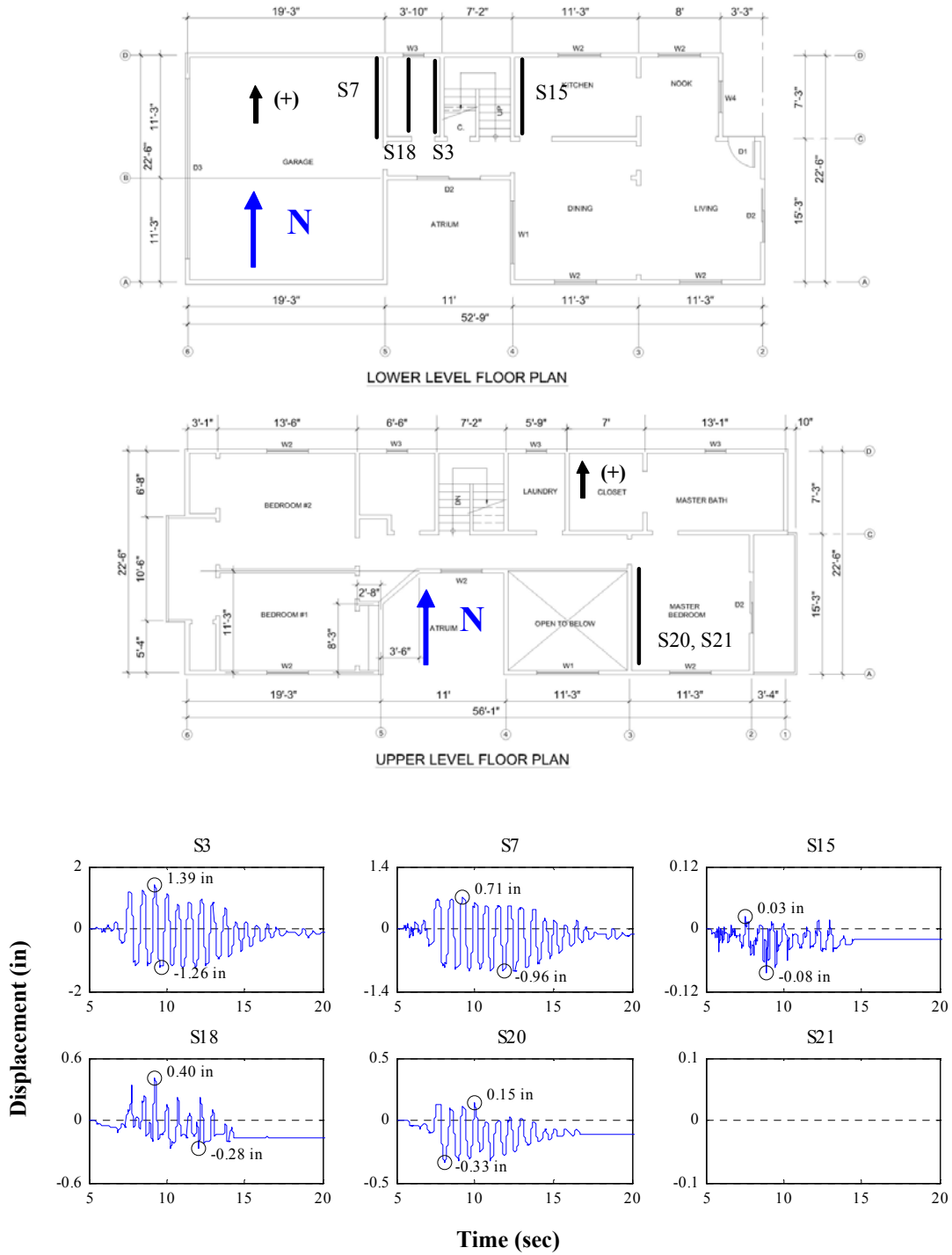


Figure M.129: Wall deformations of internal walls for Test NWP5S11

Appendix N
Selected Seismic Results:
Base Shear Force –
Displacement Hysteresis Loops

Appendix N

Phase 1, NWP1S01 Seismic Test

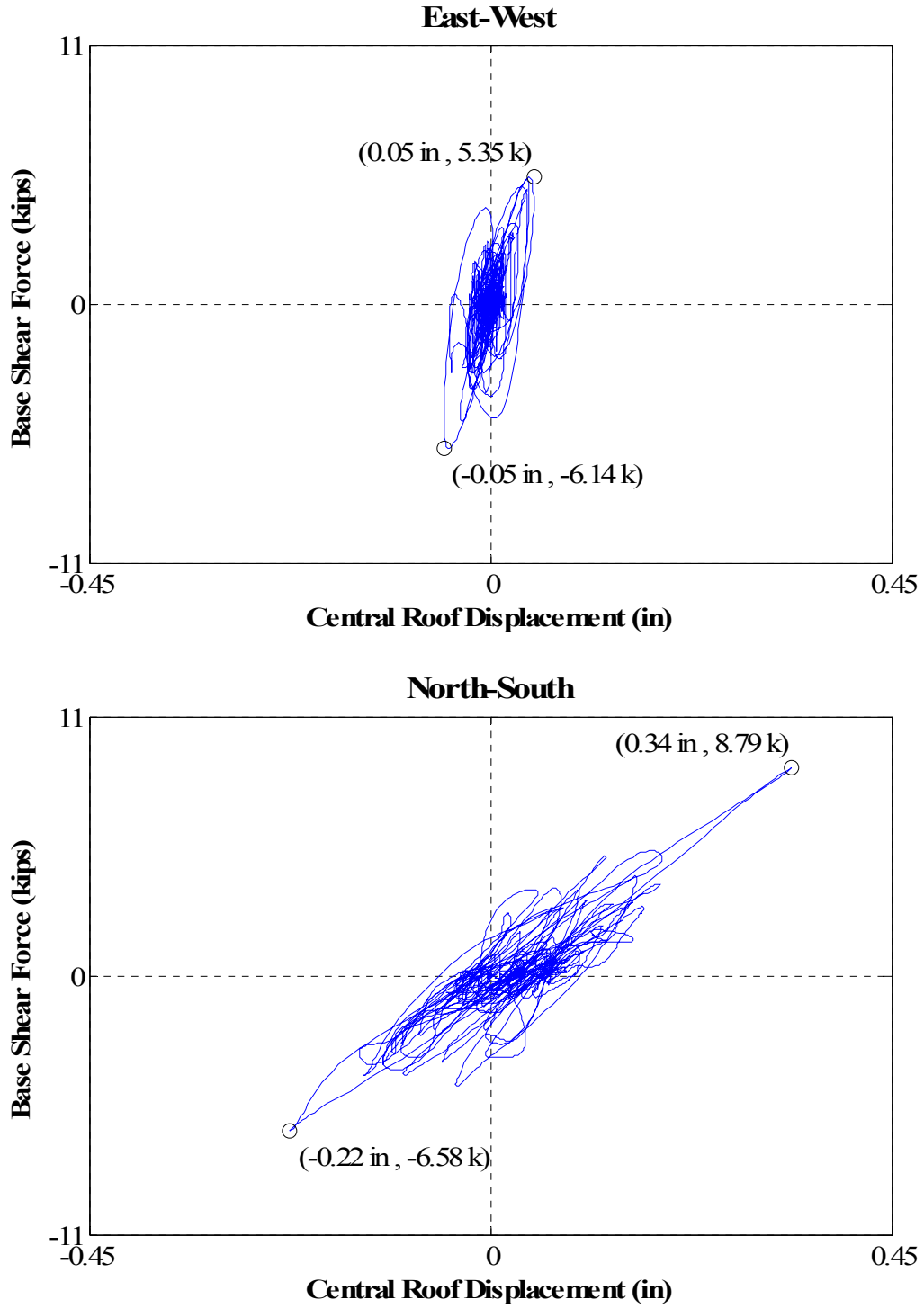


Figure N.1: Force-displacement hysteresis loops for Test NWP1S01

Appendix N

Phase 1, NWP1S02 Seismic Test

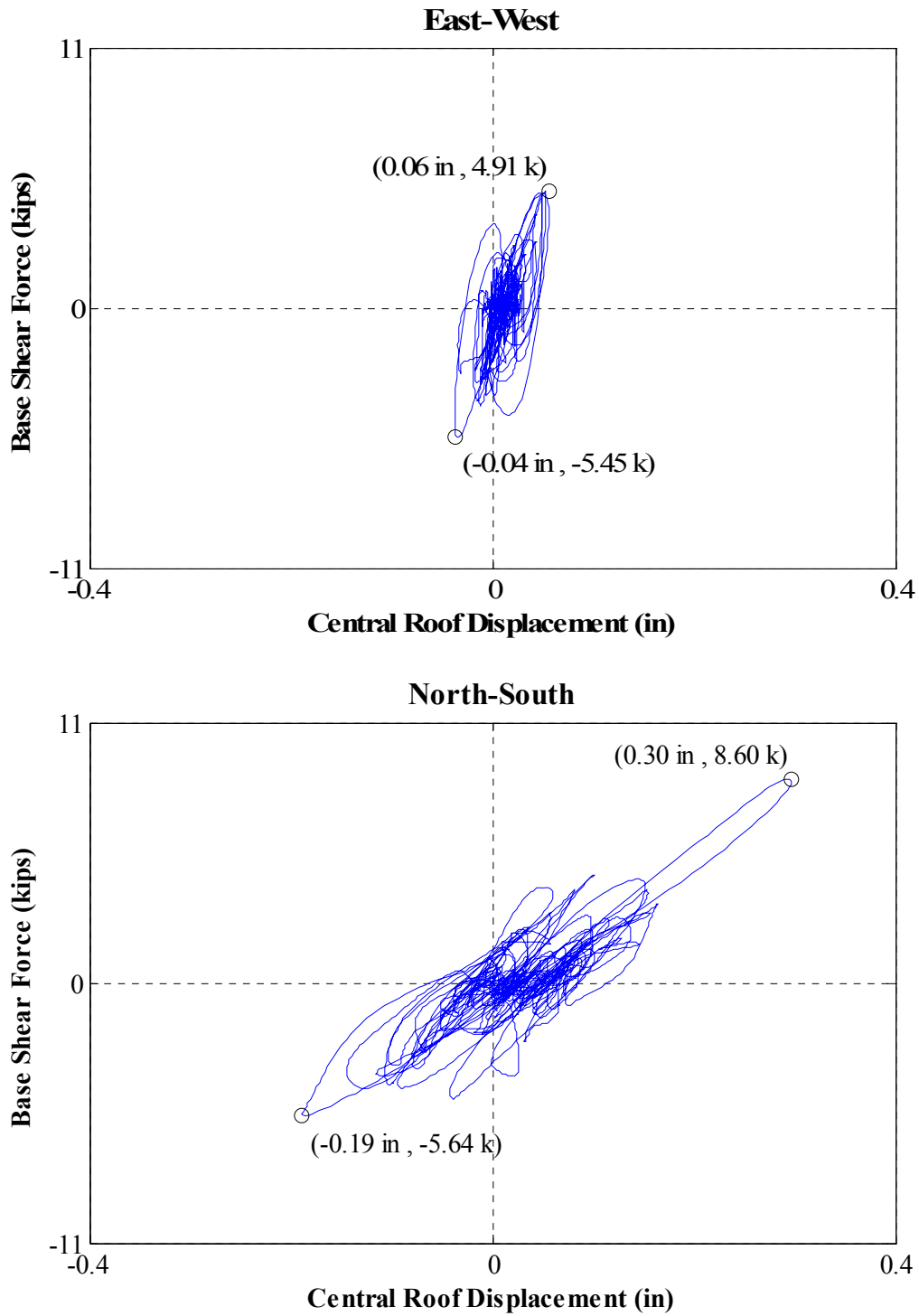


Figure N.2: Force-displacement hysteresis loops for Test NWP1S02

Appendix N

Phase 1, NWP1S03 Seismic Test

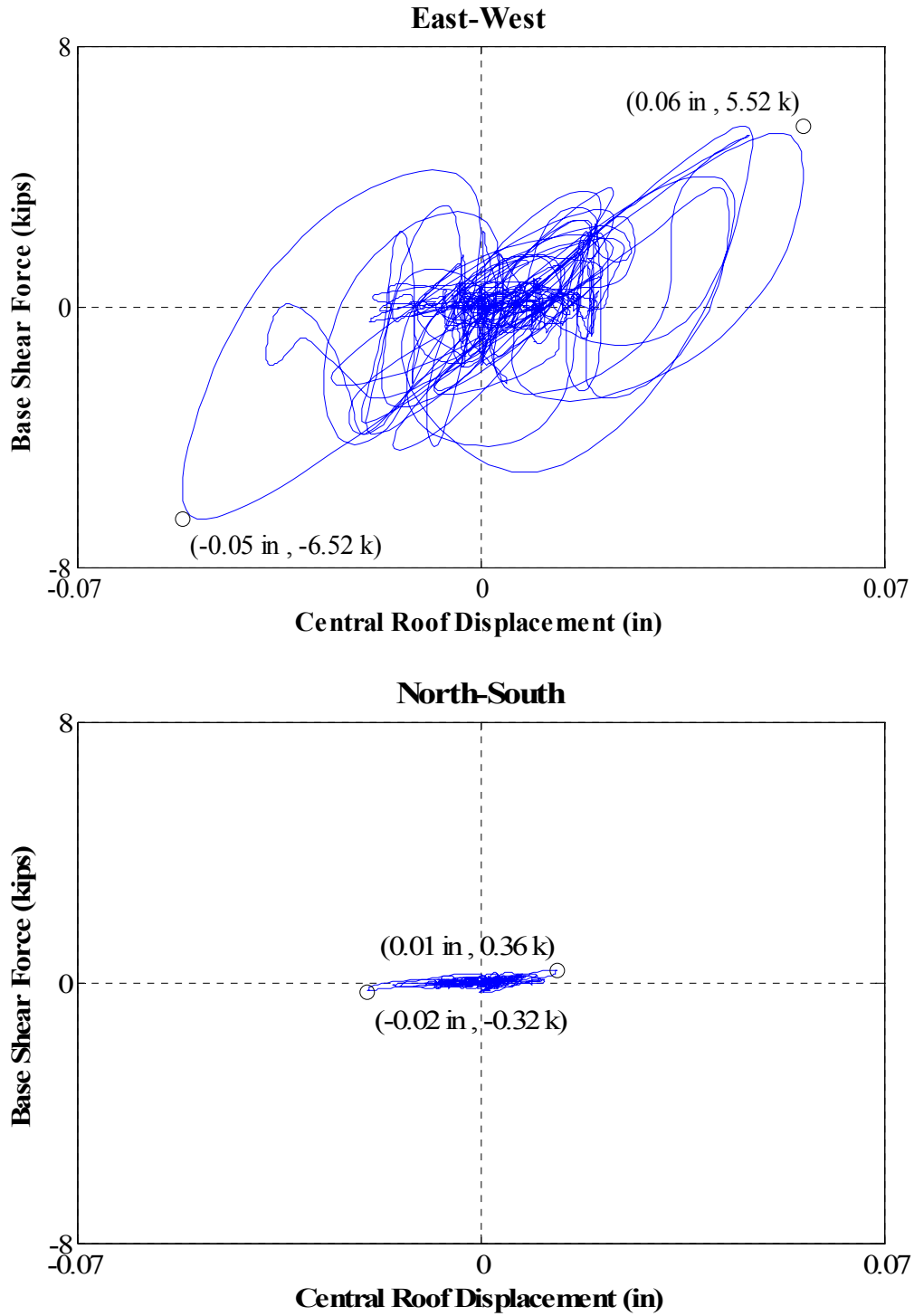


Figure N.3: Force-displacement hysteresis loops for Test NWP1S03

Appendix N

Phase 1, NWP1S04 Seismic Test

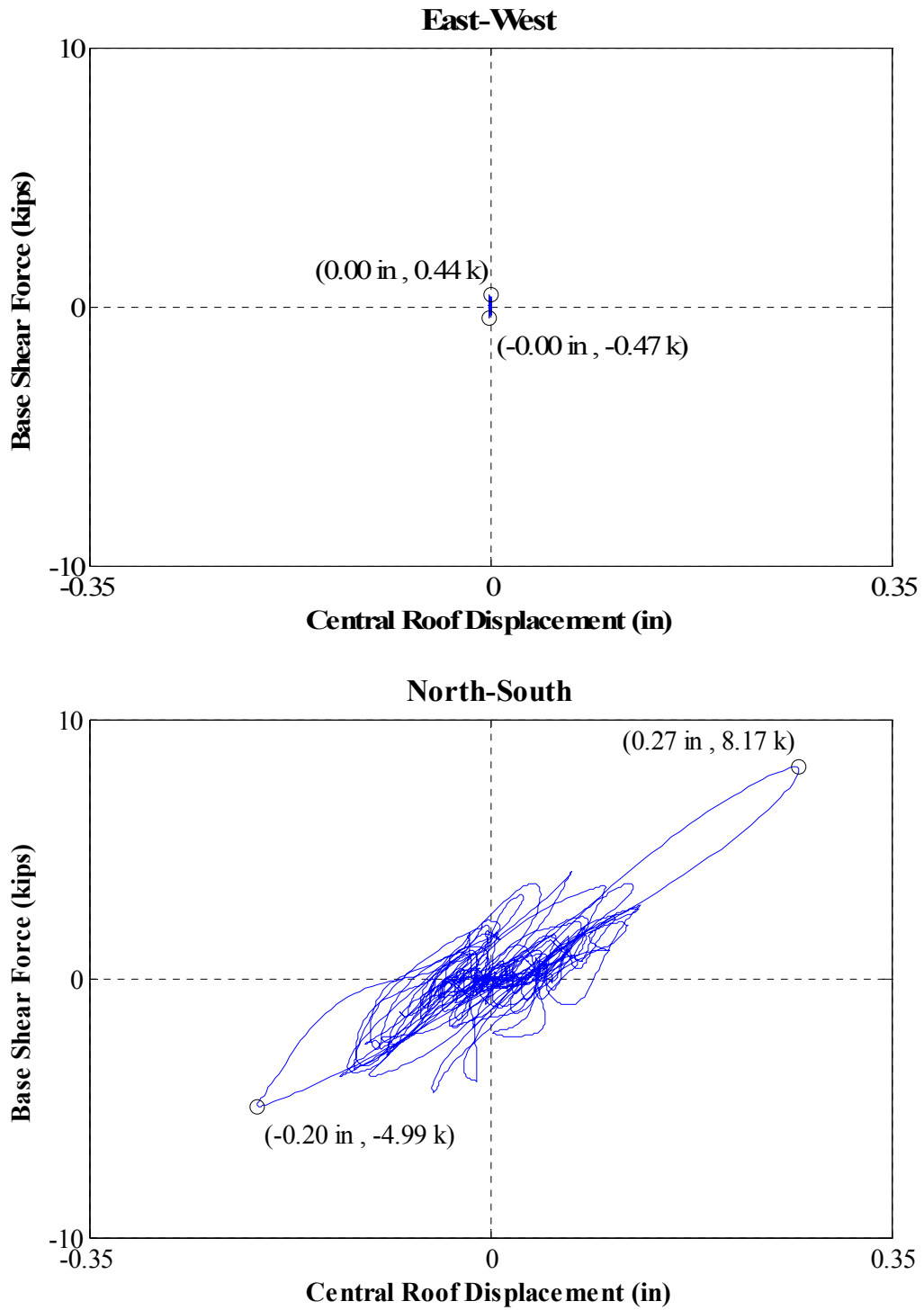


Figure N.4: Force-displacement hysteresis loops for Test NWP1S04

Appendix N

Phase 1, NWP1S05 Seismic Test

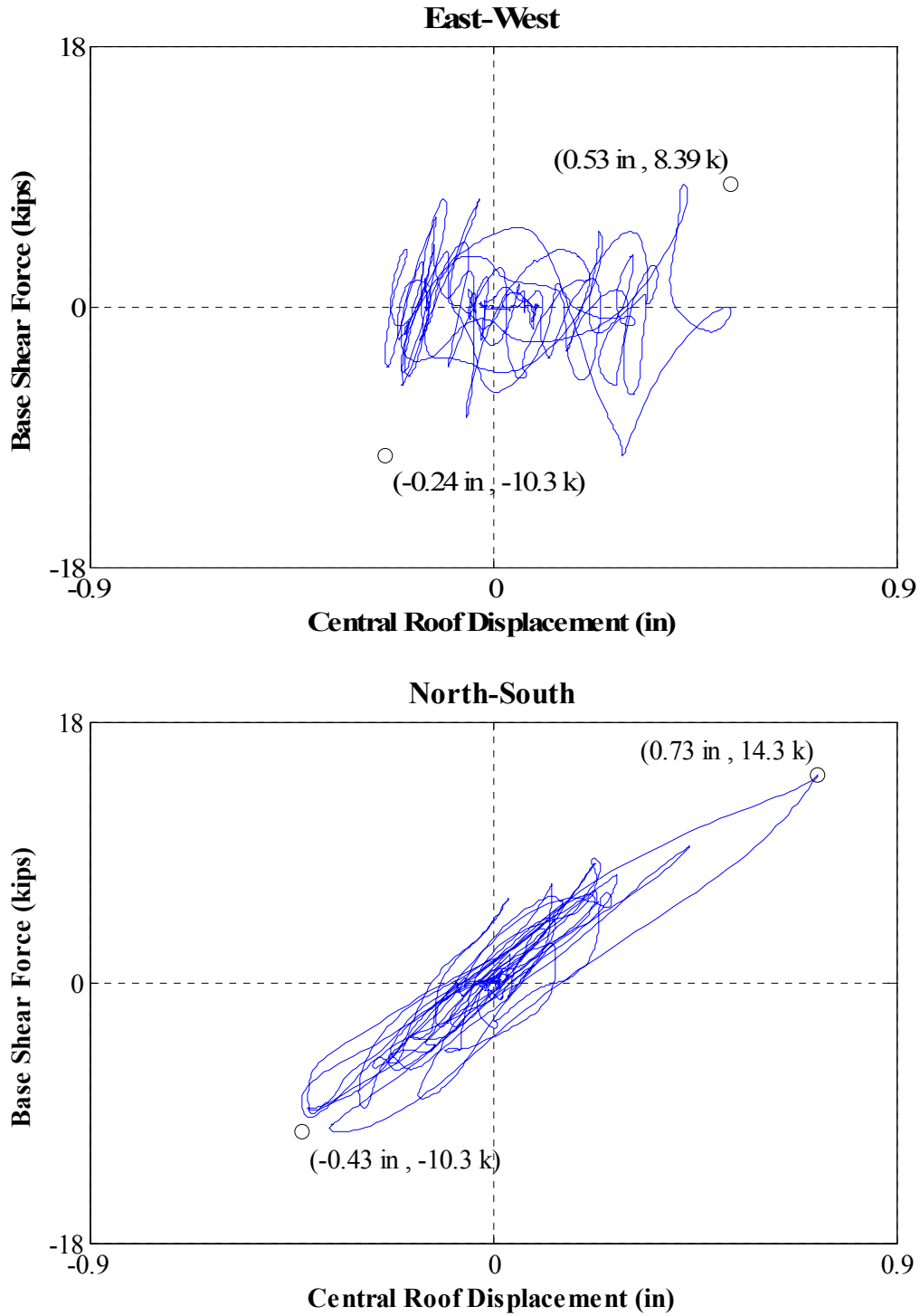


Figure N.5: Force-displacement hysteresis loops for Test NWP1S05

Appendix N

Phase 1, NWP1S17 Seismic Test

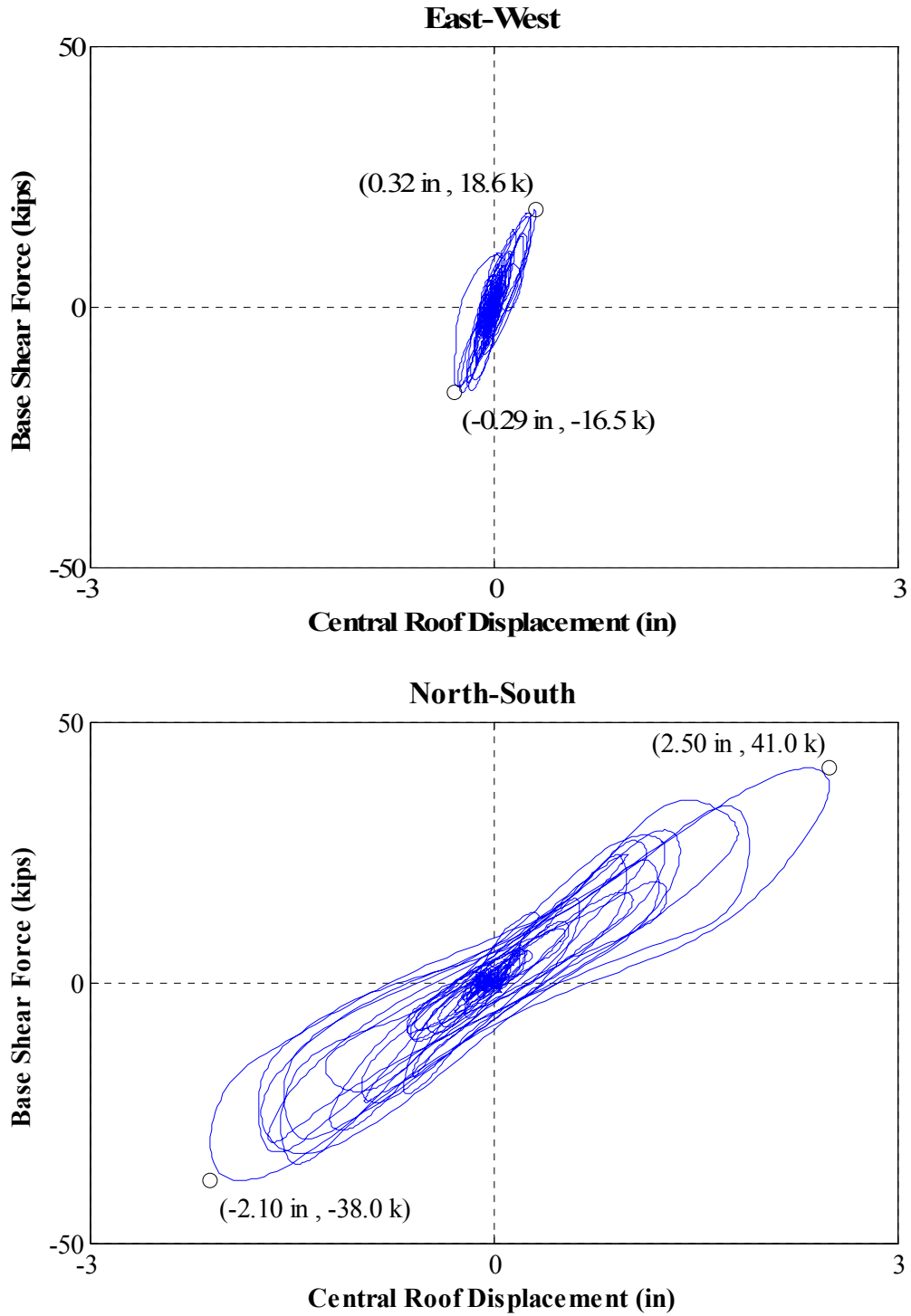


Figure N.6: Force-displacement hysteresis loops for Test NWP1S17

Appendix N

Phase 1, NWP1S07 Seismic Test

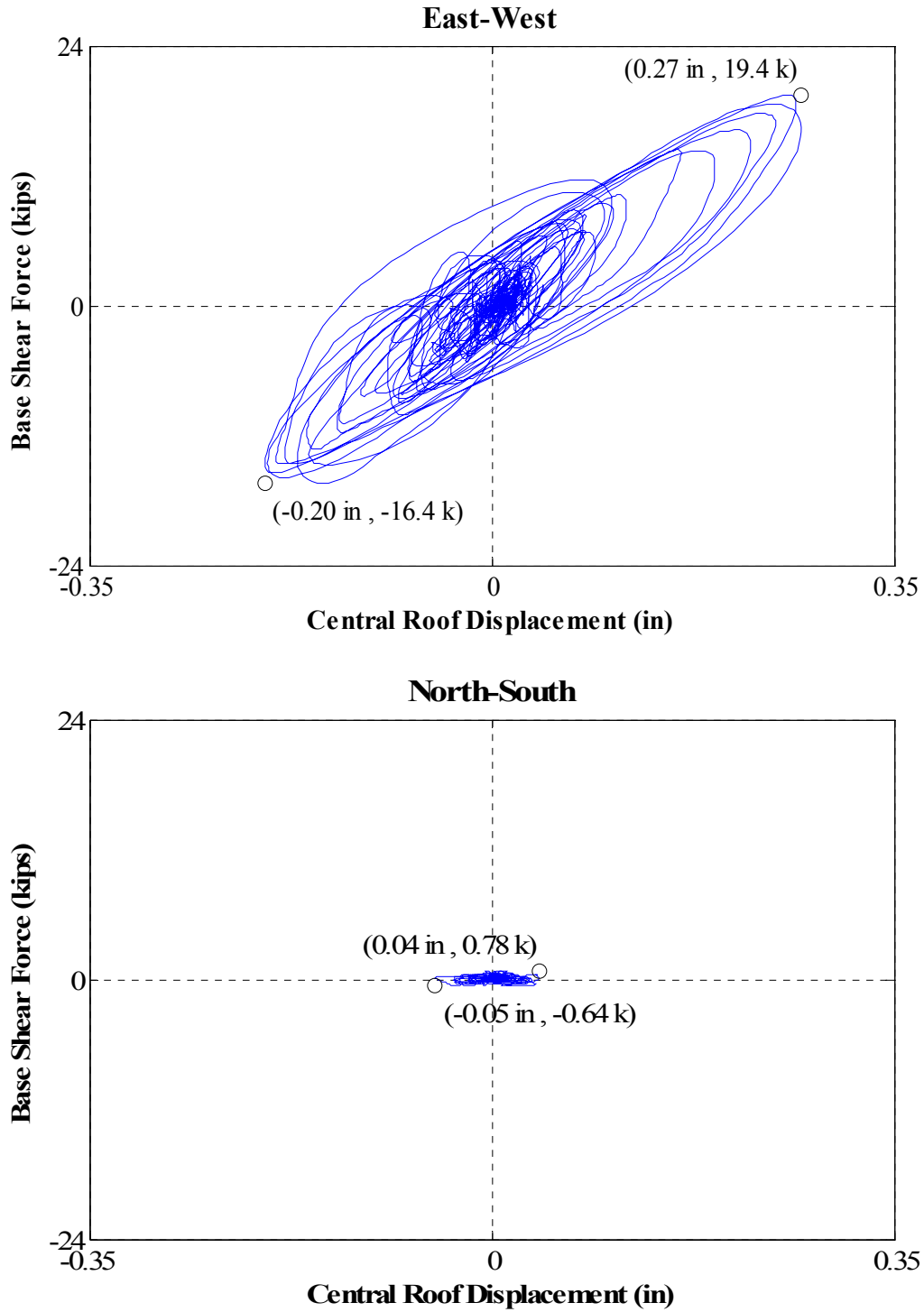


Figure N.7: Force-displacement hysteresis loops for Test NWP1S07

Appendix N

Phase 1, NWP1S06 Seismic Test

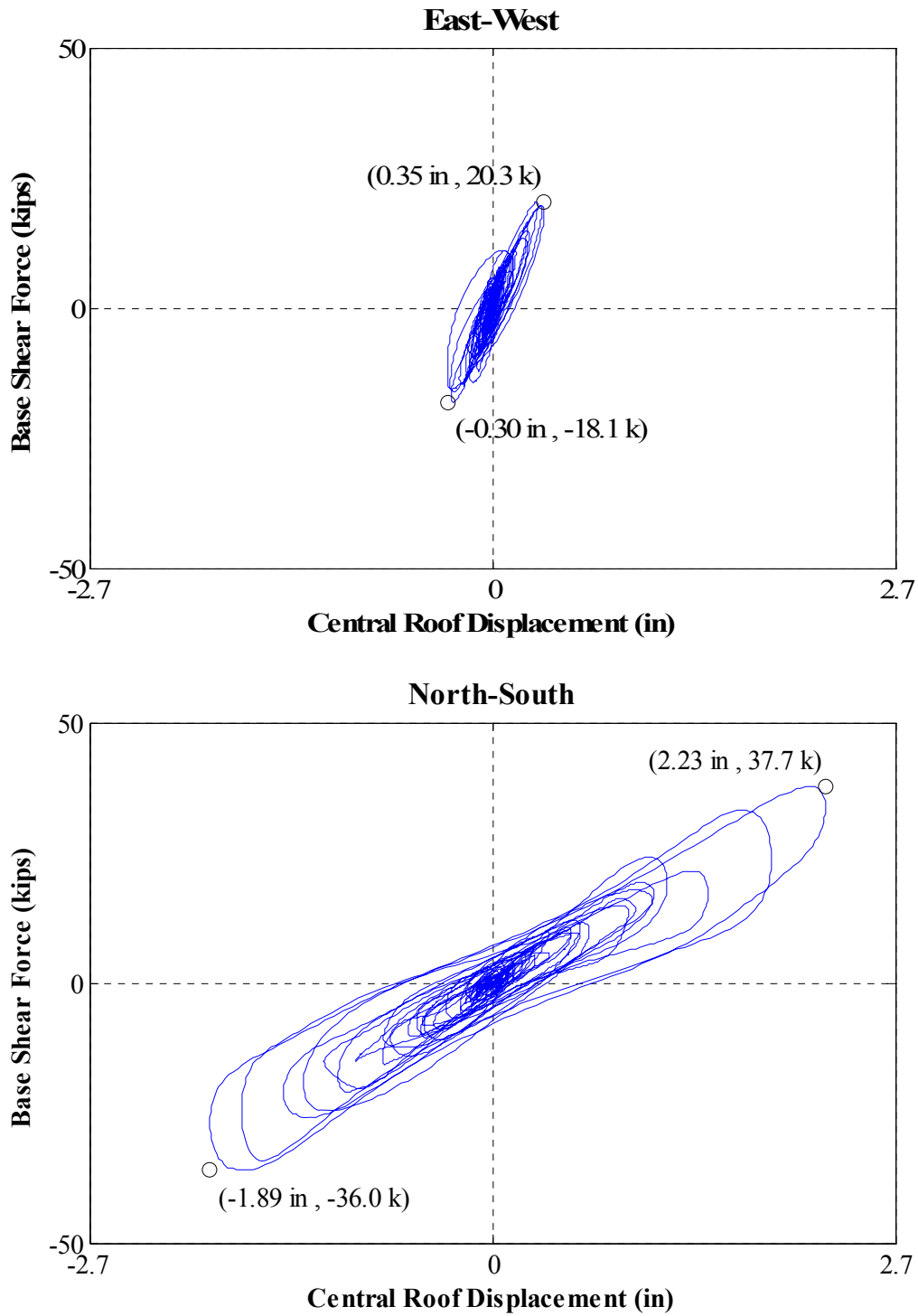


Figure N.8: Force-displacement hysteresis loops for Test NWP1S06

Appendix N

Phase 1, NWP1S10 Seismic Test

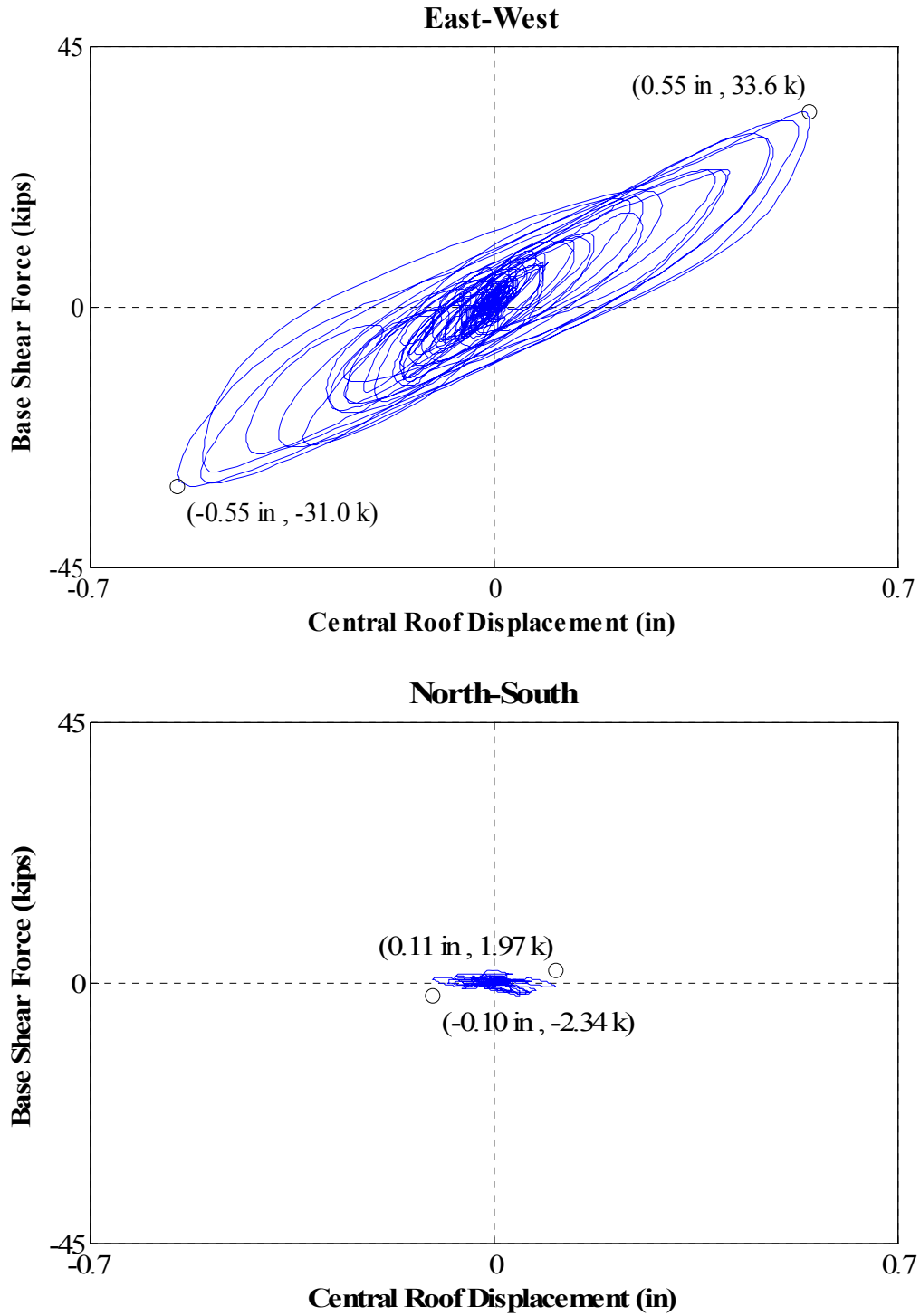


Figure N.9: Force-displacement hysteresis loops for Test NWP1S10

Appendix N

Phase 2, NWP2S01 Seismic Test

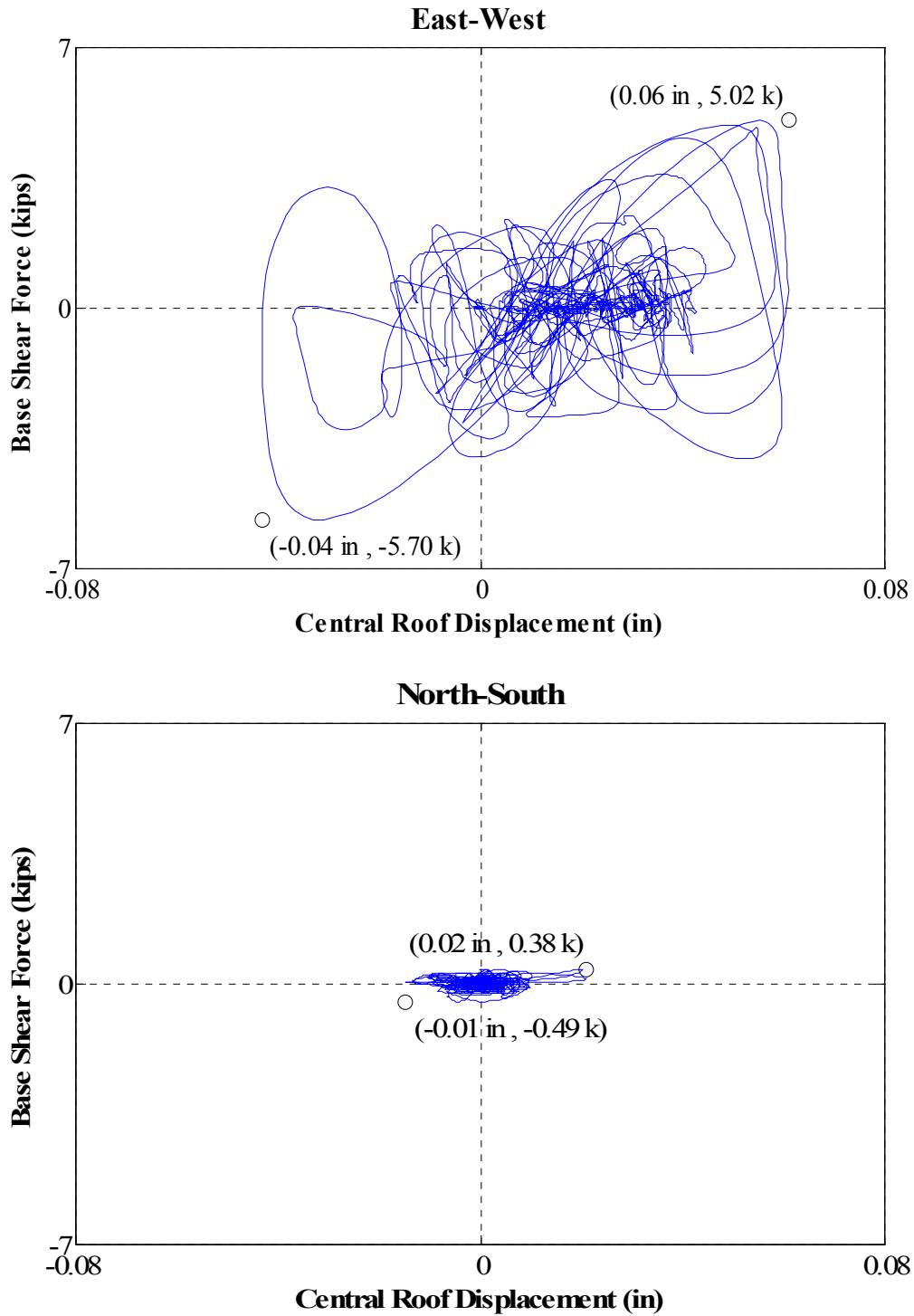


Figure N.10: Force-displacement hysteresis loops for Test NWP2S01

Appendix N

Phase 2, NWP2S02 Seismic Test

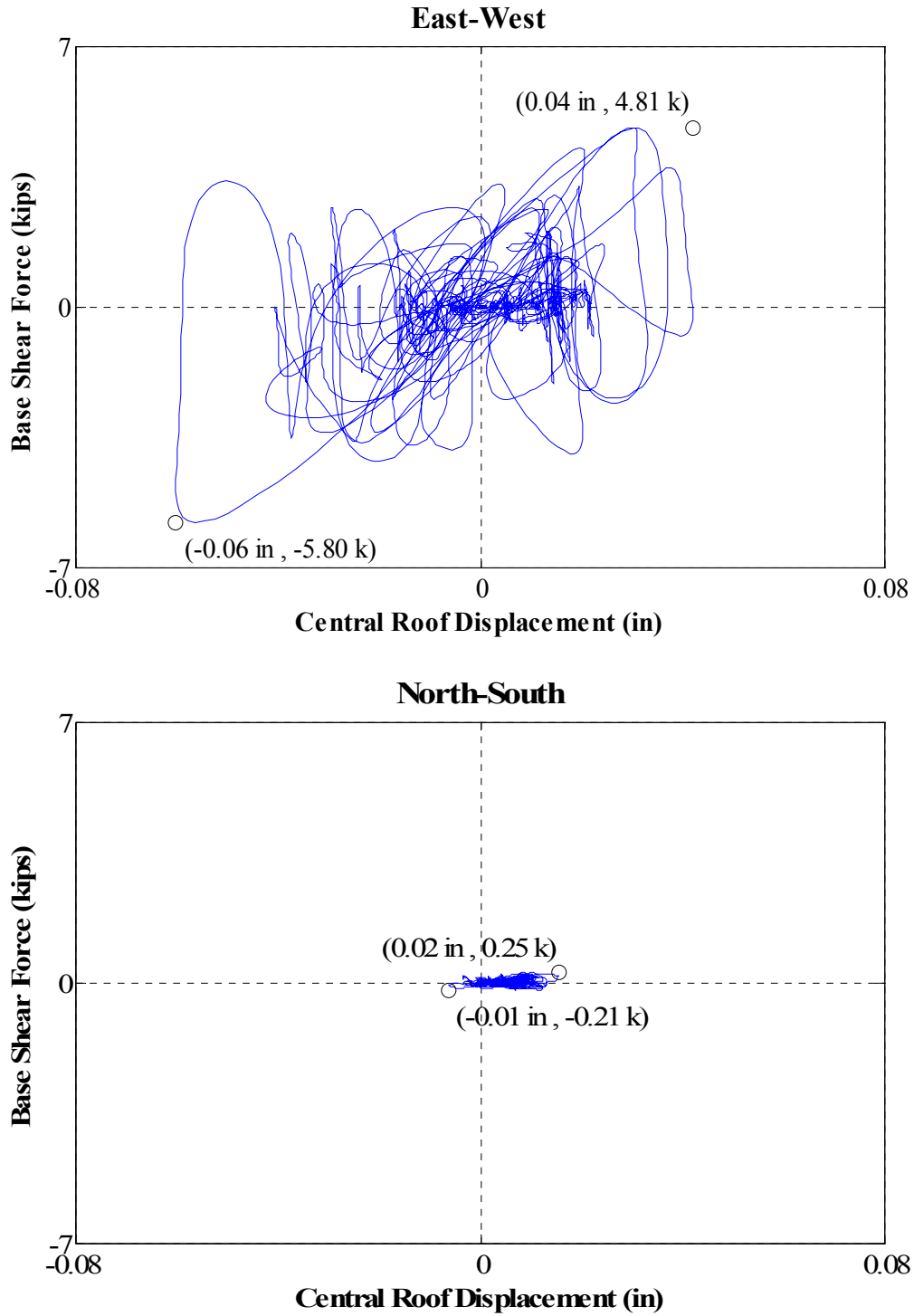


Figure N.11: Force-displacement hysteresis loops for Test NWP2S02

Appendix N

Phase 2, NWP2S03 Seismic Test

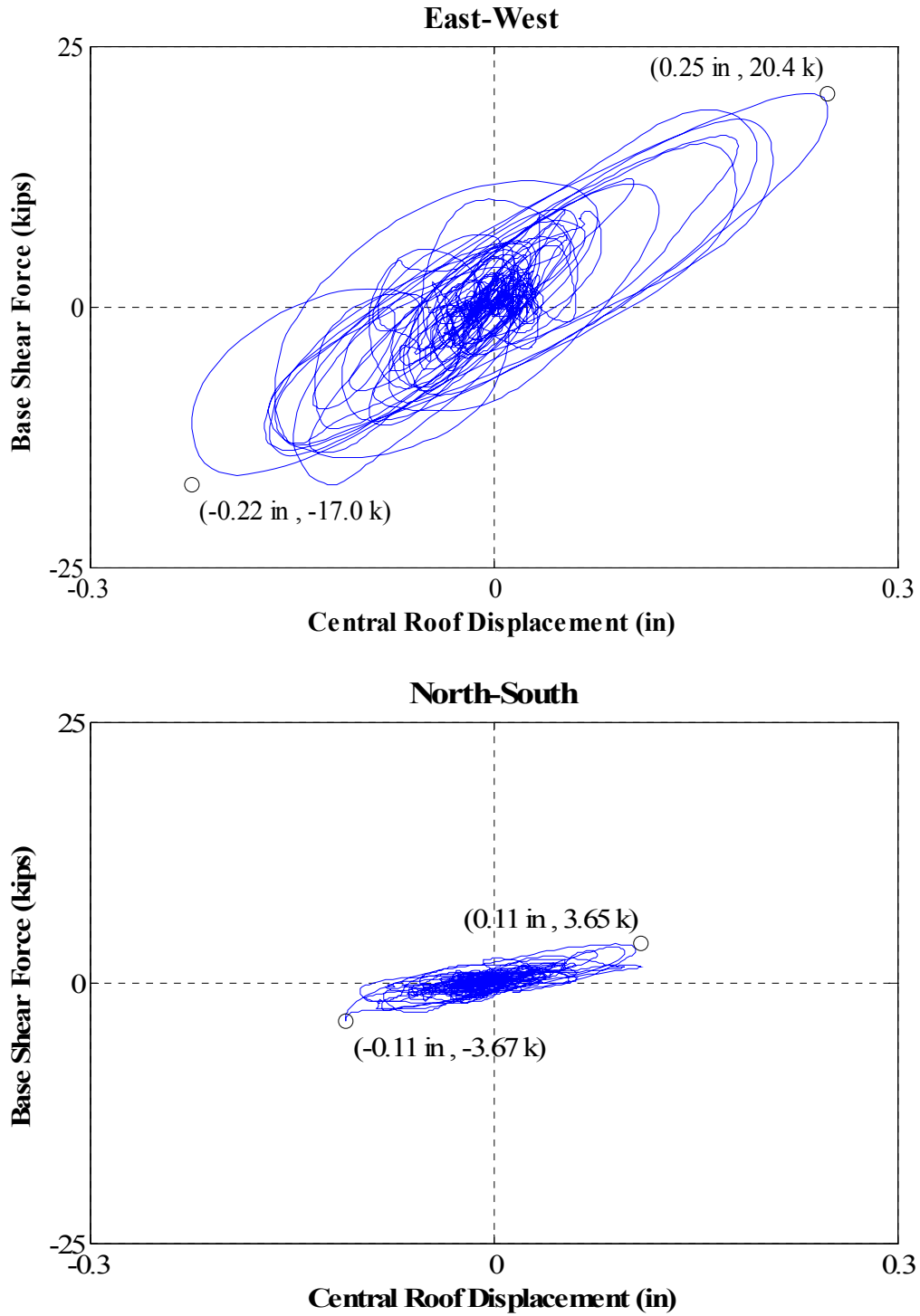


Figure N.12: Force-displacement hysteresis loops for Test NWP2S03

Appendix N

Phase 2, NWP2S04 Seismic Test

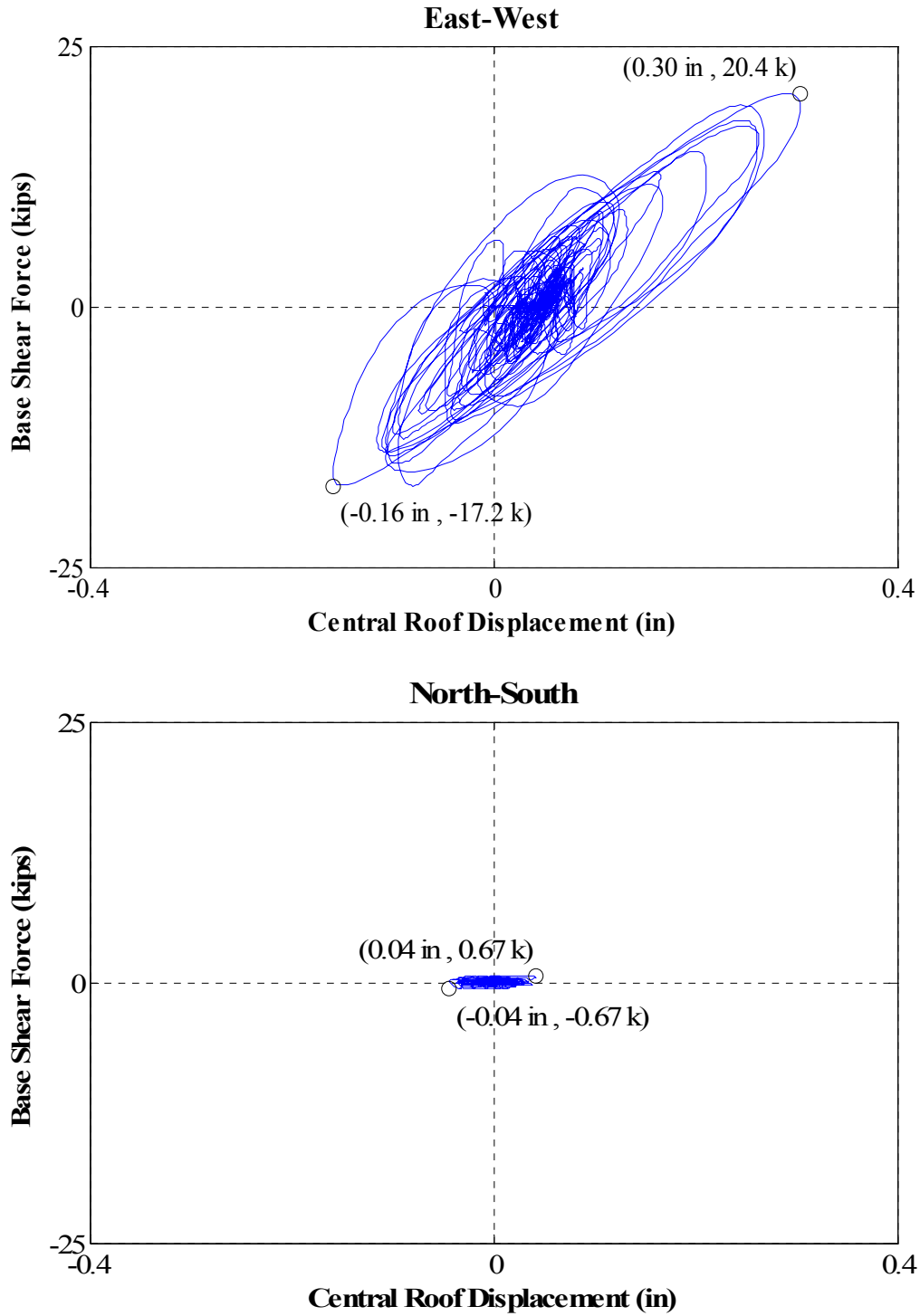


Figure N.13: Force-displacement hysteresis loops for Test NWP2S04

Appendix N

Phase 2, NWP2S05 Seismic Test

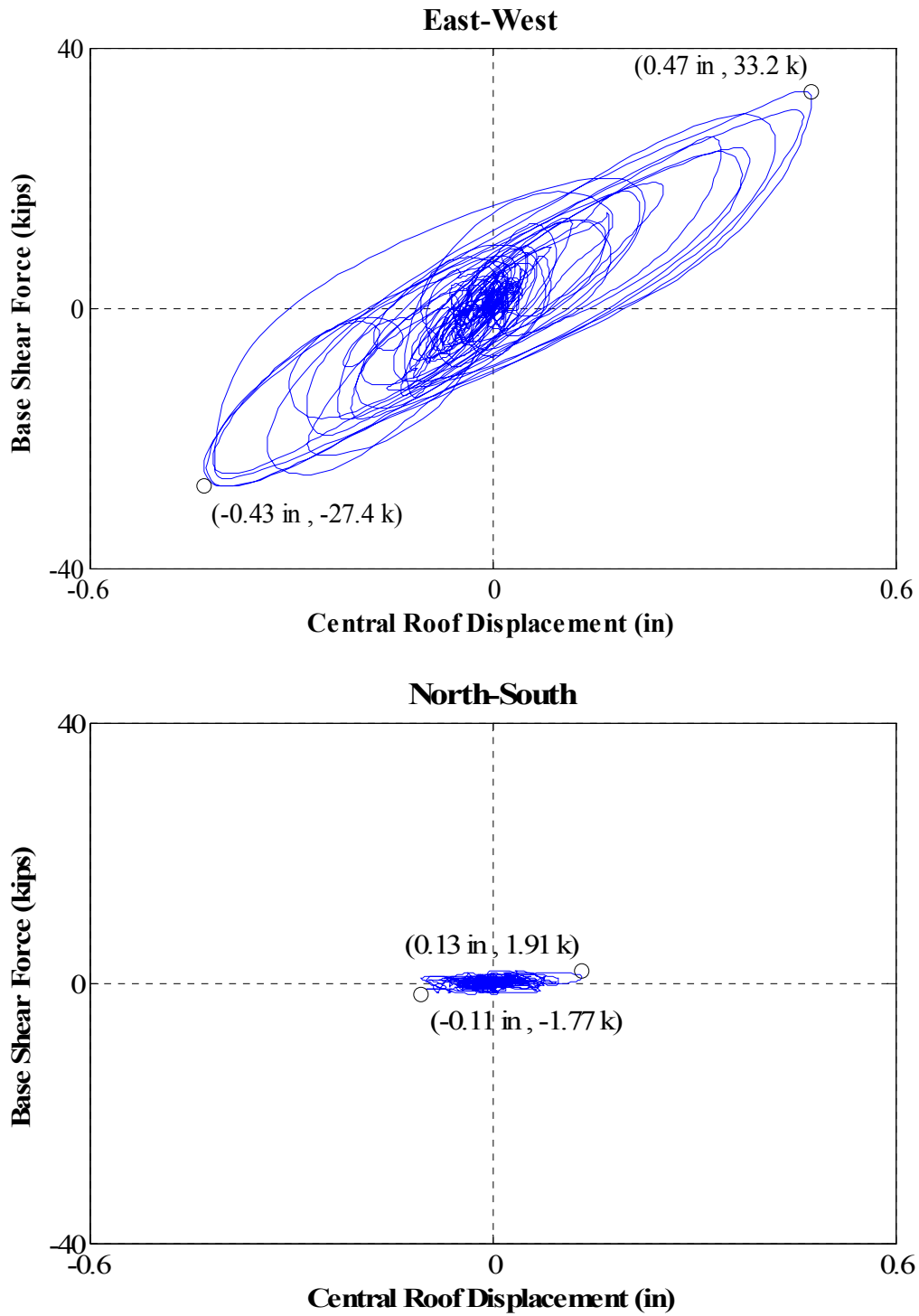


Figure N.14: Force-displacement hysteresis loops for Test NWP2S05

Appendix N

Phase 2, NWP2S06 Seismic Test

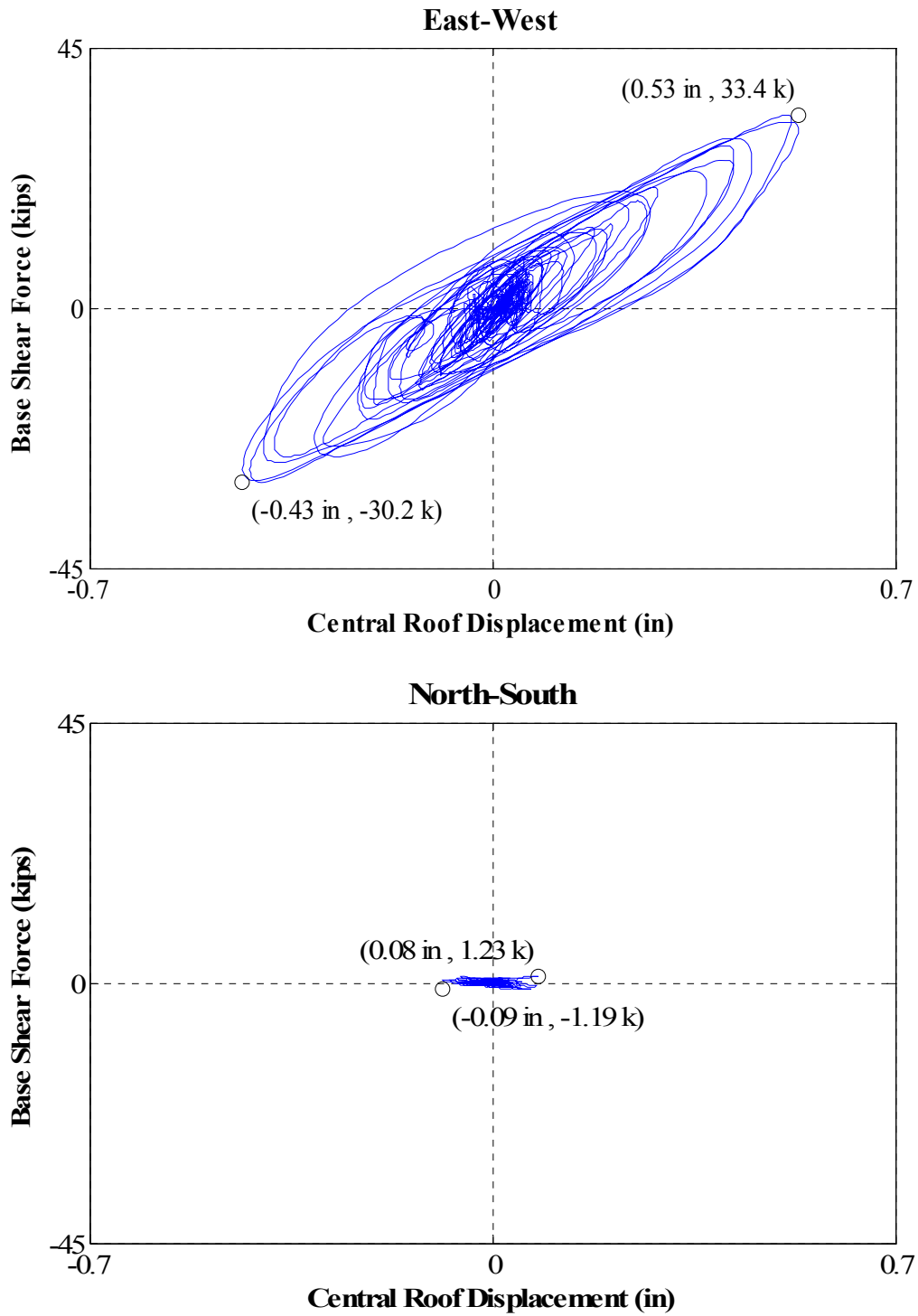


Figure N.15: Force-displacement hysteresis loops for Test NWP2S06

Appendix N

Phase 2, NWP2S07 Seismic Test

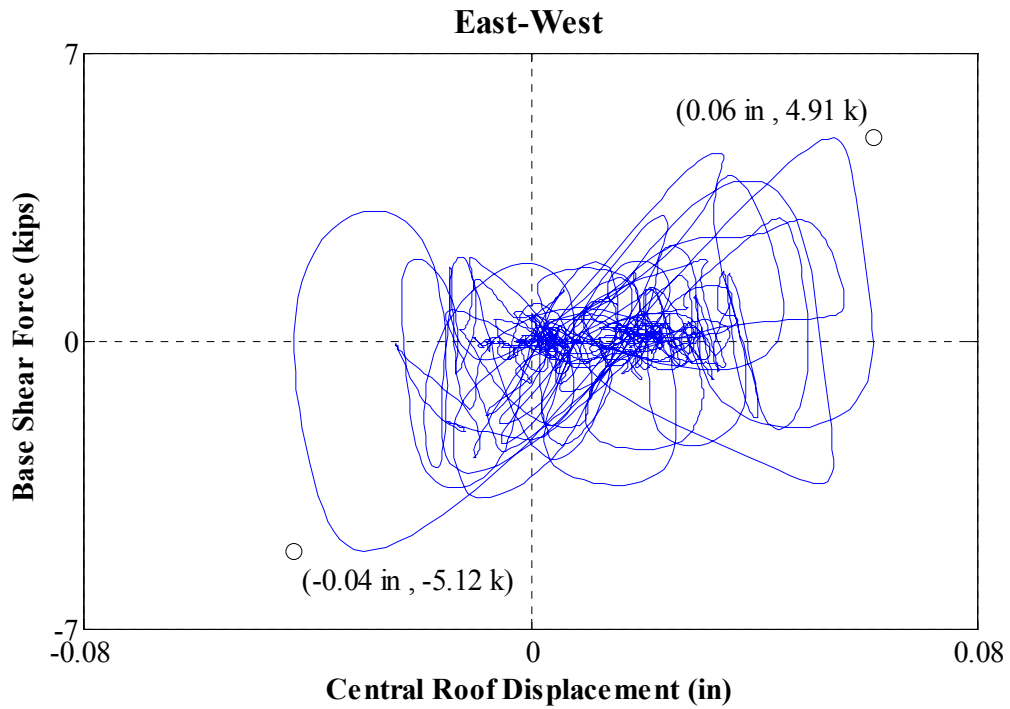


Figure N.16: Force-displacement hysteresis loop for Test NWP2S07

* Data not plotted for North-South direction due to error in recording

Appendix N

Phase 2, NWP2S08 Seismic Test

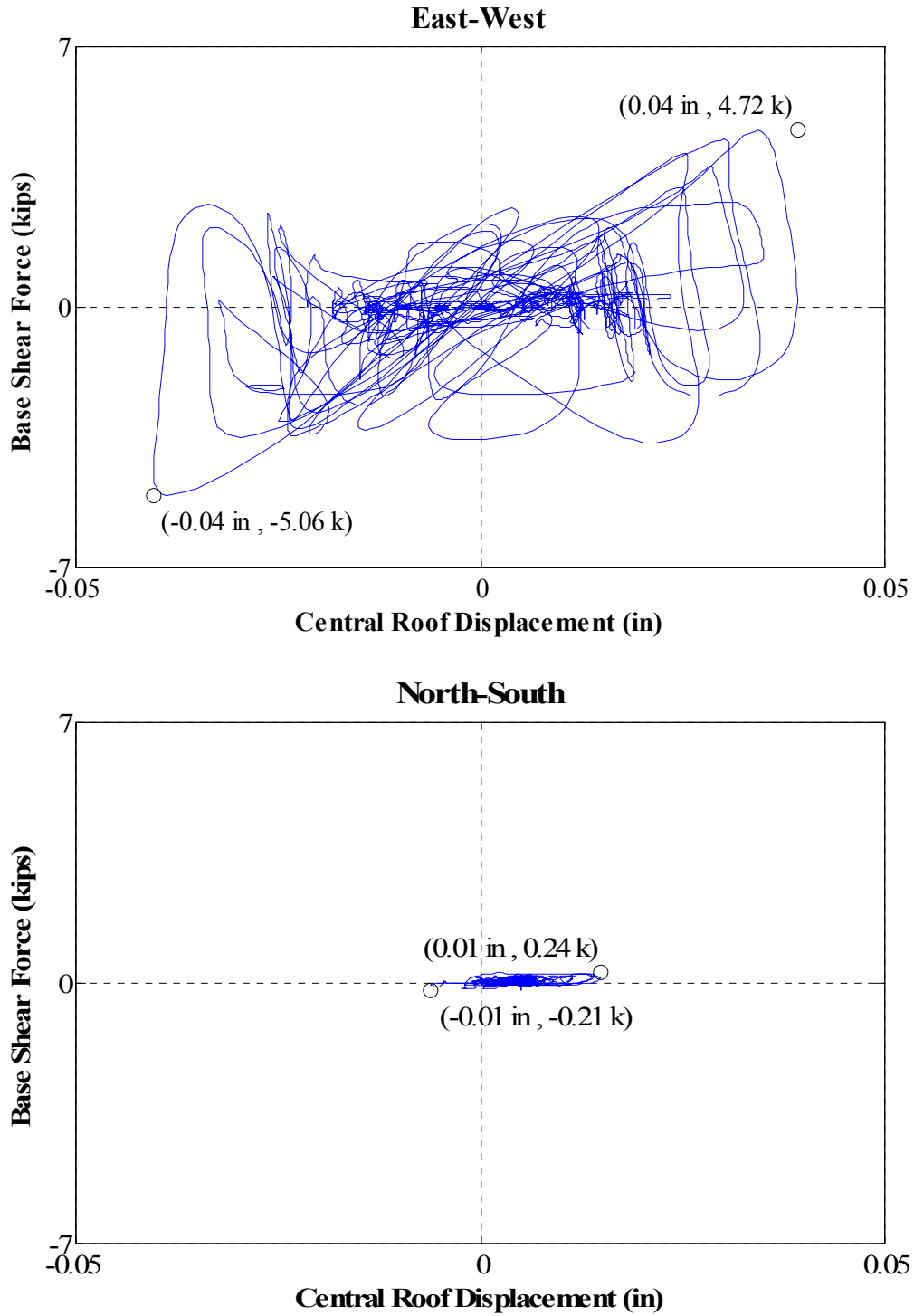


Figure N.17: Force-displacement hysteresis loops for Test NWP2S08

Appendix N

Phase 2, NWP2S09 Seismic Test

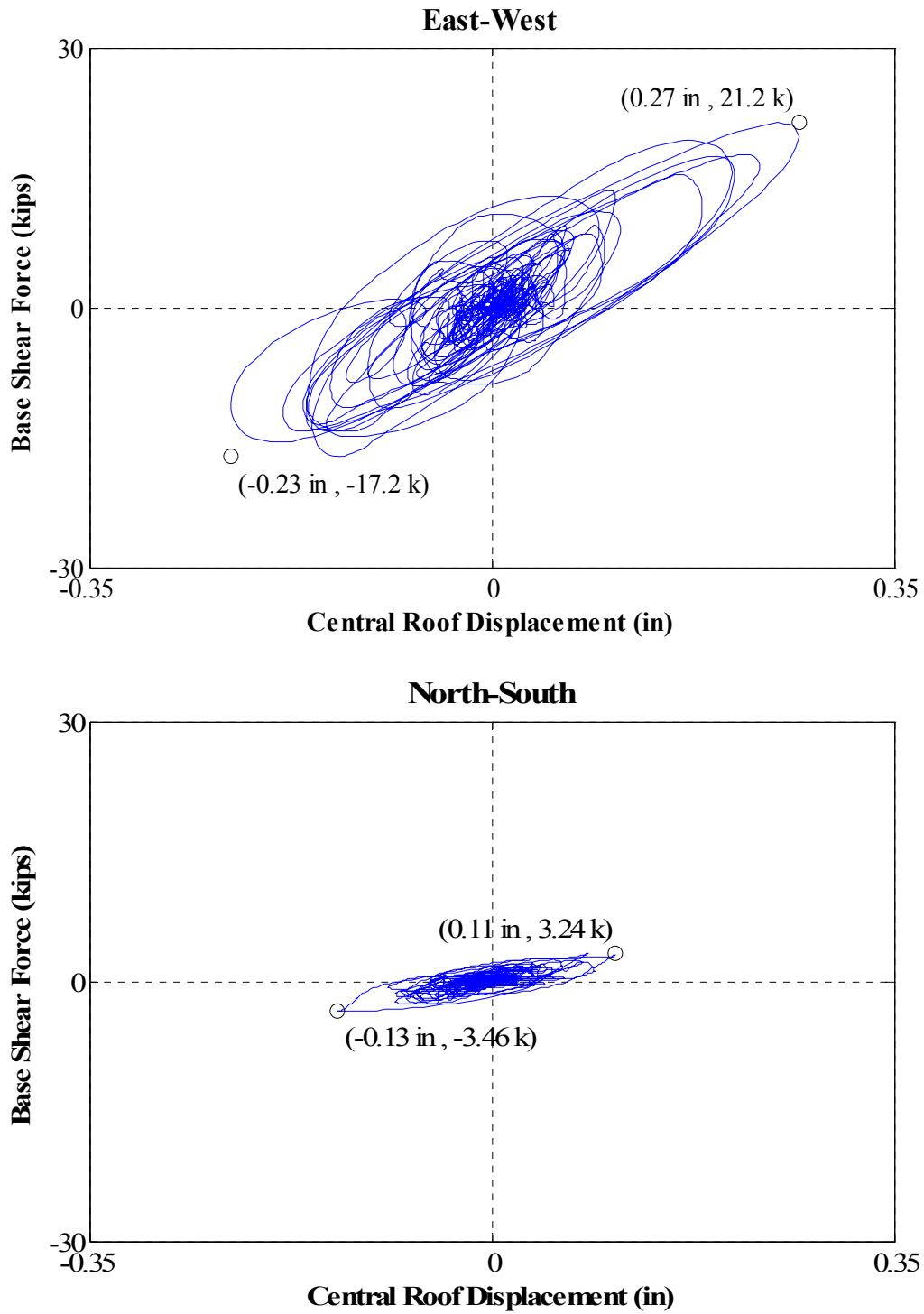


Figure N.18: Force-displacement hysteresis loops for Test NWP2S09

Appendix N

Phase 2, NWP2S10 Seismic Test

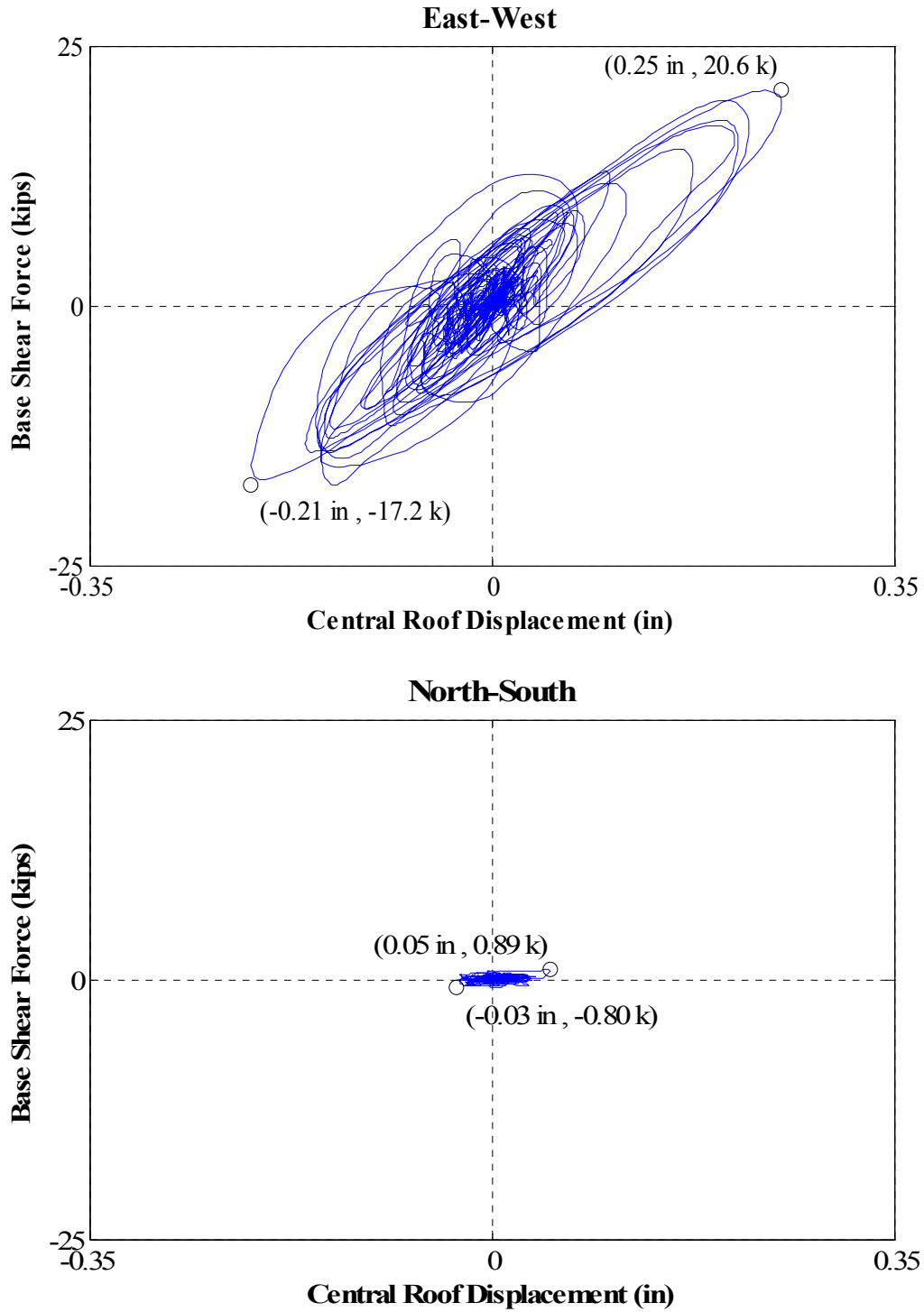


Figure N.19: Force-displacement hysteresis loops for Test NWP2S10

Appendix N

Phase 2, NWP2S11 Seismic Test

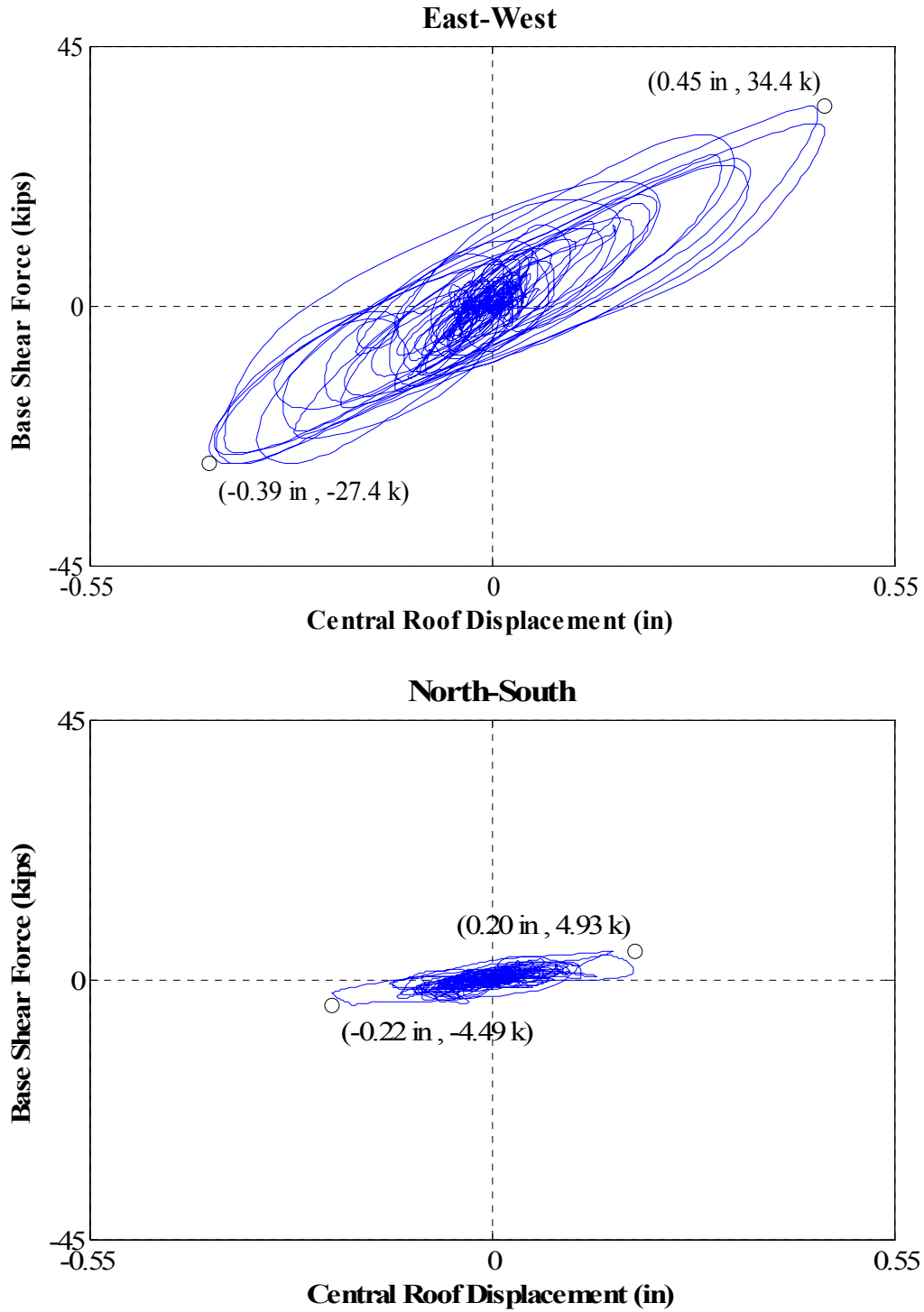


Figure N.20: Force-displacement hysteresis loops for Test NWP2S11

Appendix N

Phase 2, NWP2S12 Seismic Test

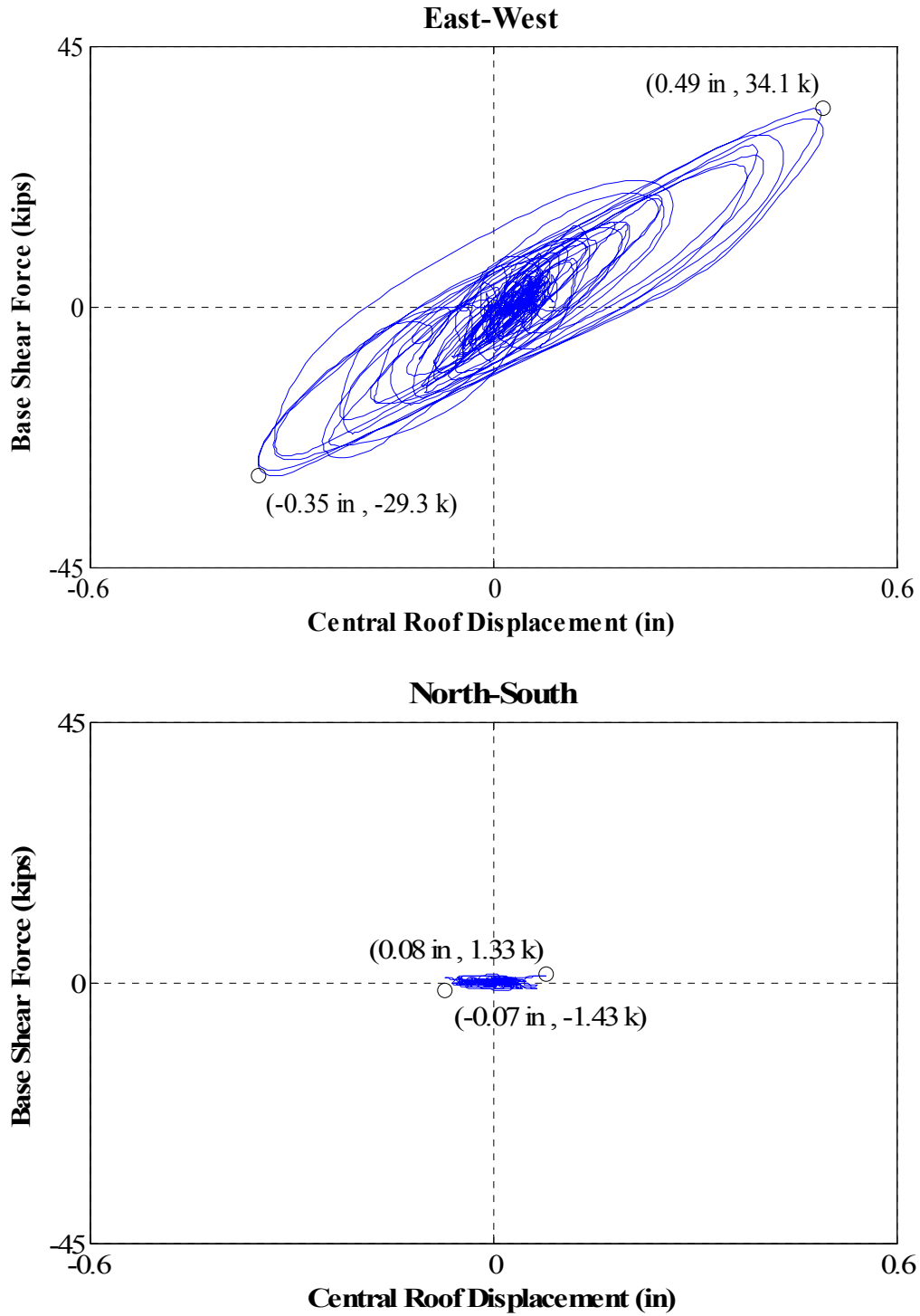


Figure N.21: Force-displacement hysteresis loops for Test NWP2S12

Appendix N

Phase 2, NWP2S13 Seismic Test

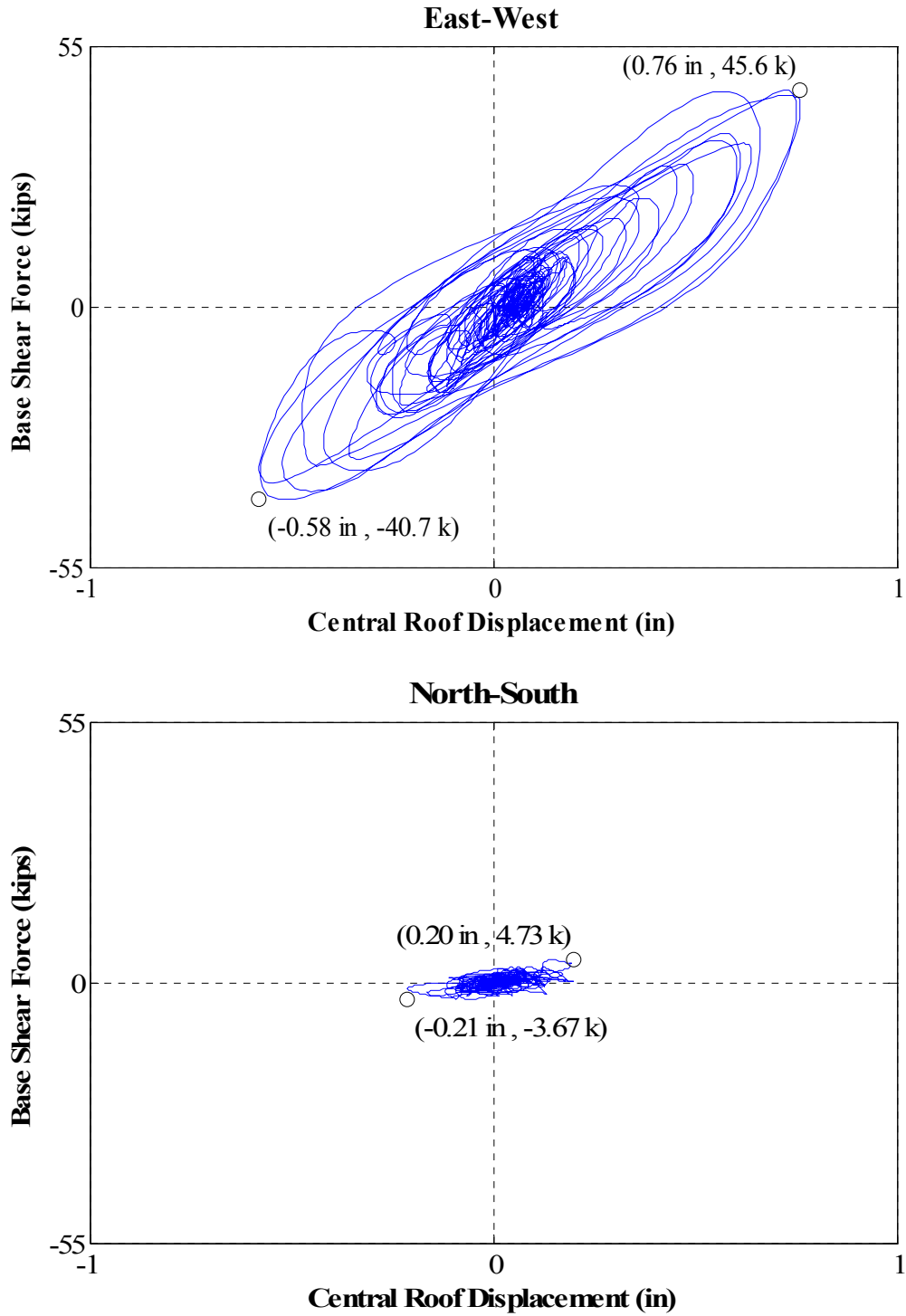


Figure N.22: Force-displacement hysteresis loops for Test NWP2S13

Appendix N

Phase 2, NWP2S14 Seismic Test

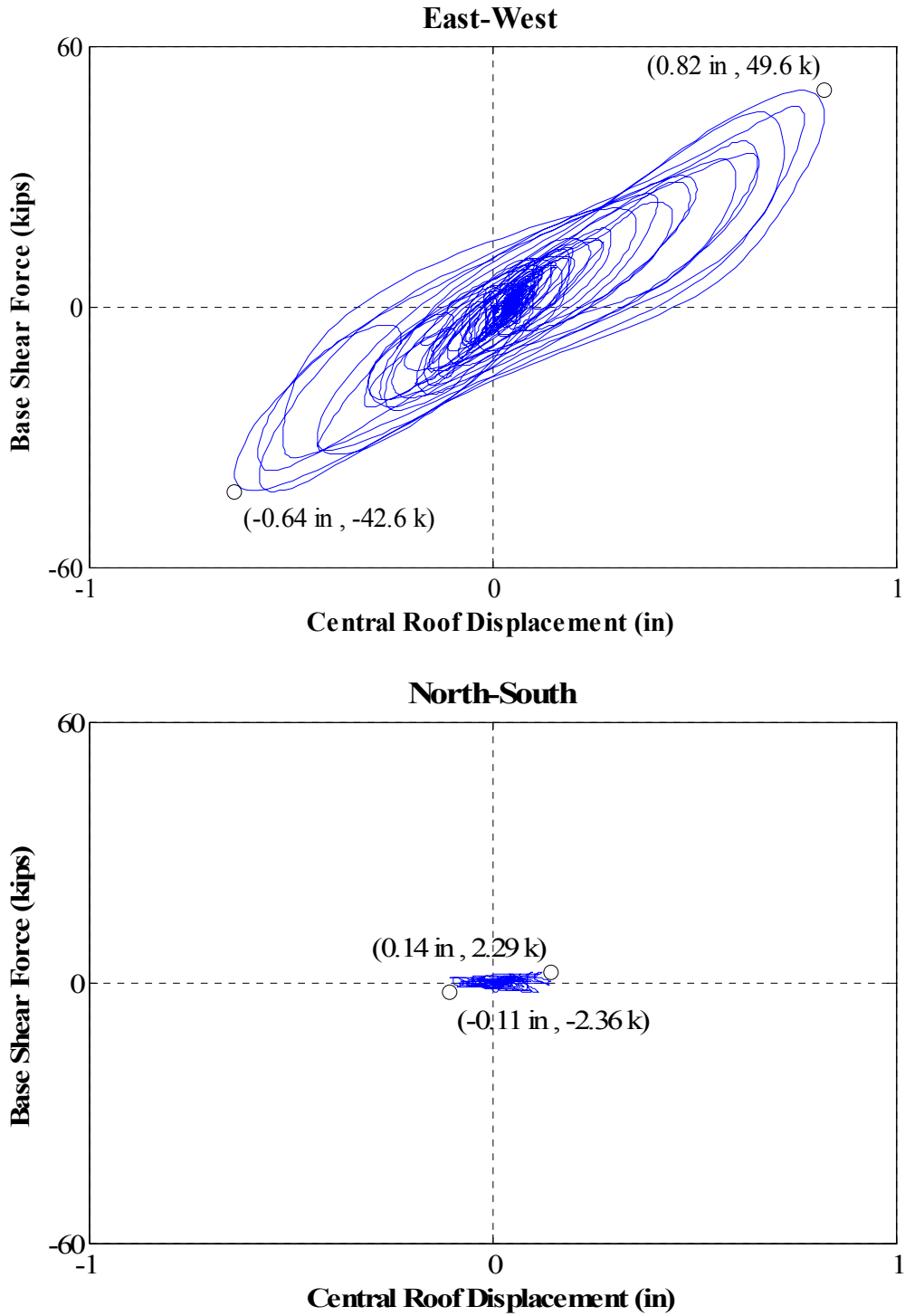


Figure N.23: Force-displacement hysteresis loops for Test NWP2S14

Appendix N

Phase 2, NWP2S16 Seismic Test

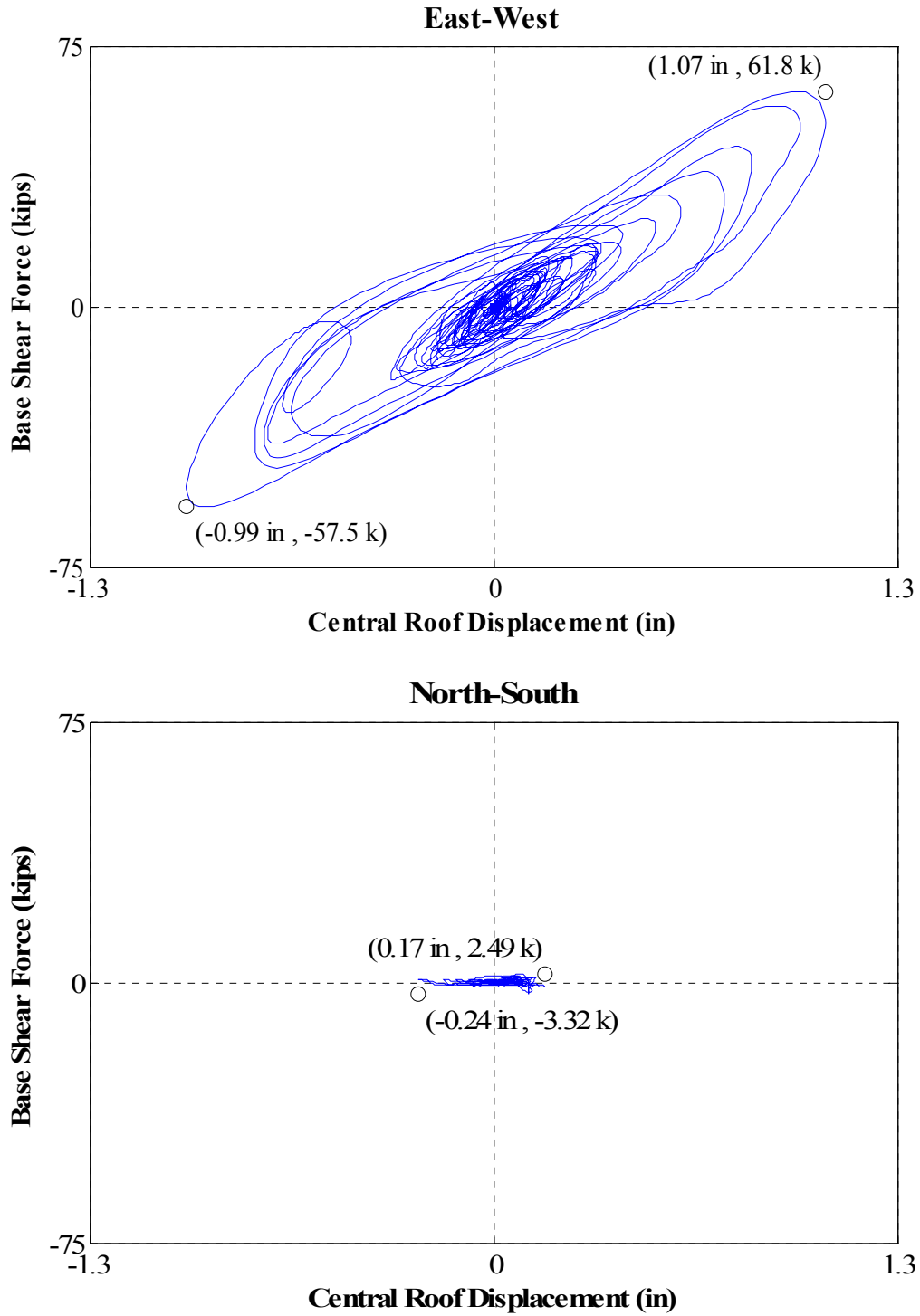


Figure N.24: Force-displacement hysteresis loops for Test NWP2S16

Appendix N

Phase 2, NWP2S17 Seismic Test

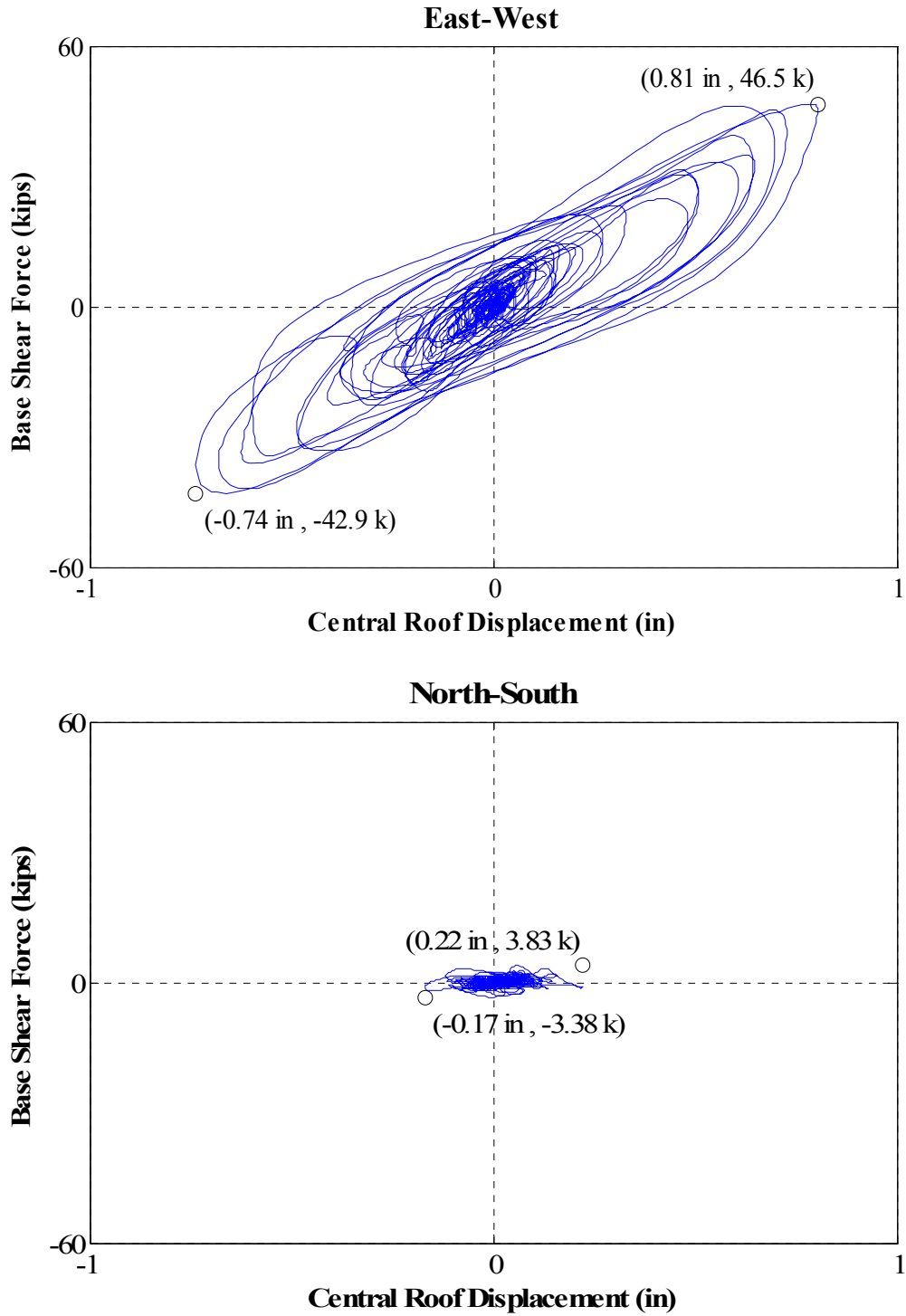


Figure N.25: Force-displacement hysteresis loops for Test NWP2S17

Appendix N

Phase 2, NWP2S21 Seismic Test

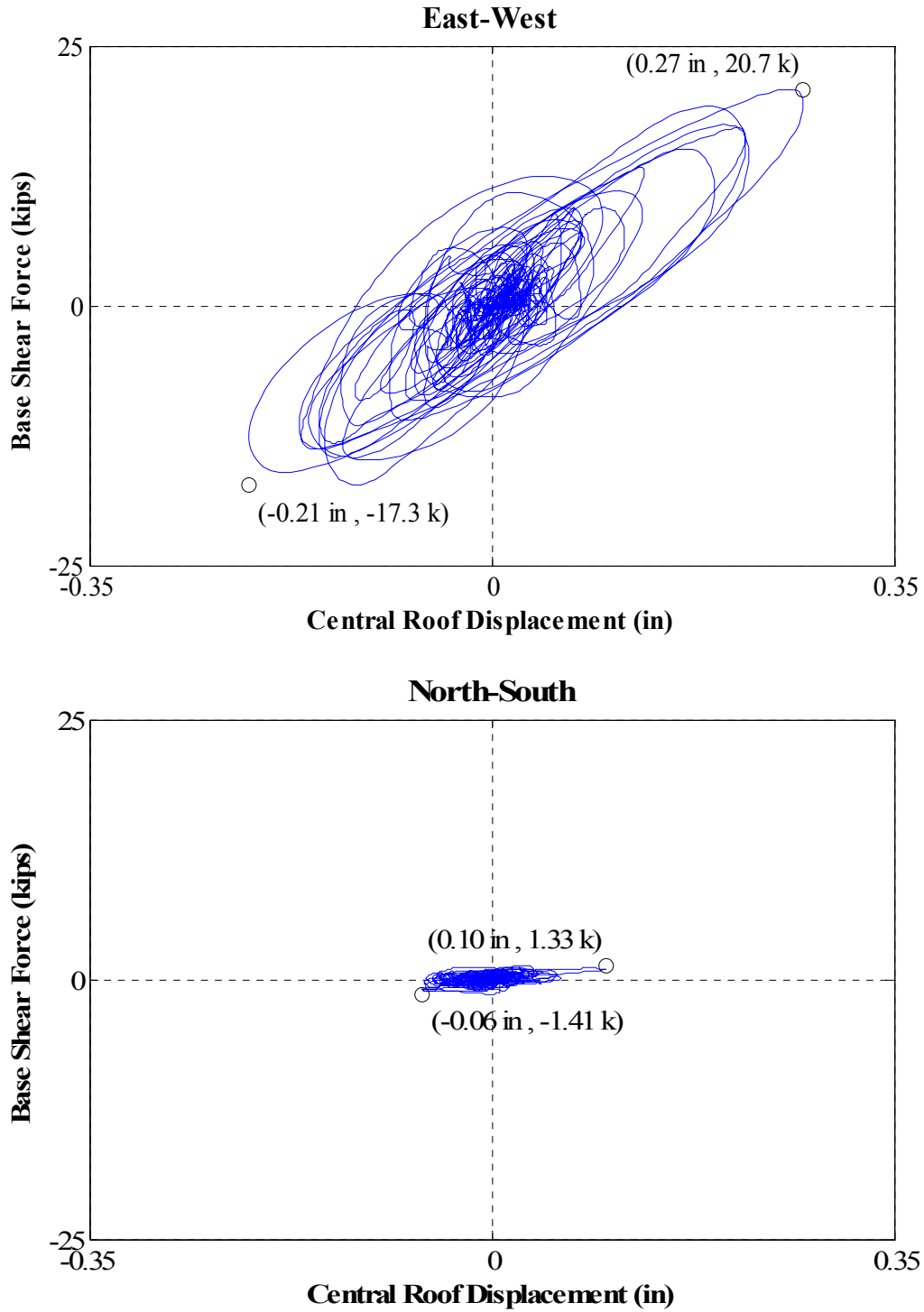


Figure N.26: Force-displacement hysteresis loops for Test NWP2S21

Appendix N

Phase 2, NWP2S24 Seismic Test

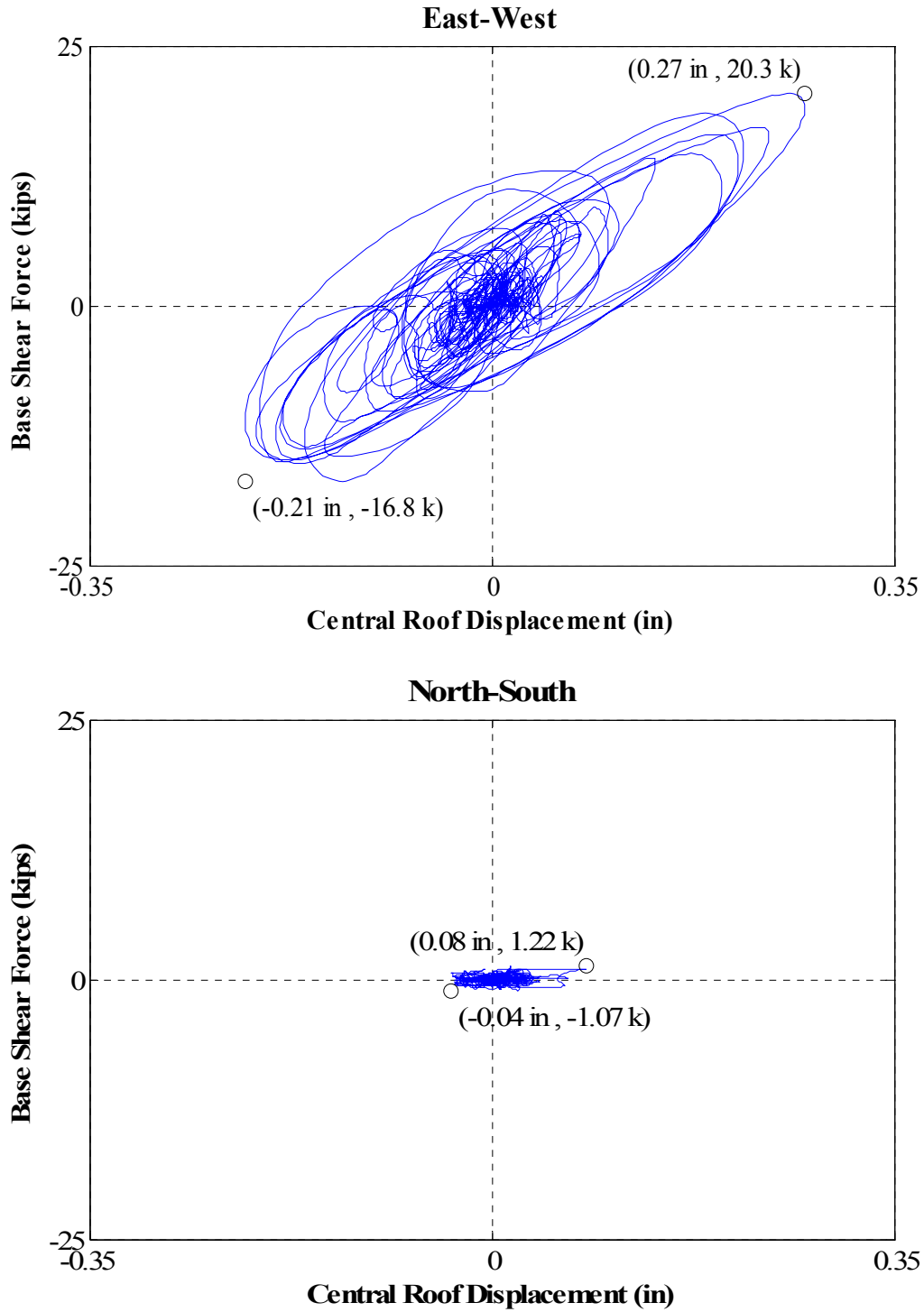


Figure N.27: Force-displacement hysteresis loops for Test NWP2S24

Appendix N

Phase 2, NWP2S25 Seismic Test

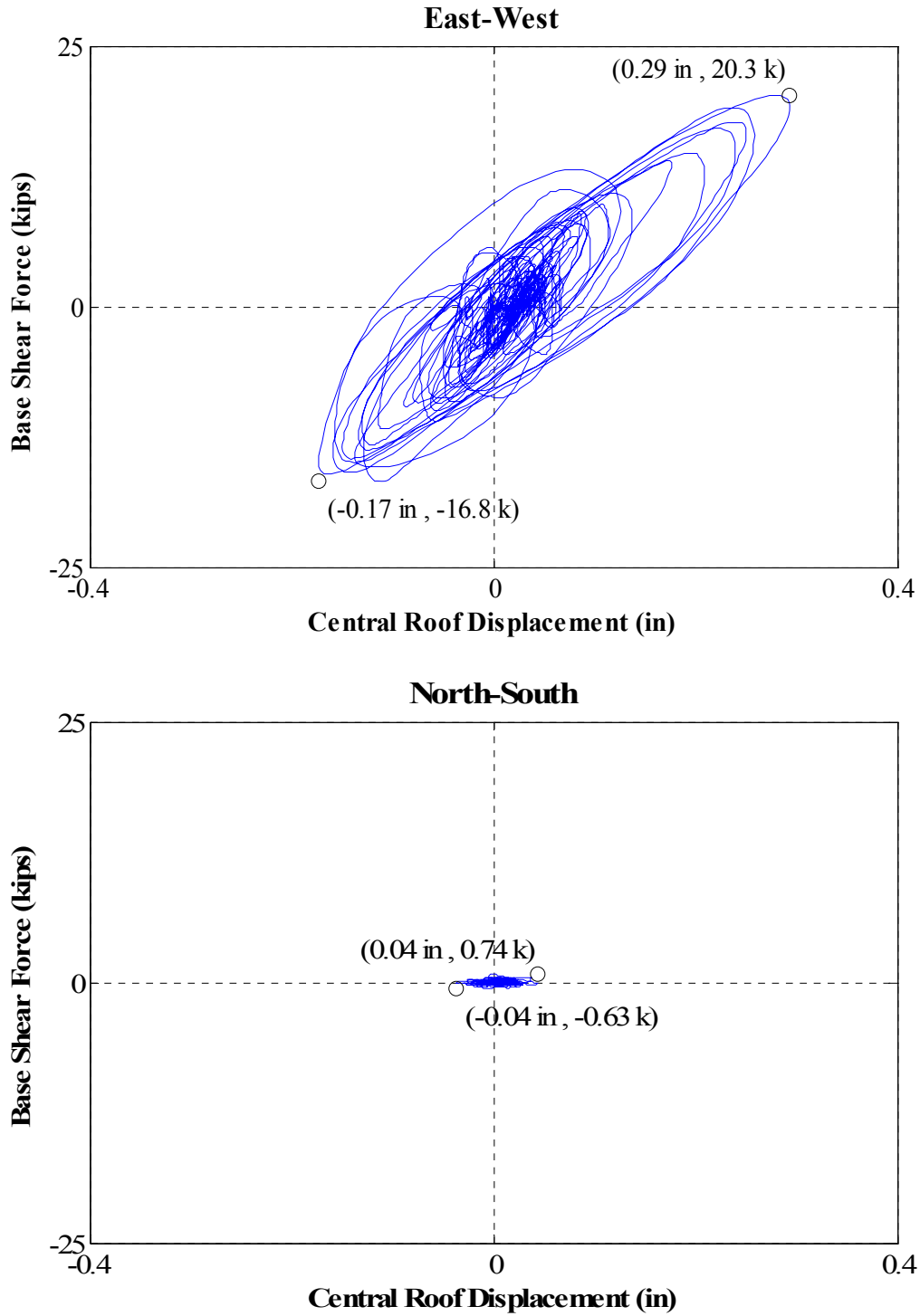


Figure N.28: Force-displacement hysteresis loops for Test NWP2S25

Appendix N

Phase 2, NWP2S26 Seismic Test

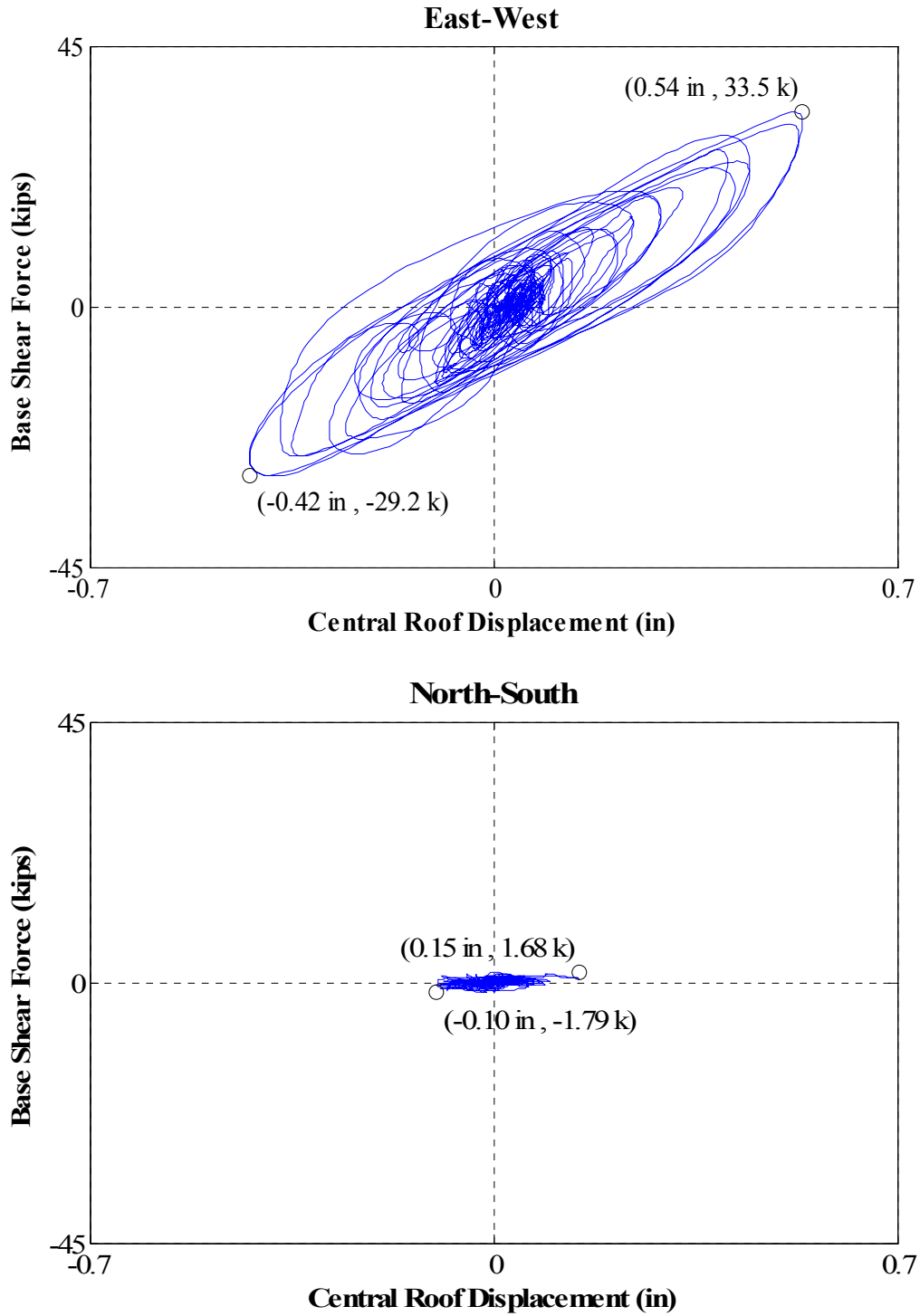


Figure N.29: Force-displacement hysteresis loops for Test NWP2S26

Appendix N

Phase 2, NWP2S27 Seismic Test

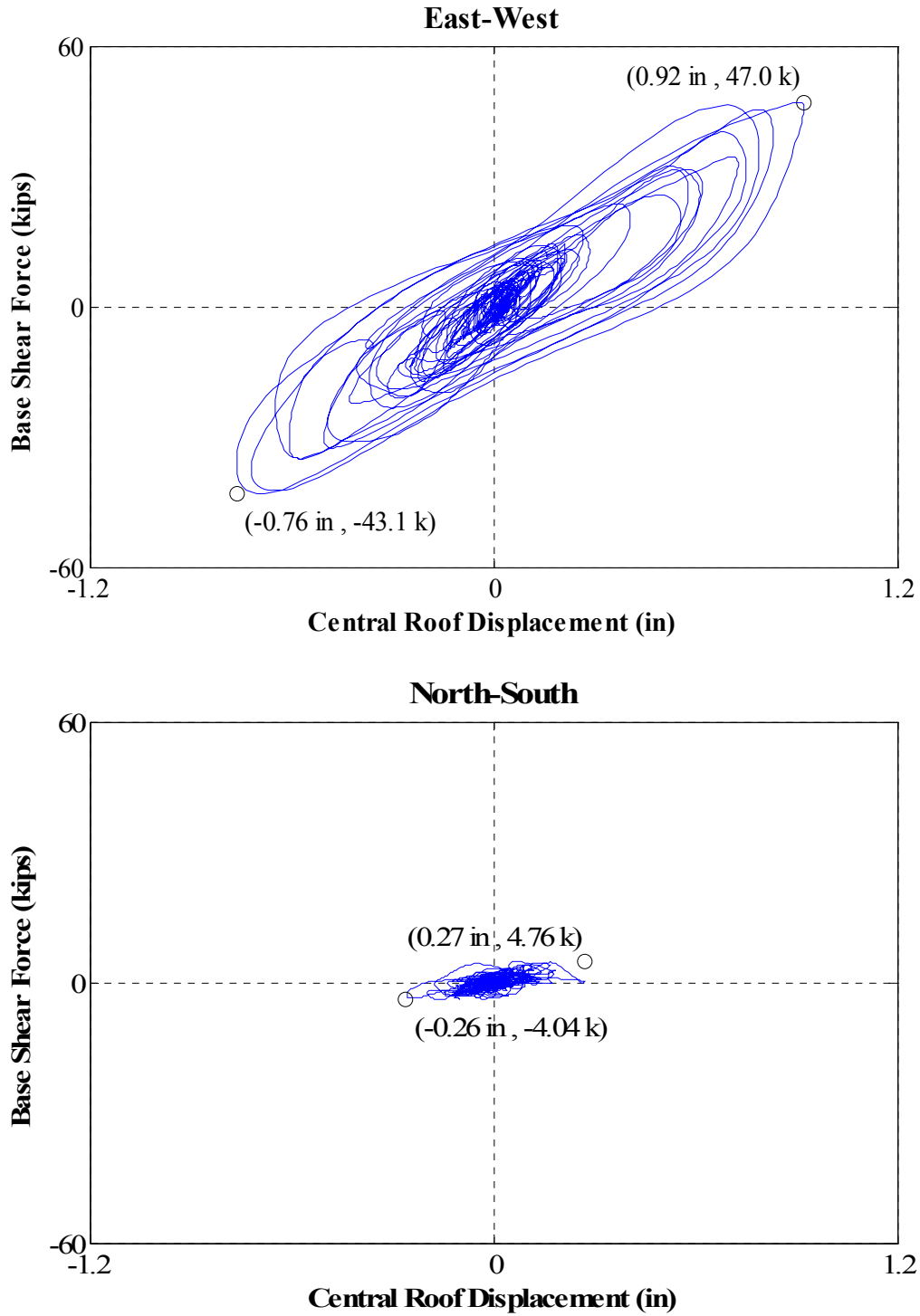


Figure N.30: Force-displacement hysteresis loops for Test NWP2S27

Appendix N

Phase 2, NWP2S28 Seismic Test

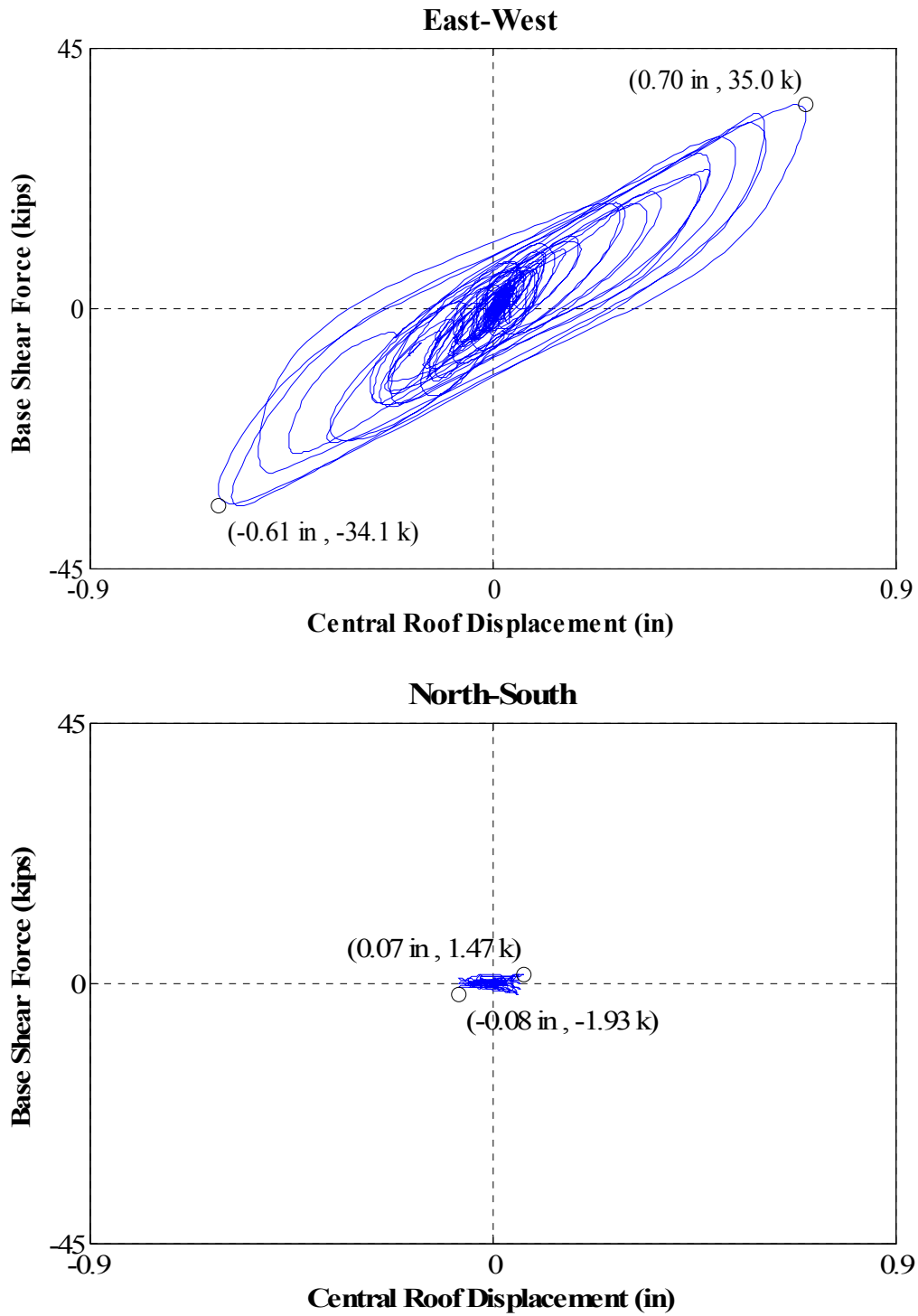


Figure N.31: Force-displacement hysteresis loops for Test NWP2S28

Appendix N

Phase 2, NWP2S29 Seismic Test

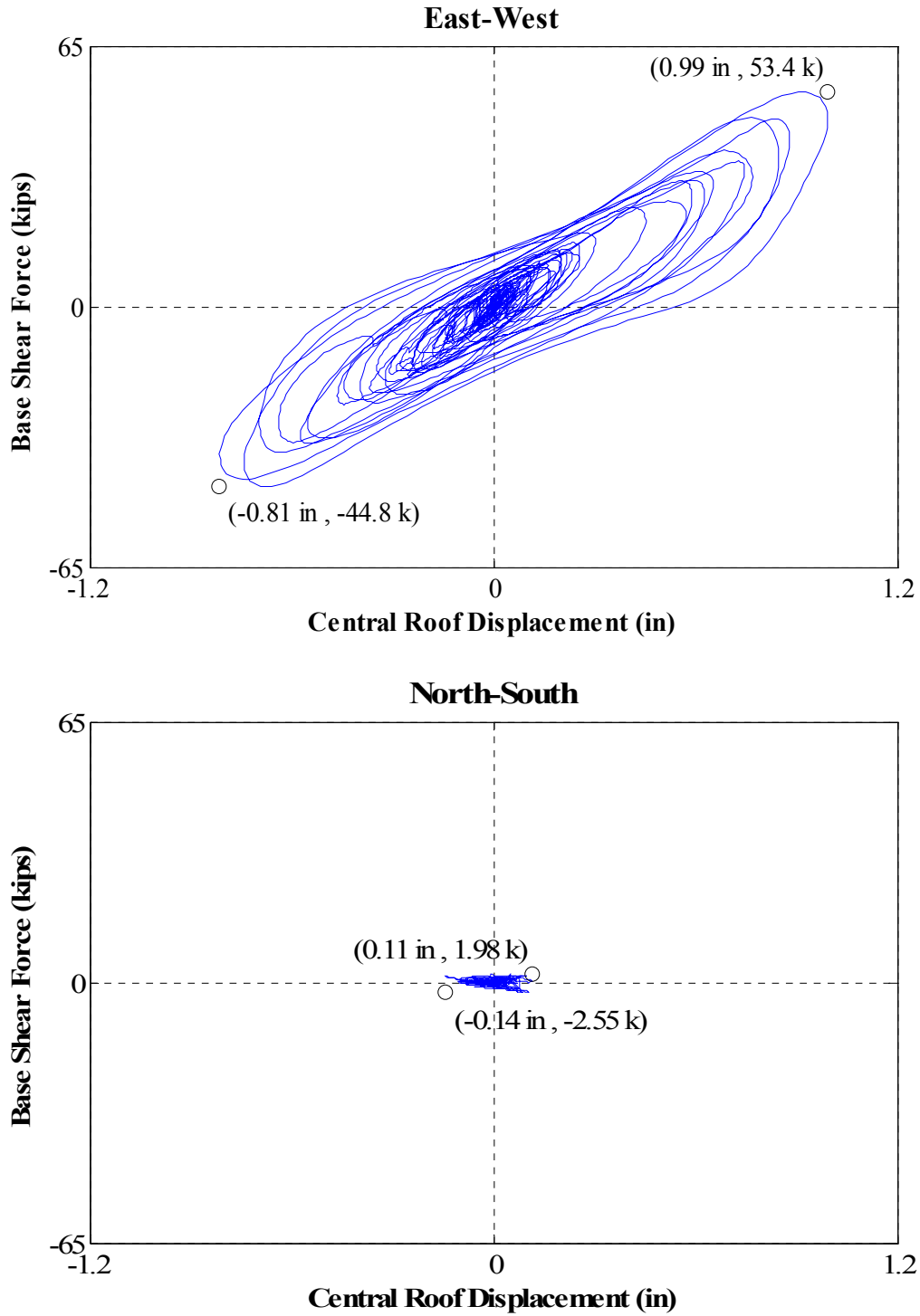


Figure N.32: Force-displacement hysteresis loops for Test NWP2S29

Appendix N

Phase 2, NWP2S30 Seismic Test

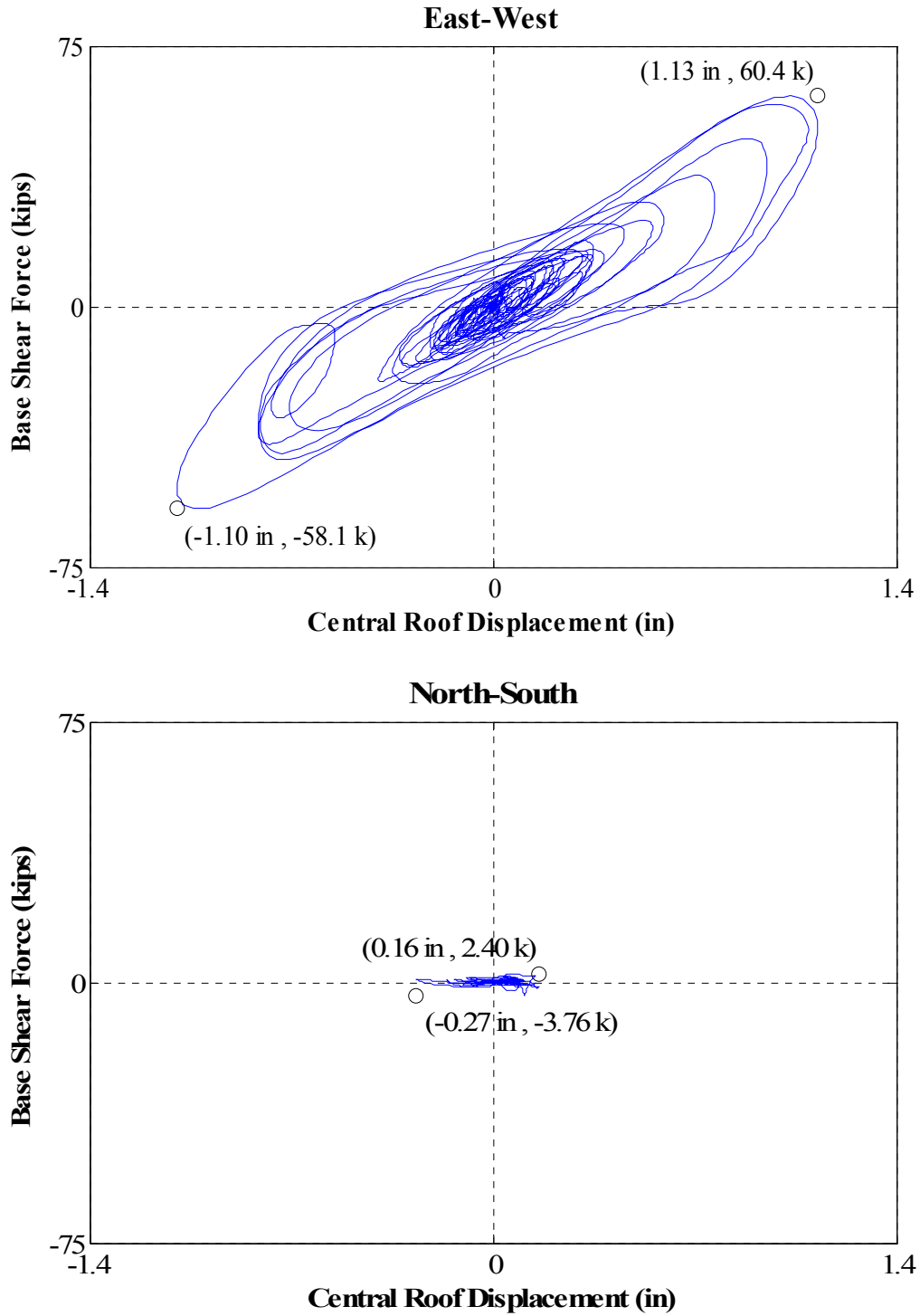


Figure N.33: Force-displacement hysteresis loops for Test NWP2S30

Appendix N

Phase 3, NWP3S01 Seismic Test

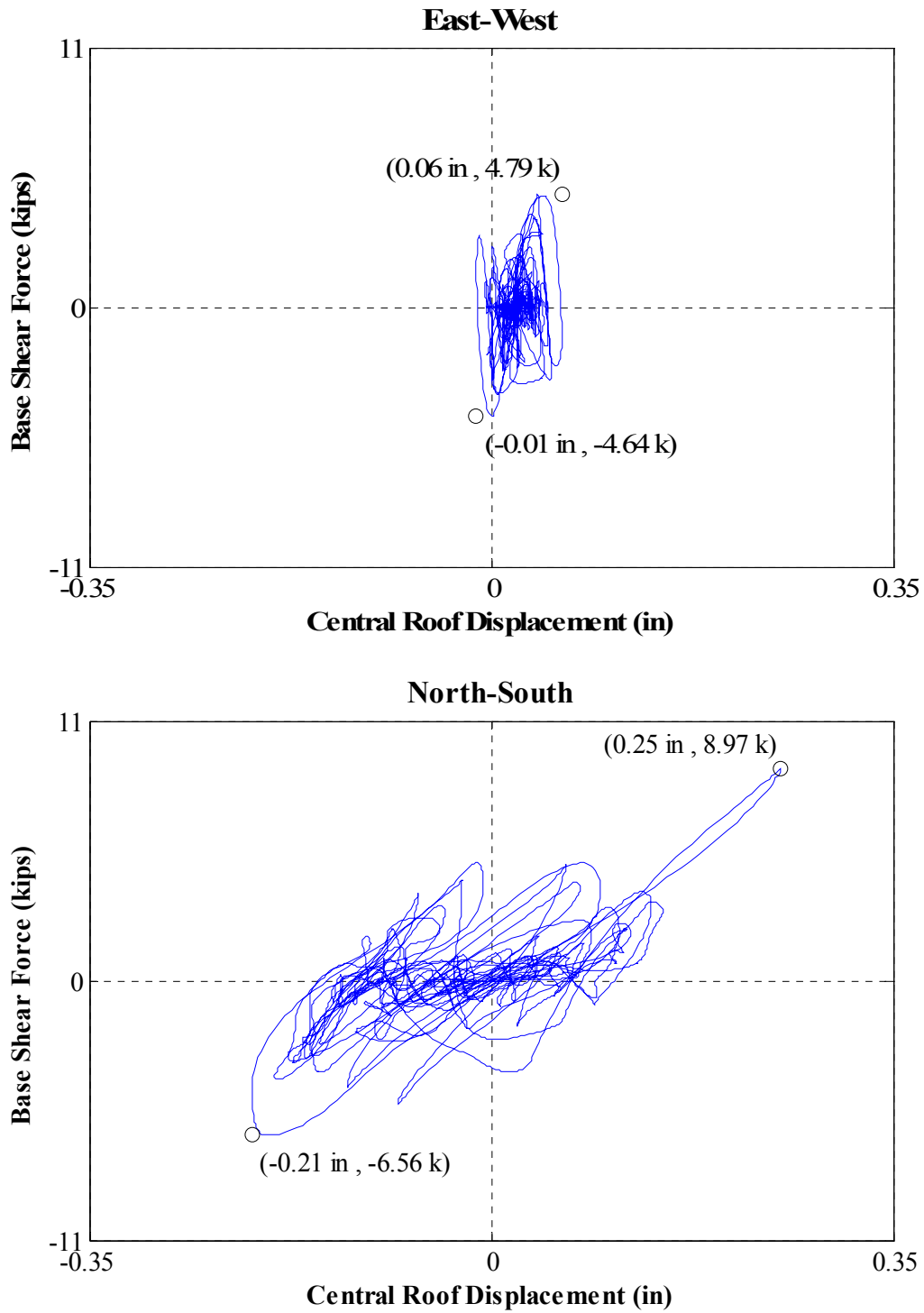


Figure N.34: Force-displacement hysteresis loops for Test NWP3S01

Appendix N

Phase 3, NWP3S02 Seismic Test

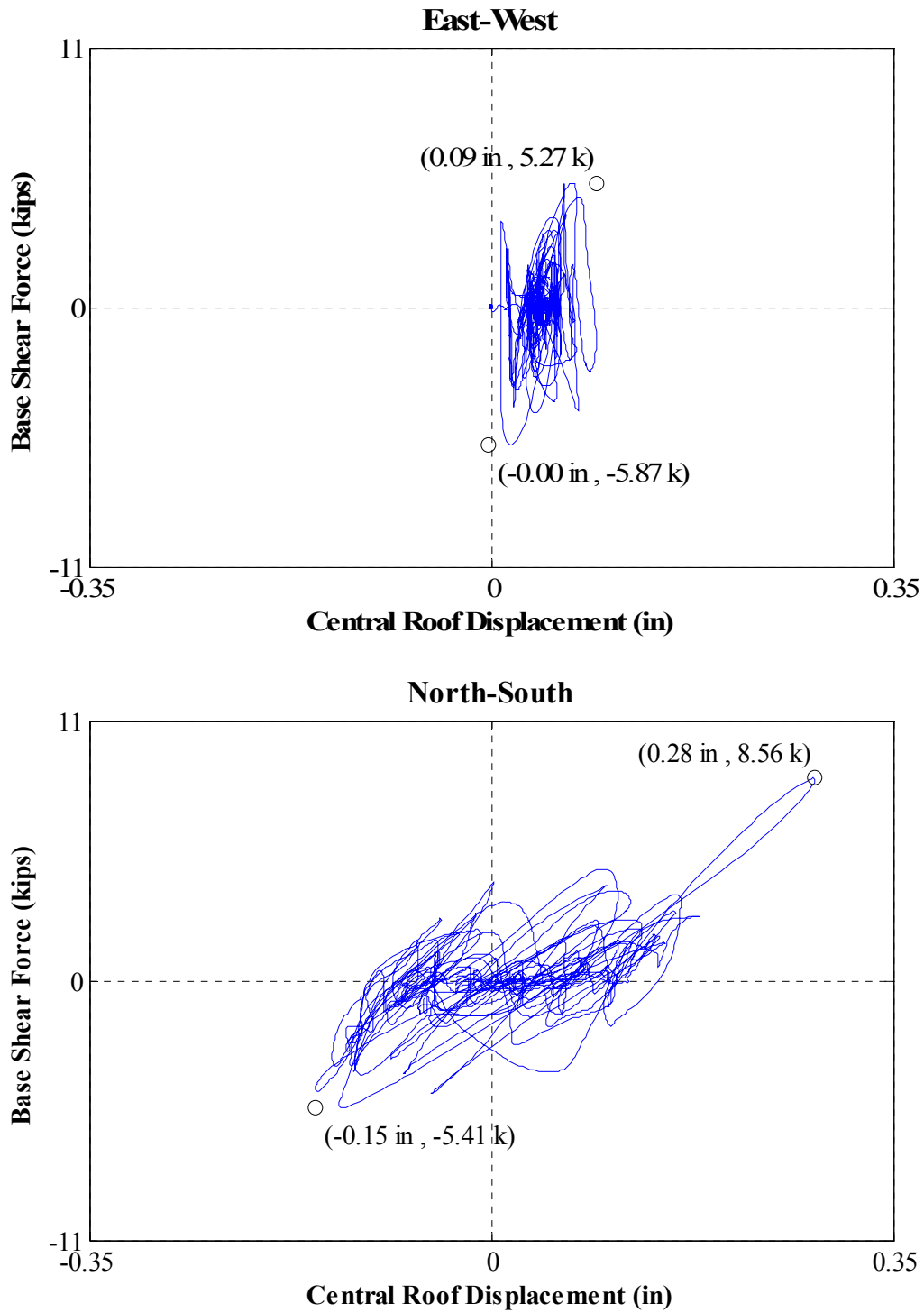


Figure N.35: Force-displacement hysteresis loops for Test NWP3S02

Appendix N

Phase 3, NWP3S03 Seismic Test

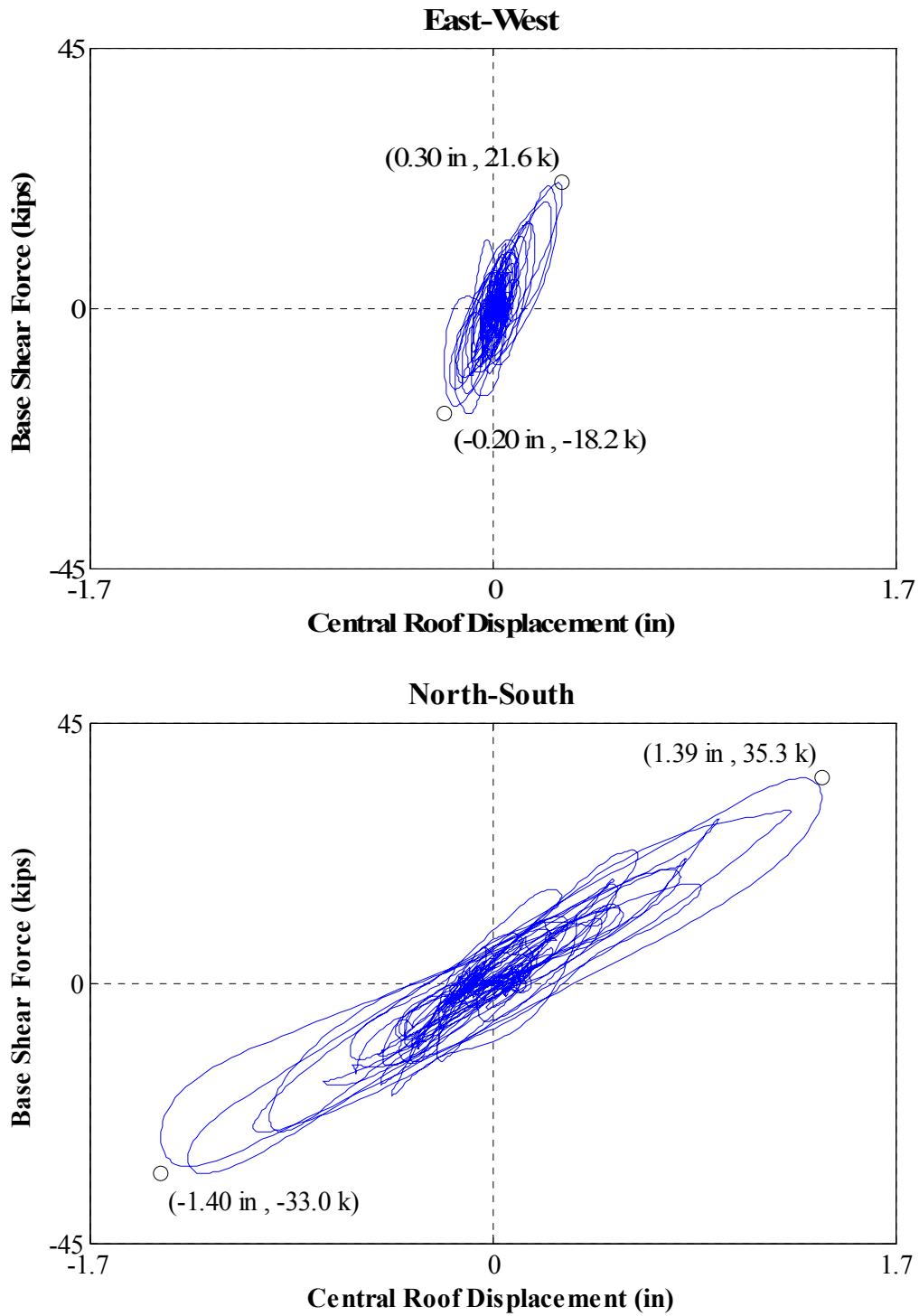


Figure N.36: Force-displacement hysteresis loops for Test NWP3S03

Appendix N

Phase 3, NWP3S04 Seismic Test

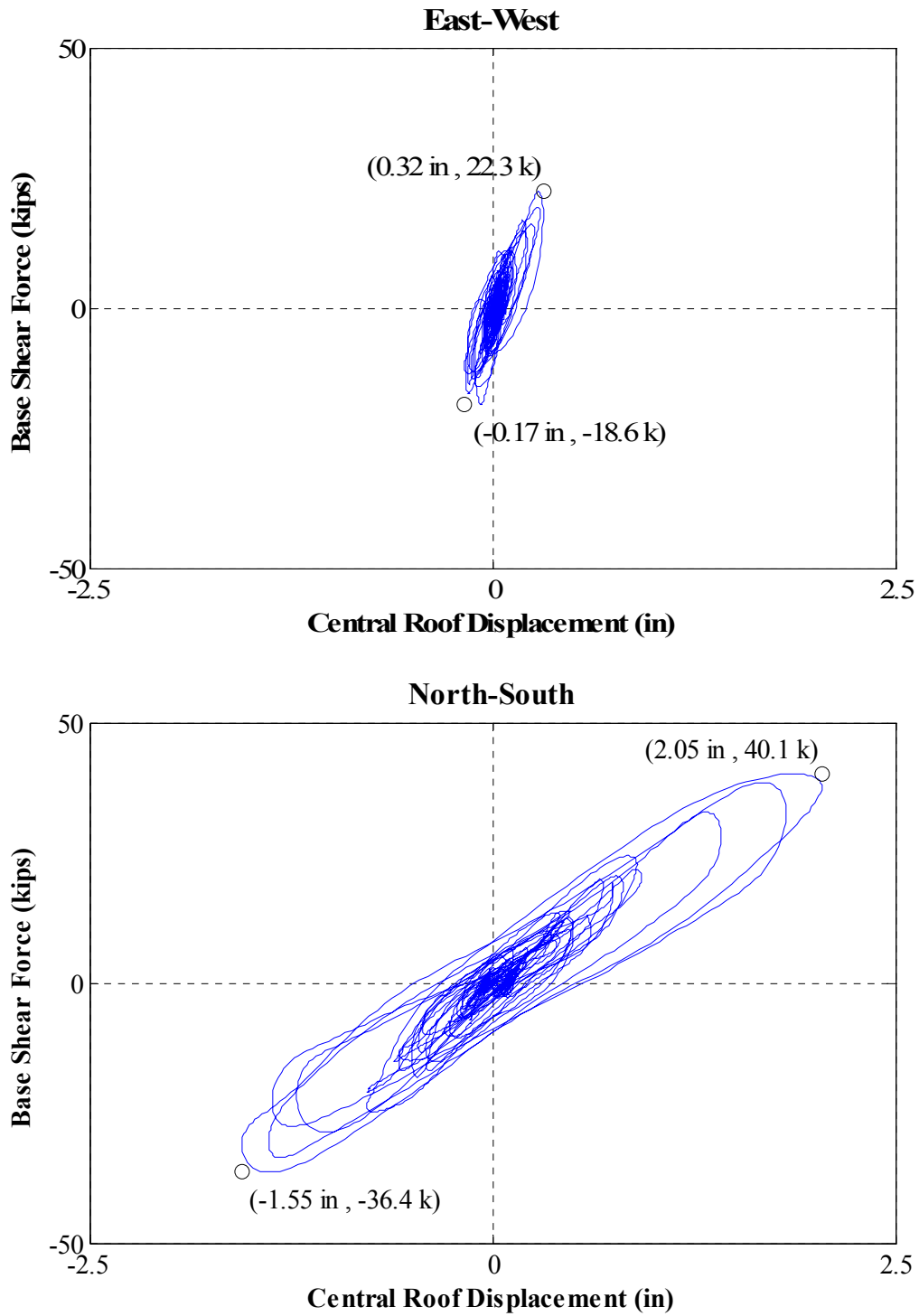


Figure N.37: Force-displacement hysteresis loops for Test NWP3S04

Appendix N

Phase 4, NWP4S01 Seismic Test

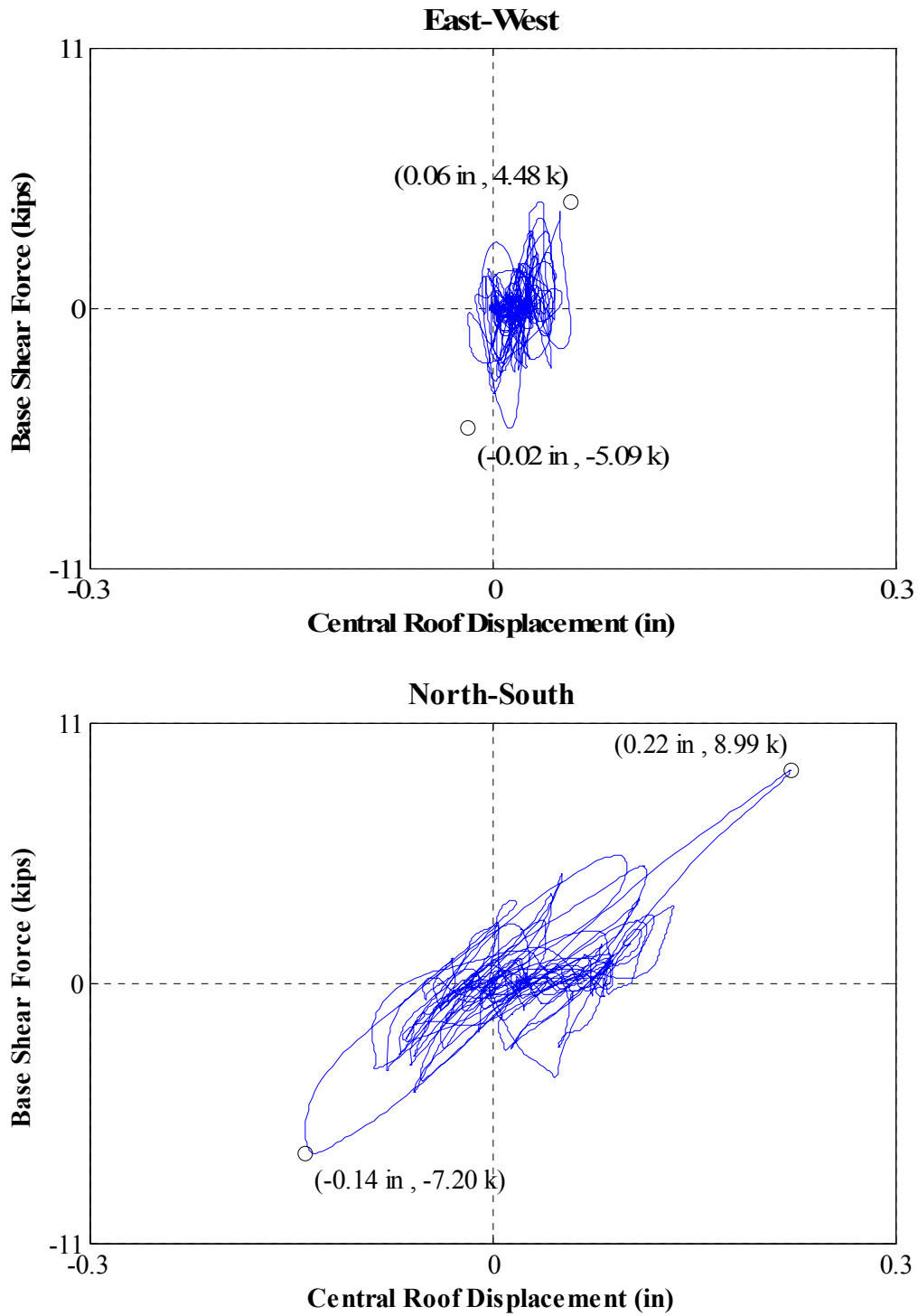


Figure N.38: Force-displacement hysteresis loops for Test NWP4S01

Appendix N

Phase 4, NWP4S02 Seismic Test

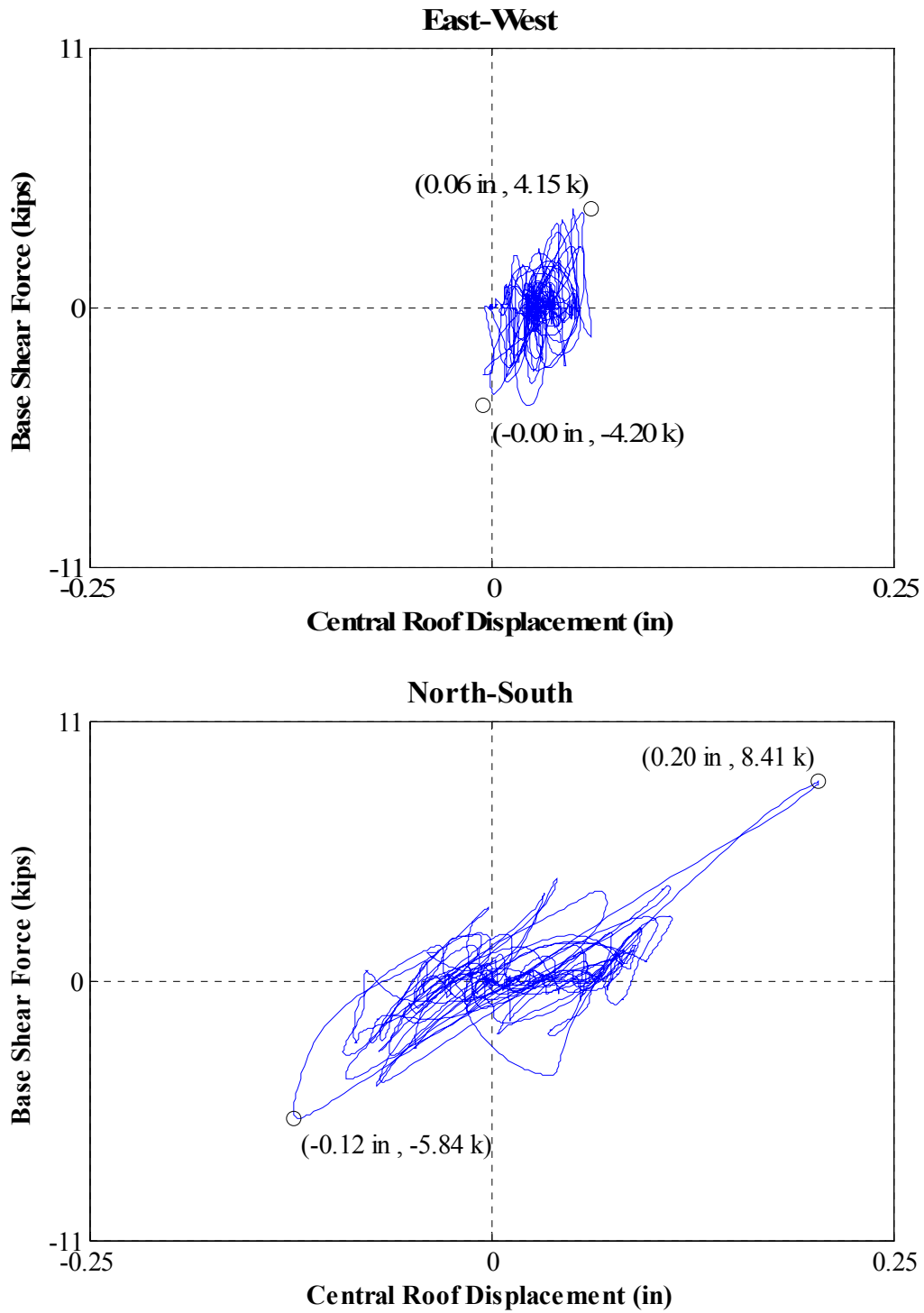


Figure N.39: Force-displacement hysteresis loops for Test NWP4S02

Appendix N

Phase 4, NWP4S03 Seismic Test

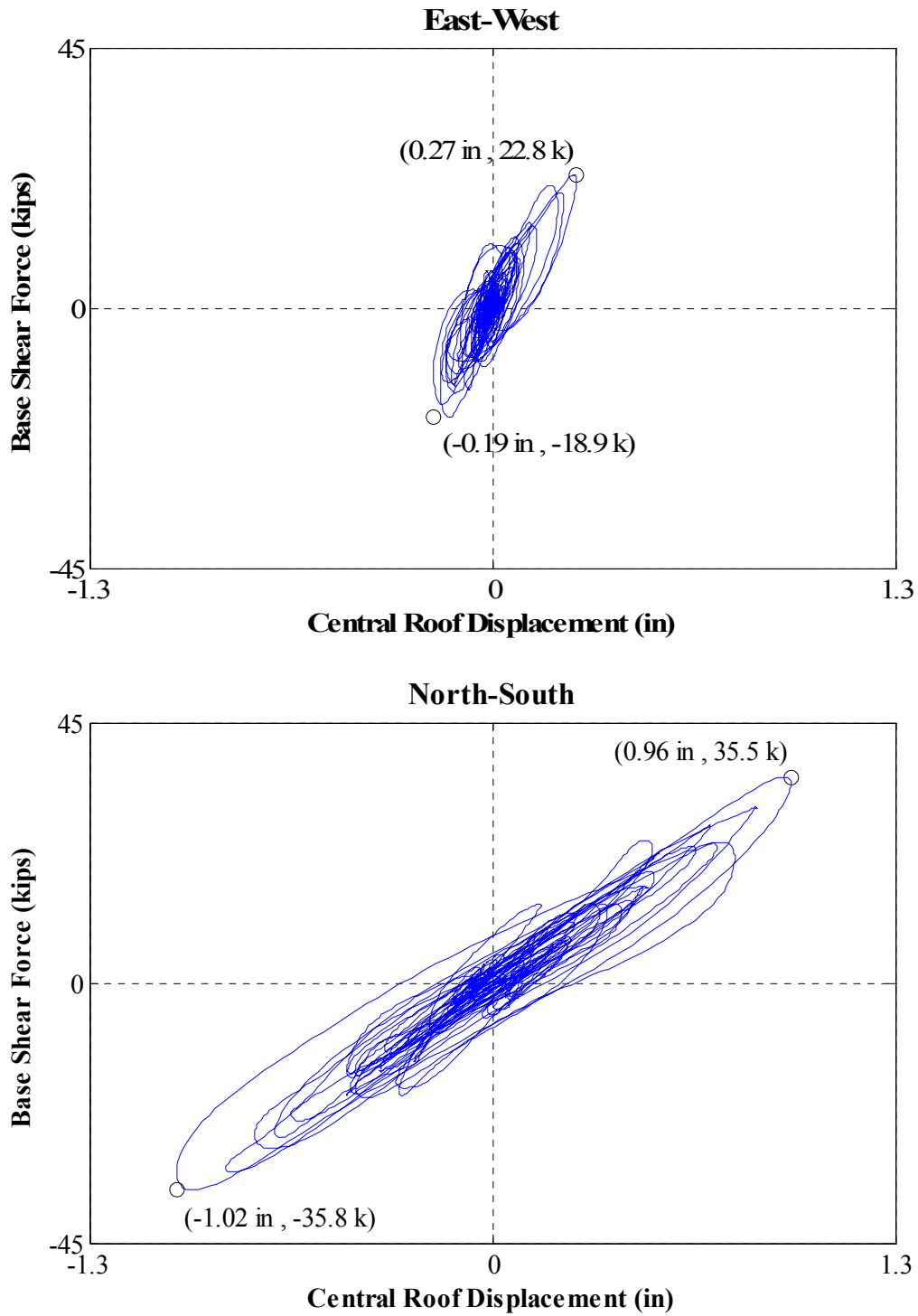


Figure N.40: Force-displacement hysteresis loops for Test NWP4S03

Appendix N

Phase 4, NWP4S04 Seismic Test

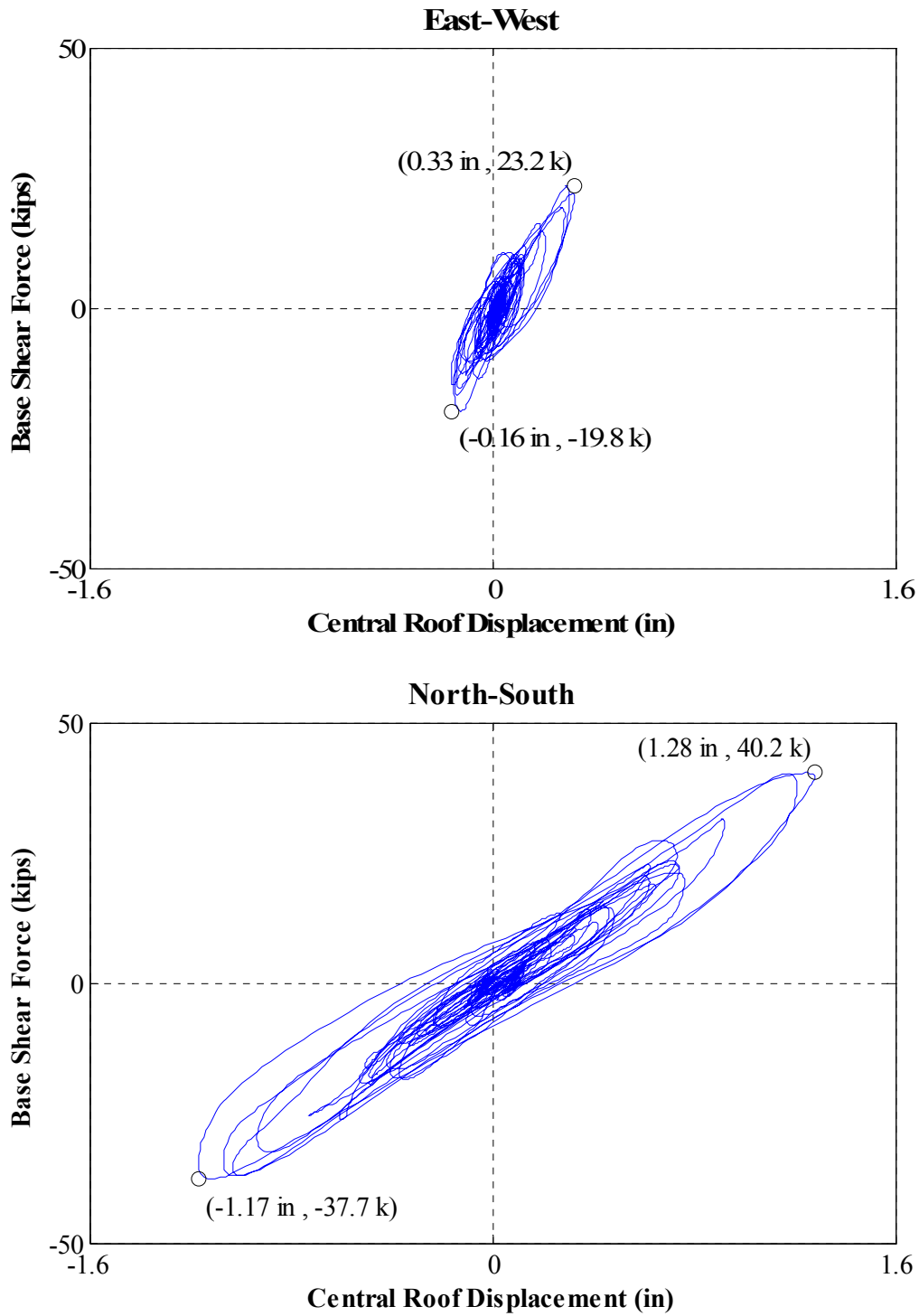


Figure N.41: Force-displacement hysteresis loops for Test NWP4S04

Appendix N

Phase 5, NWP5S01 Seismic Test

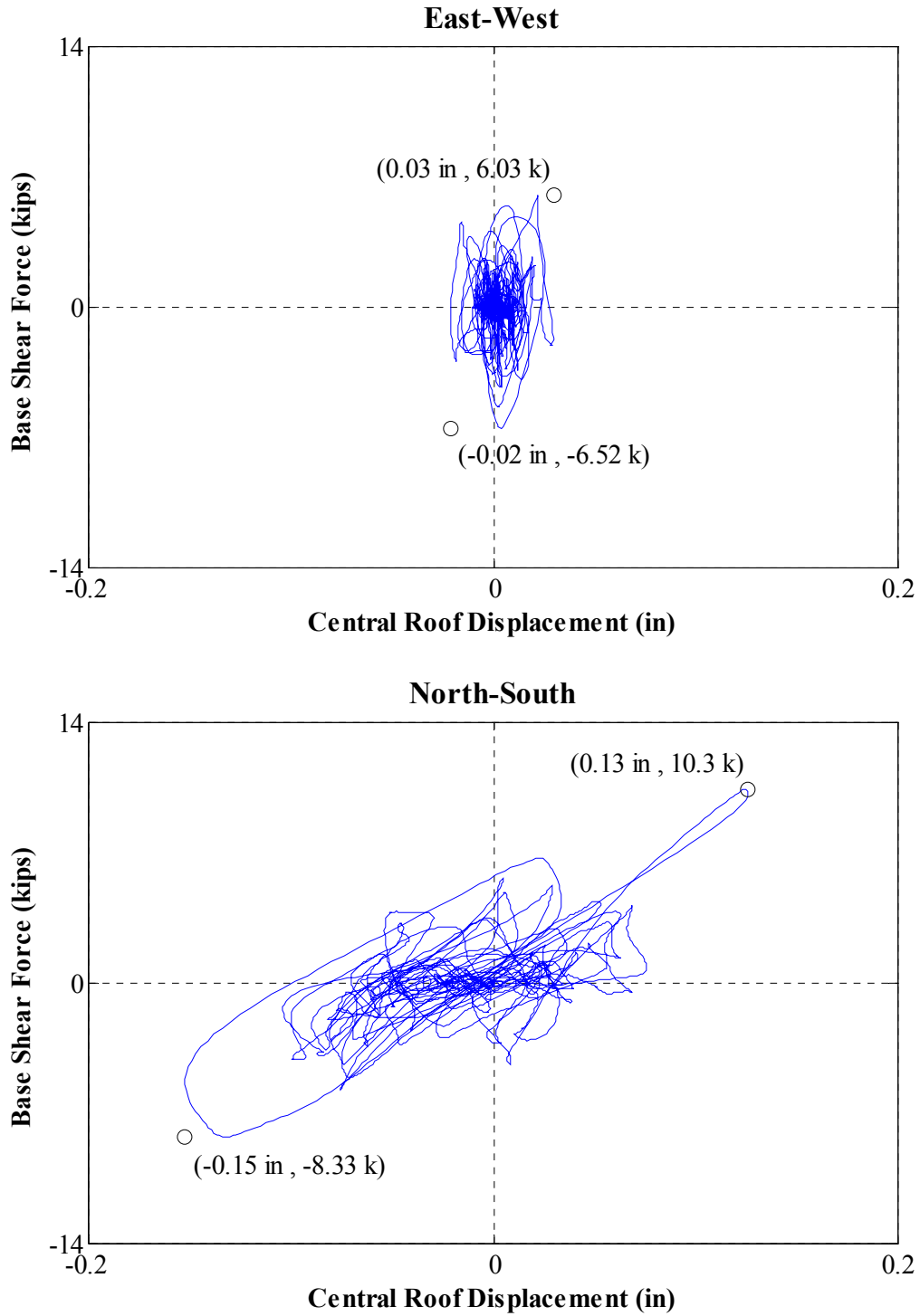


Figure N.42: Force-displacement hysteresis loops for Test NWP5S01

Appendix N

Phase 5, NWP5S02 Seismic Test

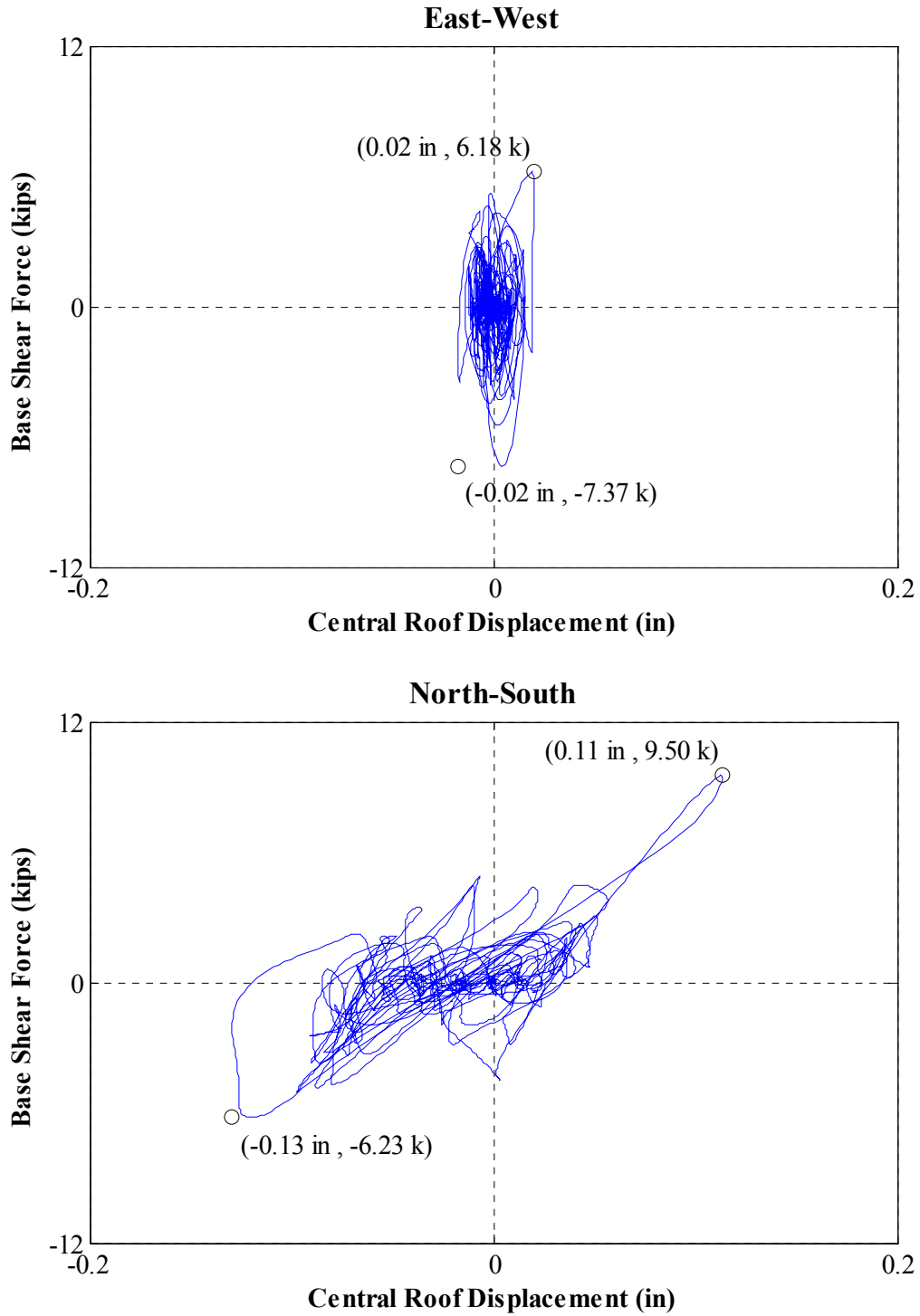


Figure N.43: Force-displacement hysteresis loops for Test NWP5S02

Appendix N

Phase 5, NWP5S03 Seismic Test

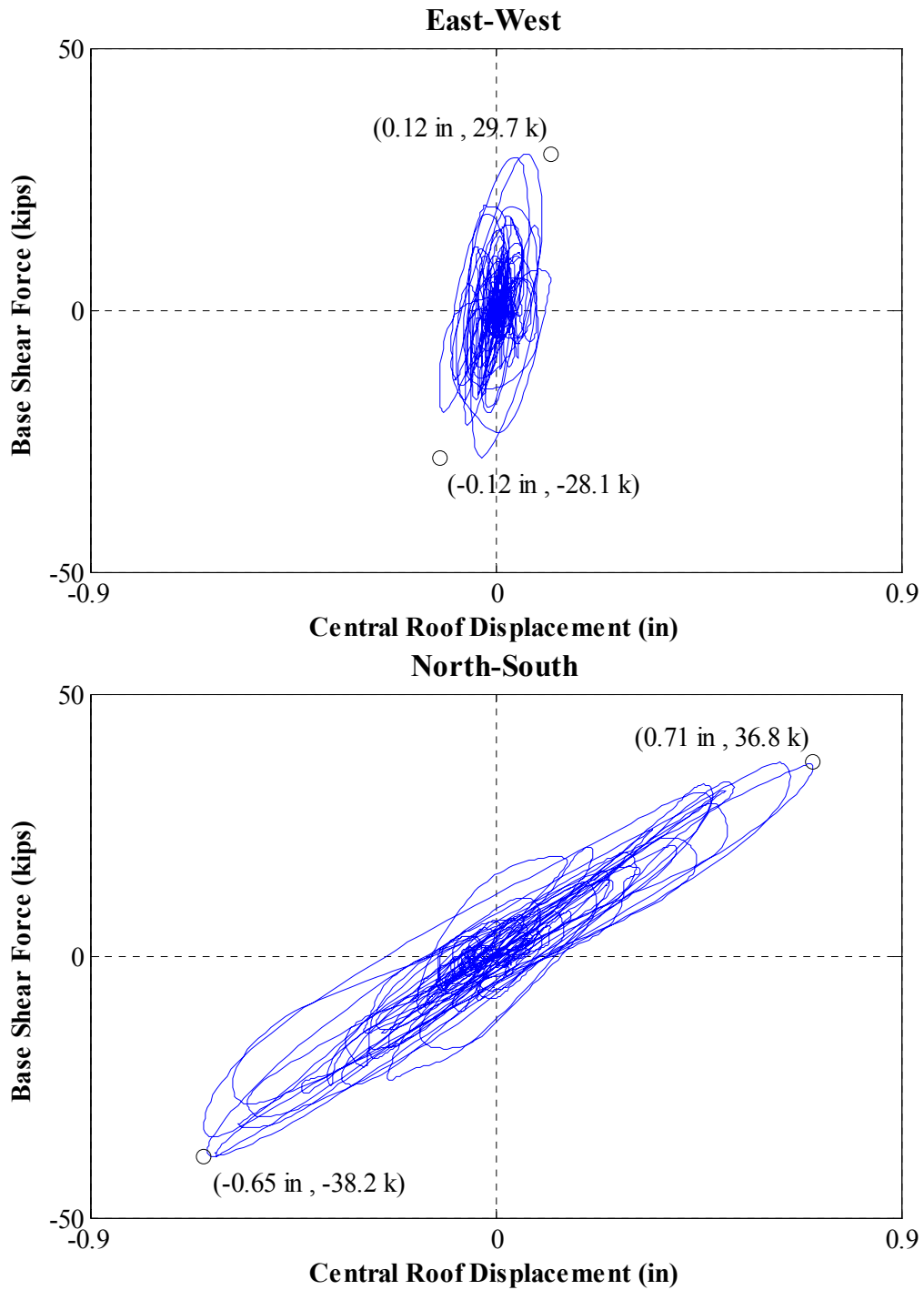


Figure N.44: Force-displacement hysteresis loops for Test NWP5S03

Appendix N

Phase 5, NWP5S04 Seismic Test

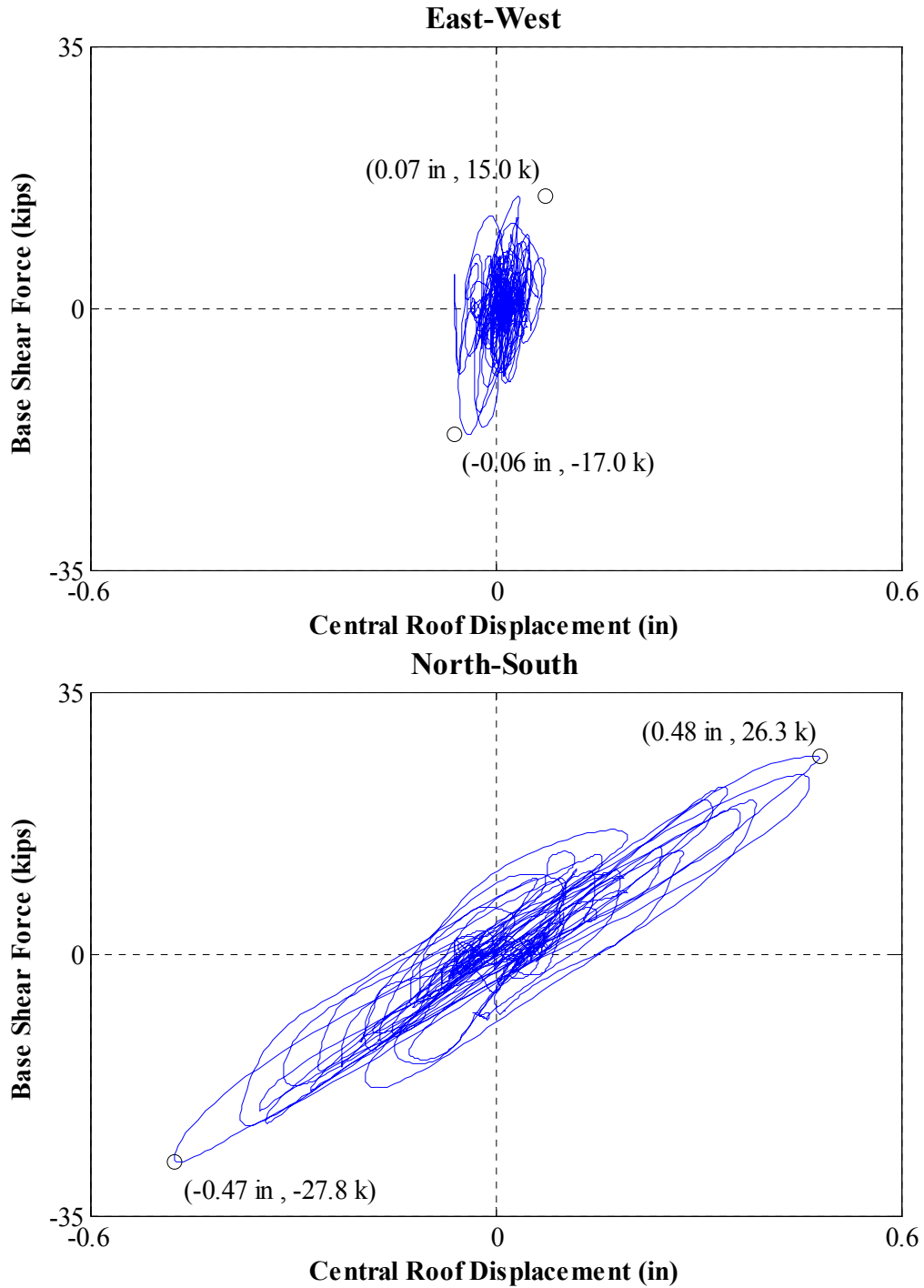


Figure N.45: Force-displacement hysteresis loops for Test NWP5S04

Appendix N

Phase 5, NWP5S05 Seismic Test

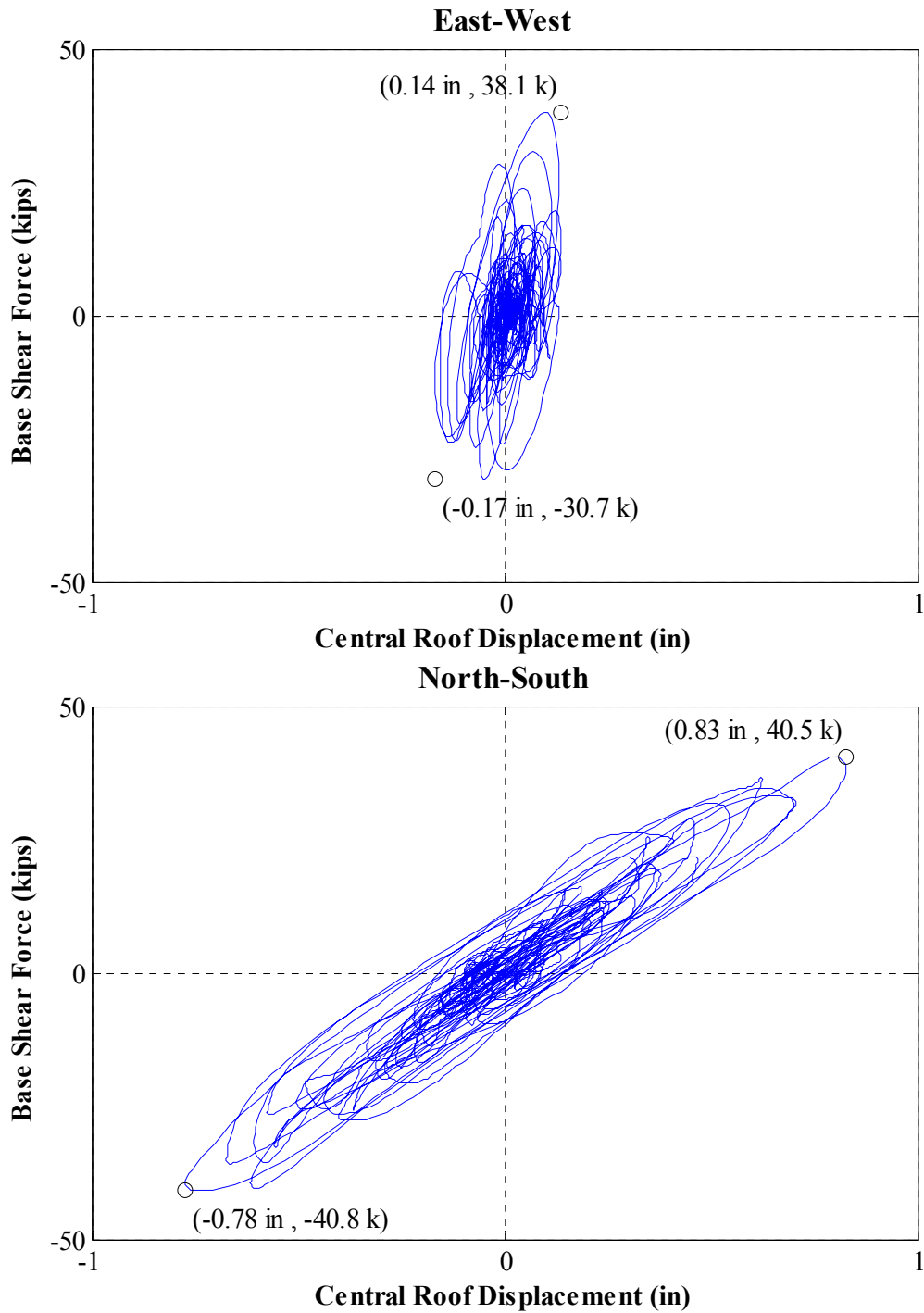


Figure N.46: Force-displacement hysteresis loops for Test NWP5S05

Appendix N

Phase 5, NWP5S06 Seismic Test

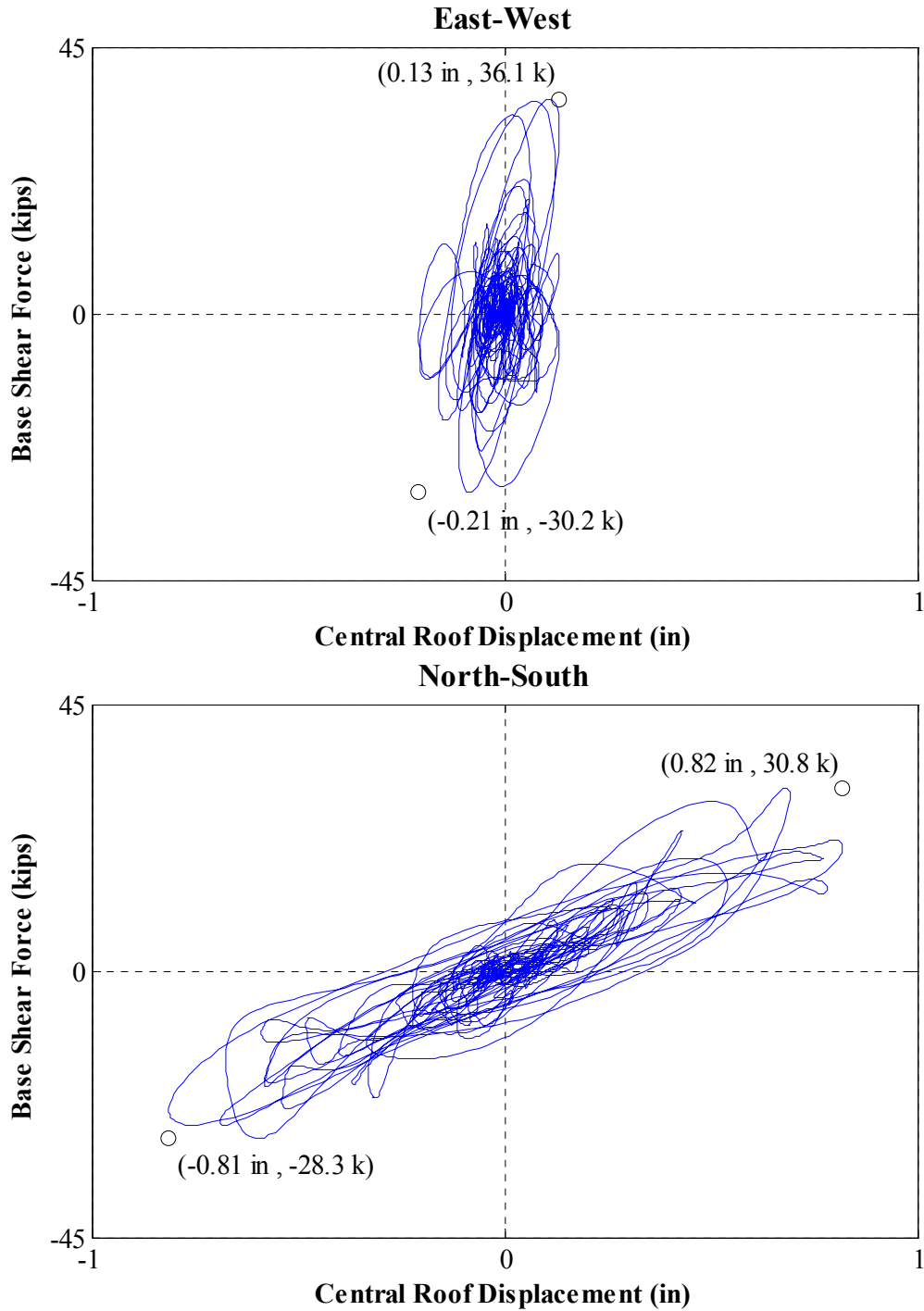


Figure N.47: Force-displacement hysteresis loops for Test NWP5S06

Appendix N

Phase 5, NWP5S07 Seismic Test

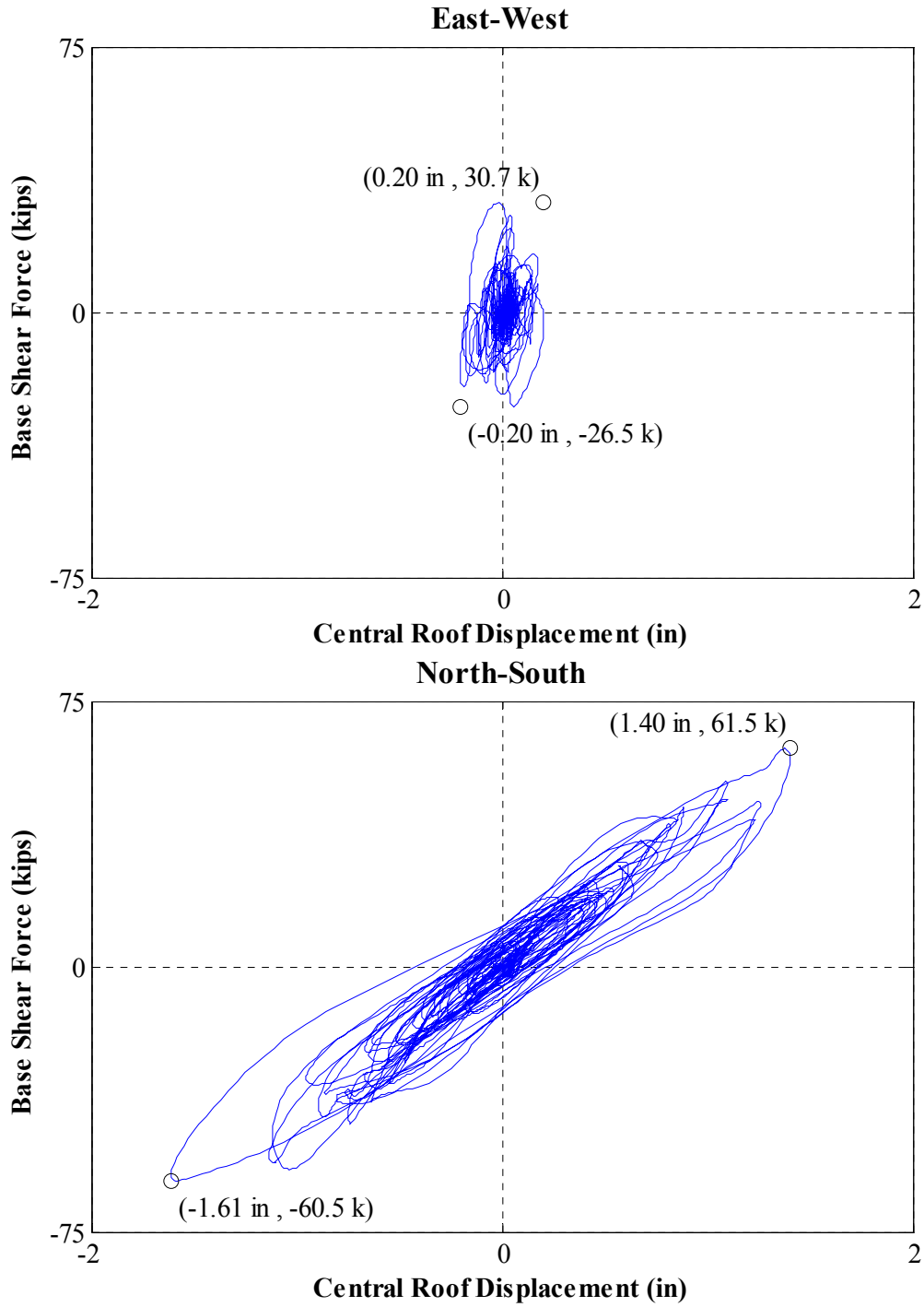


Figure N.48: Force-displacement hysteresis loops for Test NWP5S07

Appendix N

Phase 5, NWP5S08 Seismic Test

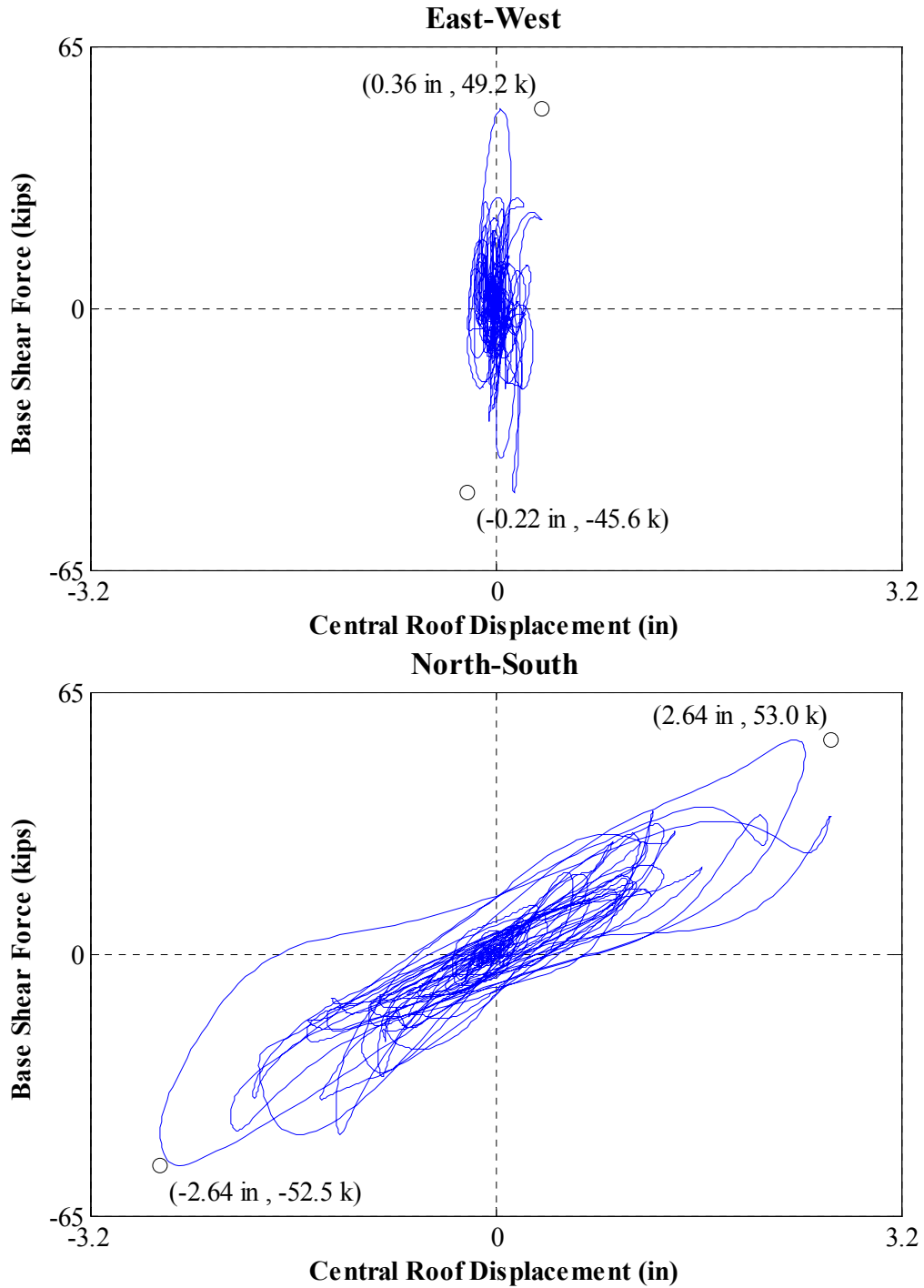


Figure N.49: Force-displacement hysteresis loops for Test NWP5S08

Appendix N

Phase 5, NWP5S09 Seismic Test

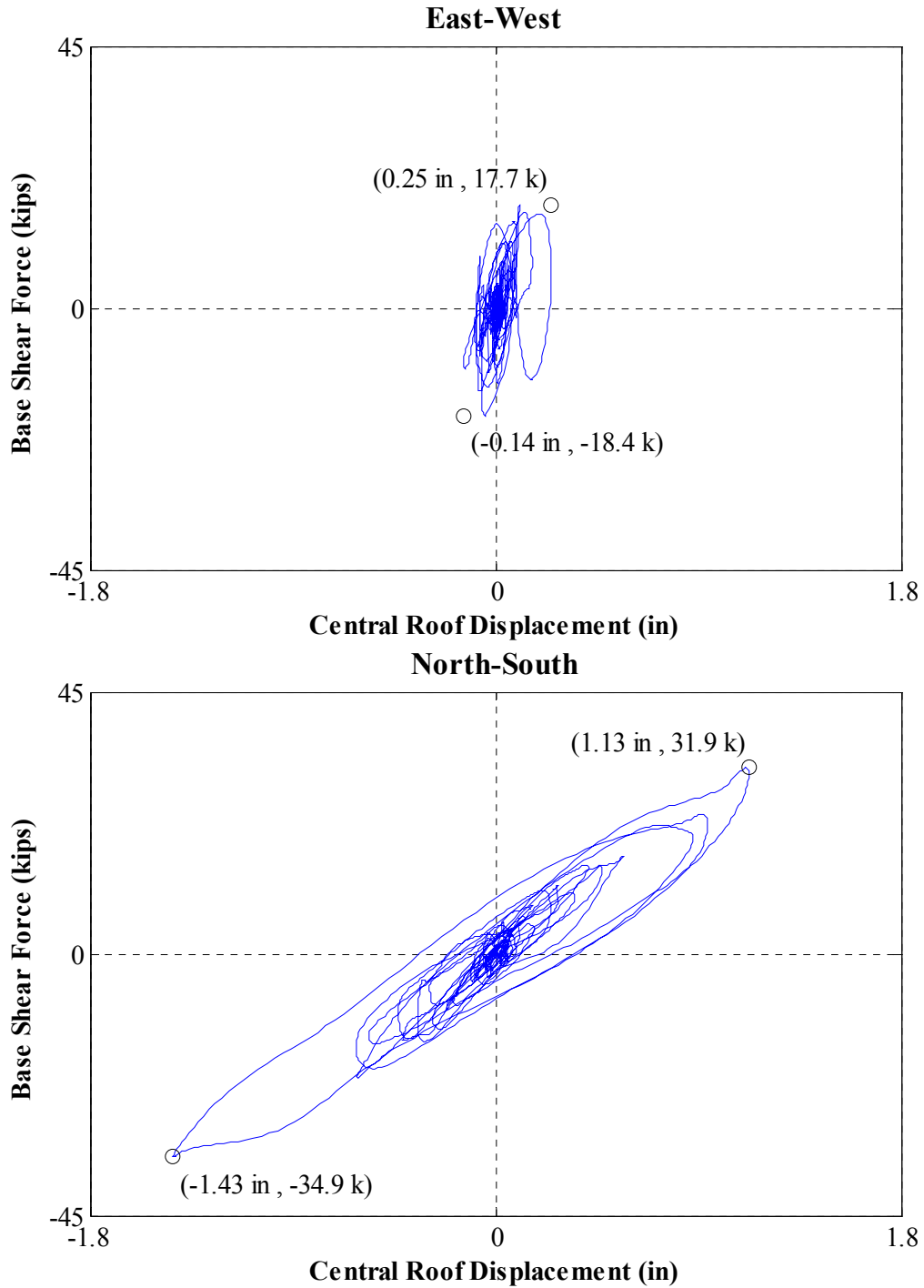


Figure N.50: Force-displacement hysteresis loops for Test NWP5S09

Appendix N

Phase 5, NWP5S11 Seismic Test

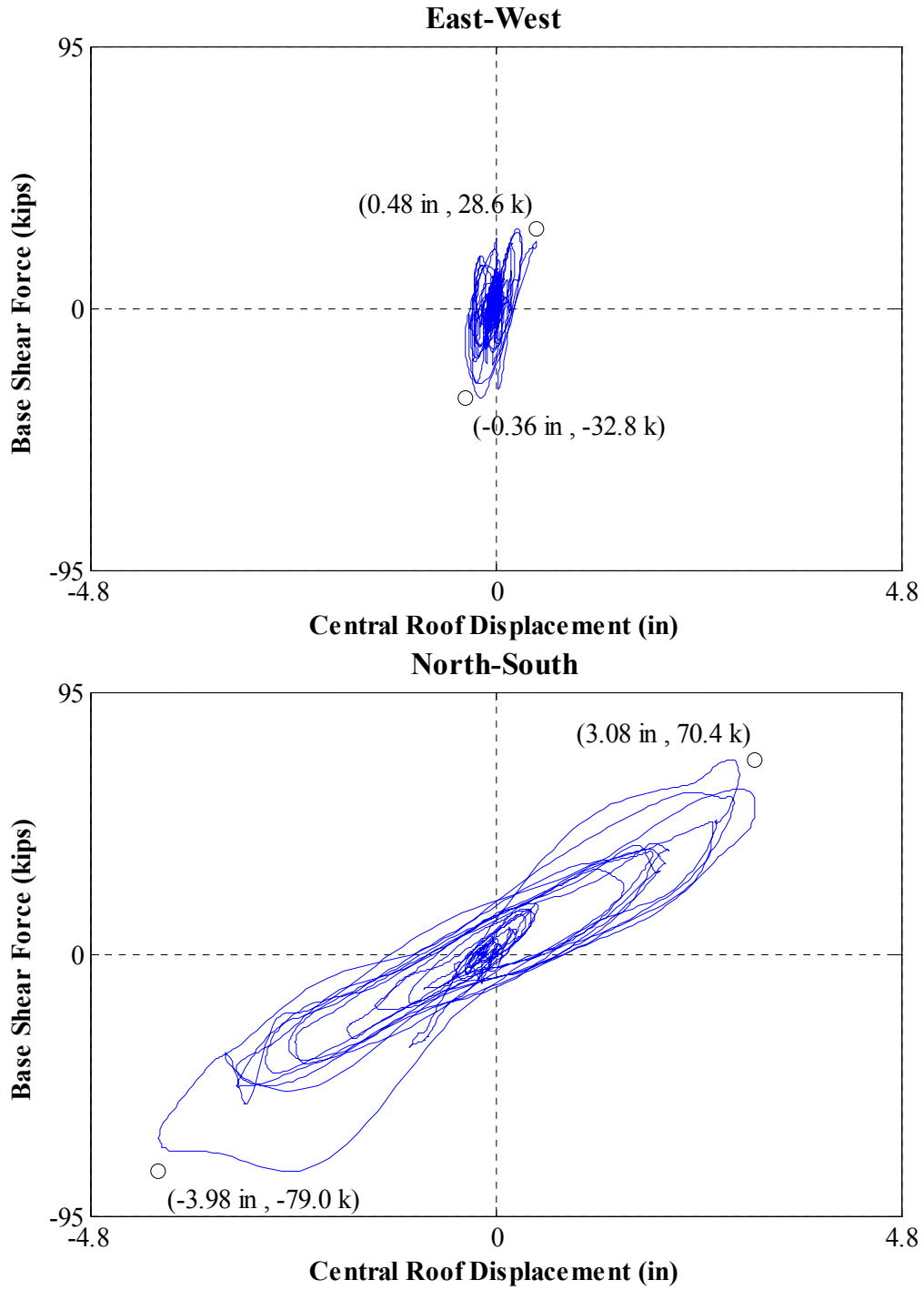


Figure N.51: Force-displacement hysteresis loops for Test NWP5S11

Appendix O
Selected Seismic Results:
Interstory Shear Force –
Displacement Hysteresis Loops

Appendix O

Phase 1, NWP1S01 Seismic Test

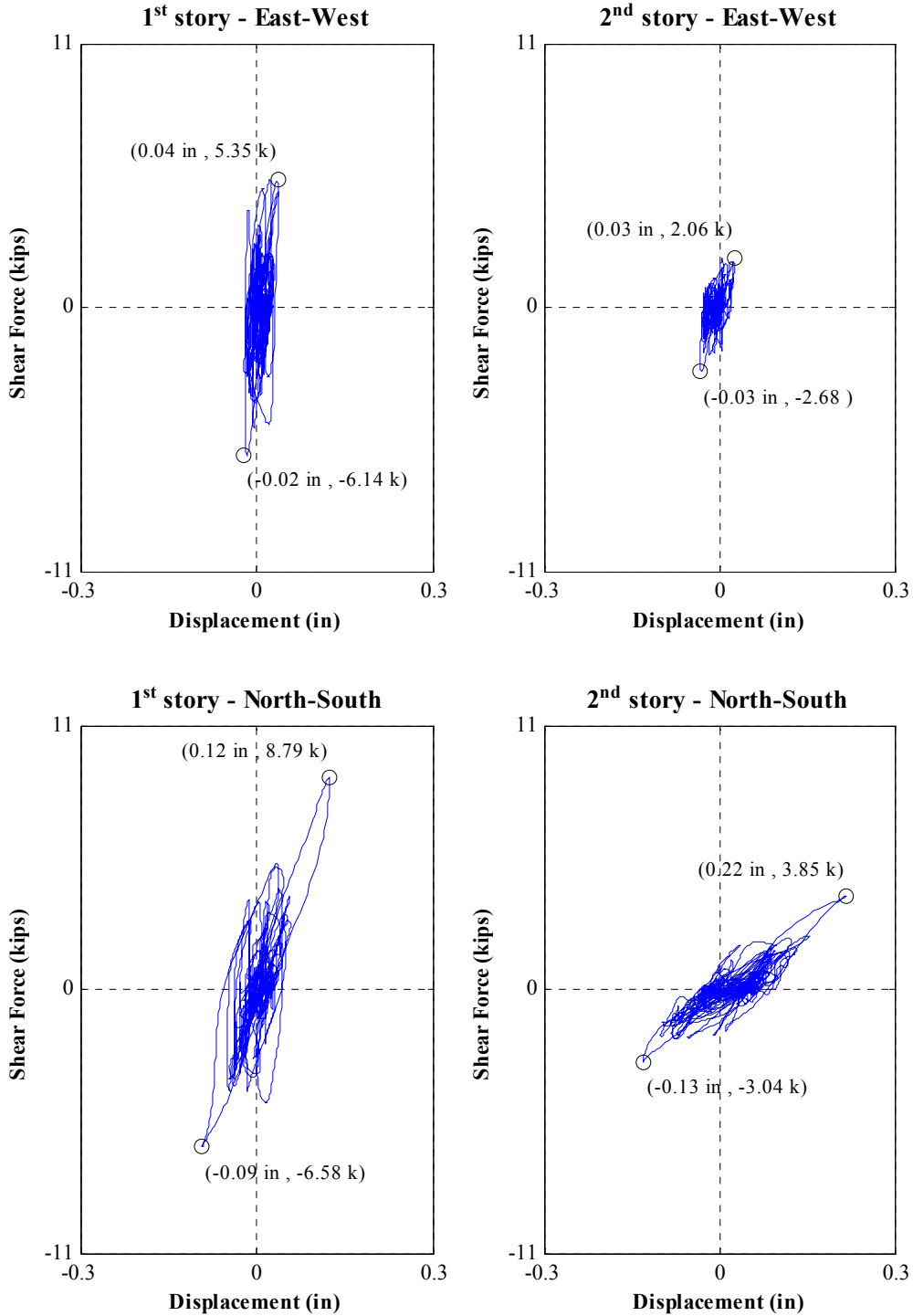


Figure O.1: Interstory force-displacement hysteresis loops for Test NWP1S01

Appendix O

Phase 1, NWP1S02 Seismic Test

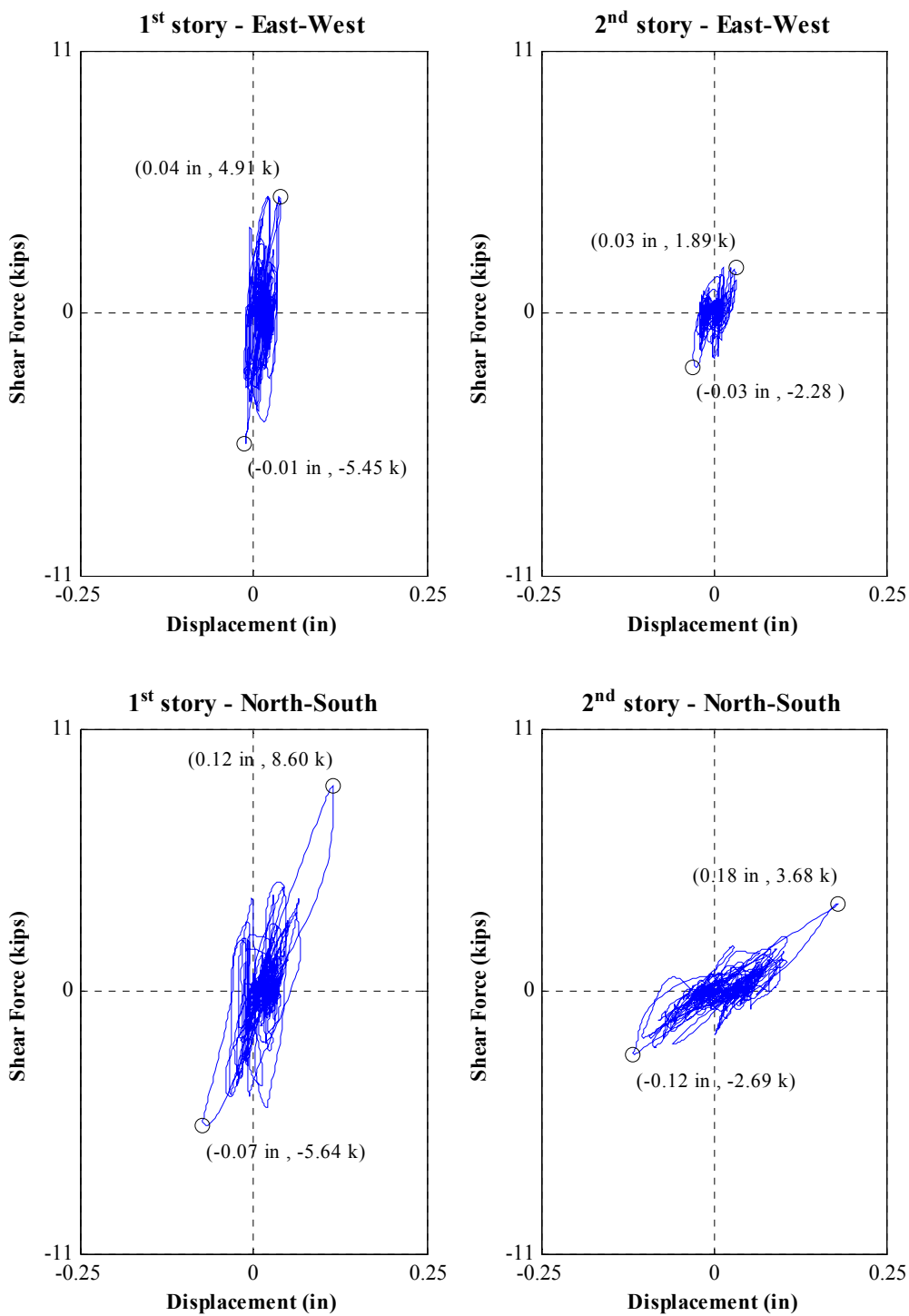


Figure O.2: Interstory force-displacement hysteresis loops for Test NWP1S02

Appendix O

Phase 1, NWP1S03 Seismic Test

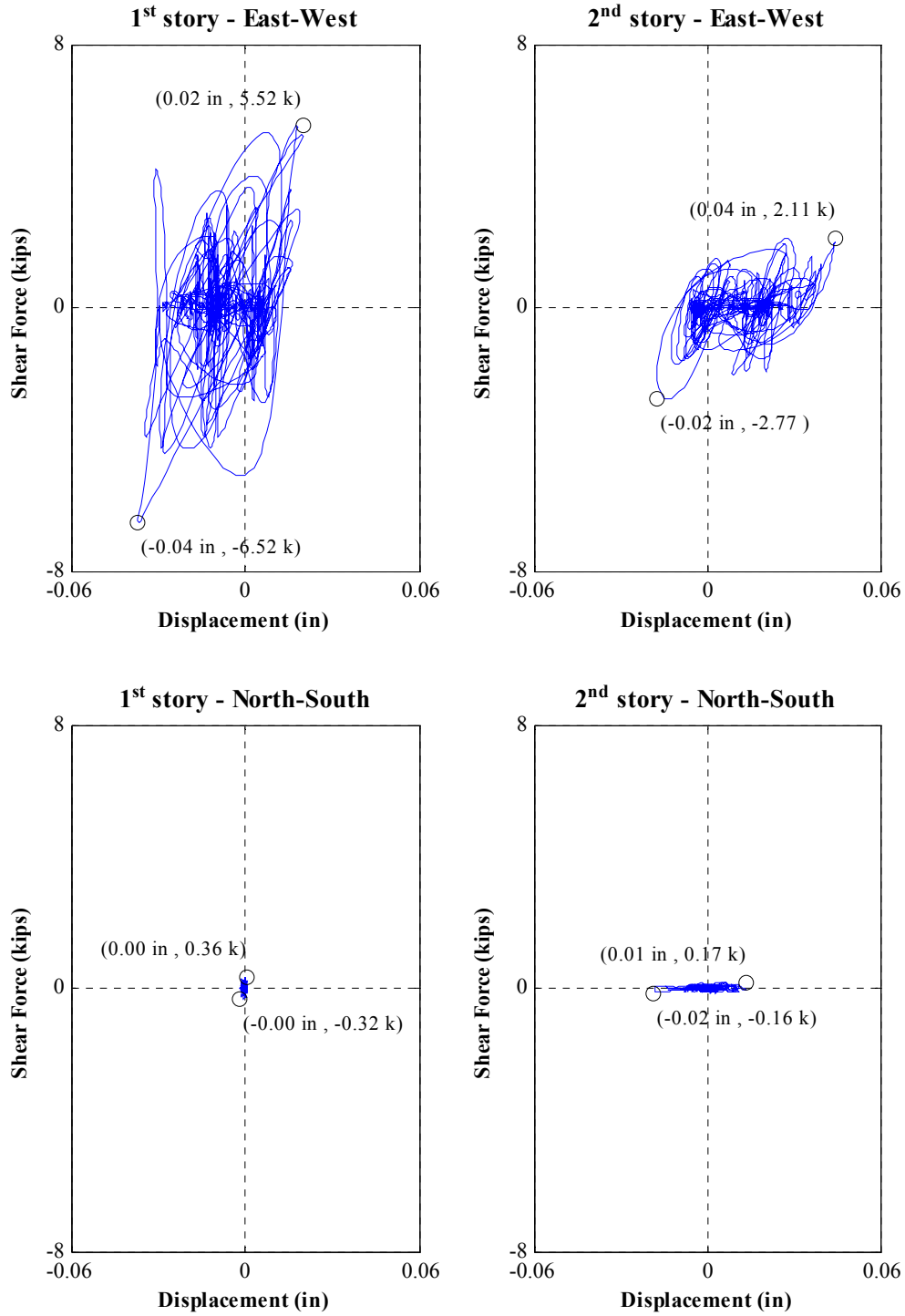


Figure O.3: Interstory force-displacement hysteresis loops for Test NWP1S03

Appendix O

Phase 1, NWP1S04 Seismic Test

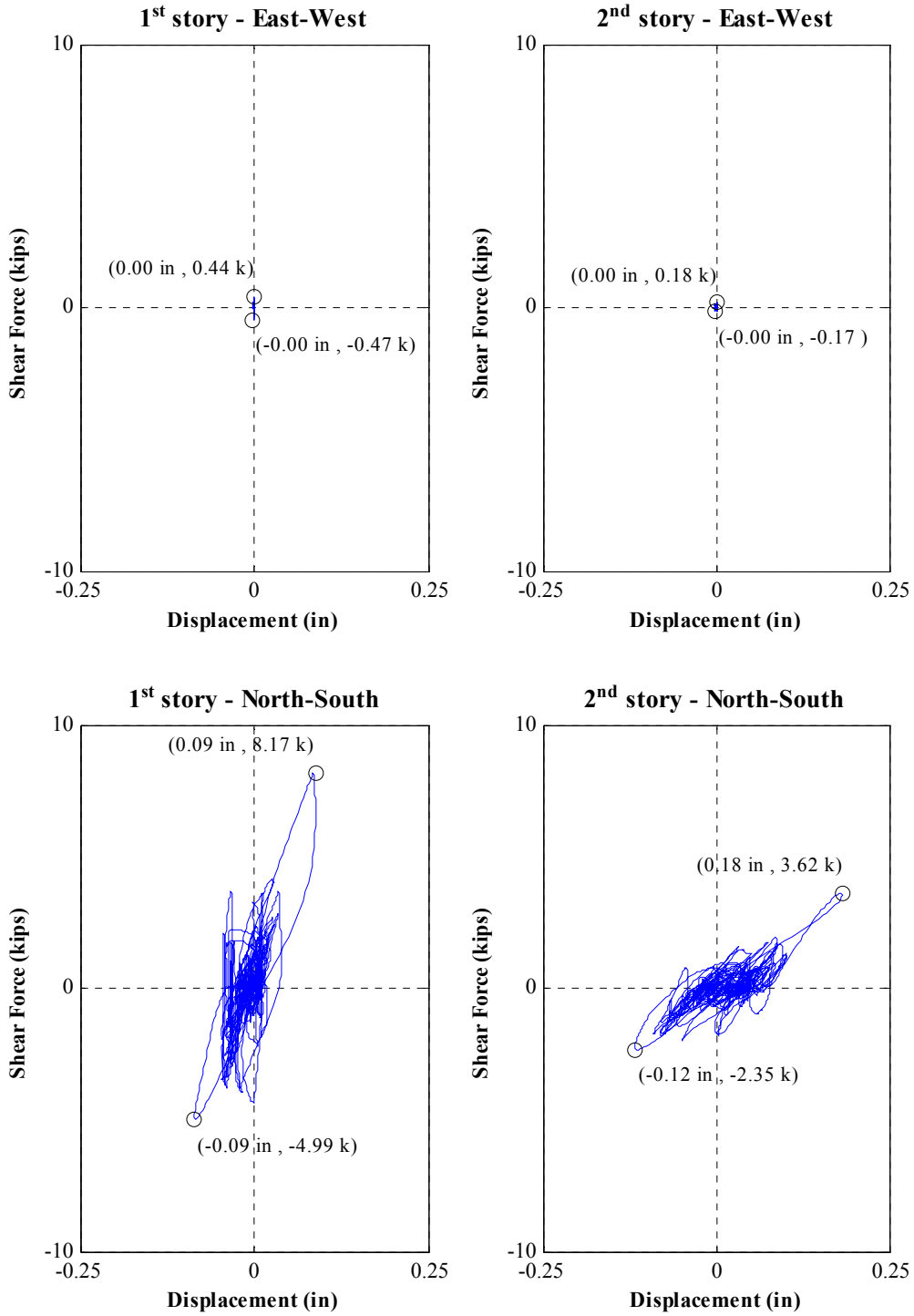


Figure O.4: Interstory force-displacement hysteresis loops for Test NWP1S04

Appendix O

Phase 1, NWP1S05 Seismic Test

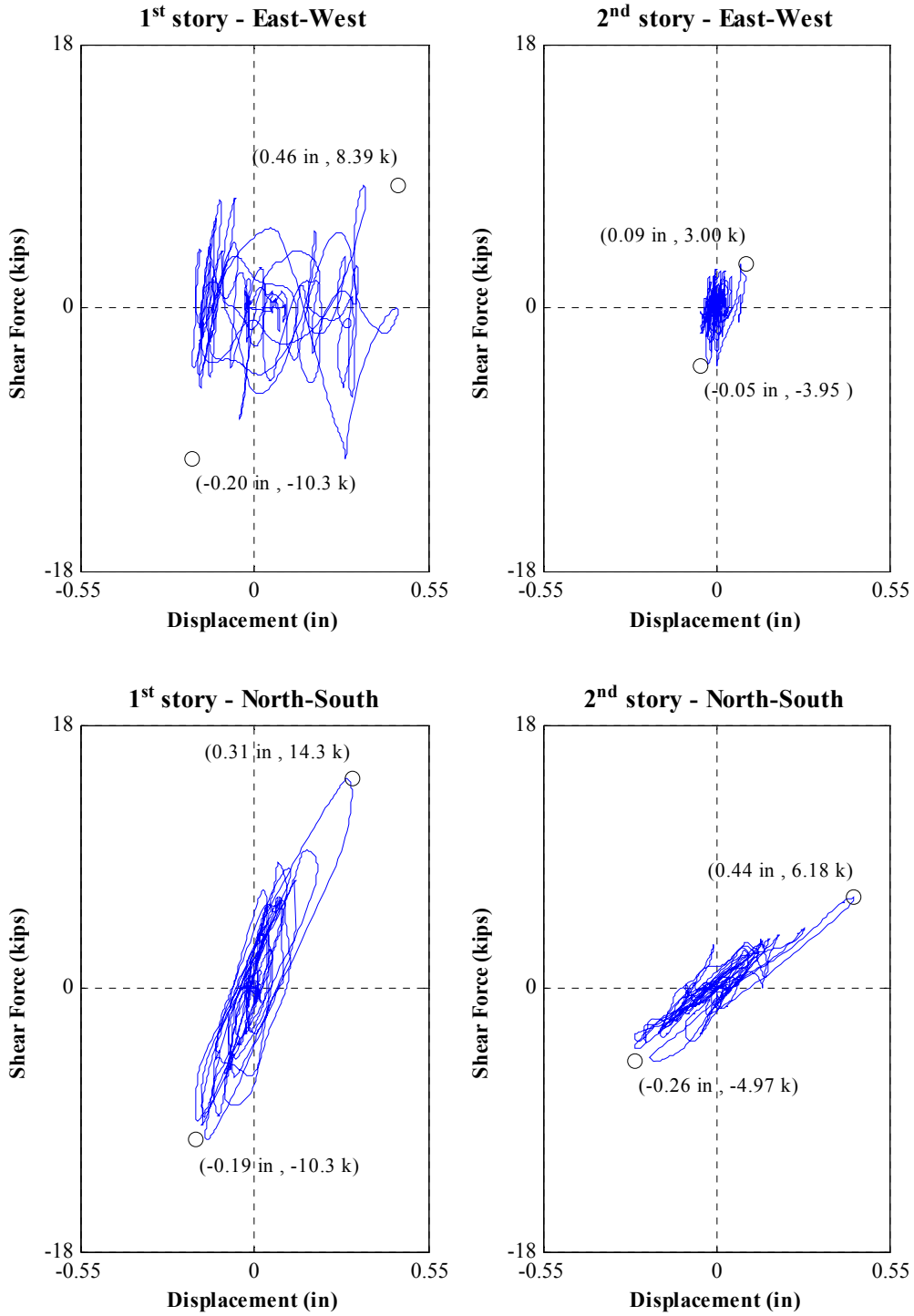


Figure O.5: Interstory force-displacement hysteresis loops for Test NWP1S05

Appendix O

Phase 1, NWP1S17 Seismic Test

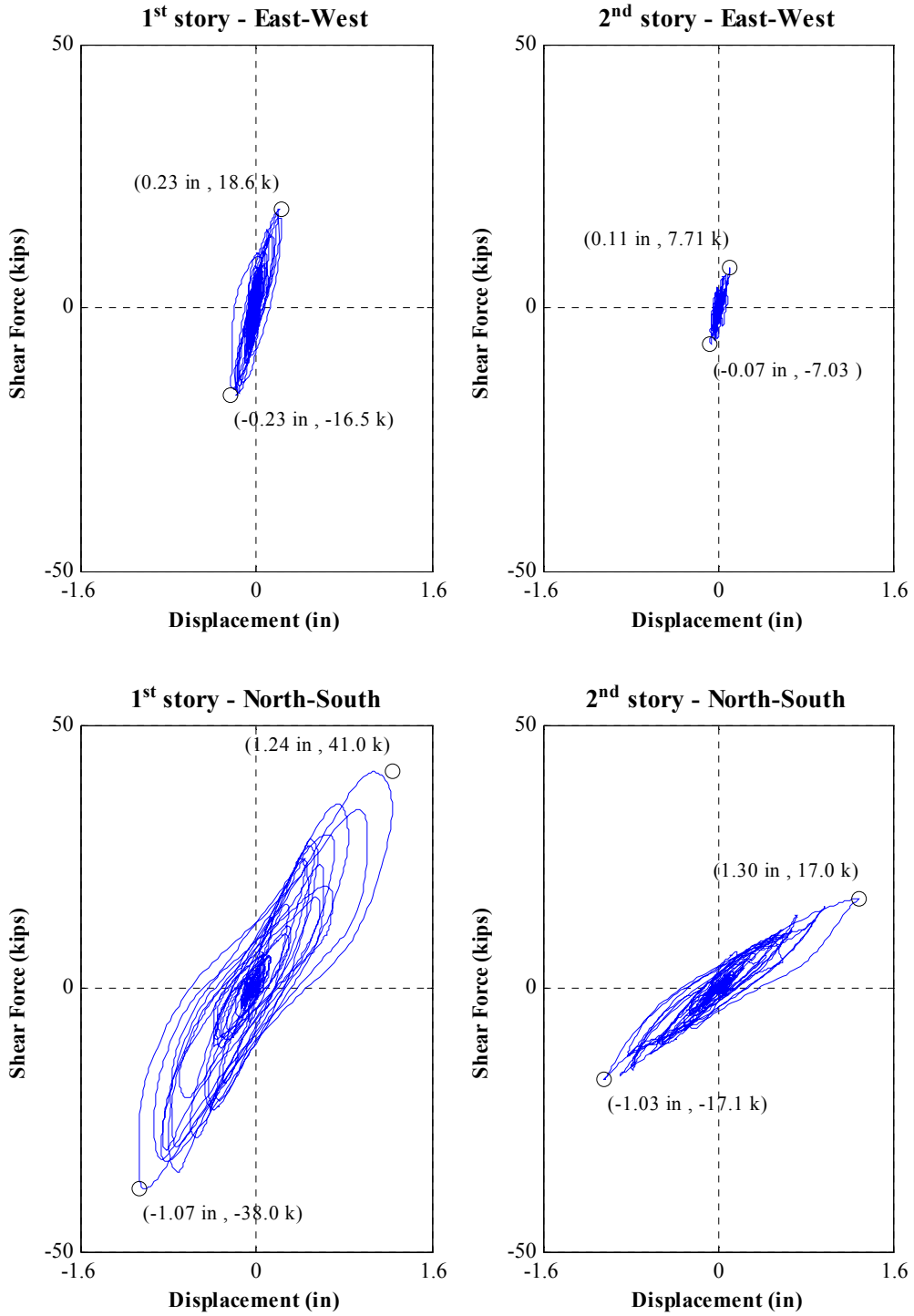


Figure O.6: Interstory force-displacement hysteresis loops for Test NWP1S17

Appendix O

Phase 1, NWP1S07 Seismic Test

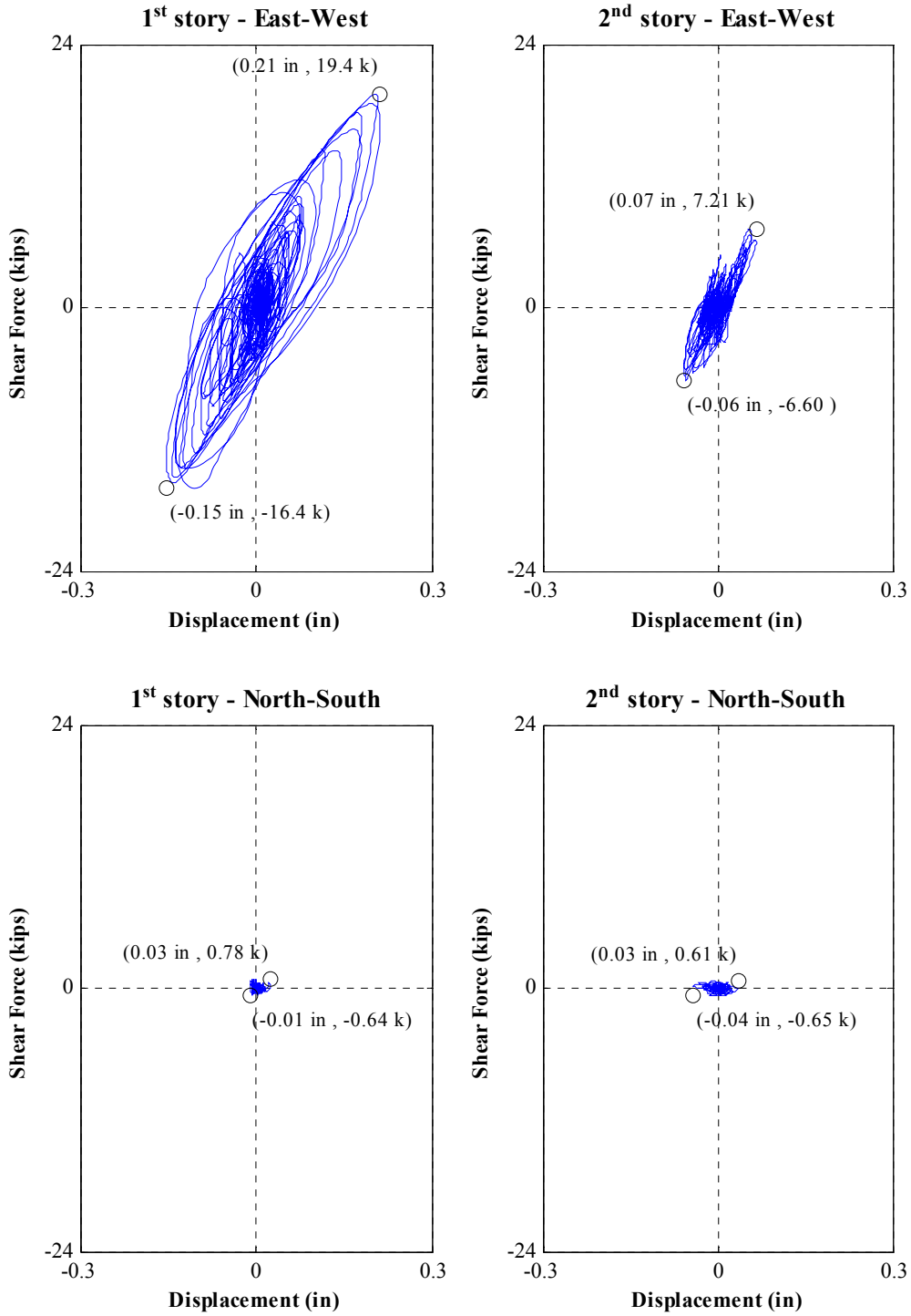


Figure O.7: Interstory force-displacement hysteresis loops for Test NWP1S07

Appendix O

Phase 1, NWP1S06 Seismic Test

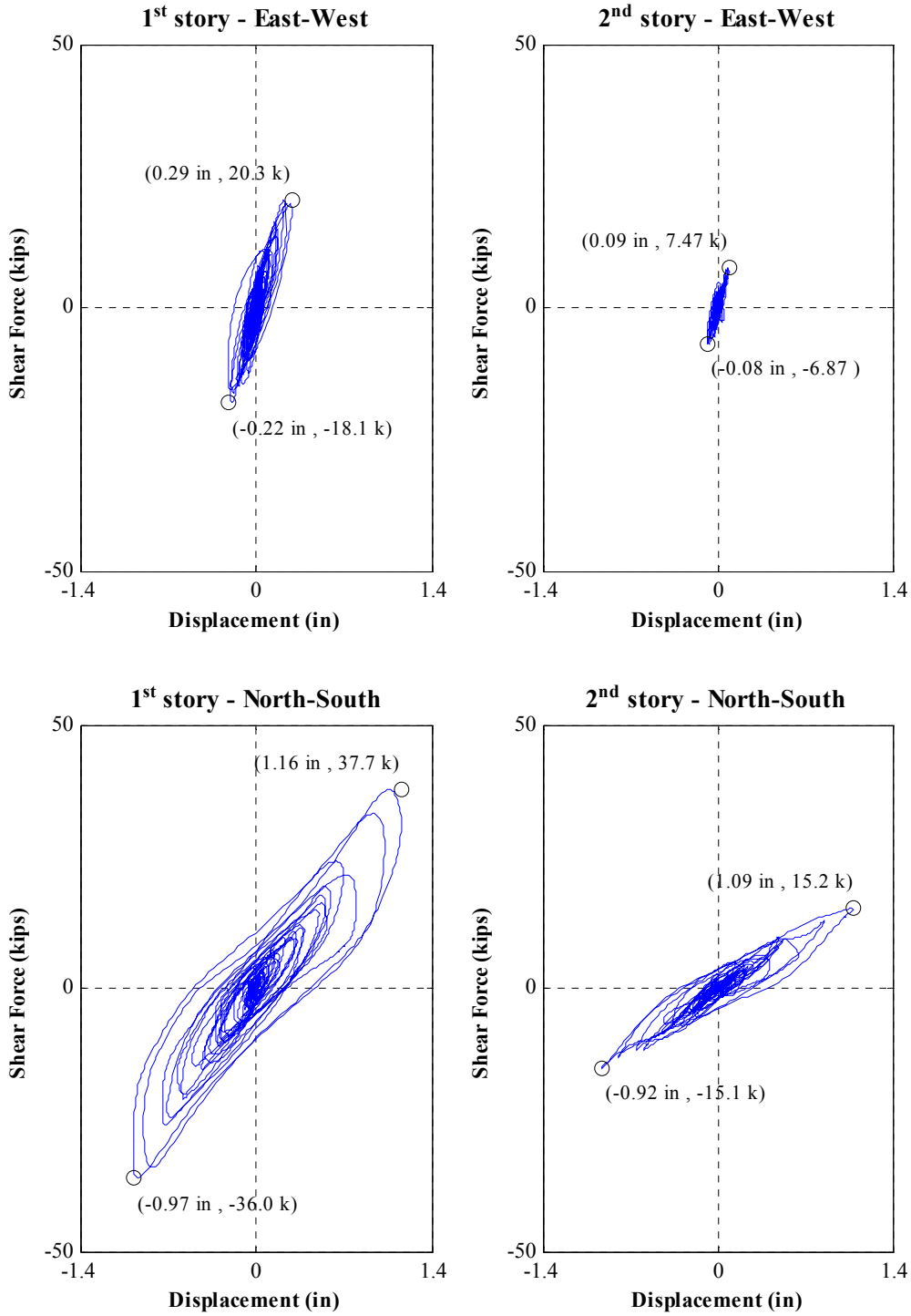


Figure O.8: Interstory force-displacement hysteresis loops for Test NWP1S06

Appendix O

Phase 1, NWP1S10 Seismic Test

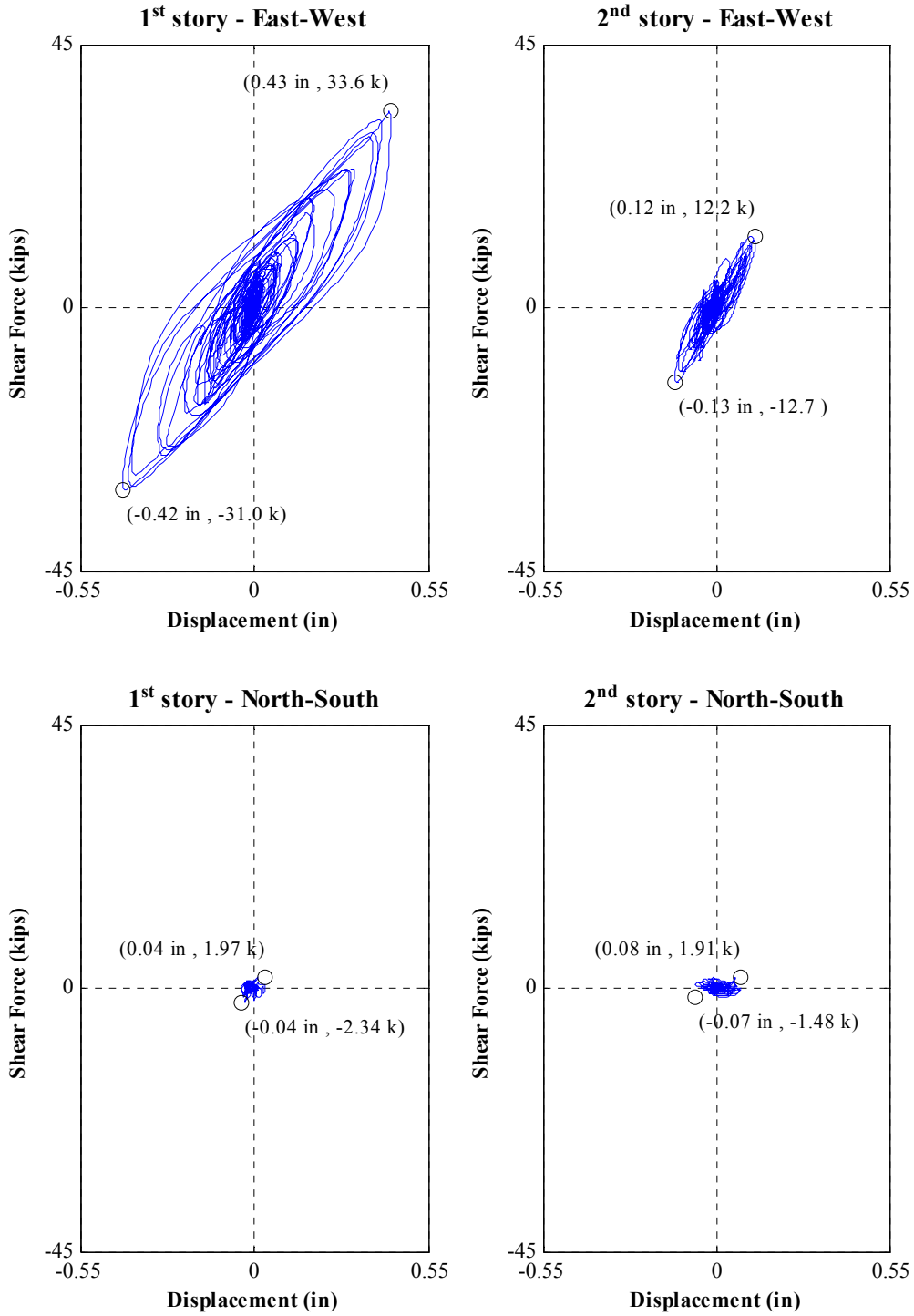


Figure O.9: Interstory force-displacement hysteresis loops for Test NWP1S10

Appendix O

Phase 2, NWP2S01 Seismic Test

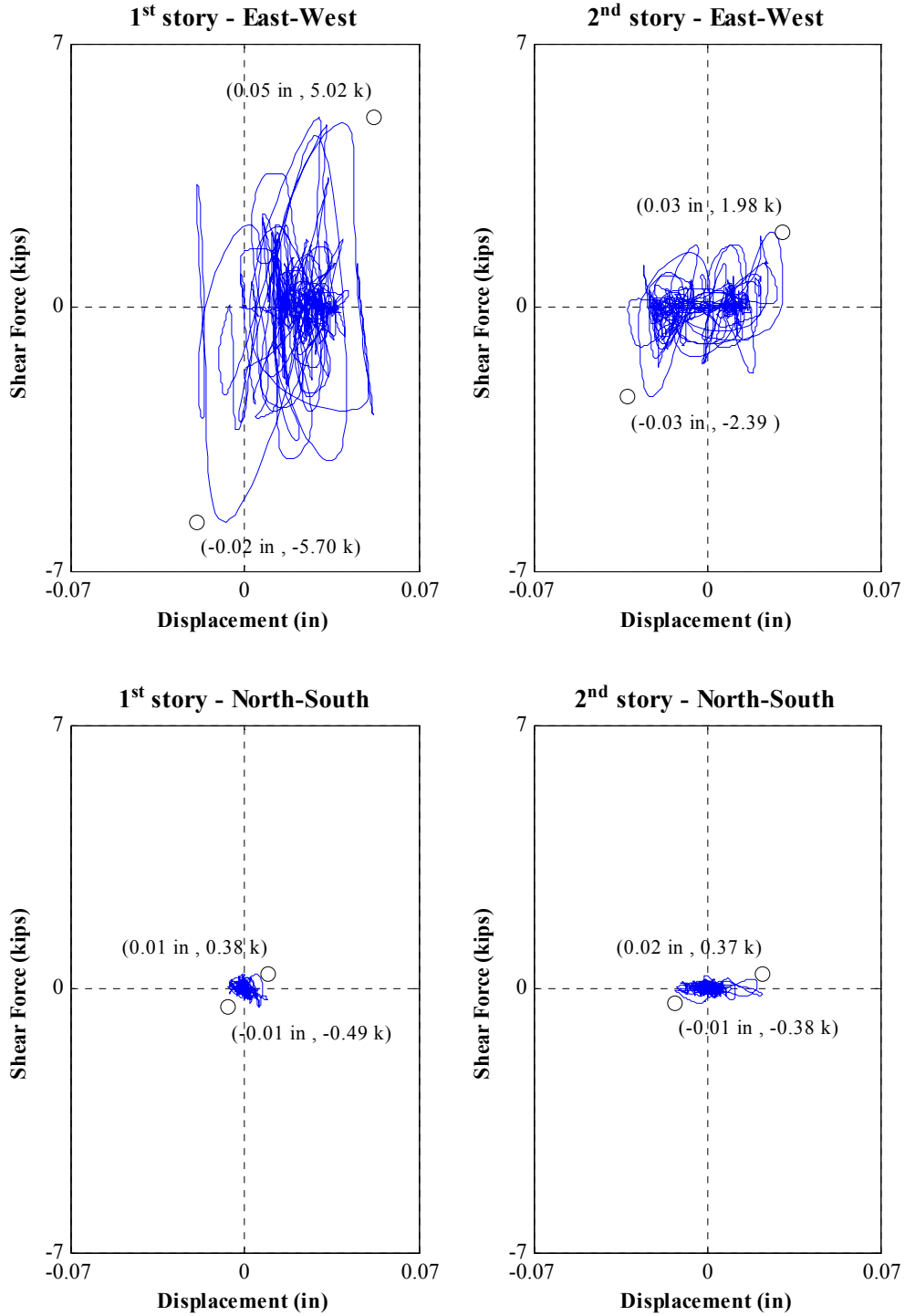


Figure O.10: Interstory force-displacement hysteresis loops for Test NWP2S01

Appendix O

Phase 2, NWP2S02 Seismic Test

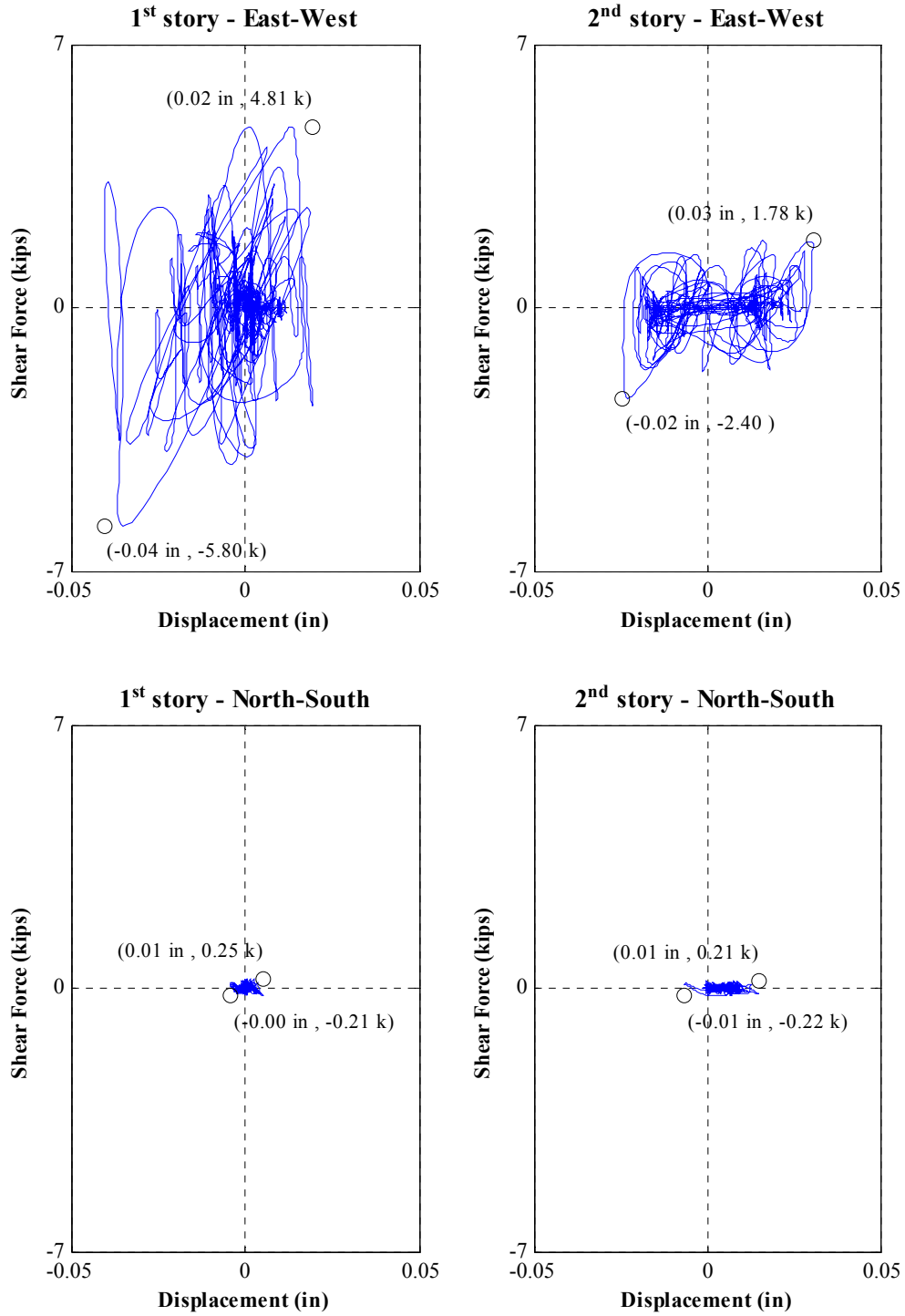


Figure O.11: Interstory force-displacement hysteresis loops for Test NWP2S02

Appendix O

Phase 2, NWP2S03 Seismic Test

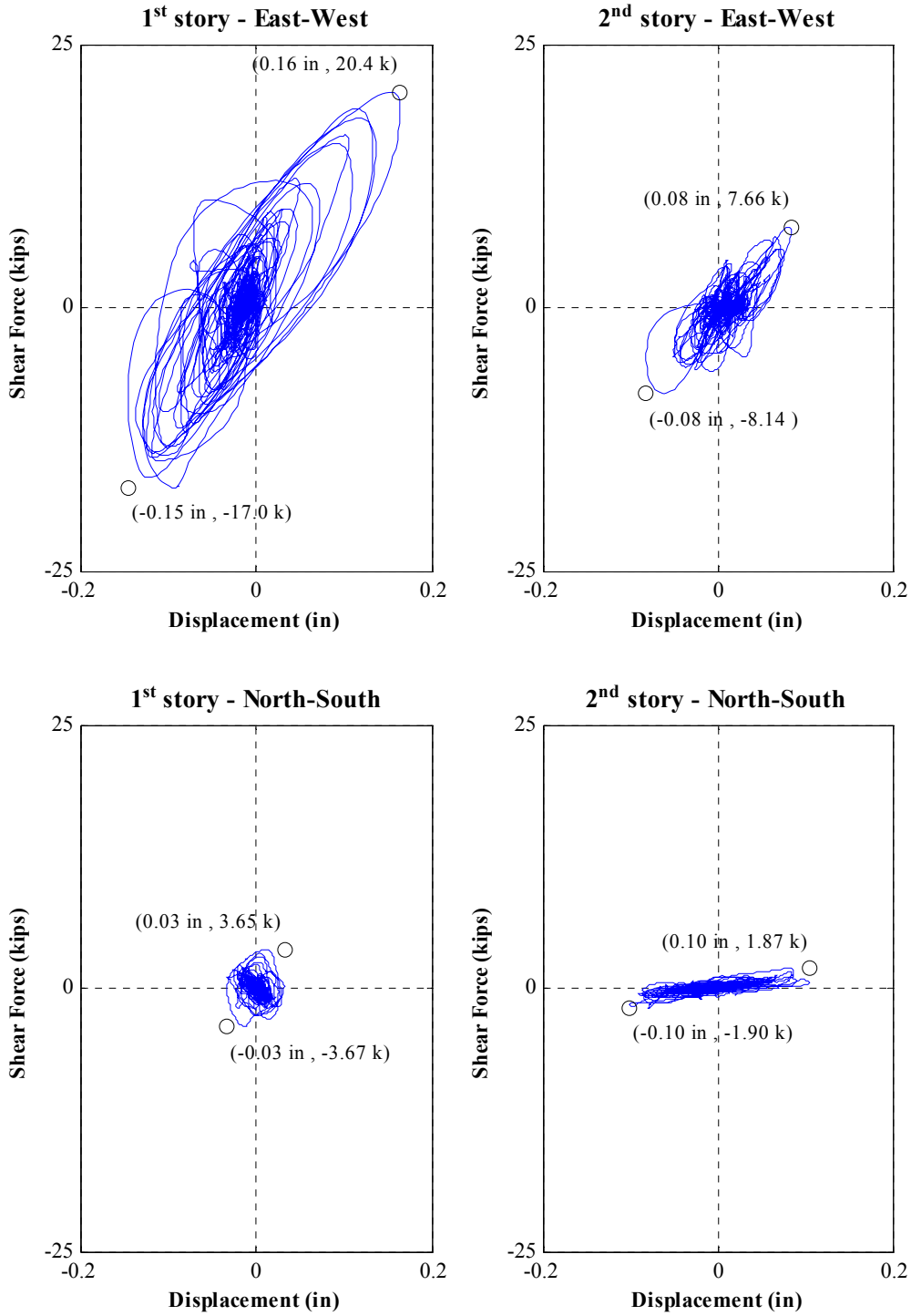


Figure O.12: Interstory force-displacement hysteresis loops for Test NWP2S03

Appendix O

Phase 2, NWP2S04 Seismic Test

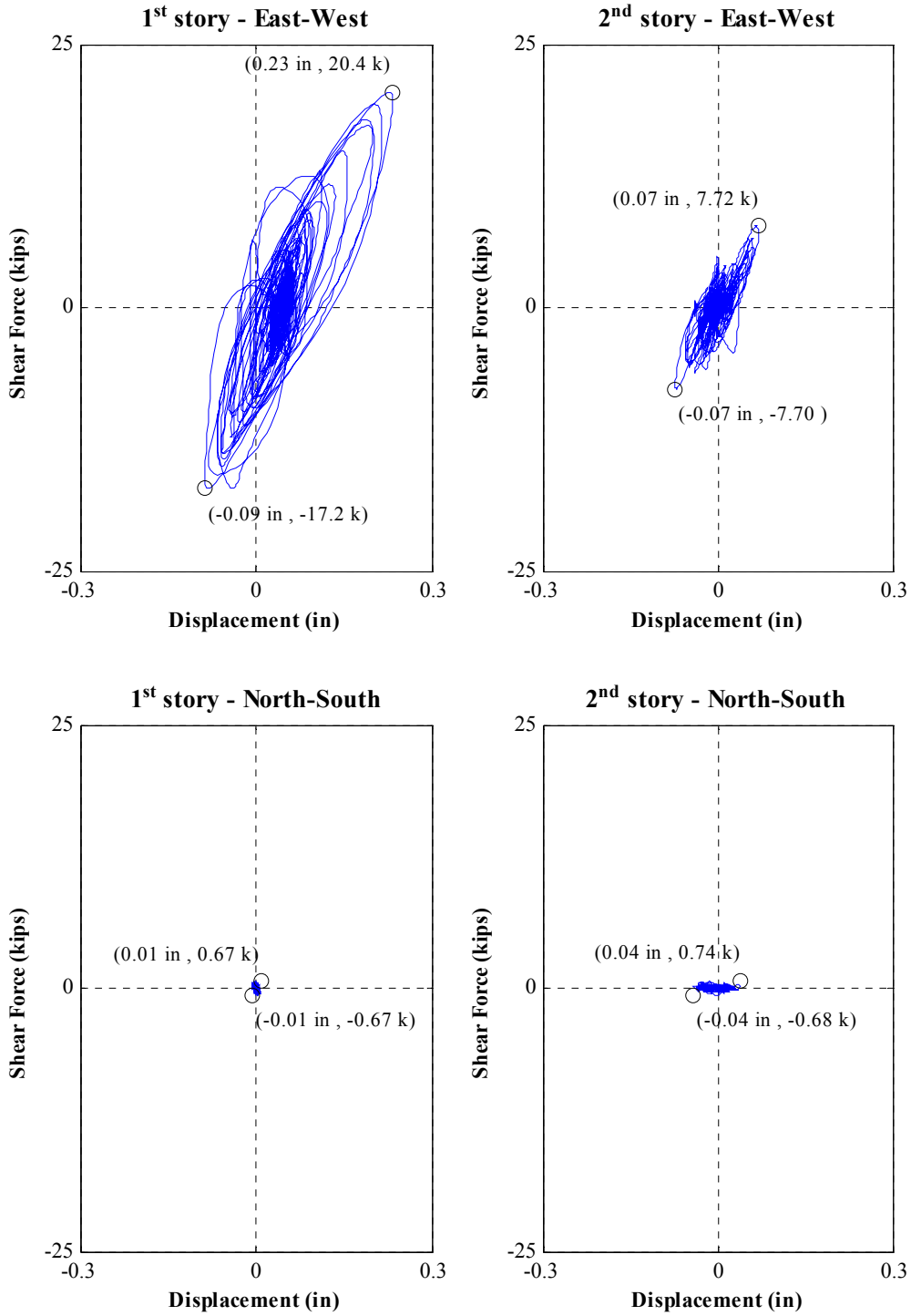


Figure O.13: Interstory force-displacement hysteresis loops for Test NWP2S04

Appendix O

Phase 2, NWP2S05 Seismic Test

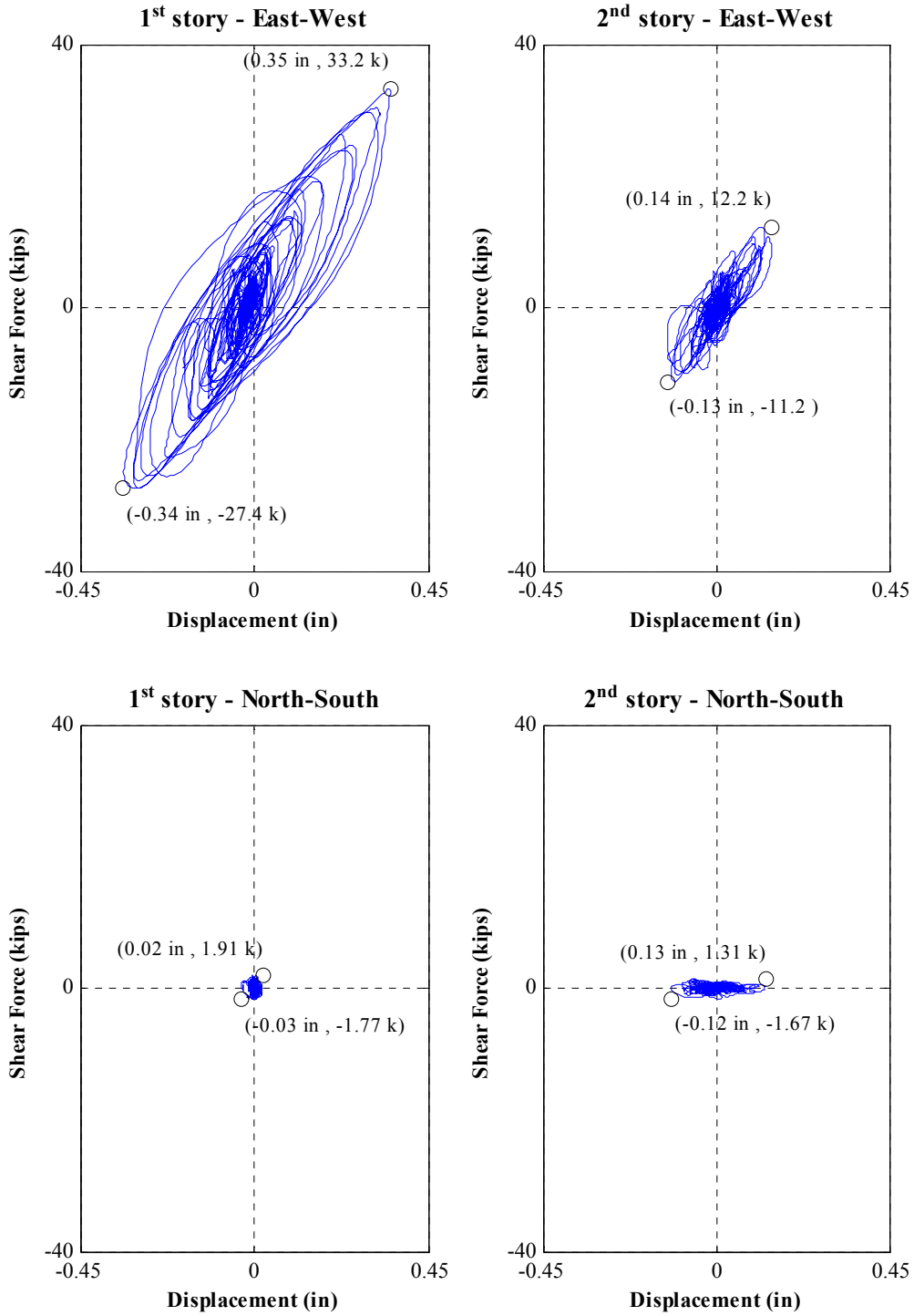


Figure O.14: Interstory force-displacement hysteresis loops for Test NWP2S05

Appendix O

Phase 2, NWP2S06 Seismic Test

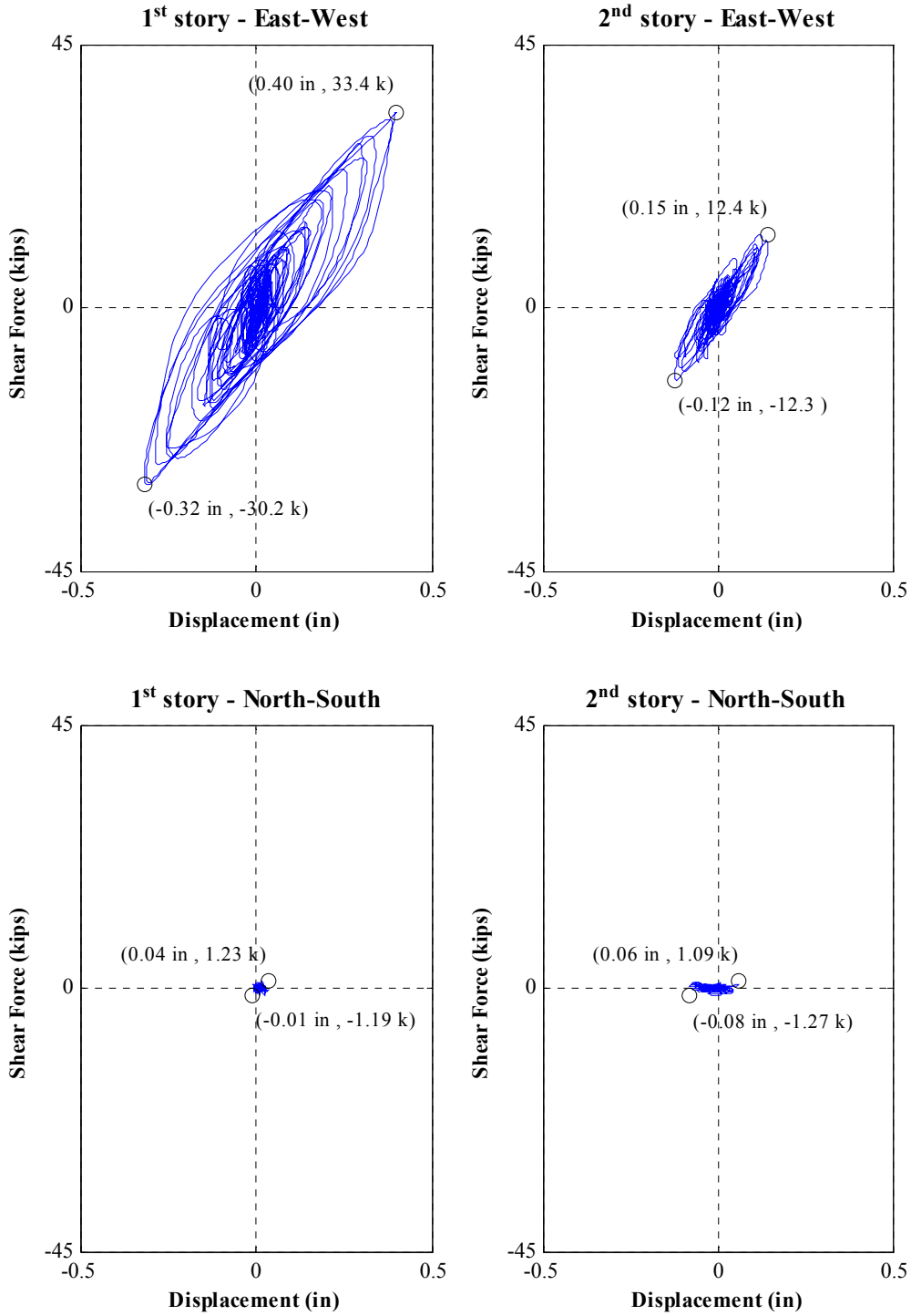


Figure O.15: Interstory force-displacement hysteresis loops for Test NWP2S06

Appendix O

Phase 2, NWP2S07 Seismic Test

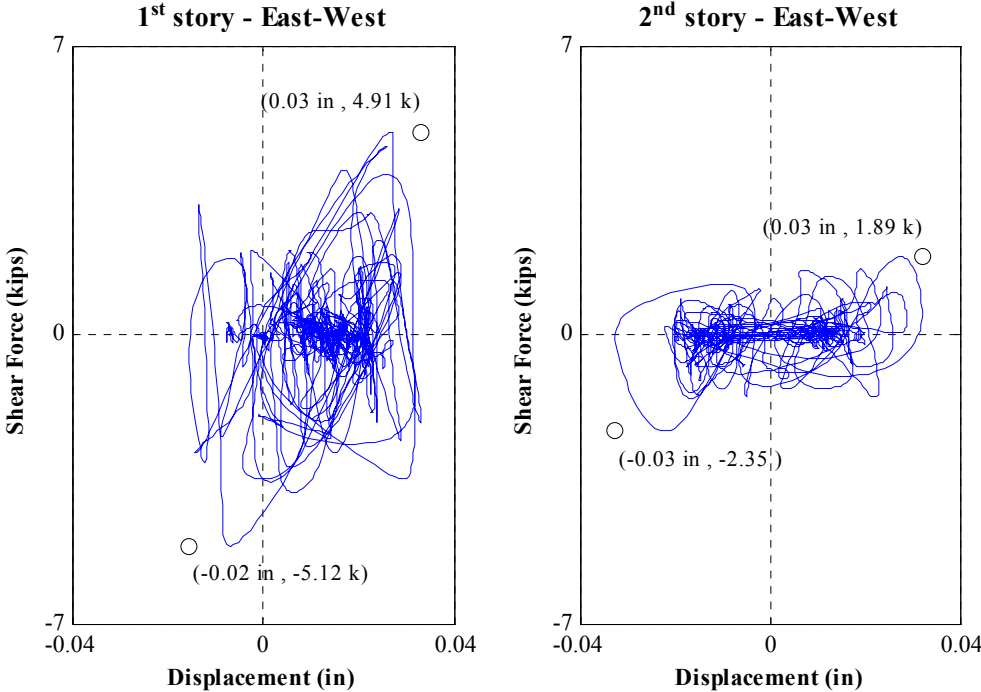


Figure O.16: Interstory force-displacement hysteresis loop for Test NWP2S07

* Data not plotted for North-South direction due to error in recording

Appendix O

Phase 2, NWP2S08 Seismic Test

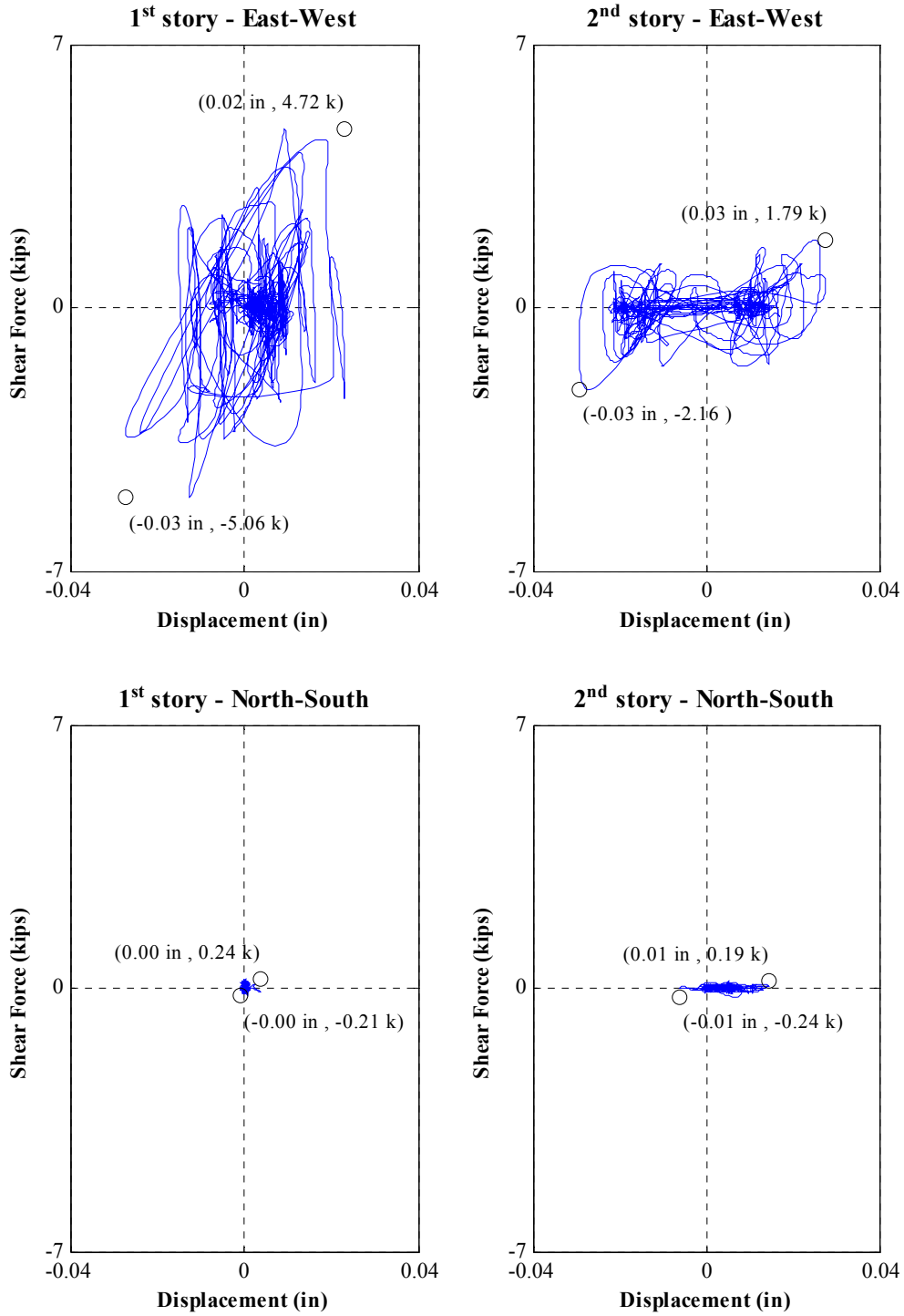


Figure O.17: Interstory force-displacement hysteresis loops for Test NWP2S08

Appendix O

Phase 2, NWP2S09 Seismic Test

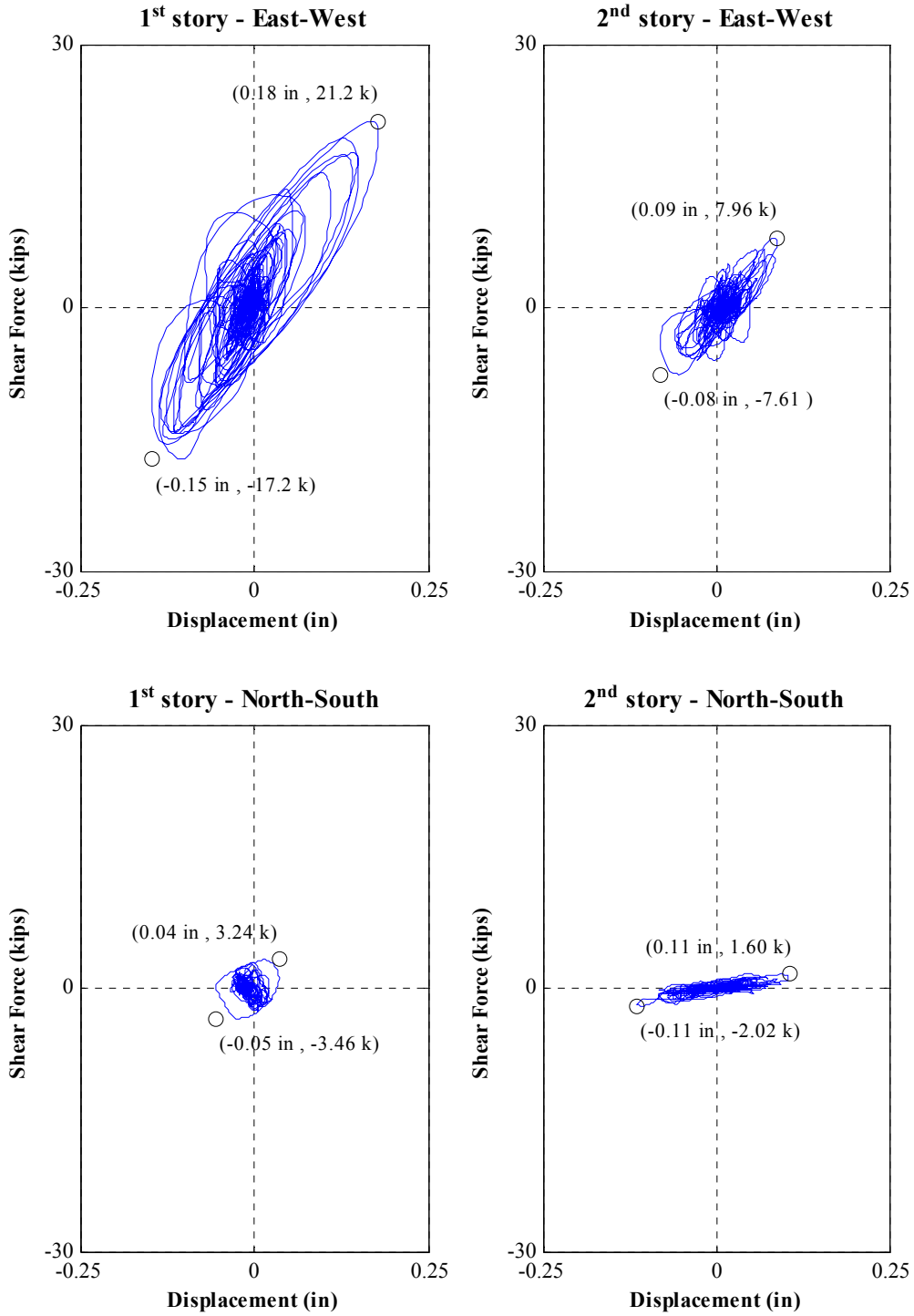


Figure O.18: Interstory force-displacement hysteresis loops for Test NWP2S09

Appendix O

Phase 2, NWP2S10 Seismic Test

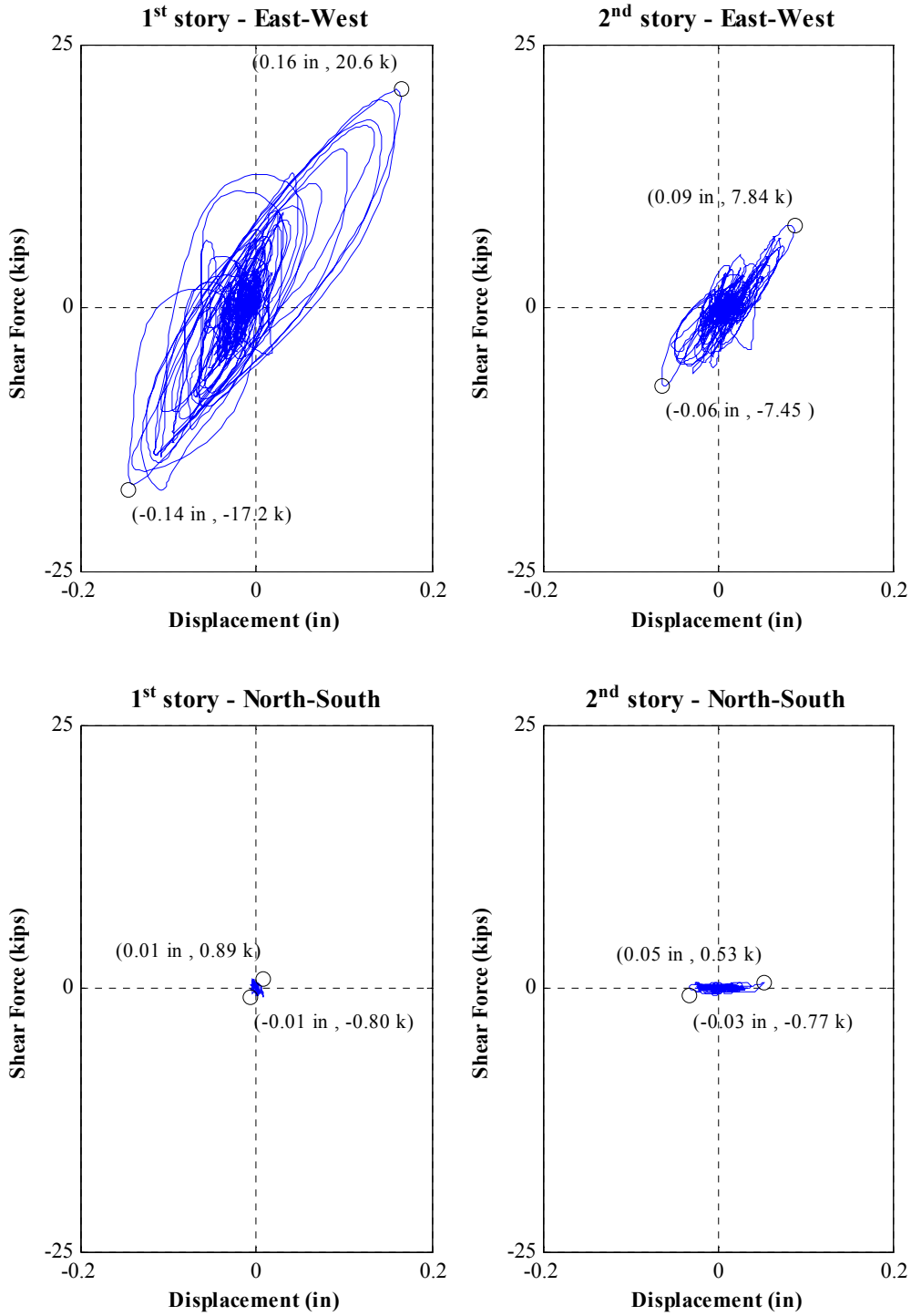


Figure O.19: Interstory force-displacement hysteresis loops for Test NWP2S10

Appendix O

Phase 2, NWP2S11 Seismic Test

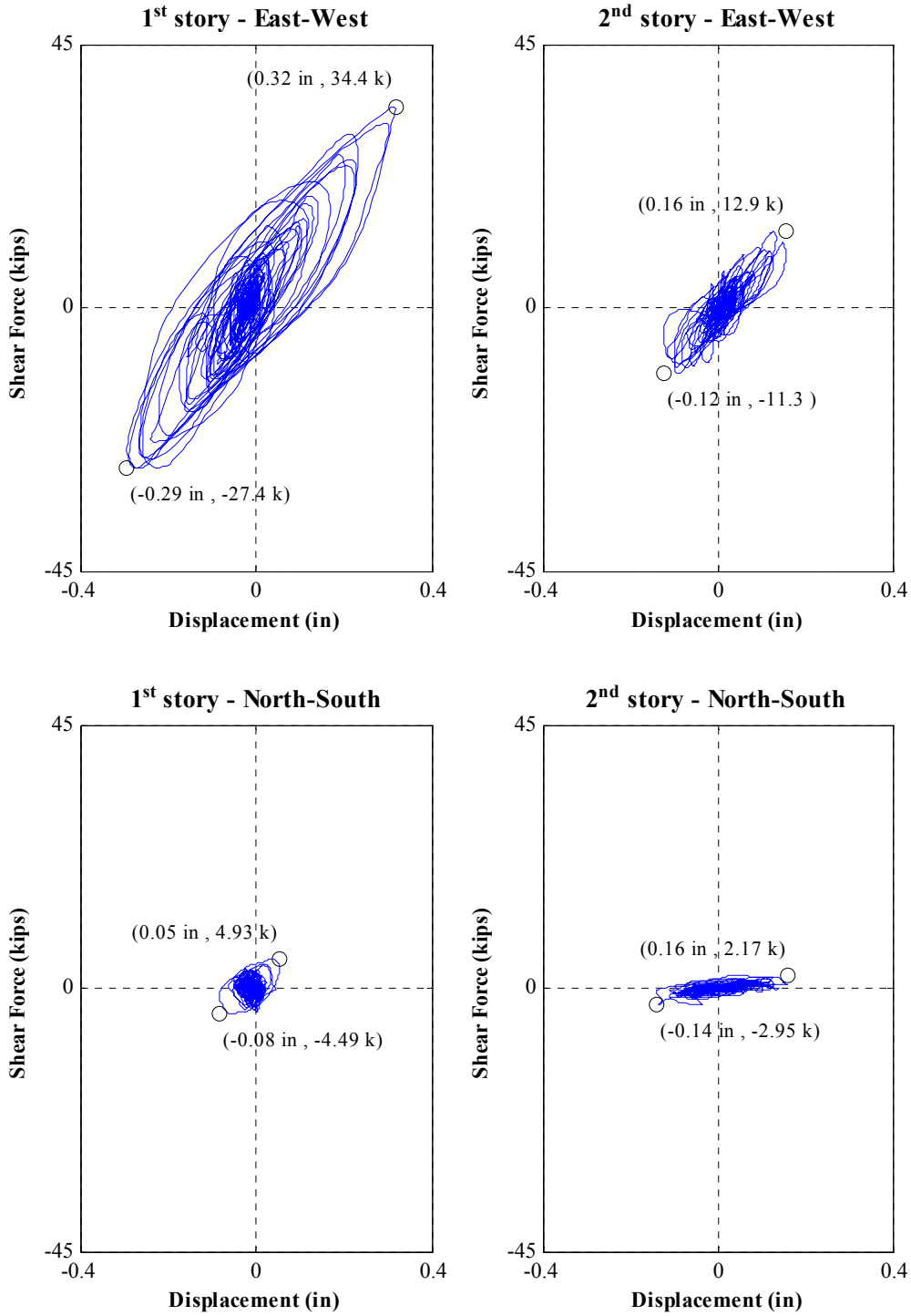


Figure O.20: Interstory force-displacement hysteresis loops for Test NWP2S11

Appendix O

Phase 2, NWP2S12 Seismic Test

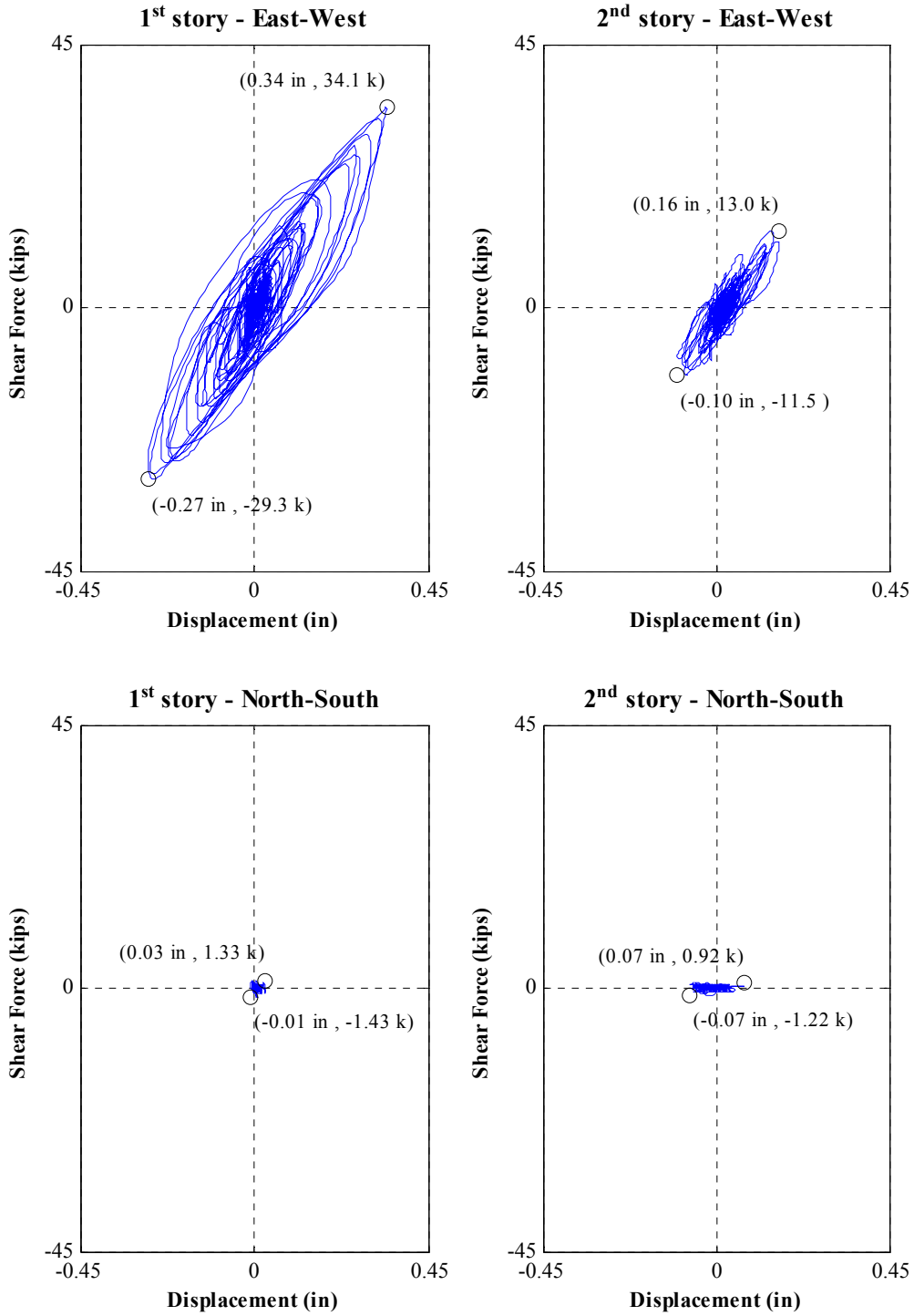


Figure O.21: Interstory force-displacement hysteresis loops for Test NWP2S12

Appendix O

Phase 2, NWP2S13 Seismic Test

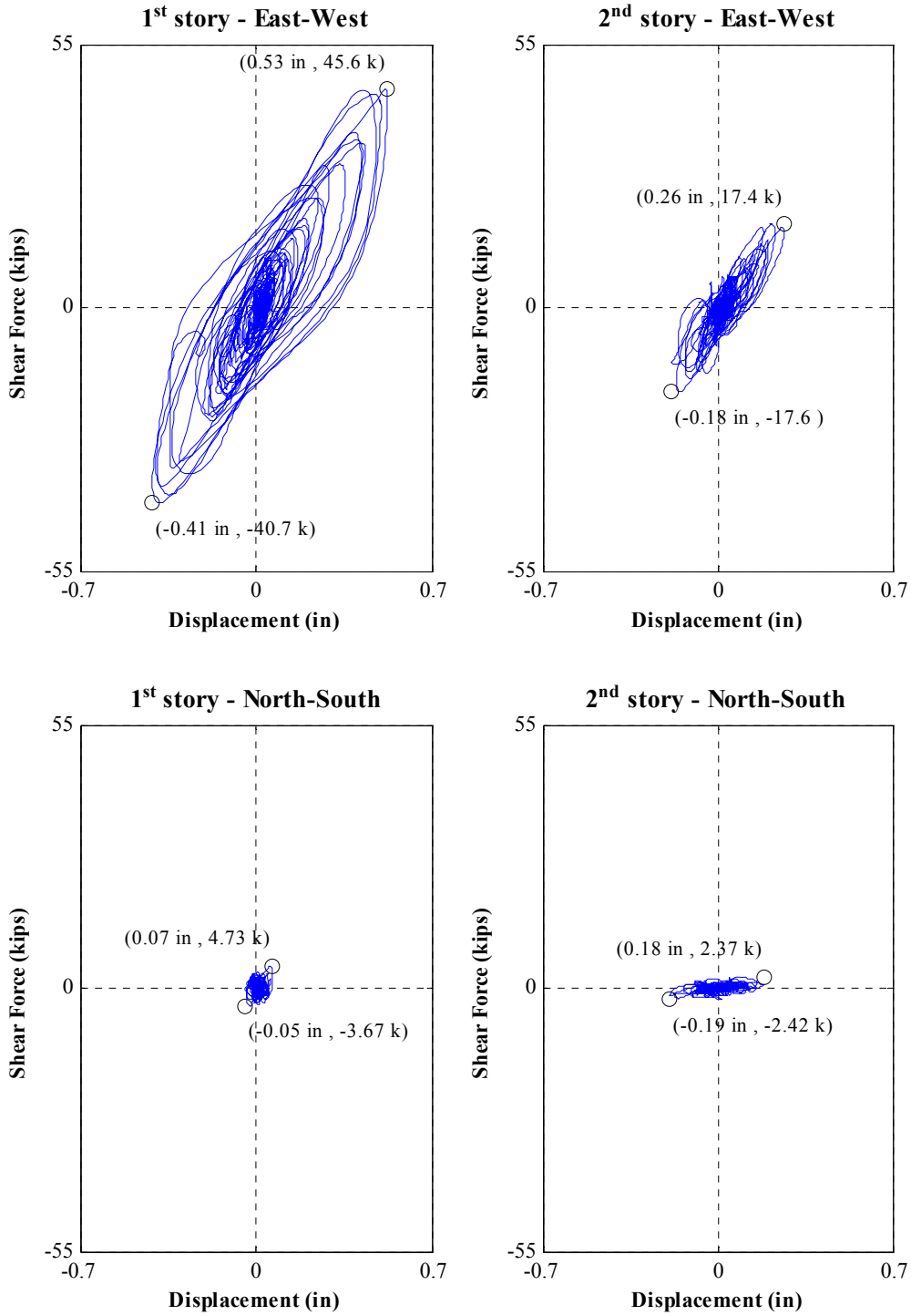


Figure O.22: Interstory force-displacement hysteresis loops for Test NWP2S13

Appendix O

Phase 2, NWP2S14 Seismic Test

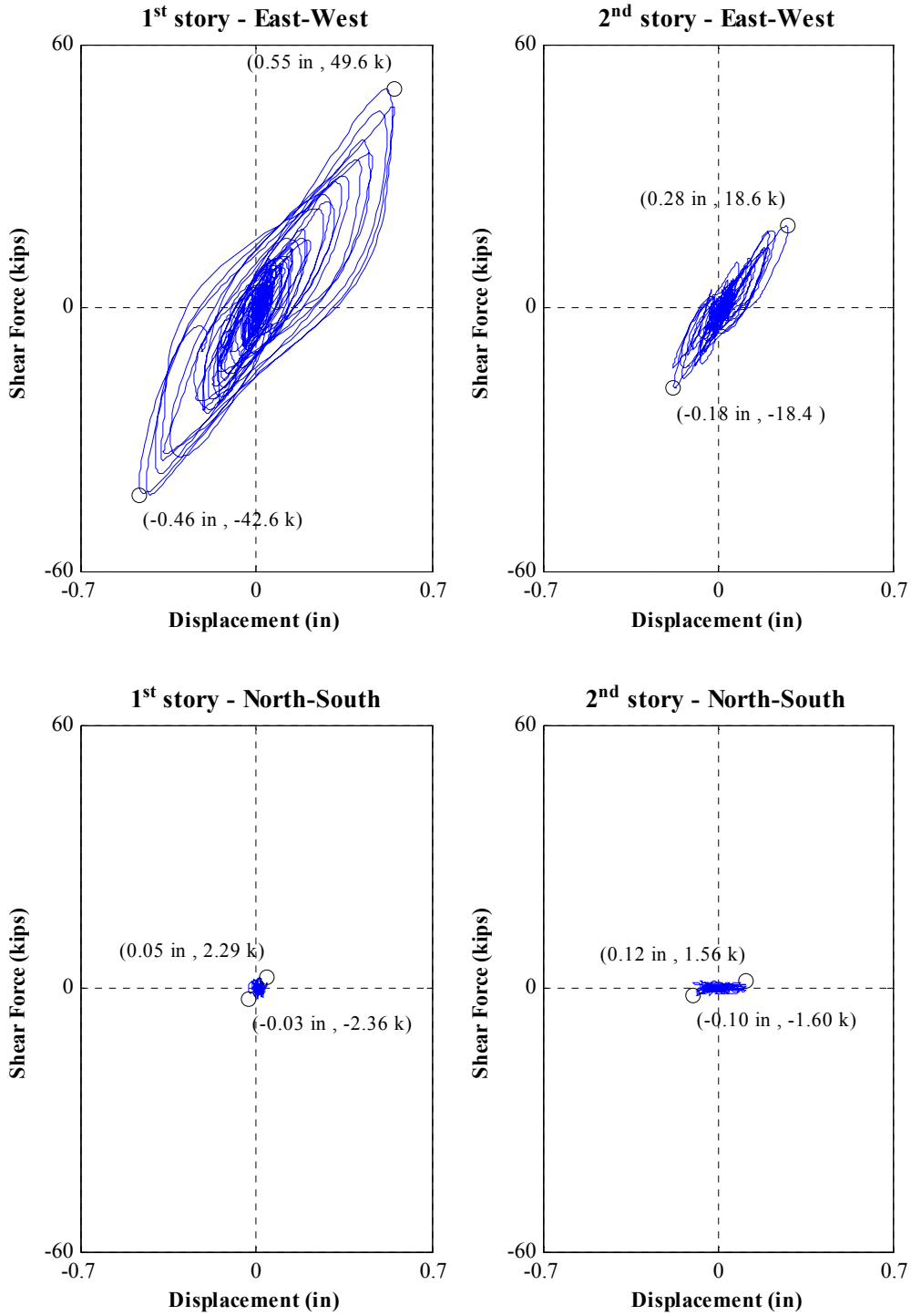


Figure O.23: Interstory force-displacement hysteresis loops for Test NWP2S14

Appendix O

Phase 2, NWP2S16 Seismic Test

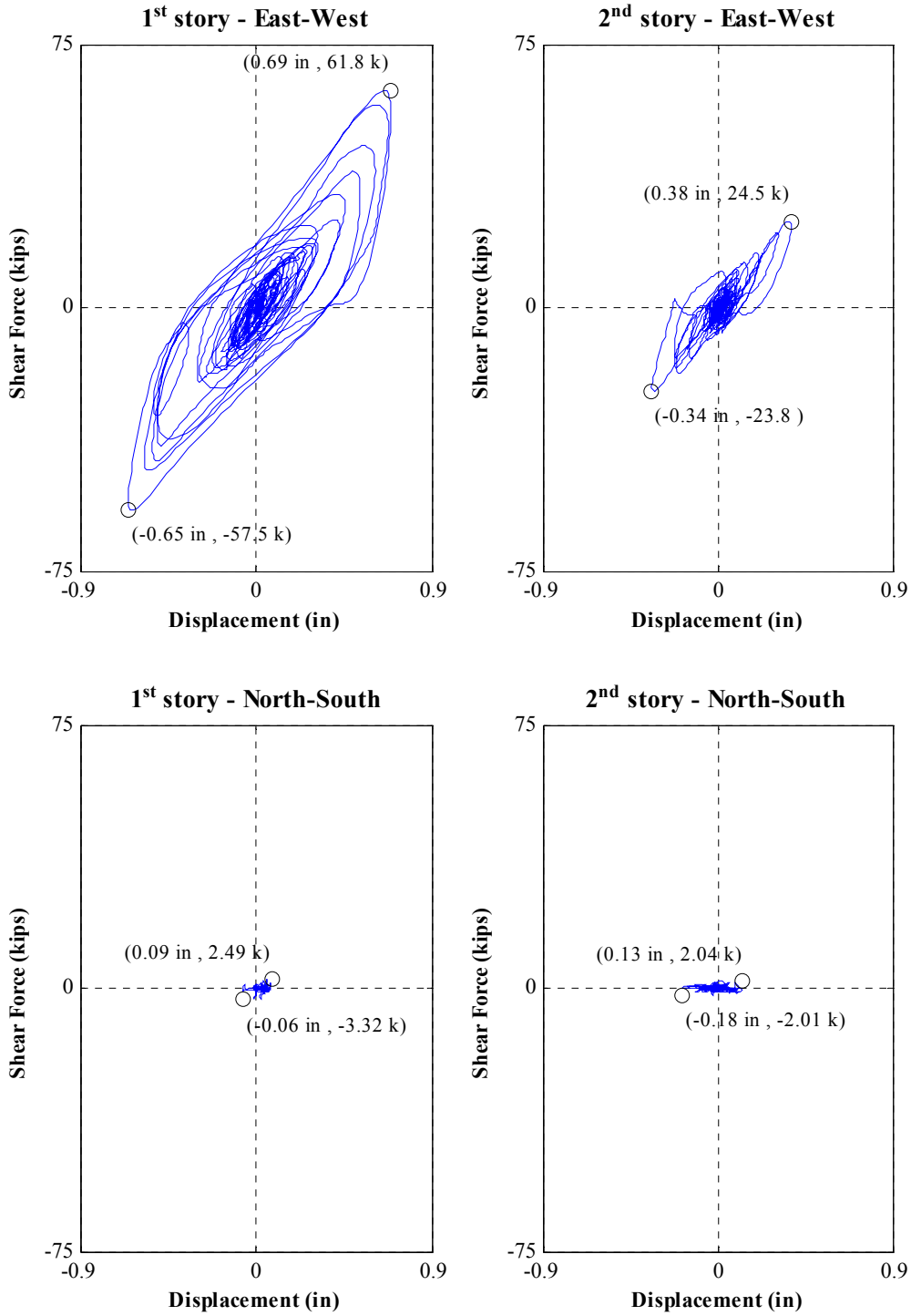


Figure O.24: Interstory force-displacement hysteresis loops for Test NWP2S16

Appendix O

Phase 2, NWP2S17 Seismic Test

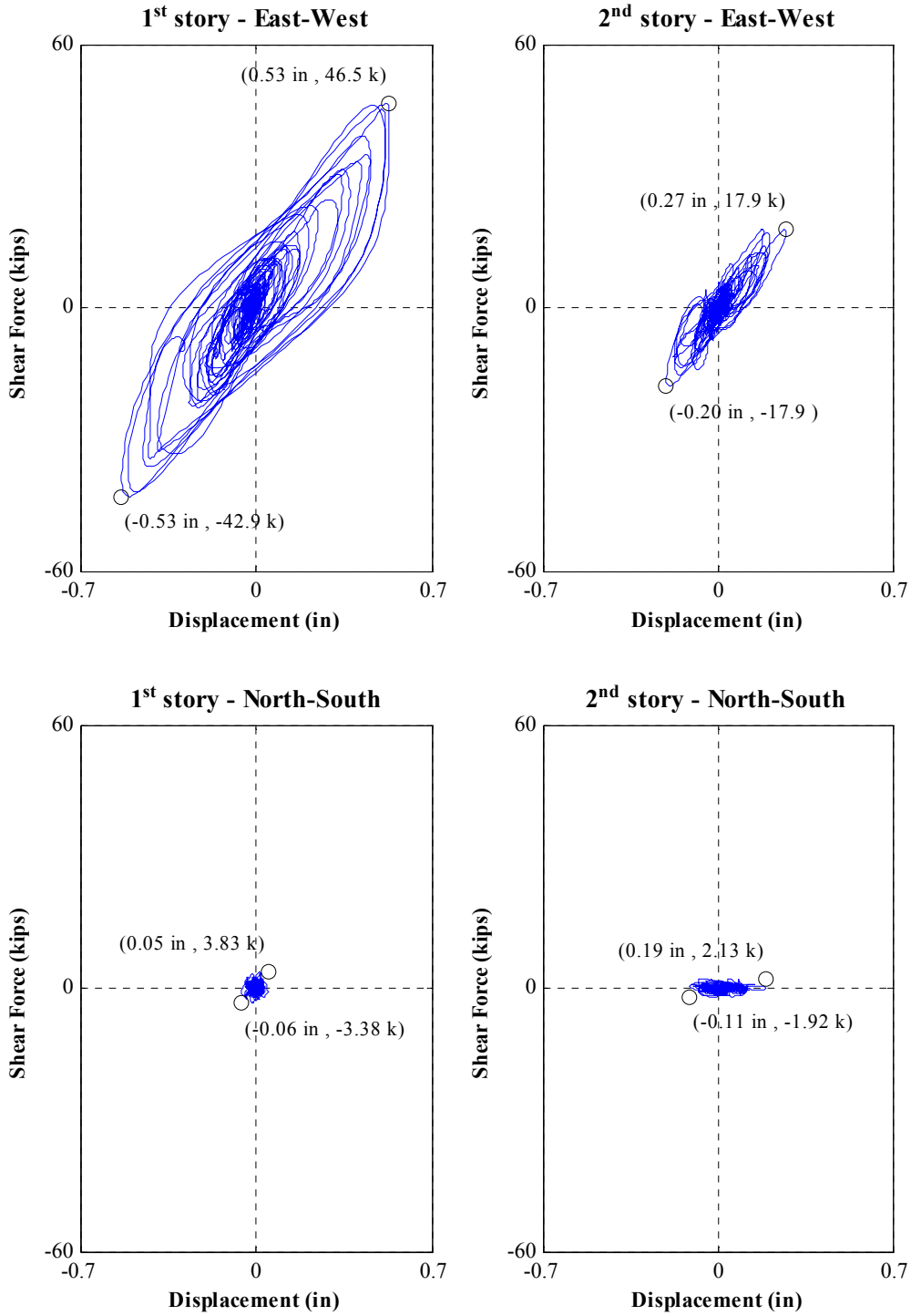


Figure O.25: Interstory force-displacement hysteresis loops for Test NWP2S17

Appendix O

Phase 2, NWP2S21 Seismic Test

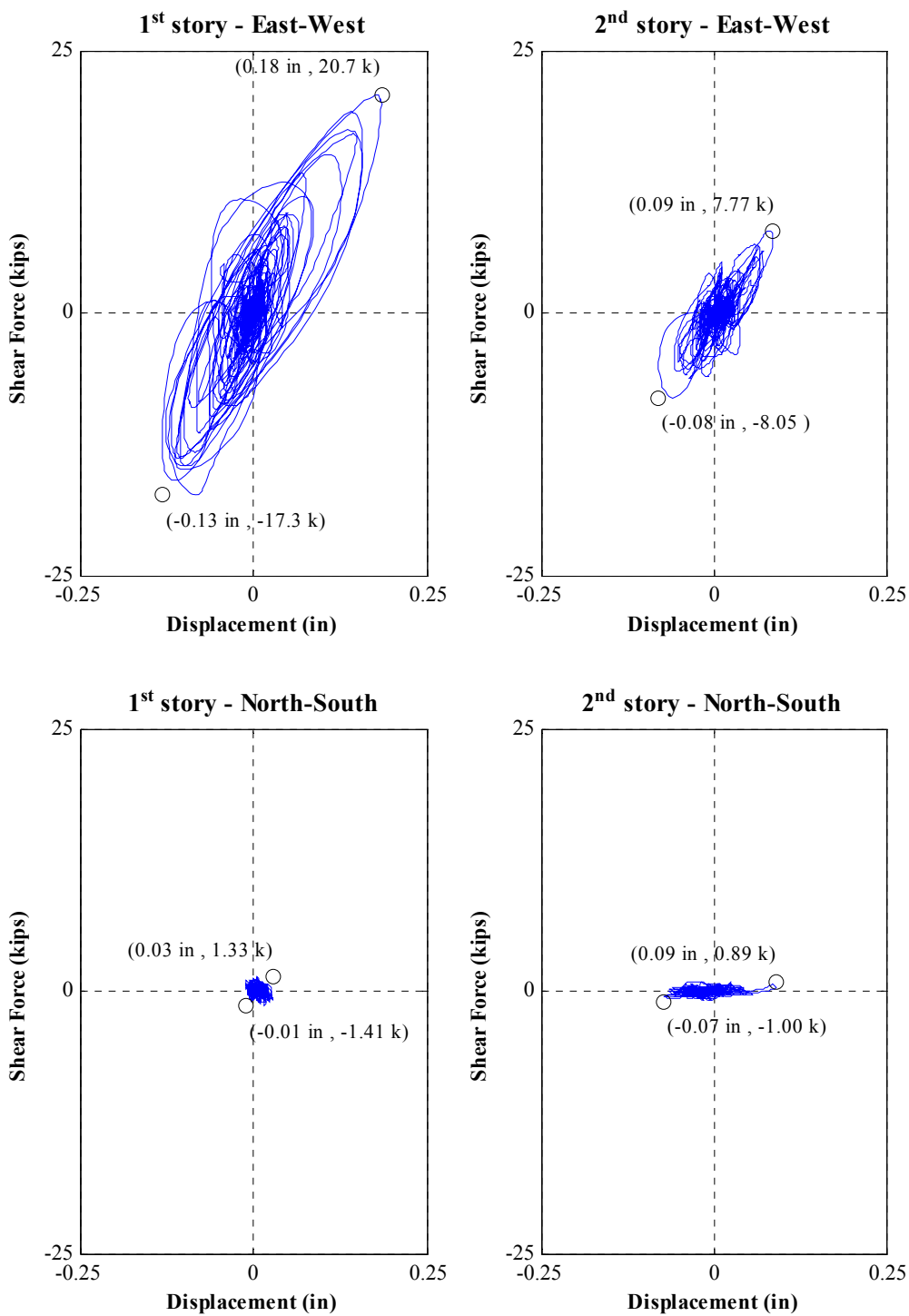


Figure O.26: Interstory force-displacement hysteresis loops for Test NWP2S21

Appendix O

Phase 2, NWP2S24 Seismic Test

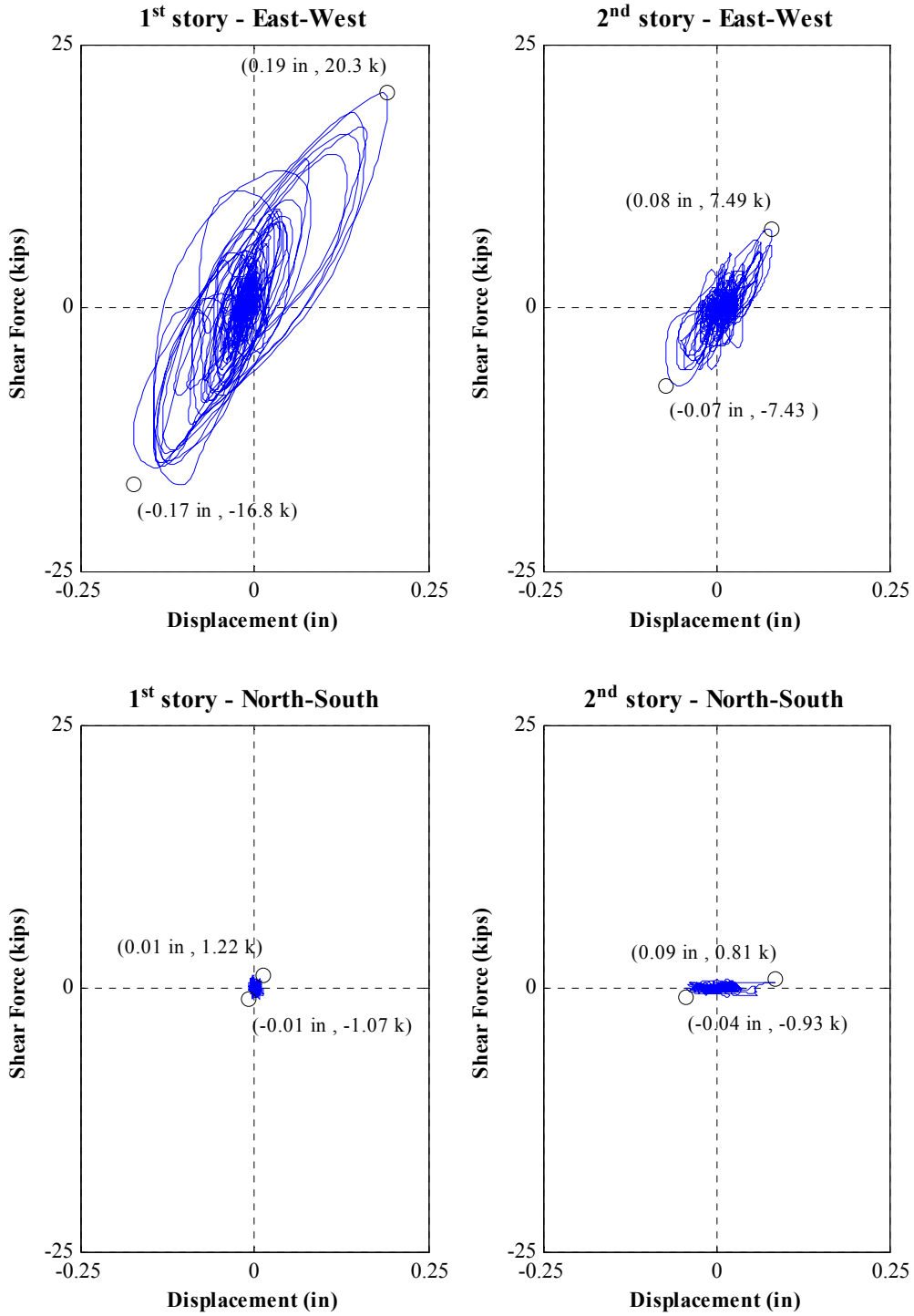


Figure O.27: Interstory force-displacement hysteresis loops for Test NWP2S24

Appendix O

Phase 2, NWP2S25 Seismic Test

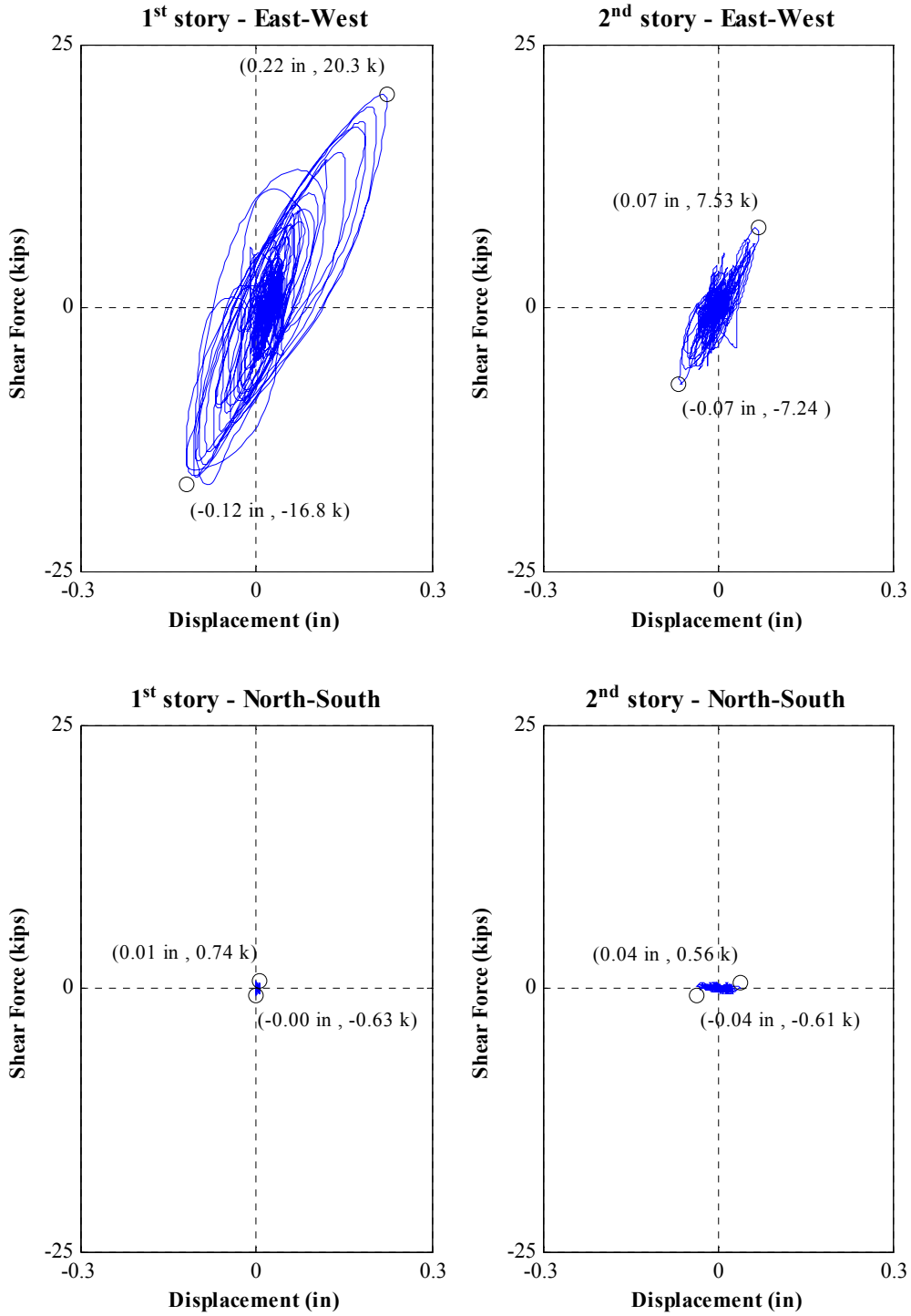


Figure O.28: Interstory force-displacement hysteresis loops for Test NWP2S25

Appendix O

Phase 2, NWP2S26 Seismic Test

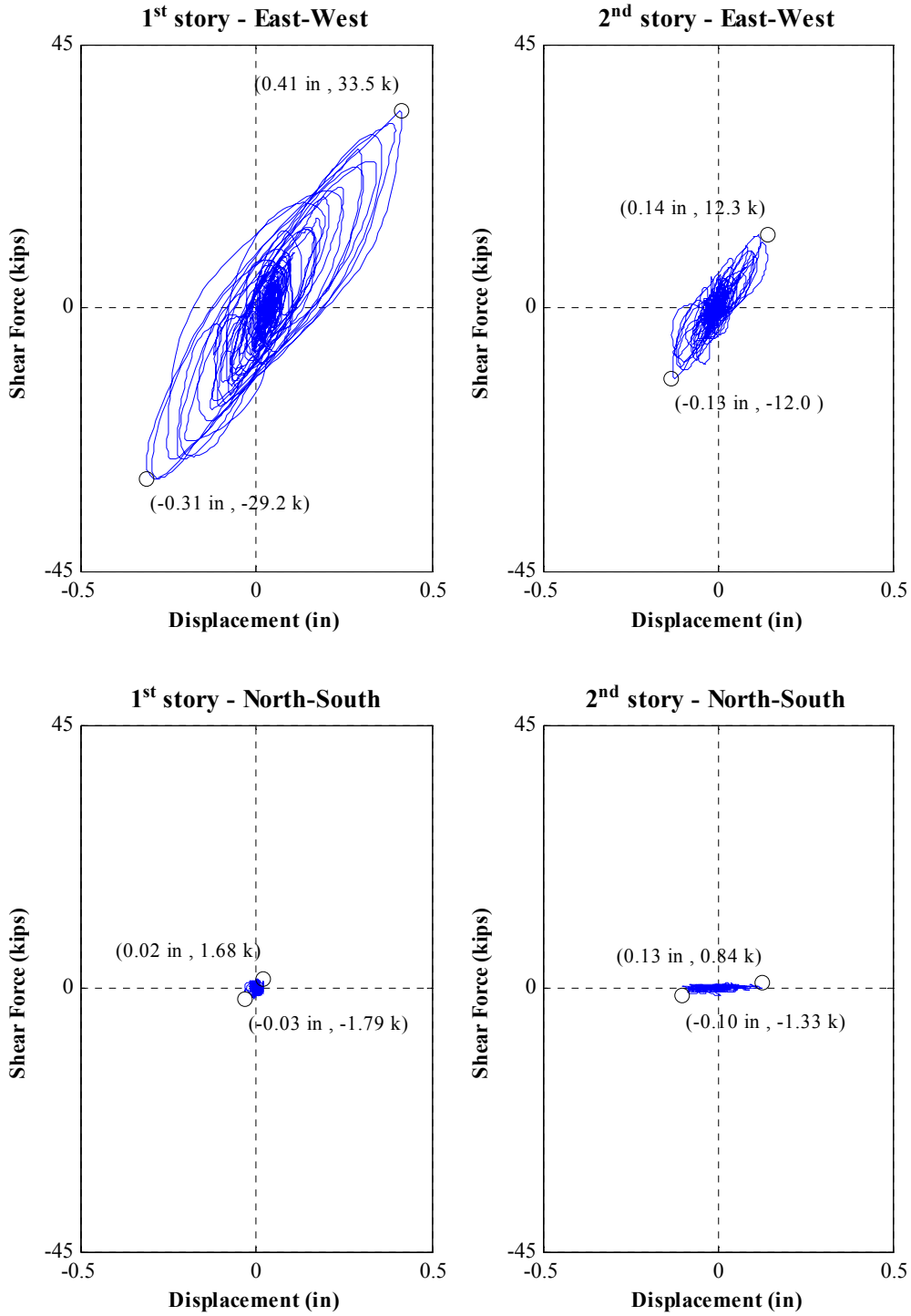


Figure O.29: Interstory force-displacement hysteresis loops for Test NWP2S26

Appendix O

Phase 2, NWP2S27 Seismic Test

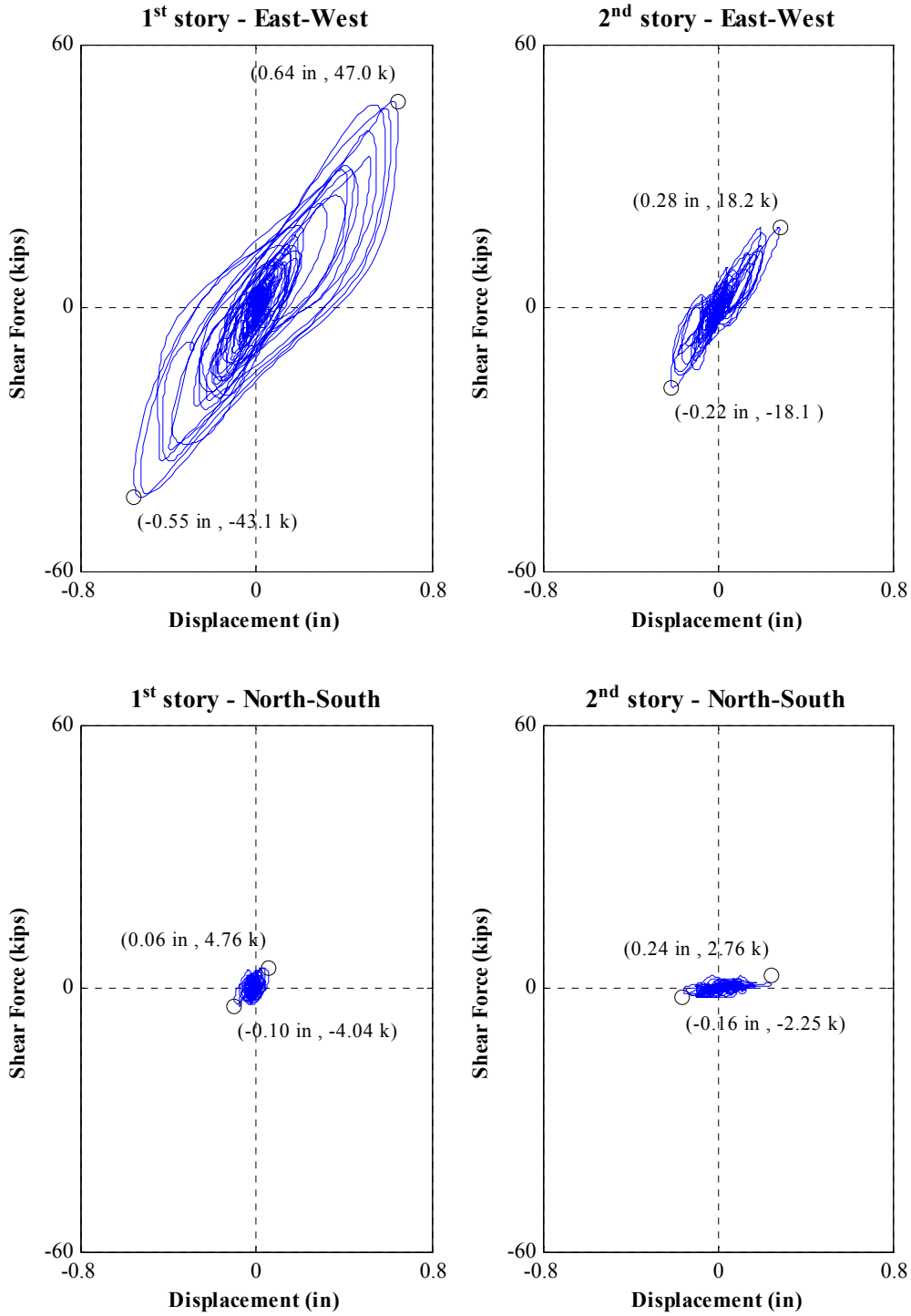


Figure O.30: Interstory force-displacement hysteresis loops for Test NWP2S27

Appendix O

Phase 2, NWP2S28 Seismic Test

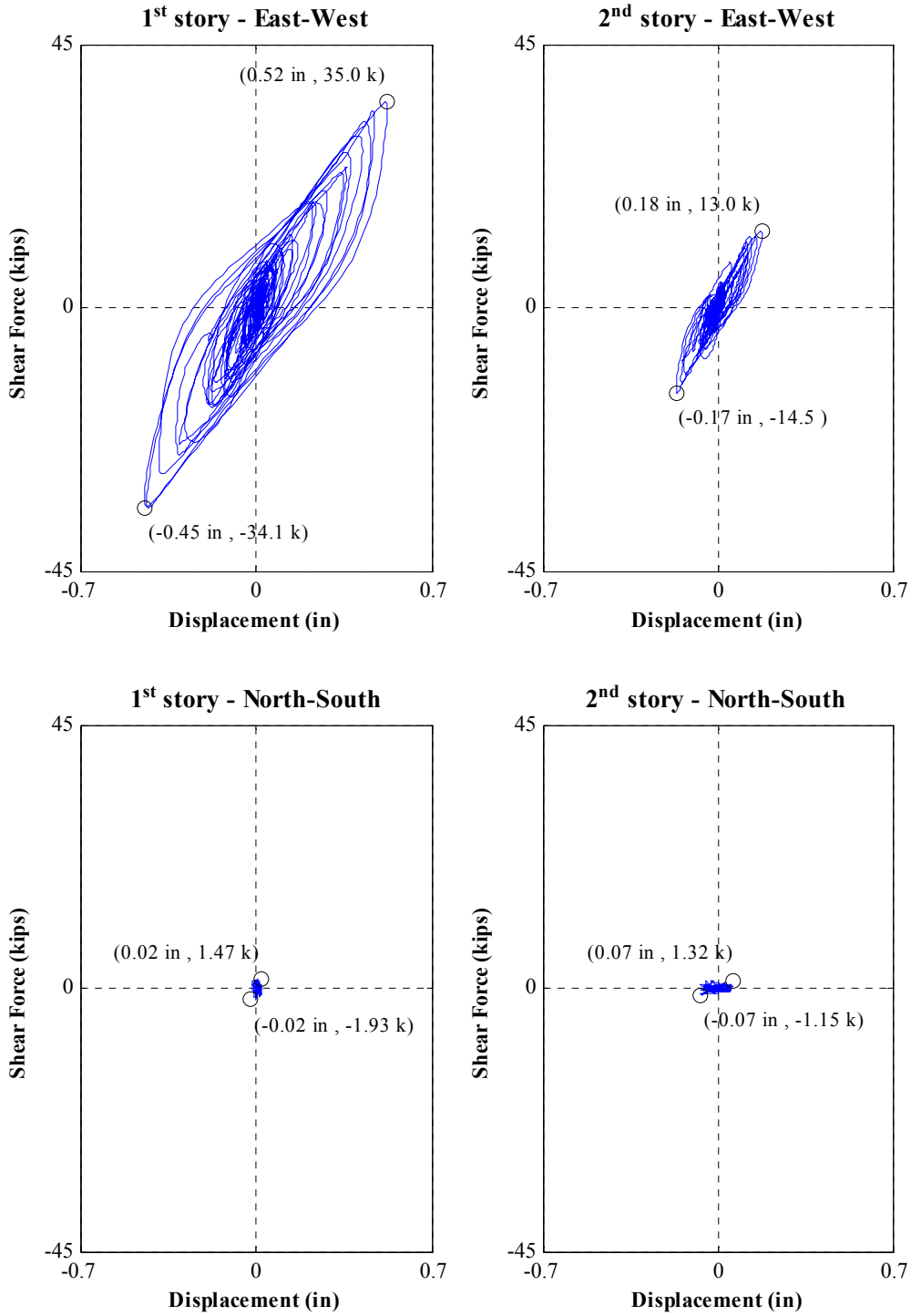


Figure O.31: Interstory force-displacement hysteresis loops for Test NWP2S28

Appendix O

Phase 2, NWP2S29 Seismic Test

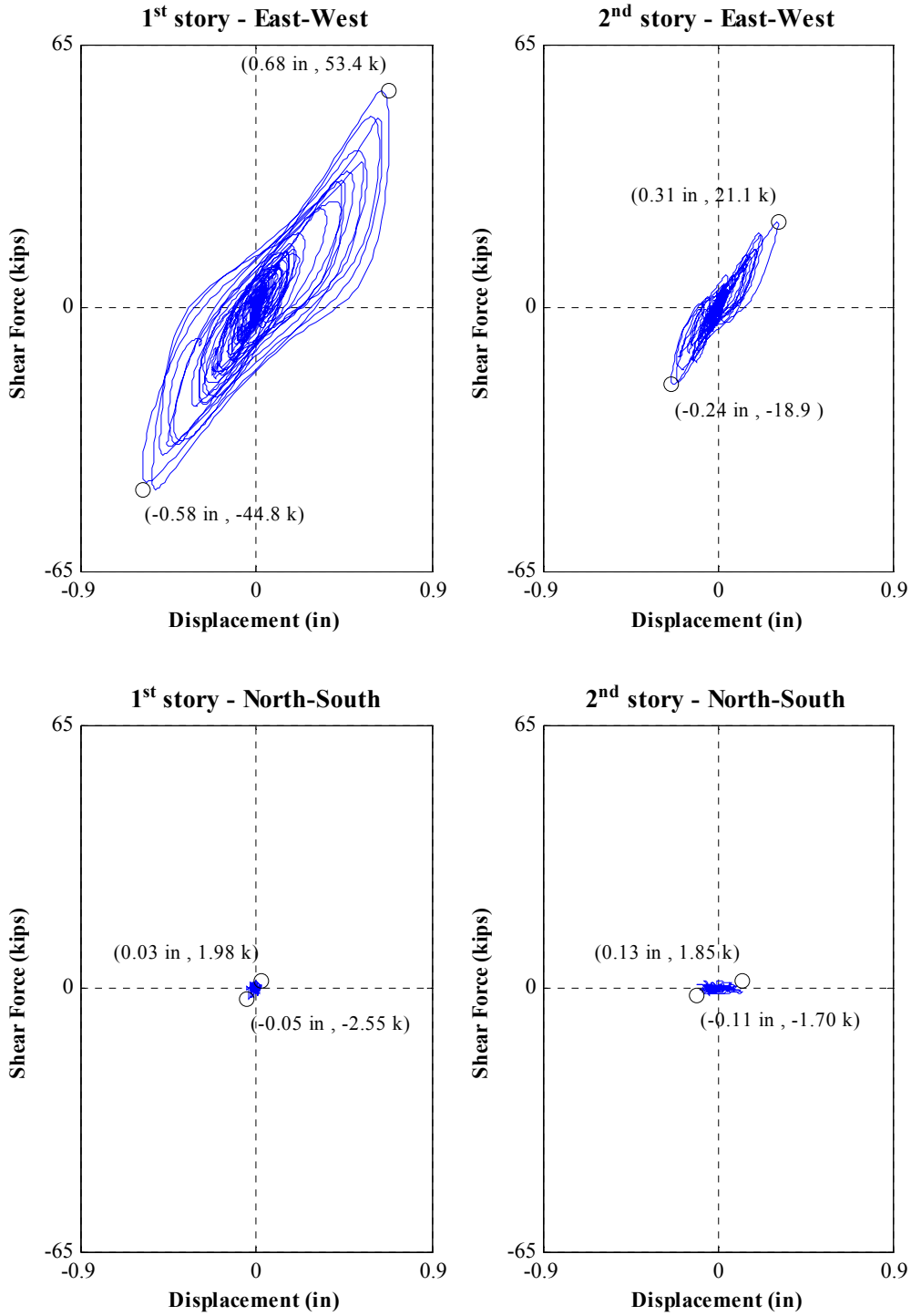


Figure O.32: Interstory force-displacement hysteresis loops for Test NWP2S29

Appendix O

Phase 2, NWP2S30 Seismic Test

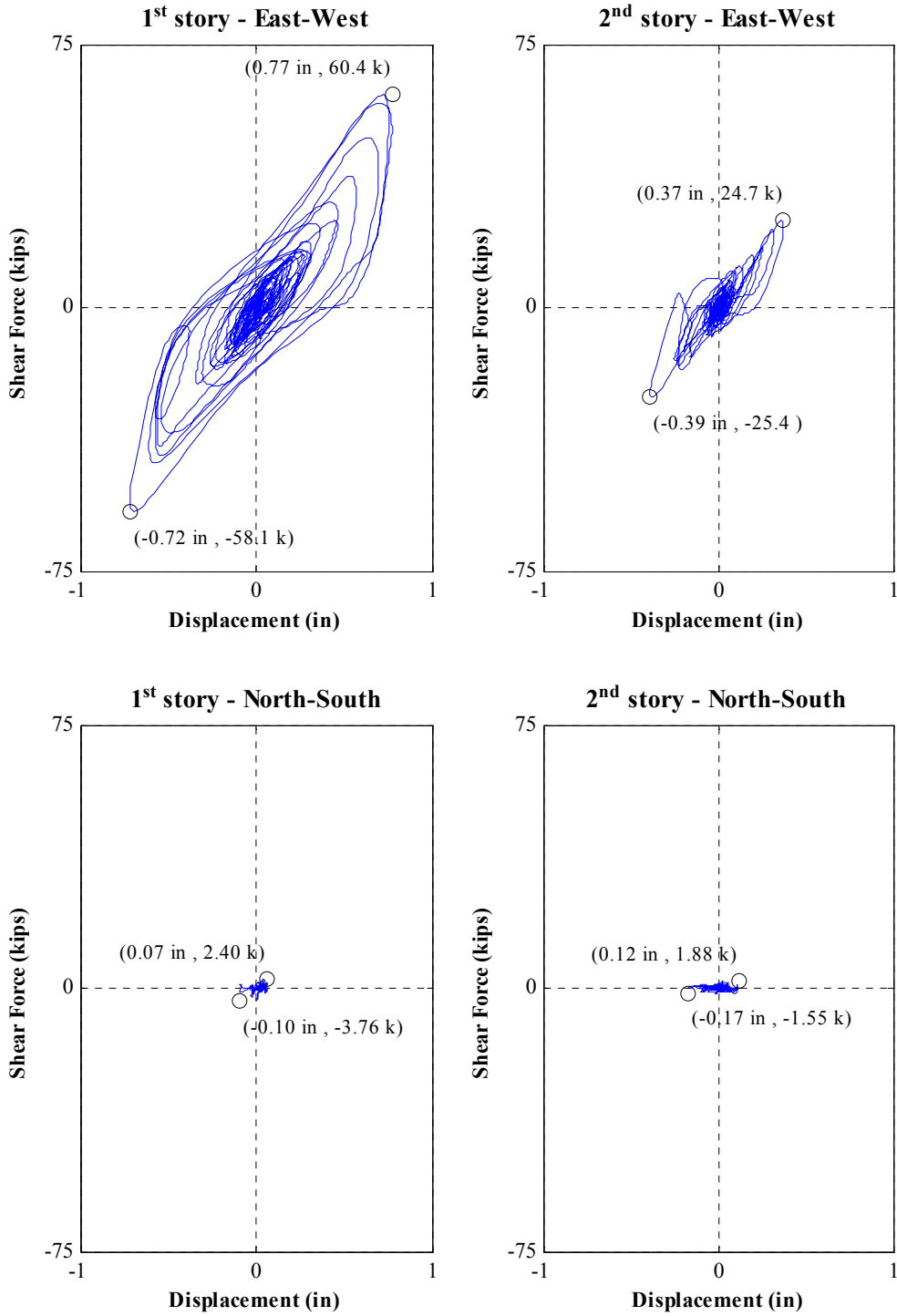


Figure O.33: Interstory force-displacement hysteresis loops for Test NWP2S30

Appendix O

Phase 3, NWP3S01 Seismic Test

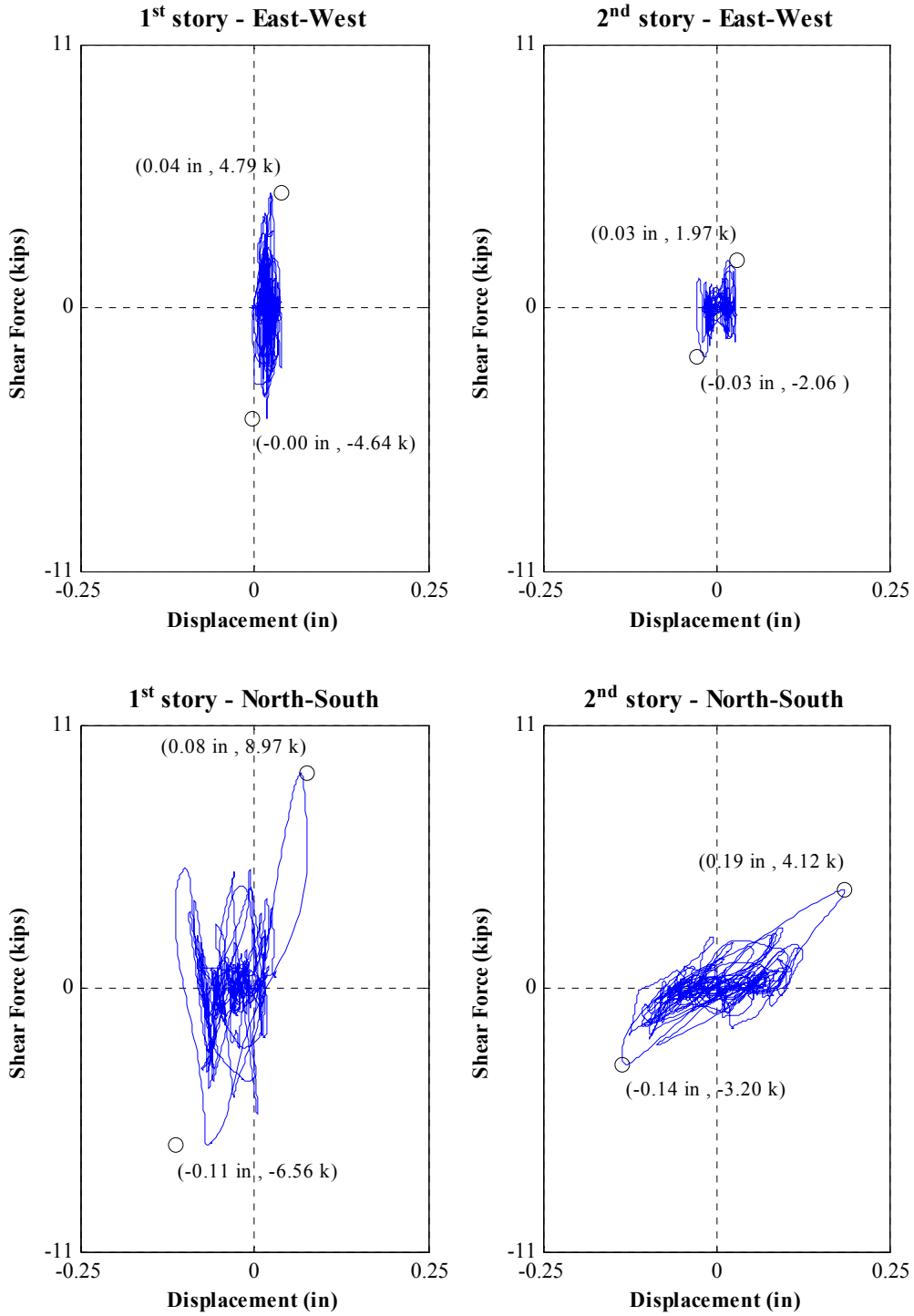


Figure O.34: Interstory force-displacement hysteresis loops for Test NWP3S01

Appendix O

Phase 3, NWP3S02 Seismic Test

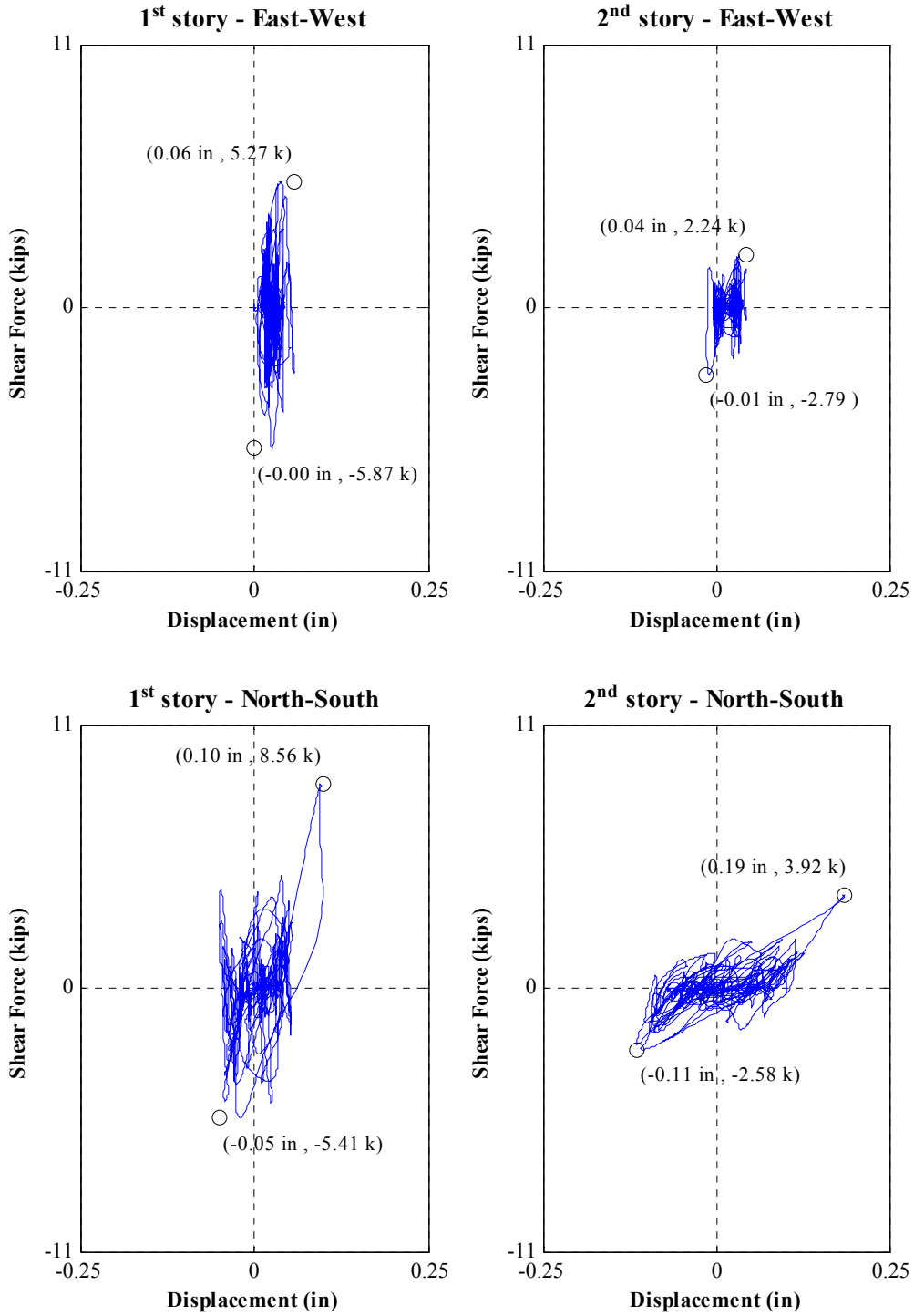


Figure O.35: Interstory force-displacement hysteresis loops for Test NWP3S02

Appendix O

Phase 3, NWP3S03 Seismic Test

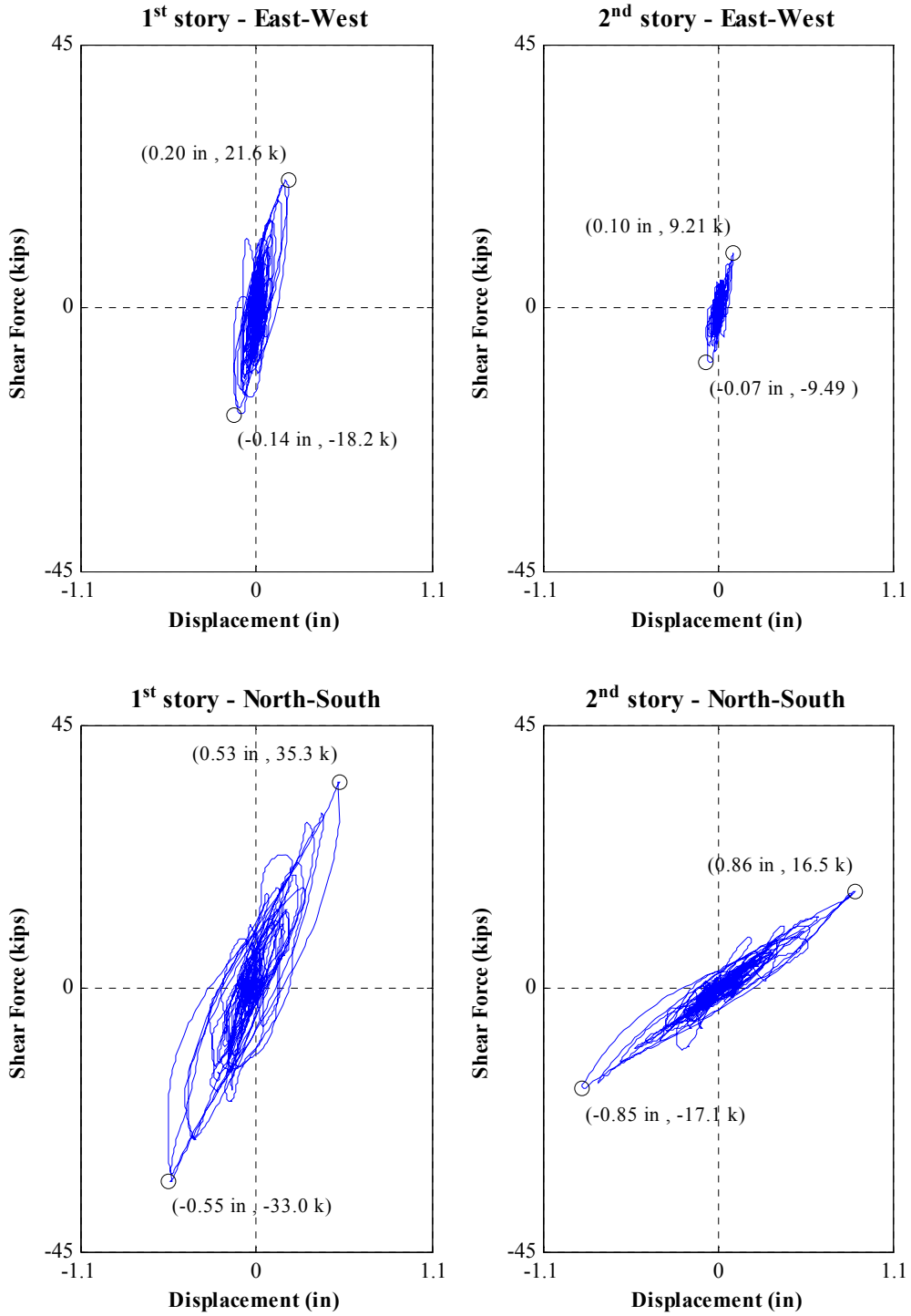


Figure O.36: Interstory force-displacement hysteresis loops for Test NWP3S03

Appendix O

Phase 3, NWP3S04 Seismic Test

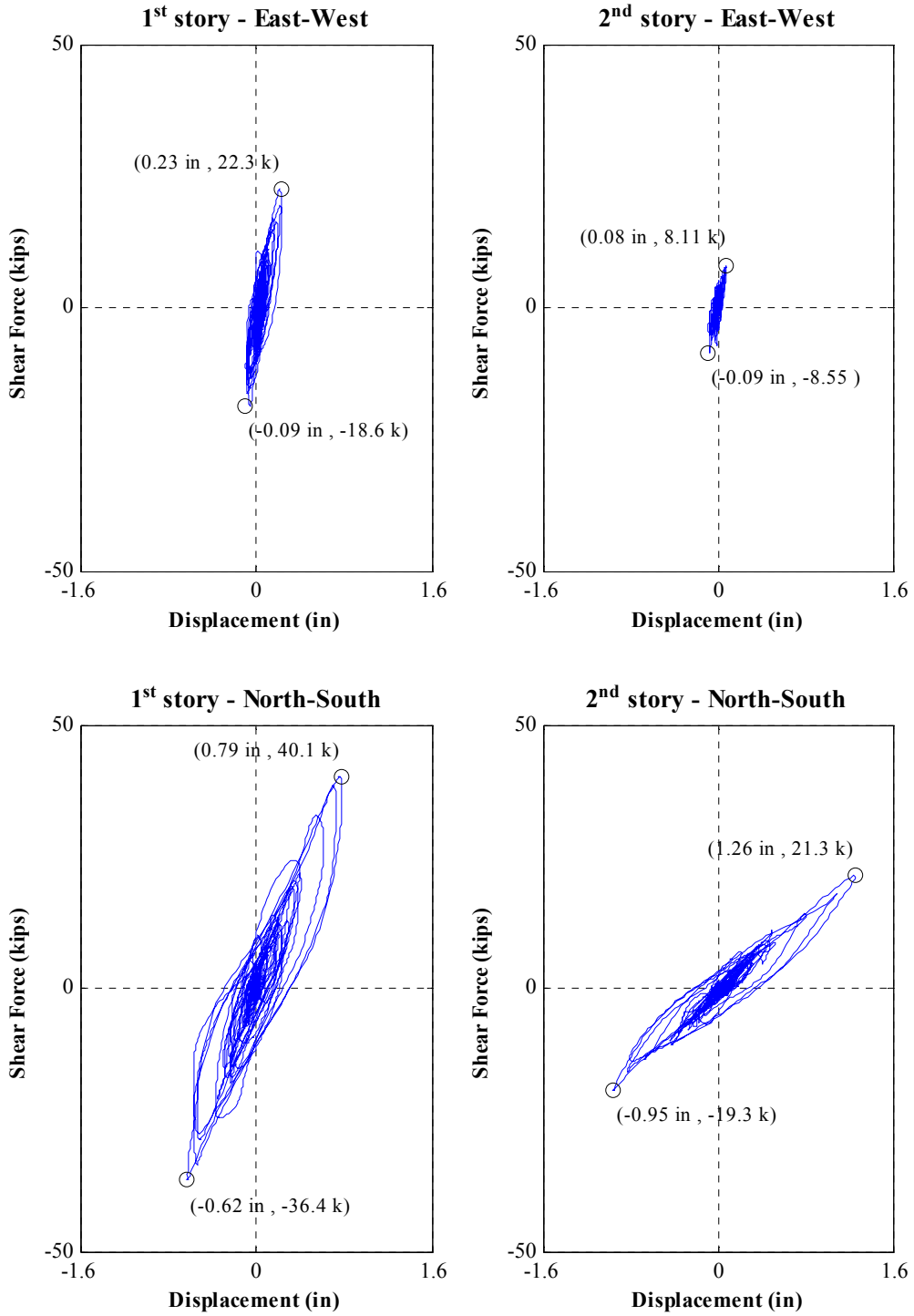


Figure O.37: Interstory force-displacement hysteresis loops for Test NWP3S04

Appendix O

Phase 4, NWP4S01 Seismic Test

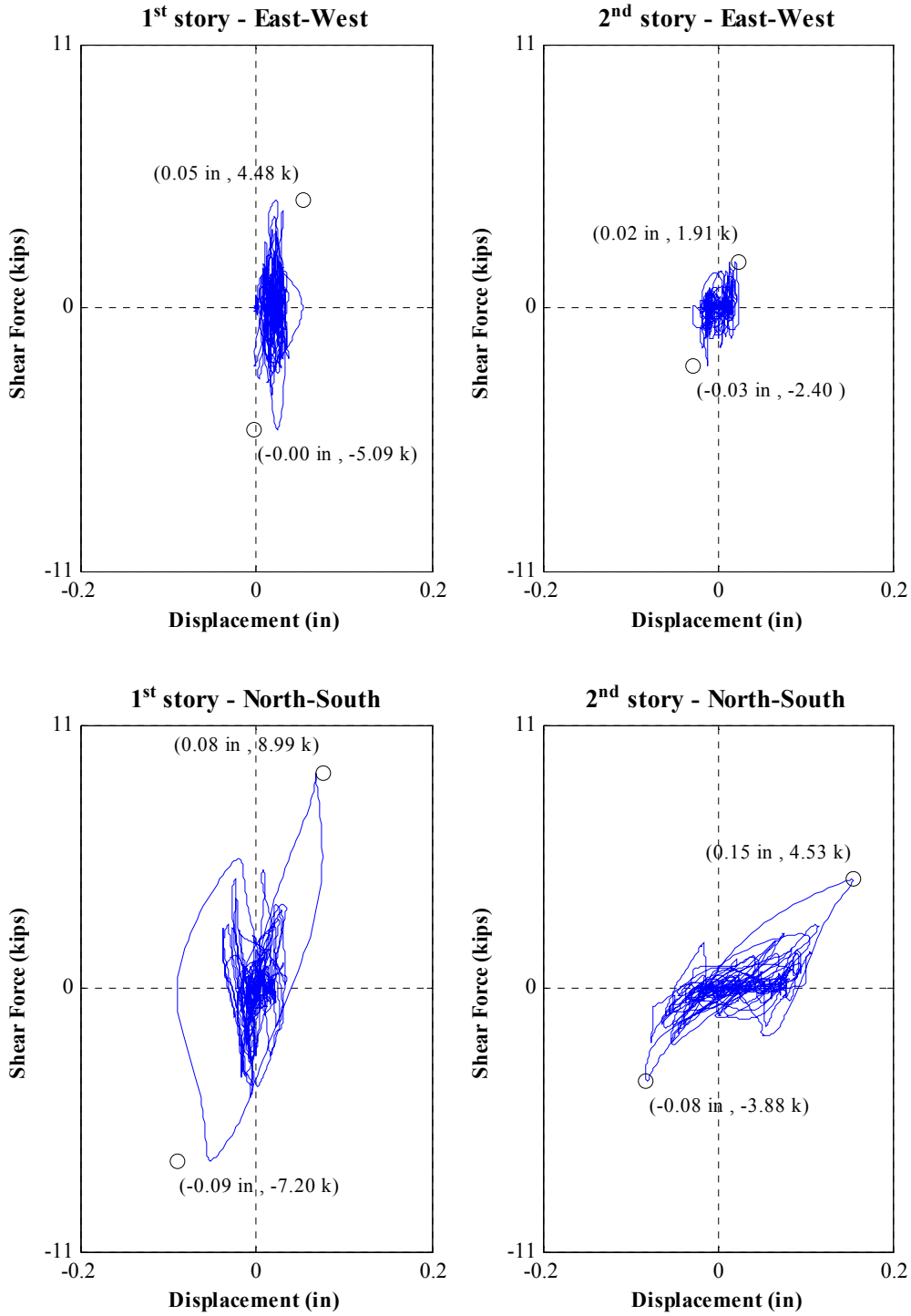


Figure O.38: Interstory force-displacement hysteresis loops for Test NWP4S01

Appendix O

Phase 4, NWP4S02 Seismic Test

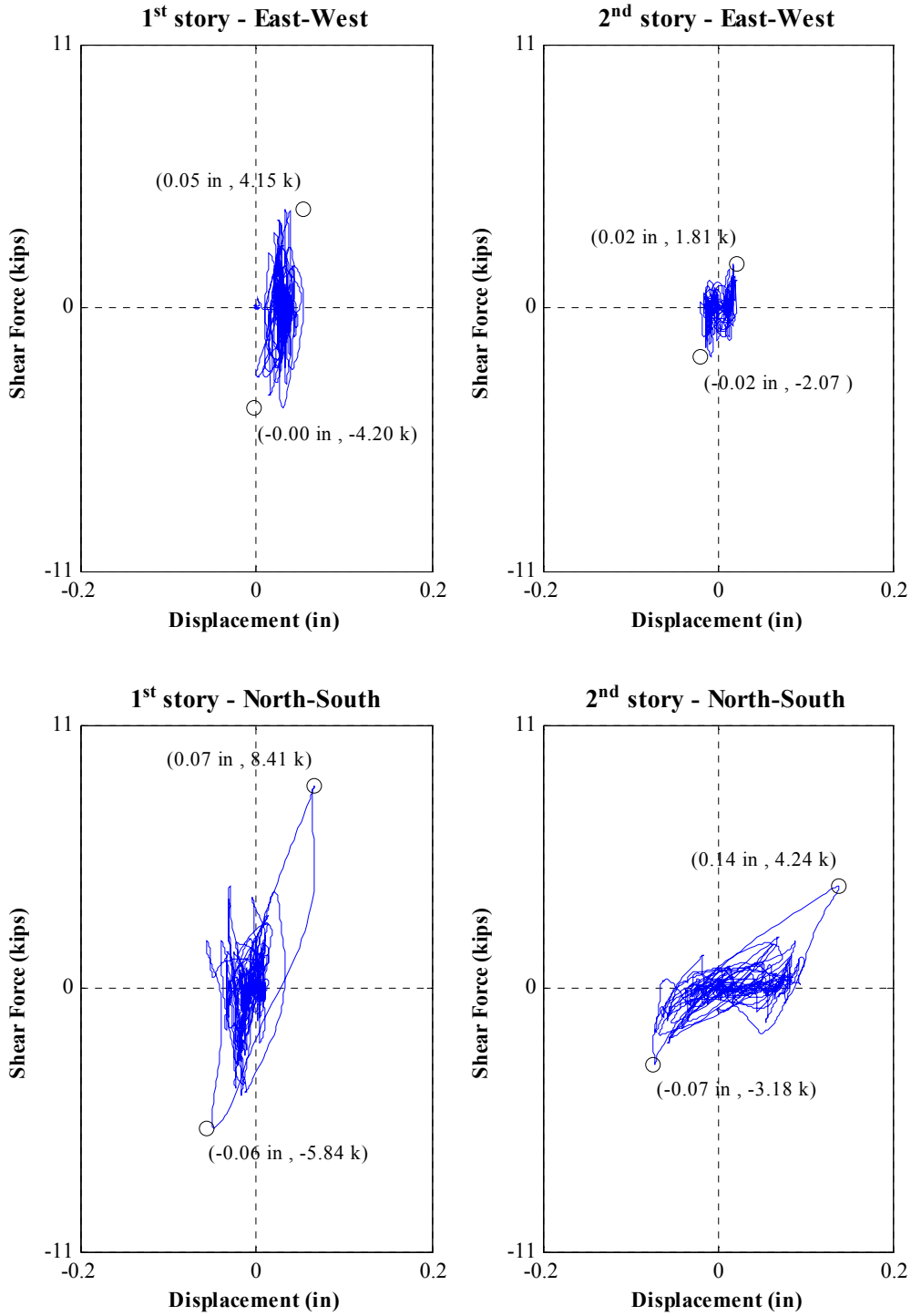


Figure O.39: Interstory force-displacement hysteresis loops for Test NWP4S02

Appendix O

Phase 4, NWP4S03 Seismic Test

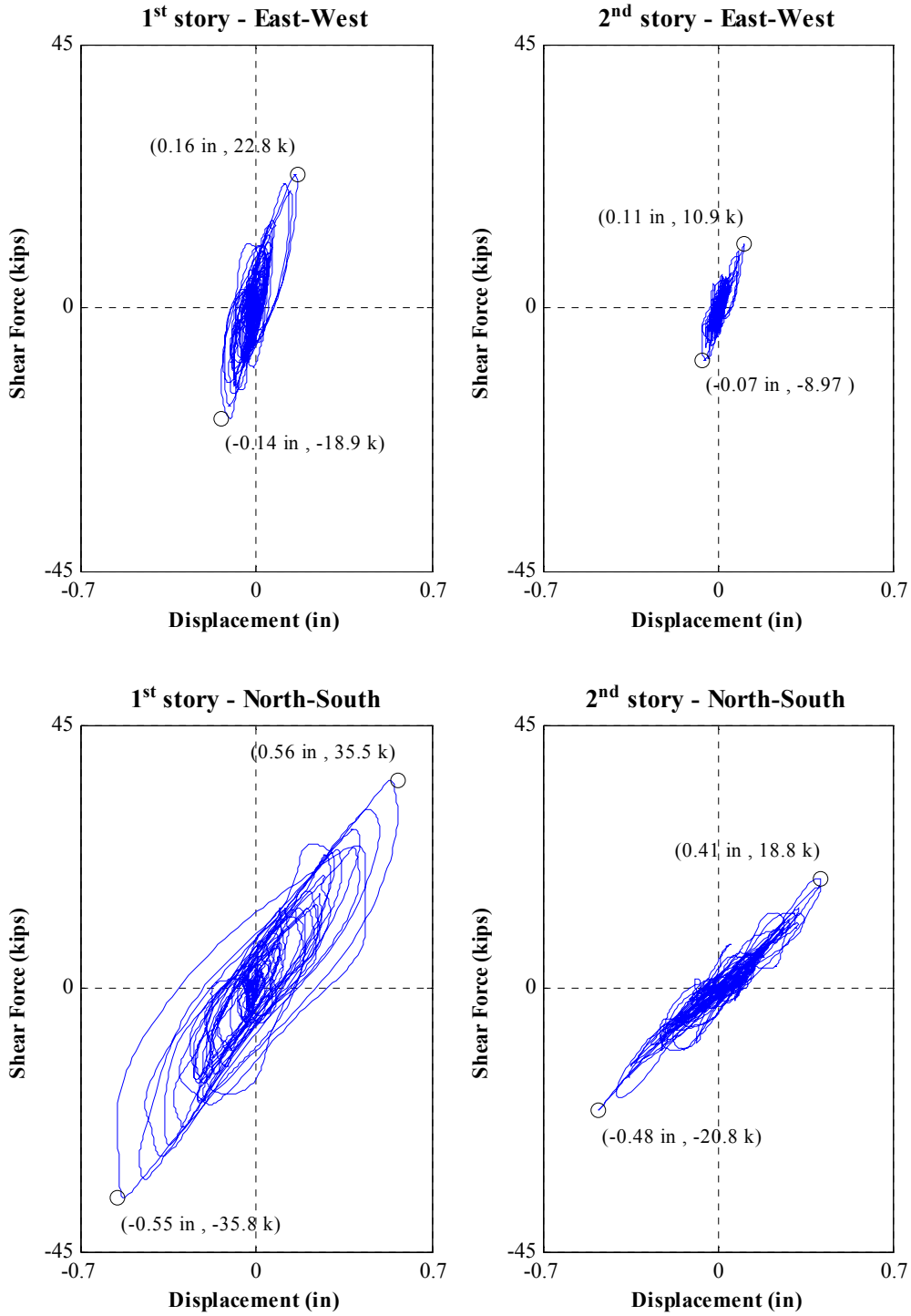


Figure O.40: Interstory force-displacement hysteresis loops for Test NWP4S03

Appendix O

Phase 4, NWP4S04 Seismic Test

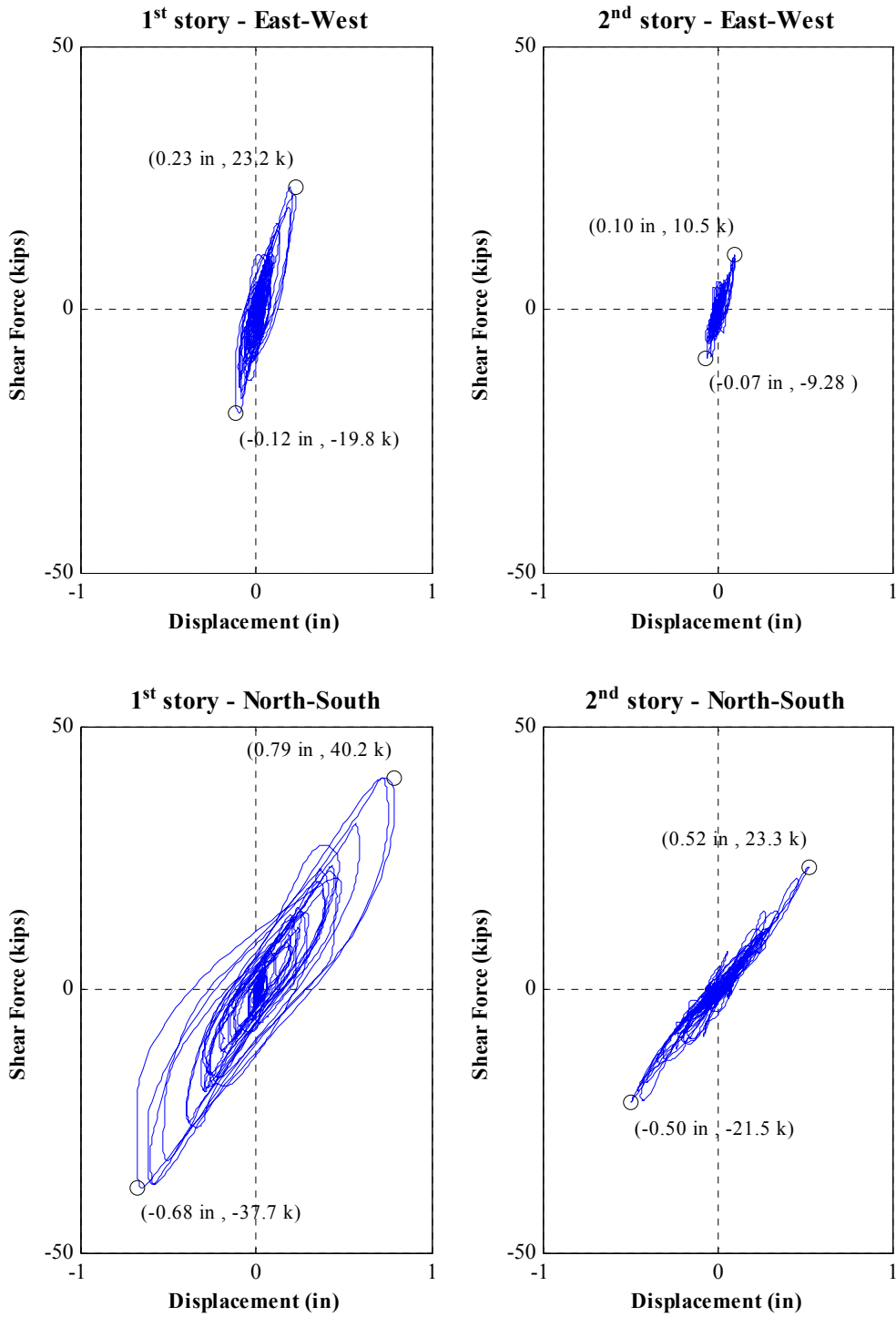


Figure O.41: Interstory force-displacement hysteresis loops for Test NWP4S04

Appendix O

Phase 5, NWP5S01 Seismic Test

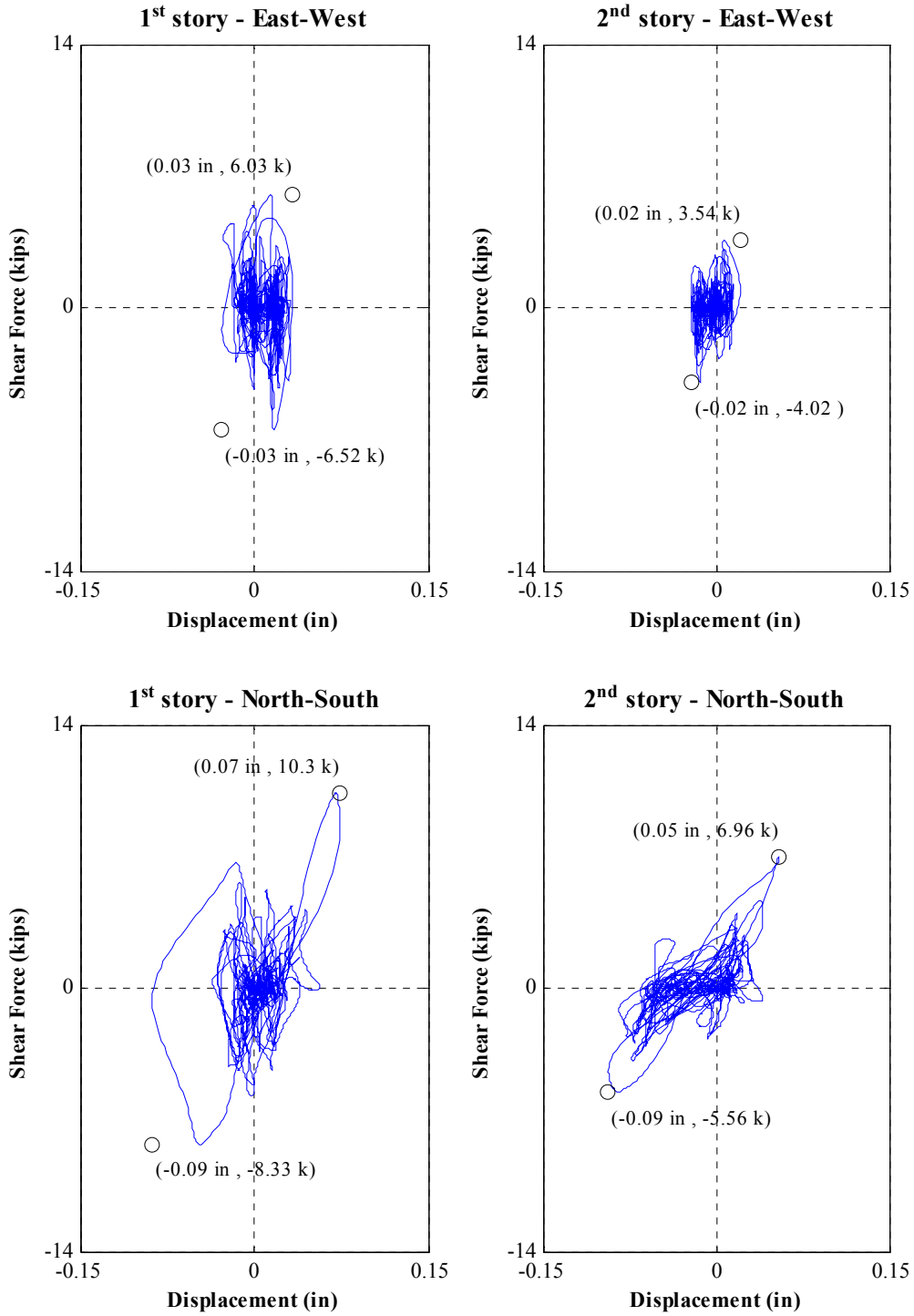


Figure O.42: Interstory force-displacement hysteresis loops for Test NWP5S01

Appendix O

Phase 5, NWP5S02 Seismic Test

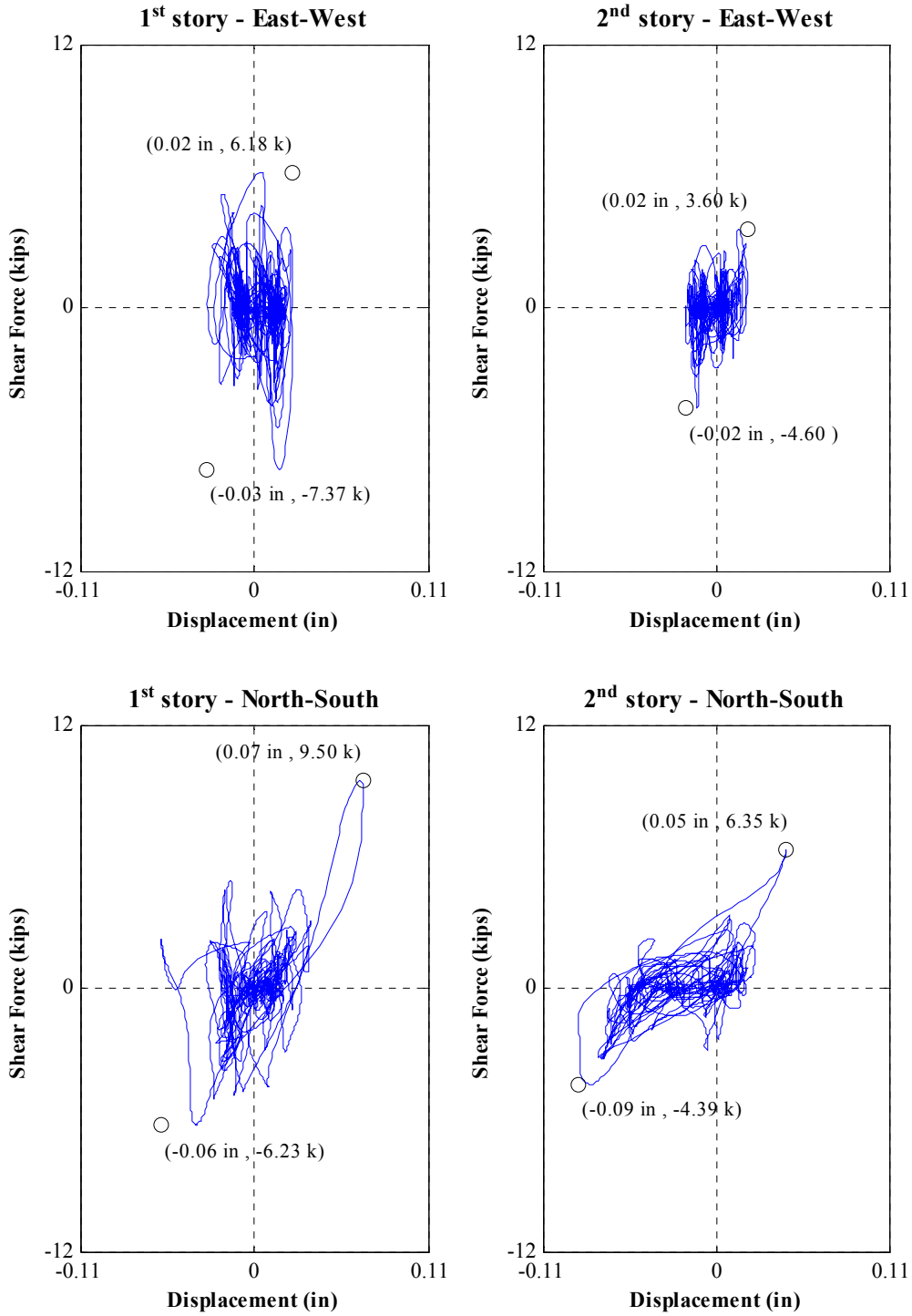


Figure O.43: Interstory force-displacement hysteresis loops for Test NWP5S02

Appendix O

Phase 5, NWP5S03 Seismic Test

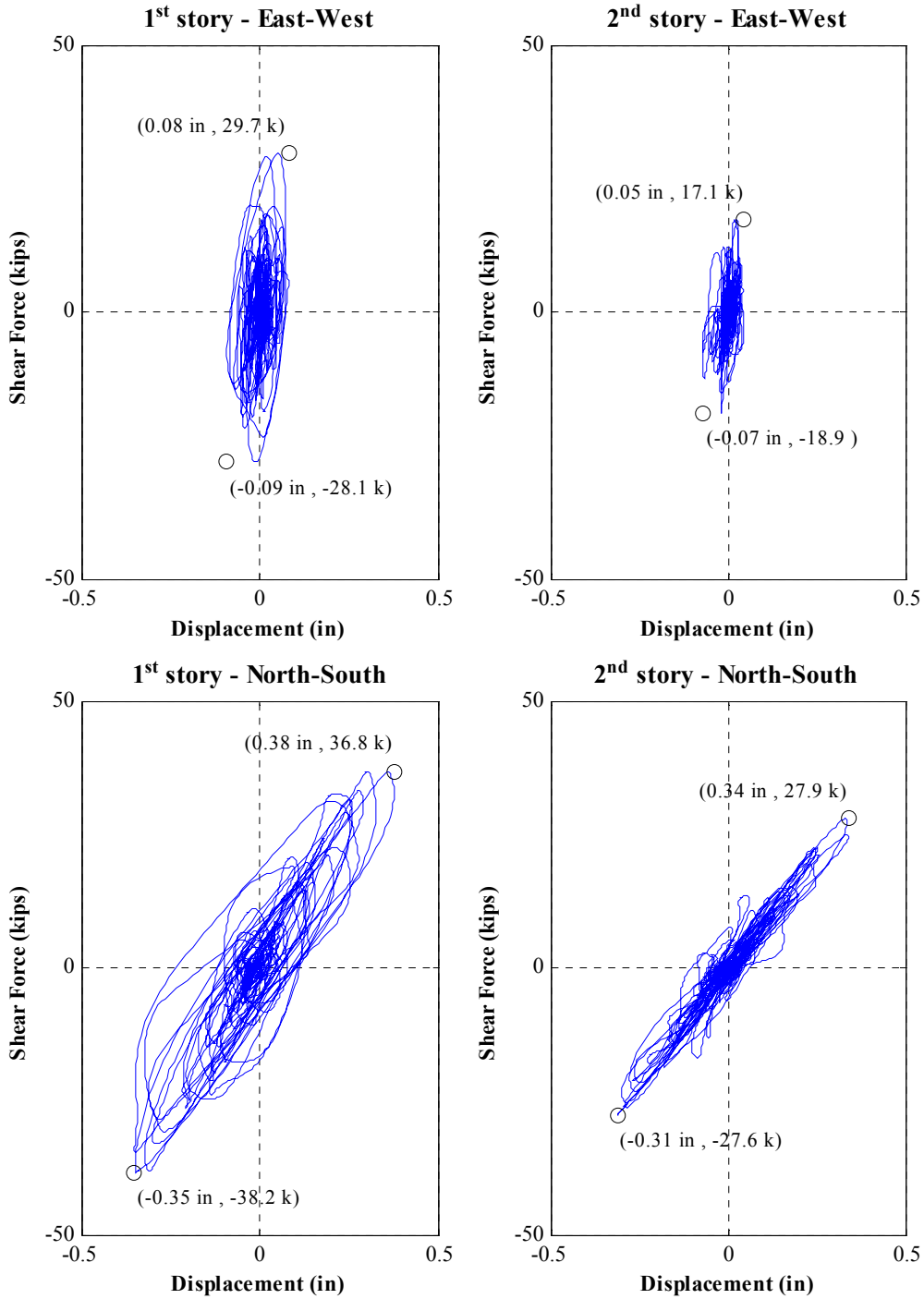


Figure O.44: Interstory force-displacement hysteresis loops for Test NWP5S03

Appendix O

Phase 5, NWP5S04 Seismic Test

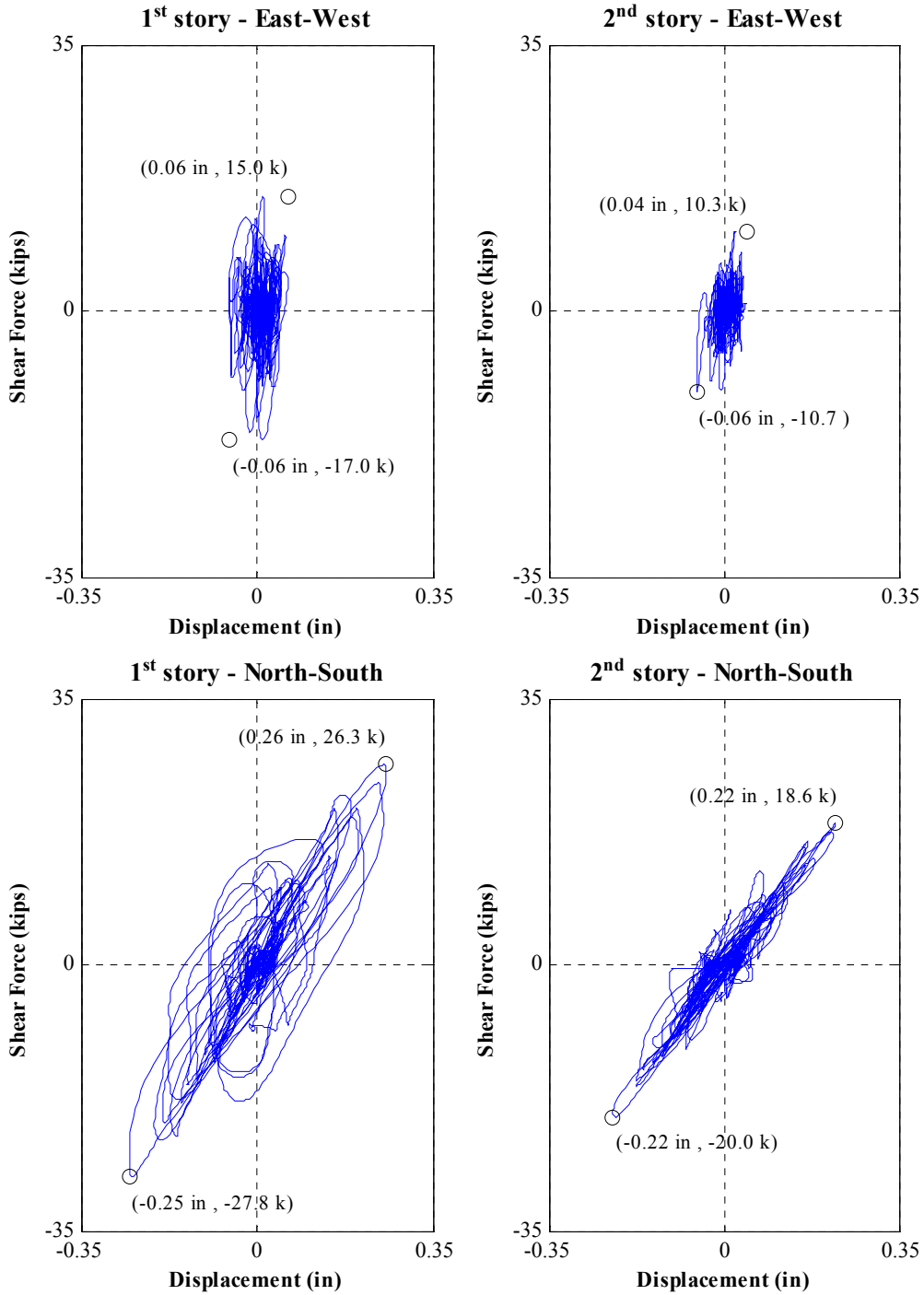


Figure O.45: Interstory force-displacement hysteresis loops for Test NWP5S04

Appendix O

Phase 5, NWP5S05 Seismic Test

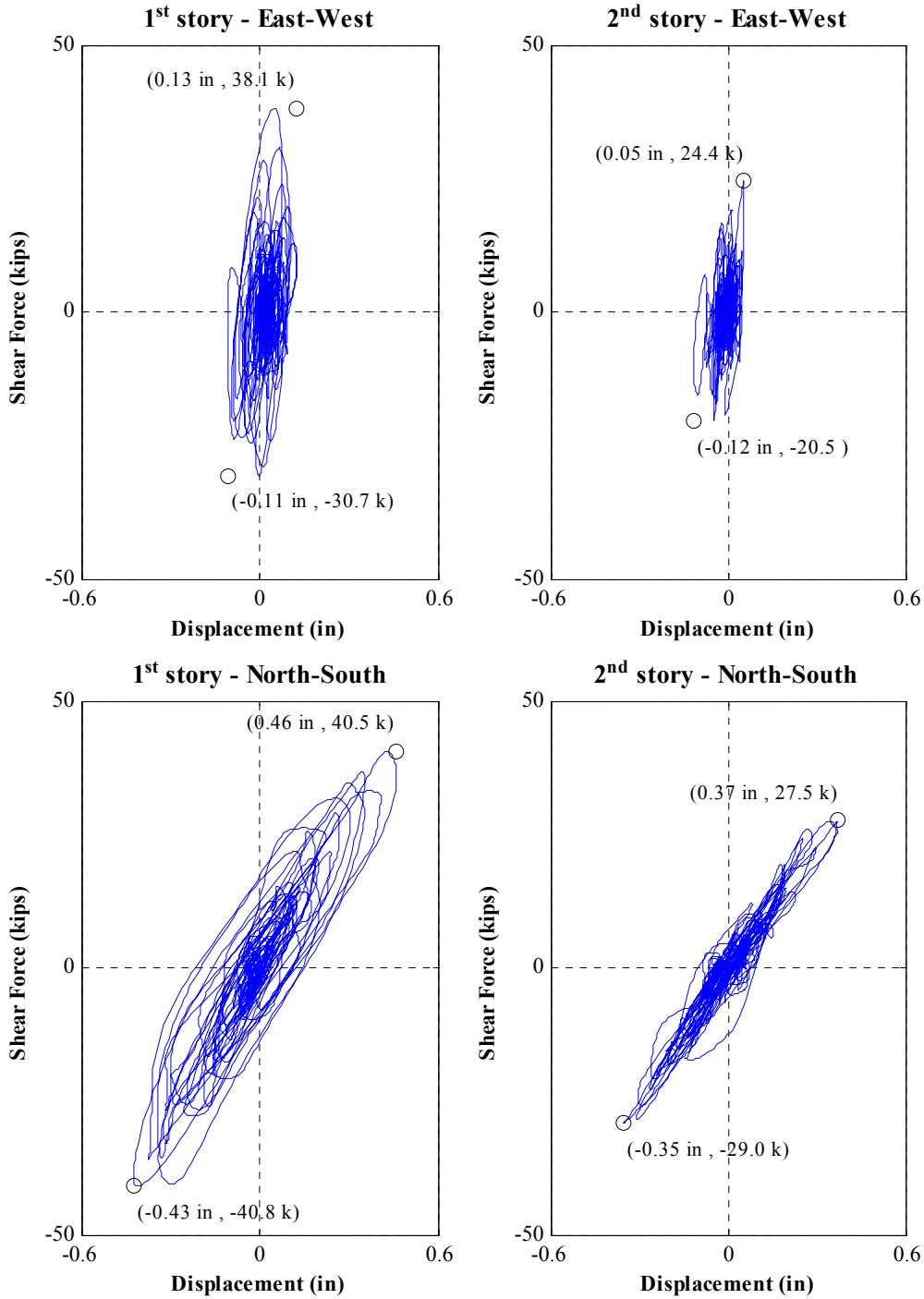


Figure O.46: Interstory force-displacement hysteresis loops for Test NWP5S05

Appendix O

Phase 5, NWP5S06 Seismic Test

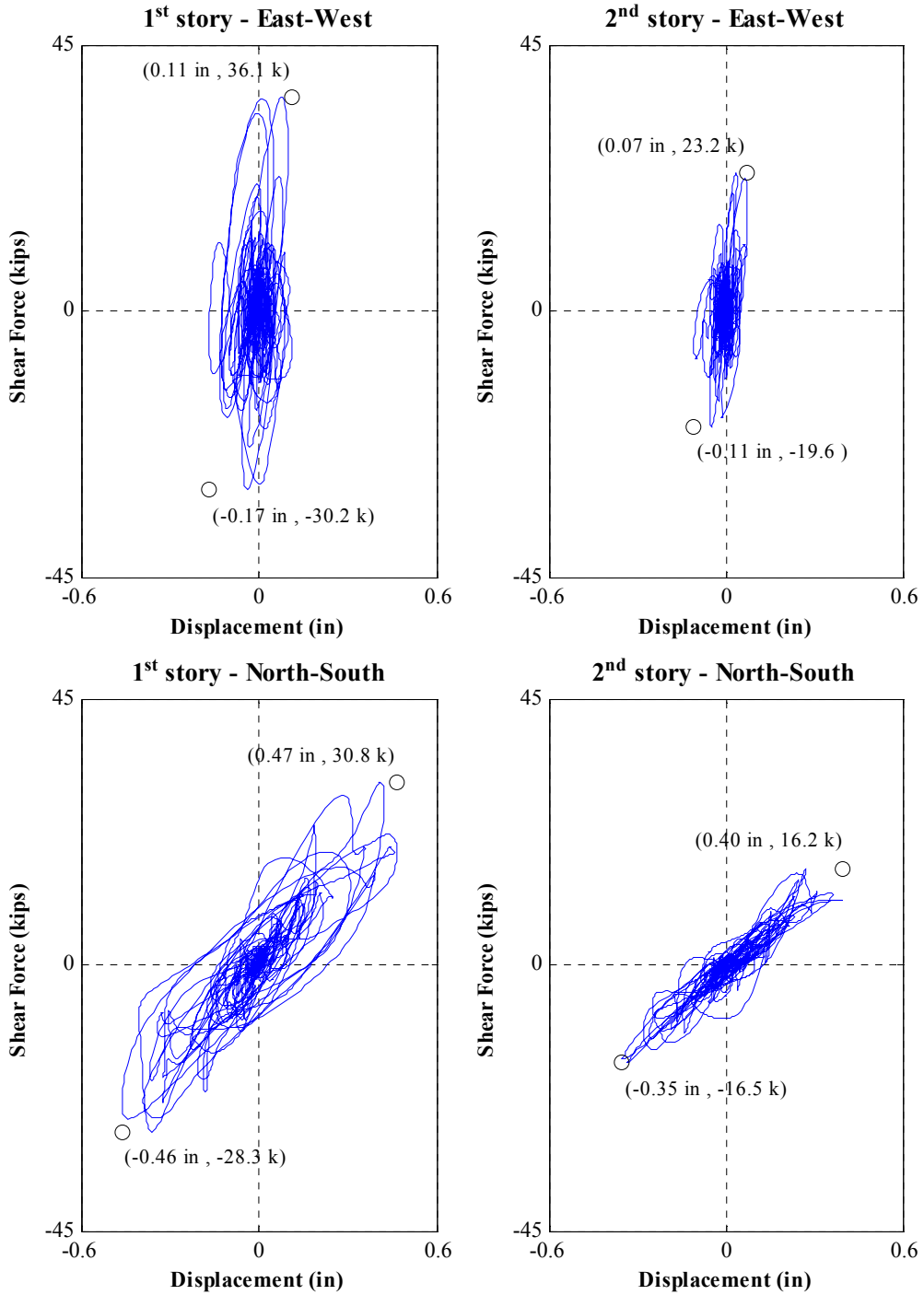


Figure O.47: Interstory force-displacement hysteresis loops for Test NWP5S06

Appendix O

Phase 5, NWP5S07 Seismic Test

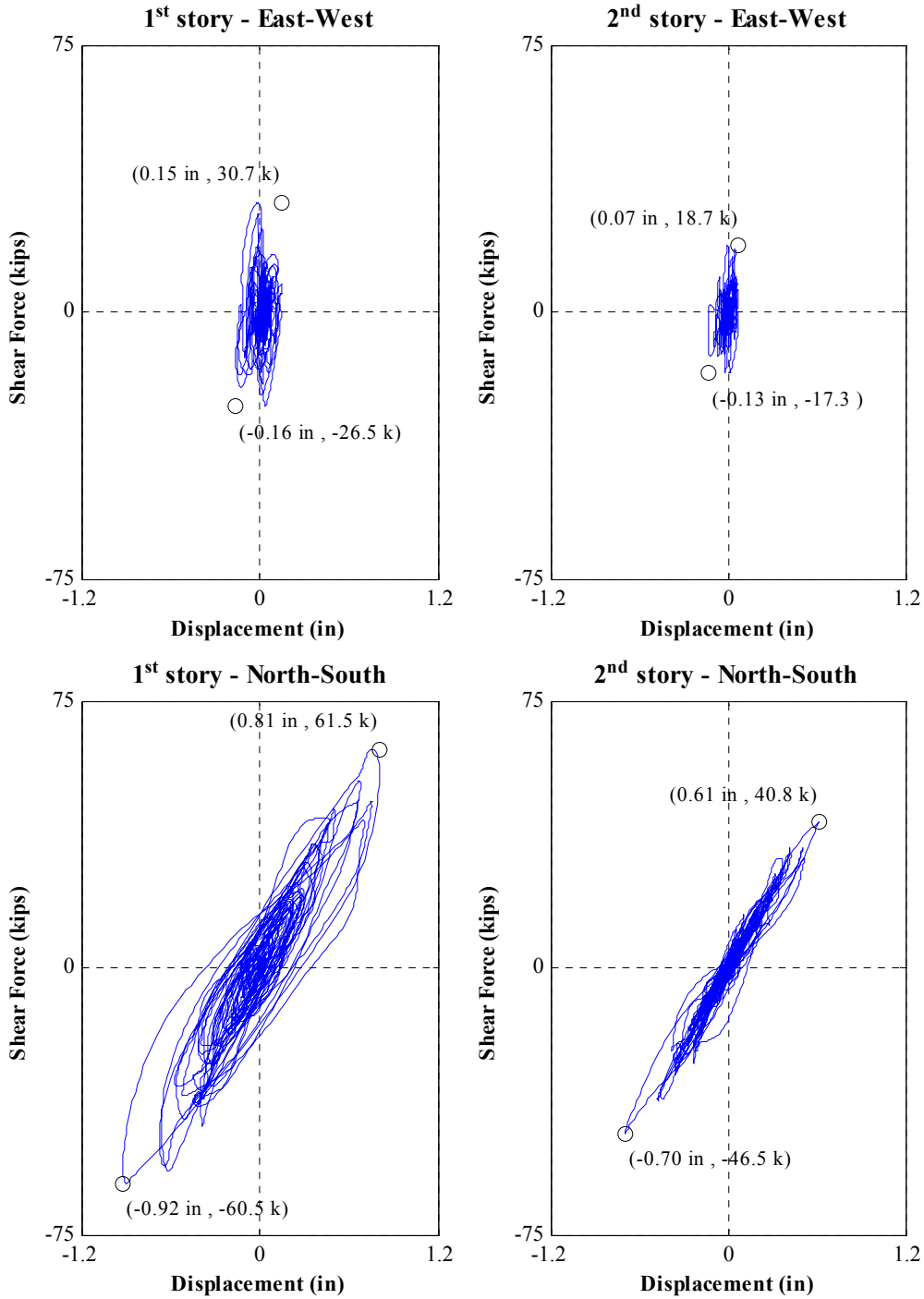


Figure O.48: Interstory force-displacement hysteresis loops for Test NWP5S07

Appendix O

Phase 5, NWP5S08 Seismic Test

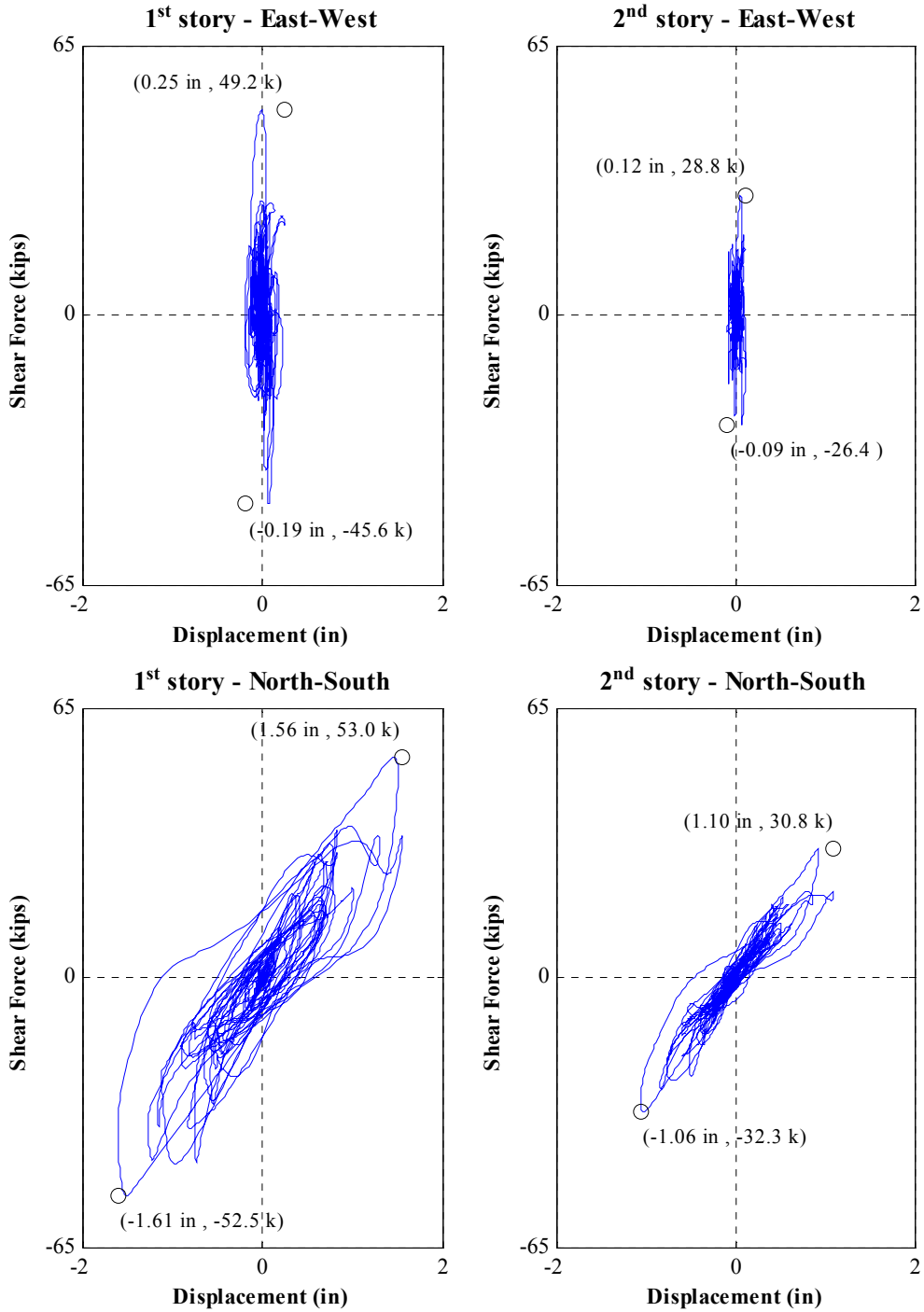


Figure O.49: Interstory force-displacement hysteresis loops for Test NWP5S08

Appendix O

Phase 5, NWP5S09 Seismic Test

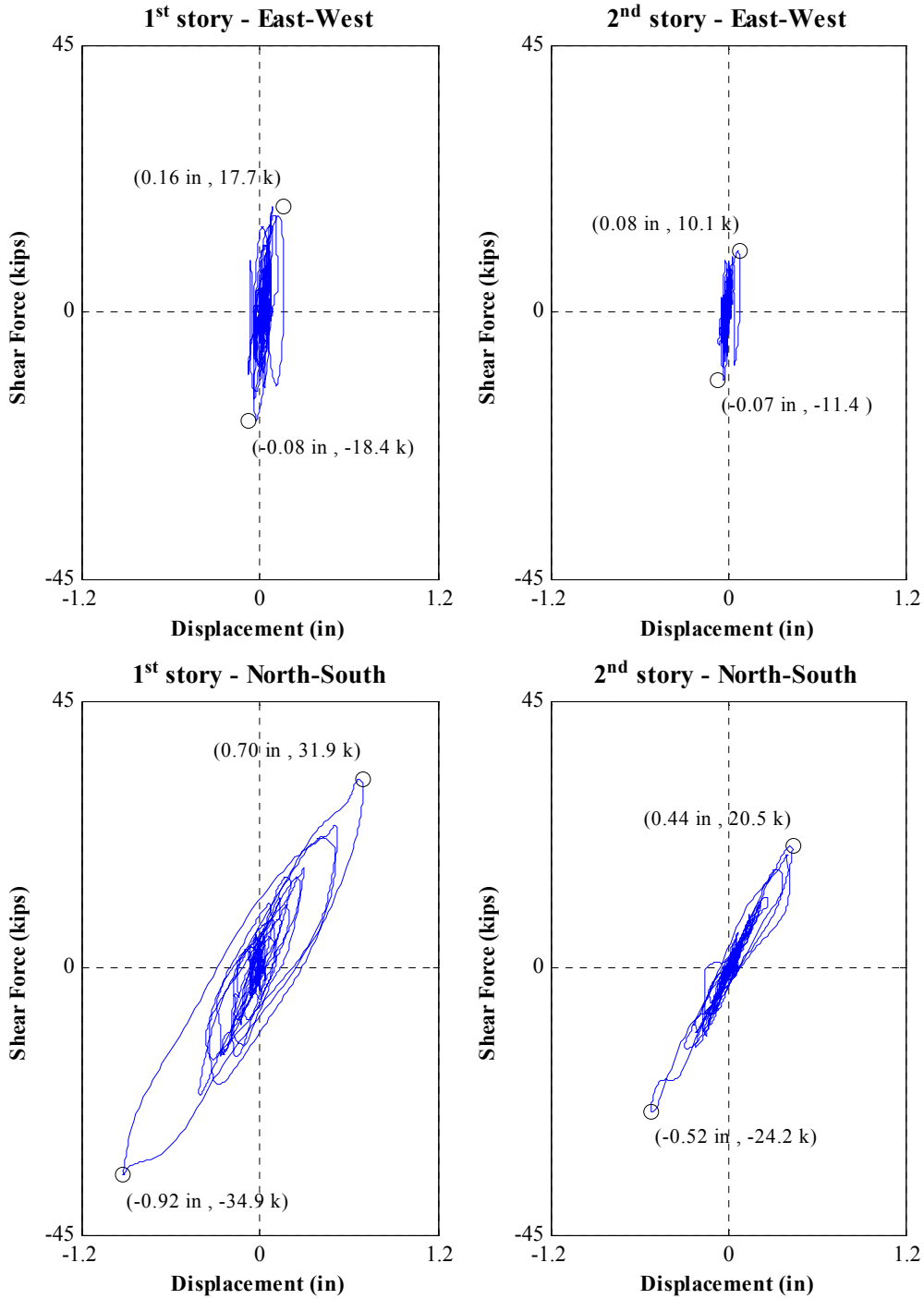


Figure O.50: Interstory force-displacement hysteresis loops for Test NWP5S09

Appendix O

Phase 5, NWP5S11 Seismic Test

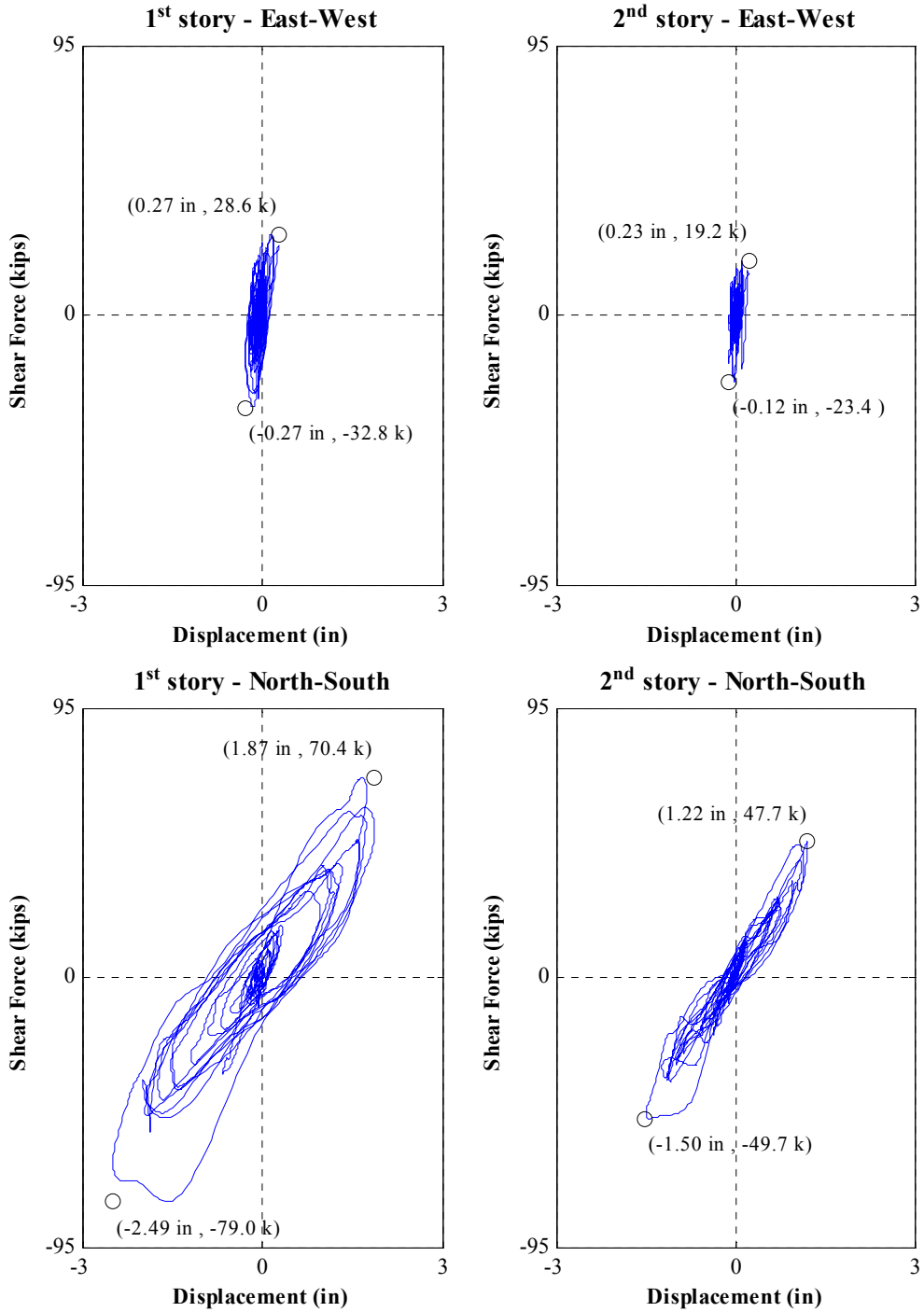


Figure O.51: Interstory force-displacement hysteresis loops for Test NWP5S11

Appendix P
Selected Seismic Results:
Sill Plate Slippage Time Histories

Appendix P

Phase 1, NWP1S01 Seismic Test

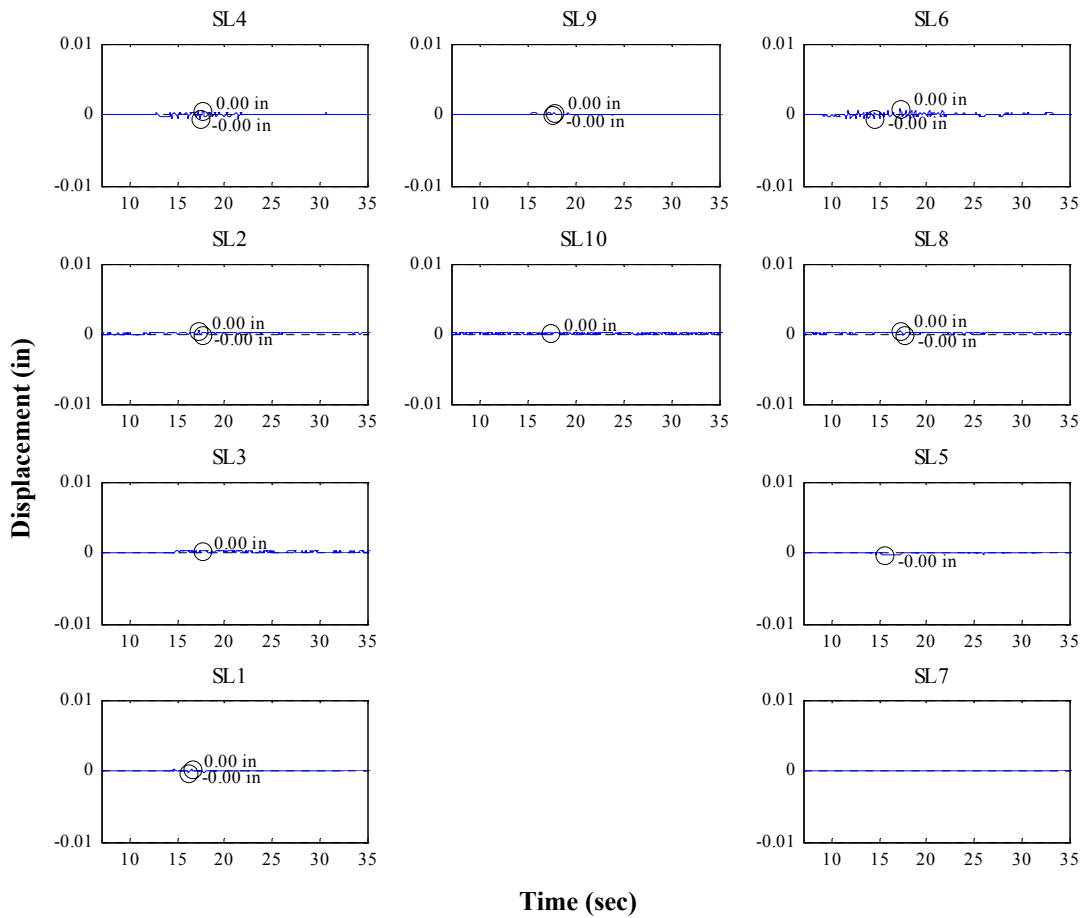
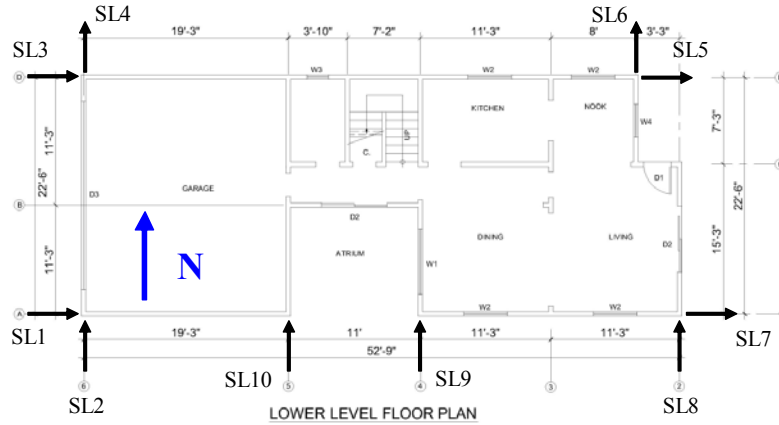


Figure P.1: Sill plate slippage time histories for Test NWP1S01

Appendix P

Phase 1, NWP1S02 Seismic Test

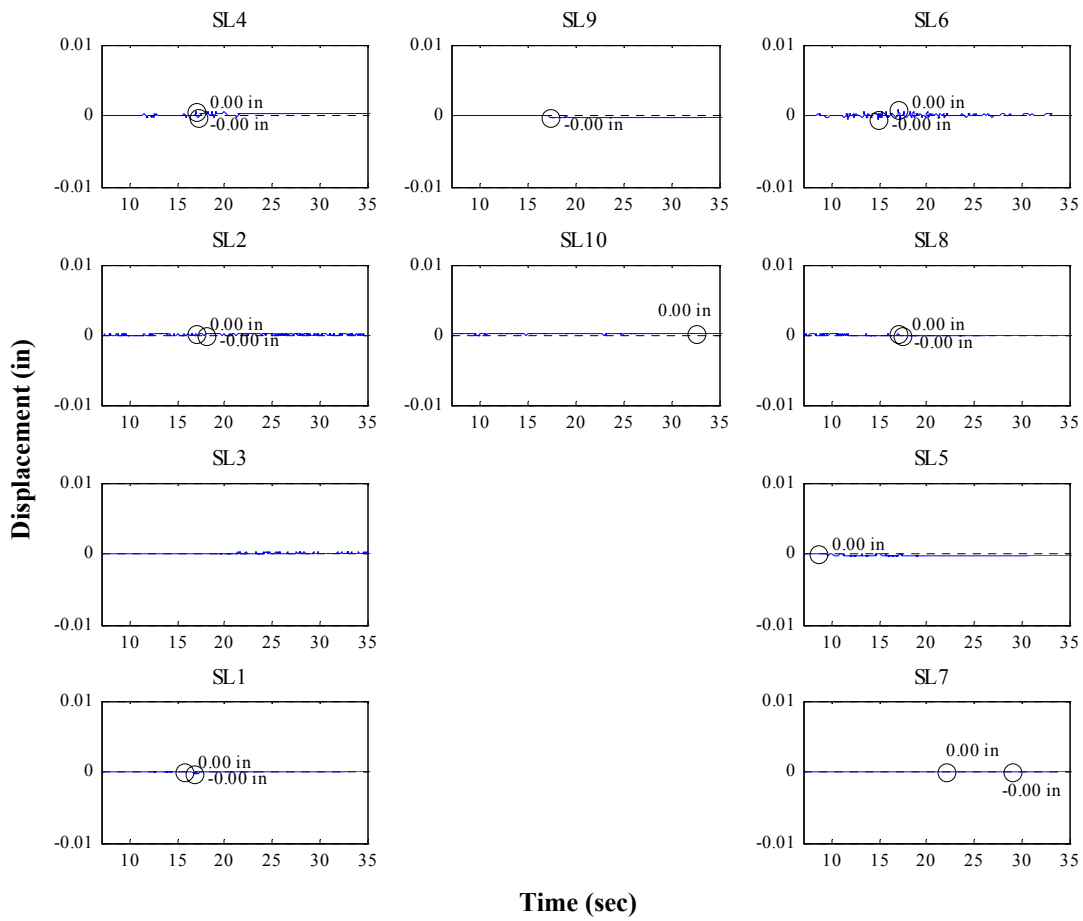
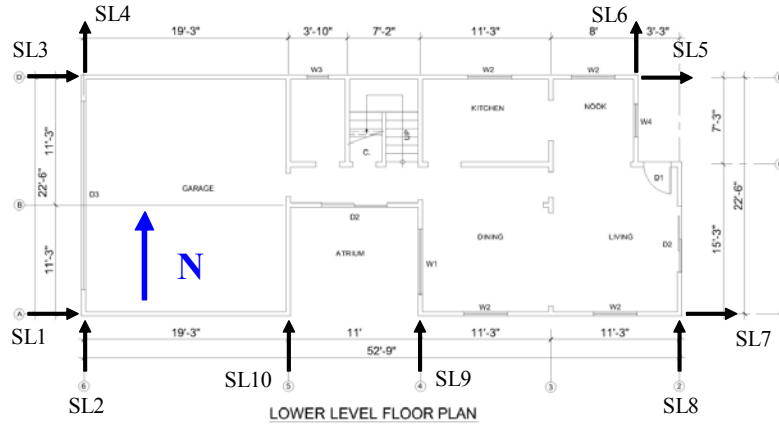


Figure P.2: Sill plate slippage time histories for Test NWP1S02

Appendix P

Phase 1, NWP1S03 Seismic Test

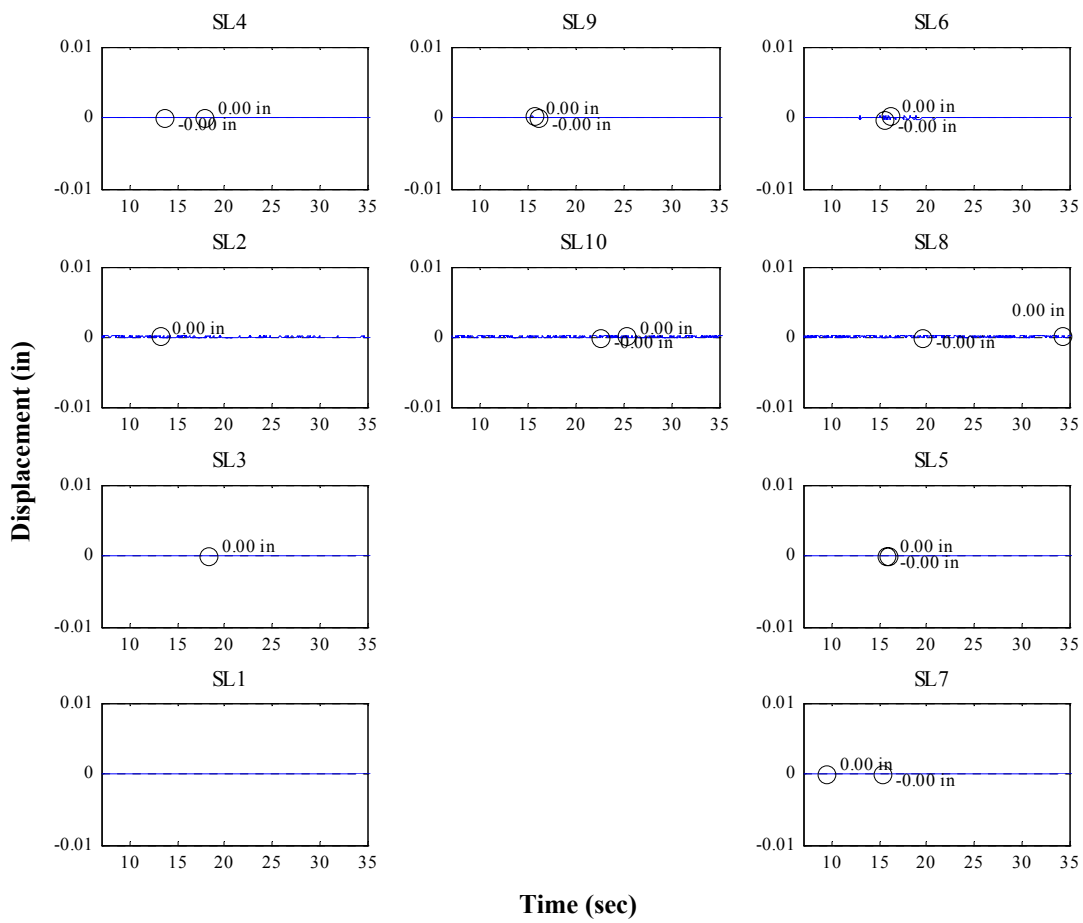
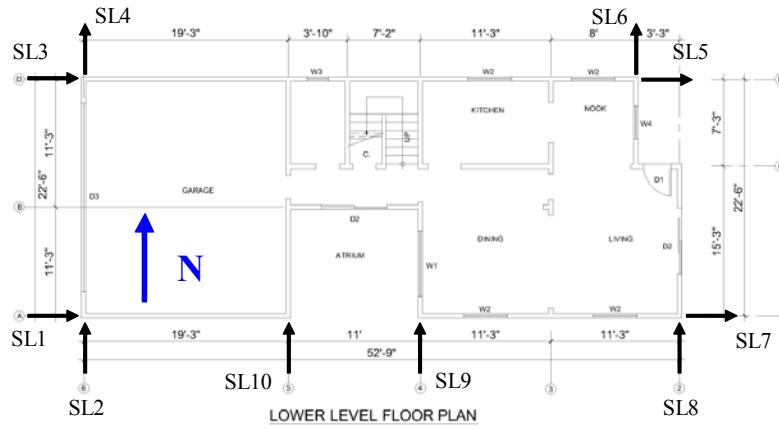


Figure P.3: Sill plate slippage time histories for Test NWP1S03

Appendix P

Phase 1, NWP1S04 Seismic Test

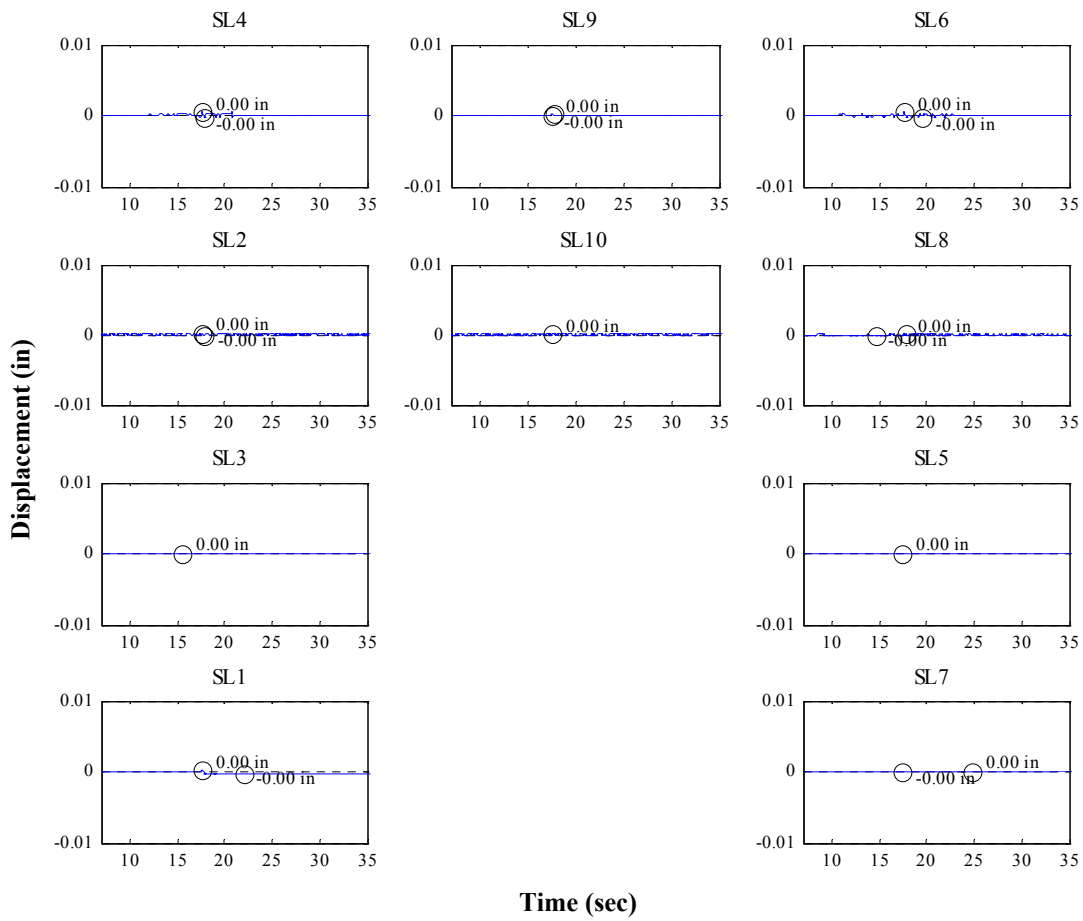
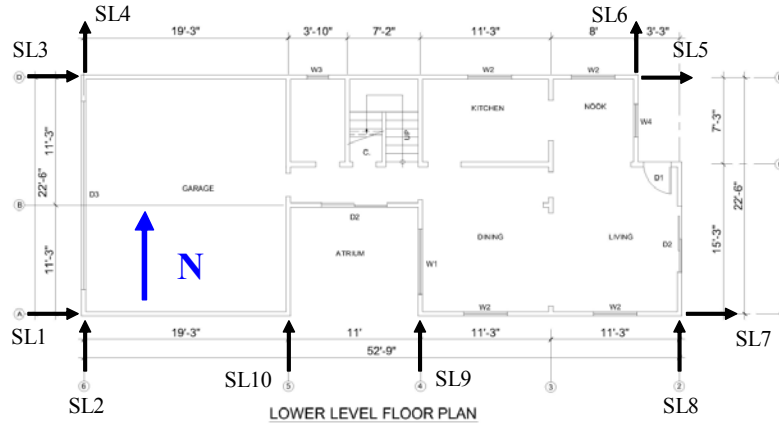


Figure P.4: Sill plate slippage time histories for Test NWP1S04

Appendix P

Phase 1, NWP1S05 Seismic Test

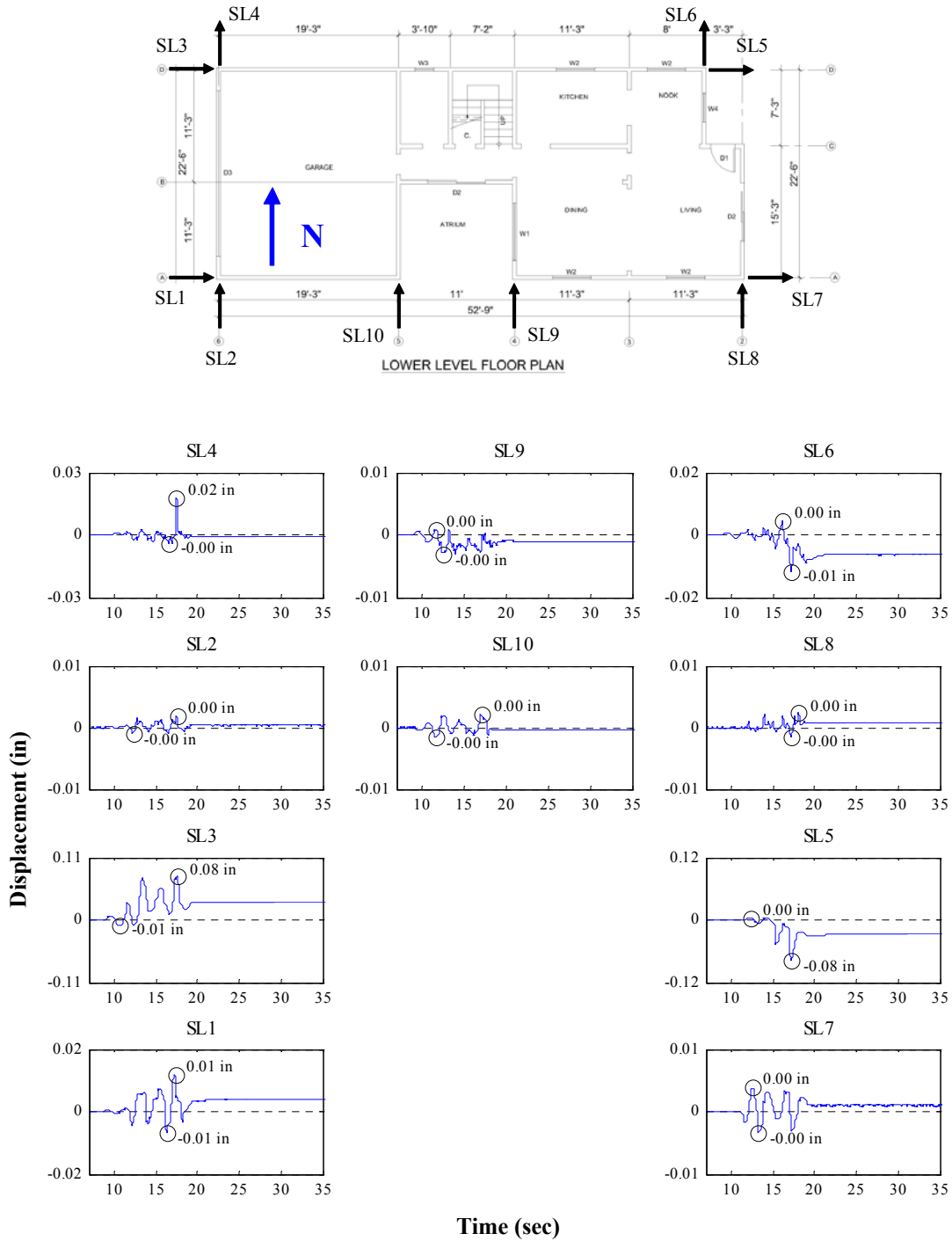


Figure P.5 Sill plate slippage time histories for Test NWP1S05

Appendix P

Phase 1, NWP1S17 Seismic Test

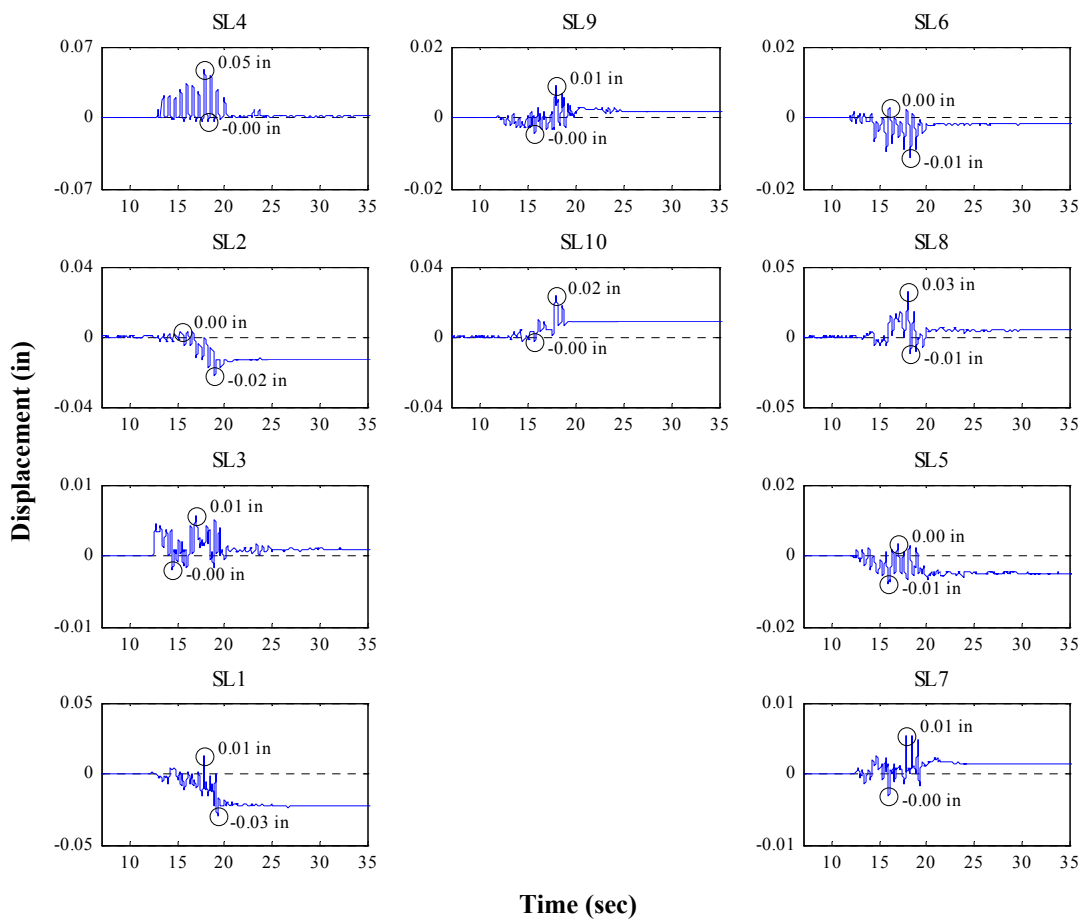
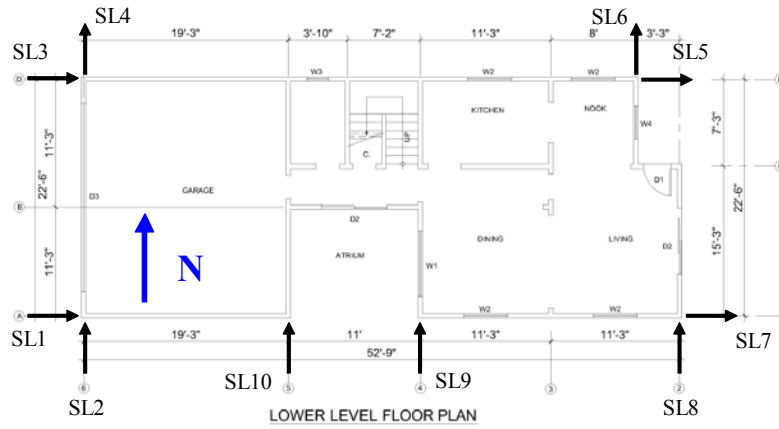


Figure P.6: Sill plate slippage time histories for Test NWP1S17

Appendix P

Phase 1, NWP1S07 Seismic Test

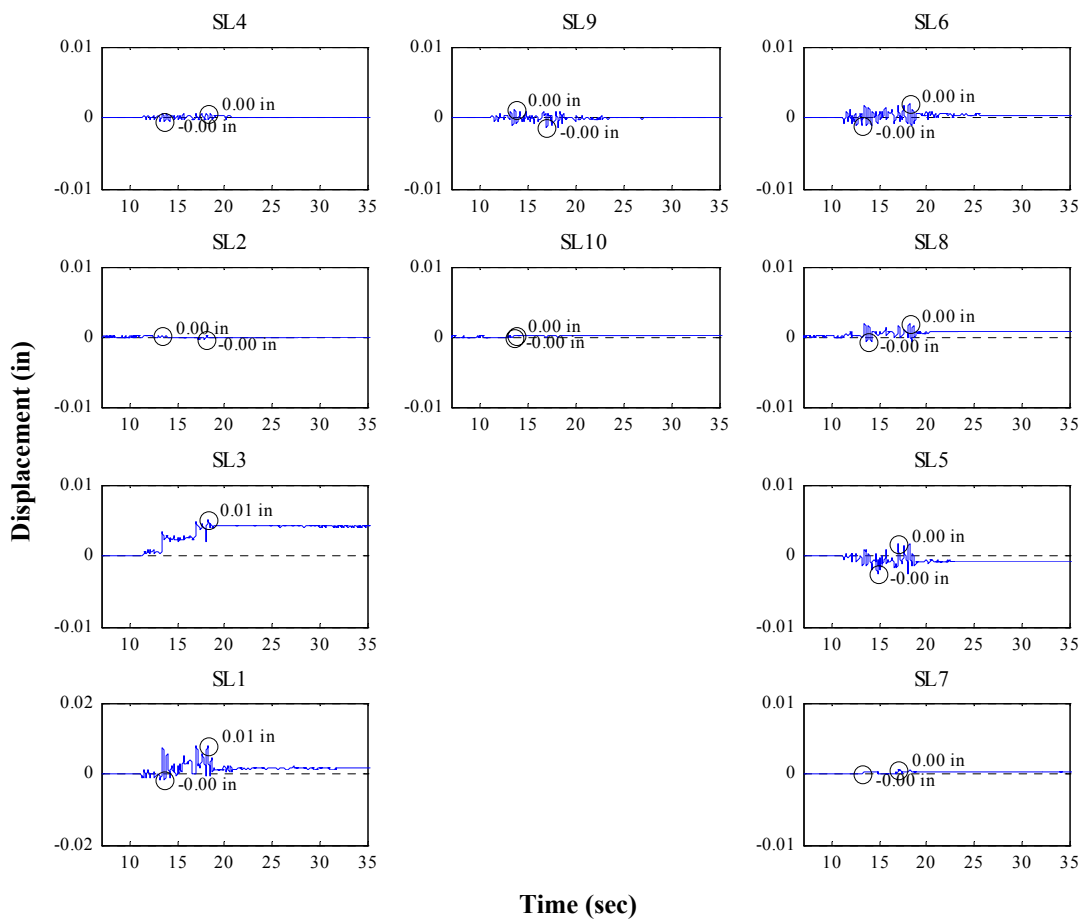
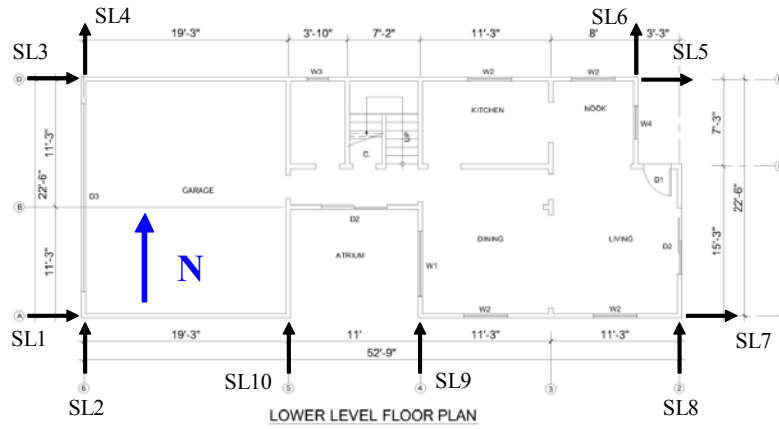


Figure P.7: Sill plate slippage time histories for Test NWP1S07

Appendix P

Phase 1, NWP1S06 Seismic Test

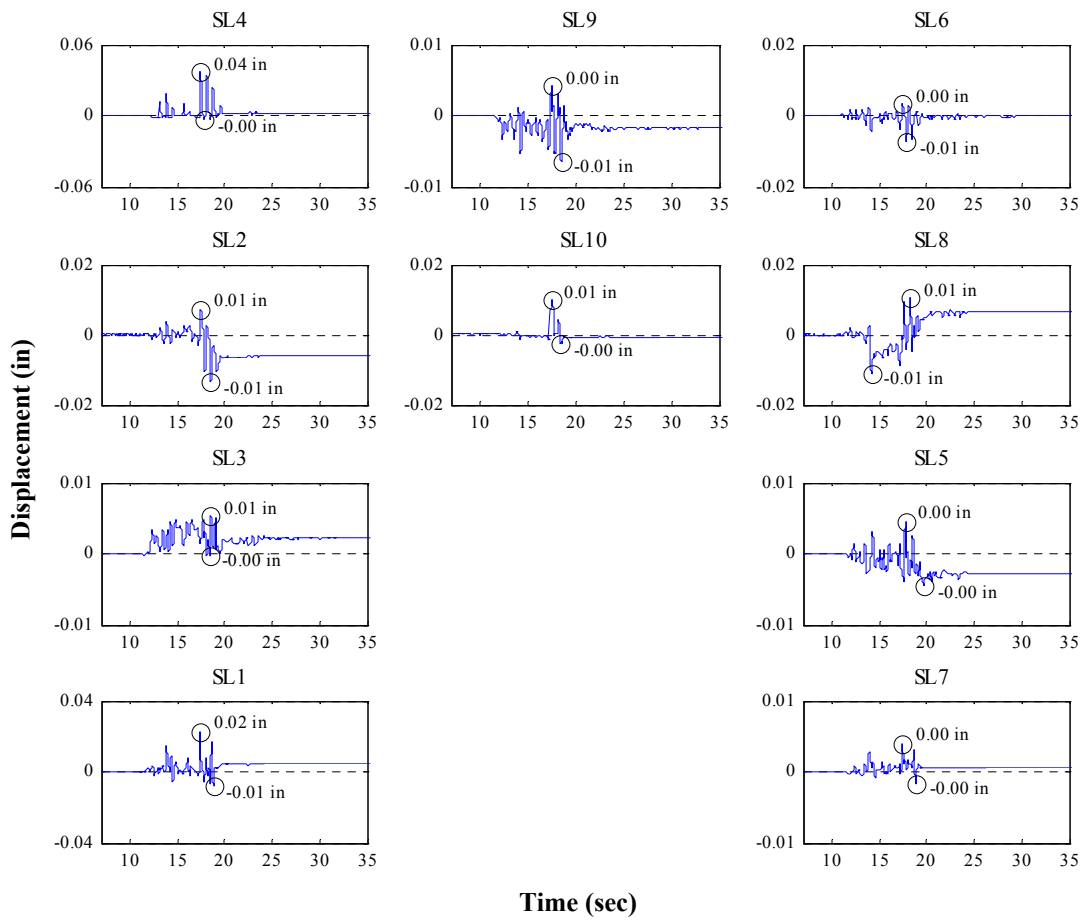
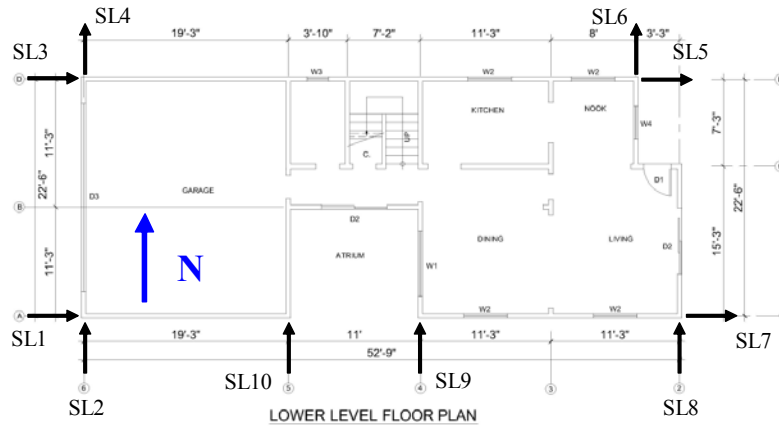


Figure P.8: Sill plate slippage time histories for Test NWP1S06

Appendix P

Phase 1, NWP1S10 Seismic Test

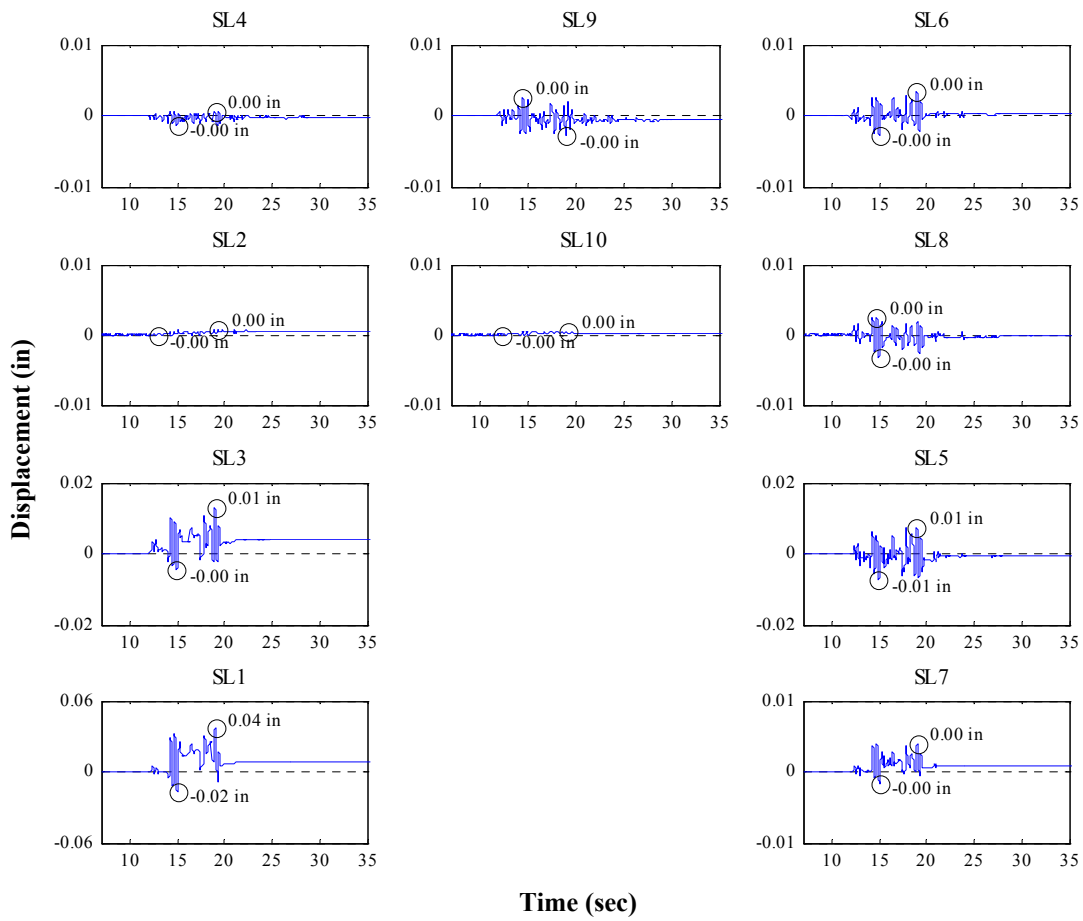
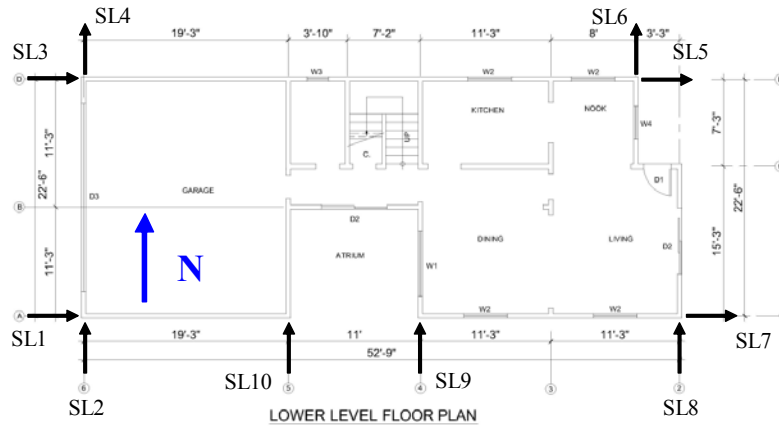


Figure P.9: Sill plate slippage time histories for Test NWP1S10

Appendix P

Phase 2, NWP2S01 Seismic Test

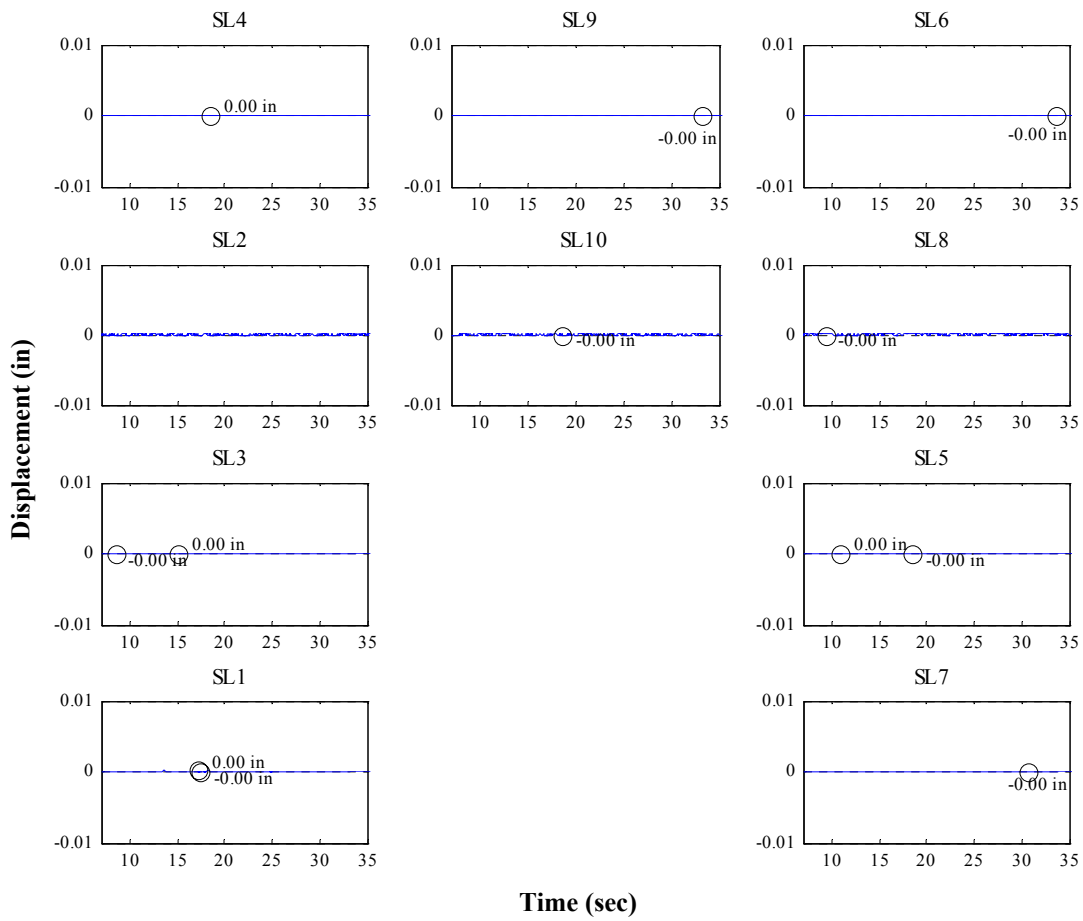
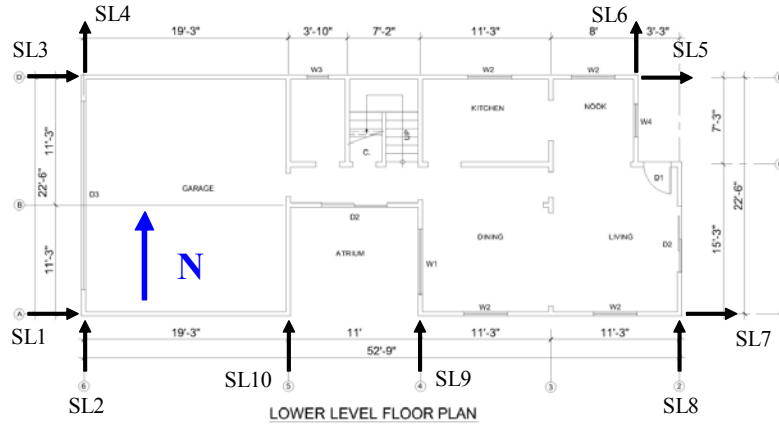


Figure P.10: Sill plate slippage time histories for Test NWP2S01

Appendix P

Phase 2, NWP2S02 Seismic Test

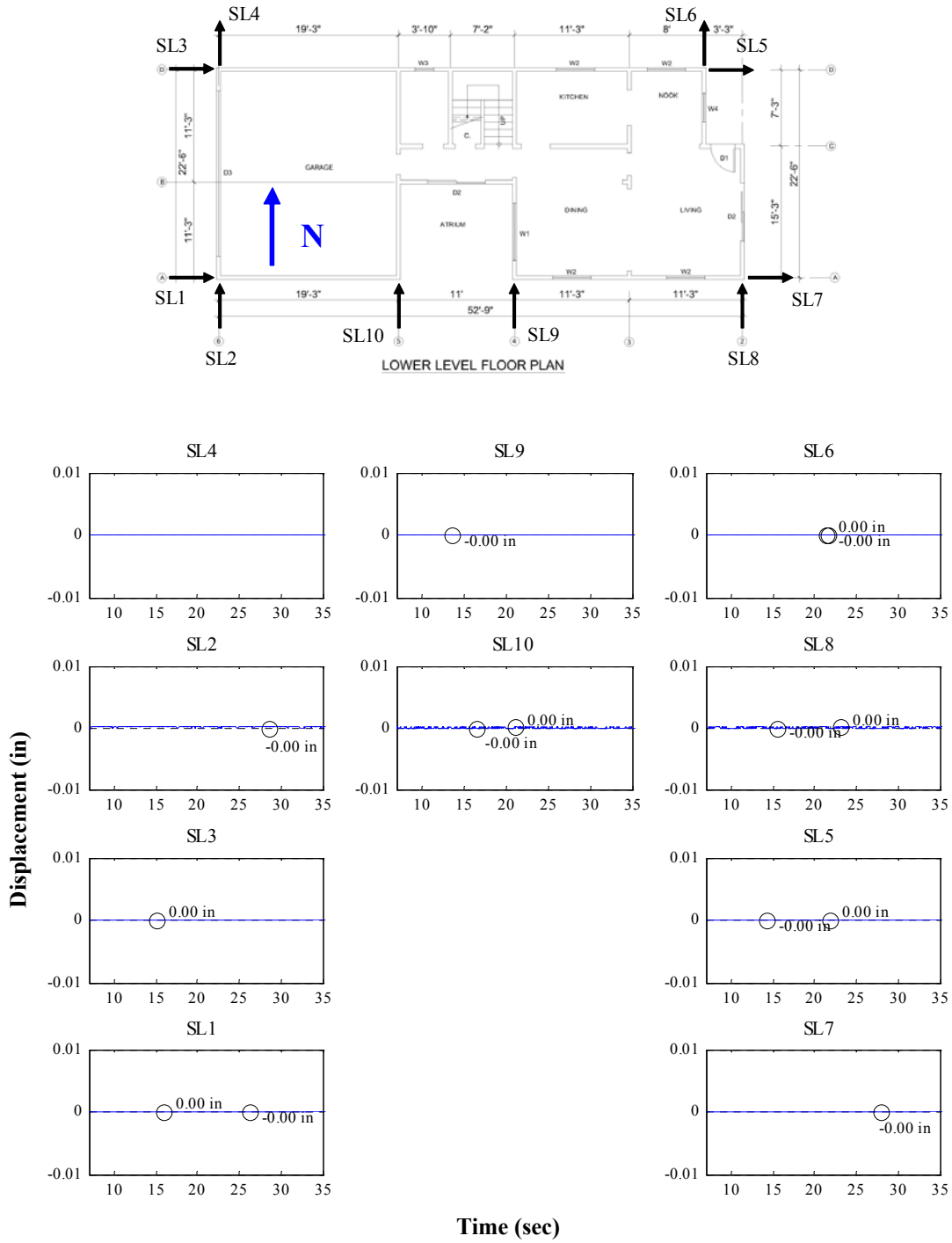


Figure P.11: Sill plate slippage time histories for Test NWP2S02

Appendix P

Phase 2, NWP2S03 Seismic Test

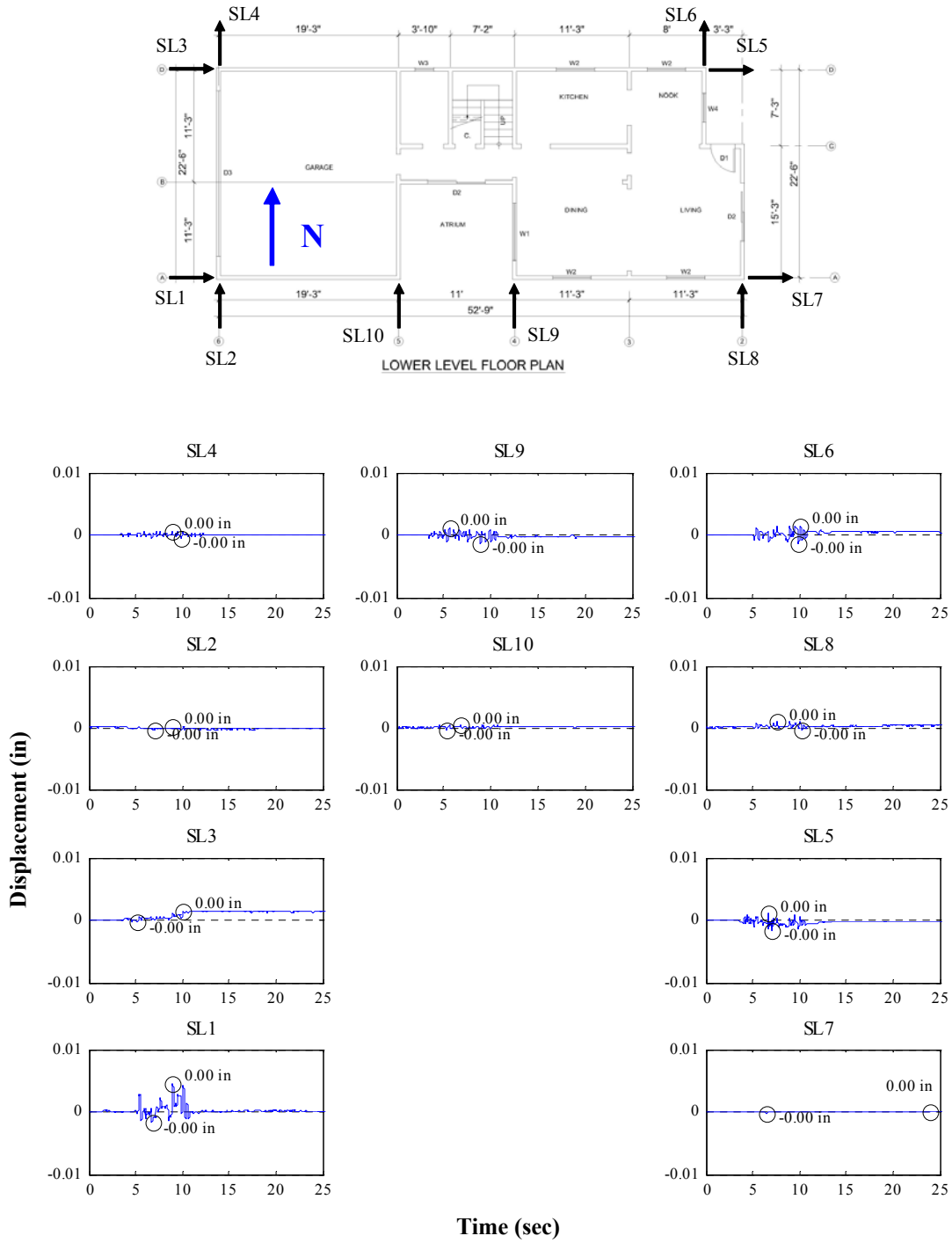


Figure P.12: Sill plate slippage time histories for Test NWP2S03

Appendix P

Phase 2, NWP2S04 Seismic Test

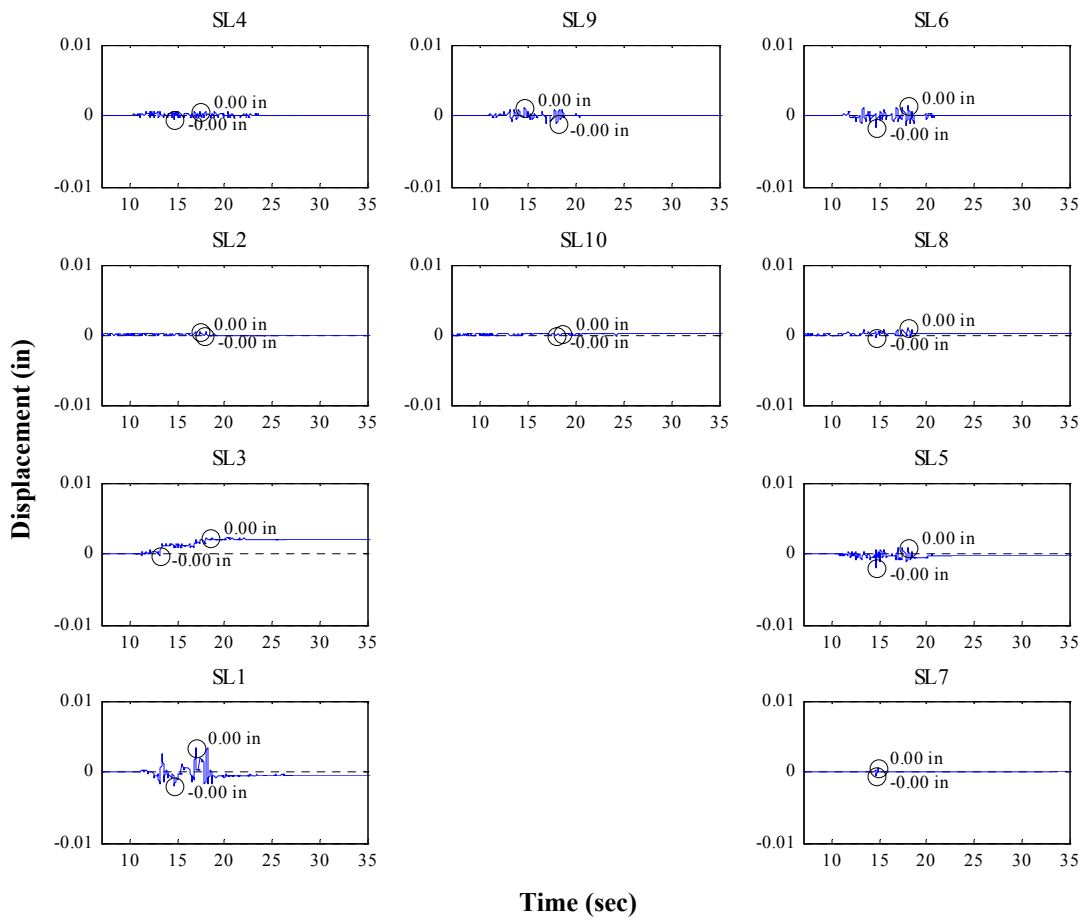
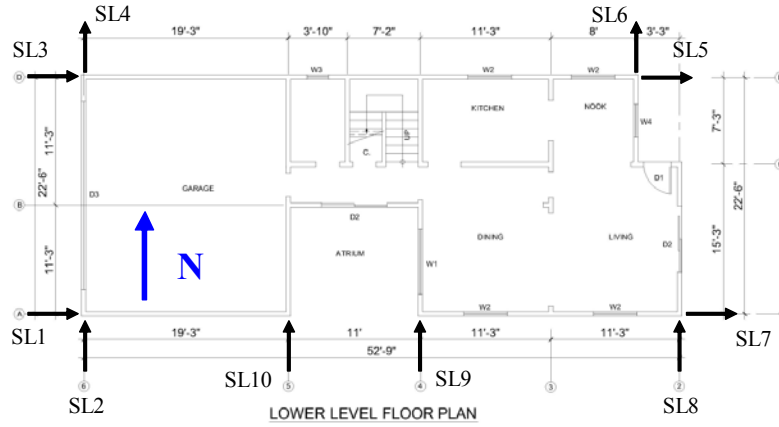


Figure P.13: Sill plate slippage time histories for Test NWP2S04

Appendix P

Phase 2, NWP2S05 Seismic Test

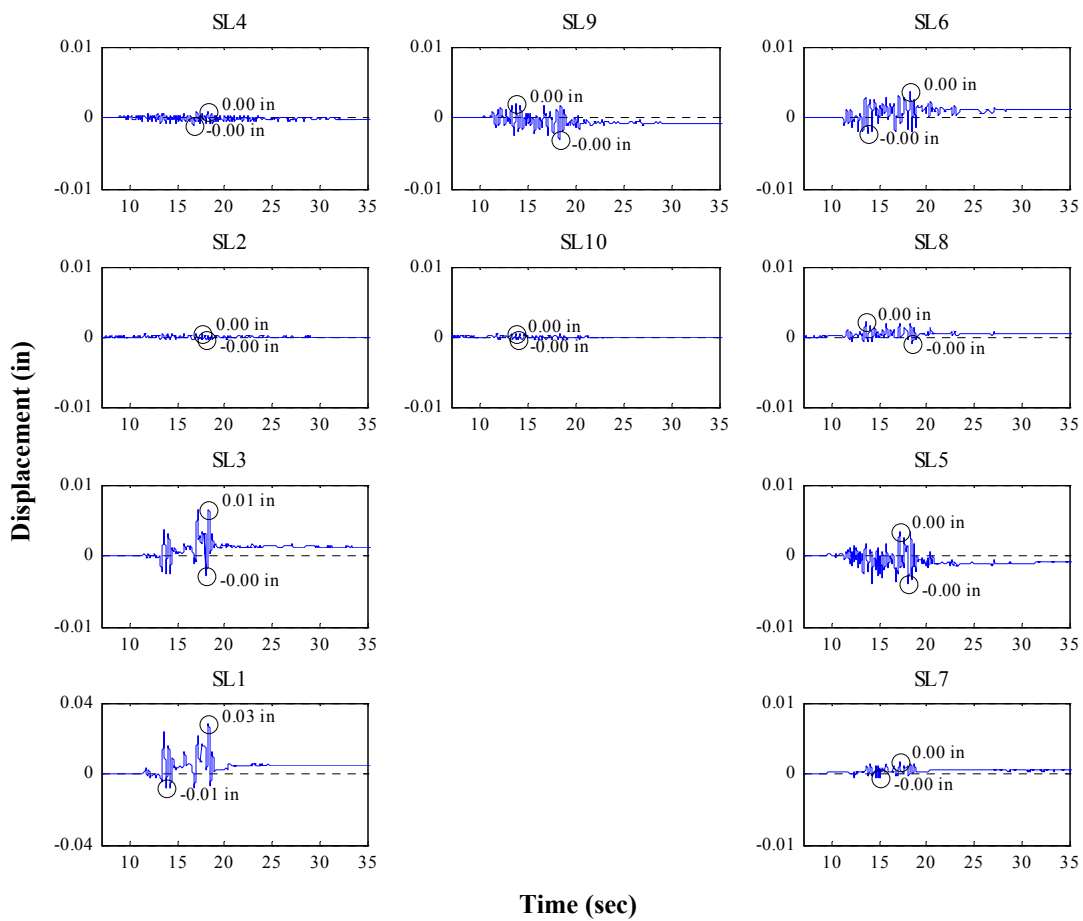
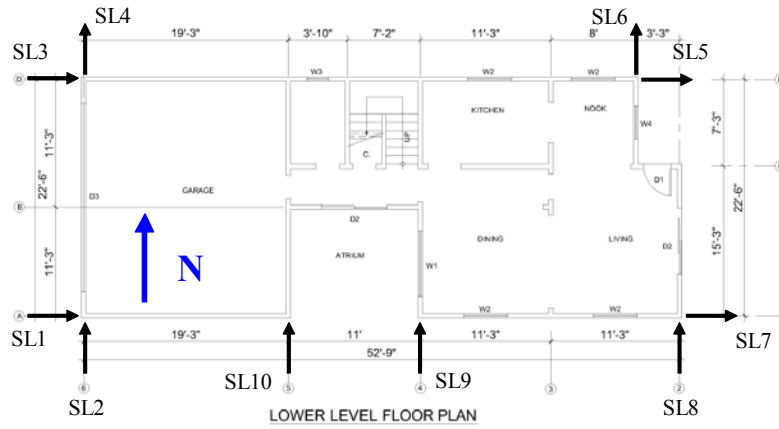


Figure P.14: Sill plate slippage time histories for Test NWP2S05

Appendix P

Phase 2, NWP2S06 Seismic Test

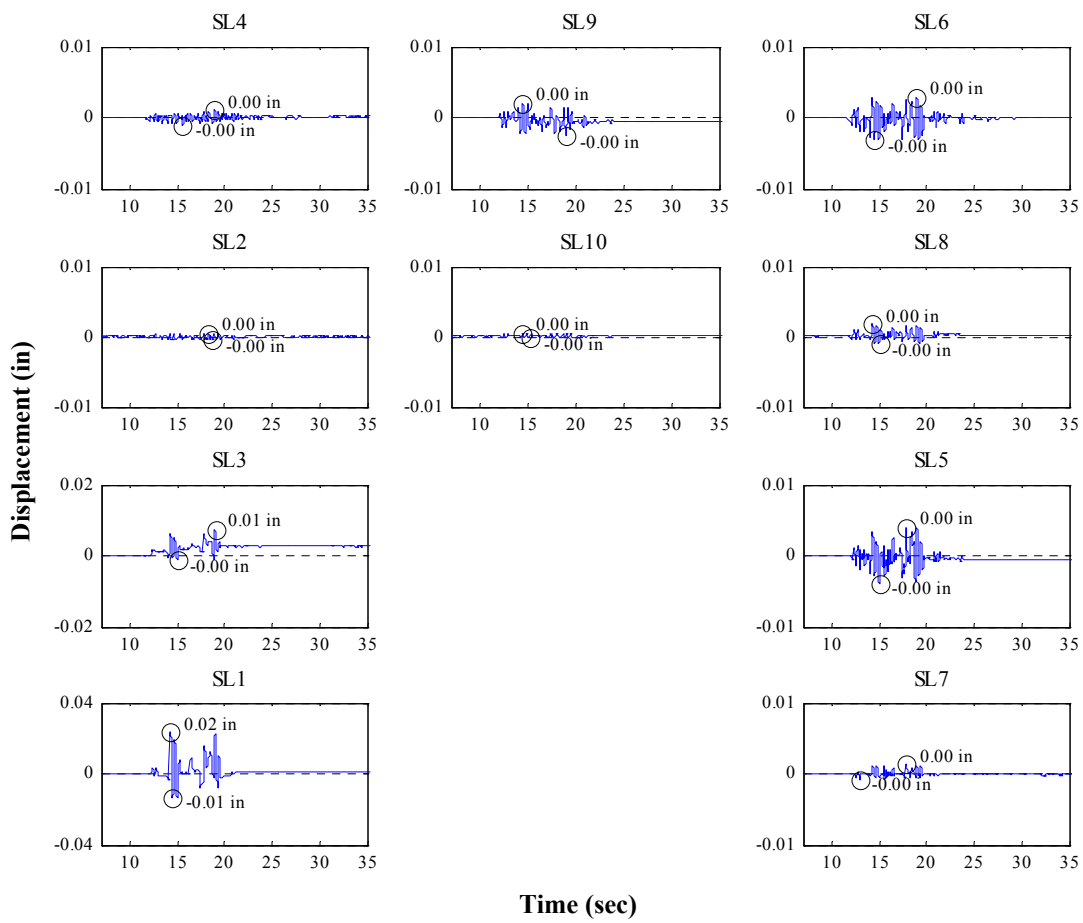
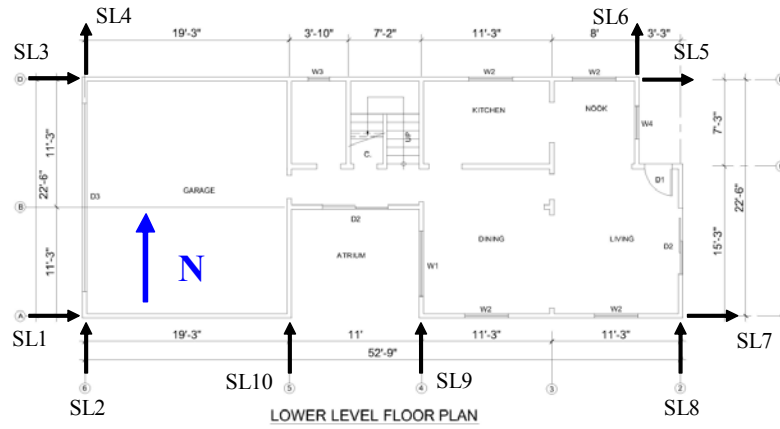


Figure P.15: Sill plate slippage time histories for Test NWP2S06

Appendix P

Phase 2, NWP2S07 Seismic Test

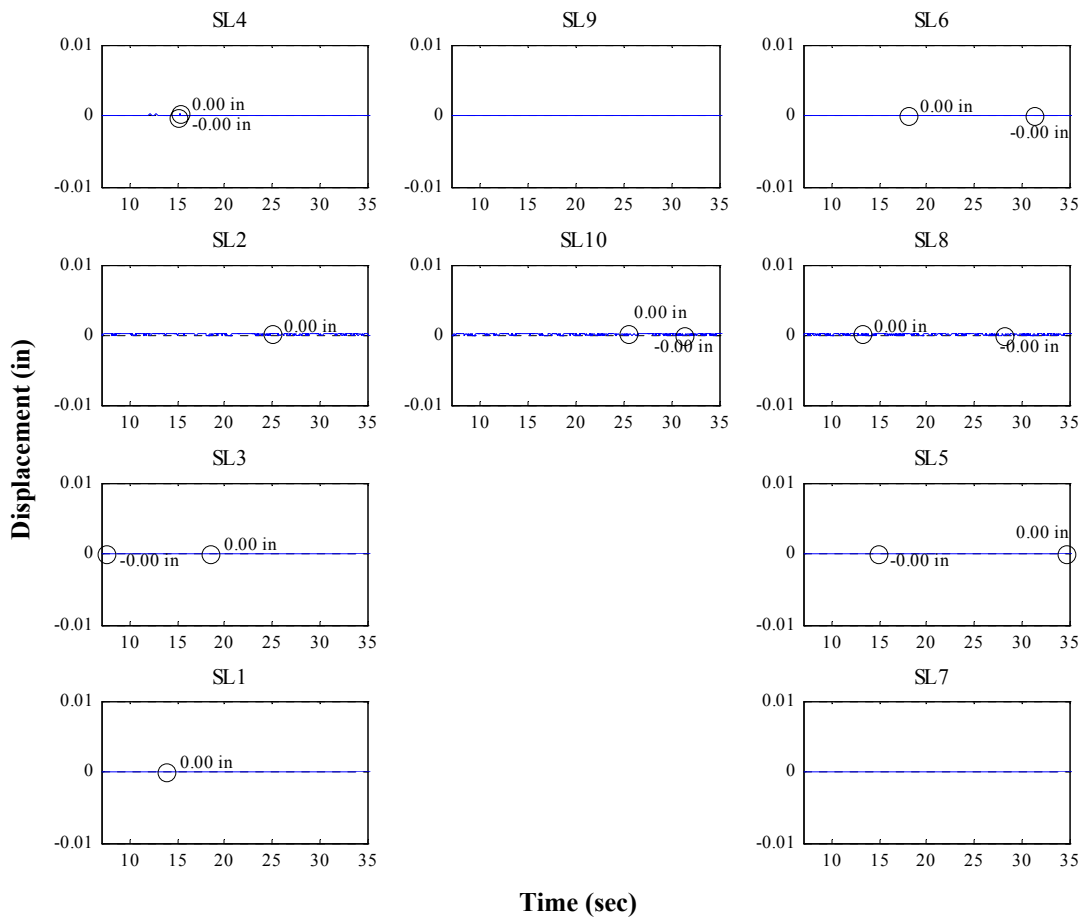
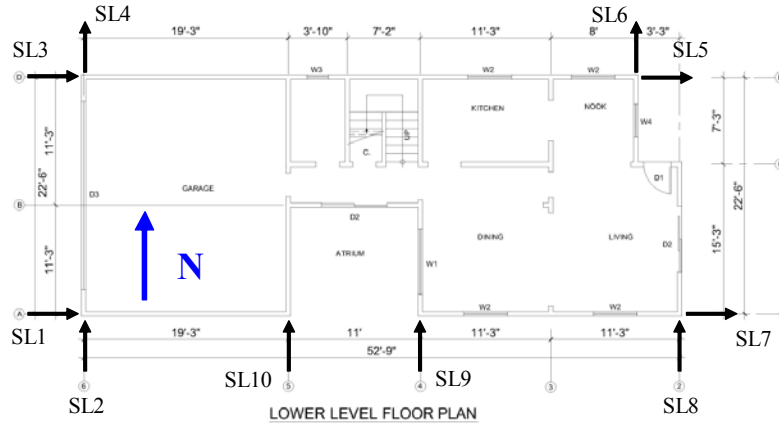


Figure P.16: Sill plate slippage time histories for Test NWP2S07

Appendix P

Phase 2, NWP2S08 Seismic Test

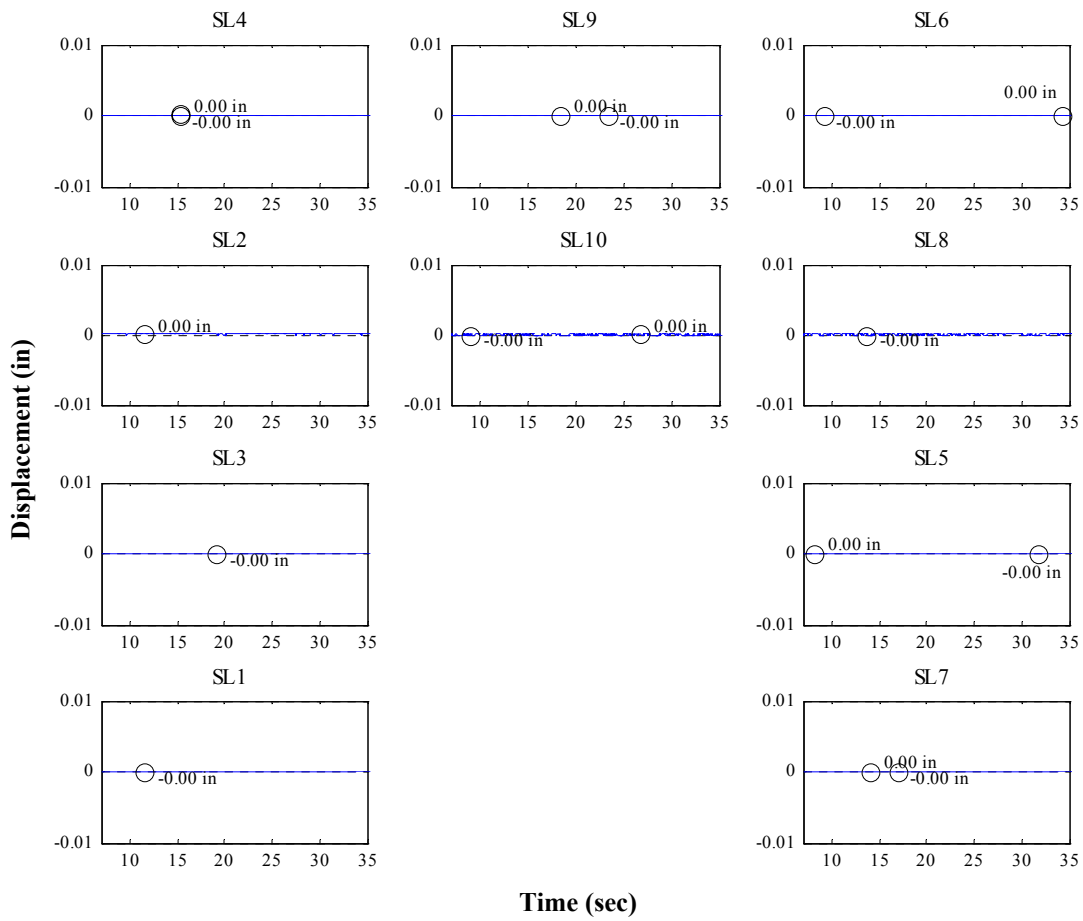
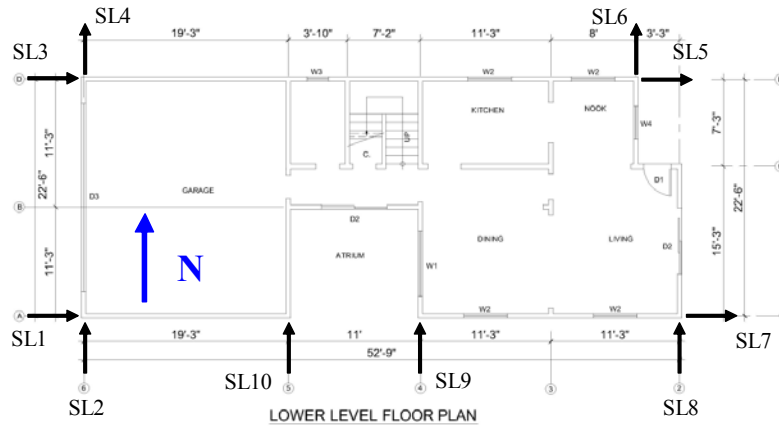


Figure P.17: Sill plate slippage time histories for Test NWP2S08

Appendix P

Phase 2, NWP2S09 Seismic Test

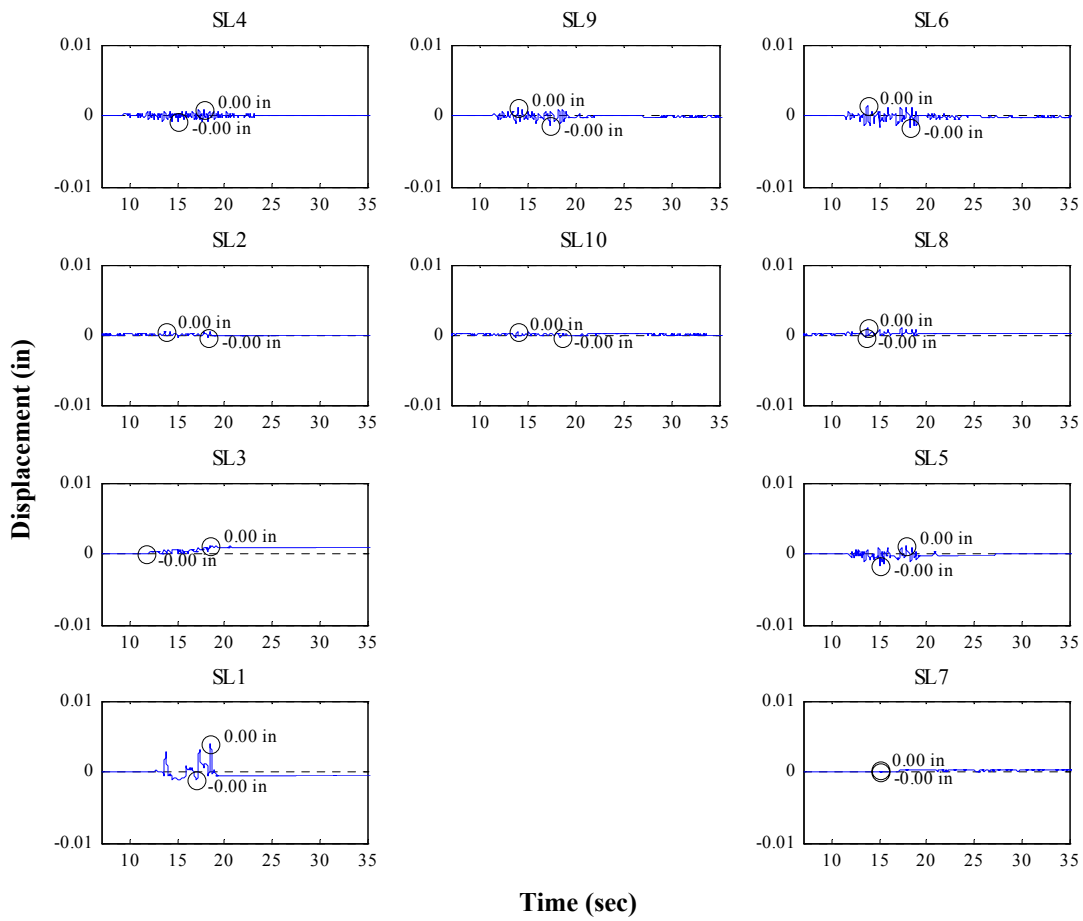
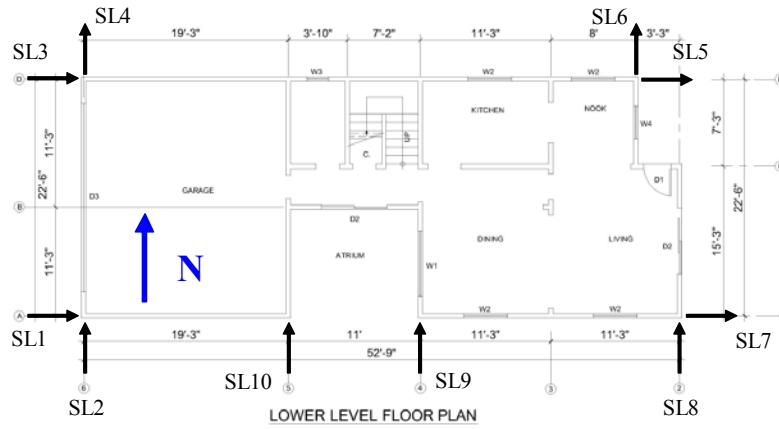


Figure P.18: Sill plate slippage time histories for Test NWP2S09

Appendix P

Phase 2, NWP2S10 Seismic Test

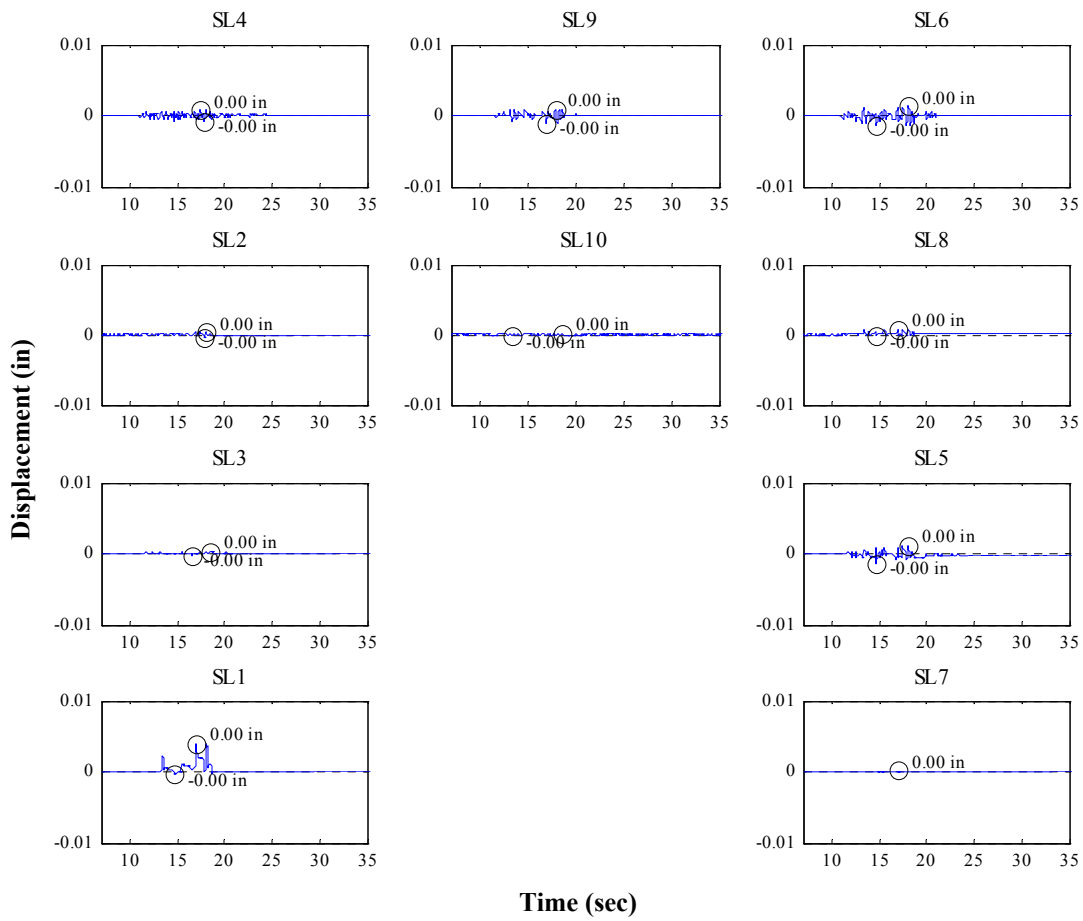
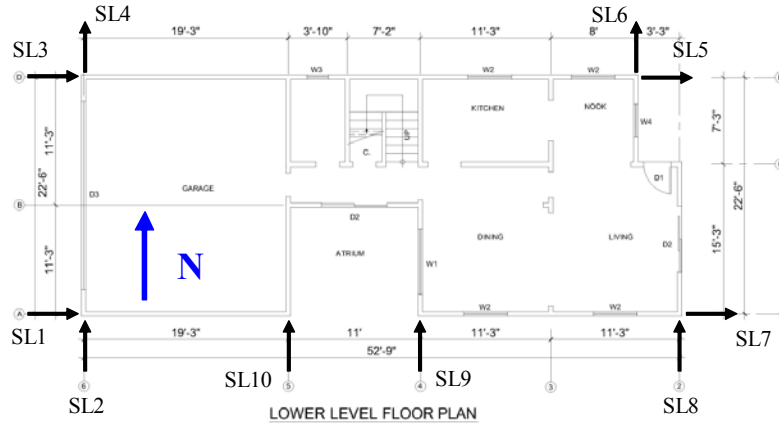


Figure P.19: Sill plate slippage time histories for Test NWP2S10

Appendix P

Phase 2, NWP2S11 Seismic Test

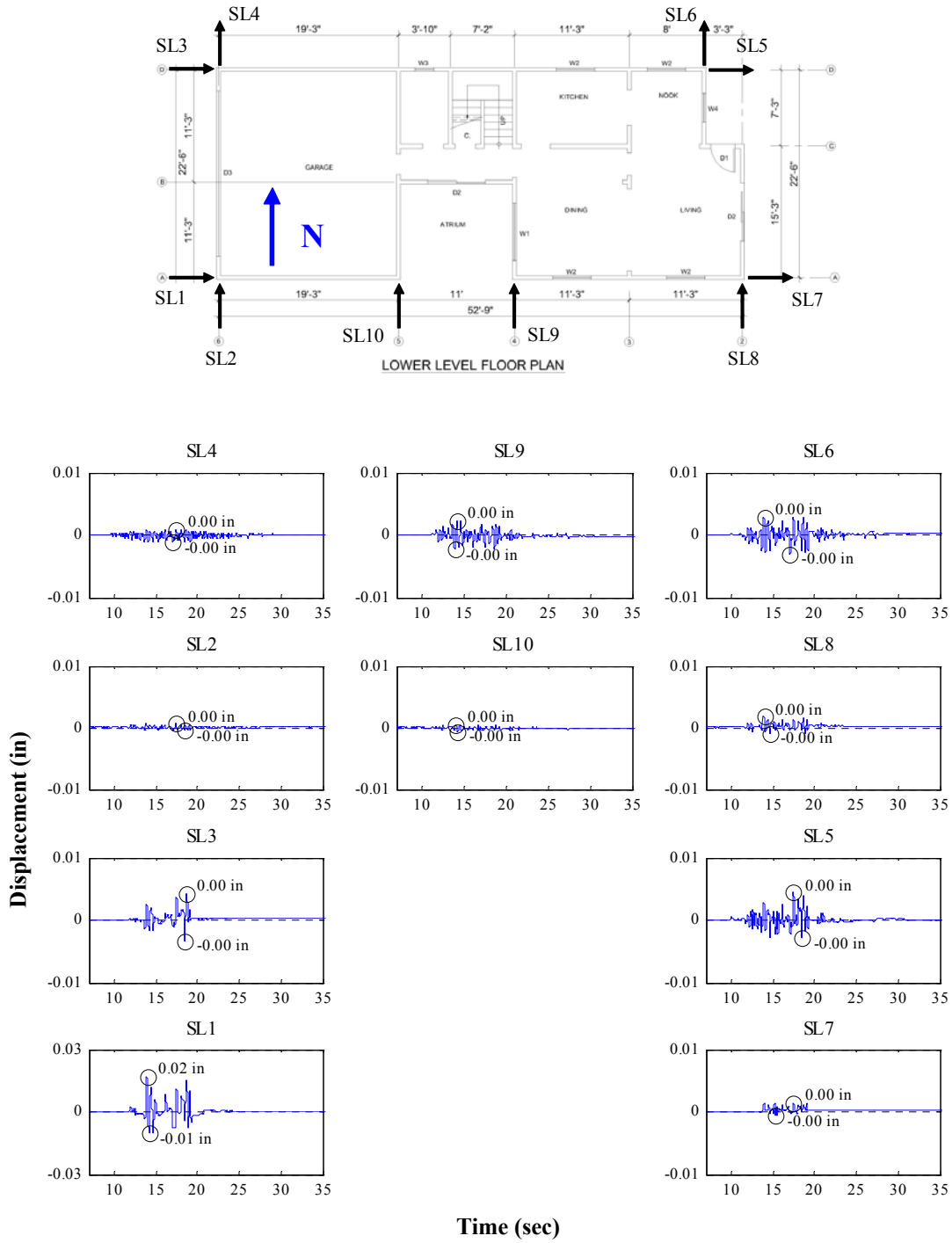


Figure P.20: Sill plate slippage time histories for Test NWP2S11

Appendix P

Phase 2, NWP2S12 Seismic Test

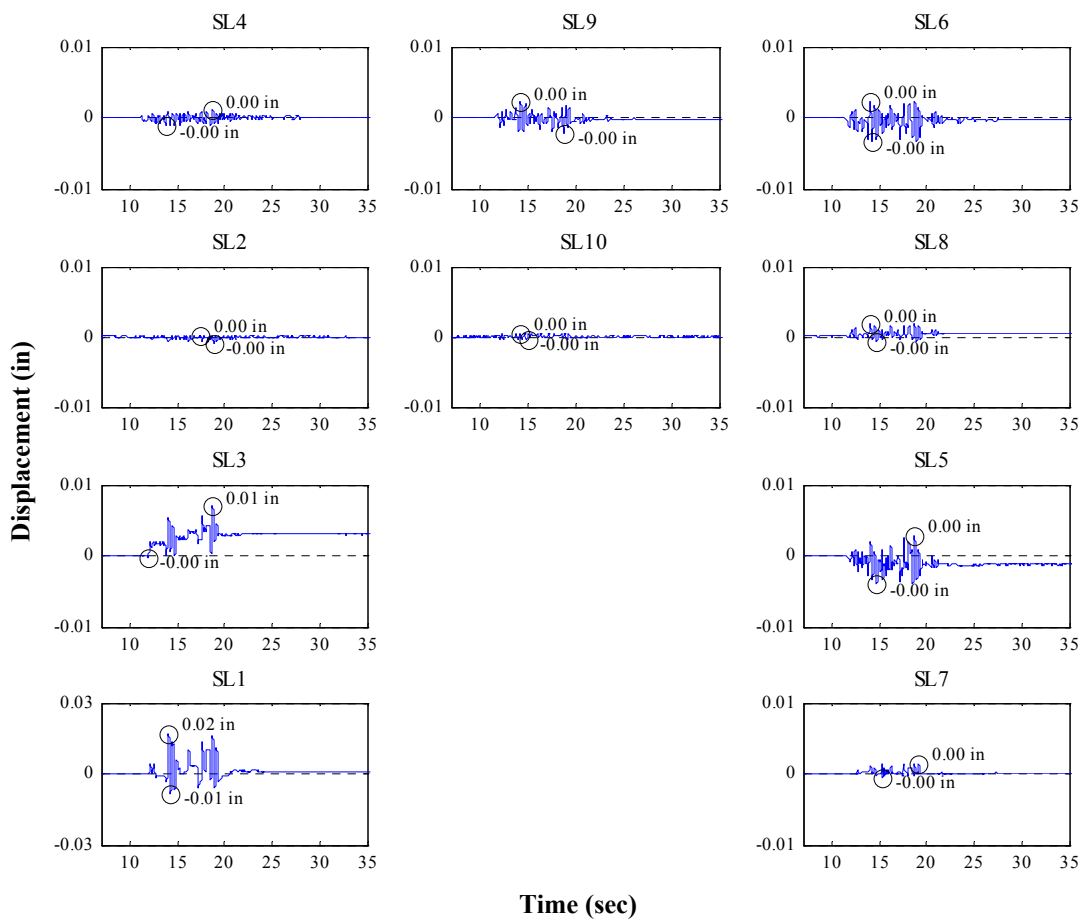
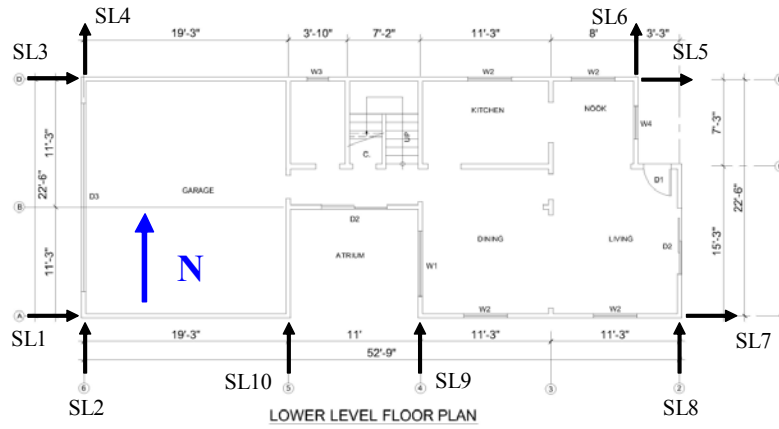


Figure P.21: Sill plate slippage time histories for Test NWP2S12

Appendix P

Phase 2, NWP2S13 Seismic Test

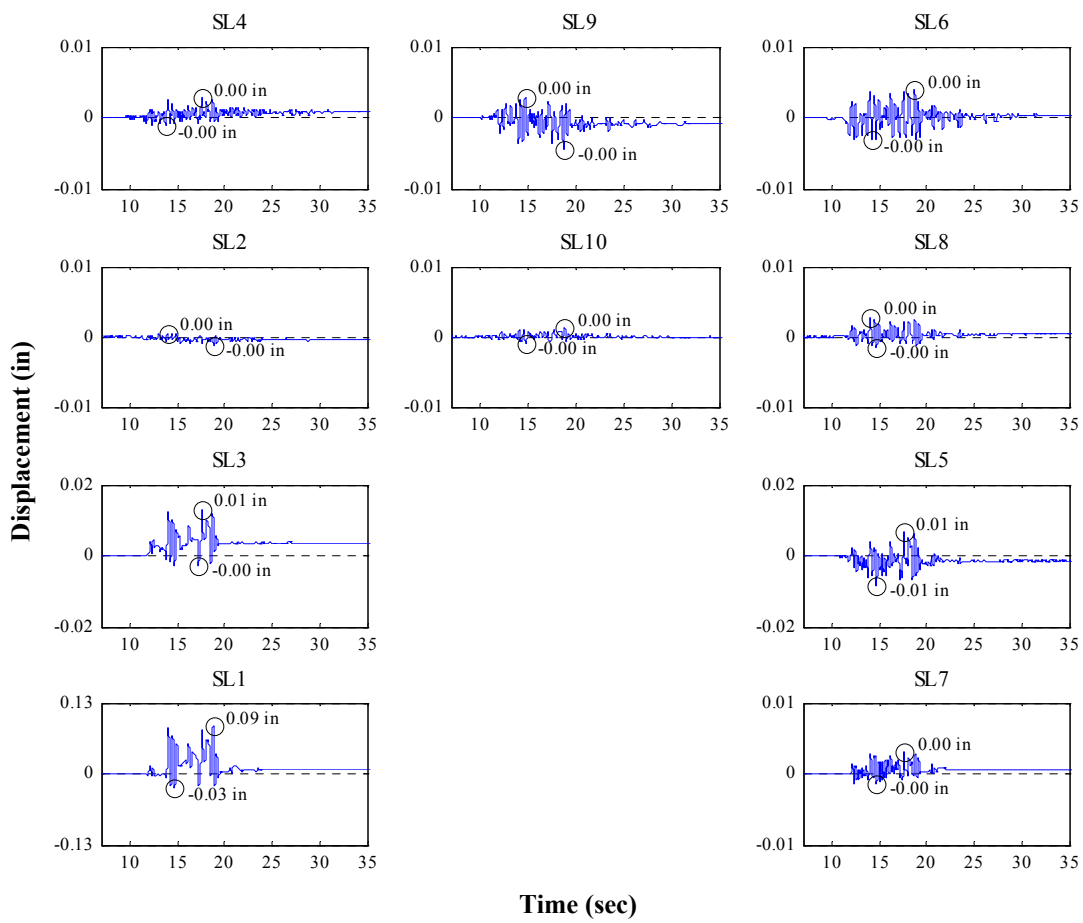
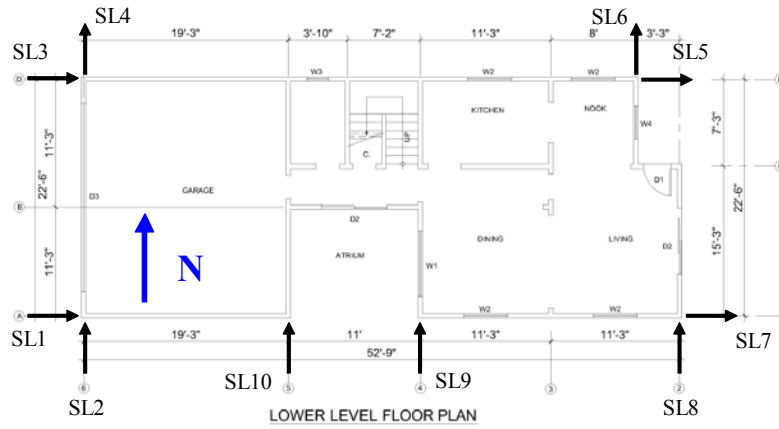


Figure P.22: Sill plate slippage time histories for Test NWP2S13

Appendix P

Phase 2, NWP2S14 Seismic Test

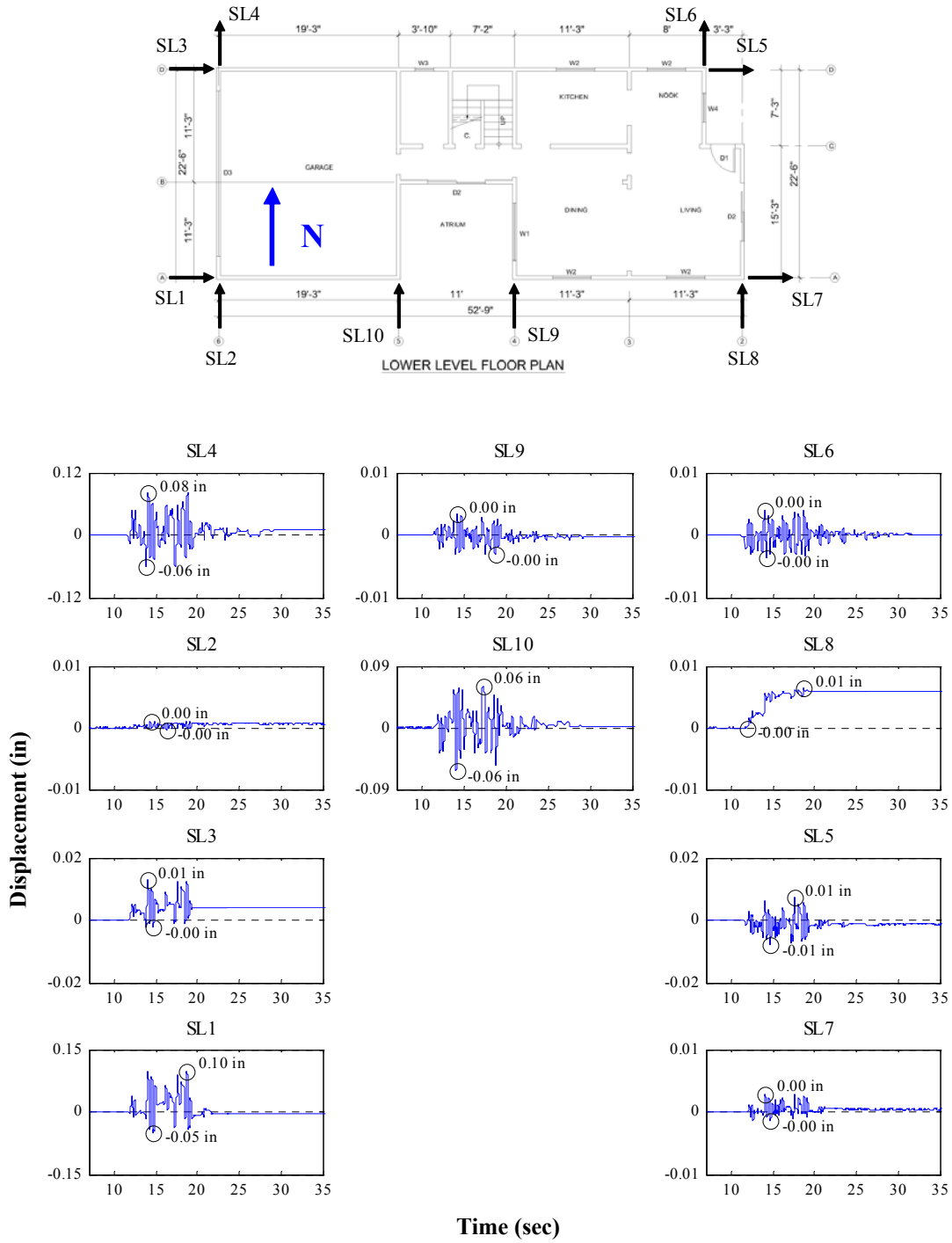


Figure P.23: Sill plate slippage time histories for Test NWP2S14

Appendix P

Phase 2, NWP2S16 Seismic Test

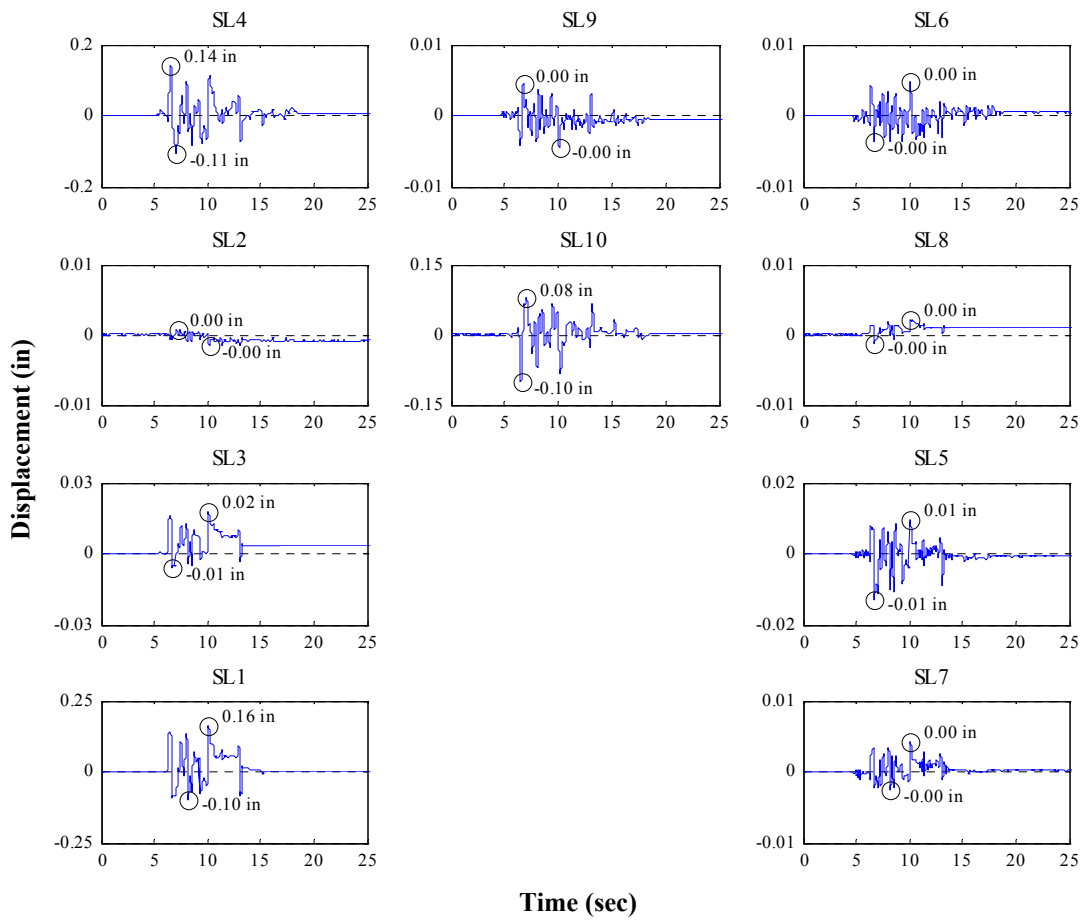
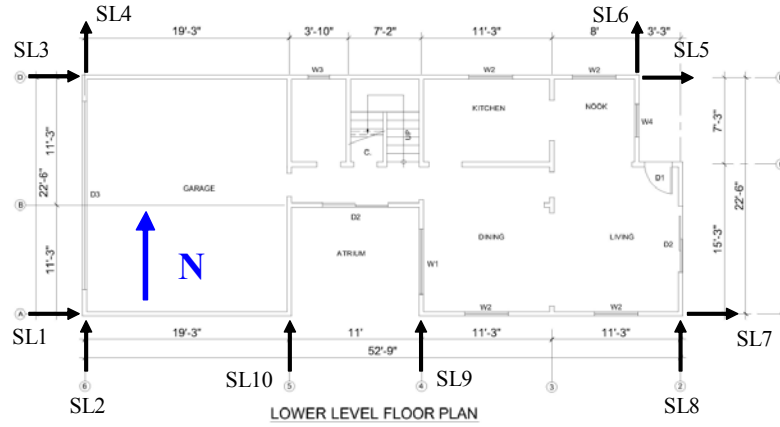


Figure P.24: Sill plate slippage time histories for Test NWP2S16

Appendix P

Phase 2, NWP2S17 Seismic Test

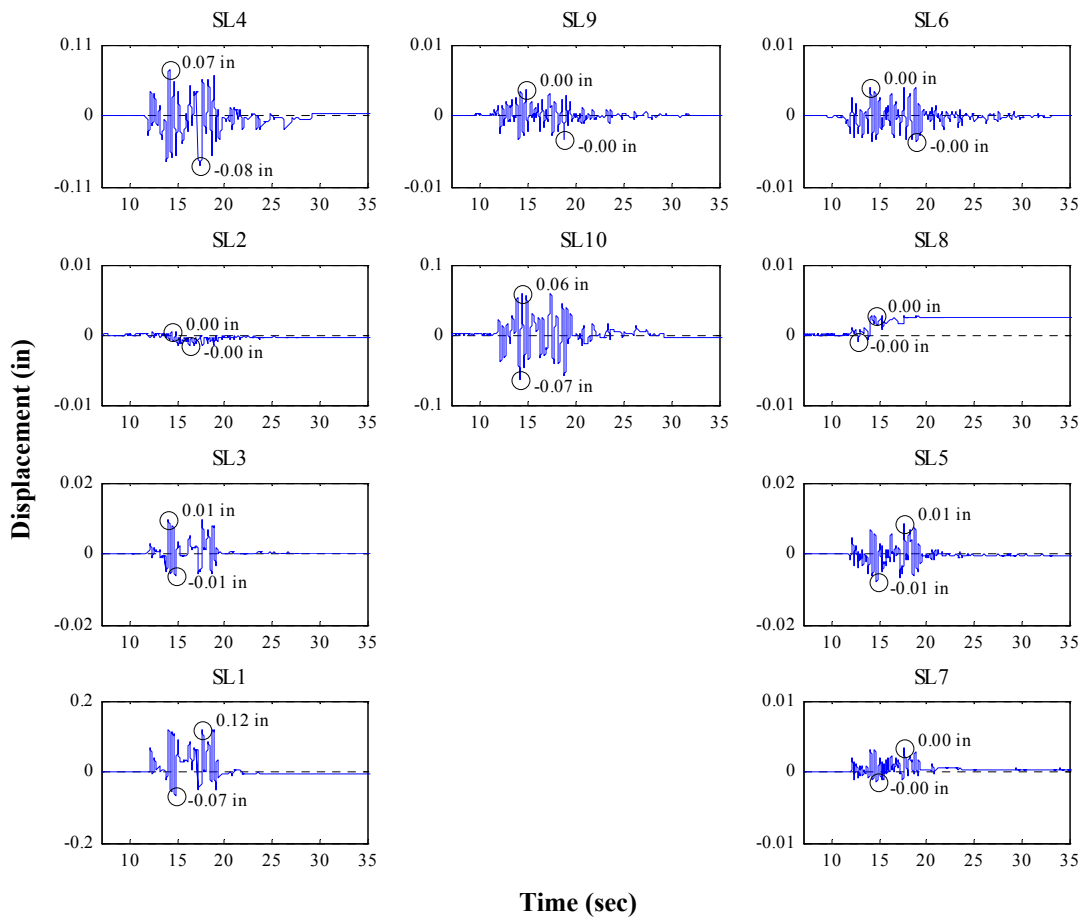
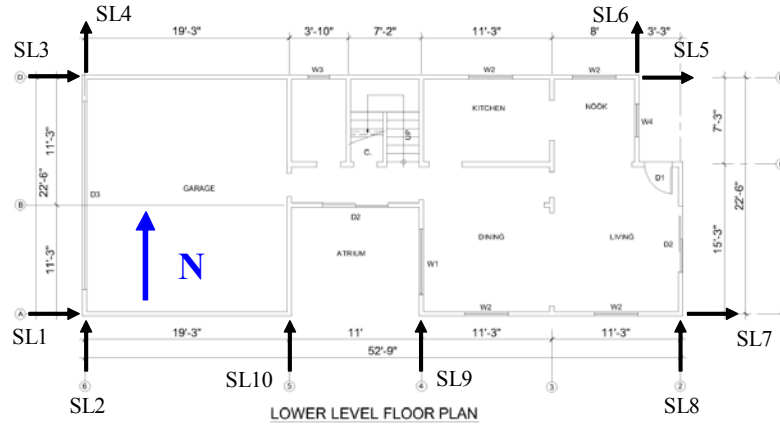


Figure P.25: Sill plate slippage time histories for Test NWP2S17

Appendix P

Phase 2, NWP2S21 Seismic Test

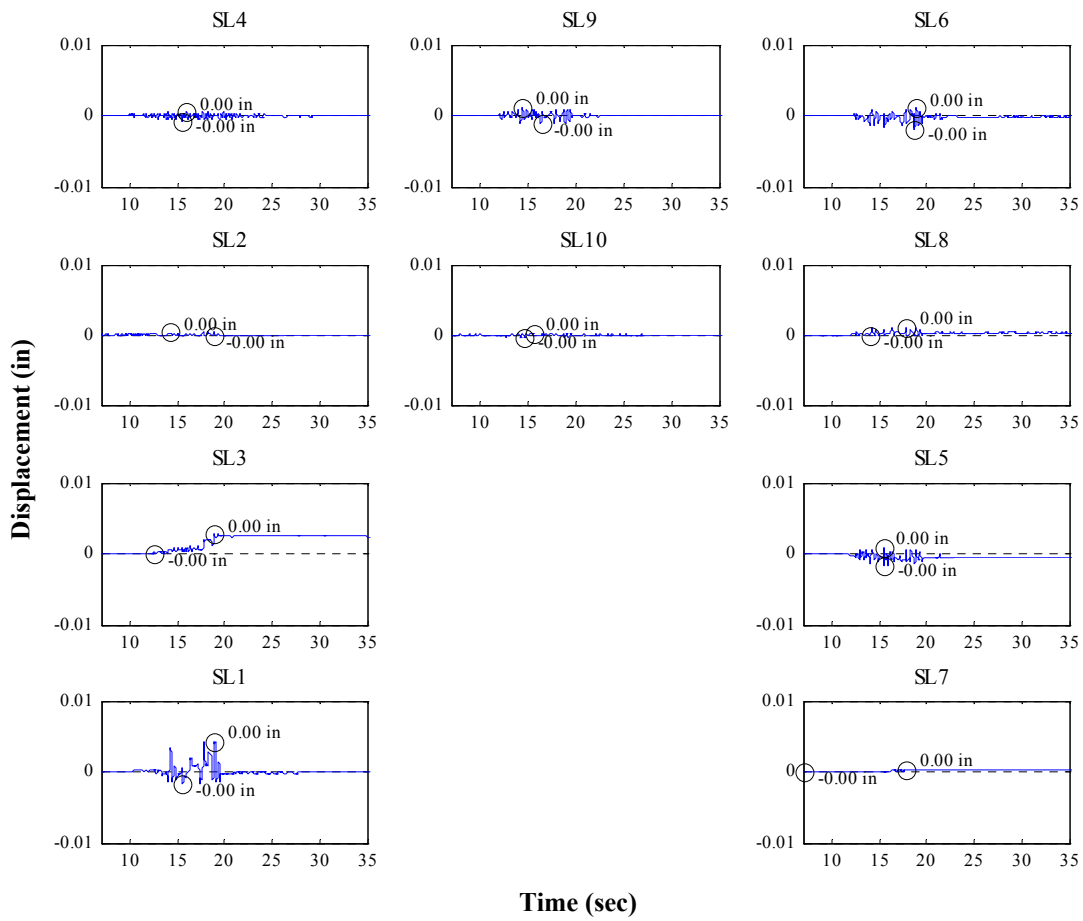
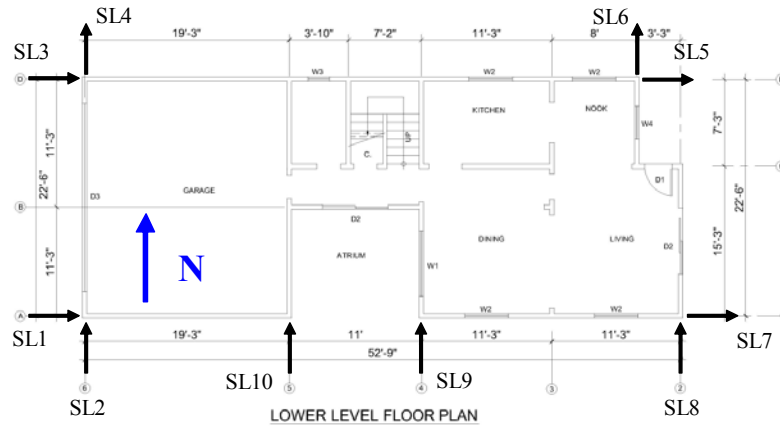


Figure P.26: Sill plate slippage time histories for Test NWP2S21

Appendix P

Phase 2, NWP2S24 Seismic Test

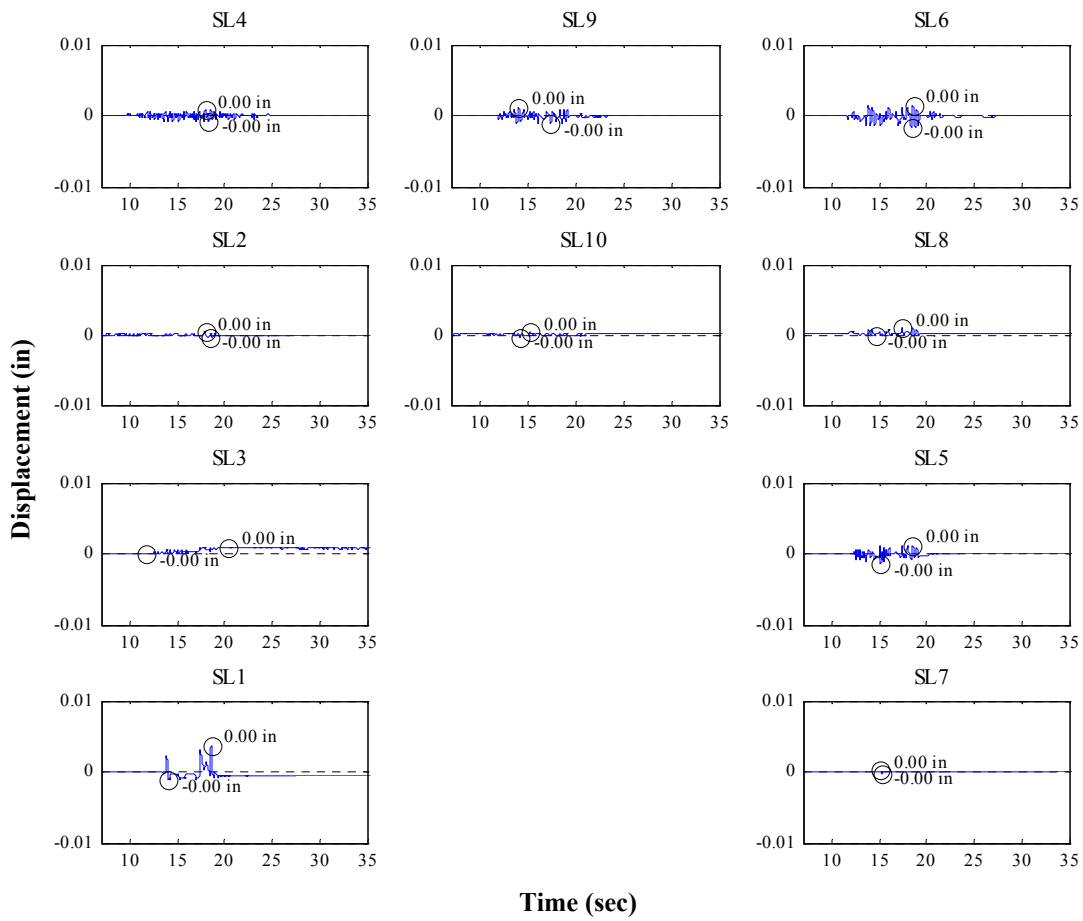
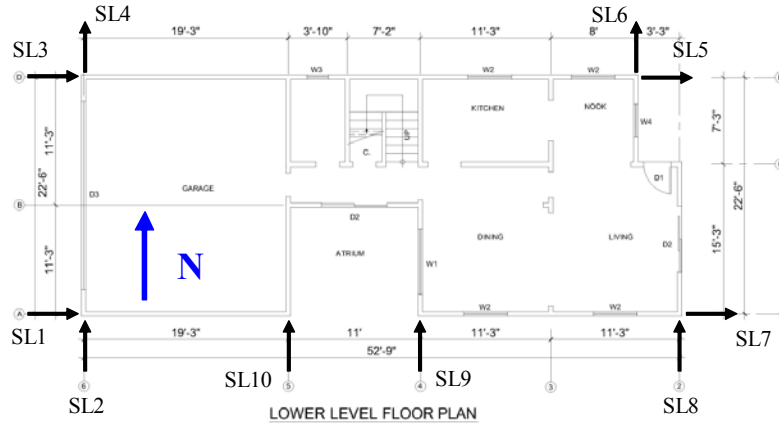


Figure P.27: Sill plate slippage time histories for Test NWP2S24

Appendix P

Phase 2, NWP2S25 Seismic Test

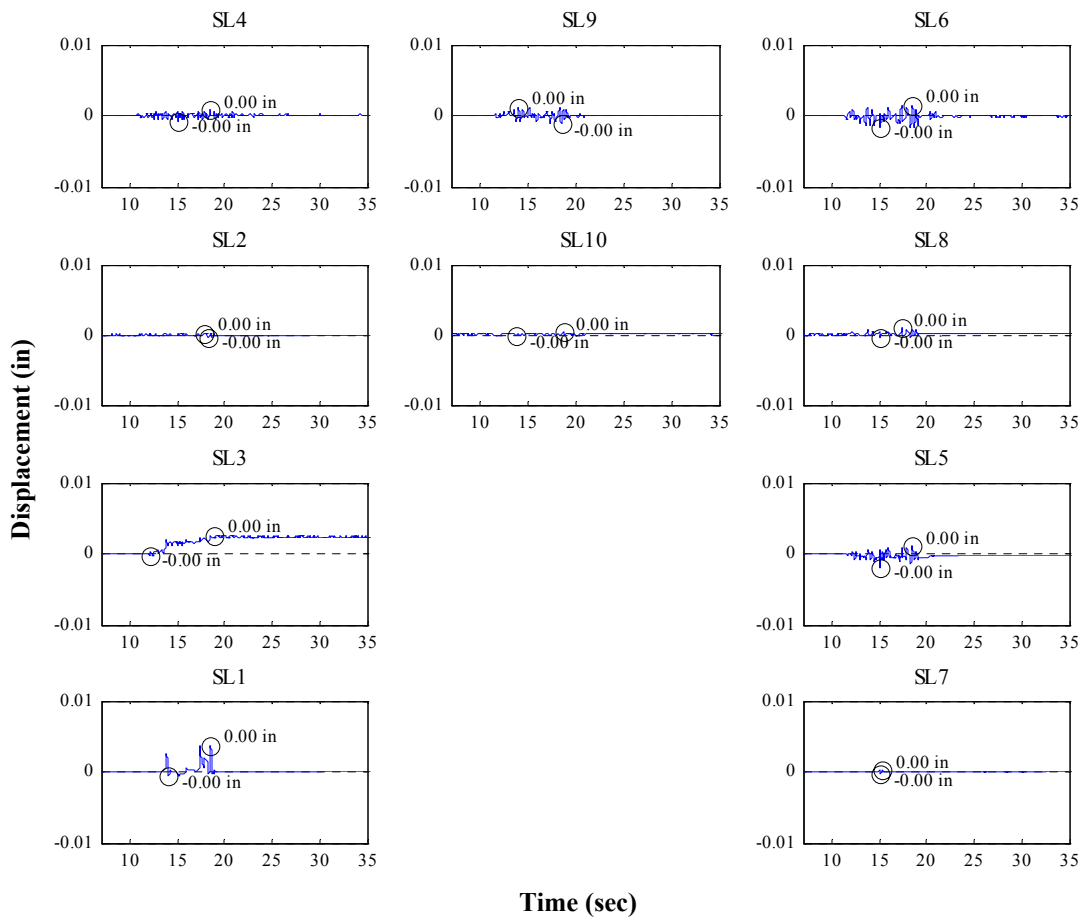
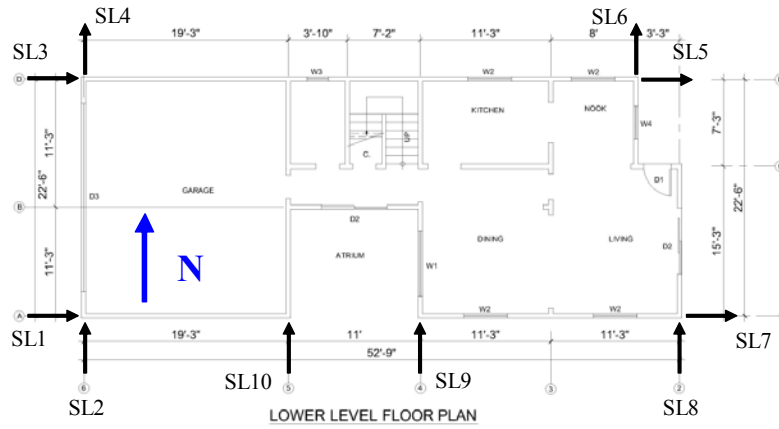


Figure P.28: Sill plate slippage time histories for Test NWP2S25

Appendix P

Phase 2, NWP2S26 Seismic Test

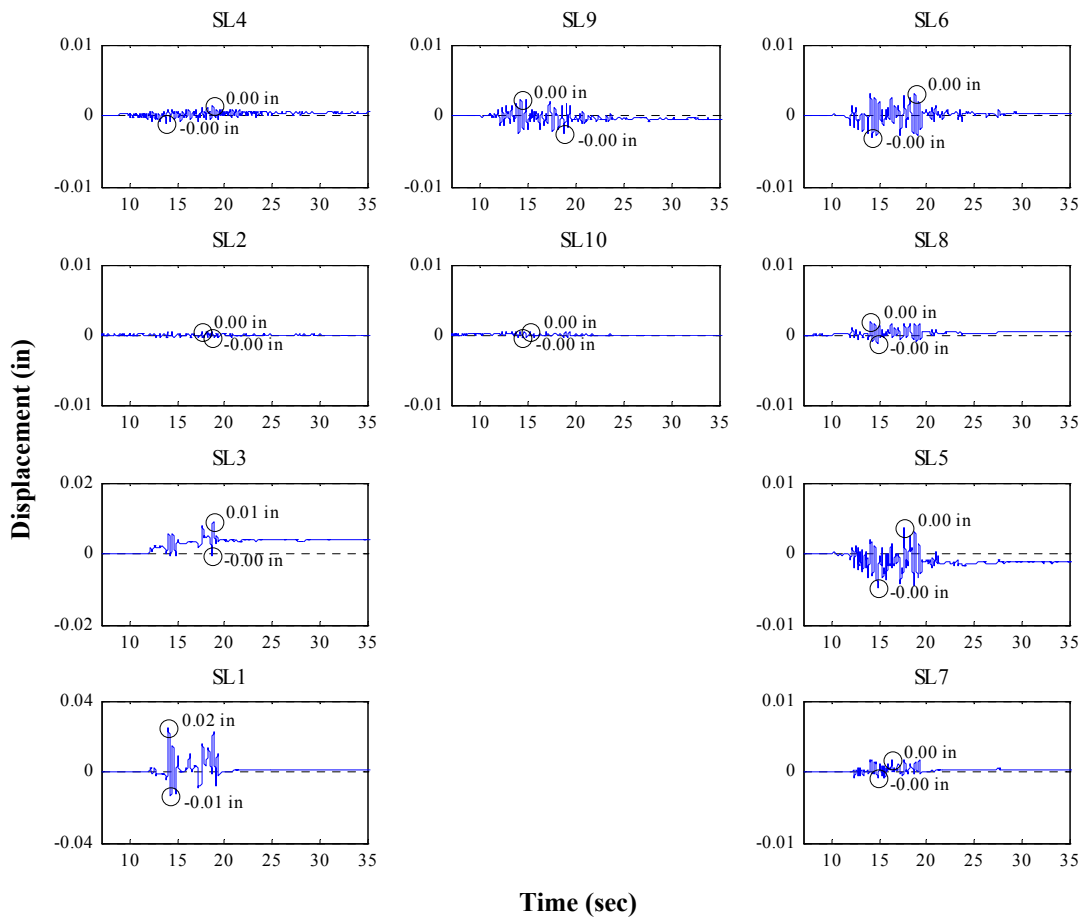
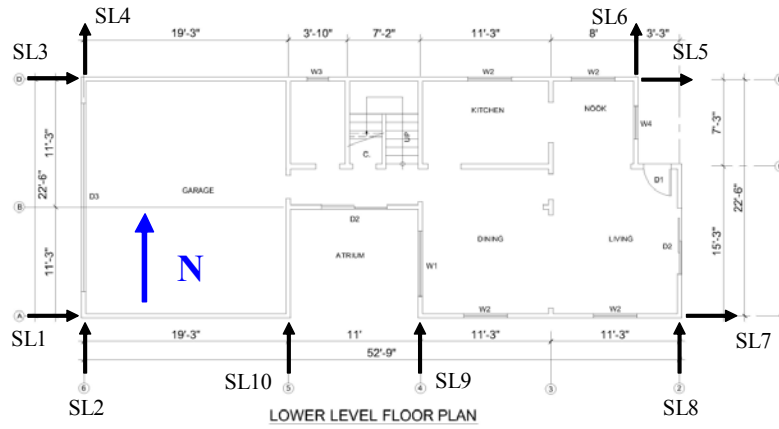


Figure P.29: Sill plate slippage time histories for Test NWP2S26

Appendix P

Phase 2, NWP2S27 Seismic Test

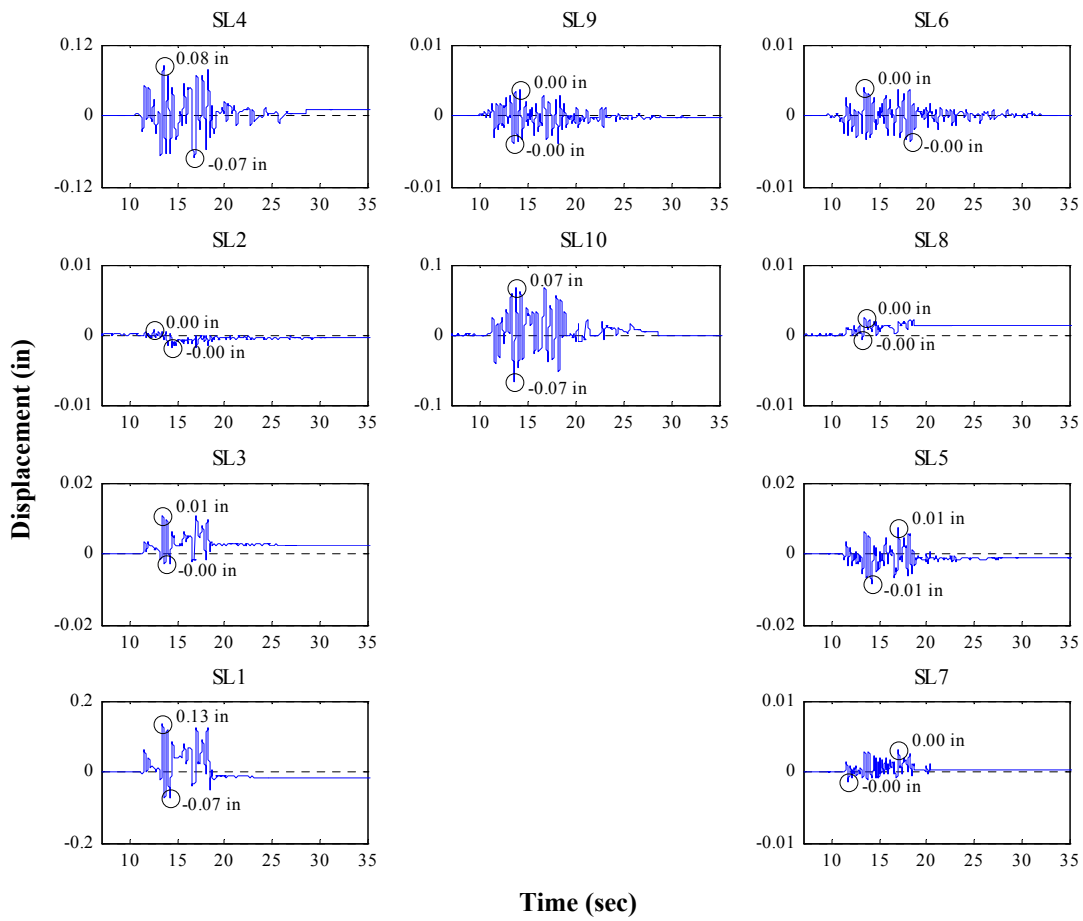
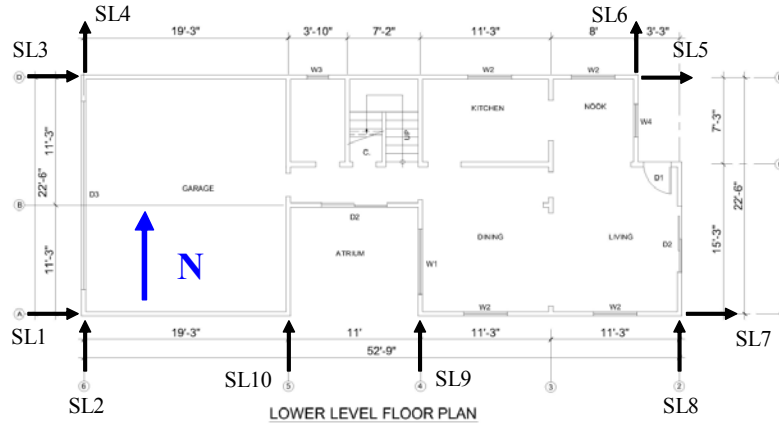


Figure P.30: Sill plate slippage time histories for Test NWP2S27

Appendix P

Phase 2, NWP2S28 Seismic Test

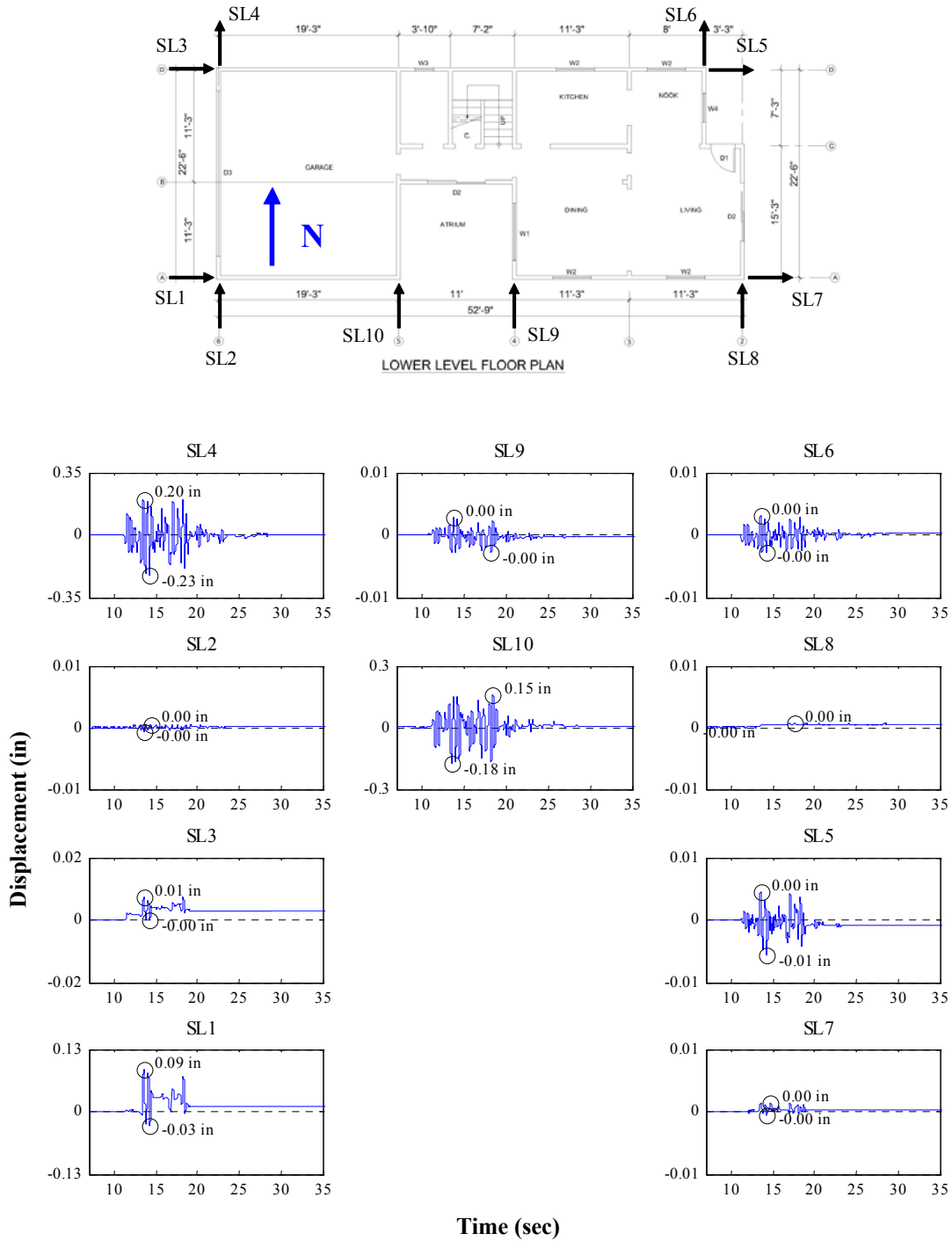


Figure P.31: Sill plate slippage time histories for Test NWP2S28

Appendix P

Phase 2, NWP2S29 Seismic Test

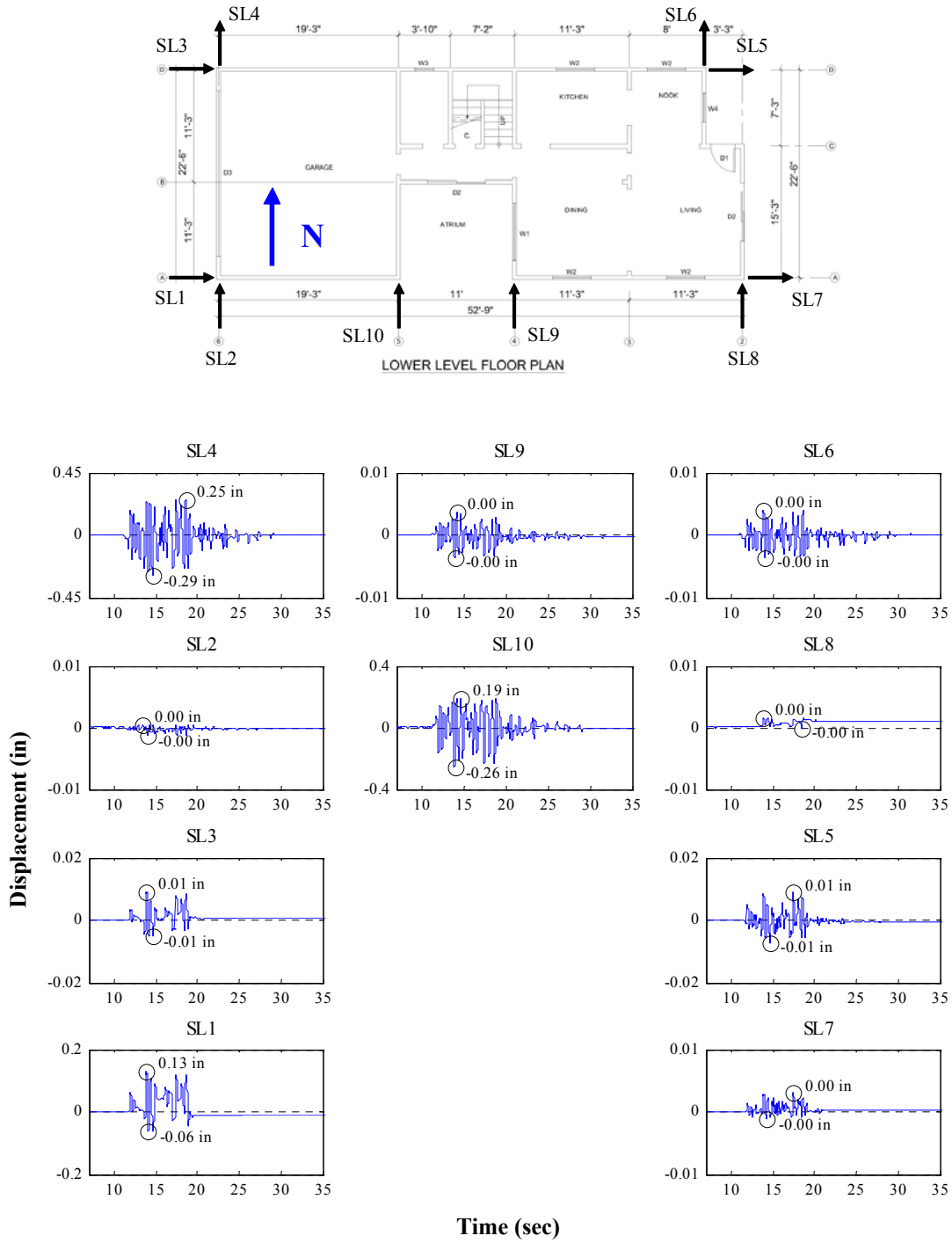


Figure P.32: Sill plate slippage time histories for Test NWP2S29

Appendix P

Phase 2, NWP2S30 Seismic Test

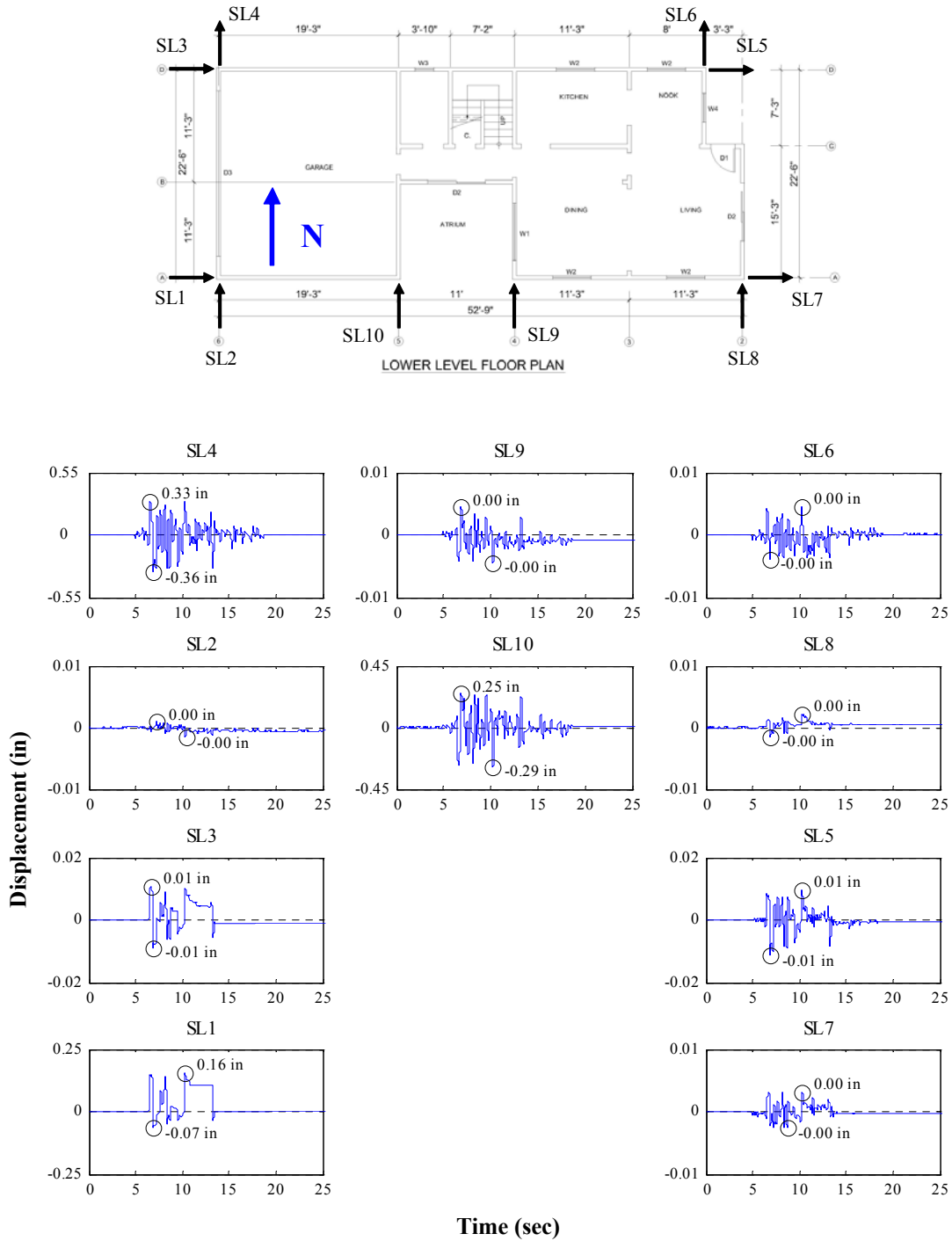


Figure P.33: Sill plate slippage time histories for Test NWP2S30

Appendix P

Phase 3, NWP3S01 Seismic Test

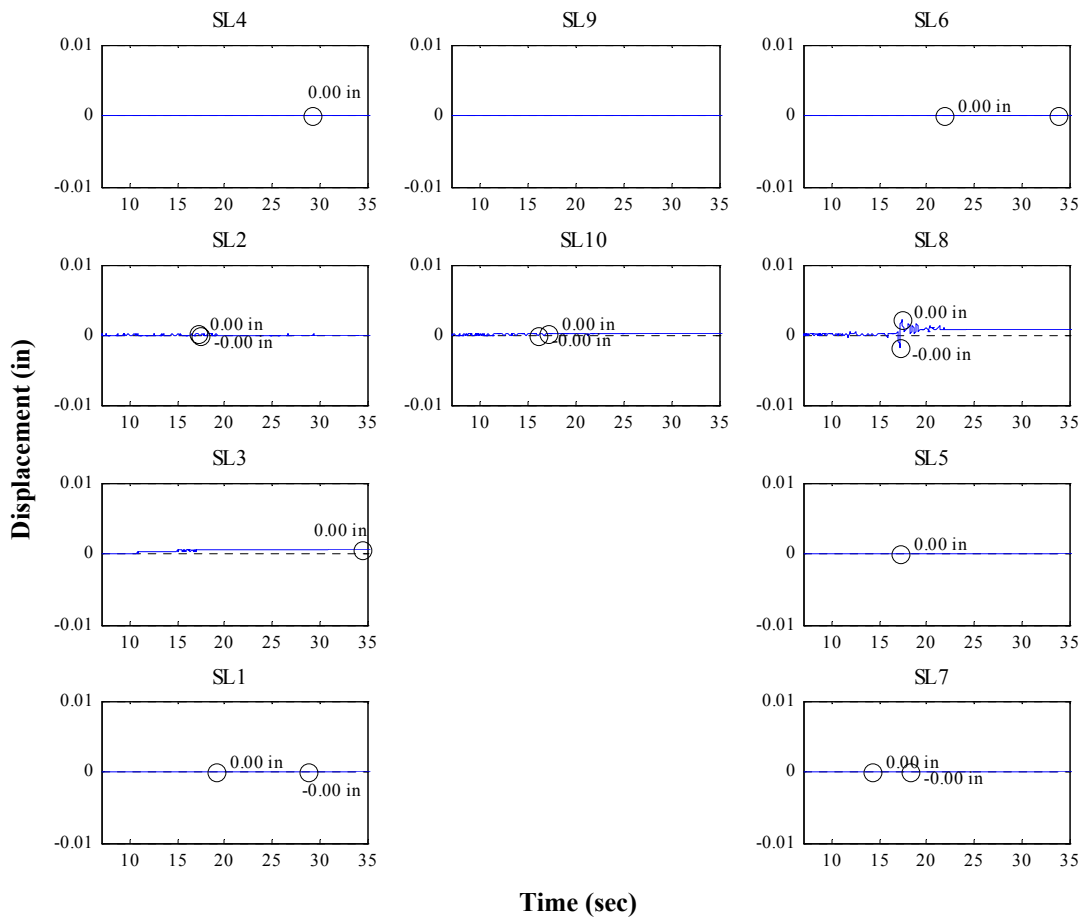
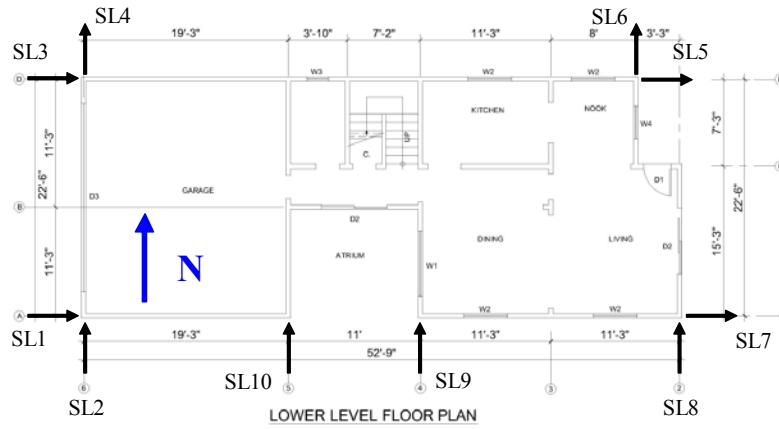


Figure P.34: Sill plate slippage time histories for Test NWP3S01

Appendix P

Phase 3, NWP3S02 Seismic Test

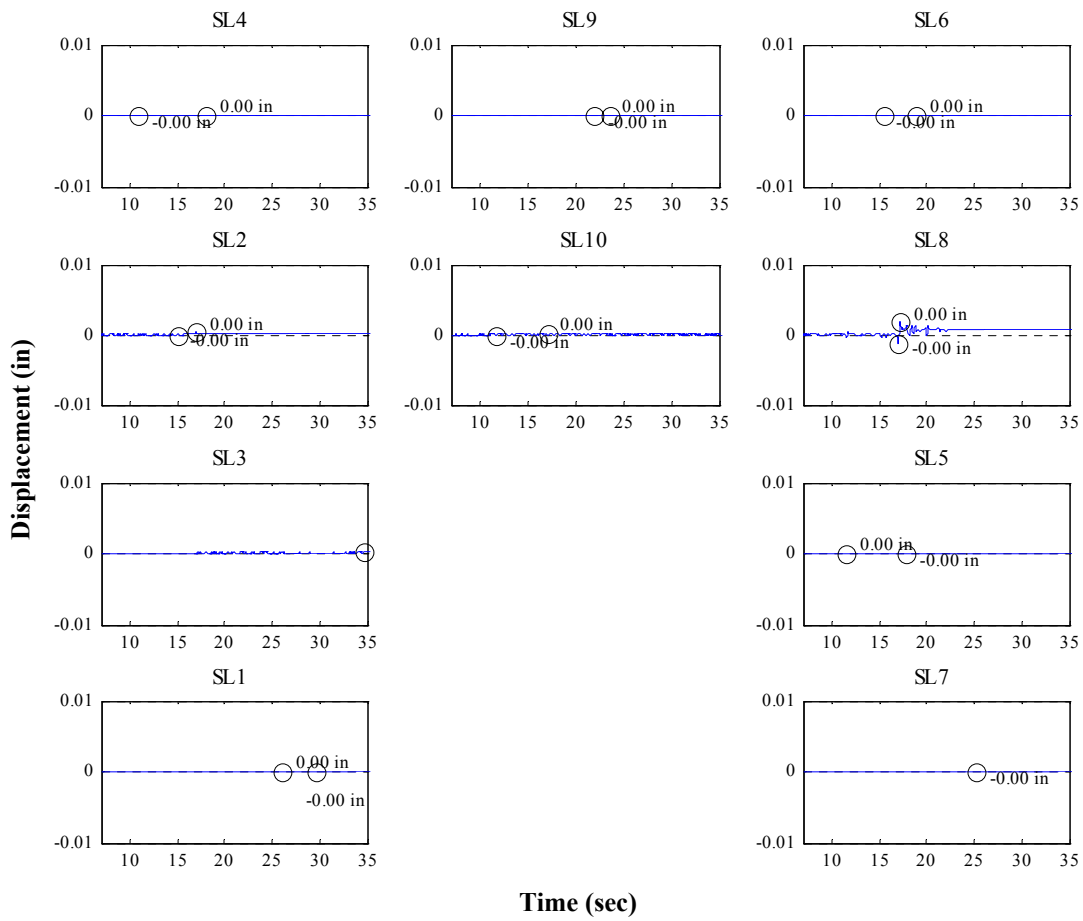
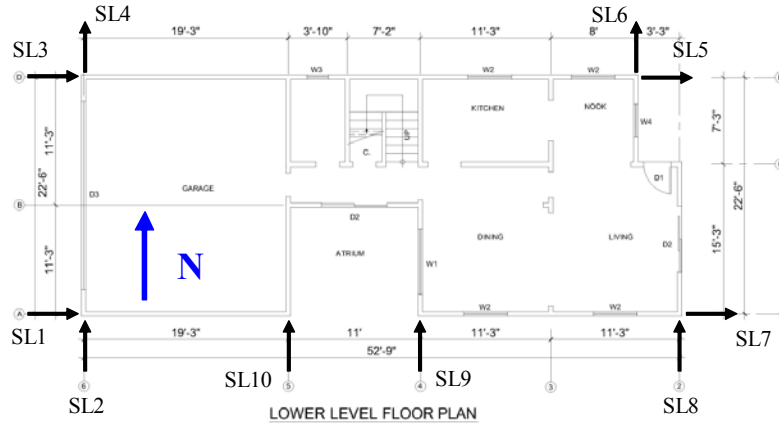


Figure P.35: Sill plate slippage time histories for Test NWP3S02

Appendix P

Phase 3, NWP3S03 Seismic Test

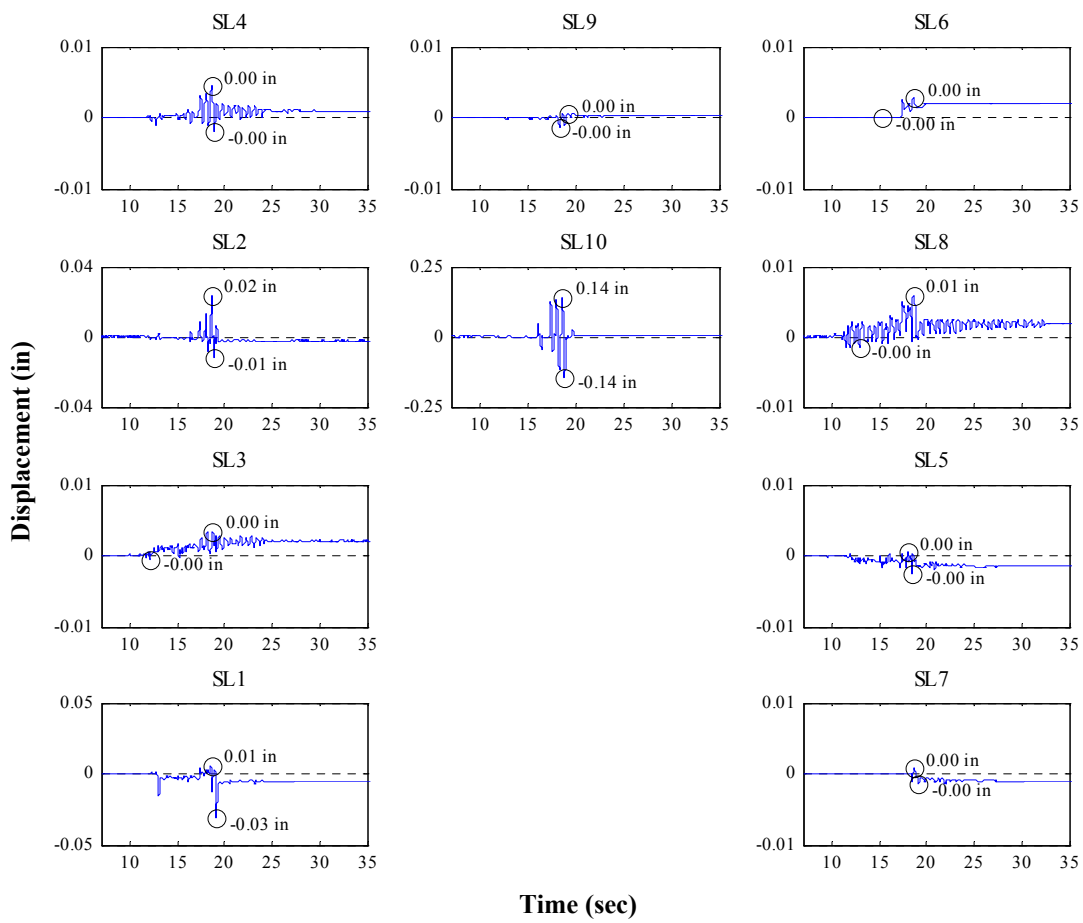
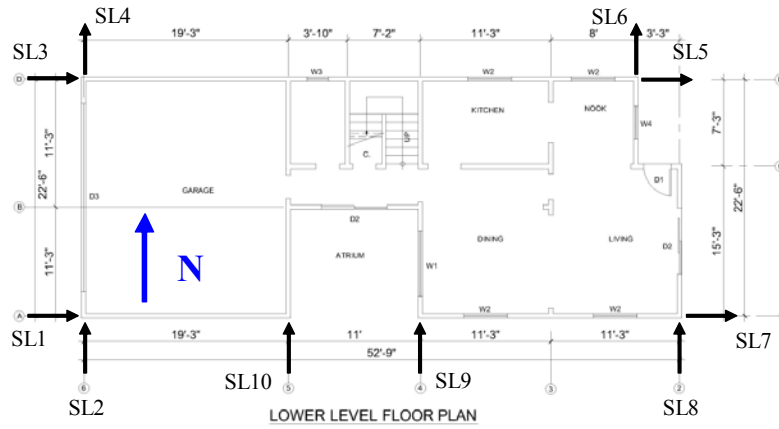


Figure P.36: Sill plate slippage time histories for Test NWP3S03

Appendix P

Phase 3, NWP3S04 Seismic Test

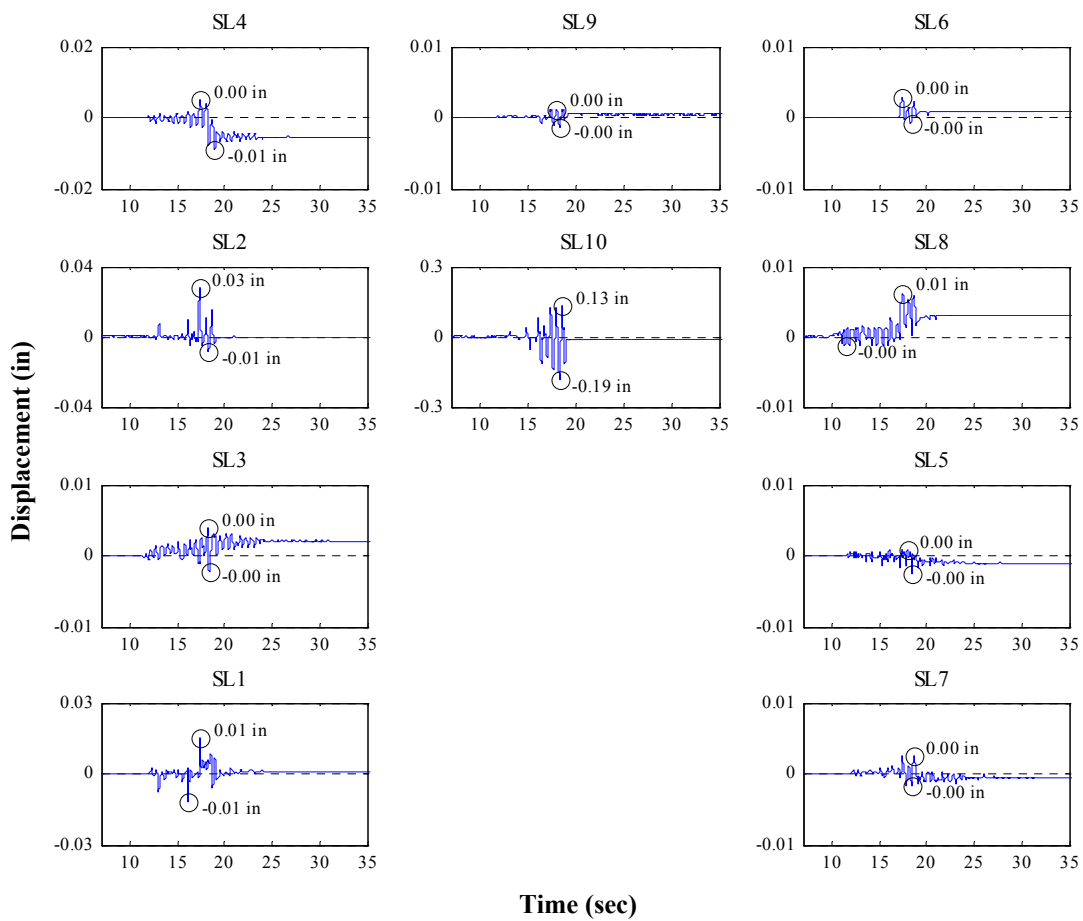
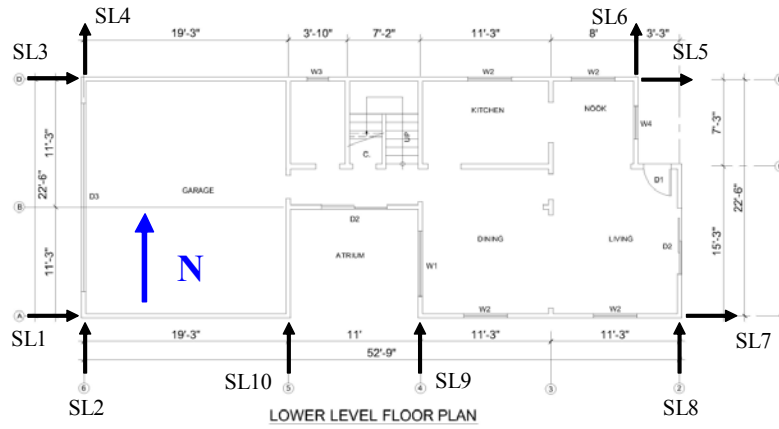


Figure P.37: Sill plate slippage time histories for Test NWP3S04

Appendix P

Phase 4, NWP4S01 Seismic Test

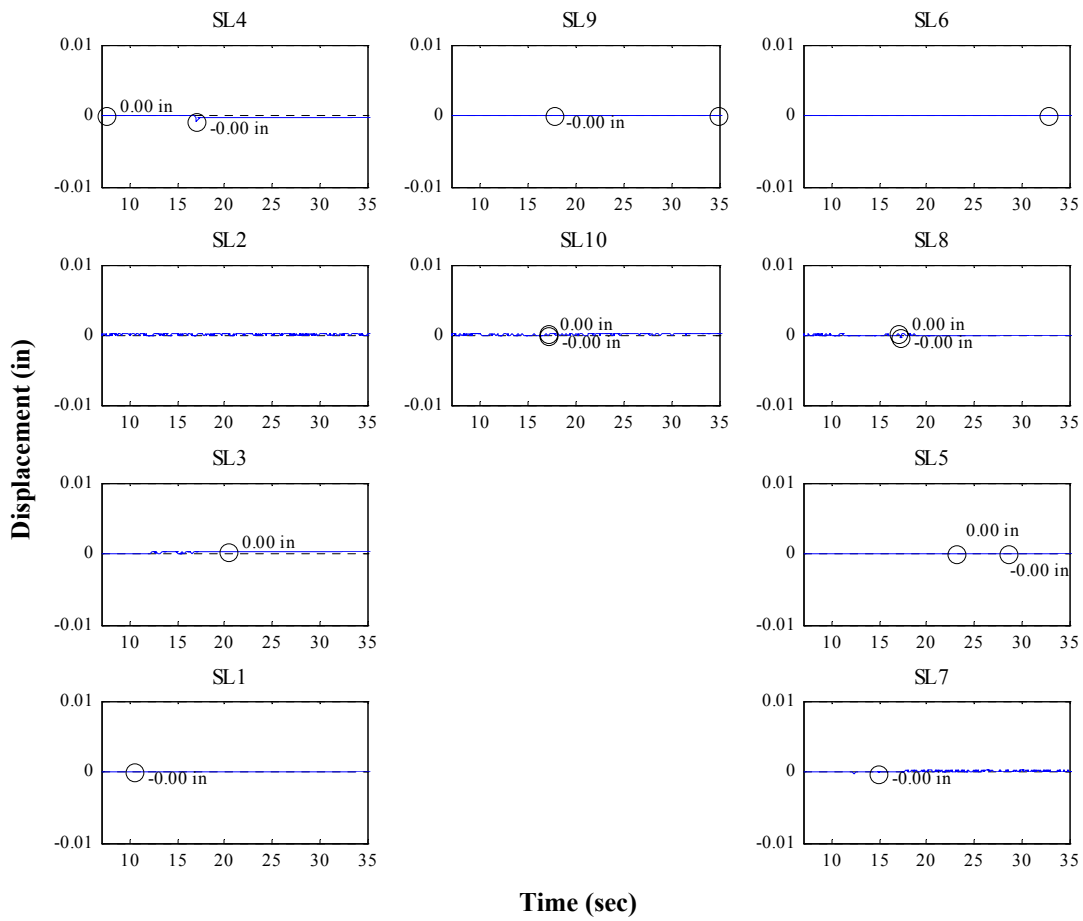
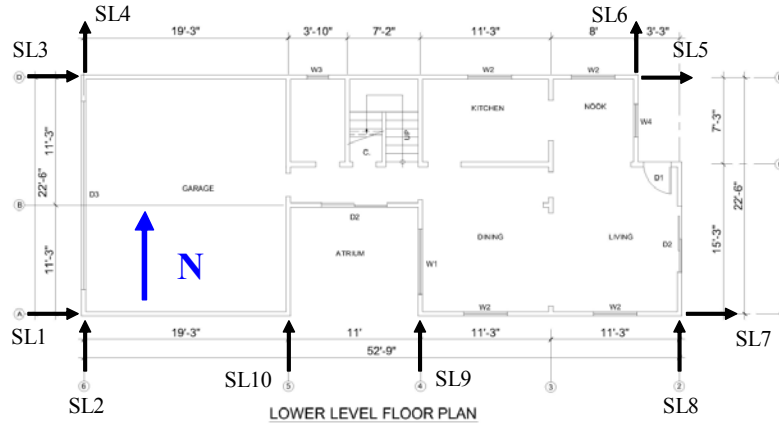


Figure P.38: Sill plate slippage time histories for Test NWP4S01

Appendix P

Phase 4, NWP4S02 Seismic Test

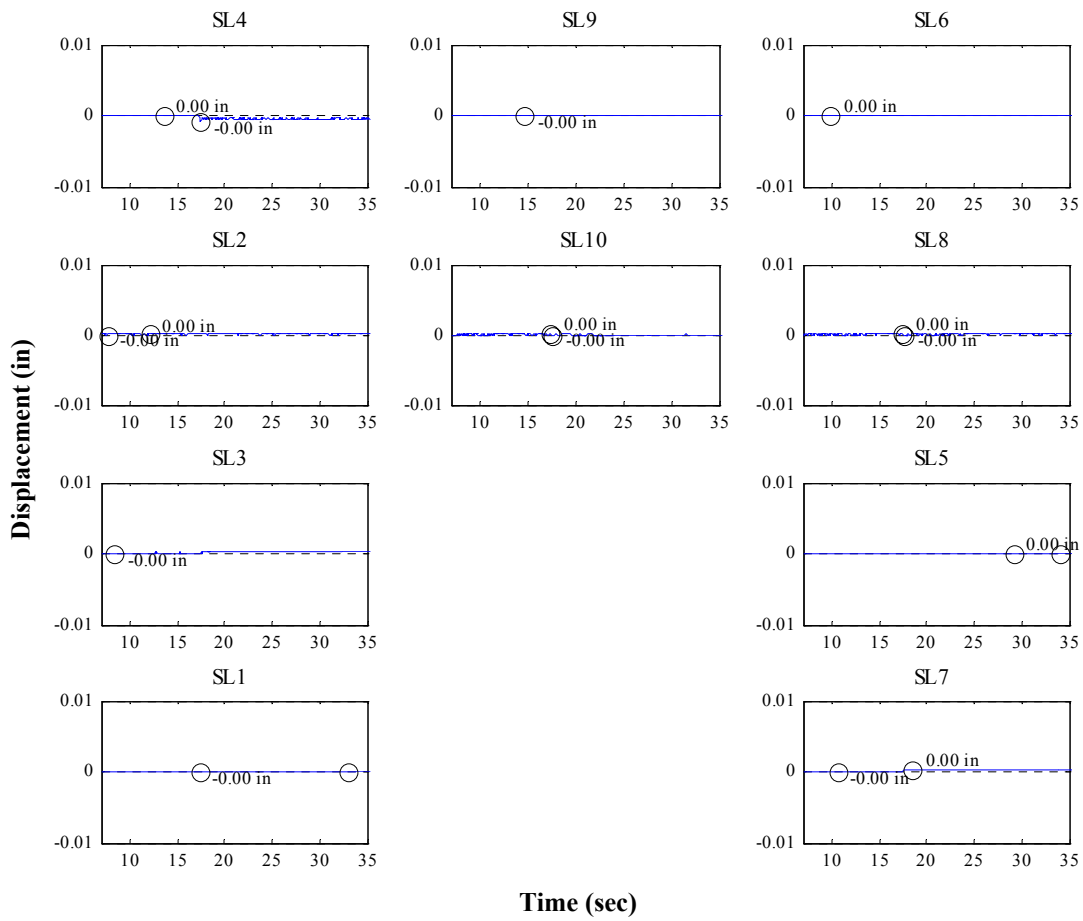
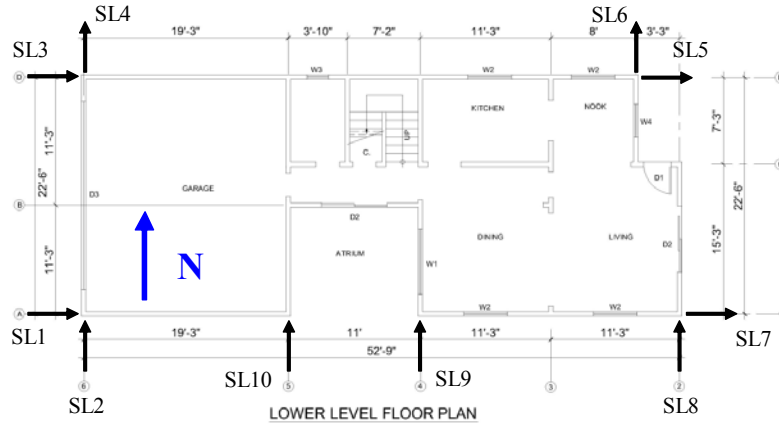


Figure P.39: Sill plate slippage time histories for Test NWP4S02

Appendix P

Phase 4, NWP4S03 Seismic Test

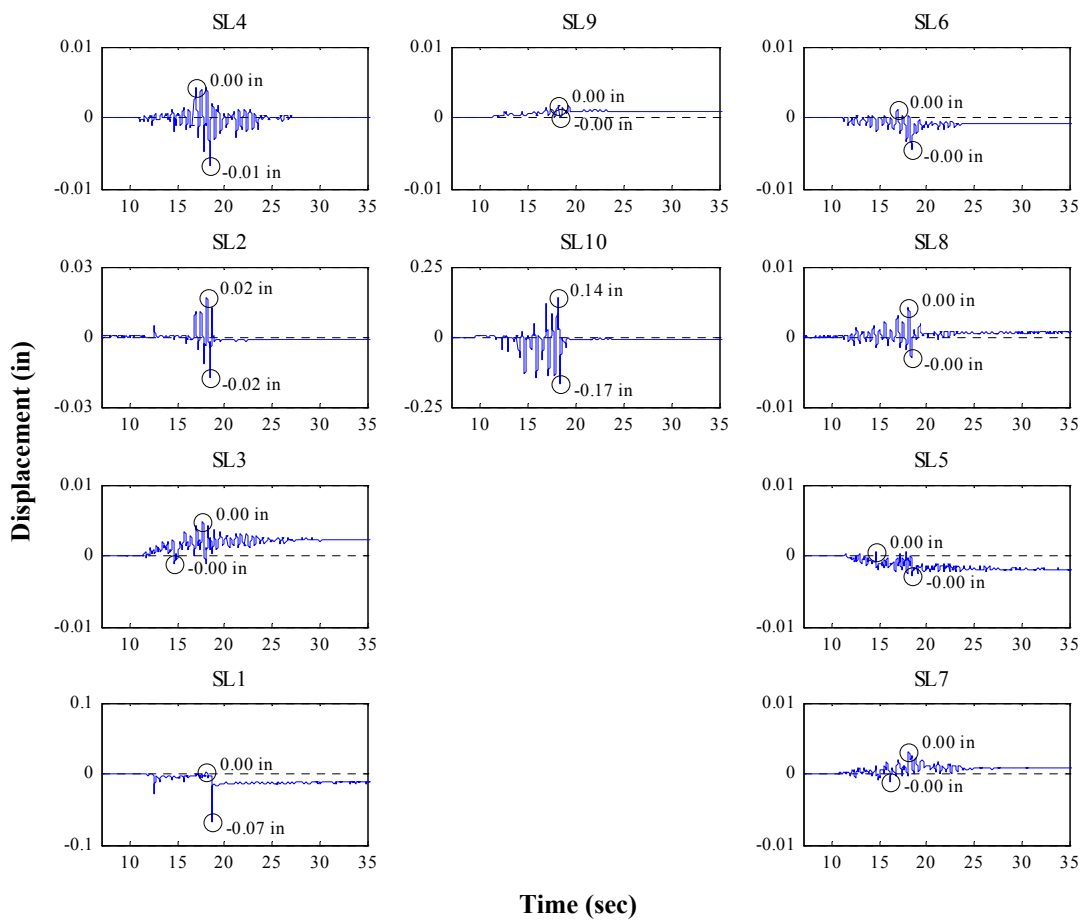
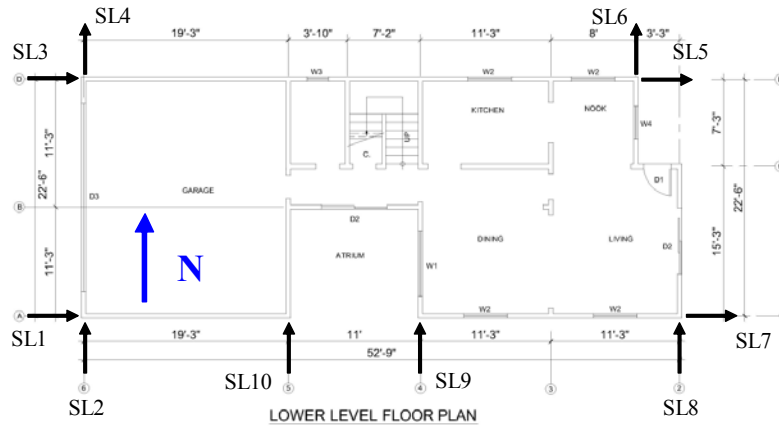


Figure P.40: Sill plate slippage time histories for Test NWP4S03

Appendix P

Phase 4, NWP4S04 Seismic Test

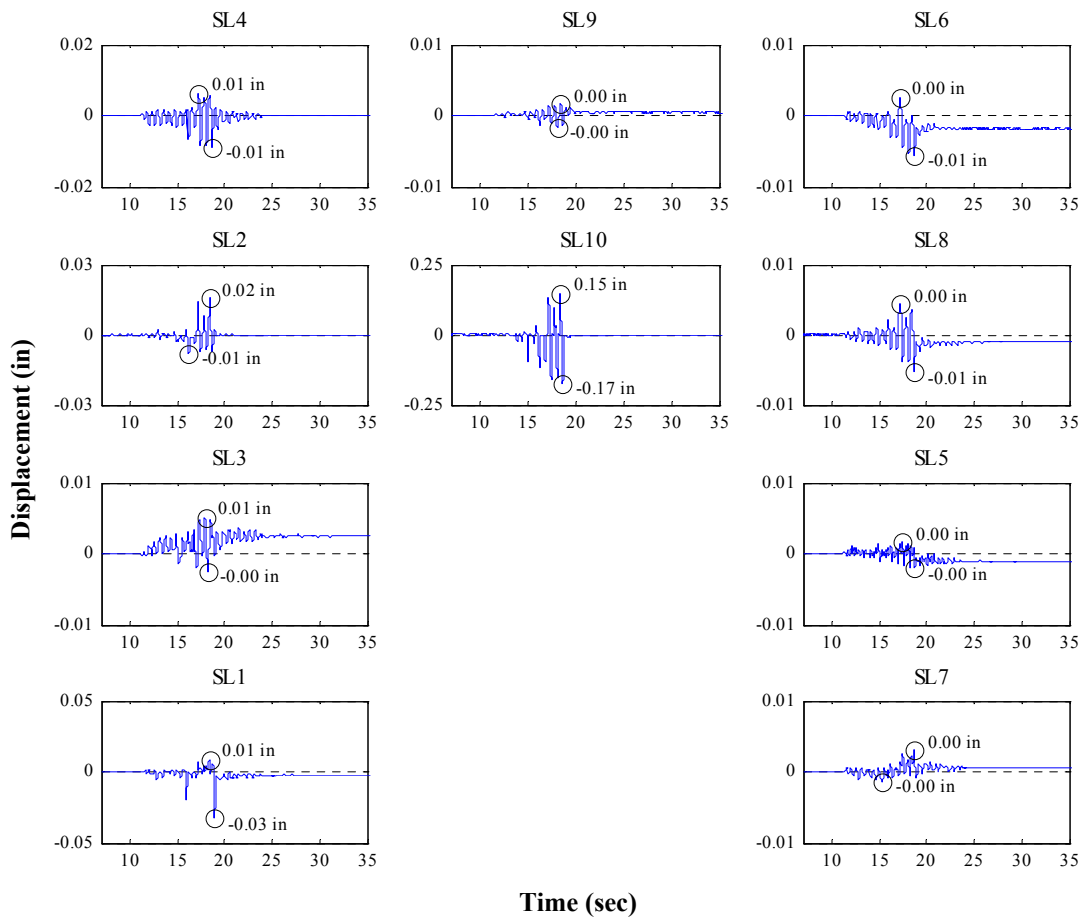
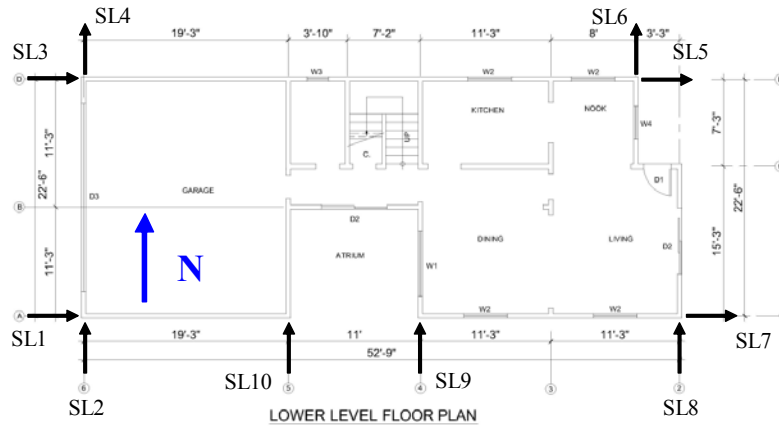


Figure P.41: Sill plate slippage time histories for Test NWP4S04

Appendix P

Phase 5, NWP5S01 Seismic Test

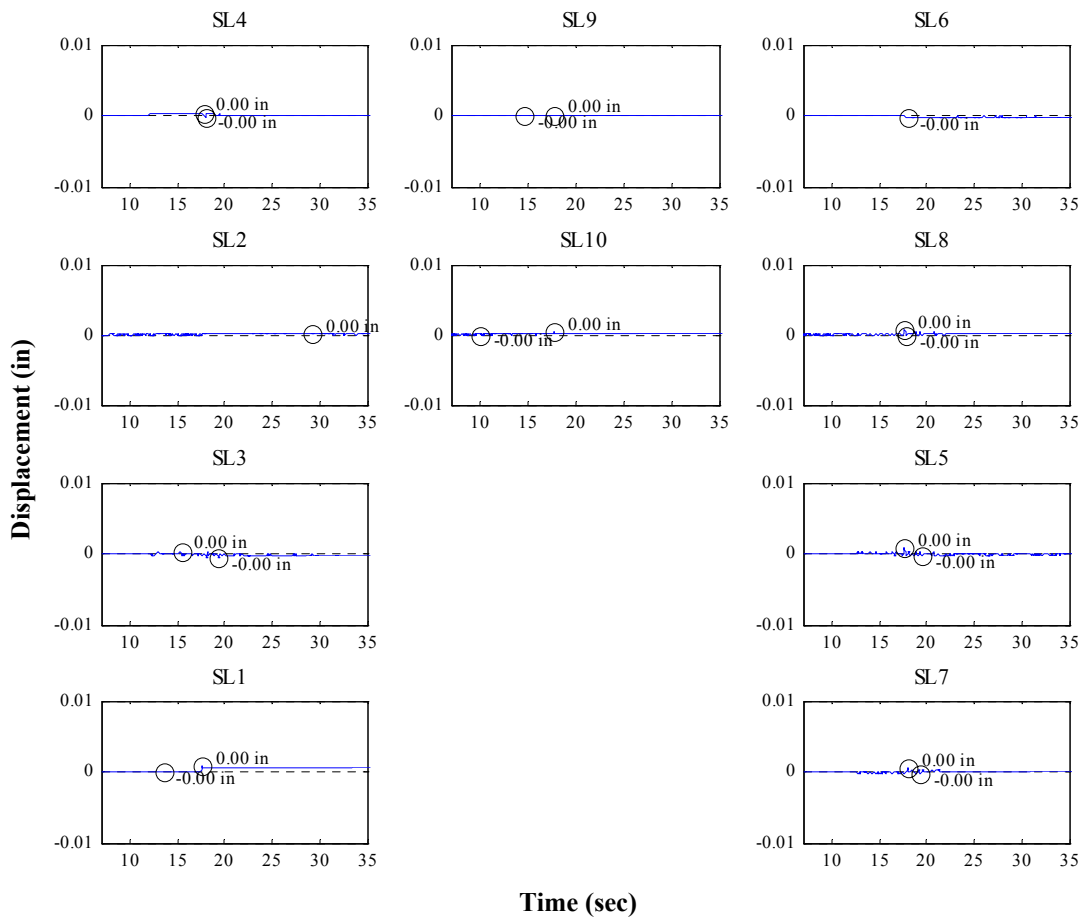
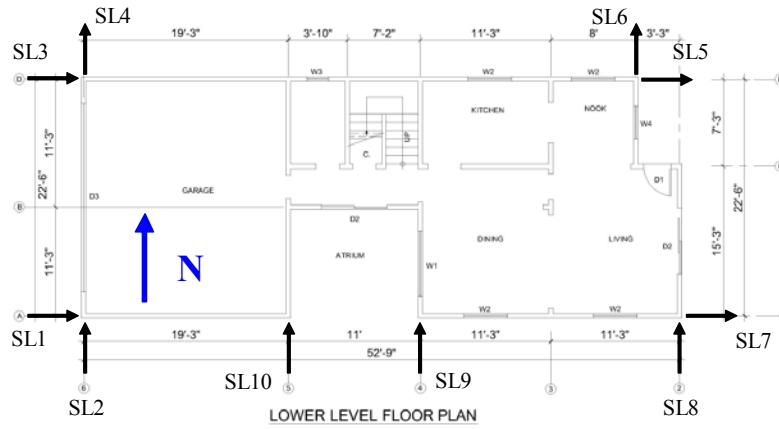


Figure P.42: Sill plate slippage time histories for Test NWP5S01

Appendix P

Phase 5, NWP5S02 Seismic Test

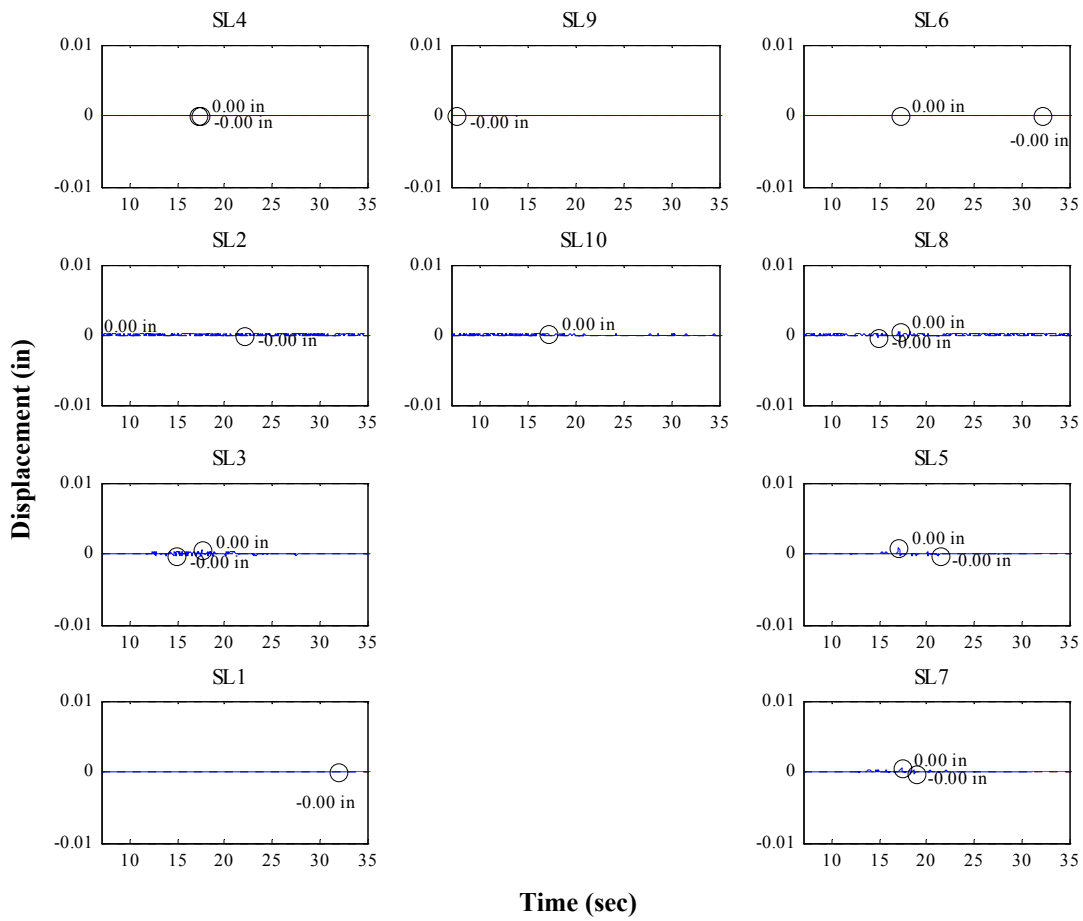
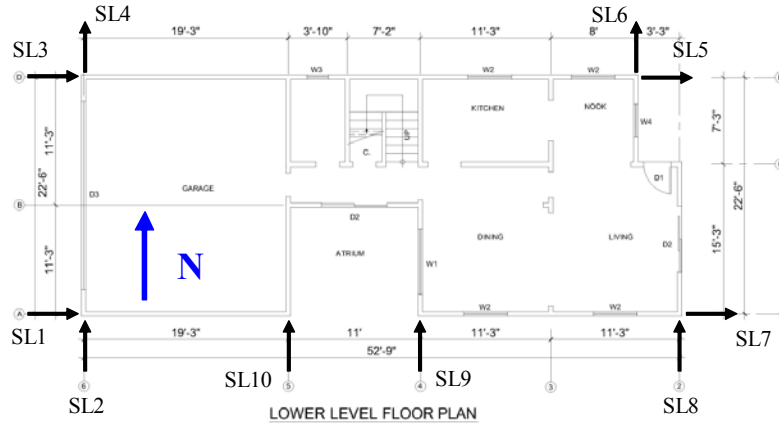


Figure P.43: Sill plate slippage time histories for Test NWP5S02

Appendix P

Phase 5, NWP5S03 Seismic Test

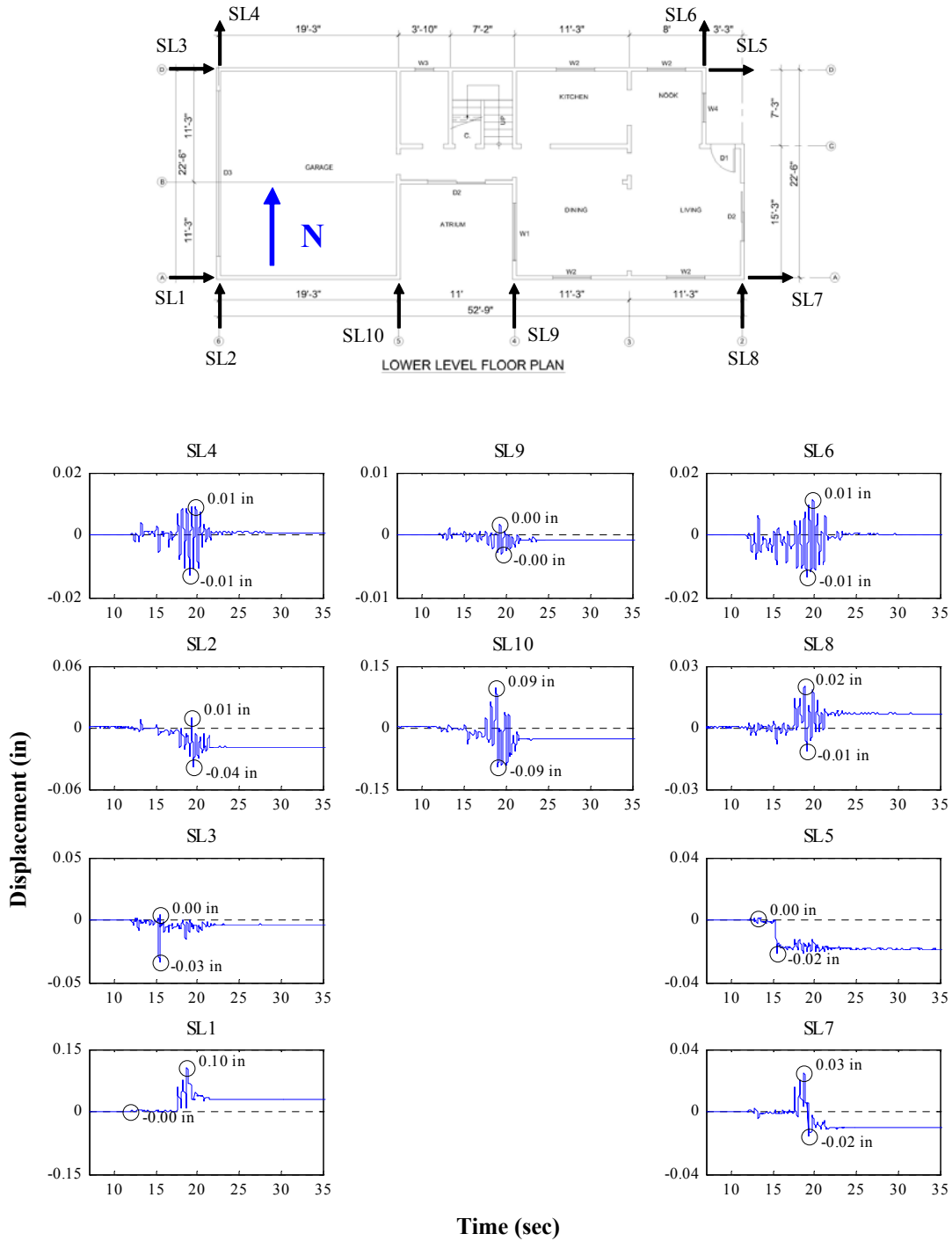


Figure P.44: Sill plate slippage time histories for Test NWP5S03

Appendix P

Phase 5, NWP5S04 Seismic Test

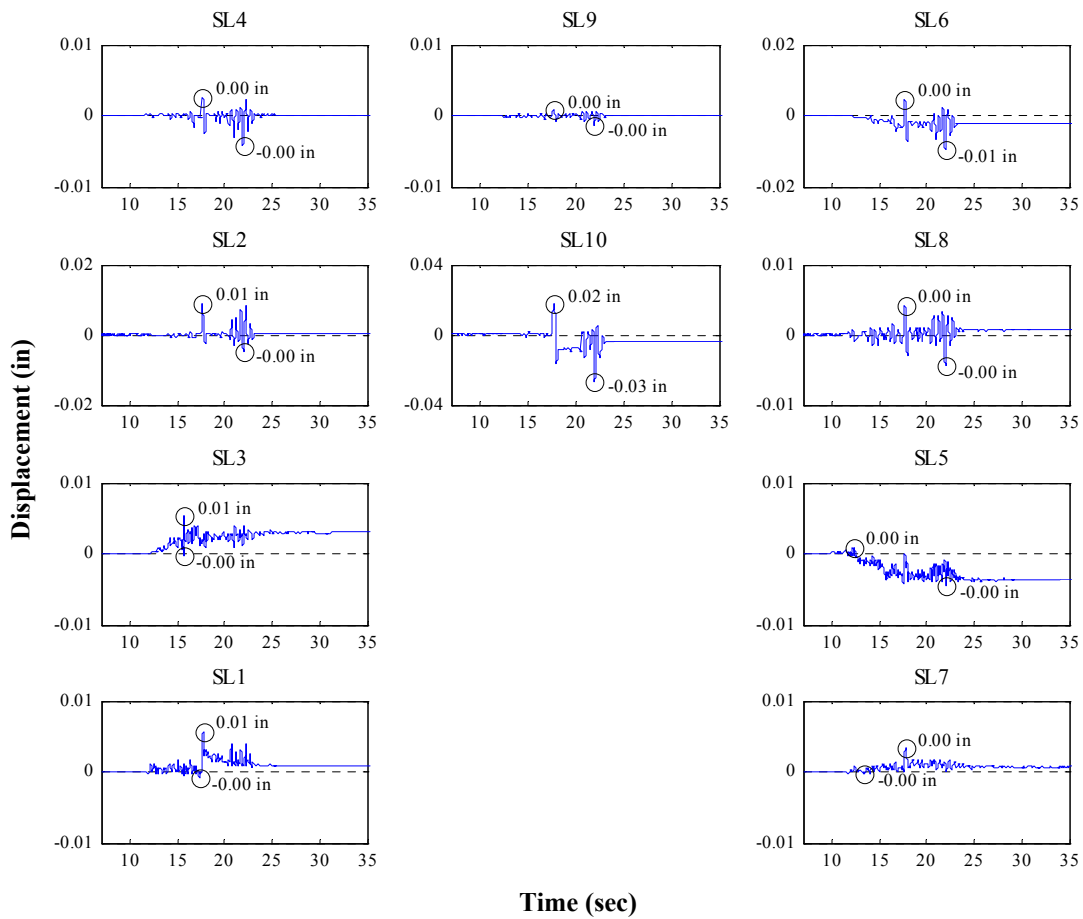
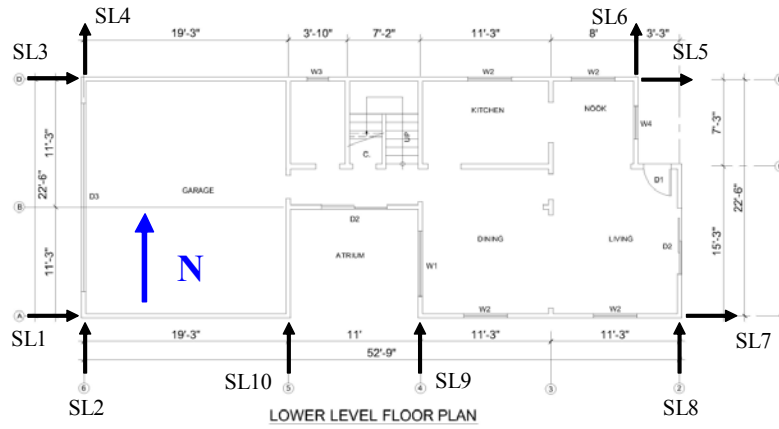


Figure P.45: Sill plate slippage time histories for Test NWP5S04

Appendix P

Phase 5, NWP5S05 Seismic Test

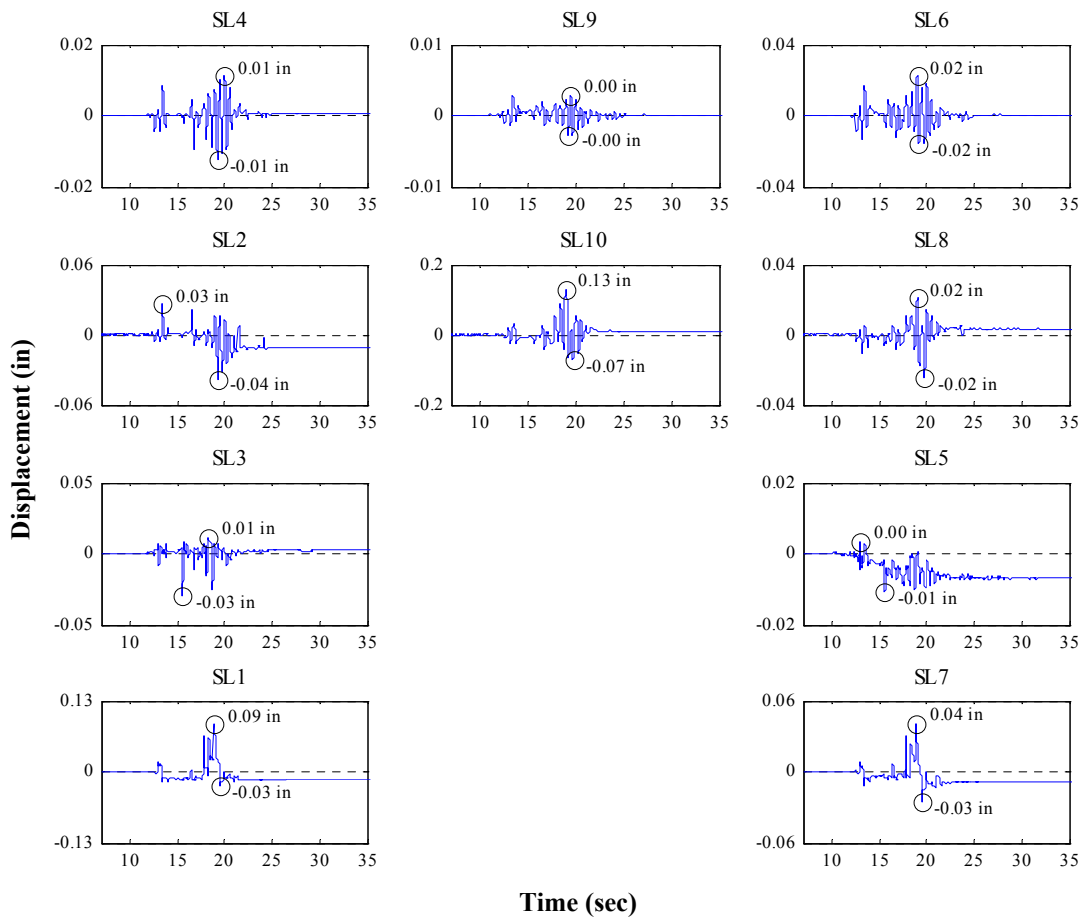
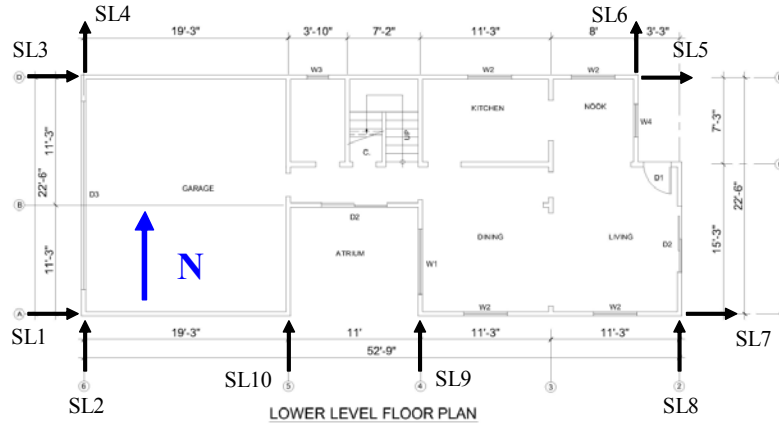


Figure P.46: Sill plate slippage time histories for Test NWP5S05

Appendix P

Phase 5, NWP5S06 Seismic Test

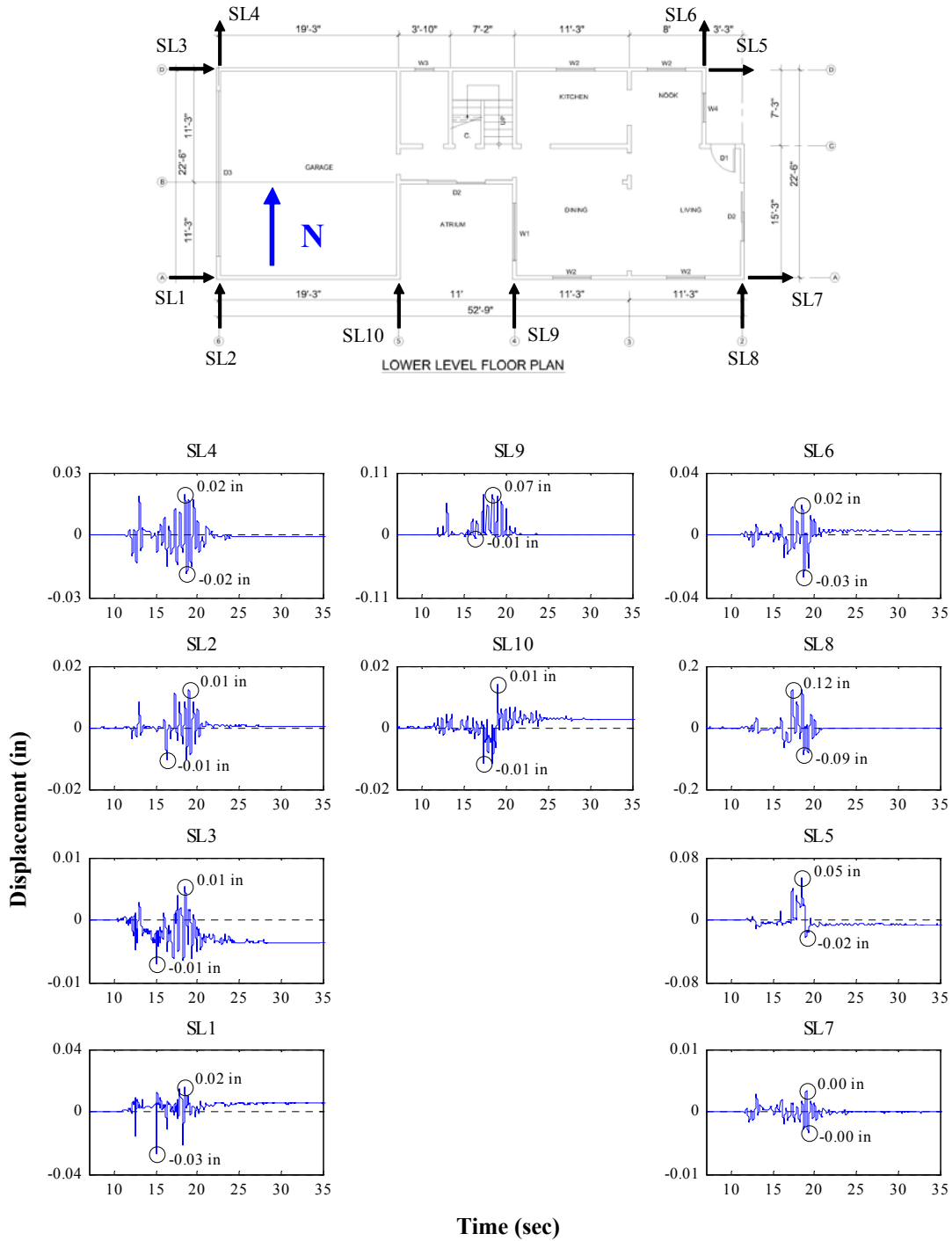


Figure P.47: Sill plate slippage time histories for Test NWP5S06

Appendix P

Phase 5, NWP5S07 Seismic Test

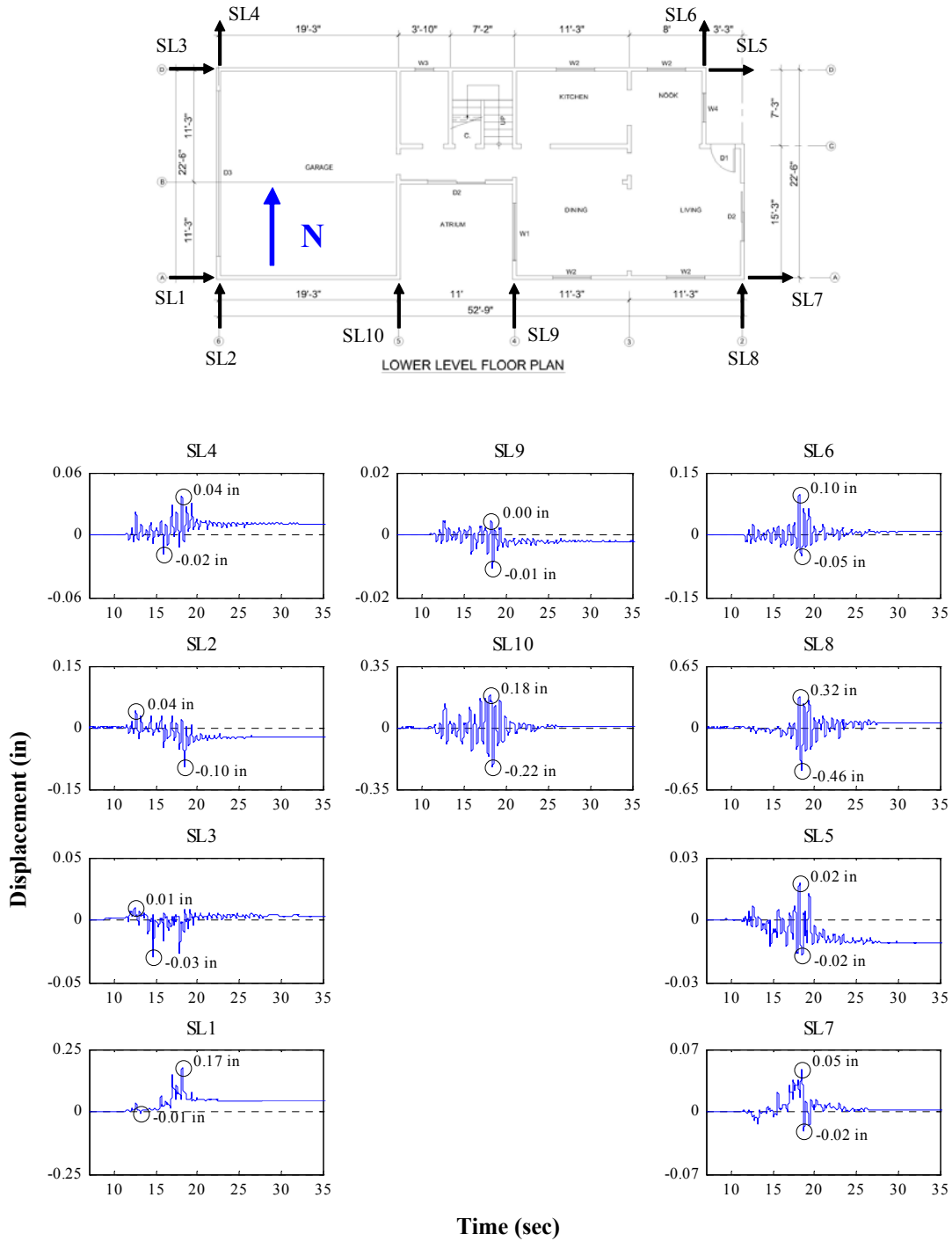


Figure P.48: Sill plate slippage time histories for Test NWP5S07

Appendix P

Phase 5, NWP5S08 Seismic Test

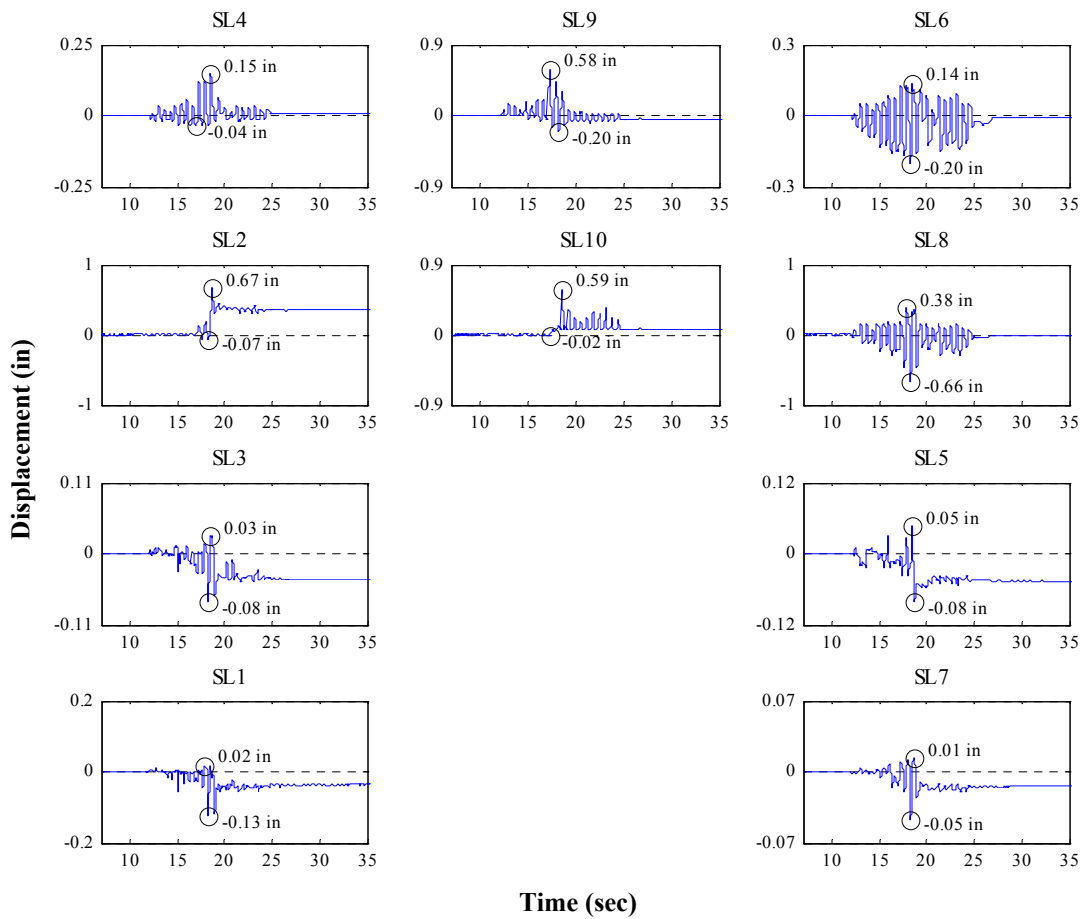
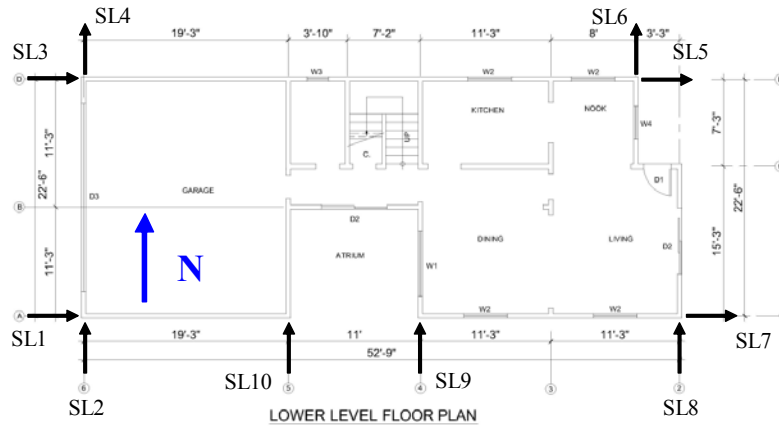


Figure P.49: Sill plate slippage time histories for Test NWP5S08

Appendix P

Phase 5, NWP5S09 Seismic Test

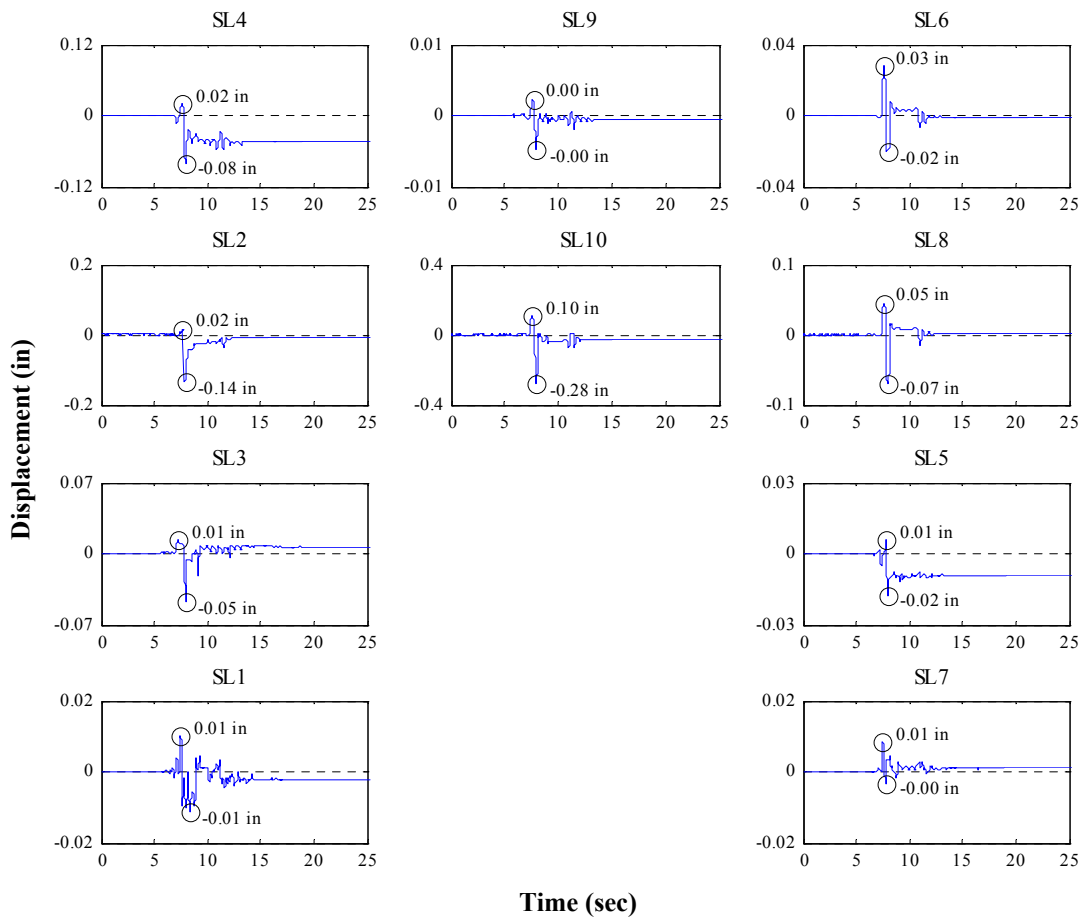
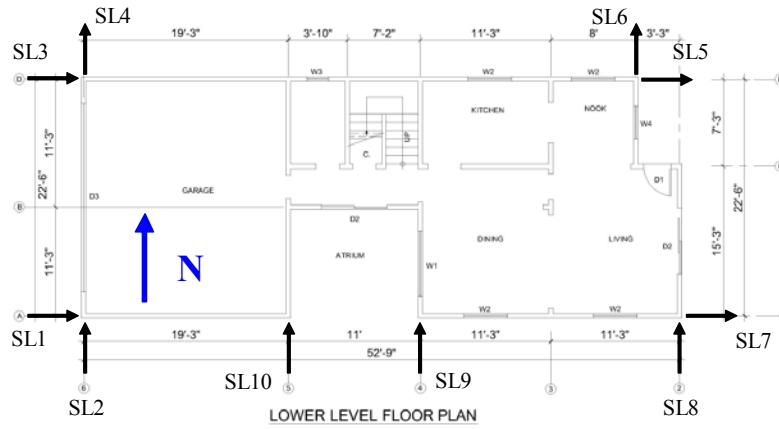


Figure P.50: Sill plate slippage time histories for Test NWP5S09

Appendix P

Phase 5, NWP5S11 Seismic Test

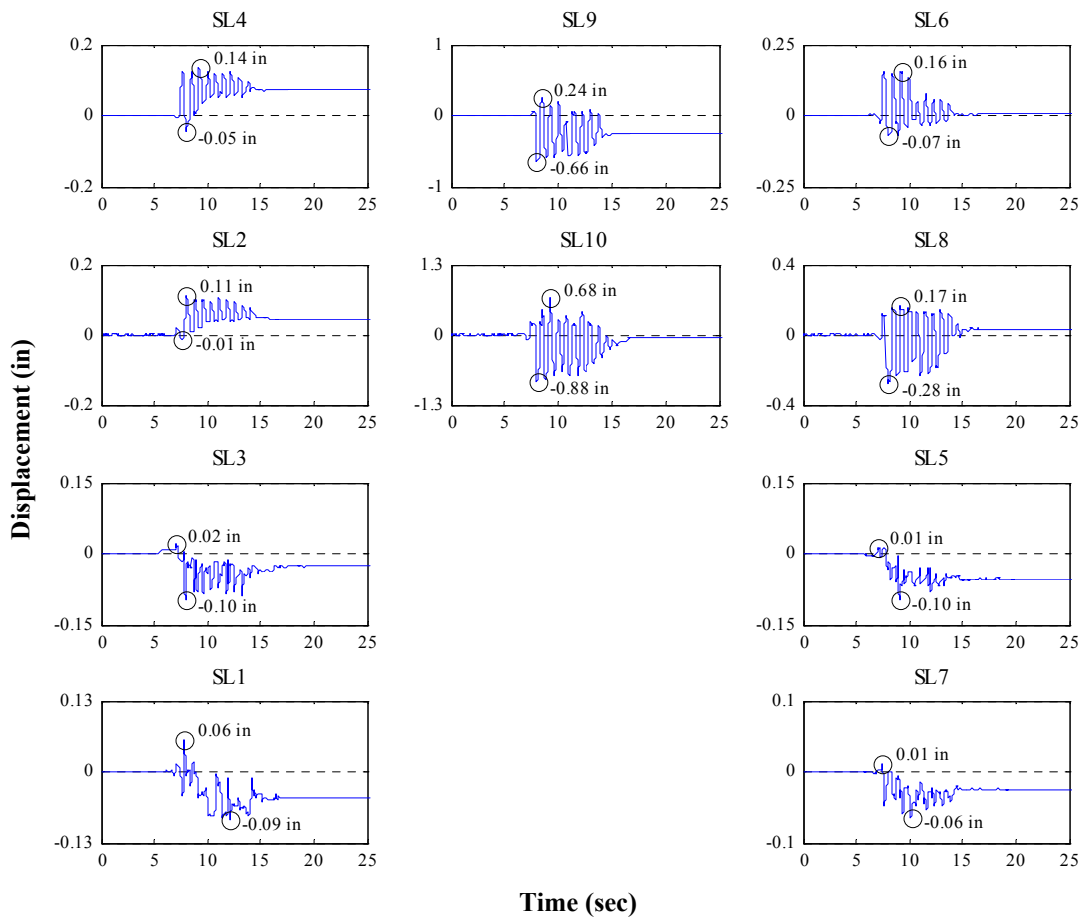
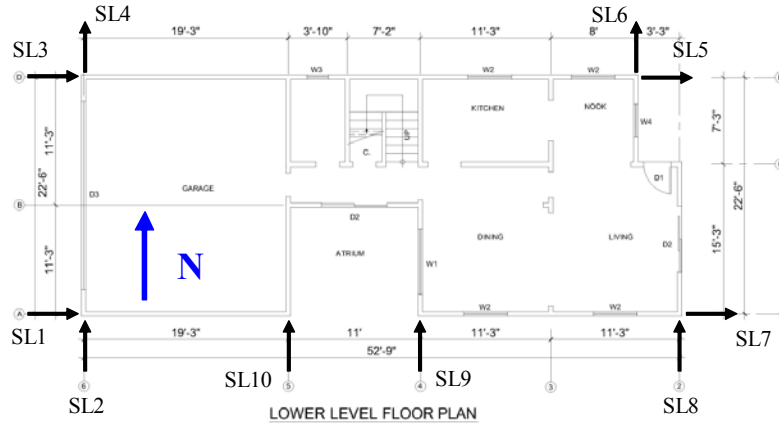


Figure P.51: Sill plate slippage time histories for Test NWP5S11

Appendix Q
Selected Seismic Results:
Peak Anchor Bolt Forces

Appendix Q

Phase 1, NWP1S01 Seismic Test

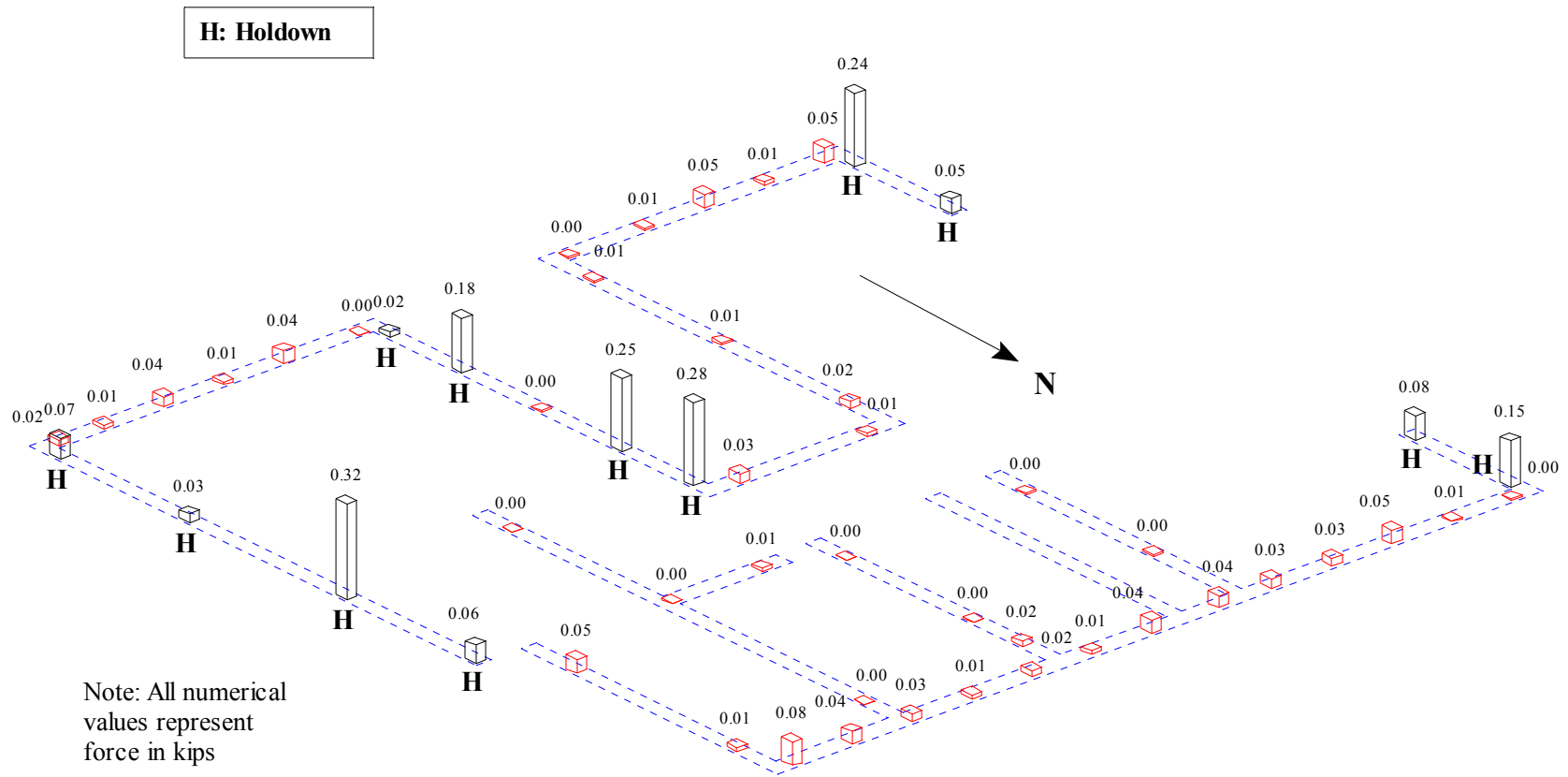


Figure Q.1: Peak anchor bolt forces for Test NWP1S01

Appendix Q

Phase 1, NWP1S03 Seismic Test

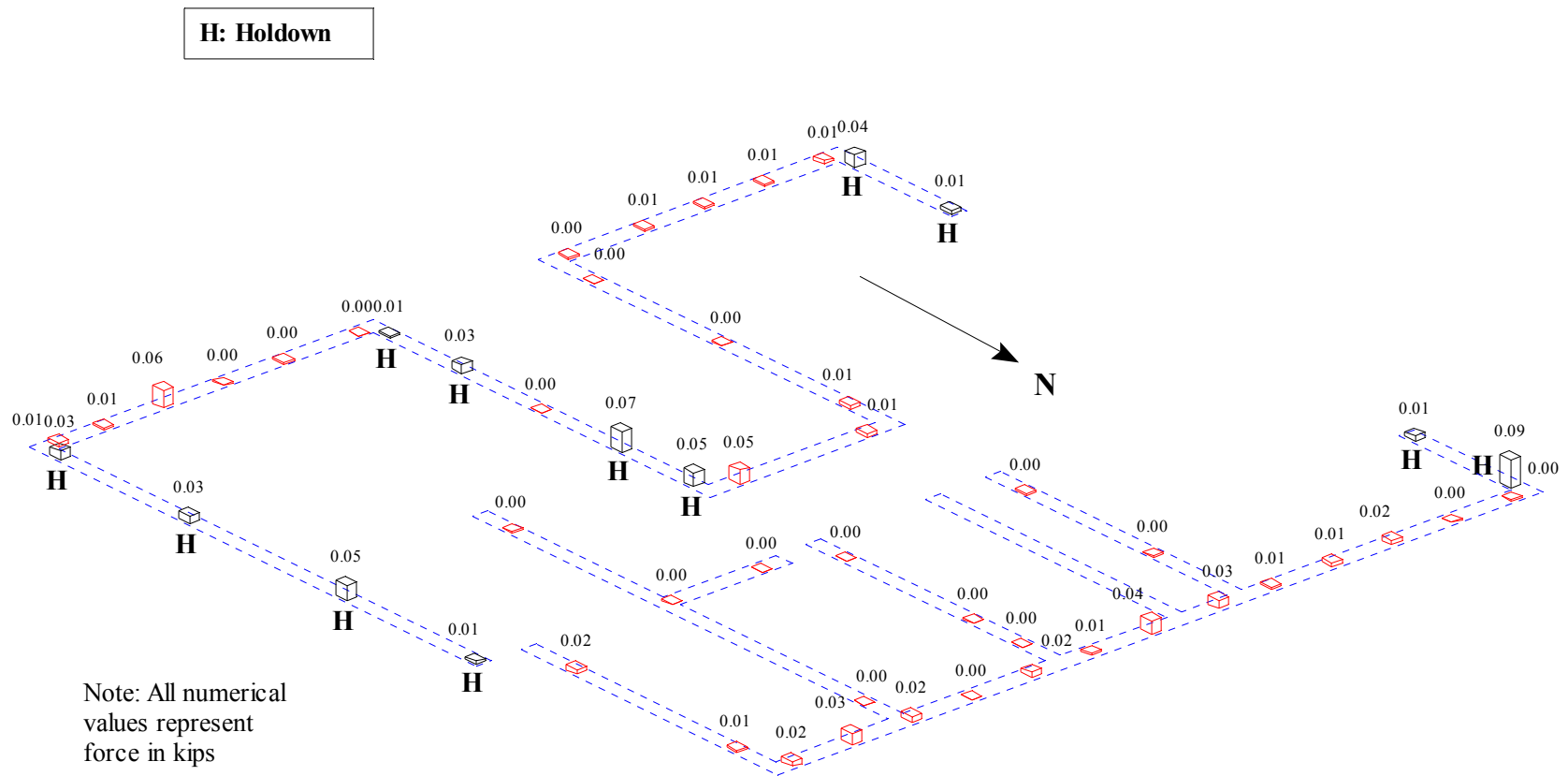


Figure Q.3: Peak anchor bolt forces for Test NWP1S03

Appendix Q

Phase 1, NWP1S04 Seismic Test

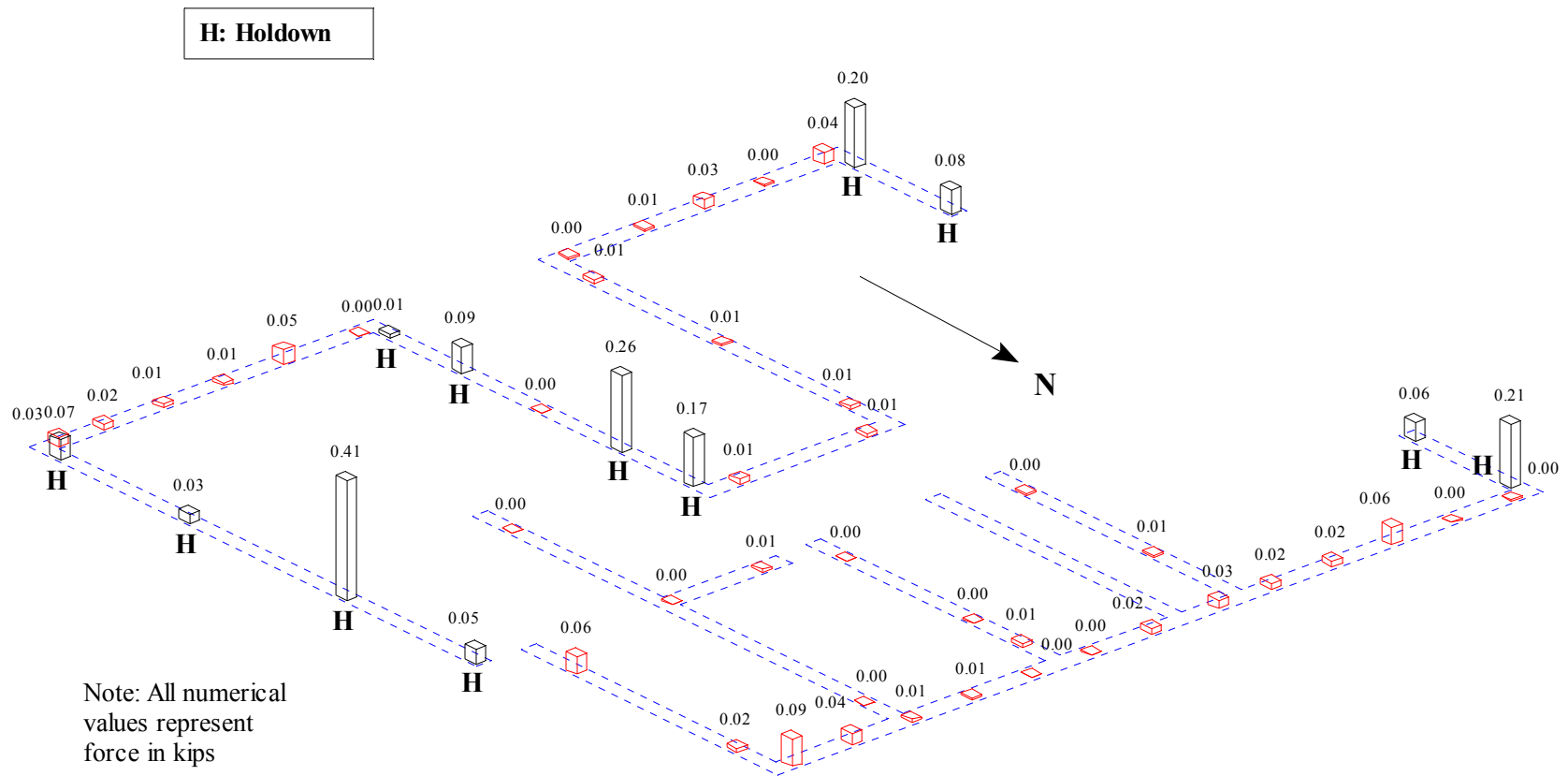


Figure Q.4: Peak anchor bolt forces for Test NWP1S04

Appendix Q

Phase 1, NWP1S05 Seismic Test

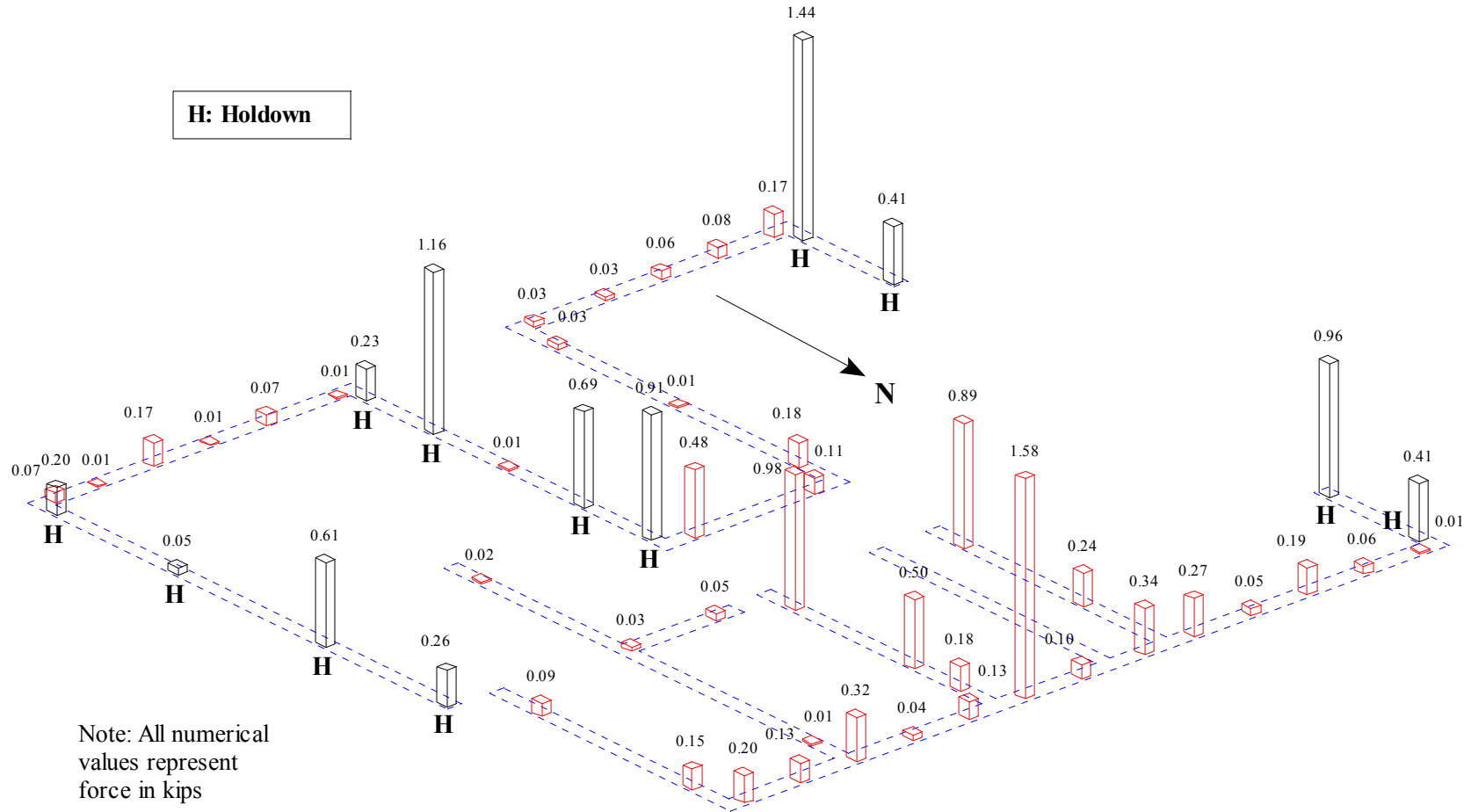


Figure Q.5: Peak anchor bolt forces for Test NWP1S05

Appendix Q

Phase 1, NWP1S17 Seismic Test

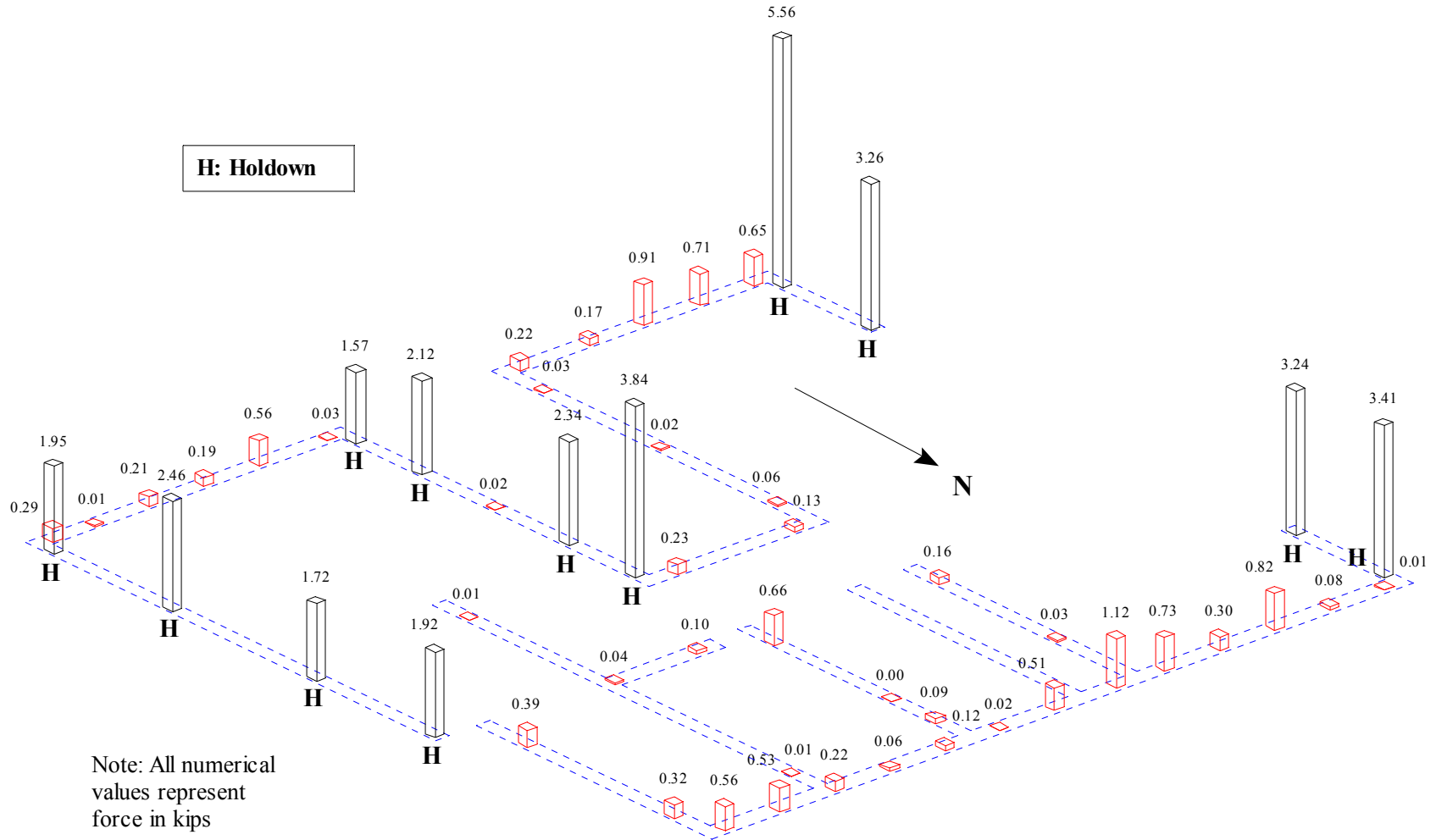


Figure Q.6: Peak anchor bolt forces for Test NWP1S17

Appendix Q

Phase 1, NWP1S07 Seismic Test

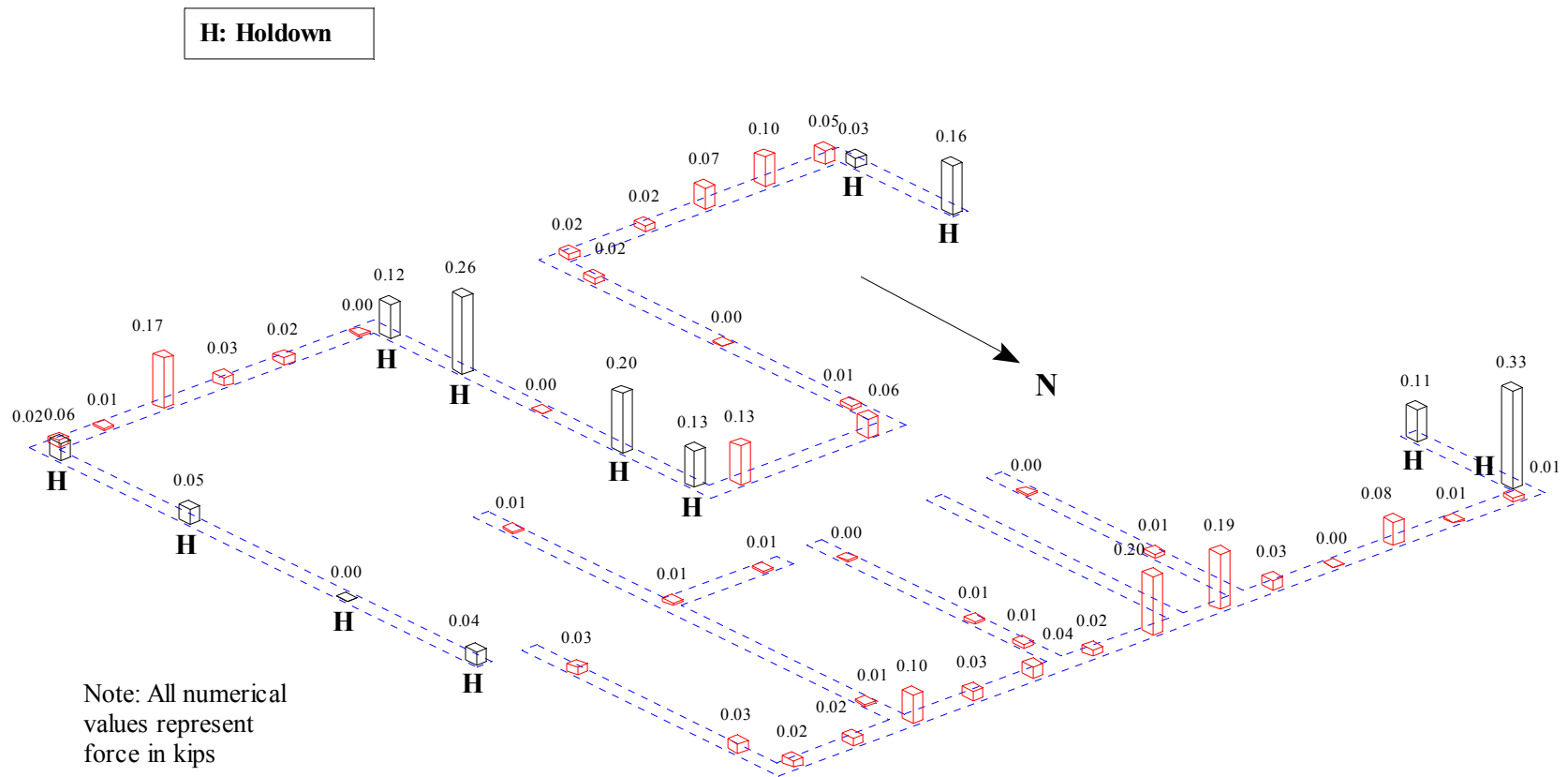


Figure Q.7: Peak anchor bolt forces for Test NWP1S07

Appendix Q

Phase 1, NWP1S06 Seismic Test

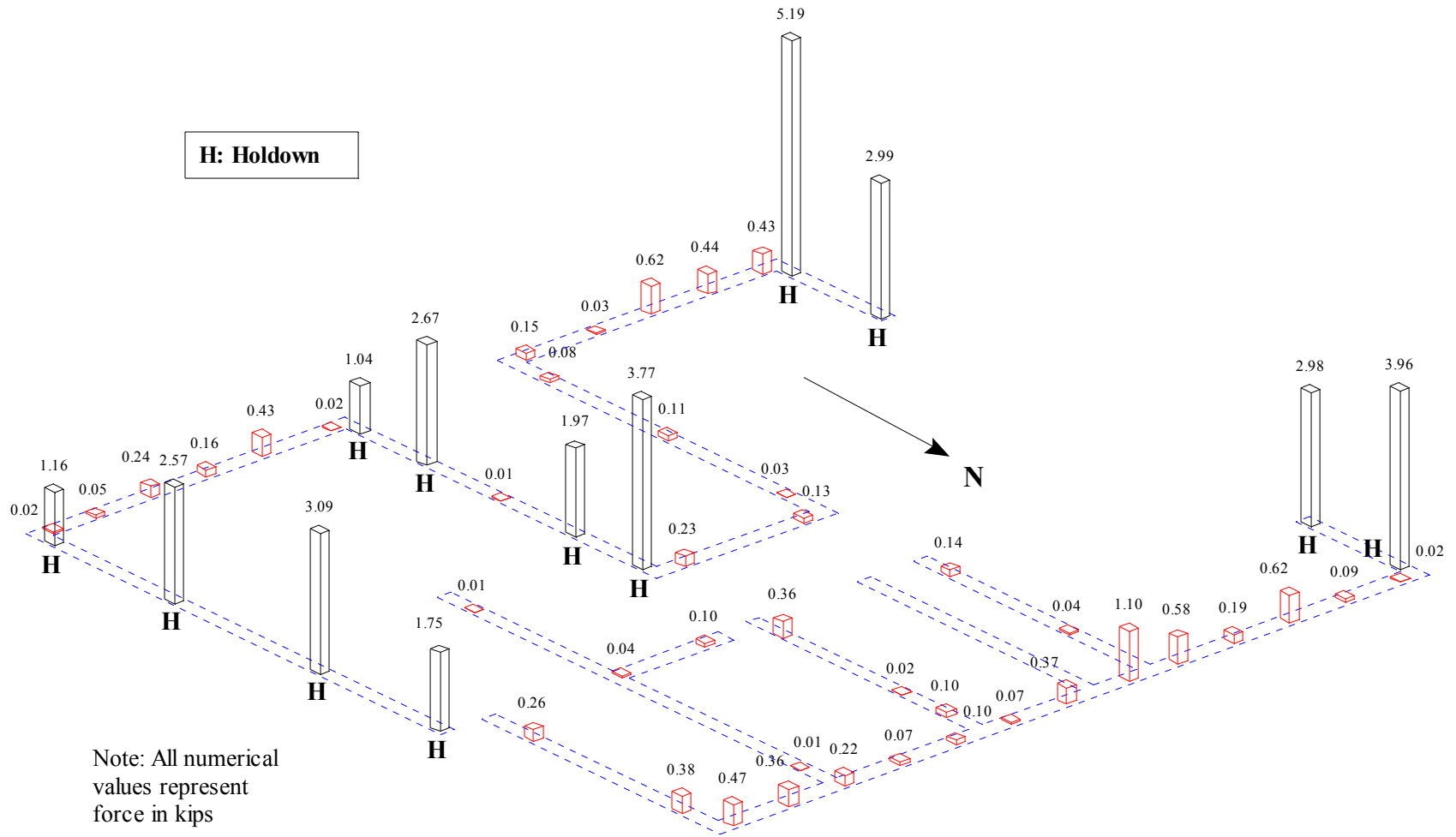


Figure Q.8: Peak anchor bolt forces for Test NWP1S06

Appendix Q

Phase 1, NWP1S10 Seismic Test

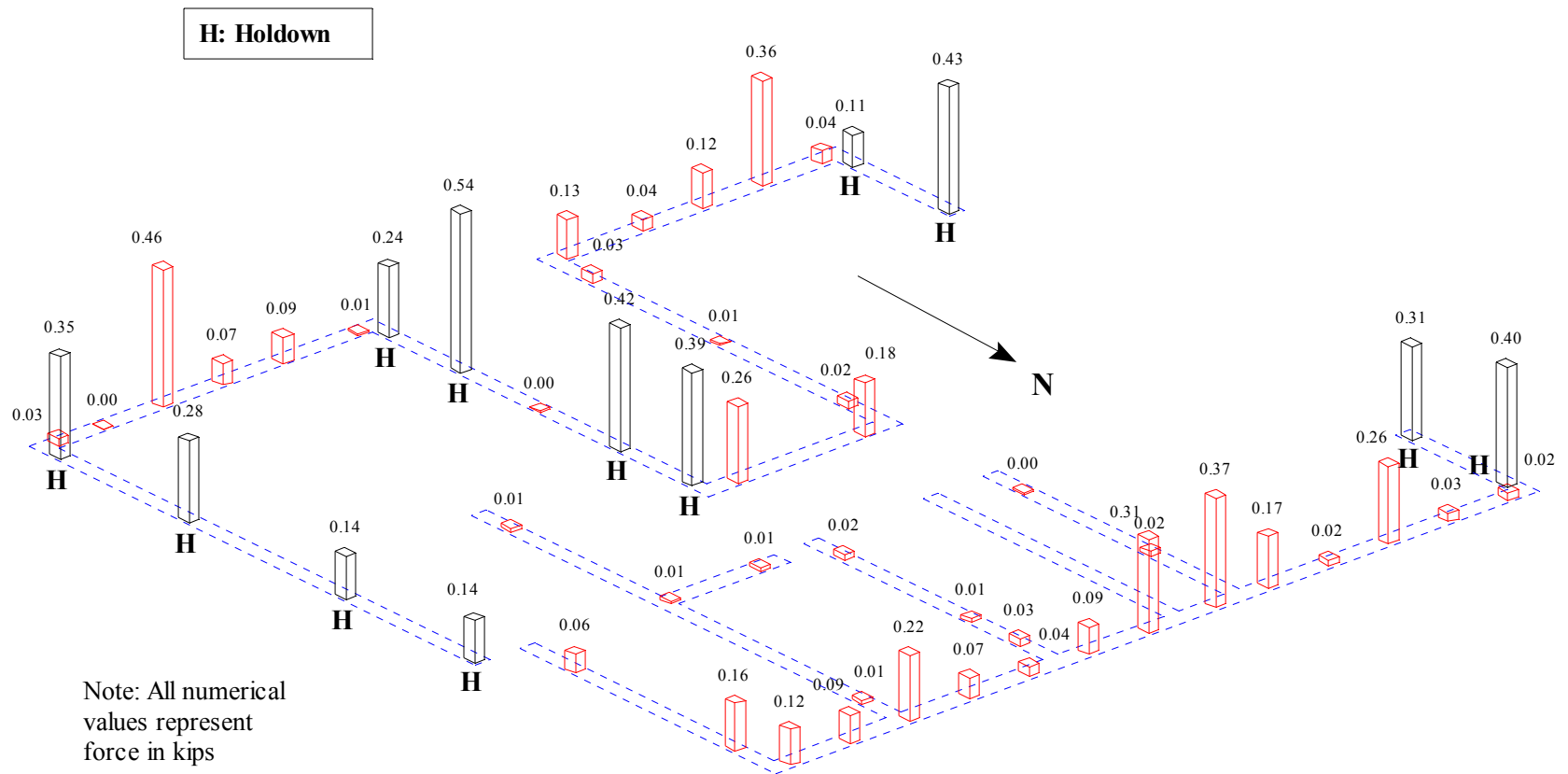


Figure Q.9: Peak anchor bolt forces for Test NWP1S10

Appendix Q

Phase 2, NWP2S01 Seismic Test

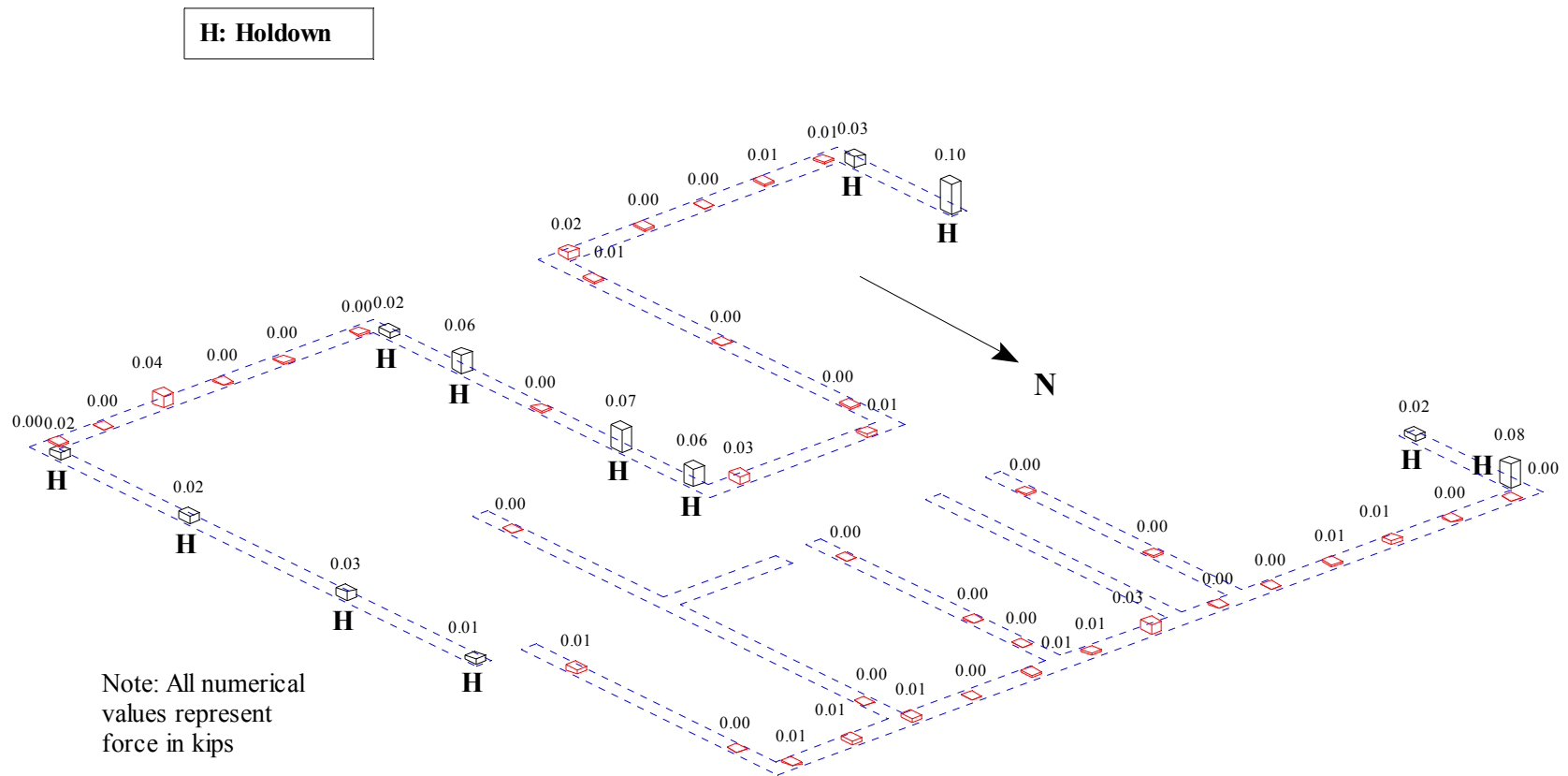


Figure Q.10: Peak anchor bolt forces for Test NWP2S01

Appendix Q

Phase 2, NWP2S02 Seismic Test

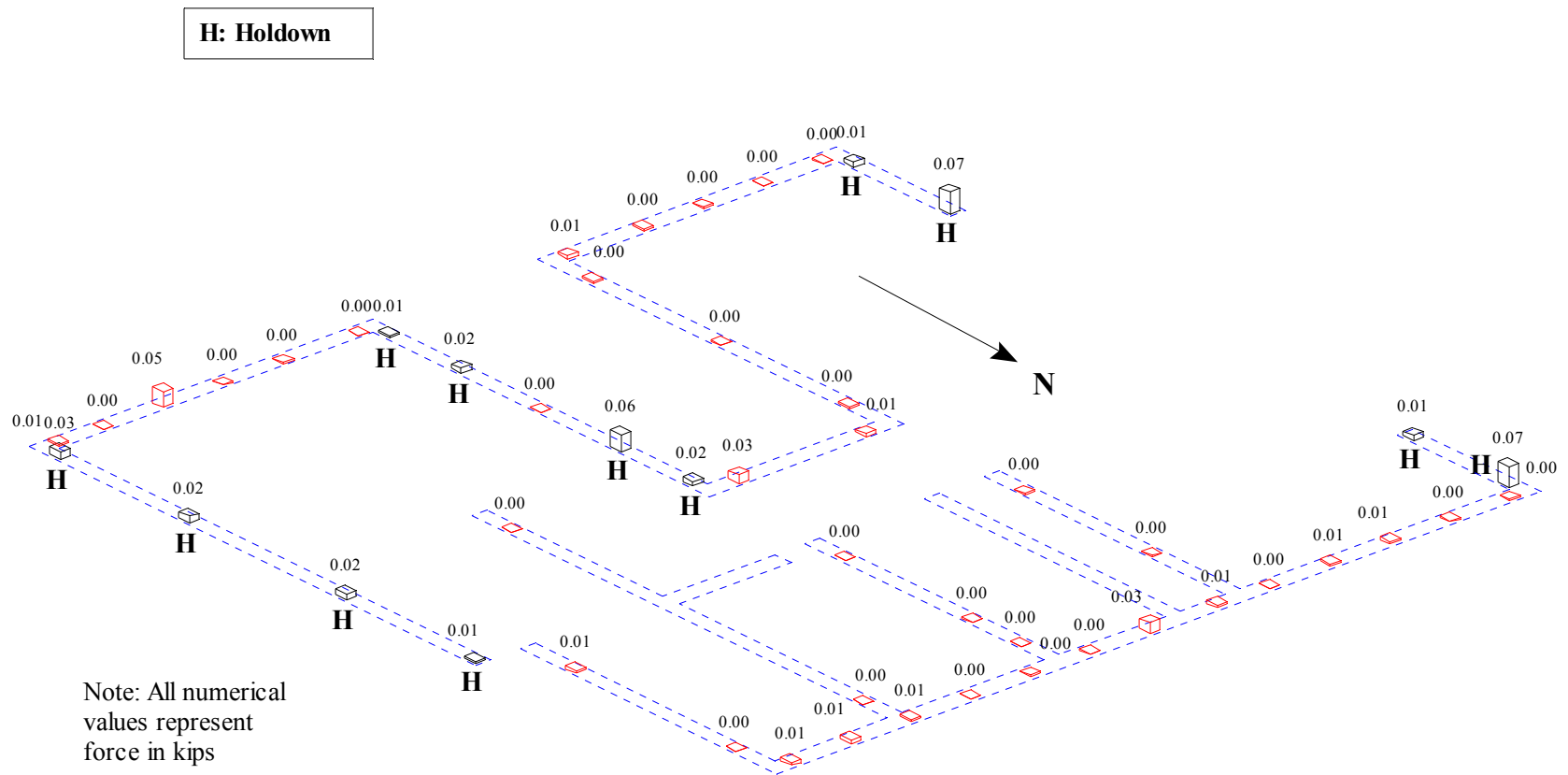


Figure Q.11: Peak anchor bolt forces for Test NWP2S02

Appendix Q

Phase 2, NWP2S05 Seismic Test

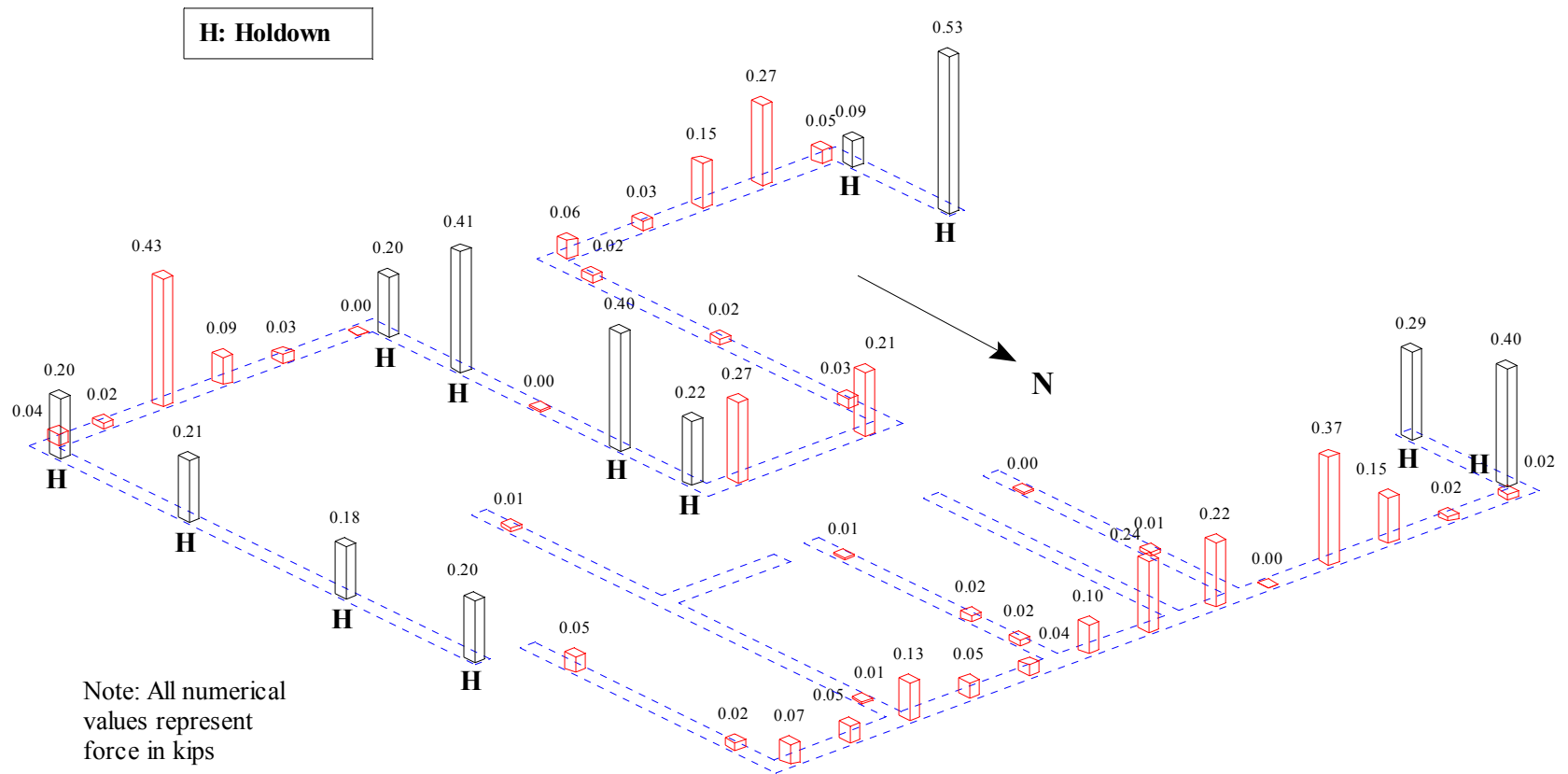


Figure Q.14: Peak anchor bolt forces for Test NWP2S05

Appendix Q

Phase 2, NWP2S06 Seismic Test

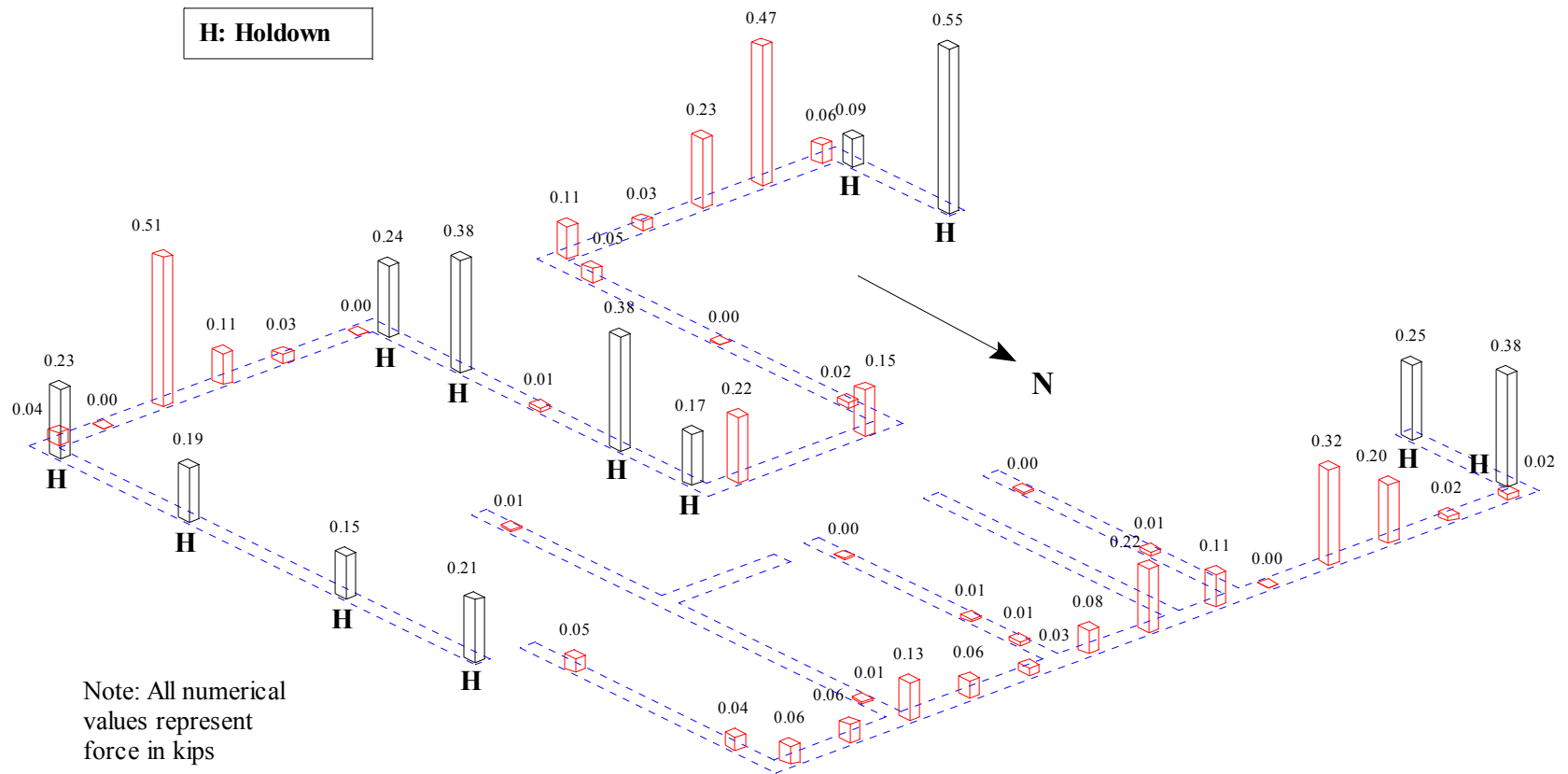


Figure Q.15: Peak anchor bolt forces for Test NWP2S06

Appendix Q

Phase 2, NWP2S07 Seismic Test

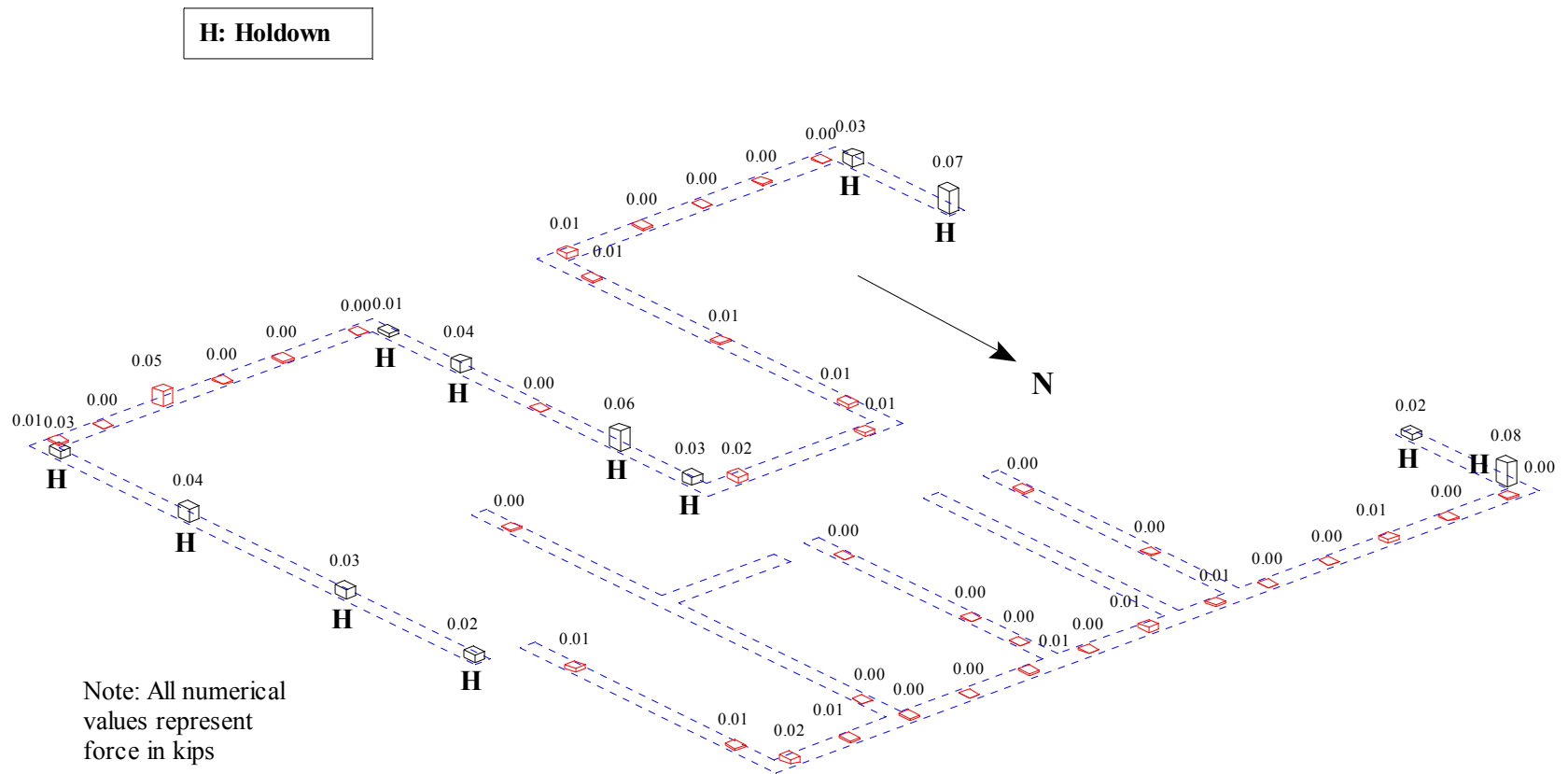


Figure Q.16: Peak anchor bolt forces for Test NWP2S07

Appendix Q

Phase 2, NWP2S08 Seismic Test

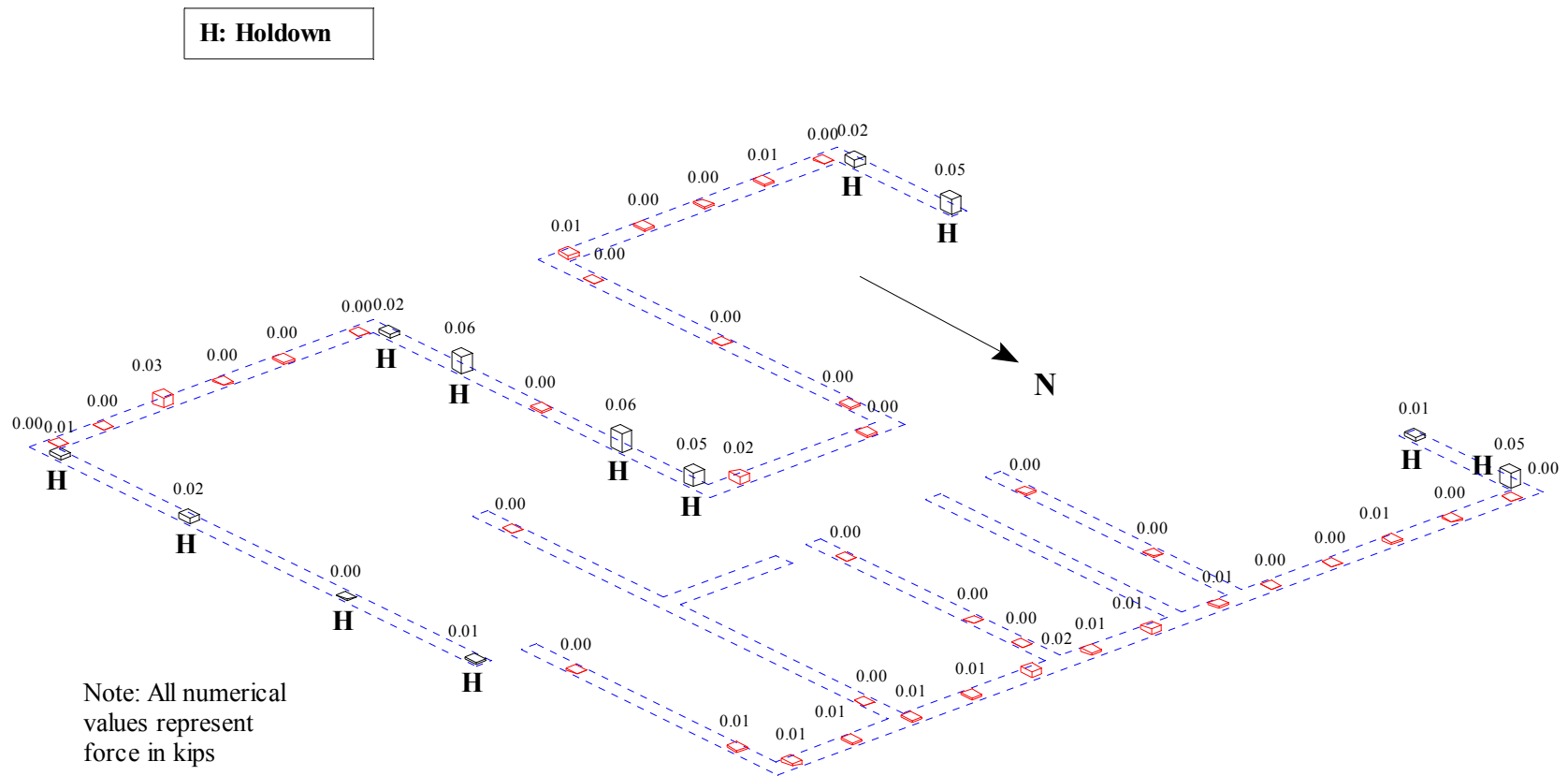


Figure Q.17: Peak anchor bolt forces for Test NWP2S08

Appendix Q

Phase 2, NWP2S12 Seismic Test

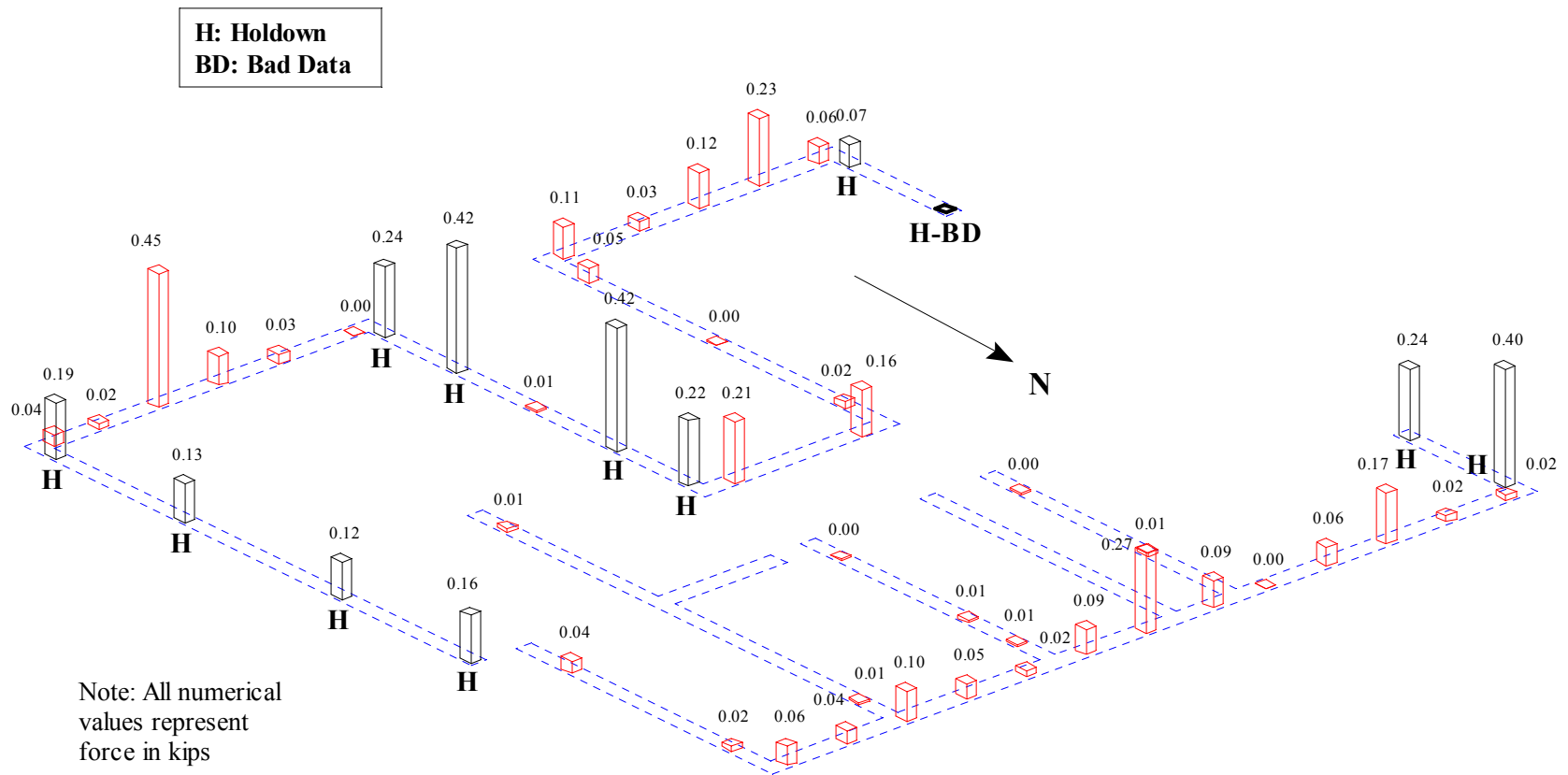


Figure Q.21: Peak anchor bolt forces for Test NWP2S12

Appendix Q

Phase 2, NWP2S13 Seismic Test

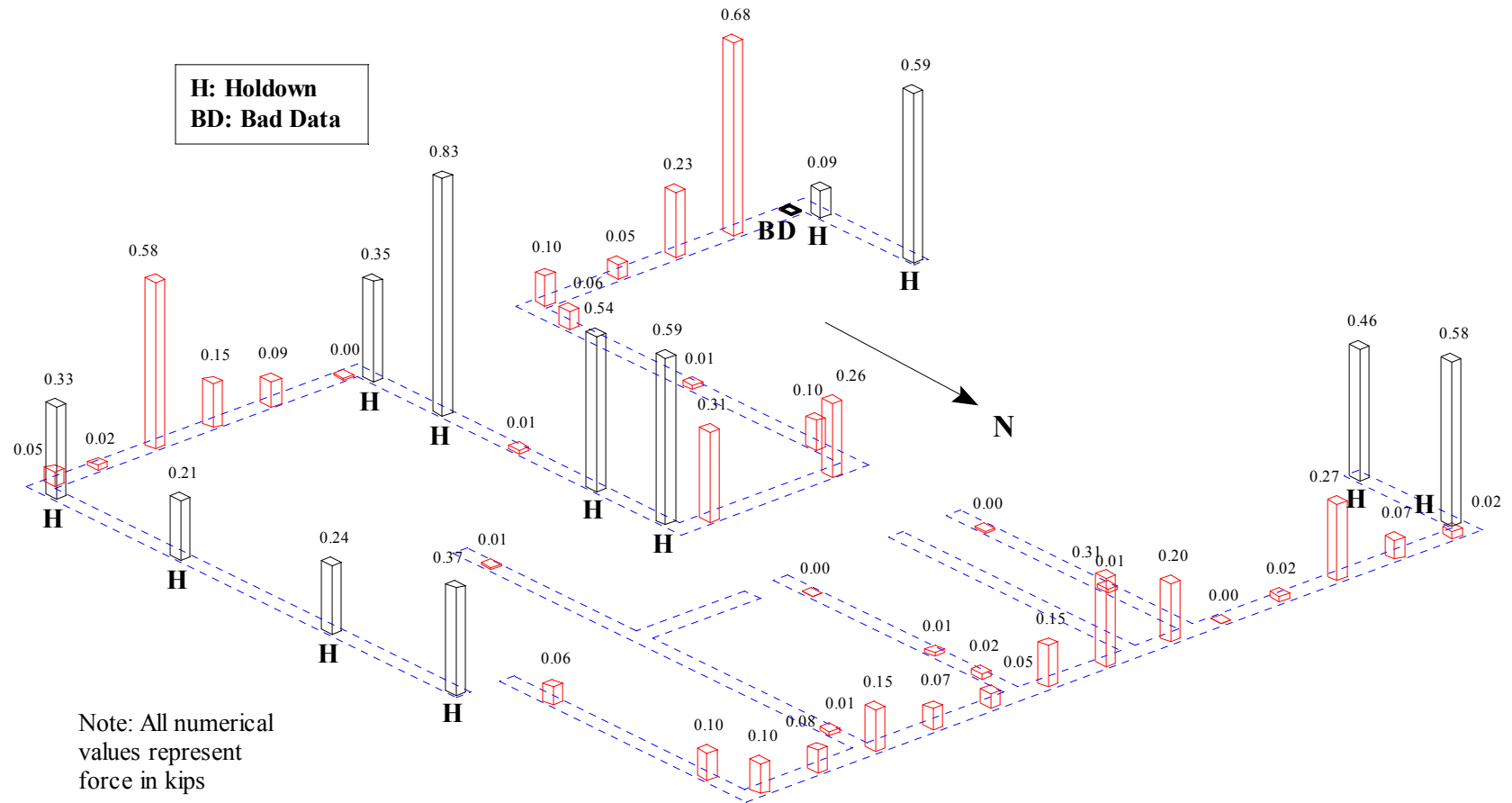


Figure Q.22: Peak anchor bolt forces for Test NWP2S13

Appendix Q

Phase 2, NWP2S14 Seismic Test

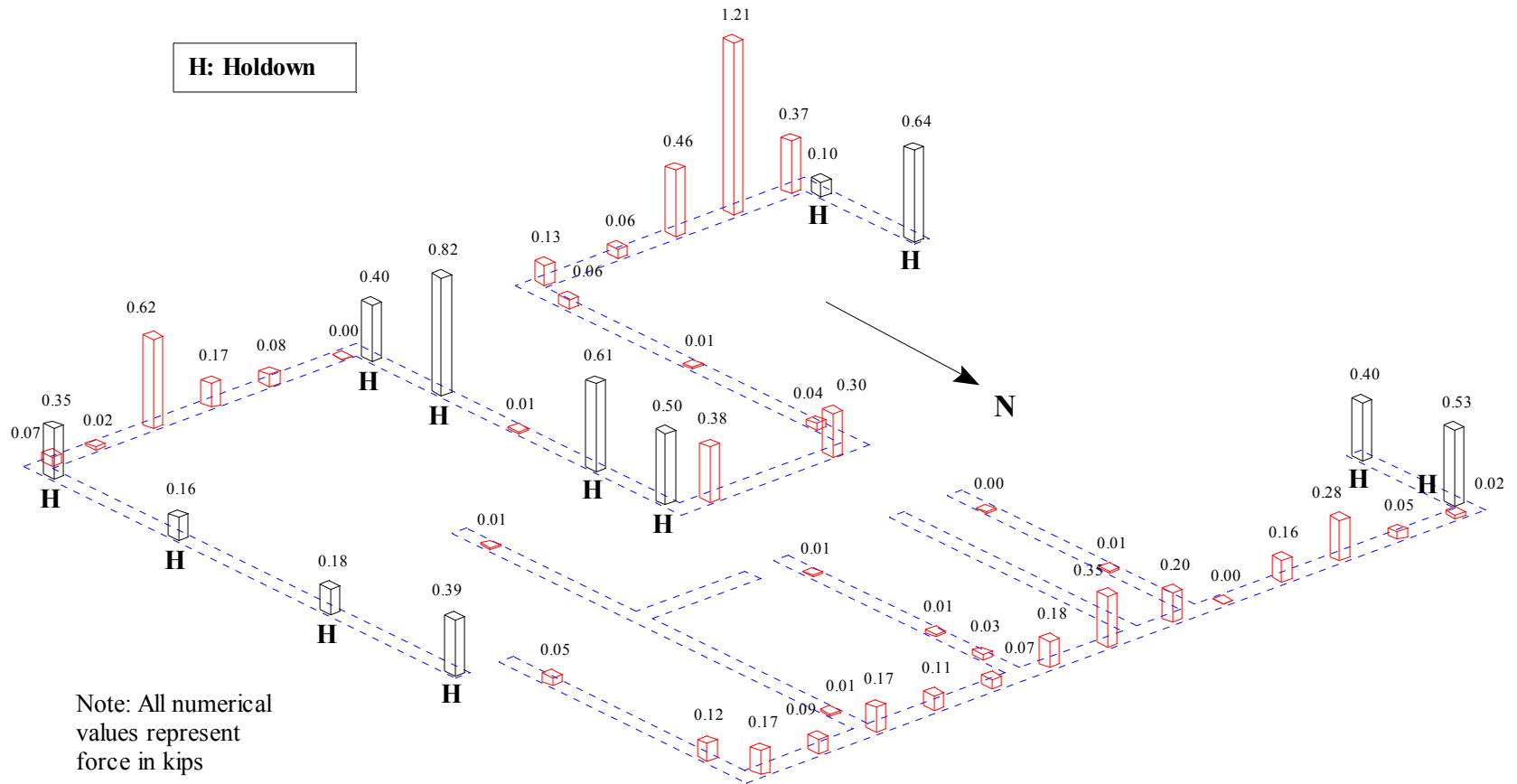


Figure Q.23: Peak anchor bolt forces for Test NWP2S14

Appendix Q

Phase 2, NWP2S16 Seismic Test

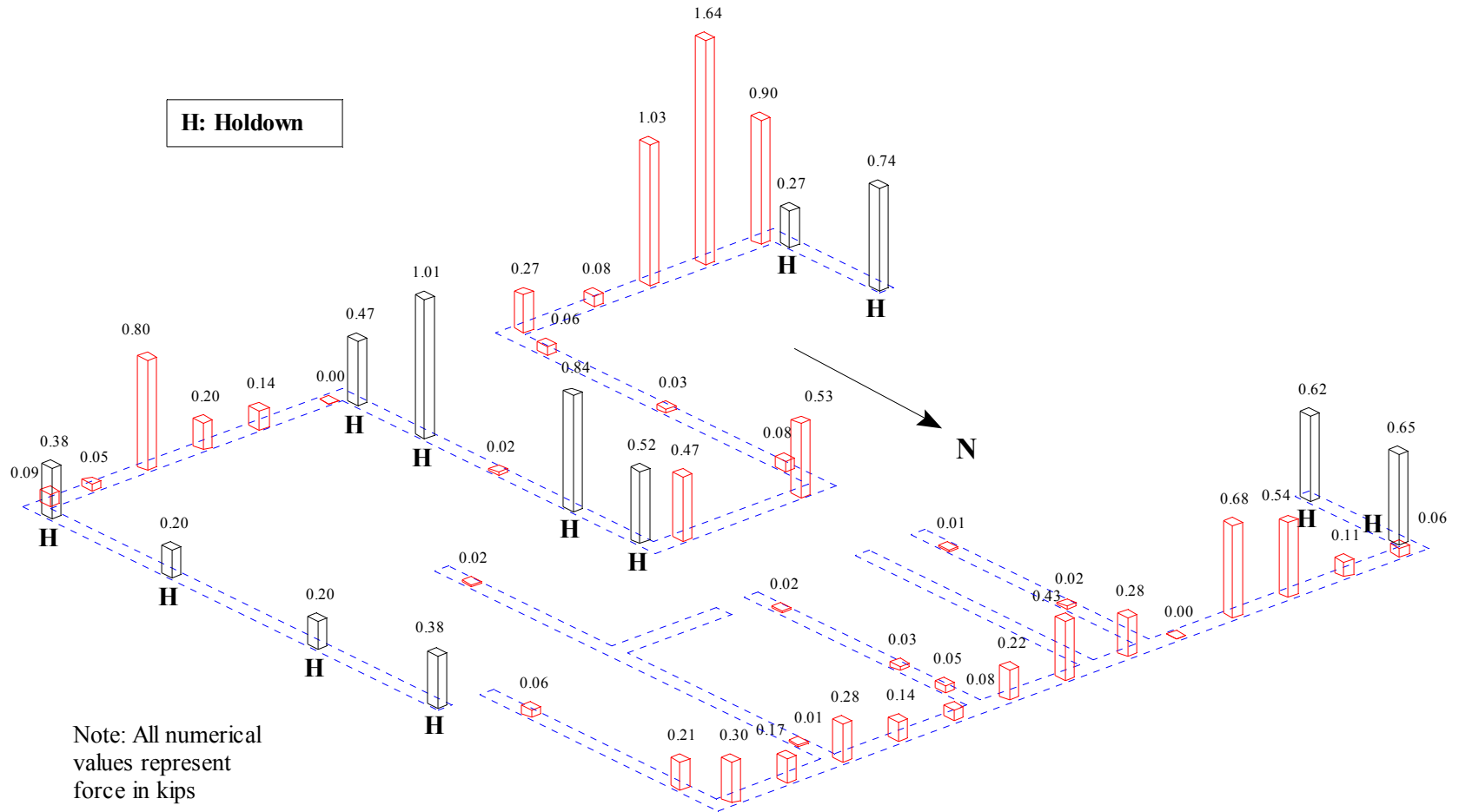


Figure Q.24: Peak anchor bolt forces for Test NWP2S16

Appendix Q

Phase 2, NWP2S17 Seismic Test

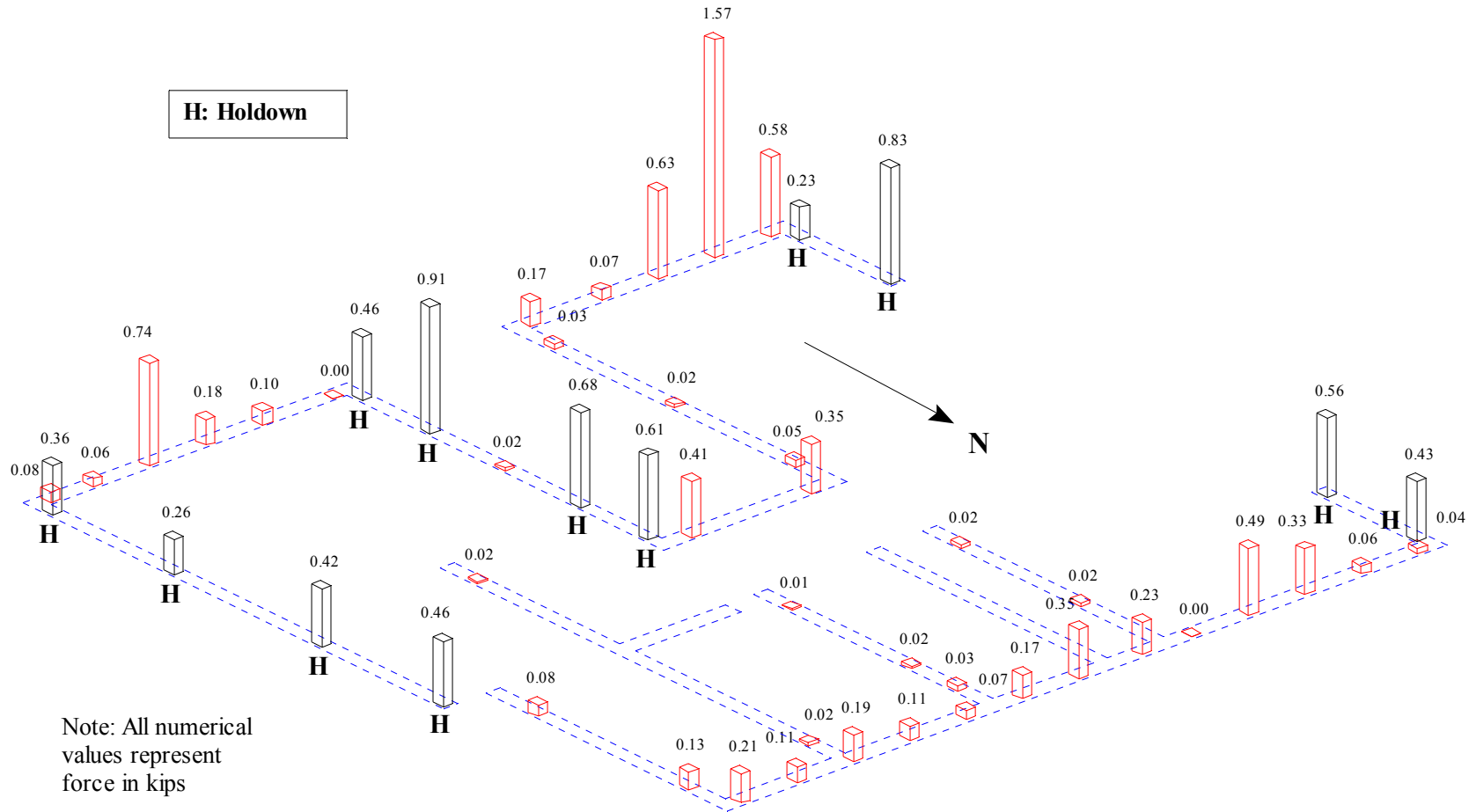


Figure Q.25: Peak anchor bolt forces for Test NWP2S17

Appendix Q

Phase 2, NWP2S25 Seismic Test

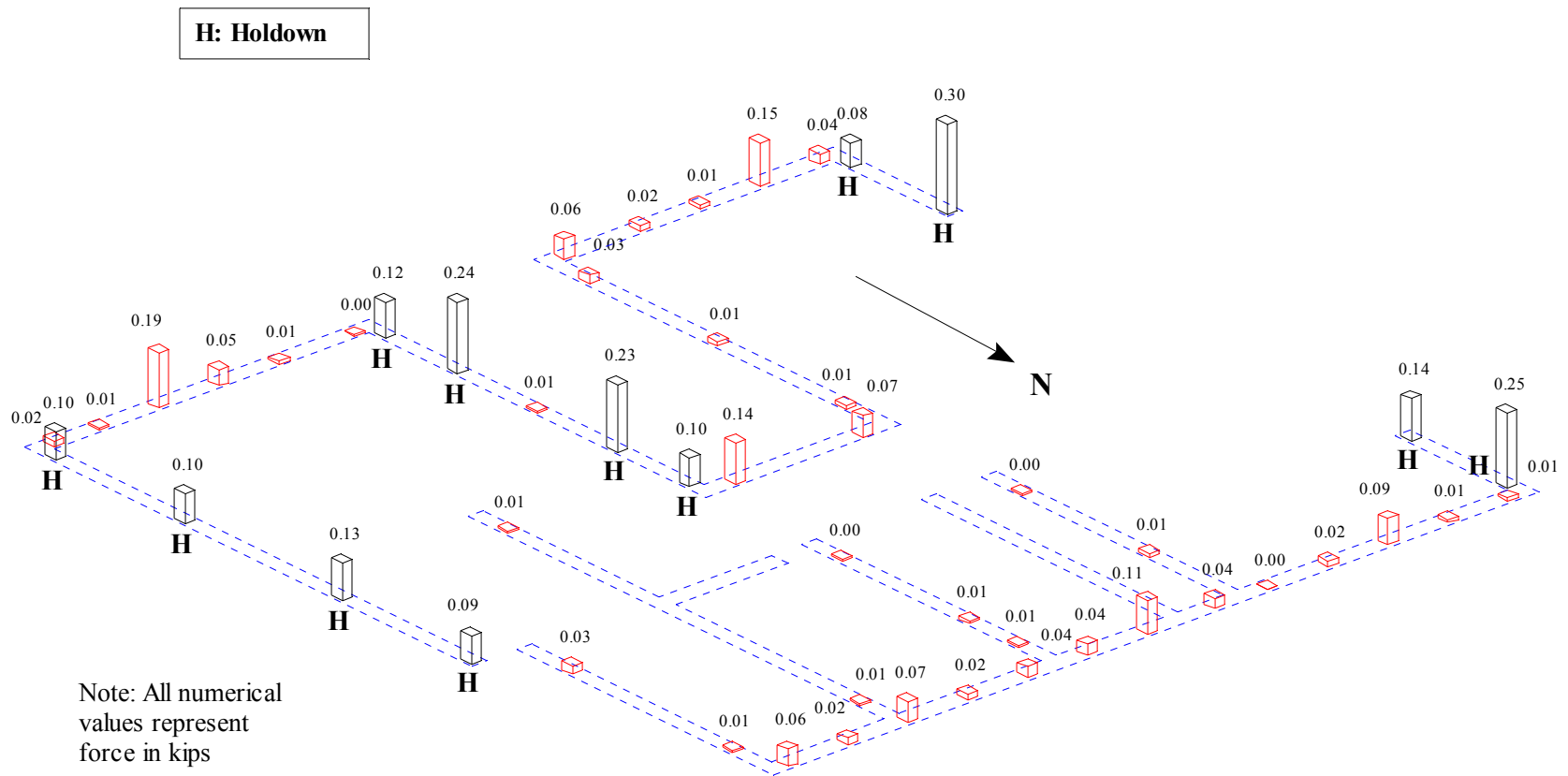


Figure Q.28: Peak anchor bolt forces for Test NWP2S25

Appendix Q

Phase 2, NWP2S27 Seismic Test

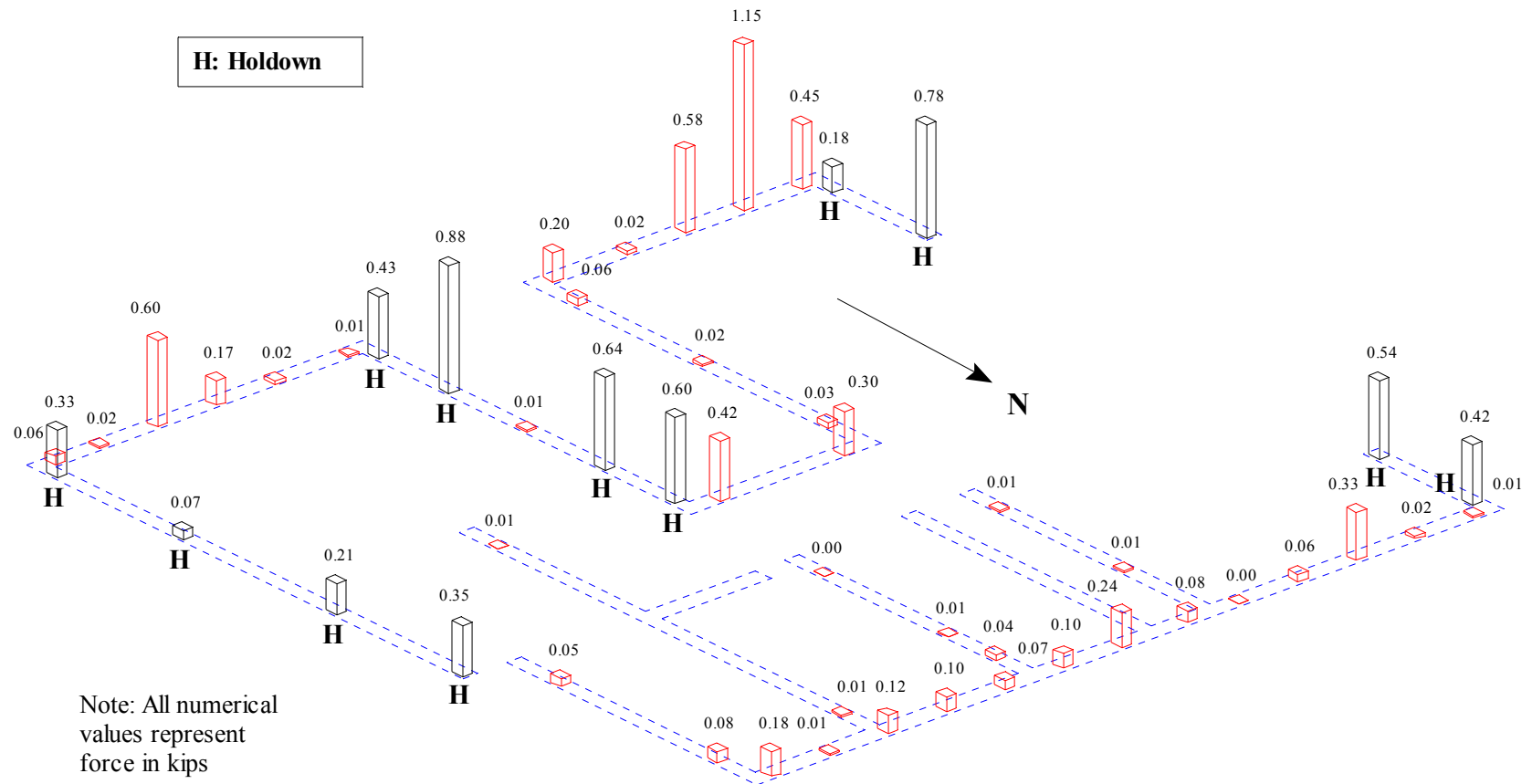


Figure Q.30: Peak anchor bolt forces for Test NWP2S27

Appendix Q

Phase 2, NWP2S29 Seismic Test

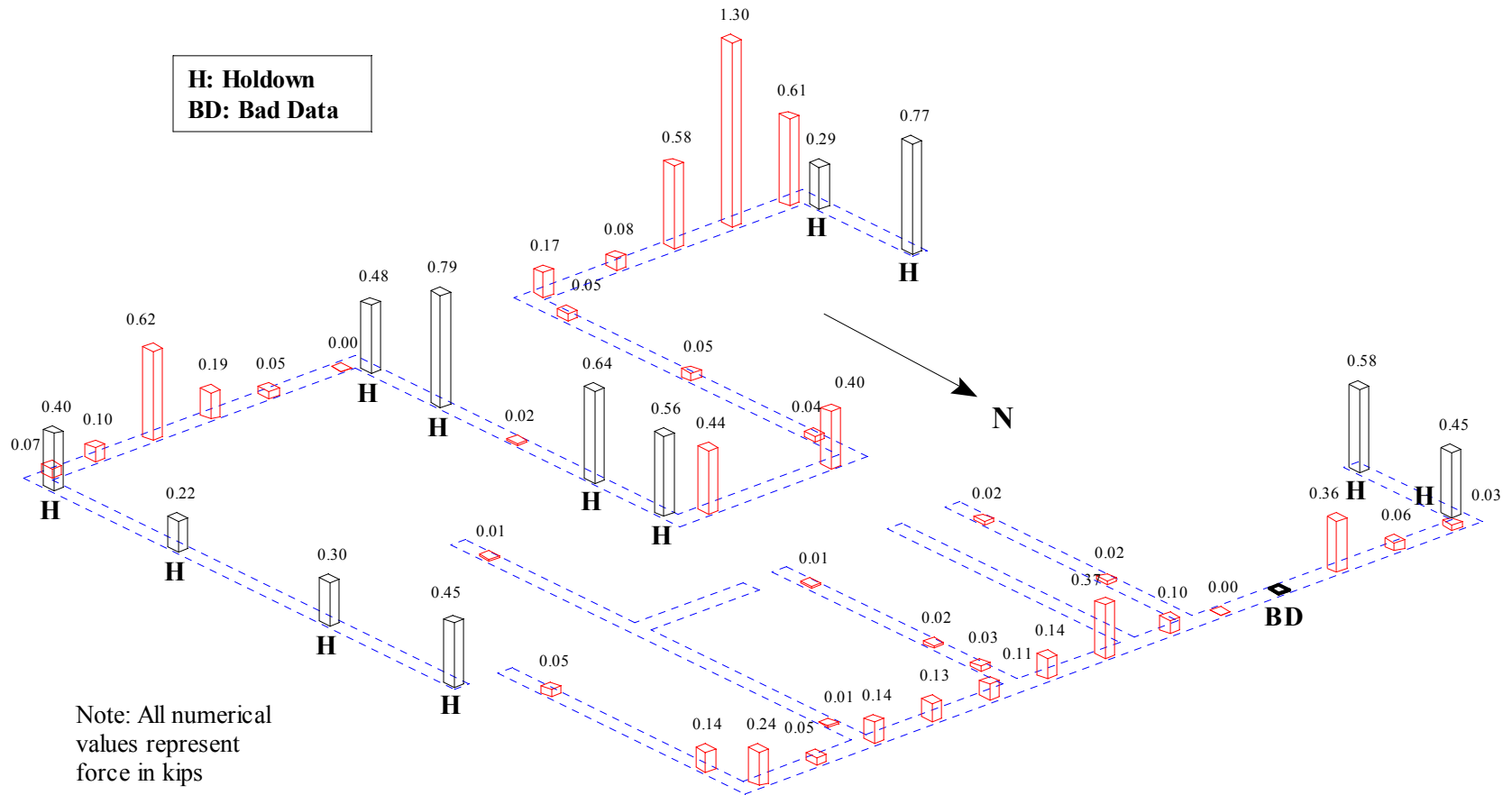


Figure Q.32: Peak anchor bolt forces for Test NWP2S29

Appendix Q

Phase 2, NWP2S30 Seismic Test

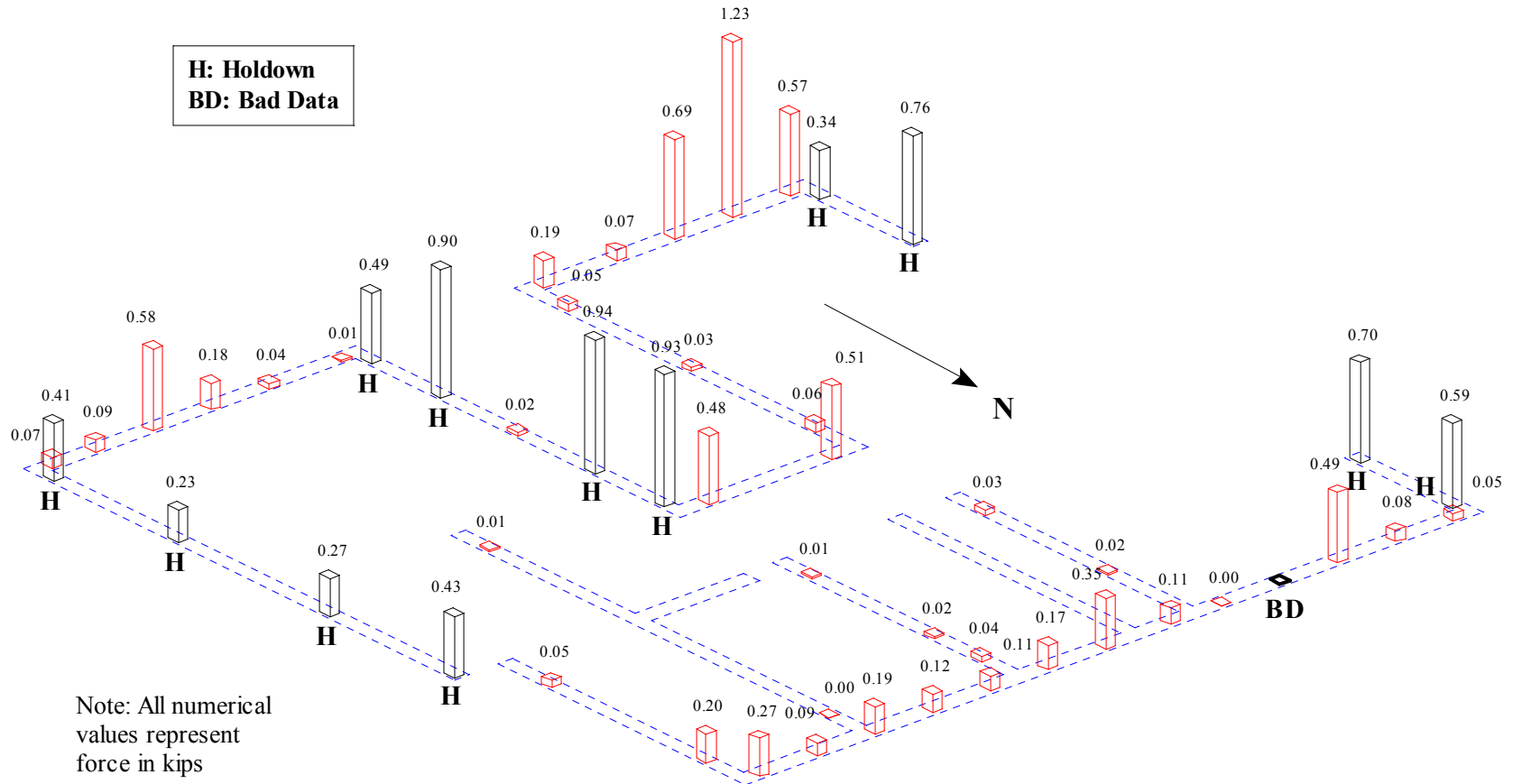


Figure Q.33: Peak anchor bolt forces for Test NWP2S30

Appendix Q

Phase 3, NWP3S01 Seismic Test

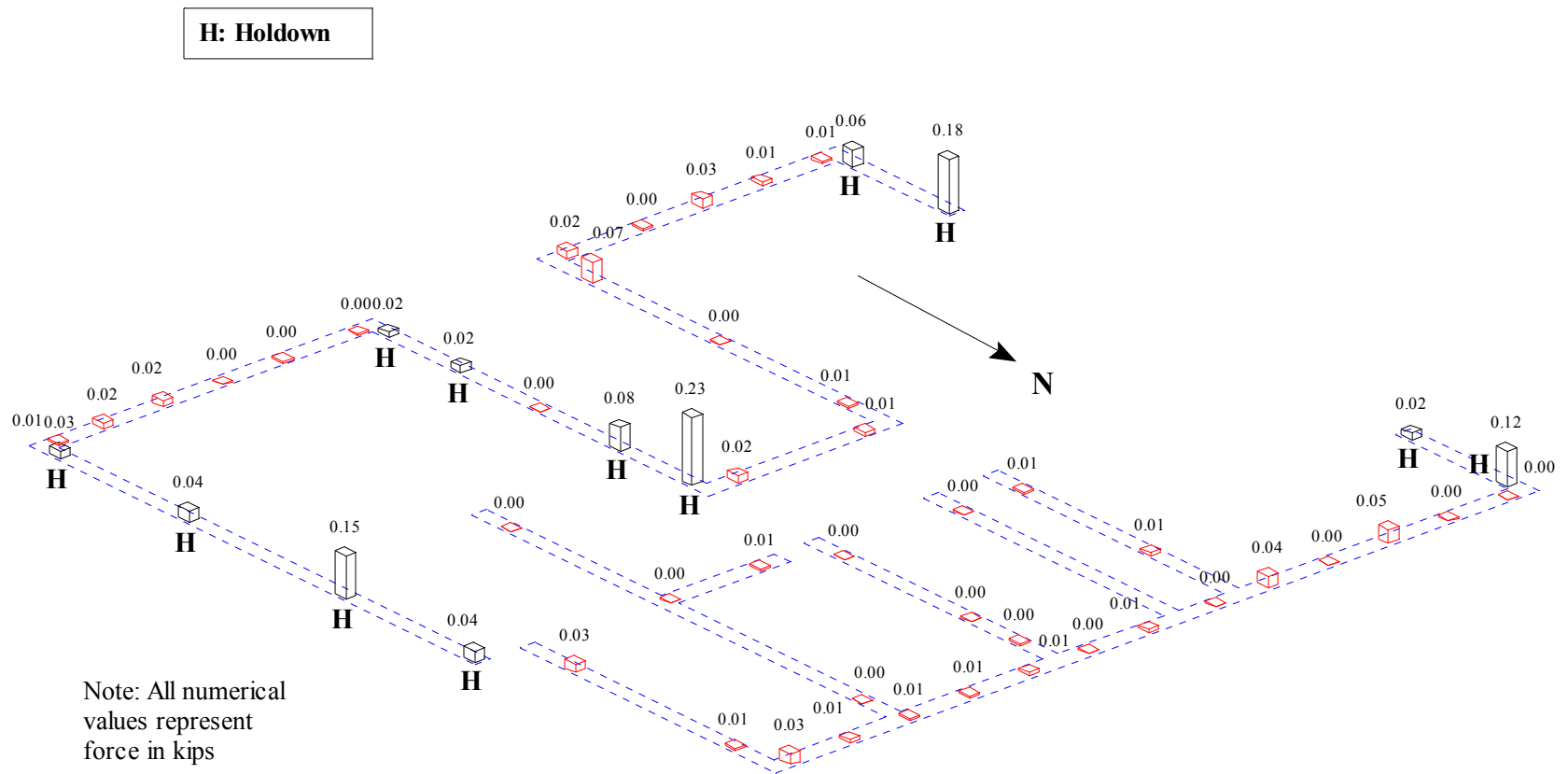


Figure Q.34: Peak anchor bolt forces for Test NWP3S01

Appendix Q

Phase 3, NWP3S02 Seismic Test

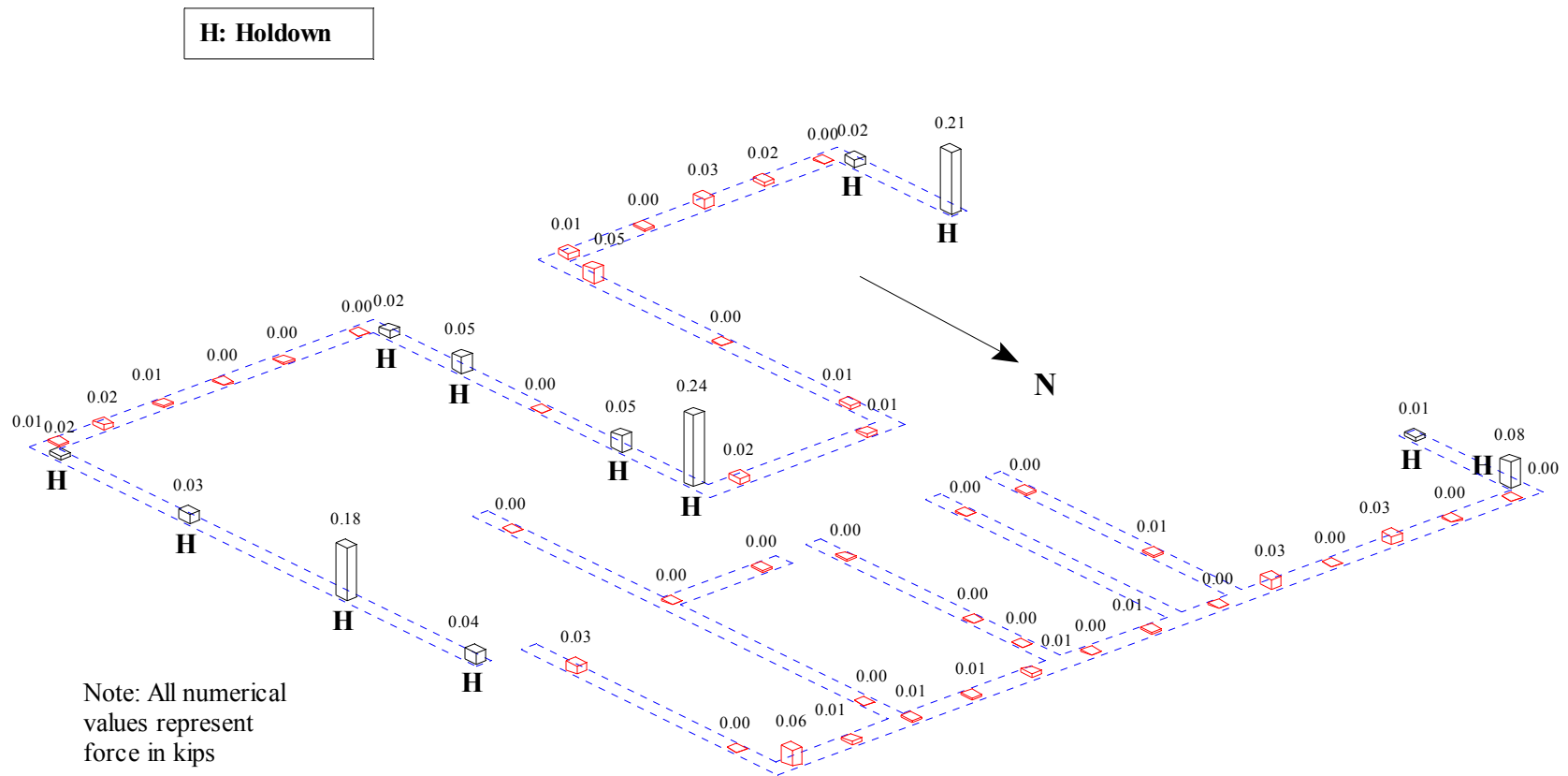


Figure Q.35: Peak anchor bolt forces for Test NWP3S02

Appendix Q

Phase 3, NWP3S03 Seismic Test

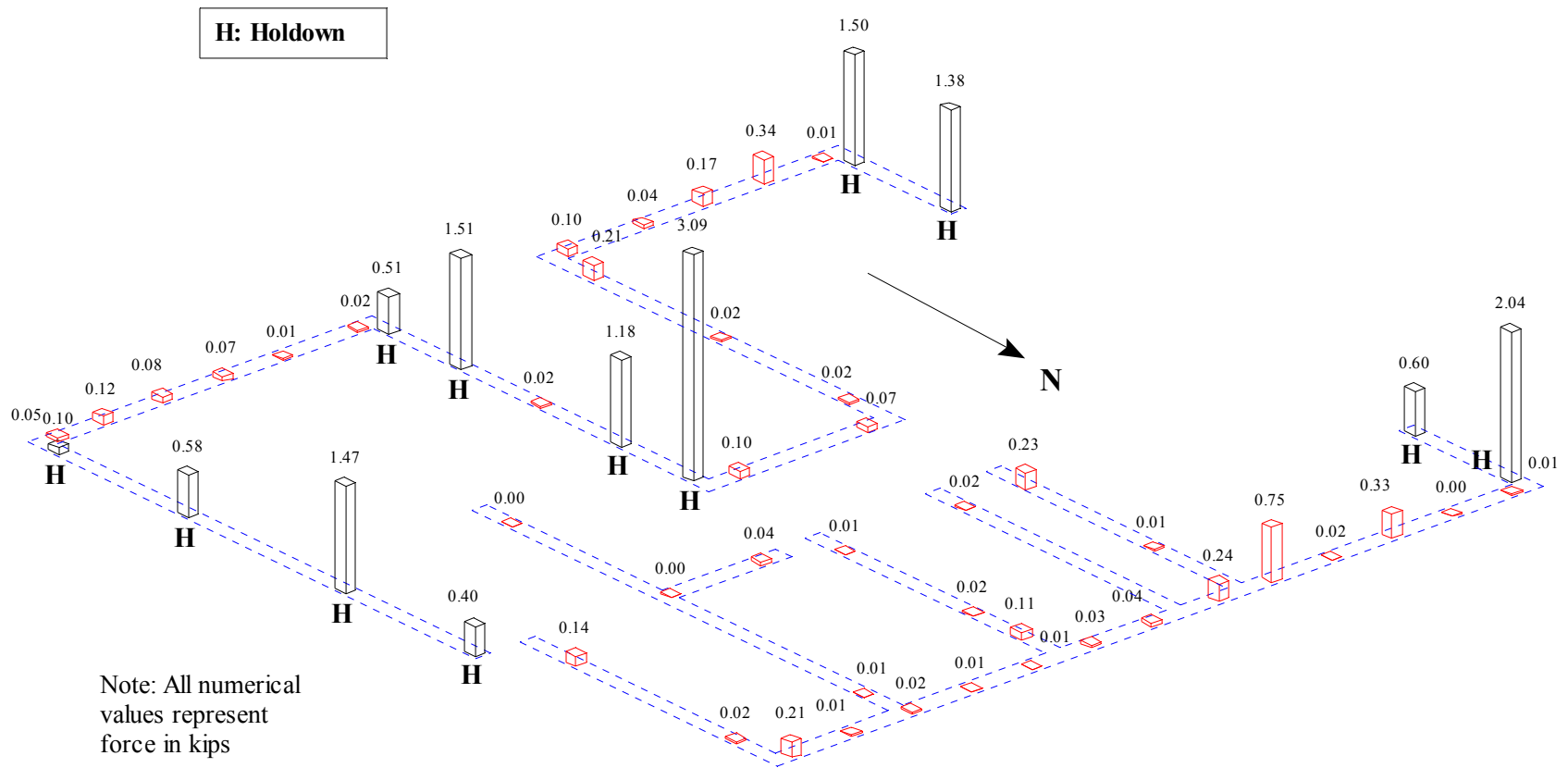


Figure Q.36: Peak anchor bolt forces for Test NWP3S03

Appendix Q

Phase 4, NWP4S01 Seismic Test

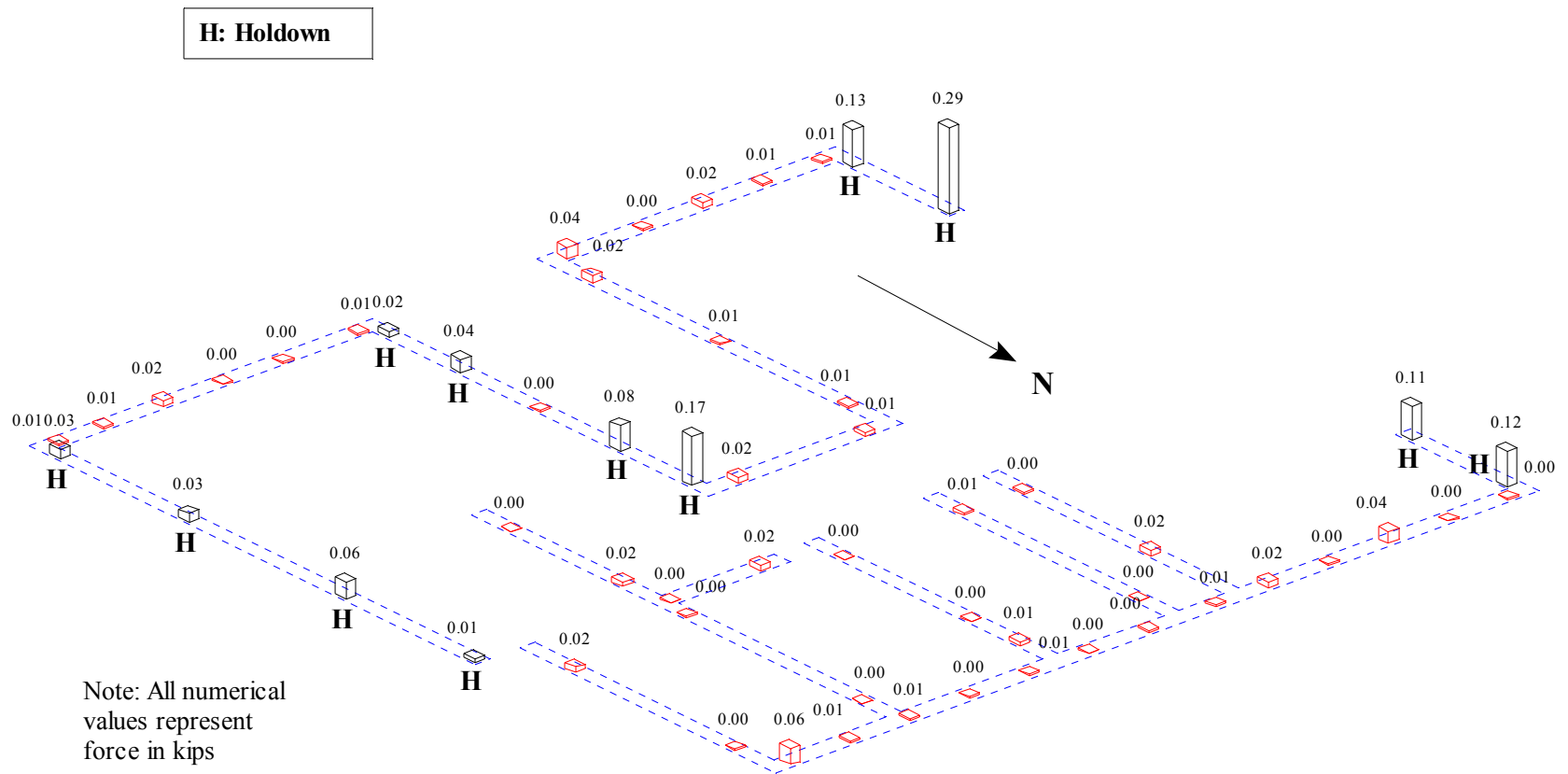


Figure Q.38: Peak anchor bolt forces for Test NWP4S01

Appendix Q

Phase 4, NWP4S02 Seismic Test

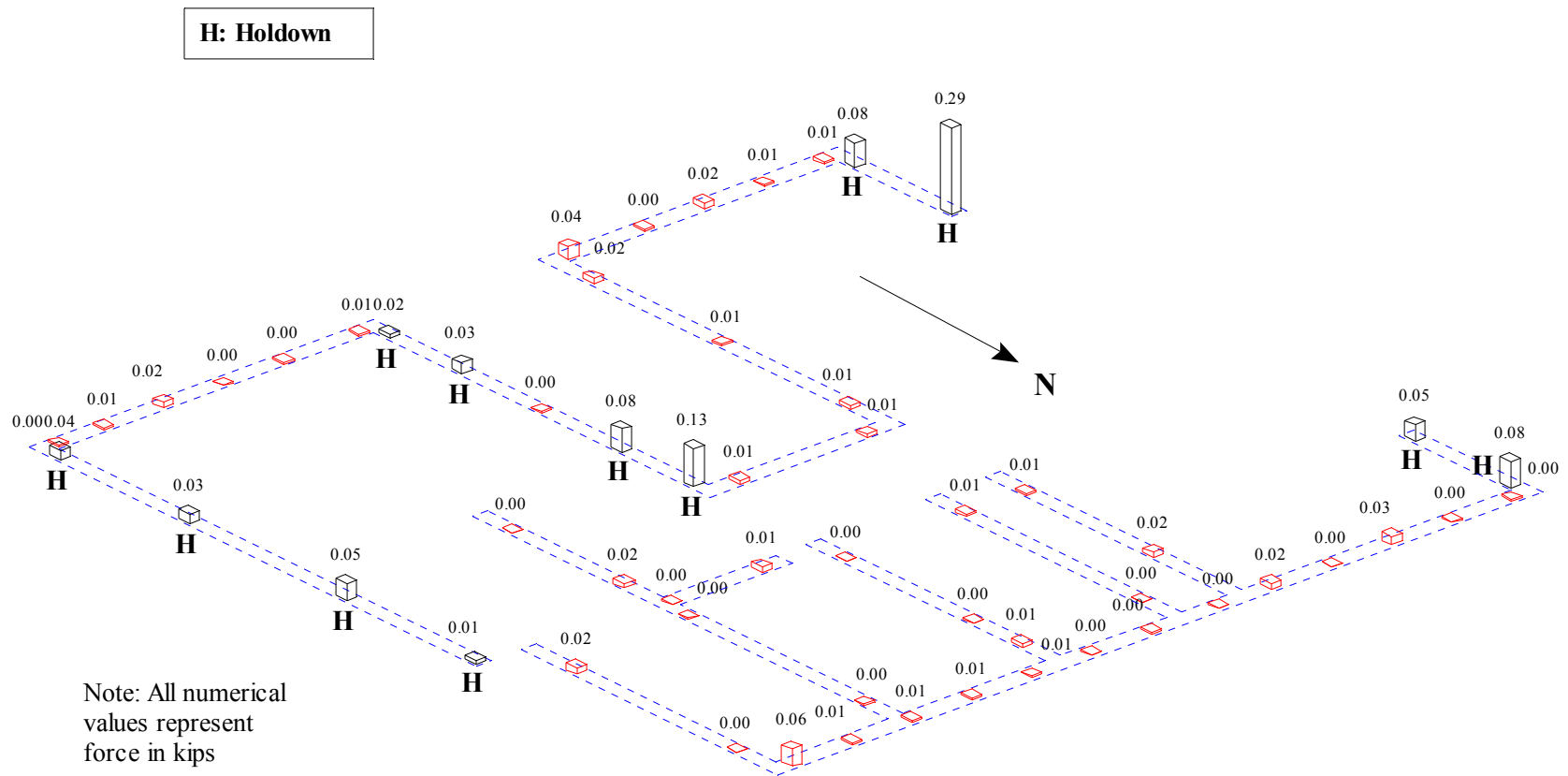
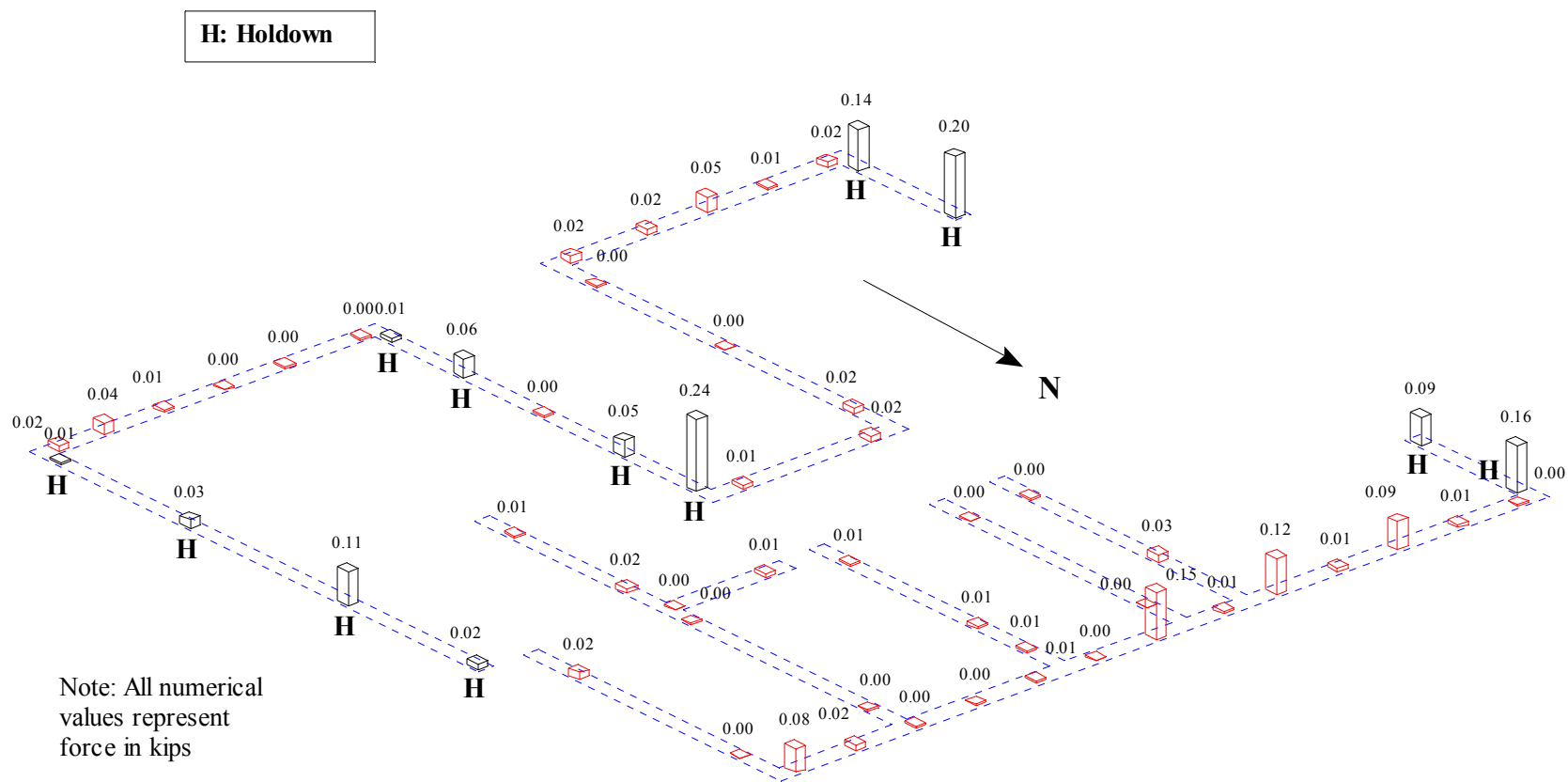


Figure Q.39: Peak anchor bolt forces for Test NWP4S02

Appendix Q

Phase 5, NWP5S01 Seismic Test



Appendix Q

Phase 5, NWP5S03 Seismic Test

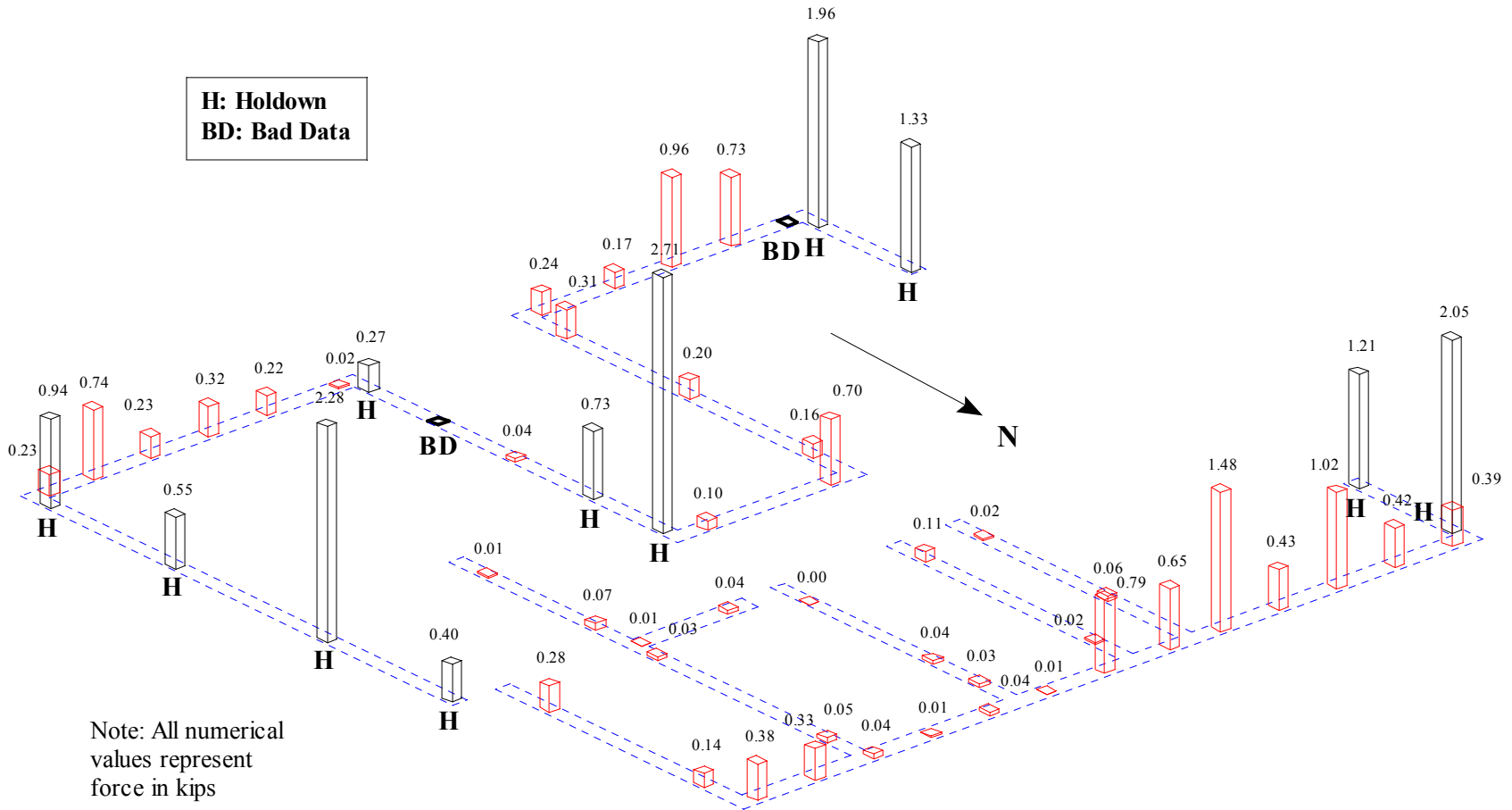
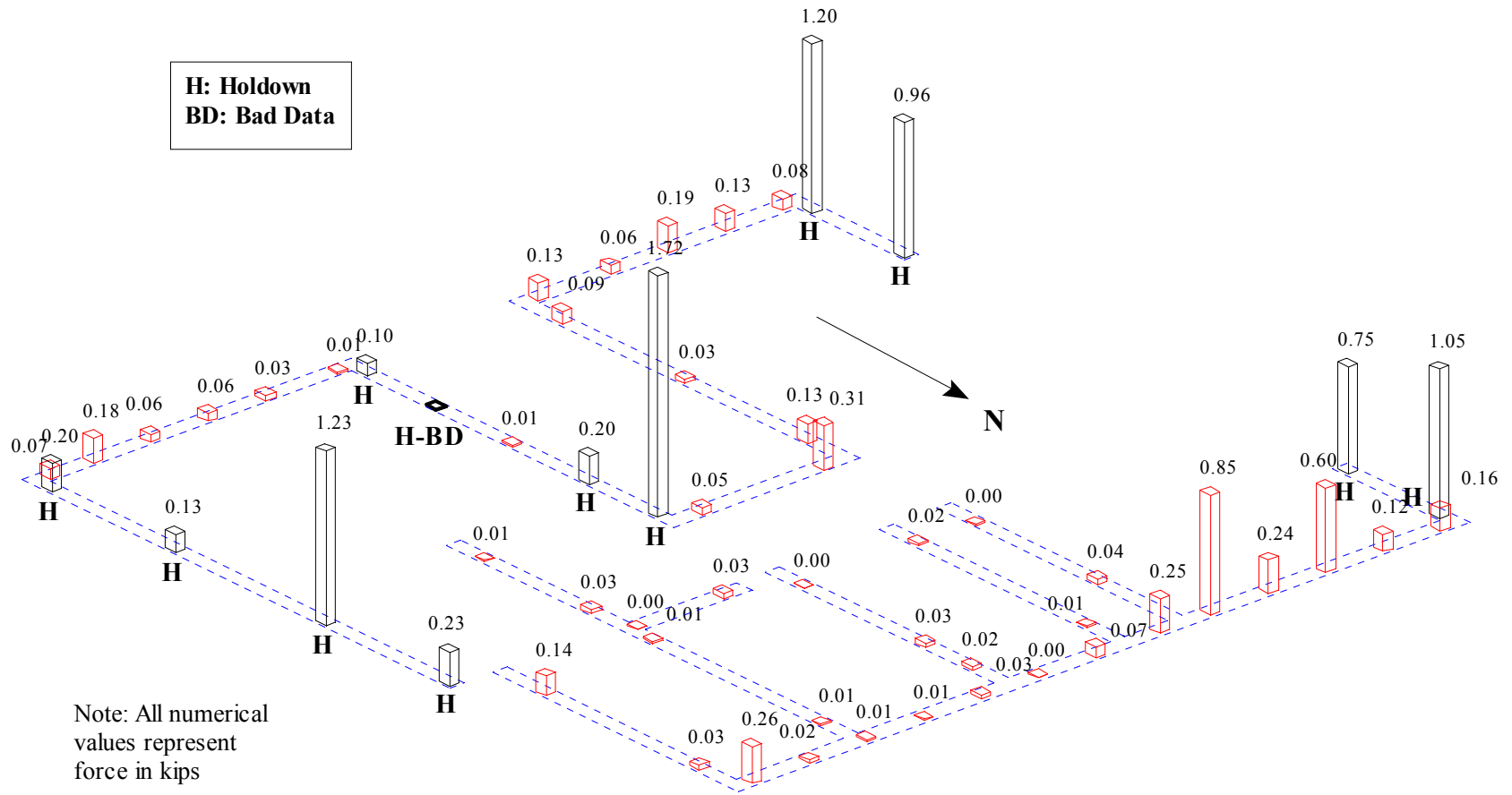


Figure Q.44: Peak anchor bolt forces for Test NWP5S03

Appendix Q

Phase 5, NWP5S04 Seismic Test



Appendix Q

Phase 5, NWP5S05 Seismic Test

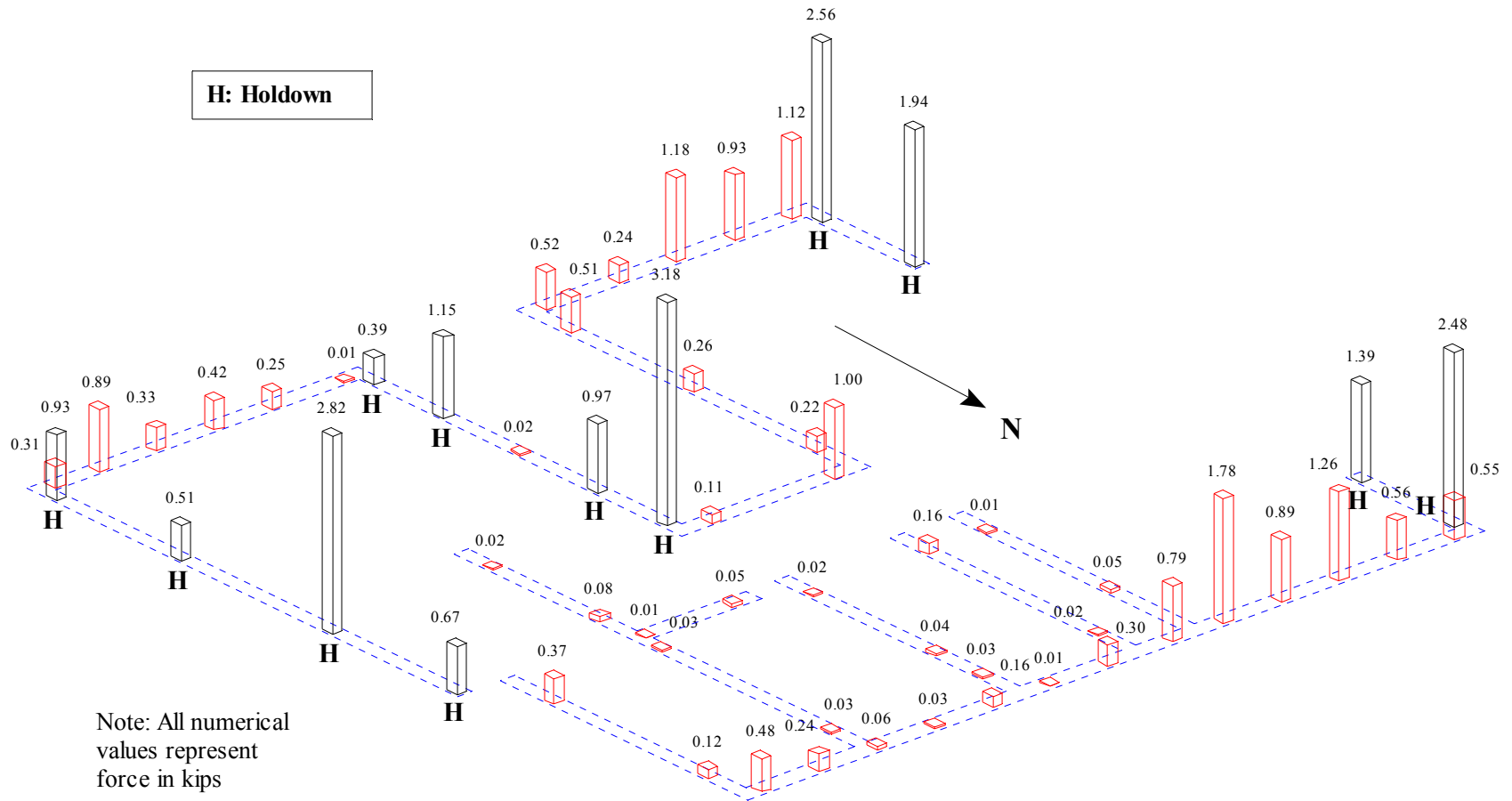


Figure Q.46: Peak anchor bolt forces for Test NWP5S05

Appendix Q

Phase 5, NWP5S06 Seismic Test

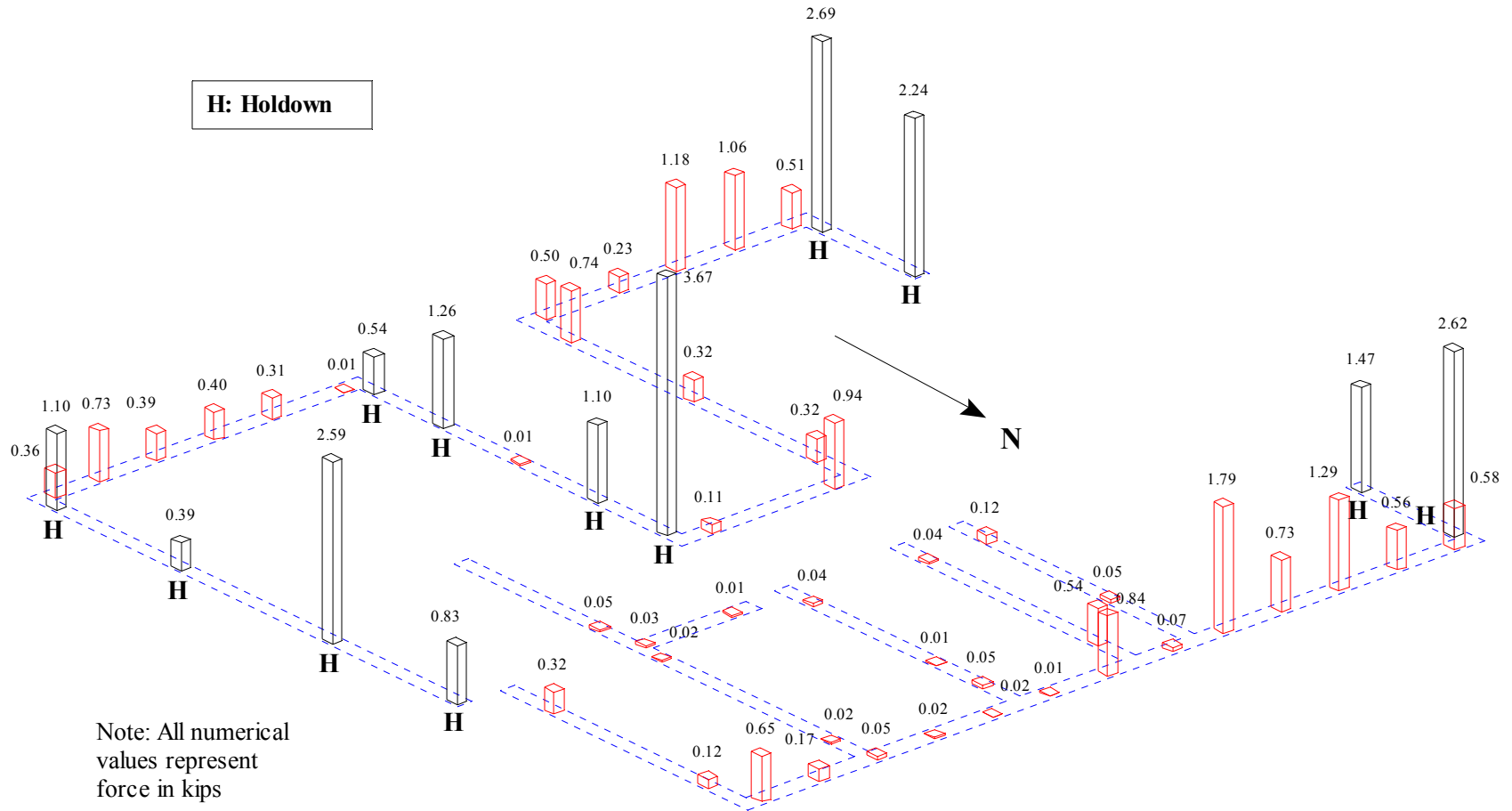


Figure Q.47: Peak anchor bolt forces for Test NWP5S06

Appendix Q

Phase 5, NWP5S07 Seismic Test

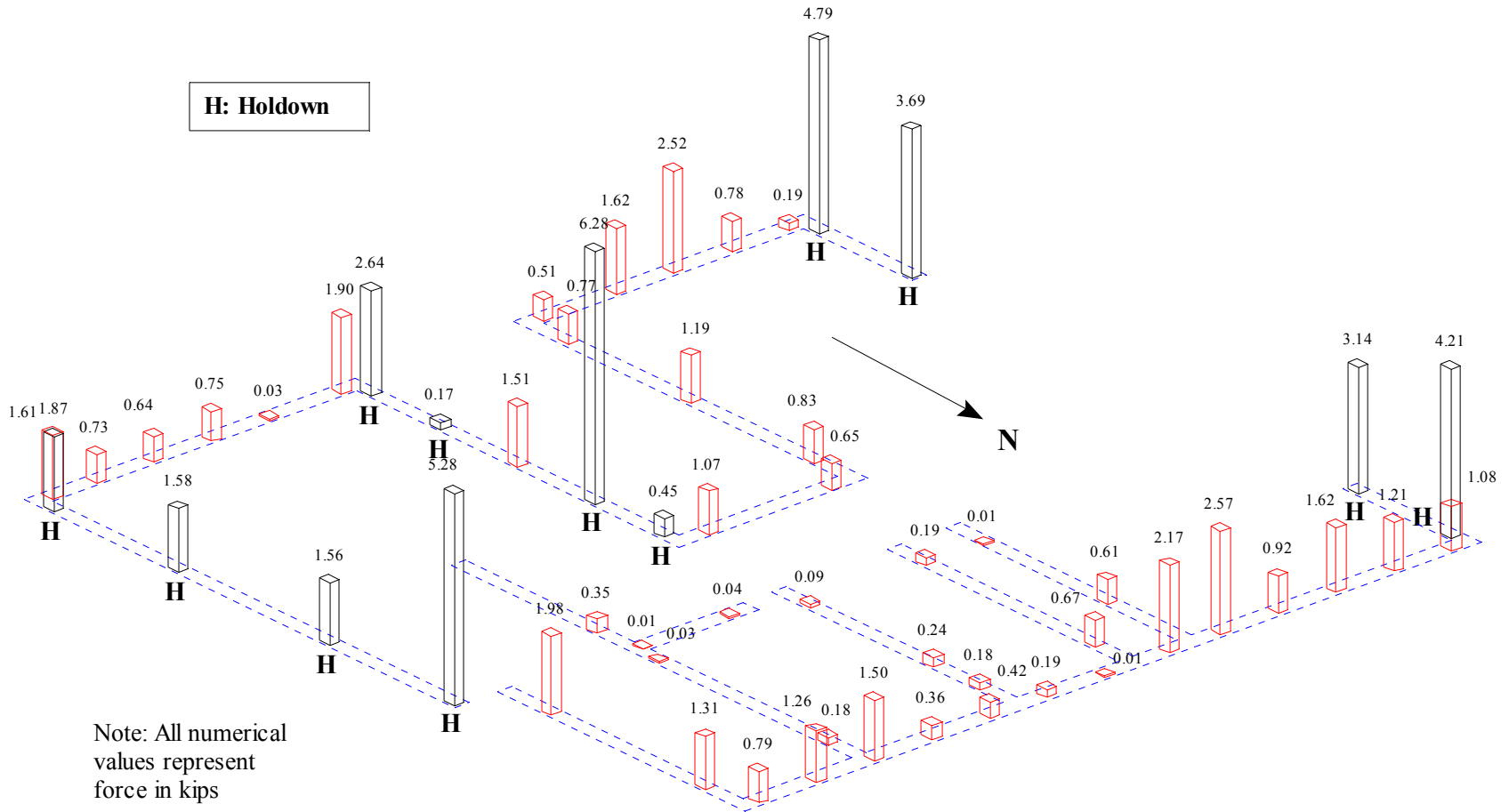


Figure Q.48: Peak anchor bolt forces for Test NWP5S07

Appendix Q

Phase 5, NWP5S08 Seismic Test

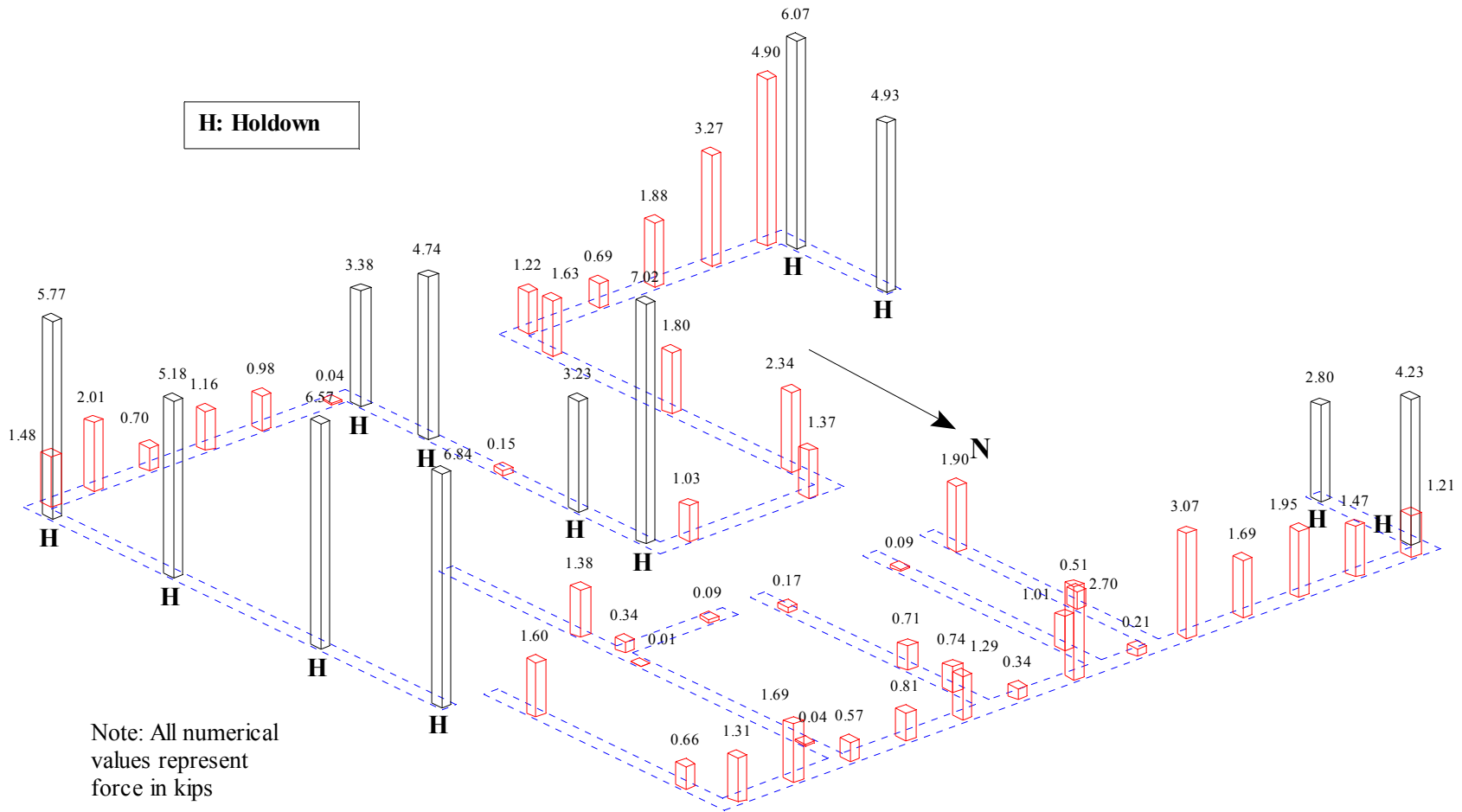


Figure Q.49: Peak anchor bolt forces for Test NWP5S08

Appendix Q

Phase 5, NWP5S09 Seismic Test

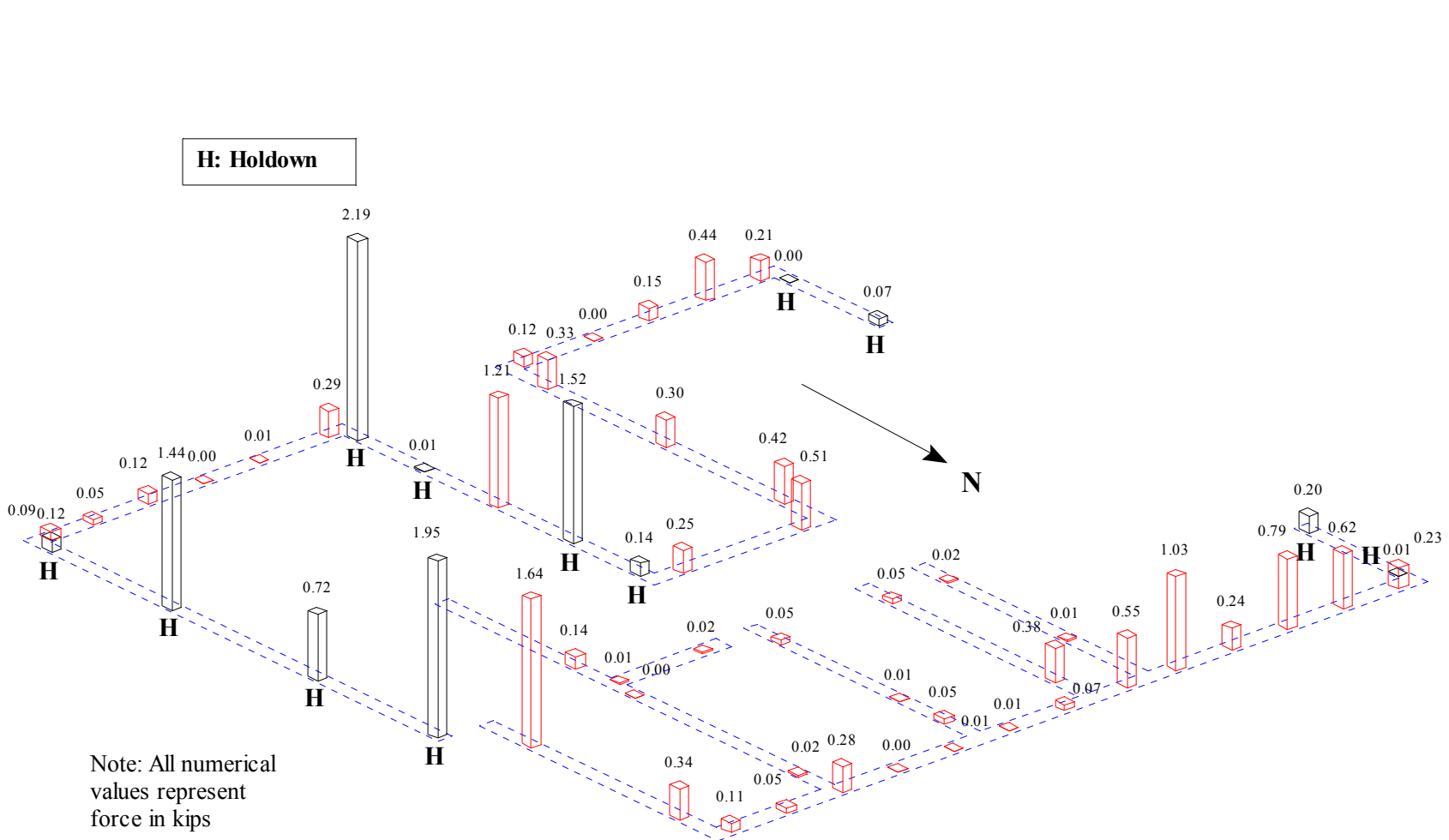


Figure Q.50: Peak anchor bolt forces for Test NWP5S09

Appendix Q

Phase 5, NWP5S11 Seismic Test

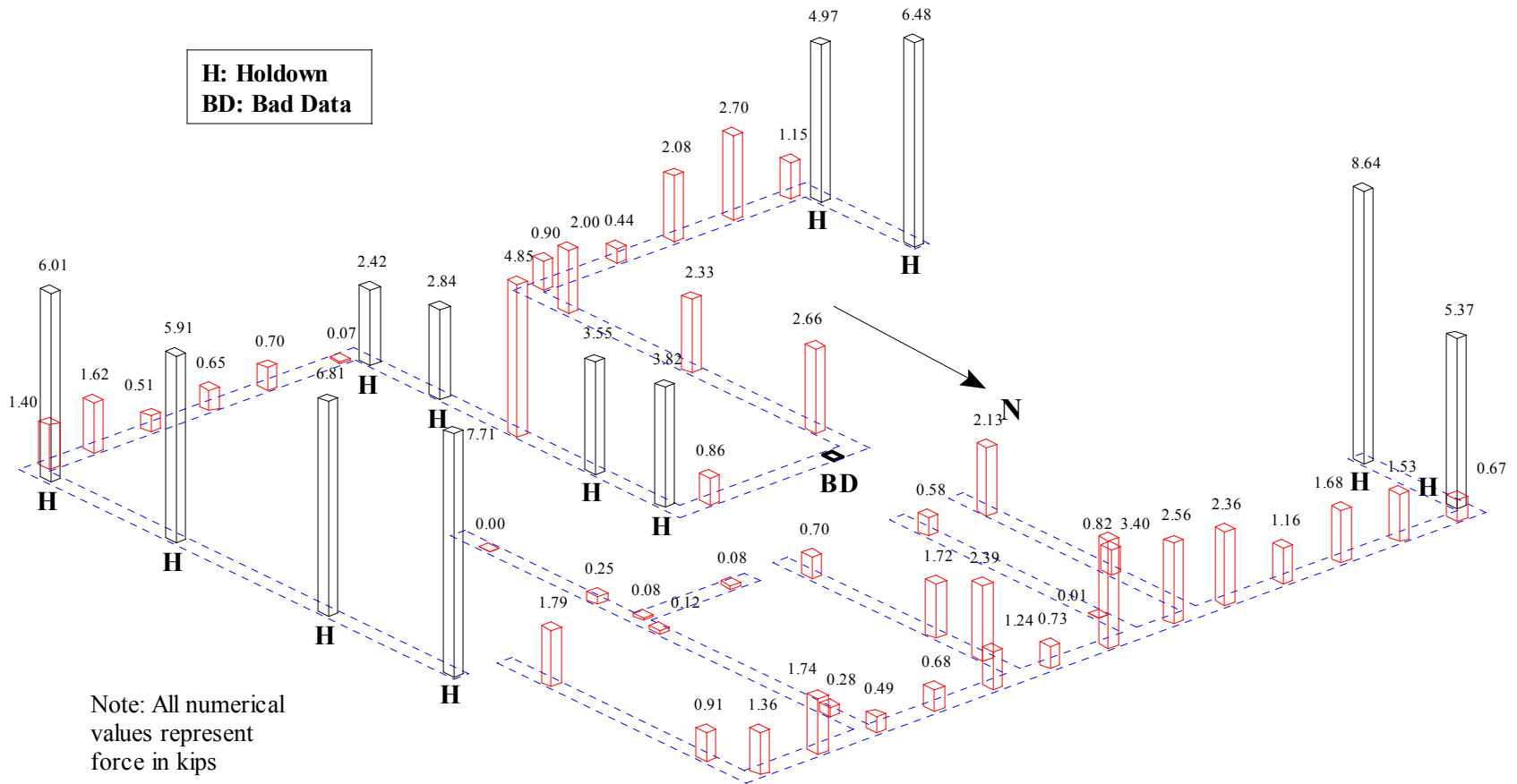


Figure Q.51: Peak anchor bolt forces for Test NWP5S11

Appendix R
Selected Seismic Results:
Peak Sill Plate and Stud Uplift

Appendix R

Phase 1, NWP1S01 Seismic Test

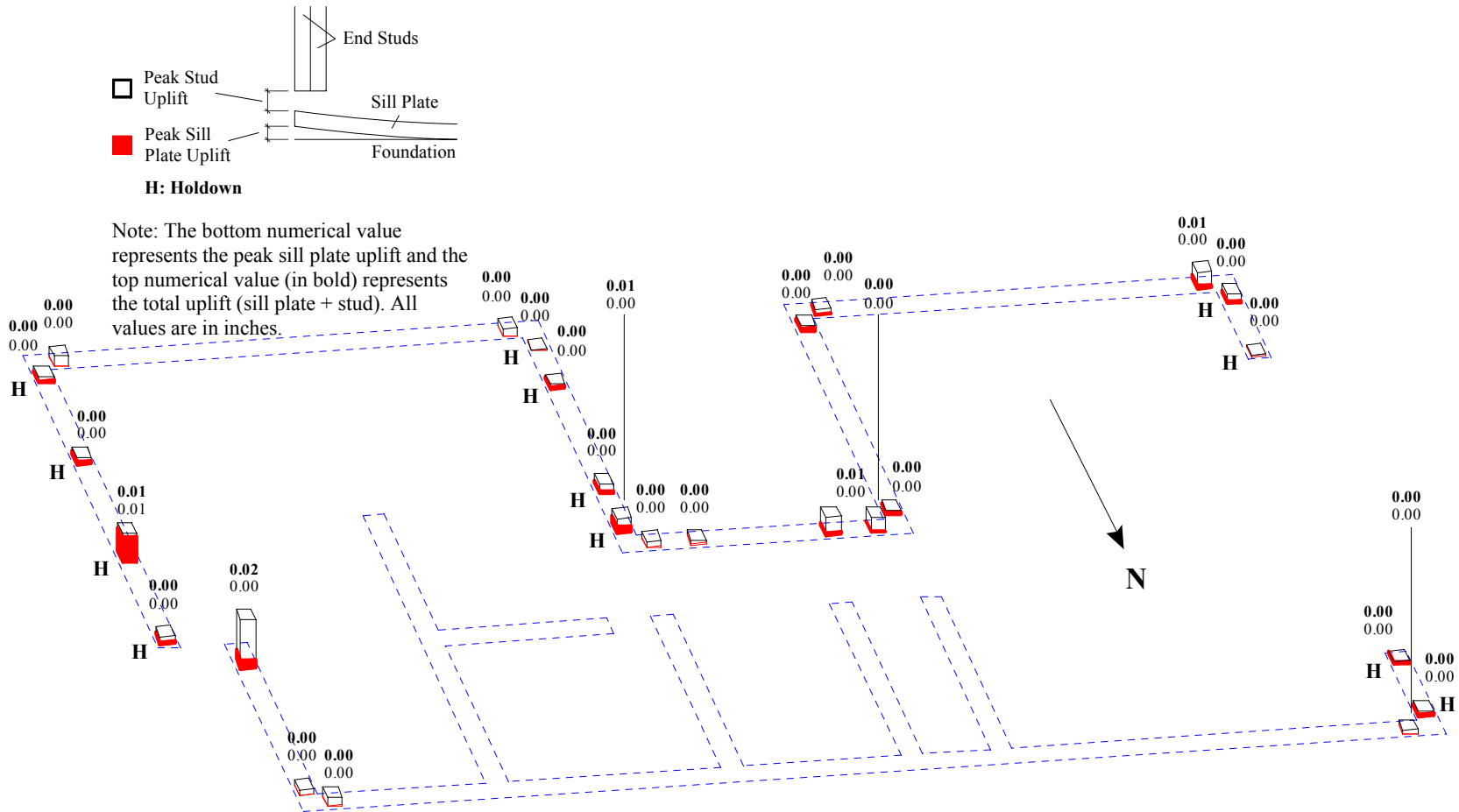


Figure R.1: Peak sill plate and stud uplift for Test NWP1S01

Appendix R

Phase 1, NWP1S02 Seismic Test

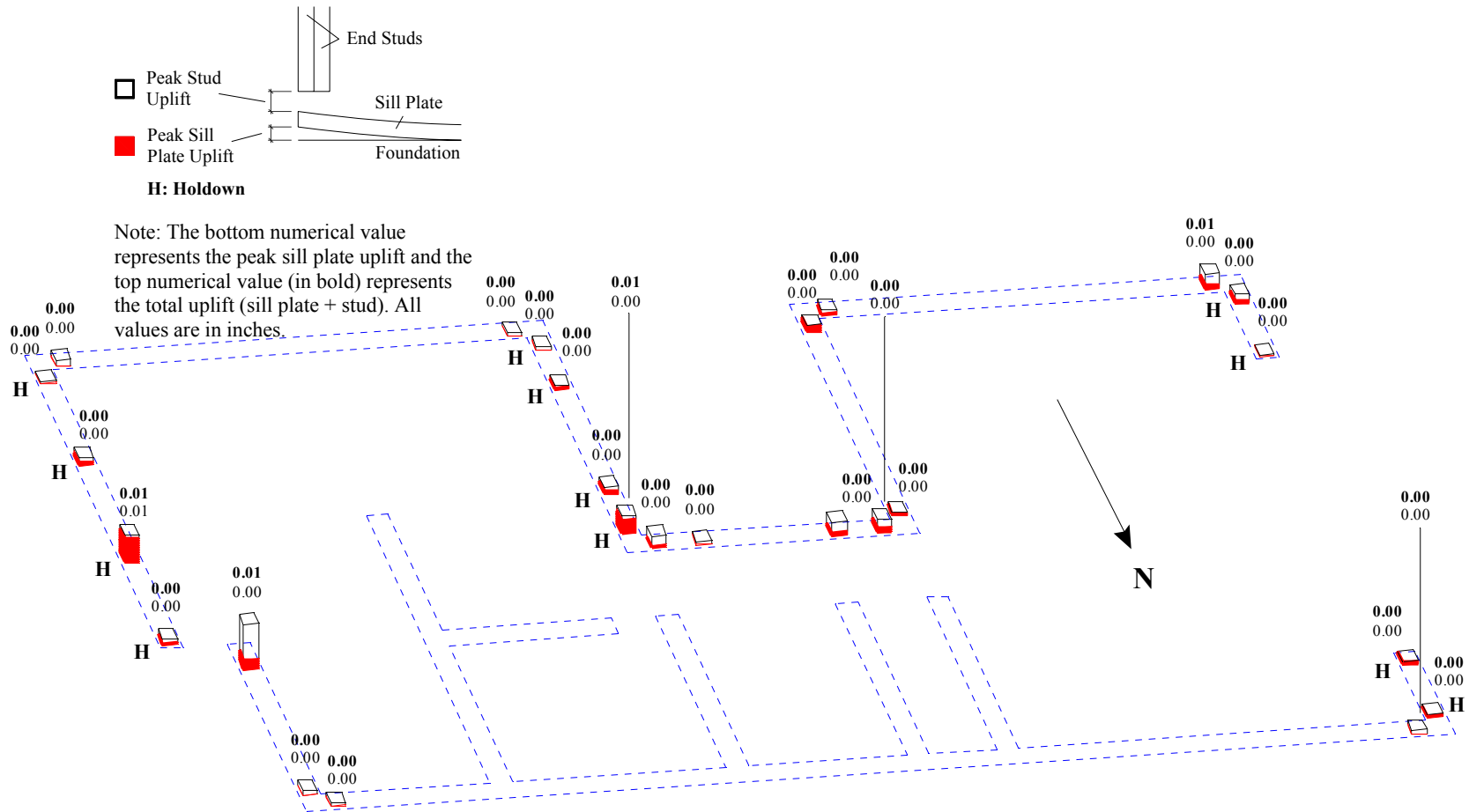


Figure R.2: Peak sill plate and stud uplift for Test NWP1S02

Appendix R

Phase 1, NWP1S03 Seismic Test

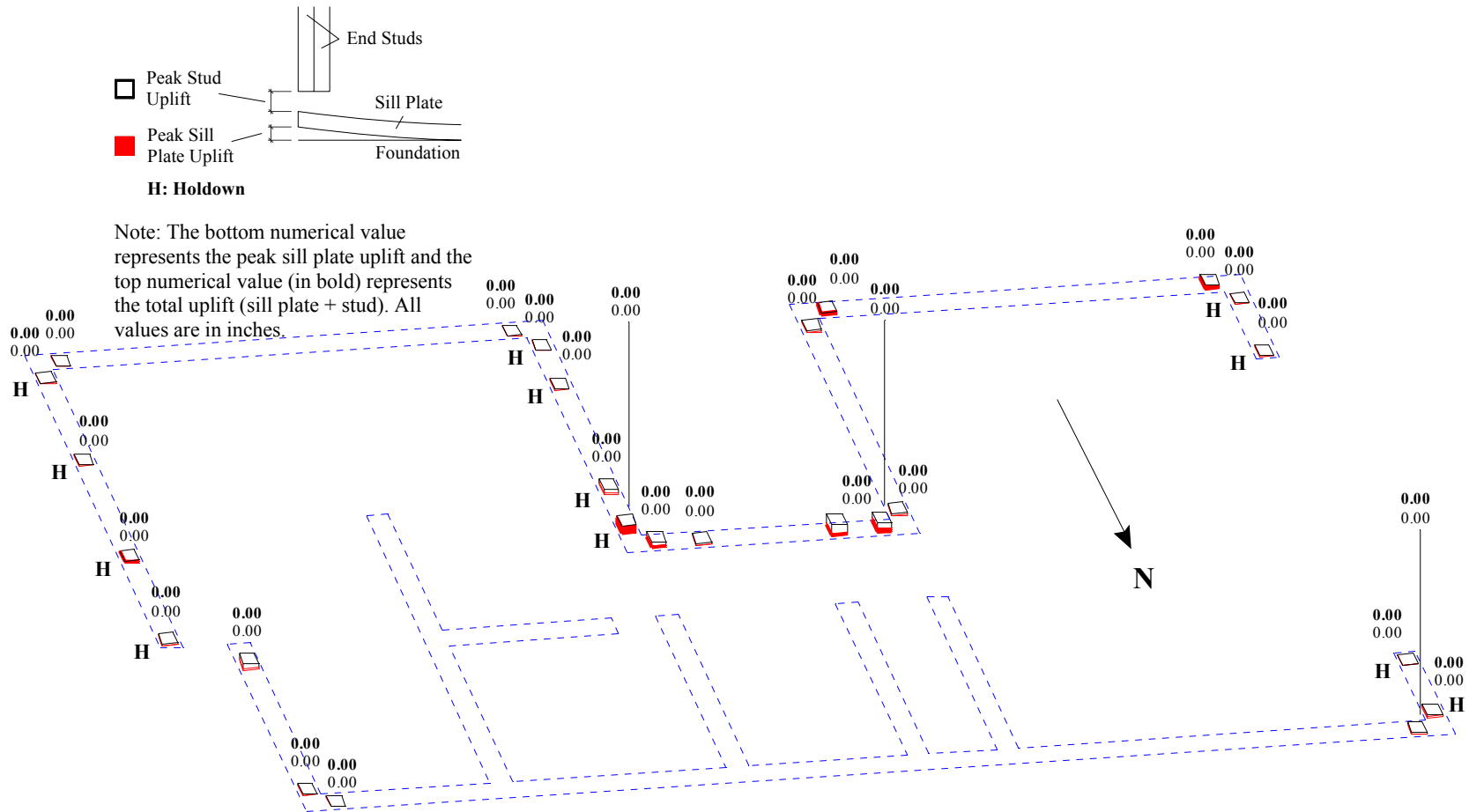


Figure R.3: Peak sill plate and stud uplift for Test NWP1S03

Appendix R

Phase 1, NWP1S04 Seismic Test

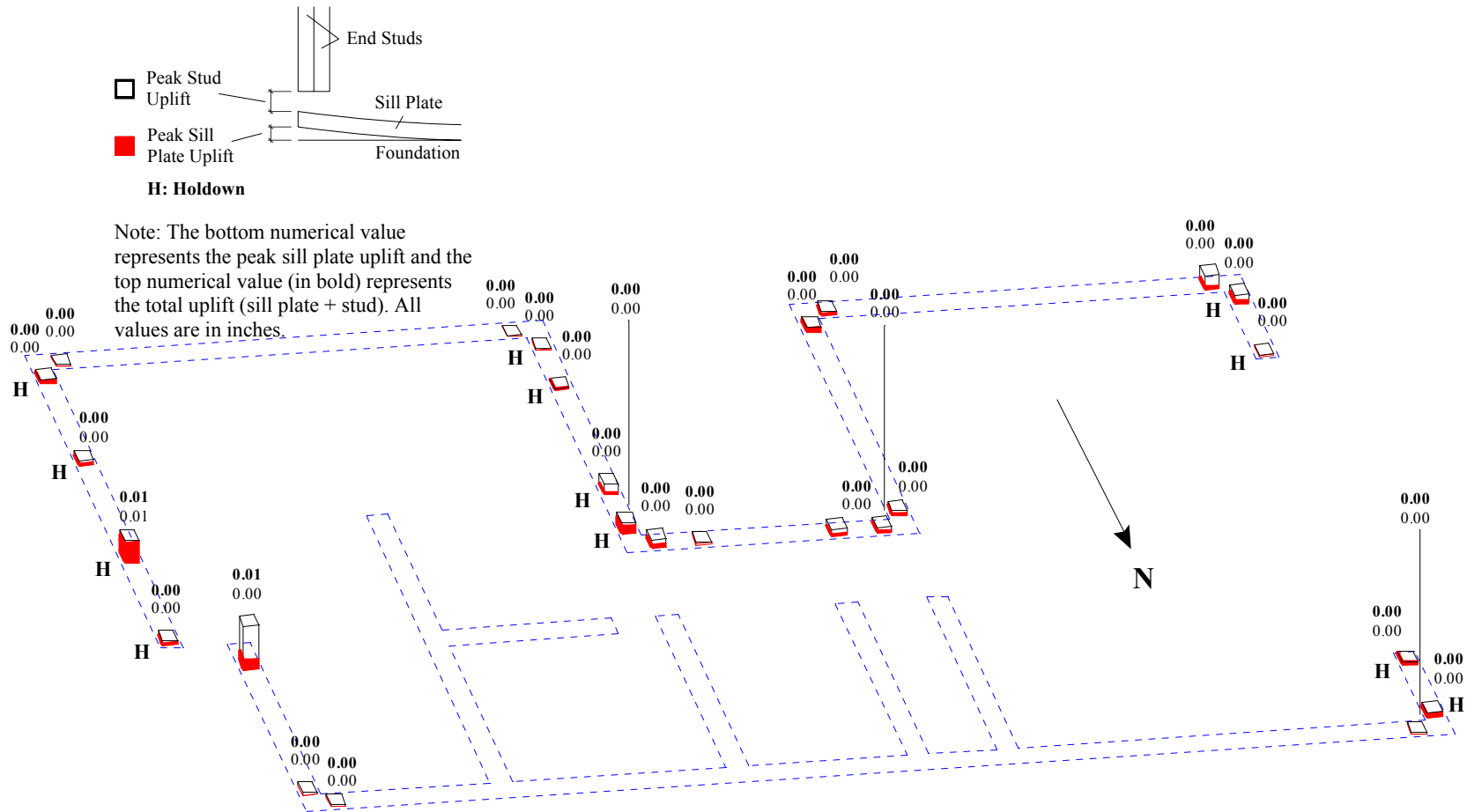


Figure R.4: Peak sill plate and stud uplift for Test NWP1S04

Appendix R

Phase 1, NWP1S05 Seismic Test

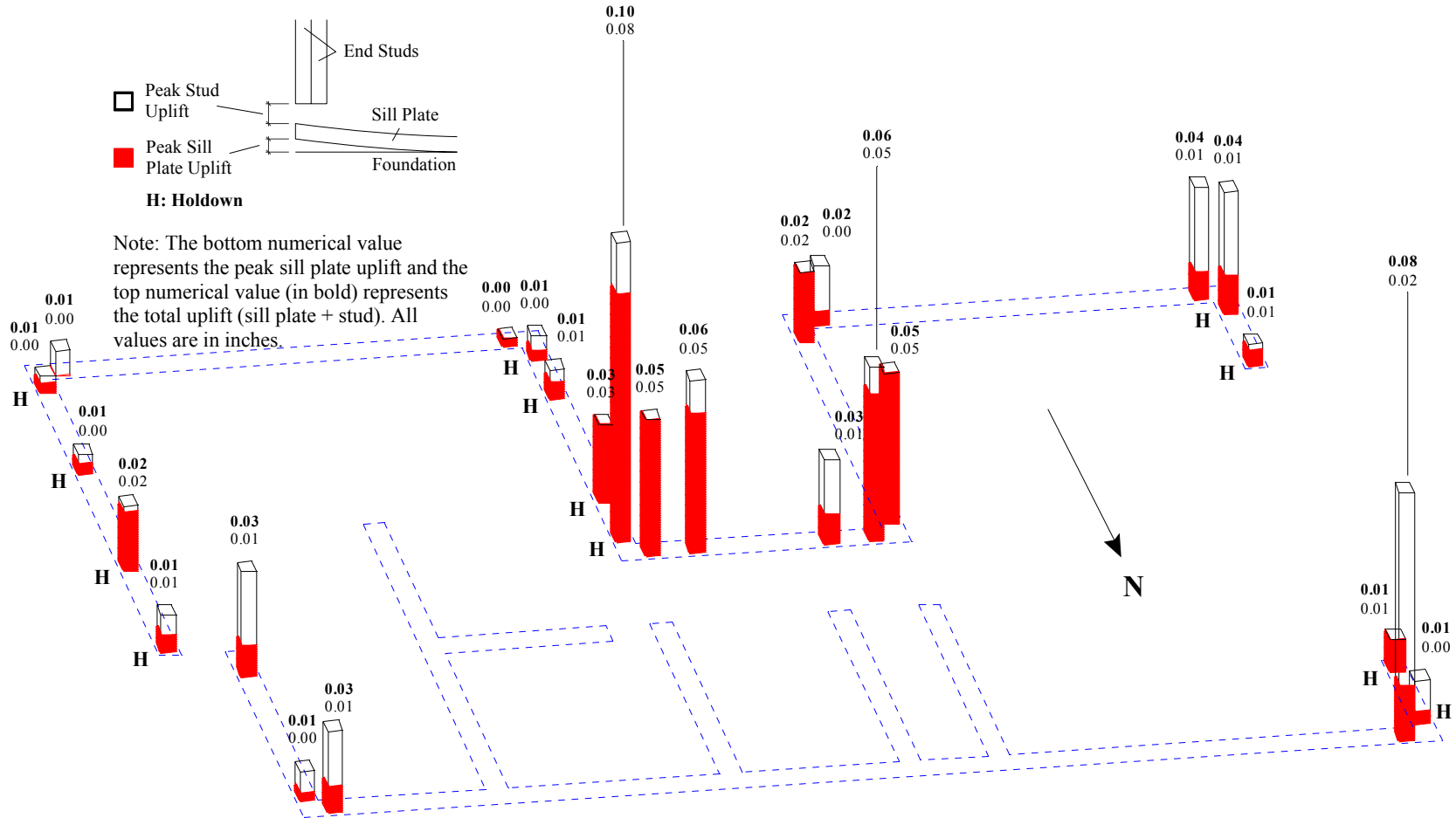


Figure R.5: Peak sill plate and stud uplift for Test NWP1S05

Appendix R

Phase 1, NWP1S17 Seismic Test

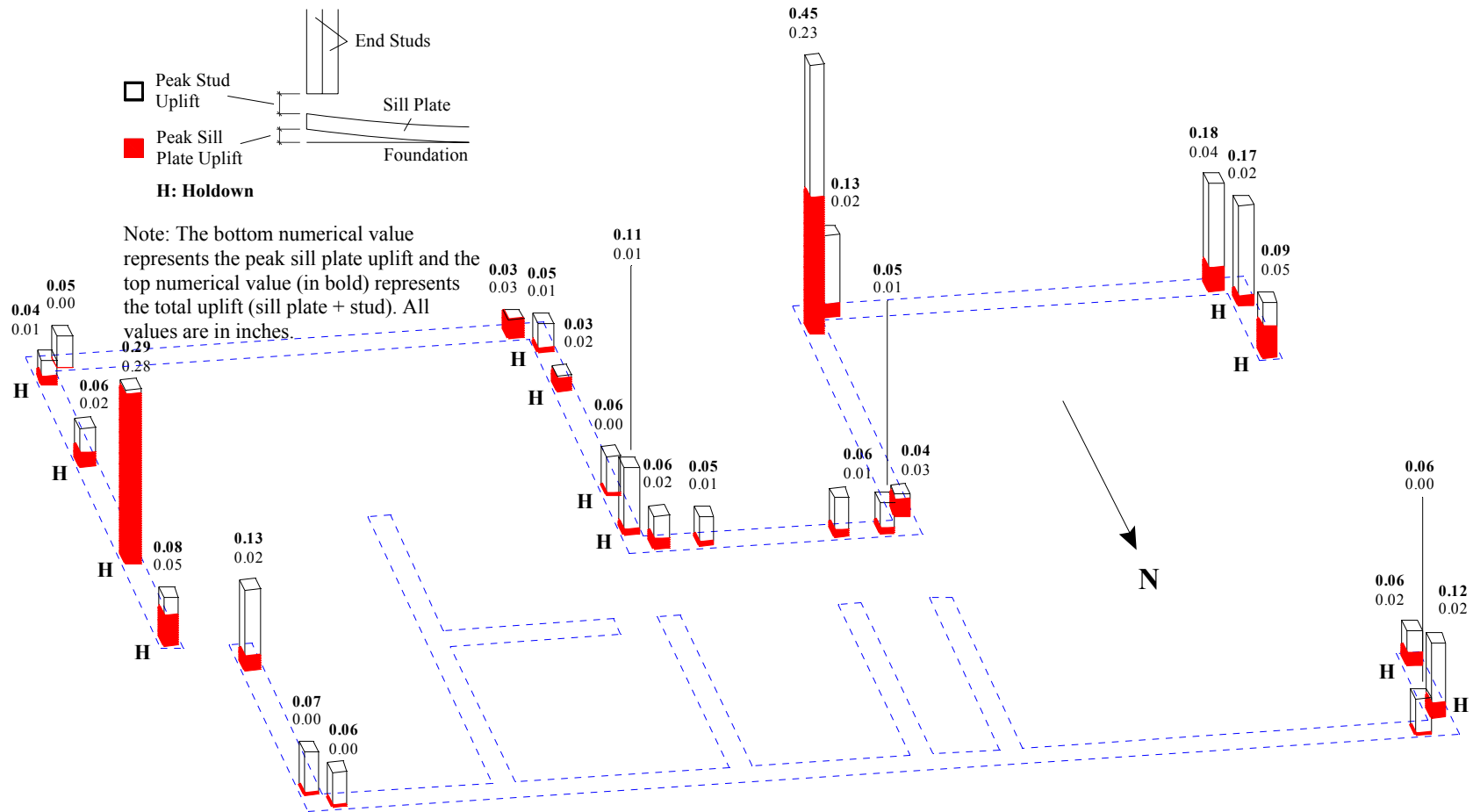


Figure R.6: Peak sill plate and stud uplift for Test NWP1S17

Appendix R

Phase 1, NWP1S07 Seismic Test

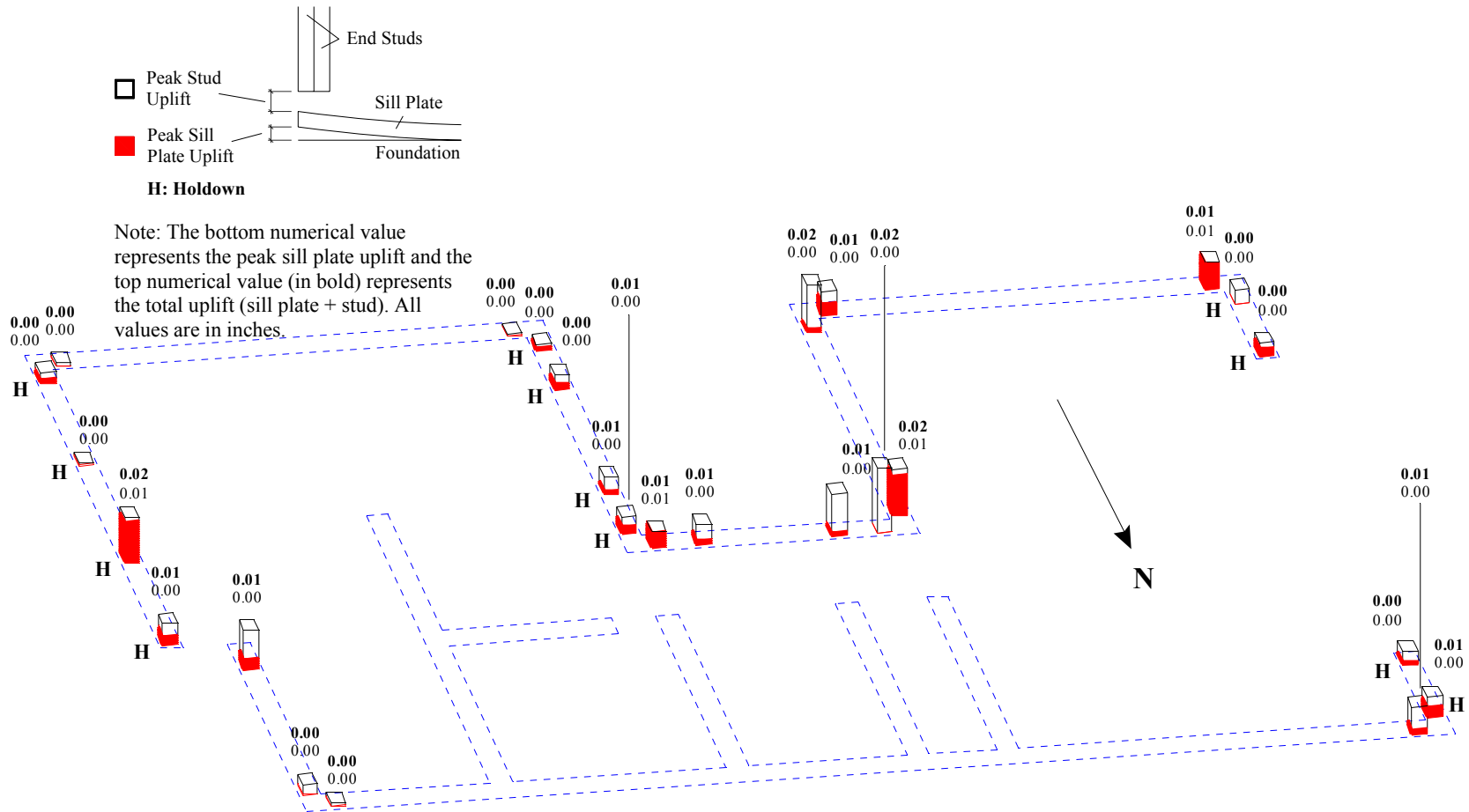


Figure R.7: Peak sill plate and stud uplift for Test NWP1S07

Appendix R

Phase 1, NWP1S06 Seismic Test

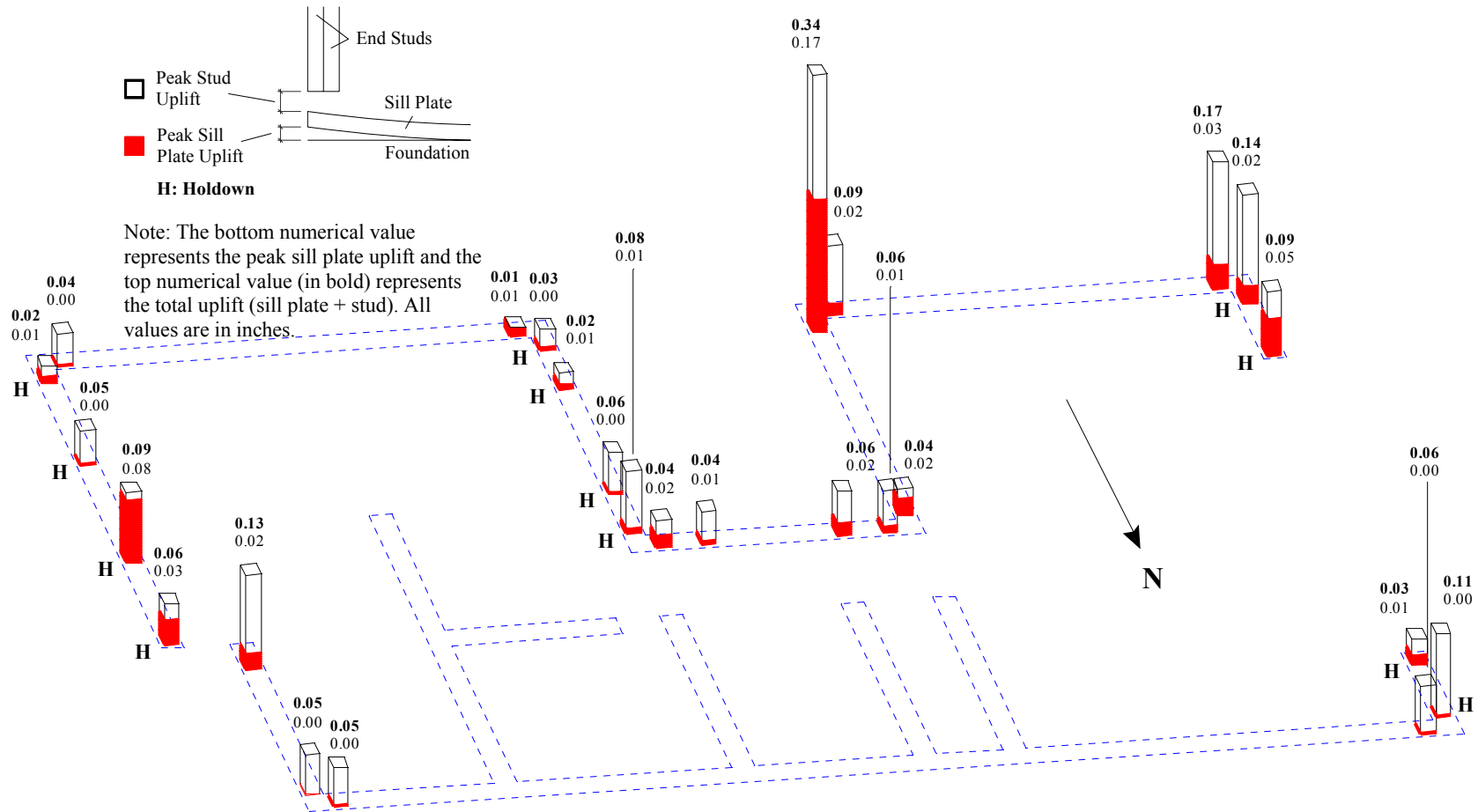


Figure R.8: Peak sill plate and stud uplift for Test NWP1S06

Appendix R

Phase 1, NWP1S10 Seismic Test

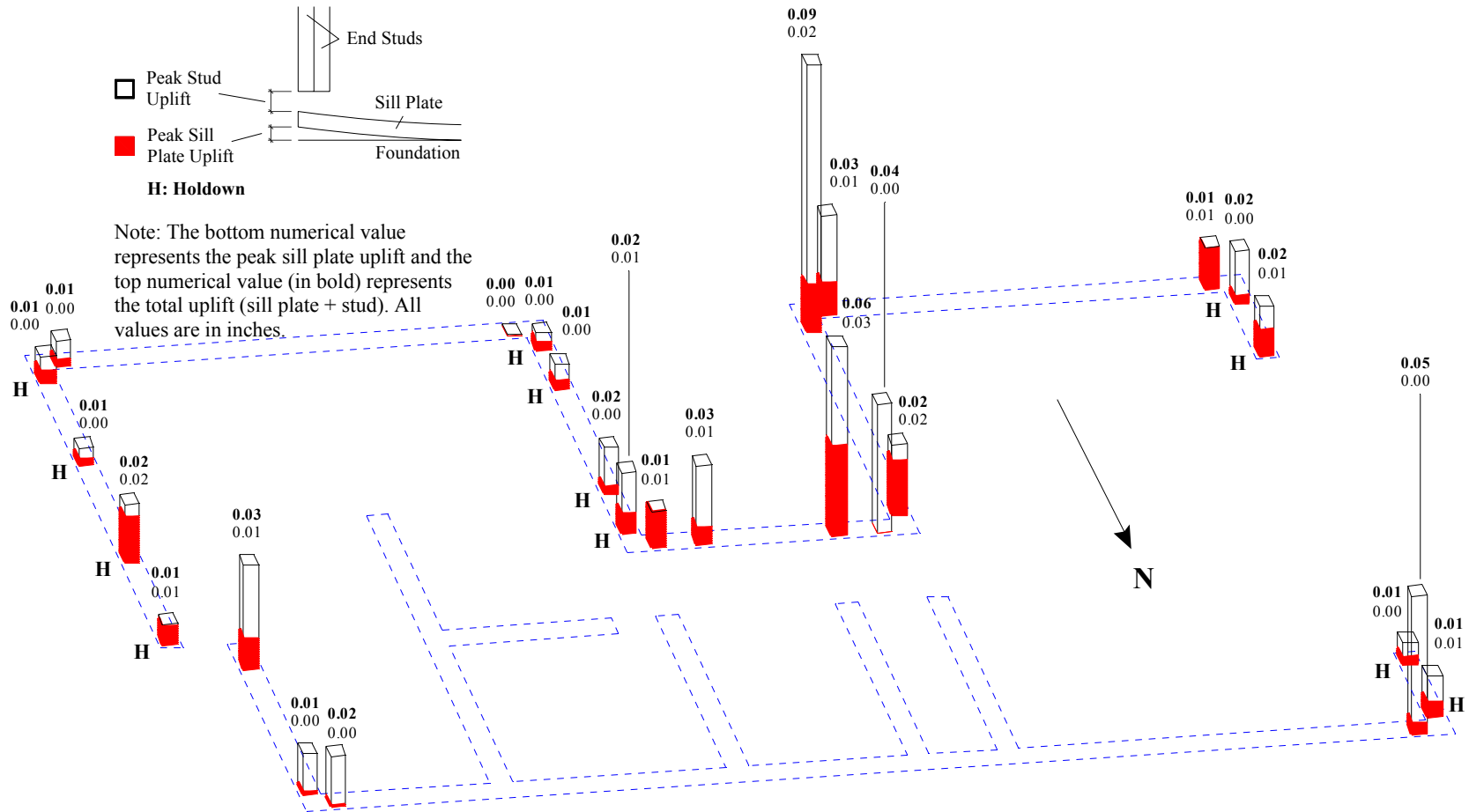


Figure R.9: Peak sill plate and stud uplift for Test NWP1S10

Appendix R

Phase 2, NWP2S01 Seismic Test

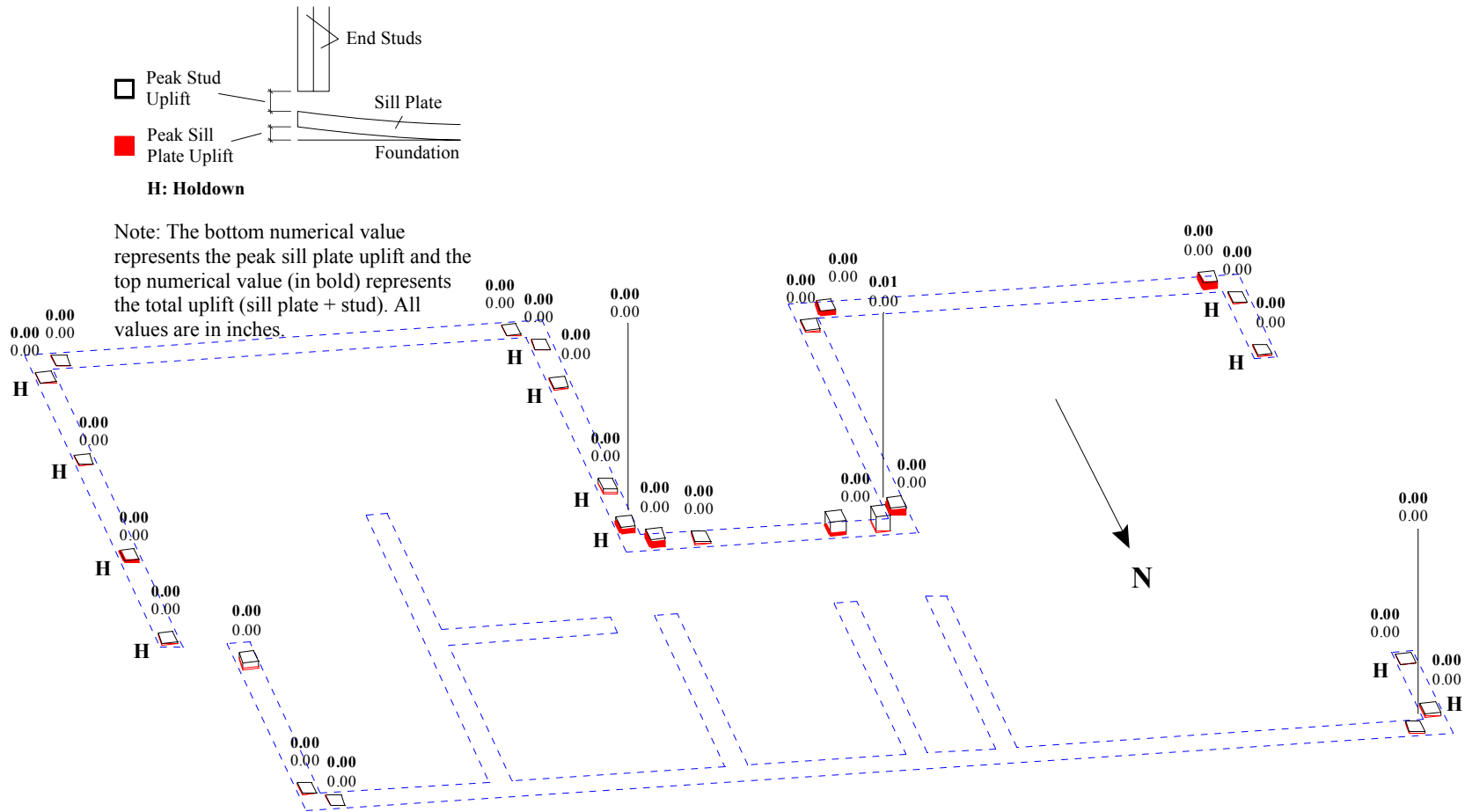


Figure R.10: Peak sill plate and stud uplift for Test NWP2S01

Appendix R

Phase 2, NWP2S02 Seismic Test

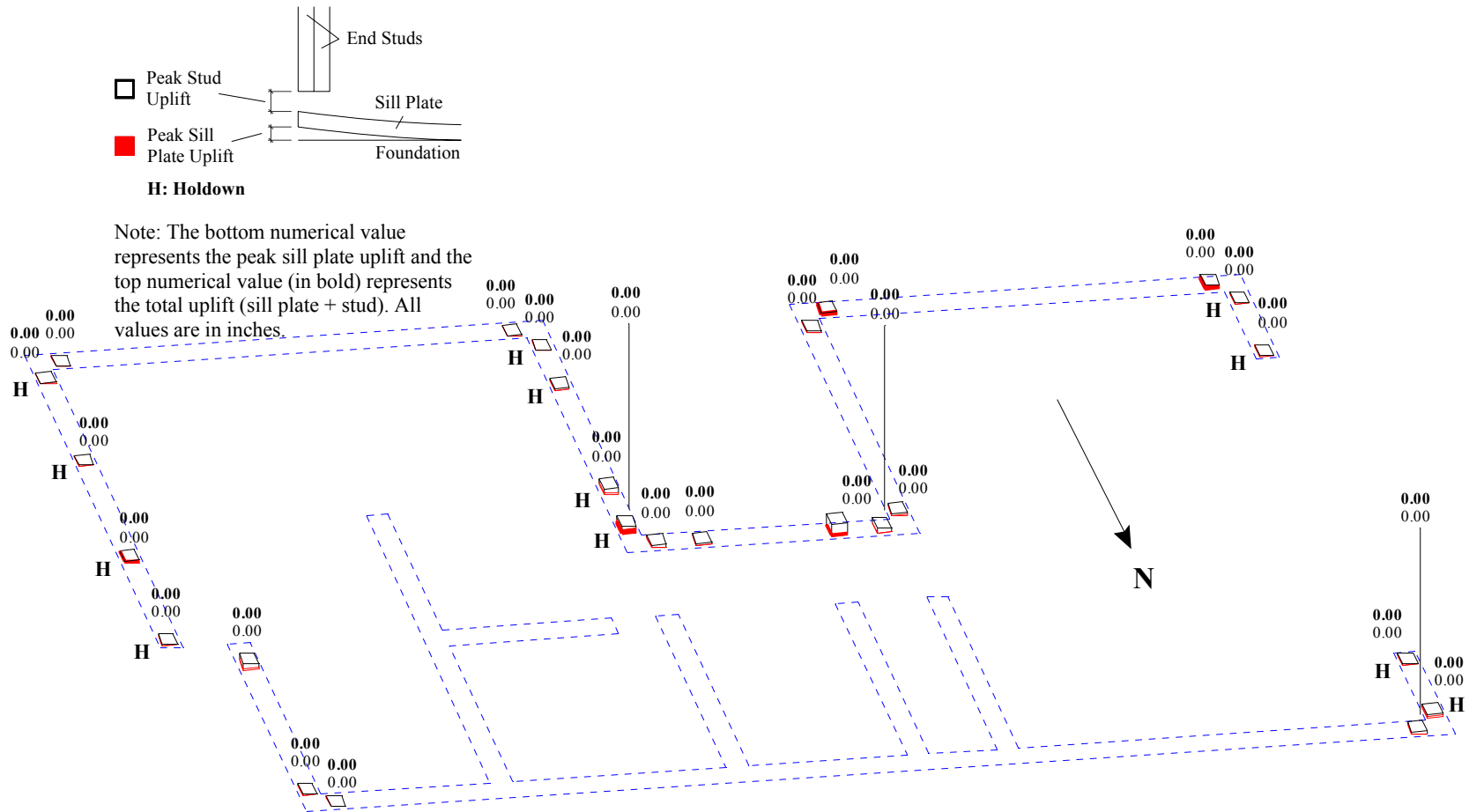


Figure R.11: Peak sill plate and stud uplift for Test NWP2S02

Appendix R

Phase 2, NWP2S03 Seismic Test

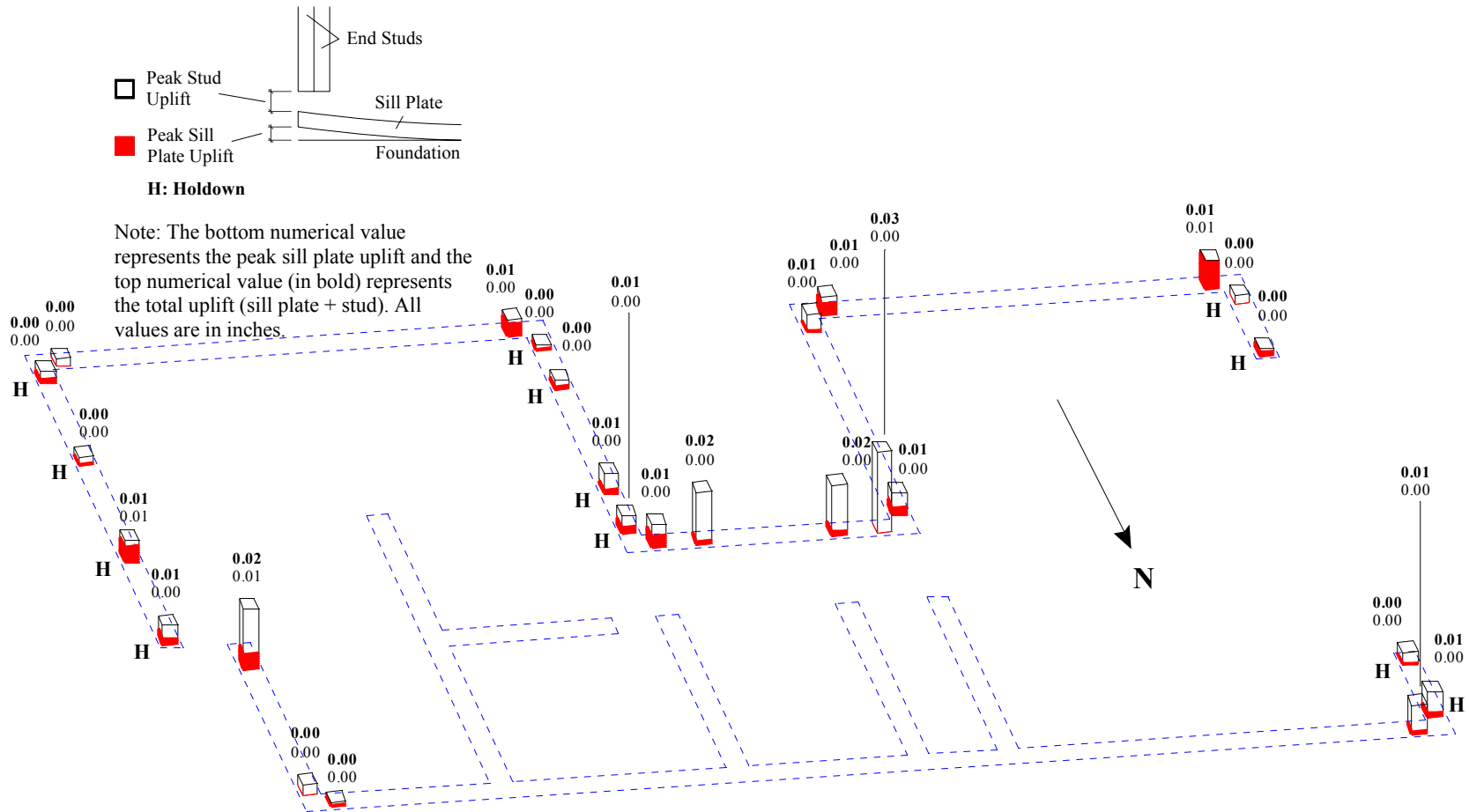


Figure R.12: Peak sill plate and stud uplift for Test NWP2S03

Appendix R

Phase 2, NWP2S05 Seismic Test

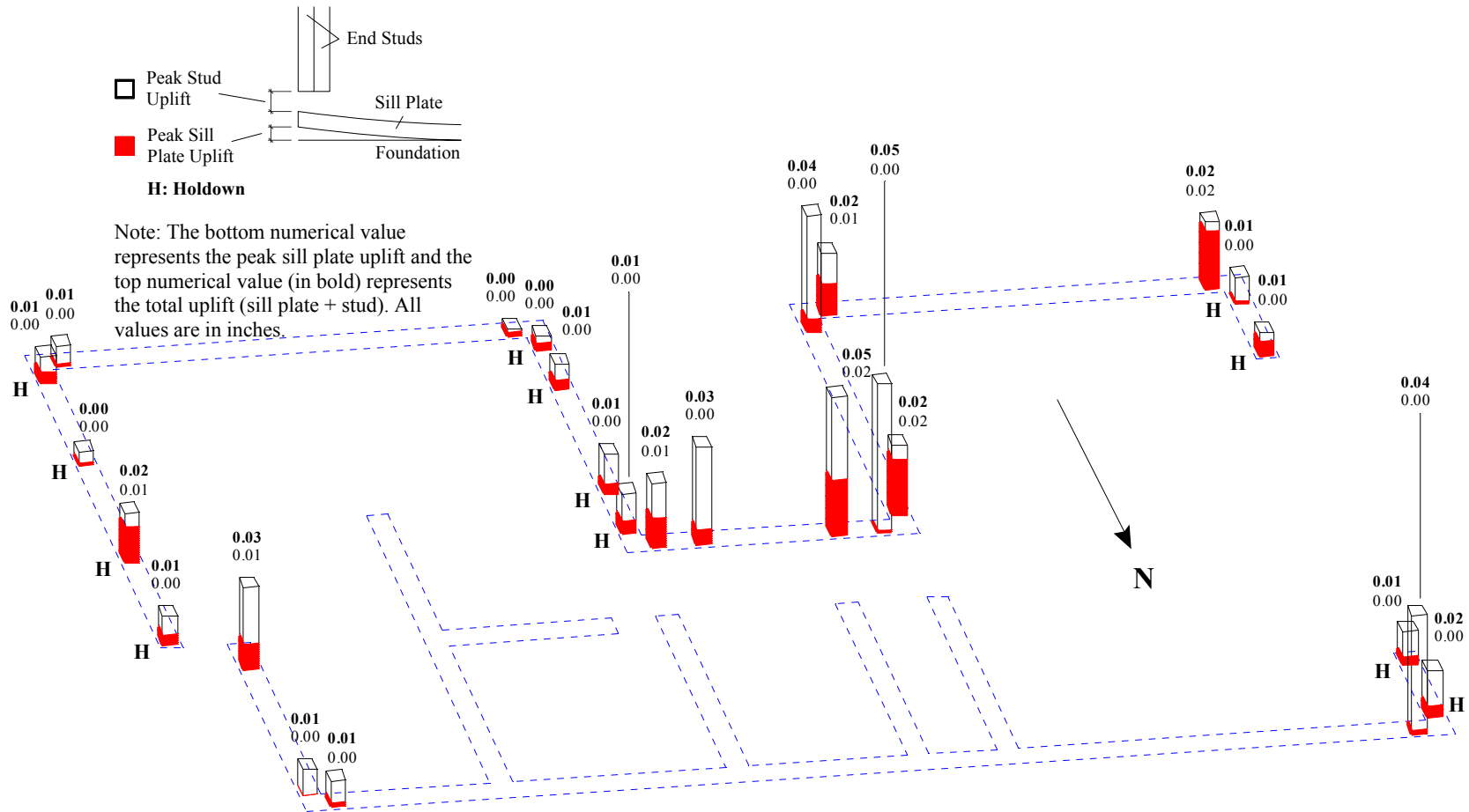


Figure R.14: Peak sill plate and stud uplift for Test NWP2S05

Appendix R

Phase 2, NWP2S06 Seismic Test

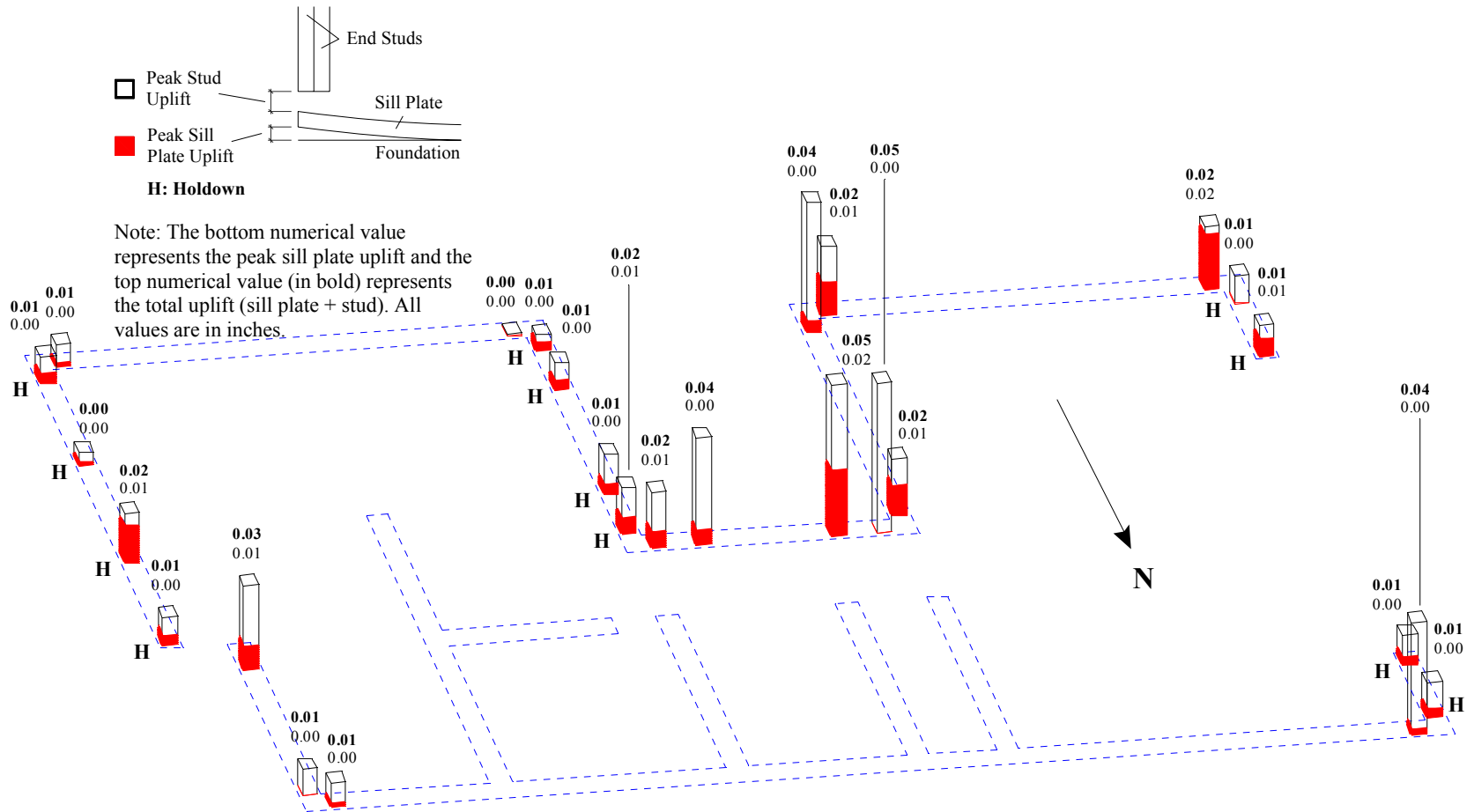


Figure R.15: Peak sill plate and stud uplift for Test NWP2S06

Appendix R

Phase 2, NWP2S07 Seismic Test

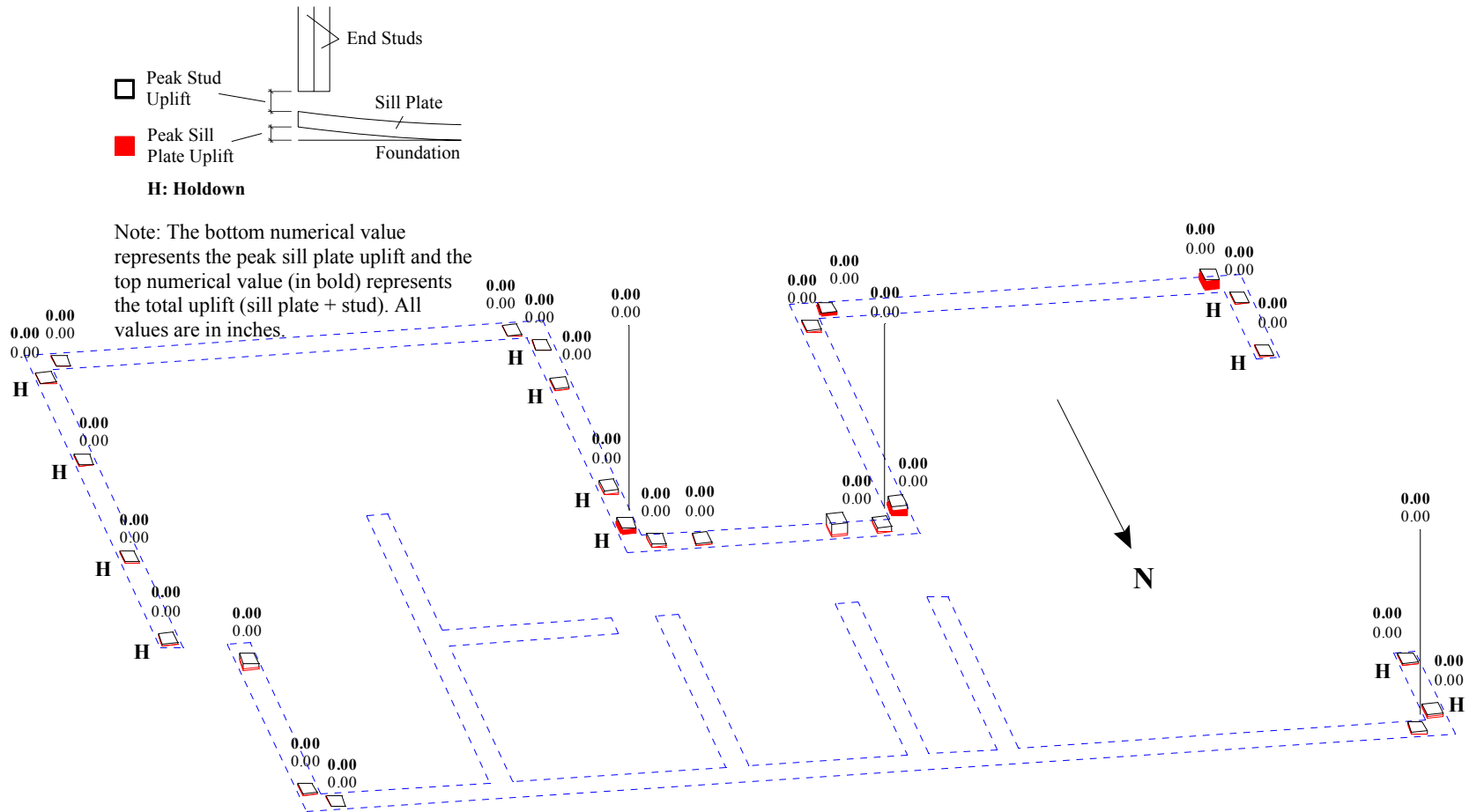


Figure R.16: Peak sill plate and stud uplift for Test NWP2S07

Appendix R

Phase 2, NWP2S08 Seismic Test

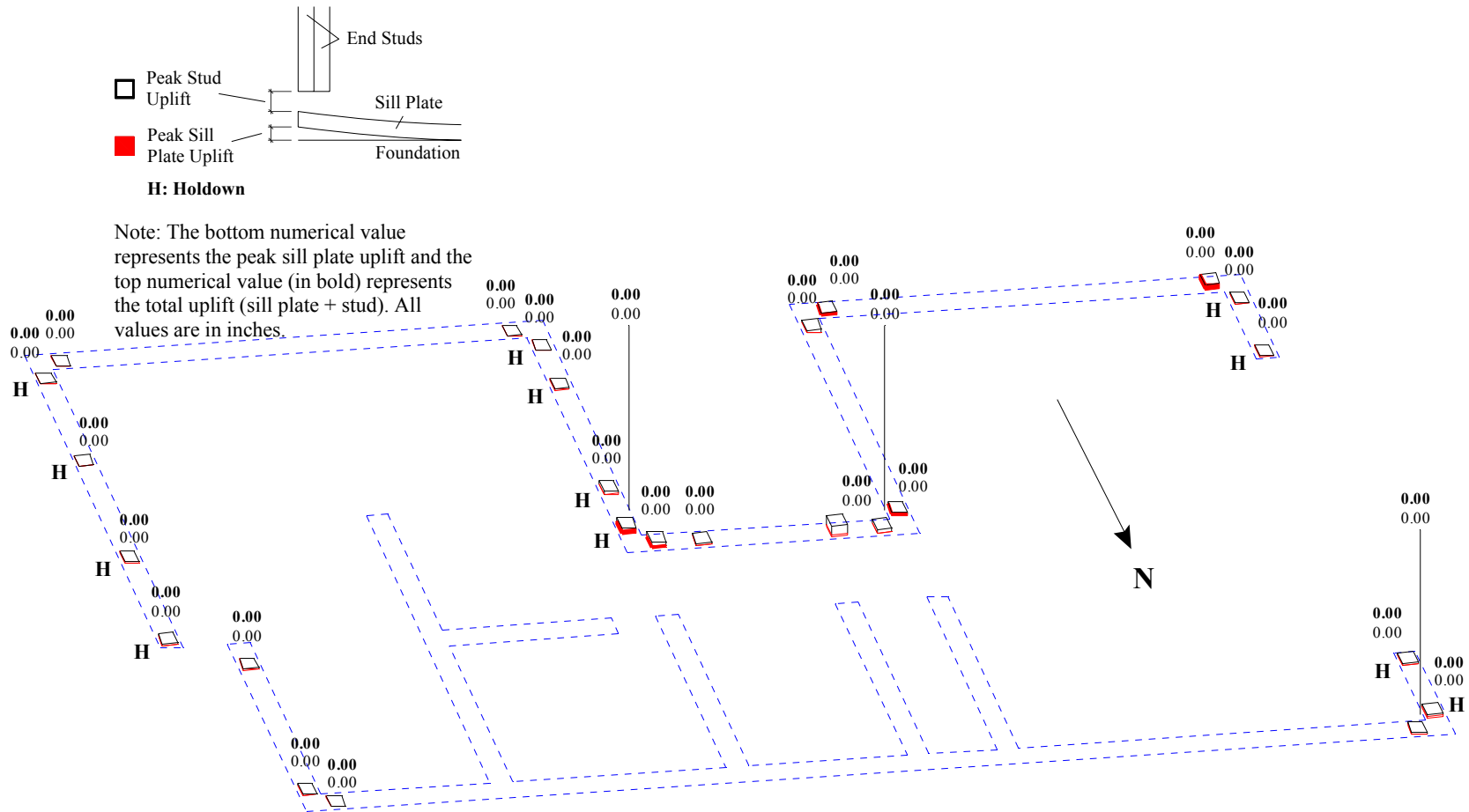


Figure R.17: Peak sill plate and stud uplift for Test NWP2S08

Appendix R

Phase 2, NWP2S09 Seismic Test

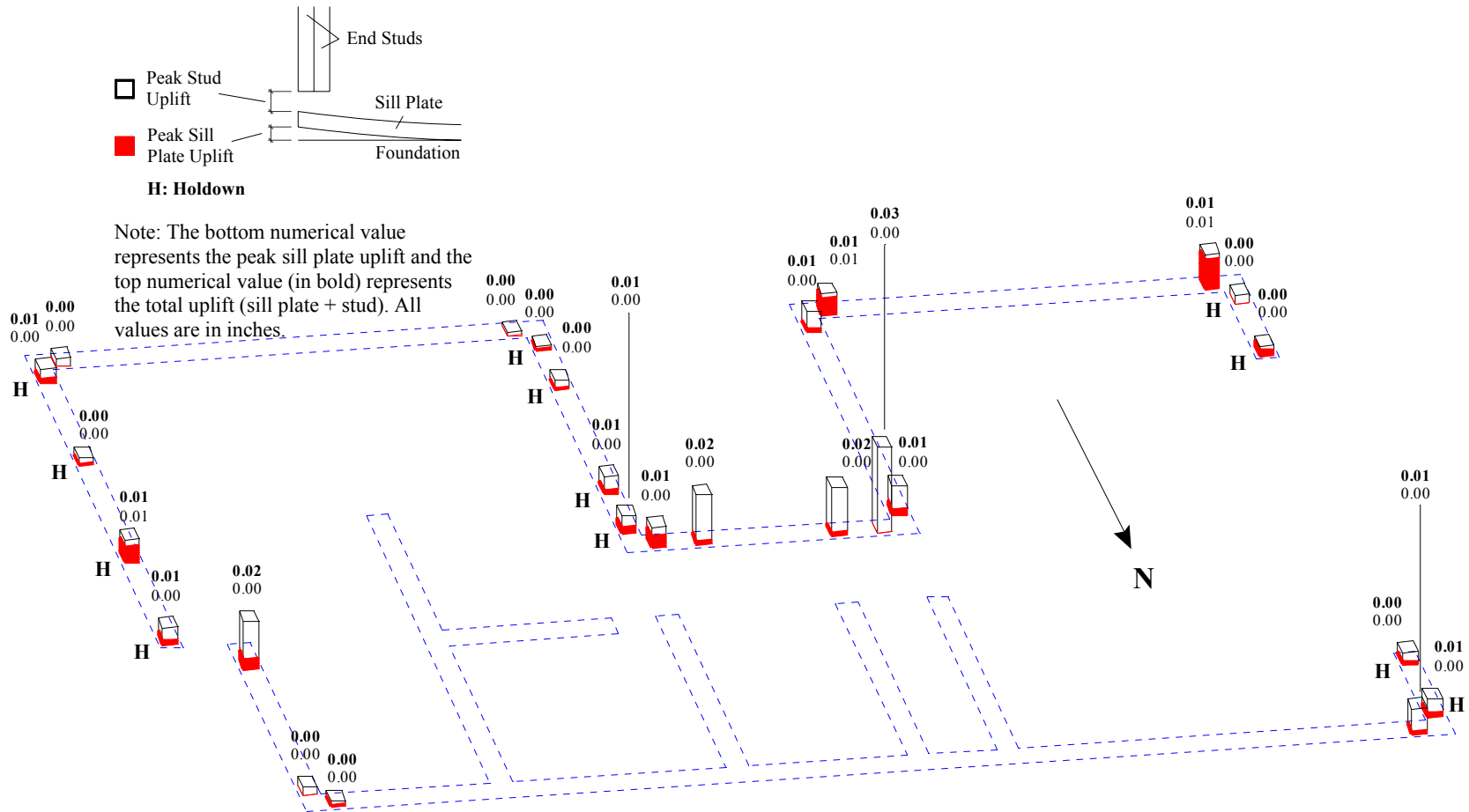


Figure R.18: Peak sill plate and stud uplift for Test NWP2S09

Appendix R

Phase 2, NWP2S10 Seismic Test

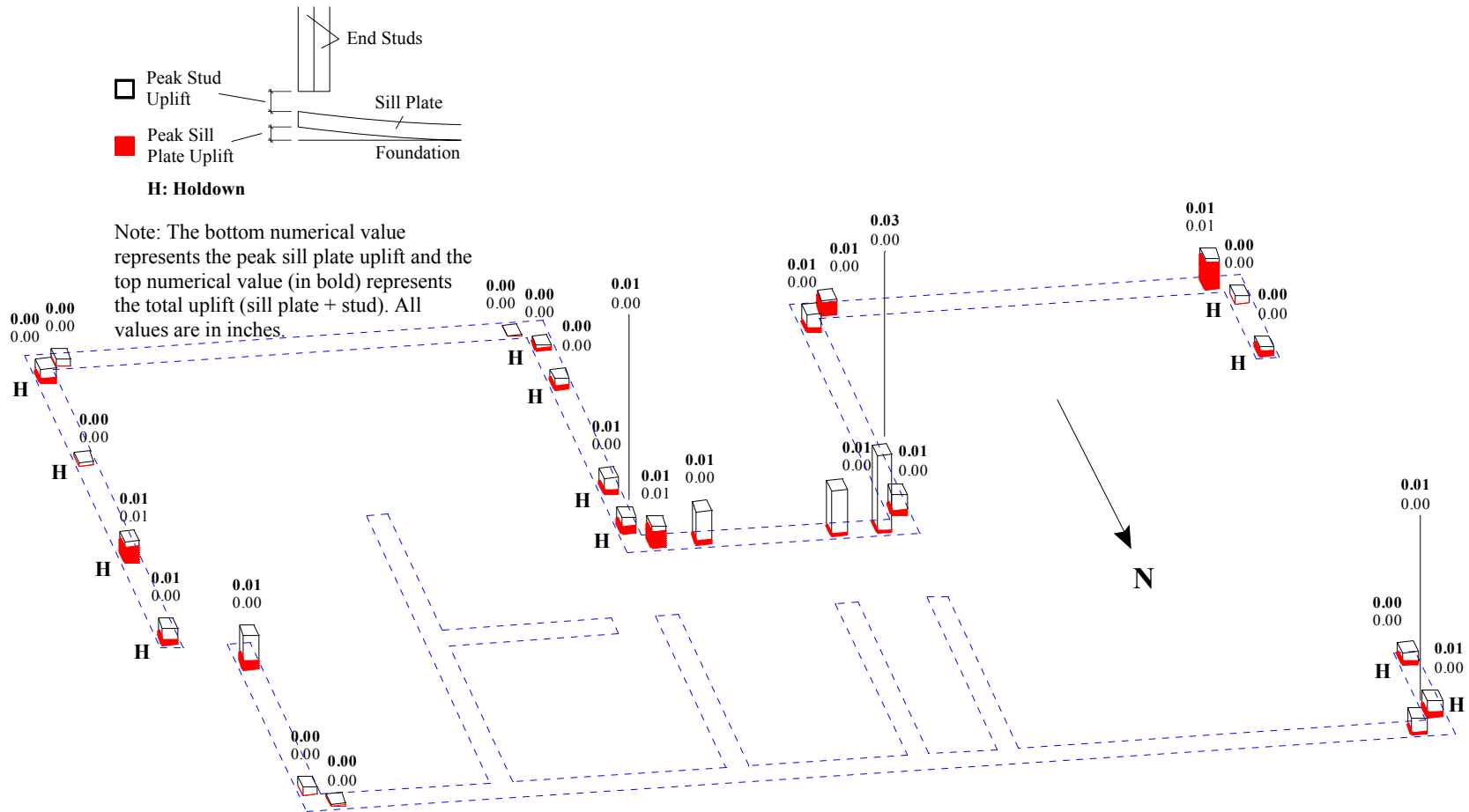


Figure R.19: Peak sill plate and stud uplift for Test NWP2S10

Appendix R

Phase 2, NWP2S12 Seismic Test

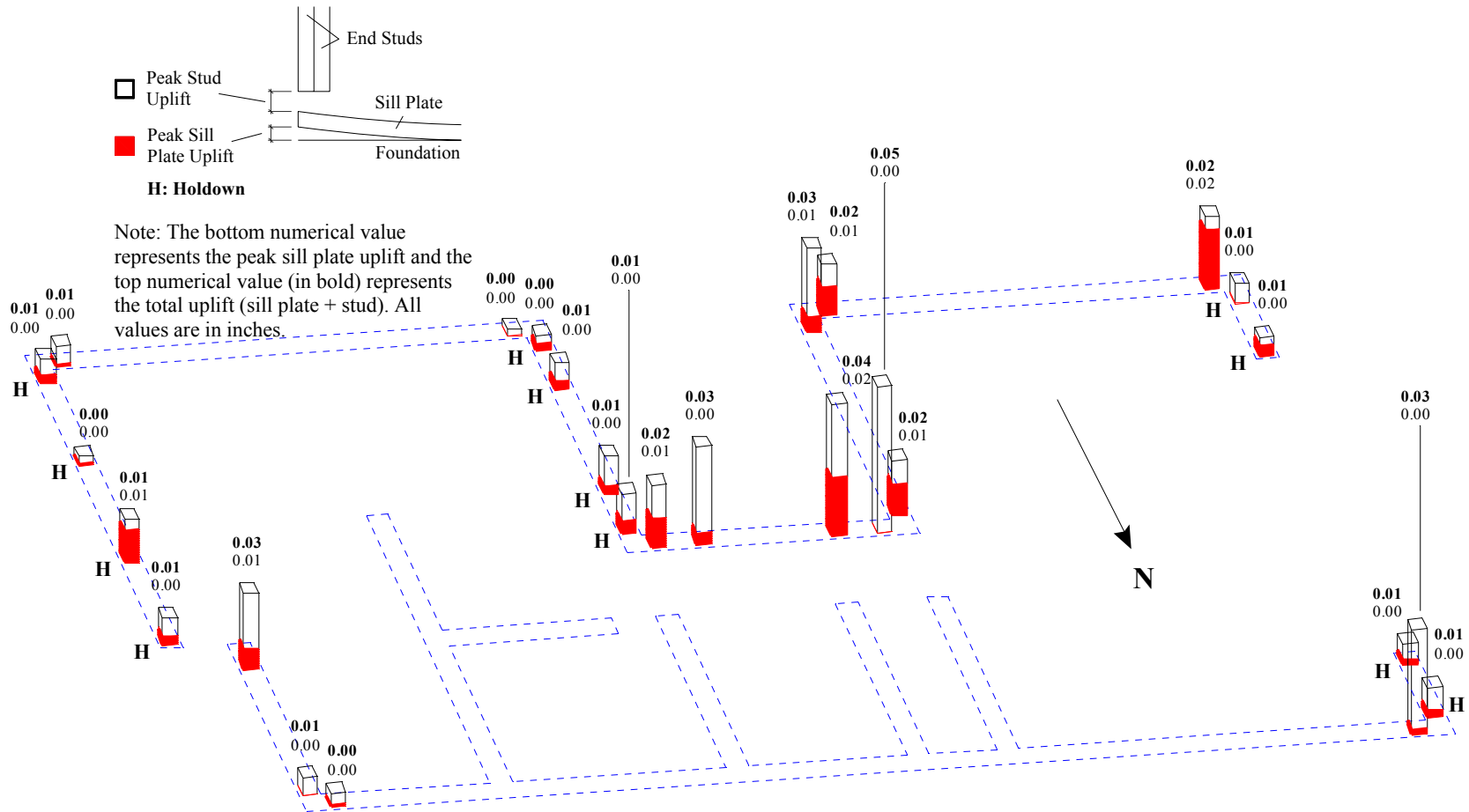


Figure R.21: Peak sill plate and stud uplift for Test NWP2S12

Appendix R

Phase 2, NWP2S13 Seismic Test

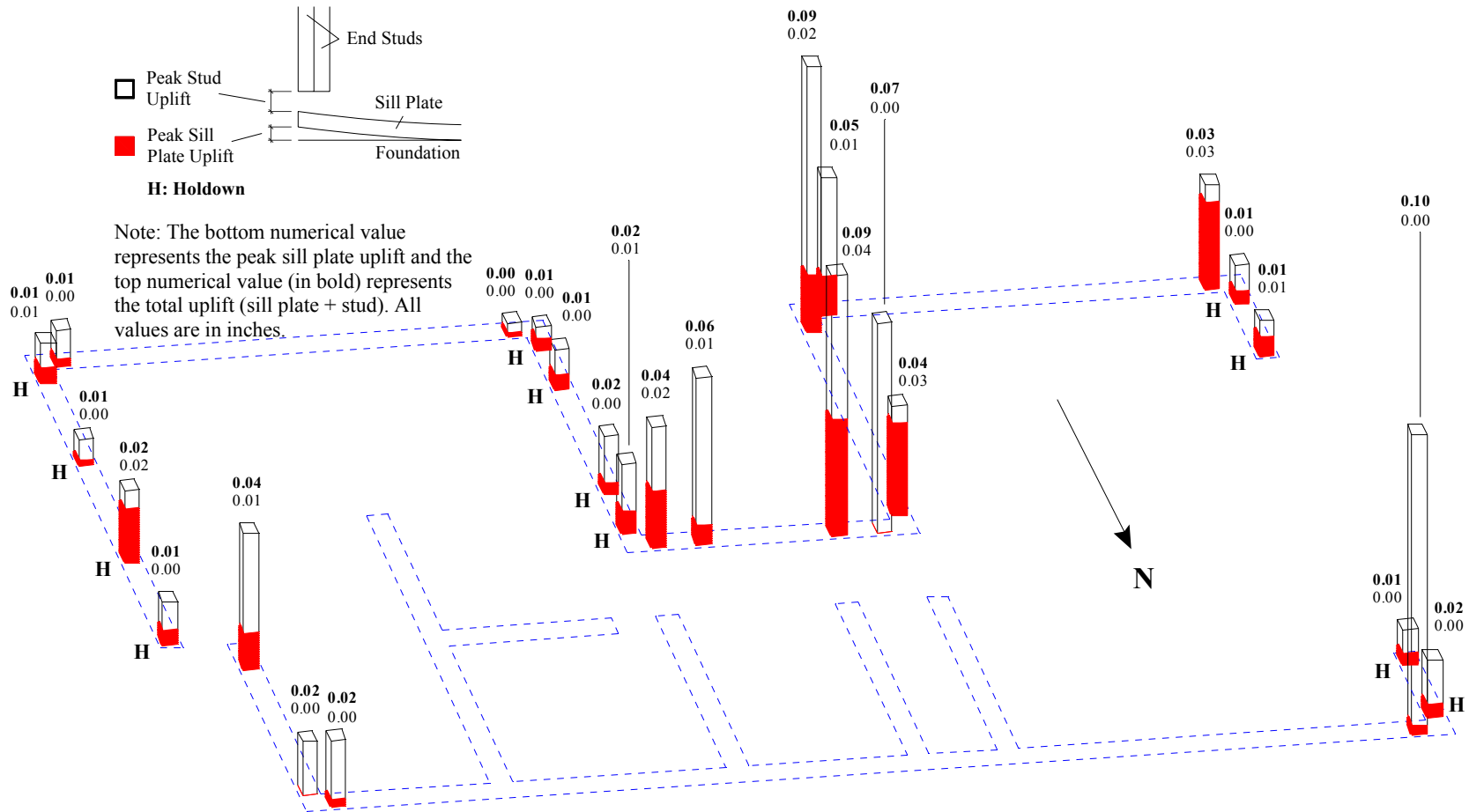


Figure R.22: Peak sill plate and stud uplift for Test NWP2S13

Appendix R

Phase 2, NWP2S17 Seismic Test

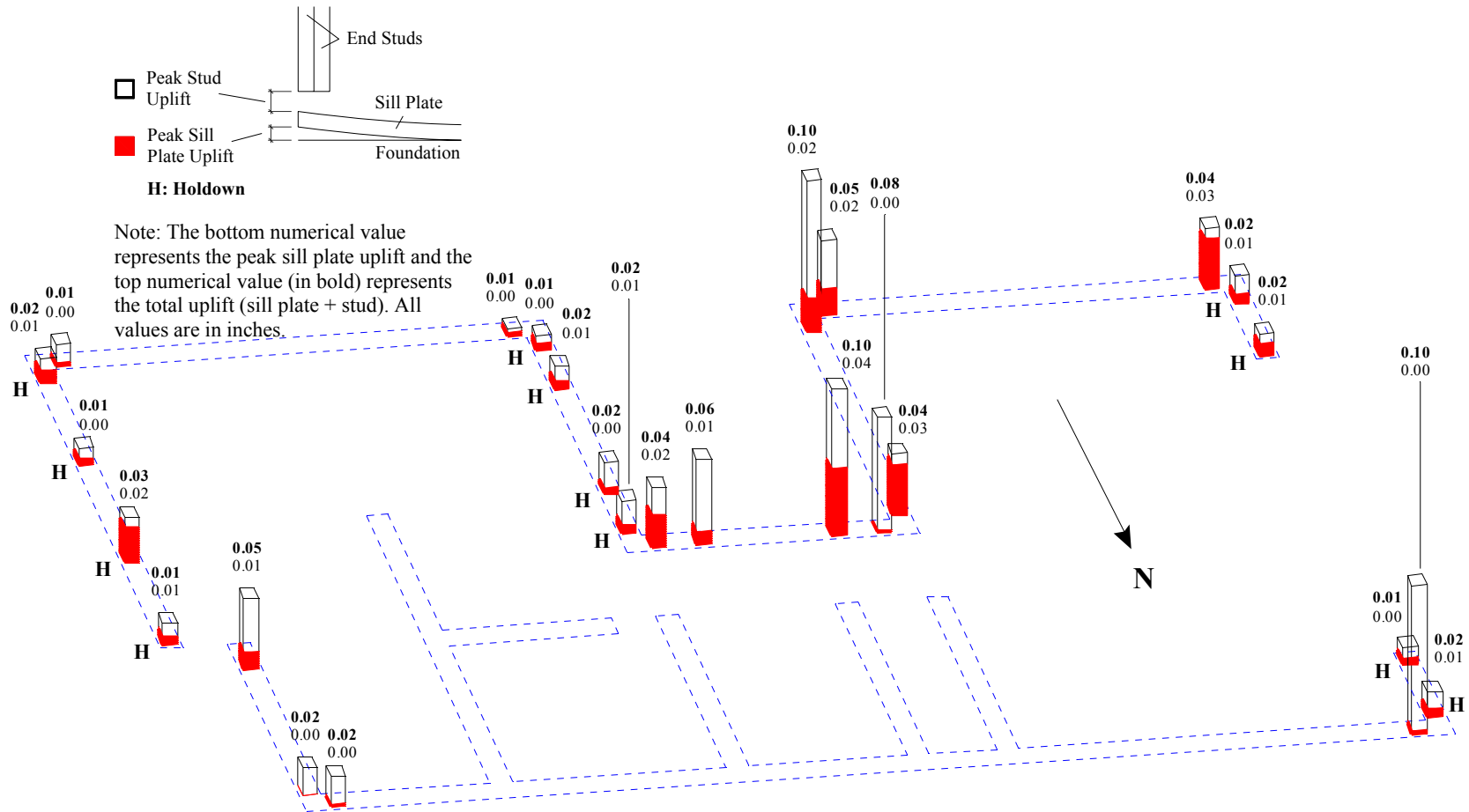


Figure R.25: Peak sill plate and stud uplift for Test NWP2S17

Appendix R

Phase 2, NWP2S21 Seismic Test

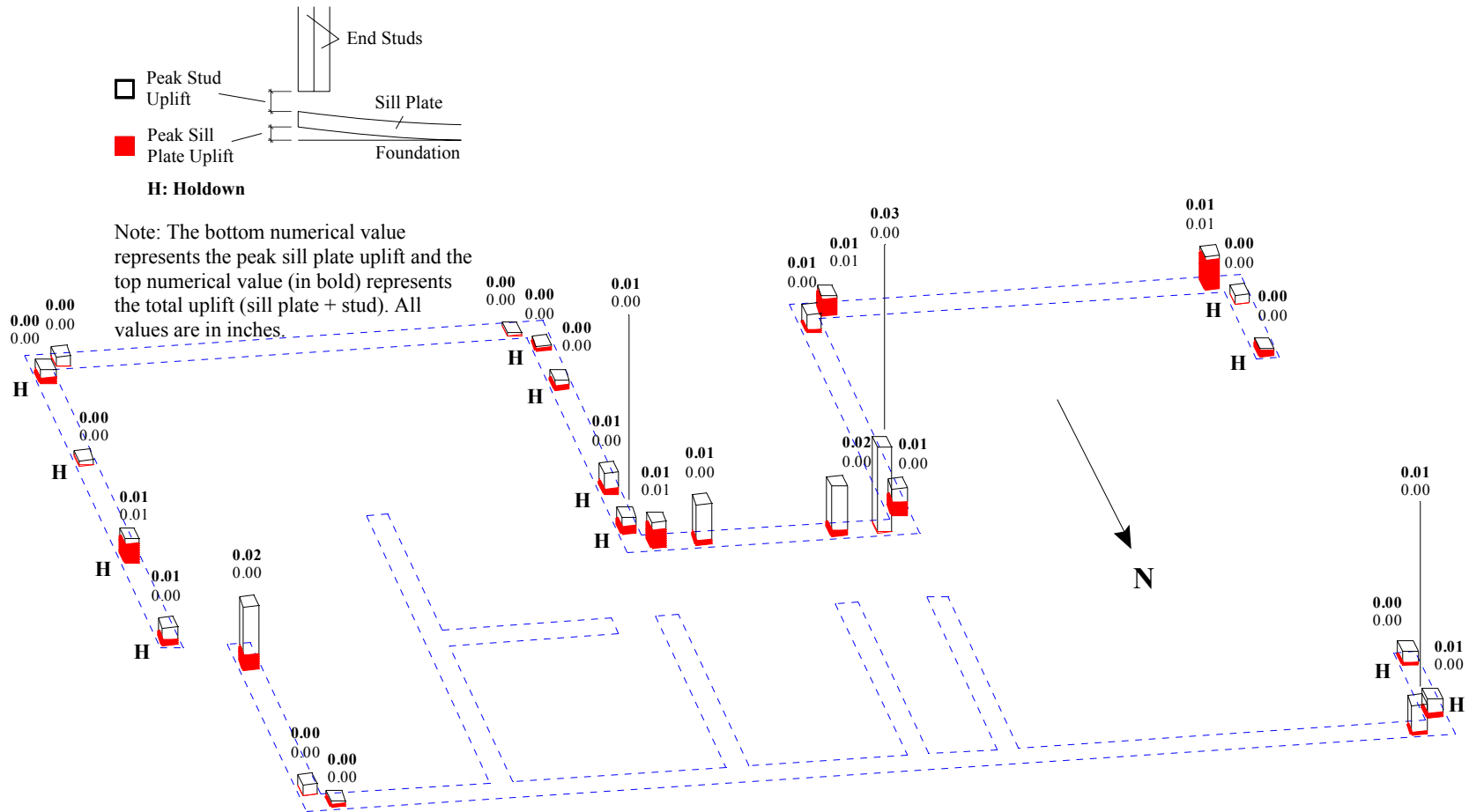


Figure R.26: Peak sill plate and stud uplift for Test NWP2S21

Appendix R

Phase 2, NWP2S24 Seismic Test

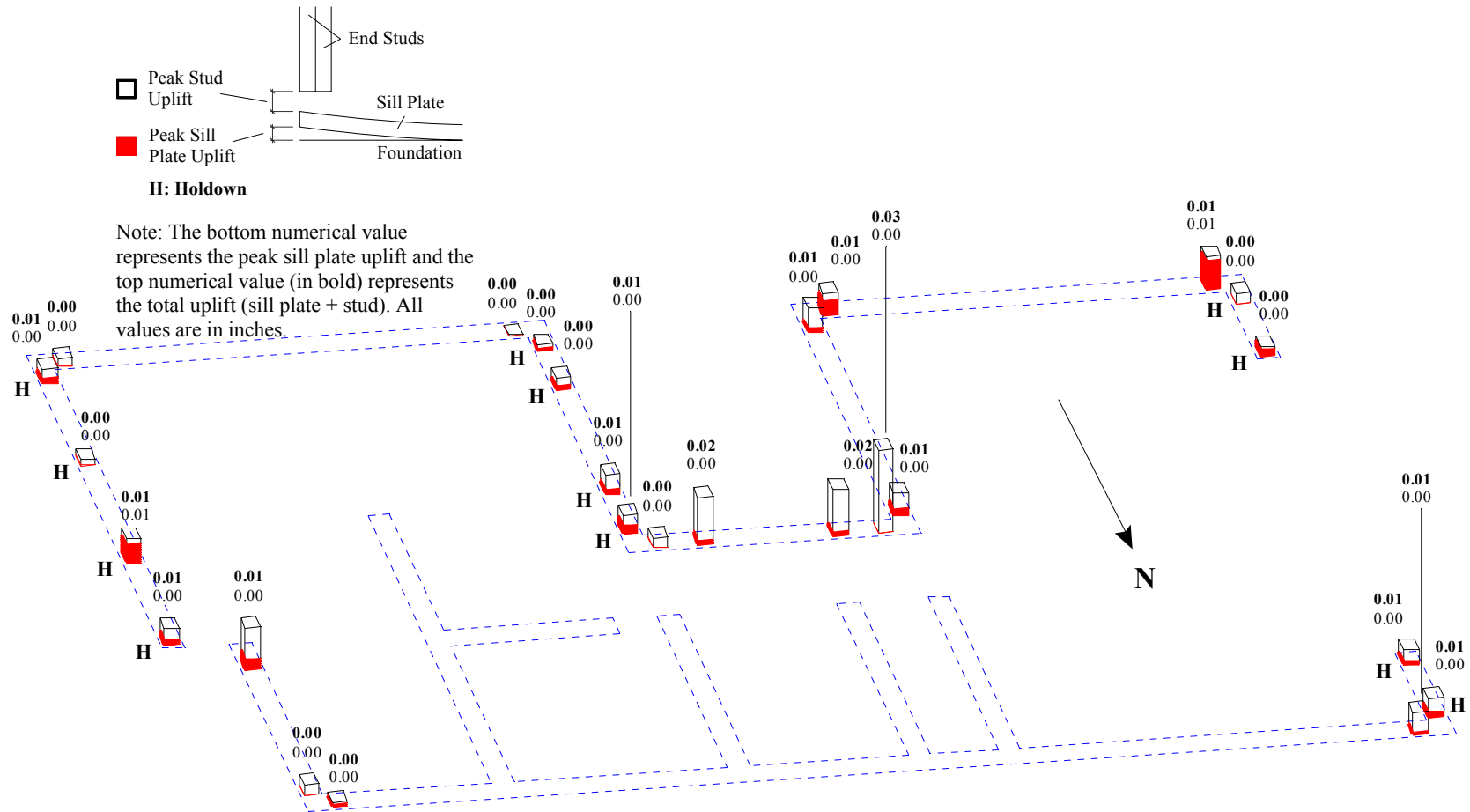


Figure R.27: Peak sill plate and stud uplift for Test NWP2S24

Appendix R

Phase 2, NWP2S26 Seismic Test

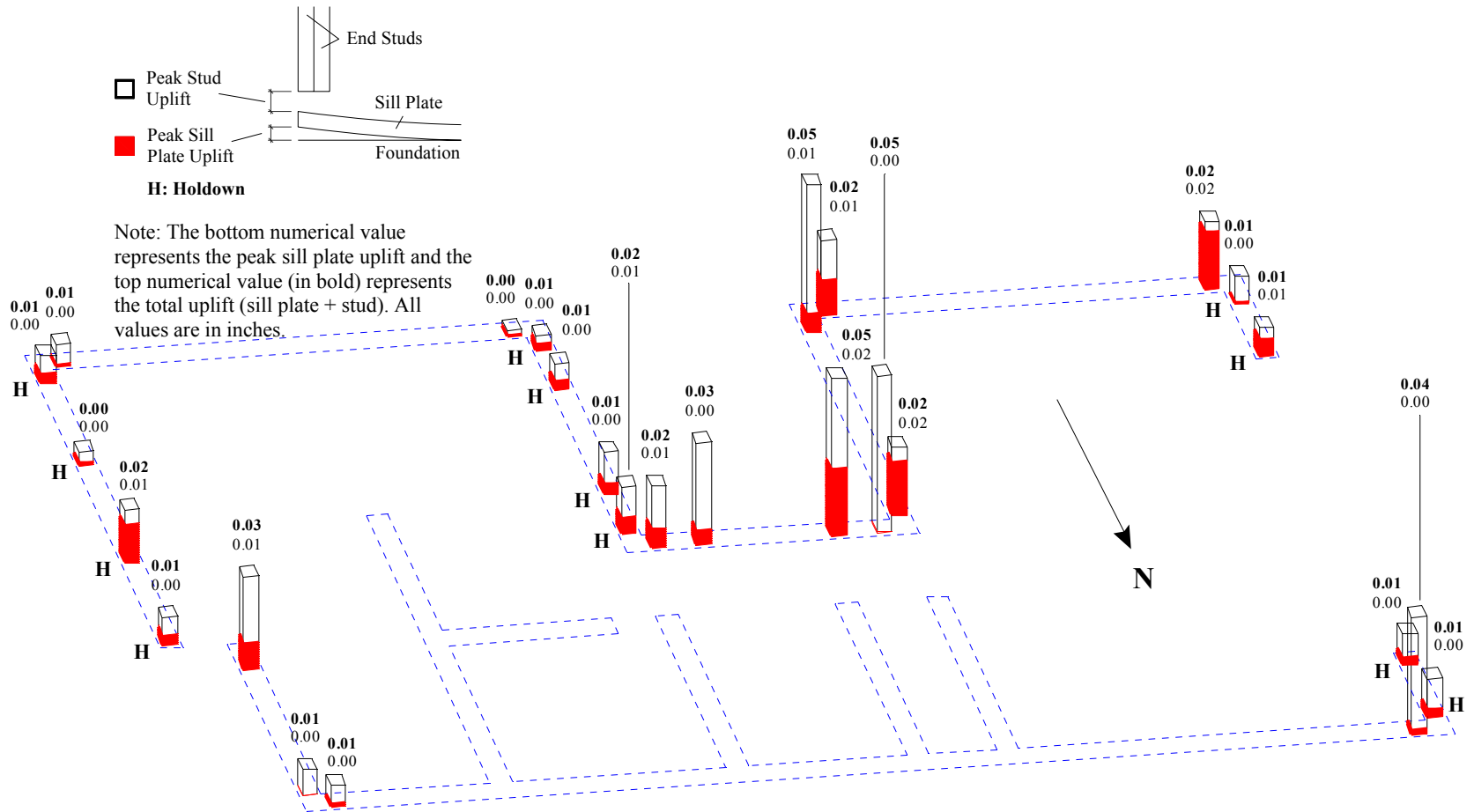


Figure R.29: Peak sill plate and stud uplift for Test NWP2S26

Appendix R

Phase 2, NWP2S27 Seismic Test

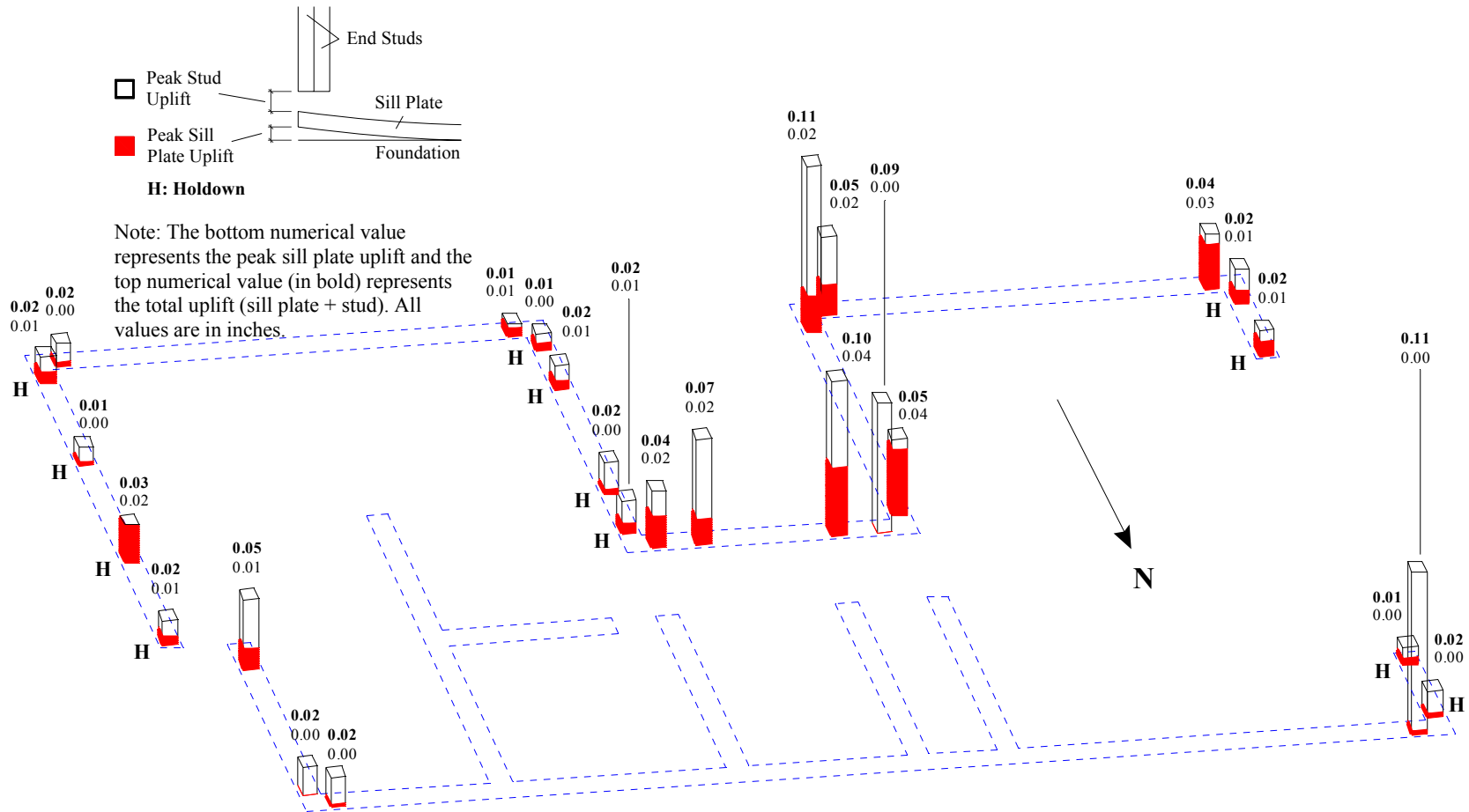


Figure R.30: Peak sill plate and stud uplift for Test NWP2S27

Appendix R

Phase 2, NWP2S29 Seismic Test

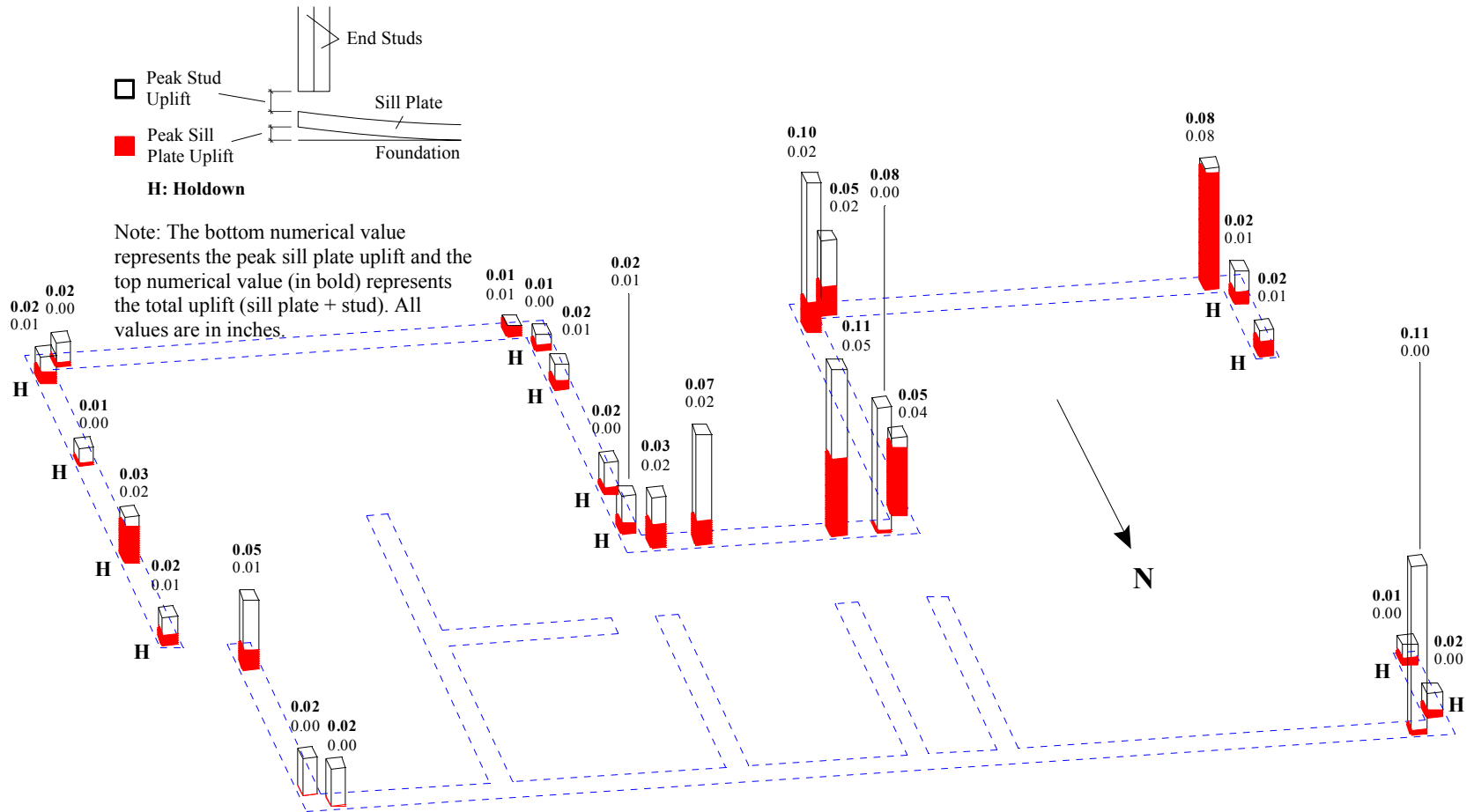


Figure R.32: Peak sill plate and stud uplift for Test NWP2S29

Appendix R

Phase 2, NWP2S30 Seismic Test

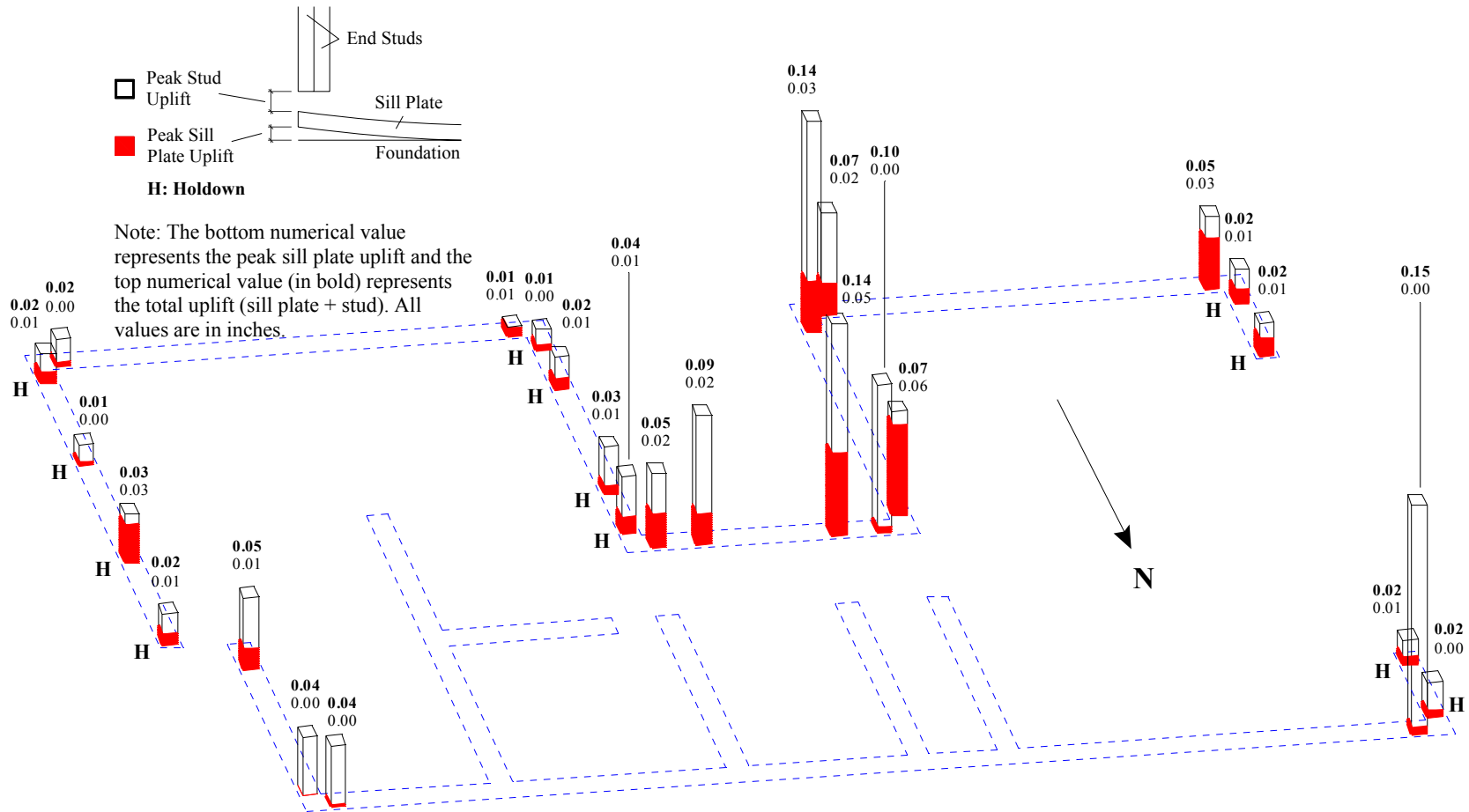


Figure R.33: Peak sill plate and stud uplift for Test NWP2S30

Appendix R

Phase 3, NWP3S01 Seismic Test

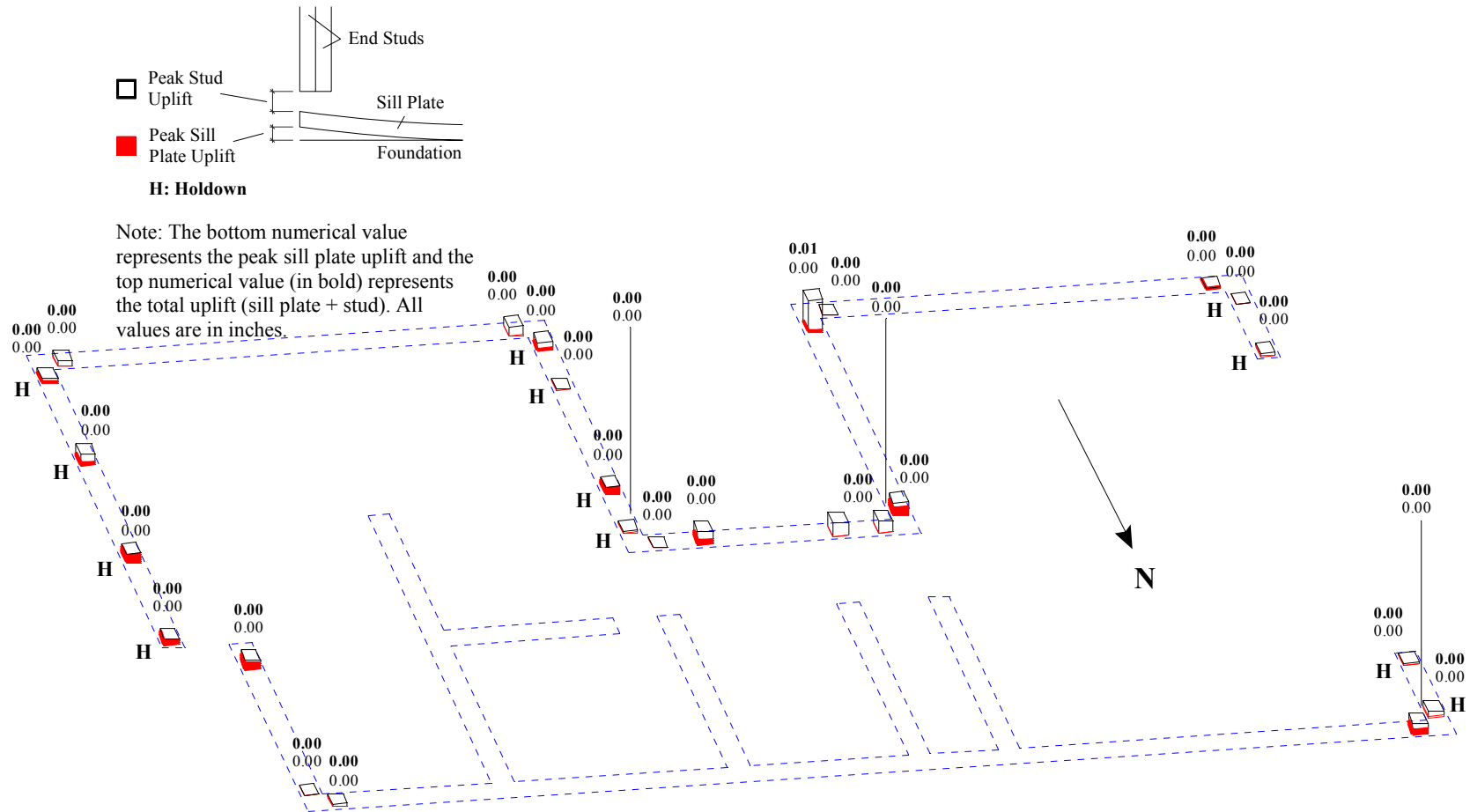


Figure R.34: Peak sill plate and stud uplift for Test NWP3S01

Appendix R

Phase 3, NWP3S02 Seismic Test

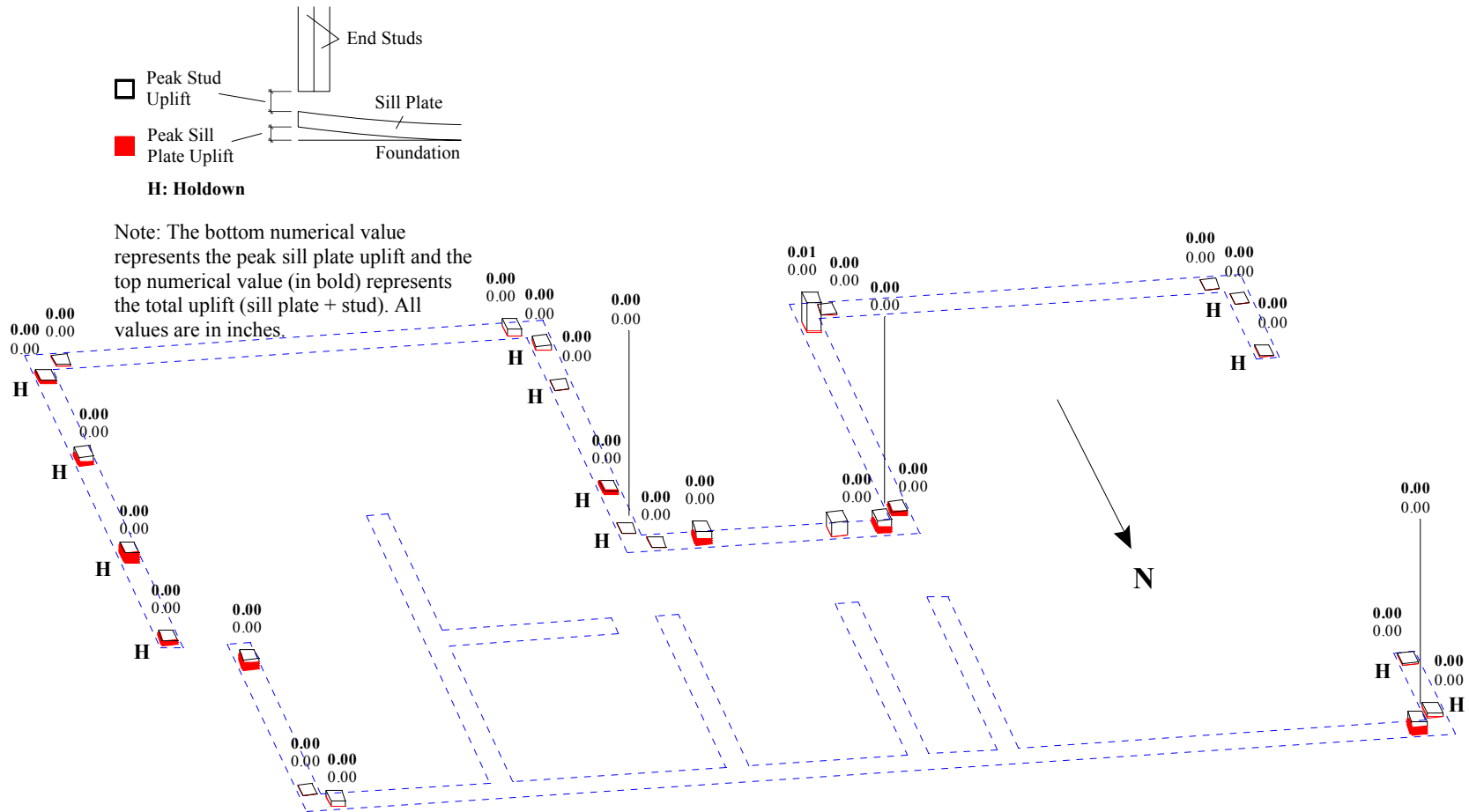


Figure R.35: Peak sill plate and stud uplift for Test NWP3S02

Appendix R

Phase 3, NWP3S03 Seismic Test

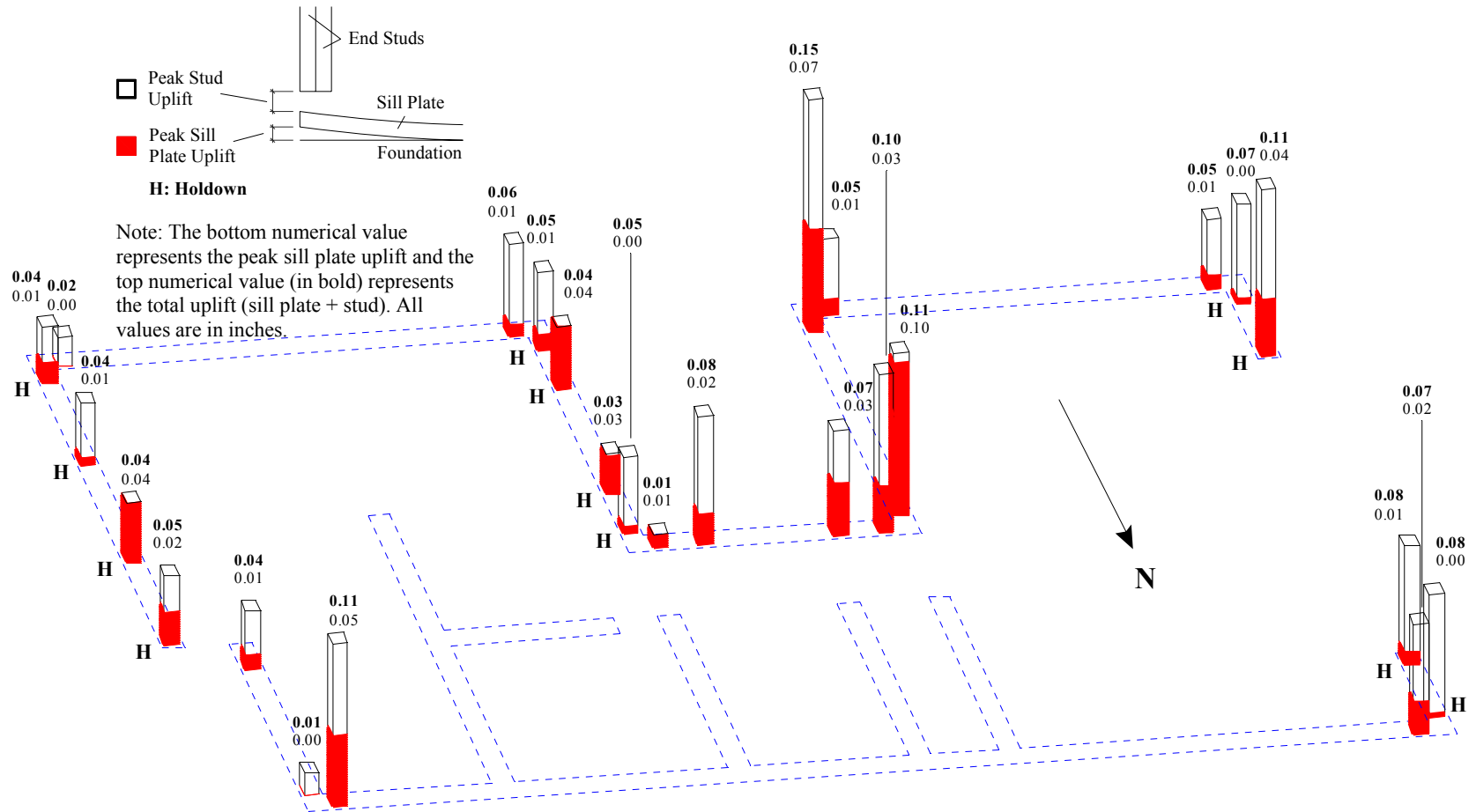


Figure R.36: Peak sill plate and stud uplift for Test NWP3S03

Appendix R

Phase 3, NWP3S04 Seismic Test

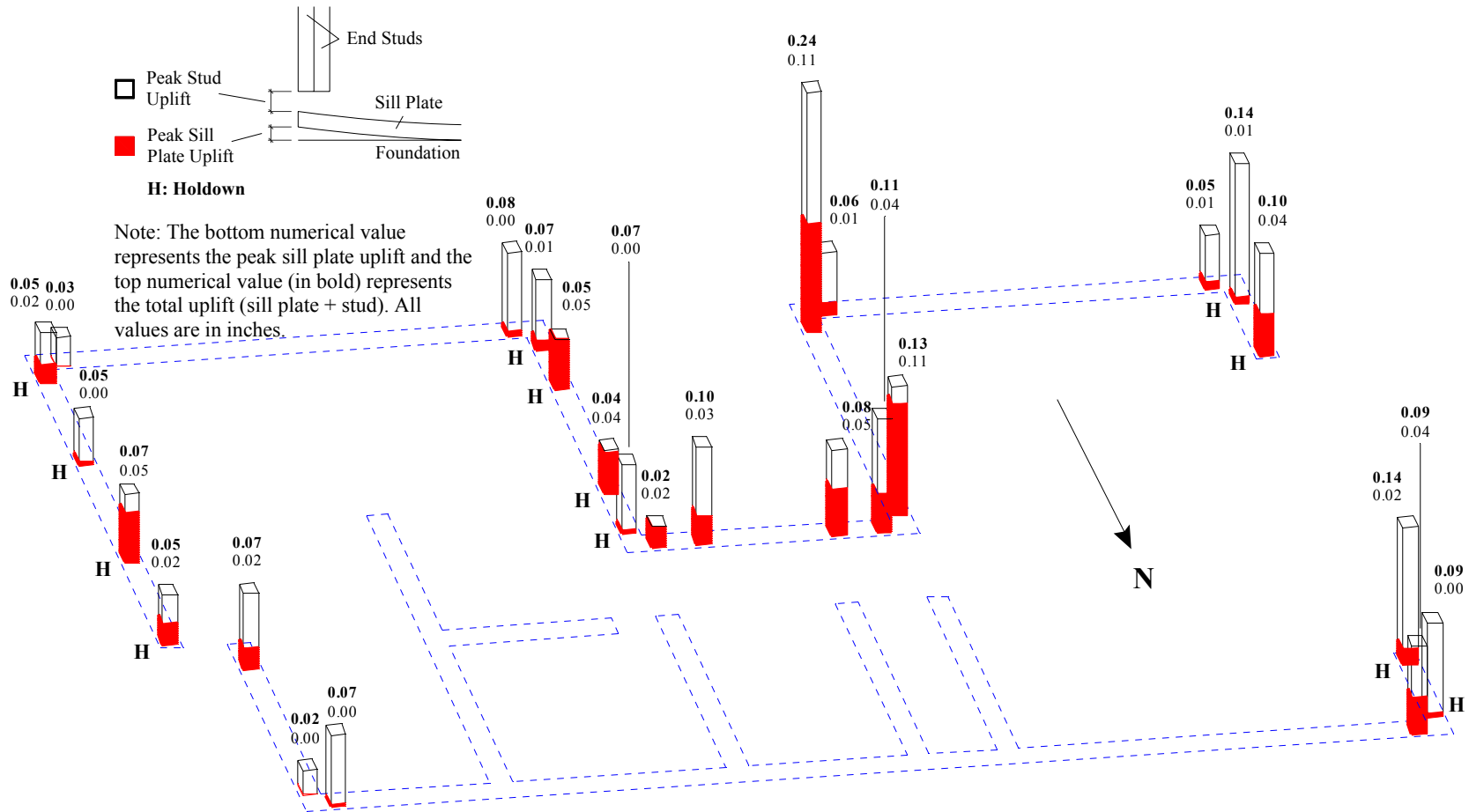


Figure R.37: Peak sill plate and stud uplift for Test NWP3S04

Appendix R

Phase 4, NWP4S01 Seismic Test

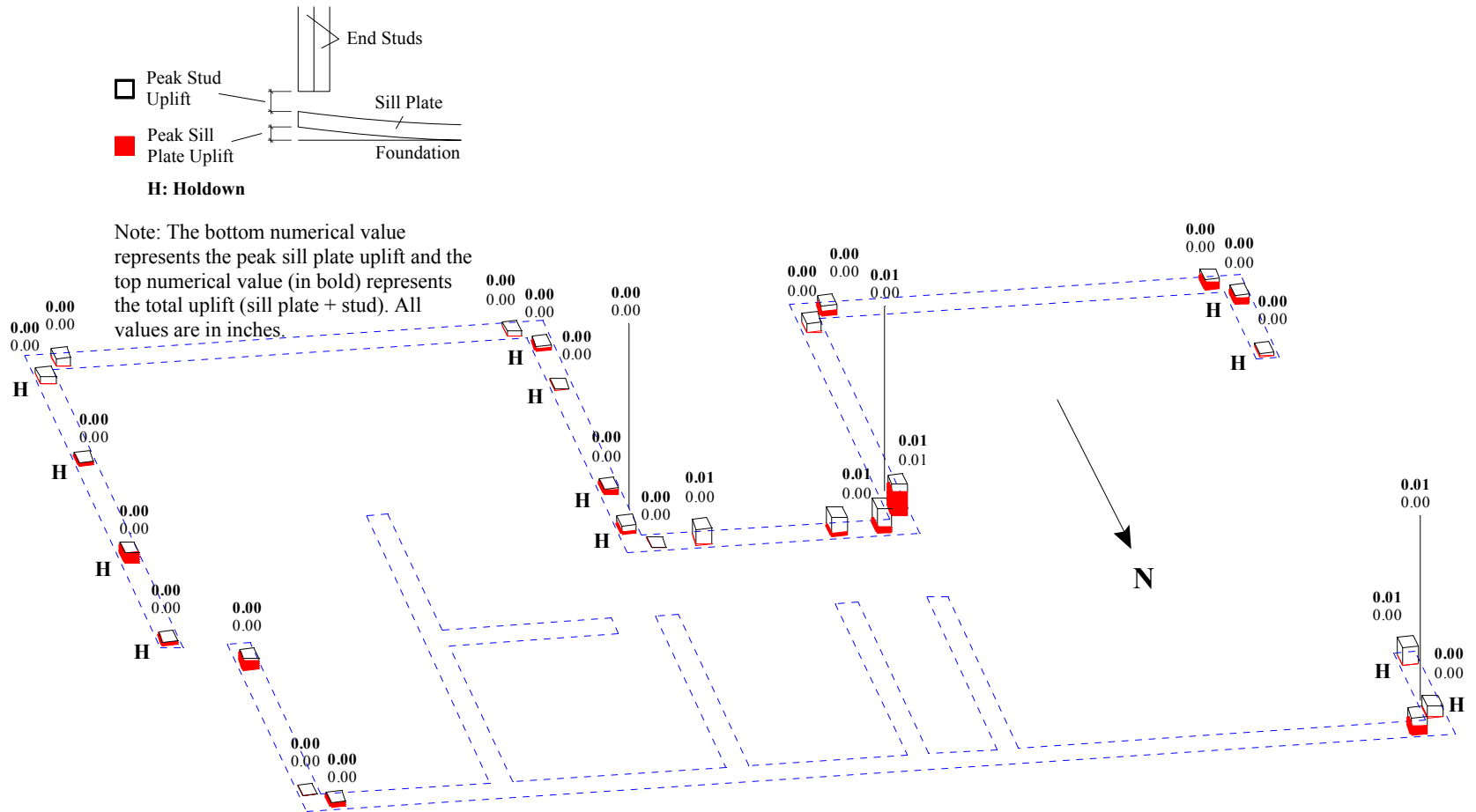


Figure R.38: Peak sill plate and stud uplift for Test NWP4S01

Appendix R

Phase 4, NWP4S02 Seismic Test

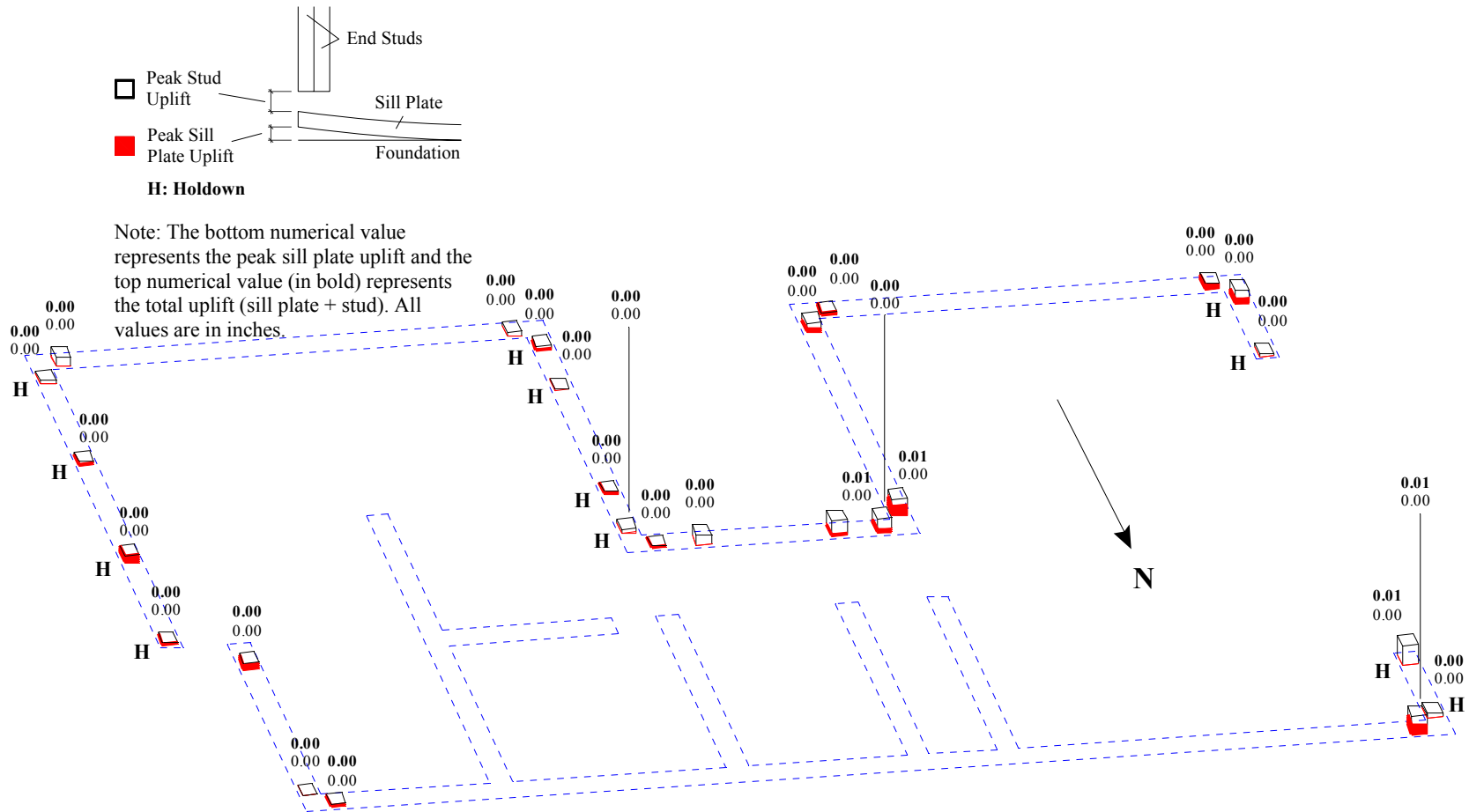


Figure R.39: Peak sill plate and stud uplift for Test NWP4S02

Appendix R

Phase 4, NWP4S03 Seismic Test

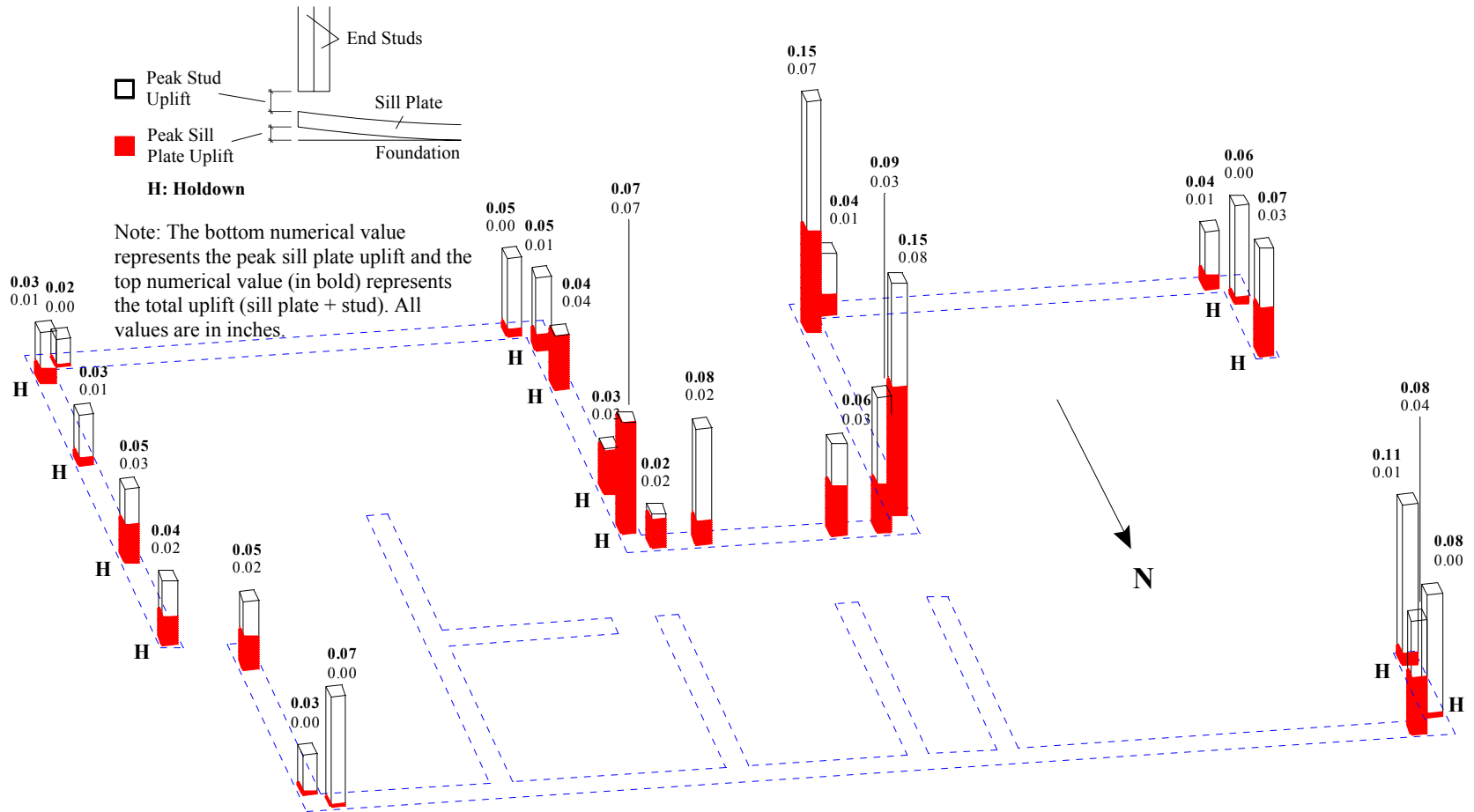


Figure R.40: Peak sill plate and stud uplift for Test NWP4S03

Appendix R

Phase 4, NWP4S04 Seismic Test

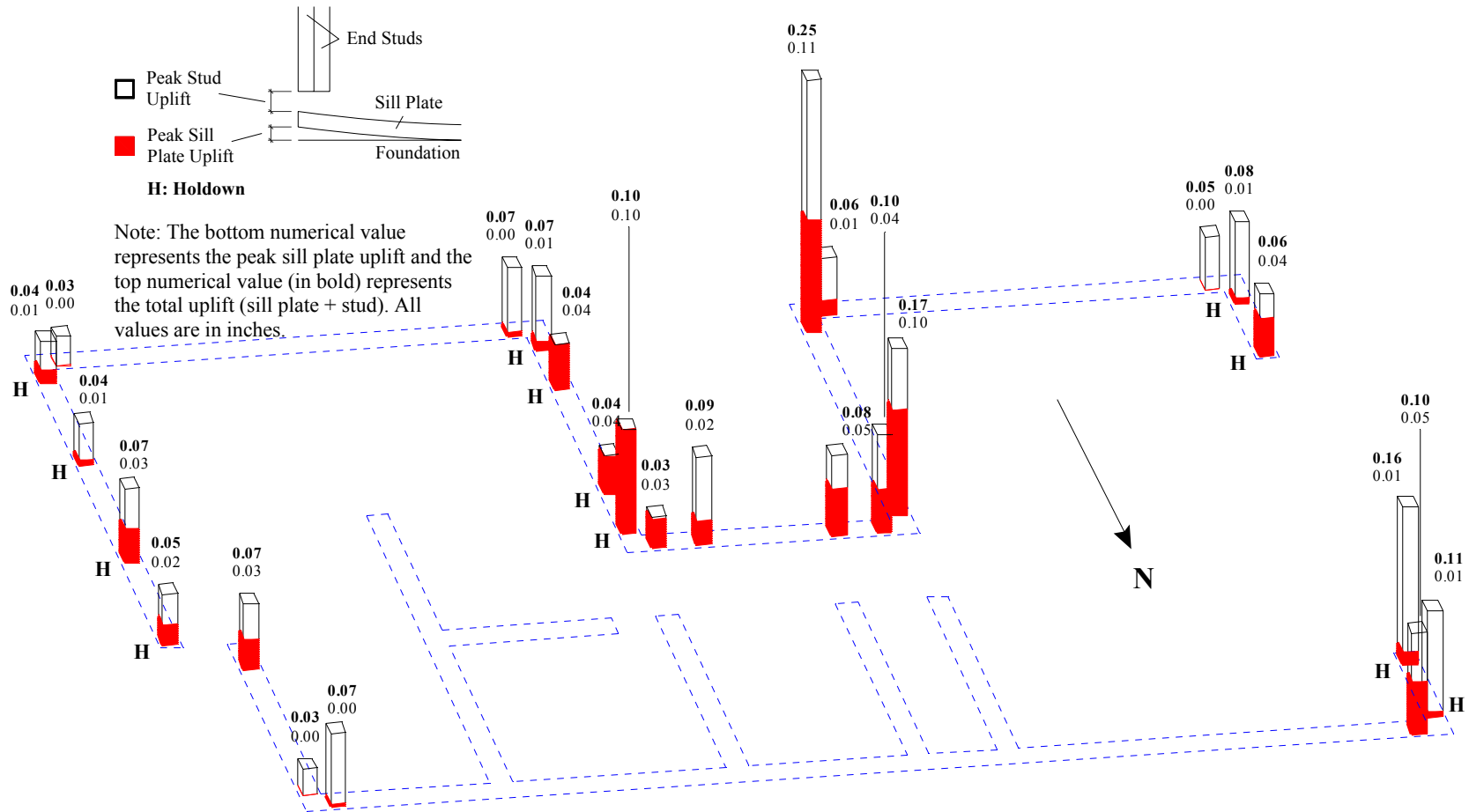


Figure R.41: Peak sill plate and stud uplift for Test NWP4S04

Appendix R

Phase 5, NWP5S01 Seismic Test

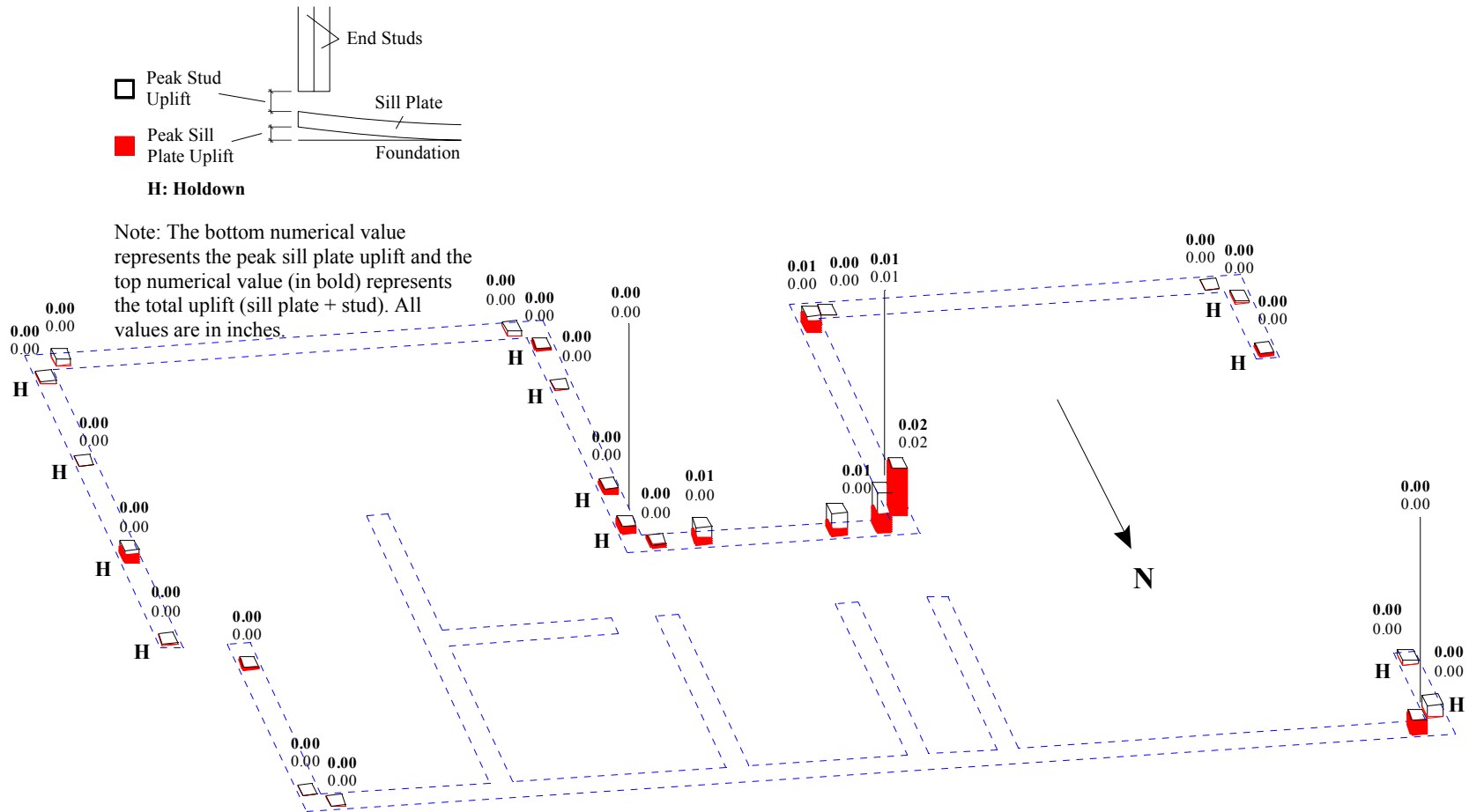


Figure R.42: Peak sill plate and stud uplift for Test NWP5S01

Appendix R

Phase 5, NWP5S02 Seismic Test

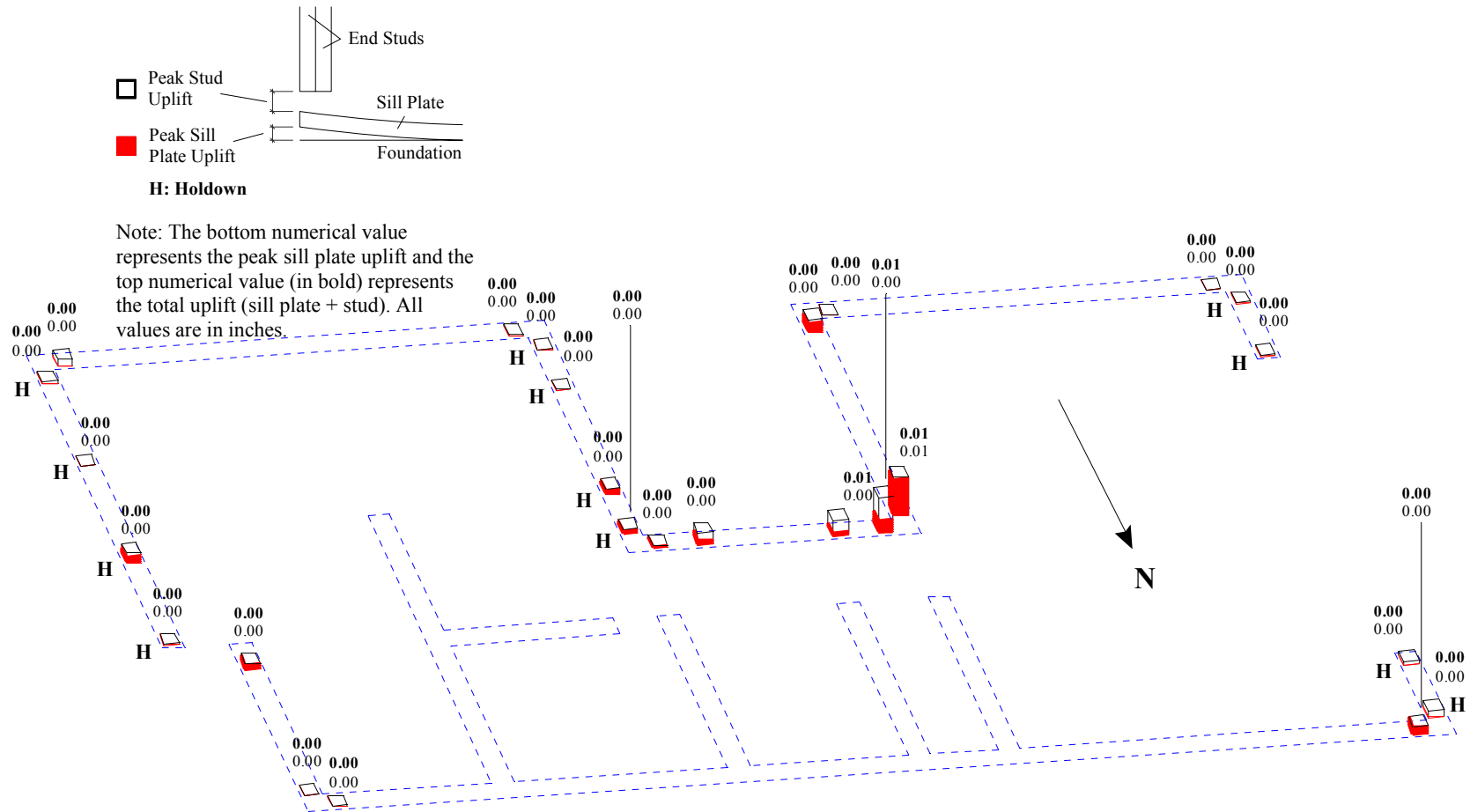


Figure R.43: Peak sill plate and stud uplift for Test NWP5S02

Appendix R

Phase 5, NWP5S03 Seismic Test

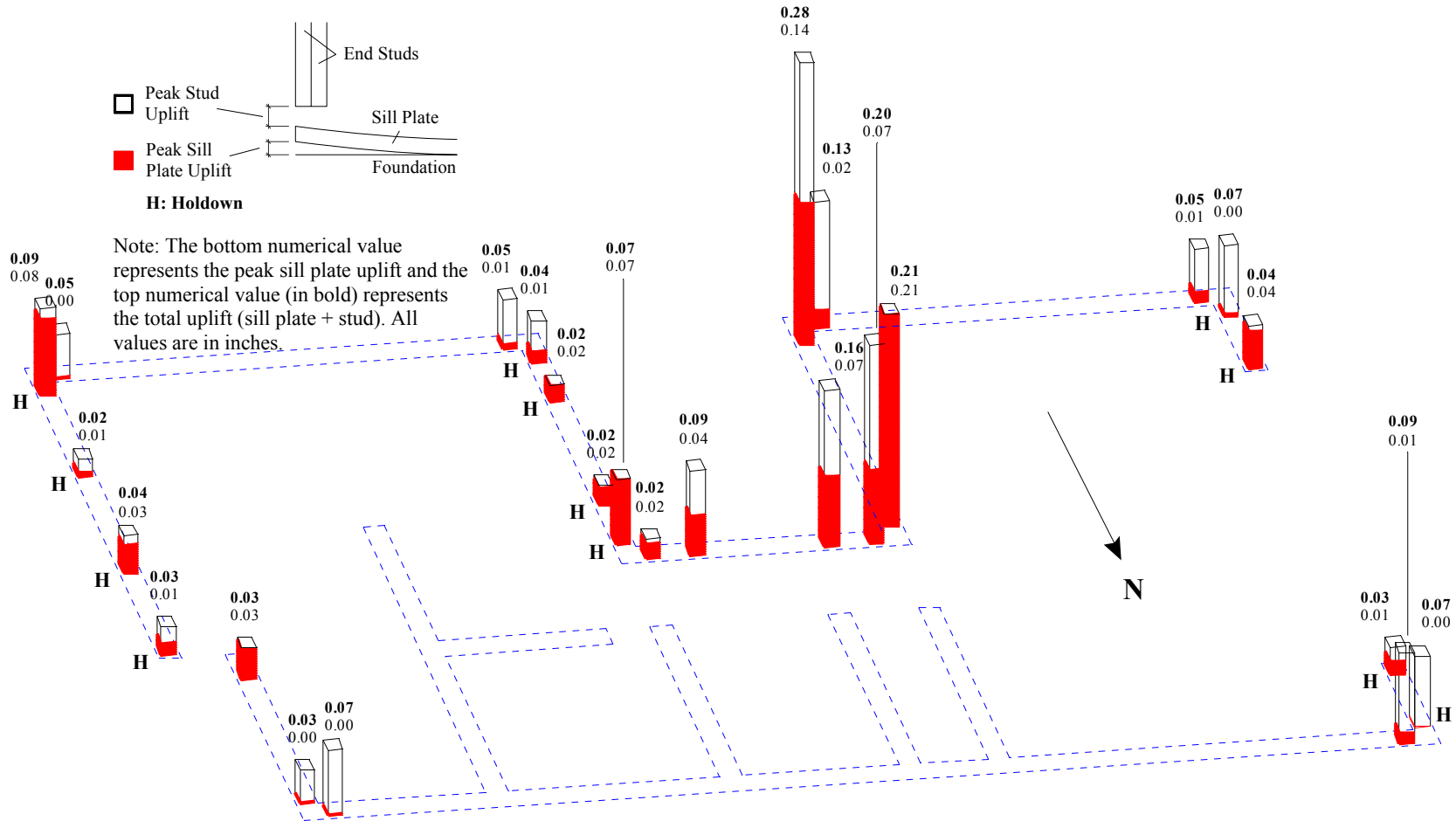


Figure R.44: Peak sill plate and stud uplift for Test NWP5S03

Appendix R

Phase 5, NWP5S04 Seismic Test

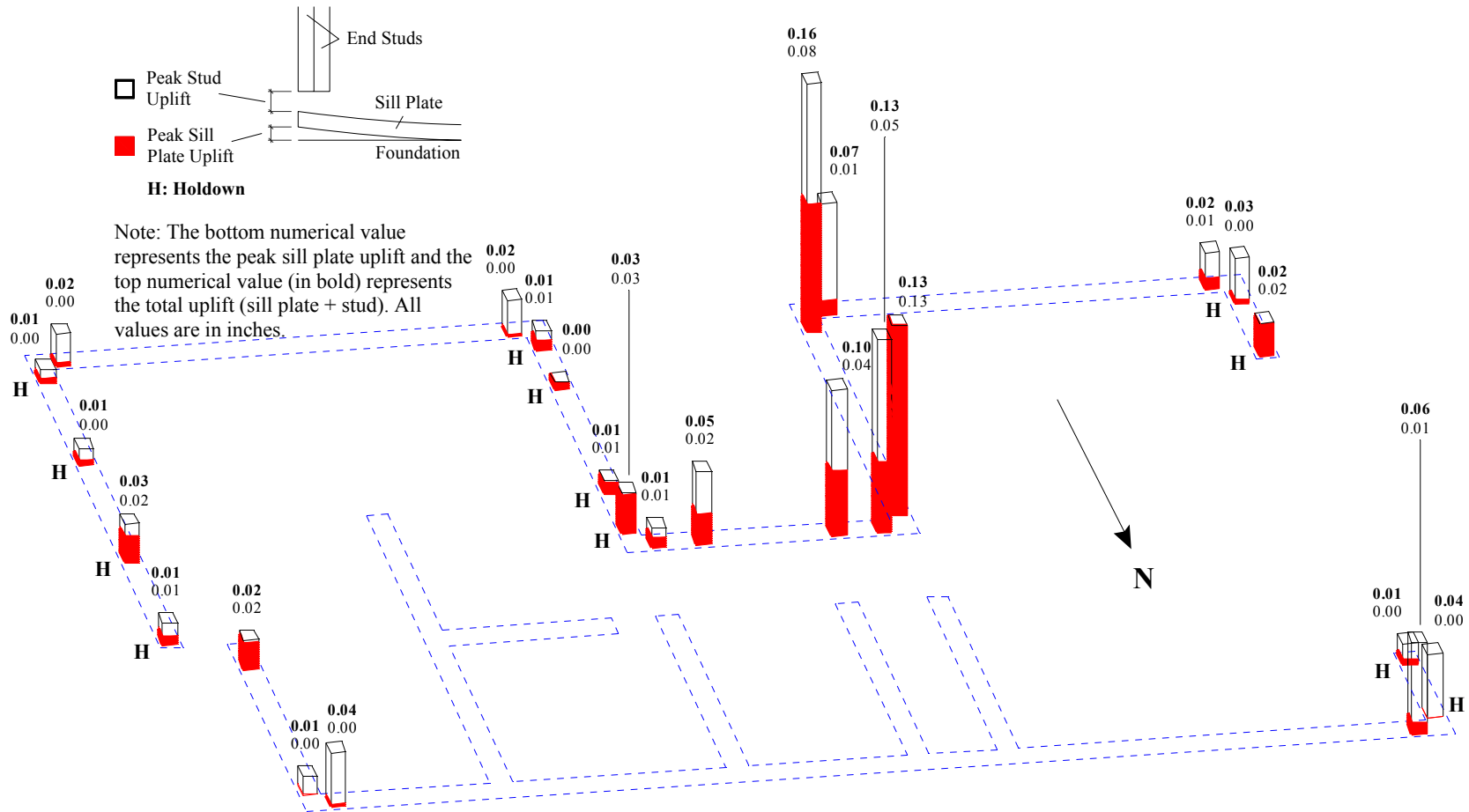


Figure R.45: Peak sill plate and stud uplift for Test NWP5S04

Appendix R

Phase 5, NWP5S05 Seismic Test

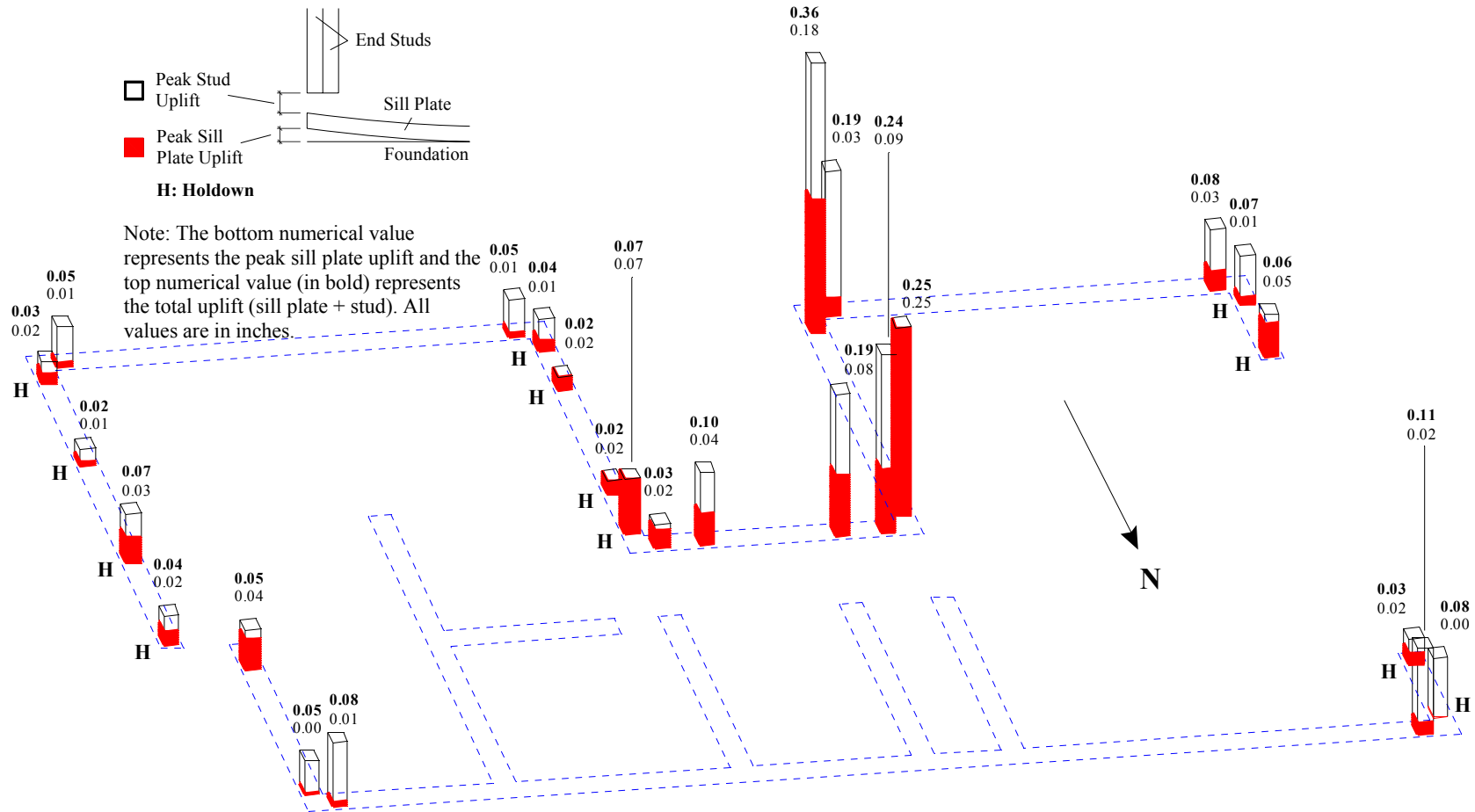


Figure R.46: Peak sill plate and stud uplift for Test NWP5S05

Appendix R

Phase 5, NWP5S06 Seismic Test

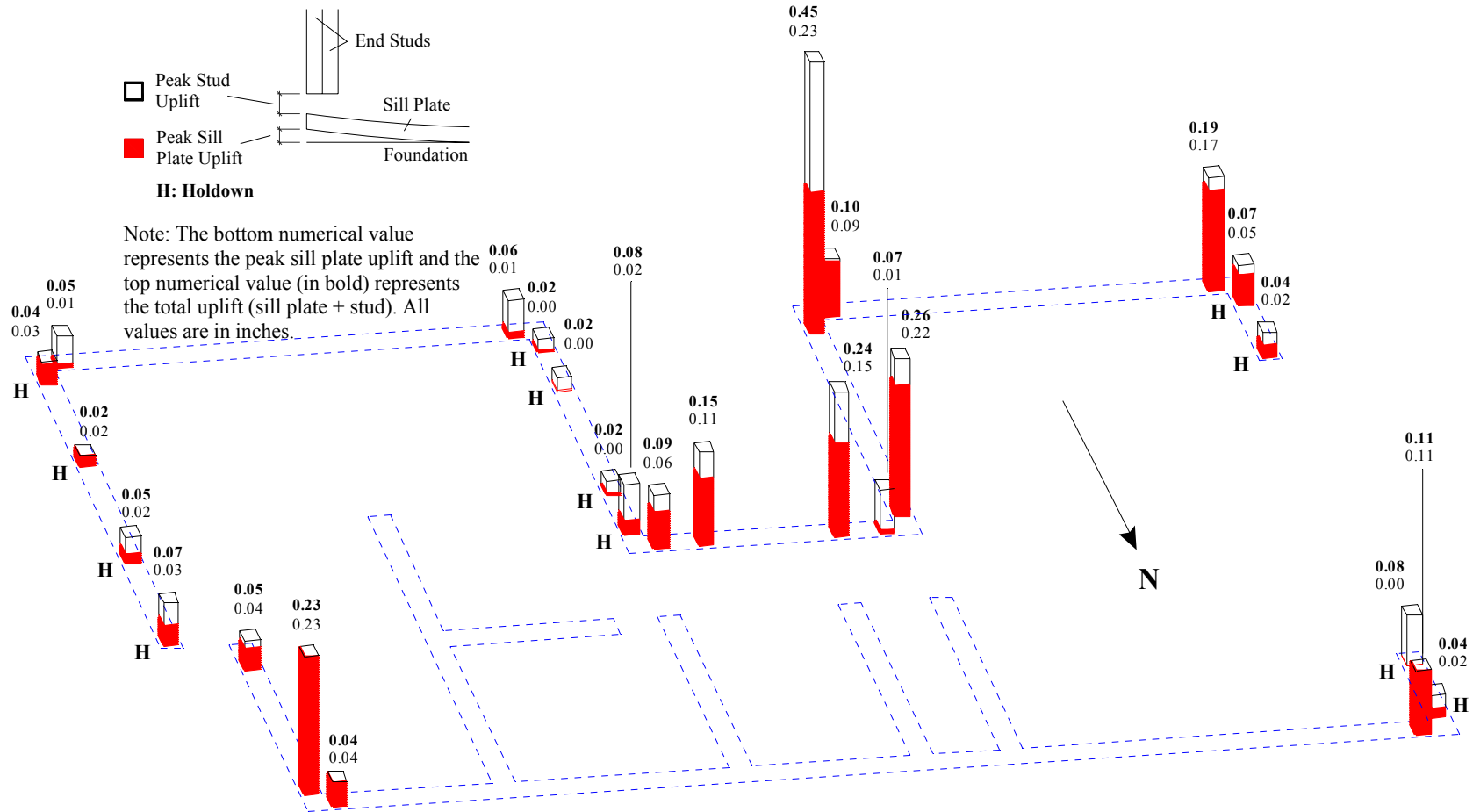


Figure R.47: Peak sill plate and stud uplift for Test NWP5S06

Appendix R

Phase 5, NWP5S07 Seismic Test

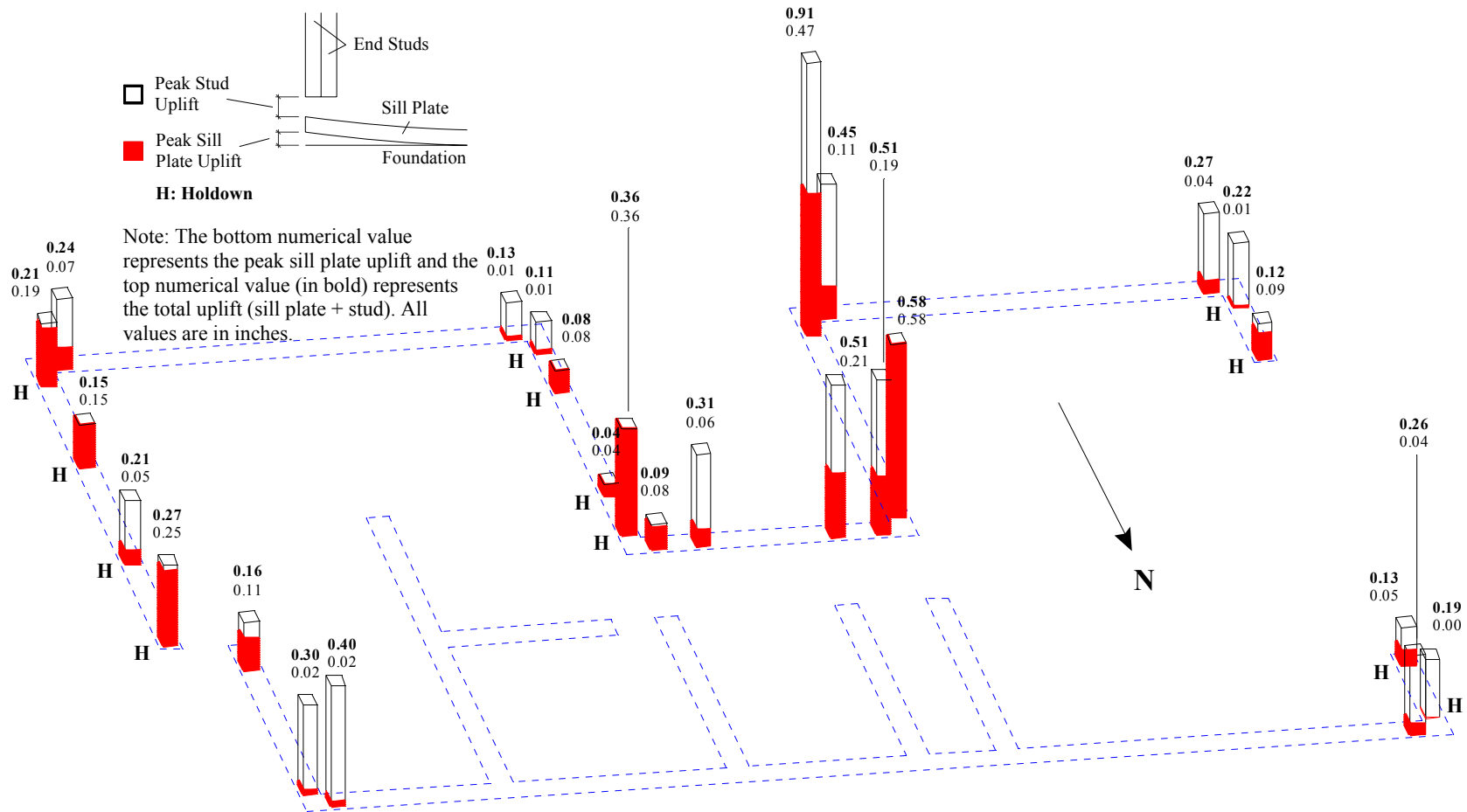


Figure R.48: Peak sill plate and stud uplift for Test NWP5S07

Appendix R

Phase 5, NWP5S08 Seismic Test

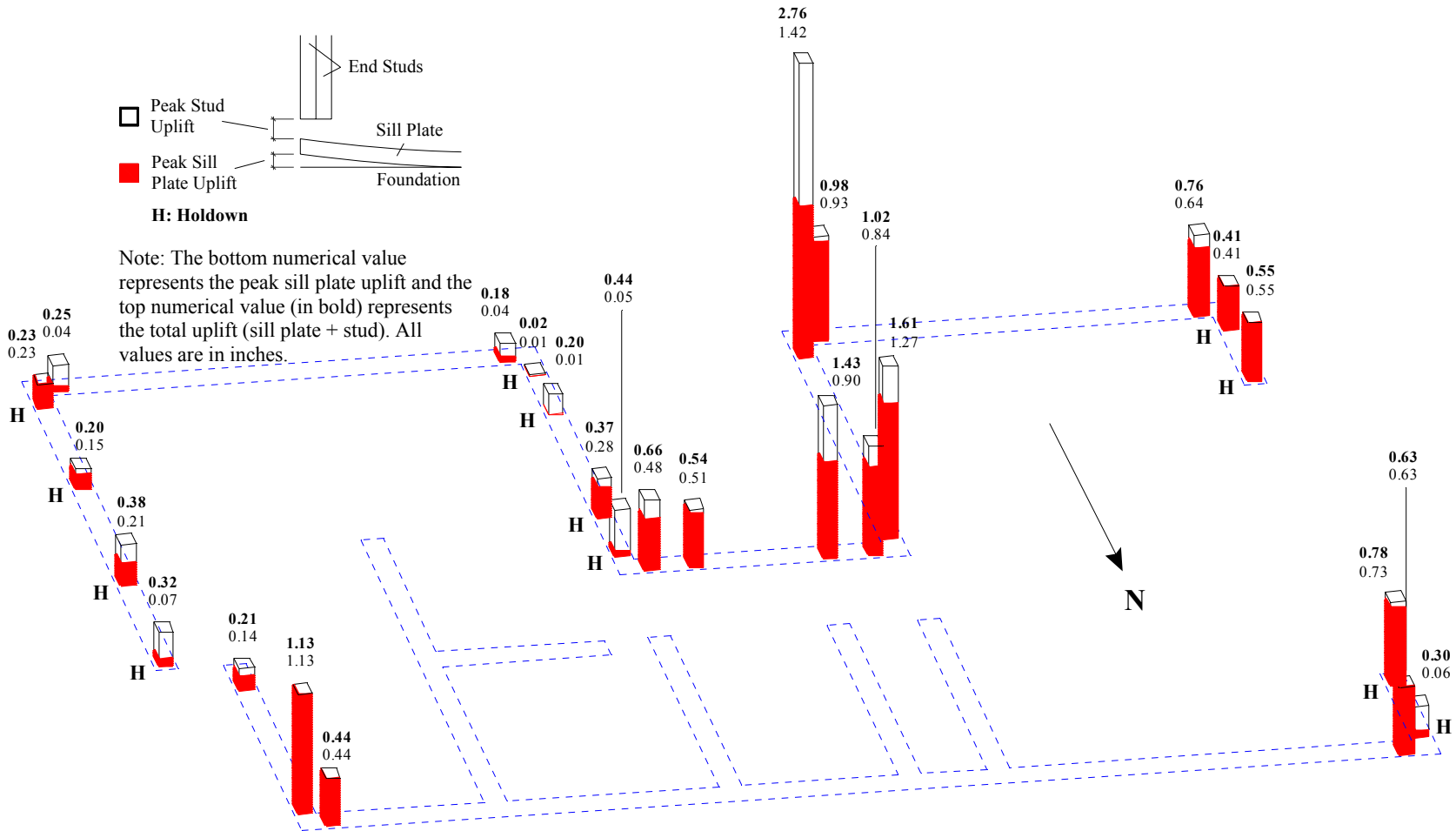


Figure R.49: Peak sill plate and stud uplift for Test NWP5S08

Appendix R

Phase 5, NWP5S09 Seismic Test

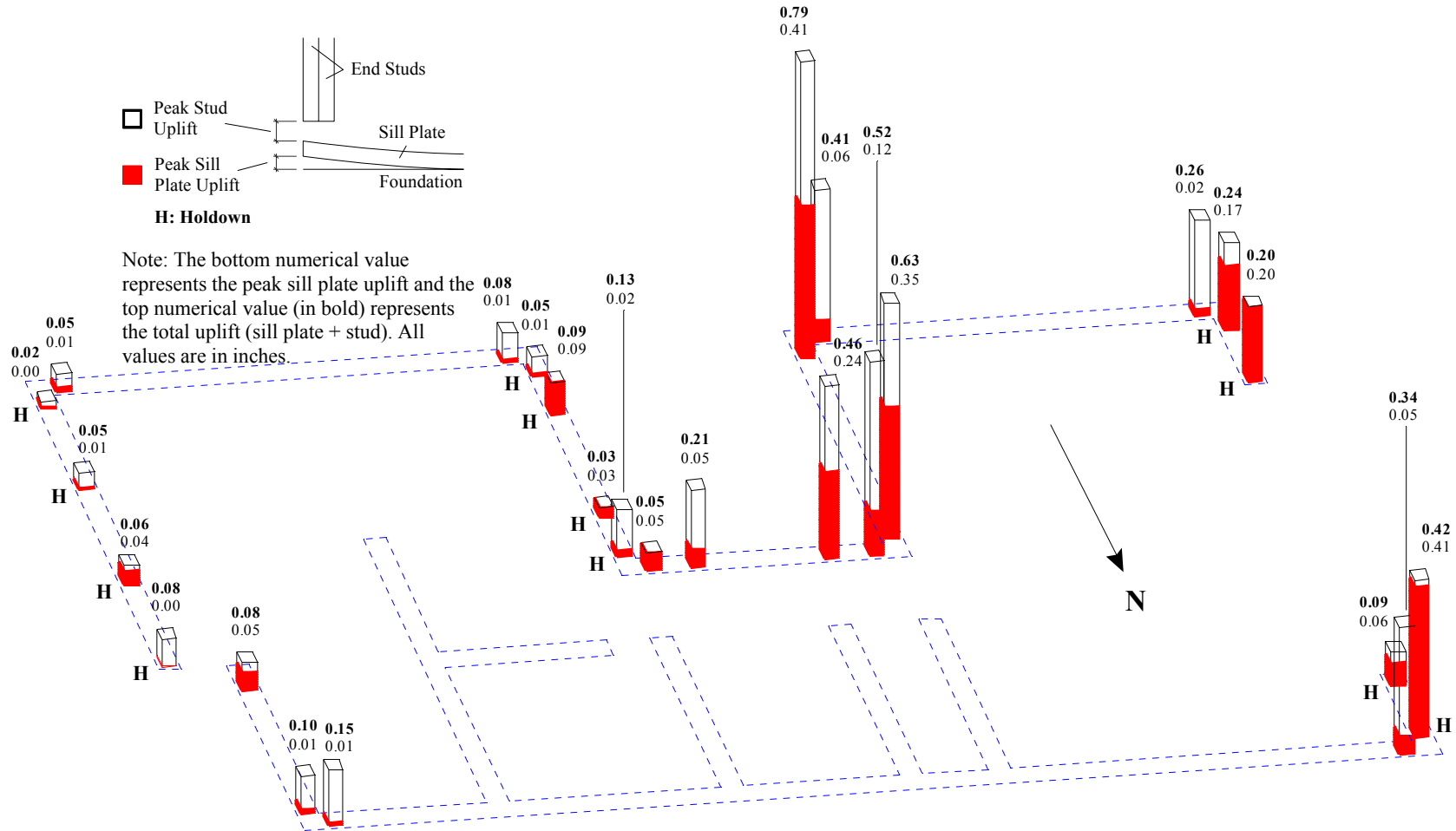


Figure R.50: Peak sill plate and stud uplift for Test NWP5S09

Appendix R

Phase 5, NWP5S11 Seismic Test

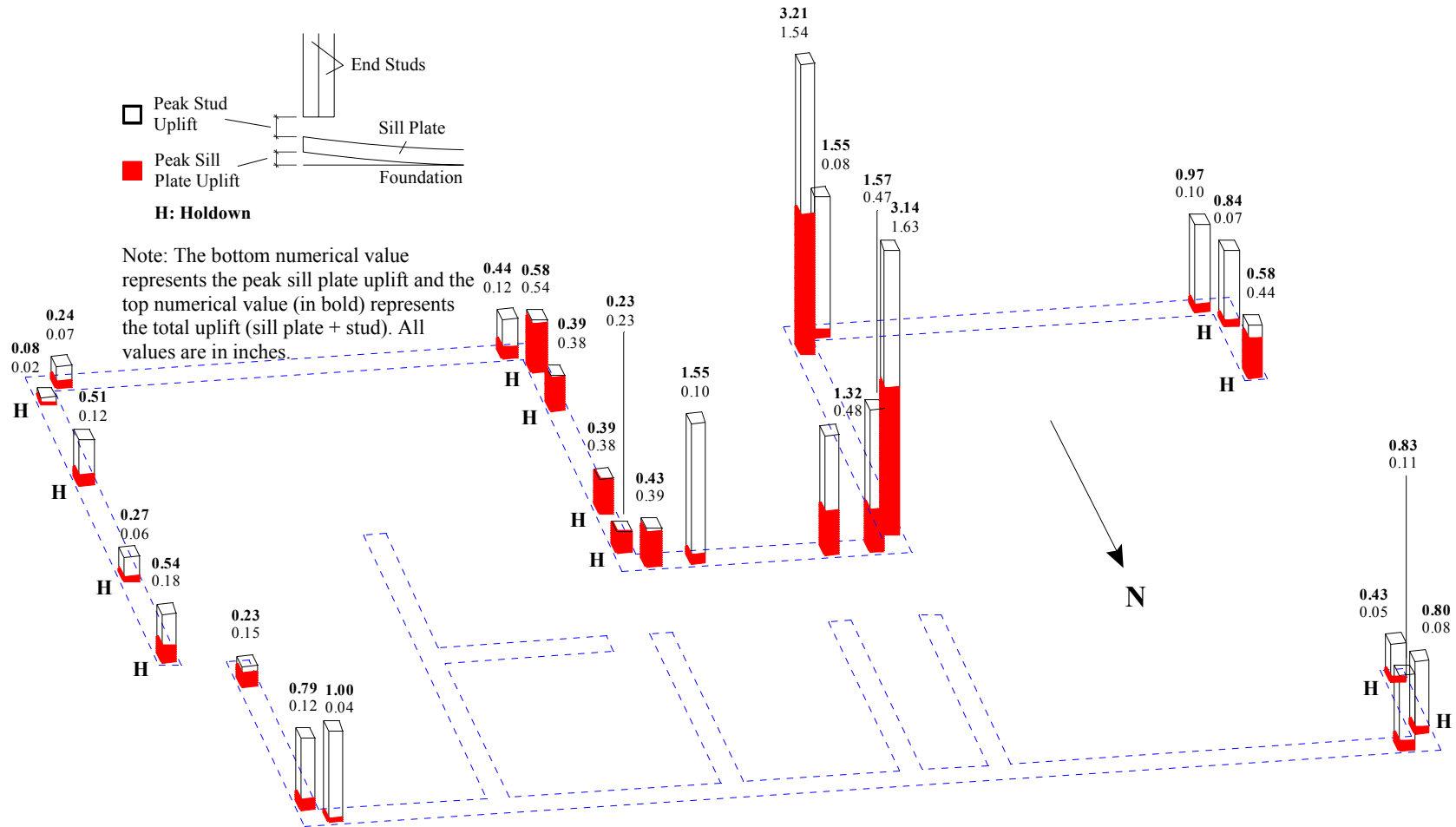


Figure R.51: Peak sill plate and stud uplift for Test NWP5S11

MCEER Technical Reports

MCEER publishes technical reports on a variety of subjects written by authors funded through MCEER. These reports are available from both MCEER Publications and the National Technical Information Service (NTIS). Requests for reports should be directed to MCEER Publications, MCEER, University at Buffalo, State University of New York, 133A Ketter Hall, Buffalo, New York 14260. Reports can also be requested through NTIS, P.O. Box 1425, Springfield, Virginia 22151. NTIS accession numbers are shown in parenthesis, if available.

- NCEER-87-0001 "First-Year Program in Research, Education and Technology Transfer," 3/5/87, (PB88-134275, A04, MF-A01).
- NCEER-87-0002 "Experimental Evaluation of Instantaneous Optimal Algorithms for Structural Control," by R.C. Lin, T.T. Soong and A.M. Reinhorn, 4/20/87, (PB88-134341, A04, MF-A01).
- NCEER-87-0003 "Experimentation Using the Earthquake Simulation Facilities at University at Buffalo," by A.M. Reinhorn and R.L. Ketter, to be published.
- NCEER-87-0004 "The System Characteristics and Performance of a Shaking Table," by J.S. Hwang, K.C. Chang and G.C. Lee, 6/1/87, (PB88-134259, A03, MF-A01). This report is available only through NTIS (see address given above).
- NCEER-87-0005 "A Finite Element Formulation for Nonlinear Viscoplastic Material Using a Q Model," by O. Gyebe and G. Dasgupta, 11/2/87, (PB88-213764, A08, MF-A01).
- NCEER-87-0006 "Symbolic Manipulation Program (SMP) - Algebraic Codes for Two and Three Dimensional Finite Element Formulations," by X. Lee and G. Dasgupta, 11/9/87, (PB88-218522, A05, MF-A01).
- NCEER-87-0007 "Instantaneous Optimal Control Laws for Tall Buildings Under Seismic Excitations," by J.N. Yang, A. Akbarpour and P. Ghaemmaghami, 6/10/87, (PB88-134333, A06, MF-A01). This report is only available through NTIS (see address given above).
- NCEER-87-0008 "IDARC: Inelastic Damage Analysis of Reinforced Concrete Frame - Shear-Wall Structures," by Y.J. Park, A.M. Reinhorn and S.K. Kunnath, 7/20/87, (PB88-134325, A09, MF-A01). This report is only available through NTIS (see address given above).
- NCEER-87-0009 "Liquefaction Potential for New York State: A Preliminary Report on Sites in Manhattan and Buffalo," by M. Budhu, V. Vijayakumar, R.F. Giese and L. Baumgras, 8/31/87, (PB88-163704, A03, MF-A01). This report is available only through NTIS (see address given above).
- NCEER-87-0010 "Vertical and Torsional Vibration of Foundations in Inhomogeneous Media," by A.S. Veletsos and K.W. Dotson, 6/1/87, (PB88-134291, A03, MF-A01). This report is only available through NTIS (see address given above).
- NCEER-87-0011 "Seismic Probabilistic Risk Assessment and Seismic Margins Studies for Nuclear Power Plants," by Howard H.M. Hwang, 6/15/87, (PB88-134267, A03, MF-A01). This report is only available through NTIS (see address given above).
- NCEER-87-0012 "Parametric Studies of Frequency Response of Secondary Systems Under Ground-Acceleration Excitations," by Y. Yong and Y.K. Lin, 6/10/87, (PB88-134309, A03, MF-A01). This report is only available through NTIS (see address given above).
- NCEER-87-0013 "Frequency Response of Secondary Systems Under Seismic Excitation," by J.A. HoLung, J. Cai and Y.K. Lin, 7/31/87, (PB88-134317, A05, MF-A01). This report is only available through NTIS (see address given above).
- NCEER-87-0014 "Modelling Earthquake Ground Motions in Seismically Active Regions Using Parametric Time Series Methods," by G.W. Ellis and A.S. Cakmak, 8/25/87, (PB88-134283, A08, MF-A01). This report is only available through NTIS (see address given above).
- NCEER-87-0015 "Detection and Assessment of Seismic Structural Damage," by E. DiPasquale and A.S. Cakmak, 8/25/87, (PB88-163712, A05, MF-A01). This report is only available through NTIS (see address given above).

- NCEER-87-0016 "Pipeline Experiment at Parkfield, California," by J. Isenberg and E. Richardson, 9/15/87, (PB88-163720, A03, MF-A01). This report is available only through NTIS (see address given above).
- NCEER-87-0017 "Digital Simulation of Seismic Ground Motion," by M. Shinozuka, G. Deodatis and T. Harada, 8/31/87, (PB88-155197, A04, MF-A01). This report is available only through NTIS (see address given above).
- NCEER-87-0018 "Practical Considerations for Structural Control: System Uncertainty, System Time Delay and Truncation of Small Control Forces," J.N. Yang and A. Akbarpour, 8/10/87, (PB88-163738, A08, MF-A01). This report is only available through NTIS (see address given above).
- NCEER-87-0019 "Modal Analysis of Nonclassically Damped Structural Systems Using Canonical Transformation," by J.N. Yang, S. Sarkani and F.X. Long, 9/27/87, (PB88-187851, A04, MF-A01).
- NCEER-87-0020 "A Nonstationary Solution in Random Vibration Theory," by J.R. Red-Horse and P.D. Spanos, 11/3/87, (PB88-163746, A03, MF-A01).
- NCEER-87-0021 "Horizontal Impedances for Radially Inhomogeneous Viscoelastic Soil Layers," by A.S. Veletsos and K.W. Dotson, 10/15/87, (PB88-150859, A04, MF-A01).
- NCEER-87-0022 "Seismic Damage Assessment of Reinforced Concrete Members," by Y.S. Chung, C. Meyer and M. Shinozuka, 10/9/87, (PB88-150867, A05, MF-A01). This report is available only through NTIS (see address given above).
- NCEER-87-0023 "Active Structural Control in Civil Engineering," by T.T. Soong, 11/11/87, (PB88-187778, A03, MF-A01).
- NCEER-87-0024 "Vertical and Torsional Impedances for Radially Inhomogeneous Viscoelastic Soil Layers," by K.W. Dotson and A.S. Veletsos, 12/87, (PB88-187786, A03, MF-A01).
- NCEER-87-0025 "Proceedings from the Symposium on Seismic Hazards, Ground Motions, Soil-Liquefaction and Engineering Practice in Eastern North America," October 20-22, 1987, edited by K.H. Jacob, 12/87, (PB88-188115, A23, MF-A01). This report is available only through NTIS (see address given above).
- NCEER-87-0026 "Report on the Whittier-Narrows, California, Earthquake of October 1, 1987," by J. Pantelic and A. Reinhorn, 11/87, (PB88-187752, A03, MF-A01). This report is available only through NTIS (see address given above).
- NCEER-87-0027 "Design of a Modular Program for Transient Nonlinear Analysis of Large 3-D Building Structures," by S. Srivastav and J.F. Abel, 12/30/87, (PB88-187950, A05, MF-A01). This report is only available through NTIS (see address given above).
- NCEER-87-0028 "Second-Year Program in Research, Education and Technology Transfer," 3/8/88, (PB88-219480, A04, MF-A01).
- NCEER-88-0001 "Workshop on Seismic Computer Analysis and Design of Buildings With Interactive Graphics," by W. McGuire, J.F. Abel and C.H. Conley, 1/18/88, (PB88-187760, A03, MF-A01). This report is only available through NTIS (see address given above).
- NCEER-88-0002 "Optimal Control of Nonlinear Flexible Structures," by J.N. Yang, F.X. Long and D. Wong, 1/22/88, (PB88-213772, A06, MF-A01).
- NCEER-88-0003 "Substructuring Techniques in the Time Domain for Primary-Secondary Structural Systems," by G.D. Manolis and G. Juhn, 2/10/88, (PB88-213780, A04, MF-A01).
- NCEER-88-0004 "Iterative Seismic Analysis of Primary-Secondary Systems," by A. Singhal, L.D. Lutes and P.D. Spanos, 2/23/88, (PB88-213798, A04, MF-A01).
- NCEER-88-0005 "Stochastic Finite Element Expansion for Random Media," by P.D. Spanos and R. Ghanem, 3/14/88, (PB88-213806, A03, MF-A01).

- NCEER-88-0006 "Combining Structural Optimization and Structural Control," by F.Y. Cheng and C.P. Pantelides, 1/10/88, (PB88-213814, A05, MF-A01).
- NCEER-88-0007 "Seismic Performance Assessment of Code-Designed Structures," by H.H-M. Hwang, J-W. Jaw and H-J. Shau, 3/20/88, (PB88-219423, A04, MF-A01). This report is only available through NTIS (see address given above).
- NCEER-88-0008 "Reliability Analysis of Code-Designed Structures Under Natural Hazards," by H.H-M. Hwang, H. Ushiba and M. Shinozuka, 2/29/88, (PB88-229471, A07, MF-A01). This report is only available through NTIS (see address given above).
- NCEER-88-0009 "Seismic Fragility Analysis of Shear Wall Structures," by J-W Jaw and H.H-M. Hwang, 4/30/88, (PB89-102867, A04, MF-A01).
- NCEER-88-0010 "Base Isolation of a Multi-Story Building Under a Harmonic Ground Motion - A Comparison of Performances of Various Systems," by F-G Fan, G. Ahmadi and I.G. Tadjbakhsh, 5/18/88, (PB89-122238, A06, MF-A01). This report is only available through NTIS (see address given above).
- NCEER-88-0011 "Seismic Floor Response Spectra for a Combined System by Green's Functions," by F.M. Lavelle, L.A. Bergman and P.D. Spanos, 5/1/88, (PB89-102875, A03, MF-A01).
- NCEER-88-0012 "A New Solution Technique for Randomly Excited Hysteretic Structures," by G.Q. Cai and Y.K. Lin, 5/16/88, (PB89-102883, A03, MF-A01).
- NCEER-88-0013 "A Study of Radiation Damping and Soil-Structure Interaction Effects in the Centrifuge," by K. Weissman, supervised by J.H. Prevost, 5/24/88, (PB89-144703, A06, MF-A01).
- NCEER-88-0014 "Parameter Identification and Implementation of a Kinematic Plasticity Model for Frictional Soils," by J.H. Prevost and D.V. Griffiths, to be published.
- NCEER-88-0015 "Two- and Three- Dimensional Dynamic Finite Element Analyses of the Long Valley Dam," by D.V. Griffiths and J.H. Prevost, 6/17/88, (PB89-144711, A04, MF-A01).
- NCEER-88-0016 "Damage Assessment of Reinforced Concrete Structures in Eastern United States," by A.M. Reinhorn, M.J. Seidel, S.K. Kunnath and Y.J. Park, 6/15/88, (PB89-122220, A04, MF-A01). This report is only available through NTIS (see address given above).
- NCEER-88-0017 "Dynamic Compliance of Vertically Loaded Strip Foundations in Multilayered Viscoelastic Soils," by S. Ahmad and A.S.M. Israil, 6/17/88, (PB89-102891, A04, MF-A01).
- NCEER-88-0018 "An Experimental Study of Seismic Structural Response With Added Viscoelastic Dampers," by R.C. Lin, Z. Liang, T.T. Soong and R.H. Zhang, 6/30/88, (PB89-122212, A05, MF-A01). This report is available only through NTIS (see address given above).
- NCEER-88-0019 "Experimental Investigation of Primary - Secondary System Interaction," by G.D. Manolis, G. Juhn and A.M. Reinhorn, 5/27/88, (PB89-122204, A04, MF-A01).
- NCEER-88-0020 "A Response Spectrum Approach For Analysis of Nonclassically Damped Structures," by J.N. Yang, S. Sarkani and F.X. Long, 4/22/88, (PB89-102909, A04, MF-A01).
- NCEER-88-0021 "Seismic Interaction of Structures and Soils: Stochastic Approach," by A.S. Veletsos and A.M. Prasad, 7/21/88, (PB89-122196, A04, MF-A01). This report is only available through NTIS (see address given above).
- NCEER-88-0022 "Identification of the Serviceability Limit State and Detection of Seismic Structural Damage," by E. DiPasquale and A.S. Cakmak, 6/15/88, (PB89-122188, A05, MF-A01). This report is available only through NTIS (see address given above).
- NCEER-88-0023 "Multi-Hazard Risk Analysis: Case of a Simple Offshore Structure," by B.K. Bhartia and E.H. Vanmarcke, 7/21/88, (PB89-145213, A05, MF-A01).

- NCEER-88-0024 "Automated Seismic Design of Reinforced Concrete Buildings," by Y.S. Chung, C. Meyer and M. Shinozuka, 7/5/88, (PB89-122170, A06, MF-A01). This report is available only through NTIS (see address given above).
- NCEER-88-0025 "Experimental Study of Active Control of MDOF Structures Under Seismic Excitations," by L.L. Chung, R.C. Lin, T.T. Soong and A.M. Reinhorn, 7/10/88, (PB89-122600, A04, MF-A01).
- NCEER-88-0026 "Earthquake Simulation Tests of a Low-Rise Metal Structure," by J.S. Hwang, K.C. Chang, G.C. Lee and R.L. Ketter, 8/1/88, (PB89-102917, A04, MF-A01).
- NCEER-88-0027 "Systems Study of Urban Response and Reconstruction Due to Catastrophic Earthquakes," by F. Kozin and H.K. Zhou, 9/22/88, (PB90-162348, A04, MF-A01).
- NCEER-88-0028 "Seismic Fragility Analysis of Plane Frame Structures," by H.H-M. Hwang and Y.K. Low, 7/31/88, (PB89-131445, A06, MF-A01).
- NCEER-88-0029 "Response Analysis of Stochastic Structures," by A. Kardara, C. Bucher and M. Shinozuka, 9/22/88, (PB89-174429, A04, MF-A01).
- NCEER-88-0030 "Nonnormal Accelerations Due to Yielding in a Primary Structure," by D.C.K. Chen and L.D. Lutes, 9/19/88, (PB89-131437, A04, MF-A01).
- NCEER-88-0031 "Design Approaches for Soil-Structure Interaction," by A.S. Veletsos, A.M. Prasad and Y. Tang, 12/30/88, (PB89-174437, A03, MF-A01). This report is available only through NTIS (see address given above).
- NCEER-88-0032 "A Re-evaluation of Design Spectra for Seismic Damage Control," by C.J. Turkstra and A.G. Tallin, 11/7/88, (PB89-145221, A05, MF-A01).
- NCEER-88-0033 "The Behavior and Design of Noncontact Lap Splices Subjected to Repeated Inelastic Tensile Loading," by V.E. Sagan, P. Gergely and R.N. White, 12/8/88, (PB89-163737, A08, MF-A01).
- NCEER-88-0034 "Seismic Response of Pile Foundations," by S.M. Mamoon, P.K. Banerjee and S. Ahmad, 11/1/88, (PB89-145239, A04, MF-A01).
- NCEER-88-0035 "Modeling of R/C Building Structures With Flexible Floor Diaphragms (IDARC2)," by A.M. Reinhorn, S.K. Kunnath and N. Panahshahi, 9/7/88, (PB89-207153, A07, MF-A01).
- NCEER-88-0036 "Solution of the Dam-Reservoir Interaction Problem Using a Combination of FEM, BEM with Particular Integrals, Modal Analysis, and Substructuring," by C-S. Tsai, G.C. Lee and R.L. Ketter, 12/31/88, (PB89-207146, A04, MF-A01).
- NCEER-88-0037 "Optimal Placement of Actuators for Structural Control," by F.Y. Cheng and C.P. Pantelides, 8/15/88, (PB89-162846, A05, MF-A01).
- NCEER-88-0038 "Teflon Bearings in Aseismic Base Isolation: Experimental Studies and Mathematical Modeling," by A. Mokha, M.C. Constantinou and A.M. Reinhorn, 12/5/88, (PB89-218457, A10, MF-A01). This report is available only through NTIS (see address given above).
- NCEER-88-0039 "Seismic Behavior of Flat Slab High-Rise Buildings in the New York City Area," by P. Weidlinger and M. Ettouney, 10/15/88, (PB90-145681, A04, MF-A01).
- NCEER-88-0040 "Evaluation of the Earthquake Resistance of Existing Buildings in New York City," by P. Weidlinger and M. Ettouney, 10/15/88, to be published.
- NCEER-88-0041 "Small-Scale Modeling Techniques for Reinforced Concrete Structures Subjected to Seismic Loads," by W. Kim, A. El-Attar and R.N. White, 11/22/88, (PB89-189625, A05, MF-A01).
- NCEER-88-0042 "Modeling Strong Ground Motion from Multiple Event Earthquakes," by G.W. Ellis and A.S. Cakmak, 10/15/88, (PB89-174445, A03, MF-A01).

- NCEER-88-0043 "Nonstationary Models of Seismic Ground Acceleration," by M. Grigoriu, S.E. Ruiz and E. Rosenblueth, 7/15/88, (PB89-189617, A04, MF-A01).
- NCEER-88-0044 "SARCF User's Guide: Seismic Analysis of Reinforced Concrete Frames," by Y.S. Chung, C. Meyer and M. Shinozuka, 11/9/88, (PB89-174452, A08, MF-A01).
- NCEER-88-0045 "First Expert Panel Meeting on Disaster Research and Planning," edited by J. Pantelic and J. Stoyke, 9/15/88, (PB89-174460, A05, MF-A01).
- NCEER-88-0046 "Preliminary Studies of the Effect of Degrading Infill Walls on the Nonlinear Seismic Response of Steel Frames," by C.Z. Chrysostomou, P. Gergely and J.F. Abel, 12/19/88, (PB89-208383, A05, MF-A01).
- NCEER-88-0047 "Reinforced Concrete Frame Component Testing Facility - Design, Construction, Instrumentation and Operation," by S.P. Pessiki, C. Conley, T. Bond, P. Gergely and R.N. White, 12/16/88, (PB89-174478, A04, MF-A01).
- NCEER-89-0001 "Effects of Protective Cushion and Soil Compliancy on the Response of Equipment Within a Seismically Excited Building," by J.A. HoLung, 2/16/89, (PB89-207179, A04, MF-A01).
- NCEER-89-0002 "Statistical Evaluation of Response Modification Factors for Reinforced Concrete Structures," by H.H-M. Hwang and J-W. Jaw, 2/17/89, (PB89-207187, A05, MF-A01).
- NCEER-89-0003 "Hysteretic Columns Under Random Excitation," by G-Q. Cai and Y.K. Lin, 1/9/89, (PB89-196513, A03, MF-A01).
- NCEER-89-0004 "Experimental Study of 'Elephant Foot Bulge' Instability of Thin-Walled Metal Tanks," by Z-H. Jia and R.L. Ketter, 2/22/89, (PB89-207195, A03, MF-A01).
- NCEER-89-0005 "Experiment on Performance of Buried Pipelines Across San Andreas Fault," by J. Isenberg, E. Richardson and T.D. O'Rourke, 3/10/89, (PB89-218440, A04, MF-A01). This report is available only through NTIS (see address given above).
- NCEER-89-0006 "A Knowledge-Based Approach to Structural Design of Earthquake-Resistant Buildings," by M. Subramani, P. Gergely, C.H. Conley, J.F. Abel and A.H. Zaghaw, 1/15/89, (PB89-218465, A06, MF-A01).
- NCEER-89-0007 "Liquefaction Hazards and Their Effects on Buried Pipelines," by T.D. O'Rourke and P.A. Lane, 2/1/89, (PB89-218481, A09, MF-A01).
- NCEER-89-0008 "Fundamentals of System Identification in Structural Dynamics," by H. Imai, C-B. Yun, O. Maruyama and M. Shinozuka, 1/26/89, (PB89-207211, A04, MF-A01).
- NCEER-89-0009 "Effects of the 1985 Michoacan Earthquake on Water Systems and Other Buried Lifelines in Mexico," by A.G. Ayala and M.J. O'Rourke, 3/8/89, (PB89-207229, A06, MF-A01).
- NCEER-89-R010 "NCEER Bibliography of Earthquake Education Materials," by K.E.K. Ross, Second Revision, 9/1/89, (PB90-125352, A05, MF-A01). This report is replaced by NCEER-92-0018.
- NCEER-89-0011 "Inelastic Three-Dimensional Response Analysis of Reinforced Concrete Building Structures (IDARC-3D), Part I - Modeling," by S.K. Kunnath and A.M. Reinhorn, 4/17/89, (PB90-114612, A07, MF-A01). This report is available only through NTIS (see address given above).
- NCEER-89-0012 "Recommended Modifications to ATC-14," by C.D. Poland and J.O. Malley, 4/12/89, (PB90-108648, A15, MF-A01).
- NCEER-89-0013 "Repair and Strengthening of Beam-to-Column Connections Subjected to Earthquake Loading," by M. Corazao and A.J. Durrani, 2/28/89, (PB90-109885, A06, MF-A01).
- NCEER-89-0014 "Program EXKAL2 for Identification of Structural Dynamic Systems," by O. Maruyama, C-B. Yun, M. Hoshiya and M. Shinozuka, 5/19/89, (PB90-109877, A09, MF-A01).

- NCEER-89-0015 "Response of Frames With Bolted Semi-Rigid Connections, Part I - Experimental Study and Analytical Predictions," by P.J. DiCorso, A.M. Reinhorn, J.R. Dickerson, J.B. Radzinski and W.L. Harper, 6/1/89, to be published.
- NCEER-89-0016 "ARMA Monte Carlo Simulation in Probabilistic Structural Analysis," by P.D. Spanos and M.P. Mignolet, 7/10/89, (PB90-109893, A03, MF-A01).
- NCEER-89-P017 "Preliminary Proceedings from the Conference on Disaster Preparedness - The Place of Earthquake Education in Our Schools," Edited by K.E.K. Ross, 6/23/89, (PB90-108606, A03, MF-A01).
- NCEER-89-0017 "Proceedings from the Conference on Disaster Preparedness - The Place of Earthquake Education in Our Schools," Edited by K.E.K. Ross, 12/31/89, (PB90-207895, A012, MF-A02). This report is available only through NTIS (see address given above).
- NCEER-89-0018 "Multidimensional Models of Hysteretic Material Behavior for Vibration Analysis of Shape Memory Energy Absorbing Devices, by E.J. Graesser and F.A. Cozzarelli, 6/7/89, (PB90-164146, A04, MF-A01).
- NCEER-89-0019 "Nonlinear Dynamic Analysis of Three-Dimensional Base Isolated Structures (3D-BASIS)," by S. Nagarajaiah, A.M. Reinhorn and M.C. Constantinou, 8/3/89, (PB90-161936, A06, MF-A01). This report has been replaced by NCEER-93-0011.
- NCEER-89-0020 "Structural Control Considering Time-Rate of Control Forces and Control Rate Constraints," by F.Y. Cheng and C.P. Pantelides, 8/3/89, (PB90-120445, A04, MF-A01).
- NCEER-89-0021 "Subsurface Conditions of Memphis and Shelby County," by K.W. Ng, T-S. Chang and H-H.M. Hwang, 7/26/89, (PB90-120437, A03, MF-A01).
- NCEER-89-0022 "Seismic Wave Propagation Effects on Straight Jointed Buried Pipelines," by K. Elhadi and M.J. O'Rourke, 8/24/89, (PB90-162322, A10, MF-A02).
- NCEER-89-0023 "Workshop on Serviceability Analysis of Water Delivery Systems," edited by M. Grigoriu, 3/6/89, (PB90-127424, A03, MF-A01).
- NCEER-89-0024 "Shaking Table Study of a 1/5 Scale Steel Frame Composed of Tapered Members," by K.C. Chang, J.S. Hwang and G.C. Lee, 9/18/89, (PB90-160169, A04, MF-A01).
- NCEER-89-0025 "DYNA1D: A Computer Program for Nonlinear Seismic Site Response Analysis - Technical Documentation," by Jean H. Prevost, 9/14/89, (PB90-161944, A07, MF-A01). This report is available only through NTIS (see address given above).
- NCEER-89-0026 "1:4 Scale Model Studies of Active Tendon Systems and Active Mass Dampers for Aseismic Protection," by A.M. Reinhorn, T.T. Soong, R.C. Lin, Y.P. Yang, Y. Fukao, H. Abe and M. Nakai, 9/15/89, (PB90-173246, A10, MF-A02). This report is available only through NTIS (see address given above).
- NCEER-89-0027 "Scattering of Waves by Inclusions in a Nonhomogeneous Elastic Half Space Solved by Boundary Element Methods," by P.K. Hadley, A. Askar and A.S. Cakmak, 6/15/89, (PB90-145699, A07, MF-A01).
- NCEER-89-0028 "Statistical Evaluation of Deflection Amplification Factors for Reinforced Concrete Structures," by H.H.M. Hwang, J-W. Jaw and A.L. Ch'ng, 8/31/89, (PB90-164633, A05, MF-A01).
- NCEER-89-0029 "Bedrock Accelerations in Memphis Area Due to Large New Madrid Earthquakes," by H.H.M. Hwang, C.H.S. Chen and G. Yu, 11/7/89, (PB90-162330, A04, MF-A01).
- NCEER-89-0030 "Seismic Behavior and Response Sensitivity of Secondary Structural Systems," by Y.Q. Chen and T.T. Soong, 10/23/89, (PB90-164658, A08, MF-A01).
- NCEER-89-0031 "Random Vibration and Reliability Analysis of Primary-Secondary Structural Systems," by Y. Ibrahim, M. Grigoriu and T.T. Soong, 11/10/89, (PB90-161951, A04, MF-A01).

- NCEER-89-0032 "Proceedings from the Second U.S. - Japan Workshop on Liquefaction, Large Ground Deformation and Their Effects on Lifelines, September 26-29, 1989," Edited by T.D. O'Rourke and M. Hamada, 12/1/89, (PB90-209388, A22, MF-A03).
- NCEER-89-0033 "Deterministic Model for Seismic Damage Evaluation of Reinforced Concrete Structures," by J.M. Bracci, A.M. Reinhorn, J.B. Mander and S.K. Kunnath, 9/27/89, (PB91-108803, A06, MF-A01).
- NCEER-89-0034 "On the Relation Between Local and Global Damage Indices," by E. DiPasquale and A.S. Cakmak, 8/15/89, (PB90-173865, A05, MF-A01).
- NCEER-89-0035 "Cyclic Undrained Behavior of Nonplastic and Low Plasticity Silts," by A.J. Walker and H.E. Stewart, 7/26/89, (PB90-183518, A10, MF-A01).
- NCEER-89-0036 "Liquefaction Potential of Surficial Deposits in the City of Buffalo, New York," by M. Budhu, R. Giese and L. Baumgrass, 1/17/89, (PB90-208455, A04, MF-A01).
- NCEER-89-0037 "A Deterministic Assessment of Effects of Ground Motion Incoherence," by A.S. Veletsos and Y. Tang, 7/15/89, (PB90-164294, A03, MF-A01).
- NCEER-89-0038 "Workshop on Ground Motion Parameters for Seismic Hazard Mapping," July 17-18, 1989, edited by R.V. Whitman, 12/1/89, (PB90-173923, A04, MF-A01).
- NCEER-89-0039 "Seismic Effects on Elevated Transit Lines of the New York City Transit Authority," by C.J. Costantino, C.A. Miller and E. Heymsfield, 12/26/89, (PB90-207887, A06, MF-A01).
- NCEER-89-0040 "Centrifugal Modeling of Dynamic Soil-Structure Interaction," by K. Weissman, Supervised by J.H. Prevost, 5/10/89, (PB90-207879, A07, MF-A01).
- NCEER-89-0041 "Linearized Identification of Buildings With Cores for Seismic Vulnerability Assessment," by I-K. Ho and A.E. Aktan, 11/1/89, (PB90-251943, A07, MF-A01).
- NCEER-90-0001 "Geotechnical and Lifeline Aspects of the October 17, 1989 Loma Prieta Earthquake in San Francisco," by T.D. O'Rourke, H.E. Stewart, F.T. Blackburn and T.S. Dickerman, 1/90, (PB90-208596, A05, MF-A01).
- NCEER-90-0002 "Nonnormal Secondary Response Due to Yielding in a Primary Structure," by D.C.K. Chen and L.D. Lutes, 2/28/90, (PB90-251976, A07, MF-A01).
- NCEER-90-0003 "Earthquake Education Materials for Grades K-12," by K.E.K. Ross, 4/16/90, (PB91-251984, A05, MF-A05). This report has been replaced by NCEER-92-0018.
- NCEER-90-0004 "Catalog of Strong Motion Stations in Eastern North America," by R.W. Busby, 4/3/90, (PB90-251984, A05, MF-A01).
- NCEER-90-0005 "NCEER Strong-Motion Data Base: A User Manual for the GeoBase Release (Version 1.0 for the Sun3)," by P. Friberg and K. Jacob, 3/31/90 (PB90-258062, A04, MF-A01).
- NCEER-90-0006 "Seismic Hazard Along a Crude Oil Pipeline in the Event of an 1811-1812 Type New Madrid Earthquake," by H.H.M. Hwang and C-H.S. Chen, 4/16/90, (PB90-258054, A04, MF-A01).
- NCEER-90-0007 "Site-Specific Response Spectra for Memphis Sheahan Pumping Station," by H.H.M. Hwang and C.S. Lee, 5/15/90, (PB91-108811, A05, MF-A01).
- NCEER-90-0008 "Pilot Study on Seismic Vulnerability of Crude Oil Transmission Systems," by T. Ariman, R. Dobry, M. Grigoriu, F. Kozin, M. O'Rourke, T. O'Rourke and M. Shinozuka, 5/25/90, (PB91-108837, A06, MF-A01).
- NCEER-90-0009 "A Program to Generate Site Dependent Time Histories: EQGEN," by G.W. Ellis, M. Srinivasan and A.S. Cakmak, 1/30/90, (PB91-108829, A04, MF-A01).
- NCEER-90-0010 "Active Isolation for Seismic Protection of Operating Rooms," by M.E. Talbott, Supervised by M. Shinozuka, 6/8/9, (PB91-110205, A05, MF-A01).

- NCEER-90-0011 "Program LINEARID for Identification of Linear Structural Dynamic Systems," by C-B. Yun and M. Shinozuka, 6/25/90, (PB91-110312, A08, MF-A01).
- NCEER-90-0012 "Two-Dimensional Two-Phase Elasto-Plastic Seismic Response of Earth Dams," by A.N. Yiagos, Supervised by J.H. Prevost, 6/20/90, (PB91-110197, A13, MF-A02).
- NCEER-90-0013 "Secondary Systems in Base-Isolated Structures: Experimental Investigation, Stochastic Response and Stochastic Sensitivity," by G.D. Manolis, G. Juhn, M.C. Constantinou and A.M. Reinhorn, 7/1/90, (PB91-110320, A08, MF-A01).
- NCEER-90-0014 "Seismic Behavior of Lightly-Reinforced Concrete Column and Beam-Column Joint Details," by S.P. Pessiki, C.H. Conley, P. Gergely and R.N. White, 8/22/90, (PB91-108795, A11, MF-A02).
- NCEER-90-0015 "Two Hybrid Control Systems for Building Structures Under Strong Earthquakes," by J.N. Yang and A. Daniellians, 6/29/90, (PB91-125393, A04, MF-A01).
- NCEER-90-0016 "Instantaneous Optimal Control with Acceleration and Velocity Feedback," by J.N. Yang and Z. Li, 6/29/90, (PB91-125401, A03, MF-A01).
- NCEER-90-0017 "Reconnaissance Report on the Northern Iran Earthquake of June 21, 1990," by M. Mehrain, 10/4/90, (PB91-125377, A03, MF-A01).
- NCEER-90-0018 "Evaluation of Liquefaction Potential in Memphis and Shelby County," by T.S. Chang, P.S. Tang, C.S. Lee and H. Hwang, 8/10/90, (PB91-125427, A09, MF-A01).
- NCEER-90-0019 "Experimental and Analytical Study of a Combined Sliding Disc Bearing and Helical Steel Spring Isolation System," by M.C. Constantinou, A.S. Mokha and A.M. Reinhorn, 10/4/90, (PB91-125385, A06, MF-A01). This report is available only through NTIS (see address given above).
- NCEER-90-0020 "Experimental Study and Analytical Prediction of Earthquake Response of a Sliding Isolation System with a Spherical Surface," by A.S. Mokha, M.C. Constantinou and A.M. Reinhorn, 10/11/90, (PB91-125419, A05, MF-A01).
- NCEER-90-0021 "Dynamic Interaction Factors for Floating Pile Groups," by G. Gazetas, K. Fan, A. Kaynia and E. Kausel, 9/10/90, (PB91-170381, A05, MF-A01).
- NCEER-90-0022 "Evaluation of Seismic Damage Indices for Reinforced Concrete Structures," by S. Rodriguez-Gomez and A.S. Cakmak, 9/30/90, PB91-171322, A06, MF-A01).
- NCEER-90-0023 "Study of Site Response at a Selected Memphis Site," by H. Desai, S. Ahmad, E.S. Gazetas and M.R. Oh, 10/11/90, (PB91-196857, A03, MF-A01).
- NCEER-90-0024 "A User's Guide to Strongmo: Version 1.0 of NCEER's Strong-Motion Data Access Tool for PCs and Terminals," by P.A. Friberg and C.A.T. Susch, 11/15/90, (PB91-171272, A03, MF-A01).
- NCEER-90-0025 "A Three-Dimensional Analytical Study of Spatial Variability of Seismic Ground Motions," by L-L. Hong and A.H.-S. Ang, 10/30/90, (PB91-170399, A09, MF-A01).
- NCEER-90-0026 "MUMOID User's Guide - A Program for the Identification of Modal Parameters," by S. Rodriguez-Gomez and E. DiPasquale, 9/30/90, (PB91-171298, A04, MF-A01).
- NCEER-90-0027 "SARCF-II User's Guide - Seismic Analysis of Reinforced Concrete Frames," by S. Rodriguez-Gomez, Y.S. Chung and C. Meyer, 9/30/90, (PB91-171280, A05, MF-A01).
- NCEER-90-0028 "Viscous Dampers: Testing, Modeling and Application in Vibration and Seismic Isolation," by N. Makris and M.C. Constantinou, 12/20/90 (PB91-190561, A06, MF-A01).
- NCEER-90-0029 "Soil Effects on Earthquake Ground Motions in the Memphis Area," by H. Hwang, C.S. Lee, K.W. Ng and T.S. Chang, 8/2/90, (PB91-190751, A05, MF-A01).

- NCEER-91-0001 "Proceedings from the Third Japan-U.S. Workshop on Earthquake Resistant Design of Lifeline Facilities and Countermeasures for Soil Liquefaction, December 17-19, 1990," edited by T.D. O'Rourke and M. Hamada, 2/1/91, (PB91-179259, A99, MF-A04).
- NCEER-91-0002 "Physical Space Solutions of Non-Proportionally Damped Systems," by M. Tong, Z. Liang and G.C. Lee, 1/15/91, (PB91-179242, A04, MF-A01).
- NCEER-91-0003 "Seismic Response of Single Piles and Pile Groups," by K. Fan and G. Gazetas, 1/10/91, (PB92-174994, A04, MF-A01).
- NCEER-91-0004 "Damping of Structures: Part 1 - Theory of Complex Damping," by Z. Liang and G. Lee, 10/10/91, (PB92-197235, A12, MF-A03).
- NCEER-91-0005 "3D-BASIS - Nonlinear Dynamic Analysis of Three Dimensional Base Isolated Structures: Part II," by S. Nagarajaiah, A.M. Reinhorn and M.C. Constantinou, 2/28/91, (PB91-190553, A07, MF-A01). This report has been replaced by NCEER-93-0011.
- NCEER-91-0006 "A Multidimensional Hysteretic Model for Plasticity Deforming Metals in Energy Absorbing Devices," by E.J. Graesser and F.A. Cozzarelli, 4/9/91, (PB92-108364, A04, MF-A01).
- NCEER-91-0007 "A Framework for Customizable Knowledge-Based Expert Systems with an Application to a KBES for Evaluating the Seismic Resistance of Existing Buildings," by E.G. Ibarra-Anaya and S.J. Fennes, 4/9/91, (PB91-210930, A08, MF-A01).
- NCEER-91-0008 "Nonlinear Analysis of Steel Frames with Semi-Rigid Connections Using the Capacity Spectrum Method," by G.G. Deierlein, S-H. Hsieh, Y-J. Shen and J.F. Abel, 7/2/91, (PB92-113828, A05, MF-A01).
- NCEER-91-0009 "Earthquake Education Materials for Grades K-12," by K.E.K. Ross, 4/30/91, (PB91-212142, A06, MF-A01). This report has been replaced by NCEER-92-0018.
- NCEER-91-0010 "Phase Wave Velocities and Displacement Phase Differences in a Harmonically Oscillating Pile," by N. Makris and G. Gazetas, 7/8/91, (PB92-108356, A04, MF-A01).
- NCEER-91-0011 "Dynamic Characteristics of a Full-Size Five-Story Steel Structure and a 2/5 Scale Model," by K.C. Chang, G.C. Yao, G.C. Lee, D.S. Hao and Y.C. Yeh," 7/2/91, (PB93-116648, A06, MF-A02).
- NCEER-91-0012 "Seismic Response of a 2/5 Scale Steel Structure with Added Viscoelastic Dampers," by K.C. Chang, T.T. Soong, S-T. Oh and M.L. Lai, 5/17/91, (PB92-110816, A05, MF-A01).
- NCEER-91-0013 "Earthquake Response of Retaining Walls; Full-Scale Testing and Computational Modeling," by S. Alampalli and A-W.M. Elgamal, 6/20/91, to be published.
- NCEER-91-0014 "3D-BASIS-M: Nonlinear Dynamic Analysis of Multiple Building Base Isolated Structures," by P.C. Tsopelas, S. Nagarajaiah, M.C. Constantinou and A.M. Reinhorn, 5/28/91, (PB92-113885, A09, MF-A02).
- NCEER-91-0015 "Evaluation of SEAOC Design Requirements for Sliding Isolated Structures," by D. Theodossiou and M.C. Constantinou, 6/10/91, (PB92-114602, A11, MF-A03).
- NCEER-91-0016 "Closed-Loop Modal Testing of a 27-Story Reinforced Concrete Flat Plate-Core Building," by H.R. Somaprasad, T. Toksoy, H. Yoshiyuki and A.E. Aktan, 7/15/91, (PB92-129980, A07, MF-A02).
- NCEER-91-0017 "Shake Table Test of a 1/6 Scale Two-Story Lightly Reinforced Concrete Building," by A.G. El-Attar, R.N. White and P. Gergely, 2/28/91, (PB92-222447, A06, MF-A02).
- NCEER-91-0018 "Shake Table Test of a 1/8 Scale Three-Story Lightly Reinforced Concrete Building," by A.G. El-Attar, R.N. White and P. Gergely, 2/28/91, (PB93-116630, A08, MF-A02).
- NCEER-91-0019 "Transfer Functions for Rigid Rectangular Foundations," by A.S. Veletsos, A.M. Prasad and W.H. Wu, 7/31/91, to be published.

- NCEER-91-0020 "Hybrid Control of Seismic-Excited Nonlinear and Inelastic Structural Systems," by J.N. Yang, Z. Li and A. Daniellians, 8/1/91, (PB92-143171, A06, MF-A02).
- NCEER-91-0021 "The NCEER-91 Earthquake Catalog: Improved Intensity-Based Magnitudes and Recurrence Relations for U.S. Earthquakes East of New Madrid," by L. Seeber and J.G. Armbruster, 8/28/91, (PB92-176742, A06, MF-A02).
- NCEER-91-0022 "Proceedings from the Implementation of Earthquake Planning and Education in Schools: The Need for Change - The Roles of the Changemakers," by K.E.K. Ross and F. Winslow, 7/23/91, (PB92-129998, A12, MF-A03).
- NCEER-91-0023 "A Study of Reliability-Based Criteria for Seismic Design of Reinforced Concrete Frame Buildings," by H.H.M. Hwang and H-M. Hsu, 8/10/91, (PB92-140235, A09, MF-A02).
- NCEER-91-0024 "Experimental Verification of a Number of Structural System Identification Algorithms," by R.G. Ghanem, H. Gavin and M. Shinozuka, 9/18/91, (PB92-176577, A18, MF-A04).
- NCEER-91-0025 "Probabilistic Evaluation of Liquefaction Potential," by H.H.M. Hwang and C.S. Lee," 11/25/91, (PB92-143429, A05, MF-A01).
- NCEER-91-0026 "Instantaneous Optimal Control for Linear, Nonlinear and Hysteretic Structures - Stable Controllers," by J.N. Yang and Z. Li, 11/15/91, (PB92-163807, A04, MF-A01).
- NCEER-91-0027 "Experimental and Theoretical Study of a Sliding Isolation System for Bridges," by M.C. Constantinou, A. Kartoum, A.M. Reinhorn and P. Bradford, 11/15/91, (PB92-176973, A10, MF-A03).
- NCEER-92-0001 "Case Studies of Liquefaction and Lifeline Performance During Past Earthquakes, Volume 1: Japanese Case Studies," Edited by M. Hamada and T. O'Rourke, 2/17/92, (PB92-197243, A18, MF-A04).
- NCEER-92-0002 "Case Studies of Liquefaction and Lifeline Performance During Past Earthquakes, Volume 2: United States Case Studies," Edited by T. O'Rourke and M. Hamada, 2/17/92, (PB92-197250, A20, MF-A04).
- NCEER-92-0003 "Issues in Earthquake Education," Edited by K. Ross, 2/3/92, (PB92-222389, A07, MF-A02).
- NCEER-92-0004 "Proceedings from the First U.S. - Japan Workshop on Earthquake Protective Systems for Bridges," Edited by I.G. Buckle, 2/4/92, (PB94-142239, A99, MF-A06).
- NCEER-92-0005 "Seismic Ground Motion from a Haskell-Type Source in a Multiple-Layered Half-Space," A.P. Theoharis, G. Deodatis and M. Shinozuka, 1/2/92, to be published.
- NCEER-92-0006 "Proceedings from the Site Effects Workshop," Edited by R. Whitman, 2/29/92, (PB92-197201, A04, MF-A01).
- NCEER-92-0007 "Engineering Evaluation of Permanent Ground Deformations Due to Seismically-Induced Liquefaction," by M.H. Baziar, R. Dobry and A-W.M. Elgamel, 3/24/92, (PB92-222421, A13, MF-A03).
- NCEER-92-0008 "A Procedure for the Seismic Evaluation of Buildings in the Central and Eastern United States," by C.D. Poland and J.O. Malley, 4/2/92, (PB92-222439, A20, MF-A04).
- NCEER-92-0009 "Experimental and Analytical Study of a Hybrid Isolation System Using Friction Controllable Sliding Bearings," by M.Q. Feng, S. Fujii and M. Shinozuka, 5/15/92, (PB93-150282, A06, MF-A02).
- NCEER-92-0010 "Seismic Resistance of Slab-Column Connections in Existing Non-Ductile Flat-Plate Buildings," by A.J. Durrani and Y. Du, 5/18/92, (PB93-116812, A06, MF-A02).
- NCEER-92-0011 "The Hysteretic and Dynamic Behavior of Brick Masonry Walls Upgraded by Ferrocement Coatings Under Cyclic Loading and Strong Simulated Ground Motion," by H. Lee and S.P. Prawl, 5/11/92, to be published.
- NCEER-92-0012 "Study of Wire Rope Systems for Seismic Protection of Equipment in Buildings," by G.F. Demetriades, M.C. Constantinou and A.M. Reinhorn, 5/20/92, (PB93-116655, A08, MF-A02).

- NCEER-92-0013 "Shape Memory Structural Dampers: Material Properties, Design and Seismic Testing," by P.R. Witting and F.A. Cozzarelli, 5/26/92, (PB93-116663, A05, MF-A01).
- NCEER-92-0014 "Longitudinal Permanent Ground Deformation Effects on Buried Continuous Pipelines," by M.J. O'Rourke, and C. Nordberg, 6/15/92, (PB93-116671, A08, MF-A02).
- NCEER-92-0015 "A Simulation Method for Stationary Gaussian Random Functions Based on the Sampling Theorem," by M. Grigoriu and S. Balopoulou, 6/11/92, (PB93-127496, A05, MF-A01).
- NCEER-92-0016 "Gravity-Load-Designed Reinforced Concrete Buildings: Seismic Evaluation of Existing Construction and Detailing Strategies for Improved Seismic Resistance," by G.W. Hoffmann, S.K. Kunnath, A.M. Reinhorn and J.B. Mander, 7/15/92, (PB94-142007, A08, MF-A02).
- NCEER-92-0017 "Observations on Water System and Pipeline Performance in the Limón Area of Costa Rica Due to the April 22, 1991 Earthquake," by M. O'Rourke and D. Ballantyne, 6/30/92, (PB93-126811, A06, MF-A02).
- NCEER-92-0018 "Fourth Edition of Earthquake Education Materials for Grades K-12," Edited by K.E.K. Ross, 8/10/92, (PB93-114023, A07, MF-A02).
- NCEER-92-0019 "Proceedings from the Fourth Japan-U.S. Workshop on Earthquake Resistant Design of Lifeline Facilities and Countermeasures for Soil Liquefaction," Edited by M. Hamada and T.D. O'Rourke, 8/12/92, (PB93-163939, A99, MF-E11).
- NCEER-92-0020 "Active Bracing System: A Full Scale Implementation of Active Control," by A.M. Reinhorn, T.T. Soong, R.C. Lin, M.A. Riley, Y.P. Wang, S. Aizawa and M. Higashino, 8/14/92, (PB93-127512, A06, MF-A02).
- NCEER-92-0021 "Empirical Analysis of Horizontal Ground Displacement Generated by Liquefaction-Induced Lateral Spreads," by S.F. Bartlett and T.L. Youd, 8/17/92, (PB93-188241, A06, MF-A02).
- NCEER-92-0022 "IDARC Version 3.0: Inelastic Damage Analysis of Reinforced Concrete Structures," by S.K. Kunnath, A.M. Reinhorn and R.F. Lobo, 8/31/92, (PB93-227502, A07, MF-A02).
- NCEER-92-0023 "A Semi-Empirical Analysis of Strong-Motion Peaks in Terms of Seismic Source, Propagation Path and Local Site Conditions, by M. Kamiyama, M.J. O'Rourke and R. Flores-Berrones, 9/9/92, (PB93-150266, A08, MF-A02).
- NCEER-92-0024 "Seismic Behavior of Reinforced Concrete Frame Structures with Nonductile Details, Part I: Summary of Experimental Findings of Full Scale Beam-Column Joint Tests," by A. Beres, R.N. White and P. Gergely, 9/30/92, (PB93-227783, A05, MF-A01).
- NCEER-92-0025 "Experimental Results of Repaired and Retrofitted Beam-Column Joint Tests in Lightly Reinforced Concrete Frame Buildings," by A. Beres, S. El-Borgi, R.N. White and P. Gergely, 10/29/92, (PB93-227791, A05, MF-A01).
- NCEER-92-0026 "A Generalization of Optimal Control Theory: Linear and Nonlinear Structures," by J.N. Yang, Z. Li and S. Vongchavalitkul, 11/2/92, (PB93-188621, A05, MF-A01).
- NCEER-92-0027 "Seismic Resistance of Reinforced Concrete Frame Structures Designed Only for Gravity Loads: Part I - Design and Properties of a One-Third Scale Model Structure," by J.M. Bracci, A.M. Reinhorn and J.B. Mander, 12/1/92, (PB94-104502, A08, MF-A02).
- NCEER-92-0028 "Seismic Resistance of Reinforced Concrete Frame Structures Designed Only for Gravity Loads: Part II - Experimental Performance of Subassemblages," by L.E. Aycaardi, J.B. Mander and A.M. Reinhorn, 12/1/92, (PB94-104510, A08, MF-A02).
- NCEER-92-0029 "Seismic Resistance of Reinforced Concrete Frame Structures Designed Only for Gravity Loads: Part III - Experimental Performance and Analytical Study of a Structural Model," by J.M. Bracci, A.M. Reinhorn and J.B. Mander, 12/1/92, (PB93-227528, A09, MF-A01).

- NCEER-92-0030 "Evaluation of Seismic Retrofit of Reinforced Concrete Frame Structures: Part I - Experimental Performance of Retrofitted Subassemblages," by D. Choudhuri, J.B. Mander and A.M. Reinhorn, 12/8/92, (PB93-198307, A07, MF-A02).
- NCEER-92-0031 "Evaluation of Seismic Retrofit of Reinforced Concrete Frame Structures: Part II - Experimental Performance and Analytical Study of a Retrofitted Structural Model," by J.M. Bracci, A.M. Reinhorn and J.B. Mander, 12/8/92, (PB93-198315, A09, MF-A03).
- NCEER-92-0032 "Experimental and Analytical Investigation of Seismic Response of Structures with Supplemental Fluid Viscous Dampers," by M.C. Constantinou and M.D. Symans, 12/21/92, (PB93-191435, A10, MF-A03). This report is available only through NTIS (see address given above).
- NCEER-92-0033 "Reconnaissance Report on the Cairo, Egypt Earthquake of October 12, 1992," by M. Khater, 12/23/92, (PB93-188621, A03, MF-A01).
- NCEER-92-0034 "Low-Level Dynamic Characteristics of Four Tall Flat-Plate Buildings in New York City," by H. Gavin, S. Yuan, J. Grossman, E. Pekelis and K. Jacob, 12/28/92, (PB93-188217, A07, MF-A02).
- NCEER-93-0001 "An Experimental Study on the Seismic Performance of Brick-Infilled Steel Frames With and Without Retrofit," by J.B. Mander, B. Nair, K. Wojtkowski and J. Ma, 1/29/93, (PB93-227510, A07, MF-A02).
- NCEER-93-0002 "Social Accounting for Disaster Preparedness and Recovery Planning," by S. Cole, E. Pantoja and V. Razak, 2/22/93, (PB94-142114, A12, MF-A03).
- NCEER-93-0003 "Assessment of 1991 NEHRP Provisions for Nonstructural Components and Recommended Revisions," by T.T. Soong, G. Chen, Z. Wu, R-H. Zhang and M. Grigoriu, 3/1/93, (PB93-188639, A06, MF-A02).
- NCEER-93-0004 "Evaluation of Static and Response Spectrum Analysis Procedures of SEAOC/UBC for Seismic Isolated Structures," by C.W. Winters and M.C. Constantinou, 3/23/93, (PB93-198299, A10, MF-A03).
- NCEER-93-0005 "Earthquakes in the Northeast - Are We Ignoring the Hazard? A Workshop on Earthquake Science and Safety for Educators," edited by K.E.K. Ross, 4/2/93, (PB94-103066, A09, MF-A02).
- NCEER-93-0006 "Inelastic Response of Reinforced Concrete Structures with Viscoelastic Braces," by R.F. Lobo, J.M. Bracci, K.L. Shen, A.M. Reinhorn and T.T. Soong, 4/5/93, (PB93-227486, A05, MF-A02).
- NCEER-93-0007 "Seismic Testing of Installation Methods for Computers and Data Processing Equipment," by K. Kosar, T.T. Soong, K.L. Shen, J.A. HoLung and Y.K. Lin, 4/12/93, (PB93-198299, A07, MF-A02).
- NCEER-93-0008 "Retrofit of Reinforced Concrete Frames Using Added Dampers," by A. Reinhorn, M. Constantinou and C. Li, to be published.
- NCEER-93-0009 "Seismic Behavior and Design Guidelines for Steel Frame Structures with Added Viscoelastic Dampers," by K.C. Chang, M.L. Lai, T.T. Soong, D.S. Hao and Y.C. Yeh, 5/1/93, (PB94-141959, A07, MF-A02).
- NCEER-93-0010 "Seismic Performance of Shear-Critical Reinforced Concrete Bridge Piers," by J.B. Mander, S.M. Waheed, M.T.A. Chaudhary and S.S. Chen, 5/12/93, (PB93-227494, A08, MF-A02).
- NCEER-93-0011 "3D-BASIS-TABS: Computer Program for Nonlinear Dynamic Analysis of Three Dimensional Base Isolated Structures," by S. Nagarajaiah, C. Li, A.M. Reinhorn and M.C. Constantinou, 8/2/93, (PB94-141819, A09, MF-A02).
- NCEER-93-0012 "Effects of Hydrocarbon Spills from an Oil Pipeline Break on Ground Water," by O.J. Helweg and H.H.M. Hwang, 8/3/93, (PB94-141942, A06, MF-A02).
- NCEER-93-0013 "Simplified Procedures for Seismic Design of Nonstructural Components and Assessment of Current Code Provisions," by M.P. Singh, L.E. Suarez, E.E. Matheu and G.O. Maldonado, 8/4/93, (PB94-141827, A09, MF-A02).
- NCEER-93-0014 "An Energy Approach to Seismic Analysis and Design of Secondary Systems," by G. Chen and T.T. Soong, 8/6/93, (PB94-142767, A11, MF-A03).

- NCEER-93-0015 "Proceedings from School Sites: Becoming Prepared for Earthquakes - Commemorating the Third Anniversary of the Loma Prieta Earthquake," Edited by F.E. Winslow and K.E.K. Ross, 8/16/93, (PB94-154275, A16, MF-A02).
- NCEER-93-0016 "Reconnaissance Report of Damage to Historic Monuments in Cairo, Egypt Following the October 12, 1992 Dahshur Earthquake," by D. Sykora, D. Look, G. Croci, E. Karaesmen and E. Karaesmen, 8/19/93, (PB94-142221, A08, MF-A02).
- NCEER-93-0017 "The Island of Guam Earthquake of August 8, 1993," by S.W. Swan and S.K. Harris, 9/30/93, (PB94-141843, A04, MF-A01).
- NCEER-93-0018 "Engineering Aspects of the October 12, 1992 Egyptian Earthquake," by A.W. Elgamal, M. Amer, K. Adalier and A. Abul-Fadl, 10/7/93, (PB94-141983, A05, MF-A01).
- NCEER-93-0019 "Development of an Earthquake Motion Simulator and its Application in Dynamic Centrifuge Testing," by I. Krstelj, Supervised by J.H. Prevost, 10/23/93, (PB94-181773, A-10, MF-A03).
- NCEER-93-0020 "NCEER-Taisei Corporation Research Program on Sliding Seismic Isolation Systems for Bridges: Experimental and Analytical Study of a Friction Pendulum System (FPS)," by M.C. Constantinou, P. Tsopelas, Y-S. Kim and S. Okamoto, 11/1/93, (PB94-142775, A08, MF-A02).
- NCEER-93-0021 "Finite Element Modeling of Elastomeric Seismic Isolation Bearings," by L.J. Billings, Supervised by R. Shepherd, 11/8/93, to be published.
- NCEER-93-0022 "Seismic Vulnerability of Equipment in Critical Facilities: Life-Safety and Operational Consequences," by K. Porter, G.S. Johnson, M.M. Zadeh, C. Scawthorn and S. Eder, 11/24/93, (PB94-181765, A16, MF-A03).
- NCEER-93-0023 "Hokkaido Nansei-oki, Japan Earthquake of July 12, 1993, by P.I. Yanev and C.R. Scawthorn, 12/23/93, (PB94-181500, A07, MF-A01).
- NCEER-94-0001 "An Evaluation of Seismic Serviceability of Water Supply Networks with Application to the San Francisco Auxiliary Water Supply System," by I. Markov, Supervised by M. Grigoriu and T. O'Rourke, 1/21/94, (PB94-204013, A07, MF-A02).
- NCEER-94-0002 "NCEER-Taisei Corporation Research Program on Sliding Seismic Isolation Systems for Bridges: Experimental and Analytical Study of Systems Consisting of Sliding Bearings, Rubber Restoring Force Devices and Fluid Dampers," Volumes I and II, by P. Tsopelas, S. Okamoto, M.C. Constantinou, D. Ozaki and S. Fujii, 2/4/94, (PB94-181740, A09, MF-A02 and PB94-181757, A12, MF-A03).
- NCEER-94-0003 "A Markov Model for Local and Global Damage Indices in Seismic Analysis," by S. Rahman and M. Grigoriu, 2/18/94, (PB94-206000, A12, MF-A03).
- NCEER-94-0004 "Proceedings from the NCEER Workshop on Seismic Response of Masonry Infills," edited by D.P. Abrams, 3/1/94, (PB94-180783, A07, MF-A02).
- NCEER-94-0005 "The Northridge, California Earthquake of January 17, 1994: General Reconnaissance Report," edited by J.D. Goltz, 3/11/94, (PB94-193943, A10, MF-A03).
- NCEER-94-0006 "Seismic Energy Based Fatigue Damage Analysis of Bridge Columns: Part I - Evaluation of Seismic Capacity," by G.A. Chang and J.B. Mander, 3/14/94, (PB94-219185, A11, MF-A03).
- NCEER-94-0007 "Seismic Isolation of Multi-Story Frame Structures Using Spherical Sliding Isolation Systems," by T.M. Al-Hussaini, V.A. Zayas and M.C. Constantinou, 3/17/94, (PB94-193745, A09, MF-A02).
- NCEER-94-0008 "The Northridge, California Earthquake of January 17, 1994: Performance of Highway Bridges," edited by I.G. Buckle, 3/24/94, (PB94-193851, A06, MF-A02).
- NCEER-94-0009 "Proceedings of the Third U.S.-Japan Workshop on Earthquake Protective Systems for Bridges," edited by I.G. Buckle and I. Friedland, 3/31/94, (PB94-195815, A99, MF-A06).

- NCEER-94-0010 "3D-BASIS-ME: Computer Program for Nonlinear Dynamic Analysis of Seismically Isolated Single and Multiple Structures and Liquid Storage Tanks," by P.C. Tsopelas, M.C. Constantinou and A.M. Reinhorn, 4/12/94, (PB94-204922, A09, MF-A02).
- NCEER-94-0011 "The Northridge, California Earthquake of January 17, 1994: Performance of Gas Transmission Pipelines," by T.D. O'Rourke and M.C. Palmer, 5/16/94, (PB94-204989, A05, MF-A01).
- NCEER-94-0012 "Feasibility Study of Replacement Procedures and Earthquake Performance Related to Gas Transmission Pipelines," by T.D. O'Rourke and M.C. Palmer, 5/25/94, (PB94-206638, A09, MF-A02).
- NCEER-94-0013 "Seismic Energy Based Fatigue Damage Analysis of Bridge Columns: Part II - Evaluation of Seismic Demand," by G.A. Chang and J.B. Mander, 6/1/94, (PB95-18106, A08, MF-A02).
- NCEER-94-0014 "NCEER-Taisei Corporation Research Program on Sliding Seismic Isolation Systems for Bridges: Experimental and Analytical Study of a System Consisting of Sliding Bearings and Fluid Restoring Force/Damping Devices," by P. Tsopelas and M.C. Constantinou, 6/13/94, (PB94-219144, A10, MF-A03).
- NCEER-94-0015 "Generation of Hazard-Consistent Fragility Curves for Seismic Loss Estimation Studies," by H. Hwang and J-R. Huo, 6/14/94, (PB95-181996, A09, MF-A02).
- NCEER-94-0016 "Seismic Study of Building Frames with Added Energy-Absorbing Devices," by W.S. Pong, C.S. Tsai and G.C. Lee, 6/20/94, (PB94-219136, A10, A03).
- NCEER-94-0017 "Sliding Mode Control for Seismic-Excited Linear and Nonlinear Civil Engineering Structures," by J. Yang, J. Wu, A. Agrawal and Z. Li, 6/21/94, (PB95-138483, A06, MF-A02).
- NCEER-94-0018 "3D-BASIS-TABS Version 2.0: Computer Program for Nonlinear Dynamic Analysis of Three Dimensional Base Isolated Structures," by A.M. Reinhorn, S. Nagarajaiah, M.C. Constantinou, P. Tsopelas and R. Li, 6/22/94, (PB95-182176, A08, MF-A02).
- NCEER-94-0019 "Proceedings of the International Workshop on Civil Infrastructure Systems: Application of Intelligent Systems and Advanced Materials on Bridge Systems," Edited by G.C. Lee and K.C. Chang, 7/18/94, (PB95-252474, A20, MF-A04).
- NCEER-94-0020 "Study of Seismic Isolation Systems for Computer Floors," by V. Lambrou and M.C. Constantinou, 7/19/94, (PB95-138533, A10, MF-A03).
- NCEER-94-0021 "Proceedings of the U.S.-Italian Workshop on Guidelines for Seismic Evaluation and Rehabilitation of Unreinforced Masonry Buildings," Edited by D.P. Abrams and G.M. Calvi, 7/20/94, (PB95-138749, A13, MF-A03).
- NCEER-94-0022 "NCEER-Taisei Corporation Research Program on Sliding Seismic Isolation Systems for Bridges: Experimental and Analytical Study of a System Consisting of Lubricated PTFE Sliding Bearings and Mild Steel Dampers," by P. Tsopelas and M.C. Constantinou, 7/22/94, (PB95-182184, A08, MF-A02).
- NCEER-94-0023 "Development of Reliability-Based Design Criteria for Buildings Under Seismic Load," by Y.K. Wen, H. Hwang and M. Shinozuka, 8/1/94, (PB95-211934, A08, MF-A02).
- NCEER-94-0024 "Experimental Verification of Acceleration Feedback Control Strategies for an Active Tendon System," by S.J. Dyke, B.F. Spencer, Jr., P. Quast, M.K. Sain, D.C. Kaspari, Jr. and T.T. Soong, 8/29/94, (PB95-212320, A05, MF-A01).
- NCEER-94-0025 "Seismic Retrofitting Manual for Highway Bridges," Edited by I.G. Buckle and I.F. Friedland, published by the Federal Highway Administration (PB95-212676, A15, MF-A03).
- NCEER-94-0026 "Proceedings from the Fifth U.S.-Japan Workshop on Earthquake Resistant Design of Lifeline Facilities and Countermeasures Against Soil Liquefaction," Edited by T.D. O'Rourke and M. Hamada, 11/7/94, (PB95-220802, A99, MF-E08).

- NCEER-95-0001 “Experimental and Analytical Investigation of Seismic Retrofit of Structures with Supplemental Damping: Part 1 - Fluid Viscous Damping Devices,” by A.M. Reinhorn, C. Li and M.C. Constantinou, 1/3/95, (PB95-266599, A09, MF-A02).
- NCEER-95-0002 “Experimental and Analytical Study of Low-Cycle Fatigue Behavior of Semi-Rigid Top-And-Seat Angle Connections,” by G. Pekcan, J.B. Mander and S.S. Chen, 1/5/95, (PB95-220042, A07, MF-A02).
- NCEER-95-0003 “NCEER-ATC Joint Study on Fragility of Buildings,” by T. Anagnos, C. Rojahn and A.S. Kiremidjian, 1/20/95, (PB95-220026, A06, MF-A02).
- NCEER-95-0004 “Nonlinear Control Algorithms for Peak Response Reduction,” by Z. Wu, T.T. Soong, V. Gattulli and R.C. Lin, 2/16/95, (PB95-220349, A05, MF-A01).
- NCEER-95-0005 “Pipeline Replacement Feasibility Study: A Methodology for Minimizing Seismic and Corrosion Risks to Underground Natural Gas Pipelines,” by R.T. Eguchi, H.A. Seligson and D.G. Honegger, 3/2/95, (PB95-252326, A06, MF-A02).
- NCEER-95-0006 “Evaluation of Seismic Performance of an 11-Story Frame Building During the 1994 Northridge Earthquake,” by F. Naeim, R. DiSulio, K. Benuska, A. Reinhorn and C. Li, to be published.
- NCEER-95-0007 “Prioritization of Bridges for Seismic Retrofitting,” by N. Basöz and A.S. Kiremidjian, 4/24/95, (PB95-252300, A08, MF-A02).
- NCEER-95-0008 “Method for Developing Motion Damage Relationships for Reinforced Concrete Frames,” by A. Singhal and A.S. Kiremidjian, 5/11/95, (PB95-266607, A06, MF-A02).
- NCEER-95-0009 “Experimental and Analytical Investigation of Seismic Retrofit of Structures with Supplemental Damping: Part II - Friction Devices,” by C. Li and A.M. Reinhorn, 7/6/95, (PB96-128087, A11, MF-A03).
- NCEER-95-0010 “Experimental Performance and Analytical Study of a Non-Ductile Reinforced Concrete Frame Structure Retrofitted with Elastomeric Spring Dampers,” by G. Pekcan, J.B. Mander and S.S. Chen, 7/14/95, (PB96-137161, A08, MF-A02).
- NCEER-95-0011 “Development and Experimental Study of Semi-Active Fluid Damping Devices for Seismic Protection of Structures,” by M.D. Symans and M.C. Constantinou, 8/3/95, (PB96-136940, A23, MF-A04).
- NCEER-95-0012 “Real-Time Structural Parameter Modification (RSPM): Development of Innervated Structures,” by Z. Liang, M. Tong and G.C. Lee, 4/11/95, (PB96-137153, A06, MF-A01).
- NCEER-95-0013 “Experimental and Analytical Investigation of Seismic Retrofit of Structures with Supplemental Damping: Part III - Viscous Damping Walls,” by A.M. Reinhorn and C. Li, 10/1/95, (PB96-176409, A11, MF-A03).
- NCEER-95-0014 “Seismic Fragility Analysis of Equipment and Structures in a Memphis Electric Substation,” by J-R. Huo and H.H.M. Hwang, 8/10/95, (PB96-128087, A09, MF-A02).
- NCEER-95-0015 “The Hanshin-Awaji Earthquake of January 17, 1995: Performance of Lifelines,” Edited by M. Shinozuka, 11/3/95, (PB96-176383, A15, MF-A03).
- NCEER-95-0016 “Highway Culvert Performance During Earthquakes,” by T.L. Youd and C.J. Beckman, available as NCEER-96-0015.
- NCEER-95-0017 “The Hanshin-Awaji Earthquake of January 17, 1995: Performance of Highway Bridges,” Edited by I.G. Buckle, 12/1/95, to be published.
- NCEER-95-0018 “Modeling of Masonry Infill Panels for Structural Analysis,” by A.M. Reinhorn, A. Madan, R.E. Valles, Y. Reichmann and J.B. Mander, 12/8/95, (PB97-110886, MF-A01, A06).
- NCEER-95-0019 “Optimal Polynomial Control for Linear and Nonlinear Structures,” by A.K. Agrawal and J.N. Yang, 12/11/95, (PB96-168737, A07, MF-A02).

- NCEER-95-0020 "Retrofit of Non-Ductile Reinforced Concrete Frames Using Friction Dampers," by R.S. Rao, P. Gergely and R.N. White, 12/22/95, (PB97-133508, A10, MF-A02).
- NCEER-95-0021 "Parametric Results for Seismic Response of Pile-Supported Bridge Bents," by G. Mylonakis, A. Nikolaou and G. Gazetas, 12/22/95, (PB97-100242, A12, MF-A03).
- NCEER-95-0022 "Kinematic Bending Moments in Seismically Stressed Piles," by A. Nikolaou, G. Mylonakis and G. Gazetas, 12/23/95, (PB97-113914, MF-A03, A13).
- NCEER-96-0001 "Dynamic Response of Unreinforced Masonry Buildings with Flexible Diaphragms," by A.C. Costley and D.P. Abrams, 10/10/96, (PB97-133573, MF-A03, A15).
- NCEER-96-0002 "State of the Art Review: Foundations and Retaining Structures," by I. Po Lam, to be published.
- NCEER-96-0003 "Ductility of Rectangular Reinforced Concrete Bridge Columns with Moderate Confinement," by N. Wehbe, M. Saiidi, D. Sanders and B. Douglas, 11/7/96, (PB97-133557, A06, MF-A02).
- NCEER-96-0004 "Proceedings of the Long-Span Bridge Seismic Research Workshop," edited by I.G. Buckle and I.M. Friedland, to be published.
- NCEER-96-0005 "Establish Representative Pier Types for Comprehensive Study: Eastern United States," by J. Kulicki and Z. Prucz, 5/28/96, (PB98-119217, A07, MF-A02).
- NCEER-96-0006 "Establish Representative Pier Types for Comprehensive Study: Western United States," by R. Imbsen, R.A. Schamber and T.A. Osterkamp, 5/28/96, (PB98-118607, A07, MF-A02).
- NCEER-96-0007 "Nonlinear Control Techniques for Dynamical Systems with Uncertain Parameters," by R.G. Ghanem and M.I. Bujakov, 5/27/96, (PB97-100259, A17, MF-A03).
- NCEER-96-0008 "Seismic Evaluation of a 30-Year Old Non-Ductile Highway Bridge Pier and Its Retrofit," by J.B. Mander, B. Mahmoodzadegan, S. Bhadra and S.S. Chen, 5/31/96, (PB97-110902, MF-A03, A10).
- NCEER-96-0009 "Seismic Performance of a Model Reinforced Concrete Bridge Pier Before and After Retrofit," by J.B. Mander, J.H. Kim and C.A. Ligozio, 5/31/96, (PB97-110910, MF-A02, A10).
- NCEER-96-0010 "IDARC2D Version 4.0: A Computer Program for the Inelastic Damage Analysis of Buildings," by R.E. Valles, A.M. Reinhorn, S.K. Kunnath, C. Li and A. Madan, 6/3/96, (PB97-100234, A17, MF-A03).
- NCEER-96-0011 "Estimation of the Economic Impact of Multiple Lifeline Disruption: Memphis Light, Gas and Water Division Case Study," by S.E. Chang, H.A. Seligson and R.T. Eguchi, 8/16/96, (PB97-133490, A11, MF-A03).
- NCEER-96-0012 "Proceedings from the Sixth Japan-U.S. Workshop on Earthquake Resistant Design of Lifeline Facilities and Countermeasures Against Soil Liquefaction, Edited by M. Hamada and T. O'Rourke, 9/11/96, (PB97-133581, A99, MF-A06).
- NCEER-96-0013 "Chemical Hazards, Mitigation and Preparedness in Areas of High Seismic Risk: A Methodology for Estimating the Risk of Post-Earthquake Hazardous Materials Release," by H.A. Seligson, R.T. Eguchi, K.J. Tierney and K. Richmond, 11/7/96, (PB97-133565, MF-A02, A08).
- NCEER-96-0014 "Response of Steel Bridge Bearings to Reversed Cyclic Loading," by J.B. Mander, D-K. Kim, S.S. Chen and G.J. Premus, 11/13/96, (PB97-140735, A12, MF-A03).
- NCEER-96-0015 "Highway Culvert Performance During Past Earthquakes," by T.L. Youd and C.J. Beckman, 11/25/96, (PB97-133532, A06, MF-A01).
- NCEER-97-0001 "Evaluation, Prevention and Mitigation of Pounding Effects in Building Structures," by R.E. Valles and A.M. Reinhorn, 2/20/97, (PB97-159552, A14, MF-A03).
- NCEER-97-0002 "Seismic Design Criteria for Bridges and Other Highway Structures," by C. Rojahn, R. Mayes, D.G. Anderson, J. Clark, J.H. Hom, R.V. Nutt and M.J. O'Rourke, 4/30/97, (PB97-194658, A06, MF-A03).

- NCEER-97-0003 "Proceedings of the U.S.-Italian Workshop on Seismic Evaluation and Retrofit," Edited by D.P. Abrams and G.M. Calvi, 3/19/97, (PB97-194666, A13, MF-A03).
- NCEER-97-0004 "Investigation of Seismic Response of Buildings with Linear and Nonlinear Fluid Viscous Dampers," by A.A. Seleemah and M.C. Constantinou, 5/21/97, (PB98-109002, A15, MF-A03).
- NCEER-97-0005 "Proceedings of the Workshop on Earthquake Engineering Frontiers in Transportation Facilities," edited by G.C. Lee and I.M. Friedland, 8/29/97, (PB98-128911, A25, MR-A04).
- NCEER-97-0006 "Cumulative Seismic Damage of Reinforced Concrete Bridge Piers," by S.K. Kunnath, A. El-Bahy, A. Taylor and W. Stone, 9/2/97, (PB98-108814, A11, MF-A03).
- NCEER-97-0007 "Structural Details to Accommodate Seismic Movements of Highway Bridges and Retaining Walls," by R.A. Imbsen, R.A. Schamber, E. Thorkildsen, A. Kartoum, B.T. Martin, T.N. Rosser and J.M. Kulicki, 9/3/97, (PB98-108996, A09, MF-A02).
- NCEER-97-0008 "A Method for Earthquake Motion-Damage Relationships with Application to Reinforced Concrete Frames," by A. Singhal and A.S. Kiremidjian, 9/10/97, (PB98-108988, A13, MF-A03).
- NCEER-97-0009 "Seismic Analysis and Design of Bridge Abutments Considering Sliding and Rotation," by K. Fishman and R. Richards, Jr., 9/15/97, (PB98-108897, A06, MF-A02).
- NCEER-97-0010 "Proceedings of the FHWA/NCEER Workshop on the National Representation of Seismic Ground Motion for New and Existing Highway Facilities," edited by I.M. Friedland, M.S. Power and R.L. Mayes, 9/22/97, (PB98-128903, A21, MF-A04).
- NCEER-97-0011 "Seismic Analysis for Design or Retrofit of Gravity Bridge Abutments," by K.L. Fishman, R. Richards, Jr. and R.C. Divito, 10/2/97, (PB98-128937, A08, MF-A02).
- NCEER-97-0012 "Evaluation of Simplified Methods of Analysis for Yielding Structures," by P. Tsopelas, M.C. Constantinou, C.A. Kircher and A.S. Whittaker, 10/31/97, (PB98-128929, A10, MF-A03).
- NCEER-97-0013 "Seismic Design of Bridge Columns Based on Control and Repairability of Damage," by C-T. Cheng and J.B. Mander, 12/8/97, (PB98-144249, A11, MF-A03).
- NCEER-97-0014 "Seismic Resistance of Bridge Piers Based on Damage Avoidance Design," by J.B. Mander and C-T. Cheng, 12/10/97, (PB98-144223, A09, MF-A02).
- NCEER-97-0015 "Seismic Response of Nominally Symmetric Systems with Strength Uncertainty," by S. Balopoulou and M. Grigoriu, 12/23/97, (PB98-153422, A11, MF-A03).
- NCEER-97-0016 "Evaluation of Seismic Retrofit Methods for Reinforced Concrete Bridge Columns," by T.J. Wipf, F.W. Klaiber and F.M. Russo, 12/28/97, (PB98-144215, A12, MF-A03).
- NCEER-97-0017 "Seismic Fragility of Existing Conventional Reinforced Concrete Highway Bridges," by C.L. Mullen and A.S. Cakmak, 12/30/97, (PB98-153406, A08, MF-A02).
- NCEER-97-0018 "Loss Assessment of Memphis Buildings," edited by D.P. Abrams and M. Shinozuka, 12/31/97, (PB98-144231, A13, MF-A03).
- NCEER-97-0019 "Seismic Evaluation of Frames with Infill Walls Using Quasi-static Experiments," by K.M. Mosalam, R.N. White and P. Gergely, 12/31/97, (PB98-153455, A07, MF-A02).
- NCEER-97-0020 "Seismic Evaluation of Frames with Infill Walls Using Pseudo-dynamic Experiments," by K.M. Mosalam, R.N. White and P. Gergely, 12/31/97, (PB98-153430, A07, MF-A02).
- NCEER-97-0021 "Computational Strategies for Frames with Infill Walls: Discrete and Smeared Crack Analyses and Seismic Fragility," by K.M. Mosalam, R.N. White and P. Gergely, 12/31/97, (PB98-153414, A10, MF-A02).

- NCEER-97-0022 "Proceedings of the NCEER Workshop on Evaluation of Liquefaction Resistance of Soils," edited by T.L. Youd and I.M. Idriss, 12/31/97, (PB98-155617, A15, MF-A03).
- MCEER-98-0001 "Extraction of Nonlinear Hysteretic Properties of Seismically Isolated Bridges from Quick-Release Field Tests," by Q. Chen, B.M. Douglas, E.M. Maragakis and I.G. Buckle, 5/26/98, (PB99-118838, A06, MF-A01).
- MCEER-98-0002 "Methodologies for Evaluating the Importance of Highway Bridges," by A. Thomas, S. Eshenaur and J. Kulicki, 5/29/98, (PB99-118846, A10, MF-A02).
- MCEER-98-0003 "Capacity Design of Bridge Piers and the Analysis of Overstrength," by J.B. Mander, A. Dutta and P. Goel, 6/1/98, (PB99-118853, A09, MF-A02).
- MCEER-98-0004 "Evaluation of Bridge Damage Data from the Loma Prieta and Northridge, California Earthquakes," by N. Basoz and A. Kiremidjian, 6/2/98, (PB99-118861, A15, MF-A03).
- MCEER-98-0005 "Screening Guide for Rapid Assessment of Liquefaction Hazard at Highway Bridge Sites," by T. L. Youd, 6/16/98, (PB99-118879, A06, not available on microfiche).
- MCEER-98-0006 "Structural Steel and Steel/Concrete Interface Details for Bridges," by P. Ritchie, N. Kaulh and J. Kulicki, 7/13/98, (PB99-118945, A06, MF-A01).
- MCEER-98-0007 "Capacity Design and Fatigue Analysis of Confined Concrete Columns," by A. Dutta and J.B. Mander, 7/14/98, (PB99-118960, A14, MF-A03).
- MCEER-98-0008 "Proceedings of the Workshop on Performance Criteria for Telecommunication Services Under Earthquake Conditions," edited by A.J. Schiff, 7/15/98, (PB99-118952, A08, MF-A02).
- MCEER-98-0009 "Fatigue Analysis of Unconfined Concrete Columns," by J.B. Mander, A. Dutta and J.H. Kim, 9/12/98, (PB99-123655, A10, MF-A02).
- MCEER-98-0010 "Centrifuge Modeling of Cyclic Lateral Response of Pile-Cap Systems and Seat-Type Abutments in Dry Sands," by A.D. Gadre and R. Dobry, 10/2/98, (PB99-123606, A13, MF-A03).
- MCEER-98-0011 "IDARC-BRIDGE: A Computational Platform for Seismic Damage Assessment of Bridge Structures," by A.M. Reinhorn, V. Simeonov, G. Mylonakis and Y. Reichman, 10/2/98, (PB99-162919, A15, MF-A03).
- MCEER-98-0012 "Experimental Investigation of the Dynamic Response of Two Bridges Before and After Retrofitting with Elastomeric Bearings," by D.A. Wendichansky, S.S. Chen and J.B. Mander, 10/2/98, (PB99-162927, A15, MF-A03).
- MCEER-98-0013 "Design Procedures for Hinge Restrainers and Hinge Sear Width for Multiple-Frame Bridges," by R. Des Roches and G.L. Fenves, 11/3/98, (PB99-140477, A13, MF-A03).
- MCEER-98-0014 "Response Modification Factors for Seismically Isolated Bridges," by M.C. Constantinou and J.K. Quarshie, 11/3/98, (PB99-140485, A14, MF-A03).
- MCEER-98-0015 "Proceedings of the U.S.-Italy Workshop on Seismic Protective Systems for Bridges," edited by I.M. Friedland and M.C. Constantinou, 11/3/98, (PB2000-101711, A22, MF-A04).
- MCEER-98-0016 "Appropriate Seismic Reliability for Critical Equipment Systems: Recommendations Based on Regional Analysis of Financial and Life Loss," by K. Porter, C. Scawthorn, C. Taylor and N. Blais, 11/10/98, (PB99-157265, A08, MF-A02).
- MCEER-98-0017 "Proceedings of the U.S. Japan Joint Seminar on Civil Infrastructure Systems Research," edited by M. Shinozuka and A. Rose, 11/12/98, (PB99-156713, A16, MF-A03).
- MCEER-98-0018 "Modeling of Pile Footings and Drilled Shafts for Seismic Design," by I. PoLam, M. Kapuskar and D. Chaudhuri, 12/21/98, (PB99-157257, A09, MF-A02).

- MCEER-99-0001 "Seismic Evaluation of a Masonry Infilled Reinforced Concrete Frame by Pseudodynamic Testing," by S.G. Buonopane and R.N. White, 2/16/99, (PB99-162851, A09, MF-A02).
- MCEER-99-0002 "Response History Analysis of Structures with Seismic Isolation and Energy Dissipation Systems: Verification Examples for Program SAP2000," by J. Scheller and M.C. Constantinou, 2/22/99, (PB99-162869, A08, MF-A02).
- MCEER-99-0003 "Experimental Study on the Seismic Design and Retrofit of Bridge Columns Including Axial Load Effects," by A. Dutta, T. Kokorina and J.B. Mander, 2/22/99, (PB99-162877, A09, MF-A02).
- MCEER-99-0004 "Experimental Study of Bridge Elastomeric and Other Isolation and Energy Dissipation Systems with Emphasis on Uplift Prevention and High Velocity Near-source Seismic Excitation," by A. Kasalanati and M. C. Constantinou, 2/26/99, (PB99-162885, A12, MF-A03).
- MCEER-99-0005 "Truss Modeling of Reinforced Concrete Shear-flexure Behavior," by J.H. Kim and J.B. Mander, 3/8/99, (PB99-163693, A12, MF-A03).
- MCEER-99-0006 "Experimental Investigation and Computational Modeling of Seismic Response of a 1:4 Scale Model Steel Structure with a Load Balancing Supplemental Damping System," by G. Pekcan, J.B. Mander and S.S. Chen, 4/2/99, (PB99-162893, A11, MF-A03).
- MCEER-99-0007 "Effect of Vertical Ground Motions on the Structural Response of Highway Bridges," by M.R. Button, C.J. Cronin and R.L. Mayes, 4/10/99, (PB2000-101411, A10, MF-A03).
- MCEER-99-0008 "Seismic Reliability Assessment of Critical Facilities: A Handbook, Supporting Documentation, and Model Code Provisions," by G.S. Johnson, R.E. Sheppard, M.D. Quilici, S.J. Eder and C.R. Scawthorn, 4/12/99, (PB2000-101701, A18, MF-A04).
- MCEER-99-0009 "Impact Assessment of Selected MCEER Highway Project Research on the Seismic Design of Highway Structures," by C. Rojahn, R. Mayes, D.G. Anderson, J.H. Clark, D'Appolonia Engineering, S. Gloyd and R.V. Nutt, 4/14/99, (PB99-162901, A10, MF-A02).
- MCEER-99-0010 "Site Factors and Site Categories in Seismic Codes," by R. Dobry, R. Ramos and M.S. Power, 7/19/99, (PB2000-101705, A08, MF-A02).
- MCEER-99-0011 "Restrainer Design Procedures for Multi-Span Simply-Supported Bridges," by M.J. Randall, M. Saiidi, E. Maragakis and T. Isakovic, 7/20/99, (PB2000-101702, A10, MF-A02).
- MCEER-99-0012 "Property Modification Factors for Seismic Isolation Bearings," by M.C. Constantinou, P. Tsopelas, A. Kasalanati and E. Wolff, 7/20/99, (PB2000-103387, A11, MF-A03).
- MCEER-99-0013 "Critical Seismic Issues for Existing Steel Bridges," by P. Ritchie, N. Kauh and J. Kulicki, 7/20/99, (PB2000-101697, A09, MF-A02).
- MCEER-99-0014 "Nonstructural Damage Database," by A. Kao, T.T. Soong and A. Vender, 7/24/99, (PB2000-101407, A06, MF-A01).
- MCEER-99-0015 "Guide to Remedial Measures for Liquefaction Mitigation at Existing Highway Bridge Sites," by H.G. Cooke and J. K. Mitchell, 7/26/99, (PB2000-101703, A11, MF-A03).
- MCEER-99-0016 "Proceedings of the MCEER Workshop on Ground Motion Methodologies for the Eastern United States," edited by N. Abrahamson and A. Becker, 8/11/99, (PB2000-103385, A07, MF-A02).
- MCEER-99-0017 "Quindío, Colombia Earthquake of January 25, 1999: Reconnaissance Report," by A.P. Asfura and P.J. Flores, 10/4/99, (PB2000-106893, A06, MF-A01).
- MCEER-99-0018 "Hysteretic Models for Cyclic Behavior of Deteriorating Inelastic Structures," by M.V. Sivaselvan and A.M. Reinhorn, 11/5/99, (PB2000-103386, A08, MF-A02).

- MCEER-99-0019 "Proceedings of the 7th U.S.- Japan Workshop on Earthquake Resistant Design of Lifeline Facilities and Countermeasures Against Soil Liquefaction," edited by T.D. O'Rourke, J.P. Bardet and M. Hamada, 11/19/99, (PB2000-103354, A99, MF-A06).
- MCEER-99-0020 "Development of Measurement Capability for Micro-Vibration Evaluations with Application to Chip Fabrication Facilities," by G.C. Lee, Z. Liang, J.W. Song, J.D. Shen and W.C. Liu, 12/1/99, (PB2000-105993, A08, MF-A02).
- MCEER-99-0021 "Design and Retrofit Methodology for Building Structures with Supplemental Energy Dissipating Systems," by G. Pekcan, J.B. Mander and S.S. Chen, 12/31/99, (PB2000-105994, A11, MF-A03).
- MCEER-00-0001 "The Marmara, Turkey Earthquake of August 17, 1999: Reconnaissance Report," edited by C. Scawthorn; with major contributions by M. Bruneau, R. Eguchi, T. Holzer, G. Johnson, J. Mander, J. Mitchell, W. Mitchell, A. Papageorgiou, C. Scaethorn, and G. Webb, 3/23/00, (PB2000-106200, A11, MF-A03).
- MCEER-00-0002 "Proceedings of the MCEER Workshop for Seismic Hazard Mitigation of Health Care Facilities," edited by G.C. Lee, M. Ettouney, M. Grigoriu, J. Hauer and J. Nigg, 3/29/00, (PB2000-106892, A08, MF-A02).
- MCEER-00-0003 "The Chi-Chi, Taiwan Earthquake of September 21, 1999: Reconnaissance Report," edited by G.C. Lee and C.H. Loh, with major contributions by G.C. Lee, M. Bruneau, I.G. Buckle, S.E. Chang, P.J. Flores, T.D. O'Rourke, M. Shinozuka, T.T. Soong, C-H. Loh, K-C. Chang, Z-J. Chen, J-S. Hwang, M-L. Lin, G-Y. Liu, K-C. Tsai, G.C. Yao and C-L. Yen, 4/30/00, (PB2001-100980, A10, MF-A02).
- MCEER-00-0004 "Seismic Retrofit of End-Sway Frames of Steel Deck-Truss Bridges with a Supplemental Tendon System: Experimental and Analytical Investigation," by G. Pekcan, J.B. Mander and S.S. Chen, 7/1/00, (PB2001-100982, A10, MF-A02).
- MCEER-00-0005 "Sliding Fragility of Unrestrained Equipment in Critical Facilities," by W.H. Chong and T.T. Soong, 7/5/00, (PB2001-100983, A08, MF-A02).
- MCEER-00-0006 "Seismic Response of Reinforced Concrete Bridge Pier Walls in the Weak Direction," by N. Abo-Shadi, M. Saiidi and D. Sanders, 7/17/00, (PB2001-100981, A17, MF-A03).
- MCEER-00-0007 "Low-Cycle Fatigue Behavior of Longitudinal Reinforcement in Reinforced Concrete Bridge Columns," by J. Brown and S.K. Kunnath, 7/23/00, (PB2001-104392, A08, MF-A02).
- MCEER-00-0008 "Soil Structure Interaction of Bridges for Seismic Analysis," I. PoLam and H. Law, 9/25/00, (PB2001-105397, A08, MF-A02).
- MCEER-00-0009 "Proceedings of the First MCEER Workshop on Mitigation of Earthquake Disaster by Advanced Technologies (MEDAT-1), edited by M. Shinozuka, D.J. Inman and T.D. O'Rourke, 11/10/00, (PB2001-105399, A14, MF-A03).
- MCEER-00-0010 "Development and Evaluation of Simplified Procedures for Analysis and Design of Buildings with Passive Energy Dissipation Systems, Revision 01," by O.M. Ramirez, M.C. Constantinou, C.A. Kircher, A.S. Whittaker, M.W. Johnson, J.D. Gomez and C. Chrysostomou, 11/16/01, (PB2001-105523, A23, MF-A04).
- MCEER-00-0011 "Dynamic Soil-Foundation-Structure Interaction Analyses of Large Caissons," by C-Y. Chang, C-M. Mok, Z-L. Wang, R. Settgast, F. Waggoner, M.A. Ketchum, H.M. Gonnermann and C-C. Chin, 12/30/00, (PB2001-104373, A07, MF-A02).
- MCEER-00-0012 "Experimental Evaluation of Seismic Performance of Bridge Restrainers," by A.G. Vlassis, E.M. Maragakis and M. Saiid Saiidi, 12/30/00, (PB2001-104354, A09, MF-A02).
- MCEER-00-0013 "Effect of Spatial Variation of Ground Motion on Highway Structures," by M. Shinozuka, V. Saxena and G. Deodatis, 12/31/00, (PB2001-108755, A13, MF-A03).
- MCEER-00-0014 "A Risk-Based Methodology for Assessing the Seismic Performance of Highway Systems," by S.D. Werner, C.E. Taylor, J.E. Moore, II, J.S. Walton and S. Cho, 12/31/00, (PB2001-108756, A14, MF-A03).

- MCEER-01-0001 “Experimental Investigation of P-Delta Effects to Collapse During Earthquakes,” by D. Vian and M. Bruneau, 6/25/01, (PB2002-100534, A17, MF-A03).
- MCEER-01-0002 “Proceedings of the Second MCEER Workshop on Mitigation of Earthquake Disaster by Advanced Technologies (MEDAT-2),” edited by M. Bruneau and D.J. Inman, 7/23/01, (PB2002-100434, A16, MF-A03).
- MCEER-01-0003 “Sensitivity Analysis of Dynamic Systems Subjected to Seismic Loads,” by C. Roth and M. Grigoriu, 9/18/01, (PB2003-100884, A12, MF-A03).
- MCEER-01-0004 “Overcoming Obstacles to Implementing Earthquake Hazard Mitigation Policies: Stage 1 Report,” by D.J. Alesch and W.J. Petak, 12/17/01, (PB2002-107949, A07, MF-A02).
- MCEER-01-0005 “Updating Real-Time Earthquake Loss Estimates: Methods, Problems and Insights,” by C.E. Taylor, S.E. Chang and R.T. Eguchi, 12/17/01, (PB2002-107948, A05, MF-A01).
- MCEER-01-0006 “Experimental Investigation and Retrofit of Steel Pile Foundations and Pile Bents Under Cyclic Lateral Loadings,” by A. Shama, J. Mander, B. Blabac and S. Chen, 12/31/01, (PB2002-107950, A13, MF-A03).
- MCEER-02-0001 “Assessment of Performance of Bolu Viaduct in the 1999 Duzce Earthquake in Turkey” by P.C. Roussis, M.C. Constantinou, M. Erdik, E. Durukal and M. Dicleli, 5/8/02, (PB2003-100883, A08, MF-A02).
- MCEER-02-0002 “Seismic Behavior of Rail Counterweight Systems of Elevators in Buildings,” by M.P. Singh, Rildova and L.E. Suarez, 5/27/02. (PB2003-100882, A11, MF-A03).
- MCEER-02-0003 “Development of Analysis and Design Procedures for Spread Footings,” by G. Mylonakis, G. Gazetas, S. Nikolaou and A. Chauncey, 10/02/02, (PB2004-101636, A13, MF-A03, CD-A13).
- MCEER-02-0004 “Bare-Earth Algorithms for Use with SAR and LIDAR Digital Elevation Models,” by C.K. Huyck, R.T. Eguchi and B. Houshmand, 10/16/02, (PB2004-101637, A07, CD-A07).
- MCEER-02-0005 “Review of Energy Dissipation of Compression Members in Concentrically Braced Frames,” by K.Lee and M. Bruneau, 10/18/02, (PB2004-101638, A10, CD-A10).
- MCEER-03-0001 “Experimental Investigation of Light-Gauge Steel Plate Shear Walls for the Seismic Retrofit of Buildings” by J. Berman and M. Bruneau, 5/2/03, (PB2004-101622, A10, MF-A03, CD-A10).
- MCEER-03-0002 “Statistical Analysis of Fragility Curves,” by M. Shinozuka, M.Q. Feng, H. Kim, T. Uzawa and T. Ueda, 6/16/03, (PB2004-101849, A09, CD-A09).
- MCEER-03-0003 “Proceedings of the Eighth U.S.-Japan Workshop on Earthquake Resistant Design of Lifeline Facilities and Countermeasures Against Liquefaction,” edited by M. Hamada, J.P. Bardet and T.D. O’Rourke, 6/30/03, (PB2004-104386, A99, CD-A99).
- MCEER-03-0004 “Proceedings of the PRC-US Workshop on Seismic Analysis and Design of Special Bridges,” edited by L.C. Fan and G.C. Lee, 7/15/03, (PB2004-104387, A14, CD-A14).
- MCEER-03-0005 “Urban Disaster Recovery: A Framework and Simulation Model,” by S.B. Miles and S.E. Chang, 7/25/03, (PB2004-104388, A07, CD-A07).
- MCEER-03-0006 “Behavior of Underground Piping Joints Due to Static and Dynamic Loading,” by R.D. Meis, M. Maragakis and R. Siddharthan, 11/17/03, (PB2005-102194, A13, MF-A03, CD-A00).
- MCEER-04-0001 “Experimental Study of Seismic Isolation Systems with Emphasis on Secondary System Response and Verification of Accuracy of Dynamic Response History Analysis Methods,” by E. Wolff and M. Constantinou, 1/16/04 (PB2005-102195, A99, MF-E08, CD-A00).
- MCEER-04-0002 “Tension, Compression and Cyclic Testing of Engineered Cementitious Composite Materials,” by K. Kesner and S.L. Billington, 3/1/04, (PB2005-102196, A08, CD-A08).

- MCEER-04-0003 "Cyclic Testing of Braces Laterally Restrained by Steel Studs to Enhance Performance During Earthquakes," by O.C. Celik, J.W. Berman and M. Bruneau, 3/16/04, (PB2005-102197, A13, MF-A03, CD-A00).
- MCEER-04-0004 "Methodologies for Post Earthquake Building Damage Detection Using SAR and Optical Remote Sensing: Application to the August 17, 1999 Marmara, Turkey Earthquake," by C.K. Huyck, B.J. Adams, S. Cho, R.T. Eguchi, B. Mansouri and B. Houshmand, 6/15/04, (PB2005-104888, A10, CD-A00).
- MCEER-04-0005 "Nonlinear Structural Analysis Towards Collapse Simulation: A Dynamical Systems Approach," by M.V. Sivaselvan and A.M. Reinhorn, 6/16/04, (PB2005-104889, A11, MF-A03, CD-A00).
- MCEER-04-0006 "Proceedings of the Second PRC-US Workshop on Seismic Analysis and Design of Special Bridges," edited by G.C. Lee and L.C. Fan, 6/25/04, (PB2005-104890, A16, CD-A00).
- MCEER-04-0007 "Seismic Vulnerability Evaluation of Axially Loaded Steel Built-up Laced Members," by K. Lee and M. Bruneau, 6/30/04, (PB2005-104891, A16, CD-A00).
- MCEER-04-0008 "Evaluation of Accuracy of Simplified Methods of Analysis and Design of Buildings with Damping Systems for Near-Fault and for Soft-Soil Seismic Motions," by E.A. Pavlou and M.C. Constantinou, 8/16/04, (PB2005-104892, A08, MF-A02, CD-A00).
- MCEER-04-0009 "Assessment of Geotechnical Issues in Acute Care Facilities in California," by M. Lew, T.D. O'Rourke, R. Dobry and M. Koch, 9/15/04, (PB2005-104893, A08, CD-A00).
- MCEER-04-0010 "Scissor-Jack-Damper Energy Dissipation System," by A.N. Sigaher-Boyle and M.C. Constantinou, 12/1/04 (PB2005-108221).
- MCEER-04-0011 "Seismic Retrofit of Bridge Steel Truss Piers Using a Controlled Rocking Approach," by M. Pollino and M. Bruneau, 12/20/04 (PB2006-105795).
- MCEER-05-0001 "Experimental and Analytical Studies of Structures Seismically Isolated with an Uplift-Restraint Isolation System," by P.C. Roussis and M.C. Constantinou, 1/10/05 (PB2005-108222).
- MCEER-05-0002 "A Versatile Experimentation Model for Study of Structures Near Collapse Applied to Seismic Evaluation of Irregular Structures," by D. Kusumastuti, A.M. Reinhorn and A. Rutenberg, 3/31/05 (PB2006-101523).
- MCEER-05-0003 "Proceedings of the Third PRC-US Workshop on Seismic Analysis and Design of Special Bridges," edited by L.C. Fan and G.C. Lee, 4/20/05, (PB2006-105796).
- MCEER-05-0004 "Approaches for the Seismic Retrofit of Braced Steel Bridge Piers and Proof-of-Concept Testing of an Eccentrically Braced Frame with Tubular Link," by J.W. Berman and M. Bruneau, 4/21/05 (PB2006-101524).
- MCEER-05-0005 "Simulation of Strong Ground Motions for Seismic Fragility Evaluation of Nonstructural Components in Hospitals," by A. Wanitkorkul and A. Filiatrault, 5/26/05 (PB2006-500027).
- MCEER-05-0006 "Seismic Safety in California Hospitals: Assessing an Attempt to Accelerate the Replacement or Seismic Retrofit of Older Hospital Facilities," by D.J. Alesch, L.A. Arendt and W.J. Petak, 6/6/05 (PB2006-105794).
- MCEER-05-0007 "Development of Seismic Strengthening and Retrofit Strategies for Critical Facilities Using Engineered Cementitious Composite Materials," by K. Kesner and S.L. Billington, 8/29/05 (PB2006-111701).
- MCEER-05-0008 "Experimental and Analytical Studies of Base Isolation Systems for Seismic Protection of Power Transformers," by N. Murota, M.Q. Feng and G-Y. Liu, 9/30/05 (PB2006-111702).
- MCEER-05-0009 "3D-BASIS-ME-MB: Computer Program for Nonlinear Dynamic Analysis of Seismically Isolated Structures," by P.C. Tsopelas, P.C. Roussis, M.C. Constantinou, R. Buchanan and A.M. Reinhorn, 10/3/05 (PB2006-111703).
- MCEER-05-0010 "Steel Plate Shear Walls for Seismic Design and Retrofit of Building Structures," by D. Vian and M. Bruneau, 12/15/05 (PB2006-111704).

- MCEER-05-0011 "The Performance-Based Design Paradigm," by M.J. Astrella and A. Whittaker, 12/15/05 (PB2006-111705).
- MCEER-06-0001 "Seismic Fragility of Suspended Ceiling Systems," H. Badillo-Almaraz, A.S. Whittaker, A.M. Reinhorn and G.P. Cimellaro, 2/4/06 (PB2006-111706).
- MCEER-06-0002 "Multi-Dimensional Fragility of Structures," by G.P. Cimellaro, A.M. Reinhorn and M. Bruneau, 3/1/06 (PB2007-106974, A09, MF-A02, CD A00).
- MCEER-06-0003 "Built-Up Shear Links as Energy Dissipators for Seismic Protection of Bridges," by P. Dusicka, A.M. Itani and I.G. Buckle, 3/15/06 (PB2006-111708).
- MCEER-06-0004 "Analytical Investigation of the Structural Fuse Concept," by R.E. Vargas and M. Bruneau, 3/16/06 (PB2006-111709).
- MCEER-06-0005 "Experimental Investigation of the Structural Fuse Concept," by R.E. Vargas and M. Bruneau, 3/17/06 (PB2006-111710).
- MCEER-06-0006 "Further Development of Tubular Eccentrically Braced Frame Links for the Seismic Retrofit of Braced Steel Truss Bridge Piers," by J.W. Berman and M. Bruneau, 3/27/06 (PB2007-105147).
- MCEER-06-0007 "REDARS Validation Report," by S. Cho, C.K. Huyck, S. Ghosh and R.T. Eguchi, 8/8/06 (PB2007-106983).
- MCEER-06-0008 "Review of Current NDE Technologies for Post-Earthquake Assessment of Retrofitted Bridge Columns," by J.W. Song, Z. Liang and G.C. Lee, 8/21/06 (PB2007-106984).
- MCEER-06-0009 "Liquefaction Remediation in Silty Soils Using Dynamic Compaction and Stone Columns," by S. Thevanayagam, G.R. Martin, R. Nashed, T. Shenthan, T. Kanagalingam and N. Ecemis, 8/28/06 (PB2007-106985).
- MCEER-06-0010 "Conceptual Design and Experimental Investigation of Polymer Matrix Composite Infill Panels for Seismic Retrofitting," by W. Jung, M. Chiewanichakorn and A.J. Aref, 9/21/06 (PB2007-106986).
- MCEER-06-0011 "A Study of the Coupled Horizontal-Vertical Behavior of Elastomeric and Lead-Rubber Seismic Isolation Bearings," by G.P. Warn and A.S. Whittaker, 9/22/06 (PB2007-108679).
- MCEER-06-0012 "Proceedings of the Fourth PRC-US Workshop on Seismic Analysis and Design of Special Bridges: Advancing Bridge Technologies in Research, Design, Construction and Preservation," Edited by L.C. Fan, G.C. Lee and L. Ziang, 10/12/06 (PB2007-109042).
- MCEER-06-0013 "Cyclic Response and Low Cycle Fatigue Characteristics of Plate Steels," by P. Dusicka, A.M. Itani and I.G. Buckle, 11/1/06 (PB2007-106987).
- MCEER-06-0014 "Proceedings of the Second US-Taiwan Bridge Engineering Workshop," edited by W.P. Yen, J. Shen, J-Y. Chen and M. Wang, 11/15/06 (PB2008-500041).
- MCEER-06-0015 "User Manual and Technical Documentation for the REDARSTM Import Wizard," by S. Cho, S. Ghosh, C.K. Huyck and S.D. Werner, 11/30/06 (PB2007-114766).
- MCEER-06-0016 "Hazard Mitigation Strategy and Monitoring Technologies for Urban and Infrastructure Public Buildings: Proceedings of the China-US Workshops," edited by X.Y. Zhou, A.L. Zhang, G.C. Lee and M. Tong, 12/12/06 (PB2008-500018).
- MCEER-07-0001 "Static and Kinetic Coefficients of Friction for Rigid Blocks," by C. Kafali, S. Fathali, M. Grigoriu and A.S. Whittaker, 3/20/07 (PB2007-114767).
- MCEER-07-0002 "Hazard Mitigation Investment Decision Making: Organizational Response to Legislative Mandate," by L.A. Arendt, D.J. Alesch and W.J. Petak, 4/9/07 (PB2007-114768).
- MCEER-07-0003 "Seismic Behavior of Bidirectional-Resistant Ductile End Diaphragms with Unbonded Braces in Straight or Skewed Steel Bridges," by O. Celik and M. Bruneau, 4/11/07 (PB2008-105141).

- MCEER-07-0004 "Modeling Pile Behavior in Large Pile Groups Under Lateral Loading," by A.M. Dodds and G.R. Martin, 4/16/07(PB2008-105142).
- MCEER-07-0005 "Experimental Investigation of Blast Performance of Seismically Resistant Concrete-Filled Steel Tube Bridge Piers," by S. Fujikura, M. Bruneau and D. Lopez-Garcia, 4/20/07 (PB2008-105143).
- MCEER-07-0006 "Seismic Analysis of Conventional and Isolated Liquefied Natural Gas Tanks Using Mechanical Analogs," by I.P. Christovasilis and A.S. Whittaker, 5/1/07.
- MCEER-07-0007 "Experimental Seismic Performance Evaluation of Isolation/Restraint Systems for Mechanical Equipment – Part 1: Heavy Equipment Study," by S. Fathali and A. Filiatrault, 6/6/07 (PB2008-105144).
- MCEER-07-0008 "Seismic Vulnerability of Timber Bridges and Timber Substructures," by A.A. Sharma, J.B. Mander, I.M. Friedland and D.R. Allicock, 6/7/07 (PB2008-105145).
- MCEER-07-0009 "Experimental and Analytical Study of the XY-Friction Pendulum (XY-FP) Bearing for Bridge Applications," by C.C. Marin-Artieda, A.S. Whittaker and M.C. Constantinou, 6/7/07 (PB2008-105191).
- MCEER-07-0010 "Proceedings of the PRC-US Earthquake Engineering Forum for Young Researchers," Edited by G.C. Lee and X.Z. Qi, 6/8/07 (PB2008-500058).
- MCEER-07-0011 "Design Recommendations for Perforated Steel Plate Shear Walls," by R. Purba and M. Bruneau, 6/18/07, (PB2008-105192).
- MCEER-07-0012 "Performance of Seismic Isolation Hardware Under Service and Seismic Loading," by M.C. Constantinou, A.S. Whittaker, Y. Kalpakidis, D.M. Fenz and G.P. Warn, 8/27/07, (PB2008-105193).
- MCEER-07-0013 "Experimental Evaluation of the Seismic Performance of Hospital Piping Subassemblies," by E.R. Goodwin, E. Maragakis and A.M. Itani, 9/4/07, (PB2008-105194).
- MCEER-07-0014 "A Simulation Model of Urban Disaster Recovery and Resilience: Implementation for the 1994 Northridge Earthquake," by S. Miles and S.E. Chang, 9/7/07, (PB2008-106426).
- MCEER-07-0015 "Statistical and Mechanistic Fragility Analysis of Concrete Bridges," by M. Shinozuka, S. Banerjee and S-H. Kim, 9/10/07, (PB2008-106427).
- MCEER-07-0016 "Three-Dimensional Modeling of Inelastic Buckling in Frame Structures," by M. Schachter and AM. Reinhorn, 9/13/07, (PB2008-108125).
- MCEER-07-0017 "Modeling of Seismic Wave Scattering on Pile Groups and Caissons," by I. Po Lam, H. Law and C.T. Yang, 9/17/07 (PB2008-108150).
- MCEER-07-0018 "Bridge Foundations: Modeling Large Pile Groups and Caissons for Seismic Design," by I. Po Lam, H. Law and G.R. Martin (Coordinating Author), 12/1/07 (PB2008-111190).
- MCEER-07-0019 "Principles and Performance of Roller Seismic Isolation Bearings for Highway Bridges," by G.C. Lee, Y.C. Ou, Z. Liang, T.C. Niu and J. Song, 12/10/07 (PB2009-110466).
- MCEER-07-0020 "Centrifuge Modeling of Permeability and Pinning Reinforcement Effects on Pile Response to Lateral Spreading," by L.L Gonzalez-Lagos, T. Abdoun and R. Dobry, 12/10/07 (PB2008-111191).
- MCEER-07-0021 "Damage to the Highway System from the Pisco, Perú Earthquake of August 15, 2007," by J.S. O'Connor, L. Mesa and M. Nykamp, 12/10/07, (PB2008-108126).
- MCEER-07-0022 "Experimental Seismic Performance Evaluation of Isolation/Restraint Systems for Mechanical Equipment – Part 2: Light Equipment Study," by S. Fathali and A. Filiatrault, 12/13/07 (PB2008-111192).
- MCEER-07-0023 "Fragility Considerations in Highway Bridge Design," by M. Shinozuka, S. Banerjee and S.H. Kim, 12/14/07 (PB2008-111193).

- MCEER-07-0024 "Performance Estimates for Seismically Isolated Bridges," by G.P. Warn and A.S. Whittaker, 12/30/07 (PB2008-112230).
- MCEER-08-0001 "Seismic Performance of Steel Girder Bridge Superstructures with Conventional Cross Frames," by L.P. Carden, A.M. Itani and I.G. Buckle, 1/7/08, (PB2008-112231).
- MCEER-08-0002 "Seismic Performance of Steel Girder Bridge Superstructures with Ductile End Cross Frames with Seismic Isolators," by L.P. Carden, A.M. Itani and I.G. Buckle, 1/7/08 (PB2008-112232).
- MCEER-08-0003 "Analytical and Experimental Investigation of a Controlled Rocking Approach for Seismic Protection of Bridge Steel Truss Piers," by M. Pollino and M. Bruneau, 1/21/08 (PB2008-112233).
- MCEER-08-0004 "Linking Lifeline Infrastructure Performance and Community Disaster Resilience: Models and Multi-Stakeholder Processes," by S.E. Chang, C. Pasion, K. Tatebe and R. Ahmad, 3/3/08 (PB2008-112234).
- MCEER-08-0005 "Modal Analysis of Generally Damped Linear Structures Subjected to Seismic Excitations," by J. Song, Y-L. Chu, Z. Liang and G.C. Lee, 3/4/08 (PB2009-102311).
- MCEER-08-0006 "System Performance Under Multi-Hazard Environments," by C. Kafali and M. Grigoriu, 3/4/08 (PB2008-112235).
- MCEER-08-0007 "Mechanical Behavior of Multi-Spherical Sliding Bearings," by D.M. Fenz and M.C. Constantinou, 3/6/08 (PB2008-112236).
- MCEER-08-0008 "Post-Earthquake Restoration of the Los Angeles Water Supply System," by T.H.P. Tabucchi and R.A. Davidson, 3/7/08 (PB2008-112237).
- MCEER-08-0009 "Fragility Analysis of Water Supply Systems," by A. Jacobson and M. Grigoriu, 3/10/08 (PB2009-105545).
- MCEER-08-0010 "Experimental Investigation of Full-Scale Two-Story Steel Plate Shear Walls with Reduced Beam Section Connections," by B. Qu, M. Bruneau, C-H. Lin and K-C. Tsai, 3/17/08 (PB2009-106368).
- MCEER-08-0011 "Seismic Evaluation and Rehabilitation of Critical Components of Electrical Power Systems," S. Ersoy, B. Feizi, A. Ashrafi and M. Ala Saadeghvaziri, 3/17/08 (PB2009-105546).
- MCEER-08-0012 "Seismic Behavior and Design of Boundary Frame Members of Steel Plate Shear Walls," by B. Qu and M. Bruneau, 4/26/08 . (PB2009-106744).
- MCEER-08-0013 "Development and Appraisal of a Numerical Cyclic Loading Protocol for Quantifying Building System Performance," by A. Filiatrault, A. Wanitkorkul and M. Constantinou, 4/27/08 (PB2009-107906).
- MCEER-08-0014 "Structural and Nonstructural Earthquake Design: The Challenge of Integrating Specialty Areas in Designing Complex, Critical Facilities," by W.J. Petak and D.J. Alesch, 4/30/08 (PB2009-107907).
- MCEER-08-0015 "Seismic Performance Evaluation of Water Systems," by Y. Wang and T.D. O'Rourke, 5/5/08 (PB2009-107908).
- MCEER-08-0016 "Seismic Response Modeling of Water Supply Systems," by P. Shi and T.D. O'Rourke, 5/5/08 (PB2009-107910).
- MCEER-08-0017 "Numerical and Experimental Studies of Self-Centering Post-Tensioned Steel Frames," by D. Wang and A. Filiatrault, 5/12/08 (PB2009-110479).
- MCEER-08-0018 "Development, Implementation and Verification of Dynamic Analysis Models for Multi-Spherical Sliding Bearings," by D.M. Fenz and M.C. Constantinou, 8/15/08 (PB2009-107911).
- MCEER-08-0019 "Performance Assessment of Conventional and Base Isolated Nuclear Power Plants for Earthquake Blast Loadings," by Y.N. Huang, A.S. Whittaker and N. Luco, 10/28/08 (PB2009-107912).

- MCEER-08-0020 “Remote Sensing for Resilient Multi-Hazard Disaster Response – Volume I: Introduction to Damage Assessment Methodologies,” by B.J. Adams and R.T. Eguchi, 11/17/08 (PB2010-102695).
- MCEER-08-0021 “Remote Sensing for Resilient Multi-Hazard Disaster Response – Volume II: Counting the Number of Collapsed Buildings Using an Object-Oriented Analysis: Case Study of the 2003 Bam Earthquake,” by L. Gusella, C.K. Huyck and B.J. Adams, 11/17/08 (PB2010-100925).
- MCEER-08-0022 “Remote Sensing for Resilient Multi-Hazard Disaster Response – Volume III: Multi-Sensor Image Fusion Techniques for Robust Neighborhood-Scale Urban Damage Assessment,” by B.J. Adams and A. McMillan, 11/17/08 (PB2010-100926).
- MCEER-08-0023 “Remote Sensing for Resilient Multi-Hazard Disaster Response – Volume IV: A Study of Multi-Temporal and Multi-Resolution SAR Imagery for Post-Katrina Flood Monitoring in New Orleans,” by A. McMillan, J.G. Morley, B.J. Adams and S. Chesworth, 11/17/08 (PB2010-100927).
- MCEER-08-0024 “Remote Sensing for Resilient Multi-Hazard Disaster Response – Volume V: Integration of Remote Sensing Imagery and VIEWS™ Field Data for Post-Hurricane Charley Building Damage Assessment,” by J.A. Womble, K. Mehta and B.J. Adams, 11/17/08 (PB2009-115532).
- MCEER-08-0025 “Building Inventory Compilation for Disaster Management: Application of Remote Sensing and Statistical Modeling,” by P. Sarabandi, A.S. Kiremidjian, R.T. Eguchi and B. J. Adams, 11/20/08 (PB2009-110484).
- MCEER-08-0026 “New Experimental Capabilities and Loading Protocols for Seismic Qualification and Fragility Assessment of Nonstructural Systems,” by R. Retamales, G. Mosqueda, A. Filiatrault and A. Reinhorn, 11/24/08 (PB2009-110485).
- MCEER-08-0027 “Effects of Heating and Load History on the Behavior of Lead-Rubber Bearings,” by I.V. Kalpakidis and M.C. Constantinou, 12/1/08 (PB2009-115533).
- MCEER-08-0028 “Experimental and Analytical Investigation of Blast Performance of Seismically Resistant Bridge Piers,” by S.Fujikura and M. Bruneau, 12/8/08 (PB2009-115534).
- MCEER-08-0029 “Evolutionary Methodology for Aseismic Decision Support,” by Y. Hu and G. Dargush, 12/15/08.
- MCEER-08-0030 “Development of a Steel Plate Shear Wall Bridge Pier System Conceived from a Multi-Hazard Perspective,” by D. Keller and M. Bruneau, 12/19/08 (PB2010-102696).
- MCEER-09-0001 “Modal Analysis of Arbitrarily Damped Three-Dimensional Linear Structures Subjected to Seismic Excitations,” by Y.L. Chu, J. Song and G.C. Lee, 1/31/09 (PB2010-100922).
- MCEER-09-0002 “Air-Blast Effects on Structural Shapes,” by G. Ballantyne, A.S. Whittaker, A.J. Aref and G.F. Dargush, 2/2/09 (PB2010-102697).
- MCEER-09-0003 “Water Supply Performance During Earthquakes and Extreme Events,” by A.L. Bonneau and T.D. O’Rourke, 2/16/09 (PB2010-100923).
- MCEER-09-0004 “Generalized Linear (Mixed) Models of Post-Earthquake Ignitions,” by R.A. Davidson, 7/20/09 (PB2010-102698).
- MCEER-09-0005 “Seismic Testing of a Full-Scale Two-Story Light-Frame Wood Building: NEESWood Benchmark Test,” by I.P. Christovasilis, A. Filiatrault and A. Wanitkorkul, 7/22/09.



EARTHQUAKE ENGINEERING TO EXTREME EVENTS

University at Buffalo, The State University of New York

Red Jacket Quadrangle ▪ Buffalo, New York 14261

Phone: (716) 645-3391 ▪ Fax: (716) 645-3399

E-mail: mceer@buffalo.edu ▪ WWW Site <http://mceer.buffalo.edu>



University at Buffalo *The State University of New York*

ISSN 1520-295X